HEALTH AND DISEASE IN FREE-RANGING AND CAPTIVE WILDLIFE

EDITED BY: Robert James Ossiboff, Nicole Indra Stacy and Francesco Carlo Origgi

PUBLISHED IN: Frontiers in Veterinary Science

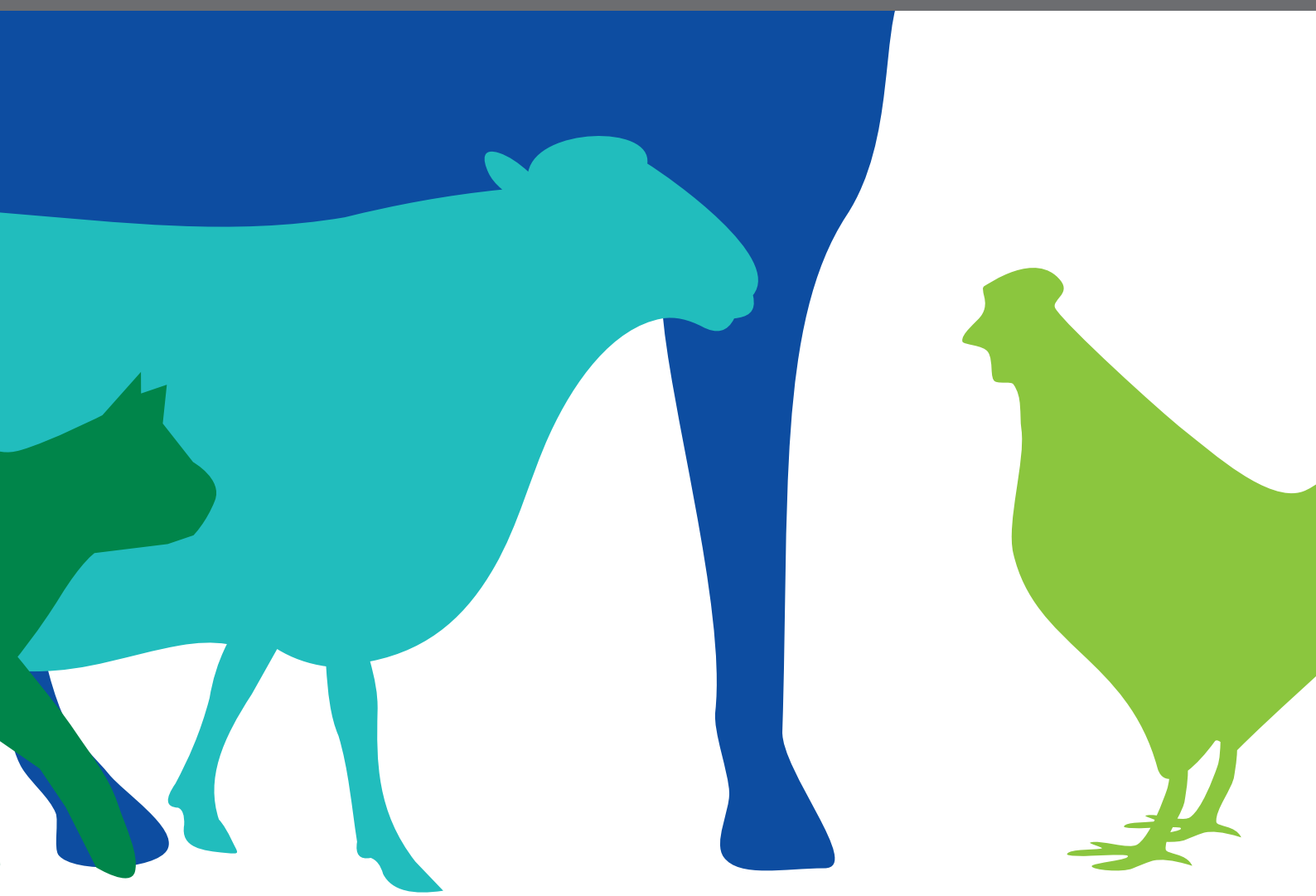

frontiers Research Topics

Frontiers eBook Copyright Statement

The copyright in the text of individual articles in this eBook is the property of their respective authors or their respective institutions or funders. The copyright in graphics and images within each article may be subject to copyright of other parties. In both cases this is subject to a license granted to Frontiers.

The compilation of articles constituting this eBook is the property of Frontiers.

Each article within this eBook, and the eBook itself, are published under the most recent version of the Creative Commons CC-BY licence. The version current at the date of publication of this eBook is CC-BY 4.0. If the CC-BY licence is updated, the licence granted by Frontiers is automatically updated to the new version.

When exercising any right under the CC-BY licence, Frontiers must be attributed as the original publisher of the article or eBook, as applicable.

Authors have the responsibility of ensuring that any graphics or other materials which are the property of others may be included in the CC-BY licence, but this should be checked before relying on the CC-BY licence to reproduce those materials. Any copyright notices relating to those materials must be complied with.

Copyright and source acknowledgement notices may not be removed and must be displayed in any copy, derivative work or partial copy which includes the elements in question.

All copyright, and all rights therein, are protected by national and international copyright laws. The above represents a summary only. For further information please read Frontiers' Conditions for Website Use and Copyright Statement, and the applicable CC-BY licence.

ISSN 1664-8714
ISBN 978-2-88966-498-6
DOI 10.3389/978-2-88966-498-6

About Frontiers

Frontiers is more than just an open-access publisher of scholarly articles: it is a pioneering approach to the world of academia, radically improving the way scholarly research is managed. The grand vision of Frontiers is a world where all people have an equal opportunity to seek, share and generate knowledge. Frontiers provides immediate and permanent online open access to all its publications, but this alone is not enough to realize our grand goals.

Frontiers Journal Series

The Frontiers Journal Series is a multi-tier and interdisciplinary set of open-access, online journals, promising a paradigm shift from the current review, selection and dissemination processes in academic publishing. All Frontiers journals are driven by researchers for researchers; therefore, they constitute a service to the scholarly community. At the same time, the Frontiers Journal Series operates on a revolutionary invention, the tiered publishing system, initially addressing specific communities of scholars, and gradually climbing up to broader public understanding, thus serving the interests of the lay society, too.

Dedication to Quality

Each Frontiers article is a landmark of the highest quality, thanks to genuinely collaborative interactions between authors and review editors, who include some of the world's best academicians. Research must be certified by peers before entering a stream of knowledge that may eventually reach the public - and shape society; therefore, Frontiers only applies the most rigorous and unbiased reviews.
Frontiers revolutionizes research publishing by freely delivering the most outstanding research, evaluated with no bias from both the academic and social point of view. By applying the most advanced information technologies, Frontiers is catapulting scholarly publishing into a new generation.

What are Frontiers Research Topics?

Frontiers Research Topics are very popular trademarks of the Frontiers Journals Series: they are collections of at least ten articles, all centered on a particular subject. With their unique mix of varied contributions from Original Research to Review Articles, Frontiers Research Topics unify the most influential researchers, the latest key findings and historical advances in a hot research area! Find out more on how to host your own Frontiers Research Topic or contribute to one as an author by contacting the Frontiers Editorial Office: frontiersin.org/about/contact

HEALTH AND DISEASE IN FREE-RANGING AND CAPTIVE WILDLIFE

Topic Editors:
Robert James Ossiboff, University of Florida, United States
Nicole Indra Stacy, University of Florida, United States
Francesco Carlo Origgi, University of Bern, Switzerland

Citation: Ossiboff, R. J., Stacy, N. I., Origgi, F. C., eds. (2021). Health and Disease in Free-Ranging and Captive Wildlife. Lausanne: Frontiers Media SA.
doi: 10.3389/978-2-88966-498-6

Table of Contents

08 ***Editorial: Health and Disease in Free-Ranging and Captive Wildlife***
Robert J. Ossiboff, Francesco C. Origgi and Nicole I. Stacy

14 ***Comparative Health Assessments of Alaskan Ice Seals***
Caroline E. C. Goertz, Colleen Reichmuth, Nicole M. Thometz, Heather Ziel and Peter Boveng

29 ***Occurrence of Rhabditid Nematodes in the Pet Giant African Land Snails (*Achatina fulica*)***
Dario d'Ovidio, Jirí Nermut, Chiara Adami and Mario Santoro

34 ***Diagnostic Performance of Clinicopathological Analytes in* Otostrongylus circumlitis*-Infected Rehabilitating Juvenile Northern Elephant Seals (*Mirounga angustirostris*)***
Julie D. Sheldon, Jorge A. Hernandez, Shawn P. Johnson, Cara Field, Sarrah Kaye and Nicole I. Stacy

40 **Trichomonas *Infection in a Community of Free-Ranging Domestic and Wild Columbiformes and Bonelli's Eagle (*Aquila fasciata*)***
Nuno Santos, José Jambas, António Monteiro, Jorge Amaral, Nuno Martins, Javier Garcia, Ana Martinez Fernández, Kevin Morris Tyler, Tereza Almeida, Joana Abrantes and Pedro J. Esteves

49 ***Abdominal Ectopic Pregnancy and Impaired Postnatal Mammary Gland Development, Consistent With Physiologic Agalactia, in a Wild European Rabbit,* Oryctolagus cuniculus**
Katherine Hughes

54 ***Keeping an Eye on Wild Brown Trout (*Salmo trutta*) Populations: Correlation Between Temperature, Environmental Parameters, and Proliferative Kidney Disease***
Aurélie Rubin, Pauline de Coulon, Christyn Bailey, Helmut Segner, Thomas Wahli and Jean-François Rubin

70 ***Molecular Detection of* Babesia *spp. (Apicomplexa: Piroplasma) in Free-Ranging Canids and Mustelids From Southern Italy***
Mario Santoro, Clementina Auriemma, Maria Gabriella Lucibelli, Giorgia Borriello, Nicola D'Alessio, Giovanni Sgroi, Vincenzo Veneziano, Giorgio Galiero and Giovanna Fusco

75 ***Assessment of the LeadCare® Plus for Use on Scandinavian Brown Bears (*Ursus arctos*)***
Amanda H. Boesen, Alexandra Thiel, Boris Fuchs, Alina L. Evans, Mads F. Bertelsen, Ilia Rodushkin and Jon M. Arnemo

82 ***Differentiating* Batrachochytrium dendrobatidis *and* B. salamandrivorans *in Amphibian Chytridiomycosis Using RNAScope® in situ Hybridization***
Robert J. Ossiboff, Anastasia E. Towe, Melissa A. Brown, Ana V. Longo, Karen R. Lips, Debra L. Miller, E. Davis Carter, Matthew J. Gray and Salvatore Frasca Jr.

92 ***Longitudinal and Cross-Sectional Sampling of Serpentovirus (Nidovirus) Infection in Captive Snakes Reveals High Prevalence, Persistent Infection, and Increased Mortality in Pythons and Divergent Serpentovirus Infection in Boas and Colubrids***

Laura L. Hoon-Hanks, Robert J. Ossiboff, Pia Bartolini, Susan B. Fogelson, Sean M. Perry, Anke C. Stöhr, Shaun T. Cross, James F. X. Wellehan, Elliott R. Jacobson, Edward J. Dubovi and Mark D. Stenglein

109 ***Fatal* Sarcocystis falcatula *Infection in Three Penguins***

Shannon G. M. Kirejczyk, Rachel E. Burns, Michael W. Hyatt, Michael J. Yabsley, Julia M. Ter Beest, Zoltan S. Gyimesi, Robert J. Ossiboff, Amelia Waltman, Tracie A. Seimon and Rita McManamon

117 ***Crude Oil and Dispersant Cause Acute Clinicopathological Abnormalities in Hatchling Loggerhead Sea Turtles (*Caretta caretta*)***

Craig A. Harms, Patricia McClellan-Green, Matthew H. Godfrey, Emily F. Christiansen, Heather J. Broadhurst and Céline A. J. Godard-Codding

128 **Caryospora-*Like Coccidia Infecting Green Turtles (*Chelonia mydas*): An Emerging Disease With Evidence of Interoceanic Dissemination***

Brian A. Stacy, Phoebe A. Chapman, Heather Stockdale-Walden, Thierry M. Work, Julie Dagenais, Allen M. Foley, Morgan Wideroff, James F. X. Wellehan Jr., April L. Childress, Charles A. Manire, Mya Rodriguez, Trevor T. Zachariah, Lydia Staggs, Bette Zirkelbach, Nina Nahvi, Whitney Crowder, Shane M. Boylan, Shelly Marquardt, Craig Pelton and Terry M. Norton

140 ***Investigating the Analytical Variability and Agreement of Manual Leukocyte Quantification Methods in Eastern Box Turtles (*Terrapene carolina carolina*)***

John M. Winter, Nicole I. Stacy, Laura A. Adamovicz and Matthew C. Allender

149 ***Evaluation of Physiological Parameters and Effectiveness of an Immobilization Protocol Using Etorphine, Azaperone, and Butorphanol in Free-Ranging Warthogs (*Phacochoerus africanus*)***

Donald Neiffer, Peter Buss, Jennie Hewlett, Guy Hausler, Leana Rossouw, Tebogo Manamela, Brittany Grenus, Emily Thulson, Francisco Olea-Popelka and Michele Miller

157 ***Effects of External Oiling and Rehabilitation on Hematological, Biochemical, and Blood Gas Analytes in Ring-Billed Gulls (*Larus delawarensis*)***

Nicholas G. Dannemiller, Katherine E. Horak, Jeremy W. Ellis, Nicole L. Barrett, Lisa L. Wolfe and Susan A. Shriner

169 ***Mortality in Three-Toed Box Turtles (*Terrapene mexicana triunguis*) at Two Sites in Missouri***

Jamie L. Palmer, Maris Brenn-White, Stephen Blake and Sharon L. Deem

175 ***Trichomonosis in Greenfinches (*Chloris chloris*) in the Netherlands 2009–2017: A Concealed Threat***

Jolianne M. Rijks, Andrea A. G. Laumen, Roy Slaterus, Julia Stahl, Andrea Gröne and Marja L. Kik

185 ***Health Assessments of Common Bottlenose Dolphins (*Tursiops truncatus*): Past, Present, and Potential Conservation Applications***
Ashley Barratclough, Randall S. Wells, Lori H. Schwacke, Teresa K. Rowles, Forrest M. Gomez, Deborah A. Fauquier, Jay C. Sweeney, Forrest I. Townsend, Larry J. Hansen, Eric S. Zolman, Brian C. Balmer and Cynthia R. Smith

203 ***Saxitoxin Poisoning in Green Turtles (*Chelonia mydas*) Linked to Scavenging on Mass Mortality of Caribbean Sharpnose Puffer Fish (*Canthigaster rostrata*-Tetraodontidae)***
Rocío González Barrientos, Gabriela Hernández-Mora, Fernando Alegre, Theresa Field, Leanne Flewelling, Sara McGrath, Jonathan Deeds, Yajaira Salazar Chacón, Karla Rojas Arrieta, Emilia Calvo Vargas, Karen Berrocal Artavia and Brian A. Stacy

209 ***Skeletal and Cardiac Rhabdomyolysis in a Live-Stranded Neonatal Bryde's Whale With Fetal Distress***
Nakita Câmara, Eva Sierra, Antonio Fernández, Cristian Manuel Suárez-Santana, Raquel Puig-Lozano, Manuel Arbelo and Pedro Herráez

217 ***Cutaneous Lesions in Freshwater Turtles (*Emydura macquarii krefftii *and* Myuchelys latisternum*) in a Rainforest Creek in North Queensland, Australia***
Wytamma Wirth, Elizabeth Elliott, Donna Rudd, Linda Hayes, Alicia Maclaine, Narges Mashkour, Shamim Ahasan, Jakob Gorm Dahl, Kezia Drane and Ellen Ariel

228 ***A Novel* Exophiala *Species Associated With Disseminated Granulomatous Inflammation in a Captive Eastern Hellbender (*Cryptobranchus alleganiensis alleganiensis*)***
Cynthia Hopf, Erin A. Graham, Connie F. C. Gibas, Carmita Sanders, James Mele, Hongxin Fan, Michael M. Garner, Nathan P. Wiederhold, Robert Ossiboff and Noha Abou-Madi

235 ***Evaluation of Severity and Factors Contributing to Foot Lesions in Endangered Ozark Hellbenders,* Cryptobranchus alleganiensis bishopi**
Rebecca H. Hardman, Kelly J. Irwin, William B. Sutton and Debra L. Miller

245 ***Clinical Manifestation and Molecular Characterization of a Novel Member of the* Nannizziopsiaceae *in a Pulmonary Granuloma From a Galapagos Tortoise (*Chelonoidis nigra*)***
Jane E. Christman, Amy B. Alexander, Kyle A. Donnelly, Robert J. Ossiboff, Nicole I. Stacy, Rebecca L. Richardson, J. Brad Case, April L. Childress and James F. X. Wellehan

252 ***Infectious Wildlife Diseases in Austria—A Literature Review From 1980 Until 2017***
Nina Eva Trimmel and Chris Walzer

275 ***Diagnosis and Surgical Management of a Paratesticular Cyst in a Rehabilitating Juvenile Male Green Turtle (*Chelonia mydas*)***
Tatiana C. Weisbrod, Nicole I. Stacy, Nancy L. Stedman and Terry M. Norton

282 ***Epidemiological Investigation of a Mortality Event in a Translocated Gopher Tortoise (*Gopherus polyphemus*) Population in Northwest Florida***
Rebecca A. Cozad, Sonia M. Hernandez, Terry M. Norton, Tracey D. Tuberville, Nicole I. Stacy, Nancy L. Stedman and Matthew J. Aresco

297 ***Coelomic Fluid Evaluation in* Pisaster ochraceus *Affected by Sea Star Wasting Syndrome: Evidence of Osmodysregulation, Calcium Homeostasis Derangement, and Coelomocyte Responses***
Sarah J. Wahltinez, Alisa L. Newton, Craig A. Harms, Lesanna L. Lahner and Nicole I. Stacy

307 ***Leukocyte and Platelet Characteristics of the Giant Panda (*Ailuropoda melanoleuca*): Morphological, Cytochemical, and Ultrastructural Features***
Spencer P. Kehoe, Nicole I. Stacy, Salvatore Frasca Jr., Tracy Stokol, Chengdong Wang, Kathryn Strayer Leach, Li Luo and Sam Rivera

319 ***Mandibular Ossifying Fibroma and Multiple Oral Papillomas in a Roe Deer (*Capreolus capreolus*)***
Samoa Zürcher-Giovannini, Thomas-Daniel Ruder, Roy Pool, Karoly Erdelyi and Francesco C. Origgi

325 ***Epitheliotropic Infections in Wildlife Ruminants From the Central Alps and Stelvio National Park***
Laura Gallina, Federica Savini, Giovanni Casà, Irene Bertoletti, Alessandro Bianchi, Lucia Rita Gibelli, Davide Lelli, Antonio Lavazza and Alessandra Scagliarini

337 ***Sarcoptic Mange in Wild Caprinae of the Alps: Could Pathology Help in Filling the Gaps in Knowledge?***
Sara Turchetto, Federica Obber, Luca Rossi, Stefano D'Amelio, Serena Cavallero, Alessandro Poli, Francesca Parisi, Paolo Lanfranchi, Nicola Ferrari, Debora Dellamaria and Carlo V. Citterio

346 ***Health Impacts and Recovery From Prolonged Freshwater Exposure in a Common Bottlenose Dolphin (*Tursiops truncatus*)***
Alissa C. Deming, Noel L. Wingers, Debra P. Moore, David Rotstein, Randall S. Wells, Ruth Ewing, Matthew R. Hodanbosi and Ruth H. Carmichael

356 ***Case Report: Invasive Pentastomes,* Raillietiella orientalis *(Sambon, 1922), in a Free-Ranging Banded Water Snake (*Nerodia fasciata*) in North Central Florida, USA***
Heather D. S. Walden, Marley E. Iredale, April Childress, James F. X. Wellehan Jr. and Robert J. Ossiboff

362 ***The Iconic Atlantic Goliath Grouper (*Epinephelus itajara*): A Comprehensive Assessment of Health Indices in the Southeastern United States Population***
Christopher R. Malinowski, Justin R. Perrault, Felicia C. Coleman, Christopher C. Koenig, Justin M. Stilwell, Carolyn Cray and Nicole I. Stacy

382 ***Concentrations of Retinol and* α*-Tocopherol in Tissue Samples From Anna's Hummingbirds (*Calypte anna*)***
Stephanie M. Diao, Robert H. Poppenga, Gwendolyne Gonzales Alarcio, Janet E. Foley, Ruta R. Bandivadekar, Linda S. Aston and Lisa A. Tell

391 ***Retrospective Study of Fishery Interactions in Stranded Cetaceans, Canary Islands***
Raquel Puig-Lozano, Antonio Fernández, Eva Sierra, Pedro Saavedra, Cristian M. Suárez-Santana, Jesús De la Fuente, Josué Díaz-Delgado, Ana Godinho, Natalia García-Álvarez, Daniele Zucca, Aina Xuriach, Marina Arregui, Idaira Felipe-Jiménez, Francesco Consoli, Pablo J. Díaz-Santana, Simone Segura-Göthlin, Nakita Câmara, Miguel A. Rivero, Simona Sacchini, Yara Bernaldo de Quirós and Manuel Arbelo

406 ***Standardization of Dolphin Cardiac Auscultation and Characterization of Heart Murmurs in Managed and Free-Ranging Bottlenose Dolphins (*Tursiops truncatus*)***
Barbara K. Linnehan, Adonia Hsu, Forrest M. Gomez, Sharon M. Huston, Ryan Takeshita, Kathleen M. Colegrove, Teri K. Rowles, Ashley Barratclough, Whitney B. Musser, Craig A. Harms, Veronica Cendejas, Eric S. Zolman, Brian C. Balmer, Forrest I. Townsend, Randall S. Wells, Eric D. Jensen, Lori H. Schwacke and Cynthia R. Smith

420 ***Case Report: Suppression of Harem Stallion Behavior and Fertility Following Anti-Gonadotropin-Releasing Hormone Vaccination of a Captive Wild Przewalski's Horse (*Equus ferus przewalskii*)***
Jérôme Ponthier, Goulven Rigaux, Sonia Parrilla-Hernandez, Sophie Egyptien, Carine Gatez, Carla Carrasco Leroy and Stéfan Deleuze

frontiers in Veterinary Science

EDITORIAL
published: 07 December 2020
doi: 10.3389/fvets.2020.620685

Editorial: Health and Disease in Free-Ranging and Captive Wildlife

Robert J. Ossiboff[1]*, *Francesco C. Origgi*[2] *and Nicole I. Stacy*[1]

[1] *Department of Comparative, Diagnostic, and Population Medicine, College of Veterinary Medicine, University of Florida, Gainesville, FL, United States,* [2] *Vetsuisse Faculty, Centre for Fish and Wildlife Health, University of Bern, Bern, Switzerland*

Keywords: wildlife health, wildlife disease, wildlife, parasite, virus, clinical pathology, anatomic pathology

Editorial on the Research Topic

Health and Disease in Free-Ranging and Captive Wildlife

Wildlife populations of wide taxonomic breadth are declining globally at an astonishing rate (1–4). Habitat loss, environmental alteration and contamination, global movement of pathogens, excessive harvesting, and other predominantly anthropogenic factors have all been implicated as contributing to the global loss of biodiversity (1, 5–7). In light of these declines, the need for improved and increased knowledge about health and disease states of both free-ranging and captive wildlife species is greater than ever. This Research Topic highlights the current state of studies of health and disease in a wide range of animal species, including invertebrates, fish, amphibians, reptiles, avians, and aquatic and terrestrial mammals.

INVERTEBRATE STUDIES

Sea Star Wasting Syndrome (SSWS) is the cause of one of the largest marine wildlife die-offs ever recorded (8). Wahltinez et al. aimed to evaluate clinical pathology-related differences between sea stars affected by SSWS and clinically healthy individuals. Compared to clinically normal ochre sea stars (*Pisaster ochraceus*), SSWS affected sea stars had significant changes to coelomic fluid chemistry and higher coelomocyte counts. Bacteria were noted in 29% coelomic fluid samples from SSWS-affected sea stars but were absent in clinically normal sea stars. These chemistry and cytological findings in coelomic fluid of SSWS-affected sea stars provide insight into the pathophysiology of SSWS.

Giant African land snails (*Achatina fulica*) are one of the most popular pet snails globally. d'Ovidio et al. investigated the occurrence of parasites of giant African land snails kept as pets in southern Italy. Fecal examinations revealed the presence of multiple species of rhabditid nematodes, including *Rhabditella axei, Rhabditis terricola, Cruznema* sp., and *Pristionchus entomophagus*. The authors highlight that given the zoonotic potential of rhabditid parasites, this finding should be considered by those who maintain or treat this species in captivity.

FISH STUDIES

Studies establishing baseline health parameters are an essential component of conservation studies (9). Malinowski et al. reported a comprehensive health assessment of the Atlantic goliath grouper (*Epinephelus itajara*). This study is the first to report a complement of health indices in free-ranging Atlantic goliath groupers from off the coasts of Florida, United States. The study also demonstrates that non-invasive blood samples can provide critical endpoint data and a wealth of health information that can be important for conservation studies.

OPEN ACCESS

Edited and reviewed by:
Andres M. Perez, University of Minnesota Twin Cities, United States

***Correspondence:**
Robert J. Ossiboff
rossiboff@ufl.edu

Specialty section:
This article was submitted to Veterinary Experimental and Diagnostic Pathology, a section of the journal Frontiers in Veterinary Science

Received: *23 October 2020*
Accepted: *17 November 2020*
Published: *07 December 2020*

Citation:
Ossiboff RJ, Origgi FC and Stacy NI (2020) Editorial: Health and Disease in Free-Ranging and Captive Wildlife. Front. Vet. Sci. 7:620685. doi: 10.3389/fvets.2020.620685

Rubin et al. aimed to evaluate the role environmental parameters play in modulating the pathogenicity of *Tetracapsuloides bryosalmonae,* the causative parasitic agent of proliferative kidney disease (PKD). PKD is an emerging disease of salmonids, and has been implicated as a major factor contributing to noted decreases of wild brown trout (*Salmo trutta*) populations in Switzerland (10). The results of the investigation highlighted that water temperature $\geq$15°C was the parameter most significantly correlated with parasite prevalence and intensity. This finding further emphasizes the importance of temperature in salmonid PKD.

AMPHIBIAN STUDIES

Chytrid fungi are important amphibian pathogens responsible for morbidity and mortality in free-ranging and captive frogs, salamanders, and caecilians (7, 11). Ossiboff et al. developed an automated dual-plex chromogenic RNAScope® *in situ* hybridization (ISH) assay for simultaneous detection and differentiation of *Batrachochytrium dendrobatidis* and *B. salamandrivorans*. The assay successfully identified organisms in tissue samples from different amphibian species preserved in formalin for up to 364 days and showed a remarkable sensitivity for the detection of *Batrachochytrium* spp.. Furthermore, this assay highlighted the infection of dermal cutaneous glands in *B. salamandrivorans* infected caudates.

Hardman et al. investigated distal limb lesions of unknown etiology in free ranging Ozark hellbenders (*Cryptobranchus alleganiensis bishopi*) in Arkansas, United States. They found a high prevalence (93.2%) of hellbenders with digit lesions characterized by swelling and often ulceration. A single infectious etiology was not determined, though mass and *Batrachochytrium dendrobatidis* infection status were significantly and positively associated with the presence of the syndrome. A multifactorial etiology was presumed for this widespread and progressive disease syndrome.

In another study of hellbenders, Hopf et al. identified a novel species of *Exophiala* in a captive Eastern hellbender (*Cryptobranchus alleganiensis alleganiensis*). Although *Exophiala* are generally considered of opportunistic significance across taxa, they can be pathogenic in aquatic and semi-aquatic species. Given the progressive growth of lesions and chronic manifestation of this novel organism without overt evidence of underlying disease, the novel organism was suggested to be a primary pathogen in this Eastern hellbender.

REPTILE STUDIES

A study by Hoon-Hanks et al. investigated specific features of serpentovirus-associated disease in snakes, including the susceptibility of different types of captive snakes to serpentovirus infection and disease, the evaluation of viral genetic diversity involved in disease, and management practices associated with disease spread. Infection was more common in pythons and boas than in colubrids; associated respiratory signs were common in infected pythons, while rare to absent in other species. Detected serpentoviruses of different snake families showed wide genetic variability, suggesting that individual viruses might vary in their ability to infect divergent snake species.

Another respiratory infectious agent of snakes was reported by Walden et al.. The case report described *Raillietiella orientalis*, a pentastome parasite with a native range in Asia and Australia, in a free-ranging banded water snake (*Nerodia fasciata*) in Northern Florida. This parasite was first documented in invasive Burmese pythons in the Everglades and nine native species in Southern Florida 2 years prior in 2017, and another report further north in 2018 in native pygmy rattlesnakes (12, 13). The identification of this organism in Northern Florida documents an additional extension of the host range of this parasite, representing a potential emerging threat to native snake species in the southeastern United States.

Stacy et al. documented the role of *Caryospora*-like coccidial infections in morbidity and mortality in green sea turtles (*Chelonia mydas*). Partial genetic characterization of *Caryospora*-like coccidia collected from turtles in the southeastern US and one green turtle found in Hawaii was performed; sequences were compared to those of *Caryospora*-like coccidia from green turtles found in Australia. The authors reported that eight distinct genotypes were present in green turtles from the southeastern US, and phylogenetic analysis were suggestive of recent interoceanic dissemination of these parasites.

Mass mortalities of the Caribbean sharpnose puffer fish (*Canthigaster rostrata*: Tetraodontidae) were linked with episodic strandings of green sea turtles (*C. mydas*) exhibiting neurological signs or mortality in Costa Rica by González Barrientos et al.. Dietary-derived saxitoxins in whole fish, ingested fish, and brain, lung, kidney, and serum from affected turtles substantially exceeded human seafood safety thresholds. In contrast, endogenous tetrodotoxins were extremely low in fish and absent in turtle stomach contents. While juvenile green sea turtles are mainly herbivorous, they will opportunistically consume fish. Such fish consumption likely occurred during the described juvenile turtle strandings that coincided with puffer fish mass mortality events.

Weisbrod et al. reported on the diagnosis and management of a paratesticular cyst in a free-ranging green sea turtle (*C. mydas*). Their report is the first documentation of a reproductive-origin cyst in a reptile species which presented a unique clinical challenge given the uncommon diagnosis and the extent of the lesion. The report also describes medical management of acute anemia in this patient.

An exposure study by Harms et al. investigated the effects of Deepwater Horizon crude oil, dispersant, and oil-dispersant mixture on loggerhead sea turtle (*Caretta caretta*) hatchlings. Compared to the control group, exposed hatchlings had various clinicopathological derangements suggesting osmoregulatory, electrolyte, mineral, and hydration imbalances. The observed abnormalities document the acute pathophysiological mechanisms associated with oil and dispersant exposure in loggerhead sea turtle hatchlings. Furthermore, the results offer guidance for treatment modalities in oiled turtles and provide an understanding of impacts on a wildlife species during an oil spill response.

A number of members of the fungal order Onygenales have been characterized as significant pathogens in reptiles (14). Christman et al. reported a novel Nannizziopsiaceae within the order Onygenales associated with disease in a captive Galapagos tortoise (*Chelonoidis nigra*). The tortoise was presented for a clinical history of chronic progressive lethargy and inappetence. Imaging revealed the presence of a single large encapsulated pulmonary granuloma. Fungal culture, cytology, histopathology, and polymerase chain reaction were performed, and phylogenetic analysis provided solid evidence of a novel fungal species within the order Onygenales.

Wirth et al. investigated the occurrence of cutaneous skin lesions in resident populations of *Myuchelys latisternum* and *Emydura macquarii krefftii* in a natural pond in Australia. The prevalence of the lesions fluctuated with season from 0 to 77 and 68%, respectively. Blood biochemical parameters, body condition and activity levels were not significantly different between affected turtles and those without lesions. While investigations into an infectious cause were unsuccessful, the position of the lesions on the turtles suggested that the initiating factor was trauma associated with behavioral, seasonal, intra-species aggression.

A study by Palmer et al. compared the survival of adult three toed box turtles (*Terrapene mexicana triunguis*) at urban and rural sites in the state of Missouri, United States. While the reasons for most turtle deaths were unknown, the authors did find that odds of annual survival were 3.5 times greater for a turtle residing in the rural site as compared to the urban site. Their data suggest that even the largest urban parks may not be able to sustain healthy populations of adult box turtles, which has severe implications in the face of ongoing habitat loss and urbanization.

While multiple protocols for quantifying leukocytes in reptiles are available, critical comparisons of these protocols are lacking. Winter et al. compared two hematological methods, Avian Leukopet™ (LO) and total white blood cell estimates from eastern box turtle (*Terrapene carolina carolina*) blood films to evaluate agreement in total leukocyte counts between the two methods, as well as to document repeatability and reproducibility of the LO assay. The authors found significant differences between the two assays as well as variability in the LO assay, highlighting the need of a gold standard for reptilian leukocyte quantification.

AVIAN STUDIES

Large scale oil spills can be a major source of morbidity and mortality in birds (15). Dannemiller et al. aimed to establish time-specific, descriptive blood analyte data following experimental sublethal oil exposure and subsequent rehabilitation in wild Ring-billed Gulls (*Larus delawarensis*). The authors reported that both sublethal oil exposure and aspects of captivity were associated with a mild non-regenerative anemia. The authors also reported that oiled gulls did not develop any clinicopathological derangements post-rehabilitation, consistent with a relatively low impact of current standard practices for rehabilitation in terms of morbidity in clinically stable and moderately oiled gulls.

Diao et al. reported on the concentrations of vitamins A and E in tissue samples from Anna's hummingbirds (*Calypte anna*). Nutritional diseases are the most common non-infectious disease in captive hummingbirds, and replicating a hummingbird's diet in captivity is challenging. Vitamin A and E levels were measured in different tissue types to provide baseline tissue concentrations which may be useful for conservation efforts to nutritional diseases of animals maintained or rehabilitated in captivity.

Finch trichomonosis is a disease of passerine birds caused by *Trichomonas gallinae*. This emerging disease has been associated with a 66% reduction of the British breeding greenfinch (*Chloris chloris*) population, while the breeding greenfinch population in the Netherlands has continued to grow. Rijks et al. investigated this discrepancy in population trends, and found that the frequency of fatal trichomonosis in the Dutch greenfinches did not differ significantly from that in Great Britain, with the parasite consistently being fatal in both bird populations. The results of the study concluded that trichomonosis is a threat concealed in Dutch breeding greenfinch census data.

Santos et al. investigated the prevalence of *Trichomonas* sp. in endangered Bonelli's eagle (*Aquila fasicata*) and several species of free-ranging and wild Colubriformes in areas of the Northwestern Iberian Peninsula via molecular testing of oro-esophageal swabs. Two genotypes appeared to be maintained in various species, with a high prevalence in Colubriformes. This study highlights the need to further investigate transmission dynamics and consider protective measures for Bonelli's eagles.

Another infectious agent of importance in avian species, *Sarcocystis falcatula*, was reported by Kirejczyk et al. in three penguins in managed care in the United States. Sarcocystosis resulted in fatal pneumonia in these intermediate aberrant hosts, as was confirmed by use of histology, immunohistochemistry, transmission electron microscopy, and PCR. Considerations for the route of infection included feces or sporozoite-containing fomite(s) shed by the definitive host, the Virginia opossum (*Didelphis virginiana)*, as well as contaminated water run-off or insects serving as mechanical vectors of opossum feces.

TERRESTRIAL MAMMAL STUDIES

Turchetto et al. carried out a broad and thorough comparative pathology investigation on sarcoptic mange, the most severe disease of wild Caprinae in Europe. The authors compared gross and histopathologic lesions of mange in different species, highlighting the known pathological and immunological aspects of the disease. The authors underlined the need to investigate the effect of immune responses on mange severity at an individual level, the main drivers in host–parasite interactions for different clinical outcomes, and the role of the immune response in determining the shift from epidemic to endemic cycle.

Blood lead levels (BLL) can be useful for monitoring environmental lead exposure in animals and investigating ecosystem health. Boesen et al. tested a specific BLL analyzer, Leadcare® Plus, against one of the gold standard measuring methods, inductively coupled plasma mass spectrometry in Scandanavian brown bears (*Ursus actos*). Their study shows

that not only are Scandanavian brown bears highly exposed to environmental lead levels, but also that BLL analysis using Leadcare® Plus can be used for monitoring lead exposure if utilizing appropriate conversion equations.

Kehoe et al. described normal morphology of blood cells in four giant pandas (*Ailuropoda melanoleuca*), a vulnerable species and a charismatic member of zoological collections worldwide. Overall, similar leukocyte and platelet staining patterns to those reported in other mammals was observed. However, a unique mononuclear cell, with a moderately indented nucleus and shared cytochemical and ultrastructural characteristics of lymphocytes and monocytes was discovered. The combined cytochemical, immunocytochemical (CD3), and ultrastructural features of these unique cells most closely resemble those of monocytes, but the definitive cell lineage remains unknown at this time.

Babesiosis is a globally emerging arthropod-borne disease. Santoro et al. investigated the prevalence of *Babesia* spp. in free-ranging canids and mustelids in southern Italy, and found that the number of *Babesia* positive carnivores in wild carnivores in Italy is higher than previously presumed. Molecular characterization of the parasites identified both *B. vulpes* and badger-associated *Babesia* for the first time in Italy and the first time in a gray wolf (*Canis lupus*).

Ponthier et al. described a non-surgical option to modulate the testicular function of wild horses. A non-surgical castration of a captive wild Przewalski's (*Equus ferus przewalskii*) stallion was performed by anti-GnRH immunization. Immuno-neutering resulted in a decrease of total spermatozoa number and motility 1 month after primary vaccination. Six months post vaccination, serum testosterone concentrations had decreased; the total spermatozoa number was near zero with no motile spermatozoa, and no offspring were sired. On the basis of these results, the authors suggested that this technique could be considered as an alternative to surgical castration in wild horses.

Extrauterine pregnancies occur when the conceptus implants outside in a location other than the uterus. Hughes described a case of extrauterine abdominal pregnancy in a wild European rabbit, *Oryctolagus cuniculus*. While such pregnancies have been described in farmed and captive *O. cuniculus*, this is the first report of the condition in a wild individual. This condition has also rarely been described in other free-ranging lagomorphs, and should be considered as a possible differential diagnosis for abdominal masses in captive and free-ranging lagomorphs.

Neiffer et al. evaluated an immobilization protocol using etorphine, azaperone, and butophanol in free-ranging warthogs (*Phacochoerus africanus*). As the most commonly used drugs for immobilization in warthogs can be associated with falling and paddling during induction and recovery and require prolonged periods of time for recovery, there is a defined need for a rapid immobilization and recovery protocol. While the evaluated protocol was effective in immobilization of free-ranging warthogs with rapid induction and recovery, it was associated with significant cardio-respiratory changes that should be considered when used in potentially compromised warthogs.

A mandibular ossifying fibroma and multiple oral papillomas are reported in a roe deer (*Capreolus capreolus*) by Zürcher-Giovannini et al. Ossifying fibromas are benign fibro-osseous neoplasms that are rarely reported in veterinary medicine, and this report is the first documentation of this tumor in a cervid. Though species-specific papillomaviruses are frequently found in association with oral papillomas, no papillomaviral DNA or antigen were identified in association with the oral growths in this deer.

Gallina et al. reported on the presence of epitheliotropic viruses in free-ranging ruminants in Italy. Epitheliotropic viruses, including poxviruses and papillomaviruses, are known to infect wild ruminants globally. A collaborative network of hunters, wildlife rangers, and institutions was established to better understand interspecies transmission and clinical diseases caused by epitheliotropic viruses in Italy. Samples from chamois, red deer, and ibex were examined by ultrastructural, histological, and molecular methods. The results of the study demonstrated spread of parapoxvirus and papillomaviruses in Italy and the potential of these viruses to cause lesions in free-ranging ruminants.

AQUATIC MAMMAL STUDIES

Otostrongylus circumlitis (OC) infections are a significant cause of mortality in northern elephant seals (NES; *Mirounga angustirostris*) (16). Sheldon et al. investigated the diagnostic performance of complete blood count, serum chemistry, acute phase proteins, protein electrophoresis, and coagulation parameters for diagnosis of OC infections in NES. The diagnostic performance was highly accurate (area under the curve $>$ 0.9) for albumin, albumin:globulin ratio, serum amyloid A, activated partial thromboplastin time, total bilirubin, and gamma-glutamyl transferase, consistent with useful indicators for systemic inflammation and DIC. These findings support previously reported clinical and gross pathological findings in NES infected with OC.

Goertz et al. reported comprehensive health assessment data for the 4 species of Alaskan ice seals, including bearded (*Erignathus barbatus*), ringed (*Pusa hispida*), spotted (*Phoca largha*), and ribbon (*Histriophoca fasciata*) seals. This publication will be a valuable reference for future investigations of mortality or disease events in these species, and for monitoring of spatial and temporal population dynamics in response to stressors such as environmental pollution and climate change.

In contrast to free-ranging pinnipeds, the common bottlenose dolphin (*Tursiops truncatus*) has been subject to population health monitoring for decades. In the review article by Barratclough et al., historical aspects, population threats, capture and handling techniques, recent technological and other methodological advancements, and the state of knowledge obtained by health assessment studies were discussed. The authors set the stage for future applications and emphasize the need for an integrative approach focused on interdisciplinary and interagency collaborations of such studies with bottlenose dolphins as a model species for marine mammal and ecosystem health and conservation.

One of the diagnostic techniques utilized in dolphin health assessments on an individual and population level is cardiac

auscultation. Linnehan et al. developed an in-water cardiac auscultation technique and propose a method for its standardized use. Furthermore, the authors document highly prevalent, subtle heart murmurs of free-ranging and managed dolphins that have not been previously reported. The majority of detected murmurs were attributed to high velocity of blood flow similar to other athletic species.

A case of prolonged freshwater exposure in a bottlenose dolphin with characteristic skin lesions, corneal edema, and mild serum biochemical derangements was reported by Deming et al.. This individual was initially rescued from a freshwater lake, released to nearby brackish water, and found dead 12 weeks post-release due to fisheries interaction. Although the initially observed freshwater skin lesions resolved at time of necropsy, the corneal edema had worsened and presumably resulted in visual impairment; it remained undetermined whether this resulted directly from freshwater exposure or other trauma. This case report contributes to understanding freshwater exposure in dolphins and demonstrates complex associations of anthropogenic effects on their habitat.

An interesting case report by Câmara et al. described skeletal and cardiac rhabdomyolysis in a newborn Bryde's whale (*Balaenoptera edeni*). The observed rhabdomyolysis likely exacerbated pre-existing fetal distress upon stranding, resulting in death. While skeletal and myocardial damage has been documented in several cetacean species, this report is the first of its kind associated with a live-stranding in a newborn Bryde's whale.

Interactions with fisheries are a global threat and challenge to populations of aquatic animals, especially marine mammals (17). To determine the prevalence of fishery interactions with marine mammal death, Puig-Lozano et al. performed an 18-year retrospective study of stranded cetaceans in the Canary Islands; the authors document that 7.4% of cases with a known cause of dead were due to fishery interactions. The most frequent types of interactions were bycatch (i.e., ingestion of longline hooks, fishing net entrapments), chronic entanglements, and fishermen aggression. Such studies are important as a baseline for the development of informed conservation policies.

REGIONAL WILDLIFE STUDIES

Trimmel and Walzer reviewed the literature of infectious diseases in terrestrial wildlife species in Austria spanning 37 years. They found a continuous increase in publication frequency across the study period. Two-hundred twenty-six publications included 131 animal species, with the majority focused on parasitic infections, and lesser studies addressing viral, bacterial, and/or fungal infections. Interestingly, no publications on prions were found. Sixty-one percent of publications discussed publications with zoonotic potential. Although spatiotemporal associations could not be addressed in this study, this literature review provides an excellent summary of the state of wildlife research in Austria and identifies areas of future interest and need of attention.

CONCLUSION

In light of recent and current declines in wildlife populations globally, there is a defined need for studies on states of health and disease in a wide taxonomic breadth of animals. Moreover, as we better understand the implications of host-pathogen interactions and the role of the ever-changing environment in shaping the disease ecology of free-ranging wildlife, there is a distinct demand for a renewed approach to characterizing mechanisms of disease and effects of stressors in non-domestic species. The papers published herein filled selective knowledge gaps while simultaneously highlighting the need for future, focused research in free-ranging and captive wildlife species: understanding basic physiology; identification and quantitative assessment of environmental factors and human stressors on wild populations; optimized preventive health measures, maintenance, and husbandry of non-domestic species in captivity; identification of novel infectious agents and their pathogenic and epidemiological significance in wild and captive populations; advancing medical and surgical management of certain conditions; mortality event investigations; and optimization of diagnostic procedures. While the editors of this Research Topic consider the pursuit a success given the variety and quality of papers and themes represented, we strongly encourage all researchers, veterinarians, and wildlife biologists to target studies that build upon these areas in need of attention for future research and to continue to publish their findings in the peer-reviewed and lay literature. Studies such as those contained in this Research Topic will be critical in the continued pursuit of global wildlife health and the preservation of biodiversity in the years to come as they can be essential tools for ongoing monitoring of populations, for identifying stressors and their effects on population dynamics, and ultimately for informing policy makers by building a basis for the development of conservation management practices that are based on high quality research answering specific population- or taxon-relevant questions.

AUTHOR CONTRIBUTIONS

RO, FO, and NS wrote and edited the article. All authors contributed to the article and approved the submitted version.

REFERENCES

1. WWF. *Living Planet Report 2020 Bending the Curve of Biodiversity Loss*. Almond REA, Grooten M, Petersen T, editors (2020).
2. Butchart SHM, Walpole M, Collen B, van Strien A, Scharlemann JPW, Almond REA, et al. Global biodiversity: indicators of recent declines. *Science*. (2010) 328:1164–8. doi: 10.1126/science.1187512
3. Stuart SN, Chanson JS, Cox NA, Young BE, Rodrigues ASL, Fischman DL, et al. Status and trends of amphibian declines and extinctions worldwide. *Science*. (2004) 306:1783–6. doi: 10.1126/science.1103538

4. Böhm M, Collen B, Baillie JEM, Bowles P, Chanson J, Cox N, et al. The conservation status of the world's reptiles. *Biol Conserv.* (2013) 157:372–85. doi: 10.1016/j.biocon.2012.07.015
5. Giam X. Global biodiversity loss from tropical deforestation. *Proc Natl Acad Sci USA.* (2017) 114:5775–7. doi: 10.1073/pnas.1706264114
6. Roll U, Feldman A, Novosolov M, Allison A, Bauer AM, Bernard R, et al. The global distribution of tetrapods reveals a need for targeted reptile conservation. *Nat Ecol Evol.* (2017) 1:1677–82. doi: 10.1038/s41559-017-0332-2
7. Scheele BC, Pasmans F, Skerratt LF, Berger L, Martel A, Beukema W, et al. Amphibian fungal panzootic causes catastrophic and ongoing loss of biodiversity. *Science.* (2019) 363:1459–63. doi: 10.1126/science.aav0379
8. Hewson I, Sullivan B, Jackson EW, Xu Q, Long H, Lin C, et al. Perspective: something old, something new? Review of wasting and other mortality in Asteroidea (Echinodermata). *Front Mar Sci.* (2019) 6:406. doi: 10.3389/fmars.2019.00406
9. Cooke SJ, O'Connor CM. Making conservation physiology relevant to policy makers and conservation practitioners. *Conserv Lett.* (2010) 3:159–66. doi: 10.1111/j.1755-263X.2010.00109.x
10. Wahli T, Knuesel R, Bernet D, Segner H, Pugovkin D, Burkhardt-Holm P, et al. Proliferative kidney disease in Switzerland: current state of knowledge. *J Fish Dis.* (2002) 25:491–500. doi: 10.1046/j.1365-2761.2002.00401.x
11. Martel A, Spitzen-van der Sluijs A, Blooi M, Bert W, Ducatelle R, Fisher MC, et al. *Batrachochytrium salamandrivorans* sp. nov. causes lethal chytridiomycosis in amphibians. *Proc Natl Acad Sci.* (2013) 110:15325–9. doi: 10.1073/pnas.1307356110
12. Farrel TM, Agugliara J, Walden HDS, Wellehan JFX, Childress AL, Lind CM. Spillover of pentastome parasites from invasive burmese pythons (*Python bivittatus*) extends beyond the geographic range of pythons in Florida. *Herp Rev.* (2019) 50:73–6.
13. Miller MA, Kinsella JM, Snow RW, Hayes MM, Falk BG, Reed RN, et al. Parasite spillover: indirect effects of invasive burmese pythons. *Ecol Evol.* (2018) 8:830–40. doi: 10.1002/ece3.3557
14. Sigler L, Hambleton S, Paré JA. Molecular characterization of reptile pathogens currently known as members of the chrysosporium anamorph of nannizziopsis vriesii complex and relationship with some human-associated isolates. *J Clin Microbiol.* (2013) 51:3338–57. doi: 10.1128/JCM.01465-13
15. Piatt JF, Lensink CJ, Butler W, Nysewander DR. Immediate impact of the "Exxon valdez" oil spill on marine birds. *Auk.* (1990) 107:387–97. doi: 10.2307/4087623
16. Colegrove KM, Greig DJ, Gulland FMD. Causes of live strandings of northern elephant seals (*Mirounga angustirostris*) and pacific harbor seals (*Phoca vitulina*) along the Central California coast, 1992-2001. *Aquat Mamm.* (2005) 31:1–10. doi: 10.1578/AM.31.1.2005.1
17. Reeves RR, McClellan K, Werner TB. Marine mammal bycatch in gillnet and other entangling net fisheries, 1990 to 2011. *Endanger Species Res.* (2013) 20:71–97. doi: 10.3354/esr00481

Conflict of Interest: The authors declare that the research was conducted in the absence of any commercial or financial relationships that could be construed as a potential conflict of interest.

Copyright © 2020 Ossiboff, Origgi and Stacy. This is an open-access article distributed under the terms of the Creative Commons Attribution License (CC BY). The use, distribution or reproduction in other forums is permitted, provided the original author(s) and the copyright owner(s) are credited and that the original publication in this journal is cited, in accordance with accepted academic practice. No use, distribution or reproduction is permitted which does not comply with these terms.

frontiers in Veterinary Science

ORIGINAL RESEARCH
published: 06 February 2019
doi: 10.3389/fvets.2019.00004

Comparative Health Assessments of Alaskan Ice Seals

Caroline E. C. Goertz[1], Colleen Reichmuth[1,2], Nicole M. Thometz[2,3], Heather Ziel[4] and Peter Boveng[4]*

[1] Alaska SeaLife Center, Seward, AK, United States, [2] Institute of Marine Sciences, University of California, Santa Cruz, Santa Cruz, CA, United States, [3] Department of Biology, University of San Francisco, San Francisco, CA, United States, [4] Polar Ecosystems Program, Marine Mammal Laboratory, Alaska Fisheries Science Center, National Oceanic and Atmospheric Administration, Seattle, WA, United States

Bearded (*Erignathus barbatus*), ringed (*Pusa hispida*), spotted (*Phoca largha*), and ribbon (*Histriophoca fasciata*) seals rely on seasonal sea-ice in Arctic and sub-Arctic regions. Many aspects of the biology and physiology of these seals are poorly known, and species-typical health parameters are not available for all species. Such information has proven difficult to obtain due to the challenges of studying Arctic seals in the wild and their minimal historic representation in aquaria. Here, we combine diagnostic information gathered between 2000 and 2017 from free-ranging seals, seals in short-term rehabilitation, and seals living in long-term human care to evaluate and compare key health parameters. For individuals in apparent good health, hematology, and blood chemistry values are reported by the source group for 10 bearded, 13 ringed, 73 spotted, and 81 ribbon seals from Alaskan waters. For a smaller set of individuals handled during veterinary or necropsy procedures, the presence of parasites and pathogens is described, as well as exposure to a variety of infectious diseases known to affect marine mammals and/or humans, with positive titers observed for *Brucella*, *Leptospira*, avian influenza, herpesvirus PhHV-1, and morbillivirus. These data provide initial baseline parameters for hematology, serum chemistries, and other species-level indicators of health that can be used to assess the condition of individual seals, inform monitoring and management efforts, and guide directed research efforts for Alaskan populations of ice-associated seals.

Keywords: ***Phoca largha*, *Histriophoca fasciata*, *Erignathus barbatus*, *Pusa hispida*, hematology, serology, fecal pathogen, parasite**

OPEN ACCESS

Edited by:
Nicole Indra Stacy,
University of Florida, United States

Reviewed by:
Sea Rogers Williams,
National Marine Life Center,
United States
Dean Konjević,
University of Zagreb, Croatia
Emily Whitmer,
Marine Mammal Center,
United States

***Correspondence:**
Colleen Reichmuth
coll@ucsc.edu

Specialty section:
This article was submitted to Zoological Medicine, a section of the journal Frontiers in Veterinary Science

Received: *21 September 2018*
Accepted: *10 January 2019*
Published: *06 February 2019*

Citation:
Goertz CEC, Reichmuth C, Thometz NM, Ziel H and Boveng P (2019) Comparative Health Assessments of Alaskan Ice Seals. Front. Vet. Sci. 6:4. doi: 10.3389/fvets.2019.00004

INTRODUCTION

Rapid environmental change threatens the stability and overall health of Arctic and sub-Arctic ecosystems (1–3). For long-lived and highly-derived species such as ice-associated marine mammals, the unprecedented rate of sea ice loss in northern latitudes may be especially devastating (4–6). A recent unusual mortality event (UME) in Alaska highlighted the potential sensitivity of Arctic and sub-Arctic pinnipeds to the effects of climate change. The Alaska Northern Pinniped UME (2011–2018) was defined by seals and walruses presenting with abnormal behavior, suspected disrupted molts, and skin lesions (7); however, the primary cause of mortality remains unknown (8, 9). The UME syndrome extended across a circumpolar arc, with cases from the Beaufort Sea, Chukchi Sea, Bering Strait, and Bering Sea in Alaska, as well as in other regions of the

Arctic Ocean extending to the North Atlantic Ocean (8). The transboundary nature of this UME increases concern that the opening of northwest and northeast passages through the Arctic, created by retreating sea ice, may result in disease transmission and possible epidemics in Alaskan marine mammals [see (10)]. This concern appears to be well founded, as nucleic acids from, and antibodies to, phocine distemper virus (PDV)—a pathogen responsible for two epidemics in northern Europe—have been detected for the first time in the North Pacific Ocean within the last decade (11), coincident with the first seasonal ice-free access routes through the Arctic from the North Atlantic Ocean (12).

In Alaska, there are four species of ice-associated seals: spotted (*Phoca largha*), ribbon (*Histriophoca fasciata*), bearded (*Erignathus barbatus*), and ringed (*Pusa hispida*) seals, often referred to collectively as "ice seals." All four species utilize sea ice during key life-history stages; however, they vary greatly in their use of, and dependence on, seasonal sea ice throughout the year. Spotted and ribbon seals use the marginal edge of the pack ice as a platform for pupping and molting annually, but individuals of these species are not generally associated with sea ice year-round (13, 14). Spotted seals use terrestrial haul-outs between foraging bouts during the summer and fall (15), while ribbon seals, the presumed deepest diving of the four species, maintain a predominately pelagic lifestyle aside from pupping and molting periods (14, 16, 17). In contrast, bearded and ringed seals are more frequently associated with sea ice throughout the year (18, 19). Bearded seals use broken and moving pack ice as a platform for pupping and molting each spring (20, 21) and are typically found on ice floes over shallow areas due to their benthic foraging habits (22, 23). Throughout much of their breeding range, ringed seals use areas of shore-fast ice, where they maintain breathing holes, and excavate subnivian lairs for pupping, nursing, and to avoid predation by polar bears. Ringed seals remain in areas of extensive fast ice for much of the year and haul out on exposed sea ice for extended periods only during the spring molt (21, 24, 25). Given the distinct ways in which Alaskan ice seals use and rely on seasonal sea ice, rapidly changing conditions in Arctic and sub-Arctic ecosystems are likely to influence these species in different ways. Such changes could relate to geographic distribution, nutritional status, pathogen exposure, and other risk factors.

There are few baseline studies available for Alaskan ice seals that could provide the critical reference values needed to assess the health of individuals and populations [for review see (10, 26)]. This is particularly true with respect to normal hematology and clinical chemistries. There are presently no published blood panels available for spotted or bearded seals. Lenfant et al. (27) reports some hematology parameters pertaining to blood oxygen storage for five ribbon seals, but no other data are available for this poorly studied species. Relatively more information is available for ringed seals. There are some data available concerning the number and type of cells present in the blood of both captive (28) and free-ranging ringed seals (29, 30), and several plasma chemistry parameters from a subset of the same wild individuals (31). A few plasma chemistry values are also reported for several captive ringed seals (28, 31). However, there is no complete data set concerning baseline blood hematology and chemistry parameters for any Alaskan ice seal.

Documentation of disease exposure and parasites in Alaskan ice seals has come primarily from healthy seals taken during subsistence hunting or handled during field research activities. These data have been reported and recently summarized in comprehensive species reviews and research reports for spotted (13, 32), ribbon (14, 33), bearded (19, 34), and ringed seals (18, 35). Microbial isolates from the target species are not commonly reported. In contrast, blood, disease, and other health parameters are readily available for more temperate-living harbor seals (*Phoca vitulina*) (36–41) whose northern range in the Pacific overlaps with that of spotted seals in the southern portion of their range.

To better understand the species-typical health and physiology of Alaskan ice seals, we describe hematological parameters, blood chemistries, serology, microbial isolates, and parasite exposure data for all four species. These data, obtained from free-ranging seals sampled during field assessments, stranded seals in short-term rehabilitation and/or at necropsy, and healthy seals living in long-term human care, provide initial reference parameters for assessing the health and overall condition of both wild and captive ice seals.

METHODS

Field-Based Studies

Source of Animals and Handling

In the spring of 2007–2010, 2014, and 2016, 80 ribbon seals and 62 spotted seals were captured at the edge of the pack ice of the Bering Sea using long-handled salmon landing nets and handled on the ice floes on which they were caught. Seals were physically restrained if <1 y old, or lightly sedated with diazepam or midazolam (0.1 mg/kg) injected intravenously into the extradural intravertebral vein. Prior to release, seals were tagged, samples were collected, and the effects of sedation were reversed with an intramuscular injection of flumazenil (0.01 mg/kg) if needed. In June 2009 and 2011, and July 2012, eight bearded seals were captured in pack ice in Kotzebue Sound, Alaska using tangle nets deployed from boats. The seals were moved to adjacent ice floes for short-term handling using the same methods as described for ribbon and spotted seals. Morphological characteristics, including size and coat condition, were used to distinguish between age groups.

Sample Collection, Processing, and Storage

Blood was collected from the extradural intravertebral vein (29) using 18-gauge, 1.5–3.5 inch needles, depending on the size of the seal, into SST and K_2EDTA-coated Vacutainer® tubes (Becton Dickinson, Franklin Lakes, New Jersey). Blood tubes were kept in insulated containers to prevent freezing before processing. Blood was processed within 6 h of collection on the main research ship (spotted and ribbon seals) or at a shore-based laboratory (bearded seals). Serum separator tubes were centrifuged for 10 min at 10,000 rpm, and 1–2 ml aliquots of serum were transferred to vials and stored at −80°C until analysis.

Laboratory Analysis

Blood samples from 62 spotted seals, 80 ribbon seals, and 8 bearded seals (**Table 1**) were analyzed for a subset of hematological parameters. Hematocrit (Hct) was determined in duplicate for each seal by filling two heparinized microhematocrit capillary tubes with whole blood from each sample and centrifuging for 10 min at 10,000 rpm. Samples were read with a microhematocrit capillary tube reader card (±1%). Hemoglobin concentration (Hb) was measured in duplicate using the cyanmethemoglobin method (Pointe Scientific, Inc.). A 10 μl aliquot of whole blood was added to 2.0 ml of cyanmethemoglobin reagent and stored in cryovials covered in aluminum foil at room temperature. Hemoglobin concentration was measured at the end of the field season (within 2 months of collection) with a Thermo Spectronic BioMate 3 spectrophotometer at λ of 540 nm. Mean corpuscular hemoglobin concentration (MCHC; average concentration of hemoglobin in a given amount of packed red blood cells) was calculated as (Hb/Hct)*100.

Archived serum from a subset of animals (33 spotted seals, 45 ribbon seals, and 5 bearded seals) was analyzed in 2017 for selected serum chemistry parameters (**Table 2**) at a commercial veterinary diagnostic laboratory (URIKA LLC, Bothell, Washington 98011) with a Beckman Coulter AU2700 Chemistry Analyzer (Beckman Coulter, Brea, California 92821). Marked to moderate hemolysis was noted in 3 of 83 samples (1 spotted seal, 2 ribbon seals). Because of the long interval between sample collection and analysis, only parameters known to be stable in samples stored at ultralow temperatures were included in the panel.

Stranded Ice Seals

Source of Animals and Handling

Ice seals in distress (9 spotted, 1 ribbon, 1 bearded, 19 ringed; **Table 3**) from across Alaska (**Figure 1**) were reported to and assessed by staff from the Alaska SeaLife Center prior to being admitted for care in coordination with NOAA's Marine Mammal Health and Stranding Response Program. Cases from 2000 to 2017 are included here. As part of their medical care, seals received initial and periodical physical examinations under physical restraint or light sedation (butorphanol 0.16–0.70 mg/kg with midazolam 0.15–0.55 mg/kg IM) to obtain biological samples for routine diagnostic analysis and disease screening. If animals died or were euthanized because of the severity of their presenting problems, additional samples were obtained post-mortem. Morphological characteristics, including size, coat condition, presence of an umbilical remnant, and time of year, were used to distinguish between age groups.

Sample Collection, Processing, and Storage

Blood was collected from the lumbar region of the extradural intravertebral vein using 18–20-gauge, 1.5–3.5 inch needles, depending on the size of the seal, directly into plain, SST, and K_2EDTA Vacutainer® tubes (BD Biosciences, Franklin Lakes, New Jersey, 07417, USA) or using a syringe and immediately transferring the blood into appropriate tubes. Whole blood was kept at room temperature and analyzed within 4 h. Plain and SST tubes were allowed to clot at room temperature then serum was separated by centrifugation for 5 min at 4,000 rpm. Serum was analyzed for chemistries or pipetted into 1 ml aliquots in cryovials and stored in a −80°C ultralow freezer until sent for further analysis. Swabs of conjunctiva and nasal passages were stored in viral transport media (Remel MicroTest M4RT Kit, Medex Supply, Passaic, New Jersey 07055) and frozen at −20°C until submitted for viral screening. Swabs of the rectum, wounds, abscesses, ears, or nares from live animals or swabs of internal organs of dead animals were collected and placed in Cary-Blair media (Becton, Dickinson & Company, Franklin Lakes, New Jersey, 07417, USA), refrigerated, and sent within 24 h to a commercial microbiology laboratory to screen for fecal pathogens or to isolate pathogenic bacteria from lesions. Fresh fecal samples were obtained opportunistically and refrigerated until on-site analysis within 4 h. While most samples for disease testing were obtained as part of admit sampling, some samples were collected later in the rehabilitation process as diseases became clinically evident or during necropsy. Tissues collected post-mortem were stored in neutral buffered formalin and later processed into slides for histopathological analysis.

Laboratory Analysis

CBC, serum chemistries, fecal parasite, and urine analyses were performed at the Alaska SeaLife Center. Only results from clinically healthy animals (9 spotted seals, 1 ribbon seal, 2 bearded seals, 10 ringed seals) were used to generate the hematology and serum chemistry tables in this report with no more than two sampling events per individual. Two microhematocrit tubes were centrifuged for 6 min at 14,000 rpm to determine Hct using a micro-capillary reader (±0.5%). Additionally, buffy coat smears obtained from spun microhematocrit tubes were examined microscopically to check for microfilaria (42). Blood smears were prepared, dried, fixed in methanol, and stained with Wright-Giemsa (Henry Schein Animal Health, Dublin, Ohio 43017) for manual white blood cell differential counts and to screen for hemoparasites. Complete blood counts were performed on an IDEXX ProCyte Dx, Heska CBC Diff, or QBC Hematology Analyzer using whole blood. Serum chemistries were performed using an IDEXX VetTest 8008.

Serum and molecular samples from the same individuals were shipped in batches about once a year on dry ice via express delivery screen for disease or exposure to disease agents. Reference laboratories and research facilities included the Oklahoma Animal Disease Diagnostic Laboratory, the Athens Veterinary Diagnostic Laboratory at the University of Georgia, University of California Davis School of Veterinary Medicine, the Animal Health Diagnostic Center at Cornell University, Kansas State Veterinary Diagnostic Laboratory, the Veterinary Diagnostic Laboratories at Colorado State University, and the Centers for Disease Control and Prevention. Thresholds established by the individual laboratories were used to determine evidence of prior natural exposure. A subset of seals were tested for microbial isolates and parasites. Culture swabs were submitted for aerobic bacterial culture at Providence Alaska Medical Center, Phoenix Central Laboratory, or the University of California Davis Veterinary Medical Teaching Hospital

TABLE 1 | Summary hematology data for live-sampled spotted seals, ribbon seals, bearded seals, and ringed seals.

Source population	Spotted seal			Ribbon seal		Bearded seal		Ringed seal	
	Rehabilitated: ASLC	**Captive: LML**	**Wild caught: bering sea (MML)**	**Rehabilitated: ASLC**	**Wild caught: bering sea (MML)**	**Wild caught: ASLC**	**Wild caught: chukchi sea, bering sea (MML)**	**Rehabilitated: ASLC**	**Captive: ASLC, LML**
Hematology values	Total range	Total range	5–95% range	Total range	5–95% range	Total range	Total range	Total range	Total range
Number individuals	$n = 9$	$n = 2$	$n = 62$	$n = 1$	$n = 80$	$n = 2$	$n = 5$–8	$n = 10$	$n = 3$
Number samples	2–18	4–6	62	2–3	79–80	4	5–8	8–19	6
Individuals—age	<1.5 y	3–5 y	Mixed[a]	1 adult	Mixed[b]	<1 y	mixed[c]	<1.5 y	mixed[d]
Individuals—sex	4 F, 5 M	2 M	33 F, 29 M	1 F	39 F, 41 M	2 M	4 F, 4 M	3 F, 7 M	1 F, 2 M
RBC (10^6/mm^3)	3.6–5.3	4.6–5.4		4.3–5.1		3.6–5.0		4.1–5.2	3.9–6.0
Hb (g/dl)	13–23	17–24	13–24[e]	29–34	13–33[e]	23–28	19–32[e]	15–26	14–30
HCT [f] (%)	32–55	52–64	45–62	68–74	45–76	57–65	52–57	39–60	42–68
MCV (fl)	79–113	101–121		140–141		119–140		98–133	95–130
MCH (pg)	30–51	37–45		66–67		55–65		38–52	33–50
MCHC (g/dl)	35–46	32–41	30–42	47–48	22–48	45–47	35–58	39–44	34–45
Platelets[g] (10^3/mm^3)	111–869	261–572		35–124		243–402		36–467	74–412
Leukocytes /μl	4,300–10,800	5,100–8,420		5,700–8,500		9,150–12,300		7,400–16,800	6,400–13,000
Neutrophil (band) /μl	0–158	0–0		0–0		0–0		0–354	0–0
Neutrophil (mature) /μl	1,806–7,560	1,224–4,884		4,218–6,035		5,582–9,401		2,966–8,409	2,405–4,158
Lymphocyte[h] /μl	972–3,456	1,616–3,021		513–1,079		1,007–1,845		950–4,233	2,368–5,670
Monocyte /μl	120–1,349	318–1,095		798–1,328		369–2,507		366–2,185	195–1,149
Eosinophil /μl	0–472	0–848		228–747		119–1,107		0–4,896	120–2,142
Basophil/ μl	0–864	0–337		0–0		0–246		0–2,352	–4

For each source population, the reported values (total range for data sets with $n < 30$ or 5–95% range for data sets with $n > 30$), numbers of individuals sampled (n), number of samples evaluated, ages of sampled individuals, and sexes of sampled individuals are provided. Source populations of sampled seals are from rehabilitation (Alaska SeaLife Center, ASLC), long-term captive (ASLC or Long Marine Lab, LML), or wild capture (ASLC or NOAA Marine Mammal Lab, MML). Hematology parameters were measured either manually or on one of several analyzers (see notations in text); thus, these can be considered combined, descriptive data, or viewed quantitatively by subgroup. Data for individual animals within each subject group are provided in ***Supplementary Table 1****.*

[a] *Age distribution of spotted seals wild-caught in the Bering Sea: 13 adults, 13 subadults, 29 young-of-year, 7 pups.*

[b] *Age distribution of ribbon seals wild-caught in the Bering Sea: 33 adults, 22 subadults, 19 young-of-year, 6 pups.*

[c] *Age distribution of bearded seals wild-caught in the Chukchi Sea, Bering Sea: 1 adult, 6 subadults, 1 pup.*

[d] *Age distribution of ringed seals sampled in long-term captivity, Alaska SeaLife Center, and Long Marine Lab: 1 subadult, 2 adults.*

[e] *Hemoglobin measured using cyanmethemoglobin method.*

[f] *HCT is reported as the directly measured packed cell volume (PCV).*

[g] *Low platelet counts (<100 10^3/mm^3) likely artifactual due to platelet clumping.*

[h] *Low lymphocyte counts (<1,000 /μl) likely attributable to stress responses.*

TABLE 2 | Summary serum chemistry data for live-sampled spotted seals, ribbon seals, bearded seals, and ringed seals.

	Spotted seal			Ribbon seal		Bearded seal		Ringed seal	
Source population	**Rehabilitated: ALSC**	**Captive:LML**	**Wild caught:bering sea[a] (MML)**	**Rehabilitated: ASLC**	**Wild caught:bering sea[a](MML)**	**Wild caught: ASLC**	**Wild caughtChukchi sea, bering sea[a] (MML)**	**Rehabilitated: ASLC**	**Captive:ASLC, LML**
Blood chemistry values	Total range	Total range	5–95% range	Total range	5–95% range	Total range	Total range	Total range	Total range
Number individuals	$n = 9$	$n = 2$	$n = 33$	$n = 1$	$n = 45$	$n = 2$	$n = 5$	$n = 10$	$n = 3$
Number samples	2–18	4–6	33	2–3	45	4	5	8–18	4–6
Individuals—age	<1.5 y	3–5y	Mixed[b]	1 adult	Mixed[c]	<1y	Mixed[d]	<1.5 y	mixed[e]
Individuals—sex	4F, 5M	2M	20F, 13M	1F	24F, 21M	2M	4F, 1M	3F, 7M	1F, 2M
Total protein (g/dl)	4.9–7.3	6.2–8.0	5.2–8.0	7.3–8.0	5.5–9.4	6.6–7.2	5.7–7.3	6.0–8.7	5.3–7.3
Albumin (g/dl)	1.7–3.5	3.0–3.9	3.2–4.1	3.0–4.4	3.3–5.0	3.0–3.3	3.2–4.0	2.6–4.0	2.0–4.0
Globulin (g/dl)	2.7–4.1	3.0–4.5	1.8–4.2	3.1–4.3	2.0–4.3	3.5–4.1	2.0–3.3	3.1–5.8	2.6–4.4
Glucose (mg/dl)	101–173	111–197	114–243	132–192	118–210	123–175	104–164	95–184	111–162
BUN (mg/dl)	23–56	29–71		41–55		12–25		19–43	36–76
Creatinine (mg/dl)	0.4–0.9	0.5–1.4	0.4–1.9	1.2–1.5	0.4–1.6	0.7–0.9	0.5–0.7	0.34–0.75	0.7–1.1
Bilirubin (mg/dl)	0.1–3.0	0.1–0.4	0.0–1.2	0.6–0.7	0.03–0.8	0.1–0.7	0.1–0.3	0.1–1.8	0.1–1.1
Cholesterol (mg/dl)	183–426	236–392	168–559	200–303	189–489	180–341	168–258	212–414	170–396
Alk phos (U/l)	113–628	77–181		32–38		105–378		75–841	71–147
ALT (U/l)	23–95	25–82		17–37		62–88		43–212	63–129
AST (U/l)	56–275	41–412		36–59		55–162		55–267	80–361
GGT (U/l)	14–37	1.0–30		11–13		5.0–7.0		6.0–139	5–55
CK (U/l)	86–991	61–2,565		357–1,320		225–820		67–1,626	178–19,967
Calcium (mg/dl)	9–12	8.2–9.6	8.8–12	9.5–10	9.3–13	8.7–9.7	9.1–11	8.6–11	8.1–9.7
Phosphorus (mg/dl)	5.1–9.6	4.3–7.8	5.7–11	4.7–6.6	6–12	5.1–8.0	8.1–11	4.7–8.8	2.7–10
Sodium (mEq/l)	150–161	152–169	145–155	156–157	147–166	152–157	147–153	148–169	154–165
Potassium (mEq/l)	3.9–5.9	5.1–5.7	3.8–5.4	4.2–4.8	3.5–4.9	3.8–4.0	3.9–5.1	3.9–5.2	3.6–6.2
Chloride (mEq/l)	107–116	108–118	97–109	112–114	95–110	107–111	98–109	104–130	109–125
Iron (mcg/dl)			141–752		146–844		214–793		
Magnesium (mg/dl)		1.5–2.1	1.8–2.8		1.9–2.7		2.0–2.8		1.8–2.4
Fibrinogen (mg/dl)	200–300							100–400	
Triglycerides (mg/dl)	22–54	121–336		21–56		34–85		22–117	54–259
Amylase (U/l)	218–398	306–459		22–35		0–35		0–49	4–46
Lipase (U/l)		19–54	25–65						6–25
Urea (mg/dl)					28–68		20–38		
LDH (U/l)	1,873–2,800			815–1,476		857–3,520		1,516–3,691	

For each source population, the reported values (total range for data sets with n < 30 or 5–95% range for data sets with n > 30), numbers of individuals sampled (n), number of samples evaluated, ages of sampled individuals, and sexes of sampled individuals are provided. Source populations of sampled seals are from rehabilitation (Alaska SeaLife Center, ASLC), long-term captive (ASLC or Long Marine Lab, LML), or wild capture (ASLC or NOAA Marine Mammal Lab, MML). Chemistry parameters were measured on one of several analyzers (see notations in text); thus, these can be considered combined, descriptive data, or viewed quantitatively by subgroup. Data for individual animals within each subject group are provided in ***Supplementary Table 2****.*

[a]*Chemistry values determined from archival (frozen) serum; enzymes excluded due to predicted degradation.*

[b]*Age distribution of spotted seals wild-caught in the Bering Sea: 10 adults, 3 subadults, 13 young-of-year, 7 pups.*

[c]*Age distribution of ribbon seals wild-caught in the Bering Sea: 17 adults, 15 subadults, 7 young-of-year, 6 pups.*

[d]*Age distribution of bearded seals wild-caught in the Chukchi Sea, Bering Sea: 4 subadults, 1 pup.*

[e]*Age distribution of ringed seals sampled in long-term captivity, Alaska SeaLife Center and Long Marine Lab: 1 subadult, 2 adults.*

TABLE 3 | Case demographics of Alaskan ice seals tested for serology (**Table 4**), microbes (**Table 5**), and parasites (**Table 6**) at the Alaska SeaLife Center.

	Spotted seal	Ribbon seal	Bearded seal	Ringed seal
Live strand	9	1	1	19
Wild caught	0	0	2	0
Males	5	0	2	10
Females	4	1	1	9
<1.5 Years old	9	0	3	19
Adult	0	1	0	0
Dead	0	0	1	8
Survivors	9	1	2	11
Total Individuals	9	1	3	19

*Individuals were live stranded with the exception of two bearded seals collected from the wild for long-term captive research. Other than one adult ribbon seal, individuals of all species were young-of-year and yearlings. Alaskan stranding locations corresponding to these cases are provided in **Figure 1**. Animals listed as Dead were deceased on arrival, died while under care, or were euthanized. Survivors are animals that were returned to health and released or retained in long-term captive care.*

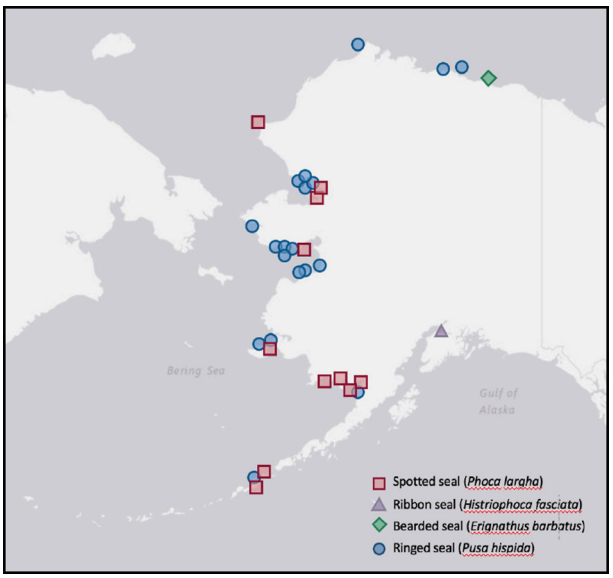

FIGURE 1 | Stranding locations of Alaskan ice seals tested for serology (**Table 4**), microbial isolates (**Table 5**), and parasites (**Table 6**) at the Alaska SeaLife Center between September 2000 and March 2017. USGS National Map (https://viewer.nationalmap.gov).

Microbiology Laboratory. Fecal pathogen screens for common enteric pathogens included *Salmonella*, *Shigella*, *Campylobacter jejuni*, and *Escherichia coli* O157. Identifications were performed on site with a Biomerieux Vitek2 GNI card or the Vitek2 NHI card (bioMérieux,Marcy-l'Etoile, France) if the organism was *Campylobacter*. Fecal samples were examined for ova and parasites using direct, float (Fecasol, Henry Schein, Melville, NY), and Baerman techniques. Other parasites were obtained by manual removal of external parasites from live animals and during necropsy. Some whole specimens or photomicrographs were sent to specialists for speciation (see acknowledgments). When available, fresh urine obtained from clean, dry surfaces was analyzed using the Urispec 11-Way Test Strips (Henry Schein Animal Health, Dublin, Ohio 43017) and a refractometer was used to determine urine specific gravity. Only urinalysis results from clinically healthy animals were used in this report. Tissue slides were examined by a pathologist (see acknowledgments) who provided histopathological diagnoses.

Captive Ice Seals

Source of Animals and Handling

Three ringed seals and four spotted seals were stranded animals that had been rehabilitated at the Alaska SeaLife Center between 2010 and 2017 but were declared non-releasable by NOAA because rehabilitation took place outside of their home range. These animals were fully recovered with no substantive medical problems. Two bearded seals were obtained in 2015 and 2016 in Kotzebue, Alaska as part of a directed capture effort to support long-term research. Captive seals participated in established husbandry programs at the Alaska SeaLife Center in Seward, Alaska or Long Marine Laboratory, in Santa Cruz, California. As part of their medical care, seals received periodic physical examinations under physical restraint or light sedation (butorphanol 0.16–0.70 mg/kg with midazolam 0.15–0.55 mg/kg IM, or diazepam 0.26–0.42 mg/kg) to obtain biological specimens for routine diagnostic and disease screening analysis.

Sample Collection, Processing, and Storage

Biological samples obtained from long-term captive seals were collected, processed, and stored in the same manner as described above for stranded animals.

Laboratory Analysis

Biological samples obtained at the Alaska SeaLife Center were analyzed in the same manner as described above for stranded animals. Whole blood and serum obtained at Long Marine Laboratory were analyzed with a Bayer Advia 120 multispecies hematology system and an Olympus AU640e blood chemistry analyzer at Antech Diagnostics (Santa Clara, California 95051) within 24 h of collection.

Analysis

Blood parameters are reported as either total ranges or trimmed ranges for each species and subject group. Where sample size is <30 individuals, minimum to maximum values are used. Where sample size is >30 individuals, 5–95% data intervals are used to reduce the influence of outliers. Hematology and serum chemistry parameters are not reported as formal species-typical reference intervals for veterinary applications, although in some cases there are sufficient underlying data to generate such intervals (43).

Hematology and serum chemistry data were evaluated using Prism 7.0 (GraphPad Software, Irvine, California 92618) and compared qualitatively among the target species or to available data for harbor seals (38). Particular note was taken when the upper value of a given parameter was 20% higher or the entire range was higher than the values reported for harbor seals; almost no lower range values reported for Alaskan ice seals were below

TABLE 4 | Disease exposure testing results for serology for Alaskan ice seals listed in **Table 3**.

Infectious Agent	Spotted seal ($n = 9$)	Ribbon seal (n=1)	Bearded seal ($n = 3$)	Ringed seal ($n = 19$)	Laboratory,[a] method,[b] (References)
MISCELLANEOUS					
Avian influenza	0/8 (0%)	–	0/3 (0%)	0/11 (0%)	Runstadler, ELISA (44, 45)
	1/5 (20%)	–	0/2 (0%)	0/3 (0%)	Runstadler, rtPCR (45)
Brucella	0/8 (0%)	1/1 (100%)	–	1/9 (11%)	Mystic, cELISA (46)
	–	–	1/3 (33%)	2/9 (22%)	OADDL, Card (47)
Coxiella	0/6 (0%)	0/1 (0%) CF	0/3 (0%)	0/15 (0%)	CDC or CSU, IFAT (48)
Herpesvirus PhHV-1	1/6 (17%)	1/1 (100%)	0/1 (0%)	2/12 (17%)	OADDL or AVDL, SN (49)
	0/2 (0%)	–	0/2 (0%)	1/3 (33%)	UC-Davis, ELISA (50)
Rabies	–	–	–	0/14 (0%)	KSU, RFFIT (56)
LEPTOSPIRA					
L. bratislava	0/9 (0%)	0/1 (0%)	0/3 (0%)	5/16 (31%)	OADDL or AVDL, MAT (51)
L. canicola	0/9 (0%)	0/1 (0%)	0/3 (0%)	0/16 (0%)	OADDL or AVDL, MAT (51)
L. grippo	0/9 (0%)	0/1 (0%)	0/3 (0%)	0/16 (0%)	OADDL or AVDL, MAT (51)
L. hardjo	1/9 (11%)	0/1 (0%)	0/3 (0%)	3/16 (19%)	OADDL or AVDL, MAT (51)
L. ictero	0/9 (0%)	0/1 (0%)	0/3 (0%)	3/16 (19%)	OADDL or AVDL, MAT (51)
L. pomona	0/9 (0%)	0/1 (0%)	0/3 (0%)	0/16 (0%)	OADDL or AVDL, MAT (51)
MORBILLIVIRUS					
Canine distemper virus	0/9 (0%)	0/1 (0%)	0/1 (0%)	0/16 (0%)	OADDL or AVDL, VNT (52)
	–	–	1/2 (50%)	–	Cornell, SN (53)
Phocine distemper virus	0/9 (0%)	0/1 (0%)	0/3 (0%)	0/16 (0%)	OADDL or AVDL, VNT (52)
Dolphin morbillivirus	0/2 (0%)	–	0/1 (0%)	0/10 (0%)	OADDL or AVDL, VNT (52)
Porpoise morbillivirus	0/1 (0%)	–	0/1 (0%)	0/10 (0%)	OADDL or AVDL, VNT (52)
PROTOZOA					
Neospora	0/5 (0%)	–	0/2 (0%)	0/3 (0%)	UCDavis, IFAT (54)
Toxoplasma gondii	–	–	0/1 (0%)	0/9 (0%)	OADDL, Latex agglutination (55)
	0/5 (0%)		0/2 IFA (0%)	0/3 (0%)	UCDavis, IFAT (54)
Sarcocystis	0/5 (0%)	–	0/2 (0%)	0/3 (0%)	UCDavis, IFAT (54)

Results are provided as number of individuals that tested positive out of number of individuals tested, and % prevalence.
[a]Laboratory abbreviations:
Runstadler, Runstadler Laboratory, Tufts University, 200 Westboro Rd, North Grafton, MA 01536 USA.
Mystic, Mystic Aquarium, 55 Coogan Blvd, Mystic, CT 06355 USA.
OADDL, Oklahoma Animal Disease Diagnostic Laboratory, W Farm Rd, Stillwater, OK 74078 USA.
AVDL, Athens Veterinary Diagnostic Laboratory, University of Georgia, 501 DW Brooks Dr., Athens, GA 30602 USA.
UCDavis, University of California Davis School of Veterinary Medicine, One Shields Avenue, Davis, CA 95616 USA.
Cornell, Animal Health Diagnostic Center, Cornell University, Ithaca, NY 14853-6401 USA.
KSU, Kansas State Veterinary Diagnostic Laboratory 1800 Denison Ave, Manhattan, KS 66506 USA.
CDC, Centers for Disease Control and Prevention, 1600 Clifton Road Atlanta, GA 30329-4027 USA.
CSU, Veterinary Diagnostic Laboratories, Colorado State University, 300 West Drake Road, Fort Collins, CO 80526 USA.
[b]Method abbreviations:
ELISA, enzyme-linked immunosorbent assay.
IFAT, immunofluorescence antibody test.
MAT, microscopic agglutination test.
SN, serum neutralization test.
RFFIT, rapid fluorescent focus inhibition test.
rtPCR, real time polymerase chain reaction.
VNT, virus neutralization test.

those reported for harbor seals. Because different laboratories and methods were used for logistical reasons, cautious indirect observational comparisons rather than statistical comparisons of blood analyte data were made within and among species.

Additional health assessment data from the subset of Alaskan seals handled during rehabilitation are reported for the target species as available and compared descriptively.

RESULTS

Summary data for hematology (**Table 1**) and serum chemistry parameters (**Table 2**) are presented for spotted, ribbon, bearded, and ringed seals as total ($n < 30$) or 5–95% ($n > 30$) ranges. The demographics for each subject group are included in the table headers. Corresponding metadata and blood panels for individual animals are provided in **Supplementary Tables 1**, **2**, respectively.

TABLE 5 | Microbial isolates identified in Alaskan ice seals listed in **Table 3**.

	Spotted seal (*n* = 7)	**Ribbon seal (*n* = 1)**	**Bearded seal (*n* = 1)**	**Ringed seal (*n* = 14)**
Positive for fecal pathogens isolates listed below	1/7 (14%)	0/1 (0%)	0/1 (0%)	4/9 (44%)
Positive for isolates from other locations, isolates listed below	2/7 (29%)	0/1 (0%)	1/1 (100%)	10/14 (71%)
No microbial cultures done, diagnosed with bacterial pneumonia	–	–	–	1
No microbial cultures done, no disease concerns	2	–	2	5
ISOLATES				
Aeromonas sp.	Feces, wound	–	–	–
Aeromonas hydrophila	–	–	–	Ear, wound*, abscess
Aeromonas veronii	–	–	–	Feces
Candida parapsilosis	–	–	–	Skin*
Citrobacter freundii	–	–	–	Ascites*
Clostridium sp	–	–	–	Ascites*
Corynebacterium sp.	–	–	–	Skin
Escherichia coli	–	–	–	Ascites*, ear
Edwardsiella tarda	Wound	–	–	–
Enterococcus faecium	Blood	–	–	–
Enterococcus sp.	–	–	–	Ascites*, lung*, wound
Enterobacter cloacae	Wound	–	–	Nares, kidney*, ear, ascites*
Fusobacterium mortiferum	–	–	–	Abscess
Hafna alvei	–	–	–	Abscess
Klebsiella pneumoniae	–	–	–	Feces, lung*
Madurella grisa	–	–	–	Hair
Methylobacterium sp	Blood	–	–	–
Plesiomonas shigelloides	Feces	–	–	Lung*, feces
Pseudomonas aeruginosa	Abscess	–	Lung*, CSF*, hilar* lymph node*, pericardium*	Lung*, ear
Pseudomonas sp.	Wound	–	–	–
Psychrobacter phenylpyruvicus	–	–	–	Skin*
Prevotella oralis	–	–	–	Abscess
Riemerella anatipestifer	–	–	–	Skin
Shewanella algae	–	–	–	Feces
Staphylococcus sp.	Abscess	–	–	–
Staphylococcus sp. (coagulase +)	–	–	–	Nares, wound
Staphylococcus aureus	Wound	–	–	–
Streptococcus phocae	–	–	–	Blood, abscess, LN*
Streptococcus sp. (β-hemolytic)	Abscess, wound	–	–	Wound
Vibrio alginolyticus	–	–	–	Ascites*
Vibrio cholerae	Feces	–	–	–

*Results for fecal and other pathogens are provided as number of individuals that tested positive out of number of individuals tested, and % prevalence. *Indicates isolates from swabs obtained at necropsy.*

Data concerning infectious disease exposure, microbiology, and parasites are reviewed for stranded ice seals from across Alaska (**Figure 1**) undergoing rehabilitation at the Alaska SeaLife Center (**Table 3**), and from the two bearded seals captured for directed research projects.

Results of tests for exposure to diseases of concern are summarized in **Table 4**. Most seals were seronegative for tested diseases. All seals were seronegative for avian influenza, phocine distemper virus, dolphin morbillivirus, porpoise morbillivirus, *Neospora, Toxoplasma, Sarcocystis, Coxiella,* and rabies. One spotted seal had a suspect positive for avian influenza on PCR testing of its fecal sample, although nasal and ocular swabs were negative. None of the spotted seals, the one ribbon seal, one of three bearded seals, and three of 18 ringed seals tested for antibodies to *Brucella* were positive. Five individuals (1 spotted, 1 ribbon, 3 ringed seals) were positive for herpesvirus. Of these, two (1 spotted, 1 ringed) were positive at admit with rising titers that decreased with subsequent testing, while

TABLE 6 | Parasites identified in Alaskan ice seals listed in **Table 3**.

	Spotted seal ($n = 9$)	Ribbon seal ($n = 1$)	Bearded seal ($n = 3$)	Ringed seal ($n = 16$)
Negative fecal exams for ova & parasites and/or none seen on post-mortem or other exam	5/9	0	0	4/16
Positive fecal exams, parasite listed below	4/9	1	3	5/16
Parasite noted on post-mortem or other exam	–	–	–	9/16
No exam for parasites performed	–	–	–	3
TREMATODES (FLUKES, NOT SPECIATED)				
Any trematode	1/9 (feces)	0/1	0/3	0/0
CESTODES (TAPEWORMS)				
Anophryocephalus sp	1/9 (feces)			
Diphyllobothrium sp	1/9 (feces)		1/3 (feces)	
Cestode, not speciated			2/3 (feces, GI*)	4/16 (feces, GI*)
Any cestode	2/9	0/1	2/3	4/16
NEMATODES (ROUNDWORMS)				
Filarioids				
Acanthocheilonema spirocauda				1/16 (blood)
Microfilaria, not speciated				3/16 (blood)
Strongylids (hookworms)				
Otostrongylus circumlitus			1/3 (feces)	2/16 (lung*)
Larva in feces, presumably lungworm	1/9 (feces)		1/3 (feces)	3/16 (feces)
Ascarids				
Anisakis sp.	1/9 (feces)			1/16 (GI)
Contracaecum sp.	1/9 (feces)			2/16 (feces, GI*)
Pseudoterranova decipiens	1/9 (feces)		1/3 (feces)	
Not speciated			1/3 (feces)	1/16 (GI)
Larva, not speciated	1/9 (feces)			1/16 (lymph node*)
Nematode, not speciated	1/9 (feces)	1/1 (feces)	2/3 (feces, GI*)	3/16 (feces, GI*)
Any nematode	4/9	1/1	3/3	11/16
ACANTHOCEPHALA (THORNY-HEADED WORMS)				
Corynosoma strumosum				1/16 (GI*)
Corynosoma semerme				1/16 (GI*)
Acanthocephala, not speciated	1/9 (feces)			2/16 (feces, GI*)
Any acanthocephala	1/9	0/1	0/3	3/16
EXTERNAL PARASITES				
Lice				
Echinophthirius horridus				2/16 (skin)
Mites	1/9 (feces)			
SUMMARY FINDINGS				
Any parasites	4/9	1/1	3/3	12/16
Multiple parasites	4/9	0/1	3/3	9/16

*Location of parasites found included the gastrointestinal system (GI), feces, lymph node, lungs, blood, or skin during diagnostic tests for parasites or opportunistically found during other exams. *Specimens obtained at necropsy.*

the other three had very low herpes titers. All seals were seronegative for *Leptosirosis canicola*, *L. grippo*, and *L. pomona*. About a third of ringed seals (5 of 16) were positive for low levels of antibodies to *L. bratislava.* Some of these ringed seals were also positive for *L. hardjo* (3) and *L. ictero* (3), which was possibly due to a cross reaction. One spotted seal was positive for *L. hardjo*. All animals tested for antibodies to canine distemper virus and other morbillivirus at the Oklahoma Animal Disease Diagnostic Laboratory (OADDL) and the Athens Veterinary Diagnostic Laboratory (AVDL) (under the same PI, J. Saliki) were negative. One of the two bearded seals tested at Cornell's Animal Health Diagnostic Center was positive for antibodies to canine distemper virus but at a low dilution that decreased with subsequent testing; this may have been due to waning maternally acquired antibodies, an original false positive, or cross reaction—and therefore not necessarily due to disease.

Results from microbial cultures are summarized in **Table 5**. A minority of animals (5 of 18) screened for pathogens from fecal samples, across all species, were positive. Seals positive for

TABLE 7 | Specific gravity of urine obtained from Alaskan ice seals listed in **Table 3**, shown with comparative data from harbor seals evaluated at Alaska SeaLife Center.

	Spotted seal	Ribbon seal	Bearded seal	Ringed seal	Harbor seal
Number Animals	6	1	2	10	29
Number Samples	9	1	4	14	37
Minimum	1.018	1.035	1.040	1.010	1.004
Maximum	1.056	1.035	1.061	1.060	1.051
Average	1.041	1.035	1.046	1.036	1.025

fecal pathogens were also positive on additional microbial testing. Most additional microbial isolates listed for spotted seals came from a single individual with only one other animal growing an isolate of concern; both of these spotted seals were very ill but survived rehabilitation. In 10 ringed seals, isolates of concern were detected in wounds, abscesses, ears, or nares or from swabs of internal organs obtained post-mortem. One additional ringed seal was diagnosed with bacterial pneumonia based on radiographs and clinical symptoms, however no specific isolate was identified. In total, 11 of 19 ringed seals were impacted by bacterial infection.

Results from parasitic examinations are summarized in **Table 6**. Half the spotted seals (5 of 9) were negative for ova and parasites on fecal exams done by any method. In contrast, parasites were found in most ringed seals (12 of 16) through fecal (any method) or other exams (grossly visible, revealed through blood tests, or microscopic review of tissues). Gastrointestinal nematodes were seen in all species. Seal lice (*Echinophthirius horridus)* and microfilaria (one was identified as *Acanthocheilonema spirocauda;* the rest were not speciated) were only seen in ringed seals.

Ranges for urinary specific gravity for the different ice seal species are provided in **Table 7** in comparison to the range seen in harbor seals (*Phoca vitulina*) treated at the same facility (C. Goertz, unpublished data).

Gross necropsy and histopathological examination of tissues from deceased ringed seals handled during rehabilitation confirmed pre-mortem diagnoses including both bacterial infections and parasitic infestations. Evidence of hepatic damage was found in some ringed seals which was consistent with derangements seen in serum enzymes associated with hepatobiliary function found during admit exams. Cases of dermal pathology were noted in ringed seals that died and those that survived, though none were afflicted with the debilitating clinical signs seen in other UME seals. Additional findings included sepsis, fat atrophy, and shock. Necropsies of spotted or ribbon seals did not occur as part of study activities.

One long-term captive bearded seal at Long Marine Laboratory died following traumatic injury. Histopathology for this nearly 2-year-old, apparently healthy individual showed systemic infection of multiple muscles (skeletal muscles, esophagus, tongue, and palate) with two forms of apicomplexan protozoal tissue cysts, in association with myositis and myophagia. A single cyst was observed in the spinal cord, with no associated inflammation. The mature cysts, mainly within myofibers, were morphologically compatible with *Sarcocystis spp.* and suggestive of subacute to chronic infection. The seal also exhibited patchy to diffuse, superficial dermal mycosis attributed to dermatophytosis and/or dermal candidiasis. Attempts at fungal isolation from cryopreserved skin were unsuccessful. As the seal died during the annual molt, it is unknown whether this condition may have been related to observed perimortem hair loss. Affected areas of skin were characterized by patchy invasion of the stratum corneum by fine, branching septate (and possibly, aseptate) fungal structures suggestive of fungal hyphae and pseudohyphae.

DISCUSSION

Knowledge of typical health indicators is an invaluable tool to assess the health of individuals and populations. The information presented here provides a set of initial baseline parameters and observations for Alaskan ice seals that may be considered in the context of emerging conservation concerns for Arctic environments, including those related to climate change and associated sea ice loss, increasing risks of contamination from oil, hazardous materials, and pollutants, introduction of pathogenic vectors including parasites and viruses, and food safety issues for subsistence communities. A discussion of key findings from the free-ranging, short-term rehabilitation, and long-term captive individuals sampled for this study follows.

Red blood cell (RBC) parameters, particularly hemoglobin (Hb) and hematocrit (Hct), are primary indicators of oxygen storage and transport capacity in marine mammals, which have substantially larger oxygen stores than their terrestrial counterparts (57). In particular, phocid seals have impressive blood oxygen stores to support prolonged breath-hold diving, with the longest and deepest diving species generally having the largest stores (58). The four species we evaluated exhibited higher values for all RBC parameters (RBC, Hb, Hct, MCV, MCH, MCHC) than more temperate living harbor seals (59, 60). When compared to other Arctic seals, the Alaskan ice seals exhibited higher RBC counts than both harp and hooded seals, and higher Hct values than harp seals (61, 62). Most notably, ribbon seals had the highest Hct values of all Arctic seals, reaching ∼75% in both captive and wild individuals. Although data on free-ranging diving behavior are limited for many Arctic phocids, high Hct, and Hb indicate that ribbon seals, the presumed deepest diver of the sampled species, also have the highest blood oxygen storage capacities. Among all Arctic seals, hooded seals are known to make the longest and deepest foraging dives, yet previously published Hb and Hct data for this species (61, 62) are lower than our values for ribbon seals. It is possible that the larger body size and robust muscle oxygen stores of hooded seals further contribute to their impressive dive profiles (63). Although there are clear differences in species-typical red blood cell indices for the target species, which vary widely in body size and routine foraging behavior,

all appear to have robust blood oxygen storage capacities. This is consistent with the thick, dark, sludgy appearance of whole blood obtained from these seals as compared to other pinnipeds.

Given that RBC indices in these species are higher than in most pinnipeds, certain conditions such as anemia may go unrecognized. Additionally, the higher RBC counts along with higher hemoglobin and iron may impact other physiological processes and serum chemistry parameters even in health (64) which may complicate veterinary assessments (i.e., hydration status, kidney function). Greater attention to RBC morphology, consistency of RBC size and color, presence of nucleated RBCs, plasma color, and reticulocyte count (not reported here) may be important, in addition to having robust age and sex specific data sets.

With respect to typical white blood cell (WBC) counts, Alaskan ice seals had more leukocytes than other seal species (60). Alaskan ice seals exhibited similar proportions of WBC types as other pinnipeds, with more neutrophils than lymphocytes and far fewer monocytes and eosinophils. Some individuals had low lymphocyte counts ($<$1,000/μl) which may be attributable to stress. Ringed seals had the highest eosinophil counts, which may correspond to a possible higher rate of parasitism in this species (see later).

Serum chemistry parameters aid in the evaluation of disease, contaminant exposure, and abnormal physiological conditions but can also change with normal development, feeding, geography, and reproductive state. In general, ice seals had similar ranges as other pinnipeds (60) though several had higher upper values. Ribbon seals had the highest total protein and albumin of the species sampled. Rehabilitated ringed seals had higher globulins; this is likely related to heightened immune stimulation and/or antigen exposure at admit from underlying disease that that was not observed in the other species.

Elevations of some blood chemistry parameters in the rehabilitation groups can be attributed to normal development of primarily young individuals (65), namely bilirubin (neonatal fetal hemoglobin turnover) and alkaline phosphatase, calcium, and phosphorus (upregulated secondary to bone growth). Several hepatobiliary-associated parameters (bilirubin, ALT, AST, and GGT) overlapped but had notably higher upper ranges in the stranded seals sampled as compared to wild Pacific harbor seal pups (39). These elevations in rehabilitated ringed seals are probably reflective of prolonged recovery from hepatobiliary disorders noted at admit and secondary to their profound morbidity and aberrant parasite migration. Alternatively, or additionally, these parameters and creatine kinase (CK) may relate to how animals are captured or handled for blood draws.

Differences in glucose, blood urea nitrogen (BUN), cholesterol, calcium, and potassium compared to other pinnipeds were considered negligible or not of physiological significance. Higher levels of sodium, and to a lesser extent chloride, were seen in spotted, ribbon, and ringed seals compared to other pinnipeds. The higher urinary specific gravity seen in Alaskan ice seals is consistent with these seals tending to have higher electrolytes, in particular sodium. As sodium levels increase, kidneys are stimulated to retain water resulting in more concentrated urine (66).

Consistent with other studies (32–35, 67–72), serological testing of Alaskan ice seals handled in rehabilitation or shortly after capture revealed little to no evidence of exposure to most diseases. While the young of the year animals in this report would not have had sufficient time in the wild to produce their own antibodies, they would have carried maternally derived antibodies. In the present study, all animals were seronegative for avian influenza, dolphin morbillivirus, phocine distemper virus, porpoise morbillivirus, *Neospora, Toxoplasma, Sarcocystis, Coxiella,* and rabies. It is notable that evidence of exposure to phocine distemper virus was not detected, although antibodies to the virus have been found in other marine mammals in some areas of the North Pacific [for review see (73)]. The few very low level positive results for antibodies to three *Leptospira* (*L. bratislava*, *L. hardjo*, and *L. ictero*), as well as the one positive result for antibodies to canine distemper, were not high enough to be consistent with disease, nor were they associated with clinical signs of infection. These findings suggest these diseases are not currently present in Alaskan ice seals, and also may indicate that these populations are immunologically naive and therefore potentially susceptible to them if introduced. An exception appears to be phocine herpesvirus and *Brucella*. The level of seroprevalence to *Brucella* is in accordance with other regional studies (32–35, 74), and while antibodies to *Brucella* were present, no seals had clinical disease. We found low to moderate levels of antibodies to phocine herpes PhHV-1 in a few stranded spotted, ribbon, and ringed seals. Two seals had rising titers on successive samples, suggesting recent disease at the time of admission, but none had clinical signs associated with herpesvirus. Chronic exposure to phocine herpes strains PhHV-1 and PhHV-2 has now been reported for spotted, ribbon, bearded, and ringed seals in the North Pacific, indicating that marine mammals in this region may be regularly exposed to the virus (32, 34, 35, 75). Prevalence and/or relative titers of PhHV-1 could be a useful adjunct to evaluating individual and population health status, as herpes has been shown to manifest more strongly in animal populations with limited resources or compromised health status (76, 77) as well as different levels of mental stress in people (78).

Bacterial isolates were more commonly obtained from ringed seals than spotted seals admitted for rehabilitation, which is consistent with greater morbidity observed in the ringed seals. More than half the ringed seal cases had clinically significant microbial infection; of these, most ultimately died or were euthanized because of the severity of their presenting problems. Isolates from spotted seals came from just two individuals that were profoundly ill prior to fully recovering from their presenting problems. In fact, all nine spotted seals handled for rehabilitation fully recovered. The single bearded seal admitted for rehabilitation succumbed to sepsis, with *Pseudomonas aeruginosa* isolated from multiple tissues. No bacterial isolates of concern were identified in the ribbon seal that was found out of range or in the two healthy bearded seals that were collected for research. Few antibiotic sensitivity tests were performed, however those results showed high sensitivity to all antibiotics tested.

There are several datasets concerning parasites in Alaskan ice seals, summarized by Geraci and St Aubin (79), Boveng et al. (13, 14), Cameron et al. (19), and Kelly et al. (18). In addition, as part of a survey for parasites in subsistence-harvested Alaskan seals (2 spotted, 36 bearded, 2 ribbon, 13 ringed seals), Tuomi et al. (personal communication, P. Tuomi) examined multiple samples (feces, gall bladder, heart, intestines, liver, lung, spleen, and stomach) for ova, larva, and whole parasites [see also (80)]. No parasites were found in the hearts or spleens of any individual sampled. Parasites were infrequently found in lungs; two bearded seals had anisakid nematodes (likely originating from the gastro-intestinal system), one ringed seal had a metastrongylid, and one spotted seal had a filaroid. While few spotted and ribbon seals were studied, all were found to have anisakids or acanthocephalalids in the stomach or intestines. Bearded seals had the greatest percentage of parasites with 81% of stomachs containing anisakids and 36% containing cestodes; 53% of gall bladder samples contained trematodes, and intestinal samples contained cestodes (83%), anisakid (11%), trematodes (6%), and acanthocephalans (3%). Bearded seal fecal samples had a similar complement of parasites with the addition of metastrongylids (6%) but no trematodes. In contrast to the present study, the ringed seals evaluated by Tuomi had lower incidences of parasite infestations, with anisakids (8%), trematodes (8%), cestodes (15%), and protozoa (8%) found only in different portions of the gastrointestinal tract; the protozoan was a coccidia oocyst morphologically consistent with *Eimeria sp*.

Of the seals handled during rehabilitation or following capture in the present study, bearded seals and ringed seals were more heavily parasitized than spotted seals. Additionally, more ringed seals had clinically significant parasites. Microfilaria—an early life stage of some parasitic nematodes which are released into the blood by adult worms, taken up by blood-feeding arthropod vectors, and develop into infective larvae that are transmitted to a new host—were only seen in ringed seals. Lungworm infections were confirmed or presumed in five ringed seal cases (31%) and one spotted seal case (11%) as well as the one bearded seal stranding case. Seal lice, *E. horridus* can serve as an intermediate host of the seal heartworm, *A. spirocauda*, which was not confirmed in any of the animals examined as part of this study, but could have been the source of the microfilaria seen in blood in a few cases. The apicomplexan protozoa seen in the captive bearded seal that died may have been acquired after leaving Alaska; however, *Sarcocystis spp*. has been previously reported in this species in the North Pacific (81).

Various degrees of alopecia and other skin conditions were observed in several animals included in this report. None, however, were consistent with the alopecia seen in the more extreme UME cases which included ulcerations as well as more profound derangements of the skin. Instead, it is the consensus of veterinarians involved with rehabilitating these animals that the alopecia was secondary to other stressors such as external wounds, chronic pulmonary disease, heavy parasitism, and/or liver disease. Additional contributors to observed hair loss may include exposure to novel environments such as warmer year-round temperatures, substrates rougher than snow or ice, and light exposure cycles different from those found in natural habitats, even when seals are housed in natural sea water with no added disinfectants. Dermal mycosis as found in the captive bearded seal that died has not been reported in bearded seals, but has been associated with persistent fresh water exposure, relatively warm water temperatures, and stress associated with seasonal molt in other pinnipeds (82, 83). When compared to other pinnipeds housed at the same facilities, Arctic ice seals appear more prone to hair loss and irregular molt (C. Goertz, unpublished data, D. Casper, personal communication, T. Schmitt personal communication).

CONCLUSIONS

The recent and unresolved unusual mortality event declared for Alaskan ice seals (2011–2018) is an alarming reminder of the challenges associated with assessing the health status of spotted, ribbon, bearded, and ringed seal populations. In particular, this event highlighted the sparsity of available data concerning health parameters and abundance estimates for these species. Given apparent low historical exposure and therefore low resistance to disease, recent extra-limital sightings of ice seals[1], and projected increases in contact between individuals and populations caused by reduced availability of sea ice (e.g., 10), it is likely that risks of epizootic events will continue to increase for these species. While still limited with respect to sample sizes and demographic groups in some cases, the hematology, and serum chemistry data provide markers for normal health status and physiology. Similar studies for other vulnerable seal species have shown that such datasets can be consistent as more individuals are added (84). Along with case-specific findings concerning disease exposure, parasite loads, and microbiology, these observations of Alaskan ice seals contribute to a much needed expanded understanding of these species.

ETHICS STATEMENT

This study was carried out in accordance with the requirements of federal marine mammal research permits 14535, 15142, 15126, 18902, 19309, or the Alaska SeaLife Center-NOAA/NMFS Stranding Agreement. Animal protocols for captive seals were approved by the Institutional Animal Care and Use Committee at the University of California Santa Cruz. Animal protocols for wild seals were approved under IACUC protocols A/NW 2010, A/NW 2016.

AUTHOR CONTRIBUTIONS

CG and CR devised the project. CG, CR, HZ, and PB were responsible for sample collection. CG, CR, NT, HZ, and PB contributed to evaluation of the data and manuscript

[1]For example, unusual sightings of ribbon seals in Wasilla and Yakutat (Alaska), and in Washington, Oregon, and California; increases in sightings and strandings of ringed seals around Unalaska Island (Aleutian Archipelago) and one stranding in Washington (National Marine Mammal Stranding Network, D. Fauquier, personal communication).

preparation. CR and PB were responsible for funding, animal welfare considerations, and project oversight.

FUNDING

The project was funded by NOAA's Alaska Pinnipeds Program (NA15NMF4390166, NA16NMF4390027). Support for stranded animal response, care, and sample analysis was provided by NOAA's Prescott Stranding Grant Program (NA03NMF4390036, NA03NMF4390357, NA04NMF4390135, NA07NMF4390218, NA07NMF4390307, NA08NMF4390527, NA09NMF4390217, NA12NMF4390164, NA14NMF4390194, NA15NMF4390043, and NA16NMF4390143) as well as donations and support from individuals and corporations. Support for veterinary care of captive seals was provided by the Joint Industry Programme on Sound and Marine Life.

ACKNOWLEDGMENTS

Field based studies: The authors thank Tracey Goldstein, Lorrie Rea, Michelle Barbieri, Deborah Fauquier, Michael Cameron, Josh London, Gavin Brady, Shawn Dahle, John Jansen, Dave Withrow, Erin Moreland, and Markus Horning for assistance in the field, the officers and crew of the NOAA ships McArthur II and Oscar Dyson for access to the Bering Sea marginal ice zone to collect ribbon and spotted seal samples. Michael Camerson, Shawn Johnson, John Jansen, Gavin Brady, Josh London, and Shawn Dahle provided assistance in obtaining bearded seal samples. Kendal Harr of URIKA Pathology provided advice and analyses of archival samples for blood chemistry values.

Stranded ice seals: The authors thank past and present husbandry, rehabilitation, and veterinary staff and volunteers at the Alaska SeaLife Center who supported seals during rehabilitation and assisted with obtaining samples. In particular, the authors thank Brett Long, Lynda Leppert, Millie Gray, Carol Stephens, Pam Tuomi, Kathy Woodie, Jane Belovarac, and Natalie Rouse. Additionally, we thank veterinary parasitologists Mike Kinsella and Ellis Greiner who speciated many parasites and pathology services (Alaska Veterinary Pathology Service; Armed Forces Institute of Pathology; University of California Davis School of Veterinary Medicine Anatomic Pathology Service, and Northwest ZooPath) that reviewed biopsies from live animals and tissues of cases post mortem.

Captive ice seals: Data collection was made possible by veterinary care and expert consultation provided by Kathy Woodie and David Casper. We thank the husbandry teams at the Alaska SeaLife Center and Long Marine Laboratory for their assistance with these seals, especially Jillian Sills, Jenna Sullivan, Sonny Knaub, Brett Long, Derek Woodie, Jamie Mullins, Brandon Russell, Juliana Kim, Shelby Burman, and Margaret Black.

The authors thank John Goodwin, Alex Whiting, David Casper, Brett Long, and Jillian Sills for their assistance with the bearded seals at the Alaska SeaLife Center. Additionally, gross necropsy and histopathological examination of tissues from the captive bearded seal that died during the study period was generously provided by veterinary pathologist Melissa Miller, California Department of Fish and Wildlife, Marine Wildlife Veterinary Care, and Research Center. We thank Lori Polasek, Brett Long, JoAnn Mellish, and Renae Sattler for helpful input to the proposal associated with this project.

Nicole Stacy, Sea Rogers Williams, Dean Konjević, and Emily Whitmer provided helpful comments that substantively improved this manuscript.

SUPPLEMENTARY MATERIAL

The Supplementary Material for this article can be found online at: https://www.frontiersin.org/articles/10.3389/fvets.2019.00004/full#supplementary-material

REFERENCES

1. Hinzman LD, Bettez ND, Bolton WR, Chapin FS, Dyurgerov MB, Fastie CL, et al. Evidence and implications of recent climate change in Northern Alaska and other Arctic regions. *Clim Change* (2005) 72:251–98. doi: 10.1007/s10584-005-5352-2
2. Overpeck JT, Sturm M, Francis JA, Perovich DK, Serreze MC, Benner R, et al. Arctic system on trajectory to new, seasonally ice-free state. *Eos* (2005) 86:309. doi: 10.1029/2005EO340001
3. Post E, Forchhammer MC, Bret-Harte MS, Callaghan TV, Christensen TR, Elberling B, et al. Ecological dynamics across the Arctic associated with recent climate change. *Science* (2009) 325:1355–8. doi: 10.1126/science.1173113
4. Laidre KL, Stirling I, Lowry LF, Wiig Ø, Heide-Jørgensen MP. Quantifying the sensitivity of Arctic marine mammals to climate-induced habitat change. *Ecol Appl.* (2008) 18:S97–125. doi: 10.1890/06-0546.1
5. McCauley DJ, Pinsky ML, Palumbi SR, Estes JA, Joyce FH, Warner RR. Marine defaunation: animal loss in the global ocean. *Science* (2015) 347: 1255641. doi: 10.1126/science.1255641
6. Moore SE, Huntington HP. Arctic marine mammals and climate change: impacts and resilience. *Ecol Appl.* (2008) 18:S157–65. doi: 10.1890/06-0282.1
7. Burek-Huntington KA, Stimmelmayr R, Herreman J, Sheffield G, Garlich-Miller J, Firth C, et al. Histopathological and ancillary diagnostic findings from 2011 northern pinnipeds UME in the Arctic and Bering Strait Regions of Alaska, USA. In: *IAAAM Conference Proceedings*. Atlanta, GA (2012). p. 3–5.
8. NOAA. *Special Notice: The Ume Involving Ice Seals With Hair Loss And Skin Lesions is Now Closed*. NOAA (2018).
9. NOAA. *Northern Pinniped Unusual Mortality Event (UME) Update* (2012). Available online at: http://www.north-slope.org/assets/images/uploads/UMEUpdate101012.pdf
10. Burek KA, Gulland FMD, O'Hara TM. Effects of climate change on Arctic marine mammal health. *Ecol Appl.* (2008) 18:S126–34. doi: 10.1890/06-0553.1
11. Goldstein T, Mazet JAK, Gill VA, Doroff AM, Burek KA, Hammond JA. Phocine distemper virus in northern sea otters in the Pacific Ocean, Alaska, USA. *Emerg Infect Dis.* (2009) 15:925–7. doi: 10.3201/eid1506.090056
12. Khon VC, Mokhov II, Latif M, Semenov VA, Park W. Perspectives of northern sea route and northwest passage in the twenty-first century. *Clim Change* (2010) 100:757–68. doi: 10.1007/s10584-009-9683-2
13. Boveng PL, Bengtson JL, Buckley TW, Cameron MF, Dahle SP, Kelly BP, et al. *Status Review of the Spotted Seal* (*Phoca largha*). *NOAA Tech Memo NMFS-AFSC* (2009) 200:i–xiii, 1–153.
14. Boveng PL, Bengtson JL, Buckley TW, Cameron MF, Dahle SP, Megrey BA, et al. *Status Review of the Ribbon Seal* (*Histriophoca fasciata*). *NOAA Tech Memo NMFS-AFSC* (2008). 191:i–xiv, 1-115.
15. Lowry LF, Frost KJ, Davis R, DeMaster DP, Suydam RS. Movements and behavior of satellite-tagged spotted seals (*Phoca largha*) in the Bering and Chukchi Seas. *Polar Biol.* (1998) 19:221–30. doi: 10.1007/s003000050238

16. Burns JJ. Remarks on the distribution and natural history of pagophilic pinnipeds in the Bering and Chukchi Seas. *J Mammal.* (1970) 51:445–54. doi: 10.2307/137838617
17. Boveng PL, Lowry LF. Ribbon seal *Histriophoca faciata*. In: Würsig B, Thewissen JGM, Kovacs K, editors. *Encyclopedia of Marine Mammals, 3rd ed*. London: Academic Press (2017). p. 811–3.
18. Kelly BP, Bentson JL, Boveng PL, Cameron MF, Dahle SP, Jansen JK, et al. *Status Review of the Ringed Seal* (*Phoca hispida*). *NOAA Tech Memo NMFS-AFSC* (2010). 212:i–xiv, 1-250.
19. Cameron MF, Bengtson JL, Boveng PL, Jansen JK, Kelly BP, Dahle SP, et al. *Status Review of the Bearded Seal* (*Erignathus barbatus*). *NOAA Tech Memo NMFS-AFSC* (2010). 211:i.
20. Kovacs KM, Lydersen C, Gjertz I. Birth-site characteristics and prenatal molting in bearded seals (*Erignathus barbatus*). *J Mammal.* (1996) 77:1085–91. doi: 10.2307/1382789
21. Bengtson JL, Hiruki-Raring LM, Simpkins MA, Boveng PL. Ringed and bearded seal densities in the eastern Chukchi Sea, 1999-2000. *Polar Biol.* (2005) 28:833–45. doi: 10.1007/s00300-005-0009-1
22. Gjertz I, Kovacs KM, Lydersen C, Wiig. Movements and diving of bearded seal (*Erignathus barbatus*) mothers and pups during lactation and post-weaning. *Polar Biol* (2000) 23:559–566. doi: 10.1007/s003000000121
23. Krafft BA, Lydersen C, Kovacs KM, Gjertz I, Haug T. Diving behaviour of lactating bearded seals (*Erignathus barbatus*) in the Svalbard area. *Can J Zool.* (2000) 78:1408–18. doi: 10.1139/cjz-78-8-1408
24. Smith TG, Stirling I. The breeding habitat of the ringed seal (*Phoca hispida*): the birth lair and associated structures. *Can J Zool.* (1975) 53:1297–305. doi: 10.1139/z75-155
25. Smith TG, Hammill MO, Taugbl G. A review of the developmental, behavioural and physiological adaptations of the ringed seal, *Phoca hispida*, to life in the Arctic winter. *Arctic* (1991) 44:124–31.
26. Bossart GD, Reidarson TH, Dierauf LA, Duffield DA. Clinical pathology. In: Dierauf LA, Gulland FMD, editors. *CRC Handbook of Marine Mammal Medicine, 2nd ed*. New York, NY: CRC Press (2001). p. 383–430.
27. Lenfant C, Johansen K, Torrance JD. Gas transport and oxygen storage capacity in some pinnipeds and the sea otter. *Respir Physiol.* (1970) 9:277–86.
28. Engelhardt FR. Hematology and plasma chemistry of captive pinnipeds and cetaceans. *Aquat Mamm.* (1979) 7:11–24.
29. Geraci J, Smith T. Functional hematology of ringed seals (*Phoca hispida*) in the Canadian Arctic. *J Fish Board Canada* (1975) 32:2559–64. doi: 10.1139/f75-302
30. Lydersen C, Ryg MS, Hammill MO, O'Brien PJ. Oxygen stores and aerobic dive limit of ringed seals (*Phoca hispida*). *Can J Zool.* (1992) 70:458–61. doi: 10.1139/z92-069
31. Geraci JR, Aubin DJ, Smith TG. Influence of age, condition, sampling time, and method on plasma chemical constiuents in free-ranging ringed seals, *Phoca hispida*. *J Fish Res Board Canada* (1979) 36:1278–82. doi: 10.1139/f79-182
32. Quakenbush L, Citta J, Crawford J. *Biology of the Spotted Seal (Phoca largha) in Alaska from 1962-2008*. Final Rep to Natl Mar Fish Serv (2009)
33. Quakenbush L, Citta J. *Biology of the ribbon seal in Alaska.* Final Rep to Natl Mar Fish Serv (2008)
34. Quakenbush L, Citta J, Crawford J. *Biology of the Bearded Seal (Erignathus barbatus) in Alaska, 1961-2009*. Final Rep to Natl Mar Fish Serv (2011)
35. Quakenbush L, Citta J, Crawford J. *Biology of the Ringed Seal (Phoca hispida) in Alaska, 1960-2010.* Final Rep to Natl Mar Fish Serv (2011)
36. Roletto J. Hematology and serum chemistry values for clinically healthy and sick pinnipeds. *J Zoo Wildl Med.* (1993) 24:145–57.
37. Trumble SJ, Castellini MA, Mau TL, Castellini JM. Dietary and seasonal influences on blood chemistry and hematology in captive harbor seals. *Mar Mammal Sci.* (2006) 22:104–23. doi: 10.1111/j.1748-7692.2006.00008.x
38. Greig DJ, Gulland FMD, Rios CA, Hall AJ. Hematology and serum chemistry in stranded and wild-caught harbor seals in Central California: reference intervals, predictors of survival, and parameters affecting blood variables. *J Wildl Dis.* (2010) 46:1172–84. doi: 10.7589/0090-3558-46.4.1172
39. Hasselmeier I, Fonfara S, Driver J, Siebert U. Differential hematology profiles of free-ranging, rehabilitated, and captive harbor seals (*Phoca vitulina*) of the German North Sea. *Aquat Mamm.* (2008) 34:149–56. doi: 10.1578/AM.34.2.2008.149
40. Vossen A, Abdulmawjood A, Lammler C, Weib R, Siebert U. Identification and molecular characterization of beta-hemolytic streptococci isolated from harbor seals (*Phoca vitulina*) and grey seals (*Halichoerus grypus*) of the German North and Baltic Seas. *J Clin Microbiol.* (2004) 42:469–73. doi: 10.1128/JCM.42.1.469
41. Bauer KL, Goertz CEC, Belovarac JA, Walton RW, Dunn JL, Tuomi P. Infectious disease and toxological monitoring of stranded Pacific harbor seals (*Phoca vitulina richardsi*) in Cook Inlet as surrogates for monitoring endangered belugas (*Delphinapterus leucas*). *J Zoo Wildl Med.* (2016) 47:770–80. doi: 10.1638/2015-0147.1
42. Marcos R, Pereira C, Santos M, Luzzago C, Lauzi S, Maia JP, et al. Buffy coat smear or Knott's test: which to choose for canine microfilaria screening in field studies? *Vet Clin Pathol.* (2016) 45:201–5. doi: 10.1111/vcp.12321
43. Friedrichs KR, Harr KE, Freeman KP, Szladovits B, Walton RM, Barnhart KF, et al. ASVCP reference interval guidelines: determination of *de novo* reference intervals in veterinary species and other related topics. *Vet Clin Pathol.* (2012) 41:441–53. doi: 10.1111/vcp.12006
44. Puryear WB, Keogh M, Hill N, Moxley J, Josephson E, Davis KR, et al. Prevalence of influenza A virus in live-captured North Atlantic gray seals: a possible wild reservoir. *Emerg Microbes Infect.* (2016) 5:1–9. doi: 10.1038/emi.2016.77
45. Spackman E. Avian influenza virus detection and quantitation by real-time RT-PCR. In: Spackman E, editors. *Animal Influenza Virus: Methods in Molecular Biology*. London: Human Press (2014). p. 105–18.
46. Meegan J, Field C, Sidor I, Romano T, Casinghino S, Smith CR, et al. Development, validation, and utilization of a competitive enzyme-linked immunosorbent assay for the detection of antibodies against brucella species in marine mammals. *J Vet Diagnostic Investig.* (2010) 22:856–62. doi: 10.1177/104063871002200603
47. Macmillan A. Conventional serological tests. In: Nielsen K, Duncan JR, editors. *Animal Brucellosis.* Boca Raton, FL: CRC Press (1990). p. 153–97.
48. Kersh GJ, Lambourn DM, Raverty SA, Fitzpatrick KA, Self JS, Akmajian AM, et al. *Coxiella burnetii* infection of marine mammals in the Pacific Northwest, 1997–2010. *J Wildl Dis.* (2012) 48:201–6. doi: 10.7589/0090-3558-48.1.201
49. Zarnke RL, Saliki JT, Macmillan AP, Brew SD, Dawson CE, Ver Hoef JM, et al. Serologic survey for *Brucella Spp*., phocid herpesvirus-1, phocid herpesvirus-2, and phocine distemper virus in harbor seals from Alaska, 1976–1999. *J Wildl Dis.* (2006) 42:290–300. doi: 10.7589/0090-3558-42.2.290
50. Goldstein T, Gulland FMD, Aldridge BM, Harvey JT, Rowles T, Lambourn DM, et al. Antibodies to phocine herpesvirus-1 are common in North American harbor seals (*Phoca vitulina*). *J Wildl Dis.* (2003) 39:487–94. doi: 10.7589/0090-3558-39.3.487
51. Colagross-Schouten AM, Mazet JAK, Gulland FMD, Miller MA, Hietala S. Diagnosis and seroprevalence of leptospirosis in California sea lions from coastal California. *J Wildl Dis.* (2002) 38:7–17. doi: 10.7589/0090-3558-38.1.7
52. Saliki JT, Lehenbauer TW. Monoclonal antibody-based competitive enzyme-linked immunosorbent assay for detection of morbillivirus antibody in marine mammal sera. *J Clin Microbiol.* (2001) 39:1877–81. doi: 10.1128/JCM.39.5.1877
53. Appel M, Robson DS. A microneutralization test for canine distemper virus. *Am J Vet Res.* (1973) 34:1459–63.
54. Miller MA, Gardner IA, Packham A, Mazet JK, Hanni KD, Jessup D, et al. Evaluation of an indirect fluorescent antibody test (IFAT) for demonstration of antibodies to *toxoplasma gondii* in the sea otter (*Enhydra lutris*). *J Parasitol.* (2002) 88:594–9.doi: 10.2307/3285456
55. Mazumder P, Chuang HYK, Wentz MW, Wiedbrauk DL. Latex agglutination test for detection of antibodies to *Toxoplasma gondii*. *J Clin Microbiol.* (1988) 26:2444–6.
56. Smith JS, Yager PA, Baer GM. A rapid reproducible test for determining rabies neutralizing antibody. *Bull World Health Organ.* (1973) 48:535–41.
57. Kooyman GL. *Diverse Divers*. New York, NY: Springer-Verlag (1989).
58. Ponganis PJ. Diving mammals. *Compr Physiol.* (2011) 1:517–35. doi: 10.1002/cphy.c091003
59. Burns JM, Costa DP, Frost K, Harvey JT. Development of body oxygen stores in harbor seals: effects of age, mass, and body composition. *Physiol Biochem Zool.* (2005) 78:1057–68. doi: 10.1086/432922

60. Gulland FMD, Dierauf LA, Whitman KL. Appendix 1: normal hematology and serum chemistry ranges. In: *CRC Handbook of Marine Mammal Medicine, 3rd ed.* New York, NY: CRC Press (2018). p. 1003–25.
61. Burns JM, Lestyk KC, Folkow LP, Hammill MO, Blix AS. Size and distribution of oxygen stores in harp and hooded seals from birth to maturity. *J Comp Physiol B* (2007) 177:687–700. doi: 10.1007/s00360-007-0167-2
62. Boily F, Beaudoin S, Measures LN. Hematology and serum chemistry of harp (*Phoca groenlandica*) and hooded seals (*Cystophora cristata*) during the breeding season, in the Gulf of St. Lawrence, Canada. *J Wildl Dis.* (2006) 42:115–32. doi: 10.7589/0090-3558-42.1.115
63. Folkow LP, Ramirez J, Ludvigsen S, Ramirez N, Blix AS. Remarkable neuronal hypoxia tolerance in the deep-diving adult hooded seal (*Cystophora cristata*). *Neurosci Lett.* (2008) 446:147–50. doi: 10.1016/j.neulet.2008.09.040
64. Tracz MJ, Alam J, Nath KA. Physiology and pathophysiology of heme: implications for kidney disease. *J Am Soc Nephrol.* (2007) 18:414–20. doi: 10.1681/ASN.2006080894
65. Morgan LW, Jakush JL, Simpson A, Norman MM, Pabst DA, Simmons S. Evaluation of hematologic and biochemical values for convalescing seals from the coast of Maine. *J Zoo Wild Med.* (2009) 40:421–9. doi: 10.1638/2007-0032.1
66. Nawata CM, Pannabecker TL. Mammalian urine concentration: a review of renal medullary architecture and membrane transporters. *J Comp Physiol B.* (2018) 188:899–918. doi: 10.1007/s00360-018-1164-3
67. Calle PP, Seagars DJ, McClave C, Senne D, House C, House JA. Viral and bacterial serology of six free-ranging bearded seals *Erignathus barbatus*. *Dis Aquat Organ.* (2008) 81:77–80. doi: 10.3354/dao01927
68. Barlough JE, Berry ES, Smith AW, Skilling DE. Prevalence and distribution of serum neutralizing antibodies to Tillamook (bovine) calicivirus in selected populations of marine mammals. *J Wildl Dis.* (1987) 23:45–51.
69. Barlough JE, Berry ES, Skilling DE, Smith AW. Prevalence and distribution of serum neutralizing antibodies to San Miguel sea lion virus types 6 and 7 in selected populations of marine mammals. *Dis Aquat Organ.* (1988) 5:75–80.
70. Osterhaus ADME, Groen J, De Vries P, UytdeHaag FGCM, Klingeborn B, Zarnke R. Canine distemper virus in seals. *Nature* (1988) 335:403–4.
71. Danner GR, McGregor MW, Zarnke RL, Olsen CW. Serologic evidence of influenza virus infection in a ringed seal (*Phoca hispida*) from Alaska. *Mar Mammal Sci.* (1998) 14:380–4.
72. Duignan PJ, Nielsen O, House C, Kovacs KM, Duffy N, Early G, et al. Epizootiology of morbillivirus infection in harp, hooded, and ringed seals from the Canadian Arctic and Western Atlantic. *J Wildl Dis.* (1997) 33:7–19. doi: 10.7589/0090-3558-33.1.7
73. Duignan P, Van Bressem M-F, Baker J, Barbieri M, Colegrove K, De Guise S, et al. Phocine distemper virus: current knowledge and future directions. *Viruses* (2014) 6:5093–134. doi: 10.3390/v6125093
74. Nymo IH, Rødven R, Beckmen K, Larsen AK, Tryland M, Quakenbush L, et al. Brucella antibodies in Alaskan true seals and eared seals—two different stories. *Front Vet Sci.* (2018) 5:8. doi: 10.3389/fvets.2018.00008
75. Zarnke RL, Harder TC, Vos HW, Ver Hoef JM, Osterhaus ADME. Serologic survey for phocid herpesvirus-1 and−2 in marine mammals From Alaska and Russia. *J Wildl Dis.* (1997) 33:459–65. doi: 10.7589/0090-3558-33.3.459
76. Costantini D, Seeber PA, Soilemetzidou S-E, Azab W, Bohner J, Buuveibaatar B, et al. Physiological costs of infection: herpesvirus replication is linked to blood oxidative stress in equids. *Sci Rep* (2018) 8:10347. doi: 10.1038/s41598-018-28688-0
77. Sebastiano M, Chastel O, De Thoisy B, Eens M, Costantini D. Oxidative stress favours herpes virus infection in vertebrates: a meta-analysis. *Curr Zool.* (2016) 62:325–32. doi: 10.1093/cz/zow019
78. Takao Y, Okuno Y, Mori Y, Asada H, Yamanishi K, Iso H. Associations of perceived mental stress, sense of purpose in life, and negative life events with the risk of incident herpes zoster and postherpetic neuralgia. *Am J Epidemiol.* (2017) 187:251–9. doi: 10.1093/aje/kwx249
79. Geraci JR, St Aubin DJ. Effects of parasites on marine mammals. *Int J Parasitol.* (1987) 5:407–14.
80. Tuomi P, McIntosh A, Leppert L, Belovarac J, Goertz, CEC Quakenbush, L Hoover-Miller A. Preliminary survey of parasite burden in subsistence harvested ice seals in Alaska. In: *Proceedings, The Alaska Marine Science Symposium*. Anchorage, AK (2011). p. 112.
81. Bishop L. Parasite-related lesions in a bearded seal, *Erignathus barbatus*. *J Wildl Dis.* (1979) 15:285–93.
82. Tanaka E, Kimura T, Wada S, Hatai K, Sonoda S. Dermatophytosis in a Steller sea lion (*Eumetopias jubatas*). *J Vet Med Sci.* (1994) 56:551–3.
83. Pollock CG, Rohrbach B, Ramsay EC. Fungal dermatitis in captive pinnipeds. *J Zoo Wildl Med.* (2000) 31:374–8. doi: 10.1638/1042-7260(2000)031[0374:FDICP]2.0.CO;2
84. Kaufman AC, Barbieri M, Robinson SJ, Baker JD, Littnan CL. Establishing hematology and serum chemistry reference intervals for wild Hawaiian monk seals (*Neomonachus schauinslandi*). *J Zoo Wildl Med.* (2018) 49:1036–40. doi: 10.1638/2017-0039.1.

Conflict of Interest Statement: The authors declare that the research was conducted in the absence of any commercial or financial relationships that could be construed as a potential conflict of interest.

Copyright © 2019 Goertz, Reichmuth, Thometz, Ziel and Boveng. This is an open-access article distributed under the terms of the Creative Commons Attribution License (CC BY). The use, distribution or reproduction in other forums is permitted, provided the original author(s) and the copyright owner(s) are credited and that the original publication in this journal is cited, in accordance with accepted academic practice. No use, distribution or reproduction is permitted which does not comply with these terms.

frontiers in Veterinary Science

ORIGINAL RESEARCH
published: 26 March 2019
doi: 10.3389/fvets.2019.00088

Occurrence of Rhabditid Nematodes in the Pet Giant African Land Snails (*Achatina fulica*)

Dario d'Ovidio[1]*, *Jirí Nermut*[2], *Chiara Adami*[3] and *Mario Santoro*[4]

[1] Private Veterinary Practitioner, Arzano, Italy, [2] Institute of Entomology, Biology Centre CAS, České Budějovice, Czechia, [3] Royal Veterinary College, University of London, Hatfield, United Kingdom, [4] Dipartimento di Sanitá Animale, Istituto Zooprofilattico Sperimentale del Mezzogiorno, Portici, Italy

Gastropods comprise nearly 60,000 species of aquatic as well as terrestrial mollusks, primarily snails and slugs. The giant African land snail (*Achatina fulica*) is one of the most popular pet snails worldwide. This gastropod mollusk is known as the intermediate host of several parasites that cause severe diseases in pets, free-ranging vertebrates, and humans. The aim of this survey was to investigate the occurrence of parasites in giant African land snails kept as pets in southern Italy. Fresh fecal samples were collected from a total of 60 giant African land snails kept in three private collections in Campania region (Italy). In addition, microscopic analysis of mucus and histological examination of biopsy samples from the foot muscle of 30 individual snails were performed. Coprological examination revealed the presence of rhabditid nematodes identified by both morphological and molecular assessment as *Rhabditella axei* in two out of three examined samples, and *Rhabditis terricola*, *Cruznema* sp., and *Pristionchus entomophagus* in one coprological sample. No parasites were detected in the muscle biopsy samples, or in the mucus. Due to the potential harm of rhabditid nematodes, their presence in giant African land snails potentially in contact with both pets and humans should not be disregarded.

Keywords: terrestrial gastropod, *Rhabditella axei*, rhabditidae, mollusk parasite, *Achatina fulica*

OPEN ACCESS

Edited by:
Robert James Ossiboff, University of Florida, United States

Reviewed by:
Elise Ladouceur, Joint Pathology Center (JPC), United States
Heather Walden, University of Florida, United States

***Correspondence:**
Dario d'Ovidio
dariodovidio@yahoo.it

Specialty section:
This article was submitted to Zoological Medicine, a section of the journal Frontiers in Veterinary Science

Received: *11 January 2019*
Accepted: *06 March 2019*
Published: *26 March 2019*

Citation:
d'Ovidio D, Nermut J, Adami C and Santoro M (2019) Occurrence of Rhabditid Nematodes in the Pet Giant African Land Snails (Achatina fulica). Front. Vet. Sci. 6:88. doi: 10.3389/fvets.2019.00088

INTRODUCTION

Invertebrates include approximately one million animal species kept both in zoological institutions and in households where they are hand raised as exotic pets (1). Gastropods comprise nearly 60,000 species of aquatic as well as terrestrial mollusks, primarily snails and slugs (1). The giant African land snail (*Achatina fulica,* syn. *Lissachatina fulica*) is native to East Africa, however it is a widespread invasive species in Asia, Oceania, and more recently in Americas, where it has been introduced accidentally or purposefully as a food source and as a pet. Its release in natural ecosystems, agricultural, and urban areas has resulted in ecological, health, and agricultural threats (2, 3). The giant African land snail is an intermediate hosts for several parasites including *Aelurostrongylus abstrusus*, *Angiostrongylus cantonensis*, *Angiostrongylus costaricensis*, *Schistosoma mansoni*, *Hymenolepis* spp., and *Fasciola hepatica* (4, 5). All the above helminths, with the exception of *A. abstrusus,* are able to cause severe diseases in humans. Specifically, the giant African land snail is the main gastropod responsible for worldwide spread of *A. cantonensis* that causes human eosinophilic meningoencephalitis in Asia and Americas (2, 6). Risk factors for infection in humans,

pets and wildlife with those helminth parasites include the ingestion of raw or undercooked infected snails or slugs, or foods contaminated by the slime of infected snails or slugs (4, 5, 7, 8).

Although the African giant land snails are among the most popular snails held as pets, and their worldwide popularity as exotic pets is growing rapidly, only a few surveys have been carried out on the occurrence of their parasites in natural conditions (2, 6, 9–11). The aim of this survey was to investigate the occurrence of parasites in giant African land snails bred as pets in southern Italy.

MATERIALS AND METHODS

General Data

In August 2018, three pools of fresh fecal samples obtained from a total of 60 giant African land snails, kept in three different private collections located in Pozzuoli, Caserta, and Naples (Italy), were investigated for parasites. From each locality we obtained a pool of feces from 20 individual snails each. The snails included in this survey had a median age of 1.6 years ranging from 0.2 to 2 years and had not received any previous anti-parasitic treatment. Snails were fed fresh vegetables and fruits; additionally, a calcium powder supplementation (Calcium, Exo Terra, Hagen Deutschland GmbH & Co. KG, Holm, Germany) was provided twice a week. All animals were bred in Italy, privately owned and kept as pets in four indoor terrariums of 60 × 30 × 45 cm in size, in groups of 10–20 animals (2 groups of 20 snails in Pozzuoli and Caserta and 2 groups of 10 snails each in Naples). An organic peat soil (Organic Coco-Peat Soil, E-Coco Products, Gloucestershire, UK), previously heat-treated (100°C for 30 min) and then free of parasites and insects, was used as substrate.

Diagnostic Procedures

Twenty grams of fresh feces were initially obtained from each of the four terrarium. When pooled feces analyzed by fresh smear, flotation and Baermann test showed positivity to rhabditid nematodes, two snails from each positive terrarium were housed individually in a sterile plastic box, and their feces were collected, immediately after defecation, in a sterile 50 ml plastic tube. Coprological examination for pooled and individual samples included fresh smear, centrifugal flotation (2 g of feces for each test) using a solution of sugar and formaldehyde (specific gravity 1.27) and Baermann test (10 g of feces for each test). Additionally, the mucus obtained during fresh smear examination was analyzed under a light microscope. Because the larval forms of several helminth species may encyst inside the foot muscle of snails, histological examination of biopsy samples harvested from the anterior and posterior areas of the foot muscle was performed in 30 snails, anesthetized with the technique described by Giannelli et al. (12) and Gilbertson and Wyatt (13). The biopsy samples were fixed in 10% neutral phosphate-buffered formalin, and processed by routine methods into paraffin blocks that were cut into 3 μm thick sections, and stained with hematoxylin and eosin. The study was performed under permission of the practice where it took place and under signed, written informed owner consent.

Morphological Identification

Temporary mounts were made by heat-killing nematodes on glass slides in a drop of water, after which a glass cover slip was applied. Nematodes were transferred into a drop of tap water on a glass slide and placed on heater (100°C) for 10 s. These specimens were used for morphological identification. An AMPLIVAL light microscope, Carl Zeiss Jena, and a Leitz Diaplan with Nomarski optics were used for observation. Morphological identification of rhabditid nematodes followed Andrassy (14) and Andrassy (15) and it was mostly based on the morphology of pharynx and stoma, and reproductive system, mainly the features of spicules, number and position of papillae or presence and size or shape of bursa for males; and tail shape, position of vulva and morphology of reproductive system for females. The identification of larvae was based on the tail shape.

Molecular Analysis

DNA was extracted from nematode specimens obtained from feces fixed in 96% ethanol collected from the three localities. Nematodes were washed in double-distilled water (ddH_2O) overnight, prior to the molecular analysis, for complete removal of residuals of ethanol. Each individual nematode was transferred into a sterile Eppendorf tube (200 μl) with 20 μl of extraction buffer (17.7 μl of ddH_2O, 2 μl of 10 × concentrated PCR buffer, 0.2 μl of 1% Tween 20 and 0.1 μl of proteinase K). Buffer and nematodes were frozen at −20°C for 20 min, and then immediately incubated at 65°C for 1 h, followed by 10 min at 95°C. The lysates were cooled on ice and then centrifuged (2 min, 9,000 g); 1 μl of supernatant was used for PCR.

A fragment of rDNA containing the internal transcribed spacer regions (ITS1, 5.8S, ITS2) was amplified using primers 18S: 5′-TTG ATT ACG TCC CTG CCC TTT-3′ (forward), and 28S: 5′-TTT CAC TCG CCG TTA CTA AGG-3′ (reverse) (16). A fragment of rDNA containing the gene for 18S rRNA was amplified using primers 22F: 5′- TCC AAG GAA GGC AGC AG GC-3′ (forward), and 1080JR: 5′- TCC TGG TGG TGC CCT TCC GTC AAT TTC-3′ (reverse) (17). The PCR master mix consisted of: ddH_2O, 7.25μl; 10 × PCR buffer, 1.25 μl; deoxynucleoside triphosphates (dNTPs), 1 μl; 0.75 μl of both forward and reverse primer; polymerase, 0.1 μl; and 1 μl of DNA-extract. The PCR profiles were used as follows: for ITS 1 cycle of 94°C for 7 min followed by 35 cycles of 94°C for 60 s, 50°C for 60 s and 72°C for 60 s, and a final elongation at 72°C for 7 min (14); for 18S 1 cycle of 94°C for 5 min, followed by 35 cycles of 94°C for 60 s, 55°C for 90 s and 72°C for 2 min and a final elongation at 72°C for 10 min. The PCR products were sequenced by GATC Biotech (Germany) and later edited and uploaded to GenBank (https://www.ncbi.nlm.nih.gov/genbank/).

RESULTS

The Baermann test revealed the presence of nematode larvae, whose length ranged from 170 to 336 μm, in all samples. Eggs, larvae and adult rhabditid nematodes were detected by fresh smear and flotation methods in all fecal samples. *Rhabditella axei* (**Figure 1**) was identified morphologically from two out of three pooled and individual fecal samples from Pozzuoli and Naples.

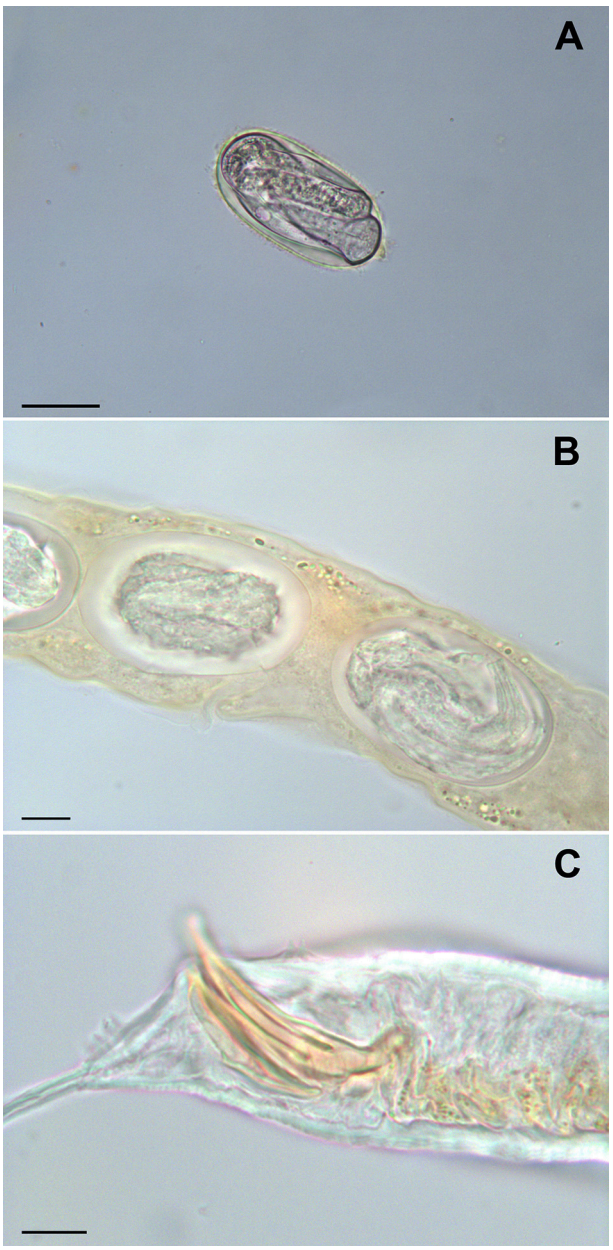

FIGURE 1 | *Rhabditella axei* obtained from the pet giant African land snails (*Achatina fulica*). An egg from coprological examination, bar = 30 μm **(A)** eggs in uterus, bar = 10 μm **(B)** caudal extremity of male, bar = 10 μm **(C)**.

In addition, *Rhabditis terricola*, *Cruznema* sp., and *Pristionchus entomophagus* were isolated from one pool and individual fecal samples from Caserta. No parasites were detected in the muscle biopsy samples or in the mucus.

Several morphological types of rhabditid nematodes were isolated from snail feces fixed in 96% ethanol. Obtained and edited sequences of ITS and 18S of these nematodes were compared (BLAST) with the material in GenBank and identified as *R. axei* (partial 18S, accession number MK124578, similarity 99%), *Rh. terricola* (partial 18S and partial ITS1, accession number MK156052, similarity 100%), *P. entomophagus* (partial 18S and partial ITS1, accession number MK156050, similarity 99%) and *Cruznema* sp. (partial 18S and partial ITS1, accession number MK156051, similarity 96–100%).

DISCUSSION

The results of this study indicate that all the examined giant African land snails lay eggs, larvae, and adult rhabditid nematodes in the feces, and may therefore represent a source of infection for other pets and humans. In order to avoid misidentification with *Strongyloides* sp., a nematode species showing close resemblance with rhabditids that has a clear parasitic zoonotic relevance (14, 15, 18), the initial morphological diagnosis of rhabditid nematodes was confirmed through molecular analyses.

Rhabditidae include free-living saprophytic nematodes, widely found in soil and organic debris where they feed mainly on bacteria. Many species of snails may serve as final definitive hosts for rhabditid nematodes (14, 15). However, a number of *Rhabditis* and *Rhabditella* species has been associated with vertebrates including humans (14, 15, 19–27). Although their presence can be the result of environmental contamination, these nematodes may cause diseases in many animals and humans. *Rhabditis elongata, Rh. hominis*, and *Rh. usuii* larvae have been isolated from human feces, urine and vaginal swabs (19–21). Nonetheless, not many cases of symptomatic infections have been reported in humans (21–24). Feng and Li (25) described two human cases of urinary infection by *R. axei* in China, and Ahn et al. (20) reported five human cases of intestinal infection with *Rhabditis* sp. in rural school children of South Korea. Similarly, two cases of human intestinal infection by *R. axei* were described in China (26), whereas another published work (21) reported a case of intestinal infection in a 5-month-old Brazilian child who was presented with fever and watery and bloody diarrhea; coprological examination revealed eggs, larvae and adults of *Rhabditis* sp. Meamar et al. (27) described the occurrence of watery diarrhea in two Iranian patients with AIDS, associated to severe intestinal infection by larvae and adult specimens of *R. axei*. Finally, Teschner et al. (24) recently described a case of outer ear canal infection in a 37 year-old man presented with purulent otorrhea from both ears and acute hearing loss caused by *Rhabditis* sp. In general, *Rhabditis* spp. are considered a common cause of external otitis in cattle living in tropical areas (*e.g.*, south America and Africa), particularly in older animals, and have been identified also in chickens, dogs and pigs with incoercible diarrhea (18, 28–30). However, asymptomatic infections have also been described and these nematodes are often considered pseudoparasites (28, 29).

Although free-living nematodes were retrieved in all fecal samples, no specimens were found in the mucus and histological samples. A possible explanation for this finding is that nematodes may locate in different tissues/organs of their hosts, depending on the type of association nematode/mollusk host (15, 31, 32). *Rhabditis* spp. complete its life cycle inside the snail, with no

damage to its molluscan host. Previous studies on the free-ranging African snails (*Archachatina* spp. and *Achatina* spp.) revealed that *R. axei* lives in the gastrointestinal tract of its snail host where the entire nematode life cycle is completed (31–33).

Although African giant snails are listed as hosts for *R. axei*, the occurrence of this nematode had been reported only in a few species of giant African snails other than *A. fulica*, namely *Archachatina marginata ovum, Ar. marginata saturalis,* and *Achatina achatina* (31). On the other hand, *P. entomophagus* has a worldwide distribution and has been mainly associated to dung beetles belonging to the superfamily Scarabaeoidea (34, 35), *R. terricola* has been found in salamanders (14, 15) and *Cruznema* spp. in the cricket *Gryllodes laplatae* (Orthoptera) (36). In all cases, transmission of the parasite occurs through the contact of the snails with contaminated moist soil that is rich in decomposing organic matter (31, 37). Although, in the present cases all the animals were kept in terraria with a heat-treated organic soil, we speculate that infection may have occurred before purchase of the animals at the pet shops or breeding facilities.

In conclusion, our results indicate that the pet giant African land snails may serve as reservoir of several rhabditid nematodes. This snail species is among the most commonly ones kept as pets, and therefore often live in close proximity to humans. As a result, the contamination of the domestic environment through their feces is possible. Although parasitic nematodes were not isolated in this study, the giant African land snails should still be considered potential carriers of nematodes able to cause opportunistic diseases in humans. Therefore, we highlight the importance of further epidemiological research on the occurrence of free-living and parasitic nematodes in gastropod snails kept in captivity, and emphasize the need for strict control measures to reduce the risk of opportunistic infection with rhabditid nematodes in pet snail owners.

AUTHOR CONTRIBUTIONS

Dd'O and MS conceived and planned the analysis. MS and JN carried out the analysis. CA helped shape the research and edited the manuscript. All authors provided critical feedback and contributed to the final manuscript.

REFERENCES

1. Zachariah T, Mitchell M. Invertebrates. In: Mitchell MA, Tully T, editors. *Manual of Exotic Pet Practice*. St. Louis, MO: Saunders Elsevier (2009). p. 11–38.
2. Ohlweiler FP, de Almeida Guimarães MC, Takahashi FY, Eduardo JM. Current distribution of *Achatina fulica*, in the state of São Paulo including records of *Aelurostrongylus abstrusus* (nematoda) larvae infestation. *Rev Inst Med Trop Sao Paulo.* (2010) 52:211–14. doi: 10.1590/S0036-46652010000400009
3. Raut SK, Baker GM. *Achatina fulica* Bowdich and other Achatinidae as pests in tropical agriculture. In: Baker GM, editor. *Molluscs as Crop Pests*. Wallingford: CAB International (2002). p. 55–114.
4. US Fish and Wildlife Service. *Giant African Snail* (*Achatina fulica*) (2015). Available online at: https://www.fws.gov/fisheries/ans/erss/highrisk/achatina-fulica-erss-june2015.pdf
5. Igbinosa IB, Isaac C, Ojagefu Adamu H, Adeleke G. Parasites of edible land snails in Edo State, Nigeria. *Helminthologia.* (2016) 53:331–5. doi: 10.1515/helmin-2016-0031
6. Vitta A, Polseela R, Nateeworanart S, Tattiyapong M. Survey of *Angiostrongylus cantonensis* in rat and giant African land snails in Phitsanulok province. *Asian Pac J Trop Med.* (2011) 4:597–9. doi: 10.1016/S1995-7645(11)60154-5
7. Alfaro-Alarcón A, Veneziano V, Galiero G, Cerrone A, Gutierrez N, Chinchilla A, et al. First report of a naturally patent infection of *Angiostrongylus costaricensis* in a dog. *Vet Parasitol.* (2015) 212:431–4. doi: 10.1016/j.vetpar.2015.08.016
8. Santoro M, Alfaro-Alarcón A, Veneziano V, Cerrone A, Latrofa MS, Otranto D, et al. The white-nosed coati (*Nasua narica*) is a naturally susceptible definitive host for the zoonotic nematode *Angiostrongylus costaricensis* in Costa Rica. *Vet. Parasitol.* (2016) 228:93–5. doi: 10.1016/j.vetpar.2016.08.017
9. Liboria M, Morales G, Carmen S, Isbelia S, Luz AP. First finding in Venezuela of *Schistosoma mansoni* eggs and other helminths of interest in public health found in faeces and mucous secretion of the mollusc *Achatina fulica* (Bowdich, 1822). *Zootecnia Trop.* (2010) 28:83–394.
10. Moreira VLC, Giese EG, Melo FTV, Simoes RO, Thiengo SC, Maldonado A, et al. Endemic angiostrongyliasis in the Brazilian Amazon: natural parasitism of *Agiostrongylus cantonensis* in *Rattus rattus* and *R. norvegicus*, and sympatric giant African land snail, *Achatina fulica*. *Acta Tropica.* (2013) 125:90–7. doi: 10.1016/j.actatropica.2012.10.001
11. Iwanowicz DD, Sanders LR, Schill WB, Xayavong MV, da Silva AJ, Qvarnstrom Y, et al. Spread of the rat lungworm (*Angiostrongylus cantonensis*) in giant African land snails (*Lissachatina fulica*) in FLorida, USA. *J Wildl Dis.* (2015) 51:749–53. doi: 10.7589/2014-06-160
12. Giannelli A, Colella V, Abramo F, do Nascimento Ramos RA, Falsone L, Brianti E, et al. Release of lungworm larvae from snails in the environment: potential for alternative transmission pathways. *PLoS Negl Trop Dis.* (2015) 9:e0003722. doi: 10.1371/journal.pntd.0003722
13. Gilbertson CR, Wyatt JD. Evaluation of euthanasia techniques for an invertebrate species, land snails (*Succinea putris*). *J Am Assoc Lab Anim Sci.* (2016) 55:577–81.
14. Andrassy I. *A Taxonomic Review of the Suborder Rhabditina* (Nematoda: Secernentia). Paris: ORSTOM (1983). p. 241.
15. Andrassy I. *Klasse Nematoda*. Berlin: Akademie Verlag (1984). p. 512.
16. Vrain TC, Wakarchuk DA, Levesque AC, Hamilton RI. Intraspecific rDNA restriction fragment length polymorphism in the *Xiphinema americanum* group. *Fundam Appl Nematol.* (1992) 15:563–73.
17. Ross JL, Ivanova ES, Spiridonov SE, Waeyenberge L, Moens M, Nicol GW, et al. Molecular phylogeny of slug-parasitic nematodes inferred from 18S rRNA gene sequences. *Mol Phylogenet Evol.* (2010) 55:738–43. doi: 10.1016/j.ympev.2010.01.026
18. Stachurska-Hagen T, Johnsen OH, Robertson LJ. Non-Strongyloides rhabditida identified in fecal samples – two case reports: lessons learned from morphological and molecular diagnostic approaches. *Parasitol Open.* (2016) 2:1–8. doi: 10.1017/pao.2016.11
19. Faust EC, Rusell PF, Jung RC. *Craig and Faust's Clinical Parasitology*. London: Kimpton (1970). p. 890.
20. Ahn YK, Chung PR, Lee KT. *Rhabditis* sp. infected cases in rural school children. *Kisaengchunghak Chapchi.* (1985) 23:1–6.
21. Campos DMB, Araújo JL, Vieira MCM, Damasceno F, Barbosa AP. A case of parasitism by *Rhabditis* sp. in a child from Goiânia, Goiás, Brazil. *Rev Soc Bras Med Trop.* (2002) 35:519–22. doi: 10.1590/S0037-86822002000500016
22. Eldridge B. Human urinary tract infection caused by *Rhabditis* sp. *PHLS Microbiol Digest.* (1993) 10:202–3.
23. He YX, Jiang H. Three human cases of urinary tract infection with *Rhabditis*. *Ji Sheng Chong Xue Yu Ji Sheng Chong Bing Za Zhi*. (1985) 3:206–8.
24. Teschner M, Würfel W, Sedlacek L, Suerba*um S, Tap*pe D, Hornef MW. Outer ear canal infection with *Rhabditis* sp. nematodes in a human. *J Clin Microbiol.* (2014) 52:1793–5.

25. Feng LC, Li, F. Two human cases of urinary tract infection with *Rhabditella axei*. *Peking Nat Hist Bull.* (1950) 18:195–202.
26. Ye LP, Zhu CG, Zhang JN. Two cases of *Rhaditis axei* infections in human digestive system. *Chin J Schistosomiasis Control.* (2002) 14:187.
27. Meamar AR, Kia EB, Zahabiun F, Jafari-Mehr A, Moghadam A, Sadjjadi SM. The occurrence of severe infections with *Rhabditis axei* in AIDS patients in Iran. *J Helminthol.* (2007) 81:351–2. doi: 10.1017/S0022149X07792301
28. Levine ND, Birch CL, Dolowy WC, McKinney RE. *Rhabditis axei*, a pseudoparasitic nematode of the dog. *J Am Vet Med Assoc.* (1963) 15:1404–6.
29. El-Azazy O, El-Gawady H, Nada, M. The occurrence of *Rhabditis* (*Rhabditella*) *axei* in the faeces of a chicken in Egypt. *J Helminthol.* (1988) 62:219–20.
30. Adewole SO, Fabumuy AO, Agunbiade RO, Ayeni, SK. Occurrence of *Rhabditis dubia* in cattle dungs in Lagos State, Nigeria. *J Environ Earth Sci.* (2014) 4:26–8.
31. Odaibo AB, Dehinbo AJ, Olofintoye LK, Falode OA. Occurrence and distribution of *Rhabditis axei* in African giant snails in southwestern Nigeria. *Helminthologia.* (2000) 37:233–5.
32. Grewal PS, Grewal SK, Tan L, Adams BJ. Parasitism of molluscs by nematodes: types of associations and evolutionary trends. *J Nematol.* (2003) 35:146–56.
33. Olofintoye LK, Olorunniyi OF. Intensity of *Rhabditis axei* at different parts of gastrointestinal tracts of *Archachatina marginata ovum* and *Achatina achatina*. *J Bio Innov.* (2016) 5:182–5.
34. Herrmann M, Mayer WE, Sommer RJ. Nematodes of the genus *Pristionchus* are closely associated with scarab beetles and theColorado potato beetle in Western Europe. *Zoology.* (2006) 109:96–108. doi: 10.1016/j.zool.2006.03.001
35. Kanzaki N, Ragsdale EJ, Herrmann M, Sommer RJ. Two new and two recharacterized species from a radiation of *Pristionchus.* (Nematoda: Diplogastridae) in Europe. *J Nematol.* (2014) 46:60–74.
36. Rebored GR, Camino NB. Two new species of nematodes (Rhabditida: Diplogasteridae and Rhabditidae) parasites of *Gryllodes laplatae.* (Orthoptera: Gryllidae) in Argentina. *Mem Inst Oswaldo Cruz.* (1998) 93:763–6.
37. Nguyen KB. Methodology, morphology and identification. In: Nguyen KB, Hunt DJ, editors. *Entomopathogenic Nematodes: Systematics, Phylogeny and Bacterial Symbionts. Nematology Monographs and Perspectives.* Leiden: Brill (2007). p. 59–119.

Conflict of Interest Statement: The authors declare that the research was conducted in the absence of any commercial or financial relationships that could be construed as a potential conflict of interest.

Copyright © 2019 d'Ovidio, Nermut, Adami and Santoro. This is an open-access article distributed under the terms of the Creative Commons Attribution License (CC BY). The use, distribution or reproduction in other forums is permitted, provided the original author(s) and the copyright owner(s) are credited and that the original publication in this journal is cited, in accordance with accepted academic practice. No use, distribution or reproduction is permitted which does not comply with these terms.

frontiers in Veterinary Science

ORIGINAL RESEARCH
published: 25 April 2019
doi: 10.3389/fvets.2019.00134

Diagnostic Performance of Clinicopathological Analytes in *Otostrongylus circumlitis*-Infected Rehabilitating Juvenile Northern Elephant Seals (*Mirounga angustirostris*)

Julie D. Sheldon [1]*, ***Jorge A. Hernandez*** [2], ***Shawn P. Johnson*** [3], ***Cara Field*** [3], ***Sarrah Kaye*** [4] ***and Nicole I. Stacy*** [5]

[1] *Illinois Zoological and Aquatic Animal Residency Program, Urbana, IL, United States,* [2] *Department of Large Animal Clinical Sciences, University of Florida College of Veterinary Medicine, Gainesville, FL, United States,* [3] *The Marine Mammal Center, Sausalito, CA, United States,* [4] *Staten Island Zoo, Staten Island, NY, United States,* [5] *Department of Comparative, Diagnostic, and Population Medicine, University of Florida College of Veterinary Medicine, Gainesville, FL, United States*

OPEN ACCESS

Edited by:
Ursula Siebert,
University of Veterinary Medicine Hanover, Germany

Reviewed by:
Adrian S. W. Tordiffe,
University of Pretoria, South Africa
Dean Konjevic,
University of Zagreb, Croatia
Nadine Lamberski,
Zoological Society of San Diego, United States

****Correspondence:***
Julie D. Sheldon
juliedsheldon@gmail.com

Specialty section:
This article was submitted to Zoological Medicine, a section of the journal Frontiers in Veterinary Science

Received: *12 November 2018*
Accepted: *09 April 2019*
Published: *25 April 2019*

Citation:
Sheldon JD, Hernandez JA, Johnson SP, Field C, Kaye S and Stacy NI (2019) Diagnostic Performance of Clinicopathological Analytes in Otostrongylus circumlitis-Infected Rehabilitating Juvenile Northern Elephant Seals (Mirounga angustirostris). Front. Vet. Sci. 6:134. doi: 10.3389/fvets.2019.00134

The nematode lungworm, *Otostrongylus circumlitis* (OC), is a significant cause of northern elephant seal (NES; *Mirounga angustirostris*) mortality at The Marine Mammal Center (TMMC, Sausalito, CA). The current lack of specific antemortem diagnostic tests for pre-patent OC infection in NES makes diagnosis, proper treatment, and assessment of efficacy of medications challenging. Severe inflammation and disseminated intravascular coagulation (DIC) develop rapidly and are difficult to treat once clinical signs develop. Certain blood inflammatory and hemostasis biomarkers for early diagnosis have recently been investigated. The objective of this study was to investigate the diagnostic performance of complete blood count, serum chemistry, acute phase proteins, protein electrophoresis, and coagulation parameters for diagnosis of OC clinical infection in NES. Samples from NES with OC infection confirmed by gross pathology with blood collected antemortem during clinical disease ($n = 9$) and NES initially admitted for malnutrition and sampled shortly before release after successful rehabilitation ($n = 20$) were included in the study. Using Receiver operator characteristic (ROC) curve analysis, the diagnostic performances (area under the curve [AUC]) of albumin (0.994), albumin:globulin ratio (0.983), serum amyloid A (0.972), activated partial thromboplastin time (0.936), total bilirubin (0.975), and gamma-glutamyl transferase (0.939) were high (AUC $>$ 0.9). These results confirm systemic inflammation and DIC, and support previously reported clinical and gross pathological findings in NES infected with

OC. In addition to AUC values, this study produced cut-off points, sensitivity, specificity, confidence intervals, and predictive values for analytes with high diagnostic performance. This data will be useful in the diagnosis and clinical management of OC-infected NES and will aid in assessment of treatment efficacy.

Keywords: clinical pathology, DIC, *Mirounga angustirostris*, Northern elephant seal, *Otostrongylus circumlitis*, ROC analysis

INTRODUCTION

The Northern elephant seal (*Mirounga angustirostris;* NES) is a phocid species inhabiting the California coast. Despite an increasing population at about 200,000 animals, this species was almost driven to extinction in the 19th century due to commercial hunting. As a result, this population underwent a bottleneck effect, decreasing the genetic diversity (1). About 150 juveniles are admitted each year to the Marine Mammal Center (TMMC) for rehabilitation due to malnutrition, trauma, human interaction, and infectious diseases (2).

Infections with the nematode lungworm, *Otostrongylus circumlitits* (OC), are responsible for 12% of NES strandings and 37% of NES mortality at TMMC (2). OC has an indirect lifecycle and a 3rd stage larvae in a fish intermediate host. Seals consume the fish and the ingested larvae migrate from the gastrointestinal tract to the liver, heart, and lungs. Once clinical signs become apparent, severe inflammation and disseminated intravascular coagulation (DIC) develop rapidly and are difficult to resolve therapeutically. Clinicopathological changes usually occur after or in concert with clinical signs (1). No antemortem diagnostic test currently exists as mortality occurs prior to ova being shed in the gastrointestinal tract, and no other pathogen identification tests have been successfully developed (1, 3).

Recent studies have evaluated the use of blood inflammatory markers, such as acute phase proteins, and hemostatic parameters, in guidance to early therapy (3, 4). However, definitive clinical diagnosis cannot be made until nematodes are grossly identified on necropsy (1, 2).

The objective of this study was to investigate the diagnostic performance of complete blood count, plasma chemistry, acute phase proteins, protein electrophoresis, and coagulation parameters for diagnosis of OC clinical infection in NES.

MATERIALS AND METHODS

The animals included in this study were retrospectively selected based on antemortem blood work and archived serum sample availability. Samples were collected in 2014–2015. The healthy group included blood samples obtained from 20 juvenile apparently healthy NES initially admitted to TMMC for malnutrition only and sampled within 3 days before release after successful rehabilitation. Animals were determined as healthy for release based on lack of historical abnormalities except for malnutrition upon admission and normal physical examination, in addition to absence of any derangements based on complete blood count (CBC) and serum chemistry. The OC-infected group included blood samples obtained from nine juvenile NES with OC infection as cause of death confirmed by gross pathology and available archived blood from antemortem collection during clinical disease.

Whole blood from all NES was previously collected antemortem under manual restraint from the extradural intervertebral sinus using a 20 Ga 1.5" needle on a Vacutainer set (Becton Dickinson, Franklin Lakes, NJ, USA) into EDTA, serum separator, and citrate tubes. The following tests were performed on all 29 samples: CBC (total leukocyte count, red blood cell count, hemoglobin concentration, hematocrit, platelet concentration, mean cell volume, mean cell hemoglobin, mean corpuscular hemoglobin concentration, red cell distribution width, mean platelet volume, and absolute differential counts for neutrophils, eosinophils, lymphocytes, monocytes, and basophils) and plasma biochemistry (gamma glutamyl transferase [GGT], alanine aminotransferase [ALT], aspartate aminotransferase [AST], alkaline phosphatase, creatine kinase, total bilirubin, glucose, phosphorus, blood urea nitrogen [BUN], creatinine, BUN:creatinine, calcium, sodium, potassium, chloride, total protein, albumin, globulin, and albumin:globulin [A:G] ratio) at TMMC, acute phase proteins serum amyloid A (SAA) and C-reactive protein (CRP) measured via immunoturbidimetric assays and protein electrophoresis (prealbumin, albumin, alpha1, alpha2, beta, and gamma globulins) at the University of Miami Avian and Wildlife Laboratory, and coagulation parameters (D-dimer, activated partial thromboplastin time [APTT], prothrombin time [PT], fibrinogen, antithrombin) at the Cornell University College of Veterinary Medicine via methods described in previous studies (3, 4).

Receiver operator characteristic (ROC) curve analysis was used to assess and compare diagnostic performance of all of the analytes listed above. Cut-off points, sensitivity (%), specificity (%), area under the curve (AUC), and 95% confidence intervals (CI) were also calculated for each analyte (MedCalc Statistical Software version 14.10.2; bvba, Ostend, Belgium; http://www.medcalc.org; 2014). Using ROC analysis, a perfect test (100% sensitivity and 0% false positives) has an AUC = 1, highly performing tests: $0.9 < \text{AUC} < 1$, moderately performing tests: $0.7 < \text{AUC} \leq 0.9$, low performing tests: $0.5 < \text{AUC} \leq 0.7$, and non-informative tests: AUC = 0.5 (5).

RESULTS

Several tests showed high diagnostic performance (AUC > 0.9) in the diagnosis of OC infection in NES. Fourteen analytes had an

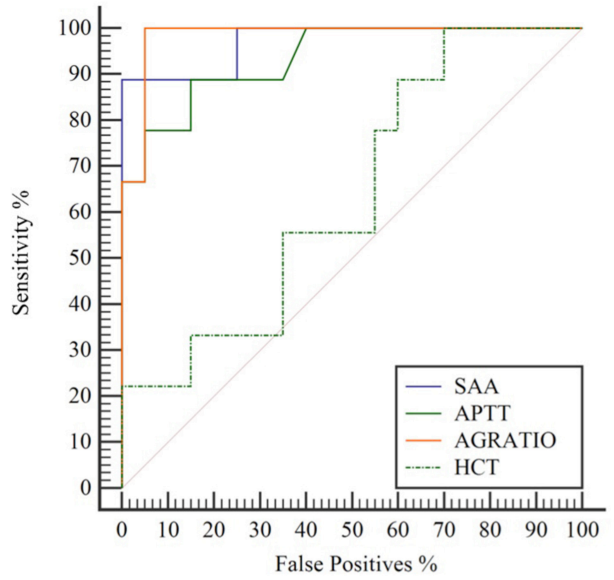

FIGURE 1 | Comparison of receiver operating characteristic (ROC) curves depicting highly accurate serum amyloid A (SAA; blue solid line), activated prothrombin time (APTT; green solid line), and albumin:globulin ratio (A:G ratio; orange solid line) in contrast to less accurate hematocrit (HCT; green dashed line) for diagnosis of *Otostrongylus circumlitis* clinical infections in Northern elephant seals (*Mirounga angustirostris*).

AUC > 0.9, and 14 had an AUC < 0.9 and >0.7. All 41 analytes evaluated had an AUC of > 0.52. A:G ratio (decreased), serum amyloid A (increased), and activated partial thromboplastin time (increased) were among the best performing analytes. Hematocrit, beta globulins, and BUN were among more poorly scoring analytes. **Figure 1** shows the ROC curve of 3 highly accurate analytes (SAA, APTT, and A:G ratio) compared to a less accurate analyte, HCT. Analyte cut-off points, sensitivity, specificity, and AUC in order of decreasing performance are listed in **Table 1**.

DISCUSSION

Diagnosis and treatment of OC infections in NES continue to pose challenges due to severity of clinical signs, difficulty of medically reversing DIC, and lack of diagnostic techniques to identify parasitic infection antemortem. This study offers new information about the diagnostic performance and cut-off points for a suite of clinicopathological analytes to aid in diagnosis, gauging disease severity, and monitoring the progress of clinical cases during rehabilitation. Treatment of suspected cases of OC in NES includes antibiotics, salicylic acid, ε-aminocaproic acid, and anti-inflammatory doses of corticosteroids. Traditionally, anthelminthic treatment has been avoided due to the risk of peracute death from rapid release of parasitic antigens (6). The pathophysiology of OC in NES resembles that of *Angiostrongylus vasorum* in dogs, which is helping to guide current investigations into appropriate anthelminthic treatment protocols in suspected OC cases at TMMC (7). However, current studies are investigating the use of anthelminthics as treatment in suspected cases of OC infected NES at the Marine Mammal Center.

Although several of the analytes performed well, they may not necessarily be specific to OC-infections given the complex sequelae of systemic inflammation and DIC. However, in using these readily available diagnostic tests collectively and in context of the identified cut-off points and clinical findings, blood analyte derangements can be used as efficient diagnostic and monitoring tools.

Among the best performing variables in this study are most inflammatory biomarkers, notably albumin, A:G ratio, SAA, and CRP, thus reflecting systemic inflammation, one of the major underlying pathophysiologic mechanisms in OC clinical cases. Both albumin and A:G ratio were decreased in OC-infected animals. Albumin is a negative acute-phase protein that is known to decrease in the presence of inflammation due to decreased hepatocyte production in response to interleukins 1 and 6 (8). Since globulins tend to increase in OC-infected animals, the A:G ratio will also drop with concurrently decreased albumin. The acute phase proteins SAA and CRP also performed well. Acute phase proteins are being utilized increasingly in wildlife species for early detection of inflammation since they have proven useful in identifying species-specific responses to inflammatory processes (9, 10). For example, they are used to characterize and monitor inflammation in several marine mammal species including manatees, dolphins, and harbor seals (11–14). One study found that SAA is significantly increased in pre-clinical and clinical OC-infected NES, while CRP protein only increased in clinical OC-infected NES; therefore, it is not surprising that SAA and CRP both performed well in this present study (3). The fact that acute phase proteins scored higher than any leukogram variables emphasizes the importance of monitoring early inflammatory markers outside of the leukogram.

The highest performing leukogram parameter was neutrophil concentration, followed by total white blood cell count and absolute band neutrophils. However, based on clinical experience at TMMC, NES generally do not show any overt leukogram changes until after clinical signs of OC-infection manifest, rendering these changes not clinically useful in early diagnosis as previously described in another study (3).

The clinical relevance of coagulopathies in OC-infected NES was supported by the well-performing analytes APTT and PT, both of which are typically prolonged in DIC. APTT measures the functionality of the surface-induced intrinsic and common pathways while PT measures that of the extrinsic and common pathways of the coagulation cascade (8). A previous study found that the OC-infected animals were hypocoagulable, mainly with prolonged APTT and PT (4). However, platelet concentration and antithrombin III did not perform as well in our study. Several OC-infected NES had platelet counts within the normal range and none suggested the animals were at risk of spontaneous hemorrhage based on coagulation physiology in domestic mammals (<30,000 cells/μL) (8).

Underlying hepatic impairment in OC-infected NES is demonstrated by the high diagnostic performance of bilirubin and liver enzymes. Increased total bilirubin in OC-infected

TABLE 1 | Cut-off points, sensitivity, specificity, area under the curve (AUC), and 95% confidence interval (CI) from highest to lowest AUC in the diagnosis of *Otostrongylus circumlitis* clinical infection in Northern elephant seals (*Mirounga angustirostris*).

Analyte	Cut-off point	Sensitivity %	Specificity %	AUC	95% CI
Calcium (mg/dl)	≤9.3	100	100	1	0.881, 1.000
Albumin (g/dl)	≤2.6	100	95	0.994	0.870, 1.000
Albumin:Globulin ratio	≤0.69	100	95	0.983	0.851, 1.000
Total bilirubin (mg/dl)	>0.7	88.9	95	0.975	0.837, 1.000
Serum amyloid A (mg/l)	>20.08	88.9	100	0.972	0.833, 1.000
Potassium (mmol/l)	≤4.5	88.9	95	0.967	0.824, 0.999
Gamma-glutamyl transferase (U/l)	>83	100	85	0.939	0.783, 0.994
Sodium (mmol/l)	≤144.5	88.9	90	0.939	0.783, 0.994
Activated partial thromboplastin time (sec)	>27	88.9	85	0.936	0.779, 0.993
Neutrophils (cells × $10^3/\mu l$)	>12.93	100	75	0.93	0.85, 1.00
White blood cell count (cells × $10^3/\mu l$)	>27.4	77.8	95	0.917	0.753, 0.986
Mean platelet volume (fl)	>9.2	88.9	95	0.914	0.749, 0.985
Band neutrophils (cellsx$10^3/\mu l$)	>1.33	88.9	100	0.91	0.76, 1.00
C-reactive protein (mg/l)	>9.04	88.9	100	0.906	0.738, 0.982
Prothrombin time (s)	>17.4	88.9	90	0.883	0.710, 0.972
Aspartate aminotransferase (U/l)	>66	88.9	90	0.878	0.703, 0.969
Alpha 2 globulins (g/dl)	>1.42	66.7	95	0.858	0.679, 0.959
Alanine aminotransferase (U/l)	>45	77.8	95	0.858	0.679, 0.959
Mean cell volume (fl)	≤179	88.9	75	0.853	0.672, 0.956
Fibrinogen (mg/dl)	≤98	77.8	100	0.839	0.656, 0.948
Alpha1 globulins (g/dl)	≤0.3	88.9	80	0.833	0.649, 0.945
Platelet count (cells × $10^3/\mu l$)	≤309	77.8	95	0.831	0.646, 0.943
Creatine kinase (U/l)	≤264	77.8	95	0.825	0.639, 0.940
Gamma globulins (g/dl)	>0.84	77.8	85	0.8	0.611, 0.924
Total protein (g/dl)	≤6	77.8	75	0.772	0.580, 0.906
Reticulocyte distribution width (%)	>5.7	100	70	0.767	0.573, 0.903
MCHC (g/dl)	>37.4	100	50	0.719	0.523, 0.869
Antithrombin III (%)	≤81	66.7	90	0.708	0.511, 0.861
Blood Urea Nitrogen:Creatinine ratio	≤100	88.9	50	0.681	0.482, 0.840
Glucose (mg/dl)	≤138	55.6	100	0.669	0.471, 0.832
Phosphorus (mg/dl)	>6.8	55.6	85	0.661	0.463, 0.825
Blood Urea Nitrogen (mg/dl)	≤28	66.6	75	0.656	0.457, 0.821
Hematocrit (%)	≤58.1	100	30	0.639	0.440, 0.808
Eosinophils (cells × $10^3/\mu l$)	≤0.00	77.8	50	0.63	0.42, 0.85
Basophils (cells × $10^3/\mu l$)	≤0.00	100	20	0.6	0.38, 0.81
Beta globulins (g/dl)	>10.7	33.3	95	0.572	0.376, 0.753
Pre-albumin (g/dl)	>0	44.4	65	0.533	0.340, 0.720
Hemoglobin (g/dl)	>21.2	66.7	55	0.522	0.330, 0.710
RBC count (cells × $10^6/\mu l$)	≤3.02	33.3	45	0.522	0.330, 0.710
Lymphocytes (cells × $10^3/\mu l$)	>2.50	66.7	0	0.52	0.24, 0.81
Monocytes (cells × $10^3/\mu l$)	≥0.38	55.6	70	0.52	0.25, 0.78

MCHC, mean corpuscular hemoglobin concentration; RBC, red blood cell.

NES could be due to decreased uptake and conjugation by hepatocytes resulting from anorexia and/or hypoxic liver damage, hepatitis/cholangitis from systemic inflammation, or extravascular hemolysis and consequent increased unconjugated bilirubin uptake (8). Increased liver enzyme activities have been described previously in OC-infected NES (1). GGT, AST, and ALT also performed well and support the conclusion of hepatocellular damage as a significant component of systemic disease. Since nematodes have not been found outside of the heart and pulmonary vasculature, these findings are presumably associated with systemic inflammation (1).

Several other analytes performed very well; although, these are generally non-specific for OC infection, are most consistent with sequelae of systemic inflammation, or reflect downstream effects of more clinically significant clinicopathological derangements. For example, calcium concentrations in OC-infected NES

ranged from 7.9–9.3 mg/dl and all healthy NES had calcium concentrations > 9.3 mg/dl. The degree of hypocalcemia in the study animals was not severe enough to cause clinical signs specific to hypocalcemia such as tremors/seizures. Hypocalcemia in these animals was likely due to decreased albumin since calcium is bound to albumin in circulation. Other possible causes of hypocalcemia include hypoparathyroidism, inadequate mobilization from bone or absorption in the intestine, or excess urinary excretion (8). Potassium and sodium both decreased in OC-infected NES and performed highly with AUCs of 0.967 and 0.939, respectively. While the magnitude of the changes were not clinically significant on their own they may reflect intra- and extracellular shifts due to loss in vomit, diarrhea, or renal excretion (8). The remaining analytes are less useful in diagnosing and monitoring disease progress of OC-infected NES but derangements thereof may be effects of severe systemic disease.

The number of highly performing analytes in this study was remarkable and highlights the severity of systemic effects of OC on NES. Results of this study support the presence of systemic inflammation and DIC in affected NES, and the previously reported pathological findings in NES infected with OC. It is presumed that NES is a relatively new host to OC and is unable to survive infection long enough for the nematodes to undergo a full lifecycle (15, 16). The data presented herein will be useful in clinical management and will aid in assessment of treatment efficacy in OC-infected NES. Acute phase proteins and coagulation parameters demonstrated superior diagnostic performance over CBC data, which emphasizes the importance of including SAA and CRP as part of the complete health evaluation in stranded NES and for early diagnosis of OC infection. Based on the results of this study and previous reports, in addition to clinical experience and anecdotal information, authors recommend that albumin, AG ratio, APTT, total bilirubin, and GGT are the most useful clinicopathological markers for the diagnosis of OC- NES. Until a definitive antemortem diagnostic test is developed, analyzing appropriate clinicopathological findings in context of all relevant clinical information is considered crucial for rapid implementation of therapy, monitoring during treatment, and assessing efficacy of various treatment modalities.

ETHICS STATEMENT

This study was carried out in accordance with the Stranding Agreement between the National Oceanic and Atmospheric Administration's National Marine Fisheries Service West Coast Region and the Marine Mammal Center approved for November 2013 through December 2015.

AUTHOR CONTRIBUTIONS

JS was responsible for primarily writing this manuscript, initial animal, and sample selection, and result interpretation. JH performed statistical analysis. SJ is veterinary director for the animals used in this study and oversaw veterinary care for them. CF is a clinical veterinarian for these animals, provided instrumental information regarding current treatment and monitoring of patients with this disease, and helped perform clinical exams and sample collections for this study. SK was responsible for performing all coagulation parameter tests and analysis. NS oversaw all aspects of the project and provided expertise in data analysis and interpretation. All coauthors played a significant role in the editing/reviewing of this paper.

ACKNOWLEDGMENTS

The authors thank the veterinary and husbandry volunteers and staff at TMMC for caring for the animals and collecting samples, the research staff at TMMC for organizing and shipping samples. The authors also thank Dr. Carolyn Cray and the University of Miami Avian and Wildlife Laboratory Team for performing protein assays. All events were performed under the Stranding Agreement between the National Oceanic and Atmospheric Administration's National Marine Fisheries Service West Coast Region and the Marine Mammal Center approved for November 2013 through December 2015.

REFERENCES

1. Gulland FM, Beckmen K, Burek K, Lowenstein L, Werner L, Spraker T, et al. Nematode (*Otostrongylus circumlitis*) infestation of Northern elephant seals (*Mirounga angustirostris*) stranded along the central California coast. *Mar Mamm Sci.* (1997) 13:446–59. doi: 10.1111/j.1748-7692.1997.tb00651.x
2. Colegrove KM, Greig DJ, Gulland FMD. Causes of live strandings of northern elephant seals (*Mirounga angustirostris*) and Pacific harbor seals (*Phoca vitulina*) along the central California coast, 1992–2001. *Aquat Mammal.* (2005) 31:1–10. doi: 10.1578/AM.31.1.2005.1
3. Sheldon JD, Johnson SP, Hernandez JA, Cray C, Stacy NI. Acute-phase responses in healthy, malnourished, and *Otostrongylus*-infected juvenile northern elephant seals (*Mirounga angustirostris*). *J Zoo Wildl Med.* (2017) 48:767–75. doi: 10.1638/2016-0267.1
4. Kaye S, Johnson S, Rios C, Fletcher DJ. Plasmatic coagulation and fibrinolysis in healthy and *Otostrongylus*-affected Northern elephant seals (*Mirounga angustirostris*). *Vet Clin Pathol.* (2017) 46:589–96. doi: 10.1111/vcp.12540
5. Greiner M, Pfeiffer D, Smith RD. Principles and practical application of the receiver-operating characteristic analysis for diagnostic tests. *Prev Vet Med.* (2000) 45, 23–41. doi: 10.1016/S0167-5877(00)00115-X
6. Kaye S, Johnson S, Arnold RD, Nie B, Davis JT, Gulland F, et al. Pharmacokinetic study of oral ε-aminocaproic acid in the northern elephant seal (*Mirounga angustirostris*). *J Zoo Wildl Med.* (2016) 47:438–46. doi: 10.1638/2015-0138.1
7. Sigrist NE, Hofer-Inteeworn N, Jud Schefer R, Kuemmerle-Fraune C, Schynder M, Kutter APN. Hyperfibrinolysis and hypofibrinogenemia diagnosed with rotational thromboelastometry in dogs naturally infected with *Angiostrongylus vasorum*. *J Vet Intern Med.* (2017) 31:1091–9. doi: 10.1111/jvim.14723
8. Stockham SL, Scott MA. *Fundamentals of Veterinary Clinical Pathology*. 2nd ed. Ames, IA: Blackwell Publishing (2008).
9. Bertelsen MF, Kjelgaard-Hansen M, Grøndahl C, Hegaard PMH, Jacobsen, S. Identification of acute phase proteins and assays applicable in nondomesticated mammals. *J Zoo Wildl Med.* (2009) 40:199–203. doi: 10.1638/2007-0125.1

10. Cray C. Acute phase proteins in animals. *Prog Mol Biol Transl Sci*. (2012) 105:113–50. doi: 10.1016/B978-0-12-394596-9.00005-6
11. Cray C, Rodriguez M, Dickey M, Brewer LB, Arheart KL. Assessment of serum amyloid A levels in the rehabilitation setting in the Florida manatee (*Trichechus manatus latirostris*). *J Zoo Wildl Med*. (2013b) 44:911–7. doi: 10.1638/2012-0270R.1
12. Funke C, King DP, Brotheridge RM, Adelung D, Stott JL. Harbor seal (Phoca vitulina) C-reactive protein (C-RP): purification, characterization of specific monoclonal antibodies and development of an immunoassay to measure serum C-RP concentrations. *Vet Immunol Immunopathol*. (1997) 59:151–62. 10.1016/S0165-2427(97)00059-7
13. Kakuschke A, Erbsloeh HB, Griesel S, Prange A. Acute phase protein haptoglobin in blood plasma samples of harbour seals (*Phoca vitulina*) of theWadden Sea and of the isle Helgoland. *Comp Biochem Physiol B Biochem Mol Biol*. (2010) 155:67–71. doi: 10.1016/j.cbpb.2009.10.002
14. Cray C, Arheart KL, Hunt M, Clauss T, Leppert LL, Roberts K, et al. Acute phase protein quantitation in serum samples from healthy Atlantic bottlenose dolphins (*Tursiops truncatus*). *J Vet Diagn Invest*. (2013a) 25:107–11. doi: 10.1177/1040638712467986
15. Toft CA, Karter AJ. Parasite-host coevolution. *Trends Ecol Evol*. (1990) 5:326–9.
16. Gerber JA, Roletto J, Morgan LE, Smith DM, Gage LJ. Findings in pinnipeds stranded along the central and northern California coast, 1984–1990. *J Wildl Dis*. (1993) 29:423–33.

Conflict of Interest Statement: The authors declare that the research was conducted in the absence of any commercial or financial relationships that could be construed as a potential conflict of interest.

The reviewer NL declared a past supervisory role with one of the author JS to the handling editor.

Copyright © 2019 Sheldon, Hernandez, Johnson, Field, Kaye and Stacy. This is an open-access article distributed under the terms of the Creative Commons Attribution License (CC BY). The use, distribution or reproduction in other forums is permitted, provided the original author(s) and the copyright owner(s) are credited and that the original publication in this journal is cited, in accordance with accepted academic practice. No use, distribution or reproduction is permitted which does not comply with these terms.

frontiers in Veterinary Science

ORIGINAL RESEARCH
published: 29 May 2019
doi: 10.3389/fvets.2019.00148

Trichomonas Infection in a Community of Free-Ranging Domestic and Wild Columbiformes and Bonelli's Eagle (*Aquila fasciata*)

Nuno Santos[1], José Jambas[2], António Monteiro[3], Jorge Amaral[3], Nuno Martins[4], Javier Garcia[5], Ana Martinez Fernández[6], Kevin Morris Tyler[7], Tereza Almeida[1,8], Joana Abrantes[1] and Pedro J. Esteves[1,8]*

[1] CIBIO/InBio—Research Center in Biodiversity and Genetic Resources, Universidade do Porto, Vairão, Portugal, [2] Oriolus Ambiente Ecoturismo Lda, Atenor, Portugal, [3] Parque Natural do Douro Internacional, Instituto de Conservação da Natureza e Florestas I.P., Mogadouro, Portugal, [4] Palombar—Associação para a Conservação da Natureza e do Património Rural, Uva, Portugal, [5] Department of Biodiversity and Environmental Management, University of León, León, Spain, [6] Servicio Territorial de Medio Ambiente, Junta de Castilla y León, Zamora, Spain, [7] Biomedical Research Centre, Norwich Medical School, University of East Anglia, Norwich, United Kingdom, [8] Departamento de Biologia, Faculdade de Ciências, Universidade do Porto, Porto, Portugal

OPEN ACCESS

Edited by:
Francesco Carlo Origgi, University of Bern, Switzerland

Reviewed by:
Bjørnar Ytrehus, Norwegian Institute for Nature Research (NINA), Norway
Nikolaus Huber, University of Veterinary Medicine, Austria

***Correspondence:**
Nuno Santos
nuno.santos@cibio.up.pt

Specialty section:
This article was submitted to Zoological Medicine, a section of the journal Frontiers in Veterinary Science

Received: *17 January 2019*
Accepted: *29 April 2019*
Published: *29 May 2019*

Citation:
Santos N, Jambas J, Monteiro A, Amaral J, Martins N, Garcia J, Fernández AM, Tyler KM, Almeida T, Abrantes J and Esteves PJ (2019) Trichomonas Infection in a Community of Free-Ranging Domestic and Wild Columbiformes and Bonelli's Eagle (Aquila fasciata). Front. Vet. Sci. 6:148. doi: 10.3389/fvets.2019.00148

Trichomonas gallinae is a pathogen of conservation relevance, whose main maintenance hosts are Columbiformes, but spillover to avian predators has been described. The goal of this study was to characterize the epidemiology of *Trichomonas* spp. in a community of free-ranging domestic and wild Columbiformes and an endangered predator, Bonelli's eagle *Aquila fasciata*. We surveyed 253 live-captured Rock doves, 16 nestling Bonelli's eagles and 41 hunted Columbiformes. Oro-esophageal swabs were incubated in culture media and *Trichomonas* spp. isolated from Bonelli's eagle (6.3%, CI_{95} 1.1-28.3), Turtle dove *Streptopelia turtur* (56.3%, CI_{95} 39.3–71.8), Wood pigeon *Columba palumbus* (83.3%, CI_{95} 43.7–97.0) and Rock dove *Columba livia* (68.4%, CI_{95} 62.4–73.8). Infected Rock doves showed significantly poorer body condition than uninfected ones ($p = 0.022$). From a subset of 32 isolates, 18S and ITS1/5.8S/ITS2 rRNA genes were sequenced and Maximum-Likelihood trees inferred. Four ribotypes of *Trichomonas* spp. were identified. In this study area *Trichomonas* spp. seem to persist in a multi-host system involving several species of Columbiformes. Conservation actions aimed at increasing the availability of trophic resources for Bonelli's eagles through Rock dove restocking should consider the risk of pathogen transmission and of introduction of alien strains.

Keywords: *Trichomonas gallinae*, Columbiformes, *Aquila fasciata*, *Streptopelia turtur*, *Columba livia*, multi-host-pathogen system, wildlife conservation

INTRODUCTION

Trichomonosis is an avian disease of conservation relevance, caused by infection with *Trichomonas gallinae* (1–3). Typical lesions in the upper digestive tract range from mild inflammation to caseous masses that can partially obstruct the digestive or respiratory tracts and progress to systemic disease (3). Trichomonosis can be present as subclinical to subacute, depending on the host species, immune status and the pathogenicity of the strain (1, 2, 4–8). Transmission can be direct, such as through "crop milk" or consumption of infected prey or indirect such as through contaminated water (3, 9–11).

Trichomonas gallinae is an important pathogen of Columbiformes, Falconiformes, and Passeriformes (3). It has been implicated in the decline of Band-tailed pigeons (*Patagioenas fasciata*) in western USA (2) and a highly pathogenic strain has recently emerged in North-Western Europe, causing population declines of finch species (3, 7, 12). Columbiformes are maintenance hosts for *T. gallinae* and the Rock dove (*Columba livia*) is considered the natural host of this pathogen (3). All species of Columbiformes occurring in Europe have been shown to harbor endemic *Trichomonas gallinae* infection (8, 13, 14). Particularly the Turtle dove (*Streptopelia turtur*) was shown to be heavily infected by *Trichomonas gallinae* (8, 15). European populations of Turtle doves heavily declined in the last decades and their migration routes pass through the Iberian Peninsula (16), with the potential of disseminating new strains. On the other hand, raptors are considered spillover hosts, acquiring infection from infected prey (3, 17).

Bonelli's eagle (*Aquila fasciata*) is a conservation priority species in Europe because of widespread declines in the last decades of the 20th century (18, 19). Most of the European population inhabits the Iberian Peninsula where its diet is based on Columbiformes, Red-legged partridge (*Alectoris rufa*) and Wild rabbit (*Oryctolagus cuniculus*) (20–22). Marginal populations of this species were shown to have low genetic variability (23), which could make them more vulnerable to emerging pathogens (24). Trichomonosis was shown to kill 2–14% of nestling Bonelli's eagles in several Iberian populations (25, 26). A marginal population of Bonelli's eagle comprising 22–24 pairs breeds in the *Douro Internacional/Arribes del Duero* natural parks and adjoining areas in northwestern Iberian Peninsula (19, 27, 28). This population is characterized by a low productivity, which has been linked to food shortage (28). Conservation management actions include supplementary feeding, either direct or through restocking of traditional pigeon lofts with Rock doves (27, 29).

Traditional pigeon lofts (TPL) are human constructions typical of Northwestern Iberian Peninsula (**Figure 1**), scattered across the landscape and originally aimed at producing Rock doves for human consumption and organic fertilizer for crops (30). These buildings provide nocturnal shelter and breeding sites for Rock doves, which are otherwise free-ranging (29, 30). Nowadays most TPL are abandoned but some have been recovered and restocked to increase prey availability for Bonelli's eagles (29).

The aim of this study was to investigate the epidemiology of *Trichomonas* spp. in the community of free-ranging domestic and wild Columbiformes and their endangered avian predator, Bonelli's eagle, in an area of Northwestern Iberian Peninsula. Additionally, we aimed to contribute to elucidating if restocking TPL with Rock doves could increase the exposure of Bonelli's eagles to infection by *Trichomonas* spp.

MATERIALS AND METHODS

Study Area

The study area consists of *Douro Internacional/Arribes del Duero* natural parks (comprising 193,000 hectares) and adjoining areas in Northwestern Iberian Peninsula (centroid 41° 11′ 36′ ′ N, 6° 45′ 49′′ W), encompassing both Portuguese and Spanish territory (**Figure 2A**). The area is an extensive plateau (600–800 m asl) where Douro river and several main tributaries (Águeda, Sabor, Côa, Tormes, and Huebra rivers) carved steep canyons in granite or shale rock. The landscape is highly fragmented, with oak (*Quercus pyrenaica*, *Q. faginea*, *Q. rotundifolia,* and *Q. suber*) and juniper (*Juniperus oxycedrus*) woods interspersed with shrub (mainly *Cytisus* sp. and *Cistus* sp.) and agricultural areas (mainly wheat *Triticum* sp., olive *Olea europaea*, vine *Vitis vinifera,* and pasture). The area is included in the Mesomediterranean and Supramediterranean bioclimatic zones showing Mediterranean-Subcontinental climate with large thermal amplitude, hot and dry summers and relatively cool and humid winters (31, 32).

Sample and Data Collection

From August 2008 to October 2009 we surveyed *Trichomonas* spp. in 253 live-captured Rock doves and 41 hunted Columbiformes, comprising 32 Turtle doves, 6 Wood pigeons (*Columba palumbus*) and 3 Rock doves. Rock doves were live-captured on 24 TPL (**Figure 2A**) by closing the exits during the night and manually capturing them inside. To prevent repeated sampling of individuals, each TPL was sampled only once and Rock doves were kept in cages and released when all were sampled (<2 h of restraint). Samples from wild Columbiformes were obtained from animals hunted for recreational purposes, according to Portuguese and European legislation. No animals were killed for the purpose of this study. This study was carried out in accordance with national and European legislation and the recommendations of the "Guidelines on the care and use of wildlife" (33).

From May 2014 to June 2016 we surveyed *Trichomonas* spp. in 16 nestling Bonelli's eagles, sampled during regular monitoring for ringing (**Figure 2A**). Samples were obtained under permits 412/2014 and 316/2016 (*Junta de Castilla y León*, Spain) and 415/2014 (*Instituto de Conservação da Natureza e Florestas*, Portugal).

An oro-esophageal swab was obtained from each bird, immediately inoculated in InPouch™ media (Biomed Diagnostics Inc., White City, OR, USA) and kept at room temperature and away from sunlight until incubation (7–50 h post collection). From individual Rock doves, we collected data on sex, age class, weight, wing length, and plumage (wild-type or other). The residuals of a linear regression between log weight and log wing length of each Rock dove were used as indicators of body condition. The presence of macroscopic lesions compatible with trichomonosis was systematically investigated in the Bonelli's eagle nestlings but not in the Columbiformes.

Data were collected on each TPL during the sampling procedure and included geographical location, number of Rock doves, presence of other avian species, provision of water, location within occupied Bonelli's eagle territories (<3 km straight line from the center of a territory occupied by a pair during the previous breeding season) and the interval between collection and incubation of the biological samples.

FIGURE 1 | Images of traditional pigeon lofts. **(A)** Landscape view; **(B)** outside view; **(C)** inside with Rock doves *Columba livia*.

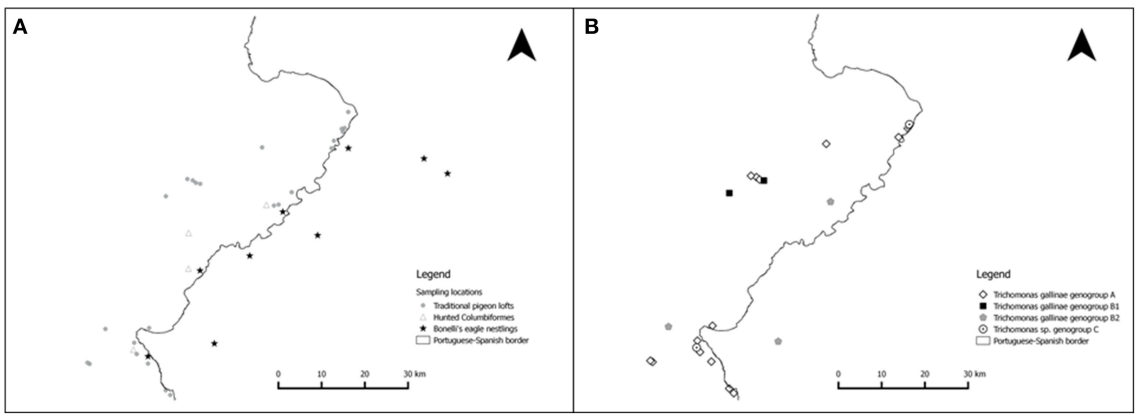

FIGURE 2 | Location of the sample collection sites and of the *Trichomonas* sp. genogroups isolated. **(A)** Sampled traditional pigeon lofts (circles), wild Columbiformes (triangles), and Bonelli's eagle nests (stars). Due to the threatened status of Bonelli's eagles and their sensitivity to disturbance, the location of the sampling sites for this species is not exact. **(B)** Geographical sampling location of the *Trichomonas* sp. genogroups identified in the study area.

Laboratory Analysis

Culture media were incubated at 37°C for 6 days and isolation of *Trichomonas* spp. was assessed by daily bright field microscopy at 100x magnification and considered positive when motile, flagellated protozoans were present in the culture media. Media containing *Trichomonas* were centrifuged at 1,430 × g for 10 min, the supernatant discarded, and the pellet re-suspended in PBS and stored at −20°C. DNA was extracted from a subset of 32 *Trichomonas* isolates, 1–2 per host species and TPL studied, with DNeasy Blood & Tissue Kit (Qiagen) and purified with Exo-AP Clean-up (Thermo Scientific), according to the manufacturer's instructions. For amplification of the 18S and ITS1/5.8S/ITS2 rRNA genes, previously established primers HM-LONG-F [5' AGGAAGCACACTATGGTCATAG 3'; (34)] and TFR1 [5' TGCTTCAGTTCAGCGGGTCTTCC 3'; (35)] were used. PCR amplification was performed with a PCR Master Mix (Phusion). Cycling parameters consisted of an initial denaturation at 98°C for 3 min, followed by 45 cycles of 98°C for 30 s, 61°C for 30 s and 72°C for 1 min, and 72°C for 5 min for the final extension step. products were purified and sequenced on an automatic sequencer PRISM 310 Genetic Analyzer (PE Applied Biosystems, Foster City, CA, USA) with the amplification primers and internal primer HM-LONG-R [5' CGTTACCTTGTTACGACTTCTCCTT 3'; (34)]. The sequences were deposited in GenBank under the following accession numbers: MK932769-773, MK932775-777. The ribotype nomenclature proposed by Gerhold et al. (36) and Grabensteiner et al. (37) is used throughout this paper.

Statistical Analysis

Differences in prevalence between TPL were analyzed by non-parametric methods (Kruskal-Wallis test). We performed a binomial GLM with *Trichomonas* spp. infection status in individual Rock doves as dependent variable and individual traits (age class, sex, body condition, and plumage type) as independent variables (**Table 1**). We performed another GLM with *Trichomonas* spp. prevalence in TPL as dependent variable and environmental and sampling features as independent variables (number of Rock doves, presence of other avian species and water availability inside the TPL, location within an occupied Bonelli's eagle territory, and interval from collection of samples to start of incubation) (**Table 1**). We considered all TPL <3 km straight distance from an occupied nest as being located within an occupied territory, based on the home ranges of breeding Bonelli's eagles in the Iberian Peninsula (38, 39). Collinearity was checked by calculating the Variance Inflation Factor with a threshold of 4 and goodness of fit assessed by calculating the Hosmer-Lemeshow χ^2. Statistical analyses were performed in R-3.3.2 (R Development Core Team). Maps were produced in QGIS 2.18.0 (QGIS Development Team). Maximum-Likelihood

TABLE 1 | Summary of the independent variables included in the statistical analysis.

Sampling unit	Independent variable	Type	*n*	Average (SD)	Categories
Rock dove	Age class	Categorical			125 adults 55 juveniles 73 n.a.
	Sex	Categorical			62 females 75 males 116 n.a.
	Weight	Continuous	126	309.9 g (69.4)	
	Wing length	Continuous	127	221.9 mm (14.8)	
	Plumage class	Categorical			41 wild-type 93 other 119 n.a.
	Interval from collection to incubation	Continuous	24	27.2 h (12.8)	
Traditional pigeon loft	Number of rock doves	Count	24	51.9 (34.4)	
	Other avian species	Categorical	24		17 no other species 7 other species[a]
	Provision of water	Categorical	24		12 yes 12 no
	Within occupied Bonelli's eagle territory (<3 km from the nest site)	Categorical	24		10 within 14 outside
	Interval from collection to incubation	Continuous	24	27.2 h (12.8)	

[a] *Sturnus unicolor, Tyto alba.*
n.a., not available.

(ML) trees were inferred for the ITS1/5.8S/ITS2 and 18S rRNA regions (**Table 2**) in MEGA6 (40) under the best-fit nucleotide substitution model determined by the same software. Node support was determined from 500 bootstrap replicates of the ML trees.

RESULTS

Descriptive Epidemiology

Trichomonas spp. were isolated from 1/16 (6.3%, CI_{95} 1.1–28.3) nestling Bonelli's eagles, 18/32 Turtle doves (56.3%, CI_{95} 39.3–71.8, $n = 32$), 5/6 Wood pigeons (83.3%, CI_{95} 43.7–97.0), and 175/256 Rock doves (68.4%, CI_{95} 62.4–73.8) (**Figure 3A**). Prevalence of *Trichomonas* spp. in TPL ranged 14.3–100% (**Figure 3B**), showing statistically significant differences between TPL ($p < 0.001$, Kruskal-Wallis test).

Determinants of Infection

In the binomial GLM with *Trichomonas* spp. isolation in individual Rock doves as dependent variable (Hosmer-Lemeshow $\chi^2 = 6.445$, $p = 0.598$), the only significant determinant of infection was the body condition, which was significantly lower ($p = 0.021$) in infected Rock doves (**Table 3** and **Figure 3C**). In the GLM with *Trichomonas* spp. prevalence in TPL as dependent variable (Hosmer-Lemeshow $\chi^2 = -1.2273$, $p = 1$), no significant determinants of prevalence of infection were identified (**Table 3**).

Molecular Epidemiology

Three ribotypes of *Trichomonas gallinae* and one ribotype of *Trichomonas* sp. were obtained from the 32 isolates that were sequenced (**Table 4** and **Figure 4**). *Trichomonas gallinae* ribotype 18S-VI, ITS-IV/B ($n = 23$) was distributed in TPL throughout the study area, while *T. gallinae* ribotype 18S-IV, ITS-I/D ($n = 3$) was detected in 2 TPL recently restocked with Rock doves acquired from a mixed-species avian collection. Both were only detected in Rock doves. *Trichomonas gallinae* ribotype 18S-II, ITS-I/D ($n = 4$) was detected in Rock doves from 2 TPL, 1 Wood pigeon and 1 nestling Bonelli's eagle, throughout the study area. Ribotype 18S-VIII, ITS-III of *Trichomonas* sp. ($n = 3$) was detected in 2 Rock doves from a single TPL and in 1 hunted Turtle dove in the northern and southern parts of the study area, respectively (**Table 4** and **Figure 2B**).

DISCUSSION

This study reports the epidemiology of *Trichomonas* spp. infection in the community of maintenance hosts for this pathogen and apparent spillover to an endangered avian predator. These results suggest that at least the *Trichomonas gallinae* ribotype 18S-II, ITS-227 I/D ($n = 4$), and ribotype 18S-VIII, ITS-III of *Trichomonas* sp. are maintained in the study area by a multi-host-pathogen system (41), where infection is likely transmitted between several species of free-ranging domestic and wild Columbiformes, as also documented in the United Kingdom (13). The inter-species transmission of *Trichomonas* spp. is supported by the high prevalence of infection in all studied Columbiformes species and particularly by the isolation of two genogroups in multiple species of Columbiformes.

Four distinct ribotypes of *Trichomonas* were detected in Rock doves, two of which are presumed to naturally occur in the study area (*T. gallinae* ribotypes 18S-VI, ITS-IV/B and 18S-II, ITS-I/D), as they were previously reported in this host species elsewhere in Europe (42). On the other hand, *T. gallinae* ribotype 18S-IV, ITS-I/D was previously reported only in Eurasian collared doves (36, 37), this being to our knowledge the first report of its isolation from Rock doves. *Trichomonas gallinae* ribotype 18S-IV, ITS-I/D was detected in the present study in two TPL recently restocked with Rock doves acquired in a mixed species collection. This observation highlights the risk of introducing new pathogen strains in local host communities by means of translocations for conservation purposes (43, 44). Here we report the first isolation in European wild Columbiformes of *Trichomonas* sp. ribotype 18S-VIII, ITS-III. This genogroup was previously detected in Europe only in 2007, in a domestic Rock dove in Austria (37).

TABLE 2 | GenBank entries used in the phylogeny of the ITS1/5.8S/ITS2 and 18S rRNA regions.

Species	Host	Origin	ITS1/5.8S/ITS2	18S rRNA
Trichomonas sp.	Pied imperial-pigeon *Ducula bicolor*	Australia	JQ755285	JQ027618
Trichomonas sp.	Chestnut-quilled Rock-pigeon *Petrophassa rufipennis*	Australia	JQ755286	JX512966
Trichomonas sp.	Racing pigeon *Columba livia*	Austria	FN433473	FN433486
Trichomonas sp.	Pied imperial-pigeon *Ducula bicolor*	Australia	JQ027616	JQ027618
Trichomonas sp.	Southern crowned pigeon *Goura scheepmakeri*	Papua New Guinea	JX512967	JX512959
Trichomonas sp.	New Zealand pigeon *Hemiphaga novaeseelandiae*	New Zealand	JQ692126	n/a
Trichomonas sp.	New Zealand pigeon *Hemiphaga novaeseelandiae*	New Zealand	JQ692128	JQ692127
Trichomonas sp.	Pheasant pigeon *Otidiphaps nobilis*	Papua New Guinea	JX512969	JX512961
Trichomonas sp.	Turtle Dove *Streptopelia turtur*	Spain	KX459488	n/a
Trichomonas sp.	Turtle Dove *Streptopelia turtur*	Italy	KX459509	n/a
Trichomonas canistomae	Dog	Czech Republic	AY244652	AY247748
Trichomonas gallinae	Broad-winged hawk *Buteo platypterus*	USA	EU215368	EU215375
Trichomonas gallinae	Budgerigar *Melopsittacus undulatus*	Austria	FN433476	FN433484
Trichomonas gallinae	Wood Pigeon *Columba oenas*	Germany	KX459442	n/a
Trichomonas gallinae	Rock Dove *Columba livia*	USA	EU215364	EU215373
Trichomonas gallinae	Eurasian collared-dove *Streptopelia decaocto*	USA	EU215364	EU215374
Trichomonas gallinae	Rock Dove *Columba livia*	Austria	FN433475	FN433480
Trichomonas gallinae	Eurasian collared-dove *Streptopelia decaocto*	Austria	FN433475	FN433482
Trichomonas sp.	Common bronzewing *Phaps chalcoptera*	Australia	JQ755275	JQ030999
Trichomonas gallinae	Turtle Dove *Streptopelia turtur*	Malta	KX844988	n/a
Trichomonas tenax	Human	USA	TTU86615	D49495
Trichomonas vaginalis	Human	USA	L29561	TVU17510
Trichomonas sp.	Rose-crowned fruit-dove *Ptilinopus regina*	Australia	JQ755274	JX512962
Trichomonas sp.	Ornate fruit-dove *Ptilinopus ornatus*	Australia	JX512968	JX512960
Tetratrichomonas sp.	Snapping turtle *Macrochelys temminckii*	Czech Republic	AY245133	AY245121
Pentatrichomonas hominis	Human	Slovakia	AY245137	AF124609

Interestingly the most common and widespread *T. gallinae* ribotype 18S-VI, ITS-IV/B was only detected in Rock doves, while the less common *T. gallinae* ribotype 18S-II, ITS-I/D was also detected in Wood pigeon and Bonelli's eagle. Whether this corresponds to a greater ability of the latter for spillover to other host species is still to be determined. Differential inter-species

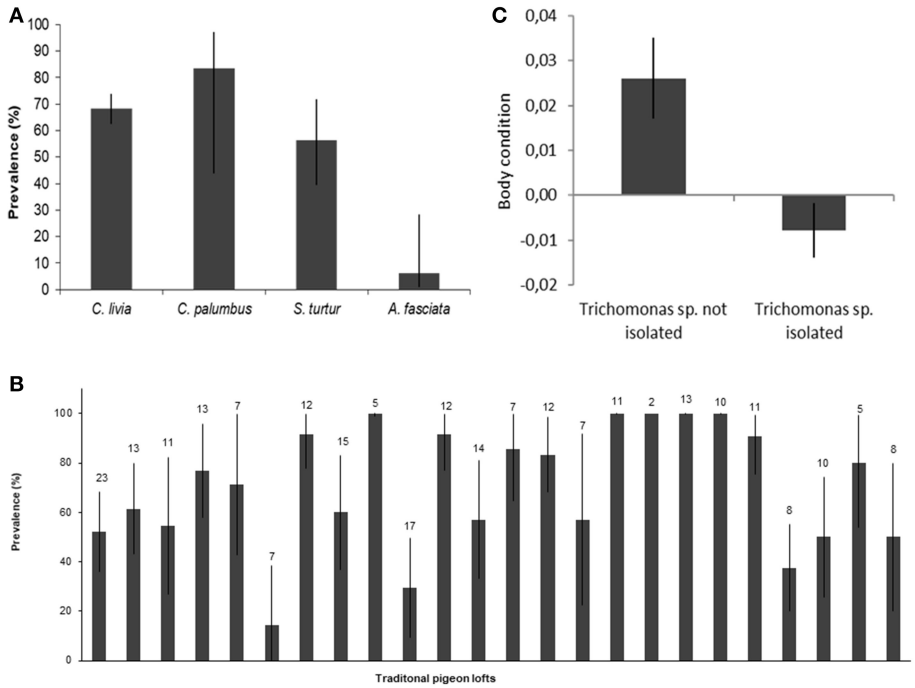

FIGURE 3 | Determinants of *Trichomonas* sp. infection**.** *Trichomonas* sp. prevalence with 95% confidence intervals by **(A)** species; **(B)** traditional pigeon loft, with the sample size for each TPL; **(C)** Rock dove body condition by *Trichomonas* sp. infection status, with standard error of the mean.

TABLE 3 | Results of the generalized linear models. Analysis of the potential determinants of *Trichomonas* sp. isolation in individual Rock doves and of prevalence in traditional pigeon lofts.

Dependent variable	Independent variable	Estimate	Statistic	*p*
Trichomonas sp. isolation in individual Rock doves (binomial)	Intercept	2.081	2.625	0.009
	Age class (juveniles)	−0.609	−0.703	0.482
	Sex (male)	−0.509	−0.818	0.413
	Body condition	−11.994	−2.304	0.021
	Interval collection to incubation	−0.020	−0.913	0.361
Trichomonas sp. prevalence in traditional pigeon lofts (proportion)	Intercept	100.068	5.923	< 0.001
	Number of Rock doves	−0.025	−0.142	0.888
	Other avian species	13.017	1.204	0.244
	Provision of water	−11.801	−1.027	0.318
	Within occupied Bonelli's eagle territory	−4.616	−0.457	0.653
	Interval from collection to incubation	−0.896	−1.906	0.073

transmission rates have been suggested for other *T. gallinae* genogroups, as well as differential pathogenicity (7, 15). As we only sequenced the 18S and ITS1/5.8S/ITS2 rRNA genes, more genetic diversity could have gone unnoticed in our sample of *Trichomonas* isolates. Furthermore, the opportunistic sampling performed in Bonelli's eagle, due to constraints in accessing nests of this endangered species, means there is no temporal overlap between samples collected from this species and those from Columbiformes.

Trichomonosis can be an important cause of mortality for nestling Bonelli's eagles; nevertheless, subclinical infections are more common than clinical ones (25, 26). In the present investigation only one nestling was shown to harbor *Trichomonas gallinae*, but no lesions were detected during handling in the nest and it survived to fledging. We could not isolate *Trichomonas* from two other nestlings with compatible lesions (oropharyngeal caseous masses), which could be due to a different etiology or a long interval between collection of samples and incubation.

TABLE 4 | Ribotypes of *Trichomonas* sp. identified in our sample based on ITS1/5.8S/ITS2 and 18S RNA sequences. Number of the isolates per species and traditional pigeon lofts (TPL). Ribotype nomenclature follows Gerhold et al. (36) and Grabensteiner et al. (37).

Ribotype	Host species	Number of isolates sequenced	Number of TPL	Representative isolates
18S-VI, ITS-IV/B	*C. livia*	22	14	*C. livia*/Portugal/115/*T. gallinae*
18S-IV, ITS-I/D	*C. livia*	3	2	*C. livia*/Portugal/290/*T. gallinae*
				C.livia/Portugal/278/*T. gallinae*
18S-II, ITS-I/D	*C. livia*	2	2	*C. livia*/Portugal/113/*T. gallinae*
	C. palumbus	1		
	A. fasciata	1		
18S-VIII, ITS-III	*C. livia*	2	1	*S. turtur*/Portugal/303/*Trichomonas* sp.
	S. turtur	1		

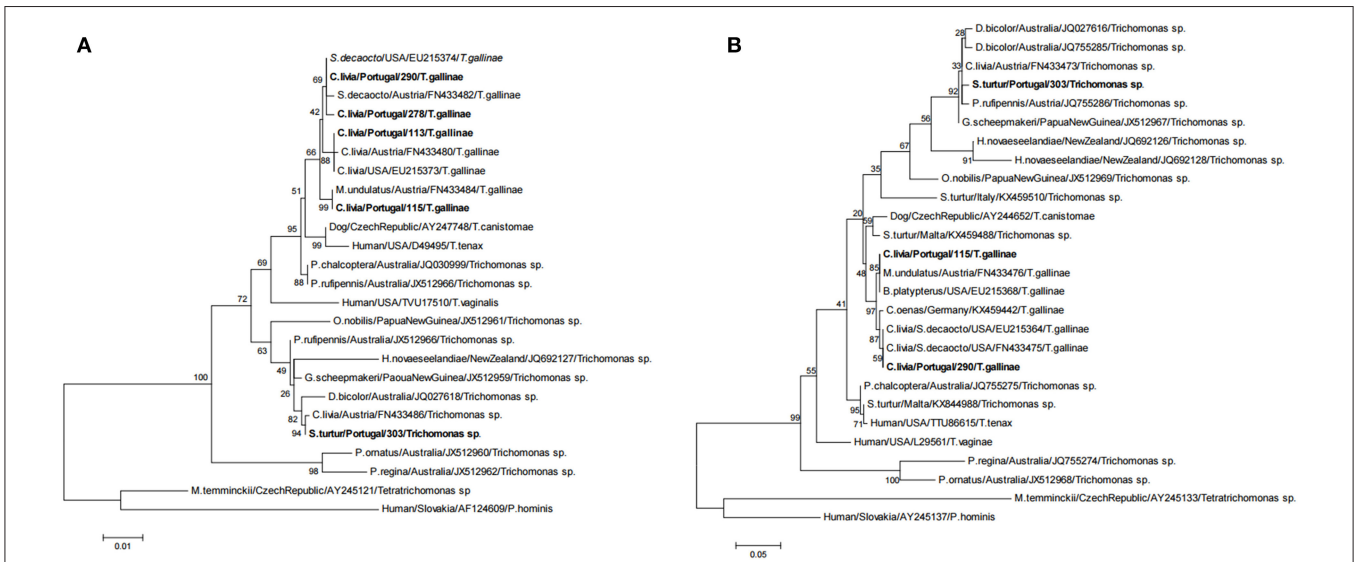

FIGURE 4 | Phylogenetic tree of the *Trichomonas* isolates based on **(A)** 18S rRNA (1155bp) and **(B)** ITS1/5.8S/ITS2 (347bp). The phylogenetic analyses were estimated using the Maximum Likelihood (ML) method available in MEGA6 (40) under the best-fit nucleotide substitution model determined by the same software. Node support was determined from 500 bootstrap replicates of the ML trees. GenBank accession numbers of the retrieved sequences are indicated.

Hernández et al. (27) also estimated a low prevalence in this same population (10%). Nevertheless, the low sample size precludes drawing conclusions on the pathogenicity and potential impact of infection by *Trichomonas gallinae* on this Bonelli's eagle population.

Comparable studies in other populations of Bonelli's eagle report higher prevalence in nestlings, which could be due to the low sample size or to the relatively long interval between collection of the samples and incubation in our study. *Trichomonas gallinae* was isolated from 36 to 68.8% of nestlings in 3 populations from Southern Iberian Peninsula (5, 25, 26), where Columbiformes are 28.5–39.2% of the prey items of Bonelli's eagles (20, 45). In our study population, Columbiformes are 20.6% of the diet of this species, with a preponderance of Rock doves over Wood pigeons (27). Given the high prevalence of infection by *Trichomonas gallinae* in all species of domestic and wild Columbiformes and the importance of these prey on the diet of Bonelli's eagles across its Iberian range, most if not all nestlings should be exposed to *Trichomonas* sp. (26). The variable prevalence of infection in nestlings from different populations could be explained by individual, regional and temporal heterogeneities in the pathogenicity of *Trichomonas gallinae* strains present in the local population of Columbiformes or the immune status of Bonelli's eagle nestlings. Marginal Iberian populations of Bonelli's eagle were shown to have low genetic diversity (23), which could impair their immune response (24). Further large-scale studies on this predator-parasite-prey system, addressing the link between diet and *Trichomonas gallinae* prevalence, are needed to elucidate the reasons for this heterogeneity in prevalence between populations of Bonelli's eagles.

One of the drivers of this study was the concern that restocking TPL with Rock doves would increase the exposure of Bonelli's eagles to *Trichomonas gallinae* (46). While this could occur if the consumption of Rock doves increases in response to this conservation action, we show that *Trichomonas* spp. infection is widespread in the wild Columbiformes community. The single case of infection in a Bonelli's eagle nestling took place in a territory where no TPL restocking was carried out. Nevertheless, emerging *Trichomonas* spp. strains might

be amplified in TPL, providing opportunity for spillover to Bonelli's eagles. Systematic disease surveillance in TPL should be implemented to detect the potential introduction of new strains and contingency plans prepared to prevent spillover to endangered avian predators.

Turtle doves in our sample showed lower prevalence than those reported elsewhere in Europe [67–100% - (8, 13–15)]. European populations of this species have undergone a sustained decline in the last decades, and trichomonosis has been suggested as contributing for this decline (8, 15, 16). The prevalence we determined in other species are comparable to those reported in the literature: 34–70% in Wood pigeon throughout Europe (8, 13, 14, 47) and 45–79% in Rock doves in Spain (5, 14).

Interestingly we observed that Rock doves from which *Trichomonas* spp. were isolated showed poorer body condition. It was shown in other host-pathogen systems that the physiological costs of immune system activation to fight infection trade-off with other physiological needs, such as reproduction, foraging and growth (48, 49). In our sample this translated into a lower body condition of infected Rock doves, as previously shown to occur in other free-ranging Columbiformes infected with *T. gallinae* (15, 47). The lower body condition of infected Rock doves could heighten the risk of predation, potentiating interspecies transmission, but being located within a Bonelli's eagle territory was not found to be a risk factor for prevalence in TPL. Studies including the whole community of avian predators of Rock doves are needed to address this question.

Trichomonas spp. seem to persist in the study area in a multi-host ecosystem, where intra- and inter-species transmission likely contribute to maintenance, making it demanding to individualize the role of each host species in the epidemiology of infection (41). More detailed molecular epidemiology tools have the potential to further contribute to unveiling the dynamics of pathogen transmission in this host community. Long-term studies will allow uncovering the origin of infection for avian predators such as the Bonelli's eagle, potentially highlighting ways to control spillover to this endangered species. Meanwhile, conservation actions aimed at increasing the availability of trophic resources for Bonelli's eagles should consider the potential risk of increased disease transmission and minimize the risk of introducing alien *Trichomonas* spp. strains.

ETHICS STATEMENT

This study was carried out in accordance with the recommendations of guidelines on the care and use of wildlife (33), Portuguese and European legislations. The study was conducted under permits 412/2014 and 316/2016 (Junta de Castilla y León, Spain) and 415/2014 (Instituto de Conservação da Natureza e Florestas, Portugal).

AUTHOR CONTRIBUTIONS

NS, JJ, AM, JG, JrA, and PE designed the study. NS, JJ, AM, JrA, NM, JG, AF, and TA performed the field and laboratory work. NS, TA, KT, JnA, and PE analyzed data and wrote the manuscript. All authors reviewed the manuscript upon submission.

FUNDING

This study was financed by the authors' institutions.

ACKNOWLEDGMENTS

We acknowledge the collaboration of *Parque Natural de los Arribes del Duero* (Spain), *Parque Natural do Douro Internacional*, *Associação Transumância e Natureza* and *Palombar* (Portugal), as well as the owners of pigeon lofts and hunters for allowing collecting samples and the volunteers who helped with sample collection. FCT supported the post-doctoral fellowship of NS (SFRH/BPD/116596/2016).

REFERENCES

1. Bunbury N, Jones CG, Greenwood AG, Bell DJ. Epidemiology and conservation implications of *Trichomonas gallinae* infection in the endangered Mauritian pink pigeon. *Biol Conserv*. (2008) 141:153–61. doi: 10.1016/j.biocon.2007.09.008
2. Robinson RA, Lawson B, Toms MP, Peck KM, Kirkwood JK, Chantrey J, et al. Emerging infectious disease leads to rapid population declines of common British birds. *PLoS ONE*. (2010) 5:e12215. doi: 10.1371/journal.pone.0012215
3. Amin A, Bilic I, Liebhart D, Hess M. Trichomonads in birds – a review. *Parasitology*. (2014) 141:733–47. doi: 10.1017/S0031182013002096
4. Höfle U, Gortázar C, Ortíz JA, Knispel B, Kaleta EF. Outbreak of trichomoniasis in a woodpigeon (*Columba palumbus*) wintering roost. *Eur J Wildl Res*. (2004) 50:73–7. doi: 10.1007/s10344-004-0043-2
5. Sansano-Maestre J, Garijo-Toledo MM, Gómez-Muñoz MT. Prevalence and genotyping of *Trichomonas gallinae* in pigeons and birds of prey. *Avian Pathol*. (2009) 38:201–7. doi: 10.1080/03079450902912135
6. Sansano-Maestre J, del Carmen Martínez-Herrero M, Garijo-Toledo MM, Gómez-Muñoz MT. RAPD analysis and sequencing of ITS1/5.8 S rRNA/ITS2 and Fe-hydrogenase as tools for genetic classification of potentially pathogenic isolates of *Trichomonas gallinae*. *Res Vet Sci*. (2016) 107:182–9. doi: 10.1016/j.rvsc.2016.05.016
7. Chi JF, Lawson B, Durrant C, Beckmann K, John S, Alrefaei AF, et al. The finch epidemic strain of *Trichomonas gallinae* is predominant in British non-passerines. *Parasitology*. (2013) 140:1234–45. doi: 10.1017/S0031182013000930
8. Marx M, Reiner G, Willems H, Rocha G, Hillerich K, Masello JF, et al. High prevalence of *Trichomonas gallinae* in wild columbids across western and southern Europe. *Parasit Vectors*. (2017) 10:242. doi: 10.1186/s13071-017-2170-0
9. Purple KE, Humm JM, Kirby RB, Saidak CG, Gerhold R. *Trichomonas gallinae* persistence in four water treatments. *J Wildl Dis*. (2015) 51:739–42. doi: 10.7589/2014-05-137
10. Sturgill F, Gerhold R. *Trichomonas gallinae* persistence in water with pH and organic material variance. *Comp Parasitol*. (2016) 83:237–9. doi: 10.1654/4799s.1
11. McBurney S, Kelly-Clark WK, Forzán MJ, Vanderstichel R, Teather K, Greenwood SJ. Persistence of *Trichomonas gallinae* in Birdseed. *Avian Dis*. (2017) 61:311–5. doi: 10.1637/11545-113016-RegR1
12. Lawson B, Robinson RA, Colvile KM, Peck KM, Chantrey J, Pennycott TW, et al. The emergence and spread of finch trichomonosis in the British Isles. *Philos Trans Royal Soc B*. (2012) 367:2852–63. doi: 10.1098/rstb.2012.0130

13. Lennon RJ, Dunn JC, Stockdale JE, Goodman SJ, Morris AJ, Hamer KC. Trichomonad parasite infection in four species of Columbidae in the UK. *Parasitology*. (2013) 140:1368–76. doi: 10.1017/S0031182013000887
14. Martínez-Herrero MC, Sansano-Maestre J, Márquez IL, Obón E, Ponce C, González J, et al. Genetic characterization of oropharyngeal trichomonad isolates from wild birds indicates that genotype is associated with host species, diet and presence of pathognomonic lesions. *Avian Pathol*. (2014) 43:535–46. doi: 10.1080/03079457.2014.967660
15. Stockdale JE, Dunn JC, Goodman SJ, Morris AJ, Sheehan DK, Grice PV, et al. The protozoan parasite *Trichomonas gallinae* causes adult and nestling mortality in a declining population of European Turtle Doves, *Streptopelia turtur*. *Parasitology*. (2015) 142:490–8. doi: 10.1017/S0031182014001474
16. Calderón L, Campagna L, Wilke T, Lormee H, Eraud C, Dunn JC, et al. Genomic evidence of demographic fluctuations and lack of genetic structure across flyways in a long-distance migrant, the European turtle dove. *BMC Evol Biol*. (2016) 16:237. doi: 10.1186/s12862-016-0817-7
17. Rogers KH, Girard YA, Woods L, Johnson CK. Avian trichomonosis in spotted owls (*Strix occidentalis*): indication of opportunistic spillover from prey. *Int J Parasitol: Parasit Wildl*. (2016) 5:305–11. doi: 10.1016/j.ijppaw.2016.10.002
18. Real J, Mañosa S. Demography and conservation of western European Bonelli's Eagle *Hieraaetus fasciatus* populations. *Biol Conserv*. (1997) 79:59–66. doi: 10.1016/S0006-3207(96)00100-0
19. Del Moral JC. *El Águila Perdicera en España. Población en 2005 y Método De Censo*. Madrid: SEO/BirdLife (2006).
20. Palma L, Beja P, Pais M, Fonseca LC. Why do raptors take domestic prey? The case of Bonelli's eagles and pigeons. *J Appl Ecol*. (2006) 43:1075–86. doi: 10.1111/j.1365-2664.2006.01213.x
21. Caro J, Ontiveros D, Pleguezuelos JM. The feeding ecology of Bonelli's eagle (*Aquila fasciata*) floaters in southern Spain: implications for conservation. *Eur J Wildl Res*. (2011) 57:729–36. doi: 10.1007/s10344-010-0480-z
22. De Juana E, Garcia E. *The Birds of the Iberian Peninsula London: Bloomsbury Publishing* (2015).
23. Mira S, Arnaud-Haond S, Palma L, Cancela ML, Beja P. Large-scale population genetic structure in Bonelli's Eagle *Aquila fasciata*. *Ibis*. (2013) 155:485–98. doi: 10.1111/ibi.12065
24. Hawley DM, Sydenstricker KV, Kollias GV, Dhondt AA. Genetic diversity predicts pathogen resistance and cell-mediated immunocompetence in house finches. *Biol Lett*. (2005) 1:326–9. doi: 10.1098/rsbl.2005.0303
25. Höfle U, Blanco J, Palma L, Melo P. Trichomoniasis in Bonelli's eagles *Hieraaetus fasciatus* nestlings in south-west Portugal. In: eds Lumeij J, Remple J, Redig P, Lierz P, Cooper M. *Raptor Biomedicine III* (Lake Worth: Zoological Education Network) (2000). p. 45–52.
26. Real J, Mañosa S, Muñoz E. Trichomoniasis in a Bonelli's eagle population in Spain. *J Wildl Dis*. (2000) 36:64–70. doi: 10.7589/0090-3558-36.1.64
27. Hernández A, Resano J, Real J. Monitorización demográfica del Águila perdicera (Aquila fasciata) en Castilla y León, análisis de la dieta, de la calidad de los pollos y aplicaciones a la conservación - informe final. *Technical Report Equip de Biologia de la Conservació, Departament de Biologia Animal, Universitat de Barcelona*. Barcelona (2012).
28. Hernández-Matías A, Real J, Moleón M, Palma L, Sánchez-Zapata JA, et al. From local monitoring to a broad-scale viability assessment: a case study for the Bonelli's Eagle in western Europe. *Ecol Monogr*. (2013) 83:239–61. doi: 10.1890/12-1248.1
29. Sousa AJG. Caracterização ecológica e genética das populações de Pombo-da-rocha (Columba livia) no Parque Natural do Douro Internacional. *Technical report, Instituto da Conservação da Natureza, Parque Natural do Douro Internacional, Figueira de Castelo Rodrigo*. Portugal (2004).
30. García JEY. *El Palomar Tradicional: Una Explotación Avícola Singular, Estúdio de Antecedentes Históricos y Aprovechamiento Humano*. Zamora: Colegio Oficial de Veterinarios de Zamora (1997).
31. Rivas-Martínez S, Cantó P, Fernandez-González F, Navarro C, Pizarro JM, Sanchez-Mata D. *Biogeografia de la Peninsula Iberica, Islas Baleares y Canarias*. Publicaciones Deptartamento Biologia Vegetal (1990).
32. Costa JC, Aguiar C, Capelo JH, Lousã M, Neto C. *Biogeografia de Portugal Continental*. Quercetea (1998).
33. CCAC *Canadian Council on Animal Care Guidelines on: The Care and Use of Wildlife*. Ontario: Canadian Council on Animal Care (2003).
34. Hess M, Kolbe T, Grabensteiner E, Prosl H. Clonal cultures of *Histomonas meleagridis*, *Tetratrichomonas gallinarum* and a *Blastocystis* sp. established through micromanipulation *Parasitology*. (2006) 133:547–54. doi: 10.1017/S0031182006000758
35. Felleisen RS. Comparative sequence analysis of 5.8S rRNA genes and internal transcribed spacer (ITS) regions of trichomonadid protozoa. *Parasitology*. (1997) 115:111–9. doi: 10.1017/S0031182097001212
36. Gerhold RW, Yabsley MJ, Smith AJ, Ostergaard E, Mannan W, Cann JD, et al. Molecular characterization of the *Trichomonas gallinae* morphologic complex in the United States. *J Parasitol*. (2008) 94:1335–41. doi: 10.1645/GE-1585.1
37. Grabensteiner E, Bilic I, Kolbe T, Hess M. Molecular analysis of clonal trichomonad isolates indicate the existence of heterogenic species present in different birds and within the same host. *Vet Parasitol*. (2010) 172:53–64. doi: 10.1016/j.vetpar.2010.04.015
38. Bosch R, Real J, Tinto A, Zozaya EL, Castell C. Home-ranges and patterns of spatial use in territorial Bonelli's Eagles *Aquila fasciata*. *Ibis*. (2010) 152:105–17. doi: 10.1111/j.1474-919X.2009.00985.x
39. Pérez-García JM, Margalida A, Afonso I, Ferreiro E, Gardiazábal A, et al. Interannual home range variation, territoriality and overlap in breeding Bonelli's eagles (*Aquila fasciata*) tracked by GPS satellite telemetry. *J Ornithol*. (2012) 154:63–71. doi: 10.1007/s10336-012-0871-x
40. Tamura K, Stecher G, Peterson D, Filipski A, Kumar S. MEGA6: Molecular Evolutionary Genetics Analysis version 6.0. *Mol Biol Evol*. (2013) 30:2725–9. doi: 10.1093/molbev/mst197
41. Holt RD, Dobson AP, Begon M, Bowers RG, Schauber EM. Parasite establishment in host communities. *Ecol Lett*. (2003) 6:837–42. doi: 10.1046/j.1461-0248.2003.00501.x
42. Ganas P, Jaskulska B, Lawson B, Zadravec M, Hess, M, Bilic I. Multi-locus sequence typing confirms the clonality of *Trichomonas gallinae* isolates circulating in European finches. *Parasitology*. (2014) 141:652–61. doi: 10.1017/S0031182013002023
43. Cunningham AA. Disease risks of wildlife translocations. *Conserv Biol*. (1996) 10:349–53. doi: 10.1046/j.1523-1739.1996.10020349.x
44. Walker SF, Bosch J, James TY, Litvintseva AP, Valls JAO, Piña S, et al. Invasive pathogens threaten species recovery programs. *Curr Biol*. (2008) 18:853–4. doi: 10.1016/j.cub.2008.07.033
45. Resano-Mayor J, Hernández-Matías A, Real J, Parés F, Inger R, Bearhop S. Comparing pellet and stable isotope analyses of nestling Bonelli's Eagle A*quila fasciata* diet. *Ibis*. (2014) 156:176–88. doi: 10.1111/ibi.12095
46. Rollan À, Hernández-Matías A, Real J. *Guidelines for the Conservation of Bonelli's Eagle Populations*. Barcelona: Universitat de Barcelona. (2016). Available online at: http://hdl.handle.net/2445/69446 (accessed April 2, 2019).
47. Villanúa D, Höfle U, Pérez-Rodríguez L, Gortázar C. *Trichomonas gallinae* in wintering common wood pigeons *Columba palumbus* in Spain. *Ibis*. (2006) 148:641–8. doi: 10.1111/j.1474-919X.2006.00561.x
48. Van der Most PJ, de Jong B, Parmentier HK, Verhulst S. Trade-off between growth and immune function: a meta-analysis of selection experiments. *Funct Ecol*. (2011) 25:74–80. doi: 10.1111/j.1365-2435.2010.01800.x
49. Demas GE, Greives TJ, Chester EM, French SS. The energetics of immunity: mechanisms mediating trade-offs in eco-immunology. In: eds Demas GE, Nelson RJ. *Ecoimmunology* (New York, NY: Oxford University Press) (2012), 257–296.

Conflict of Interest Statement: The authors declare that the research was conducted in the absence of any commercial or financial relationships that could be construed as a potential conflict of interest.

Copyright © 2019 Santos, Jambas, Monteiro, Amaral, Martins, Garcia, Fernández, Tyler, Almeida, Abrantes and Esteves. This is an open-access article distributed under the terms of the Creative Commons Attribution License (CC BY). The use, distribution or reproduction in other forums is permitted, provided the original author(s) and the copyright owner(s) are credited and that the original publication in this journal is cited, in accordance with accepted academic practice. No use, distribution or reproduction is permitted which does not comply with these terms.

frontiers in Veterinary Science

CASE REPORT
published: 07 August 2019
doi: 10.3389/fvets.2019.00254

Abdominal Ectopic Pregnancy and Impaired Postnatal Mammary Gland Development, Consistent With Physiologic Agalactia, in a Wild European Rabbit, *Oryctolagus cuniculus*

*Katherine Hughes**

Department of Veterinary Medicine, University of Cambridge, Cambridge, United Kingdom

OPEN ACCESS

Edited by:
Robert James Ossiboff, University of Florida, United States

Reviewed by:
Martha Ann Delaney, University of Illinois at Urbana-Champaign, United States
Steven H. Weisbroth, Consultant, McLean, VA, United States
John Ford Roberts, University of Florida, United States

***Correspondence:**
Katherine Hughes
kh387@cam.ac.uk
orcid.org/0000-0002-3331-1249

Specialty section:
This article was submitted to Veterinary Experimental and Diagnostic Pathology, a section of the journal Frontiers in Veterinary Science

Received: *22 May 2019*
Accepted: *17 July 2019*
Published: *07 August 2019*

Citation:
Hughes K (2019) Abdominal Ectopic Pregnancy and Impaired Postnatal Mammary Gland Development, Consistent With Physiologic Agalactia, in a Wild European Rabbit, Oryctolagus cuniculus. Front. Vet. Sci. 6:254. doi: 10.3389/fvets.2019.00254

A wild European rabbit, *Oryctolagus cuniculus*, was diagnosed with an abdominal pregnancy due to the presence of a single abdominal lithopedion attached by a thin fibrovascular stalk to the left uterine horn, which was distorted by the tension of the adhesion. Evidence of mineralized remnants, chronic inflammation, and fibrosis in the left uterine endometrium and myometrium suggested that the lithopedion had arisen as a secondary abdominal pregnancy. The right uterine horn contained two macroscopically normal fetuses. The mammary gland exhibited notably retarded development in relation to the size of the fetuses. Histologically, mammary alveoli lacked evidence of intraluminal secretory product, and ducts lacked prominence and contained clusters of small numbers of macrophages. The doe also exhibited mild granulomatous and heterophilic pneumonia with rare intralesional adiaspores, suggesting infection with *Emmonsia* spp. as an incidental finding. This case documents secondary abdominal pregnancy in a wild lagomorph not subjected to artificial insemination procedures suggested to increase the occurrence of this condition in farmed rabbits. An abdominal pregnancy is one of a number of factors that should be considered as a potential factor in the etiology of impaired postnatal mammary development or reduced milk yield in a breeding doe, although no causative association is demonstrated in this case. Abdominal ectopic pregnancy is one possible differential diagnosis in the investigation of the presence of a palpable abdominal mass or masses in *O. cuniculus*.

Keywords: abdominal pregnancy, ectopic pregnancy, extrauterine pregnancy, lithopedion, mammary gland, *Oryctolagus cuniculus*, pregnancy, rabbit

BACKGROUND

Extrauterine pregnancy, often used synonymously with the term "ectopic pregnancy," describes a pregnancy occurring outwith the uterus (1). Four subtypes are recognized (**Table 1**) but the most common subtype arising in animals, particularly in species other than non-human primates, is abdominal pregnancy. Primary abdominal pregnancy arises when the conceptus implants within the abdomen due to escape from the fallopian tube, for example following retrograde movement

TABLE 1 | Tabular representation of subtypes of extrauterine pregnancy, as recognized in human medicine, with selected case examples from humans and animals.

Extrauterine pregnancy Often used synonymously with the term "ectopic pregnancy" to describe a pregnancy occurring outwith the uterus (1).				
Tubal The fertilized ovum implants in the fallopian tube, most frequently in the ampulla in humans (2, 3).	**Ovarian** The ovary is the site of implantation, growth, and development of the gestational sac (4).	**Cervical** The site of implantation is the cervical canal—a rare form of ectopic pregnancy in humans (5).	**Abdominal [peritoneal]** The fertilized ovum implants in the abdomen. The most common subtype of ectopic pregnancy recognized in animals other than non-human primates (1).	
			Primary Abdominal implantation is due to the fertilized ovum entering the peritoneal cavity, such as through the fimbria. Lack of lesions in the reproductive tract is suggestive of primary extrauterine pregnancy, but the possibility of repair cannot be discounted (6).	**Secondary** Uterine or tubal trauma leads to oocyte release into the abdomen (7).

through the fimbria. By contrast, secondary abdominal pregnancy occurs following uterine or tubal trauma that results in abdominal implantation.

Abdominal pregnancies have been previously described in laboratory (8), pet (9–11), and farmed *Oryctolagus cuniculus* (1, 12, 13). Indeed, in farmed rabbits, use of artificial insemination has been postulated to be a factor in the pathogenesis of some cases (12). Abdominal pregnancy in wild lagomorphs is likely under-reported, although two cottontail rabbits (*Sylvilagus floridanus*) (14), two European hares (*Lepus europaeus*) (15), and a mountain hare (*Lepus timidus scoticus*) (16) are amongst the reports of abdominal pregnancies in this group of animals. The present report describes a case of secondary abdominal pregnancy in a wild European rabbit, *O. cuniculus*, with concurrent impaired mammary gland development.

CASE PRESENTATION

The cadaver of a wild female European rabbit, *O. cuniculus*, was one of a group shot for population management and donated for research and teaching to the veterinary anatomic pathology service of the Department of Veterinary Medicine, University of Cambridge (UK). The rabbit weighed 1.78 kg. Post mortem examination revealed a very firm, irregular mass with a smooth, gray/pink surface in the left abdomen. The mass had average dimensions 40 × 35 × 30 mm and had thin, tough, translucent adhesions to the left abdominal wall and the left uterine horn, the latter adhesion exhibiting evidence of vascularity, and the tension of the adhesion causing distortion of the left uterine horn (**Figures 1A,B**). On cut section, the mass was dry and multifocally gritty, but contained clearly discernable fetal remnants, including skin, hair, hard palate, and bone surrounded by lamellated fibrous tissue and fetal membranes (**Figure 1C**). The mass was interpreted to be a lithopedion, or mineralized abdominal ectopic pregnancy (17).

At the point of attachment to the left uterine horn, the uterine lumen contained an irregular, cream, 12 × 8 × 5 mm concretion and a circumferential 10 mm band of the uterine endometrium was dark red at this focus. The right uterine horn contained two fetuses, with crown-rump lengths 55 and 53 mm. Macroscopically, the mammary gland exhibited some evidence of development consistent with early pregnancy, such as prominent vasculature and mild parenchymal development, but this was considered markedly less than expected for this stage of pregnancy based on previous analyses (18). The gastrointestinal tract, in particular the stomach, was subjectively less full than the majority of wild rabbits from the same region examined as part of ongoing studies (18, 19) and scarce fecal pellets were present in the rectum. No other abnormalities were detected macroscopically.

Tissues were fixed in 10% neutral buffered formalin, and histological sections were prepared following standard procedures. The lithopedion was composed of amorphous eosinophilic material, indicative of degeneration and autolysis, which was multifocally heavily mineralized. Although nuclei were multifocally apparent, the degree of degeneration was such that cell populations were not identifiable and the presence of an inflammatory infiltrate could not be assessed. The uterus at the point of attachment of the lithopedion exhibited a locally extensive endometrial infiltrate of moderate numbers of lymphocytes, plasma cells, heterophils, and fewer macrophages, with locally extensive ulceration. Underlying this focus, there was a loss of distinction of the myometrial layers and locally extensive, mild to moderate, fibrosis. Together with the presence of the small concretion of mineralized material within the uterine lumen, this was considered strong evidence of abdominal pregnancy and formation of a lithopedion secondary to uterine rupture.

The macroscopic impression that the mammary gland was markedly under-developed for the stage of pregnancy was confirmed histologically, with only a thin layer of mammary tissue present and mammary lobules interspersed by prominent, wide, bands of connective tissue. The mammary alveoli frequently lacked intraluminal proteinaceous material and ducts

FIGURE 1 | Presence of a lithopedion in a wild European rabbit**. (A)** A firm mass with a smooth surface is present in the abdomen of a female rabbit (white arrow). Asterisk denotes fetus in right uterine horn; arrowhead indicates left ovary. **(B)** A thin fibrovascular band (purple arrow) connects the lithopedion to the left uterine horn, which is distorted as a result. Arrowhead indicates left ovary. **(C)** On cut surface the lithopedion contains fetal remnants including skin, hair, bone, and hard palate (partially fixed tissue).

were generally empty except for small numbers of macrophages and desquamated epithelial cells. The lack of mammary development was particularly pronounced when compared with mammary tissue from another female carrying a litter of similarly developed fetuses (crown-rump length median: 51 cm; mean: 50 cm; $n = 8$; **Figure 2**).

Histologically the lungs exhibited multifocal, mild, granulomatous and heterophilic pneumonia with multinucleated giant cells and very rare adiaspores, with morphology consistent with *Emmonsia* spp. There were no other significant findings on histological examination.

DISCUSSION

This report describes a case of secondary abdominal pregnancy in a wild rabbit. Secondary abdominal pregnancy is considered to arise as a consequence of traumatic injury to the reproductive tract, leading to a communication between the uterus or vagina and the peritoneal cavity, and the subsequent propulsion of a conceptus or fetus into the abdomen, potentially as a result of contractions associated with parturition in some cases (7, 12). In this case, the lithopedion was a similar size to the fetuses in the unaffected right uterine horn. It is therefore tempting to speculate that, given the degree of fetal maceration, the abdominal pregnancy originally arose during a previous pregnancy. This scenario is also consistent with the lack of detectable communication between the left uterine horn and the peritoneal cavity, and the presence of chronic inflammation and fibrosis in the myometrium suggestive of a chronic reparative process. The mineralized concretion within the uterus at this site likely represented residual material associated with the fetus expelled into the abdomen.

Studies in farmed or laboratory rabbits, for which dates of insemination are recorded, have facilitated accurate description of concurrent abdominal pregnancies and intrauterine fetuses of differing ages (13), suggesting that it is indeed feasible that the abdominal fetus described in this report originally arose during a previous pregnancy. This raises the question of whether the wild rabbit described here would have exhibited clinical signs associated with the presence of the lithopedion. Interestingly, during post mortem examination, it was felt that the stomach was less full than usual for rabbits examined as part of a cohort culled for population management, and the rectum was largely devoid of feces. It is therefore tentatively suggested that the lithopedion and associated adhesions were impacting the rabbit to a degree, supporting previous assertions that abdominal pregnancy may be associated with clinical signs in some cases: one pet rabbit diagnosed with an abdominal pregnancy was

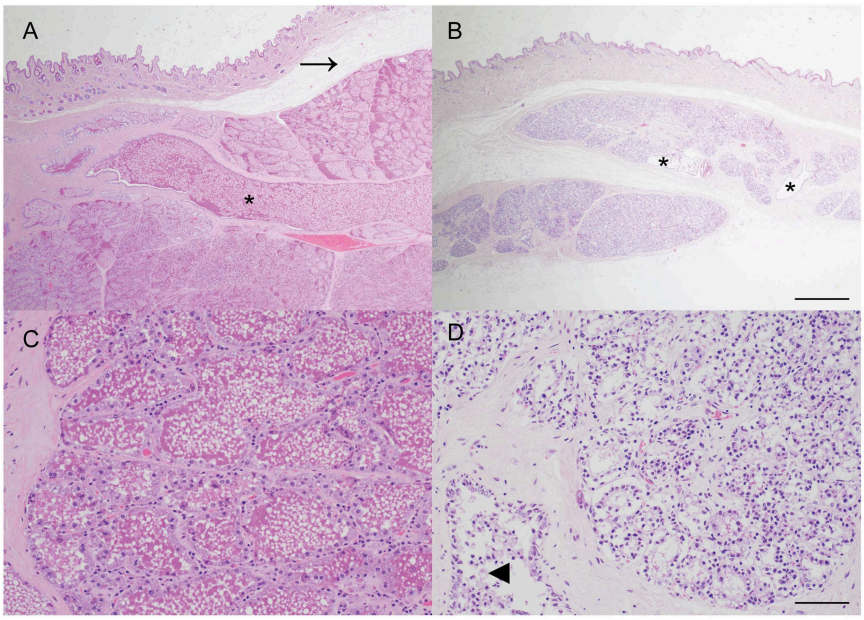

FIGURE 2 | Impaired postnatal mammary development, consistent with physiologic agalactia, in a wild European rabbit with an abdominal pregnancy. **(A,C)** Mammary tissue from a doe with fetuses of a similar gestational age to the affected doe exhibits extensive alveolar development, and large amounts of eosinophilic proteinaceous material within mammary alveoli and ducts (asterisk). Arrow indicates artifactual separation of skin from underlying mammary tissue. **(B,D)** Mammary tissue from a female rabbit with an abdominal pregnancy exhibits alveoli with reduced diameter and lacking secretion, and small, largely empty ducts (asterisks). Some ducts contain small clusters of macrophages (arrowhead). Haematoxylin and eosin stain. Scale bars indicate 800 microns **(A,B)** and 80 microns **(C,D)**.

presented with inappetance and lethargy and subsequently died. Three mummified abdominal fetuses were detected during a post mortem examination, and although no definitive association with the death of the rabbit was described, no alternative cause of death was discovered (9). A further laboratory rabbit later discovered to have multiple abdominal lithopedions also exhibited anorexia (8). However, in another case in a pet rabbit, no clinical signs were noted (10).

Although no definitive relationship to the abdominal pregnancy can be inferred from this case, it is tempting to speculate on a potential relationship between the presence of the lithopedion and the impaired mammary development. Agalactia has been previously described in a laboratory rabbit with an extrauterine pregnancy although no description of the mammary gland was provided (8). In the present case, the relative lack of mammary development, when compared to an unaffected doe pregnant with similarly sized fetuses, is striking (**Figure 2**). One limitation of this case is that as the rabbit was wild, no reproductive history or details regarding concurrent lactation are available. The lack of postnatal mammary development, consistent with physiologic agalactia, may be attributable to a postulated lack of concurrent lactation due to loss of the previous litter, or the presence of just two viable fetuses, but it also seems possible that stress, resulting from the abdominal pregnancy and leading to elevated blood cortisol, may have played a more direct role. Secretion of prolactin, a key regulator of development of the milk secreting mammary epithelial cells via activation of Signal Transducer and Activator of Transcription 5 (STAT5) (20), is reduced in a rabbit model of critical illness using deep dermal burns (21). The impact of other stressors, such as heat stress, on postnatal mammary gland development are widely recognized in production ruminants (22). In this case there was no evidence of inflammation within the mammary gland and thus an infectious cause of agalactia was considered unlikely. This case highlights that further investigation of a potential link between abdominal pregnancy and impaired mammary gland development in rabbits may be merited.

The rabbit in this report was microscopically diagnosed with mild granulomatous and heterophilic pneumonia with multinucleated giant cells and very rare adiaspores, with morphology consistent with *Emmonsia* spp. We have recently described adiaspiromycosis in a wild European rabbit with a much higher burden of adiaspores and marked granulomatous pneumonia which was grossly apparent (19). By comparison, in this case the pathology was subtle, only appreciable histologically, and was considered to be most likely an incidental finding of no clinical consequence. Such incidental diagnosis of adiaspiromycosis has also been reported in other small mammal species such as moles (*Talpa europaea*) (23). DNA extraction and subsequent PCR amplification and sequencing would have been the optimal approach to attempt to definitively confirm the diagnosis of adiaspiromycosis in this rabbit, particularly as culture is oftentimes unrewarding (24).

This case report illustrates that, although abdominal pregnancies in rabbits may be associated with artificial insemination procedures in some farmed rabbits (12), they may also occur in wild *O. cuniculus*. This report also suggests that an abdominal pregnancy should be considered as a differential diagnosis in the investigation of a palpable abdominal mass or masses in *O. cuniculus*. Larger scale studies examining

ectopic pregnancy in rabbits may reveal further insights into the pathogenesis of this condition.

DATA AVAILABILITY

All datasets analyzed for this study are included in the manuscript.

ETHICS STATEMENT

The animal study was reviewed and approved by University of Cambridge Department of Veterinary Medicine Ethics and Welfare Committee.

AUTHOR CONTRIBUTIONS

KH performed the gross and histological post mortem examination, conceived the study, collected and collated the data, and wrote the manuscript.

FUNDING

Publication costs were supported by Girton College, University of Cambridge. The funder had no role in study design, data collection and analysis, decision to publish, or preparation of the manuscript.

ACKNOWLEDGMENTS

The author thanks the pest controller who donates wild rabbit cadavers to the University of Cambridge for teaching and research purposes. The author gratefully acknowledges the technical expertise of Mrs. Debbie Sabin in the preparation of tissue sections. The rabbit described here was part of a post mortem study of the pathology of wild rabbits, and the author thanks the Ethics and Welfare Committee of the Department of Veterinary Medicine, University of Cambridge for their review of the study plan (reference: CR240).

REFERENCES

1. Corpa JM. Ectopic pregnancy in animals and humans. *Reproduction.* (2006) 131:631–40. doi: 10.1530/rep.1.00606
2. Gauvin C, Amberger M, Louie K, Argeros O. Previously asymptomatic ruptured tubal ectopic pregnancy at over 10weeks' gestation: Two case reports. *Case Rep Womens Health.* (2019) 21:e00089. doi: 10.1016/j.crwh.2018.e00089
3. Stremick JK, Couperus K, Ashworth SW. Ruptured tubal ectopic pregnancy at fifteen weeks gestational age. *Clin Pract Cases Emerg Med.* (2019) 3:62–4. doi: 10.5811/cpcem.2019.1.40860
4. Ge L, Sun W, Wang L, Cheng L, Geng C, Song Q, et al. Ultrasound classification and clinical analysis of ovarian pregnancy: a study of 12 cases. *J Gynecol Obstet Hum Reprod.* (2019). doi: 10.1016/j.jogoh.2019.04.003. [Epub ahead of print].
5. Mouhajer M, Obed S, Okpala AM. Cervical ectopic pregnancy in resource deprived areas: a rare and difficult diagnosis. *Ghana Med J.* (2017) 51:94–7. doi: 10.4314/gmj.v51i2.8
6. Hong CC, Armstrong ML. Ectopic pregnancy in 2 guinea-pigs. *Lab Anim.* (1978) 12:243–4. doi: 10.1258/002367778781088567
7. Bland-Sutton J. Abdominal pregnancy in women, cats, dogs, and rabbits. *Lancet.* (1904) 164:1625–7.
8. Tena-Betancourt E, Tena-Betancourt CA, Zuniga-Munoz AM, Hernandez-Godinez B, Ibanez-Contreras A, Graullera-Rivera V. Multiple extrauterine pregnancy with early and near full-term mummified fetuses in a New Zealand white rabbit (*Oryctolagus cuniculus*). *J Am Assoc Lab Anim Sci.* (2014) 53:204–7.
9. Arvidsson A. Extra-uterine pregnancy in a rabbit. *Vet Rec.* (1998) 142:176.
10. Beddow BA. Ectopic pregnancy in a rabbit. *Vet Rec.* (1999) 144:624.
11. Turner PV, Brash ML, Smith DA. Rabbits. In: Turner PV, Brash ML, Smith DA, editors. *Pathology of Small Mammal Pets.* Hoboken, NJ: John Wiley & Sons, Inc. (2018). p. 11.
12. Segura Gil P, Peris Palau B, Martinez Martinez J, Ortega Porcel J, Corpa Arenas JM. Abdominal pregnancies in farm rabbits. *Theriogenology.* (2004) 62:642–51. doi: 10.1016/j.theriogenology.2003.11.005
13. Marco-Jimenez F, Garcia-Dominguez X, Valdes-Hernandez J, Vicente JS. Extra-uterine (abdominal) full term foetus in a 15-day pregnant rabbit. *BMC Vet Res.* (2017) 13:307. doi: 10.1186/s12917-017-1229-7
14. Jacobson HA, Kibbe DP, Kirkpatrick RL. Ectopic fetuses in two cottontail rabbits. *J Wildl Dis.* (1975) 11:540–2.
15. Stott P, Wight N. Female reproductive tract abnormalities in European hares (*Lepus europaeus*) in Australia. *J Wildl Dis.* (2004) 40:696–703. doi: 10.7589/0090-3558-40.4.696
16. Van der Merwe M, Racey PA. Abdominal foetus in the hare (*Lepus timidus scoticus*). *J Zool.* (1981) 197:309–11.
17. Holdt Somer SJ. Lithopedion: an unexpected finding. *Am J Obstet Gynecol.* (2016) 215:524 e521–2. doi: 10.1016/j.ajog.2016.06.056
18. Hughes K, Watson CJ. Sinus-like dilatations of the mammary milk ducts, Ki67 expression, and CD3-positive T lymphocyte infiltration, in the mammary gland of wild European rabbits during pregnancy and lactation. *J Anat.* (2018) 233:266–73. doi: 10.1111/joa.12824
19. Hughes K, Borman AM. Adiaspiromycosis in a wild European rabbit, and a review of the literature. *J Vet Diagn Invest.* (2018) 30:614–8. doi: 10.1177/1040638718772631
20. Shin HY, Hennighausen L, Yoo KH. STAT5-driven enhancers tightly control temporal expression of mammary-specific genes. *J Mammary Gland Biol Neoplasia.* (2019) 24:61–71. doi: 10.1007/s10911-018-9418-y
21. Weekers F, Van Herck E, Coopmans W, Michalaki M, Bowers CY, Veldhuis JD, et al. A novel in vivo rabbit model of hypercatabolic critical illness reveals a biphasic neuroendocrine stress response. *Endocrinology.* (2002) 143:764–74. doi: 10.1210/endo.143.3.8664
22. Tao S, Dahl GE, Laporta J, Bernard JK, Orellana Rivas RM, Marins TN. Effects of heat stress during late gestation on the dam and its calf. *J Anim Sci.* (2019) 96:351. doi: 10.1093/jas/skz061
23. Simpson VR, Davison NJ, Dagleish MP. Causes of mortality and lesions observed post mortem in European moles (*Talpa europaea*) in Cornwall, South-west England. *J Comp Pathol.* (2019) 167:18–25. doi: 10.1016/j.jcpa.2018.11.006
24. Borman AM, Simpson VR, Palmer MD, Linton CJ, Johnson EM. Adiaspiromycosis due to Emmonsia crescens is widespread in native British mammals. *Mycopathologia.* (2009) 168:153–63. doi: 10.1007/s11046-009-9216-6

Conflict of Interest Statement: The author declares that the research was conducted in the absence of any commercial or financial relationships that could be construed as a potential conflict of interest.

Copyright © 2019 Hughes. This is an open-access article distributed under the terms of the Creative Commons Attribution License (CC BY). The use, distribution or reproduction in other forums is permitted, provided the original author(s) and the copyright owner(s) are credited and that the original publication in this journal is cited, in accordance with accepted academic practice. No use, distribution or reproduction is permitted which does not comply with these terms.

frontiers in Veterinary Science

ORIGINAL RESEARCH
published: 22 August 2019
doi: 10.3389/fvets.2019.00281

Keeping an Eye on Wild Brown Trout (*Salmo trutta*) Populations: Correlation Between Temperature, Environmental Parameters, and Proliferative Kidney Disease

Aurélie Rubin[1,2,3]*, *Pauline de Coulon*[4], *Christyn Bailey*[1,5], *Helmut Segner*[1], *Thomas Wahli*[1] *and Jean-François Rubin*[2,3]

[1] Department of Infectious Diseases and Pathobiology, Centre for Fish and Wildlife Health, University of Bern, Bern, Switzerland, [2] La Maison de la Rivière, Tolochenaz, Switzerland, [3] Land, Nature, Environment Institute, University of Applied Sciences and Arts Western Switzerland, Geneva, Switzerland, [4] Department of Ecology and Evolution, Faculty of Biology and Medicine, University of Lausanne, Lausanne, Switzerland, [5] Fish Immunology and Pathology Laboratory, Animal Health Research Center (CISA-INIA), Madrid, Spain

OPEN ACCESS

Edited by:
Robert James Ossiboff, University of Florida, United States

Reviewed by:
Franz Lahnsteiner, Bundesamt für Wasserwirtschaft, Austria
Bartolomeo Gorgoglione, Michigan State University, United States

***Correspondence:**
Aurélie Rubin
aurelie.rubin@students.unibe.ch

Specialty section:
This article was submitted to Zoological Medicine, a section of the journal Frontiers in Veterinary Science

Received: 03 May 2019
Accepted: 07 August 2019
Published: 22 August 2019

Citation:
Rubin A, de Coulon P, Bailey C, Segner H, Wahli T and Rubin J-F (2019) Keeping an Eye on Wild Brown Trout (Salmo trutta) Populations: Correlation Between Temperature, Environmental Parameters, and Proliferative Kidney Disease. Front. Vet. Sci. 6:281. doi: 10.3389/fvets.2019.00281

Proliferative kidney disease (PKD) is an emerging disease of salmonids caused by the myxozoan parasite *Tetracapsuloides bryosalmonae*, which plays a major role in the decrease of wild brown trout (*Salmo trutta*) populations in Switzerland. Strong evidence demonstrated that water temperature modulates parasite infection. However, less knowledge exists on how seasonal water temperature fluctuations influence PKD manifestation under field conditions, how further environmental factors such as water quality may modulate the disease, and whether these factors coalesce with temperatures role possibly giving rise to cumulative effects on PKD. The aims of this study were to (1) determine the correlation between seasonal course of water temperature and PKD prevalence and intensity in wild brown trout populations, (2) assess if other factors such as water quality or ecomorphology correlate with the infection, and (3) quantitatively predict the implication of these factors on PKD prevalence with a statistical model. Young-of-the-year brown trout were sampled in 45 sites through the Canton of Vaud (Switzerland). For each site, longitudinal time series of water temperature, water quality (macroinvertebrate community index, presence of wastewater treatment plant effluent) and ecomorphological data were collected and correlated with PKD prevalence and intensity. 251 *T. bryosalmonae*-infected trout of 1,118 were found (overall prevalence 22.5%) at 19 of 45 study sites (42.2%). Relation between PKD infection and seasonal water temperature underlined that the mean water temperature for June and the number of days with mean temperature $\geq$15°C were the most significantly correlated parameters with parasite prevalence and intensity. The presence of a wastewater treatment plant effluent was significantly correlated with the prevalence and infection intensity. In contrast, macroinvertebrate diversity and river ecomorphology were shown to have little impact on disease parameters. Linear and logistic regressions highlighted quantitatively the prediction of PKD prevalence depending on environmental parameters at a given site and

its possible increase due to rising temperatures. The model developed within this study could serve as a useful tool for identifying and predicting disease hot spots. These results support the importance of temperature for PKD in salmonids and provides evidence for a modulating influence of additional environmental stress factors.

Keywords: proliferative kidney disease, *Salmo trutta*, *Tetracapsuloides bryosalmonae*, water temperature, water quality, ecomorphology, wild fish population, aquatic fieldwork

INTRODUCTION

Beginning in the 1980s, the catch of brown trout *Salmo trutta* in Switzerland experienced a massive decline of up to 50% (1–4). This process is still ongoing. Hence, the wild salmonid populations are considered to be threatened (5–7). Investigations within a nationwide project suggested the decrease was due to multifactorial drivers (2). Among the parameters involved, a parasitic disease of salmonids, proliferative kidney disease (PKD) was considered to play a major role (2, 3, 8–10).

The causative agent of PKD is the myxozoan parasite *Tetracapsuloides bryosalmonae* (11, 12). The life cycle of the parasite comprises salmonid fish species as vertebrate hosts and bryozoans, mainly *Fredericella sultana* (Blumenbach), as invertebrate hosts (13–16). Spores, which have developed in bryozoans, are released into the water and upon contact with a suitable vertebrate host, infect the fish through skin and gills (14, 17). Via the circulatory system, the parasites eventually reach the target organs, mainly the kidney. The infection may cause renal swelling (18–20). In the kidney, the parasite normally develops sporogonic stages in the tubuli, from where spores are released via the urine and can infect bryozoans again (15, 21, 22). Depending on host susceptibility and seasonal conditions, extrasporogonic stages might instead proliferate in the interstitial tissue causing PKD, which may lead to high mortality rates (18, 19, 23). Juvenile fish getting in contact with the parasite for the first time appear to be particularly susceptible to the infection and to PKD pathogenesis (8, 19, 24, 25).

Several freshwater fish diseases are suggested to be sensitive to the rising temperatures associated with climate change (26–30). Also for PKD, water temperature is a key parameter for the disease prevalence and intensity for Swiss wild brown trout populations (8–10, 31), wild Atlantic salmon *Salmo salar* L. in Norway (32), and brown trout (33) and rainbow trout *Oncorhynchus mykiss* (Walbaum) from laboratory experiments (34–37) as examples. Renal pathology and trout mortalities are enhanced at water temperatures of $\geq$15°C (19, 23, 25, 38, 39). Consequently, PKD-associated mortalities and disease symptoms show a seasonal occurrence and appear to be most pronounced during summer and early autumn (8, 32, 34, 40). Temperature could act directly or indirectly on this host-parasite system. Indeed, high temperature could promote spore production by bryozoans (41), accelerate parasite proliferation in fish (18, 23, 36), modulate the host immune response (37) and modify the parasite transmission opportunities (33).

Abbreviations: PKD, Proliferative kidney disease; IBCH, Swiss biological index; WWTP, Wastewater treatment plant; N days $\geq$ x, Number of days with a daily mean temperature $\geq$ x°C.

In addition, freshwater fish diseases can be influenced by a multitude of stressors besides temperature (27, 42, 43), such as habitat quality, water levels, pH, and water quality (26, 44, 45). This last factor might indeed have an influence on PKD prevalence, intensity and mortality as previously investigated (31, 46, 47).

To date, data on the influence of temperature on *T. bryosalmonae* infection of fish is largely derived from laboratory experiments using constant temperature(s). In the wild, the influence of long-term water temperature measurements on the development of the disease has rarely been investigated. Besides temperature, other environmental factors have been individually revealed to influence *T. bryosalmonae* infection, but seldom in a combined way. In addition, rainbow trout is often used as a model species for laboratory investigations of fish disease, including to reproduce PKD in controlled conditions [e.g., (14, 17, 18, 23, 34–37)]. Though, rainbow trout and brown trout react differently to *T. bryosalmonae* infection, in terms of sensitivity to infectious agent and environmental stress (46), intensity of *T. bryosalmonae* infection (48), or temperature-dependant modulation of the parasite (49) for example. Therefore, some of the conclusions based on experiments with rainbow trout might not correspond to the situation of wild brown trout populations in their natural habitat with fluctuating temperatures. Thus, the influence of the course of water temperature over time, with its seasonal, local and diurnal variations, on PKD infection in wild brown trout populations need to be investigated. Moreover, the possible cumulative effects of other environmental factors and their predicted consequences on the disease should also be taken under consideration. Field investigations are therefore of crucial importance for a better understanding of the brown trout—*T. bryosalmonae* host parasite system and possible future implications by the global warming on population dynamics.

The aims of the present study were to (1) determine the correlation between seasonal course of water temperature and PKD prevalence and intensity in wild brown trout populations, (2) identify if additional environmental parameters, such as water quality or ecomorphology, might have cumulative effects on PKD infection, and (3) quantitatively predict the combined consequences of these environmental parameters on the disease prevalence.

MATERIALS AND METHODS

Study Sites

Forty five stations located over 18 rivers of the Canton of Vaud in Switzerland were analyzed (**Figure 1**). For each station, data on *T. bryosalmonae* infection status of fish (prevalence and

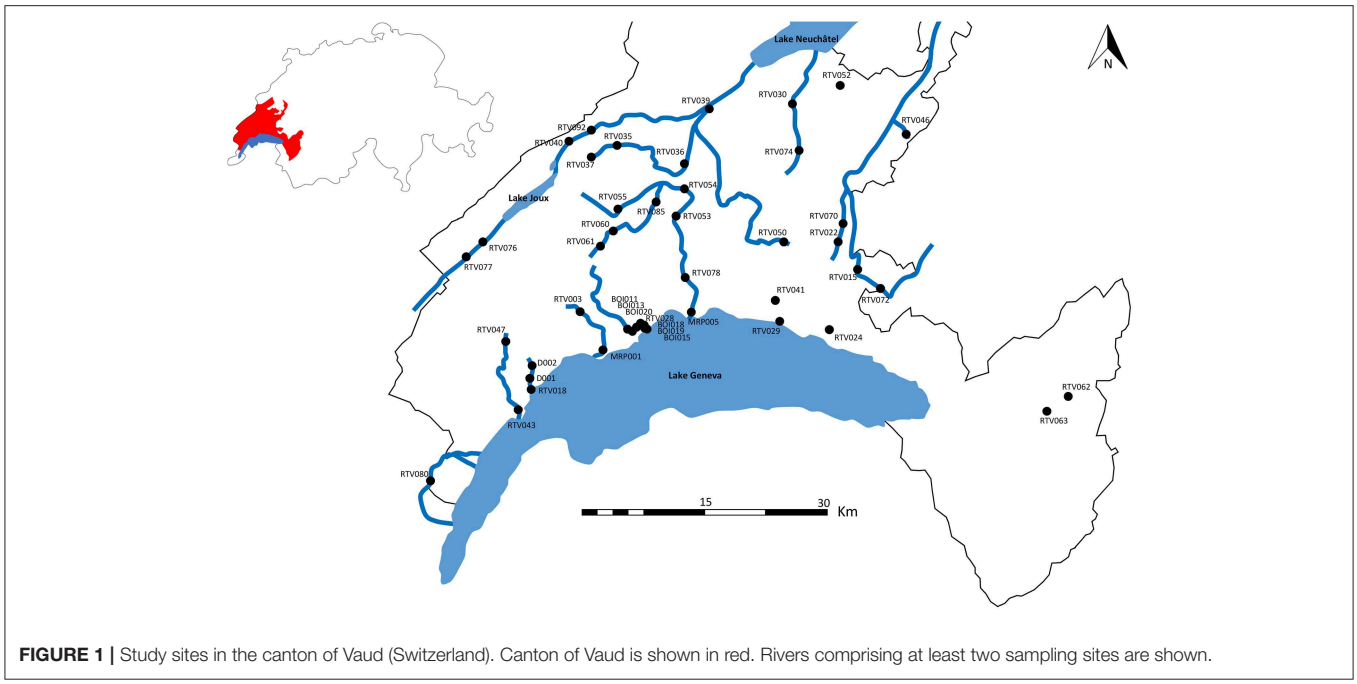

FIGURE 1 | Study sites in the canton of Vaud (Switzerland). Canton of Vaud is shown in red. Rivers comprising at least two sampling sites are shown.

intensity), water temperature, biological water quality assessed through macroinvertebrate sensitivity, presence/absence of a wastewater treatment plant (WWTP) and ecomorphology were collected (**Table 1**).

Temperature Data

Water temperature was measured with temperature loggers (HOBO® Water Temp Pro v2 Data Logger, Onset, Cape Cod Massachusetts, USA) recording the water temperature every 15 min. Before placing the loggers into the water and upon sampling, they were compared to a reference thermometer to determine possible drifts which could then be considered for the temperature values. Temperature measurements were selected from the 1st of March 2014, which was considered as the fry emergence date for streams of the Midlands (Rubin, pers. obs.), until the 31st of August 2014 since fish were sampled at the beginning of September. For two sites (RTV063 and RTV022), water temperatures were extrapolated with upstream or downstream loggers. No temperature data were available for RTV092.

Six types of temperature values are described in the study: (1) the monthly mean temperature from March to August, (2) the mean temperature from the "spring" period (March–May), the mean temperature from the "summer" period (June–August) and the total mean during the whole period, (3) the maximum temperature (absolute maximum and daily mean maximum), (4) the number of days with a daily mean temperature $\geq$ 13°C to $\geq$ 19°C, and (5) the degree days, calculated as the sum of the daily mean temperature values from the 1st of March to the 31st of August 2014.

Additional Environmental Factors

Macroinvertebrate Analysis

A good indicator for the assessment of water quality and ecological quality is the macroinvertebrate community, depending on the observed taxa and their sensitivity to pollutants (50–56). The standardized method "IBCH" (Swiss biological index) developed by the Swiss Federal Office for the Environment (53) is used to determine the biological water quality and ecological status through assessment of the macroinvertebrate community. This method, also applied in Bailey et al. (31), was performed at all 45 study sites except the station RTV41, where water was loaded with a huge amount of sediment due to construction works preventing sample collection. For an assessment of the biological water quality during the life period of sampled fish (March to September 2014), macrozoobenthos samplings were performed between the 12th of March and 22nd of April 2015, following the favorable sampling periods in function of the altitude, defined by the method (53). 35 macroinvertebrates samplings were performed by our team and eight stations were analyzed by collaborators of the department of water protection from the General Directorate of the Environment from the canton of Vaud.

This standardized method (53) consisted of eight macroinvertebrate samplings with a normalized net in function of the substratum and waterflow. After capture, all material was fixed in a container filled with 85% ethanol. In the laboratory, the material was sorted and determined using a binocular loupe. The determination of each individual was performed until family taxonomic level, using the reference book of Tachet et al. (50). Abundance of all taxa was recorded. Finally, the IBCH index, a score between 0 (very low water quality) and 20 (excellent), was calculated based on the diversity of observed taxa and their sensitivity to water quality. Based

TABLE 1 | Study sites, PKD status, temperature, and environmental data.

	PKD data				Environmental data			Temperature data				
Site index	**Number of infected fish**	**PKD prevalence (%)**	**Infection degree**	**Alteration degree**	**IBCH note**	**Upstream WWTP**	**Ecomorphology**	**Mean June [°C]**	**Mean Summer (June-July-August) [°C]**	**Days with daily mean ≥ 14°C**	**Days with daily mean ≥ 15°C**	**Days with daily mean ≥ 16°C**
BOI011	0	0	0.0	0.0	13	Yes	1	13.9	14.5	62	35	4
BOI013	0	0	0.0	0.0	9	Yes	1	14.7	15.1	72	54	24
BOI020	0	0	0.0	0.0	9	No	1	15.0	16.2	85	82	56
RTV028	3	13	3.7	3.7	14	Yes	1	15.3	15.6	83	65	38
BOI018	17	68	3.8	3.5	12	Yes	1	15.0	15.8	84	81	41
BOI019	22	88	4.6	4.4	7	Yes	1	15.1	15.9	85	80	47
BOI015	22	88	4.6	4.4	12	Yes	1	15.7	16.2	86	83	60
D002	0	0	0.0	0.0	8	No	4	15.2	16.3	86	83	68
D001	0	0	0.0	0.0	7	No	1	12.6	13.3	11	1	0
RTV018	0	0	0.0	0.0	6	No	1	11.8	11.3	4	0	0
RTV063	0	0	0.0	0.0	13	No	1	8.5	8.6	0	0	0
RTV062	0	0	0.0	0.0	13	No	1	9.3	9.3	0	0	0
RTV003	0	0	0.0	0.0	14	Yes	2	10.2	7.3	0	0	0
MRP001	0	0	0.0	1.7	17	Yes	1	10.6	9.4	0	0	0
RTV072	1	4	3.0	3.0	17	Yes	1	15.3	15.0	70	50	20
RTV015	1	4	3.0	2.0	17	Yes	1	15.3	15.0	68	50	20
RTV022	8	31	4.4	4.4	12	No	1	14.1	14.4	63	31	10
RTV070	6	24	3.7	3.8	12	No	1	14.4	14.6	67	40	12
RTV046	0	0	0.0	0.0	11	No	1	13.3	14.1	55	19	1
RTV074	24	96	3.0	2.6	11	Yes	1	15.0	15.1	70	55	26
RTV030	12	48	1.8	2.0	15	Yes	1	15.9	15.9	79	67	51
RTV037	0	0	0.0	0.0	15	No	1	11.1	9.7	0	0	0
RTV035	0	0	0.0	0.0	13	Yes	1	13.4	12.4	16	5	0
RTV036	0	0	0.0	0.0	13	Yes	3	14.2	13.5	41	14	1
RTV077	10	38	3.3	2.7	17	No	1	17.5	16.3	79	64	49
RTV076	19	70	3.0	3.1	16	No	2	15.3	13.8	38	30	15
RTV040	0	0	0.0	0.0	14	No	1	10.0	9.7	0	0	0
RTV092	0	0	0.0	0.0	15	No	2	NA	NA	NA	NA	NA
RTV039	1	4	3.0	2.0	8	Yes	4	15.0	13.7	45	31	7
RTV055	0	0	0.0	0.0	14	Yes	3	11.8	10.3	0	0	0
RTV054	8	32	2.3	2.3	14	Yes	2	14.4	13.2	33	12	2
RTV053	23	92	3.7	3.7	13	Yes	4	16.5	15.0	62	48	33
RTV078	9	38	2.8	3.2	8	Yes	1	16.3	15.5	84	59	35
MRP005	18	72	3.9	3.9	9	Yes	2	18.0	16.7	90	74	59
RTV061	0	0	0.0	0.0	11	Yes	1	13.6	12.7	14	6	1

(Continued)

TABLE 1 | Continued

Site index	PKD data				Environmental data			Temperature data				
	Number of infected fish	PKD prevalence (%)	Infection degree	Alteration degree	IBCH note	Upstream WWTP	Ecomorphology	Mean June [°C]	Mean Summer (June-July-August) [°C]	Days with daily mean ≥ 14°C	Days with daily mean ≥ 15°C	Days with daily mean ≥ 16°C
RTV060	21	81	4.0	4.2	15	Yes	1	14.5	13.2	39	13	6
RTV085	26	100	3.7	3.8	15	Yes	1	14.0	13.8	47	23	3
RTV024	0	0	0.0	0.0	10	No	1	15.0	15.1	82	50	17
RTV029	0	0	0.0	0.0	8	No	1	15.3	15.2	71	53	28
RTV041	0	0	0.0	0.0	NA	No	2	14.7	14.7	67	44	20
RTV043	0	0	0.0	0.0	16	No	1	13.6	12.5	17	2	0
RTV047	0	0	0.0	0.0	13	No	1	13.2	13.5	33	2	0
RTV050	0	0	0.0	0.0	15	No	1	13.0	13.1	25	3	0
RTV052	0	0	0.0	0.0	10	No	1	12.3	13.3	22	3	0
RTV080	0	0	0.0	0.0	10	No	1	7.8	7.7	0	0	0

NA, no data for this site.

on this index, a water quality class was assigned to each station, with the scale: very good water quality = index 17–20, good = 13–16, medium = 9–12, poor = 5–8, bad = 0–4. The macrozoobenthos samplings were performed relating to ethical approvals (permission delivered by the Service of Hunting, Fishing and Surveillance of the Biodiversity and Landscape Division from the General Directorate of the canton of Vaud).

Wastewater Treatment Plant

The presence/absence of a wastewater treatment plant effluent upstream of the study site was also determined using topographic maps.

Ecomorphology

Ecomorphology is also a potential stressor affecting fish health (57–59) and fish density in streams (60–62). The ecomorphology was determined using the standardized method "Ecomorphology" from the Swiss Federal Office for the Environment (63). This method aims to determine the structural diversity of the stream, its connectivity and interactions with the surrounding area. A class was attributed to each of 45 river sections depending on the state of the riverbed, riverbank and shore, following the scale 1 = natural, 2 = little affected, 3 = very affected, 4 = artificial, 5 = underground pipe. These data were obtained from the geodatabase from the Federal Office of Topography (Swisstopo) (64).

Fish Analysis

Twenty five young-of-the-year (YOY) brown trout were sampled by electrofishing at each site, resulting in a total number of 1,118 fish. The sampling campaign took place over a period of 10 days, between the 1st and 11th of September 2014. This period was chosen based on previous PKD studies in Swiss streams (8–10) and PKD analysis in the river Boiron de Morges (Rubin, unpublished data), showing that the peak of *T. bryosalmonae* infection in brown trout occurs in late August, beginning of September. After this period, typical PKD kidney alterations could still be visible but parasites might already have been cleared out by the immune system of the fish or have left the fish, causing therefore difficulties for the diagnosis (10).

After electrofishing, juvenile brown trout (total body length 40–118 mm, mean of 76 mm ± standard deviation of 13 mm) were euthanized with an overdose of MS222 (3-aminobenzoic acid ethyl ester, 300 mg l-1, Argent Chemical Laboratories). The fish body cavity was opened, and whole animals were fixed in 4% buffered formalin until later kidney removal in the laboratory. Whole fixed kidneys were embedded in paraffin. Organs were cut using routine histological methods and stained with haematoxylin and eosin (H&E). One section of the full length of the kidney was prepared per fish. Thus, one slide per fish was examined for the presence of *T. bryosalmonae*. The degree of infection (infection intensity corresponding to an estimation of the numbers of observed parasites) and the alteration degree (tissue proliferation due to pathological alterations) were recorded for each sample using a microscope. For each slide a common score system from 0 (no parasite/no

alteration) to 6 (at least 10 parasites per high power field with 400x magnification/severe alteration) was applied as in Bettge et al. (18) and Schmidt-Posthaus et al. (39). If at least one parasite was observed, the slide was considered as histologically positive. The infection/alteration degree per station were then calculated as the mean of all infection/alteration scores from a site. The prevalence of PKD (%) was calculated as the percentage of *T. bryosalmonae* infected individuals within all sampled animals at a particular site.

Histology was chosen for PKD diagnosis instead of Polymerase Chain Reaction (PCR) due to time, material and crew resources in the field. This method also permits to assess the severity of pathological response and the state of the disease. However, histological examination may have missed the parasites for fish with very low infection levels. Thus, immunohistochemistry was performed on three randomly selected fish per station where no *T. bryosalmonae* parasites were observed on any H&E stained slide, in order to corroborate negative results. Therefore, immunohistochemistry was performed on 78 samples using an anti-*T. bryosalmonae* (PKX) monoclonal antibody (AquaMab-P01, Aquatic Diagnostic Ltd., Stirling, Scotland) applying the method described by Bettge et al. (18).

Fish samplings were performed relating to ethical approvals (permission number VD2871 delivered by the Service of Consumption and Veterinary business of the canton of Vaud).

Statistical Analysis

The sample size used for the statistical analysis, contains 1,068 samples. Data of sites RTV041 and RTV092 were excluded because of the absence of, respectively, IBCH index and temperature data.

The software RStudio (version 1.1.463) was used to perform the statistical analysis. An univariate analysis was conducted using Pearson's coefficient to investigate the correlation between the prevalence of *T. bryosalmonae* infected fish, infection degree, alteration degree and temperature data, as well as potentially aggravating environmental parameters. Student's *t*-test was also applied to test the significant differences ($p < 0.05$) in the means of temperature variables and other environmental factors between *T. bryosalmonae* positive fish and PKD healthy trout from all sampling sites.

Multivariate analysis was applied using a linear probability model (LPM) and a logistic model (Logit) that quantified the implication of the different parameters on the PKD infection. The following equation was applied for the linear regression:

$$PKD_i = \beta_0 + \beta_1 * Temp_j + \beta_2 * IBCH_j + \beta_3 * WWTP_j + \beta_4 * Ecomorphology_j + \epsilon_i$$

Where:

PKDi is a binary variable taking the value of 1 if the trout *i* is infected with *T. bryosalmonae*, and 0 otherwise,
Temp is an indicator of temperature,
IBCH is the value of the IBCH index,
WWTP is a binary variable with a value of 1 if a WWTP is present upstream the study site, and 0 otherwise,
Ecomorphology is a categorial variable (from 1 for a natural section to 4 for a very anthropized sector),
ϵ is the error term or the residual variation that the model cannot explain,
Index *i* represents variable at the trout level and index *j* represents variable at the site level.

The average marginal effect was applied for the Logit model, in order to get comparable results and not "log odd ratio" data. The conditional expectation was also applied to predict the variation of PKD prevalence due to temperature, while controlling the other environmental factors.

RESULTS

Water Temperature

A selection of the temperature results is given in **Table 1** (all temperature data are given in **Supplementary Material**). Highest mean temperature during the study period (March to August 2014), and during the summer (June to August) was observed

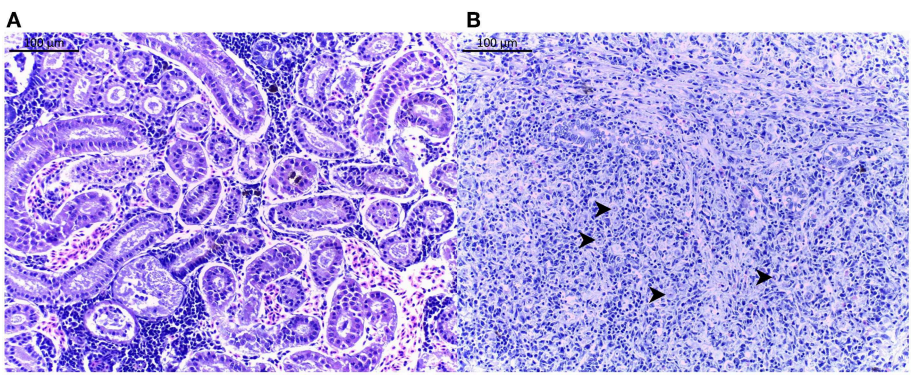

FIGURE 2 | Histological pictures of brown trout *Salmo trutta* posterior kidney. **(A)** Histological assessment of an infection score of 0 (no parasite). **(B)** Histological assessment of an infection score of 6 (severe infection). Some parasites *Tetracapsuloides bryosalmonae* are shown (arrows). Scale bar = 100 µm. Pictures are taken from H&E stained slides.

TABLE 2 | Pearson's correlation between *T. bryosalmonae* infected brown trout prevalence, infection degree, alteration degree, and variables.

Variables	PKD prevalence	Infection degree	Alteration degree
Mean temperature of march [°C]	0.069	0.091	0.098
Mean temperature of April [°C]	0.209	0.209	0.199
Mean temperature of May [°C]	0.311	0.296	0.286
Mean temperature of June [°C]	0.406	0.366	0.351
Mean temperature of July [°C]	0.304	0.289	0.267
Mean temperature of August [°C]	0.307	0.297	0.276
Mean temperature of spring (March–May) [°C]	0.213	0.216	0.211
Mean temperature of summer (June–August) [°C]	0.346	0.325	0.304
Total mean temperature [°C]	0.306	0.294	0.279
Maximum temperature [°C]	0.146	0.114	0.106
Maximum daily mean temperature [°C]	0.315	0.307	0.301
Days with daily mean temperature ≥ 13°C	0.315	0.298	0.282
Days with daily mean temperature ≥ 14°C	0.358	0.343	0.322
Days with daily mean temperature ≥ 15°C	0.373	0.363	0.337
Days with daily mean temperature ≥ 16°C	0.360	0.350	0.323
Days with daily mean temperature ≥ 17°C	0.308	0.288	0.266
Days with daily mean temperature ≥ 18°C	0.224	0.202	0.187
Days with daily mean temperature ≥ 19°C	0.150	0.138	0.116
Degree days	0.307	0.295	0.277
IBCH note	0.044	0.002	−0.001
WWTP	0.321	0.303	0.295
Ecomorphology	0.041	0.026	0.042

at the outlet of the river Venoge (MRP005) with a value of, respectively, 13.8 and 16.7°C. Mean temperature of June reached <10°C in three stations, was comprised between 10 and 15°C in 28 cases, and surpassed 15°C in 13 stations. The warmest daily mean temperature (20.6°C) was observed in the Orbe (RTV077) and the Venoge (MRP005). Some stations never reached a daily mean temperature of ≥15°C, while a maximum of 83 days was measured in the Boiron (BOI015) and the Dullive (D002). The degree days varied from 1,090 (RTV063) to 2,539 (MRP005).

Additional Environmental Factors

IBCH scores were calculated for each site (**Table 1**) based on the sensitivity and abundance of macroinvertebrate taxa. The lowest obtained IBCH score was 6 (RTV018) and the highest IBCH score obtained was 17 (MRP001, RTV015, RTV072, and RTV077). Four stations corresponded to the water quality class "very good," 20 belonged to the class "good," 13 sites were classified as "medium" and seven were in the class "poor." Thus, all water quality classes were represented in the samples, except the poorest class.

A WWTP was present upstream at 24 of the study sites (53.3%) (**Table 1**). Among them, 15 stations were assessed as PKD-positive (62.5%), with prevalence ranging from 4 to 100% (mean of 52 ± 34%) of *T. bryosalmonae* infected fish.

The ecomorphology class indicates the condition of the riverbed. Thirty four stations belonged to the class 1, six were in the class 2, two belonged to class 3 and three were considered as anthropized (class 4) (**Table 1**). No site belonged to the class 5.

PKD Manifestation

Stocking of fry or juvenile brown trout for sustaining natural populations was performed since several years in 16 study sites (stocking performed at a maximum of 2 km upstream the study site). Thus, for a comparison of wild fish between all sites, no stocking took place before our fish sampling in 2014, in agreement with the fish inspectorship of the canton of Vaud. All YOY caught here originate therefore from natural spawning. Among the 45 sampled sites, 19 stations (42.2%) were assessed as *T. bryosalmonae*-positive (**Table 1**). The disease was present in the rivers Boiron de Morges, Broye, Flon de Carrouge, Mentue, Orbe, Venoge, and Veyron. Presence of *T. bryosalmonae* was observed in 251 brown trout from the 1,118 sampled animals (22.5%). The observed prevalence ranged from 0 to 100%. Among the 19 PKD-positive sites, the highest site-specific infection degree (score of 4.64) was found in the Boiron (BOI019), while the lowest (score of 1.84) was seen in the Mentue (RTV030) (**Figure 2**). However, even if PKD prevalence was low (≤10%), infected fish showing high infection degree (≥3.0) were found. When considering the degree of alteration, mean values between 1.7 to 4.4 at sites with infected fish were found.

Correlation of Environmental Variables and PKD

Pearson's correlation coefficient between *T. bryosalmonae* prevalence/infection degree/alteration degree and temperature parameters/other environmental variables is given in **Table 2**. A positive linear relation appeared between infected fish/infection degree/alteration degree and every temperature variable but remained rather low ($r < 0.5$). The strongest correlation was obtained with the mean temperature of June ($r = 0.406$ with prevalence, 0.366 with infection degree, 0.351 with alteration degree), followed by the number of days with a daily mean temperature ≥15°C (N days ≥ 15) ($r = 0.373$ with prevalence, 0.363 with infection degree, 0.337 with alteration degree). No correlation was found between PKD data and IBCH index ($r = 0.044$ with prevalence, 0.002 with infection degree, −0.001 with alteration degree) and ecomorphology ($r = 0.041$ with prevalence, 0.026 with infection degree, 0.042 with alteration degree), in contrast to the presence of an upstream WWTP ($r = 0.321$ with prevalence, 0.303 with infection degree, 0.295 with alteration degree). Site-specific infection degree and

prevalence of infected fish were positively correlated ($r = 0.808$), as well as alteration degree and prevalence of infected fish ($r = 0.750$). Infection degree and alteration degree were strongly correlated ($r = 0.952$).

Average Differences

Significant differences in the means of temperature parameters between sites with infected and not infected fish were observed. Mean temperature of June was significantly higher (mean of 15.4°C) for sites with infected fish than for sites with trout without parasites (mean of 13.4°C) (**Figure 3A**). The same applied for the N days ≥ 15 (**Figure 3B**).

The presence of an upstream WWTP significantly positively influenced the PKD prevalence (**Figure 4A**). On the contrary, no significant difference appeared between sites with infected and sites with parasite-free fish for IBCH score (**Figure 4B**) and ecomorphology (**Figure 4C**).

Quantification of the Predicted Effect of Temperature and Additional Environmental Factors on PKD Prevalence

Two models, a linear model (LPM) and a logistic model (Logit), were compared to quantify the predicted variation of PKD prevalence due to an increase of one unit of the temperature variables and other environmental factors. These analyses were performed by separating the temperature variables in two categories (temperature means and N days ≥ x°C), which permit an estimate of the best temperature indicator.

Table 3a (LPM results) and **Table 3b** (Logit results) show the estimated effect of an increase of 1°C of the different means of temperatures on the prevalence of infected fish. All mean temperature parameters were significantly associated with infection prevalence ($p < 0.001$). For example, the predictions showed that a one-degree increment elevation in the mean temperature of June induces an increase of 6.9% of the prevalence of infected fish for the LPM [**Table 3a**, Model (1)] and an increase of 9.9% for the Logit [**Table 3b**, Model (1)].

The temperature parameter that explained at best the variance of the prevalence of infected fish (R2) was obtained with the model using the mean temperature of June [**Table 3a**, Model (1), R2 = 0.211] followed by the model taking into account the mean temperature of summer [Model (4), R2 = 0.196] for the LPM. The same findings appeared for the Logit [**Table 3b**, Model (1), Pseudo R2 = 0.373; Model (4), Pseudo R2 = 0.339]. **Table 4a** (LPM) and **Table 4b** (Logit) give the quantification of the average influence of the N days ≥ x°C and other environmental factors on the prevalence of the disease. Every temperature variable was significant ($p < 0.01$). For the LPM model, the N days ≥ 16 appeared to be the best explanatory temperature variable (R2 = 0.208), followed by the N days ≥ 15 (R2 = 0.203). The N days ≥ 14 (Pseudo R2 = 0.313) and then the N days ≥ 15 (Pseudo R2 = 0.309) had the higher Pseudo R2 for the Logit models. Therefore, all models showed that an increase in water temperature induced an increment in the predicted prevalence of infected fish. For the mean temperature category, the mean temperature of June and the mean temperature of the summer period explained at best the variance of the infection prevalence, both LPM and Logit combined. For the number of days with a daily mean temperature ≥ x°C, the LPM and Logit did not result in the same findings for the best explanatory variable for the variance of PKD prevalence (respectively, N days ≥ 16 and N days ≥ 14) but were coincident for the second explanatory variable (N days ≥ 15). Variance of each parameter was better explained with the Logit model than with the LPM model. However, R2 and Pseudo R2 remained low for every model.

Concerning the additional environmental parameters, the IBCH index was significantly associated with PKD prevalence ($p < 0.05$) only in Logit models (four out of five models dealing with means of temperature and in five of the eight models of the number of days with a daily mean ≥ x°C). An increase of one unit in the IBCH score induced a predicted increase smaller than 2.1% in the PKD prevalence. The presence of an upstream WWTP was significantly linked to the disease ($p < 0.01$) in all models. The presence of such a facility increased the predicted PKD prevalence between 18 and 30.8% at a given site. On the contrary, ecomorphology was never significantly linked to PKD prevalence ($p < 0.05$). Therefore, presence of an upstream WWTP seemed to play a role in the predicted PKD prevalence, while IBCH score and ecomorphology had less influence.

Since both LPM and Logit models predicted that the mean temperature of June and the N days ≥ 15 explained well the variance of the infection prevalence, these two parameters were chosen for the following graphs. The LPM and Logit predicted PKD prevalence depending on the mean temperature of June, with study sites projection, are shown (**Figures 5A,B**). Infected fish were detected in stations with a mean temperature in June of 14°C at least. LPM predicted negative prevalence for temperature below 10°C, which highlighted limits of the model. On the contrary, the prediction issued from the Logit better corresponds to the observations. The predicted prevalence started to be positive from a mean temperature of June at 13°C and then increased. This model predicted a marked threshold effect from which infected fish may be found in the wild. The predictions of LPM and Logit models in function of the N days ≥ 15 are shown (**Figures 6A,B**). Infected fish were observed at sites with a mean temperature of ≥15°C for at least 12 days. The difference between the LPM and Logit model was weaker compared to the prediction of the mean temperature of June.

DISCUSSION

We performed a large-scale field investigation with longitudinal temperature measurements to demonstrate that temperature does indeed influence PKD prevalence and intensity in the wild. The possible combined influence of additional environmental parameters upon disease dynamics was also tested. Moreover, we developed a statistical model to highlight the predicted increase of PKD prevalence with rising water temperatures and/or additional environmental factors. Our analysis confirmed a positive relationship existing between water temperature and PKD prevalence and intensity in wild trout. The mean temperature of June and the N days ≥ 15 were the two parameters

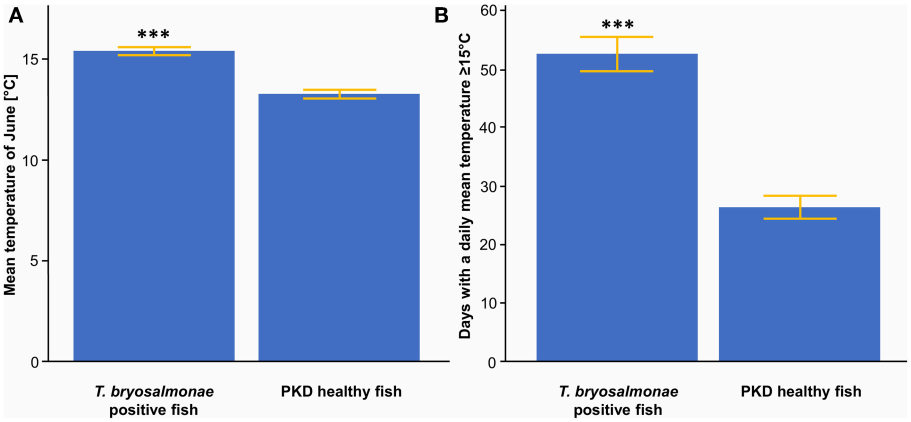

FIGURE 3 | (A) Mean temperature of June between *T. bryosalmonae* infected and PKD healthy fish. **(B)** Number of days with a daily mean temperature ≥ 15°C between *T. bryosalmonae* infected and PKD healthy fish. Yellow lines indicate standard error, asterisks indicate levels of significance (*t*-Test), ***$p < 0.001$.

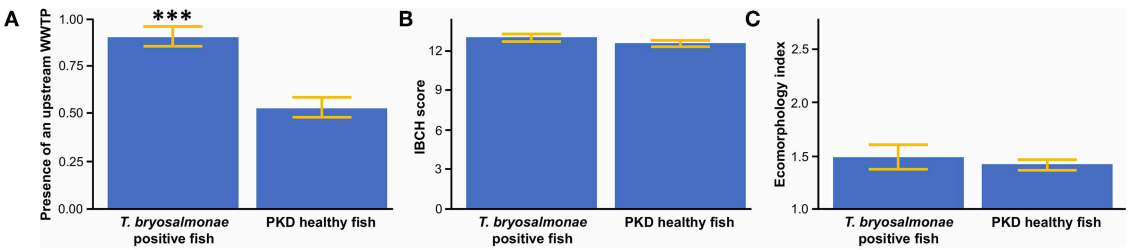

FIGURE 4 | (A) Mean presence of an upstream wastewater treatment plant (WWTP) between *T. bryosalmonae* infected and PKD healthy fish. **(B)** Mean biological score (IBCH) between *T. bryosalmonae* infected and PKD healthy fish. **(C)** Mean ecomorphology index between *T. bryosalmonae* infected and PKD healthy fish. Yellow lines indicate standard error, asterisks indicate levels of significance (*t*-test), ***$p < 0.001$.

that were most strongly associated with PKD prevalence. The mean temperature of the summer period (June to August) was also a strong indicator for the prevalence of infected fish. Depending on the models, the macroinvertebrate index might sometimes have a positive correlation with the disease prevalence. The presence of an upstream WWTP showed significant aggravating influence on the infection prevalence, while the ecomorphology had less importance. Logistic model had a better explanatory power than linear model. However, the variance of the models remained low, suggesting that other parameters than the factors tested here might also have an influence on the disease. Thus, our findings (1) increased the knowledge of the implication of water temperature in PKD prevalence and intensity by investigating the impact of long-term temperature data, with seasonal, diurnal and site-specific changes, on PKD infection, in a large number of field sites within a specific region, (2) determined other disease modulating factors, such as water quality, and (3) quantitatively predicted the further impact of environmental parameters on the given prevalence.

PKD Manifestation

In our study, PKD infected fish were generally detected in the downstream part of the rivers, while stations close to the source were free of the disease, as observed in the Boiron (upstream sites BOI011 and BOI013 were PKD free, while infected fish were found from the site RTV028 and downstream), the Venoge (no infected fish were observed in the site RTV055 but *T. bryosalmonae* positive fish appeared from station RTV054 and downstream) and the Veyron (upstream site RTV061 was free of the disease while parasites were found in downstream stations RTV060 and RTV085). Based on a study of 287 sampling sites throughout Switzerland, Wahli et al. (38) observed that the disease was present at an altitude lower than 800 m in most cases. Feist et al. (65) observed PKD prevalence ranging from 0 to 43% in England, which corresponds also to the findings of Peeler et al. (66) (PKD prevalence ranging from 2.5 to 36%). In our study, PKD prevalence ranged from 0 to 100% at a scale level of one canton, as observed by Wahli et al. (38) at a scale of a country. Therefore, PKD prevalence is also highly spatially variable, even within the same region.

Relationship Between Temperature and PKD Infection

The influence of water temperature on PKD infection has been investigated mostly in laboratory with rainbow trout as model species, but studies comprising *in situ* water temperature data sets over seasons and their impact on wild brown trout populations

Table 3a | Linear predicted increase/decrease of *T. bryosalmonae* infected fish prevalence due to an increase of 1 unit in the mean temperature variables and additional environmental parameters.

	Model 1	Model 2	Model 3	Model 4	Model 5
Mean temperature June	0.069*** (0.005)				
Mean temperature July		0.048*** (0.004)			
Mean temperature August			0.050*** (0.004)		
Mean temperature Summer				0.057*** (0.004)	
Total mean temperature					0.063*** (0.005)
IBCH (note)	0.006 (0.004)	0.013** (0.005)	0.014** (0.005)	0.012** (0.004)	0.013** (0.005)
WWTP	0.181*** (0.027)	0.230*** (0.026)	0.235*** (0.026)	0.216*** (0.026)	0.212*** (0.027)
Ecomorphology	−0.030* (0.014)	0.001 (0.015)	0.002 (0.015)	−0.006 (0.015)	−0.014 (0.015)
N	1,068	1,068	1,068	1,068	1,068
R2	0.211	0.181	0.188	0.196	0.169

Robust standard error in parentheses.
**p < 0.10, **p < 0.05, ***p < 0.01.*

Table 3b | Logistic predicted increase/decrease of *T. bryosalmonae* infected fish prevalence due to an increase of 1 unit in the mean temperature variables and additional environmental parameters.

	Model 1	Model 2	Model 3	Model 4	Model 5
Mean temperature June	0.099*** (0.007)				
Mean temperature July		0.065*** (0.006)			
Mean temperature August			0.069*** (0.006)		
Mean temperature Summer				0.084*** (0.007)	
Total mean temperature					0.100*** (0.010)
IBCH (note)	0.006 (0.004)	0.016*** (0.004)	0.019*** (0.004)	0.016*** (0.004)	0.020*** (0.004)
WWTP	0.190*** (0.025)	0.225*** (0.024)	0.235*** (0.024)	0.213*** (0.084)	0.206*** (0.250)
Ecomorphology	−0.021* (0.012)	0.021* (0.012)	0.026* (0.012)	0.015 (0.012)	0.001 (0.012)
N	1,068	1,068	1,068	1,068	1,068
Pseudo R2	0.373	0.299	0.315	0.339	0.296

Robust standard error in parentheses.
**p < 0.10, **p < 0.05, ***p < 0.01.*

are scarce. Wahli et al. (38) correlated PKD prevalence with altitude (as a substitution for temperature) in a wide variety of sites spread all over Switzerland, but they found no relationship between these two elements. On the contrary, in this study, a relationship between longitudinal temperature data and PKD prevalence and intensity was assessed within a field setting. *T. bryosalmonae* infection might appear when temperature reaches 9°C (36). Clinical signs and mortality are enhanced when the water temperature is >15°C (19, 23, 25, 39). Bettge et al. (18) showed that renal pathology of rainbow trout and parasite numbers were more intense at elevated temperature. Immune response strategy chosen by rainbow trout is also dependant of water temperature (37). Moreover, high temperature results in an accelerated rate for parasite release of brown trout, modifying therefore the parasite transmission period (33).

Our results do not support the findings of Gay et al. (36) since infected fish were observed in sites with warmer temperature than 9°C, even if trout were also sampled in colder streams. However, Gay et al. used rainbow trout as model species and experiments were performed in the laboratory. We also observed infected fish in sites with a minimum of 12 days with a daily mean of ≥15°C, which is slightly < the 14 to 28 days at 15°C predicted by Fischnetz (67) for PKD development in the wild. Lewisch et al. (68) found a significant increased number of *T. bryosalmonae* infected brown trout in Austria at sampling sites comprising a minimum of 115 days with at least 1 hourly maximum water temperature measurement exceeding 15°C. However, no long-term water temperature measurements at the precise sampling sites were used for these two studies, which might explain the differences with our results.

Based on statistical analysis, we observed that, when comparing the LPM and Logit, the Logit seemed to better fit to the data. This model should therefore be favored for further investigations. We found that the explanatory power of the variance from the mean temperature of summer (Pseudo R2 = 0.373) was also very close to the mean temperature of June results (Pseudo R2 = 0.339). Therefore, for a more global approach, the mean temperature of the summer period might also be a good indicator, instead of a precise month. Indeed, monthly temporal variations are more likely to depend in a particular

Table 4a | Linear predicted increase/decrease of *T. bryosalmonae* infected fish prevalence due to an increase of 1 unit in the in the number of days with a daily mean ≥ x°C variables and additional environmental parameters.

	Model 1	Model 2	Model 3	Model 4	Model 5	Model 6	Model 7	Model 8
Days with daily mean ≥ 13°C	0.004*** (0.000)							
Days with daily mean ≥ 14°C		0.004*** (0.000)						
Days with daily mean ≥ 15°C			0.005*** (0.000)					
Days with daily mean ≥ 16°C				0.007*** (0.001)				
Days with daily mean ≥ 17°C					0.012*** (0.001)			
Days with daily mean ≥ 18°C						0.016*** (0.003)		
Days with daily mean ≥ 19°C							0.035*** (0.007)	
Degree days								0.004*** (0.000)
IBCH (note)	0.012* (0.005)	0.012** (0.004)	0.014** (0.004)	0.012** (0.004)	0.004 (0.004)	−0.001 (0.004)	−0.004 (0.004)	0.015** (0.005)
WWTP	0.222*** (0.026)	0.200*** (0.026)	0.191*** (0.027)	0.221*** (0.026)	0.265*** (0.026)	0.272*** (0.026)	0.290*** (0.026)	0.209*** (0.026)
Ecomorphology	−0.002 (0.015)	−0.002 (0.015)	−0.009 (0.015)	−0.024 (0.015)	−0.028 (0.015)	−0.02 (0.015)	−0.016 (0.016)	−0.018 (0.015)
N	1,068	1,068	1,068	1,068	1,068	1,068	1,068	1,068
R2	0.18	0.194	0.203	0.208	0.191	0.148	0.133	0.171

Robust standard error in parentheses.
**p < 0.10, **p < 0.05, ***p < 0.01.*

Table 4b | Logistic predicted increase/decrease of *T. bryosalmonae* infected fish prevalence due to an increase of 1 unit in the in the number of days with a daily mean ≥ x°C variables and additional environmental parameters.

	Model 1	Model 2	Model 3	Model 4	Model 5	Model 6	Model 7	Model 8
Days with daily mean ≥ 13°C	0.005*** (0.000)							
Days with daily mean ≥ 14°C		0.005*** (0.000)						
Days with daily mean ≥ 15°C			0.005*** (0.000)					
Days with daily mean ≥ 16°C				0.006*** (0.001)				
Days with daily mean ≥ 17°C					0.010*** (0.001)			
Days with daily mean ≥ 18°C						0.013*** (0.002)		
Days with daily mean ≥ 19°C							0.031*** (0.005)	
Degree days								0.005*** (0.001)
IBCH (note)	0.015** (0.004)	0.017*** (0.004)	0.017*** (0.004)	0.014*** (0.004)	0.005 (0.004)	0.001 (0.004)	−0.002 (0.004)	0.021*** (0.004)
WWTP	0.225*** (0.024)	0.203*** (0.024)	0.201*** (0.025)	0.234*** (0.025)	0.282*** (0.026)	0.285*** (0.026)	0.308*** (0.027)	0.204*** (0.028)
Ecomorphology	0.017 (0.012)	0.022* (0.012)	0.015 (0.012)	−0.003 (0.012)	−0.013 (0.013)	−0.019 (0.014)	−0.015 (0.014)	−0.001 (0.001)
N	1,068	1,068	1,068	1,068	1,068	1,068	1,068	1,068
Pseudo R2	0.299	0.313	0.309	0.304	0.277	0.214	0.201	0.298

Robust standard error in parentheses.
**p < 0.10, **p < 0.05, ***p < 0.01.*

year than the mean of the whole summer season. Taking into account the summer mean temperature is therefore a possibility to reduce the influence of a specific month, in particular for year to year comparisons. Given the water temperature regime of a stream is known, our results permit to assess if the thermal conditions are reached for the development of the infection or to estimate the predicted increase of PKD prevalence following rising water temperature due to global warming. Solutions to prevent this increase of water temperature might therefore be proposed to counteract the possible spread of the disease. Our model estimated that an increase of one degree in the mean temperature of summer might result in an increase of 5.7% in infection prevalence. Therefore, with rising temperature in Switzerland (69–71) due to the ongoing global warming (72), the PKD infection prevalence might intensify in already infected zones possibly leading to the parasite colonizing new areas, thus, extending the geographic range of *T. bryosalmonae* (16, 19, 29). This phenomenon is also relevant for other emerging diseases sensitive to temperature (28, 30), such as furunculosis caused by the bacterium *Aeromonas salmonicida* (73) or enteric redmouth disease due to *Yersinia ruckeri* (74).

The Relationship Between Additional Environmental Factors and PKD Infection Prevalence

Studies have shown that low water quality can induce a decrease in freshwater biodiversity, such as macroinvertebrate community (56, 75, 76) or fish diversity (77, 78). In this study, we investigated

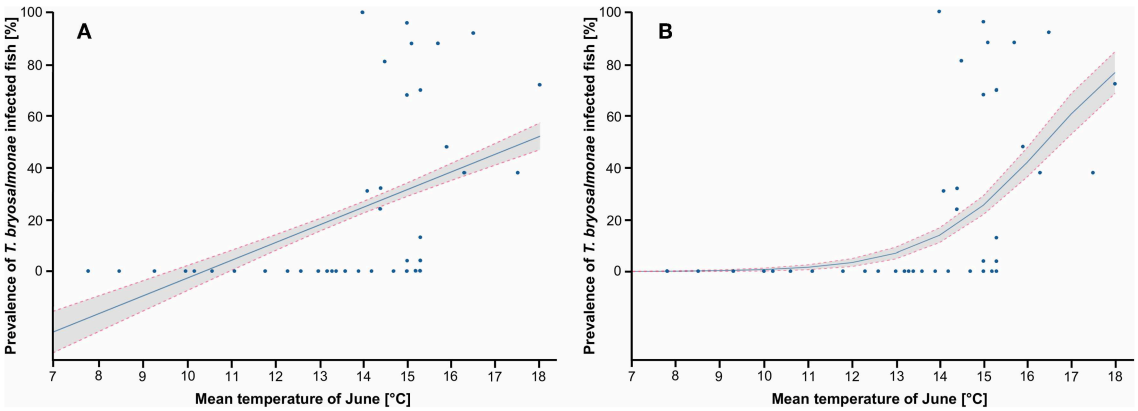

FIGURE 5 | Prediction of the prevalence of *T. bryosalmonae* infected fish depending on the mean temperature of June. **(A)** Prediction of the linear probability model (LPM), R2 is 0.211. **(B)** Prediction of the logistic model (Logit), Pseudo R2 is 0.373. Blue points correspond to study sites, blue line corresponds to the prediction, gray zone corresponds to the 95% confidence intervals.

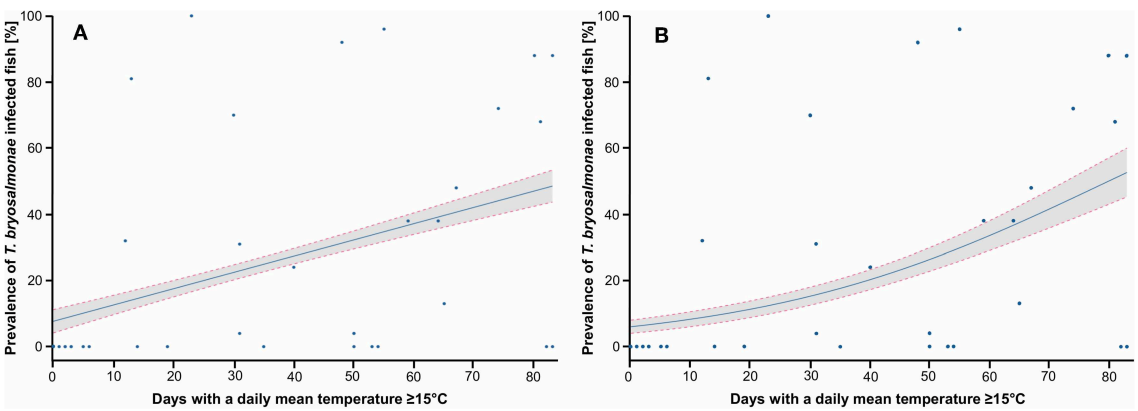

FIGURE 6 | Prediction of the prevalence of *T. bryosalmonae* infected fish depending on the number of days with a daily mean temperature ≥ 15°C. **(A)** Prediction of the linear probability model (LPM), R2 is 0.203. **(B)** Prediction of the logistic model (Logit), Pseudo R2 is 0.309. Blue points correspond to study sites, blue line corresponds to the prediction, gray zone corresponds to the 95% confidence intervals.

the combined effect of different environmental factors and their relationship with PKD disease dynamics. Our analyses revealed that PKD prevalence was not strongly influenced by the state of the macroinvertebrate community measured by means of the Swiss biological index "IBCH," which assessed water quality depending on the presence or absence of taxon sensitive to pollutants, as stoneflies for example. The presence of macroinvertebrate community is also driven by other factors, such as hydrology and habitat of a stream and does not focus only on water pollutants. The benthic fauna might therefore not be an ideal predictor for the disease presence.

We also analyzed the presence of an upstream WWTP as in indicator for water quality. Schmidt et al. (79) explored the effect of a sewage plant effluent on rainbow and brown trout health. When comparing trout kept in tap water and fish raised in water with an input of water coming from the WWTP, they found some alterations in internal organs but nothing that highlighted a real impact of low water quality on the decrease of brown trout populations. Bernet et al. (80) observed a decrease in brown trout health due to wastewater effluent. El-Matbouli and Hoffman (47) investigated the influence of water quality on *T. bryosalmonae*-rainbow and brown trout system. A significant difference in the PKD prevalence from sampled trout upstream and downstream of a WWTP effluent was observed. Significant differences in PKD prevalence and parasite intensity also appeared between two environmentally similar sites distant of 400 m, upstream and downstream of a WWTP in Switzerland (31). Our results corroborate these findings, since the presence of a WWTP appeared to be a significant aggravating parameter. Indeed, PKD prevalence increased by 20% if there was a WWTP present. However, the present study as well as the abovementioned referenced reports do not allow to assess if the decrease in water quality influences the disease prevalence either by directly affecting the fish health making them more vulnerable to the parasite infection, or influenced indirectly *T. bryosalmonae* infection by favoring the presence of

bryozoans, since polluted water seems to favor the proliferation of filter feeding bryozoans (19, 36) which, in turn, increases the number of parasites in water. For instance, Hartikainen et al. (81) showed that an increase in nutrient concentration promotes bryozoan biomass and growth rates of *Fredericella sultana*, the most common bryozoan hosting *T. bryosalmonae*. Moreover, the concentration of statoblast was significantly promoted by phosphorus concentrations. A possibility for discriminating these two hypotheses would be to test the direct impact of water quality on fish health by performing a controlled experiment with infected trout raised in good and low water quality. Therefore, even if water quality has been considerably improved by sewage treatment in Switzerland (60) and the majority of WWTP effluent respect the Swiss legislation (82), we found that WWTP effluents play a role in the infection and might thus be considered when studying PKD in the wild. However, the variable used here was "presence" or "absence" of a WWTP, therefore more detailed investigations of this factor should be conducted, such as taking into account the dilution ratio of the effluent in the stream, the distance between the WWTP and the study site or the inhabitant equivalent of WWTP, which might reveal further information on the influence of WWTP effluents.

We observed that ecomorphology was not a discriminant factor for PKD prevalence. Thus, this parameter does not seem to act directly on the infection. However, this factor might characterize the habitat complexity of the stream, which could impact the trout density (61–63). Moreover, a stream with canalized riverbanks without trees could lead to higher water temperature. With rising temperature due to global change, this situation could become even worse. Therefore, especially in the downstream part of anthropized rivers, some habitats are susceptible to turn thermally unsuitable for brown trout, which could lead to a population decrease (6), as suspected in the southern periphery of brown trout distribution range (83–85). Thus, restoration measures should be taken in rivers, as planting trees along open streams, which will thus reduce the temperature increase by making shadow or remove physical barriers to restore the migration to upstream thermal refuges.

CONCLUSION

Our results highlight the combined influence of water temperature, water quality and ecomorphology on PKD prevalence and intensity in wild brown trout populations. Water temperature appeared to be the major factor for PKD prevalence. When the necessary water temperature conditions are reached, the presence of an upstream WWTP might also play a role. These findings are crucial, especially in the context of global warming. Indeed, an increase in summer mean temperature and temperature variability might have consequences in the *T. bryosalmonae*-brown trout system, together with the potential geographical expansion of PKD. Therefore, knowing the significant parameters influencing the infection will allow to identify and to predict the potential disease hot spots in the future. Solutions to prevent this temperature increase and actions against the further spread of the disease might be proposed in terms of river management, mainly in downstream parts of river where water temperatures are higher and water quality is reduced.

DATA AVAILABILITY

The datasets generated for this study are available on request to the corresponding author.

ETHICS STATEMENT

This study was carried out in accordance with the recommendations of the Swiss Confederation. The protocol of macrozoobenthos sampling was approved by the Service of Hunting, Fishing, and Surveillance of the Biodiversity and Landscape Division from the General Directorate of the canton of Vaud, and the protocol of fish sampling was approved by the Service of Consumption and Veterinary business of the canton of Vaud (permission number VD2871).

AUTHOR CONTRIBUTIONS

AR, J-FR, and TW conceived the experiment. PdC, AR, and J-FR performed the sampling. PdC and AR carried out the laboratory analysis. CB, PdC, AR, J-FR, HS, and TW analyzed the data. AR wrote the draft of the paper. All authors commented on the manuscript.

FUNDING

This study was partly funded by the General Directorate of the Environment from the canton of Vaud (DGE) and partly by the Federal Food Safety and Veterinary Office (FSVO) through the pilot program Adaptation to climate change. CB was funded by SNF Post Doc Mobility Fellowship number P400PB_183824.

ACKNOWLEDGMENTS

The authors wish to thank the department of Water Protection from the General Directorate of the Environment from the canton of Vaud (DGE-DIREV-PRE) for providing the IBCH index from eight stations and the fish-rangers for their help in the fish sampling. We also thank Quentin Gallea for his instruction in the statistical analysis.

SUPPLEMENTARY MATERIAL

The Supplementary Material for this article can be found online at: https://www.frontiersin.org/articles/10.3389/fvets.2019.00281/full#supplementary-material

REFERENCES

1. Burkhardt-Holm P. Peter A, Segner H. Decline of fish catch in Switzerland. *Aquatic Sci.* (2002) 64:36–54. doi: 10.1007/s00027-002-8053-1
2. Burkhardt-Holm P, Giger W, Güttinger H, Peter A, Scheurer K, Suter MJF, et al. Where have all the fish gone? The reasons why fish catches in Swiss rivers are declining. *Environ Sci Technol.* (2005) 39:441–7. doi: 10.1021/es053375z
3. Burkhardt-Holm P, Scheurer K. Application of the weight-of-evidence approach to assess the decline of brown trout (*Salmo trutta*) in Swiss rivers. *Aquatic Sci.* (2007) 69:51–70. doi: 10.1007/s00027-006-0841-6
4. Burkhardt-Holm P. Decline of brown trout (*Salmo trutta*) in Switzerland - How to assess potential causes in a multi-factorial cause-effect relationship. *Mar Environ Res.* (2008) 66:181–2. doi: 10.1016/j.marenvres.2008.02.055
5. Borsuk ME, Reichert P, Peter A, Schager E, Burkhardt-Holm P. Assessing the decline of brown trout (*Salmo trutta*) in Swiss rivers using a Bayesian probability network. *Ecol Model.* (2006) 192:224–44. doi: 10.1016/j.ecolmodel.2005.07.006
6. Hari RE, Livingstone DM, Siber R, Burkhardt-holm P, Güttinger H. Consequences of climatic change for water temperature and brown trout populations in Alpine rivers and streams. *Glob Change Biol.* (2006) 12:10–26. doi: 10.1111/j.1365-2486.2005.001051.x
7. Zimmerli S, Bernet D, Burkhardt-Holm P, Schmidt-Posthaus H, Vonlanthen P, Wahli T, et al. Assessment of fish health status in for Swiss rivers showing a decline of brown trout catches. *Aquatic Sci.* (2007) 69:11–25. doi: 10.1007/s00027-006-0844-3
8. Wahli T, Knuesel R, Bernet D, Segner H, Pugovkin D, Burkhardt-Holm P, et al. Proliferative kidney disease in Switzerland: current state of knowledge. *J Fish Dis.* (2002) 25:491–500. doi: 10.1046/j.1365-2761.2002.00401.x
9. Schager E, Peter A, Burkhardt-Holm P. Status of young-of-the-year brown trout (*Salmo trutta fario*) in Swiss streams: factors influencing YOY trout recruitment. *Aquatic Sci.* (2007) 69:41–50. doi: 10.1007/s00027-007-0845-x
10. Wahli T, Bernet D, Steiner PA, Schmidt-Posthaus H. Geographic distribution of *Tetracapsuloides bryosalmonae* infected fish in Swiss rivers: an update. *Aquatic Sci.* (2007) 69:3–10. doi: 10.1007/s00027-006-0843-4
11. Canning E, Curry A, Feist S, Longshaw M, Okamura B. *Tetracapsula bryosalmonae* N. SP. for PKX organism, the cause of PKD in salmonid fish. *Bull Eur Assoc Fish Pathol.* (1999) 19:203–6.
12. Canning E, Tops S, Curry A, Wood T, Okamura B. Ecology, development and pathogenicity of *Buddenbrockia plumatellae* Schröder, 1910 (*Myxozoa,* Malacosporea) (syn. *Tetracapsula bryozoides*) and establishment of *Tetracapsuloides* n. gen. for *Tetracapsula bryosalmonae*. *J Eucaryotic Microbiol.* (2002) 49:280–95. doi: 10.1111/j.1550-7408.2002.tb00371.x
13. Anderson CL, Canning EU, Okamura B. Molecular data implicate bryozoans as hosts for PKX (phylum Myxozoa) and identify a clade of bryozoan parasites within the *Myxozoa*. *Parasitol.* (1999) 119:555–61. doi: 10.1017/S003118209900520X
14. Longshaw M, Le Deuff RM, Harris AF, Feist SW. Development of proliferative kidney disease in rainbow trout, *Oncorhynchus mykiss* (Walbaum), following short-term exposure to *Tetracapsula bryosalmononae* infected bryozoans. *J Fish Dis.* (2002) 25:443–9. doi: 10.1046/j.1365-2761.2002.00353.x
15. Morris DJ, Adams A. Transmission of *Tetracapsuloides bryosalmonae* (*Myxozoa*: Malacosporea), the causative organism of salmonid proliferative kidney disease, to the freshwater bryozoan *Fredericella sultana*. *Parasitology.* (2006) 133:701–9. doi: 10.1017/S003118200600093X
16. Tops S, Hartikainen H, Okamura B. The effect of infection by *Tetracapsuloides bryosalmonae* (*Myxozoa*) and temperature on *Fredericella sultana* (Bryozoa). *Int J Parasitol.* (2009) 39:1003–10. doi: 10.1016/j.ijpara.2009.01.007
17. Grabner DS, El-Matbouli M. *Tetracapsuloides bryosalmonae* (*Myxozoa*: Malacosporea) portal of entry into the fish host. *Dis Aquatic Organ.* (2010) 90:197–206. doi: 10.3354/dao02236
18. Bettge K, Wahli T, Segner H, Schmidt-Posthaus H. Proliferative kidney disease in rainbow trout: time- and temperature-related renal pathology and parasite distribution. *Dis. Aquatic Organ.* (2009) 83:67–76. doi: 10.3354/dao01989
19. Okamura B, Hartikainen HL, Schmidt-Posthaus H, Wahli T. Life cycle complexity, environmental change and the emerging status of salmonid proliferative kidney disease. *Freshw Biol.* (2011) 56:735–53. doi: 10.1111/j.1365-2427.2010.02465.x
20. Schmidt-Posthaus H, Hirschi R, Schneider E. Proliferative kidney disease in brown trout: infection level, pathology and mortality under field conditions. *Dis Aquatic Organ.* (2015) 114:139–46. doi: 10.3354/dao02855
21. Abd-Elfattah A, Kumar G, Soliman H, El-Matbouli M. Persistence of *Tetracapsuloides bryosalmonae* (*Myxozoa*) in chronically infected brown trout *Salmo trutta*. *Dis Aquatic Organ.* (2014) 111:41–9. doi: 10.3354/dao02768
22. Soliman H, Kumar G, El-Matbouli M. *Tetracapsuloides bryosalmonae* persists in brown trout *Salmo trutta* for five years post exposure. *Dis Aquatic Organ.* (2018) 127:151–6. doi: 10.3354/dao03200
23. Bettge K, Segner H, Burki R, Schmidt-Posthaus H, Wahli T. Proliferative kidney disease (PKD) of rainbow trout: temperature- and time-related changes of *Tetracapsuloides bryosalmonae* DNA in the kidney. *Parasitology.* (2009) 136:615–25. doi: 10.1017/S0031182009005800
24. Feist SW, Longshaw M. Phylum *myxozoa*. In: Woo PTK, editor. *Fish Diseases and Disorders. Protozoan and Metazoan Infections*, Vol. 1, 2nd ed. Oxfordshire: CAB International (2006). p. 230–96.
25. Bruneaux M, Visse M, Gross R, Pukk L, Saks L, Vasmägi A. Parasite infection and decrease thermal tolerance: impact of proliferative kidney disease on a wild salmonid fish in the context of climate change. *Funct Ecol.* (2017) 31:216–26. doi: 10.1111/1365-2435.12701
26. Marcogliese D. Implications of climate change for parasitism of animals in the aquatic environment. *Can J Zool.* (2001) 79:1331–52. doi: 10.1139/cjz-79-8-1331
27. Marcos-López M, Gale P, Oidtmann B, Peeler E. Assessing the impact of climate change on disease emergence in freshwater fish in the United Kingdom. *Transbound Emerg Dis.* (2010) 57:293–304. doi: 10.1111/j.1865-1682.2010.01150.x
28. Adlard R, Miller T, Smit N. The butterfly effect: parasite diversity, environment, and emerging disease in aquatic wildlife. *Trends Parasitol.*(2015) 31:160–6. doi: 10.1016/j.pt.2014.11.001
29. Carraro L, Bertuzzo E, Mari L, Fontes I, Hartikainen H, Strepparava N, et al. Integrated field, laboratory, and theoretical study of PKD spread in a Swiss prealpine river. *PNAS.* (2017) 114:11992–7. doi: 10.1073/pnas.1713691114
30. Debes PV, Gross R, Vasemägi A. Quantitative genetic variation in, and environmental effects on, pathogen resistance and temperature-dependent disease severity in a wild trout. *Am Natural.* (2017) 190:244–65. doi: 10.1086/692536
31. Bailey C, Rubin A, Strepparava N, Segner H, Rubin J-F, Wahli T. Do fish get wasted? Assessing the influence of effluents on parasitic infection of wild fish. *Peer J.* (2018) 6:e5956. doi: 10.7717/peerj.5956
32. Sterud E, Forseth T, Ugedal O, Poppe TT, Jørgensen A, Bruheim T, et al. Severe mortality in wild Atlantic salmon *Salmo salar* due to proliferative kidney disease (PKD) caused by *Tetracapsuloides bryosalmonae* (*Myxozoa*). *Dis Aquatic Organ.* (2007) 77:191–8. doi: 10.3354/dao01846
33. Strepparava N, Segner H, Ros A, Hartikainen H, Schmidt-Posthaus H, Wahli T. Temperature-related parasite infection dynamics: the case of proliferative kidney disease of brown trout. *Parasitology.* (2017) 145:281–91. doi: 10.1017/S0031182017001482
34. Foott JS, Hedrick RP. Seasonal occurrence of the infectious stage of proliferative kidney disease (PKD) and resistance of rainbow trout, *Salmo gairdneri* Richardson, to reinfection. *J Fish Biol.* (1987) 30:477–83. doi: 10.1111/j.1095-8649.1987.tb05771.x
35. De Kinkelin P, Loriot B. A water temperature regime which prevents the occurrence of proliferative kidney disease (PKD) in rainbow trout, *Oncorhynchus mykiss* (Walbaum). *J Fish Dis.* (2001) 24:489–93. doi: 10.1046/j.1365-2761.2001.00312.x
36. Gay M, Okamura B, De Kinkelin P. Evidence that infectious stages of *Tetracapsula bryosalmonae* for rainbow trout *Oncorhynchus mykiss* are present throughout the year. *Dis Aquatic Organ.* (2001) 46:31–40. doi: 10.3354/dao046031
37. Bailey C, Segner H, Casanova-Nakayama A, Wahli T. Who needs the hotspot? The effect of temperature on the fish host immune response to *Tetracapsuloides bryosalmonae* the causative agent of proliferative kidney disease. *Fish Shellfish Immunol.* (2017) 63:424–37. doi: 10.1016/j.fsi.2017.02.039
38. Wahli T, Bernet D, Segner H, Schmidt-Posthaus H. Role of altitude and water temperature as regulating factors for the geographical distribution

of *Tetracapsuloides bryosalmonae* infected fishes in Switzerland. *J Fish Biol.* (2008) 73:2184–97. doi: 10.1111/j.1095-8649.2008.02054.x
39. Schmidt-Posthaus H, Bettge K, Forster U, Segner H, Wahli T. Kidney pathology and parasite intensity in rainbow trout *Oncorhynchus mykiss* surviving proliferative kidney disease: time course and influence of temperature. *Dis Aquatic Organ.* (2012) 97:207–18. doi: 10.3354/dao02417
40. Dash M, Vasemägi A. Proliferative kidney disease (PKD) agent *Tetracapsuloides bryosalmonae* in brown trout populations in Estonia. *Dis Aquatic Organ.* (2014) 109:139–48. doi: 10.3354/dao02731
41. Tops S, Lockwood W, Okamura B. Temperature-driven proliferation of *Tetracapsuloides bryosalmonae* in bryozoan hosts portends salmonid declines. *Dis Aquatic Organ.* (2006) 70:227–36. doi: 10.3354/dao070227
42. Jacobson KC, Arkoosh MR, Kagley AN, Clemons ER, Collier TK, Casillas E. Cumulative effects of natural and anthropogenic stress on immune function and disease resistance in juvenile Chinook salmon. *J Aquatic Anim Health.* (2003) 15:1–12. doi: 10.1577/1548-8667(2003)015<0001:CEONAA>2.0.CO;2
43. Thrush M, Murray A, Brun E, Wallace S, Peeler E. The application of risk and disease modelling to emerging freshwater diseases in wild aquatic animals. *Freshw Biol.* (2011) 56:658–75. doi: 10.1111/j.1365-2427.2010.02549.x
44. Graham DA, Staples C, Wilson CJ, Jewhurst H, Cherry K, Gordon A, et al. Biophysical properties of salmonid alphaviruses: influence of temperature and pH on virus survival. *J Fish Dis.* (2007) 30:533–43. doi: 10.1111/j.1365-2761.2007.00811.x
45. Marcogliese D. The impact of climate change on the parasites and infectious diseases of aquatic animals. *OIE Rev Sci Tech.* (2008) 27:467–84. doi: 10.20506/rst.27.2.1820
46. Schmidt-Posthaus H, Bernet D, Wahli T, Burkhardt-Holm, P. Morphological organ alterations and infectious diseases in brown trout *Salmo trutta* and rainbow trout *Oncorhynchus mykiss* exposed to polluted river water. *Dis Aquatic Organ.* (2001) 44:161–70. doi: 10.3354/dao044161
47. El-Matbouli M, Hoffmann RW. Influence of water quality on the outbreak of proliferative kidney disease - field studies and exposure experiments. *J Fish Dis.* (2002) 25:459–67. doi: 10.1046/j.1365-2761.2002.00393.x
48. Kumar G, Abd-Elfattah A, Saleh M, El-Matbouli M. Fate of *Tetracapsuloides bryosalmonae* (*Myxozoa*) after infection of brown trout *Salmo trutta* and rainbow trout *Oncorhynchus mykiss*. *Dis Aquatic Organ.* (2013) 107:9–18. doi: 10.3354/dao02665
49. Bailey C, Schmidt-Posthaus H, Segner H, Wahli T, Strepparava N. Are brown trout *Salmo trutta fario* and rainbow trout *Oncorhynchus mykiss* two of a kind? A comparative study of salmonids to temperature-influenced *Tetracapsuloides bryosalmonae* infection. *J Fish Dis.* (2018) 41:191–8. doi: 10.1111/jfd.12694
50. Tachet H, Richoux P, Bournaud M, Usseglio Polatera P. *Invertébrés D'eau Douce, Systématique, Biologie, Écologie*. Paris: CNRS&Editions (2000). p. 588.
51. Liess M, Von Der Ohe P. Analyzing effects of pesticides on invertebrate communities in stream. *Environ Toxicol Chem.* (2005) 24:954–65. doi: 10.1897/03-652.1
52. Schriever C, Hansler Ball M, Holmes C, Maund S, Liess M. Agricultural intensity and landscape structure: influences on the macroinvertebrate assemblages of small streams in northern Germany. *Environ Toxicol Chem.* (2007) 26:346–57. doi: 10.1897/05-629R.1
53. Federal Office for the Environment (FOEN). *Méthodes D'analyse et D'appréciation des cours d'eau, Macrozoobenthos—Niveau R (Région) (in French)*. Bern. (2010). Available online at: https://www.bafu.admin.ch/bafu/fr/home/themes/eaux/publications/publications-eaux/methodes-d-analyse-et-d-appreciation-des-cours-d-eau-en-suisse-macrozoobenthos.html
54. Marcel R, Bouchez A, Rimet F. Influence of herbicide contamination on diversity and ecological guilds of river diatoms. *Cryptogam Algol.* (2013) 34:169–83. doi: 10.7872/crya.v34.iss2.2013.169
55. Malaj E, Von der Ohea P, Groted M, Kühnee R, Mondyf C, Usseglio-Polaterag P, et al. Organic chemicals jeopardize the health of freshwater ecosystems on the continental scale. *PNAS.* (2014) 111:9549–54. doi: 10.1073/pnas.1321082111
56. Kattwinkel M, Reichert P, Rüegg J, Liess M, Schuwirth N. Modelling macroinvertebrate community dynamics in stream mesocosms contaminated with a pesticide. *Environ Sci Technol.* (2016) 50:3165–73. doi: 10.1021/acs.est.5b04068
57. Näslund J, Rosengren M, Del Villar D, Gansel L, Norrgård J, Persson L, et al. Hatchery tank enrichment affects cortisol levels and shelter-seeking in Atlantic salmon (*Salmo salar*). *Can J Fish Aquatic Sci.* (2013) 70:585–90. doi: 10.1139/cjfas-2012-0302
58. Rosengren M, Kvingedal E, Näslund J, Johnsson J, Sundell K. Born to be wild: effects of rearing density and environmental enrichment on stress, welfare, and smolt migration in hatchery-reared Atlantic salmon. *J Can Sci Halieutiq Aquatiq.* (2017) 74:396–405. doi: 10.1139/cjfas-2015-0515
59. Cogliati K, Herron C, Noakes D, Schreck C. Reduced stress response in juvenile Chinook Salmon reared with structure. *Aquaculture.* (2019) 504:96–101. doi: 10.1016/j.aquaculture.2019.01.056
60. Federal Office for the Environment (FOEN). *NADUF–Messresultate 1977–1998. Schriftenreihe Umwelt Nr.319 (in German)*. Bern: Federal Office for the Environment (FOEN); Swiss Federal Institute of Aquatic Science and Technology (EAWAG) (2000).
61. Horan D, Kershner J, Hawkins C, Crowl T. Effects of Habitat area and complexity on colorado river cutthroat trout density in uinta mountain streams. *Trans Am Fish Soc.* (2000) 129:1250–63. doi: 10.1577/1548-8659(2000)129<1250:EOHAAC>2.0.CO;2
62. Ayllón D, Almodóvara A, Nicolab G, Parraa I, Elvira B. Modelling carrying capacity dynamics for the conservation and management of territorial salmonids. *Fish Res.* (2012) 134–6:95–103. doi: 10.1016/j.fishres.2012.08.004
63. Federal Office for the Environment (FOEN). *Ecomorphologie des cours D'eau Suisses (in French)*. Bern (2009). Available online at: https://www.bafu.admin.ch/bafu/fr/home/themes/eaux/publications/publications-eaux/ecomorphologie-cours-eau-suisses.html
64. Federal Office of Topography (Swisstopo). *Ecomorphology Map of Switzerland*. Available online at: https://map.geo.admin.ch/ (accessed September 27, 2018).
65. Feist SW, Peeler E, Gardiner R, Smith E, Longshaw M. Proliferative kidney disease and renal myxosporidiosis in juvenile salmonids from rivers in England and Wales. *J Fish Dis.* (2002) 25:451–8. doi: 10.1046/j.1365-2761.2002.00361.x
66. Peeler EJ, Feist SW, Thrush MA, St-Hilaire S. An assessment of the variation in the prevalence of renal myxosporidiosis and hepatitis in wild brown trout, *Salmo trutta* L., within and between rivers in South-West England. *J Fish Dis.* (2008) 31:719–28. doi: 10.1111/j.1365-2761.2008.00942.x
67. Fischnetz. *Final Report of Project Fischnetz (in French)*. Bern: Eawag Dübendorf and BUWAL (2004).
68. Lewisch E, Unfer G, Pinter K, Bechter T, El-Matbouli M. Distribution and prevalence of *T. bryosalmonae* in Austria: a first survey of trout from rivers with a shrinking population. *J Fish Dis.* (2018) 41:1549–57. doi: 10.1111/jfd.12863
69. Federal Office of Meteorology and Climatology (MeteoSwiss). *Climate change in Switzerland*. Available online at: https://www.meteoswiss.admin.ch/home/climate/climate-change-in-switzerland.html (accessed June 6, 2019).
70. Beniston M. *Changements Climatiques et Impacts*. Lausanne: Presses Polytechniques et Universitaires Romandes (2012). p. 247.
71. Rebetez M. *La Suisse se Réchauf*fe. Lausanne: Presses Polytechniques et Universitaires Romandes (2014). p. 144.
72. IPCC. Summary for policymakers. In: *Global Warming of 1.5°C. An IPCC Special Report on the Impacts of Global Warming of 1.5°C Above Pre-Industrial Levels and Related Global Greenhouse Gas Emission Pathways, in the Context of Strengthening the Global Response to the Threat of Climate Change, Sustainable Development, and Efforts to Eradicate Poverty*. Geneva: World Meteorological Organization (2018). p. 32.
73. Nordmo R, Ramstad A. Variables affecting the challenge pressure of *Aeromonas salmonicidae* and *Vibrio salmonicida* in Atlantic salmon (*Salmo salar* L.). *Aquaculture.* (1999) 171:1–12. doi: 10.1016/S0044-8486(98)00426-8
74. Tobback E, Decostere A, Hermans K, Haesebrouck F, Chiers K. *Yersinia ruckeri* infections in salmonid fish. *J Fish Dis.* (2007) 30:257–68. doi: 10.1111/j.1365-2761.2007.00816.x
75. Duan X, Wang Z, Xu M. Effects of fluvial processes and human activities on stream macro-invertebrates. *Int J Sediment Res.* (2011) 26:416–30. doi: 10.1016/S1001-6279(12)60002-X
76. Chiu M, Hunt L, Resh V. Response of macroinvertebrate communities to temporal dynamics of pesticide mixtures: a case study from the Sacramento River watershed, California. *Environ Pollut.* (2016) 219:89–98. doi: 10.1016/j.envpol.2016.09.048

77. Shetty A, Venkateshwarlu M, Muralidharan M. Effect of water quality on the composition of fish communities in three coastal rivers of Karnataka, India. *Int J Aquatic Biol.* (2015) 3:42–51. doi: 10.22034/ijab.v3i1.46
78. Guo Q, Liu X, Ao X, Qin J, Wu X, Ouyang S. Fish diversity in the middle and lower reaches of the Ganjiang River of China: threats and conservation. *PLoS ONE.* (2018) 13:e0205116. doi: 10.1371/journal.pone.0205116
79. Schmidt H, Bernet D, Wahli T, Meier W, Burkhardt-Holm, P. Active biomonitoring with brown trout and rainbow trout in diluted sewage plant effluents. *J Fish Biol.* (1999) 54:585–96. doi: 10.1111/j.1095-8649.1999.tb00637.x
80. Bernet D, Schmidt H, Bernet D, Wahli T, Burkhardt-Holm P. Effects of treated waste water on infectious agents in brown trout. *Fish Ecol.* (2001) 12:1–16.
81. Hartikainen H, Johnes P, Moncrieff C, Okamura B. Bryozoan populations reflect nutrient enrichment and productivity gradients in rivers. *Freshw Biol.* (2009) 54:2320–34. doi: 10.1111/j.1365-2427.2009.02262.x
82. *Ordinance on Water Protection (in French)*. (1998). Available online at: https://www.admin.ch/opc/fr/classified-compilation/19983281/201401010000/814.201.pdf
83. Jonsson B, Jonsson N. A review of the likely effects of climate change on anadromous Atlantic salmon *Salmo salar* and brown trout *Salmo trutta*, with particular reference to water temperature and flow. *J Fish Biol.* (2009) 75:2381–447. doi: 10.1111/j.1095-8649.2009.02380.x
84. Lassalle G, Rochard E. Impact of twenty-first century climate change on diadromous fish spread over Europe, North Africa and the Middle East. *Glob Change Biol.* (2009) 15:1072–89. doi: 10.1111/j.1365-2486.2008.01794.x
85. Almodóvar A, Nicola GG, Ayllón D, Elvira B. Global warming threatens the persistence of Mediterranean brown trout. *Glob Change Biol.* (2012) 18:1549–60. doi: 10.1111/j.1365-2486.2011.02608.x

Conflict of Interest Statement: The authors declare that the research was conducted in the absence of any commercial or financial relationships that could be construed as a potential conflict of interest.

Copyright © 2019 Rubin, de Coulon, Bailey, Segner, Wahli and Rubin. This is an open-access article distributed under the terms of the Creative Commons Attribution License (CC BY). The use, distribution or reproduction in other forums is permitted, provided the original author(s) and the copyright owner(s) are credited and that the original publication in this journal is cited, in accordance with accepted academic practice. No use, distribution or reproduction is permitted which does not comply with these terms.

frontiers in Veterinary Science

ORIGINAL RESEARCH
published: 23 August 2019
doi: 10.3389/fvets.2019.00269

Molecular Detection of *Babesia* spp. (Apicomplexa: Piroplasma) in Free-Ranging Canids and Mustelids From Southern Italy

Mario Santoro[1], Clementina Auriemma[1], Maria Gabriella Lucibelli[1], Giorgia Borriello[1], Nicola D'Alessio[1], Giovanni Sgroi[2], Vincenzo Veneziano[2], Giorgio Galiero[1] and Giovanna Fusco[1]*

[1] *Istituto Zooprofilattico Sperimentale del Mezzogiorno, Portici, Italy,* [2] *Department of Veterinary Medicine and Animal Productions, Università degli Studi di Napoli "Federico II", Naples, Italy*

Babesiosis is an emerging tick-borne disease caused by apicomplexan parasites with widespread geographical distribution and various wildlife species as reservoir hosts. The aims of this study were to investigate the prevalence and assess the role of free-ranging canids and mustelids in the maintenance of *Babesia* spp. in southern Italy. PCR analysis of splenic samples targeting the 18S rRNA gene revealed the presence of *Babesia* spp. in 36 of 82 (43.9%) red foxes (*Vulpes vulpes*) including 29 (58%) from Campania region and seven (21.8%) from Calabria region, in seven of 13 (53.8%) Eurasian badgers (*Meles meles*), and in one of 13 (7.7%) gray wolves (*Canis lupus*). Samples from other host species including 9 Eurasian otters (*Lutra lutra*), 1 stone marten (*Martes foina*), 1 least weasel (*Mustela nivalis*), and 1 European polecat (*Mustela putorius*) tested *Babesia* spp. negative. Sequence analysis of the 18S rRNA gene demonstrated the presence of *B. vulpes* in the red fox and two sequence types of badger-associated *Babesia* spp. in the Eurasian badger. The *Babesia* sp. sequence detected in the gray wolf was identical to a badger-associated *Babesia* sp. This study shows that the number of *Babesia* spp. infecting free-ranging carnivores in Italy is higher than currently believed, and suggests that these hosts may play an important role in the maintenance of the sylvatic cycle of these parasites. It is the first report of badger-associated *Babesia* spp. in Italy and in a gray wolf.

Keywords: *Vulpes vulpes*, *Meles meles*, *Canis lupus*, *Babesia vulpes*, badger-associated *Babesia* spp., babesiosis, tick-borne disease

OPEN ACCESS

Edited by:
Robert James Ossiboff, University of Florida College of Veterinary Medicine, United States

Reviewed by:
Steven Victor Kubiski, University of California, Davis, United States
Nikolaus Huber, University of Veterinary Medicine, Austria

****Correspondence:***
Mario Santoro
mario.santoro@izsmportici.it

Specialty section:
This article was submitted to Zoological Medicine, a section of the journal Frontiers in Veterinary Science

Received: *19 June 2019*
Accepted: *05 August 2019*
Published: *23 August 2019*

Citation:
Santoro M, Auriemma C, Lucibelli MG, Borriello G, D'Alessio N, Sgroi G, Veneziano V, Galiero G and Fusco G (2019) Molecular Detection of Babesia spp. (Apicomplexa: Piroplasma) in Free-Ranging Canids and Mustelids From Southern Italy. Front. Vet. Sci. 6:269. doi: 10.3389/fvets.2019.00269

INTRODUCTION

Babesiosis is a tick-borne disease caused by haemoprotozoan organisms of the genus *Babesia* (Apicomplexa: Piroplasma), and several wildlife species may represent important reservoir hosts. According to the most recent studies, *Babesia* spp. of carnivore mammals are divided into three main groups including the *Babesia microti* group infecting felids, canids, mustelids and procyonids; the prototheilerid group infecting felids, canids, herpestids and hyaenids; and *Babesia* sensu stricto group infecting canids, procyonids, and ursids (1–3).

In free-ranging carnivores in Europe, infection with at least three *Babesia* spp. has been documented including *B. canis* in the gray wolf (*Canis lupus*) (4), *B. canis* and *B. vulpes* (this latter reported in the literature as *B.* "Spanish dog isolate," *B. microti*-like, *B. annae*, and *Theileria annae*)

(5) in the red fox (*Vulpes vulpes*), and *B. vogeli* in a stone marten (*Martes foina*). Moreover, at least two genotypes named badger-associated *Babesia* spp. in the Eurasian badger (*Meles meles*) (1, 3, 6) and a genotype that clustered together to *B. vulpes* isolates [FJ225390.1 (7)] have been reported. An additional *Babesia* genotype in the European wildcat (*Felis silvestris silvestris*) from Bosnia and Herzegovina (8) has been also reported. *B. vulpes* and badger-associated *Babesia* spp. are included in the *B. microti* group; *B. canis* and *B. vogeli* are included in the *Babesia* sensu stricto group (1–3).

There are few studies focusing on the *Babesia* spp. in free-ranging carnivores other than red fox in Europe, and none in Italy (1, 3, 6, 8). Due to recent reports of DNA sequences than could represent new species and the overall lack of prevalence surveys in most carnivore species and geographic locations, it is likely that the number of *Babesia* spp. infecting free-ranging carnivores is higher that currently believed (1, 6–10).

Among *Babesia* species in free-ranging carnivores in Italy, only three recently studies from northern and central Italy reported the presence of *B. vulpes* in the red fox (11–13). All those studies suggested that regional factors as climatic and landscape variables linked to tick vector abundance and wild carnivore population densities may exist (11–13). Here we perform a molecular survey to study the occurrence of *Babesia* spp. in free-ranging canids and mustelids in the southern Italy where emerging tick-borne pathogens (i.e., *B. canis*, *B. gibsoni, B. vogeli*, *Ehrlichia canis*, *Anaplasma* spp., *Borrelia burgdorferi* spp., and *Rickettia* spp.) have been recently reported in domestic and free-ranging carnivores (14–18).

MATERIALS AND METHODS

Sample Collection

Carcasses of 120 free-ranging carnivores including members of two families (Canidae and Mustelidae) obtained from the southern Italy were used for this study (**Table 1**). Carcasses were all road-killed animals except for the red foxes obtained during the official hunting season from local hunters. Carcasses were all obtained between January 2017 and December 2018 except for six Eurasian otters (*Lutra lutra*) obtained between March 2004 and December 2016 [see also (16)].

Molecular Analyses

Spleen samples were collected at post-mortem examination and stored at −20°C for a week until DNA extraction. Genomic DNA was extracted from 25 mg of spleen with the QIAamp DNA mini KIT (QIAGEN) following manufacturer's instructions. All samples were screened for the presence of *Babesia* spp. by PCR targeting the 18S rRNA gene as described by Casati et al. (19). To assess the analytical sensitivity of the PCR assay, the DNA concentration was determined by biophotometry (BioPhotometer plus, Eppendorf, Italy). The extract was then serially diluted 10-fold in sterile water starting from 774 μg/ml, and each dilution was used as template for the PCR reaction. Briefly, reactions were performed in a total volume of 25 μL containing HotStar HiFidelity PCR Buffer 1X, 1 ul of HotStar HiFidelity DNA Polymerase, 0.6 μM of each primer, and 3.5 μL of DNA. The primers used were BJ1 (5′-GTC TTGTAATTGGAATGATGG-3′) and BN2 (5′-TAGTTTATGGTTAGGACTACG-3'). Amplification conditions included an initial denaturation/activation step at 95 °C for 5 min, followed by 35 cycles of denaturation at 94 °C for 1 min, annealing at 55 °C for 1 min and extension at 72°C per 2 min, and a final extension step at 72°C for 5 min. Amplicons (486–520 bp) were resolved by automated capillary electrophoresis with the instrument QIAxcel (QIAGEN). Amplicons were subsequently purified and sequenced in both directions using the same primers as for PCR, employing the Big Dye Terminator Cycle Sequencing Kit v1.1 (Thermo Fischer Scientific, USA) in the automated sequencer 3500 Genetic Analyzer (ThermoFisher). Sequences were aligned using BIOEDIT software and compared with those available in GenBank (BLAST—http://blast.ncbi.nlm.nih.gov/Blast.cgi). Phylogenetic analyses were performed with the Neighbor-Joining method, using MEGA 6.0 (20, 21).

TABLE 1 | Carnivore species, region of sampling and positive individuals for *Babesia* spp. in southern Italy.

Host species	Locality	*n*	Positive n	Prevalence of infection (%)
Red fox (*Vulpes vulpes*)	Calabria	32	7	21.8
	Campania	50	29	58
Gray wolf (*Canis lupus*)	Campania	13	1	7.7
Eurasian badger (*Meles meles*)	Campania	13	7	53.8
Eurasian otter (*Lutra lutra*)	Basilicata	1	0	0
	Calabria	2	0	0
	Campania	6	0	0
Stone marten (*Martes foina*)	Campania	1	0	0
European polecat (*Mustela putorius*)	Campania	1	0	0
Least weasel (*Mustela nivalis*)	Campania	1	0	0

RESULTS

Among DNA extracts, 36 of 82 (43.9%) samples of red fox, seven of 13 (53.8%) samples of Eurasian badger, and one of 13 (7.7%) samples of gray wolf were PCR-positive for *Babesia* spp. (**Table 1**). The amplicon detection limit for the PCR assay was 77.4 μg/ml corresponding to 1.9 μg/reaction.

Sequences from the red foxes (520 bp) were all identical and shared a similarity of 100% with *B. vulpes* 18S rRNA gene sequences found in GenBank (KY175167.1, KY175166.1). In the Eurasian badger and gray wolf we obtained six sequences belonging to two sequence types. The first type (515 bp) was found in four Eurasian badgers and a gray wolf (from MK742770 to MK742774) and showed a similarity of 100% with *Babesia* sp. badger type A 18S rRNA gene sequences found in China (MG799845.1, MH844530.1) and Spain (KT223484.1). The second one (486 bp) was found in a single Eurasian badger (MK742775), and showed a similarity of 100% with a *Babesia* sp. 18S rRNA gene sequence (JX679177.1) found in nymph individuals of the tick *Ixodes canisuga* collected from a red fox in Germany, and in an Eurasian badger in China (MG799847.1).

A Phylogenetic tree of the 18S rRNA gene of *Babesia* spp. of *microti* group using the Neighbor-Joining method, showed

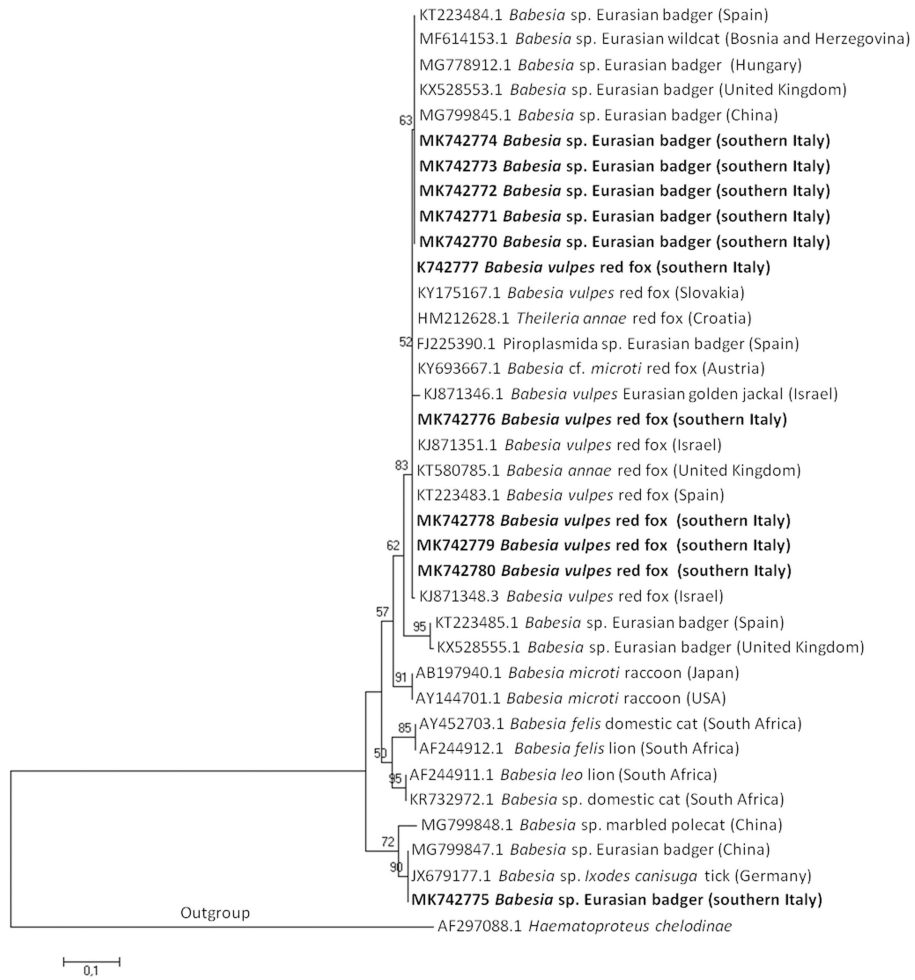

FIGURE 1 | The evolutionary history of *Babesia microti* group DNA sequences was inferred using the Neighbor-Joining method. The optimal tree with the sum of branch length = 1,76412028 is shown. The percentage of replicate trees in which the associated taxa clustered together in the bootstrap test (1,000 replicates) is shown above the branches. The tree is drawn to scale, with branch lengths in the same units as those of the evolutionary distances used to infer the phylogenetic tree. The evolutionary distances are in the units of the number of base substitutions per site. Sequences are presented by GenBank accession number, *Babesia* species, host species, and geographical location in brackets. Isolate from this study are in bold.

that *B. vulpes* sequences from this study clustered together with *B. vulpes*, *B.* sp. Spanish dog isolate, *B. annae*, *T. annae,* and *B. microti*-like piroplasm confirming the synonymy with those species. The first type sequence detected in the Eurasian badger and gray wolf clustered together with *Babesia* sp. badger type A and *Babesia* sp. Meles Hu1 found in European countries; the second type sequence detected in a Eurasian badger clustered together with a *Babesia* sp. found in Germany and China (**Figure 1**).

DISCUSSION

In this study, the splenic samples of seven free-ranging carnivore species from the southern Italy were molecularly screened for the presence of *Babesia* spp. The DNA of three *Babesia* spp. all belonging to the *B. microti* group was detected.

Published data regarding *Babesia* spp. in free-ranging carnivores in Italy is limited to few studies that detected *B. vulpes* in the red fox only. In the red fox in Italy, *B. vulpes* prevalence was highly variable: 0.98% in north-western (11), 54% in north-eastern (13), and 22.88% in central Italy (12). PCR prevalence of *B. vulpes* in this survey differed depending on geographical locality. In Campania region, *B. vulpes* prevalence was almost three times higher than that reported in Calabria region (58 vs. 21.8%), but it was lower than prevalence found in Portugal [69.2% (22)] and Galicia, Spain [from 61 to 79.8% (23)].

Prevalence of badger-associate *Babesia* spp. in the Eurasian badger has been reported to range from 21.3 to 53.2% in Scotland (9), from 20 to 35.2% in Spain (6, 7), and it was 66.7% in Hungary (3). Prevalence of badger-associated *Babesia* spp. in the Eurasian badger in this study was among the higher prevalence values recorded to date.

Difference in *Babesia* spp. prevalence suggests regional differences in tick species diversity and abundance, and infection rate of the pathogen in ticks may influence the dynamic of *Babesia* spp. infection in mammalian hosts. In a recent study

from Spain, Checa et al. (23) found significant differences in prevalence of *B. vulpes* infection among red fox populations of Galicia provinces suggesting that humid climates found in those provinces with highest prevalence rates are capable of sustaining higher burdens of ixodid ticks, which in turn may lead to the increased risk of tick-borne diseases. Differences in prevalence of *B. vulpes* between Campania and Calabria regions indicate a lower circulation of the parasite in Calabria region and could be related to the highest red fox density and tick vector abundance in those localities of the Campania region where the red foxes were obtained. A great abundance of potential hosts is an important factor for tick expansion and a potential for the spread of babesiosis (3, 4, 23). Southern Italy represents an endemic area for several tick-borne pathogens infecting domestic and free-ranging carnivores showing distribution corresponding to known distribution of its tick vectors (14–18). DNA of *B. vulpes* has been detected in many European countries in few tick species infecting the red fox including *I. canisuga*, *I. hexagonus*, *I. ricinus*, *Rhipicephalus sanguineus* s.l., and *Dermacentor reticulatus;* all these species are present in southern Italy except the last one. *I. hexagonus* is considered the most likely vector for *B. vulpes* (23, 24).

Despite the frequent contacts occurring between domestic dogs (as hunting dogs and sheepdogs) and red foxes, and the few ixodid tick vectors they share, infection of dogs and other free-ranging carnivores with *B. vulpes* occurred occasionally suggesting the red fox as its main natural host (1, 25). A recent survey of *Babesia* spp. in 1,311 hunting dogs in the Campania region of southern Italy revealed only the presence of *B. canis*, *B. gibsoni*, and *B. vogeli* (18). It suggests that at least in this region the red foxes and hunting dogs tend to acquire different *Babesia* spp.

In Europe, at least two DNA sequences of badger-associated *Babesia* spp. that could be undescribed *Babesia* species (named *Babesia* sp. isolate badger type A or *Babesia* sp. isolate Meles Hu1, and *Babesia* sp. isolate badger type B) have been reported in the Eurasian badger in Spain (6), Scotland (9), and Hungary (3) (see phylogenetic tree in **Figure 1**). An additional sequence type available in GenBank corresponds to a *Babesia* sequence detected in a Eurasian badger in Xinjiang, China (*Babesia* sp. badger isolate Badger-1; MG799847.1), and in an *I. canisuga* tick collected in a red fox in Germany (*Babesia* sp. 4 NAN2012; JX679177.1). Four out of five badger-associated *Babesia* spp. sequences detected in the present study in the Eurasian badger were identical to type A sequences found in China and Spain; the other one (MK742775) was identical to those found in China (MG799847.1) and Germany (JX679177.1). The high homology among sequences here found and those deposited in GenBank suggests that the parasites may circulate among Eurasian badgers across Europe.

Contrary to that observed for *B. vulpes*, a recent study demonstrated that the infection of badger-associated *Babesia* spp. may occur in dogs showing clinical signs of babesiosis (3). The usage of dogs during badger hunting in Hungary was considered as a plausible explication for the dog infections (3), since few *Babesia* spp. within the *microti* group may be transmitted orally by direct contact with infected blood (26, 27). The absence of the badger-associated *Babesia* spp. infection in hunting dogs from southern Italy may be linked to two main facts: (a) in Italy the badger hunting is an unperformed practice; (b) the hunters treated regularly their dogs with ectoparasiticides, as a result of being informed of the risks of pathogen transmission by ticks and other vectors (17, 18).

To our knowledge there are only two previous reports of *Babesia* infection in the gray wolf (4, 28). Erdelyi et al. (28) described a fatal infection by *B. canis* in two male captive gray wolves in a private farm in Hungary. Beck et al. (4) reported the infection by *B. canis* in seven of 108 gray wolves (including one captive and six free-ranging) in Croatia. The *Babesia* positive gray wolf found in the present study was a road killed adult female collected in January 2017 in Montemarano (Avellino municipality). It represents the first molecular confirmed case of a badger associated *Babesia* infection in a free-ranging gray wolf. It is plausible to suppose that the gray wolf was infected via blood-sucking ticks or alternatively preying on an infected Eurasian badger similarly to that hypothesized by Hornok et al. (3) for hunting dogs in Hungary.

In conclusion, the red fox and the Eurasian badger in southern Italy exhibit a high prevalence of infection caused by *B. vulpes* and badger-associated *Babesia* spp., respectively. It suggests that these hosts may play an important role in the maintenance of the sylvatic cycle of these parasites. This represents the first detection of badger-associated *Babesia* spp. in Italy. The detection of a badger-associated *Babesia* sp. in a gray wolf deserves further studies to understand the gray wolf role in the maintenance of this *Babesia* strain in the wild.

DATA AVAILABILITY

Representative nucleotide sequences of *Babesia* spp. found in this study have been submitted to GenBank and are available with the following accession numbers: from MK742776 to MK742780 for B. vulpes; MK742775 for the Babesia sequence detected from a single Eurasian badger; from MK742770 to MK742774 for the Babesia sequences detected in four Eurasian badger and a gray wolf.

ETHICS STATEMENT

Ethical review and approval was not required for the animal study because The IZSM is accredited by the Italian Ministry of Health to perform systematic surveys on infectious diseases of domestic and free-ranging animals. Procedures for this study were performed in accordance with the guide for the care and use of animals by the Italian Ministry of Health.

AUTHOR CONTRIBUTIONS

MS, GG, and GF: experimental conception and design. GS, ND, and VV: collection of samples. CA, ML, and GB: molecular analysis. MS: paper writing. All authors read and approved the final manuscript.

ACKNOWLEDGMENTS

This study was partially funded by the grant from the Ministry of Health of the Italian Republic (IZS ME 05/16 RC).

REFERENCES

1. Alvarado-Rybak M, Solano-Gallego L, Millán J. A review of piroplasmid infections in wild carnivores worldwide: importance for domestic animal health and wildlife conservation. *Parasit Vectors*. (2016) 9:538. doi: 10.1186/s13071-016-1808-7
2. Schreeg ME, Marr HS, Tarigo JL, Cohn LA, Bird DM, Scholl EH, et al. Mitochondrial genome sequences and structures aid in the resolution of Piroplasmida phylogeny. *PLoS ONE*. (2016) 11:e0165702. doi: 10.1371/journal.pone.0165702
3. Hornok S, Horváth G, Takács N, Kontschán J, Szőke K, Farkas R. Molecular identification of badger-associated *Babesia* sp. DNA in dogs: updated phylogeny of piroplasms infecting Caniformia. *Parasit Vectors*. (2018) 11:235. doi: 10.1186/s13071-018-2794-8
4. Beck A, Huber D, Polkinghorne A, Kurilj AG, Benko V, Mrljak V, et al. The prevalence and impact of Babesia canis and *Theileria* sp. in free-ranging grey wolf (*Canis lupus*) populations in Croatia. *Parasit Vectors*. (2017) 10:168. doi: 10.1186/s13071-017-2106-8
5. Baneth G, Florin-Christensen M, Cardoso L, Schnittger L. Reclassification of Theileria annae as *Babesia vulpes* sp. nov. *Parasit Vectors*. (2015) 8:207. doi: 10.1186/s13071-015-0830-5
6. Barandika JF, Espí A, Oporto B, Del Cerro A, Barral M, Povedano I, et al. Occurrence and genetic diversity of piroplasms and other apicomplexa in wild carnivores. *Parasitol Open*. (2016) 2:1–7. doi: 10.1017/pao.2016.4
7. Gimenez C, Casado N, Criado-Fornelio A, de Miguel FA, Dominguez-Peñafiel G. A molecular survey of Piroplasmida and Hepatozoon isolated from domestic and wild animals in Burgos (northern Spain). *Vet Parasitol*. (2009) 162:147–50. doi: 10.1016/j.vetpar.2009.02.021
8. HodŽić A, Alić A, Duscher GG. High diversity of blood-associated parasites and bacteria in European wild cats in Bosnia and Herzegovina: a molecular study. *Ticks Tick Borne Dis*. (2018) 9:589–93. doi: 10.1016/j.ttbdis.2018.01.017
9. Bartley PM, Wilson C, Innes EA, Katzer F. Detection of Babesia DNA in blood and spleen samples from Eurasian badgers (*Meles meles*) in Scotland. *Parasitology*. (2017) 144:1203–10. doi: 10.1017/S0031182017000476
10. Liu X, Yang M, Liu G, Zhao S, Yuan W, Xiao R, et al. Molecular evidence of Rickettsia raoultii, "Candidatus Rickettsia barbariae" and a novel Babesia genotype in marbled polecats (Vormela peregusna) at the China-Kazakhstan border. *Parasit Vectors*. (2018) 11:450. doi: 10.1186/s13071-018-3033-z
11. Zanet S, Trisciuoglio A, Bottero E, de Mera IG, Gortazar C, Carpignano MG, et al. Piroplasmosis in wildlife: Babesia and Theileria affecting free-ranging ungulates and carnivores in the Italian Alps. *Parasit Vectors*. (2014) 7:70. doi: 10.1186/1756-3305-7-70
12. Ebani VV, Rocchigiani G, Nardoni S, Bertelloni F, Vasta V, Papini RA, et al. Molecular detection of tick-borne pathogens in wild red foxes (Vulpes vulpes) from Central Italy. *Acta Trop*. (2017) 172:197–200. doi: 10.1016/j.actatropica.2017.05.014
13. Da Rold G, Ravagnan S, Soppelsa F, Porcellato E, Soppelsa M, Obber F, et al. Ticks are more suitable than red foxes for monitoring zoonotic tick-borne pathogens in northeastern Italy. *Parasit Vectors*. (2018) 11:137. doi: 10.1186/s13071-018-2726-7
14. René-Martellet M, Lebert I, Chêne J, Massot R, Leon M, Leal A, et al. Diagnosis and incidence risk of clinical canine monocytic ehrlichiosis under field conditions in Southern Europe. *Parasit Vectors*. (2015) 8:3. doi: 10.1186/s13071-014-0613-4
15. Santoro M, Veneziano V, D'Alessio N, Di Prisco F, Lucibelli MG, Borriello G, et al. Molecular survey of Ehrlichia canis and Coxiella burnetii infections in wild mammals of southern Italy. *Parasitol Res*. (2016) 115:4427–31. doi: 10.1007/s00436-016-5213-0
16. Santoro M, D'Alessio N, Cerrone A, Lucibelli MG, Borriello G, Aloise G, et al. The Eurasian otter (*Lutra lutra*) as a potential host for rickettsial pathogens in southern Italy. *PLoS ONE*. (2017) 12:e0173556. doi: 10.1371/journal.pone.0173556
17. Piantedosi D, Neola B, D'Alessio N, Di Prisco F, Santoro M, Pacifico L, et al. Seroprevalence and risk factors associated with Ehrlichia canis, *Anaplasma* spp., Borrelia burgdorferi sensu lato, and D. immitis in hunting dogs from southern Italy. *Parasitol Res*. (2017) 116:2651–60. doi: 10.1007/s00436-017-5574-z
18. Veneziano V, Piantedosi D, Ferrari N, Neola B, Santoro M, Pacifico L, et al. Distribution and risk factors associated with *Babesia* spp. infection in hunting dogs from Southern Italy. *Ticks Tick Borne Dis*. (2018) 9:1459–63. doi: 10.1016/j.ttbdis.2018.07.005
19. Casati S, Sager H, Gern L, Piffaretti JC. Presence of potentially pathogenic *Babesia* spp. for human in Ixodes ricinus in Switzerland. *Ann Agric Environ Med*. (2006) 13:65–70.
20. Saitou N, Nei M. The neighbor-joining method: a new method for reconstructing phylogenetic trees. *Mol Biol Evol*. (1987) 4:406–25.
21. Tamura K, Stecher G, Peterson D, Filipski A, Kumar S. MEGA6: molecular evolutionary genetics analysis version 6.0. *Mol Biol Evol*. (2013) 30:2725–9. doi: 10.1093/molbev/mst197
22. Cardoso L, Cortes HC, Reis A, Rodrigues P, Simões M, Lopes AP, et al. Prevalence of Babesia microti-like infection in red foxes (Vulpes vulpes) from Portugal. *Vet Parasitol*. (2013) 196:90–5. doi: 10.1016/j.vetpar.2012.12.060
23. Checa R, López-Beceiro AM, Montoya A, Barrera JP, Ortega N, Gálvez R, et al. Babesia microti-like piroplasm (syn. Babesia vulpes) infection in red foxes (Vulpes vulpes) in NW Spain (Galicia) and its relationship with Ixodes hexagonus. *Vet Parasitol.* (2018) 252:22–8. doi: 10.1016/j.vetpar.2018.01.011
24. Camacho AT, Pallas E, Gestal JJ, Guitián FJ, Olmeda AS, Telford SR, et al. Ixodes hexagonus is the main candidate as vector of Theileria annae in northwest Spain. *Vet Parasitol*. (2003) 112:157–63. doi: 10.1016/S0304-4017(02)00417-X
25. Nayyar Ghauri H, Ijaz M, Farooqi SH, Ali A, Ghaffar A, Saleem S, et al. A comprehensive review on past, present and future aspects of canine theileriosis. *Microb Pathog*. (2018) 126:116–22. doi: 10.1016/j.micpath.2018.10.033
26. Malagon F, Tapia JL. Experimental transmission of Babesia microti infection by the oral route. *Parasitol Res*. (1994) 80:645–8. doi: 10.1007/BF00932947
27. Jefferies R, Ryan UM, Jardine J, Broughton DK, Robertson ID, Irwin PJ. Blood, bull terriers and babesiosis: further evidence for direct transmission of Babesia gibsoni in dogs. *Aust Vet J*. (2007) 85:459–63. doi: 10.1111/j.1751-0813.2007.00220.x
28. Erdélyi K, Mezősi L, Vladov S, Földvári G. Fatal acute babesiosis in captive grey wolves (*Canis lupus*) due to Babesia canis. *Ticks Tick Borne Dis*. (2014) 5:281–3. doi: 10.1016/j.ttbdis.2013.11.003

Conflict of Interest Statement: The authors declare that the research was conducted in the absence of any commercial or financial relationships that could be construed as a potential conflict of interest.

Copyright © 2019 Santoro, Auriemma, Lucibelli, Borriello, D'Alessio, Sgroi, Veneziano, Galiero and Fusco. This is an open-access article distributed under the terms of the Creative Commons Attribution License (CC BY). The use, distribution or reproduction in other forums is permitted, provided the original author(s) and the copyright owner(s) are credited and that the original publication in this journal is cited, in accordance with accepted academic practice. No use, distribution or reproduction is permitted which does not comply with these terms.

frontiers in Veterinary Science

ORIGINAL RESEARCH
published: 28 August 2019
doi: 10.3389/fvets.2019.00285

Assessment of the LeadCare® Plus for Use on Scandinavian Brown Bears *(Ursus arctos)*

Amanda H. Boesen[1], Alexandra Thiel[1], Boris Fuchs[1], Alina L. Evans[1], Mads F. Bertelsen[2], Ilia Rodushkin[3] and Jon M. Arnemo[1,4]*

[1] Department of Forestry and Wildlife Management, Faculty of Applied Ecology, Agricultural Sciences and Biotechnology, Inland Norway University of Applied Sciences, Koppang, Norway, [2] Center for Zoo and Wild Animal Health, Copenhagen Zoo, Frederiksberg, Denmark, [3] ALS Scandinavia AB, Luleå University of Technology, Luleå, Sweden, [4] Department of Wildlife, Fish and Environmental Studies, Faculty of Forest Sciences, Swedish University of Agricultural Sciences, Umeå, Sweden

Lead (Pb) exposure is associated with adverse health effects in both humans and wildlife. Blood lead levels (BLL) of sentinel wildlife species can be used to monitor environmental lead exposure and ecosystem health. BLL analyzers, such as the LeadCare®, are validated for use in humans, assessed for use in some avian species and cattle, and are increasingly being used on wildlife to monitor lead exposure. The LeadCare® analyzers use a technique called anodic stripping voltammetry (ASV). Species-specific conversion equations have been proposed to approximate the levels found with gold standard measuring methods such as inductively coupled plasma mass spectrometry (ICP-MS) because the ASV method has been shown to underestimate BLL in some species. In this study we assessed the LeadCare® Plus (LCP) for use on Scandinavian brown bears (*Ursus arctos*). LCP measurements were correlated with ICP-MS with a Bland-Altman analyzed bias of 16.3–22.5%, showing a consistent overestimation of BLL analyzed with LCP. Based on this analysis we provide conversion equations for calculating ICP-MS BLL based on the LCP results in Scandinavian brown bears. Our study shows that the LeadCare® Plus can be used for monitoring of lead exposure by approximating gold standard levels using conversion equations. This enables comparison with other gold standard measured BLL within the observed range of this study (38.20–174.00 μg/L). Our study also found that Scandinavian brown bears are highly exposed to environmental lead.

Keywords: blood lead, lead exposure, *Ursus*, anodic stripping voltammetry, Pb

OPEN ACCESS

Edited by:
Nicole Indra Stacy, University of Florida, United States

Reviewed by:
Nadine Lamberski, Zoological Society of San Diego, United States
Enrique Yarto, Centro Veterinario Mexico, Mexico

****Correspondence:***
Amanda H. Boesen
ahb.gorm@gmail.com

Specialty section:
This article was submitted to Zoological Medicine, a section of the journal Frontiers in Veterinary Science

Received: *06 June 2019*
Accepted: *12 August 2019*
Published: *28 August 2019*

Citation:
Boesen AH, Thiel A, Fuchs B, Evans AL, Bertelsen MF, Rodushkin I and Arnemo JM (2019) Assessment of the LeadCare® Plus for Use on Scandinavian Brown Bears (Ursus arctos). Front. Vet. Sci. 6:285. doi: 10.3389/fvets.2019.00285

INTRODUCTION

Environmental contamination with and subsequent exposure to lead (Pb) impacts both humans and animals living in a polluted ecosystem. In humans lead has been associated with a wide range of harmful health effects, including reduced IQ (1) and cardiovascular disease (2, 3). The World Health Organization states that there are no safe levels of lead in the body (4) and even low level exposure poses a health risk, especially during developing stages (5). Although the harmful effects of lead exposure in humans are well-documented, these results have yet to be applied in legislation and regulation on all areas of lead usage, e.g., lead-based ammunition for hunting. The European Food Safety Authority (EFSA) has set the blood lead level (BLL) of concern for

developmental neurotoxicity in humans to 12 μg/L (6). The level of concern of the American Centers for Disease Control and Prevention (CDC), now termed the "reference level" under the current US administration, is 50 μg/L (7, 8).

Lead is absorbed through ingestion and inhalation (9), with higher absorption from the gastrointestinal tract in children than in adults (10). Lead can be measured in the blood (11). Lead compounds are inorganic, organic or ionic, where organic lead can be metabolized to inorganic and ionic lead (12). Ionic lead exerts similar toxicities as inorganic lead. As a bio accumulative toxicant, 94% of the lead body burden is stored in bone (13). The half-life for inorganic lead is 30 days in blood and 10–30 years in bone (6, 10). The half-life seems to be positively correlated to the length of exposure (14) and varies with age and sex (15).

Lead follows a three-compartment distribution model between blood, soft tissue and bone (11). Lead is excreted via urine and feces as well as in hair, sweat and nails (11). BLL can be used to measure recent exposure, but bone-stored lead can be reabsorbed and become an endogenous source of lead, keeping the blood level elevated. Increased calcium mobilization through bone resorption and concurrent reabsorption of lead to the blood is seen during pregnancy and lactation in humans (16), with highest mobilization of bone stored lead in the postpartum period (17). This causes prenatal and neonatal exposure through the placenta (18) and nursing in humans (19) and mice (20). The lactose content of the milk promotes calcium absorption in the gut, and thereby also increases lead absorption (21).

The gold standard of lead analysis in blood or tissue is generally accepted to be graphite-furnace atomic absorption spectrometry (GFAAS) or inductively coupled plasma mass spectrometry (ICP-MS) (22). ICP-MS and GFAAS has been determined to be statistically equivalent when measuring BLLs for clinical use and biomonitoring (23, 24). Both methods are expensive and time-consuming and require laboratory involvement. An alternative analytical method that both simplifies the process and lowers the cost of determining BLL has been introduced: Anodic stripping voltammetry (ASV) is a relatively new method that uses electrochemistry to measure lead in blood (25).

The LeadCare® analyzers from Magellan Diagnostics Inc. (North Billerica, MA, USA) apply ASV technology. These analyzers are validated for humans (26), some avian species (27, 28) and in cattle (29) by comparison to the GFAAS and/or ICP-MS. Furthermore, ASV has been used in studies investigating lead exposure in grizzly bears (*Ursus arctos*), black bears (*U. americanus*), gray wolves (*Canis lupus*) and cougars (*Puma concolor*) (30), and multiple avian species (31, 32). The analyzers are portable and require little training to operate. This is beneficial in wildlife research and biomonitoring of lead exposure in the field.

In studies comparing the LeadCare® systems with GFAAS or ICP-MS, the ASV analyzers had a negative bias (i.e., underestimation) when measuring the BLL of avian wildlife (27, 33) and cattle (29). Validation for each species has been proposed to verify the conversion rate when using the LeadCare® to monitor exposure (23). No significant difference was found between the different LeadCare® systems in birds (23). In the present study, the LeadCare® Plus (LCP) was used as it has the lowest detection range of the currently available LeadCare® analyzers.

The objective of this study was to compare LCP and ICP-MS for measurement of BLL in Scandinavian brown bears. Based on previous studies on hunting with lead-based ammunition in Scandinavia (34), the scavenging behavior of Scandinavian brown bears (35) and assessment of the LeadCare® system in other species, we predicted (1) to find detectable levels of lead in blood of some bears and (2) to find that LCP was negatively biased when compared to ICP-MS.

METHODS AND MATERIALS

The present study was conducted in Dalarna and Gävleborg counties in south-central Sweden (61°N 15°E) and Hedmark County in south-eastern Norway (61°N 18°E) as part of the Scandinavian Brown Bear Research Project (36). Captures, handling and sampling of bears were approved by the Swedish Ethical Committee on Animal Research (Uppsala, Sweden; #C18/15), the Swedish Environmental Protection Agency (Stockholm, Sweden; NV-0758-14), and the Swedish Board of Agriculture (#31-11102/12) and were carried out according to an established protocol (37).

Blood was collected from the jugular vein in 4 ml EDTA tubes using the Vacuette® system (Greiner Bio-One, Kremsmünster, Austria) from 54 bears captured during April-May 2018. The blood samples were analyzed on the LCP according to the protocol for the analyzer, either within 6 h of sampling, or after refrigeration at 4°C for up to 72 h. In addition, 70 frozen samples stored at −20°C for 1 to 8 years (2010: $N = 11$, 2013: $N = 23$, 2017: $N = 36$) were analyzed. The frozen samples were thawed at room temperature and inverted to homogenize the content before being tested on the LCP with the same method as the fresh blood samples.

Fifty microliter whole blood was transferred using a calibrated autopipette (Eppendorf Research® 10–100 μL, pipette tips 10–100 μL, Eppendorf, Hamburg, Germany) into a test vial provided in the test kit for the analyzer. Test vials contain hydrochloric acid solution that breaks down the red blood cells. The vial was inverted 8–10 times, then stored out of sunlight at room temperature for 24 h. After 24 h, the test vial was inverted 8–10 times and 30 μL was transferred with the autopipette to the test strip of the analyzer. The analysis took 3 min and the result was provided in μg/dL. The analyzer does not have memory, so the result was written down before the used sample strip was removed.

For each day of analysis with the LCP a quality control set from the test kit was analyzed. All quality controls analyzed during this study were within the control range given for the respective test kits used.

After analysis on the LCP, the samples were stored at −20°C in the collection tubes. The samples were then sent for analysis at ALS Scandinavia AB (Luleå, Sweden) to determine the BLL with ICP-MS. The freezing chain was not further interrupted. The samples were thawed, inverted for several

minutes, and an aliquot of whole blood was digested with concentrated nitric acid (closed vessel, MW-assisted digestion using Mars5 laboratory digestion system from CEM) followed by dilution with distilled, de-ionized water. Diluted digests were analyzed by ICP-SFMS (ELEMENT2, ThermoScientific, Bremen, Germany), using combination of internal standardization and external calibration. Details on preparation method, measuring parameters and operation conditions can be found elsewhere (38, 39). Method blanks prepared and analyzed alongside with blood samples contain <0.5 μg/L Pb. Accuracy of the method in Pb concentration range 10–460 μg/L was controlled using reference materials from Sero AS (Oslo, Norway, Seronorm Trace elements in Human Whole Blood, Lot 1702826A, L1, L2, and L3) reconstituted according to the manufacturer's instructions.

Statistical Method

All statistical analyses were carried out with R (40). Linear regression modeling was used to assess the agreement between the LCP and the ICP-MS concentrations. BLL_{ICP-MS} was modeled as response with BLL_{LCP} as explanatory variable. Regression coefficients of the model outputs were used to develop conversion equations. The LCP and the ICP-MS BLLs were log transformed to improve normality of error and distribution.

The BLLs were analyzed both pooled and separated into fresh and frozen. One sample was excluded as an extreme outlier with $BLL_{LCP} > 650$ μg/L (over detection limit of the analyzer) and $BLL_{ICP-MS} = 174$ μg/L. The final sample size was $n = 124$ with 54 fresh and 70 frozen samples. The LCP concentration in μg/dL was converted to μg/L. As quantity of frozen samples from each sample year was not enough to analyse each year statistically, all frozen samples were analyzed as one category.

Previous wildlife studies have identified a bias of the ASV method, so Bland-Altman method comparison analysis (41) using R package *blandr* (42) was used to determine a potential bias on BLL of Scandinavian brown bears between the analysis methods of ASV and ICP-MS.

Models tested on log-transformed data:

$$\text{Model 1 } BLL_{ICP-MS\ pooled} = \beta_0 + \beta_1 \left(BLL_{LCP\ pooled}\right) + \epsilon$$

$$\text{Model 2 } BLL_{ICP-MS\ fresh} = \beta_0 + \beta_1 \left(BLL_{LCP\ fresh}\right) + \epsilon$$

$$\text{Model 3 } BLL_{ICP-MS\ frozen} = \beta_0 + \beta_1 \left(BLL_{LCP\ frozen}\right) + \epsilon$$

Significance for analysis was set at $\alpha = 0.05$. Diagnostics plots for the regression models were checked.

RESULTS

BLL analyzed with the LCP had a median of 99 μg/L (mean 106.3 μg/L) in a range of 40–231 μg/L. BLL analyzed with ICP-MS had a mean of 88.1 μg/L (median 83 μg/L) in a range of 32.5–173.0 μg/L.

The LCP was significantly correlated to the ICP-MS BLL both for overall as well as fresh and frozen samples separately (**Table 1**, **Figure 1**) and conversion equations were based on the models 1, 2 and 3. An overall positive bias of the LCP was found with Bland-Altman analysis. For pooled samples, 19.01% (CI: 16.62–21.40%), for fresh samples at 22.50% (CI: 19.53–25.47%), and for frozen samples 16.32% (CI: 12.83–19.82%) (**Figure 2**) showing an overestimation of the BLL compared to ICP-MS results.

When applying the conversion equation on the BLL_{LCP}, the new, calculated BLL was not significantly different from the BLL_{ICP-MS} (pooled, $P = 0.933$; fresh, $P = 0.978$; frozen, $P = 0.988$) with similar range.

DISCUSSION

The results showed a high correlation between LCP and ICP-MS, although with a linear positive bias (overestimation) of 16.3–22.5% of the LCP. Conversion equations for BLL_{LCP} were established to estimate BLL_{ICP-MS} in brown bears for the observed range of this study. Furthermore, the results indicate that Scandinavian brown bears are exposed to elevated BLL.

The positive bias of the LCP contrasts with all other comparison studies conducted on wildlife and cattle, as these studies found a negative bias on the analyzers using the same method (ASV). The frozen samples of our study had a smaller bias when compared to the gold standard which is in alignment with findings by Herring et al. (23) in avian species. Conversion equations for the LCP results to estimate ICP-MS BLL both for pooled, fresh and frozen samples were made, which can be used for future studies in brown bears to approximate the gold standard levels. The pooled conversion formula was provided for the use with a small sample size comprising of both fresh and frozen samples. The higher r^2-value of the pooled conversion formula could be influenced by the larger sample size in this group.

The BLLs of this study were higher than the levels Rogers et al. (30) found in black bears and grizzly bears in Yellowstone, however these levels were only analyzed on a LeadCare® system, and were not validated.

BLLs cannot be directly compared with levels measured using other methods because of the identified bias. Using LCP BLL without correcting for the bias could lead to an overestimation of the actual lead exposure within the observed range of this study.

Factors Affecting BLL or Measurements

The LeadCare® manufacturer recommends to use fresh blood samples, and the FDA permits the use of the machine when used for capillary samples for humans (43). Freezing has been shown to impact the results of BLLs in wildlife (23) and humans (44), and the length of freezing may have had an effect on the measured BLL in this study as the freezing causes evaporation. We saw a smaller bias between the LCP and the ICP-MS in our samples that had been stored frozen prior to LCP analysis, with cause yet to be identified. To examine possible evaporation due to freezing, the samples could in future analysis be weighed before freezing and after thawing for reanalysis after long term storage.

Packed cell volume (PCV) could affect the measured BLLs, as stress throughout the capture, and especially during the chasing period, can cause dehydration and contraction of the spleen during exertion (45). A higher PCV likely gives a higher BLL reading using any analysis method, because of a relatively higher

TABLE 1 | Model parameters with *P*-values, r^2 and Bland-Altman analyzed bias showing a positive bias of the LeadCare® Plus (LCP) for pooled ($N = 124$), fresh ($N = 54$), and frozen ($N = 70$) samples of blood lead levels in Scandinavian brown bear (*Ursus arctos*) and conversion equation based on the regression coefficients for the models 1, 2, and 3 to estimate blood lead levels when analyzed with Inductively coupled plasma mass spectrometry (ICP-MS).

ICP-MS as a function of LCP	*P*	r^2	Bland-Altman bias [CI95]	Conversion equation
Model 1—Pooled	<0.001	0.864	0.1901 [0.1662–0.2140]	logy = 0.0279 + 0.9527(log x)
Model 2—Fresh	<0.001	0.923	0.2250 [0.1953–0.2547]	logy = −0.0779 + 0.9684(log x)
Model 3—Frozen	<0.001	0.817	0.1632 [0.1283–0.1982]	logy = 0.0292 + 0.9579(log x)

CI95: 95% confidence interval.

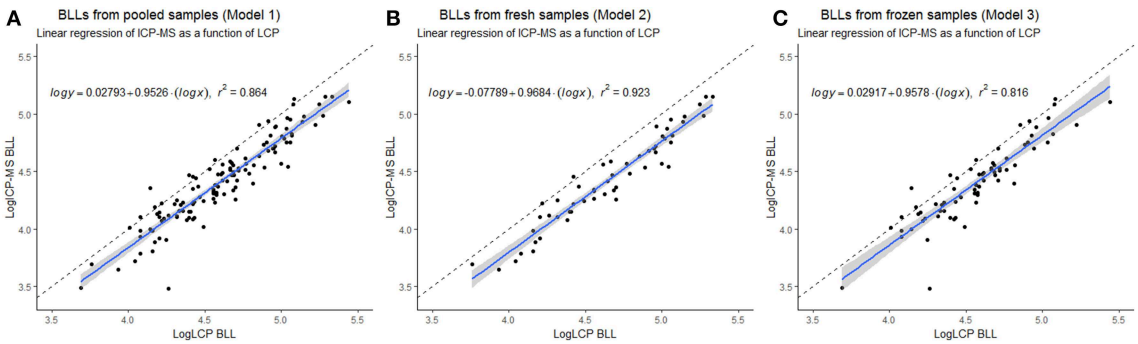

FIGURE 1 | Linear regression of pooled, Model 1 **(A)**, fresh, Model 2 **(B)**, and frozen, Model 3 **(C)** blood lead levels (BLL) of Scandinavian Brown bear (*Ursus arctos*) (sampled 2010–2018) measured with inductively coupled plasma mass spectrometry (ICP-MS) as a function of BLL measured with LeadCare® Plus (LCP). Linear regression model (blue) with 95% confidence interval (gray) and added dashed line of optimal 1 to 1 comparison, and equation of the model with r^2. Plotted with log transformed data.

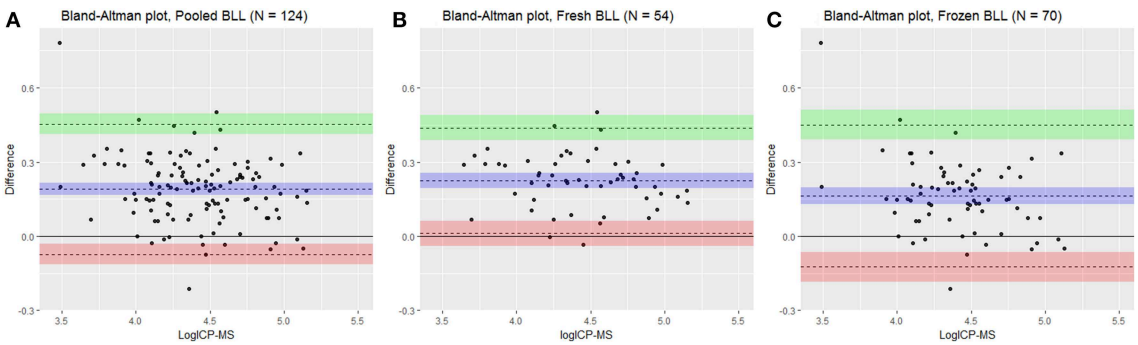

FIGURE 2 | Bland-Altman plot for log transformed pooled **(A)**, fresh **(B)**, and frozen **(C)** blood lead levels (BLL) in Scandinavian brown bear *(Ursus arctos)* comparing analysis methods Inductively coupled plasma mass spectrometry (ICP-MS) and LeadCare® Plus (LCP). X axis shows the log ICP-MS as gold standard reference and Y axis shows differences ($logBLL_{LCP}$-$logBLL_{ICP-MS}$). Represented is mean difference (bias) in blue line with 95% confidence interval in shaded blue with upper limit of agreement of Bland-Altman analysis in green line with 95% confidence interval in shaded green (+1.96*standard deviation) and lower limit of agreement (−1-96*standard deviation) in red line with 95% confidence interval in shaded red.

concentration of red blood cells, to which a majority of the lead is bound. Reference PCV for free-ranging brown bears is 0.41–0.54% (46) following the same capture methods as used in this study, with a seasonal variation of higher PCV in winter compared to summer (47, 48).

BLLs show recent lead exposure or endogenous lead remobilised due to bone resorption. During hibernation, the bear maintains bone mass through balanced bone resorption and formation activity (49, 50). Continuous endogenous exposure could keep the BLLs elevated during hibernation and possibly result in the high concentrations observed in the spring.

A trend of higher bone resorption is seen in bears that give birth (51). As lead is transferred through the placenta and through the milk during the lactational period (18), there could be a higher endogenous exposure in females but overall lower body lead burden because of higher excretion compared to males. The accumulative body lead burden can be measured in bone to investigate life history exposure and sex differences of the bears.

However, accumulation site depends on bone formation activity at time of exposure (52). This is in alignment with findings by Herring et al. (53) that measured bone lead in the femoral bone of brown bears in Croatia. They found differing concentrations within the same individual, dependent on location of sampling site for both trabecular and compact bone.

The LeadCare® analyzers were recalled in May 2017 (54) due to underestimations of BLLs when using venous blood samples in humans. Caldwell et al. (55) reported that the CDC quality assurance program in the last five quality challenges found that participating laboratories were able to accurately analyse BLLs with a LeadCare® Ultra or Plus in 70% of the cases with a set evaluation criteria limit of ±20 μg/L on bovine venous samples that had been stored frozen until distribution. In the same study, overall accuracy of all participating laboratories with no distinction between methods was 89% with the same evaluation criteria limit of ±20 μg/L. This inaccuracy is to be kept in mind when analyzing LCP results.

Perspectives

Lead exposure from spent hunting ammunition is considered a major ecological and One Health concern (56). Ingestion of lead ammunition has not definitively been identified in bears (30). However, novel ways to identify source of exposure from other wildlife studies can be implemented, like measuring antimony (Sb) (57), another component of lead alloy in lead ammunition (58, 59). As lead is present in the environment, other food sources such as berries and ants should be investigated as potential sources, as well as exposure from active lead mines and secondary lead smelters.

The BLLs found in this study show a significant exposure to lead with unknown behavioral or physiological impact on the bears. Accurate monitoring of lead exposure in wildlife species is essential for identifying risks associated with toxicants that are proven harmful. The bear could be used as a sentinel species, as it is an opportunistic omnivore (60) and scavenger (35, 61). Using bear blood as a biomarker for recent exposure, or to compare temporal studies before and after legislative changes, is a relatively easy and readily available tool in biomonitoring.

Monitoring of acute or endogenous lead exposure in individuals, for health assessment, as well as on population level can be carried out using portable lead analyzers such as the LeadCare® Plus with provided conversion equations to approximate gold standard levels within the observed range of this study.

This is the initiating study on lead in Scandinavian brown bears and further research is necessary to investigate potential harmful effects and possible sources of exposure.

DATA AVAILABILITY

The dataset for this study is available upon request.

AUTHOR CONTRIBUTIONS

JA: study design. AB, AT, BF, AE, and JA: capture and sampling. AB, AT, and AE: LeadCare® analysis. IR: inductively coupled plasma mass spectrometry analysis. AB, AT, and BF: data analysis. AB: drafting of manuscript. AB, AT, BF, AE, MB, IR, and JA: revision of manuscript and approval of submitted version.

FUNDING

The present study was mainly funded by the Inland Norway University of Applied Sciences, with contributions from the ALS Scandinavia AB. The Scandinavian Brown Bear Research Project is primarily funded by the Swedish Environmental Protection Agency, the Norwegian Environment Agency, the Austrian Science Fund, the Swedish Association for Hunting and Wildlife Management and the research council of Norway.

ACKNOWLEDGMENTS

We thank the veterinarians, biologists, technicians, students and helicopter pilots who participated in the field work. This is scientific paper no. 280 from the Scandinavian Brown Bear Research Project.

REFERENCES

1. Lanphear BP, Hornung R, Khoury J, Yolton K, Baghurst P, Bellinger DC, et al. Low-level environmental lead exposure and children's intellectual function: an international pooled analysis. *Environ Health Perspect.* (2005) 113:894–9. doi: 10.1289/ehp.7688
2. Lanphear BP, Rauch S, Auinger P, Allen RW, Hornung RW. Low-level lead exposure and mortality in US adults: a population-based cohort study. *Lancet Public Health.* (2018) 3:e177–84. doi: 10.1016/S2468-2667(18)30025-2
3. Nawrot TS, Staessen JA. Low-level environmental exposure to lead unmasked as silent killer. *Circulation.* (2006) 114:1347–9. doi: 10.1161/CIRCULATIONAHA.106.650440
4. WHO. *Lead Poisoning and Health*. (2018). Available online at: http://www.who.int/news-room/fact-sheets/detail/lead-poisoning-and-health (accessed September 11, 2018).
5. Liu J, Gao D, Chen Y, Jing J, Hu Q, Chen Y. Lead exposure at each stage of pregnancy and neurobehavioral development of neonates. *Neurotoxicology.* (2014) 44:1–7. doi: 10.1016/j.neuro.2014.03.003
6. EFSA and Panel on Contaminants in the Food Chain (CONTAM). Scientific opinion on lead in food. *EFSA J.* (2013) 2013:1–321. doi: 10.2903/j.efsa.2010.1570
7. CDC. *Response to Advisory Committee on Childhood Lead Poisoning Prevention Recommendations in "Low Level Lead Exposure Harms Children: A Renewed Call of Primary Prevention"*. (2012). Available online at: http://www.cdc.gov/nceh/lead/ACCLPP/CDC_Response_Lead_Exposure_Recs.pdf (accessed September 11, 2018).
8. CDC. *New Blood Lead Level Information—What Do Parents Need to Know to Protect Their Children?* (2017). Available online at: https://www.cdc.gov/nceh/lead/acclpp/blood_lead_levels.htm (accessed November 20, 2018).
9. Chamberlain AC. Effect of airborne lead on blood lead. *Atmos Environ.* (1982) 17:677–92. doi: 10.1016/0004-6981(83)90415-8

10. Agency for Toxic Substances and Disease Registry. *Toxicological Profile for Lead*. ATSDR (2007). Available online at: https://europepmc.org/books/NBK158766 (accessed December 5, 2018).
11. Rabinowitz MB, Wetherill GW, Kopple JD. Kinetic analysis of lead metabolism in healthy humans. *J Clin Invest.* (1976) 58:260–70. doi: 10.1172/JCI108467
12. International Agency for Research on Cancer. (2006). *Inorganic and Organic Lead Compounds* (IARC). Available online at: www.inchem.org/documents/iarc/vol87/volume87.pdf (accessed May 22, 2019).
13. Barry PSI, Mossman DB. Lead concentrations in human tissues. *Br J Ind Med.* (1970) 27:339–51. doi: 10.1136/oem.27.4.339
14. O'flaherty EJ, Hammond PB, Lerner SI. Dependence of apparent blood lead half-life on the length of previous lead exposure in humans. *Toxicol Sci.* (1982) 2:49–54. doi: 10.1093/toxsci/2.1.49
15. Gulson B. Stable lead isotopes in environmental health with emphasis on human investigations. *Sci Total Environ.* (2008) 400:75–92. doi: 10.1016/j.scitotenv.2008.06.059
16. Silbergeld EK. Lead in bone: implications for toxicology during pregnancy and lactation. *Environ Health Perspect.* (1991) 91:63–70. doi: 10.1289/ehp.919163
17. Gulson BL, Mahaffey KR, Jameson CW, Mizon KJ, Korsch MJ, Cameron MA, et al. Mobilization of lead from the skeleton during the postnatal period is larger than during pregnancy. *J Lab Clin Med.* (1998) 133:324–9. doi: 10.1016/S0022-2143(98)90182-2
18. Xie X, Ding G, Cui C, Chen L, Gao Y, Zhou Y, et al. The effects of low-level prenatal lead exposure on birth outcomes. *Environ Pollut.* (2013) 175:30–4. doi: 10.1016/j.envpol.2012.12.013
19. Ettinger AS, Roy A, Amarasiriwardena CJ, Smith D, Lupoli N. Maternal blood, plasma, and breast milk lead: lactational transfer and contribution to infant exposure. *Environ Health Perspect.* (2014) 122:87–92. doi: 10.1289/ehp.1307187
20. Keller CA, Doherty RA. Bone lead mobilization in lactating mice and lead transfer to suckling offspring. *Top Catal.* (1980) 55:220–8. doi: 10.1016/0041-008X(80)90083-6
21. Bushnell PJ, DeLuca HF. Lactose facilitates the intestinal absorption of lead in weanling rats. *Science.* (1981) 211:61–3. doi: 10.1126/science.7444448
22. Bonnefoy C, Menudier A, Moesch C, Lachâtre G, Mermet JM. Validation of the determination of lead in whole blood by ICP-MS. *J Anal Atom Spectrom.* (2002) 17:1161–5. doi: 10.1039/b201889f
23. Herring G, Eagles-Smith CA, Bedrosian B, Craighead D, Domenech R, Langner HW, et al. Critically assessing the utility of portable lead analyzers for wildlife conservation. *Wildl Soc Bull.* (2018) 42:284–94. doi: 10.1002/wsb.892
24. Palmer CD, Lewis ME, Geraghty CM, Barbosa F, Parsons PJ. Determination of lead, cadmium and mercury in blood for assessment of environmental exposure: a comparison between inductively coupled plasma-mass spectrometry and atomic absorption spectrometry. *Spectrochim Acta Part B Atom Spectrosc.* (2006) 61:980–90. doi: 10.1016/j.sab.2006.09.001
25. Barón-Jaimez J, Joya MR, Barba-Ortega J. Anodic stripping voltammetry—ASV for determination of heavy metals. *J Phys Conf Ser.* (2013) 466:2023. doi: 10.1088/1742-6596/466/1/012023
26. Pineau A, Fauconneau B, Rafael M, Viallefont A, Guillard O. Determination of lead in whole blood: comparison of the leadCare blood lead testing system with Zeeman longitudinal electrothermal atomic absorption spectrometry. *J Trace Elem Med Biol.* (2002) 16:113–7. doi: 10.1016/S0946-672X(02)80037-2
27. Craighead D, Bedrosian B. Blood lead levels of common ravens with access to big-game offal. *J Wildl Manag.* (2008) 72:240–5. doi: 10.2193/2007-120
28. Langner HW, Domenech R, Slabe VA, Sullivan SP. Lead and mercury in fall migrant golden eagles from western North America. *Arch Environ Contam Toxicol.* (2015) 69:54–61. doi: 10.1007/s00244-015-0139-6
29. Bischoff K, Gaskill C, Erb HN, Ebel JG, Hillebrandt J. Comparison of two methods for blood lead analysis in cattle: graphite-furnace atomic absorption spectrometry and leadcare(R) II system. *J Vet Diagn Invest.* (2010) 22:729–33. doi: 10.1177/104063871002200510
30. Rogers TA, Bedrosian B, Graham J, Foresman KR. Lead exposure in large carnivores in the greater Yellowstone ecosystem. *J Wildl Manag.* (2012) 76:575–82. doi: 10.1002/jwmg.277
31. Brown CS, Luebbert J, Mulcahy D, Schamber J, Rosenberg DH. Blood lead levels of wild Steller's Eiders (Polysticta stelleri) and black scoters (Melanitta nigra) in Alaska using a portable blood lead analyzer. *J Zoo Wildl Med.* (2006) 37:361–5. doi: 10.1638/05-092.1
32. González F, López I, Suarez L, Moraleda V, Rodríguez C. Levels of blood lead in Griffon vultures from a Wildlife Rehabilitation Center in Spain. *Ecotoxicol Environ Saf.* (2017) 143:143–50. doi: 10.1016/j.ecoenv.2017.05.010
33. Bedrosian B, Parish CN, Craighead D. Differences between blood lead level detection techniques: Analysis within and among three techniques and four avian species. In: Watson RT, Fuller M, Pokras M, Hunt WG, editors. *Ingestion of Lead from Spent Ammunition: Implications for Wildlife and Humans*. Boise, ID: The Peregrine Fund (2009). doi: 10.4080/ilsa.2009.0122
34. Stokke S, Brainerd S, Arnemo JM. Metal deposition of copper and lead bullets in moose harvested in Fennoscandia. *Wildl Soc Bull.* (2017) 41:98–106. doi: 10.1002/wsb.731
35. Rauset GR, Kindberg J, Swenson JE. Modeling female brown bear kill rates on moose calves using global positioning satellite data. *J Wildl Manag.* (2012) 76:1597–606. doi: 10.1002/jwmg.452
36. SBBRP. *Scandinavian Brown Bear Research Project*. (2019). Available online at: http://bearproject.info/about-the-project/ (accessed March 7, 2019).
37. Arnemo JM, Evans AL. Biomedical protocols for free-ranging brown bears, wolves, wolverines and lynx. *Inl Norw Univ Appl Sci.* (2017) 2017:1–16. doi: 10.13140/RG.2.1.2717.7120
38. Rodushkin I, Ödman F, Branth S. Multi-element analysis of environmental samples by high resolution inductively coupled plasma mass spectrometry. *Fresenius J Anal Chem.* (1999) 364:338–46. doi: 10.1007/s002160051346
39. Rodushkin I, Ödman F, Olofsson R, Axelsson MD. Determination of 60 elements in whole blood by sector field inductively coupled plasma mass spectrometry. *J Anal At Spectrom.* (2000) 15:937–44. doi: 10.1039/B201889F
40. R Core Team. *R: A Language and Environment for Statistical Computing*. (2018). Available online at: https://www.r-project.org/ (accessed September 7, 2018).
41. Bland JM, Altman DG. Measuring agreement in method comparison studies. *Stat Methods Med Res.* (1999) 8:135–60. doi: 10.1177/096228029900800204
42. Datta D. *Blandr: A Bland-Altman Method Comparison Package for R*. (2017).
43. FDA UFDA. *Recalls LeadCare Plus and Ultra Testing Systems due to Inaccurate Test Results*. Magellan Diagnostics Inc. fda.gov (2018). Available online at: https://www.fda.gov/MedicalDevices/Safety/ListofRecalls/ucm560534.htm (accessed March 7, 2019).
44. Wang S, Peter F. The stability of human blood lead in storage. *J Anal Toxicol.* (1985) 9:85–8.
45. Vatner SF, Higgins CB, Millard RW, Franklin D. Role of the spleen in the peripheral vascular response to severe exercise in untethered dogs. *Cardiovasc Res.* (1974) 8:276–82. doi: 10.1093/cvr/8.2.276
46. Græsli AR, Fahlman Å, Evans AL, Bertelsen MF, Arnemo JM, Nielsen SS. Haematological and biochemical reference intervals for free-ranging brown bears (*Ursus arctos*) in Sweden. *BMC Vet Res.* (2014) 10:1–9. doi: 10.1186/s12917-014-0183-x
47. Evans AL, Sahlén V, Støen OG, Fahlman Å, Brunberg S, Madslien K, et al. Capture, anesthesia, and disturbance of free-ranging brown bears (*Ursus arctos*) during hibernation. *PLoS ONE.* (2012) 7:1–8. doi: 10.1371/journal.pone.0040520
48. Græsli AR, Evans AL, Fahlman Å, Bertelsen MF, Blanc S, Arnemo JM. Seasonal variation in haematological and biochemical variables in free-ranging subadult brown bears (*Ursus arctos*) in Sweden. *BMC Vet Res.* (2015) 11:1–9. doi: 10.1186/s12917-015-0615-2
49. Donahue SW, Galley SA, Vaughan MR, Patterson-Buckendahl P, Demers LM, Vance JL, et al. Parathyroid hormone may maintain bone formation in hibernating black bears (*Ursus americanus*) to prevent disuse osteoporosis. *J Exp Biol.* (2006) 209:1630–8. doi: 10.1242/jeb.02185
50. Hellgren EC. Physiology of hibernation in bears. *Ursus*. (1998) 10:467–77.
51. Donahue SW, Vaughan MR, Demers LM, Donahue HJ. Serum markers of bone metabolism show bone loss in hibernating bears. *Clin Orthop Relat Res.* (2003) 295–301. doi: 10.1097/00003086-200303000-00040
52. Tarragó O, Brown MJ. Case studies in environmental medicine (CSEM). *Lead Toxicity*. (2017) P. 66. Available online at: https://www.atsdr.cdc.gov/csem/csem.asp?csem=34&po=0
53. Lazarus M, Orct T, Reljić S, Sedak M, Bilandžić N, Jurasović J, et al. Trace and macro elements in the femoral bone as indicators of long-term environmental

exposure to toxic metals in European brown bear (Ursus arctos) from Croatia. *Environ Sci Pollut Res.* (2018) 25:21656–70. doi: 10.1007/s11356-018-2296-4
54. FDA UFDA. (2017). FDA Warns Against Using Magellan Diagnostics LeadCare Testing Systems with Blood Obtained from a Vein: FDA Safety Communication. Available online at: https://www.fda.gov/MedicalDevices/Safety/AlertsandNotices/ucm558733.htm (accessed February, 9, 2019).
55. Caldwell KL, Cheng P, Vance KA, Makhmudov A, Jarrett JM, Caudill SP, et al. LAMP : a CDC program to ensure the quality of blood-lead laboratory *Measurements*. (2019) 25:23–30. doi: 10.1097/PHH.0000000000000886
56. Hampton JO, Laidlaw M, Buenz E, Arnemo JM. Heads in the sand : public health and ecological risks of lead-based bullets for wildlife shooting in Australia. *Wildl Res.* (2018) 45:287–306. doi: 10.1071/WR17180
57. French AD. *Toxicokinetics and Sources of Lead in American Woodcock (Scolopax minor)*. (2017) Available online at: http://hdl.handle.net/2346/73544 (accessed December 3, 2018).
58. Anderson CG. The metallurgy of antimony. *Chemie Erde.* (2012) 72:3–8. doi: 10.1016/j.chemer.2012.04.001
59. Storgaard S, Willems M, Storgaard BS. The fate of lead in soils: the transformation of lead pellets in shooting-range soils. *R Swedish Acad Sci.* (1987) 16:11–5.
60. Stenset NE, Lutnæs PN, Bjarnadóttir V, Dahle B, Fossum KH, Jigsved P, et al. Seasonal and annual variation in the diet of brown bears *Ursus arctos* in the boreal forest of southcentral Sweden. *Wildl Biol.* (2016) 22:107–16. doi: 10.2981/wlb.00194
61. Legagneux P, Suffice P, Messier JS, Lelievre F, Tremblay JA, Maisonneuve C, et al. High risk of lead contamination for scavengers in an area with high moose hunting success. *PLoS ONE.* (2014) 9:e111546. doi: 10.1371/journal.pone.0111546

Conflict of Interest Statement: The authors declare that the research was conducted in the absence of any commercial or financial relationships that could be construed as a potential conflict of interest.

Copyright © 2019 Boesen, Thiel, Fuchs, Evans, Bertelsen, Rodushkin and Arnemo. This is an open-access article distributed under the terms of the Creative Commons Attribution License (CC BY). The use, distribution or reproduction in other forums is permitted, provided the original author(s) and the copyright owner(s) are credited and that the original publication in this journal is cited, in accordance with accepted academic practice. No use, distribution or reproduction is permitted which does not comply with these terms.

frontiers in Veterinary Science

ORIGINAL RESEARCH
published: 12 September 2019
doi: 10.3389/fvets.2019.00304

Differentiating *Batrachochytrium dendrobatidis* and *B. salamandrivorans* in Amphibian Chytridiomycosis Using RNAScope® *in situ* Hybridization

Robert J. Ossiboff[1], Anastasia E. Towe[2], Melissa A. Brown[1], Ana V. Longo[3,4], Karen R. Lips[4], Debra L. Miller[2,5], E. Davis Carter[5], Matthew J. Gray[5] and Salvatore Frasca Jr.[1]*

[1] Department of Comparative, Diagnostic, and Population Medicine, College of Veterinary Medicine, University of Florida, Gainesville, FL, United States, [2] Department of Biomedical and Diagnostic Sciences, College of Veterinary Medicine, University of Tennessee, Knoxville, Knoxville, TN, United States, [3] Department of Biology, University of Florida, Gainesville, FL, United States, [4] Department of Biology, University of Maryland College Park, College Park, MD, United States, [5] Center for Wildlife Health, University of Tennessee Institute of Agriculture, Knoxville, TN, United States

OPEN ACCESS

Edited by:
Erica Leigh Behling-Kelly, Cornell University, United States

Reviewed by:
Steven Victor Kubiski, University of California, Davis, United States
Jose Guillermo Vilches-Moure, Stanford University, United States

***Correspondence:**
Robert J. Ossiboff
rossiboff@ufl.edu

Specialty section:
This article was submitted to Veterinary Experimental and Diagnostic Pathology, a section of the journal Frontiers in Veterinary Science

Received: *16 July 2019*
Accepted: *28 August 2019*
Published: *12 September 2019*

Citation:
Ossiboff RJ, Towe AE, Brown MA, Longo AV, Lips KR, Miller DL, Carter ED, Gray MJ and Frasca S Jr (2019) Differentiating Batrachochytrium dendrobatidis and B. salamandrivorans in Amphibian Chytridiomycosis Using RNAScope® in situ Hybridization. Front. Vet. Sci. 6:304. doi: 10.3389/fvets.2019.00304

Batrachochytrium dendrobatidis and *B. salamandrivorans* are important amphibian pathogens responsible for morbidity and mortality in free-ranging and captive frogs, salamanders, and caecilians. While *B. dendrobatidis* has a widespread global distribution, *B. salamandrivorans* has only been detected in amphibians in Asia and Europe. Although molecular detection methods for these fungi are well-characterized, differentiation of the morphologically similar organisms in the tissues of affected amphibians is incredibly difficult. Moreover, an accurate tool to identify and differentiate *Batrachochytrium* in affected amphibian tissues is essential for a specific diagnosis of the causative agent in chytridiomycosis cases. To address this need, an automated dual-plex chromogenic RNAScope® *in situ* hybridization (ISH) assay was developed and characterized for simultaneous detection and differentiation of *B. dendrobatidis* and *B. salamandrivorans*. The assay, utilizing double Z target probe pairs designed to hybridize to 28S rRNA sequences, was specific for the identification of both organisms in culture and in formalin-fixed paraffin-embedded amphibian tissues. The assay successfully identified organisms in tissue samples from five salamander and one frog species preserved in formalin for up to 364 days and was sensitive for the detection of *Batrachochytrium* in animals with qPCR loads as low as 1.1×10^2 zoospores/microliter. ISH staining of *B. salamandrivorans* also highlighted the infection of dermal cutaneous glands, a feature not observed in amphibian *B. dendrobatidis* cases and which may play an important role in *B. salamandrivorans* pathogenesis in salamanders. The developed ISH assay will benefit both amphibian chytridiomycosis surveillance projects and pathogenesis studies by providing a reliable tool for *Batrachochytrium* differentiation in tissues.

Keywords: chytrid, dermal glands, frog, fungus, ISH, pathology, salamander

INTRODUCTION

Chytridiomycosis is a devastating fungal disease causing substantial and ongoing global amphibian biodiversity loss (1–4). Two fungal pathogens have been identified as agents of amphibian chytridiomycosis, *Batrachochytrium dendrobatidis* (*Bd*), and *B. salamandrivorans* (*Bsal*) (1, 5, 6). Both species are believed to have originated in Asia, and have been spread globally as a result of anthropogenic factors (2, 7). *Bd* was first identified in 1998 (5); it can cause clinical disease in all orders of amphibians, including frogs, salamanders, and caecilians, and can be found on all continents where amphibians occur (8).

In contrast, *Bsal* was first documented in 2013, and while it can be detected on some frog species, reports of clinical disease are restricted to salamanders (1, 9, 10). The documented distribution is limited to Asia and Europe (1, 11, 12). Given the potential for widespread *Bsal*-associated mortalities on other continents with high salamander biodiversity, like the Americas, there is a critical and urgent need for accurate, specific, and sensitive molecular and tissue-based diagnostic tests for identification of *Bsal* (2, 13). The case definition for confirmed *Bsal* chytridiomycosis includes histopathology consistent with *Bsal* infection with correlating molecular diagnostics (14). While there are some unique morphologic features particular to each *Bd* and *Bsal* in culture (15), differentiation in tissues can be difficult. As natural mixed *Bd*/*Bsal* infections are likely given the high prevalence of *Bd* in some wild American salamander populations if *Bsal* was ever to be introduced, there is a distinct need for tissue-level differentiation of *Bd* and *Bsal* (16–18).

Identification and differentiation of pathogens in tissue section are primarily achieved by either antibody- or nucleic acid-based modalities. In antibody-based assays, such as immunohistochemistry, unique protein epitopes to a target pathogen are required. Differentiation of closely related pathogens using IHC can be difficult due to conserved amino acid sequence, and polyclonal anti-*Bd* antibodies cross-react with *Bsal* (1). Even a monoclonal antibody, 5C4, specific for *Bd* and *Bsal*, binds to proteins from both organisms in western blots (19). While the western blot banding profile for each of the two organisms was unique, the antibody would be unlikely to differentiate *Bd* and *Bsal* in tissue section given its dual reactivity. In contrast, nucleic acid-based tissue-based detection modalities, namely *in situ* hybridization (ISH), utilize specific, and unique stretches of genomic or expressed RNA sequence. Recent advances in ISH, namely RNAScope® technology, have improved the sensitivity and specificity of the technique as well as developing methodologies for simultaneous detection of multiple nucleic acid targets (20–22).

To simultaneously detect and differentiate *Bd* and *Bsal* organisms in formalin-fixed, paraffin-embedded skin sections from amphibians, an automated dual-plex chromogenic RNAScope® ISH was developed and characterized. The specificity of the assay was tested on both pure cultures of *Bd* and *Bsal* and infected animals, the effect of formalin-fixation time and *Bd*/*Bsal* loads on ISH results was compared, and the technique was utilized to assess the distribution of *Bd* and *Bsal* in infected animals.

MATERIALS AND METHODS

Batrachochytrium dendrobatidis (*Bd*) and *B. salamandrivorans* (*Bsal*) Culture

Bd isolate ALKL1 (isolated from an eastern newt [*Notophthalmus viridescens*] from Virginia, USA) and *Bsal* isolate AMFP (isolated from a morbid wild fire salamander [*Salamandra salamandra*] from Bunderbos, The Netherlands) were grown on 1% tryptone plates (1, 23). The cultures were individually scraped and placed in a 1.5 ml microcentrifuge tube containing approximately 0.7 ml 70% ethanol. Additional aliquots of scraped *Bd* and *Bsal* were combined and fixed in 70% ethanol together. Microcentrifuge tubes were briefly centrifuged, ethanol was removed, and the fixed fungi were suspended in Histogel (Richard-Allan Scientific, Kalamazoo, Michigan), processed routinely and embedded in paraffin.

Experimental Infection of Eastern Newts (*Notophthalmus viridescens*) With *Bd* and *Bsal*

Adult eastern newts were collected from Maryland, screened for *Bd* and *Bsal*, treated with itraconazole, and experimentally infected with *Bd*, *Bsal*, or both *Bd* and *Bsal* as previously described (23). All *Batrachochytrium* infected newts died during the experiment, and uninfected control newts were euthanized using benzocaine hydrochloride. Postmortem swabs were screened for *Bd* and *Bsal* by qPCR as previously described (23). Newts were collected under MD Department of Natural Resources permit No. 56,427. Lab protocols were performed under University of Maryland IACUC protocol R-15-15.

Newts were fixed in 10% neutral buffered formalin for ∼48 h before being transferred to 70% ethanol. Two newts from each experimental group (*Bd*-/*Bsal*-; *Bd*+/*Bsal*-; *Bd*-/*Bsal*+; *Bd*+/*Bsal*+) were decalcified in 0.5 M ethylenediamine tetraacetate acid (EDTA), ph 8.0 for ∼24 h. Serial transverse sections of the body and sagittal sections of all limbs and the tail were taken and submitted for routine processing and paraffin embedding.

Experimental Infection of Large-Blotched Ensatinas (*Ensatina eschscholtzii klauberi*), Red Salamanders (*Pseudotriton ruber*), Eastern Newts (*Notophthalmus viridescens*), Red-Legged False Brook Salamanders (*Aquiloeurycea cephalica*), and Yellow-Eyed Ensatinas (*Ensatina eschscholtzii xanthoptica*) With *Bsal*

Large-blotched ensatinas (*E. e. klauberi*) and red salamanders (*Pseudotriton ruber*) were raised in captivity by Indoor Ecosystems LLC (Whitehouse, OH, USA). Eastern newts (*N. viridescens*), yellow-eyed ensatinas (*Ensatina eschscholtzii xanthoptica*), and red-legged false brook salamanders (*Aquiloeurycea cephalica*) and were collected from the wild (Tennessee, USA, California, USA, and Mexico, respectively). *Notophthalmus viridescens* were collected under Tennessee

Wildlife Resources Agency Scientific Collection Permit #1990. *Ensatina eschscholtzii xanthoptica* were collected under California Department of Fish and Wildlife Scientific Collection Permit #SC-11505. *Aquiloeurycea cephalica* were collected under permit from the Agriculture, Stockbreeding, Rural Development, Fishing and Food Ministry of Mexico and import permit #MA87825B-1 from the United States Fish and Wildlife Service. The *A. cephalica* were determined to be naturally infected with *Bd* by qPCR using previously described methods, which provided an opportunity for a natural co-exposure experiment (24). All other animals were verified as *Bd* qPCR negative.

Bsal isolate AMFP was grown on tryptone gelatin hydrolysate plates and flooded to create serial dilutions from 5×10^3 to 5×10^6 *Bsal* zoospores/mL. Individuals from each species were exposed to *Bsal* in 100-mL containers for 24 h that contained 1 mL of inoculum and 9 mL of autoclaved water. After the *Bsal* challenge, salamanders were housed in husbandry containers with moist paper towel and a cover object. Salamanders were humanely euthanized using benzocaine hydrochloride upon loss of righting ability. All husbandry and euthanasia procedures followed the Amphibian Husbandry Resource Guide of the Association of Zoos and Aquariums and the Guide for Euthanasia by the American Veterinary Medical Association. All animal procedures were approved by University of Tennessee Institutional Animal Care and Use Committee protocol #2395.

At necropsy, all animals were swabbed to test for the presence of *Bsal* DNA (and *Bd* for *A. cephalica* co-exposure experiments). Genomic DNA was extracted (Qiagen DNeasy Blood and Tissue Kit, Hilden, Germany) and quantitative PCR performed using an Applied Biosystems Quantstudio 6 Flex system (Thermo Fisher Scientific, USA) using previously described methods (24). All swabs were run in duplicate, and the number of *Batrachochytrium* zoospore copies/μl was calculated using serial dilutions of synthetic *Bsal* and *Bd* DNA.

After necropsy, samples were preserved in 10% neutral buffered formalin until processing (2–364 days). The length of formalin storage was varied to examine potential effects of fixation time on ISH sensitivity. Animals were then decalcified in 0.5M EDTA, ph 8.0 for ∼24 h. Serial transverse sections of the body and sagittal sections of all limbs and the tail were taken and submitted for routine processing and paraffin embedding.

Naturally Occurring Little Devil Poison Frog (*Oophaga sylvatica*) Chytridiomycosis

A captive born and bred little devil poison frog (*Oophaga sylvatica*) was submitted to the Aquatic, Amphibian, and Reptile Pathology Service at the University of Florida's College of Veterinary Medicine for diagnostic necropsy. The frog arrived in 70% ethanol, was transferred to 10% neutral buffered formalin for 24 h, and then decalcified in 0.5M EDTA, ph 8.0 for ∼24 h. Serial transverse sections of the body and sagittal sections of all limbs and the tail were taken and submitted for routine processing and paraffin embedding. Histopathologic findings were consistent with *Bd* chytridiomycosis, and the sample was utilized for ISH as an anuran (frog) chytridiomycosis sample.

RNAScope® Dual-Plex Chromogenic *in situ* Hybridization (ISH)

Custom RNAScope® target-specific oligonucleotide (ZZ) probes were designed by Advanced Cell Diagnostics (Advanced Cell Diagnostics, Newark, California). Two ZZ probes, complementary to nucleotides 452-555 of *B. dendrobatidis* JEL 197 (NG_027619.1) and nucleotides 444-584 of *Batrachochytrium salamandrivorans* isolate AMFP (KC762293.1) 28S rRNA sequences, were designed each for *Bd* and *Bsal*, respectively. Chromogenic ISH was performed on a Leica BOND RX Fully Automated Research Stainer (Leica Biosystems, Buffalo Grove, Illinois) using RNAscope technology (22). Formalin-fixed paraffin-embedded tissue blocks were sectioned at 4 μm and mounted on Fisherbrand SuperFrost Plus glass slides (Fisher Scientific, Pittsburgh, PA). Automated, dual-plex, chromogenic RNAscope using methodology based on Anderson et al. (20) was performed using both *Bd* [LS, catalog #527278] and *Bsal* [LS, catalog #527288-C2] ISH probes. Pretreatment, hybridization, signal amplification, and detection (RNAscope Reference Guide, ACD/Biotechne) were performed on the Leica BOND RX. Pretreatment conditions included sequential deparaffinization, target retrieval using Leica Epitope Retrieval Buffer at 95°C for 15 m, protease digestion at 40°C for 15 min, and endogenous enzyme block. *Bd* and *Bsal* probes were hybridized at 42°C for 120 min, followed by signal development. After hybridization, serial signal amplification reactions were followed by online fast red chromogenic development of the *Bsal* probe. PermaGreen/HRP (Diagnostic Biosystems, Pleasanton, CA) was manually applied for 3 min to visualize the *Bd* probe. Slides were counterstained with hematoxylin, ImmunoHisto-Sealer (Diagnostic BioSystems, Pleasonton, CA) was applied for long-term retention of the green signal, and coverslips were mounted with Vectamount Permanent (Vector Laboratories, Burlingame, CA). The dihydrodipicolinate reductase (dapB) probe [LS, catalog #320758] was used as a negative control probe and was applied to separate histologic sections processed concurrently and in the same manner as those that received the *Bd* and *Bsal* probes. Glass slides were visualized on an Olympus BX43 microscope (Olympus Corporation, Tokyo, Japan); photomicrographs were captured with a Spot Insight 12 Mp sCMOS Color Camera (Spot Imaging, Sterling Heights, Michigan) and SPOT Imaging software (v5.4.3; Spot Imaging, Sterling Heights, Michigan).

RESULTS

Specificity of *Bd*/*Bsal* ISH on Cultured *Batrachochytrium*

To determine the specificity of the dual-plex chromogenic ISH assay, staining of *Bd* and *Bsal* cultures was performed (**Figure 1**), including hematoxylin and eosin (**Figure 1A**) which did not differentiate both fungi in mixed samples due to similar morphologic features. Pure cultures of *Bd* (**Figure 1B**) and *Bsal* (**Figure 1C**) demonstrated strong, positive green or red staining, respectively, of all fungal life stages including zoospores,

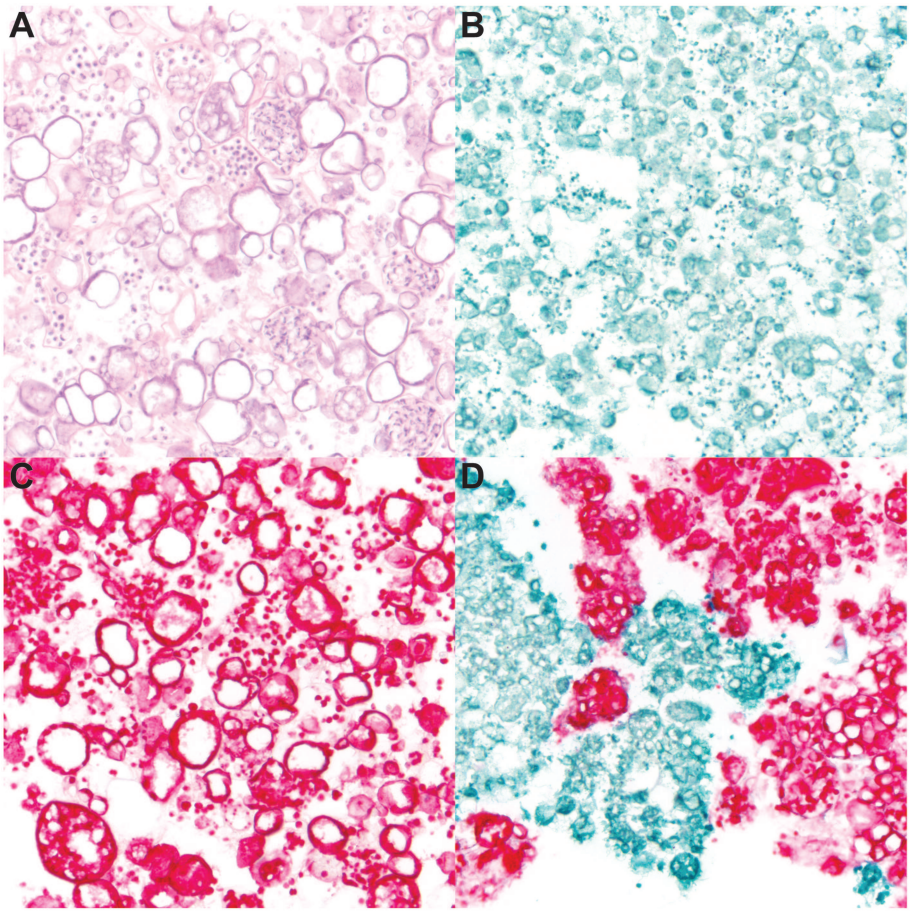

FIGURE 1 | RNAScope® *in situ* hybridization (ISH) of cultured *Batrachochytrium dendrobatidis* (*Bd*) and *B. salamandrivorans* (*Bsal*). Ethanol fixed samples of mixed *Bd*/*Bsal* **(A,D)**, *Bd* alone **(B)**, or *Bsal* alone **(C)** were suspended in Histogel sample processing matrix and processed for histology. Samples were then stained with hematoxylin and eosin **(A)** and dual-plex chromogenic *Bd*/*Bsal* RNAScope® ISH targeting the 28S rRNA gene. *Bd* probe binding is visualized by green staining **(B,D)** and *Bsal* probe binding is visualized by red staining **(C,D)**. Intact fungal sporangia containing zoospores, empty sporangia, and free zoospores are present in all samples. All images are at 600x magnification.

mature zoosporangia, and empty, discharged sporangia. In a mixed sample, *Bd* and *Bsal* organisms were clearly differentiated by ISH (**Figure 1D**), with little to no cross reactivity or non-specific background staining. No positive staining was noted in the dapB stained negative control slides (data not shown).

Specificity of *Bd*/*Bsal* ISH on Experimentally Infected Eastern Newts (*Notophthalmus viridescens*)

To confirm *Bd* and *Bsal* ISH probe reactivity on formalin-fixed paraffin-embedded tissue sections, automated dual-plex chromogenic ISH was carried out on slides of *N. viridescens* experimentally infected with *Bd* and/or *Bsal* (23). Newts were preserved with limited formalin fixation time (∼48 h) before transfer to 70% ethanol for long term storage, and as such were ideal for RNAScope® ISH validation per manufacturer's recommendations. Dual *Bd*/*Bsal* infected salamanders provided material to assess diagnostic specificity of the probe, and the small size of the newts also permitted screening of all tissues to assess for non-specific probe binding (**Figure 2**). Skin sections from uninfected newts (**Figures 2A–C**) stained with H&E, GMS, and ISH served as controls. *N. viridescens* infected with *Bd* alone, *Bsal* alone, or both *Bd*/*Bsal* all showed histopathologic changes consistent with chytridiomycosis, including epidermal hyperplasia, hyperkeratosis, and intralesional fungus (**Figures 2D,G,J**). *Batrachochytrium* zoosporangia and zoospores were absent in uninfected animals (**Figure 2B**), but present in all infected salamanders as highlighted by GMS staining (**Figures 2E,H,K**). No ISH reactivity was detected in the skin of *Bd*-/*Bsal*- newts (**Figure 2C**). In *Bd*+/*Bsal*- newts, zoosporangia exhibited green *Bd* probe staining (**Figure 2F**), while only red *Bsal* probe staining was detected in the fungus present within *Bd*-/*Bsal*+ newts (**Figure 2I**). In dual infected animals, both red *Bsal* and green *Bd* probe staining was present throughout the skin sections, and in some foci, *Bd,* and

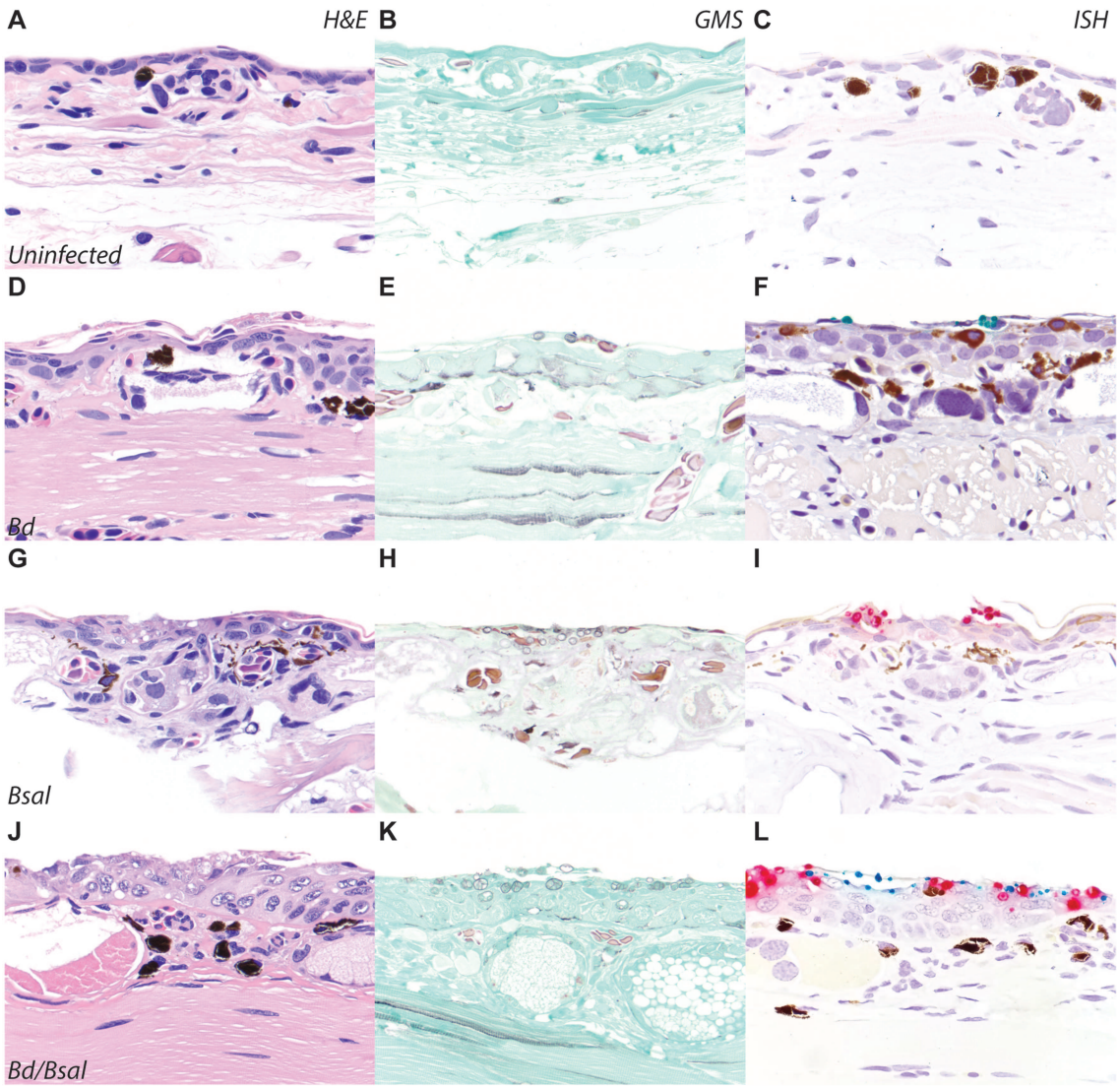

FIGURE 2 | *Bd/BSal* RNAScope® ISH of eastern newts (*Notophthalmus viridescens*). Skin sections from uninfected **(A–C)**, *Bd*-infected **(D–F)**, *Bsal*-infected **(G–I)**, or *Bd/Bsal* infected **(J–L)** are stained with hematoxylin and eosin **(A,D,G,J)**, Gomori methenamine silver to highlight fungal organisms **(B,E,H,K)**, or *Bd/Bsal* ISH **(C,F,I,L)**. *Bd* probe binding is visualized by green staining **(F,L)** and *Bsal* probe binding is visualized by red staining **(I,L)**. In all cases of chytridiomycosis, the presence of fungal organisms is accompanied by epidermal hyperplasia and hyperkeratosis. All images are at 200x magnification.

Bsal zoosporangia were intermingled amongst each other (**Figure 2L**). Mature fungal zoosporangia with a discharge tube, morphologically consistent with *B. dendrobatidis,* were highlighted by green *Bd* probe staining, while zoosporangia with prominent, multifocal septation (colonial zoosporangia), morphologically consistent with *B. salamandrivorans*, were highlighted by red *Bsal* probe staining (1, 5, 6). No non-specific staining of the *Bd* probe was noted in any of tissues of the examined newts; mild non-specific staining of the *Bsal* probe was noted in the retina and occasionally arthropod chitin (ingesta) in the gastrointestinal tract (data not shown). DapB control probe staining was uniformly negative in all animals (**Supplementary Figure 1A**).

Validation of *Bd/Bsal* ISH in Other Amphibian Species

Four additional species of salamander and one frog species were used for automated dual-plex chromogenic *Bd/Bsal* ISH testing to confirm probe specificity in other amphibian species. Red-legged false brook salamanders (*A. cephalica*; $n = 3$), large-blotched ensatinas (*E. e. klauberi;* $n = 5$), yellow-eyed ensatinas (*E. e. xanthoptica*; $n = 6$), red salamanders (*P. ruber*; $n = 3$), and a little devil poison frog (*O. sylvatica*; $n = 1$). All salamanders ($n = 17$) were experimentally infected with *Bsal*, and necropsy fungal loads ranged from 1.4×10^2 to 2.1×10^5 genome copies per microliter (**Table 1**). The three *A. cephalica* were naturally infected with *Bd* at collection, with necropsy *Bd*

TABLE 1 | Summary of animals used for *Bd*/*Bsal* RNAScope® ISH validation.

Species	Days in Formalin	qPCR loads (copies or zoospores/μL)		ISH	
		Bd	***Bsal***	***Bd***	***Bsal***
Eastern newt (*Notophthalmus viridescens*)	2	–	–	–	–
	2	–	–	–	–
	2	70,851[Z]	–	+	–
	2	33,608[Z]	–	+	–
	2	–	268,366[Z]	–	+
	2	–	103,125[Z]		
	2	43,850[Z]	108[Z]	+	+
	2	140,944[Z]	59,838[Z]	+	+
	2	–	4,003[C]	–	+
	331	–	4,687[C]	–	+
	2	–	10,690[C]	–	+
	2	–	12,892[C]	–	+
	364	–	22,316[C]	–	+
	8	–	118,881[C]	–	+
	7	–	186,371[C]	–	+
	8	–	292,173[C]	–	+
Red-legged false brook salamander (*Aquiloeurycea cephalica*)	154	182,448[C]	208,652[C]	+	+
	154	2246,063[C]	139[C]	+	–
	154	622[C]	54,748[C]	–	+
Large-blotched ensatina (*Ensatina eschscholtzii klauberi*)	2	–	44,132[C]	–	+
	2	–	70,830[C]	–	+
	2	–	163,558[C]	–	+
	131	–	5,252[C]	–	+
	104	–	8,488[C]	–	+
Yellow-eyed ensatina (*Ensatina eschscholtzii xanthoptica*)	104	–	432[C]	–	+
	104	–	1,095[C]	–	+
	104	–	1,963[C]	–	+
	104	–	2,634[C]	–	+
	2	–	29,886[C]	–	+
	2	–	92,294[C]	–	+
Red salamander (*Pseudotriton ruber*)	120	–	70,723[C]	–	+
	120	–	87,258[C]	–	+
	120	–	234,771[C]	–	+
Little devil poison frog (*Oophaga sylvatica*)	1	*NP*	*NP*	+	–

Length of tissue storage time in formalin prior to processing, quantitative PCR loads of Bd ± Bsal, and Bd/Bsal ISH results are shown.
[Z], zoospore equivalents; [C], copies; NP, Not performed.

fungal loads ranging from 6.2×10^2 to 2.2×10^6 (**Table 1**). No PCR was performed on the poison frog with chytridiomycosis on diagnostic necropsy. Positive ISH staining was observed in all species tested (**Figure 3**). Of the 17 qPCR *Bsal* positive salamanders, 16 salamanders were *Bsal* ISH positive (94.1%; **Figures 3A–C**). The *Bsal* ISH negative animal had the second lowest *Bsal* load of animals tested (1.4×10^2 copies/μl). Of the 3 qPCR *Bd* positive salamanders, 2 salamanders were *Bd* ISH positive (66.7%; **Figure 3A**). The *Bd* ISH negative animal had the lowest *Bd* load of animals tested (6.2×10^2 copies/μl). Both salamanders with discordant qPCR/ISH results were of the same species (*A. cephalica*) and had a formalin fixation time of 154 days (**Table 1**). However, positive *Bd* and *Bsal* probe staining was noted in one *A. cephalica* with higher fungal loads (**Figure 3A**). Both *Bsal* and *Bd* probe staining, when present, was strong, even in animals stored in formalin for up to 154 days. The one frog tested exhibited positive *Bd* probe staining (**Figure 3D**). Occasional non-specific staining of the retina and ingested chitin was noted as for *N. viridescens*. DapB control probe staining was uniformly negative in all animals (**Supplementary Figures 1B–D** and data not shown).

Effect of Formalin Fixation Time on *Bd*/*Bsal* ISH

Given the finding that animals with formalin fixation times up to 154 days could still exhibit positive *Bd*/*Bsal* ISH staining, two additional eastern newts (*N. viridescens*) with formalin fixation times of 331 (*Bsal* load−4.7×10^3) and 364 (*Bsal* load 2.2×10^4) days, respectively, were tested. Both animals were *Bsal* ISH positive, with no dramatic difference in staining distribution and intensity (data not shown).

Sensitivity of *Bd*/*Bsal* ISH

To approximate the sensitivity of *Bd*/*Bsal* ISH in comparison to qPCR *Bd*/*Bsal* loads in salamanders, staining results from 33 salamanders representing 5 species were compared. *Bsal* loads ranged from 1.1×10^2 to 2.7×10^5 (zoospore equivalents) or 1.4×10^2 to 2.9×10^5 (ITS-1 copies) per microliter. Positive *Bsal* probe staining was present in tissue sections of animals with qPCR *Bsal* levels as low as 1.1×10^2 zoospore equivalents (formalin fixation time, 2 days) or 4.3×10^2 ITS-1 copies (formalin fixation time, 104 days) per microliter. *Bd* loads ranged from 3.4×10^4 to 1.4×10^5 (zoospore equivalents) or 6.2×10^2 to 2.2×10^6 (ITS-1 copies) per microliter. Positive *Bd* probe staining was present in tissue sections of animals with qPCR *Bd* levels as low as 3.4×10^4 zoospore equivalents (formalin fixation time, 2 days) or 1.8×10^5 ITS-1 copies (formalin fixation time, 104 days) per microliter.

Distribution of *Bd*/*Bsal* Organisms in Tissue

The high contrast of particularly the red staining *Bsal* organisms, but also the green staining *Bd* organisms, in this assay afforded additional advantages for the identification of even low numbers of zoosporangia in tissues over routine and histochemical stains (**Figure 2**). The distribution of *Bd* and *Bsal* was compared in sections stained of all 32 positive amphibians in this study. *Bd* organisms were present primarily within the stratum corneum (**Figures 2F,L, 3A**), as has been previously reported (5, 6). *Bsal* organisms were predominantly found in clusters or plaques that extended down to the deeper levels of the epidermis (**Figures 2I,L, 3A–C**). The highest distribution of lesions were present on the distal limbs, tail, and head (data not shown), though foci of *Bsal* chytridiomycosis could be found in the epidermis throughout the body, consistent with previous reports (1). In some animals, *Bsal* zoosporangia were noted to extend

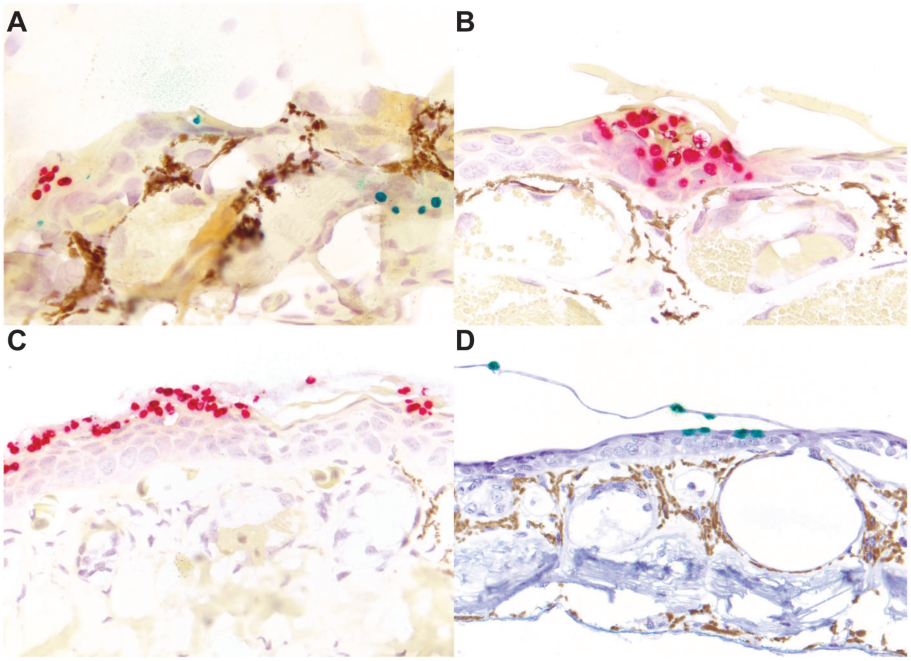

FIGURE 3 | *Bd*/*BSal* RNAScope® ISH of skin sections of mixed species with chytridiomycosis. Concurrent *Bd* and *Bsal* chytridiomycosis in an experimentally infected red-legged false brook salamander (*Aquiloeurycea cephalica*; **A**). *Bsal* chytridiomycosis in an experimentally infected large-blotched ensatina (*Ensatina eschscholtzii klauberi*; **B**) and a red salamander (*Pseudotriton ruber*; **C**). *Bd* chytridiomycosis in a naturally infected little devil poison frog (*Oophaga sylvatica;* **D**). *Bd* probe binding is visualized by green staining **(A,D)** and *Bsal* probe binding is visualized by red staining **(A–C)**. The golden tinctorial property of (**A–C**) is an artifact of the counterstain occasionally seen. **(A,B)** are at 400x magnification; **(C,D)** are at 200x magnification.

into the neck and secretory epithelial cells of underlying dermal glands (**Figure 4**). The density of glandular *Bsal* zoosporangia ranged from low (**Figure 4B**) to moderate (**Figures 4C,D**) within individual glands, and sometimes to multifocal glands within a small area of skin (**Figure 4D**). *Bsal* zoosporangia were not noted in any other epithelial cells of the body other than the epidermis and dermal glands.

DISCUSSION

Accurate diagnosis of chytridiomycosis due to *B. salamandrivorans* (*Bsal*) in free-ranging salamanders, particularly given the high potential for natural co-infections with *B. dendrobatidis* (*Bd*), may not always be possible with routine histopathology and PCR alone. For this reason, we developed an automated, dual-plex chromogenic RNAScope® *in situ* hybridization (ISH) assay for rapid, accurate, and simultaneous differentiation and co-localization of *Bd* and *Bsal* in tissue section.

The developed assay was highly specific for both *Bd* and *Bsal* in comparison to each other and amphibian tissues, with minimal cross-reactivity to host tissues from five species of salamander and one species of frog. Though any staining should always be interpreted with appropriate controls, the minimal non-specific reactivity in the examined salamanders and frogs suggests it is unlikely for other species to be dramatically different. The noted non-specific reactivity of the *Bsal* probe to the retina and to arthropod ingesta should not impair interpretation of cutaneous lesions typical of chytridiomycosis.

The assay detected *Bsal* in samples that remained in fixative for up to 364 days and *Bd* in tissues that remained in fixative up to 154 days. Though manufacturer's recommendations for optimal storage and handling of tissues are either 70% ethanol indefinitely or formalin fixation for <48 h, the ability of this assay to detect *Bsal* and *Bd* after extended (>48 h) formalin fixation will make it more useful for surveillance projects when samples may be archived for some time before submission. *Bsal* ISH staining was positive in sample fixed in formalin for 2 days with 1.1×10^2 zoospore equivalents/μl (postmortem skin swab) and 104 days with 4.3×10^2 ITS-1 copies/μl (postmortem skin swab), but negative in a sample fixed in formalin for 154 days with 1.4×10^2 ITS-1 copies/μl (postmortem skin swab). This indicates that the *Bsal* ISH can be highly sensitive even after extended fixation times. Moreover, the high contrast between the light blue hematoxylin counterstain and the red *Bsal* probe staining may make diagnosis easier than more traditional histochemical special stains (such as GMS or periodic acid Schiff). As such, ISH may be advantageous over routine and histochemical stains for the identification of organisms in low-level or subclinical *Bsal* infections as identified by molecular diagnostics. Interpretation of the sensitivity of the *Bd* ISH is more difficult, as it was not a primary focus in this study and there is limited load distribution in the examined samples, particularly at lower levels. There was no detection of *Bd* probe signal in *A. cephalica* with

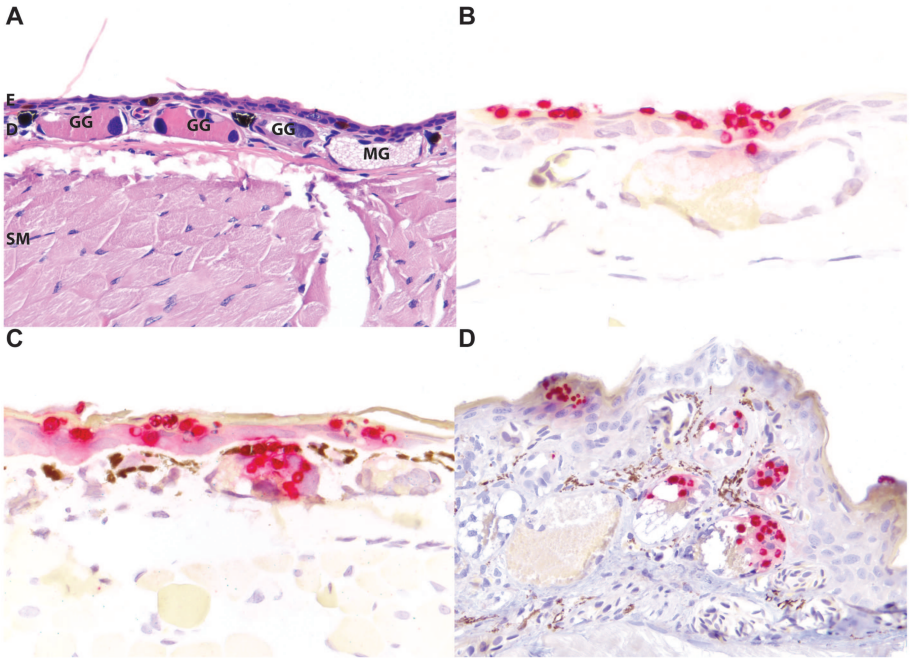

FIGURE 4 | *Bsal* infection of dermal glandular epithelial cells in salamanders. Normal, uninfected eastern newt (*Notophthalmus viridescens*) skin stained with hematoxylin and eosin highlighting the epidermis [E], dermis [D], dermal glands (granular glands [GG] and mucus glands [MG]), and subcuticular skeletal muscle [SM] **(A)**. In experimentally infected red salamanders (*Pseudotriton ruber*; **B**), yellow-eyed ensatinas (*Ensatina eschscholtzii xanthoptica;* **C**), and large-blotched ensatinas (*E. e. klauberi*; **D**), positive red ISH staining of *Bsal* organisms extends down from the epidermis into the epithelial cells of dermal glands. In the most severely affected regions, abundant organisms may be present in multiple glands **(C)**. **(A,D)** are at 200x magnification; **(B,C)** are at 400x magnification.

6.2×10^2 ITS-1 copies/microliter of a postmortem skin swab, suggesting a lower sensitivity of the dual assay for *Bd* than *Bsal*. However, more samples representing a wider range of fixation times and *Bd* loads are necessary for a more definitive *Bd* sensitivity.

Little modification of previously published techniques for automated dual-plex chromogenic RNAScope® ISH was required (20, 22). Three chromogenic options are available for dual-plex RNAScope from the manufacturer: brown and green in channel one (*Bd* probe), red in channel two (*Bsal* probe). Due to the presence of abundant melanocytes in the amphibian epidermis, the HRP-based green chromogen as provided in the RNAScope® LS Green Accessory pack was selected for visualization of *Bd* probe binding. However, rapid and significant fading and stain dissolution was noted starting as soon as 48 h after processing with this chromogen. For long-term retention of the green signal of the *Bd* probe, an alternative green chromogen (PermaGreen/HRP) and the use of an additional preservation solution (Immunohisto-Sealer) were used. Neither of these modifications had an effect on the *Bsal* probe fast red signal. The cost of performing this assay is not without consideration, at approximately $100–200 USD per slide, depending on single- or dual-plex and automated or manual staining. The use of ISH may not be appropriate or necessary in all instances. However, for high profile diagnostic cases it can provide important etiologic confirmation of *Batrachochytrium* infections, and for pathogenesis studies, it can provide specific pathogen/lesion co-localization.

One of the most noteworthy findings in this study was the identification of *Bsal* zoosporangia not only within the epithelial cells of the epidermis but within the epithelial cells of dermal glands. In *Bd* infections, zoosporangia invade mature cells of the epidermal stratum granulosum and stratum corneum, sparing the basal epidermis and any underlying structures (25, 26). Fungal infection can result in epidermal hyperplasia and hyperkeratosis significant enough to disrupt cutaneous electrolyte transport, gas exchange, and osmoregulation and cause death (27). The pathogenesis of *Bsal* chytridiomycosis, however, has not been elucidated. As the distribution of lesions associated with *Bsal* infection can be considerably patchier than the more generalized skin response in *Bd* infections, it is possible if not likely that *Bsal* mortalities involve a different underlying pathogenesis. There are two primary types of dermal glands in amphibians: mucus and granular (serous or poison) glands (**Figure 4A**). The glands are divided into three parts: (i) the duct which is lined by modified keratinocytes and serves as the conduit from the gland to the epidermal surface; (ii) the intercalary region lined by reserve blastic epidermal cells; and (iii) the gland alveolus lined by secretory epithelium (28). While it would not be unexpected to see *Batrachochytrium* zoosporangia in the keratinized ducts of dermal glands (**Figure 4B**), in some animals fungal organisms extended down into the gland alveoli

within secretory epithelial cells (**Figures 4C,D**). The presence of *Bsal* zoosporangia within glandular epithelial cells may affect the secretory function of these glands. Cutaneous glandular secretions assist in maintaining the skin as a moist surface for gas exchange, preventing water loss, and as a source of active and passive defense in the form of noxious or poisonous substances, or antimicrobial compounds (29–32). Additional studies to investigate the effects of *Bsal* infection on cutaneous mucus and granular gland function are needed to identify the role of the infection of these glands on the pathogenesis of *Bsal* infections.

This report describes the development and characterization of an automated, dual-plex, chromogenic RNAScope® ISH assay for simultaneous detection and differentiation of *Bd* and *Bsal* in tissue sections. In combination with molecular diagnostics and routine histopathology, this assay represents an important tool for definitive diagnosis of *Bsal* chytridiomycosis. Such multimodal confirmation may be useful in high profile or complicated in diagnostic cases and/or surveillance studies. The assay also will also be a useful tool in the study of laboratory infections of *Bsal* in salamanders and other amphibian hosts to better understand the potential host range, tissue tropism, and pathogenesis of the emerging fungal disease of amphibians, as well as the potential interaction of *Bsal* and *Bd* in mixed infections.

DATA AVAILABILITY

All datasets generated for this study are included in the manuscript/**Supplementary Files**.

ETHICS STATEMENT

The animal study was reviewed and approved by University of Maryland IACUC protocol R-15-15. University of Tennessee Institutional Animal Care and Use Committee protocol #2395. Written informed consent was obtained from the owners for the participation of their animals in this study.

AUTHOR CONTRIBUTIONS

RO and SF designed the experiments. MB performed and optimized the ISH staining. RO and AT interepreted the ISH staining. AL, KL, DM, EC, and MG performed experimental infections of the animals. RO drafted the manuscript and created the figures. All authors reviewed the manuscript.

FUNDING

A portion of this research was supported by NSF Division of Environmental Biology grant #1814520 and USDA National Institute of Food and Agriculture Hatch Project 1012932 awarded to MG and DM. The North Carolina Wildlife Resources Commission (project #WM-0309), Tennessee Wildlife Resources Agency (project #52537), and Liquid Spark, Inc. (Bryson City, NC, USA) provided funds for testing *Pseuodtriton ruber*. AT was funded through the Summer Student Research Program by the University of Tennessee Center of Excellence in Livestock Diseases and Human Health. AL was supported by NSF Postdoctoral Fellowship in Biology (DEB-1523551). BAND Foundation provided funds for this project as part of *Bsal* susceptibility trials for species of concern.

ACKNOWLEDGMENTS

The authors thank the staff of the Histology Laboratory at University of Florida's College of Veterinary Medicine. We thank Dr. Gabriella Parra Olea and Dr. Rebecca Hardman for help with collecting *A. cephalica* and Lawrence Erickson and Laura Patterson for collecting *E. e. xanthoptica*. We thank Tim Herman for providing captive *Ensatina eschscholtzii klauberi* and *Pseuodtriton ruber*. We thank the following technical staff for help with experiments at the University of Tennessee: Christian Yarber, Ciara Sheets, Joseph Whipple, Jacob Wessels, and Markese Bohanon.

SUPPLEMENTARY MATERIAL

The Supplementary Material for this article can be found online at: https://www.frontiersin.org/articles/10.3389/fvets.2019.00304/full#supplementary-material

Supplementary Figure 1 | DapB negative control staining of amphibian tissues. No positive signal is seen in DapB control staining of skin from an eastern newt (*Notophthalmus viridescens*; **A**), a yellow-eyed ensatina (*Ensatina eschscholtzii xanthoptica;* **B**), a red salamander (*Pseudotriton ruber*; **C**), or a little devil poison frog (*Oophaga sylvatica;* **D**). All images are at 400x magnification.

REFERENCES

1. Martel A, Spitzen-van der Sluijs A, Blooi M, Bert W, Ducatelle R, Fisher MC, et al. *Batrachochytrium salamandrivorans* sp. nov. causes lethal chytridiomycosis in amphibians. *Proc Natl Acad Sci USA*. (2013) 110:15325–9. doi: 10.1073/pnas.1307356110
2. Martel A, Blooi M, Adriaensen C, Van Rooij P, Beukema W, Fisher MC, et al. Recent introduction of a chytrid fungus endangers Western Palearctic salamanders. *Science*. (2014) 346:630–1. doi: 10.1126/science.1258268
3. Scheele BC, Pasmans F, Skerratt LF, Berger L, Martel A, Beukema W, et al. Amphibian fungal panzootic causes catastrophic and ongoing loss of biodiversity. *Science*. (2019) 363:1459–63. doi: 10.1126/science.aav0379
4. Skerratt LF, Berger L, Speare R, Cashins S, McDonald KR, Phillott AD, et al. Spread of chytridiomycosis has caused the rapid global decline and extinction of frogs. *Ecohealth*. (2007) 4:125–34. doi: 10.1007/s10393-007-0093-5
5. Berger L, Speare R, Daszak P, Green DE, Cunningham AA, Goggin CL, et al. Chytridiomycosis causes amphibian mortality associated with population declines in the rain forests of Australia and Central America. *Proc Natl Acad Sci USA*. (1998) 95:9031–6. doi: 10.1073/pnas.95.15.9031
6. Pessier AP, Nichols DK, Longcore JE, Fuller MS. Cutaneous chytridiomycosis in poison dart frogs (*Dendrobates* spp.) and White's tree frogs (*Litoria caerulea*). *J Vet Diagnostic Investig*. (1999) 11:194–9. doi: 10.1177/104063879901100219

7. O'Hanlon SJ, Rieux A, Farrer RA, Rosa GM, Waldman B, Bataille A, et al. Recent Asian origin of chytrid fungi causing global amphibian declines. *Science.* (2018) 360:621–7. doi: 10.1126/science.aar1965
8. Lips KR. Overview of chytrid emergence and impacts on amphibians. *Philos Trans R Soc B Biol Sci.* (2016) 371:20150465. doi: 10.1098/rstb.2015.0465
9. Blooi M, Martel A, Haesebrouck F, Vercammen F, Bonte D, Pasmans F. Treatment of urodelans based on temperature dependent infection dynamics of *Batrachochytrium salamandrivorans*. *Sci Rep.* (2015) 5:8037. doi: 10.1038/srep08037
10. Nguyen TT, Nguyen T, Van ZT, Pasmans F, Martel A. Trade in wild anurans vectors the urodelan pathogen *Batrachochytrium salamandrivorans* into Europe. *Amphibia-Reptilia.* (2017) 38:554–6. doi: 10.1163/15685381-00003125
11. Laking AE, Ngo HN, Pasmans F, Martel A, Nguyen TT. *Batrachochytrium salamandrivorans* is the predominant chytrid fungus in Vietnamese salamanders. *Sci Rep.* (2017) 7:44443. doi: 10.1038/srep44443
12. Sabino-Pinto J, Veith M, Vences M, Steinfartz S. Asymptomatic infection of the fungal pathogen *Batrachochytrium salamandrivorans* in captivity. *Sci Rep.* (2018) 8:11767. doi: 10.1038/s41598-018-30240-z
13. Gray MJ, Lewis JP, Nanjappa P, Klocke B, Pasmans F, Martel A, et al. *Batrachochytrium salamandrivorans*: The North American Response and a call for action. *PLOS Pathog.* (2015) 11:e1005251. doi: 10.1371/journal.ppat.1005251
14. White CL, Forzán MJ, Pessier AP, Allender MC, Ballard JR, Catenazzi A, et al. Amphibian: a case definition and diagnostic criteria for *Batrachochytrium salamandrivorans* chytridiomycosis. *Herpetol Rev.* (2016) 47:207.
15. Van Rooij P, Martel A, Haesebrouck F, Pasmans F. Amphibian chytridiomycosis: a review with focus on fungus-host interactions. *Vet Res.* (2015) 46:137. doi: 10.1186/s13567-015-0266-0
16. Chatfield MWH, Moler P, Richards-Zawacki CL. The amphibian chytrid fungus, *Batrachochytrium dendrobatidis*, in Fully Aquatic Salamanders from Southeastern North America. *PLoS One*. (2012). doi: 10.1371/journal.pone.0044821
17. Pullen KD, Best AM, Ware JL. Amphibian pathogen *Batrachochytrium dendrobatidis* prevalence is correlated with season and not urbanization in central Virginia. *Dis Aquat Organ.* (2010) 91:9–16. doi: 10.3354/dao02249
18. Rothermel BB, Walls SC, Mitchell JC, Dodd CK, Irwin LK, Green DE, et al. Widespread occurrence of the amphibian chytrid fungus *Batrachochytrium dendrobatidis* in the southeastern USA. *Dis Aquat Organ.* (2008) 82:3–18. doi: 10.3354/dao01974
19. Dillon MJ, Bowkett AE, Bungard MJ, Beckman KM, O'Brien MF, Bates K, et al. Tracking the amphibian pathogens *Batrachochytrium dendrobatidis* and *Batrachochytrium salamandrivorans* using a highly specific monoclonal antibody and lateral-flow technology. *Microb Biotechnol.* (2017) 10:381–94. doi: 10.1111/1751-7915.12464
20. Anderson CM, Zhang B, Miller M, Butko E, Wu X, Laver T, et al. Fully automated rnascope *in situ* hybridization assays for formalin-fixed paraffin-embedded cells and tissues. *J Cell Biochem.* (2016) 117:2201–8. doi: 10.1002/jcb.25606
21. Chan S, de L'Etang AF, Rangell L, Caplazi P, Lowe JB, Romeo V. A method for manual and automated multiplex RNAscope *in situ* hybridization and immunocytochemistry on cytospin samples. *PLoS ONE.* (2018) 13:e0207619. doi: 10.1371/journal.pone.0207619
22. Wang F, Flanagan J, Su N, Wang LC, Bui S, Nielson A, et al. RNAscope: a novel *in situ* RNA analysis platform for formalin-fixed, paraffin-embedded tissues. *J Mol Diagnostics.* (2012) 14:22–9. doi: 10.1016/j.jmoldx.2011.08.002
23. Longo AV, Fleischer RC, Lips KR. Double trouble: co-infections of chytrid fungi will severely impact widely distributed newts. *Biol Invasions.* (2019) 21:2233–45. doi: 10.1007/s10530-019-01973-3
24. Blooi M, Pasmans F, Longcore JE, Spitzen-Van Der Sluijs A, Vercammen F, Martel A. Duplex real-Time PCR for rapid simultaneous detection of *Batrachochytrium dendrobatidis* and *Batrachochytrium salamandrivorans* in amphibian samples. *J Clin Microbiol.* (2013) 51:4173–7. doi: 10.1128/JCM.02313-13
25. Berger L, Hyatt AD, Speare R, Longcore JE. Life cycle stages of the amphibian chytrid *Batrachochytrium dendrobatidis*. *Dis Aquat Organ.* (2005) 68:51–63. doi: 10.3354/dao068051
26. Longcore JE, Pessier AP, Nichols DK. *Batrachochytrium Dendrobatidis* gen. et sp. nov., a chytrid pathogenic to amphibians. *Mycologia*. (1999) 91:219–27. doi: 10.1080/00275514.1999.12061011
27. Voyles J, Young S, Berger L, Campbell C, Voyles WF, Dinudom A, et al. Pathogenesis of chytridiomycosis, a cause of catastrophic amphibian declines. *Science.* (2009) 326:582–5. doi: 10.1126/science.1176765
28. Toledo RC, Jared C. Cutaneous granular glands and amphibian venoms. *Comp Biochem Physiol – Part A Physiol.* (1995) 111:1–29. doi: 10.1016/0300-9629(95)98515-I
29. Arifulova I, Delfino G, Dujsebayeva T, Fedotovskikh G, Nosi D, Terreni A. Serous cutaneous glands in the South American horned frog Ceratophrys ornata (Leptodactylformes, Chthonobatrachia, Ceratophrydae): ultrastructural expression of poison biosynthesis and maturation. *J Morphol.* (2007) 268:690–700. doi: 10.1002/jmor.10541
30. Daly JW, Spande TF, Garraffo HM. Alkaloids from amphibian skin: a tabulation of over eight-hundred compounds. *J Nat Prod.* (2005) 68:1556–75. doi: 10.1021/np0580560
31. Page Fredericks L, Dankert JR. Antibacterial and hemolytic activity of the skin of the terrestrial salamander, Plethodon cinereus. *J Exp Zool.* (2000) 287:340–5. doi: 10.1002/1097-010X(20001001)287:5<340::AID-JEZ2>3.3.CO;2-0
32. Quay WB. Integument and the environment glandular composition, function, and evolution. *Integr Comp Biol.* (1972) 12:95–108. doi: 10.1093/icb/12.1.95

Conflict of Interest Statement: The authors declare that the research was conducted in the absence of any commercial or financial relationships that could be construed as a potential conflict of interest.

Copyright © 2019 Ossiboff, Towe, Brown, Longo, Lips, Miller, Carter, Gray and Frasca. This is an open-access article distributed under the terms of the Creative Commons Attribution License (CC BY). The use, distribution or reproduction in other forums is permitted, provided the original author(s) and the copyright owner(s) are credited and that the original publication in this journal is cited, in accordance with accepted academic practice. No use, distribution or reproduction is permitted which does not comply with these terms.

frontiers in Veterinary Science

ORIGINAL RESEARCH
published: 03 October 2019
doi: 10.3389/fvets.2019.00338

Longitudinal and Cross-Sectional Sampling of Serpentovirus (Nidovirus) Infection in Captive Snakes Reveals High Prevalence, Persistent Infection, and Increased Mortality in Pythons and Divergent Serpentovirus Infection in Boas and Colubrids

*Laura L. Hoon-Hanks[1], Robert J. Ossiboff[2], Pia Bartolini[3], Susan B. Fogelson[4], Sean M. Perry[5], Anke C. Stöhr[5], Shaun T. Cross[1], James F. X. Wellehan[2], Elliott R. Jacobson[2], Edward J. Dubovi[6] and Mark D. Stenglein[1]**

[1] Department of Microbiology, Immunology, and Pathology, College of Veterinary Medicine and Biomedical Sciences, Colorado State University, Fort Collins, CO, United States, [2] Department of Comparative Diagnostic and Population Medicine, College of Veterinary Medicine, University of Florida, Gainesville, FL, United States, [3] Terrestrial & Arboreal, LLC, Melrose, FL, United States, [4] Fishhead Labs LLC, Stuart, FL, United States, [5] Department of Veterinary Clinical Sciences, School of Veterinary Medicine, Louisiana State University, Baton Rouge, LA, United States, [6] Animal Health Diagnostic Center, College of Veterinary Medicine, Cornell University, Ithaca, NY, United States

The aim of this study of serpentovirus infection in captive snakes was to assess the susceptibility of different types of snakes to infection and disease, to survey viral genetic diversity, and to evaluate management practices that may limit infection and disease. Antemortem oral swabs were collected from 639 snakes from 12 US collections, including 62 species, 28 genera, and 6 families: Pythonidae ($N = 414$ snakes; pythons were overrepresented in the sample population), Boidae (79), Colubridae (116), Lamprophiidae (4), Elapidae (12), and Viperidae (14). Infection was more common in pythons (38%; 95% CI: 33.1–42.4%), and in boas (10%; 95% CI: 5.2–18.7%) than in colubrids (0.9%, 95% CI: <0.01–4.7%); infection was not detected in other snake families (lamprophiids 0/4, 95% CI: 0–49%; elapids 0/12, 95% CI: 0–24.2%; and vipers 0/14, 95% CI: 0–21.5%), but more of these snakes need to be tested to confirm these findings. Clinical signs of respiratory disease were common in infected pythons (85 of 144). Respiratory signs were only observed in 1 of 8 infected boas and were absent in the single infected colubrid. Divergent serpentoviruses were detected in pythons, boas, and colubrids, suggesting that different serpentoviruses might vary in their ability to infect snakes of different families. Older snakes were more likely to be infected than younger snakes (p-value < 0.001) but males and females were equally likely to be infected (female prevalence: 23.4%, 95% CI 18.7–28.9%; male prevalence: 23.5%, 95% CI 18–30.1%; p-value $= 0.144$). Neither age (p-value $= 0.32$) nor sex (p-value $= 0.06$) was statistically

OPEN ACCESS

Edited by:
Kathryn Christine Gamble, Lincoln Park Zoo, United States

Reviewed by:
Dean Konjević, University of Zagreb, Croatia
Nuno Santos, University of Porto, Portugal
Eva Dervas, University of Zurich, Switzerland

***Correspondence:**
Mark D. Stenglein
mark.stenglein@colostate.edu

Specialty section:
This article was submitted to Zoological Medicine, a section of the journal Frontiers in Veterinary Science

Received: *30 May 2019*
Accepted: *19 September 2019*
Published: *03 October 2019*

Citation:
Hoon-Hanks LL, Ossiboff RJ, Bartolini P, Fogelson SB, Perry SM, Stöhr AC, Cross ST, Wellehan JFX, Jacobson ER, Dubovi EJ and Stenglein MD (2019) Longitudinal and Cross-Sectional Sampling of Serpentovirus (Nidovirus) Infection in Captive Snakes Reveals High Prevalence, Persistent Infection, and Increased Mortality in Pythons and Divergent Serpentovirus Infection in Boas and Colubrids. Front. Vet. Sci. 6:338. doi: 10.3389/fvets.2019.00338

associated with disease severity. Longitudinal sampling of pythons in a single collection over 28 months revealed serpentovirus infection is persistent, and viral clearance was not observed. In this collection, infection was associated with significantly increased rates of mortality (p-value = 0.001) with death of 75% of infected pythons and no uninfected pythons over this period. Offspring of infected parents were followed: vertical transmission either does not occur or occurs with a much lower efficiency than horizontal transmission. Overall, these findings confirm that serpentoviruses pose a significant threat to the health of captive python populations and can cause infection in boa and colubrid species.

Keywords: captive, epidemiology, nidovirus, pythons, respiratory disease, serpentovirus, snake

INTRODUCTION

The order *Nidovirales* historically included viruses infecting mammals, birds, fish, crustaceans, and insects. With the increasing availability and affordability of metagenomic sequencing, this order has seen marked expansion in the recent years [e.g. (1–3)]. A distinct clade of nidoviruses now classified as belonging to the suborder *Tornidovirineae* family *Tobaniviridae* began with the discovery of novel nidoviruses in pythons, marking the first example of nidoviruses in reptilian hosts (4–6). Since this initial discovery, related nidoviruses have been discovered in additional snake species, lizards, turtles, cattle, and snake-associated nematodes (1, 2, 7–11). Several of these viruses have been associated with significant disease, particularly respiratory disease, highlighting this virus family as a source of potential emerging pathogens that warrant additional investigation (4–8, 10, 11). With recent taxonomic reclassification of the order *Nidovirales*, reptile-associated nidoviruses are classified within the *Serpentovirinae* subfamily and will be referred following to as serpentoviruses (12).

Snake-associated (ophidian) serpentoviruses were discovered in 2014 and were indirectly linked to respiratory disease in pythons (4–6, 10). Subsequent experimental infections of ball pythons confirmed a causal relationship between serpentovirus infection and respiratory disease, emphasizing the importance of these emerging viruses in veterinary medicine (13). Experimentally infected pythons developed antemortem hyperemia of the choanal and oral mucosa with or without mucosal hemorrhages, abundant oral mucus secretion, excessive swallowing, increased respiratory effort and rate, open-mouthed breathing, and anorexia. Postmortem findings included chronic-active mucinous and proliferative rhinitis, stomatitis, glossitis, tracheitis, esophagitis, and interstitial pneumonia (13). Related viruses have been detected in snake species, with or without evidence of respiratory disease, spanning multiple families within the *Serpentes* suborder throughout North America, Europe, and Asia. These include *Pythonidae* species [ball python (*Python regius*), Indian python (*Python molurus*), Burmese python (*Python bivittatus*), green tree python (*Morelia viridis*), and carpet python (*Morelia spilota*)]; *Boidae* species [boa constrictor (*Boa constrictor*)]; *Colubridae* species [Pope's keelback (*Hebius popei*), red-banded snake (*Lycodon rufozonatus*), and Mandarin rat snake (*Euprepiophis mandarinus*)]; and *Homalopsidae* species [Chinese water snake (*Myrrophis chinensis*)] (2, 4–6, 9, 10, 14). Despite this growing list of susceptible hosts, the prevalence and clinical significance of serpentovirus infection in most snakes remains unknown, and no published study has tested snakes in the families *Viperidae* or *Elapidae*, two large families that include the majority of venomous snake species. Therefore, despite mounting evidence that serpentoviruses are common and potentially significant pathogens of snakes, the extent of species susceptibility to infection and disease remains poorly understood.

The purpose of this study was to evaluate the epidemiology of serpentovirus infection in captive snakes. Mixed captive snake collections with both known and unknown serpentovirus infection status were selected. The collections included snakes from the major snake families: *Pythonidae*, *Boidae*, *Colubridae*, *Lamprophiidae*, *Viperidae*, and *Elapidae*. Data from individual snakes within each collection was collected to assess correlations between species, age, sex, and clinical signs with serpentovirus status. Furthermore, sequencing data was generated to investigate serpentovirus genetic diversity and whether strains clustered by collection, species, and disease state. Longitudinal sampling was performed to determine persistence and progression of infection within a collection and evaluate the potential for viral clearance and vertical transmission.

MATERIALS AND METHODS

Ethical Statement

All samples were considered non-invasive clinical samples collected by veterinarians or veterinary technicians from client-owned animals for the purpose of diagnostic testing for snake pathogens; an ethical review was not performed for this reason.

Snake Collections/Populations

Eleven collections (A–K) were tested, either in entirety (all the snakes were tested) or partially (a subset of snakes). A twelfth, collective group (L) included snakes from a variety of sources that were individually submitted by veterinarians or owners following suspicion of serpentovirus-associated respiratory disease. One collection was sampled longitudinally (collection A) while the remaining collections were sampled once. Species, age, sex, clinical signs, and a respiratory score (see below) were recorded

for each snake, when available. Snakes were recorded as either the species or subspecies depending on the information provided by the owner. If known, exact ages were recorded; in cases where only the age category was noted a standard age was provided (hatchling: ∼1 month [0.1 year] and juvenile: 6 months [0.5 year]; adults were not estimated). If an age or age category was not provided, these snakes were not included in analyses where age was a variable. Sex was recorded as male, female, or unknown. Following evaluation of snakes and discussion with owners, veterinarians or veterinary technicians provided a respiratory score based on a specific rubric: 0—no respiratory signs; 1—mild respiratory signs (e.g., increased mucus in the oral cavity or hyperemia of the oral mucosa but otherwise acting normally); 2—moderate respiratory signs (e.g., wheezing, coughing); and 3—severe respiratory signs (e.g., open-mouthed breathing, respiratory distress). Summary data for each collection can be found in **Supplemental Table S1**.

Longitudinal Sampling

Collection A was tested longitudinally following an outbreak of serpentovirus-associated respiratory disease. The first pythons in this collection were tested by in 2015 by PCR and metagenomic sequencing in the Stenglein laboratory (see below), at which point serpentovirus was determined to be established in the collection, but an overt outbreak had not occurred. In December 2015, a group of green tree pythons were purchased from another state. The purchased green tree pythons were acquired from the seller in July 2016, by which time approximately 9 of the purchased snakes had died of undiagnosed respiratory disease. None of the deceased snakes underwent postmortem examination by the sellers during this time (December 2015–July 2016), but two snake carcasses (A98 and A99) were frozen. Upon acquisition of the remaining live snakes, a quarantine area was established. The newly arriving snakes were placed in a large room that was partially separated from the main collection of pythons (i.e., quarantined pythons were housed in one room and the main collection pythons were housed in another room of the house, which was separated by space but not physical barriers); all venomous snakes were housed in rooms separated by walls and doors from the quarantined and main collection pythons. Two weeks into the quarantine period, purchased snakes began to show signs of respiratory disease; snakes began to die at 3 weeks into quarantine. Shortly after, pythons in the main collection also exhibited signs of respiratory disease. At this point, all pythons in the collection were sampled and any snakes found to be serpentovirus-positive, or had significant risk of exposure to serpentovirus (e.g., were part of the purchased collection, were housed in the quarantine area, were exhibiting signs of respiratory disease but initial testing yielded negative PCR results, or had any direct or indirect contact with purchased snakes) were separated from the main collection and placed in a separate building away from the house where more rigorous quarantine and disinfection measures were undertaken. These included separate tools and supplies that remained in quarantine, cleaning tools and surfaces with a quaternary ammonium compound (Simple Green d Pro 3 Plus), outer clothing and footwear specific for the quarantine area, only one designated caretaker for infected snakes, showering directly after exiting the quarantine area, and air filters placed on all vents leading out of the quarantine building. All pythons within the collection had continued testing over the course of 28 months at approximately 4-month intervals. Furthermore, the two snake carcasses that were frozen by the seller were acquired and postmortem oral swabs were collected. In contrast to the sampling of the python species within the collection, only a subset of venomous snakes (12 elapids and 13 vipers) were tested and snakes were only tested once.

During the 28 months, a serpentovirus-positive male and female green tree python were bred in the quarantine area, resulting in a clutch of eggs. The eggs were removed from the parents and artificially incubated in the main collection area. Egg surfaces were cleaned by exposure to UV light (Zoo Med brand 5.0 light) for 1 min, 3–4 inches away. Following hatching, eggs were frozen and egg shells/remaining contents were submitted for sampling, along with choanal swabs from the hatchlings. Hatchlings were sampled at approximately 4-month intervals for 20 months.

Similarly, a serpentovirus-positive male and female jungle carpet python (*Morelia spilota cheynei*) were bred in quarantine, resulting in a clutch of eggs. The eggs were removed from the parents and artificially incubated in the quarantine area. Egg surfaces were briefly cleaned with a quaternary ammonium compound. Upon hatching, offspring were removed from quarantine and placed in a separate room away from both serpentovirus-positive snakes and the main collection. Eggs were tested following hatching and offspring were tested twice during a 6-month interval.

Postmortem Examination

A necropsy was performed on a subset of snakes from collection A, H, and L that died during the study. Fresh frozen and formalin-fixed tissues were collected. Formalin-fixed tissues were processed routinely and histopathology was performed on an a select few of these cases, as previously described (13).

Snake Sampling

Swabs

All antemortem samples were collected by a veterinarian or certified veterinary technician. Swabs from the choana or oral cavity were collected from each individual snake using cotton- or rayon-tipped swabs (**Figure 1**). Dry swabs were then placed in either a 1.5 ml Eppendorf tube or 2 ml screw-cap conical tube and frozen at −20°C for 1–14 days. Samples were then shipped overnight on ice to the Stenglein laboratory. At the time of arrival, swabs were suspended in 1 ml of brain heart infusion (BHI) broth (Becton Dickinson) and vortexed prior to storage at −80°C.

Tissues

Samples from post mortem analysis of collection A, H, and L (see above) were submitted as fresh-frozen tissues (−20 or −80°C). Lung, trachea, and esophagus were pooled or submitted as individual samples. Additionally, to assess vertical transmission in Collection A, eggs collected post-hatching were submitted

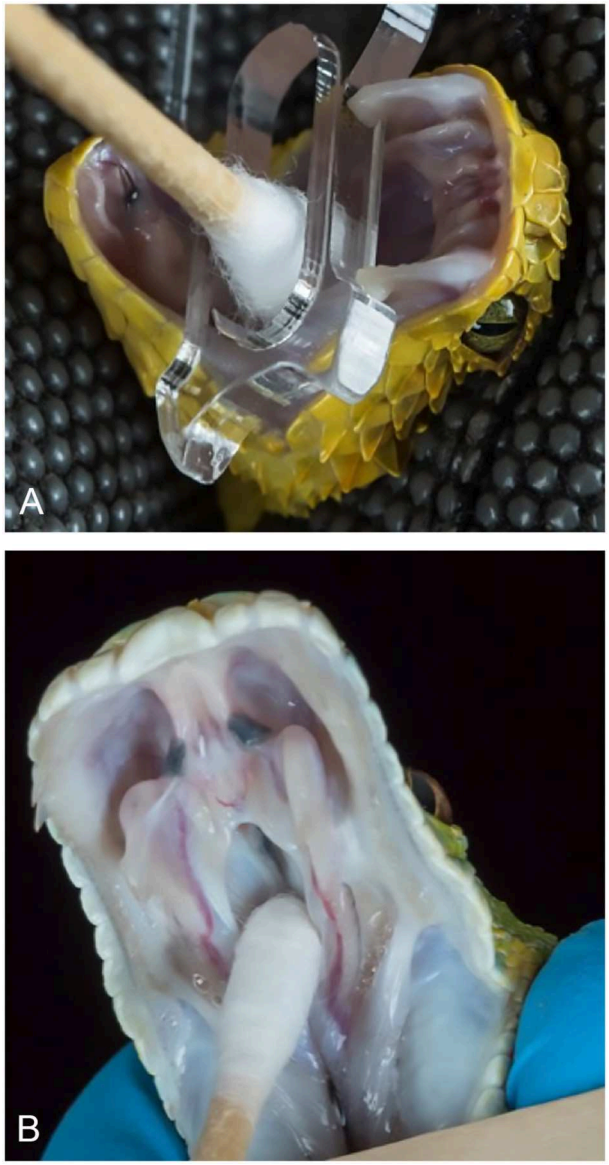

FIGURE 1 | Oral (top) and choanal (bottom) swabbing of captive snakes. Variable bush viper *(Atheris squamigera)* **(A)**. Green tree python (*Morelia viridis*) **(B)**. Photos courtesy of Greg Lepara.

frozen (−20°C). Tissue and egg samples were stored at −80°C upon arrival to the Stenglein laboratory.

RNA Extraction

Swabs

Viral RNA was extracted from swabs in BHI using Zymo Research viral RNA kit with either individual columns or in a 96-well plate. Approximately 200 μl of BHI was processed according to the manufacturer's instructions. RNA was eluted in 30 μl of RNase/DNase-free water. Extracted RNA was stored at −80°C.

Tissues

Total RNA was extracted from tissues and pooled eggs (shell and remaining contents; 4 eggs per pool) using a combination of TRIzol (Ambion Life Technologies) with RNA clean and concentrator columns (CC-5; Zymo Research) as previously described (13). Extracted RNA was stored at −80°C.

Viral RNA Detection

RNA extracted from snake samples was tested for serpentovirus RNA multiple times by independent methods. First, a hemi-nested polymerase chain reaction (PCR) was performed. Round 1, a reverse transcription quantitative PCR (RT-qPCR), was performed using Luna Universal One-Step RT-qPCR kit (New England BioLabs). Twelve microliter reactions included a final concentration of 1x Luna Universal One-Step Reaction Mix, 1x Luna WarmStart RT Enzyme Mix, and 0.3 μM of each degenerate serpentovirus primer (BarniPVTF and BarniGGTR; **Table 1**) mixed with 4 μl of RNA template. Reaction mixtures were run in a Roche LightCycler 480 II with the following cycle parameters: 55°C for 10 min; 95°C for 1 min; 95°C for 10 s and 60°C for 30 s with 45 cycles; and a melting curve (95°C for 5 s; 65°C for 1 min; ramp to 97°C with a rate of 0.11°C/s; and 40°C for 30 s). A no-template water control and positive RNA control from previous experiments with serpentovirus positive snakes (13) were included with each plate. Round 2, a qPCR, was performed using Luna Universal qPCR Master Mix. Twelve microliter reactions included a final concentration of 1x Luna Universal Master Mix and 0.3 μM of each degenerate serpentovirus primer (BarniPVTF and BarniDYTR; **Table 1**) mixed with 5 μl of PCR product from round 1 diluted 1:10 in water. Reaction mixtures were run with the following cycle parameters: 95°C for 1 min; 95°C for 15 s and 60°C for 30 s with 45 cycles; and a melting curve. Both round 1 and round 2 PCR products were run on a 1.5% agarose gel with ethidium bromide for confirmation of amplification and assessment of amplicon size.

RNA from all positive samples from the first hemi-nested PCR was re-tested by a second PCR protocol to confirm results. Reverse transcription from RNA to complementary DNA (cDNA) was performed using random priming as previously described (13). The heminested PCR described above was then repeated using the same primers (round 1: Barni PVTF and BarniGGTR; round 2: BarniPVTF and BarniDYTR) but utilizing the Luna Universal qPCR Master Mix reaction parameters and cycle conditions for both rounds.

A subset of samples with inconclusive PCR results were selected for an additional PCR using the internal primer set (BarniPVTF and BarniDYTR) in a non-nested reaction; this primer set was found to provide increased sensitivity for more divergent serpentoviruses when used independently of the outer primer set. PCR was performed as described above, beginning with diluted cDNA as template. Cycle parameters were altered as follows: 95°C for 1 min; 95°C for 15 s, 46°C for 20 s, and 60°C for 20 s with 45 cycles; and a melting curve.

To confirm previous positive results were not the outcome of PCR contamination during round 1 or round 2 of the hemi-nested reactions and to achieve a longer amplicon sequence for phylogenetic analysis, new primers were designed that flanked

TABLE 1 | Primer sets targeting snake serpentoviruses.

Primer	F/R	Sequence (5′-3′)	Target	Pair	Amplicon (bp)
BarniPVTF (MDS-1222)	F	GAGCACTCCACAARCCAGTCAC	RdRp	BarniGGTR	353
				BarniDYTR	185
BarniGGTR (MDS-1224)	R	KGCATCRCCRCTACTTGTGCCTCC	–	–	–
BarniDYTR (MDS-1223)	R	RCTRCGGTCGCATTTCGTRTARTC	–	–	–
MDS-1529	F	GCAGCACCAGACAACTTCAT	ORF1B/RdRp	MDS-1530	536
				BarniDYTR	385
MDS-1530	R	TTGTACAGWGTGTTGGCGAA	–	–	–

F, forward; R, reverse; RdRp, RNA-dependent RNA polymerase; ORF1B, open reading frame 1B; Bp, basepairs.

the previous hemi-nested set using partial or full-length ophidian serpentovirus sequences available in this laboratory from python hosts (MDS-1529 and MDS-1530; **Table 1**). Positive samples were tested as previously described using the new primers and beginning with random-primed cDNA as template. Cycle parameters were as follows: 95°C for 1 min; 95°C for 15 s and 60°C for 30 s with 45 cycles; and a melting curve.

Sanger Sequencing

Samples that were positive by qPCR and demonstrated the correct amplicon size by gel electrophoresis were Sanger sequenced. Samples were submitted to GENEWIZ (San Diego, California) as premixed samples with the appropriate forward primer (BarniPVTF or MDS-1529); sequencing reactions with the reverse primer were not performed.

Metagenomic Sequencing

A subset of samples with inconclusive PCR results were targeted for shotgun metagenomic sequencing (**Supplemental Table S2**). RNA libraries were generated using the Kapa RNA HyperPrep Kit (Kapa Biosystems) according to the manufacturer's instructions with an input concentration of approximately 100 ng of RNA and 8 rounds of amplification. Kapa Dual-Indexed Adapter Kit Illumina Platform (Kapa Biosystems) was used for adapter ligation and barcoding. Equivalent masses of DNA from each sample were pooled and libraries were size selected (200–600 bp, including Illumina adapters) by gel electrophoresis on a 2% agarose gel. Gel extraction was performed using the Zymo Gel DNA Recovery Kit (Zymo Research) according the manufacturer's instructions. Library quantification was performed with the Kapa Biosystems Illumina library quantification kit according the manufacturer's instructions. Dual indexed, single-end 1 × 75 or 1 × 150 sequencing was performed on an Illumina NextSeq 500 instrument with a NextSeq 500/550 High Output Kit v2 (75 cycles) or Mid Output v2 (150 cycles), respectively. Sequencing analysis was performed as previously described (13).

Sequences were deposited in the GenBank database and short read archive (SRA). Short sequences of ORF1B: GenBank MN117077-MN117130. Partial or full-length genomic sequences generated by metagenomic sequencing: Genbank MN161558-MN161572. Raw data from metagenomic sequencing: BioProject PRJNA555716, BioSample SAMN12358419-SAMN12358456, SRA SRR9921013-SRR9921050.

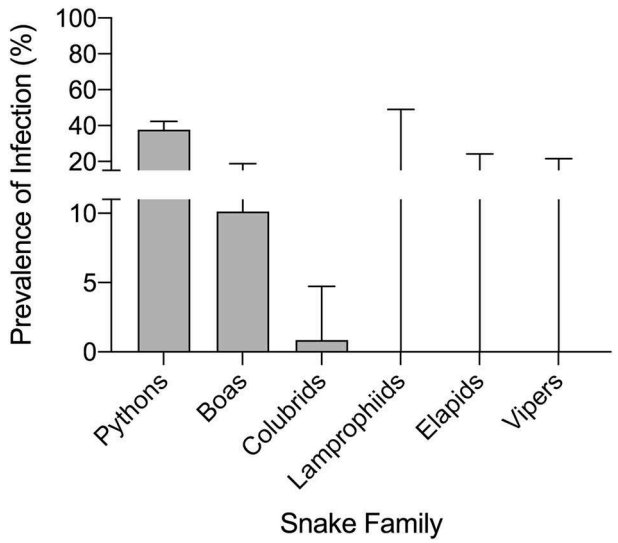

FIGURE 2 | Captive pythons in some collections have a high prevalence of serpentovirus infection. A significant association was observed between infection status and snake family (p-value $\leq$ 0.001). Prevalence of serpentovirus in snakes of each family: pythons 37.7% (156 infected/414 total snakes tested; 95% confidence interval [CI]: 33.1–42.4%), boas 10.1% (8/79; 95% CI: 5.2–18.7%), colubrids 0.9% (1/116; 95% CI: <0.01–4.7%); infection was not detected in lamprophiids (0/4; 95% CI: 0–49%), elapids (0/12; 95% CI: 0–24.2%), or vipers (0/14; 95% CI: 0–21.5%). Bars indicate 95% CI.

Data Analysis

Statistical Analyses

Overall prevalence with 95% confidence intervals (CI) was assessed within each snake family (*Pythonidae, Boidae, Colubridae, Lamprophiidae, Elapidae, Viperidae*). The association between infection status and age, sex, respiratory score, and phylogenetic family were evaluated by a binary logistic

TABLE 2 | Prevalence of serpentovirus by snake species, family, and total.

Common name	Scientific name	Total # tested	# Positive	Positive (%)
Pythons (*Pythonidae* family)				
Children's python	*Antaresia childreni*	1	0	0%
Spotted python	*Antaresia maculosa*	3	0	0%
Anthill python	*Antaresia perthensis*	2	1	50%
Stimson's python	*Antaresia stimsoni*	1	1	100%
Black-Headed python	*Aspidites melanocephalus*	2	0	0%
Woma python	*Aspidites ramsayi*	3	1	33%
Bismarck ring python	*Bothrochilus boa*	2	0	0%
Savu python	*Liasis mackloti*	4	0	0%
Olive python	*Liasis olivaceus*	3	0	0%
Reticulated python	*Malayopython reticulatus*	14	6	43%
Rough scaled python	*Morelia carinata*	2	2	100%
Carpet python	*Morelia spilota*	13	8	62%
Jungle carpet python	*Morelia spilota cheynei*	8	6	75%
Inland carpet python	*Morelia spilota metcalfei*	2	2	100%
Diamond python	*Morelia spilota spilota*	4	4	100%
Green tree python	*Morelia viridis*	120	91	76%
Angolan python	*Python anchietae*	6	1	17%
Burmese python	*Python bivittatus*	2	0	0%
Borneo python	*Python breitensteini*	20	2	10%
Blood python	*Python brongersmai*	45	16	36%
Sumatran python	*Python curtus*	20	7	35%
Indian rock python	*Python molurus*	1	1	100%
Ball python	*Python regius*	136	7	5%
	Totals	**414**	**156**	**37.7%**
Boids (*Boidae family*)				
Dumeril's boa	*Acrantophis dumerili*	2	1	50%
Boa constrictor	*Boa contrictor*	16	0	0%
Puerto Rican boa	*Chilabothrus inornatus*	1	1	100%
Emerald tree boa	*Corallus caninus*	29	5	17%
Amazon tree boa	*Corallus hortulanus*	2	1	50%
Brazilian rainbow boa	*Epicrates cenchria*	5	0	0%
Kenyan sand boa	*Gongylophis colubrinus*	11	0	0%
West African sand boa	*Gongylophis muelleri*	10	0	0%
Rosy boa	*Lichanura trivirgata*	3	0	0%
	Totals	**79**	**8**	**10.1%**
Colubrids (*Colubridae* family)				
Western hognose	*Heterodon nasicus*	7	0	0%
CA kingsnake	*Lampropeltis getula californiae*	16	0	0%
Nuevo Leon kingsnake	*Lampropeltis exicana thayeri*	17	0	0%
AZ mountain kingsnake	*Lampropeltis pyromelana*	9	0	0%
Milksnake	*Lampropeltis triangulum*	1	0	0%
LA milksnake	*Lampropeltis t. amaura*	2	0	0%
Pueblan milksnake	*Lampropeltis t. campbelli*	3	0	0%
Honduran milksnake	*Lampropeltis t. hondurensis*	4	1	25%
Nelson's milksnake	*Lampropeltis t. nelsoni*	1	0	0%
Sinaloan milksnake	*Lampropeltis t. sinaloae*	6	0	0%
Baja CA mountain kingsnake	*Lampropeltis zonata algama*	3	0	0%
Tricolor hognose	*Lystrophis pulcher*	7	0	0%
Cornsnake	*Pantherophis guttatus*	34	0	0%

(Continued)

TABLE 2 | Continued

Common name	Scientific name	Total # tested	# Positive	Positive (%)
Bullsnake	*Pituophis catenifer sayi*	2	0	0%
Cape gopher snake	*Pituophis vertebralis*	4	0	0%
	Totals	**116**	**1**	**0.9%**
Lamprophiids (*Lamprophiidae* family)				
African house snake	*Boaedon filiginosus*	4	0	0%
	Totals	**4**	**0**	**0%**
Elapids (*Elapidae* family)				
Death adder	*Acanthophis rogosus*	1	0	0%
Angolan coral cobra	*Aspidelaps lubricus cowlesi*	1	0	0%
Shield-nosed cobra	*Aspidelaps scutatus*	1	0	0%
Blackbacked Jameson's mamba	*Dendroaspis jamesoni jamesoni*	3	0	0%
Black mamba	*Dendroaspis polylepis*	1	0	0%
Western green mamba	*Dendroaspis viridis*	3	0	0%
Eastern green mamba	*Dendroaspis angusticeps*	1	0	0%
Rinkhal's spitting cobra	*Hemachatus haemachatus*	1	0	0%
	Totals	**12**	**0**	**0%**
Vipers (*Viperidae* family)				
Usambara eyelash bush viper	*Atheris ceratophora*	3	0	0%
Mexican nomad viper	*Atropoides nummifer*	1	0	0%
Speckled forest pit viper	*Bothriopsis taeniata*	4	0	0%
Brazilian lance-head pit viper	*Bothrops moojeni*	2	0	0%
Sumatran pit viper	*Trimeresurus sumatranus*	1	0	0%
Sri Lankan palm pit viper	*Trimeresurus trigonocephalus*	3	0	0%
	Totals	**14**	**0**	**0%**
	Totals	**639**	**165**	**25.8%**

regression. Age and sex were also independently compared to the respiratory score (0, 1, 2, 3) by a Kruskal-Wallis test and Mann-Whitney *U* test, respectivley.

Phylogenetic Analyses

Sequences generated by either Sanger sequencing or metagenomic sequencing were utilized for phylogenetic analysis. Sequences spanning a 467 bp region of ORF1B, including the RNA-dependent RNA polymerase, were aligned using MAFFT software with default parameters (E-INS-i algorithm, 200PAM/$k = 2$ scoring matrix, gap open penalty of 3, and offset value of 0) in Geneious 11.0.4 (15, 16). A phylogenetic tree was generated using PhyML in Geneious with Hasegawa-Kishino-Yano (HKY, nst = 2) substitution model, with 1000 bootstrap replicates, an estimated transition/transversion rate, a fixed proportion of invariable sites (0), 4 substitution rate categories, and a fixed gamma distribution parameter (1, 17, 18).

RESULTS

Prevalence

Serpentovirus infection was detected in all snake collections except collection J, and prevalence within each serpentovirus-positive collection ranged from 5 to 100% (**Supplemental Table S1**). In total, 165 snakes out of 639 were found to be positive for serpentovirus (26%). Prevalence among pythons was markedly higher (37.7%; 156 infected/414 total; 95% CI 33.1–42.4%) compared to boas (10.1%; 8/79; 95% CI: 5.2–18.7%) and colubrids (<1%; 1/116; 95% CI: <0.01–4.7%); infection was not detected in lamprophiids (0/4; 95% CI: 0–49%), elapids (0/12; 95% CI: 0–24.2%), or vipers (0/14; 95 CI: 0–21.5%; **Figure 2**). Prevalence in individual species ranged from 0 to 100% (**Table 2**). A significant association was observed between infection status and snake family (p-value ≤ 0.001).

In collections A and H, physical separation of infected snakes from the rest of the collection and strict sterility practices resulted in high prevalence of infection in quarantined snakes and low prevalence in the main collection. In these two collections, quarantined snakes were relocated to a separate building from the main collection that included its own separate air-flow/venting. Quarantine practices included designated individuals or days for managing quarantined snakes, shower-out procedures, quarantine-specific clothes, shoes, equipment, and instruments, one-way flow of bedding and feeder rodents, disposable glove changes between racks and hand sanitizer disinfection of gloves between breed rotations in racks, and disinfection of all surfaces and instruments with quaternary ammonium compound (Simple Green or F10) following use. In collection A, the prevalence

of serpentovirus in quarantined snakes (A1–9 and 13–36) was 94% (31/33). Prevalence within the primary collection was 4%: only 1 of 25 pythons became positive (a green tree python; see "Long-Term Sequential Sampling"). In collection H, prevalence in quarantined snakes (H118–154) was 68.4% (26/38) and prevalence in the main collection (H1–117) was 4.3% (5/117). The quarantine practices for other collections were unknown or quarantine of infected snakes did not occur.

Morbidity and Mortality

Clinical signs noted at the time of sampling included increased oral hyperemia and increased oral and nasal mucus (respiratory score 1; **Figure 3**), wheezing and/or audible breathing (respiratory score 2), open-mouthed breathing or difficulty breathing (respiratory score 3), and other non-specific signs such as anorexia, inappropriate shedding, difficulty perching in arboreal snakes, and spectaculitis. Respiratory scores were compared between snakes in each genus with at least one positive result (**Figure 4**). Scores ranged from 0 (absent disease) to 3 (severe disease) within snakes of the *Pythonidae* family, including within each genus. In contrast, only 1 out of 8 snakes within the *Boidae* family had a non-zero respiratory score. Only one snake from the *Colubridae* family was found to be positive and had no apparent signs of disease (respiratory score of 0). Statistical comparisons were not performed due to the low number of snakes available in each genus other than *Morelia* and *Python*. Low numbers of snakes that were serpentovirus-negative also exhibited signs of respiratory disease (**Supplemental Table S1**).

Mortality rates were high in three examined collections. In collection A, the mortality rate of serpentovirus-infected snakes was 75% (30/40). Within 20 months of initial sampling, 50% of infected pythons in collection A had died, in comparison to none of the uninfected pythons, which were all still alive at the end of the study (**Figure 5**). In collection G, the mortality rate of infected snakes was 45% (9/20); euthanasia of some serpentovirus-uninfected snakes due to a *Cryptosporidium* outbreak, as well as the sale of uninfected snakes and loss to follow-up, precluded assessment of serpentovirus-uninfected snake mortality. In collection H, 5 infected snakes were found dead and 51 snakes with either confirmed serpentovirus-infection or contact with infected snakes were euthanized. The total loss in the collection was 36% (56/155); the mortality rate of uninfected snakes was 0%.

A subset of snakes that were PCR positive for serpentovirus by oral swab and/or tissue pools (lung, trachea, esophagus) were assessed by gross, histopathologic, or complete postmortem evaluation from collections A (15 pythons), H (1 python), and L (7 pythons). Collection A included 11 green tree pythons (*Morelia viridis*), 2 carpet pythons (*Morelia spilota*), and 2 rough scaled pythons (*Morelia carinata*); a single blood python (*Python brongersmai*) was evaluated in collection H; and collection L included 4 green tree pythons, 1 rock python (Python molurus), 1 Stimson's python (*Antaresia stimsoni*), and 1 Dumeril's boa (*Acrantophis dumerili*). All pythons (total 23) exhibited evidence of respiratory disease consistent with serpentovirus infection as previously described (4–6, 10, 13). Findings included chronic-active and mucinous rhinitis, stomatitis, esophagitis, tracheitis, and proliferative interstitial pneumonia. Representative gross and histologic images are presented in **Figure 6**. Moderate to severe pneumonia was determined to be a primary contributor to the cause of death in most snakes (all except 4 green tree pythons) and these snakes exhibited a respiratory score of 2 (moderate) or 3 (severe) around the time of death. Secondary lesions detected by histopathology ($n = 10$) included bacterial and/or fungal colonization of the upper and lower respiratory tract and esophagus ($n = 7$), sepsis ($n = 3$), and systemic gout (likely associated with emaciation and dehydration; $n = 1$). Bacterial culture of the lung or liver from two snakes yielded heavy growth of *Pseudomonas aeruginosa* and moderate growth of *Escherichia coli*, *Providencia rettgeri*, and/or *Citrobacter* species. In the 4 green tree pythons with minimal to mild pneumonia, lesions in the upper respiratory tract (rhinitis, stomatitis, esophagitis, tracheitis) were more pronounced and were accompanied by evidence of emaciation, gout, or sepsis that was determined to be a likely cause of death. These snakes exhibited respiratory scores of 1 (mild) around the time of death.

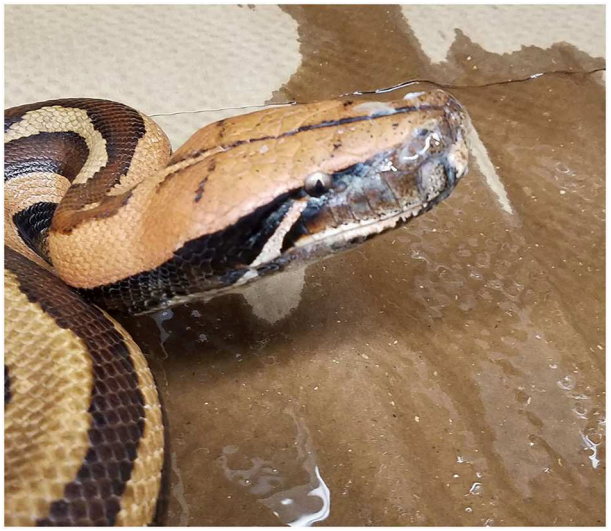

FIGURE 3 | Excessive oral and nasal mucus production in a serpentovirus-positive snake. Blood python; Collection H.

Age and Sex

Infection status was compared to age (range of 0.1–22 years) and sex (male or female). A statistically significant association was observed between age and infection status in snakes (p-value $\leq$ 0.001; **Figure 7A**). No significant association was observed between the sex and infection status (p-value = 0.144; **Figure 7B**). Neither age (**Figure 7C**) nor sex (**Figure 7D**) were statistically associated with respiratory score (p-value = 0.32 and p-value = 0.06, respectively).

Phylogenetic Analysis

Viral sequences were phylogenetically analyzed to assess overall genetic diversity, to reconstruct possible transmission events, and to test for associations between viral genotypes

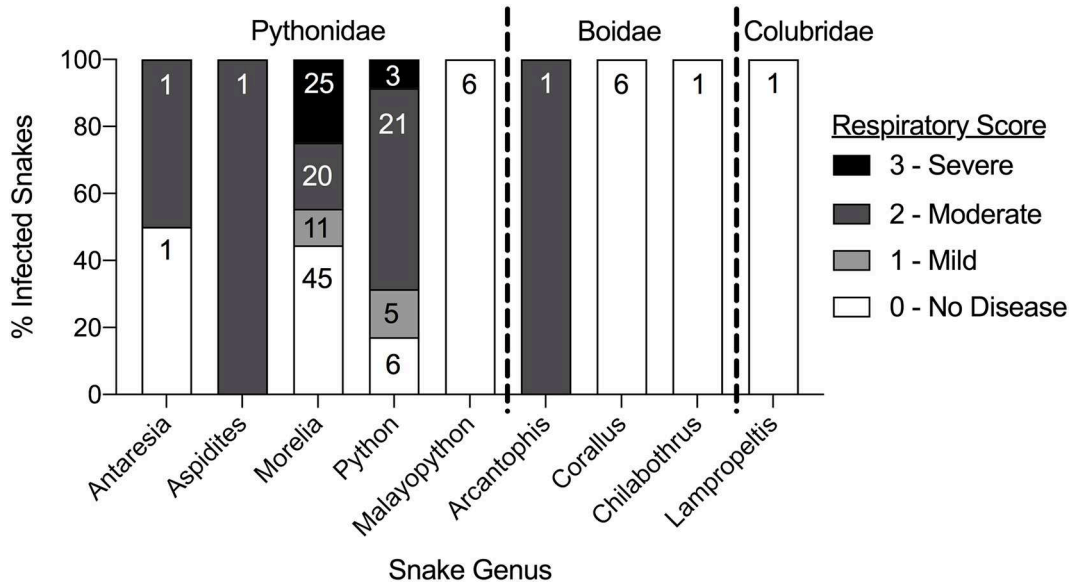

FIGURE 4 | Clinical disease varies by individuals within each snake genus and amongst snake families. Comparison of the respiratory scores of individual serpentovirus-positive snakes within each snake genus. Data is represented as a stacked bar graph totaling 100% of infected snakes in each snake genus. Each respiratory score is represented as a percentage of the total. Values within each fraction of the total indicate the sample size (N).

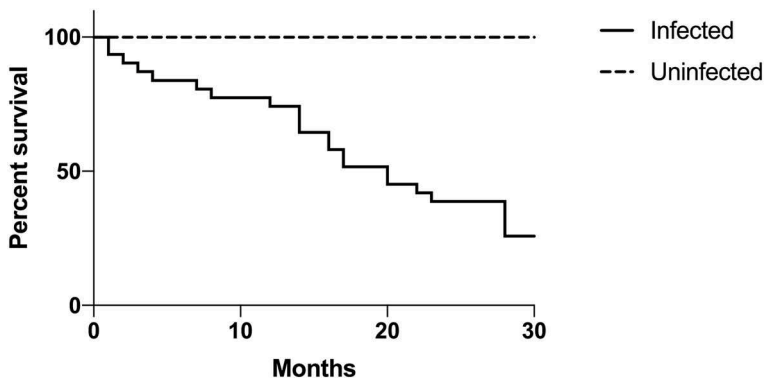

FIGURE 5 | Infected snakes are statistically more likely to experience mortality than uninfected snakes. Longitudinal assessment of mortality between infected and uninfected snakes in collection A. Time is represented in months and begins at the onset of a serpentovirus outbreak (September 2016). Kaplan-Meier survival curve; p-value = 0.001.

and host species or disease (**Figure 8**; Genbank accession numbers MN117077-MN117130).

Two serpentovirus groups were evident. One definitive clade, which accounted for most of the sequences generated in this study, contained sequences recovered from python species in the genera *Morelia*, *Python*, *Aspidites*, and *Antaresia* (**Figure 8**). This clade included the serpentoviruses previously associated with respiratory disease in pythons, such as ball python nidovirus (4–6, 10, 13). The sequences in this python-only clade shared >80% pairwise nucleotide identity in the aligned ORF1B region.

The other group contained sequences from boas (genera *Corallus* and *Chilabothrus*), a colubrid (genus *Lampropeltis)*, and reticulated pythons (genus *Malayopython)* in addition to sequences that were identified by metagenomic surveys of colubrid and homalopsid snakes in China (2). This second group was less well-supported phylogenetically and contained more overall genetic diversity than the python-only clade, with sequences sharing ≥57% pairwise nucleotide identity. These sequences were identified using metagenomic sequencing of samples from snakes for which PCR results had been negative or inconclusive (**Supplemental Table S2**).

Although the virus phylogeny did not form well-supported monophyletic clades by host, viruses with more similar sequences were generally found in snakes of the same species or genus. Exceptions to this included closely related viruses that infected pythons of multiple genera in the same collection. For example, virtually identical viruses (≥99.8% pairwise identity in the region used to make the tree) were recovered from three snakes of different genera from collection G: G47 (*Morelia viridis*), G58 (*Antaresia perthensis*), and G59 (*Python regius*). Similar examples

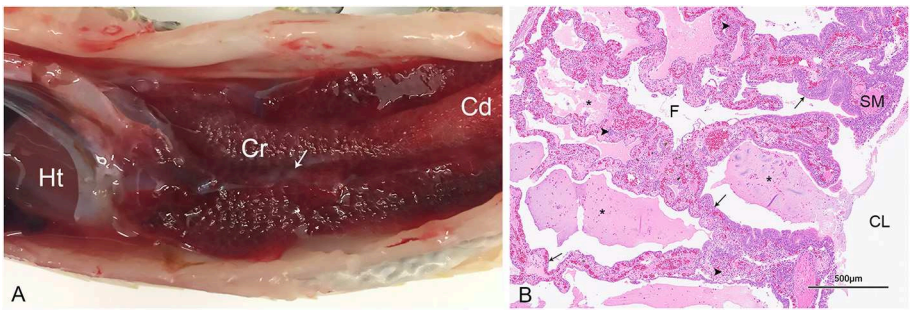

FIGURE 6 | Gross and histologic pulmonary lesions in a serpentovirus-positive green tree python from collection A (snake A26). **(A)** The lungs are markedly thickened and dark red, especially in the cranial (Cr) lung compared to the caudal (Cd) lung. Small mucoid aggregates are present within the central lumen of the lung (arrow). The heart (Ht) is indicated for orientation. **(B)** Histopathology of the lung revealing proliferative and interstitial mucinous pneumonia characterized by excessive mucus, edema, and necrotic debris (asterisks) within the central lumen (CL) and faveoli (F), marked epithelial hypertrophy and hyperplasia lining faveoli (arrows), and mixed chronic-active inflammation within thickened faveolar septa (arrowheads). These lesions are consistent with serpentovirus infection. SM, smooth muscle. Hematoxylin and Eosin. 40× magnification.

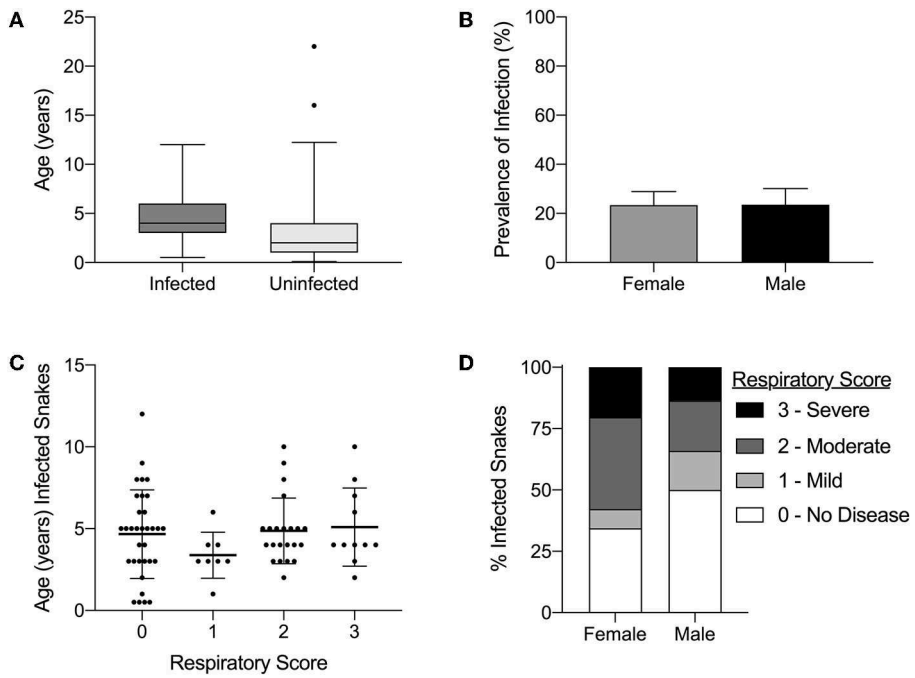

FIGURE 7 | Serpentovirus infection is statistically associated with age but not with sex; clinical signs are not statistically associated with age or sex. **(A)** Comparison of ages between serpentovirus-infected and uninfected snakes. Average ages: 4.7 (infected) and 2.6 (uninfected). Binary logistic regression; p-value ≤ 0.001. Box and whisker plot 1–99 percentile. **(B)** Prevalence of infection in male and female snakes. Female prevalence: 23.4%, 95% CI 18.7–28.9%. Male prevalence: 23.5%, 95% CI 18–30.1%. Binary logistic regression; p-value $= 0.144$. **(C)** Comparison of respiratory score to age in serpentovirus-positive snakes. Kruskal-Wallis test (one-way ANOVA on ranks, non-parametric); p-value $= 0.32$. Scatter dot plot mean with standard deviation. **(D)** Comparison of respiratory score with sex in serpentovirus-positive snakes. Mann-Whitney U test; p-value $= 0.06$. Stacked bar graph representing the number of snakes with each respiratory score as a fraction of the total (100%).

included the viruses from snakes G42, G50, and G61, and those from L14 and L23. Genetically distinct serpentovirus sequences were recovered from all positive collections, except collection I.

The possibility that some viral genotypes were more pathogenic than others was also investigated. In the python-only clade, respiratory score ranged from 0 to 3 and an overt association between viral genotype and clinical disease was not evident. In contrast, respiratory scores were 0 for all boas, colubrids, and reticulated pythons outside the python-only clade. The only boa in this study that was documented to have clinical disease (L22, Dumeril's boa; respiratory score of 2) was not included in this phylogeny due to sequence length limitations (155 bp available compared to 467 bp for sequences in the phylogeny). Alignment of the short Dumeril's boa sequence revealed it to be slightly more related to the viruses in the python-only clade, with which it shared ∼70–77% nucleotide identity,

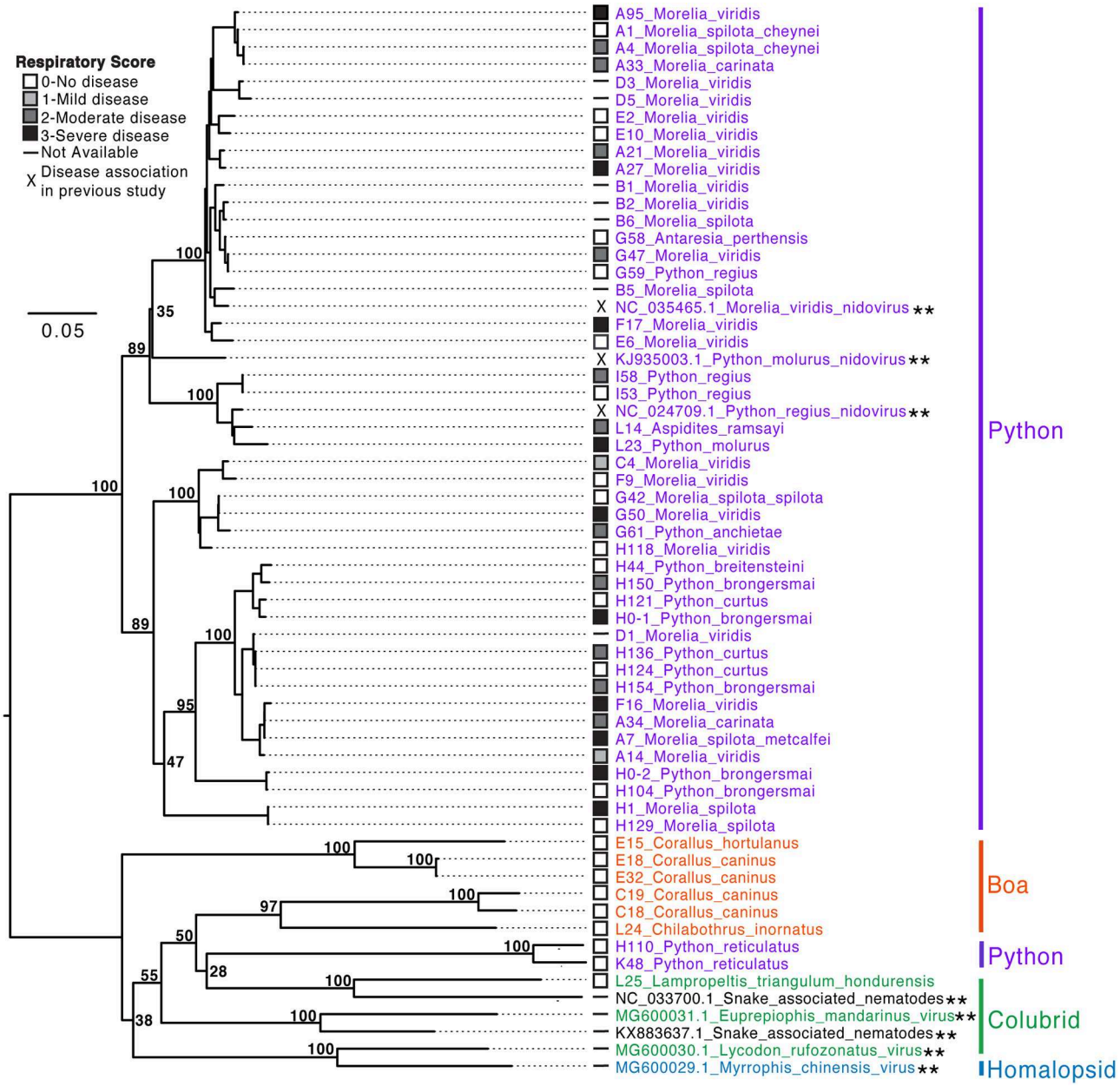

FIGURE 8 | Serpentovirus phylogeny reveals implications regarding species susceptibility to infection and disease. Snake IDs are indicated by collection letter (A–L) and number followed by genus and species. Snake families are indicated to the right: Python (*Pythonidae*, purple), Boa (*Boidae*, orange), Colubrid (*Colubridae*, green), and Homalopsid (*Homalopsidae*, blue). Reference sequences identified in previous studies and available in GenBank (double asterisks: **) are indicated by accession number followed by the genus and species of the host, except snake-associated nematode viruses in which the host species was unknown. Nucleotide sequences (467 basepairs; ORF1B) aligned and analyzed with PhyML with HKY85 substitution model and 1,000 bootstrap replicates; bootstrap values (%) included at major nodes. The tree was semi-subjectively rooted, this was partially based on protein alignments of ORF1B of serpentovirus reference sequences in GenBank and partially to highlight differences between the python-only clade and more divergent viral sequences of boas, colubrids, homalopsids, and reticulated pythons; a definitive monophyletic clade of these divergent viruses is poorly supported by bootstrap values and should not be interpreted as such. Short sequences of the ORF1B detected during the study and used to generate this phylogeny were deposited in GenBank (MN117077-MN117130).

in contrast to 49–62% identity to viruses derived from boas, colubrids, and reticulated pythons.

Partial or complete genome sequences derived from metagenomic sequencing were globally aligned to ball python nidovirus (BPNV; NC_024790.1) and percent nucleotide identity was assessed (**Supplemental Table S2**). Python serpentoviruses (A93–95, F17, H0–1,−2, L1, 3, 4, 8, 14) ranged from 62 to 94% nucleotide identity; boa serpentoviruses (C18–19) ranged

from 31 to 43% nucleotide identity; the colubrid serpentovirus (L25) exhibited 30% nucleotide identity; the reticulated python serpentovirus (K48) exhibited 31% nucleotide identity. These new serpentovirus genomes had similar overall genome structures to that of BPNV at the 5' end: two large overlapping open reading frames, ORF1A and ORF1B, separated by a ribosomal frameshift signal (AAAAAC) that together encode a large polyprotein of non-structural proteins. These large ORFs were immediately followed by a spike protein gene (ORF2). The 3' end of the genomes of the viruses in the python-only clade were similarly organized to BPNV with five predicted ORFs encoding: a transmembrane protein, matrix protein, nucleoprotein, and 2 additional predicted transmembrane proteins. The other serpentoviruses outside the python-only clade for which near-complete genomes were obtained had more variable 3′ end gene content, but all had predicted matrix and nucleoprotein genes flanked by variable numbers of genes encoding proteins with predicted transmembrane domains.

Co-infection

Serpentovirus co-infection in a blood python from collection H (snake H0) was detected. One complete coding genome (H0–1) and one nearly complete coding genome (H0–2) were generated from sequencing reads (**Supplemental Table S2**). These sequences shared approximately 71% global nucleotide identity. When a short nucleotide sequence from each H0 serpentovirus was compared to other snakes in the collection (**Figure 8**), H0–1 shared >99% nucleotide identity to H121 and only 90% to H0–2 and H104, respectively; H0–2 shared >99% identity to H104. Possible coinfections were also detected in two other snakes (H136 and L21) in which low numbers of unique serpentovirus reads detected by metagenomic sequencing did not align to the primary assembled serpentovirus genome.

Long-Term Sequential Sampling of Collection A

Forty pythons in collection A were sampled longitudinally at approximately 4-month intervals over 28 months following an outbreak of serpentovirus that began in 2016. The infection status and clinical progression of individual snakes (**Figure 9**), and horizontal transmission (**Figure 10**) were assessed. Three snakes that were part of the original collection (introduced in 2008) were diagnosed with serpentovirus in 2015 and died (A93–95). Snakes A1–9, 30–31, and 33–36 were introduced between 2013 and 2015 and their infection status was unknown prior to the 2016 outbreak. Snakes A10–29 and 32 were purchased and introduced to the collection in 2016, after which the outbreak of serpentovirus-associated respiratory disease occurred. Snakes A98 and A99 were also purchased from the same seller and had contact with A10–29 and 32 but died prior to introduction into collection A. Positive snakes (tested at 0 and 4 months into the outbreak; A1–9 and 13–34) were quarantined away from remainder of collection. Snakes A37–40 were purchased after the outbreak (2017) and were never directly exposed to serpentovirus-positive snakes in the collection.

Overall, positive snakes remained positive during the 28-month period (**Figure 9**); no snakes were seen to transition from consistently positive to consistently negative. Snakes A11–12 (green tree pythons) were serpentovirus-negative at initial sampling were housed with the main collection and remained negative. Only one snake in the main collection converted to positive (A66); see "Vertical Transmission." Two snakes (A35–36, olive pythons) that were initially negative, but potentially exposed to serpentovirus, were housed in the quarantine area; these snakes remained negative throughout the study. In a subset of quarantined snakes (A13–18), intermittent negative results were obtained despite overall positivity. These negative results primarily, but not exclusively occurred in snakes exhibiting lower respiratory scores (0–1). Sanger sequencing of PCR amplicons before and after time points with negative results yielded identical viral sequences.

Phylogenetic analysis of viral sequences from snakes in collection A was performed on 26 of 40 positive snakes; 5 viral genotype groups were detected, three of which were present in the 2016 outbreak (**Figure 10**). The first viral genotype group was found in one of the initial snakes diagnosed with serpentovirus (A95) and was also detected in other snakes from the original collection (A1–6, 8–9, 33), but not in any purchased snakes. The second and third viral genotypes were found in the purchased snakes that died before introduction into the collection (A98 and 99). These genotypes were also detected in the purchased snakes that were introduced (A21, 26, 27, 66) as well as snakes from the original collection (A7 and 34), consistent with transmission from the purchased snakes to the original collection. Longer viral sequences for phylogenetic analysis were not collected from all positive snakes in the collection, therefore, the presence of other viral genotypes not represented in the phylogeny cannot be ruled out.

Vertical Transmission

During the longitudinal sampling of collection A, two separate serpentovirus-positive mating pairs (green tree pythons A27 and A29; jungle carpet pythons A1 and A3) were bred and resulted in a clutch of eggs. The green tree python mating pair resulted in 17 eggs and 16 viable hatchlings which were sampled orally at 4-month intervals for 20 months; 7 of these were only tested once due to donation to a separate collection and loss to follow-up within the first 4 months. The egg shells and liquid contents (post hatching) were pooled (4 eggs per pool) and all were found to be serpentovirus RNA positive. All offspring were negative at each sampling time-point except one (A66) that became serpentovirus-positive between 8 and 12 months of age. Sanger sequencing was performed on oral/choanal swabs from the adult male, female, and positive offspring, and the pooled egg shell/contents. Viral sequences from the adult female and the egg shell/contents were >99% similar to each other but only 84% similar to the viral sequences detected in the adult male and positive offspring, which were >98% similar to each other. A second mating pair of jungle carpet pythons produced a clutch of 9 eggs and 2 viable offspring that were sampled twice during a 6-month period. Egg pools were again found to be positive but the offspring remained negative during the sampling period.

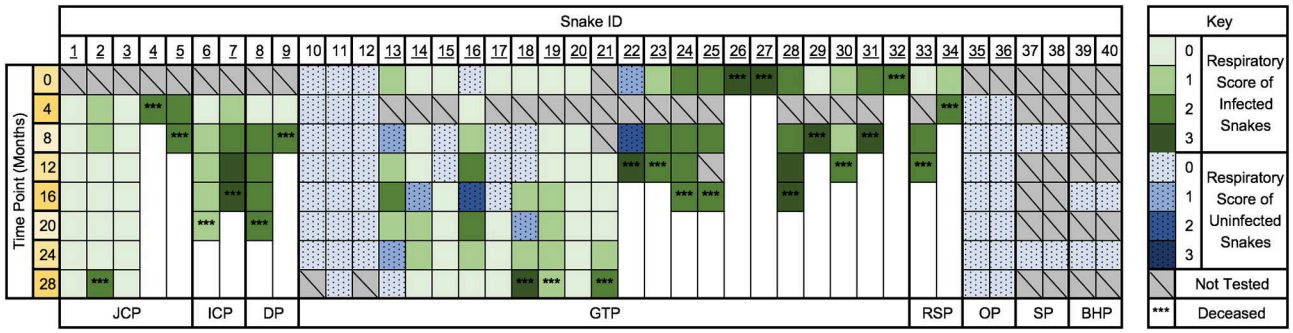

FIGURE 9 | The progression of serpentovirus infection and disease within a single collection (A) over 28 months. Time points begin September 2016 (0 months) and end December 2018 (28 months). Green indicates a serpentovirus-positive result (infected). Blue indicates a serpentovirus-negative result (uninfected). Shades of blue and green indicate respiratory score at the time of sampling. ***Indicate the approximate time of death. Snakes in quarantine are indicated by underlining of the snake ID number. JCP, jungle carpet python (*Morelia spilota cheynei*). ICP, inland carpet python (*Morelia spilota metcalfei*). GTP, green tree python (*Morelia viridis*). RSP, rough-scaled python (*Morelia carinata*). OP, olive python (*Liasis olivaceus*). SP, savu python (*Liasis mackloti savuensis*). BHP, blackhead python (*Aspidites melanocephalus*).

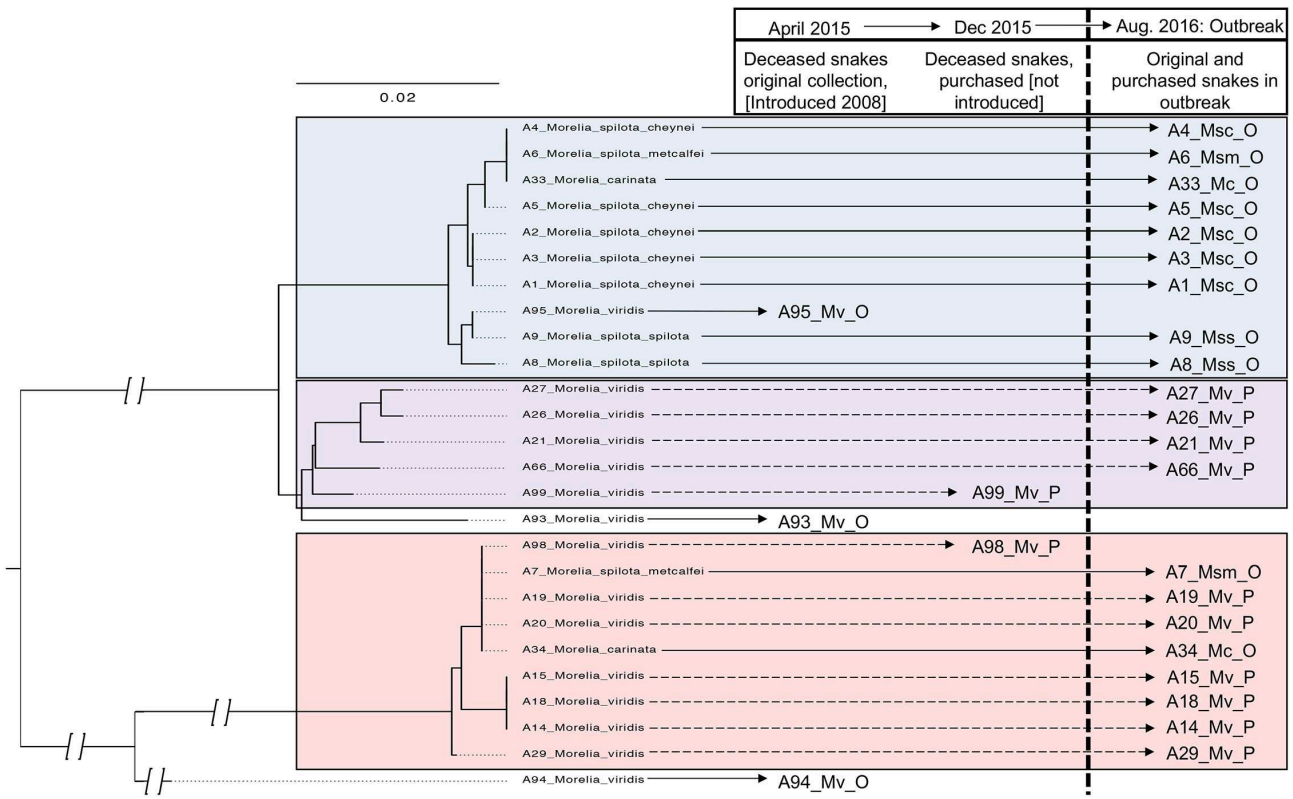

FIGURE 10 | Phylogeny and proposed horizontal transmission in collection A. Nucleotide sequences (467 basepairs) aligned and analyzed with PhyML with HKY85 substitution model and 1,000 bootstrap replicates; arbitrary rooting; discontinuous scale in branches closer to root indicated by branch breaks. Snake ID denoted by A and number; Mv, *Morelia viridis*; Msc, *Morelia spilota cheynei*; Msm, *Morelia spilota metcalfei*; Mc, *Morelia carinata*. O, original collection. P, purchased.

DISCUSSION

In this study, 639 snakes from 62 species were screened for infection with ophidian serpentoviruses. Prevalence of infection was highest in pythons (nearly 40%) and serpentoviruses were detected in pythons in the *Morelia, Python, Malayopython, Antaresia*, and *Aspidites* genera. This finding agrees with reports in the literature that many python species are susceptible to serpentovirus infection (4–6, 9, 10). Most positive pythons in this study were *Morelia* species. The veterinary community has anecdotally regarded these pythons as being more predisposed to respiratory infection. It is possible that this belief reflected

an increased susceptibility and high prevalence of serpentovirus infection in captive *Morelia* species. It is important to note that 5 of the collections in this study were known to have serpentovirus infections, which could have biased the sample set to increase prevalence measures. Nonetheless, these findings highlight the high rate of infection that can occur in collections in which serpentoviruses have been introduced.

In contrast to a high prevalence in pythons, serpentoviruses were detected at a significantly lower rate in snakes from the *Boidae* and *Colubridae* families and not detected in any snakes from the *Lamprophiidae*, *Elapidae*, or *Viperidae* families. These findings could indicate a reduced susceptibility or resistance to infection in these species. However, small sample sizes and targeted PCR assays may have impacted these results. Combined, only 30 lamprophiids, elapids, and vipers were tested and all were negative. Additionally, only 8 boas and 1 colubrid were found to be serpentovirus-positive out of 79 and 116, respectively. Based on the genetic diversity of serpentoviruses described in this study, it is possible that the PCR assay used may not have detected more divergent serpentoviruses in some of these species. Overall, these conclusions regarding species susceptibility and species specificity in non-python snakes must therefore be interpreted with caution and PCR-based diagnostics may need to be updated to account for the newfound diversity of serpentoviruses in snakes.

What can be concluded from these results is that non-python snakes are potentially less susceptible or resistant to infection by serpentoviruses that readily infect pythons. Phylogenetic analysis revealed that the same python serpentoviruses can infect pythons from multiple genera. But these viruses were never found to infect boas and colubrids in the same collections that had been exposed to infected pythons. In contrast, the viruses found in boas and colubrids (and reticulated pythons) belonged to distinct evolutionary lineages from those found in pythons. Therefore, although python serpentoviruses can infect pythons of multiple genera, barriers to infection may be too great for them to infect boas or colubrids, and vice versa. Interestingly, evolutionarily distinct serpentoviruses found in reticulated pythons were more closely related to viruses from boas and colubrids and an evolutionarily distinct serpentovirus found in a Dumeril's boa was more closely related to viruses from pythons (non-reticulated). Sampling of wild-caught snakes will provide insight into the origins and natural hosts of these distinct serpentoviruses.

Clinical disease was consistently observed for all virus genotypes detected in the clade of python-associated serpentoviruses, whereas clinical disease was absent in boas, colubrids, and reticulated pythons (serpentoviruses outside the python-only clade). The virus detected in a Dumeril's boa was the only virus associated with clinical disease in a boa species. Its closer relation to python viruses may provide evidence that certain genotypic lineages are more likely to cause disease in snakes, or that certain snakes are more susceptible to disease with these viruses. However, this hypothesis will likely be altered as a greater number of serpentoviruses in non-python species or divergent serpentoviruses are discovered.

The single serpentovirus sequence found in a colubrid in the study (L25) was most closely related a sequenced recovered from a snake-associated nematode (1). Previously it was shown that serpentovirus is detectable in gastrointestinal tissue and feces in infected ball pythons (13) and it is hypothesized that these putative worm viruses (1) actually represent snake viruses that were ingested by or contaminated the surface of intestinal nematodes.

Previous studies evaluating the prevalence of viral infections or respiratory disease in pythons and boas found a greater prevalence in pythons, as well as correlations with older age and specific husbandry practices (9, 19, 20). Similarly, the study found older snakes were more likely to be infected, but increasing age did not increase the likelihood of clinical disease. Therefore, infection in older animals is suspected to be due to increasing time of potential exposure, rather than physiologic changes that accompany age. Husbandry was not directly assessed in this study but it is a significant variable in the health of captive reptiles and suboptimal practices can result in stress and alterations in immunity (21, 22). If one can assume similar husbandry practices within a collection, it would be expected that snakes of the same species infected with the same or highly similar viruses would exhibit similar degrees of clinical disease. In some collections, this trend was observed (e.g., Collection H), whereas in others, clinical disease was more variable (e.g., Collection A). Beyond husbandry, individual animal factors that could have played a role in disease variability include length of time infected and exposure dose, co-morbidities (both infectious and non-infectious), reproductive stage/status, and genetic background of the host (23). Other inciting stress events could have also affected groups of snakes within a collection, including seasonal or environmental change, relocation/shipping, breeding, and increased handling or showing (23).

Coinfections have been documented in natural infections of viruses related to serpentoviruses, such as toroviruses and coronaviruses, and have been associated with viral recombination and evolution (24, 25). The snake in which serpentovirus coinfection was detected (H0) died from severe respiratory disease, but it is unknown if coinfection altered the disease course or pathologic progression. Coinfections with other known and unknown non-serpentovirus snake pathogens may also have played roles in disease progression. Other agents including paramyxoviruses, orthoreoviruses, sunshine virus, and *Mycoplasma* species have been associated with, or shown to cause respiratory disease in snakes (20, 26–28). The ecological interactions of serpentoviruses with other pathogens and the host immune system merits further study.

One of the primary goals of this project was to assess aspects of disease that may lend themselves to better management strategies including quarantine practices, the potential for viral clearance, the frequency of diagnostic testing, and the risk of transmission to offspring following breeding.

In two collections a significantly lower rate of infection in the main population compared to infected snakes in quarantine was observed. Collection A and H removed infected snakes and snakes that had been in direct or close contact with infected snakes, from the main collection and placed them in separate

quarantine buildings. A single designated caretaker was assigned, either indefinitely or each day, for quarantine management. Quarantine-specific clothes and equipment, separate air-flow and ventilation, and rigorous disinfection practices of the facility were utilized (see prevalence results). In both cases, infection rates were high in quarantined snakes (68–100%) and remained low (<5%) in the main collection. These findings indicate that transmission occurs at a higher rate between snakes of close-proximity and that proper quarantine practices that limit the spread of infectious agents can be highly effective. Possible routes of transmission are speculated to include fecal-oral or respiratory fomite transmission or direct contact during breeding events, which have the potential to be limited or eliminated through quarantine measures (13).

Phylogenetic analysis of a single collection (A) over time revealed that existing infected snakes and introduced infected snakes could both contribute to overall serpentovirus burden. Furthermore, longitudinal testing of this same collection revealed that serpentovirus infection can persist over long periods and infection can result in overt or subclinical disease. In this study, intermittent negative results in a low number of snakes were initially thought to represent viral clearance, but sampling of these snakes over time revealed continued evidence of infection. Negative PCR results could represent episodes of viral clearance followed by re-infection or periods of reduced shedding below the limit of detection. No snakes were observed to transition from consistently positive to consistently negative test results, indicating complete clearance may not be possible. Technical factors could also play a role in "false-negative" results, such as insufficient swabbing or sample handling. Independent of the underlying cause of intermittent negative results, the chronicity of disease and the potential for negative test results in infected snakes highlights two important management strategies: the need for longer periods of quarantine prior to the introduction of potentially infected snakes (at least 3 months) and the requirement of multiple negative diagnostic tests over time to ensure true serpentovirus-negativity in individual snakes.

Also in collection A, infected snakes that exhibited moderate to severe respiratory signs were treated with antibiotics (enrofloxacin and ceftazidime) following bacterial culture of sterile lung washes that yielded heavy growth of *Pseudomonas* species and moderate growth of *Escherichia coli* and *Citrobacter* species. Additionally, subcutaneous lactated ringers fluid therapy and an increased thermal gradient were provided. Secondary bacterial infections have been observed in association with serpentovirus infection (4, 6, 13). In some cases, treated snakes exhibiting moderate to severe clinical signs lived up to 16 months post-diagnosis, which could be associated with antibiotic treatment and supportive therapy. Although this observation was only anecdotal and not a monitored aspect of this study, it is possible that treatment of sequelae could contribute to prolonged lifespan in persistently serpentovirus-infected collections.

Vertical transmission is a natural route of spread for some nidoviruses (e.g., equine arteritis virus, gill-associated virus) (29, 30). In this study, vertical transmission was evaluated in the eggs and offspring of serpentovirus-positive mating pairs. Viral RNA was detected in/on most eggs, which was suspected to represent contamination from feces within the cloaca rather than infection of the embryo or egg contents. In offspring, all but one remained negative following hatching (1/19). In the one positive offspring, the viral genotype was more closely related to the male parent than the female parent. Therefore, these findings may support vertical transmission of serpentoviruses from the male, but at a significantly lower rate than horizontal transmission. Furthermore, in this study eggs were artificially incubated and sterilized with UV or a quaternary ammonium compound and hatchlings were housed separately from other infected snakes. The prevalence of infection in offspring hatched under natural conditions was not examined, but could provide insight into the likelihood of horizontal transmission from parent to offspring under more typical conditions. Lastly, a low rate of hatching was observed in one clutch (2/9), which was suspected to be due to artificial incubation errors, but this cannot be confirmed.

Serpentoviruses are significant respiratory pathogens of pythons and introduction into collections can be devastating. Due to the chronicity and variability in clinical signs during infection with serpentoviruses, stringent management strategies are recommended. These include prolonged quarantine practices with multiple negative test results prior to the introduction of new snakes into the collection, the immediate removal or separation of any positive snakes from the main collection with strict quarantine measures to prevent continued spread, and understanding the risk of horizontal and vertical transmission when purchasing, selling, or breeding snakes. The clinical importance of serpentovirus infection in boas and colubrids remains poorly understood, but infection is possible and should be perceived as a potential respiratory pathogen. Serpentovirus infection in other snake species continues to be an ongoing field of research.

DATA AVAILABILITY STATEMENT

The datasets generated for this study can be found in the GenBank and BioProject/BioSample/Short Read Archive.

ETHICS STATEMENT

Ethical review and approval was not required for the animal study because non-invasive samples were collected by owners and submitted to our laboratory. No animal handling, manipulation, or sampling was performed in our laboratory on live animals.

AUTHOR CONTRIBUTIONS

LH-H was responsible for performing experiments, analyzing and interpreting the data, and drafting of the manuscript. RO, PB, SF, SP, AS, and EJ provided samples and collected epidemiologic data for the study. JW, ED, and RO provided primers and protocols for the study. SC and MS performed metagenomic sequencing and data analysis. All authors contributed to manuscript revision, read, and approved the submitted version.

FUNDING

Funding for this project was provided by Colorado State University, the Alvin Hoerlein fellowship to LH-H, and gracious donations from reptile enthusiasts; Computational resources were supported by NIH/NCATS Colorado CTSA Grant Number UL1 TR002535.

ACKNOWLEDGMENTS

The authors would like to thank the following groups and individuals: Justin Lee and Marylee Layton at the CSU Next Generation Sequencing facility; Dr. Whitney Zoll, Dr. Stephen Barten, Dr. Mike Corcoran, Dr. Kelsie Stoval, the veterinary pathologists at Colorado State University Veterinary Diagnostic Lab, Cody Bartolini, Steven Tillis, Joshua Doss, Jordan Padlo, Raul Diaz, and numerous anonymous reptile owners for providing samples; Greg Lepara for photographs of swabbing technique.

SUPPLEMENTARY MATERIAL

The Supplementary Material for this article can be found online at: https://www.frontiersin.org/articles/10.3389/fvets.2019.00338/full#supplementary-material

REFERENCES

1. Shi M, Lin X-D, Tian J-H, Chen L-J, Chen X, Li C-X, et al. Redefining the invertebrate RNA virosphere. *Nature.* (2016) 540:539–43. doi: 10.1038/nature20167
2. Shi M, Lin X-D, Chen X, Tian J-H, Chen L-J, Li K, et al. The evolutionary history of vertebrate RNA viruses. *Nature.* (2018) 556:197–202. doi: 10.1038/s41586-018-0012-7
3. Saberi A, Gulyaeva AA, Brubacher JL, Newmark PA, Gorbalenya AE. A planarian nidovirus expands the limits of RNA genome size. *PLoS Pathog.* (2018) 14:e1007314. doi: 10.1371/journal.ppat.1007314
4. Bodewes R, Lempp C, Schurch AC, Habierski A, Hahn K, Lamers M, et al. Novel divergent nidovirus in a python with pneumonia. *J Gen Virol.* (2014) 95 (Pt 11):2480–5. doi: 10.1099/vir.0.068700-0
5. Stenglein MD, Jacobson ER, Wozniak EJ, Wellehan JFX, Kincaid A, Gordon M, et al. Ball python nidovirus: a candidate etiologic agent for severe respiratory disease in *Python regius*. *mBio.* (2014) 5:e01484-01414. doi: 10.1128/mBio.01484-14
6. Uccellini L, Ossiboff RJ, de Matos REC, Morrisey JK, Petrosov A, Navarrete-Macias I, et al. Identification of a novel nidovirus in an outbreak of fatal respiratory disease in ball pythons (*Python regius*). *Virol J.* (2014) 11:144. doi: 10.1186/1743-422X-11-144
7. Tokarz R, Sameroff S, Hesse RA, Hause BM, Desai A, Jain K, et al. Discovery of a novel nidovirus in cattle with respiratory disease. *J Gen Virol.* (2015) 96:2188–93. doi: 10.1099/vir.0.000166
8. O'Dea MA, Jackson B, Jackson C, Xavier P, Warren K. Discovery and partial genomic characterisation of a novel nidovirus associated with respiratory disease in wild shingleback lizards (*Tiliqua rugosa*). *PLoS ONE.* (2016) 11:e0165209. doi: 10.1371/journal.pone.0165209
9. Marschang RE, Kolesnik E. Detection of nidoviruses in live pythons and boas. Tierarztl Prax Ausg K Kleintiere Heimtiere. (2017) 45:22–6. doi: 10.15654/TPK-151067
10. Dervas E, Hepojoki J, Laimbacher A, Romero-Palomo F, Jelinek C, Keller S, et al. Nidovirus-associated proliferative pneumonia in the green tree python (*Morelia viridis*). J Virol. (2017) 91:e00718-17. doi: 10.1128/JVI.00718-17
11. Zhang J, Finlaison DS, Frost MJ, Gestier S, Gu X, Hall J, et al. Identification of a novel nidovirus as a potential cause of large scale mortalities in the endangered Bellinger River snapping turtle (*Myuchelys georgesi*). *PLoS ONE.* (2018) 13:e0205209. doi: 10.1371/journal.pone.0205209
12. Ziebuhr J, Baric RS, Baker S, de Groot RJ, Drosten C, Gulyaeva A, et al. Reorganization of the family Coronaviridae into two families, Coronaviridae (including the current subfamily Coronavirinae and the new subfamily Letovirinae) and the new family Tobaniviridae (accommodating the current subfamily Torovirinae and three other subfamilies), revision of the genus rank structure and introduction of a new subgenus rank. In: *International Committee on Taxonomy of Viruses* (2018).
13. Hoon-Hanks LL, Layton ML, Ossiboff RJ, Parker JSL, Dubovi EJ, Stenglein MD. Respiratory disease in ball pythons (*Python regius*) experimentally infected with ball python nidovirus. *Virology.* (2018) 517:77–87. doi: 10.1016/j.virol.2017.12.008
14. Rampacci E, Masi M, Origgi FC, Stefanetti V, Bottinelli M, Selleri P, et al. First molecular detection of ball python nidovirus in Italy—short communication. *Acta Vet Hung.* (2019) 67:127–34. doi: 10.1556/004.2019.014
15. Katoh K, Standley DM. MAFFT multiple sequence alignment software version 7: improvements in performance and usability. *Mol Biol Evol.* (2013) 30:772–80. doi: 10.1093/molbev/mst010
16. Misawa K, Katoh K, Kuma K, Miyata T. MAFFT: a novel method for rapid multiple sequence alignment based on fast Fourier transform. *Nucleic Acids Res.* (2002) 30:3059–66. doi: 10.1093/nar/gkf436
17. Guindon S, Dufayard J-F, Lefort V, Anisimova M, Hordijk W, Gascuel O. New algorithms and methods to estimate maximum-likelihood phylogenies: assessing the performance of PhyML 3.0. *Syst Biol.* (2010) 59:307–21. doi: 10.1093/sysbio/syq010
18. Hasegawa M, Kishino H, Yano T. Dating of the human-ape splitting by a molecular clock of mitochondrial DNA. *J Mol Evol.* (1985) 22:160–74. doi: 10.1007/BF02101694
19. Pees M, Schmidt V, Marschang RE, Heckers KO, Krautwald-Junghanns M-E. Prevalence of viral infections in captive collections of boid snakes in Germany. *Vet Rec.* (2010) 166:422. doi: 10.1136/vr.b4819
20. Schmidt V, Marschang RE, Abbas MD, Ball I, Szabo I, Helmuth R, et al. Detection of pathogens in Boidae and Pythonidae with and without respiratory disease. *Vet Rec.* (2013) 172:236. doi: 10.1136/vr.100972
21. DeNardo D. Chapter 9—Stress in captive reptiles A2—Mader. In: Douglas R, editor. *Reptile Medicine and Surgery, 2nd ed*. Saint Louis, WB: Saunders (2006). p. 119–23. Available online at: http://www.sciencedirect.com/science/article/pii/B072169327X500134
22. Murray MJ. Chapter 65—Pneumonia and lower respiratory tract disease A2—Mader. In: Douglas R, editor. *Reptile Medicine and Surgery, 2nd ed*. Saint Louis, WB: Saunders (2006). p. 865–77. Available online at: http://www.sciencedirect.com/science/article/pii/B072169327X500699
23. Jacobson ER. *Infectious Diseases and Pathology of Reptiles. Chapter 2. Reptile Immunology*. Oxford: CRC Press (2007).
24. Chu DKW, Peiris JSM, Chen H, Guan Y, Poon LLM. Genomic characterizations of bat coronaviruses (1A, 1B and HKU8) and evidence for co-infections in Miniopterus bats. *J Gen Virol.* (2008) 89:1282–7. doi: 10.1099/vir.0.83605-0
25. Smits SL, Lavazza A, Matiz K, Horzinek MC, Koopmans MP, de Groot RJ. Phylogenetic and evolutionary relationships among torovirus field variants: evidence for multiple intertypic recombination events. *J Virol.* (2003) 77:9567. doi: 10.1128/JVI.77.17.9567-9577.2003
26. Penner JD, Jacobson ER, Brown DR, Adams HP, Besch-Williford CL. A novel Mycoplasma sp. associated with proliferative tracheitis and pneumonia in a Burmese python (*Python molurus bivittatus*). *J Comp Pathol.* (1997) 117:283–8. doi: 10.1016/S0021-9975(97)80024-2

27. Hyndman TH, Marschang RE, Wellehan JFXJ, Nicholls PK. Isolation and molecular identification of Sunshine virus, a novel paramyxovirus found in Australian snakes. *Infect Genet Evol J Mol Epidemiol Evol Genet Infect Dis.* (2012) 12:1436–46. doi: 10.1016/j.meegid.2012.04.022
28. Lamirande EW, Nichols DK, Owens JW, Gaskin JM, Jacobson ER. Isolation and experimental transmission of a reovirus pathogenic in ratsnakes (Elaphe species). *Virus Res.* (1999) 63:135–41. doi: 10.1016/S0168-1702(99)00067-2
29. Cowley JA, Hall MR, Cadogan LC, Spann KM, Walker PJ. Vertical transmission of gill-associated virus (GAV) in the black tiger prawn Penaeus monodon. *Dis Aquat Organ.* (2002) 50:95–104. doi: 10.3354/dao050095
30. Vaala WE, Hamir AN, Dubovi EJ, Timoney PJ, Ruiz B. Fatal, congenitally acquired infection with equine arteritis virus in a neonatal Thoroughbred. *Equine Vet J.* (1992) 24:155–8. doi: 10.1111/j.2042-3306.1992.tb02803.x

Conflict of Interest: PB is a co-founder and owner of Terrestrial & Arboreal. SF is the founder and owner of Fishhead Labs.

The remaining authors declare that the research was conducted in the absence of any commercial or financial relationships that could be construed as a potential conflict of interest.

The handling editor declared a past co-authorship with one of the authors RO.

Copyright © 2019 Hoon-Hanks, Ossiboff, Bartolini, Fogelson, Perry, Stöhr, Cross, Wellehan, Jacobson, Dubovi and Stenglein. This is an open-access article distributed under the terms of the Creative Commons Attribution License (CC BY). The use, distribution or reproduction in other forums is permitted, provided the original author(s) and the copyright owner(s) are credited and that the original publication in this journal is cited, in accordance with accepted academic practice. No use, distribution or reproduction is permitted which does not comply with these terms.

frontiers in Veterinary Science

CASE REPORT
published: 10 October 2019
doi: 10.3389/fvets.2019.00340

Fatal *Sarcocystis falcatula* Infection in Three Penguins

Shannon G. M. Kirejczyk[1†], Rachel E. Burns[2†], Michael W. Hyatt[3†], Michael J. Yabsley[4,5], Julia M. Ter Beest[6], Zoltan S. Gyimesi[6], Robert J. Ossiboff[7†], Amelia Waltman[7†], Tracie A. Seimon[7] and Rita McManamon[1,8]*

[1] Department of Pathology, College of Veterinary Medicine, University of Georgia, Athens, GA, United States, [2] Connecticut Veterinary Medical Diagnostic Laboratory, Department of Pathobiology and Veterinary Science, College of Agriculture, Health and Natural Resources, University of Connecticut, Storrs, CT, United States, [3] Adventure Aquarium, Camden, NJ, United States, [4] Southeastern Cooperative Wildlife Disease Study, College of Veterinary Medicine, University of Georgia, Athens, GA, United States, [5] Warnell School of Forestry and Natural Resources, University of Georgia, Athens, GA, United States, [6] Louisville Zoological Garden, Louisville, KY, United States, [7] The Wildlife Conservation Society, Bronx, NY, United States, [8] Zoo and Exotic Animal Pathology Service and Infectious Diseases Laboratory, Department of Small Animal Medicine and Surgery, College of Veterinary Medicine, University of Georgia, Athens, GA, United States

Sarcocystis falcatula is a well-known cause of fatal pneumonia in some birds, particularly Old World psittacines. Here we describe fatal sarcosystosis due to *S. falcatula* in 3 penguins (Family Spheniscidae) under managed care, including one African penguin (*Spheniscus demersus*), and two Southern rockhopper penguins (*Eudyptes chrysocome*). Randomly distributed foci of necrosis, inflammatory cell infiltrates, edema, and variable numbers of round to elongated protozoal schizonts were observed in sections of lung. Protozoal organisms exhibited strong immunoreactivity for *Sarcocystis* sp. antigen by immunohistochemistry. Apicomplexan and *Sarcocystis* genus-specific PCR assays and sequence analysis confirmed *S. falcatula* as the etiologic agent. These cases of fatal pneumonia attributed to *S. falcatula* expand the list of aberrant intermediate avian hosts, with particular implications for penguins.

Keywords: penguin, protozoal pneumonia, *Sarcocystis falcatula*, apicomplexa, *Spheniscus demersus*, *Eudyptes chrysocome*

OPEN ACCESS

Edited by:
Amy Louise Warren, University of Calgary, Canada

Reviewed by:
Frederique Nguyen, Agroalimentaire et de l'alimentation de Nantes-Atlantique, France
Francisco Ruben Carvallo Chaigneau, Virginia Tech, United States

***Correspondence:**
Shannon G. M. Kirejczyk
skirejc@emory.edu

†Present address:
Shannon G. M. Kirejczyk, Division of Pathology, Yerkes National Primate Research Center, Emory University, Atlanta, GA, United States
Rachel E. Burns, Disease Investigations, Institute for Conservation Research, San Diego Zoo Global, San Diego, CA, United States
Michael W. Hyatt, Wildlife Conservation Society, New York Aquarium, Brooklyn, NY, United States
Robert Ossiboff, Aquatic, Amphibian, and Reptile Pathology Program, College of Veterinary Medicine, University of Florida, Gainesville, FL, United States
Amelia Waltman, Pritzker School of Medicine, University of Chicago, Chicago, IL, United States

Specialty section:
This article was submitted to Veterinary Experimental and Diagnostic Pathology, a section of the journal Frontiers in Veterinary Science

Received: *16 July 2019*
Accepted: *20 September 2019*
Published: *10 October 2019*

BACKGROUND

Causes of protozoal pneumonia in birds include *Sarcocystis falcatula*, *Toxoplasma gondii*, *Plasmodium* spp., *Haemoproteus* spp., and *Isospora* (formerly *Atoxoplasma*) spp. Such infections are characterized by necrotizing interstitial pneumonia, with air capillaries containing tachyzoites (*T. gondii*) or meronts/schizonts (*S. falcatula* and *Plasmodium* spp.) within endothelial cells and/or macrophages. Malaria and toxoplasmosis are well-described causes of interstitial pneumonia in penguins (1, 2). Although molecular evidence of *Sarcocystis* spp. infection was recently reported in Magellenic penguins in Brazil (3), fatal disease due to pulmonary sarcocystosis has not previously been described in penguins. In this case series, we report the clinical, gross, microscopic, and ultrastructural features of fatal *S. falcatula* infections in 3 penguins under managed care.

CASE PRESENTATIONS

Case 1 was a 27-year-old, male African penguin (*Spheniscus demersus*) housed at an aquarium in the United States. The bird was at the end of a molting period and had been depressed and lethargic for a couple days before being found dead. Necropsy revealed congested lungs, and a complete set of formalin-fixed tissues was submitted to the Connecticut Veterinary Medical Diagnostic Laboratory for histopathology. Opossums had been seen on the property where this penguin was housed, but not inside the exhibit.

Case 2 was a 5-year-old, female, Southern rockhopper penguin (*Eudyptes chrysocome*) from a different zoological institution. Due to renovation of the birds' indoor exhibit, the penguin and its flock were temporarily housed outdoors for 6 weeks in a completely meshed enclosure with access to a temperature-regulated pool. Penguins were given oral itraconazole[1] (15 mg, once daily) for aspergillosis prophylaxis for the duration of the relocation. Two days prior to its death, the bird's appetite declined and it was observed floating in water, rather than exhibiting normal swimming and diving behavior. Physical examination revealed severe dyspnea and generalized weakness. The bird was anesthetized for further diagnostics but died shortly after induction. Post-mortem radiographs revealed increased soft tissue opacity in the lungs. Necropsy revealed dark red, wet lungs that sank in formalin (**Figure 1A**), a friable spleen, and edematous pericardial sac. There was a well-demarcated, 1-cm-diameter, white to yellow, raised, coelomic plaque on the inner surface of the ribs and a moderate amount of green fecal staining around the cloacal orifice. Following the death of this bird and the onset of warmer spring temperatures, the remaining flock was moved to an indoor, chilled holding area.

Five days later, a 32-year-old, female, Southern rockhopper penguin (case 3) from the same institution began to exhibit weakness, anorexia and dyspnea, and auscultation revealed harsh lung sounds. The bird was treated with ponazuril[2] (25 mg/kg PO, once), enrofloxacin[3] (15 mg/kg SC, once), meloxicam[4] (0.5 mg/kg IM, once), and furosemide[5] (0.2 mg/kg IM, once) for presumed pulmonary edema, but died 1 h later. Necropsy examination revealed dark red, wet lungs, and an enlarged, nodular spleen. The caudal aspect of the left lung contained a small, focal, tan to brown, firm area.

Cytologic examination of lung tissue imprints from case 3 showed crescent-shaped, 2 × 4–8 μm protozoal zoites (**Figure 1B**), toxic heterophils and multinucleated giant cells. A complete set of tissues from cases 2 and 3 were fixed in 10% neutral-buffered formalin and submitted to the University of Georgia Zoo and Exotic Animal Pathology Service for histopathology. Fresh spleen from case 2 was submitted to Athens Veterinary Diagnostic Laboratory for aerobic and anaerobic cultures. Fresh lung and liver from Cases 2 and 3 were submitted to the Southeastern Cooperative Wildlife Disease Study (SCWDS, Athens, GA) for molecular testing.

LABORATORY INVESTIGATIONS AND DIAGNOSTIC TESTS

Histopathology and Immunohistochemistry

Representative sections of all submitted tissues were routinely processed, embedded in paraffin wax, and 4–5-micron-thick sections were stained with Hematoxylin and Eosin (H&E) for light microscopy. For case 1, the only relevant immunohistochemical stain available at the Connecticut Veterinary Medical Diagnostic Laboratory was a rabbit polyclonal antibody against *T. gondii* (BioGenex, San Ramon, CA). Additional stains for *Sarcocystis* sp. (rabbit polyclonal antibody) and *T. gondii* (rabbit polyclonal antibody) were performed at the California Animal Health & Food Safety Laboratory System, Davis, CA as previously described (4). For cases 2 and 3, immunohistochemistry was performed at the University of Georgia College of Veterinary Medicine Histology Laboratory using antibodies for *S. neurona* (rabbit polyclonal antibody, 1:500 dilution for 60 min), *Neospora caninum* (goat polyclonal antibody[6], 1:300 dilution for 30 min) and *T. gondii* (mouse monoclonal antibody[6], 1:1,0000 dilution for 10 min).

The clinical, histologic, immunohistochemical, and molecular findings for three penguins with fatal *S. falcatula* infection are summarized in **Table 1**. All penguins had severe, necrotizing and lymphohistiocytic interstitial pneumonia. Parabronchi were flooded with hemorrhage, edema, and fibrin (**Figure 1C**). Air capillaries were obscured by foci of necrosis with fibrin exudation, and accumulations of heterophils, hemorrhage, and protozoal schizonts (**Figure 1D**). Air spaces were multifocally lined by hypertrophied epithelial cells (**Figure 1E**). In cases 2 and 3, schizonts were numerous and elongate, often conforming to the shape of capillaries (**Figure 1D**, inset), while schizonts were fewer and this classic serpentine morphology of *S. falcatula* was not observed in case 1. In all cases, schizonts occasionally exhibited a "sunburst" arrangement, in which merozoites radiated around a centralized clearing (**Figure 1E**, inset).

A full set of tissues, including lung, liver, brain, skeletal muscle, and heart was examined for case 1. No extrapulmonary schizonts or sarcocysts were seen, and additional immunohistochemical stains were not pursued. Cases 2 and 3 exhibited mild lymphohistiocytic myocarditis and myositis and schizonts were observed in multiple tissues in these birds (**Table 1**). Protozoa stained variably PAS-positive on Periodic acid-Schiff reaction stains, and did not stain with Giemsa. On immunohistochemistry, protozoa exhibited strong immunoreactivity (**Figure 1F**) for polyclonal *S. neurona*

[1]Janssen Ortho LLC, Stateroad 933 Km 0 1 Street Statero, Gurabo, Puerto Rico 00778 USA. 100 mg capsules were opened and weighed out into 15 mg capsule doses by JT or ZG or by a compounding pharmacy (Taylors Pharmacy, 306 South Park Avenue, Winter Park, FL 32789 USA).

[2]Compounded by Taylors Pharmacy, 306 South Park Avenue, Winter Park, FL 32789 USA. 50 mg/ml suspension.

[3]Manufactured by Norbrook Laboratories Limited, Newry, BT35 6PU, Co. Down, Northern Ireland. 22.7 mg/ml.

[4]Manufactured by Norbrook Laboratories Limited, Newry, BT35 6PU, Co. Down, Northern Ireland. 5 mg/ml.

[5]Manufactured by Boehringer Ingelheim Vetmedica, Inc. 2621 North Belt Hwy, St. Joseph, MO 64506, USA.

[6]Veterinary Medical Research & Development, 425 NW Albion Dr, Pullman, WA, 99163, U.S.A.

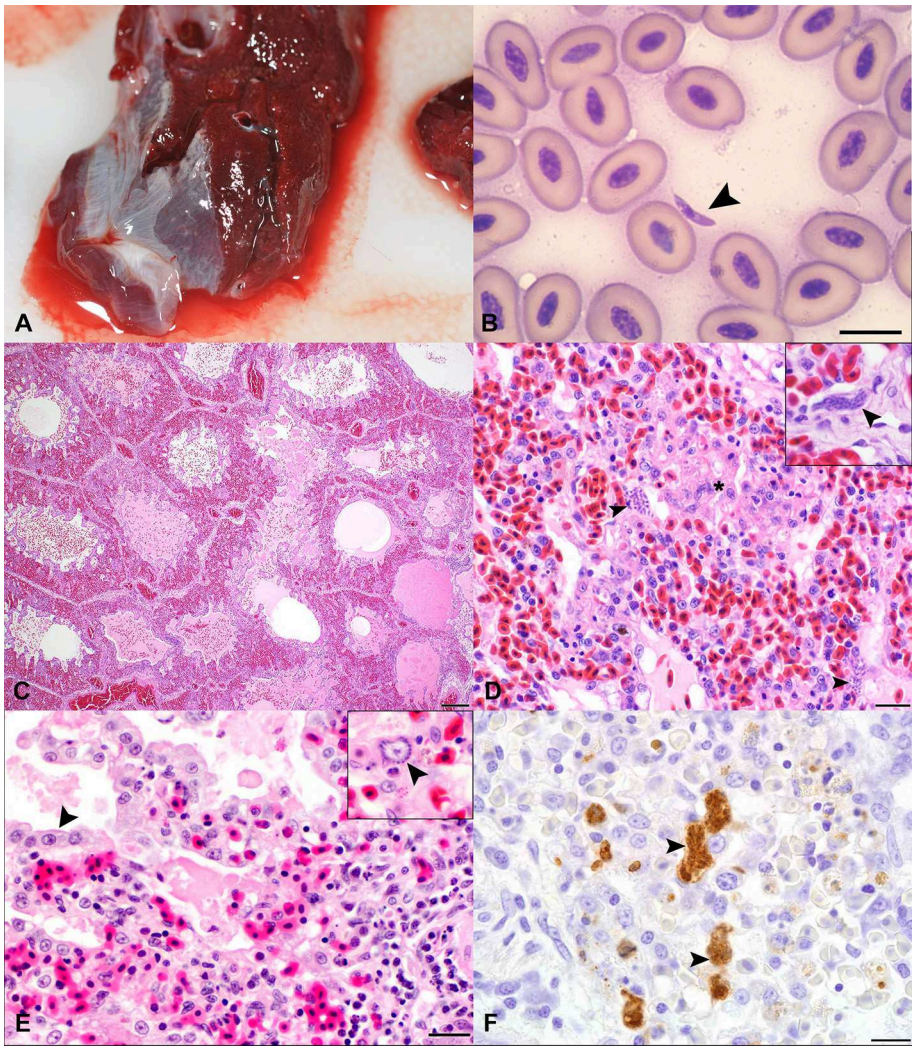

FIGURE 1 | Gross, cytological, histopathologic, and immunohistochemical features of *Sarcocystis falcatula* infection in the lung of Southern rockhopper (*Eudyptes chrysocome*) and African (*Spheniscus demersus*) penguins. **(A)** Gross appearance of lung tissue from case 2 at necropsy. The lungs are dark red and edematous, with red-tinged fluid oozing along the periphery of the tissue. The lungs sank in formalin. **(B)** Cytology of tissue imprint from the lung of case 3 obtained at necropsy. The vast majority of cells are erythrocytes. A single, 2 × 8 micron, elongate to crescent-shaped tachyzoite with a small, round, slightly off-center nucleus is present at the center of the image (arrowhead). Bar = 10 μm. **(C)** Lung, from a 5-year-old, female, Southern rockhopper penguin (case 2), with *S. falcatula* pneumonia. Parabronchi and atria are frequently flooded by edema, hemorrhage and fibrin. H&E. Bar = 200 μm. **(D)** Lung, case 2. Air capillaries are multifocally obscured by foci of necrosis (*) containing protozoal schizonts (arrowheads), fibrin, hemorrhage, and low numbers of heterophils. The interstitium is hypercellular due to low numbers of lymphocytes and macrophages. H&E. Bar = 20 μm. Inset: High magnification image highlights the elongate to serpentine appearance of an intracellular schizont (case 3). **(E)** Lung, case 1. Pneumocytes lining the parabronchus in the top left of the image are hypertrophied (arrowhead) and the air space is filled with edema, fibrin, macrophages, and scant hemorrhage. The interstitium is expanded by inflammatory cell infiltrates, and multifocally obscured by necrosis, hemorrhage, and an accumulation of fibrin and edema. H&E. Bar = 20 μm. Inset: High magnification image with a schizont (arrowhead), which exhibits a "sunburst" pattern, with merozoites radiating around a clear zone. **(F)** Immunohistochemistry for *S. neurona* polyclonal antibody on lung tissue (case 2) demonstrates strongly immunoreactive, elongate to serpentine schizonts (arrowheads), free merozoites, and macrophages containing phagocytosed debris. DAB chromogen with hematoxylin counterstain. Bar = 10 μm.

antibodies and variable immunoreactivity for *N. caninum* and *T. gondii* antibodies (**Table 1**).

Cases 2 and 3 had markedly hypercellular spleens with foci of extramedullary granulopoiesis. There were also coalescing foci of coagulative to lytic necrosis, and case 3 had scattered, intraendothelial schizonts (**Figure 2A**). Under anaerobic conditions, *Clostridium perfringens* was cultured from the spleen of case 2. Splenic tissue from case 3 was not available for culture. Low numbers of schizonts were present in foci of splenic necrosis for case 3, so sarcosporidiosis is the most likely explanation for this lesion. However, given that low numbers of gram-positive bacilli in one section of skeletal muscle, septicemia cannot entirely be ruled out in case 3.

All cases had multifocal lymphohistiocytic portal hepatitis and extramedullary granulopoiesis (**Figure 2B**); cases 2 and 3 had low numbers of schizonts within sinusoids (**Figure 2B**, right inset).

TABLE 1 | Signalment, clinical history, gross pathology, histopathology, immunohistochemistry, and molecular findings for 3 penguins with *S. falcatula* infection.

Case	Signalment	Clinical history and gross pathology	Histopathology	Immunohistochemistry			PCR results	
				Sarcocystis	*Neospora*	*Toxoplasma*	*Sarcocystis*	*Plasmodium*
1	27-year-old, male African penguin (*Spheniscus demersus)*	Several days of depression and lethargy; found dead Congested lungs	*Lymphohistiocytic and necrotizing pneumonia with protozoal schizonts Lymphohistiocytic hepatitis Pulmonary anthracosis	+++	ND	±	*S. falcatula*	ND
2	5-year-old, female, Southern rockhopper penguin (*Eudyptes chrysocome*)	Housed outdoors for 6 weeks in meshed enclosure; access to temperature-regulated pool; itraconazole[1] prophylaxis (9 mg/kg) Anorexia, abnormal swimming, and severe dyspnea; died while anesthetized for exam Dark red, wet lungs Friable spleen	*Necrotizing pneumonia with protozoal schizonts Splenic necrosis Sepsis (*Clostridium perfringens* cultured from spleen). Lymphohistiocytic myocarditis Lymphohistiocytic myositis Lymphohistiocytic hepatitis Lymphohistiocytic ventriculitis Extramedullary granulopoiesis in liver and spleen Schizonts in lung, heart, skeletal muscle, liver, proventriculus, ventriculus, duodenum, pancreas, adrenal, and kidney Small fungal granuloma (coelomic plaque)	+++	ND	ND	*S. falcatula*	–
3	32-year-old, female, Southern rockhopper penguin (*Eudyptes chrysocome*)	Housed outdoors for 6 weeks in meshed enclosure; access to temperature-regulated pool; itraconazole prophylaxis (6.5 mg/kg) Anorexia and severe dyspnea; given ponazuril (25 mg/kg PO), enrofloxacin (15 mg/kg SC), meloxicam (0.5 cm/kg IM), and furosemide (0.2 mg/kg IM); died 1 h post-exam Dark red, wet lungs Spleen enlarged, mottled, and nodular	*Necrotizing pneumonia with protozoal schizonts Splenic necrosis Lymphohistiocytic myocarditis Lymphohistiocytic myositis Lymphohistiocytic hepatitis Koilin degeneration Extramedullary granulopoiesis in liver and spleen Schizonts in lung, heart, skeletal muscle, spleen, liver, brain, and kidney Pulmonary granuloma and air sacculitis	+++	+	–	*S. falcatula*	–

**Presumptive cause of death; –, Immunonegative; +, Weakly immunopositive; +++, Strongly immunopositive; ND, not done.*

All cases also had moderate numbers of sinusoidal macrophages containing fragments of erythrocytes and intracytoplasmic hemosiderin (**Figure 2B**, left inset).

In addition to fulminant pulmonary sarcocystosis, case 2 had a small, coelomic fungal granuloma. Aspergillosis is suspected but fungal culture and/or PCR would be required for definitive diagnosis and further testing was not pursued. Case 3 had mild air sacculitis and a focal heterophilic granuloma at the caudal aspect of the left lung lobe. This lesion is believed to be related to a prior aspiration event, given the presence of foreign material and lack of microorganisms on special stains for fungi (Gomori Methenamine Silver), bacteria (modified Brown and Brenn Gram), and acid-fast bacilli (Ziehl-Neelsen).

Transmission Electron Microscopy

Formalin-fixed lung tissue from case 3 was trimmed into two, 2-mm-thick pieces and transferred to 2% paraformaldehyde, 2% glutaraldehyde in 0.1 M phosphate buffer, pH 7.25. After overnight fixation, tissue was rinsed in 0.1 M phosphate buffer, post-fixed for 1 h with 1% buffered osmium tetroxide (OsO_4), then rinsed in deionized water and dehydrated in an ascending ethanol series before infiltration with propylene oxide and Mollenhauer's Epon-Araldite resin mixture (5). Tissue samples were embedded in fresh resin mixture and allowed to polymerize in a 70°C oven. One-micron-thick sections were stained with Toluidine Blue O to select areas of interest before 60 nm sections were obtained and placed on grids. Grid sections were stained with uranyl acetate and lead citrate before examination with a JEOL JEM 1011 transmission electron microscope at 80 kV. Images were captured with an XR80M wide-angle multi-discipline mid-mount CCD camera[7].

Transmission electron microscopy revealed protozoa with ultrastructural features compatible with *Sarcocystis* spp. (**Figure 3**) (6–8). Capillary endothelial cells occasionally

[7]Advanced Microscopy Techniques, 242 West Cummings Park, Woburn, MA, 01801, U.S.A.

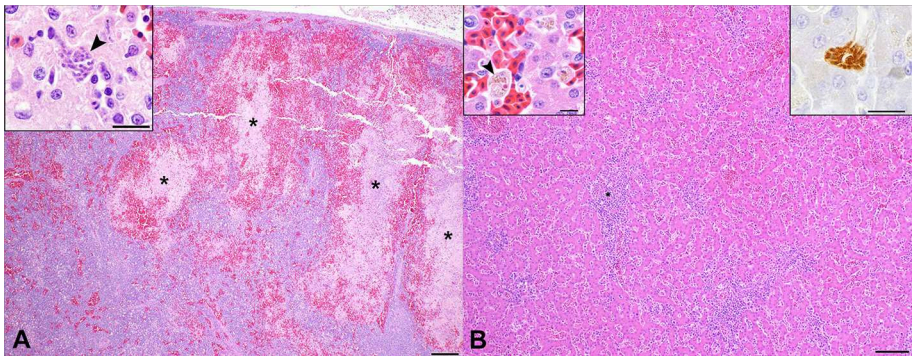

FIGURE 2 | Hepatic and splenic pathology in Southern rockhopper penguins with fatal *Sarcocystis falcatula* infection. **(A)** Spleen, case 2. The splenic parenchyma is markedly hypercellular, with numerous hematopoietic cell precursors, lymphocytes, histiocytes, and plasma cells. There are multifocal to coalescing zones of coagulative to lytic necrosis (*) surrounded by a rim of hemorrhage. H&E. Bar = 200 μm. Inset: High magnification image of a *S. falcatula* schizont (arrowhead) within an area of necrosis in the spleen of case 3. Bar = 10 μm. **(B)** Liver, case 2. Portal regions are hypercellular, with moderate numbers of lymphocytes, plasma cells, macrophages and granulocytic precursor cells, which compress hepatocytes multifocally. Bar = 100 μm. Left insert: Sinusoids are congested, with macrophages containing phagocytosed cell debris, erythrocyte fragments and hemosiderin (arrowhead). H&E. Bar = 10 μm. Right inset: Immunohistochemistry for *S. neurona* highlights a schizont with radially arranged merozoites. Bar = 10 μm.

contained an intracytoplasmic, serpentine schizont, which conformed to the cell shape. One schizont had a multilobulated nucleus with nuclear spindles arranged along the periphery (**Figures 3A,B**). Merozoites had a round, central nucleus, an anterior conoid and several tear-shaped, electron-dense micronemes at the posterior end (**Figures 3C,D**) (6).

Polymerase Chain Reaction (PCR) Analysis and Sequencing

For case 1, formalin-fixed, paraffin-embedded (FFPE) lung tissue was submitted to the Wildlife Conservation Society (Bronx, NY) and DNA was extracted using a QIAamp DNA FFPE Tissue Kit[8]. Extracts were tested by conventional PCR using both pan-apicomplexan and *Sarcocystis*-specific assays targeting the 18S rRNA and internal transcribed spacer 1 (ITS-1) regions, respectively. A small portion of the 18S rRNA gene was amplified as previously described (9). A portion of the ITS-1 region was amplified using primer P-ITSF and a degenerate primer (ShortITSR; 5′-GGGATTCARTKGYYGAAA-3′) designed based on publicly available Sarcocystis ITS-1 sequences (10). Amplicons were bi-directionally sequenced commercially, analyzed using Geneious R7 (Auckland, New Zealand) to generate a consensus sequence, trimmed of their primers, and analyzed by BLASTn.

The DNA sequence from the 18S gene was 100% identical to *Sarcocystis falcatula* in Genbank (MH626537, isolate Lorikeet ID #205850) but also identical to numerous other *Sarcocystis* isolates in GenBank. The DNA sequence from the ITS-1 region was 100% identical to *Sarcocystis falcatula* in GenBank (MH626538, isolate Lorikeet ID #205850) and *Sarcocystis cf. falcatula* in GenBank (AF389339) (11, 12). The next closest match for the ITS-1 region was *Sarcocystis speeri* and *Sarcocystis neurona* (98–99% identity).

For cases 2 and 3, DNA was extracted from fresh lung and liver using a commercial DNA extraction kit[8] at SCWDS. The genus of the organism was determined by screening tissues with primers that amplify a short portion of the 18S rRNA gene of numerous apicomplexan parasites as previously described (13). Amplification products were visualized in 2% agarose gels stained with GelRed[9]. Amplicons were gel-purified using a kit[8] and bi-directionally sequenced at the University of Georgia Genomics Facility (Athens, Georgia). Chromatograms were analyzed using Geneious R7 and the consensus sequence was compared to other sequences in GenBank.

To further characterize the *Sarcocystis* sp. in cases 2 and 3, partial cytochrome b gene was amplified with primers CYTB-F and CYTB-R, the ITS-1 region was amplified with primers ITS-234F19 and ITS-720R19, and the partial surface antigen 2 gene was amplified with primers SAG2-F1 and SAG2-R1 as previously described (14, 15). Amplicons were purified, sequenced, and analyzed as described above. To rule out the possibility of *Plasmodium* and/or *Haemoproteus* spp. infection in cases 2 and 3, a nested PCR targeting the mitochondrial cytochrome b (*cytb*) gene was conducted as previously described using primary primers HaemNFI and HaemNR3 and nested primers HaemF and HaemR2 (16).

For cases 2 and 3, liver and lung samples from both penguins were positive using the Tg18s58F and Tg18s348R PCR protocol and the resulting sequences (302 bp) were identical to each other and 100% similar to numerous *Sarcocystis* spp. The cytb gene sequences (580 bp) obtained from liver and spleen of cases 2 and 3 were identical and 100% similar to *S. falcatula* from captive bare-faced ibis (*Phimosus infuscatus*) from Brazil (KX265018) and Virginia opossum from California, USA (KP871704). The ITS-1 (287 bp) sequences were identical to each other and contained two polymorphic bases. These sequences were 98–99%

[8]QIAGEN, Inc, 27220 Turnberry Lane 200, Valencia, CA 91355, U.S.A.

[9]Biotium, Inc. 46117 Landing Pkwy, Fremont, CA 94538, U.S.A.

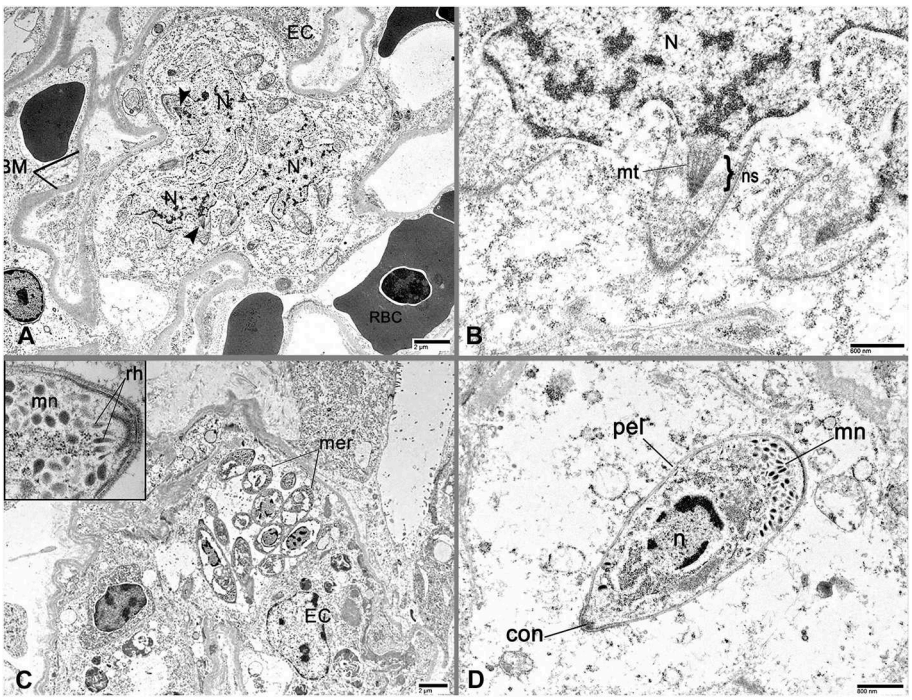

FIGURE 3 | Ultrastructure of *Sarcocystis falcatula* asexual life stages by Transmission Electron Microscopy (TEM) in the lung of a 32-year-old, female, Southern rockhopper penguin (case 3). **(A)** TEM demonstrates an intraendothelial *S. falcatula* schizont. The schizont expands the endothelial cell (EC), is irregularly shaped and is separated from the EC cytoplasm by a thin membrane. Several nuclear spindles (arrowheads) project from the schizont nucleus (N). The endothelial cell abuts a capillary containing erythrocytes (RBC) and is supported by a basement membrane (BM). Bar = 2 μm. **(B)** Higher magnification TEM image of the *S. falcatula* schizont nucleus (N) from **(A)**. Several conically arranged microtubules (mt) comprise the nuclear spindle (ns) of a developing merozoite. Bar = 600 nm. **(C)** TEM shows numerous, up to 2 × 6 μm merozoites clustered within an endothelial cell (EC). Inset: Higher magnification of a merozoite showing rhoptries (rh) and micronemes (mn). Bar = 2 μm. **(D)** A mature merozoite is present in a focus of necrotic lung tissue on TEM. The merozoite has a central, round nucleus (n), an anterior conoid (con), numerous micronemes (mn) at the posterior pole, and a double-membrane pellicle (pel). Bar = 800 nm.

similar to numerous *S. falcatula* strains from Brazil and the U.S.A. with some only differing at those two polymorphic bases. The four SAG2 sequences (402 bp) were identical and were 100% similar to the only *S. falcatula* (GQ851953) sequence available in GenBank. All four tissues were positive for the rpoB gene. The sequences were identical to each other and 100% similar to one *S. falcatula* (440 bp, KX265017) strain and >99% similar to several other *S. falcatula* sequences in GenBank (495 bp, e.g., AY164999).

DISCUSSION

Death of these penguins was attributed to severe pneumonia caused by *S. falcatula*. The diagnosis was supported by IHC and confirmed by PCR. The differential diagnosis for apicomplexan pneumonia in penguins includes malaria, toxoplasmosis, and sarcocystosis. Fatal pulmonary infection with *S. falcatula* has been reported most often in psittacines (17–20), and the current report is believed to be the first in Spheniscidae. The histopathologic features of pneumonia in these penguins were similar to that described in other avian species infected with *S. falcatula*, namely necrosis, edema, fibrin deposition, congestion, hemorrhage, heterophilic, and mononuclear inflammatory infiltrates, endothelial cell lysis, and pneumocyte hyperplasia (7, 20–22).

The life cycle of *Sarcocystis* spp. involves definitive and intermediate hosts. In North America, the definitive host for *S. falcatula* and the closely related *S. neurona* is the Virginia opossum (*Didelphis virginiana*), which sheds infective sporocysts in feces (8). Infection of intermediate hosts typically occurs through ingestion of food contaminated with opossum feces, but insects can serve as mechanical vectors (17). In case 1, opossums were seen on the premises but not in the bird's enclosure, so ingestion of feces or sporozoite-containing fomite(s) is considered most likely. Contaminated water run-off or insect entry into the enclosure are additional possibilities.

In contrast to case 1 (African penguin), cases 2 and 3 (Southern rockhopper penguins) had disseminated infections with large numbers of schizonts. Potential factors that may have influenced the progression of disease in these animals include the dose of sporozoites ingested, time elapsed since infection, differences in host species susceptibility or pathogen virulence, and concomitant sepsis in case 2.

Acosta et al. (3) recently provided molecular evidence of *Sarcocystis* spp. infection in a cohort of Magellanic

penguins (*Spheniscus magellanicus*) in Brazil. A *Sarcocystis* sp. closely related to *S. falcatula* was isolated from the pectoral muscle of 16 penguins, which were undergoing rehabilitation and died due to other causes. Given the tissue of origin (pectoral muscle), the authors postulated that the genetic material originated from tissue cysts, suggesting that the penguins survived an acute infection and formed sarcocysts. Sarcocysts were not identified in the penguins of the current report.

Cross-reactivity between cyst-forming apicomplexans has been reported for polyclonal antibodies targeting *T. gondii*, *N. caninum*, and *Sarcocystis* sp. (23–25). Although a previous study has shown a lack of cross-reactivity between a polyclonal *S. neurona* antibody and *S. falcatula* schizonts in budgerigars (*Melopsittacus undulatus*) (26), the *S. neurona* antibody used in all cases strongly reacted with *S. falcatula* in the tissue sections, which highlights the variability that can occur between IHC results based on different polyclonal antibodies.

This report expands the list of intermediate hosts for *S. falcatula* and underscores the importance of excluding opossums, their feces, and potential vectors from penguin enclosures. Additional studies are needed to determine individual and species-specific susceptibilities among penguins and whether or not infection and survival confers protective humoral immunity in individual birds. Prophylactic treatment for surviving penguins may be considered if sarcocystosis is diagnosed in a collection.

DATA AVAILABILITY STATEMENT

All datasets generated for this study are included in the manuscript/supplementary files.

ETHICS STATEMENT

All animals included in this study were treated with the standard of care at each institution, as set forth by the Association of Zoos and Aquariums. An ethical review process was not required for this study, as the methods described herein were part of the routine diagnostic process to determine the cause of death of these penguins. All biological samples were obtained from penguins at postmortem exam, following the natural death of these animals.

AUTHOR CONTRIBUTIONS

SK and RB drafted the manuscript. MH provided clinical care for case 1 and performed the post mortem exam. JT and ZG provided clinical care for cases 2 and 3 and performed the post mortem exams. RB performed the histopathology on case 1. SK and RM performed the histopathology on cases 2 and 3 and TEM on case 3. RO, TS, and AW designed and performed the PCR and sequencing and analyzed the sequencing data for case 1. MY designed and performed the PCR and sequencing and analyzed the sequencing data for cases 2 and 3. All authors assisted with writing and critically reviewing the manuscript.

ACKNOWLEDGMENTS

The authors wish to thank Denise Long and Ione Jackman from the CVMDL and Santiago Diab and Karen Sverlow from CAHFS-Davis for histology and immunohistochemistry of case 1. We also thank the staff of the UGA CVM Histology Laboratory for immunohistochemistry (cases 2 and 3), and Mary Ard at the Georgia Electron Microscopy Laboratory for assistance with Transmission Electron Microscopy.

REFERENCES

1. Ploeg M, Ultee T, Kik M. Disseminated toxoplasmosis in black-footed penguins (*Spheniscus demersus*). *Avian Dis.* (2011) 55:701–3. doi: 10.1637/9700-030411-Case.1
2. Vanstreels RE, da Silva-Filho RP, Kolesnikovas CK, Bhering RC, Ruoppolo V, Epiphanio S, et al. Epidemiology and pathology of avian malaria in penguins undergoing rehabilitation in Brazil. *Vet Res.* (2015) 46:30. doi: 10.1186/s13567-015-0160-9
3. Acosta ICL, Soares RM, Mayorga L, Alves BF, Soares HS, Gennari SM. Occurrence of tissue cyst forming coccidia in Magellanic penguins (*Spheniscus magellanicus*) rescued on the coast of Brazil. *PLoS ONE.* (2018) 13:e0209007. doi: 10.1371/journal.pone.0209007
4. Miller MA, Sverlow K, Crosbie PR, Barr BC, Lowenstine LJ, Gulland FM, et al. Isolation and characterization of two parasitic protozoa from a pacific harbor seal (*Phoca vitulina richardsi*) with meningoencephalomyelitis. *J Parasitol.* (2001) 87:816–22. doi: 10.1645/0022-3395(2001)087[0816:IACOTP]2.0.CO;2
5. Mollenhauer HH. Plastic embedding mixtures for use in electron microscopy. *Stain Technol.* (1964) 39:111–4.
6. Dubey JP. General biology. In: Dubey JPCS, and Fayer R, editors. *Sarcocystosis of Animals and Man*. 1st ed. Boca Raton, FL: CRC Press (1989). p. 1–81.
7. Smith JH, Meier JL, Neill PJG, Box ED. Pathogenesis of *Sarcocystis falcatula* in the budgerigar. II. Pulmonary pathology. *Lab Invest.* (1987) 56:72–84.
8. Smith JH, Meier JL, Neill PJG, Box ED. Pathogenesis of *Sarcocystis falcatula* in the budgerigar. I. Early pulmonary schizogony. *Lab Invest.* (1987) 56:60–71.
9. Sledge DG, Bolin SR, Lim A, Kaloustian LL, Heller RL, Carmona FM, et al. Outbreaks of severe enteric disease associated with *Eimeria furonis* infection in ferrets (*Mustela putorius furo*) of 3 densely populated groups. *J Am Vet Med Assoc.* (2011) 239:1584–8. doi: 10.2460/javma.239.12.1584
10. Kutkiene L, Prakas P, Sruoga A, Butkauskas D. The mallard duck (*Anas platyrhynchos*) as intermediate host for *Sarcocystis wobeseri* sp. nov. from the barnacle goose (*Branta leucopsis*). *Parasitol Res.* (2010) 107:879–88. doi: 10.1007/s00436-010-1945-4
11. Verma SK, Trupkiewicz JG, Georoff T, Dubey JP. Molecularly confirmed acute, fatal *Sarcocystis falcatula* infection in the rainbow lorikeets (*Trichoglossus moluccanus*) at the Philadelphia Zoo. *J Parasitol.* (2018) 104:710–2. doi: 10.1645/18-78
12. Dubey JP, Lindsay DS, Rosenthal BM, Kerber CE, Kasai N, Pena HFJ, et al. Isolates of *Sarcocystis falcatula*–like organisms from South American opossums *Didelphis Marsupialis* and *Didelphis Albiventris* from SÃo Paulo, Brazil. *J Parasitol.* (2001) 87:1449–53. doi: 10.1645/0022-3395(2001)087[1449:IOSFLO]2.0.CO;2
13. Su C, Shwab EK, Zhou P, Zhu XQ, Dubey JP. Moving towards an integrated approach to molecular detection and identification of *Toxoplasma gondii*. *Parasitology.* (2010) 137:1–11. doi: 10.1017/S0031182009991065
14. Cesar MdO. *Sarcocystis sp Eliminados por Didelphis aurita e Didelphis albiventris (Gambás) de vida livre no Estado de São Paulo: Infecção Experimental em Periquitos Australianos (Melopsittacus undulatus) e Camundongos Balb/c nude*. São Paulo: Faculdade de Medicina Veterinária e Zootecnia da Universidade de São Paulo (2011).

15. Valadas SYOB. *Caracterização Molecular de Isolados de SARCOCYSTIS spp. Obtidos de Marsupiais do Gênero Didelphis spp. Pela Análise de Gene Mitocondrial, Gene de Apicoplasto, Espaçador Interno Transcrito (ITS-1) e Genes Codificadores de Antígenos de Superfície (SAGs) [Doctoral]*. São Paulo: Universidade de São Paulo. Faculdade de Medicina Veterinária e Zootecnia (2015).
16. Hellgren O, Waldenström J, Bensch S. A new PCR assay for simultaneous studies of leucocytozoon, plasmodium, and haemoproteus from avian blood. *J Parasitol*. (2004) 90:797–802. doi: 10.1645/GE-184R1
17. Clubb SL, Frenkel JK. *Sarcocystis falcatula* of opossums: transmission by cockroaches with fatal pulmonary disease in psittacine birds. *J Parasitol*. (1992) 78:116–24. doi: 10.2307/3283697
18. Godoy SN, De Paula CD, Cubas ZS, Matushima ER, Catao-Dias JL. Occurrence of *Sarcocystis falcatula* in captive psittacine birds in Brazil. *J Avian Med Surg*. (2009) 23:18–23. doi: 10.1647/2008-006R.1
19. Hillyer EV AM, Greiner EC, Atkinson CT, Frenkel JK. An Outbreak of *Sarcocystis* in a collection of psittacines. *J Zoo Wildl Med*. (1991) 22:434–45.
20. Villar D KM, Howard L, Hammond E, Cray C, Latimer K. Clinical presentation and pathology of sarcocystosis in psittaciform birds: 11 cases. *Avian Dis*. (2008) 52:187–94. doi: 10.1637/8104-090207-Case
21. Smith JH NP, Dillard EA, Box ED. Pathology of experimental *Sarcocystis falcatula* infections of canaries (*Serinus canarius*) and pigeons (*Columba livia*). *J Parasitol*. (1990) 76:59–68. doi: 10.2307/3282628
22. Smith JH, Craig TM, Dillard EA, Neill PJG, Jones LP. Naturally occurring apicomplexan acute interstitial pneumonitis in thick-billed parrots (*Rhynchopsitta pachyrhyncha*). *J Parasitol*. (1990) 76:285–8. doi: 10.2307/3283038
23. Barr BC, Conrad PA, Dubey JP, Anderson ML. Neospora-like encephalomyelitis in a calf: pathology, ultrastructure, and immunoreactivity. *J Vet Diagn Invest*. (1991) 3:39–46. doi: 10.1177/104063879100300109
24. Sundermann CA, Estridge BA, Branton MS, Bridgman CR, Lindsay DS. Immunohistochemical diagnosis of *Toxoplasma gondii*: potential for cross-reactivity with *Neospora caninum*. *J Parasitol*. (1997) 83:440–3. doi: 10.2307/3284407
25. Uzeda RS, Schares G, Ortega-Mora LM, Madruga CR, Aguado-Martinez A, Corbellini LG, et al. Combination of monoclonal antibodies improves immunohistochemical diagnosis of *Neospora caninum*. *Vet Parasitol*. (2013) 197(3–4):477–86. doi: 10.1016/j.vetpar.2013.07.008
26. Marsh AE, Barr BC, Tell L, Koski M, Greiner E, Dame J, et al. *In vitro* cultivation and experimental inoculation of *Sarcocystis falcatula* and *Sarcocystis neurona* merozoites into budgerigars (*Melopsittacus undulatus*). *J Parasitol*. (1997) 83:1189–92. doi: 10.2307/3284386

Conflict of Interest: The authors declare that the research was conducted in the absence of any commercial or financial relationships that could be construed as a potential conflict of interest.

Citation: Kirejczyk SGM, Burns RE, Hyatt MW, Yabsley MJ, Ter Beest JM, Gyimesi ZS, Ossiboff RJ, Waltman A, Seimon TA and McManamon R (2019) Fatal Sarcocystis falcatula Infection in Three Penguins. Front. Vet. Sci. 6:340. doi: 10.3389/fvets.2019.00340

Copyright © 2019 Kirejczyk, Burns, Hyatt, Yabsley, Ter Beest, Gyimesi, Ossiboff, Waltman, Seimon and McManamon. This is an open-access article distributed under the terms of the Creative Commons Attribution License (CC BY). The use, distribution or reproduction in other forums is permitted, provided the original author(s) and the copyright owner(s) are credited and that the original publication in this journal is cited, in accordance with accepted academic practice. No use, distribution or reproduction is permitted which does not comply with these terms.

frontiers in Veterinary Science

ORIGINAL RESEARCH
published: 15 October 2019
doi: 10.3389/fvets.2019.00344

Crude Oil and Dispersant Cause Acute Clinicopathological Abnormalities in Hatchling Loggerhead Sea Turtles (*Caretta caretta*)

Craig A. Harms[1]*, *Patricia McClellan-Green*[2†], *Matthew H. Godfrey*[1,3,4], *Emily F. Christiansen*[1‡], *Heather J. Broadhurst*[1‡] and *Céline A. J. Godard-Codding*[5]

[1] Department of Clinical Sciences and Center for Marine Sciences and Technology, College of Veterinary Medicine, North Carolina State University, Morehead City, NC, United States, [2] Department of Biological Sciences and Center for Marine Sciences and Technology, North Carolina State University, Morehead City, NC, United States, [3] North Carolina Wildlife Resources Commission, Beaufort, NC, United States, [4] Nicholas School of the Environment, Duke University Marine Lab, Beaufort, NC, United States, [5] The Institute of Environmental and Human Health, Texas Tech University and TTU Health Sciences Center, Lubbock, TX, United States

OPEN ACCESS

Edited by:
Nicole Indra Stacy,
University of Florida, United States

Reviewed by:
Emma Hooijberg,
University of Pretoria, South Africa
Meera Heller,
University of California, Davis, United States

***Correspondence:**
Craig A. Harms
craig_harms@ncsu.edu

[†]Deceased

[‡]**Present address:**
Emily F. Christiansen and Heather J. Broadhurst, North Carolina Aquariums, Center for Marine Sciences and Technology, Morehead City, NC, United States

Specialty section:
This article was submitted to Veterinary Experimental and Diagnostic Pathology, a section of the journal Frontiers in Veterinary Science

Received: 24 May 2019
Accepted: 23 September 2019
Published: 15 October 2019

Citation:
Harms CA, McClellan-Green P, Godfrey MH, Christiansen EF, Broadhurst HJ and Godard-Codding CAJ (2019) Crude Oil and Dispersant Cause Acute Clinicopathological Abnormalities in Hatchling Loggerhead Sea Turtles (Caretta caretta). Front. Vet. Sci. 6:344. doi: 10.3389/fvets.2019.00344

Following the explosion of the *Deepwater Horizon* MC252 oil rig in 2010, 319 live sea turtles exposed to crude oil and oil-dispersant (Corexit) combinations were admitted to rehabilitation centers for decontamination and treatment. Treatment of oiled sea turtles was guided by expected physiological and pathological effects of crude oil exposure extrapolated from studies in other species and from a single loggerhead sea turtle (*Caretta caretta*) study. While invaluable starting points, inherent limitations to extrapolation, and small sample size of the experimental exposure study, reduce their utility for clinical guidance and for assessing oil spill impacts. Effects of dispersants were not included in the previous experimental exposure study, and cannot be effectively isolated in the analysis of field data from actual spills. A terminal study of pivotal temperature of sex determination using eggs salvaged from doomed loggerhead nests provided an opportunity for an ancillary exposure study to investigate the acute effects of crude oil, dispersant, and a crude oil/dispersant combination in sea turtle hatchlings. Eggs were incubated at 27.2–30.8°C, and hatchlings were randomly assigned to control, oil, dispersant, and combined oil/dispersant exposures for 1 or 4 days. Contaminant exposures were started after a 3 day post-hatching period simulating nest emergence. Turtles were placed in individual glass bowls containing aged seawater and exposed to oil (Gulf Coast—Mixed Crude Oil Sweet, CAS #8002-05-9, 0.833 mL/L) and/or dispersant (Corexit 9500A, 0.083 mL/L), replicating concentrations encountered during oil spills and subsequent response. Statistically significant differences between treatments and non-exposed controls were detected for PCV, AST, uric acid, glucose, calcium, phosphorus, total protein, albumin, globulin, potassium, and sodium. The principal dyscrasias reflected acute osmolar, electrolyte and hydration challenges that were more numerous and greater in combined oil/dispersant exposures at 4 days. Clinicopathological findings were supported by a failure to gain weight (associated with normal hatchling hydration

in seawater) in dispersant and combination exposed hatchlings. These findings can help guide clinical response for sea turtles exposed to crude oil and crude oil/dispersant combinations, and indicate potential impacts on wildlife to consider when deploying dispersants in an oil spill response.

Keywords: *Caretta caretta*, corexit, crude oil, dispersant, hematology, loggerhead sea turtle, plasma biochemistry

INTRODUCTION

For 87 days following the explosion of the *Deepwater Horizon* (DWH) MC252 oil rig in 2010, an estimated 134 million gallons (500,000 m^3) of crude oil were released into the Gulf of Mexico, with 1.8 million gallons (7,000 m^3) of surface and subsurface chemical dispersants (Corexit 9500A and Corexit 9527A) applied in an attempt to mitigate impact (1). A calculated estimate of 402,000 surface-pelagic juvenile sea turtles (Kemp's ridleys *Lepidochelys kempii*, green turtles *Chelonia mydas*, loggerheads *Caretta caretta*, and hawksbills *Eretmochelys imbricata*) were exposed to oil, with about 54,800 likely to have been heavily oiled (2). Turtles admitted to rehabilitation centers for decontamination and treatment numbered only 319 (3). Physiological and pathological effects expected from crude oil exposure used to guide treatment of oiled sea turtles came from extrapolation of studies in other species (4) and from one experimental *in vivo* loggerhead sea turtle oil exposure study (5). Effects reasonably expected from crude oil exposure include gastrointestinal pathology, adrenal, and salt gland dysfunction, kidney, and liver pathology, anemia, increased white blood cell (WBC) counts, pneumonia and skin sloughing (4, 5). While invaluable starting points, inherent limitations to extrapolation and small sample size of the loggerhead study limit utility for clinical guidance and for assessing oil spill impacts. For instance, some expected abnormalities such as hemolytic anemia and extensive skin sloughing previously reported in sea turtles exposed to crude oil were not observed in the case of the DWH spill (3, 6). Subsequent to the DWH oil spill, clinicopathological effects on spill-exposed sea turtles have been published from the Canary Islands (7) and from the DWH spill itself (3, 6) that provide further insights on spill impacts to sea turtles. Dispersants, however, were not included in the previous sea turtle oil exposure study, were not a component of spill exposures in the Canary Islands, and cannot be effectively isolated in the analysis of field data from the DWH incident. The combined effects of crude oil and dispersant on sea turtles have not previously been documented.

A terminal study of pivotal temperature of sex determination using loggerhead eggs salvaged from doomed nests provided a rare opportunity for an ancillary exposure study to investigate the acute effects of crude oil, dispersant, and a crude oil/dispersant combination in sea turtle hatchlings. The impact of oil and other environmental pollution in reptiles, and particularly in sea turtles, is little understood due to a scarcity of toxicity data in this taxon (8). Here, we present findings that will prove useful for guiding diagnostics and therapeutics of sea turtles in future oil spills, and inform decisions on whether or not to deploy chemical dispersants.

MATERIALS AND METHODS

This study was conducted under endangered species permit 13ST50 from the North Carolina Wildlife Resources Commission, with federal authority delegated from the U.S. Fish and Wildlife Service, and with approval of the North Carolina State University Institutional Animal Care and Use Committee (11-078-O, 11-103-O).

Eggs from loggerhead nests destined to fail from timing or position of nesting and invasive species predation (feral hogs) on a barrier island were salvaged and transported for a terminal pivotal temperature study in 2013. Eggs were incubated under controlled conditions of 27.2–30.8°C following previously described methods for the pivotal temperature study. These temperatures bracket previously reported pivotal temperatures for loggerheads (9). Hatchlings came from 3 clutches, ranging from 106 to 136 eggs, with 56–68% hatch success. Prior to hatching, a subset of eggs was assigned to one of eight treatment groups using a pseudo-random number generator (Windows Excel, Microsoft Corporation, Redmond, WA, USA). After emerging from its eggshell, each hatchling entered its predetermined treatment group 3 days post-hatching, simulating the time expected for emergence from the nest (10). The eight treatment groups ($n = 15$ or 16 per group) were exposed to crude oil (Gulf Coast—Mixed Crude Oil Sweet, CAS #8002-05-9, hereafter referred to simply as crude oil or oil), dispersant product Corexit 9500A (Nalco, Sugar Land, TX; hereafter referred to simply as Corexit), crude oil and Corexit combined, and a negative control (sea water only), for 1 or for 4 days. Sample size was limited to available hatchlings in the primary pivotal temperature study for this pilot study. Each treatment and duration represents a different group of turtles. Sampling occurred at only one time point per group, as indicated (1 or 4 days). Exposures were carried out in flat-bottomed glass bowls (19 cm diameter × 7 cm tall) containing 600 mL aged and filtered seawater at a salinity of 36 ppt and 26°C, one turtle per container, in a room set to a 16:8 h light:dark cycle. Crude oil exposure treatment was 0.833 mL/L and Corexit was 0.083 mL/L, replicating concentrations reasonably encountered during oil spills and subsequent response with a recommended ratio of 1:10 Corexit: oil by the Chemical Response to Oil Spills: Ecological Effects Research Forum (11, 12). Calculated thickness of the crude oil layer resulting from 0.5 ml spread over a surface area of 283 cm^2, assuming uniform distribution, is 0.018 mm. Turtles were not fed, consistent with their residual yolk dependency

for the first few days of life (13), and were monitored 6–10 times daily. Hatching and exposure treatments spanned 28 days. Turtles were weighed, and straight carapace length (SCL) and straight carapace width (SCW) were measured at the beginning and at the end of exposures. At the conclusion of exposures, hatchlings were euthanized by decapitation and pithing (14), gross necropsies were performed, and samples were split among multiple planned studies.

Blood (∼0.25 ml) was collected directly from cervical vessels into lithium-heparinized tubes (Terumo™ Capiject™, Fisher Scientific, catalog number 22-256536) at the time of euthanasia and processed within 30 min. Blood smears were stained with a rapid blood stain (HemacolorR, EMD Millipore Corp., Bilerica, MA). Packed cell volume (PCV) was determined using a microhematocrit mini-centrifuge (International Medical Assistance, Inc., Indianapolis, IN). A plasma biochemical panel was performed on a clinical analyzer (VetScan, Abaxis, Union City, CA, with an Avian/Reptile Profile Plus reagent rotor) (15). The biochemical panel included aspartate aminotransferease (AST), creatine kinase (CK), uric acid, glucose, calcium, phosphorus, total protein (TP), albumin, globulin (by calculation), potassium, and sodium. Blood smears were evaluated by a single observer (CAH) blinded to treatment. Estimated WBC count was determined by the formula

$$\text{WBC estimate } (/\mu L) = \text{average WBC per high power field (10 fields)} \times (\text{objective power})^2$$

where the objective power was 40x (and ocular was 10x), and differential counts were determined from counts of 100 cells based on described leukocyte morphology (16).

Statistical analyses were performed using a commercial statistics software package (JMP® Pro 13.2.0, SAS Inc., Cary, NC). Distribution of data was assessed by the Shapiro-Wilk test. Because many data were not normally distributed, non-parametric statistics were employed throughout for uniformity. Results were compared among treatment groups using the Kruskal-Wallis test. If significant differences were detected, multiple comparisons were performed with Wilcoxon rank sums test between treatment and control corresponding to the day of exposure, and between day 4 and day 1 within each treatment. Changes in weight, SCL and SCW before and after exposures were compared within groups by the Wilcoxon matched pairs signed ranks test. Indices of hemolysis, lipemia and icterus, as determined by the VetScan analyzer, were compared among groups by Fisher's exact test, followed by correspondence analysis if a significant difference was detected. An apparent association between plasma calcium and potassium was assessed by Kendall's τ coefficient. An $\alpha < 0.05$ was accepted as significant.

RESULTS

Turtles remained active or resting and responsive to stimuli throughout the exposure period. No skin sloughing, skin lesions, or significant internal gross lesions were observed. Oil was present in the GI tracts of all oil-exposed turtles. Results of morphometrics (**Table 1**), hematology (**Table 2**), and plasma biochemistry (**Table 3**) are shown by treatment group. Statistically significant differences between exposure treatment groups and non-exposed controls, and between 1 and 4 day exposure groups within treatments, were detected for weight, estimated WBC, some differential counts, heterophil/lymphocyte (H/L) ratio, PCV, AST, uric acid, glucose, calcium, phosphorus, total protein, albumin, globulin, potassium, and sodium. Plasma calcium and potassium were significantly positively associated ($\tau = 0.5052$, $p < 0.0001$).

Weight increased significantly between initial and final measurements for the control day 1 group (median 4% increase, $p = 0.0031$), the control day 4 group (median 6% increase, $p = 0.0006$), and the Corexit exposure day 1 group (median 4% increase, $p = 0.0191$) but not for the oil exposure day 1 group (median 2% increase, $p = 0.0753$) or day 4 group (median 6% increase, $p = 0.0561$), the Corexit exposure day 4 group (median 2% decrease, $p = 0.3363$), or the combined oil and Corexit day 1 (median 0% change) or day 4 (median 2% decrease, $p = 0.1140$) groups. The SCL increased significantly between initial and final measurements for the control day 1 group ($p = 0017$) the control day 4 group ($p = 0.0023$), the oil exposure day 1 ($p = 0.012$) and day 4 ($p < 0.0001$) groups, the Corexit exposure day 1 group ($p = 0.0313$), and the combined oil and Corexit exposure day 1 group ($p = 0.0203$), but not for the Corexit exposure day 4 group or for the combined oil and Corexit exposure day 4 group. The SCW did not differ between initial and final measurements for any treatment group.

Findings consistent with osmotic, electrolyte, mineral and hydration challenges included (1) significantly higher PCV in combination exposures at days 1 and 4 compared with corresponding controls (**Table 2**); (2) significantly higher plasma uric acid concentrations in oil exposures at days 1 and 4, Corexit exposures at day 4 (which increased significantly from Corexit at day 1), and combination exposures at day 1 and day 4 (which increased significantly from combination exposures at day 1); (3) significantly lower calcium concentration in oil exposures at day 1; (4) significantly higher phosphorus concentrations in oil exposures at day 4 and combination exposures at day 1; (5) significantly higher TP in Corexit exposures at day 4 (which increased significantly from Corexit exposures at day 1) and combination exposures at days 1 and 4; (6) significantly higher albumin concentration in combination exposures at day 4; (7) significantly higher potassium concentrations in Corexit and combination exposures at day 4 (which increased significantly from their respective exposures at day 1); and (8) significantly lower sodium concentrations in combination exposures at day 1 but sodium concentrations that increased significantly in Corexit and combination exposures on day 4 compared with their concentrations on day 1 (**Table 3**).

There was no difference in indices of hemolyis (median 0, range 0–2+) or icterus (median 1+, range 0–1+) among groups. There was a significant difference in lipemia index, with the greatest proportion of 1+ lipemia occurring in turtles exposed to both oil and Corexit for 4 days (80 vs. 20% with no lipemia), the next highest proportion of 1+ lipemia being in turtles exposed to oil for 4 days (33%) ($p < 0.0001$). Heinz bodies and morphological changes in WBCs were not observed in blood smears.

TABLE 1 | Morphometrics results by treatment groups, before and after exposures.

Analyte	Control 1 day	Control 4 days	Oil 1 day	Oil 4 days	Corexit 1 day	Corexit 4 days	Both 1 day	Both 4 days
Initial Weight (g)	18.5 (17.0 to 20.1)	19 (16.9 to 20.9)	18.7 (17.1 to 21.0)	18.9 (17.3 to 21.3)	18.5 (17.1 to 19.7)	19.0 (16.8 to 20.0)	18.9 (17.1 to 20.3)	18.6 (16.8 to 20.1)
Final Weight (g)	19.2 (18.0 to 20.9)	19.8 (18.6 to 21.7)	19.0 (17.9 to 20.7)	20.0 (17.0 to 21.9)	19.0 (17.3 to 20.7)	**19.0 (16.2 to 20.4)***	18.9 (17.5 to 20.6)	**18.2 (16.4 to 20.1)***
Δ Weight (g)	0.8 (−0.5 to 1.8)	1.1 (−0.1 to 1.9)	0.3 (−0.7 to 1.3)	1.2 (−1.1 to 2.2)	0.8 (−0.6 to 1.6)	***−0.4 (−1.0 to 1.4)**+*	**0.0 (−0.6 to 0.8)***	**−0.3 (−1.2 to 0.7)***
Initial SCL (mm)	45.8 (43.4 to 47.7)	45.7 (42.7 to 47.4)	46.1 (44.6 to 48.2)	46.9 (42.7 to 48.2)	45.7 (42.7 to 48.2)	46.2 (42.2 to 47.1)	45.8 (42.3 to 47.4)	46.0 (42.5 to 47.5)
Final SCL (mm)	46.2 (44.2 to 48.4)	46.9 (43.3 to 48.0)	45.8 (44.5 to 48.4)	47.3 (43.3 to 49.6)	46.3 (43.4 to 47.5)	46.4 (42.4 to 47.8)	45.9 (42.3 to 47.7)	46.2 (42.4 to 48.0)
Δ SCL (mm)	0.40 (−0.16 to 1.1)	0.46 (−0.12 to 2.2)	0.29 (−0.30 to 0.62)	0.35 (0.05 to 1.60)	0.30 (−0.38 to 1.04)	0.22 (−0.50 to 1.00)	0.33 (−0.60 to 1.16)	0.06 (−0.23 to 1.24)
Initial SCW (mm)	35.3 (34.0 to 37.1)	35.2 (33.2 to 37.2)	35.8 (34.6 to 36.9)	35.8 (31.8 to 37.3)	35.6 (32.5 to 37.0)	35.6 (31.8 to 37.3)	35.5 (32.0 to 37.2)	35.0 (32.7 to 36.9)
Final SCW (mm)	35.1 (34.4 to 36.3)	36.0 (33.7 to 37.5)	35.7 (33.2 to 37.2)	35.9 (32.1 to 37.4)	35.8 (32.4 to 36.6)	35.6 (32.7 to 36.9)	35.5 (31.7 to 37.1)	35.0 (33.0 to 36.9)
Δ SCW (mm)	−0.44 (−1.21 to 1.53)	0.41 (−0.68 to 2.50)	−0.12 (−1.72 to 1.47)	0.29 (−0.84 to 1.98)	−0.02 (−0.52 to 0.72)	−0.02 (−0.97 to 1.20)	0.01 (−1.18 to 1.12)	−0.06 (−1.68 to 1.20)

*Bold and * indicate significant difference with the control group for the corresponding day.*
Italics and + indicate the day 4 group differs significantly from the day 1 group for that treatment.
N = 14–16 (12–14 for SCW); median (10–90th percentiles).

TABLE 2 | Hematological results by treatment groups.

Analyte	Control 1 day	Control 4 days	Oil 1 day	Oil 4 days	Corexit 1 day	Corexit 4 days	Both 1 day	Both 4 days
PCV[a] (%)	25 (19–32)	27 (21–29)	27 (20–33)	28 (22–32)	24 (22–31)	*30 (22–34)+*	**28 (23–33)***	**30 (23–33)***
WBC Estimate ($\times 10^3/\mu L$)	6.1 (3.3–14.2)	*3.7 (2.5–8.1)+*	**11.0 (4.6–14.6)***	**10.1 (7.3–22.6)***	5.9 (3.7–13.0)	**10.7 (3.2–21.5)***	10.7 (4.1–19.7)	**14.2 (5.4–25.5)***
Heterophils (%)	69 (55–86)	67 (47–80)	75 (65–88)	70 (63–80)	70 (53–89)	***80 (71–92)*+***	**81 (65–90)***	**75 (54–92)***
Eosinophils (%)	0 (0–1.0)	0 (0–1.0)	0 (0–0.8)	0 (0–1.3)	0 (0–1.4)	0 (0–1.0)	0 (0–0.3)	0 (0–0.50)
Basophils (%)	0 (0–0)	0 (0–0.4)	0 (0–1.4)	0 (0–0)	0 (0–0)	0 (0–0.5)	0 (0–0)	0 (0–0.5)
Lymphocytes (%)	21 (9–34)	21 (14–40)	**15 (3–28)***	20 (10–31)	20 (8–40)	***14 (5–24)*+***	**13 (6–20)***	*20 (8–35)+*
Monocytes (%)	9 (3–16)	7 (2–20)	8 (2–22)	10 (2–20)	8 (1–15)	4 (0–12)	6 (1–23)	4 (0–17)
Heterophils ($\times 10^3/\mu L$)	5.0 (2.3–15.3)	*3.5 (1.6–7.5)+*	**10.2 (4.5–14.9)***	**9.5 (6.1–21.1)***	5.0 (2.8–13.5)	***10.3 (2.8–23.0)*+***	**10.3 (3.8–20.2)***	**12.8 (4.7–26.0)***
Eosinophils ($\times 10^3/\mu L$)	0 (0–0.1)	0 (0–0)	0 (0–0)	0 (0–0.2)	0 (0–0.1)	0 (0–0.1)	0 (0–0)	0 (0–0.1)
Basophils ($\times 10^3/\mu L$)	0 (0–0)	0 (0–0)	0 (0–0.2)	0 (0–0)	0 (0–0)	0 (0–0)	0 (0–0)	0 (0–0.1)
Lymphocytes ($\times 10^3/\mu L$)	1.7 (0.8–3.3)	1.1 (0.6–2.2)	1.8 (0.3–3.7)	***2.4 (1.2–5.1)*+***	1.7 (0.8– 3.3)	1.5 (0.5– 3.3)	1.4 (0.6–2.6)	***3.4 (1.1–5.2)*+***
Monocytes ($\times 10^3/\mu L$)	0.7 (0.2– 1.1)	0.4 (0.1– 1.2)	1.3 (0.2–3.6)	0.9 (0.2–3.4)	0.5 (0.1– 2.0)	0.4 (0.1– 1.4)	0.6 (0.1–4.8)	0.7 (0–3.0)
Heterophil/ Lymphocyte Ratio	3.4 (1.7–10.5)	3.0 (1.2– 5.4)	**4.8 (2.4–28.6)***	3.8 (2.0–7.9)	3.5 (1.4–10.2)	***5.8 (3.1–19.4)*+***	**6.5 (3.9–13.5)***	*4.0 (1.8–12.6)+*

*Bold and * indicate significant difference with the control group for the corresponding exposure duration.*
Italics and + indicate the day 4 group differs significantly from the day 1 group for that treatment.
N = 14–16; median (10–90th percentiles).
[a]*Packed Cell Volume.*

TABLE 3 | Plasma biochemical results by treatment groups.

Analyte	Control 1 day	Control 4 days	Oil 1 day	Oil 4 days	Corexit 1 day	Corexit 4 days	Both 1 day	Both 4 days
AST[a] (U/L)	157 (132–207)	161 (131–206)	186 (129–267)	171 (138–221)	164 (135–225)	***200 (140–244)*+**	173 (138–240)	**196 (169–275)***
CK[b] (U/L)	4,234 (2,919–6,153)	3,440 (1,864–6,190)	3,716 (1,222–6,403)	4,496 (2,752–5,852)	4,287 (2,415–7,536)	5,901 (2,408–8,252)	3,432 (1,897–6,996)	5,114 (3,049–8,177)
Uric Acid (mg/dL)	0.7 (0.3–2.1)	0.6 (0.4–1.3)	**1.2 (0.6–4.8)***	**1.0 (0.6–2.7)***	0.5 (0.3–2.3)	***1.2 (0.6–3.4)*+**	**1.3 (0.6–2.6)***	***2.5 (0.7–8.0)*+**
Glucose (mg/dL)	128 (102–222)	122 (105–149)	129 (105–191)	130 (108–162)	128 (97– 130)	**134 (111–200)***	134 (104–212)	***155 (128–241)*+**
Ca++ (mg/dL)	8.8 (7.5–10.8)	8.2 (6.4–12.5)	**7.6 (7.3–10.6)***	7.8 (6.7–11.0)	9.1 (6.8–11.1)	10.2 (7.4–17.6)	8.0 (7.3–11.8)	9.8 (7.1–17.2)
Phosphorus (mg/dL)	6.8 (5.1–9.5)	*8.0 (7.2–9.6)+*	7.3 (5.7–10.3)	**8.8 (7.4–12.3)***	7.0 (6.2–10.2)	*8.9 (6.6–11.0)+*	**8.5 (6.6–12.8)***	8.4 (6.4–9.9)
Total Protein (g/dL)	2.8 (2.5–3.5)	2.7 (2.4–2.9)	3.0 (2.5–3.9)	2.7 (2.4–3.4)	2.7 (2.5–3.2)	***3.2 (2.6–3.6)*+**	**3.1 (2.7–3.6)***	**3.3 (2.7–3.8)***
Albumin (g/dL)	1.6 (1.4–2.0)	1.5 (1.2–1.8)	1.7 (1.4–2.0)	1.6 (1.4–1.9)	1.5 (1.3–1.8)	1.7 (1.2–2.0)	1.8 (1.4–2.1)	**1.7 (1.1–2.0)***
Globulin (g/dL)	1.2 (1.1–1.4)	1.2 (1.0–1.3)	1.2 (1.1–2.0)	1.3 (1.0–1.6)	1.2 (1.1–1.4)	***1.5 (1.2–1.6)*+**	**1.4 (1.2–1.7)***	**1.5 (1.2–2.3)***
K+ (mmol/L)	5.5 (4.7–6.0)	4.8 (3.6–7.0)	5.6 (4.2–7.1)	4.7 (3.9–6.8)	5.3 (4.1–7.0)	***6.6 (4.1–9.7)*+**	5.6 (3.8–6.9)	***6.2 (4.9–9.4)*+**
Na+ (mmol/L)	162 (148–170)	165 (152–180)	155 (146–169)	156 (149–171)	162 (151–171)	*172 (157–180)+*	**150 (148–169)***	*165 (149–180)+*

*Bold and * indicate significant difference with the control group for the corresponding exposure duration.*
Italics and + indicate the day 4 group differs significantly from the day 1 group for that treatment.
N = 14–16; median (10–90th percentiles).
[a]*Aspartate Aminotransferase.*
[b]*Creatine Kinase.*

DISCUSSION

Interpretation of Findings

The principal alterations found in the present study reflect osmotic, electrolyte, mineral, and hydration challenges that collectively were worst in the 4-day combined oil/dispersant exposure treatment. There were additionally indications of a hypothalamic-pituitary-adrenal (HPA) stress response, and potential hepatocellular toxicity. Specifics for each category are addressed in turn, then compared with previous reports. Conclusions from plasma biochemical results are drawn from an in-house clinical analyzer that can vary somewhat from core diagnostic laboratory instruments (15), but performance is consistent and minimal sample volume is required (100 μl whole blood), a distinct advantage when volumes are small and further split for multiple companion studies [e.g., (17, 18)]. Sample size limited power of statistical analysis, particularly with highly variable analytes such as CK and Ca.

Osmotic, electrolyte, mineral, and hydration balance is maintained by the salt gland, kidneys, intestinal epithelium, and skin (19). Fluid loss from any source could result in hemoconcentration, as reflected in increased PCV and TP. The elevations in TP were driven primarily by globulins, which could instead indicate an inflammatory response (although this was not supported by the hematological findings) (16). Albumin determined by the bromocresol green dye binding method (used by the VetScan Analyzer, 15) is less reliable in non-mammalian plasma (20), and globulin is a calculated value from TP and albumin, therefore relative values of these components of TP must be interpreted with caution. Plasma protein electrophoresis is preferred for determining albumin and globulin values in reptile plasma (20), but sample volumes in the present study were insufficient for electrophoresis. Uric acid is the plasma analyte considered to be the best indicator of renal function in reptiles, with even marginal increases in sea turtles serving as a marker of dehydration or renal dysfunction (19). Elevated potassium, sodium, and phosphorus are also consistent with renal dysfunction (16). Potassium may also increase with hemolysis, metabolic acidosis or myopathy (16), but there was virtually no detectable hemolysis and no difference in hemolysis among groups. Acid-base status was not assessed. Phosphorus changes may be dietary in origin, but these turtles were still yolk-dependent and not fed. The lower calcium in day 1 oil exposures is unexplained, but can be seen concurrently with derangements in other electrolytes and minerals (16). It may also represent a statistical anomaly resulting from limited sample size and high variability. Calcium concentrations were also highly variable in other treatment groups, but included some markedly high values (>15 mg/dL) in the Corexit and combined 4 day exposures that could be clinically significant. The lower sodium in combined 1 day exposures also reflects an inconsistency that can be seen with hydration abnormalities in sea turtles (16). This dysregulation could potentially derive from renal, salt gland, or adrenal (via mineralocorticoid) sources. Clinicopathological findings related to hydration challenges were also supported by a failure of hatchlings to gain weight associated with normal hatchling hydration in seawater (21) in Corexit 4 day exposure at and oil and Corexit combination 1 and 4 day exposures. Weight gain of controls was consistent with previously reported hydration-associated weight gain of hatchlings in seawater (21). Increased SCL observed in most groups was associated with normal gradual flattening of the carapace curvature after hatching.

A HPA stress response is suggested by (1) a higher estimated leukocyte count with a higher estimated heterophil count and elevated heterophil/lymphocyte ratio in oil and combined exposures at both time points and Corexit 4 day exposures, (2) higher H/L ratios in oil and combined 1 day exposures and Corexit 4 day exposures (which increased significantly from the 1 day exposure group) (**Table 2**) and (3) significantly higher glucose in Corexit and combined 4 day exposures compared with controls (which for combined exposure increased significantly from 1 to 4 day exposure groups) (**Table 3**). An elevated H/L ratio is an indication of a glucocortioid response in multiple taxa (22) that has been evaluated in sea turtles with variable results (23–26). The higher estimated leukocyte and heterophil counts could also have resulted from an inflammatory reaction, however, given that it was not accompanied by a corresponding reduction in lymphocytes. Absence of toxic heterophils and reactive lymphocytes make an inflammatory response less likely. Eosinophils were uncommon in all treatment groups, so reduced eosinophils as a further indication of a glucocorticoid response could not be assessed. Increased plasma glucose is commonly observed as part of an HPA stress response, secondary to increased endogenous glucocorticoids (16). Small sample volumes precluded measurement of plasma corticosterone.

The possibility of hepatocellular toxicity is suggested by higher AST activities for Corexit and combination exposures at 4 days in the absence of differences in CK. Activities for CK, however, were highly variable, and AST elevations were not major.

Comparison With Prior Studies

Comparing with prior studies of experimental (5) and spill exposures to crude oil (3, 27), several similarities and differences are noted. Differences in exposure conditions and sea turtle life stage likely account for some of the inconsistencies. In the exposure study (5), sample size was even smaller ($n = 6$) than in the current study, limiting statistical power, turtles were older, and larger loggerheads (15–18 mo, 8–12 kg) that would normally be feeding but were fasted, oil thickness at the surface was greater (0.5 vs. 0.018 mm in the present study), and no Corexit was included. In the DWH oil spill exposure (3), animals were primarily pelagic phase Kemp's ridleys and green turtles with only a few loggerheads, larger [0.34–4.0 kg, (28)] but of undetermined ages, degree of exposure was of varying severity and duration for both oil and Corexit, and turtles were evaluated after the additional effects of rescue and extended transport and following through decontamination and rehabilitation. In the Canary Islands, juvenile and subadult pelagic loggerheads (mean weight 9.16 ± 7.74 sd kg) exposed to smaller scale spills from shipping lanes (25) were evaluated as a subset of stranded rescued turtles (7/149) with regards to clinicopathological alterations (27). In this case, exposures were similarly variable, and there was

no Corexit exposure. Turtles in these prior studies were well-past yolk-dependence. Clinical chemistry analyzers differed among studies, which can also affect results (15).

In both experimental (5) and spill exposures of sea turtles to crude oil (3, 27), there were indications of anemia. However, in the experimental exposure (5), blood was collected in EDTA, which can artifactually lyse red blood cells of sea turtles, and although erythrocyte counts appeared to decrease, PCV did not, which is inconsistent with a true anemia (3). In spill exposures, anemia may have been associated with comorbidities such as trauma, pneumonia, or gastrointestinal disease (6), some of which could have been independent of oiling, or that developed as later sequelae of oiling. In the case of the DWH oil spill, onset of anemia was variable, and was non-hemolytic, in contrast with previous findings in sea birds that develop hemolytic anemia (3). Additionally, PCV at the time of rescue was highly variable, and included values as high as 47% (6), suggesting at least some turtles experienced hemoconcentration. In the current study, PCV was higher in exposures than in controls, consistent with hemoconcentration, and there was likewise no indication of hemolysis. Anemia may have developed following longer term exposures.

Initially elevated electrolytes and uric acid were commonly observed in sea turtles rescued in the DWH spill (3), consistent with findings in the current study, and with osmotic, electrolyte, and hydration challenges. In the previous experimental crude oil exposure study, authors speculated that there could have been salt gland dysfunction in two of five oil-exposed turtles based on incidental analysis of salt gland secretion, but this was not systematically evaluated and no plasma electrolyte values were presented (5). These plasma electrolyte and uric acid alterations could result from dehydration, or renal, salt gland or adrenal dysfunction. Dehydration might also result from severe epithelial damage, either intestinal or dermal, but in contrast with the previous exposure study and in spill exposure in the Canary Islands in which skin sloughing was prominent (5, 25), no skin sloughing was observed in the current study, and only rarely observed during the DWH spill (6). Presence, absence and degree of skin sloughing in different contexts may result from differences in crude oil composition, weathering, and duration and amount of exposure. For instance, oil depth in the previous crude oil exposure study was 0.5 (5), vs. 0.018 mm in the current study. Lower plasma calcium was observed in oiled turtles in the Canary Islands compared with controls (27), as was hypocalcemia in a number of green turtles following rescue in the DWH spill (6), similar to oil exposure alone at day 1 in the current study. Because sea turtles in the current study were still yolk-dependent, however, malnutrition would not have been responsible for the lower calcium concentrations, as suggested in the field exposure studies. In other treatments in the current study, plasma calcium concentrations were highly variable, but included some markedly high values in some turtles that could be of clinical significance. Both hyper- and hypokalemia were observed in sea turtles rescued in the DWH spill (16), compared with hyperkalemia in Corexit and combined exposures in the current study. A positive association of plasma calcium and potassium, with clinically significant high values of both, is consistent with simultaneously high values reported in a case of sea turtle exertional myopathy (29). In that case it was attributed to cellular degradation, renal dysfunction or both, which could also be factors in oil and dispersant exposure, albeit from different root causes. A companion study of NMR metabolomics using samples from the current exposure study found depletion of the osmolyte taurine in muscle samples that may further reflect osmotic stress of crude oil exposure (18).

Leukocytosis was reported in experimental oil exposure (5) and specifically a heterophilic leukocytosis in spill exposures (3, 27), similar to the higher estimated leukocyte and heterophil counts in the current findings. This was interpreted as most likely a stress leukogram, without ruling out an inflammatory component (3, 5). Over half of turtles rescued in the DWH spill exhibited elevated glucose concentrations, as seen in Corexit and combined exposures at 4 days in the current study, similarly consistent with an HPA stress response. However, hypoglycemia was also observed in several turtles in the DWH response (3, 6), as well as in spill exposures in the Canary Islands (27), attributed to anorexia or exhaustion. Decreases in skeletal muscle lactate and creatinine detected by NMR metabolomic analysis may reflect energy depletion (18), which an HPA response would help mitigate.

Elevated plasma activities of various tissue enzymes (ALP, ALT, AST, CK, LDH) consistent with non-specific tissue damage have been reported in spill exposures (3, 27), but were inconsistently observed and confounded by effects of exertion, rescue, handling, and transport (3). Higher plasma AST activities in Corexit and combined exposures in the current study were minor.

Clinical Relevance of Findings

Clinical relevance of statistically significant differences in exposure groups may appear minor from a cursory comparison of medians, many of which fall within reference intervals for multiple size classes of loggerheads sampled under varied conditions (16, 30). Some upper 10th percentile values, however, would be of considerable concern for morbidity or potential pending mortality, including uric acid (8.0 mg/dL), potassium (9.7 mmol/L), and phosphorus (12.8 mg/dL). While not statistically significantly different, the same holds true for upper 10th percentile values of plasma calcium (17.7 mg/dL). Plasma uric acid concentrations >2.0 mg/dL are considered problematic in sea turtles (19), and hyperkalemia may lead to fatal cardiac arrhythmias (31). Survival of cold-stunned Kemp's ridleys is lower for turtles presenting with higher plasma uric acid, potassium and phosphorus (32). Plasma uric acid concentration was one of three main determinants of survival in a multispecies model of rehabilitating sea turtles in Taiwan, along with plasma creatinine and presence or absence of a buoyancy disorder (33). Plasma potassium was one of three main determinants in a model of mortality probability for cold-stunned Kemp's ridleys, along with pH and pO_2 (34). This model was later extended to Kemp's ridleys from the DWH oil spill to calculate that 25% of rescued oiled turtles had physiological derangement putting them at high risk of

mortality absent therapeutic intervention (3). No turtles in the current study exhibited a buoyancy disorder, and creatinine, blood pH and pO_2 were not measured, therefore, neither model could be applied. Nonetheless, even median values of plasma uric acid and potassium in the combined exposure, along with failure to gain weight from normal hydration following immersion, suggest a substantially increased risk of mortality when comparing qualitatively to outcomes in previous studies (32–34).

Results from spill responses indicate that despite dyscrasias associated with oil exposure, there can be a high rate of recovery and release of oiled sea turtles (>88%) if they are rescued, decontaminated and treated (3, 6, 25). However, in the DWH spill, only 574 turtles were rescued and examined, with 319 oiled turtles admitted to rehabilitation centers, out of a calculated estimate of 402,000 surface-pelagic sea turtles that were exposed (2, 3). Approximately 30% of exposed oceanic sea turtles minimally to moderately oiled and 100% of heavily mired turtles are expected to have died (28). More abnormalities were observed with longer (4 days) and combined oil and Corexit exposures in the current study, and these could be expected to exacerbate with more prolonged exposure. Corexit alone after 4 days exposure was associated with more abnormalities than crude oil exposure alone. Combinations of crude oil and Corexit have exhibited enhanced toxicity in a wide range of organisms and cells, including rotifers, corals, fish embryos, juvenile mullet, lymphoproliferative response of dolphins, and others (1, 35–39). Corexit by itself damages epithelia (38), which could include skin, conjunctiva and gastrointestinal epithelia, consistent with observed hydration-related clinicopathological abnormalities. Although skin was not grossly affected in the current study, permeability could have been impacted, as could permeability of the gastrointestinal epithelium. When combined with oil, dispersants increase exposure of organism to crude oil hydrocarbons (38), which could affect renal, adrenal, or salt gland function. Although little to no dioctyl sodium sulfosuccinate (DOSS, used as a marker for Corexit exposure) was detected in turtles that died during the DWH spill, that may have resulted from a relatively high lower limit of quantification, and photo- and bio-degradation in surface waters could have decreased exposure by the time of sampling (40). Corexit was also applied at a lower target dispersant to oil ratio than in the current study [1:20 vs. 1:10 (41)]. Application and exposure were likely heterogeneous, however, and combined exposures early in the event could have persistent effects.

Variability in clinicopathological values of oiled sea turtles within and among studies indicate the need for basic diagnostics on at least a subset of turtles arriving in cohorts during a mass casualty event in order to guide appropriate treatments. This particularly applies to electrolytes, glucose and calcium, in order to tailor fluid therapy. Point of care analyzers requiring only small volumes of blood and yielding rapid results are helpful in this regard (6, 15).

Exposure to crude oil, Corexit, and crude oil-Corexit combined result in osmotic, electrolyte, hydration, HPA and potentially hepatocellular responses and dyscrasias in hatchling loggerheads. These abnormalities were greater and more numerous in 4 day exposures than 1 day exposures, and greater with the combined exposures than single agent exposures. These findings highlight potential hazards to consider when deploying dispersants during an oil spill mitigation response.

DATA AVAILABILITY STATEMENT

The datasets generated for this study are available on request to the corresponding author.

ETHICS STATEMENT

The animal study was reviewed and approved by North Carolina State University Institutional Animal Care and Use Committee.

AUTHOR CONTRIBUTIONS

CH designed the clinicopathological component of the overall exposure study reported here, collected and analyzed samples, analyzed results, and wrote the paper. PM-G conceived the overall exposure study, conducted the exposures, collected and distributed samples to collaborators, and contributed to data analysis and initial writing. MG conducted the pivotal temperature study that provided the opportunity for this ancillary study, acquired the doomed eggs, carried out the egg incubation, collected and processed samples and contributed to writing. EC and HB collected and processed samples and contributed to writing. CG-C conceived the overall exposure study, supported the collection and distribution of samples to collaborators and contributed to writing.

FUNDING

Support for the pivotal temperature study came from a NOAA Section 6 Research Grant (NA10NMF4720035). Support for the add-on exposure study came from the state of North Carolina.

ACKNOWLEDGMENTS

We thank B. Phillips, E. McCarthy, R. Pezdek, and S. Webb for technical assistance, and J. Griffitt for providing crude oil. The authors recognize the controversial nature of an investigation such as this Holden (42) and deliberated before proceeding. In the context of eggs from doomed nests being used in a NOAA-approved and sponsored ongoing terminal study, and the paucity of toxicological data for sea turtles exposed to crude oil and dispersants, we opted to maximize use of these turtles destined for euthanasia in order to advise science-based treatment and conservation of sea turtles affected in future oil spills.

REFERENCES

1. Beyer J, Trannum HC, Bakke T, Hodson PV, Collier TK. Environmental effects of the Deepwater Horizon oil spill: a review. *Mar Pollut Bull*. (2016) 110:28–51 doi: 10.1016/j.marpolbul.2016.06.027
2. McDonald TL, Schroeder BA, Stacy BA, Wallace BP, Starcevich LA, Gorham J, et al. Density and exposure of surface-pelagic juvenile sea turtles to Deepwater Horizon oil. *Endang Species Res.* (2017) 33:69–82. doi: 10.3354/esr00771
3. Stacy NI, Field CL, Staggs L, MacLean RA, Stacy BA, Keene J, et al. Clinicopathological findings in sea turtles assessed during the Deepwater Horizon oil spill response. *Endang Species Res*. (2017) 33:25–37. doi: 10.3354/esr00769
4. Shigenaka G (editor). *Oil and Sea Turtles: Biology, Planning, and Response*. National Oceanic and Atmospheric Administration, NOAA's National Ocean Service, Office of Response and Restoration, Silver Spring, Maryland (2003). p. 112. Available online at: https://response.restoration.noaa.gov/sites/default/files/Oil_Sea_Turtles.pdf (accessed 25 April 2019).
5. Lutcavage ME, Lutz PL, Bossart GD, Hudson DM. Physiologic and clinicopathologic effects of crude oil on loggerhead sea turtles. *Arch Environ Contam Toxicol*. (1995) 28:417–422. doi: 10.1007/BF00211622
6. Field CL, Staggs L, Godard-Codding C. Sea turtles and oil. In: Manire CA, Norton TM, Stacy BA, Innis CJ, Harms CA, editors. *Sea Turtle Health & Rehabilitation*. Plantation, FL: J. Ross Publishing (2017). p. 899–931.
7. Orós J, Montesdeoca N, Camacho M, Arencibia A, Calabuig P. Causes of stranding and mortality, and final disposition of loggerhead sea turtles (*Caretta caretta*) admitted to a wildlife rehabilitation center in Gran Canaria Island, Spain (1998-2014): a long-term retrospective study. *PLoS ONE*. (2016) 11: e0149398. doi: 10.1371/journal.pone.0149398
8. Zychowski GV, Godard-Codding CAJ. Reptilian exposure to polycyclic aromatic hydrocarbons and associated effects. *Environ Toxicol Chem*. (2017) 36:25–35. doi: 10.1002/etc.3602
9. Mrosovsky N. Pivotal temperatures for loggerhead turtles from northern and southern nesting beaches. *Can J Zool*. (1988) 66:661–9. doi: 10.1139/z88-098
10. Godfrey MH, Mrosovsky N. Estimating the time between hatching of sea turtles and their emergence from the nest. *Chelonian Conserv Biol*. (1997) 2:581–5.
11. Barron, MG, Ka'aihue L. Critical evaluation of CROSERF test methods for oil dispersant toxicity testing under subarctic conditions. *Mar Pollut Bull*. (2003) 46:1191–9. doi: 10.1016/S0025-326X(03)00125-5
12. Hemmer MJ, Barron MG, Greene RM. Comparative toxicity of eight oil dispersants, Louisiana sweet crude oil (Lsc), and chemically dispersed Lsc to two aquatic test species. *Environ Toxicol Chem*. (2011) 30:2244–52. doi: 10.1002/etc.619
13. Wyneken J, Salmon M. Frenzy and postfrenzy swimming activity in loggerhead green, and leatherback hatchling sea turtles. *Copeia*. (1992) 1992:478–84. doi: 10.2307/1446208
14. Leary S, Underwood W, Anthony R, Cartner S, Corey D, Grandin T, et al. *AVMA Guidelines for the Euthanasia of Animals, 2013*. Shaumburg, IL: American Veterinary Medical Association (2013). p. 102.
15. Wolf KN, Harms CA, Beasley JF. Evaluation of five clinical chemistry analyzers for use in health assessment in sea turtles. *J Am Vet Med Assoc*. (2008) 233:470–5. doi: 10.2460/javma.233.3.470
16. Stacy NI, Innis CJ. Clinical pathology. In: Manire CA, Norton TM, Stacy BA, Innis CJ, Harms CA, editors. *Sea Turtle Health & Rehabilitation*. Plantation, FL: J. Ross Publishing (2017). p. 147–207.
17. Bailey SAB, Niemuth JN, McClellan-Green PD, Godfrey MH, Harms CA, Stoskopf MK. 1H-NMR metabolomic study of whole blood from hatchling loggerhead sea turtles (*Caretta caretta*) exposed to crude oil and/or Corexit. *R Soc Open Sci*. (2017) 4:171433. doi: 10.1098/rsos.171433
18. Bembenek-Bailey SA, Niemuth JN, McClellan-Green PD, Godfrey MH, HarmsCA, Gracz H, et al. NMR metabolomic analysis of skeletal muscle, heart, and liver of hatchling loggerhead sea turtles (*Caretta caretta*) experimentally exposed to crude oil and/or Corexit. *Metabolites*. (2019) 9:21. doi: 10.3390/metabo9020021
19. Innis CJ, Valente ALS, Stacy BA, Wyneken J. Urogenital and lacrimal systems. In: Manire CA, Norton TM, Stacy BA, Innis CJ, Harms CA, editors. *Sea Turtle Health & Rehabilitation*. Plantation, FL: J. Ross Publishing (2017). p. 381–415.
20. Gicking JC, Foley AM, Harr KE, Rasking RE, Jacobson E. Plasma protein electrophoresis of the Atlantic loggerhead sea turtle, *Caretta caretta*. *J Herp Med Surg*. (2004) 14:13–8. doi: 10.5818/1529-9651.14.3.13
21. Bennet JM, Taplin LE, Grigg GC. Sea water drinking as a homeostatic response to dehydration in hatchling loggerhead turtles *Caretta caretta*. *Comp Biochem Physiol*. (1986) 83A:507–13. doi: 10.1016/0300-9629(86)90137-4
22. Davis AK, Maney DL, Maerz JC. The use of leukocyte profiles to measure stress in vertebrates: a review for ecologists. *Funct Ecol*. (2008) 22:760–72. doi: 10.1111/j.1365-2435.2008.01467.x
23. Keller JM, Kucklick JR, Stamper MA, Harms CA, McClellan-Green PD. Associations between organochlorine contaminant concentrations and clinical health parameters in loggerhead sea turtles from North Carolina, USA. *Environ Health Persp*. (2004) 112:1074–9. doi: 10.1289/ehp.6923
24. Harris HS, Benson SR, Gilardi KV, Poppenga RH, Work TM, Dutton PH, et al. Comparative health assessment of Western Pacific leatherback turtles (*Dermochelys coriacea*) foraging off the coast of California, 2005-2007. *J Wildl Dis*. (2011) 47:321–37. doi: 10.7589/0090-3558-47.2.321
25. Camacho M, Orós J, Boada LD, Zaccaroni A, Silvi M, Formigaro C, et al. Potential adverse effects of inorganic pollutants on clinical parameters of loggerhead sea turtles (*Caretta caretta*): results from a nesting colony from Cape Verde, West Africa. *Mar Environ Res*. (2013) 92:15–22. doi: 10.1016/j.marenvres.2013.08.002
26. Hunt KE, Innis CJ, Kennedy AE, McNally KL, Davis DG, Burgess EA, et al. Assessment of ground transportation stress in juvenile Kemp's ridley sea turtles (*Lepidochelys kempii*). *Conserv Physiol*. (2016) 4:cov071. doi: 10.1093/conphys/cov071
27. Casal AB, Orós J. Plasma biochemistry and haematology values in juvenile loggerhead sea turtles undergoing rehabilitation. *Vet Rec*. (2009) 164:663–5. doi: 10.1136/vr.164.21.663
28. Mitchelmore CL, Bishop CA, Collier TK. Toxicological estimation of mortality of oceanic sea turtles oiled during the Deepwater Horizon oil spill. *Endang Species Res*. (2017) 33:39–50. doi: 10.3354/esr00758
29. Phillips BE, Cannizzo SA, Godfrey MH, Stacy BA, Harms CA. Exertional myopathy in a juvenile green sea turtle (*Chelonia mydas*) entangled in a large mesh gillnet. *Case Reports Vet Med*. (2015) 2015:604320. doi: 10.1155/2015/604320
30. Rousselet E, Stacy NI, LaVictoire K, Higgins BM, Tocidlowski ME Flanagan JP, et al. Hematology and plasma biochemistry analytes in five age groups of immature, captive-reared loggerhead sea turtles (*Caretta caretta*). *J Zoo Wildl Med*. (2013) 44:859–74. doi: 10.1638/2012-0162R1.1
31. Mitchell M. Reptile cardiology. *Vet Clin N Am: Exotic Anim Pract*. (2009) 12:65–79. doi: 10.1016/j.cvex.2008.10.001
32. Innis CJ, Ravich JB, Tlusty MF, Hoge MS, Wunn DS, Boerner-Neville LB, et al. Hematologic and plasma biochemical findings in cold-stunned Kemp's ridley turtles: 176 cases (2001-2005). *J Am Vet Med Assoc*. (2009) 235:426–32. doi: 10.2460/javma.235.4.426
33. Li TH, Chang CC, Cheng IJ, Lin SC. Development of a summarized health index (SHI) for use in predicting survival in sea turtles. *PLoS ONE*. (2015) 10:e0120796. doi: 10.1371/journal.pone.0120796
34. Stacy NI, Innis CJ, Hernandez JA. Development and evaluation of three mortality prediction indices for cold-stunned Kemp's ridley sea turtles (*Lepidochelys kempii*). *Conserv Physiol*. (2013) 1:cot003. doi: 10.1093/conphys/cot003
35. Shafir S, Rijn JV, Rinkevich B. Short and long term toxicity of crude oil and oil dispersants to two representative coral species. *Environ Sci Tech*. (2007) 41:5571–4. doi: 10.1021/es0704582
36. Milinkovitch T, Kanan R, Thomas-Guyon H, Le Floch S. Effects of dispersed oil exposure on the bioaccumulation of polycyclic aromatic hydrocarbons and

the mortality of juvenile *Liza ramada*. *Sci Total Environ*. (2011) 409:1643–50. doi: 10.1016/j.scitotenv.2011.01.009
37. Rico-Martínez R, Snell TW, Shearer TL. Synergistic toxicity of Macondo crude oil and dispersant Corexit 9500A® to the *Brachionus plicatilis* species complex (Rotifera). *Environ Pollut*. (2013) 173:5–10. doi: 10.1016/j.envpol.2012.09.024
38. Adams J, Sweezey M, Hodson PV. Oil and oil dispersant do not cause synergistic toxicity to fish embryos. *Environ Toxicol Chem*. (2014) 33:107–14. doi: 10.1002/etc.2397
39. White ND, Godard-Codding C, Webb SJ, Bossart GD, Fair PA. Immunotoxic effects of *in vitro* exposure of dolphin lymphocytes to Louisiana sweet crude oil and Corexit™. *J Appl Toxicol*. (2016) 37:676–82. doi: 10.1002/jat.3414
40. Ylitalo GM, Collier TK, Anulacion BF, Juaire K, Boyer RH, da Silva DAM, et al. Determining oil and dispersant exposure in sea turtles from the northern Gulf of Mexico resulting from the *Deepwater Horizon* oil spill. *Endang Spec Res*. (2017) 33:9–24. doi: 10.3354/esr00762
41. Passow U, Sweet J, Quigg A. How the dispersant Corexit impacts the formation of sinking marine oil snow. *Mar Pollut Bull*. (2017) 125:139–45. doi: 10.1016/j.marpolbul.2017.08.015
42. Holden C. Random samples. *Science*. (1994) 263:1566–7. doi: 10.1126/science.263.5153.1566-c

Conflict of Interest: CH has previously consulted with counsel for British Petroleum on sea turtle health matters. CG-C previously conducted research on sea turtle health following the Deepwater Horizon oil spill event funded from the Natural Resource Damage Assessment Trustees and is currently conducting research on marine mammal health funded by Exxon Neftegas Limited and the Sakhalin Energy Investment. The content herein is solely the responsibility of the authors and does not represent the official views of any past or current funding parties associated with the authors.

The remaining authors declare that the research was conducted in the absence of any commercial or financial relationships that could be construed as a potential conflict of interest.

The handling Editor declared a past co-authorship with one of the authors CH.

Copyright © 2019 Harms, McClellan-Green, Godfrey, Christiansen, Broadhurst and Godard-Codding. This is an open-access article distributed under the terms of the Creative Commons Attribution License (CC BY). The use, distribution or reproduction in other forums is permitted, provided the original author(s) and the copyright owner(s) are credited and that the original publication in this journal is cited, in accordance with accepted academic practice. No use, distribution or reproduction is permitted which does not comply with these terms.

frontiers in Veterinary Science

ORIGINAL RESEARCH
published: 22 October 2019
doi: 10.3389/fvets.2019.00372

Caryospora-Like Coccidia Infecting Green Turtles (*Chelonia mydas*): An Emerging Disease With Evidence of Interoceanic Dissemination

Brian A. Stacy[1], Phoebe A. Chapman[2], Heather Stockdale-Walden[3], Thierry M. Work[4], Julie Dagenais[4], Allen M. Foley[5], Morgan Wideroff[5], James F. X. Wellehan Jr.[3], April L. Childress[3], Charles A. Manire[6], Mya Rodriguez[7], Trevor T. Zachariah[8], Lydia Staggs[9], Bette Zirkelbach[10], Nina Nahvi[11], Whitney Crowder[12], Shane M. Boylan[13], Shelly Marquardt[14], Craig Pelton[15] and Terry M. Norton[10,16]*

[1] National Marine Fisheries Service, Office of Protected Resources, University of Florida (Duty Station), Gainesville, FL, United States, [2] Veterinary-Marine Animal Research Teaching and Investigation Unit, School of Veterinary Science, University of Queensland, Gatton, QLD, Australia, [3] Department of Comparative, Diagnostic, and Population Medicine, College of Veterinary Medicine University of Florida, Gainesville, FL, United States, [4] US Geological Survey, National Wildlife Health Center, Honolulu Field Station, Madison, WI, United States, [5] Florida Fish and Wildlife Conservation Commission, Jacksonville Field Laboratory, Fish and Wildlife Research Institute, Jacksonville, FL, United States, [6] Loggerhead Marinelife Center, Juno Beach, FL, United States, [7] Miami Seaquarium, Miami, FL, United States, [8] Sea Turtle Healing Center, Brevard Zoo, Melbourne, FL, United States, [9] Veterinary Services, Zoological Operations, SeaWorld Orlando, Orlando, FL, United States, [10] The Turtle Hospital, Marathon, FL, United States, [11] Sea Turtle, Inc., South Padre Island, TX, United States, [12] Gumbo Limbo Nature Center, Sea Turtle Rehabilitation Facility, Boca Raton, FL, United States, [13] South Carolina Aquarium, Charleston, SC, United States, [14] Clearwater Marine Aquarium, Clearwater, FL, United States, [15] Volusia Marine Science Center, Ponce Inlet, FL, United States, [16] Georgia Sea Turtle Center, Jekyll Island, GA, United States

OPEN ACCESS

Edited by:
Francesco Carlo Origgi, University of Bern, Switzerland

Reviewed by:
Mario Santoro, Stazione Zoologica Anton Dohrn, Italy
Wendi D. Roe, Massey University, New Zealand
Jorge Orós, University of Las Palmas de Gran Canaria, Spain

***Correspondence:**
Brian A. Stacy
brian.stacy@noaa.gov

Specialty section:
This article was submitted to Zoological Medicine, a section of the journal Frontiers in Veterinary Science

Received: *08 August 2019*
Accepted: *08 October 2019*
Published: *22 October 2019*

Citation:
Stacy BA, Chapman PA, Stockdale-Walden H, Work TM, Dagenais J, Foley AM, Wideroff M, Wellehan JFX Jr, Childress AL, Manire CA, Rodriguez M, Zachariah TT, Staggs L, Zirkelbach B, Nahvi N, Crowder W, Boylan SM, Marquardt S, Pelton C and Norton TM (2019) Caryospora-Like Coccidia Infecting Green Turtles (Chelonia mydas): An Emerging Disease With Evidence of Interoceanic Dissemination. Front. Vet. Sci. 6:372. doi: 10.3389/fvets.2019.00372

Protozoa morphologically consistent with *Caryospora* sp. are one of the few pathogens associated with episodic mass mortality events involving free-ranging sea turtles. Parasitism of green turtles (*Chelonia mydas*) by these coccidia and associated mortality was first reported in maricultured turtles in the Caribbean during the 1970s. Years later, epizootics affecting wild green turtles in Australia occurred in 1991 and 2014. The first clinical cases of *Caryospora*-like infections reported elsewhere in free-ranging turtles were from the southeastern US in 2012. Following these initial individual cases in this region, we documented an epizootic and mass mortality of green turtles along the Atlantic coast of southern Florida from November 2014 through April 2015 and continued to detect additional, sporadic cases in the southeastern US in subsequent years. No cases of coccidial disease were recorded in the southeastern US prior to 2012 despite clinical evaluation and necropsy of stranded sea turtles in this region since the 1980s, suggesting that the frequency of clinical coccidiosis has increased here. Moreover, we also recorded the first stranding associated with infection by a *Caryospora*-like organism in Hawai'i in 2018. To further characterize the coccidia, we sequenced part of the 18S ribosomal and mitochondrial cytochrome oxidase I genes of coccidia collected from 62 green turtles found in the southeastern US and from one green turtle found in Hawai'i. We also sequenced the ribosomal internal transcribed spacer regions from selected cases and compared all results with those obtained from *Caryospora*-like coccidia collected from green turtles found in Australia. Eight distinct genotypes were represented in green turtles from the southeastern US. One genotype predominated and was identical to that

of coccidia collected from the green turtle found in Hawai'i. We also found a coccidian genotype in green turtles from Florida and Australia with identical 18S and mitochondrial sequences, and only slight inter-regional differences in the internal transcribed spacer 2. We found no evidence of geographical structuring based on phylogenetic analysis. Low genetic variability among the coccidia found in green turtle populations with minimal natural connectivity suggests recent interoceanic dissemination of these parasites, which could pose a risk to sea turtle populations.

Keywords: *Caryospora*, Eimeriidae, sea turtle, mortality, stranding, pathogen pollution

INTRODUCTION

The genus *Caryospora* are coccidian parasites in the order Eucoccidiorida, family Eimeriidae. A key feature for morphologic identification is that sporulated oocysts have a single sporocyst with eight sporozoites. The type species is *Caryospora simplex*, which uses snakes in the genus *Vipera* as definitive hosts and can use rodents as intermediate hosts (1). There are at least 81 morphologically described species in the genus (2), but of these, only five named species have available DNA sequence data, and these five do not include the type species, *C. simplex*. Phylogenetic analyses show that *Caryospora* are paraphyletic, with *C. bigemina*, *Caryospora*-like coccidia from sea turtles, *C. ernsti*, and *C. daceloe*/*C. neofalconis* representing four distinct clades in the coccidian tree, with *C. daceloe*/*C. neofalconis* actually clustering in the family Sarcocystidae rather than Eimeriidae (3–6). Although the use of European viper hosts suggests that *C. bigemina* may represent the correct cluster, until reference sequence is available for *C. simplex*, it is not possible to say which one of these clades is actually *Caryospora*.

Caryospora cheloniae was first described in the 1970s during the investigation of an epizootic of enterocolitis characterized by dilation, mucosal hyperplasia, and ulceration of the distal small intestine and colon coincident with the presence of numerous coccidia in hatchling and juvenile maricultured green turtles (*Chelonia mydas*) at a facility in the Caribbean (7, 8). Almost 20 years later, a coccidiosis epizootic occurred in wild immature green turtles in Moreton Bay in southeast Queensland, Australia (9). In addition to enterocolitis, extra-intestinal schizonts were found in the brain, thyroid gland, and kidney. Some turtles exhibited abnormal neurological signs attributed to meningoencephalitis from the protozoal infection. Sporadic cases were documented in Australia during subsequent years (10) and another epizootic occurred there in 2014 (4).

Gordon et al. (9) identified the coccidia associated with the first reported Australian epizootic as *C. cheloniae* based on morphology; however, there was no apparent connection between the Australian population of green turtles and the captive-bred green turtles of the original Caribbean report, which were descendants of stock collected from Atlantic nesting assemblages. Genetic characterization of the coccidia from the 2014 Australian epizootic identified two genotypes based on partial sequencing of the ribosomal 18S gene. One genotype was found in coccidia from the gastrointestinal tract, brain, and lung and a second genotype was found in coccidia from the thyroid gland and kidney (4). Phylogenetic analysis suggested that these two genotypes have different relations to other coccidia, highlighting problems with *Caryospora* taxonomy and the putative identification of *C. cheloniae* in sea turtles. As Chapman et al. (4) note, the absence of genetic data from the original Caribbean *C. cheloniae* epizootic and the aforementioned taxonomic uncertainty around recognized *Caryspora* spp. present a formidable barrier to resolving taxonomy and to making a genus or species diagnosis. In acknowledgment of their undefined taxonomic status, hereafter we refer to coccidia found in sea turtles morphologically resembling the original description of *C. cheloniae* as *Caryospora*-like organisms (CLOs).

Coccidia with *Caryospora*-like morphology were not reported in free-ranging sea turtles outside of the Southwest Pacific for years following the initial Australian epizootic despite extensive long-term mortality surveillance efforts in other areas, including the western Atlantic and Hawai'i. To our knowledge, the earliest record of a CLO in another region was the detection of oocysts in a green turtle fecal sample collected from a foraging area near the Marquesas Keys, Florida, US in 2007 (B. Stacy, unpublished data). Four cases of CLO infections were next encountered in green turtles captured in the Gulf of Venezuela from 2011–2013 (11). Around the same time, the first wild green turtles with clinically significant CLO infections were found in the Northwest Atlantic (12, 13). Shortly thereafter, we documented a CLO epizootic concurrent with increased green turtle strandings in southeastern Florida during the fall of 2014 and the winter and spring of 2015. In 2018, we discovered a moribund juvenile green turtle in Hawai'i with severe enteritis associated with a CLO; the first case in this region.

Collectively, this increase in diagnoses within US waters of the Northwest Atlantic and Central Pacific over the last decade suggested a recent change in parasitism or disease occurrence within these areas. These findings prompted a broader collaborative study encompassing locations of known CLO infections in green turtles within the US and Australia to better understand the genetic diversity and distribution of these parasites, and attempt to explain the recent emergence of this disease in the northern hemisphere. Here we describe cases of CLO infection in green turtles, including the epizootic in southeastern Florida, and results of genetic characterization and phylogenetic analysis primarily based on the 18S ribosomal and mitochondrial cytochrome oxidase I (MT-*coI*) genes.

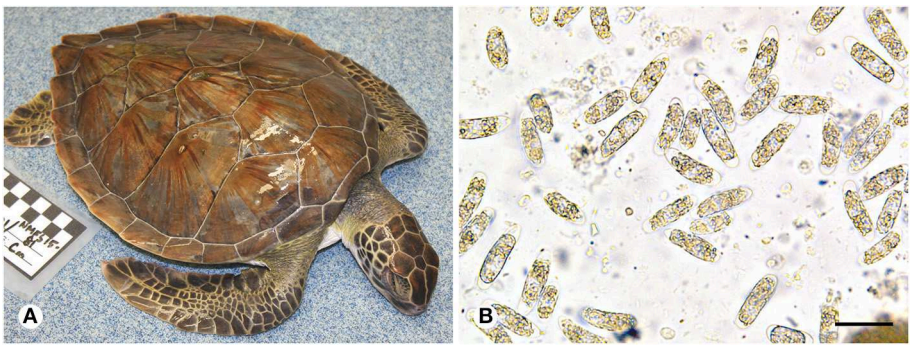

FIGURE 1 | (A) Green turtle (*Chelonia mydas*) with coccidiosis found during a 2014/2015 epizootic in southeastern Florida. The frequent presentation of turtles found during this event was absence of injuries, other apparent causes of stranding, or accumulated epibiota. Note the sunken eyes and gaunt neck and shoulder regions due to dehydration or diminished nutritional condition. **(B)** Oocysts morphologically consistent with *Caryospora* sp. (genotype US1) in feces from a green turtle that stranded in Florida. Scale = 40 μm.

MATERIALS AND METHODS

Sea Turtle Evaluation and Sampling

Participants in the Sea Turtle Stranding and Salvage Network (STSSN) documented stranded sea turtles on the Atlantic and Gulf of Mexico coasts of the US and recorded date, location, species, carapace length [including straight carapace length (SCL) from the nuchal notch to the caudal-most tip], and any apparent external abnormalities as described by Foley et al. (14). Sea turtles were similarly documented by the stranding responders in Hawai'i.

Diagnosis of CLO infection was based on detection of oocysts in fecal samples or by histopathology consistent with published reports (8, 9) (**Figures 1–3**). In the southeastern US, live turtles were taken to authorized rehabilitation facilities where diagnostic evaluation included fecal examination for endoparasites by direct smear and flotation. Necropsies were performed on turtles that died during rehabilitation or that were found deceased. Tissues for histopathology were fixed in neutral phosphate buffered formalin, processed into paraffin blocks, sectioned onto glass slides, and stained with hematoxylin and eosin using routine methods. These tissues typically included all major organ systems, including the brain, heart, lungs, liver, gastrointestinal tract, kidneys, spleen, pancreas, thyroid gland, and adrenal glands, but were limited to enteric lesions in some instances due to postmortem condition. For a subset of cases, sections of enteric contents or feces were frozen at −4 or −80°C for genetic study.

For the 2014/15 Florida epizootic, we developed a general case definition that characterized many of the increased strandings during this period. The intent of this case definition was to estimate the total number of stranded animals that may have been affected, but were not examined due to postmortem condition or other logistical reasons, and to examine the role of CLO infection. Our case definition criteria included stranded turtles without any traumatic injury or other external anomaly, including unusual epibiotic accumulation (an indication of chronic illness). In addition, we excluded clearly emaciated turtles but included those with indications of severe dehydration or lesser degrees of weight loss (based on subjective assessment), which are often externally difficult to distinguish and are evidenced by sunken eyes and gaunt neck, shoulder, and prefemoral regions (**Figure 1**).

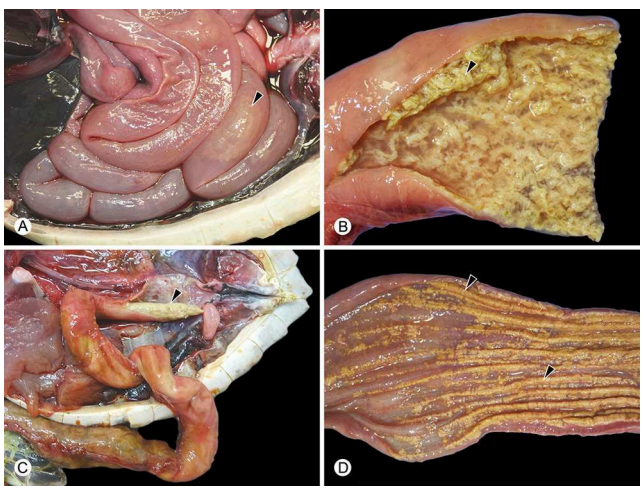

FIGURE 2 | Examples of gross findings in green turtles (*Chelonia mydas*) with enteric *Caryospora*-like coccidiosis. The genotype characterized during this study is provided in parentheses. **(A)** Abnormal watery enteric contents with gas formation (arrowhead) (US1). **(B)** Hyperplasia and sloughing (arrowhead) of the mucosa (US1). **(C)** Colitis (US2) resulting in formation of intraluminal casts of inflammatory exudate (arrowhead). **(D)** Colitis (US1) accompanied by multifocal or diffuse ulceration (arrowheads).

Genetic Characterization and Phylogenetic Analysis

We extracted DNA from enteric contents or feces of green turtles with CLOs using two types of commercial kits (DNeasy® Blood and Tissue Kit, Qiagen, Valencia, California, USA; ZR Fecal DNA Miniprep™ Zymo Research, Irvine, California, USA). The latter was used if failure to amplify DNA was suspected to have resulted from PCR inhibitors in feces. When possible, we concentrated oocysts for DNA extraction using Sheather's sugar flotation and

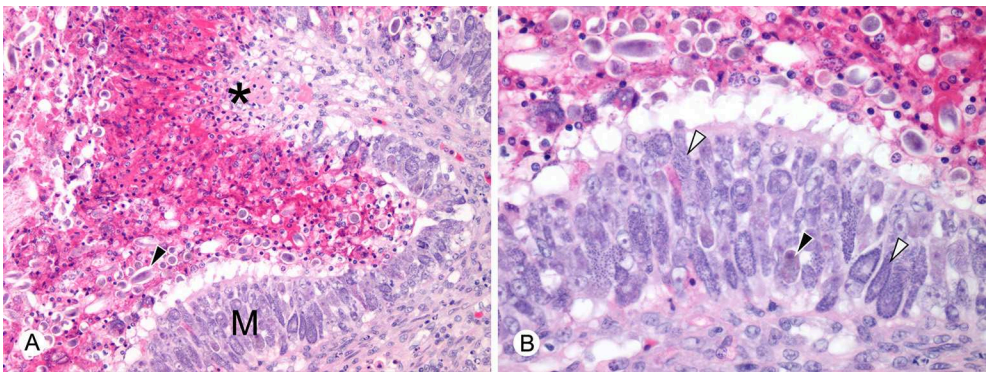

FIGURE 3 | Histopathological lesions in green turtles (*Chelonia mydas*) with enteric *Caryospora*-like coccidiosis (US1 genotype). **(A)** There is hyperplasia of enteric mucosa (M) bordering an area of ulceration (*). Numerous oocysts (arrowhead) are dispersed with heterophilic inflammation in the lumen. Scale bar = 98 μm. **(B)** At higher magnification, large numbers of macrogamonts (black arrowhead) and microgamonts (white arrowheads) are visible within enterocytes. Scale bar = 50 μm. Hematoxylin and eosin.

centrifugation (15). In addition, for comparative purposes, we also extracted DNA from CLOs found in feces from loggerhead (*Caretta caretta*) and Kemp's ridley turtles (*Lepidochelys kempii*), as well as an example of *Eimeria carettae* (16) from a loggerhead, the only described eimeriid species other than *C. cheloniae* reported in a sea turtle.

For genetic characterization, we targeted portions of the 18S ribosomal and MT-*coI* genes, and the ribosomal internal transcribed spacer regions (ITS1 and ITS2) (**Table 1**). For PCR reactions, we used Invitrogen Platinum Taq DNA polymerase (ThermoFisher Scientific, Massachusetts, USA) and the following parameters: denaturation at 94°C for 5 min, then 40 cycles of denaturation at 94°C (45 s), annealing temperature set at 5°C below primer melting temperatures (30 s), and extension at 72°C (60 s). The final extension step was at 72°C for 10 min. Amplicons of the expected size were submitted for Sanger sequencing in both directions (Genewiz, South Plainfield, New Jersey, USA). Sequence of the same genes was obtained from samples from a stranded turtle in Hawai'i and previously reported cases from Australia (4) using separate laboratories at those locations and similar methods.

Chromatographs were evaluated using Finch TV Version 14.0 (Geospiza, Inc., Seattle, Washington, USA). We used Clustal Omega to perform nucleotide sequence alignments and pairwise comparisons (17). Based on previous studies of inter- and intraspecific variation in the 18S and MT-*coI* genes of other apicomplexans (18, 19), unique genotypes were given numeric designations based on MT-*coI* sequence. If any variability was found in the 18S gene from samples with like MT-*coI* sequences, the organism was considered a variant and given an alphanumeric identifier (e.g., 9A, 9B). Genotypes were confirmed by sequences derived from multiple samples. If a genotype was represented by a single example, PCR and sequencing were repeated for confirmation. All chromatographs were reviewed for any nucleotide ambiguity as evidence of potential mixed infections. We required unambiguous 18S and MT-*coI* sequences to designate genotypes to help avoid mismatching of genetic data between types, which is an inherent risk of working with fecal samples that may include different coccidia.

We used the 18S for the phylogenetic analysis based on the additional variation observed in this gene as compared with the MT-*coI*, and the greater availability of 18S sequences of other coccidia in public databases. Five hundred and thirty-four positions were available for analysis after alignment. Smart Model Selection (20) was used to select TN93 as the most appropriate model, with a proportion of invariant sites and gamma distribution. Bayesian inference (BI) analysis was conducted using Mr.Bayes 3.2.6 (21). Three million generations were run, with samples taken every 300 generations. The first 10% of trees were discarded as burn-in, with convergence confirmed using Tracer 1.6 (22). Maximum likelihood (ML) analyses were performed using PhyML 3.0 (23) using the same model and 1,000 bootstrap replicates.

RESULTS

Description of 2014–2015 Epizootic and Other Reported US Cases

In November 2014, rehabilitation facilities began reporting stranded green turtles with coccidiosis along the southern Atlantic coast of Florida (Brevard County through Monroe County). Frequent reporting of these cases continued over the next several months, peaked in April 2015, and tapered off quickly thereafter. This epizootic coincided with a 36.1% increase in stranded green turtles ($n = 366$) relative to the previous 5-year average ($n = 269$) for the same area and time. Ninety-eight of these strandings met our case definition; 60 were found alive, 38 were deceased. The median SCL of these turtles was 27.9 cm (SE = 0.73, range = 13.2–55.5). This was less than that of other stranded green turtles found in these counties during the same time (39.9 cm, SE = 0.88, range = 21.9–71.0; Mann-Whitney U Test, $P < 0.001$) (**Figure 4**). Fifty of the turtles that met the case definition were screened for coccidia by fecal examination ($n = 13$), histopathology ($n = 33$), or both methods ($n = 4$); 45 were

TABLE 1 | Oligonucleotide primers used to amply the partial 18S ribosomal gene, mitochondrial cytochrome oxidase I gene (MT-*col*), and ribosomal internal transcribed spacer regions (ITS1 and 2).

Gene	Forward	F sequence	Reverse	R sequence
18S	Cary.18SF	5′-AGTTTCGAGGTAGTGACGAGA-3′	Cary.18S.R2	5′-CCTATCTCTAGTCGGCATAGTTT-3′
	Cary.18S.F2	5′-ACGAACTACTGCGAAAGCAT-3′	Cary.18SR	5′-CATCACAGACCTGTTATTGCCT-3′
	STCoccF	5′-CAAGAACGACAGTAGGGGGT-3′	STCoccR	5′- AGTGATGCGGAAACCAAAGT-3′
ITS1	Coc.NEW.18S.F	5′-CGGAAGGATCATTCACACGT-3′	Coc.ITS2.R	5′-GATGGTTCACTGAAATCTGCAA-3′
	Coc.NEW.18S.F	5′-CGGAAGGATCATTCACACGT-3′	Cary.5.8s.R	5′-CACTGAAATCTGCAATTCACAAT-3′
ITS2	Coc.5.8s.F	5′-ATGAAGRRCGCAGCGAA-3′	Coc.28s.R	5′-TCCTCCRCTTARTAATATGCTTAA-3′
MT-*col*	Cary.COI.F	5′-ATTTAATTGTAATTGGATTGGCT-3′	Cary.COI.R	5′-CTGTAGGGATAGCAATCATCAT-3′
	Cary.COI.F.2	5′-GTCTATTCACTTGGGCTATTGTATT-3′	Cary.COI.R	5′-CTGTAGGGATAGCAATCATCAT-3′

positive for CLOs. Nine of these turtles were found dead, 25 were found alive and later died, and 11 survived and were released following treatment at sea turtle rehabilitation facilities. Of the five turtles meeting the case definition in which CLOs were not detected, two had severe bacterial infections. A cause of stranding was not identified for the other three turtles.

During the epizootic, an additional 13 cases of CLO infection were detected in stranded green turtles that did not meet our case definition, including three turtles found in nearby counties of Volusia and St. Johns. These turtles were either emaciated and had abundant epibiota, or had other apparent causes of stranding, such as advanced fibropapillomatosis, vessel strike injuries, or shark bite wounds. These cases suggest that additional turtles that did not meet our case definition likely had clinically significant CLO infection; however, the numbers of turtles with these other issues that were found during the epizootic were not unusually high (i.e., did not account for the unusually high numbers of strandings during this time).

Turtles diagnosed with CLO infection by histopathology ($n = 31$) had enterocolic lesions like those previously described (8, 9). Grossly, the enterocolic contents were often watery and straw-colored with various degrees of gas formation (**Figures 2A,B**). Mucosal lesions ranged from hyperplasia to ulceration and were most consistently severe in the distal half of the small intestine, which was filled with fluid and sloughed mucosa. Developing stages of coccidia were numerous within enterocytes and were observed by histology in all areas of the intestine. Myriad oocysts were dispersed among sloughed cells and in the exudate within ulcerated areas (**Figure 3**). Histopathological examination included brain and other major organs in all 31 cases; no extra-intestinal coccidia were observed.

We concluded that CLO infections were a significant contributing cause of the elevated numbers of strandings during the epizootic based on the frequency of infection among examined stranded turtles (45/50 turtles) and the severity of enterocolic lesions in necropsied individuals. As will be reported elsewhere, some stranded turtles, including those with coccidiosis, also had concentrations of domoic acid or saxitoxins in organs and digestive contents exceeding 200 ng/g, which is above concentrations previously interpreted as asymptomatic exposure in marine mammals [e.g., (24, 25)]; thus, other factors in addition to coccidiosis may have played a causative role in the strandings during this period. Of particular relevance to comparison with prior CLO outbreaks, 24 of 35 live stranded turtles with coccidiosis exhibited lethargy, weakness, and abnormal neurological signs including loss of coordination and abnormal head movements, often in conjunction with severe hypoglycemia (<2 mg/dl). However, we found no histopathological evidence of neurological protozoal infection. Considerations for causes of the neurological abnormalities included hypoglycemia associated with protozoal enterocolitis, as well as biotoxicosis.

Following the 2014/15 coccidiosis epizootic, necropsies conducted by resource agencies and voluntary reporting of coccidial infections diagnosed at rehabilitation facilities throughout the southeastern US (Virginia to Texas) yielded 49 cases of CLO infection in green turtles through December 2018. Additional unreported cases were likely. The stranding locations of most of the infected turtles were distributed along the Atlantic coast of Florida, and included Georgia ($n = 1$) and South Carolina ($n = 2$). Some cases were reported in the Gulf of Mexico, including one case in Florida (Pinellas County) and four from Texas (Cameron County). In contrast to the relatively frequent diagnosis of fatal enterocolitis during the epizootic, most of the subsequent cases were live turtles with infections of indeterminate clinical significance due to multiple concurrent health problems or without any apparent clinical signs. Veterinarians specifically attributed clinical signs (including lethargy, dehydration, and weight loss) to coccidiosis in only 3 of 46 live turtles diagnosed with CLO infection based on fecal examination. To our knowledge, only three green turtles in which coccidiosis was identified as the cause of death have been recorded in the southeastern US since the epizootic (among 226 necropsies conducted in a manner where fatal coccidiosis would have been confidently detected). In addition, a stranded green turtle that died from severe enteric coccidiosis was found on Oahu, Hawai'i on March 8, 2018 representing the first case documented in the Central Pacific region.

In total, a review of available data yielded 113 confirmed cases of CLO infections in green turtles in US waters, including 5 cases prior to the 2014/15 epizootic, 58 during the epizootic, and 49 from subsequent years, as well as the single case from Hawai'i. We were able to genetically characterize the coccidia in 62 of these cases. In addition, we sequenced 18S and MT-*coI*

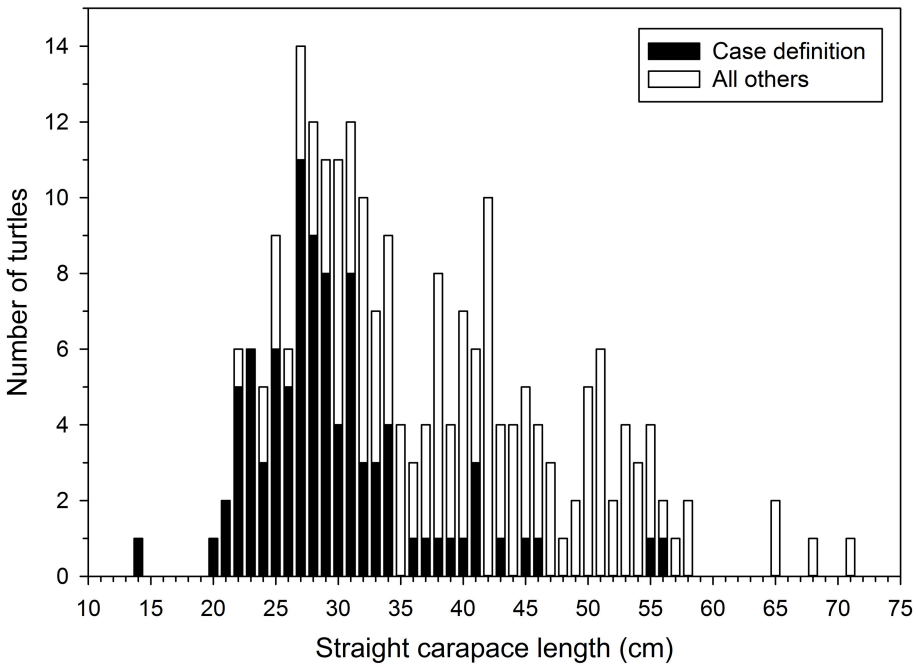

FIGURE 4 | Straight carapace lengths (SCL, nuchal notch to pygal tip) of stranded green turtles (*Chelonia mydas*) found in southeastern Florida during November 2014 through April 2015. The median SCL of turtles matching our case definition for suspected clinically significant *Caryspora*-like organism infections was less than that of all other green turtles that stranded during this same period and area.

genes from CLOs detected in five loggerhead turtles and two Kemp's ridleys, as well as coccidia from a loggerhead diagnosed as *E. carettae* based on oocyst morphology. As the general parasitological, clinical, and pathological findings associated with CLOs have been previously described, the remaining results focus on those cases in which genetic characterization of the coccidia was possible.

Genetic Characterization

Genotypic Variation

We sequenced a homologous 525 bp partial segment of the 18S gene and 344 bp of the MT-*coI* gene from all genotypes. We were able to sequence larger 810 bp sequences of the 18S gene from some cases and included this extra sequence data in our comparisons and submissions to GenBank; however, almost all of the variability within the 18S gene was present within the most consistently amplified shorter segment. We found 11 distinct genotypes among US samples, eight in green turtles, two in loggerheads (including that of *E. carettae*), and one in both loggerheads and Kemp's ridleys (**Table 2**). Pairwise percent identity comparisons are shown in **Table 3**. Most examples of each genotype were represented by identical 18S and MT-*coI* sequences; however, some variability was present within the 18S of coccidia with the same MT-*coI* sequence. These exceptions included US6 and 9, which had 2 and 3 variants, respectively, of the 18S gene. We were able to sequence the larger 18S partial sequence from most examples. The US9 18S variants had between 1 and 6 nucleotide differences; a single nucleotide difference was found between variants of US6. The single base position difference in US6 variants was within the additional larger sequence that was inconsistently available for all genotypes, thus individual US6 variants do not appear in the tables. Similar to US genotypes and as noted by Chapman et al. (4), there are 4 variants of the Australian genotype 1, designated here (with GenBank accession numbers) as Aus1A (KT361639), Aus1B (MN450829), Aus1C (MN450830), and Aus1D (MN450831), with up to 4 nucleotide differences within the 18S and identical MT-*coI* sequence (MN450846). We also sequenced the MT-*coI* gene (MN450847) from the previously reported Australian genotype 2 (KT361640).

We found evidence of additional genetic diversity among cases from the southeastern US, but did not designate more genotypes because we were either unable to obtain unambiguous sequence, likely due to mixed infections, or we could not sequence either the 18S or MT-*coI* for undetermined reasons. These instances included loggerheads with US4. Although we were able to repeatedly obtain unambiguous MT-*coI* sequence from one loggerhead and both Kemp's ridleys with US4, three other loggerheads had ambiguous peaks at several positions suggesting the presence of other genotypes. In addition, there were two unique genotypes found in individual green turtles represented by 18S or MT-*coI* sequence only (MN450828 and MN450845, respectively).

Comparison of Genotypes With Life History, Geography, and Disease

The species, SCLs, and locations where infected turtles were found are given for each US genotype in **Table 2**. Most genotypes

TABLE 2 | Genotypes of coccidia found in stranded sea turtles in the US by host species (Cm = *Chelonia mydas*; Cc = *Caretta caretta*; Lk = *Lepidochelys kempii*), turtle straight carapace length (measured from nuchal notch to caudal suprapygal scute, median given if $n > 4$), locations of discovery, number of examples representing each genotype, and GenBank accession numbers for corresponding 18S ribosomal and mitochondrial cytochrome oxidase I gene (MT-col) genes.

Genotype	Host species	SCL median	SCL range	Location(s)	No. of turtle hosts	GeneBank (18S)	GenBank (MT-*col*)
1	Cm	28.6	17.4–50.4	US-Atl;HW	24	MN450815	MN450832
2	Cm	25.4	19.9–68.4	US-Atl	9	MN450816	MN450833
3	Cm	30.3	22.1–52.5	US-Atl,GoM	12	MN450817	MN450834
4	Cc	69.7	7.6–80.9	US-Atl	4	MN450818	MN450835
	Lk	-	34.0–52.4	US-Atl	2		
5[a]	Cc	68.2	-	US-Atl	1	MN450819	MN450836
6	Cm	27.3	23.7–49.7	US-Atl	5	MN450820	MN450837
7	Cm	49.2	-	US-Atl	1	MN450821	MN450838
8	Cm	49.5	-	US-GoM	1	MN450822	MN450839
9[b]	Cm	30.8	27.5–104.2	US-Atl;Aus	9[b]	MN450823-25	MN450840-42
10	Cm	32.1	-	US-GoM	1	MN450826	MN450843
11	Cc	72.7	-	US-GoM	1	MN450827	MN450844

Locations are provided as the Atlantic coast of the US (US-Atl), Gulf of Mexico coast of the US (US-GoM), Hawai'i (HW), and eastern Australia (Aus).

[a] *Corresponds to Eimeria carettae.*

[b] *The following are the number of individual cases for each of 3 variants of this genotype: 9A (n = 2); 9B (n = 4); 9C (n = 2).*

were only found in one host species; US4 was found in both loggerheads and Kemp's ridleys. All but two infected turtles were neritic phase juveniles within the size range typically found within habitat near where they stranded. Infected sea turtles of other life phases that we documented included a post-hatchling loggerhead (SCL = 7.6 cm) with US4 and an adult green turtle (SCL = 104.2 cm) with US9.

Coccidia from green turtles found prior to the Florida epizootic, including the first detected case in a free-ranging green turtle in 2007 and one of the initial stranded green turtles found in Florida in 2012, were genotypes US6 and 3, respectively. Of the 19 cases with sequence data from the 2014/15 Florida epizootic, all but one was US1. In contrast, of sequences from 35 green turtles found after the Florida epizootic, four were US1, seven were US2, eight were US3, four were US6, eight were US9, one each were US7, US8, and US10, and one was a mixed infection of US2 and US3 evidenced by clear double peaks at the expected locations in the chromatographs.

Coccidia infecting the stranded green turtle found in Hawai'i were also US1. As we were surprised to find identical genotypes in different ocean basins, we also sequenced the two ITS regions to further examine genetic similarity. Examples of US1 from the southeastern US and Hawai'i were identical across 18S, MT-*coI*, and both ribosomal spacer regions (MN450848).

In addition, the 18S and MT-*coI* of US9C genotype were identical to a genotype found in Australia, Aus1C. We were able to sequence most of the ITS2 and found 4/382 nucleotide differences between US9C (MN450849) and Aus1C (MN450850). Multiple attempts to obtain sequences for the ITS1 of these genotypes failed.

When genotypes were compared with clinical history and necropsy findings, some infections with US1 ($n = 16$), US2 ($n = 4$), US3 ($n = 1$), US9B ($n = 1$), US11 ($n = 1$), and a mixed infection of US2 and US3 ($n = 1$) were regarded as clinically significant. Clinical significance of the remainder was unclear. Coccidial enterocolitis was confirmed by histopathology in turtles parasitized by US1 ($n = 16$), 2 ($n = 2$), and 9B ($n = 1$) with the small intestine being the most affected in examples of US1 and 9B (**Figures 2A,B**). In three cases with US1 or US2, the most prominent gross lesion was ulcerative colitis covered by tenacious exudate (**Figures 2C,D**). Histopathological examination included the brain and other major organs of 14 turtles infected with US1 and one turtle with US9B; no coccidia were found in extra-intestinal tissues. All other genotypes were derived from coccidia found in feces of live turtles that survived, thus necropsy data were not available.

Phylogenetic Analysis

The Bayesian Inference and Maximum Likelihood analyses using the 18S gene produced phylogenetic trees of similar topology (**Figures 5**, **6**). The US and Australian sequences included in this study formed two clades. The first, containing all Australian genotype 1 variants and all US genotypes but one, was sister to another clade containing the *Schellackia* and several species of *Eimeria* infecting amphibians and reptiles. The second clade was comprised of US Type 7, Australian Type 2, and two Eimeriid coccidian sequences obtained from leatherback turtles (KT956976 and KT956977), and was basal to another containing species of *Isospora* and *Eimeria*. Notably, two sequences from apicomplexans infecting green turtles in Australia, obtained from Genbank, were split between the first, larger clade containing our sea turtle coccidia (KY046255) and the *Schellackia*/*Eimeria* clade (KY046254). Similar analysis of the MT-*coI* did not yield additional resolution (data not shown).

DISCUSSION

We describe the first epizootic of CLOs in free-ranging sea turtles in the northern hemisphere and report observations related to coccidial infections among stranded turtles in the US in recent

TABLE 3 | Percentage identity matrix of partial 18S ribosomal (above diagonal line) and mitochondrial cytochrome oxidase I (MT-*coI*, below diagonal line) genes of coccidia from green turtles (*Chelonia mydas*), loggerhead turtles (*Caretta caretta*), and Kemp's ridley turtles (*Lepidochelys kempii*) collected in the southeastern US and Australia (Aus).

	US.1	US.2	US.3	US.4	US.5	US.6	US.7	US.8	US.9A	US.9B	US.9C	US.10	US.11	Aus.1A	Aus.1B	Aus.1C	Aus.1D	Aus.2
US.1		98.86	98.86	99.24	98.86	99.43	92.57	98.48	98.67	98.86	99.05	99.43	99.60	99.43	100.00	99.05	99.24	91.79
US.2	99.47		99.24	99.62	99.24	99.43	92.95	99.62	99.05	99.24	99.05	99.43	99.20	99.43	98.86	99.05	99.62	92.18
US.3	98.55	95.35		99.62	99.62	99.43	92.76	98.86	98.86	99.05	99.05	99.05	99.20	99.43	98.86	99.05	99.24	91.98
US.4	96.80	95.06	97.67		99.62	99.81	92.95	99.24	99.05	99.24	99.43	99.43	99.60	99.81	99.24	99.43	99.62	92.18
US.5	97.67	95.93	98.55	99.13		99.43	92.76	98.86	98.86	99.05	99.05	99.05	99.20	99.43	98.86	99.05	99.24	91.98
US.6	97.97	94.77	97.67	96.22	97.09		92.76	99.05	99.24	99.43	99.62	99.60	99.80	100.00	99.43	99.62	99.81	91.98
US.7	88.37	87.79	88.08	87.79	88.37	88.37		92.57	92.38	92.57	92.38	92.95	92.61	92.76	92.57	92.38	92.95	99.05
US.8	95.35	99.42	95.93	95.06	95.93	95.06	87.50		99.05	99.24	98.67	99.05	98.80	99.05	98.48	98.67	99.24	91.79
US.9A	99.42	95.06	99.13	97.38	98.26	97.97	88.95	95.64		99.81	98.86	99.24	99.00	99.24	98.67	98.86	99.43	91.60
US.9B	99.42	95.06	99.13	97.38	98.26	97.97	88.95	95.64	100.00		99.05	99.43	99.20	99.43	98.86	99.05	99.62	91.79
US.9C	99.42	95.06	99.13	97.38	98.26	97.97	88.95	95.64	100.00	100.00		99.24	99.40	99.62	99.05	100.00	99.43	91.60
US.10	99.71	95.06	98.84	97.09	97.97	98.26	88.66	95.64	99.71	99.71	99.71		99.40	99.62	99.43	99.24	99.81	92.18
US.11	99.42	95.35	99.13	97.38	98.26	98.55	88.37	95.93	99.42	99.42	99.42	99.71		99.80	99.60	99.40	99.60	91.80
Aus.1A	99.42	95.06	99.13	97.38	98.26	97.97	88.95	95.64	100.00	100.00	100.00	99.71	99.42		99.43	99.62	99.81	91.98
Aus.1B	99.42	95.06	99.13	97.38	98.26	97.97	88.95	95.64	100.00	100.00	100.00	99.71	99.42	100.00		99.05	99.24	91.79
Aus.1C	99.42	95.06	99.13	97.38	98.26	97.97	88.95	95.64	100.00	100.00	100.00	99.71	99.42	100.00	100.00		99.43	91.60
Aus.1D	99.42	95.06	99.13	97.38	98.26	97.97	88.95	95.64	100.00	100.00	100.00	99.71	99.42	100.00	100.00	100.00		92.18
Aus.2	89.24	87.50	88.95	88.66	89.24	89.24	97.38	87.79	89.83	89.86	89.83	89.53	89.24	89.83	89.83	89.83	89.83	

Genotype numbers reflect MT-coI sequences; letters are assigned to variants with variable 18S sequences, but identical MT-coI sequences. US5 corresponds to Eimeria carettae. All other genotypes are Caryospora-like based on morphological similarity to C. cheloniae.

years. Although we detected inter- and intraregional genetic variation among coccidia with oocysts that resemble previous descriptions of *C. cheloniae*, we found identical or highly similar genotypes in both Atlantic and Pacific green turtles based on genes known to exhibit interregional diversity in other species of Apicomplexa (18, 19, 26). Of particular concern with regard to wildlife health is that these genotypes were found during epizootics involving green turtles in the US and Australia.

The first report of *C. cheloniae* in maricultured turtles at a facility in the Cayman Islands predated molecular methods. Researchers relied on morphology for later comparisons and attributed the first epizootic involving wild green turtles in Australia to *C. cheloniae* based on the original description (9). Chapman et al. (4) provided the first genetic data on CLOs in Australian green turtles from a later epizootic, demonstrating genetic differences among organisms associated with the outbreak and noting problems with the current taxonomy. Our analyses are in agreement with previous studies, showing at least three distinct clades in the Eimeriidae that are all called *Caryospora*, in addition to the paraphyly of *Eimeria*, *Schellackia*, *Lankesterella*, and *Isospora*. Phylogenetic classification of coccidia based on sporulation patterns has proven problematic due to significant homoplasy in this characteristic. Gene sequence data have often been useful in determining which morphologic/life cycle characteristics of coccidians are phylogenetically informative. Using molecular data, organisms previously all labeled as *Isospora* based on sporulation patterns were recognized as *Isospora* and *Cystoisospora*, indicating that the presence or absence of Stieda bodies, the use of paratenic hosts, and avian or mammalian host specificity, are more phylogenetically informative than the number of sporocysts or sporozoites for these genera (27). Indeed, some of the *Cystoisospora* inconsistently undergo sporulation patterns that would cause them to be misidentified as *Caryospora* (28, 29). Revision of current taxonomy is expected, and the CLOs of sea turtles may well prove to be a novel genus; this will require sequence data of *C. simplex* to determine.

In the US, resource agencies, academic programs, and rehabilitation organizations have studied sea turtle strandings through clinical evaluation and necropsy in the decades following the original Caribbean epizootic. Although there have been parasitological descriptions of coccidia in loggerheads and leatherbacks (16, 30) and numerous studies of diseases affecting green turtles in the Northwest Atlantic and Central Pacific [e.g., (31, 32)], there were no reports of enteric coccidiosis associated with morbidity or mortality of wild sea turtles in these regions prior to 2012. Recent attention resulting from the 2014/15 US coccidiosis epizootic undoubtedly facilitated discovery of subsequent cases detected in our study; however, given the previous surveillance effort, we believe clinically significant enteric coccidiosis is a newly emergent disease of green turtles in the northern hemisphere.

Genetic characterization allowed us to demonstrate that the Florida epizootic was largely attributable to coccidia of a single genotype, US1, and that this genotype also was linked to the first case of enteric coccidiosis identified in Hawai'i. In addition, we found another coccidian genotype in two stranded green

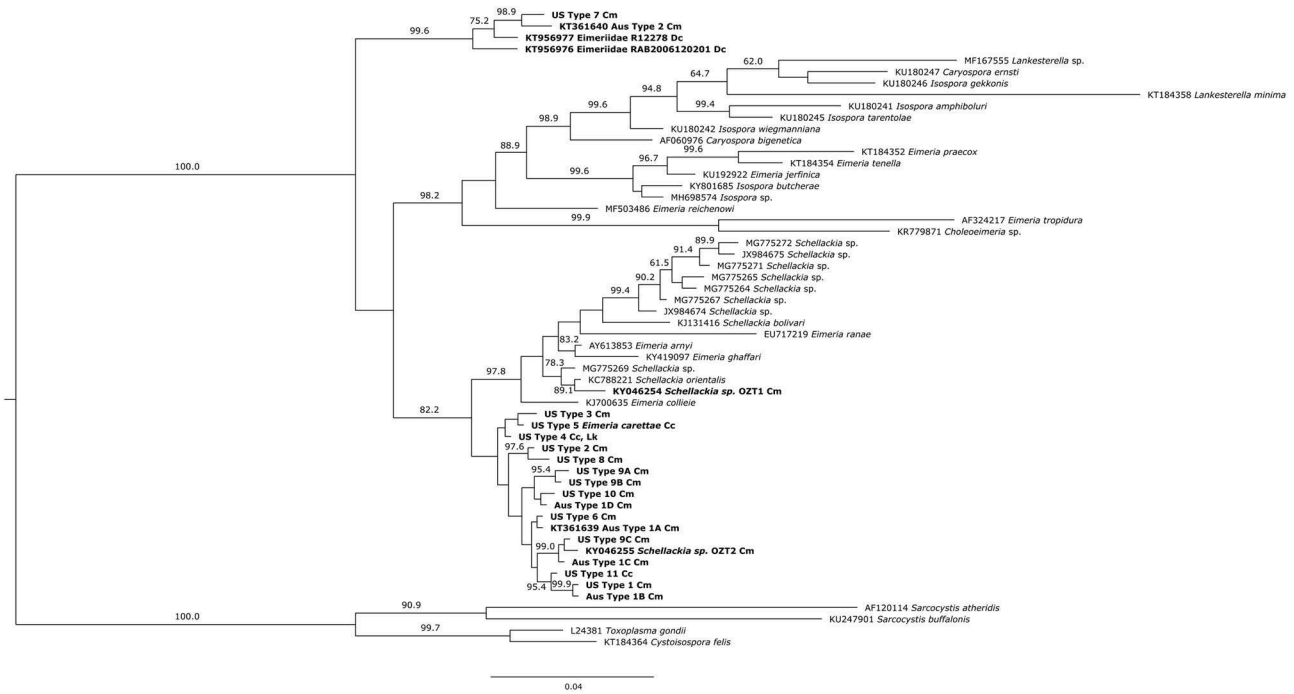

FIGURE 5 | Bayesian inference analysis of partial 18S sequences from sea turtle coccidia and related taxa. Bold type indicates sequences obtained from sea turtle coccidia; host species is indicated by abbreviations following sequence name (Cm = *Chelonia mydas*; Cc = *Caretta caretta*; Dc = *Dermochelys coriacea*; Lk = *Lepidochelys kempii*). Numbers on branches indicate posterior probabilities as a percentage; values under 60% are not shown. Scale bar indicates the number of nucleotide substitutions per site.

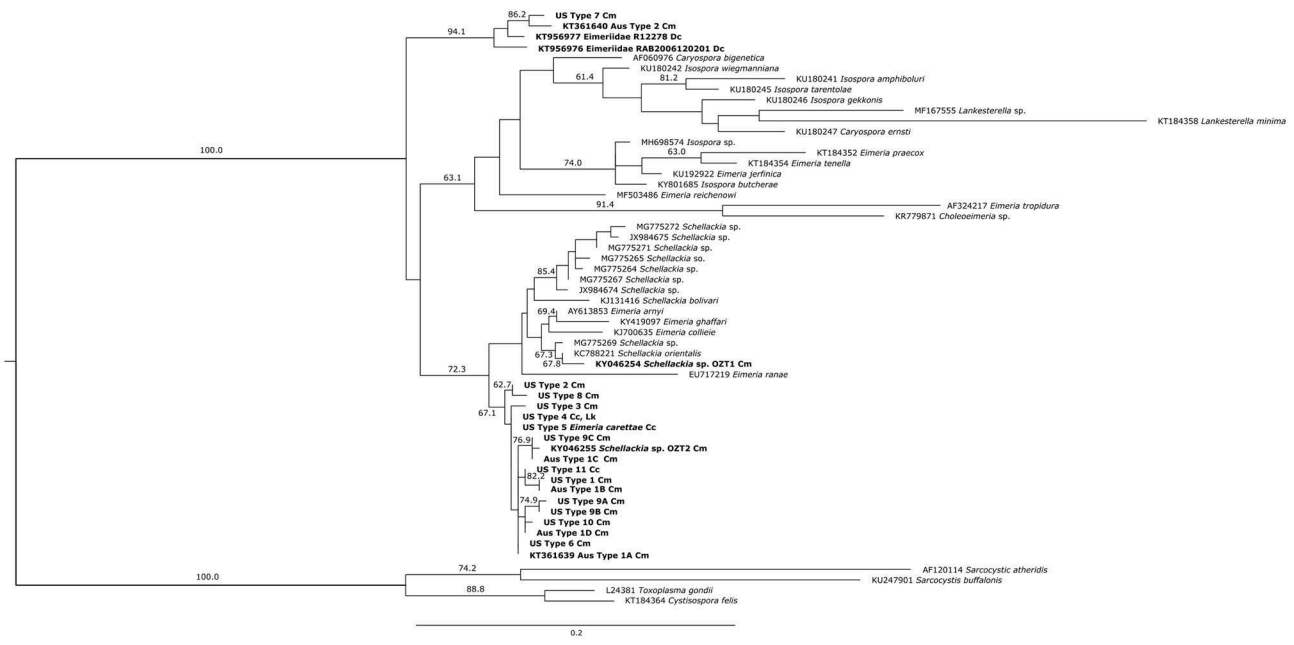

FIGURE 6 | Maximum likelihood analysis of partial 18S sequences from sea turtle coccidia and related taxa. Bold type indicates sequences obtained from sea turtle coccidia; host species is indicated by abbreviations following sequence name (Cm = *Chelonia mydas*; Cc = *Caretta caretta*; Dc = *Dermochelys coriacea*; Lk = *Lepidochelys kempii*). Numbers on branches indicate bootstrap values as a percentage; values under 60% are not shown. Scale bar indicates the number of nucleotide substitutions per site.

turtles in Florida that was highly similar to one characterized during an Australian epizootic in 2014. These findings show lack of variability across the three different genetic loci most commonly used to study intraspecific diversity in a variety of taxa. Limited genetic diversity among parasites and lack of geographical relation are indications of pathogen emergence and anthropogenic spread (33, 34). Although additional studies are prudent, our findings indicate a substantial probability that pathogenic coccidia of sea turtles have undergone recent dissemination among ocean basins.

Large-scale spread of coccidia could occur though transportation or migration of infected hosts or transport of oocysts. Although movement or comingling of infected sea turtles within ocean basins is possible, interoceanic movement is highly improbable. The separation of Atlantic and Indo-Pacific green turtle populations is ancient with minimal recent gene flow (35). Infected intermediate hosts also may spread coccidia. Low intraspecific variation is described in *Sarcocystis* spp. that use birds as intermediate hosts (36). It is unknown whether CLOs found in sea turtles have direct or indirect life cycles (4). Regardless, we are unaware of any candidate intermediate hosts that naturally move between the Pacific and Atlantic Oceans. There are numerous examples of recent range shifts by marine organisms associated with warming sea temperatures that could influence pathogen distribution; however, most of the shifts studied to date have been latitudinal within ocean basins (37).

Anthropogenic transport of oocysts or infected intermediate hosts is another possibility. The resilience of *Caryospora* oocysts have not been specifically studied, but coccidian oocysts in general are well-known for their stability in the environment and resistance to chemical disinfection (38). It is plausible that oocysts or infected intermediate hosts could be transported between distant locations in ballast water aboard ships. Ballast water is known to be a potential means of transport of marine organisms, including protozoa, algae, and invertebrates (39–41). Examination of seawater, ballast water, and potential intermediate hosts for CLOs would be valuable in exploring possible avenues of transmission and associated potential risks of human-mediated dissemination of coccidia.

As with locality, there was no apparent phylogenetic structuring of the coccidia by host species, which suggests a history of host switching rather than diversification through prolonged species coevolution. Detection of US4 in both loggerhead and Kemp's ridley turtles was somewhat unsurprising as these species have similar diets and are hosts for a number of the same metazoan parasites (42, 43). In addition, our phylogenetic analyses did not provide further insight into apparent differences in tissue distribution of coccidia, which is one of the most remarkable dissimilarities among reports from Australia and those from the northern hemisphere. Coccidia have been consistently described in extra-intestinal locations, including the brain, thyroid gland, and kidneys in Australian epizootics, accompanied by neurological signs, whereas organisms have only been observed thus far in the mucosa of the digestive tract in US cases. Histopathological findings from green turtles found in the US with confirmed CLO infection included examination of the brain and other organs from a total of 38 green turtles, including 14 with US1, one with US9B, and 23 from the 2014/15 epizootic where genotype was not identified, but was most likely US1. Because many of the US genotypes were found in live turtles that survived, including US9C with its high similarity to Aus1C, additional study of tissue distribution is required.

We do not yet have enough information to compare differences in pathogenicity among the coccidian genotypes. Some of the genotypes, especially US1 and those found in Australia, clearly cause significant disease in some sea turtles, but others were detected without clinically apparent effect or possible masking of any signs by concurrent health problems, including coccidia found in loggerheads and Kemp's ridleys. Turtles without evident clinical signs that are shedding oocytes may have had enteric lesions of limited distribution or that were uncomplicated by secondary bacterial infection. Subclinical shedding may pose a risk to other sea turtles, especially in captive situations, thus regular fecal examinations using flotation methods are a sensible component of initial clinical evaluation and subsequent assessments.

Stranded sea turtles with coccidia have occurred in Australia during spring, leading to a hypothesis that warming water temperatures may play a role in development of clinical disease (4). However, at least in the southeastern US, sea turtle strandings peak in the spring regardless of cause, so it is unclear whether seasonality of coccidial infections exists in this region.

Previous reports of CLO infections in sea turtles include all life stages from hatchlings to adults (4, 8, 9). In the first reported Australia epizootic, most affected turtles were immature (9), whereas adult turtles were thought more susceptible during a subsequent large outbreak (4). The median SCL of green turtles affected during the Florida epizootic was lower than concurrent strandings of the same species that did not meet our case definition, suggesting that smaller juveniles were disproportionately affected. However, we did not sufficiently screen turtles of other sizes during the epizootic to explore more confidently the relationship between size and CLO infection. Given the inherent biases related to study of stranded sea turtles, future studies examining parasite prevalence in free-ranging sea turtles during the course of in-water sea turtle research are needed in order to better understand prevalence among size classes.

Enteric coccidiosis resulting from CLOs is one of very few known infectious causes of episodic mass stranding and mortality events involving sea turtles. Although study of epizootics has characterized the pathology of CLO infections and the demography of affected turtles, many aspects of these parasites remain poorly understood, including their life cycle and dynamics of infection in free-ranging sea turtle populations. Multi-institutional, international collaboration in the current study allowed us to examine CLO infections for the first time over a large spatial scale and to undertake intensive screening

and sampling of stranded turtles to gain a more complete appreciation of the genetic diversity of these parasites and their global distribution. Moreover, the discovery of genetically identical organisms in different ocean basins raises significant concerns regarding the potential for human-mediated spread of these sea turtle pathogens.

DATA AVAILABILITY STATEMENT

The raw data supporting the conclusions of this manuscript will be made available by the authors, without undue reservation, to any qualified researcher.

ETHICS STATEMENT

The animal study was reviewed and approved by University of Florida IACUC.

AUTHOR CONTRIBUTIONS

All authors contributed to data and sample collection and review and preparation of the manuscript. In addition, data analyses were conducted by BS, PC, HS-W, TW, JD, AF, MW, and JW.

FUNDING

The Australian Research Council (Linkage Grant LP110100569) provided funding for characterization of Australian samples.

ACKNOWLEDGMENTS

We thank the participants in the sea turtle stranding networks in the southeastern US, Hawai'i, and Australia for information collected from stranded sea turtles. We also thank staff of the Turtle Hospital, Miami Seaquarium, Loggerhead Marinelife Center, Volusia Marine Science Center, Sea World Orlando, Sea Turtle, Inc., South Carolina Aquarium, Gumbo Limbo Nature Center, Brevard Zoo, Clearwater Marine Aquarium, and Georgia Sea Turtle Center that participated in data and sample collection. In addition, we appreciate the valuable contributions of Leanne Flewelling, Nina Thompson, Shanon Gann, Jessica Patterson, and Melanie Stadler related to sampling and lab analyses and thank Christine Sundermann for her review of the manuscript.

REFERENCES

1. Léger L. Protozoaires parasites des vipéres (Vipera aspis). *Bulletin Mensuel, Association Francaise pour l'avancement des Sciences (Abstract)*. (1904) 9:268.
2. Duszynski DW, Couch L, Upton, S.J. *The Coccidia of the World. Supported by NSF grant PEET DEB 9521687* (1998).
3. Yang R, Brice B, Ryan U. A new *Caryospora* coccidian species (Apicomplexa: Eimeriidae) from the laughing kookaburra (*Dacelo novaeguineae*). *Exp Parasitol*. (2014) 145:68–73. doi: 10.1016/j.exppara.2014.07.008
4. Chapman PA, Owen H, Flint M, Traub RJ, Cribb TH, Mills PC. Molecular characterization of coccidia associated with an epizootic in green sea turtles (*Chelonia mydas*) in South East Queensland, Australia. *PLoS ONE*. 11:e0149962. doi: 10.1371/journal.pone.0149962
5. Santana-Sánchez G, Flores-Valle IT, González-Gómez M, Vega-Sánchez V, Salgado-Miranda C, Soriano-Vargas E. *Caryospora neofalconis* and other enteroparasites in raptors from Mexico. *Int J Parasitol Parasites Wildl*. (2015) 22:351–5. doi: 10.1016/j.ijppaw.2015.08.004
6. Megía-Palma RM, Martinez JD, Nasri I, Cuervo JJ, Martín JM, Acevedo ID, et al. Phylogenetic relationships of *Isospora*, *Lankesterella*, and *Caryospora* species (Apicomplexa: Eimeriidae) infecting lizards. *Org Divers Evol*. (2016) 16:275–88. doi: 10.1007/s13127-015-0253-3
7. Rebell G, Rywlin A, Ulrich G. Coccidiosis in the green turtle in mariculture (*Chelonia mydas*). *J World Aquacult Soc*. (1974) 5:197–204. doi: 10.1111/j.1749-7345.1974.tb00190.x
8. Leibovitz L, Rebell G, Boucher GC. *Caryospora cheloniae* sp. *n: A coccidial pathogen of mariculturereared green sea turtles (Chelonia mydas mydas). J Wildl Dis*. (1978) 14:269–75. doi: 10.7589/0090-3558-14.2.269
9. Gordon AN, Kelly WR, Lester RJG. Epizootic mortality of free-living green turtles, *Chelonia mydas*, due to coccidiosis. *J Wildl Dis*. (1993) 29:490–4. doi: 10.7589/0090-3558-29.3.490
10. Flint M, Patterson-Kane JC, Limpus CJ, Work TM, Blair D, Mills PC. Postmortem diagnostic investigation of disease in free-ranging marine turtle populations: a review of common pathologic findings and protocols. *J Vet Diagn Investig*. (2009) 21:733–59. doi: 10.1177/104063870902100601
11. Conde B, Alvarado MC, Espinoza-Ridríguez N, Barrios-Garrido H. Primer reporte de coccidiosis en tortugas verdes (*Chelonia mydas*) del Golfo de Venezuela. *Zoología*. (2019) 42:278–88. doi: 10.15446/caldasia.v41n2.66421
12. Pelton CA, Boylan B, Stacy N, McIntosh A, Walsh M, Ranly M, et al. The use of triazinones for the treatment of coccidia morphologically resembling *Caryospora cheloniae* in green sea turtles (*Chelonia mydas*). In: *International Association of Aquatic Animal Veterinarians 44th Annual Conference Proceedings, April 21–26, 2013*. Sausalito, CA (2013). p. 81–2.
13. Manire CA, Montgomery NB. Intestinal coccidia resembling *Caryospora* spp. in green and loggerhead sea turtles: occurrence and effective treatment. In: *International Association of Aquatic Animal Veterinarians 45th Annual Conference Proceedings, May 17–21, 2014*. Gold Coast, QLD (2014). Available online at: https://www.vin.com/apputil/content/defaultadv1.aspx?id=6251967&pid=11397 (accessed September 27, 2019).
14. Foley AM, Schroeder BA, Redlow AE, Fick-Child KJ, Teas WG. Fibropapillomatosis in stranded green turtles (*Chelonia mydas*) from the eastern United States (1980–98): trends and associations with environmental factors. *J Wildl Dis*. (2005) 41:29–41. doi: 10.7589/0090-3558-41.1.29
15. Zajac AM, Conboy GA. *Veterinary Clinical Parasitology*. 8th ed. Ames, IA: Blackwell Publishing (2012). p. 368.
16. Upton SJ, Odell DK, Walsh MT. *Eimeria caretta* sp.nov. (Apicomplexa: Eimeriidae) from the loggerhead sea turtle, *Caretta caretta* (Testudines). *Can J Zoolog*. (1990) 68:1268–9. doi: 10.1139/z90-189
17. Chojnacki S, Cowley A, Lee J, Foix A, Lopez, R. Programmatic access to bioinformatics tools from EMBL-EBI update. *Nucleic Acids* Res. (2017) 45:W550–3. doi: 10.1093/nar/gkx273
18. Gjerde B, Luzón M, Alunda JM, de la Fuente C. Morphological and molecular characteristics of six *Sarcocystis* spp. from red deer (*Cervus elaphus*) in Spain, including *Sarcocystis cervicanis* and three new species. *Parasitol Res*. (2017) 116:2795–811. doi: 10.1007/s00436-017-5590-z
19. Murata R, Suzuki J, Hyuga A, Shinkai T, Sadamasu K. Molecular identification and characterization of *Sarcocystis* spp. in horsemeat and beef marketed in Japan. *Parasite*. (2018) 25:27. doi: 10.1051/parasite/2018026
20. Lefort V, Longueville JE, Gascuel O. SMS: smart model selection in PhyML. *Mol Biol Evol*. (2017) 34:2422–4. doi: 10.1093/molbev/msx149
21. Ronquist F, Teslenko M, van der Mark P, Ayres DL, Darling A, Höhna S, et al. MrBayes 3.2: efficient Bayesian phylogenetic inference and model choice across a large model space. *Syst Biol*. (2012) 61:539–42. doi: 10.1093/sysbio/sys029

22. Rambaut A, Suchard M, Drummond AJ. *Tracer v1.6* (2014). Available online at: http://beast.bio.ed.ac.uk/Tracer/ (accessed April 19, 2019).
23. Guindon S, Dufayard JF, Lefort V, Anisimova M, Hordijk W, Gascuel, O. New algorithms and methods to estimate maximum-likelihood phylogenies: assessing the performance of PhyML 3.0. *Mol Biol Evol*. (2010) 34:2422–4. doi: 10.1093/sysbio/syq010
24. Fire SE, Wang Z, Byrd M, Whitehead HR, Paternoster J, Morton SL. Co-occurrence of multiple classes of harmful algal toxins in bottlenose dolphins (*Tursiops truncatus*) stranding during an unusual mortality event in Texas, USA. *Harmful Algae*. (2011) 10:330–6. doi: 10.1016/j.hal.2010.12.001
25. Twiner MJ, Schwacke L, Davidson L, Wang Z, Morton S, Roth S, et al. Concurrent exposure of bottlenose dolphins (*Tursiops truncatus*) to multiple algal toxins in Sarasota Bay, Florida, USA. *PLoS ONE*. (2011) 6:e17394. doi: 10.1371/journal.pone.0017394
26. El-Sherry S, Ogedengbe ME, Hafeez MA, Barta JR. Divergent nuclear 18S rDNA paralogs in a turkey coccidium, *Eimeria meleagrimitis*, complicate molecular systematics and identification. *Int J Parasitol*. (2013) 43:679–85. doi: 10.1016/j.ijpara.2013.03.005
27. Barta JR, Schrenzel MD, Carreno R, Rideout BA. The genus *Atoxoplasma* (Garnham 1950) as a junior objective synonym of the genus *Isospora* (Schneider 1881) species infecting birds and resurrection of *Cystoisospora* (Frenkel 1977) as the correct genus for Isospora species infecting mammals. *J. Parasitol*. (2005) 91:726–7. doi: 10.1645/GE-3341.1
28. Houk AE, O'Connor T, Pena HF, Gennari SM, Zajac AM, Lindsay DS. Experimentally induced clinical *Cystoisospora canis* coccidiosis in dogs with prior natural patent *Cystoisospora ohioensis*-like or *C. canis* infections. *J Parasitol*. (2013) 99:892–5. doi: 10.1645/13-197.1
29. Jongwutiwes S, Putaporntip C, Charoenkorn M, Iwasaki T, Endo T. Morphologic and molecular characterization of *Isospora belli* oocysts from patients in Thailand. *Am J Trop Med Hyg*. (2007) 77:107–12. doi: 10.4269/ajtmh.2007.77.107
30. Ferguson SD, Wellehan JF Jr, Frasca S Jr, Innis CJ, Harris HS, Miller M, et al. Coccidial infection of the adrenal glands of leatherback sea turtles (*Dermochelys coriacea*). *J Wildl Dis*. (2016) 52:874–82. doi: 10.7589/2015-11-310
31. Stacy BA, Foley AM, Greiner E, Herbst LH, Bolten A, Klein P, et al. Spirorchiidiasis in stranded loggerhead *Caretta caretta* and green turtles *Chelonia mydas* in Florida (USA): host pathology and significance. *Dis Aquat Organ*. (2010) 89:237–59. doi: 10.3354/dao02195
32. Work TM, Balazs GH, Summers TM, Hapdei JR, Tagarino AP. Causes of mortality in green turtles from Hawaii and the insular Pacific exclusive of fibropapillomatosis. *Dis Aquat Organ*. (2015) 115:103–10. doi: 10.3354/dao02890
33. Rosenthal BM, Dunams DB, Pritt B. Restricted genetic diversity in the ubiquitous cattle parasite, *Sarcocystis cruzi*. *Infect Genet Evol*. (2008) 8:588–92. doi: 10.1016/j.meegid.2008.04.004
34. Maharramov J, Meeus I, Maebe K, Arbetman M, Morales C, Graystock P, et al. Genetic variability of the neogregarine *Apicystis bombi*, an etiological agent of an emergent bumblebee disease. *PLoS One*. (2013) 8:e81475. doi: 10.1371/journal.pone.0081475
35. Bowen BW, Karl SA. Population genetics and phylogeography of sea turtles. *Mol Ecol*. (2007) 16:4886–907. doi: 10.1111/j.1365-294X.2007.03542.x
36. Prakas P, Oksanen A, Butkauskas D, Sruoga A, Kutkiene L, ŠvaŽas S, et al. Identification and intraspecific genetic diversity of *Sarcocytsis rileyi* from ducks, *Anas* spp., in Lithuania and Finland. *J Parasitol*. (2014) 100:657–61. doi: 10.1645/13-395.1
37. Sorte CJB, Williams SL, Carlton JT. Marine range shifts and species introductions: comparative spread rates and community impacts. *Global Ecol Biogeogr*. (2010) 19:3030–316. doi: 10.1111/j.1466-8238.2009.00519.x
38. Daugschies A, Bangoura B, Lendner M. Inactivation of exogenous endoparasite stages by chemical disinfectants: current state and perspectives. *Parasitol Res*. (2013) 112:917–32. doi: 10.1007/s00436-013-3324-4
39. Galil BS, Hülsmann N. Protist transport via ballast water - biological classification of ballast tanks by food web interactions. *Europ J Protistol*. (1997) 33:244–53. doi: 10.1016/S0932-4739(97)80002-8
40. Bax N, Williamson A, Aguero M, Gonzalez E, Geeves W. Marine invasive alien species: a threat to global biodiversity. *Mar Policy*. (2003) 27:313–23. doi: 10.1016/S0308-597X(03)00041-1
41. Shaw JLA, Weyrich LS, Hallegraeff G, Cooper A. Retrospective eDNA assessment of potentially harmful algae in historical ship ballast tank and marine port sediments. *Mol Ecol*. (2019) 28:2476–85. doi: 10.1111/mec.15055
42. Greiner EC. Parasites of Sea Turtles. In: Wyneken J, Lohmann KJ, Musick JA, editors. *The Biology of Sea Turtles*, Vol. III. Boca Raton, FL: CRC Press (2013). p. 427–46.
43. Stacy BA, Chapman PA, Foley AM, Greiner EC, Herbst LH, Bolten AB, et al. Evidence of diversity, site, and host specificity of sea turtle blood flukes (Digenea: Schistosomatoidae: "Spirorchiidae"): a molecular prospecting study. *J Parastol*. (2017) 103:756–67. doi: 10.1645/16-31

Disclaimer: The statements and findings are those of the authors and do not necessarily reflect the view of NOAA or the US Department of Commerce.

Conflict of Interest: MR is employed by Miami Seaquarium and LS is employed by SeaWorld Orlando.

The remaining authors declare that the research was conducted in the absence of any commercial or financial relationships that could be construed as a potential conflict of interest.

Copyright © 2019 Stacy, Chapman, Stockdale-Walden, Work, Dagenais, Foley, Wideroff, Wellehan, Childress, Manire, Rodriguez, Zachariah, Staggs, Zirkelbach, Nahvi, Crowder, Boylan, Marquardt, Pelton and Norton. This is an open-access article distributed under the terms of the Creative Commons Attribution License (CC BY). The use, distribution or reproduction in other forums is permitted, provided the original author(s) and the copyright owner(s) are credited and that the original publication in this journal is cited, in accordance with accepted academic practice. No use, distribution or reproduction is permitted which does not comply with these terms.

frontiers in Veterinary Science

ORIGINAL RESEARCH
published: 12 November 2019
doi: 10.3389/fvets.2019.00398

Investigating the Analytical Variability and Agreement of Manual Leukocyte Quantification Methods in Eastern Box Turtles (*Terrapene carolina carolina*)

John M. Winter[1], *Nicole I. Stacy*[2], *Laura A. Adamovicz*[1] *and Matthew C. Allender*[1]*

[1] *Wildlife Epidemiology Laboratory, College of Veterinary Medicine, University of Illinois, Urbana, IL, United States,*
[2] *Department of Diagnostic, Comparative, and Population Medicine, College of Veterinary Medicine, University of Florida, Gainesville, FL, United States*

OPEN ACCESS

Edited by:
Jennifer Johns,
Oregon State University, United States

Reviewed by:
Jennifer Steinberg,
IDEXX Laboratories, Inc., United States
Gabriele Rossi,
Murdoch University, Australia

***Correspondence:**
Matthew C. Allender
mcallend@illinois.edu

Specialty section:
This article was submitted to Veterinary Experimental and Diagnostic Pathology, a section of the journal Frontiers in Veterinary Science

Received: *30 August 2019*
Accepted: *28 October 2019*
Published: *12 November 2019*

Citation:
Winter JM, Stacy NI, Adamovicz LA and Allender MC (2019) Investigating the Analytical Variability and Agreement of Manual Leukocyte Quantification Methods in Eastern Box Turtles (Terrapene carolina carolina). Front. Vet. Sci. 6:398. doi: 10.3389/fvets.2019.00398

Leukogram evaluation provides valuable information about inflammation, infection, and stress in free-living and zoo-maintained wildlife. While multiple protocols for quantifying leukocytes are available in reptiles, agreement between methods is infrequently described and analytical variability (including repeatability and reproducibility) has not been critically evaluated. This study addresses these knowledge gaps for two hematological methods in eastern box turtles (*Terrapene carolina carolina*): Avian Leukopet^{TM} (LO) and total white blood cell (WBC) estimates from blood films (EST). The objectives of this study were (1) to evaluate agreement in total WBC and individual leukocyte counts between the LO and EST methods, (2) to document repeatability (intra-assay variability) and reproducibility (inter-assay variability) for the LO method, and (3) to investigate whether biological drivers of WBC counts differ between quantification methods. Box turtles ($n = 120$) were sampled from five study sites in Illinois during the 2018 active season. The LO method produced significantly higher WBC counts than the EST method, and constant and proportional error was variable for each leukocyte type. The LO method demonstrated an intra-assay variability of 8.2% and an inter-assay variability of 12%, independent of biological variation. WBC counts were significantly affected by age class using both LO and EST methods, but WBC differences between locations and sexes were only observed using the LO method. These findings emphasize the importance of considering leukocyte determination method when analyzing reptilian hematology results. The inherent variability in currently available methods creates uncertainty in resulting data and highlights the need of a gold standard for reptilian WBC quantification.

Keywords: hemacytometer, hematology, manual methodology, reptile, white blood cell count, white blood cell estimate

INTRODUCTION

Monitoring health is critical to the conservation of any wild species, as the viability of a population is inseparable from its health status (1). However, baseline health data including clinical pathology values (e.g., hematology, plasma biochemistries, protein electrophoresis), pathogen prevalence, and contaminant concentrations are infrequently available for free-living animals. This lack of information can complicate the design and interpretation of comprehensive health studies. Establishing baseline clinical pathology data facilitates monitoring for trends in overall health status and can inform more effective conservation management strategies (2). Hematology is one of the most commonly-used veterinary health assessment tools due to ease of performance, cost-effectiveness, and wide availability in diagnostic and research settings.

Leukogram changes can indicate inflammation, infection, and stress associated with poor health or unsuitable environmental conditions, highlighting the utility of hematologic indices for health assessment in sentinel species like reptiles (3, 4). While mammalian hematology can be performed using automated cell counters, reptilian hematologic analyses require manual methods due to their characteristic nucleated erythrocytes and thrombocytes. Manual leukocyte counting methods used in reptiles include total white blood cell (WBC) estimates from blood films (EST), Natt and Herrick's (NH) direct counts, and indirect leukocyte quantification using the Avian Leukopet kit (LO). The proper application of manual hematology methods is technically challenging and produces more imprecise leukocyte estimates than automated analyzers in mammals (5). However, the analytical variability of these methods has not yet been assessed in reptiles; limiting our understanding of the random error inherent in these approaches.

Similarly, hematologic method comparison studies are limited in reptiles. In Galápagos tortoises (*Chelonoidis* spp.), significant differences in leukocyte quantification were reported between the NH and LO quantification methods and the NH method exhibited better agreement with the EST method (6). Discrepancies in leukocyte counts between different methods have also been documented in loggerhead sea turtles (*Caretta caretta*) (7, 8) and leatherback sea turtles (*Dermochelys coriacea*) (9). However, the degree to which different hematologic methods agree has not yet been determined in terrestrial turtles.

Conclusions drawn from studies investigating hematologic variation due to temporal, spatial, and demographic factors assume that measurements accurately reflect the true value of the analyte. Thus, understanding method-based variability in leukocyte quantification is critical for appropriately interpreting wildlife health data and comparing health status between populations and studies. Characterizing the analytical variability of hematologic assays may encourage researchers to use the most appropriate leukocyte quantification methods, reduce the occurrence of erroneous findings, and consequently allow for more accurate conclusions to be drawn leading to improved wildlife health research.

This study addressed the following specific objectives using blood samples from free-living eastern box turtles (*Terrapene carolina carolina*): (1) Determine level of agreement between the EST and the LO methods, (2) Determine repeatability (intra-assay variability) and reproducibility (inter-assay variability) of the LO method, and (3) Assess whether biological drivers of leukocyte counts are similar between hematologic methods.

MATERIALS AND METHODS

Field Techniques

Eastern box turtles (EBT) were collected from five field sites in Illinois (Collison, Forest Glen, Kennekuk, Kickapoo, and Forbes) using dog-assisted capture as previously described (10). Turtles were weighed, assigned to an age class (adults were >200 g, juveniles were <200 g), and sexed using a combination of sexually dimorphic traits (11). Complete physical examinations were conducted by a single observer (LA). Turtles with clinical signs of illness (ocular/nasal discharge, oral plaques, open-mouth breathing, etc.) or active injuries were categorized as "unhealthy," while turtles with no clinical signs of illness or fully-healed injuries were considered "apparently healthy."

Blood (<0.08% body weight) was collected via the subcarapacial sinus, immediately placed into lithium heparin microtainers (Becton, Dickinson and Company, 1 Becton Drive, Franklin Lakes, NJ), and stored on ice packs until processing (2–6 h after collection). Blood that was obviously lymph contaminated or clotted was not used in analyses. All activities involving live animals were approved by the University of Illinois Institutional Animal Care and Use Committee (Protocol 18000).

Complete Blood Counts

Blood smears were made using heparinized samples immediately upon arrival at the laboratory. Slides were air-dried, then stained using a modified Wright-Giemsa method (Hema 3™ Stat Pack, Fisher Scientific, 300 Industry Drive, Pittsburgh, PA). Total leukocyte quantification was then performed using two methods: (1) the Avian Leukopet™ Kit (Vetlab Supply, Palmetto Bay, FL) with 100-WBC differential counts from corresponding blood films, and (2) WBC estimates and 100-WBC differential counts from blood films. The LO procedure was performed per manufacturer's instructions and read on a Bright-line hemacytometer (Hausser Scientific, Horsham, PA, USA). Briefly, blood samples were repeatedly inverted to ensure a homogeneous blood cell mixture, 25 μL of heparinized whole blood was gently mixed with 750 μL of phloxine stain, the mixture was incubated for 10 min, equal volume aliquots were loaded into each hemacytometer chamber, and the hemacytometer was left undisturbed for 10 min prior to cell counting. Stained heterophils and eosinophils were counted in all nine squares of the hemacytometer grids, and total WBC count was determined using the following equation (12):

$$\left[\frac{Hemacytometer\ side\ 1 + Hemacytometer\ 2}{\underset{(from\ differential\ count)}{\%Heterophils + \%Eosinophils}} \times 1.1 \times 16 \times 100\right]$$

Total white blood cell estimates (EST) were performed by a single observer (JW) at 40x magnification by counting all leukocytes

across 10 different fields of the monolayer. The results were averaged and multiplied by 2000 to calculate the number of white blood cells per microliter (13). One-hundred WBC differentials were performed under oil immersion by a single observer (LA).

Intra-Assay Variability of the Avian Leukopet™

Three hemacytometers were loaded and reviewed from a single phloxine-blood tube to determine intra-assay variability (repeatability). All loading and cell-counting for this portion of the study was performed by a single observer (JW).

Inter-assay Variability of the Avian Leukopet™

For each blood sample included in the intra-assay variability portion of the study, a second phloxine-blood mixture was mixed, loaded, and read to determine inter-assay variability (reproducibility). These samples were prepared and counted by multiple different individuals to capture inherent inter-observer variability. Only one hemacytometer was read for each blood sample by one individual from the group of different individuals.

Statistical Analysis

Statistical analysis was conducted in the following manner to test study hypotheses: (1) Assess agreement between hematology parameters determined by EST and LO methods; (2) Determine the analytical variability of the LO method; and (3) Investigate whether biological drivers of leukocyte counts differ between quantification methods. All statistical assessments were performed using commercial software at an alpha value of 0.05 (14) (MedCalc version 18.9, MedCalc software bvba, Ostend, Belgium; R version 3.5.1).

Objective 1. Agreement Between Avian Leukopet™ and WBC Estimates

Agreement in hematological counts from the LO and EST methods was evaluated using Passing-Bablok regression, Bland-Altman plots, and paired Wilcoxon-Signed Rank tests. Passing-Bablok analysis constructs a linear regression model between the results of two diagnostic methods performed on paired data. Ninety-five percent confidence intervals (95% CI) are produced for the slope and the y-intercept of this model. If the 95% CI for the slope contains one and the 95% CI for the y-intercept contains zero, the diagnostic methods agree. If the CI for the slope does not contain one, proportional error is present and if the CI for the y-intercept does not contain zero, constant error is present. Passing-Bablok is robust to outliers, allows for measurement errors, and makes no distributional assumptions, however, it does assume a high positive correlation between the diagnostic methods (15, 16). To test this assumption, Kendall's tau was determined for each set of test results.

Bland-Altman figures plot the differences between paired results produced by different diagnostic methods against the mean of those results. Limits of agreement (LOA), defined as the mean difference ±1.96 times the standard deviation of the differences, are also plotted. Values above or below the LOA demonstrate poor agreement, and patterns in the data can indicate proportional and systematic error.

Objective 2. Avian Leukopet Analytical Variability

Intra-assay variability (repeatability) was determined by calculating the coefficient of variation (CV) for three replicates performed by a single observer. Inter-assay variability (reproducibility) was determined by calculating the CV of those same three replicates read by a single observer and one replicate from a different phloxine-blood mixture made using blood from the same turtle read by an individual from a rotating group of observers. The values used to calculate this inter-assay variability were the average of the first three replicates and the single value produced by the second phloxine-blood mixture. The analytical coefficient of variation (CV_A) was calculated based on the difference between hemacytometer readings within the same individuals, and the between-turtle coefficient of variation (CV_G) was calculated as the variation between different blood samples. Generalized linear models were used to determine whether inter or intra-assay variability was associated with turtle health status.

Objective 3. Biological Predictors of WBC Data Produced by Different Methods

Continuous variables (hematological values) were assessed for normality using skewness, kurtosis, Q-Q plots, and the Shapiro–Wilk test. Descriptive statistics (mean, standard deviation, and range for normally distributed variables, median, 10th and 90th percentiles for non-normally distributed variables) were tabulated. General linear models were constructed separately for each WBC quantification method using the glm function in R (17). Hematological values were the dependent variables, and independent variables included demographic factors (sex, age class), spatiotemporal factors (month, location), and health classification (apparently healthy vs. unhealthy). Akaike information criterion (AIC) model rankings, used to determine relative quality of statistical models, were then performed to determine the most parsimonious model for each hematological value and leukocyte quantification method using AICmodavg (18).

RESULTS

Sample Population

A total of 120 EBT including 46 females, 56 males, and 18 turtles of unknown sex were sampled in May, June July, and August, 2018 at Collison ($n = 26$), Forest Glen ($n = 17$), Kennekuk ($n = 24$), Kickapoo ($n = 17$), and Forbes ($n = 27$). One hundred turtles were classified as adults, 20 were juveniles. Eighteen turtles were classified as unhealthy due to the presence of ocular discharge ($n = 1$), nasal discharge ($n = 2$), aural abscesses ($n = 2$), nodular or erosive lesions on the carapace or hard palate ($n = 5$), fresh injuries ($n = 4$), limb swelling ($n = 2$), and oral plaques ($n = 2$).

Agreement Analysis

The LO method (performed by a single observer) resulted in consistently higher absolute leukocyte numbers than the EST method (**Table 1**, **Figures 1A**, **2A**). Passing-Bablok regression revealed constant and/or proportional error between the LO and EST methods for all leukocytes except eosinophils (**Table 2A**,

TABLE 1 | Descriptive statistics for leukogram data determined by three different manual count methodologies: estimated leukocyte count from blood films (WBC Estimate), Avian Leukopet™ using an average of three replicates performed by a single observer (LO1), and Avian Leukopet™ using a single replicate from multiple observers (LO2) for 120 free-living eastern box turtles (*Terrapene carolina carolina*).

		WBC estimate	Avian leukopet™ (LO1)	Avian leukopet™ (LO2)
Parameter	**N**	**Measure of central tendency and dispersion**	**Measure of central tendency and dispersion**	**Measure of central tendency and dispersion**
White blood cells (/μL)	120	16,000 (8,800–24,200)	19,236 (10,321–32,087)	17,129 (9,888–28,800)
Heterophils (H) (/μL)	120	2,553 (847–5,262)	2,811 (1,233–5,709)	2,557 (1,214–4,747)
Lymphocytes (L) (/μL)	120	9,110 (5,176–14,450)	10,844 (5,679–20,364)	10,031 (4,743–19,551)
Monocytes (/μL)	120	290 (0–674)	355 (0–867)	304 (0–850)
Eosinophils (/μL)	120	1,832 (796–4,260)	2,194 (970–4,954)	2,005 (848–4,455)
Basophils (/μL)	120	1,387 (1,156–1,618)	1,688 (1,408–1,967)	1,192 (367–2568)
H:L ratio	120		0.32 (0.28–0.37)	

Mean and 95% confidence intervals (CI) are presented for normally-distributed parameters, while median and 10th−90th percentiles are presented for non-normally distributed parameters. LO1 values were significantly higher than WBC estimates for each parameter ($P < 0.005$).

Figure 1A). Data for WBC, monocytes, and basophils were proportionally higher in the LO method, heterophils were constantly higher in the LO method, and lymphocytes were both constantly and proportionally increased in the LO method when compared to the EST method.

There was agreement between LO data determined by a single individual and the group of individuals for total WBC, lymphocytes, and basophils (**Table 2B**, **Figure 1B**). The single observer produced proportionally higher values for heterophils, eosinophils, and monocytes. Although, the confidence intervals for these values were narrower than those comparing the LO and EST methods and the observed differences may not equate to significant biological variability (**Figure 2B**).

Avian Leukopet™ Analytical Variability

Intra-assay variability was 8.2%, while inter-assay variability was 12% (**Table 3**). Health classification did not significantly impact inter ($p = 0.99$) or intra-assay ($p = 0.97$) CV values.

Biological Effects on Hematological Values Produced Using Different Methods

There was no single general linear model predicting WBC that had overwhelming support (AICcwt > 0.5) for any of the determination methods. In the univariate analysis, age was the only predictor significantly associated with WBC using all three determination methods; juvenile turtles consistently had higher WBC than adults (**Tables 4**, **5**). Location and sex were significant predictors of WBC from the single observer using the LO method but were not statistically significant predictors of WBC using the EST method or the multi-observer LO method.

DISCUSSION

This study assessed analytical variability in the Avian Leukopet™, compared leukocyte values resulting from two commonly-used quantification methods, and investigated whether methodological differences affected conclusions about biological variation and the health of free-living eastern box turtles. The LO method demonstrated an intra-assay variability of 8.2% and an inter-assay variability of 12%, independent of biological variation. The LO method yielded significantly higher leukocyte numbers than the EST method in an observer-dependent fashion. Similarly, associations between biological predictors and WBC counts differed based on method and observer. This highlights the importance of considering methodology when interpreting hematologic data and underscores the inherent variability of manual hematologic methods in reptiles.

Manual leukocyte quantification is technically challenging, and each method has a different set of benefits and limitations. Both the EST and LO methods require a high-quality blood smear with an even cell distribution along with a knowledgeable slide reader to discern between cells of similar appearance (e.g., lymphocytes vs. thrombocytes). The EST method is inexpensive, requires only a drop of blood to make a smear, and allows for the observation of leukocyte abnormalities such as toxic heterophils or intra-cellular inclusions; however, poor quality smears and anticoagulant artifacts may affect the accuracy of this approach. The advantages of the LO method include rapid identification of stained leukocytes that can be performed by an observer without advanced training or knowledge of hematology if a knowledgeable observer performs the accompanying 100-WBC differential count. However, this method can be time-consuming due to the series of 10 min incubations during phloxine staining and hemacytometer loading. Errors can be made at multiple stages including improper mixing of blood into the stain, error in dilution, and improper charging of the hemacytometer. The EST method has been previously recommended to be routinely run in conjunction with the LO method for verification (19, 20). However, a gold-standard hematological method has yet to be identified in reptiles. Until a gold-standard is available, research efforts should focus on quantifying analytical variability in manual methods to better understand their potential impact on clinical decision-making.

Method-based variation in leukocyte quantification has been previously described in other species with nucleated erythrocytes (6–9, 21). All leukocyte quantification methods in the present study identified significantly higher WBC counts in juvenile turtles. The single-observer LO method also detected associations between location, sex, and WBC count; however, the effects of these variables were small compared to the effect of age class and may represent statistical significance without accompanying biological importance.

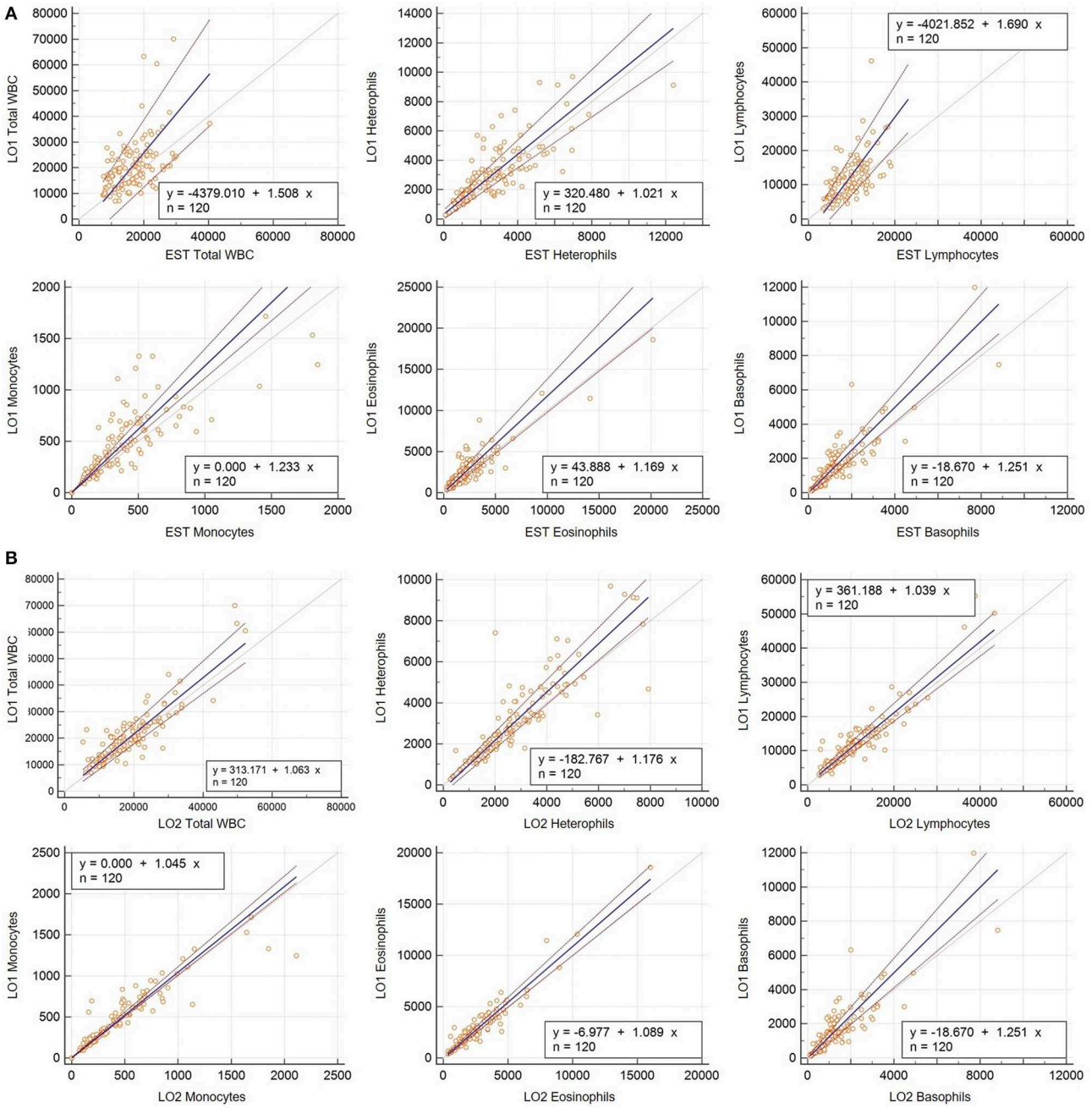

FIGURE 1 | (A) Passing-Bablok regression analyses for hematology parameters determined using the Avian Leukopet method with the average of three replicates performed by a single observer (LO1) and the WBC estimation method (EST) in 120 free-living eastern box turtles (*Terrapene carolina carolina*). Solid lines depict linear regression lines and dashed lines depict the 95% confidence intervals around the linear regression line. **(B)** Passing-Bablok regression analyses for hematology parameters determined using the Avian Leukopet method from one observer (LO1) and a group of observers (LO2) in 120 free-living eastern box turtles (*Terrapene carolina carolina*). Solid lines depict linear regression lines and dashed lines depict the 95% confidence intervals around the linear regression line.

Deem et al. (8) also found that leukogram interpretation varied based on hematologic method; specifically, WBC counts differed between turtle groups using the Eosinophilic Unopette method (foraging < nesting and stranded), but not the EST method. These findings indicate that hematologic method may influence clinical assessment of reptilian patients, potentially affecting our understanding of biology, physiology, and health at the individual and population levels.

Previous studies have also documented higher WBC counts using phloxine-based stains (Eopettes, eosinophilic Unopettes) compared to EST methods in Galápagos tortoises (6), leatherback

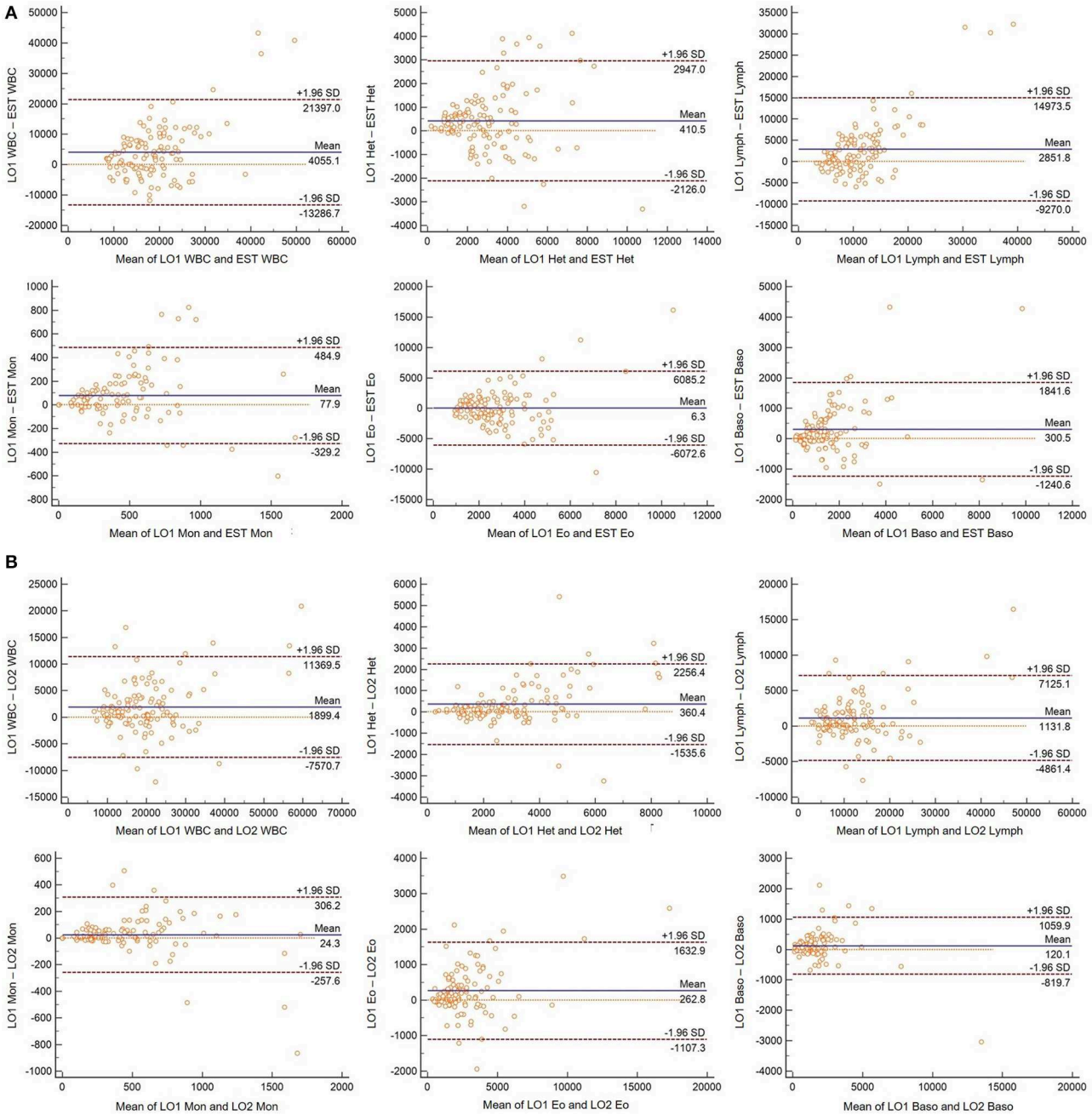

FIGURE 2 | (A) Bland-Altman plots for hematology parameters determined using the Avian Leukopet method from one observer (LO1) and the WBC estimation method (EST) in 120 free-living eastern box turtles (*Terrapene carolina carolina*). Central lines depict the mean difference between the two methods, upper and lower lines represent limits of agreement (LOA), defined as the mean difference ±1.96 times the standard deviation of the differences. **(B)** Bland-Altman plots for hematology parameters determined using the Avian Leukopet method from one observer (LO1) and a group of observers (LO2) in 120 free-living eastern box turtles (*Terrapene carolina carolina*). Central lines depict the mean difference between the two methods, upper and lower lines represent limits of agreement (LOA), defined as the mean difference ±1.96 times the standard deviation of the differences.

sea turtles (9), macaws (21), and loggerhead sea turtles (8). The reason for leukocyte overestimation in the LO method is unknown, but it has been reported that the total WBC can be artificially elevated when using the LO method if the heterophil count is low (22). Many reptiles, including eastern box turtles, have been reported to be predominantly lymphocytic (23–31) which may help explain this finding, although a more recent study reported heterophils as the dominant leukocyte in eastern box turtles (32). These discrepancies indicate that comparing hematologic

TABLE 2A | Passing-Bablok regression parameters and Kendall's Tau values for leukogram data determined using the Avian Leukopet™ method (average of three replicates performed by a single observer) and white blood cell estimate from blood films in 120 free-living eastern box turtles (*Terrapene carolina carolina*).

Parameter	Kendall's Tau (*P*-value)	Slope (95% CI)	Y-Intercept (95% CI)	Error present
White blood cells (/μL)	0.377 ($p < 0.0001$)	1.51 (1.18–1.91)	−4,379 (−11,363, 315)	P
Heterophils (/μL)	0.769 ($p < 0.0001$)	1.02 (0.87–1.20)	320 (4, 598)	C
Lymphocytes (/μL)	0.736 ($p < 0.0001$)	1.69 (1.40–2.03)	−4,021 (−6,992, −1,693)	C, P
Monocytes (/μL)	0.742 ($p < 0.0001$)	1.23 (1.12–1.39)	0 (0, 5)	P
Eosinophils (/μL)	0.773 ($p < 0.0001$)	1.17 (1.00–1.35)	44 (−277, 331)	None
Basophils (/μL)	0.837 ($p < 0.0001$)	1.25 (1.07–1.44)	−19 (−198, 88)	P

C, constant error; P, proportional error.

TABLE 2B | Passing-Bablok regression parameters and Kendall's Tau values for leukocyte counts determined using the Avian Leukopet™ (single observer vs. group of observers) in 120 free-living eastern box turtles (*Terrapene carolina carolina*).

Parameter	Kendall's Tau (P-value)	Slope (95% CI)	Y-Intercept (95% CI)	Error present
WBC (/μL)	0.671 ($p < 0.0001$)	1.06 (0.95–1.18)	313 (−1345, 1814)	None
Heterophils (/μL)	0.624 ($p < 0.0001$)	1.18 (1.08–1.27)	−183 (−410, 19)	P
Lymphocytes (/μL)	0.493 ($p < 0.0001$)	1.04 (0.95–1.14)	361 (−431, 1039)	None
Monocytes (/μL)	0.856 ($p < 0.0001$)	1.04 (1.01–1.11)	0 (0, 6)	P
Eosinophils (/μL)	0.613 ($p < 0.0001$)	1.09 (1.01–1.17)	−7 (−117, 107)	P
Basophils (/μL)	0.673 ($p < 0.0001$)	1.06 (1.00–1.14)	14 (−38, 68)	None

C, constant error; P, proportional error.

TABLE 3 | Analytical variability of Avian Leukopet™ in eastern box turtles (*Terrapene carolina carolina*).

	Intra-assay variability	Inter-assay variability
N	120	120
Analyzed in triplicate	Yes	No
Mean	20,630	20,155
SD	10,233	9,662
Min	7,016	6,861
Max	70,044	64,826
CV_G	49.6%	47.9%
CV_A	8.2%	12.0%
Minimum	0.7%	1.3%
Maximum	21.5%	44.8%

N, number of samples; Mean, average of total WBC; CV_G, between-turtle coefficient of variation; CV_A, analytical coefficient of variation.

TABLE 4 | Statistical significance of demographic and spatiotemporal factors predicting total white blood cell counts (WBC) in 120 eastern box turtles (*Terrapene carolina carolina*) using three methods for determining WBC.

	LO1	LO2	Est
Month	$P = 0.499$	$P = 0.34$	$P = 0.46$
Location	$\mathbf{P = 0.03}$	$P = 0.279$	$P = 0.069$
Sex	$\mathbf{P = 0.011}$	$P = 0.0837$	$P = 0.26$
Age class	$\mathbf{P = 0.0002}$	$\mathbf{P = 0.0014}$	$\mathbf{P = 0.00123}$
Disease	$P = 0.51$	$P = 0.81$	$P = 0.685$

P-values are from ANOVAs for month and location and independent t-tests for sex and age class. LO1 = Avian Leukopet method determined in triplicate by a single observer; LO2 = Avian Leukopet method determined by a group of individuals a single time; Est = estimate method to determine total WBC. P-values less than the alpha level (0.05) are bolded.

indices between studies with different methodologies should be approached with caution.

The coefficient of variation is used as a measurement of analytical imprecision in method validation studies (33). The present study is the first to report intra (8.2%) and inter-assay (12%) CV for the LO method in reptiles. These values are consistent with the 6.8% intra-assay CV reported by Dein et al. (34) for avian leukocytes using the BD Unopette method, and with four additional avian studies that reported intra-assay CV values of 11–34%. While box turtle CV values are similar to those in birds, it is unclear whether this level of inherent variability is acceptable for medical use. Criteria for determining acceptable analytical precision can be derived from biological variation data (intra-individual variation; CVi), with the maximum allowable imprecision (CVmax) equating to less than half the CVi (5). Based on human CVi data, manual leukocyte quantification methods produce an unacceptable level of imprecision for clinical decision-making in dogs and cats (5). While CVi data are not currently available for box turtle hematologic indices, these values would be useful to further contextualize and interpret the Avian Leukopet CV values determined in the present study.

Coefficients of variation (analytical imprecision) and bias (systematic error) are also used to calculate total error (TE); a value that represents the entire analytical uncertainty in a diagnostic test (35). Total allowable error (TEa) is defined as the amount of medically tolerable variation for a given clinical pathology analyte. Comparing observed total error (TEobs) for a new diagnostic method to TEa provides an objective means of determining whether the diagnostic method's analytical performance is clinically acceptable (TEobs < TEa) (35). While TEa guidelines have been produced for hematologic indices in veterinary species, bias estimates for the Avian Leukopet in box turtles are unavailable. Determining bias involves comparing paired test results between a new diagnostic method and a gold-standard method using commercially-produced quality control material (QCM) that is not yet available

TABLE 5 | Descriptive statistics for total leukocyte counts which differed by age class in 120 free-living eastern box turtles (*Terrapene carolina carolina*).

		N	Mean	Std. deviation	95% confidence interval for mean		Minimum	Maximum
					Lower bound	Upper bound		
LO1	Adult	100	19,248	9,390	17,385	21,111	7,017	70,044
	Juvenile	20	27,541	11,669	22,080	33,003	13,830	63,267
	Total	120	20,630	10,234	18,780	22,480	7,017	70,044
LO2	Adult	100	17,620	8,147	16,004	19,237	5,312	52,218
	Juvenile	20	24,282	9,818	19,687	28,877	12,133	49,800
	Total	120	18,731	8,765	17,146	20,315	5,312	52,218
Est	Adult	100	15,848	6,150	14,628	17,068	7,400	40,400
	Juvenile	20	20,210	4,351	18,174	22,246	10,200	28,800
	Total	120	16,575	6,095	15,473	17,677	7,400	40,400

Mean, standard deviation, 95% confidence interval, and minimum/maximum are presented. LO1 = Total leukocyte count determined using the Avian Leukopet^{TM} method determined in triplicate by a single observer; LO2 = Total leukocyte count determined using the Avian Leukopet^{TM} method determined by a group of individuals; EST = Total leukocyte count determined using the estimate method.

for reptiles (36). Alternative methods for determining bias are recommended when QCM and gold-standard diagnostic methods do not exist, however, these were not pursued in the present study (36). While determining bias and calculating TEobs and TEa was outside the scope of this study, future investigation of these values would be useful for evaluating the clinical validity of the Avian Leukopet in box turtles.

Future directions for research include determining CVi and bias for different hematologic methods in box turtles and other reptiles. This information will enable a more objective comparison between methods and help identify the most valid diagnostic option for clinical assessment. Developing a gold-standard hematologic method is another important milestone which will advance clinical pathology interpretation in reptile patients.

Researchers and clinicians must be cognizant of the potential for method-generated variability when comparing results between diagnostic assays and making clinical decisions. As demonstrated in this study, commonly used methods for reptile hematology may produce significantly different results and biological associations. The analytical variability values documented in this study are an important first step toward understanding the inherent variation in reptile hematologic indices, however, a gold standard method for reptile hematology needs to be established to facilitate method comparison. Continued characterization of manual hematologic methods will ultimately improve clinical case assessment, direct research methodology, and lead to better reptile health management.

DATA AVAILABILITY STATEMENT

The datasets generated for this study are available on request to the corresponding author.

ETHICS STATEMENT

The animal study was reviewed and approved by University of Illinois Institutional Animal Care and Use Committee.

AUTHOR CONTRIBUTIONS

MA and NS: experimental conception and design. MA, LA, JW: sample collection. LA and JW: hematology. MA and LA: statistical analysis. JW, LA, MA, and NS: paper writing.

FUNDING

The present study was partially funded by a grant (D18ZO-607) through the Morris Animal Foundation Veterinary Student Scholars program to JW. Funding for turtle capture was provided by a State Wildlife Grant (T104-R1) from the Illinois Department of Natural Resources.

ACKNOWLEDGMENTS

The authors would like to thank John Rucker and his turtle dogs, Bayer for providing flea and tick preventive for the dogs, and the University of Illinois veterinary students who helped find and sample turtles.

REFERENCES

1. Karesh WB, Cook RA. Applications of veterinary medicine to in situ conservation efforts. *Oryx*. (1995) 29:244–52. doi: 10.1017/S0030605300021232
2. Deem SL, Karesh WB, Weisman W. Putting theory into practice: wildlife health in conservation. *Conserv Biol.* (2001) 15:1224–33. doi: 10.1046/j.1523-1739.2001.00336.x
3. Sleeman JM. Use of wildlife rehabilitation centers as monitors of ecosystem health. In: Fowler ME, Miller RE, editors. *Zoo and Wild Animal*

Medicine, 6th Edn. Saint Louis, MO: Saunders Elsevier (2008). p. 97–104. doi: 10.1016/B978-141604047-7.50015-4
4. Johnstone CP, Lill A, Reina RD. Does habitat fragmentation cause stress in the agile antechinus? A haematological approach. *J Comp Physiol B*. (2012) 182:139–55. doi: 10.1007/s00360-011-0598-7
5. Kjelgaard-Hansen M, Jensen AL. Is the inherent imprecision of manual leukocyte differential counts acceptable for quantitative purposes? *Vet Clin Pathol*. (2006) 35:268–70. doi: 10.1111/j.1939-165X.2006.tb00128.x
6. Sheldon JD, Stacy NI, Blake S, Cabrera F, Deem SL. Comparison of total leukocyte quantification methods in free-living Galapagos tortoises (*Chelonoidis* spp.). *J Zoo Wildl Med.* (2016) 47:196–205. doi: 10.1638/2015-0159.1
7. Arnold J. White blood cell count discrepancies in Atlantic loggerhead sea turtles: Natt-Herrick vs. Eosinophil Unopette. In: *Proceedings of the 14th Annual Conference of the Association of Zoo Veterinary Technicians*. Cleveland, OH (1994). p. 15–22.
8. Deem SL, Norton TM, Mitchell M, Segars AL, Alleman AR, Cray C, et al. Comparison of blood values in foraging, nesting, and stranded loggerhead turtles (*Caretta caretta*) along the coast of Georgia, USA. *J Wildl Dis.* (2009) 45:41–56. doi: 10.7589/0090-3558-45.1.41
9. Deem SL, Dierenfeld ES, Sounguet GP, Alleman, AR, Cray C, Poppenga RH, et al. Blood values in free-ranging nesting leatherback sea turtles (*Dermochelys coriacea*) on the coast of the Republic of Gabon. *J Zoo Wildl Med*. (2006) 37:464–71. doi: 10.1638/05-102.1
10. Boers K, Leister K, Byrd J, Band M, Phillips CA, Allender MC. Capture effort, rate, demographics, and potential for disease transmission in wild eastern box turtles (*Terrapene carolina carolina*) captured through canine directed searches. *Herpetol Rev*. (2017) 48:300–4.
11. Dodd CK. *North American Box Turtles: A Natural History*. Norman, OK: University of Oklahoma Press (2001).
12. *Avian Leukopet^{TM} [package insert]*. Palmetto Bay, FL: Vetlab Supply (2015).
13. Campbell T. Hematology of birds. In: Thrall MA, Weiser G, Allison R, Campbell T, editors. *Veterinary Hematology and Clinical Chemistry*, 2nd Edn. Ames, IA: John Wiley & Sons (2012). p. 238–76.
14. R Core Team. *R: A Language and Environment for Statistical Computing*. Vienna: R Foundation for Statistical Computing (2018). Available online at: https://www.R-project.org/
15. Passing H. A new biometrical procedure for testing the equality of measurements from two different analytical methods application of linear regression procedures for method comparison studies in clinical chemistry, part I. *J Clin Chem Clin Biochem*. (1983) 21:709–20. doi: 10.1515/cclm.1983.21.11.709
16. Bablok W, Passing H, Bender R, Schneider B. A general regression procedure for method transformation application of linear regression procedures for method comparison studies in clinical chemistry, part III. *J Clin Chem Clin Biochem*. (1988) 26:783–90. doi: 10.1515/cclm.1988.26.11.783
17. R Core Team. *R: A Language and Environment for Statistical Computing*. Vienna: R Foundation for Statistical Computing (2016). Available online at: https://www.R-project.org/
18. Mazerolle MJ. *AICcmodavg: Model Selection and Multimodel Inference Based on (Q)AIC(c). R Package Version 2.1-1*. (2017). Available online at: https://cran.r-project.org/package=AICcmodavg
19. Stacy NI, Alleman AR, Sayler KA. Diagnostic hematology of reptiles. *Clin Lab Med.* (2011) 31:87–108. doi: 10.1016/j.cll.2010.10.006
20. Strik NI, Alleman AR, Harr KE. Circulating inflammatory cells. In: Jacobson ER, editor. *Infectious Diseases and Pathology of Reptiles: Color Atlas and Text*. Boca Raton, FL: CRC Press (2007). p. 167–218. doi: 10.1201/9781420004038.ch3
21. Russo EA, McEntee L, Applegate L, Baker JS. Comparison of two methods for determination of white blood cell counts in macaws. *J Am Vet Med Assoc*. (1986) 189:1013.
22. Sykes JM, Klaphake E. Reptile hematology. *Clin Lab Med*. (2015) 35:661–80. doi: 10.1016/j.cll.2015.05.014
23. Sypek J, Borysenko M. Reptiles. In: Rowley AF, Ratcliffe NA, editors. *Vertebrate Blood Cells*. Cambridge, UK: Cambridge University Press (1998). p. 211–56.
24. Alleman AR, Jacobson ER, Raskin RE. Morphologic, cytochemical staining and ultrastructural characteristics of blood from eastern diamondback rattlesnakes (*Crotalus adamanteus*). *Am J Vet Res*. (1999) 60:507–14.
25. Work TM, Raskin RE, Balazs GH, Whittaker SD. Morphologic and cytochemical characteristics of blood cells from Hawaiian green turtles. *Am J Vet Res*. (1998) 59:1252–7.
26. Divers SJ, Redmayne G, Aves EK. Haematological and biochemical values of 10 green iguanas (*Iguana iguana*). *Vet Rec*. (1996) 138:203–5. doi: 10.1136/vr.138.9.203
27. Lamirande EW, Bratthauer AD, Fisher DC, Nichols DK. Reference hematologic and plasma chemistry values of brown tree snakes (*Boiga irregularis*). *J Zoo Wildl Med*. (1999) 30:516–20.
28. Troiano JC, Vidal JC, Gould J, Gould E. Haematological reference intervals of the South American rattlesnake (*Crotalus durissus terrificus*, Laurenti, 1768) in captivity. *Comp Haematol Int*. (1997) 7:109–12. doi: 10.1007/BF02652577
29. Minter LJ, Dombrowski DS, Stoskopf MK, Purnell CA, Loomis MR, De Voe RS. Hematology and plasma biochemical values for free ranging cottonmouths (*Agkistrodon piscivorus*) in Central North Carolina, USA. *Herpetol Conserv Biol*. (2013) 8:321–34.
30. Adamovicz L, Bronson E, Barrett K, Deem SL. Health assessment of free-living eastern box turtles (*Terrapene carolina carolina*) in and around the Maryland zoo in Baltimore 1996–2011. *J Zoo Wildl Med*. (2015) 46:39–51. doi: 10.1638/2014-0066R.1
31. Way Rose BM, Allender MC. Health assessment of wild eastern box turtles (*Terrapene carolina carolina*) in east Tennessee. *J Herpetol Med Surg*. (2011) 21:107–12. doi: 10.5818/1529-9651-21.4.107
32. Lloyd TC, Allender MC, Archer G, Phillips CA, Byrd J, Moore AR. Modeling hematologic and biochemical parameters with spatiotemporal analysis for the free-ranging eastern box turtle (*Terrapene carolina carolina*) in Illinois and Tennessee, a potential biosentinel. *EcoHealth*. (2016) 13:467–79. doi: 10.1007/s10393-016-1142-8
33. Flatland B, Freeman KP, Friedrichs KR, Vap LM, Getzy KM, Evans EW, et al. ASVCP quality assurance guidelines: control of general analytical factors in veterinary laboratories. *Vet Clin Pathol.* (2010) 39:264–77. doi: 10.1111/j.1939-165X.2010.00251.x
34. Dein FJ, Wilson A, Fischer D, Langenberg P. Avian leucocyte counting using the hemocytometer. *J Zoo Wildl Med.* (1994) 25:432–7.
35. Nabity MB, Harr KE, Camus MS, Flatland B, Vap LM. ASVCP guidelines: allowable total error hematology. *Vet Clin Pathol.* (2018) 47:9–21. doi: 10.1111/vcp.12583
36. Vap LM, Harr KE, Arnold JE, Freeman KP, Getzy K, Lester S, et al. ASVCP quality assurance guidelines: control of preanalytical and analytical factors for hematology for mammalian and nonmammalian species, hemostasis, and crossmatching in veterinary laboratories. *Vet Clin Pathol*. (2012) 41:8–17. doi: 10.1111/j.1939-165X.2012.00413.x

Conflict of Interest: The authors declare that the research was conducted in the absence of any commercial or financial relationships that could be construed as a potential conflict of interest.

Copyright © 2019 Winter, Stacy, Adamovicz and Allender. This is an open-access article distributed under the terms of the Creative Commons Attribution License (CC BY). The use, distribution or reproduction in other forums is permitted, provided the original author(s) and the copyright owner(s) are credited and that the original publication in this journal is cited, in accordance with accepted academic practice. No use, distribution or reproduction is permitted which does not comply with these terms.

frontiers in Veterinary Science

ORIGINAL RESEARCH
published: 14 November 2019
doi: 10.3389/fvets.2019.00402

Evaluation of Physiological Parameters and Effectiveness of an Immobilization Protocol Using Etorphine, Azaperone, and Butorphanol in Free-Ranging Warthogs (*Phacochoerus africanus*)

Donald Neiffer[1], Peter Buss[2], Jennie Hewlett[2†], Guy Hausler[3], Leana Rossouw[2], Tebogo Manamela[2], Brittany Grenus[4], Emily Thulson[5], Francisco Olea-Popelka[5†] and Michele Miller[3]*

[1] Wildlife Health Sciences, National Zoological Park, Smithsonian Conservation Biology Institute, Washington, DC, United States, [2] Veterinary Wildlife Services, South African National Parks, Kruger National Park, Skukuza, South Africa, [3] Division of Molecular Biology and Human Genetics, Department of Science and Technology-National Research Foundation Centre of Excellence for Biomedical Tuberculosis Research, Faculty of Medicine and Health Sciences, Medical Research Council Centre for Tuberculosis Research, Stellenbosch University, Cape Town, South Africa, [4] Cummings School of Veterinary Medicine at Tufts University, North Grafton, MA, United States, [5] Department of Clinical Sciences and Mycobacteria Research Laboratories, College of Veterinary Medicine and Biomedical Science, Colorado State University, Fort Collins, CL, United States

Twenty free-ranging warthogs (*Phacochoerus africanus*) in the Kruger National Park, South Africa, were immobilized with a combination of etorphine (0.039 ± 0.005 mg/kg) and azaperone (0.44 ± 0.06 mg/kg) administered intramuscularly by dart. Butorphanol (1 mg per mg etorphine) was administered intravenously at $t = 5$ min. A standardized scoring system was used to record induction, immobilization and recovery characteristics. Physiological parameters were recorded at 5 min intervals and an arterial sample collected for blood gas analyses every 15 min. At 45 min after butorphanol administration, immobilization was partially reversed by administering naltrexone (40x etorphine dose in mg) intravenously. Overall, induction quality was good, with the mean time to safe handling 5.9 ± 1.4 min. The majority of immobilization scores (54%) over the entire monitoring period (40 min) were at level 3, consistent with a light plane in which palpebral and laryngeal reflexes were still present but the animal could be safely handled. Overall mean heart rate was 94.7 ± 15.3 beats per min, mean respiratory rate was 14.7 ± 9.8 breaths per min, and the mean rectal temperature was 38.5 ± 1.0°C. Significant hypoxia (overall mean oxygen arterial partial pressure 38.8 ± 8.4 mmHg), hypercapnia (mean carbon dioxide arterial partial pressure 63.3 ± 7.8 mmHg), and acidosis (mean pH 7.28 ± 0.04) were observed in immobilized warthogs. Following antagonist administration, warthogs were standing within 1.0 ± 0.4 min, with the majority of recoveries scored as excellent. The drug combination proved to be effective in the

OPEN ACCESS

Edited by:
Nicole Indra Stacy, University of Florida, United States

Reviewed by:
Nuno Santos, University of Porto, Portugal
Dean Konjević, University of Zagreb, Croatia

***Correspondence:**
Donald Neiffer
neifferd@si.edu

†Present address:
Jennie Hewlett, Pharmacology Department, Faculty of Veterinary Science, University of Pretoria, Onderstepoort, South Africa
Francisco Olea-Popelka, Schulich School of Medicine and Dentistry, Western University, London, ON, Canada

Specialty section:
This article was submitted to Zoological Medicine, a section of the journal Frontiers in Veterinary Science

Received: *29 July 2019*
Accepted: *28 October 2019*
Published: *14 November 2019*

Citation:
Neiffer D, Buss P, Hewlett J, Hausler G, Rossouw L, Manamela T, Grenus B, Thulson E, Olea-Popelka F and Miller M (2019) Evaluation of Physiological Parameters and Effectiveness of an Immobilization Protocol Using Etorphine, Azaperone, and Butorphanol in Free-Ranging Warthogs (Phacochoerus africanus). Front. Vet. Sci. 6:402. doi: 10.3389/fvets.2019.00402

immobilization of free-ranging warthogs with rapid induction and recovery, but with significant cardio-respiratory changes. Therefore, this drug combination may be useful when rapid immobilization and recovery are indicated, but should be used cautiously in compromised warthogs.

Keywords: azaperone, butorphanol, etorphine, immobilization, *Phacochoerus africanus*, warthog

INTRODUCTION

Warthogs (*Phacochoerus africanus)* are popular inhabitants at zoos and widely distributed in sub-Saharan Africa. However, handling and immobilization can be challenging due to their size, strength and presence of tusks. They can also be difficult to capture due to their acute awareness of their surroundings. Like other suids, they are also susceptible to injury and hyperthermia associated with immobilization (1, 2). Therefore, rapid induction and recovery are important components when choosing an immobilizing drug for these species.

The most common drugs reported for use in warthogs are ketamine (K) and tiletamine-zolazepam (TZ), often combined with medetomidine (M), or azaperone (A) (1, 3). However, these combinations commonly result in falling and paddling during induction and recovery, as well as prolonged periods before animals are recovered sufficiently for release.

Etorphine is a highly potent opioid commonly used for immobilization of wildlife (1). This drug is commonly combined with azaperone to counteract opioid-induced hypertension and lower the dose of etorphine required for immobilization. Etorphine administration results in rapid induction and complete reversibility with naltrexone. However, significant physiological changes including hypoxia, hypercapnia and acidemia are well-documented side effects (4). There are limited reports of etorphine immobilization of warthogs and even less information on physiological responses in this species (2, 5–7). Due to the potential for severe respiratory depression and cardiac arrest, publications that are more recent recommend avoiding its use or completely fail to mention potent opioids as an option for any suid anesthesia (1, 3, 8). This total avoidance of etorphine is not warranted in our experience. Given its availability and since successful immobilization of free-ranging warthogs requires both rapid induction and recovery, etorphine may be a suitable choice, particularly if other drugs can be used to mitigate side effects. Therefore, the aim of this study was to evaluate the effects and suitability of an etorphine, azaperone, butorphanol drug combination in free-ranging warthogs.

MATERIALS AND METHODS

The study was conducted in the Kruger National Park (24.9948°S, 31.5969°E) in April 2017. The research protocol was approved by the South African National Parks Animal Use and Care Committee.

Adult warthogs were administered immobilizing drugs into the muscles of the hindquarters using a 3.0 ml plastic dart with 30–40 mm collared needle, propelled by a compressed air dart rifle (DAN-INJECT, International S.A., Skukuza 1350, South Africa). Drug doses were calculated, based on visual estimation of weight, to deliver 0.035 mg/kg etorphine (9.8 mg/ml, M99, Ilanco, Kempton Park 1619, South Africa) and 0.40 mg/kg azaperone (40 mg/ml, Janssen Pharmaceutical Ltd., Halfway House 1685, South Africa). The etorphine dose chosen was based on both experience of the authors and published recommendations (2, 5, 7). After a pilot study, butorphanol (50 mg/ml, Kyron Laboratories, Benrose 2011, South Africa) was added to the immobilization protocol by administering 1:1 butorphanol (mgs) to etorphine (mgs) intravenously 5 min after animal could be safely handled.

Once a warthog was immobilized and safe to handle, it was blindfolded, cotton wool earplugs inserted, and placed in lateral recumbency. Monitoring was started 10 min after initial handling ($t = 5$) to allow repositioning, instrumentation, and butorphanol administration. After induction, study animals were placed in the shade, weighed, and their ears notched for identification to prevent re-darting. At $t = 45$ (∼50 min after initial handling), naltrexone (40 mg/ml, Kyron Laboratories), at 40 times the etorphine dose (mgs), was administered into an auricular vein.

Induction times and quality (using a previously described subjective scoring system), immobilization quality, and recovery times and quality were recorded (9). Induction quality was assessed using a scale of 1 (excellent) to 4 (poor). Immobilization depth was scored on a scale of 1–6, with light immobilization equal to a score of 3 (**Table 1**). Depth was assessed at each 5 min interval during the 40 min monitoring period. Quality of recovery was scored with a 1–4 scale, similar to induction (**Table 2**).

Physiological parameters were recorded at 5 min intervals. Heart rate (HR) was measured by auscultation; respiratory rate (RR) by counting thoracic/abdominal excursions and air movement at the nares; and body temperature (BT)

TABLE 1 | Immobilization scoring system for warthogs.

1. Not achieved	Further dosing required for recumbency.
2. Sedated	Responds to manipulation and painful stimulus, voluntary movement, and reflexes present.
3. Light	Safely handled, muscle tone present in jaw and limbs, palpebral, and laryngeal reflexes present.
4. Moderate	No voluntary movement, reduced palpebral and pedal reflexes, relaxed jaw tone, no reaction to sampling.
5. Surgical	Loss of palpebral and pedal reflexes, absent jaw tone, fixed pupils, regular breathing, no reaction to sampling/ear notching.
6. Deep	No reflexes, central miotic pupil, shallow breathing and cardio-respiratory depression.

TABLE 2 | Recovery scoring system.

1. Excellent	Sternal score	Antagonist administration to sternal <10 min.
	Standing score	Minimal struggling/stands without falling after minimal attempts.
	Ambulating score	Minimal or no ataxia when walking.
2. Good	Sternal score	Antagonist administration to sternal in 10–20 min.
	Standing score	Transitions to standing with only a few falls before standing successfully.
	Ambulating score	Mild ataxia when walking with few falls.
3. Fair	Sternal score	Antagonist administration to sternal in 20–30 min.
	Standing score	Multiple unsuccessful attempts at standing before able to stand without falling.
	Ambulating score	Moderately ataxic when walking and falls occasionally.
4. Poor	Sternal score	Antagonist administration to sternal >30 min or remained in lateral recumbency.
	Standing score	Unable to stand without falling.
	Ambulating score	Unable to ambulate or falls frequently.

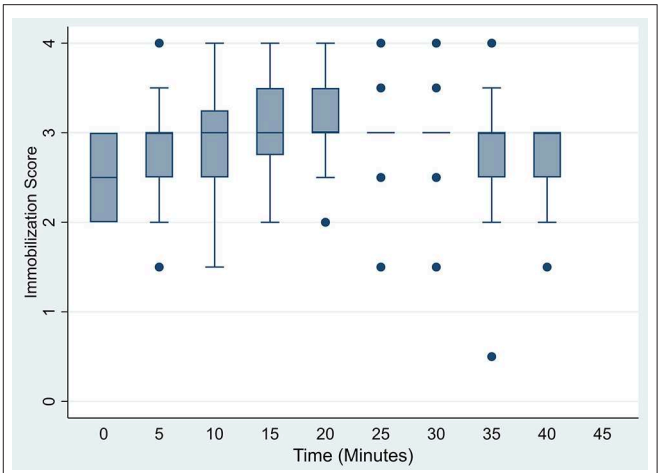

FIGURE 1 | Box plots of immobilization scores for warthogs *(Phacochoerus africanus)* immobilized with etorphine, azaperone, and butorphanol evaluated at 5 min intervals. Horizontal bars represent median values with brackets indicating 95% confidence intervals.

using a digital thermometer placed against the rectal wall. Hemoglobin saturation (SpO_2) was measured by using a pulse oximeter reflectance probe (TidalGuard SP, SHARN Veterinary Inc., Tampa, Florida 33634, USA) positioned on the conjunctival membranes.

Arterial blood samples, collected from the medial saphenous artery at $t = 5$, $t = 20$, and $t = 35$, were immediately analyzed using a portable blood gas analyzer (iSTAT®1 Handheld Clinical Analyzer, Heska Corporation, Loveland, Colorado 80538, USA) with a CG4+ cartridge (iSTAT CG4+ cartridges, Heska Corporation). Parameters included arterial partial pressure of oxygen (PaO_2), carbon dioxide ($PaCO_2$), pH, lactate, base excess (BE_{ecf}), bicarbonate (HCO_3^-), and arterial hemoglobin saturation (SaO_2).

Descriptive statistics (mean, standard deviation, minimum, median, and maximum values) were calculated at different sampling points for induction, immobilization, recovery scores, and physiological and blood gas parameters, using STATA 14 software (Stata Statistical Software, College Station, Texas 77845, USA). Normality of data was assessed by visualizing histograms and using the Shapiro-Wilk test. A linear regression model using ranks was used to evaluate the effect of time (compare values) on the cardiorespiratory and blood gas values including the sample intervals as a fixed effect and using $t = 5$ as the reference values. Non-parametric analysis results were considered statistically significant at $p < 0.05$.

RESULTS

Twenty free-ranging warthogs (4 males, 16 females), with mean weight of 68.0 kg (range 43.5–105.5 kg), were immobilized using the etorphine, azaperone, and butorphanol drug combination. Mean drug dosages, based on actual body mass, were etorphine 0.039 ± 0.005 mg/kg (range 0.030–0.046 mg/kg), azaperone 0.44 ± 0.06 mg/kg (range 0.35–0.54 mg/kg), and butorphanol 0.39 ± 0.005 mg/kg (range 0.030–0.046 mg/kg).

Induction was rapid with ataxia occurring at 2.1 ± 0.5 min (range 1.1–3.0 min). Initial recumbency occurred at 4.8 ± 1.5 min (range 2.4–9.3 min), followed by immobilization (sufficient to allow safe handling) at 5.9 ± 1.4 min (range 3.5–9.6 min). Induction was considered excellent (score 1) in 3 animals, good (score 2) in 16, and fair in 1 warthog of the 20 immobilizations. At initial assessment ($t = 0$), warthogs had immobilization scores of 2–3, with warthogs assessed as sedated to light immobilization (**Figure 1**). Sedated animals responded to stimuli and had some voluntary movement. Lightly immobilized warthogs maintained some muscle tone and reflexes but could be safely handled. Median immobilization scores increased between $t = 0$ and $t = 20$, with the majority of animals (53–70%) at a light immobilization plane (score 3) between $t = 20$ and $t = 40$. None of the warthogs had an immobilization score of 5 (surgical) or 6 (deep).

Figure 2 illustrates cardiorespiratory and BT changes over time (all values are summarized in **Supplementary Table 1**). Over the 40 min immobilization, there was no significant changes in overall HR, RR and BT. The overall mean HR was 94.7 ± 15.3 beats per min (bpm), with a median of 96 bpm and a range of 57–130 bpm. Overall mean RR was 14.7 ± 9.8 breaths per min (btpm) (median 13 btpm, range 3–60 btpm). Overall mean BT was 38.5 ± 1.0°C (median 38.6°C, range 35.5–40.9°C). The overall mean SpO_2 value was at 74.0 ± 13.5% (range 41–99%).

Figure 3 illustrates arterial blood gas changes over time (all values are summarized in **Supplementary Table 2**). Warthogs were acidotic with a borderline significant increase in median pH values over time (median pH 7.254 at $t = 5$; 7.302 at $t = 35$; $p = 0.054$). Significant hypoventilation was present at the first time point with median $PaCO_2$ and PaO_2 values

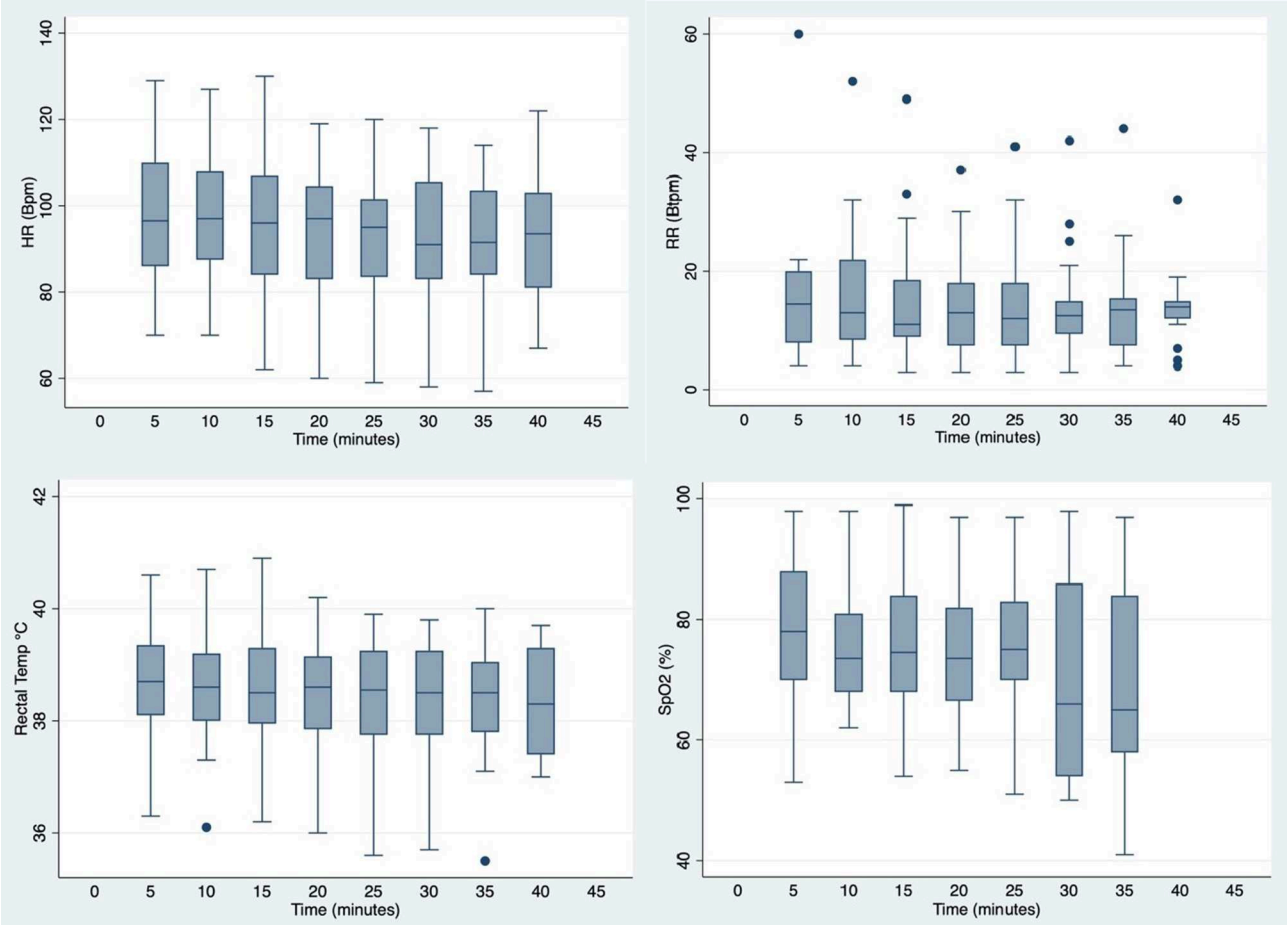

FIGURE 2 | Box plots showing distribution of cardiorespiratory and body temperature values measured at 5 min intervals in warthogs *(Phacochoerus africanus)* immobilized with etorphine, azaperone, and butorphanol. The box represents the interquartile range (25th and 75th percentile) with the horizontal bars inside the box representing median values. The bars represent the lower and upper adjacent values, and outside values are represented by dots.

of 61.3 mmHg and 44 mmHg, respectively at $t = 5$. These values significantly worsened over time with median values for $PaCO_2$ and PaO_2 at 67.3 and 36.5 mmHg, respectively at $t = 35$ ($p = 0.045$). Median lactate values decreased significantly over time from 3.7 to 0.8 mmol/L between $t = 5$ and $t = 35$ ($p = 0.001$).

Naltrexone was administered to reverse the effects of the etorphine at a mean dosage of 1.64 ± 0.44 mg/kg (range 1.05–3.24 mg/kg). Recovery was rapid with warthogs voluntarily rolling into sternal at a mean time of 0.8 ± 0.4 min (range 0.2–1.8 min) after antidote administration. Sternal recovery was scored as excellent in all but two animals. First attempts to stand occurred at a mean time of 1.0 ± 0.4 min (range 0.2–1.8 min), and successful standing and walking at 1.4 ± 0.5 min (range 0.3–2.1 min). Due to the rapid transition from sternal to standing and walking, the majority of warthogs had a score of 1 for these categories (89, 84, and 89%, respectively). No mortalities or morbidities were observed in any of the immobilized warthogs in this study.

DISCUSSION

The combination of etorphine, azaperone, and butorphanol administered to free-ranging warthogs consistently produced rapid induction with adequate immobilization to perform minor procedures, including ear notching and arterial blood collection. However, significant hypoventilation with respiratory acidosis was present. In addition, although respiratory rate and body temperature were relatively stable, persistent tachycardia was present for the duration of the immobilization. Recovery was smooth, with rapid controlled transition from recumbency to standing and walking after antidote administration.

Rapid inductions are crucial to immobilizing free-ranging warthogs since they can disappear into the bush after darting. In this study, drug effects were observed by approximately 2 min and warthogs were recumbent and could be handled within 5–6 min. Although a different cohort of warthogs was used, a previous study using free-ranging warthogs in Kruger National Park showed that a combination of medetomidine, butorphanol, tiletamine-zolazepam, and ketamine (MBTZK)

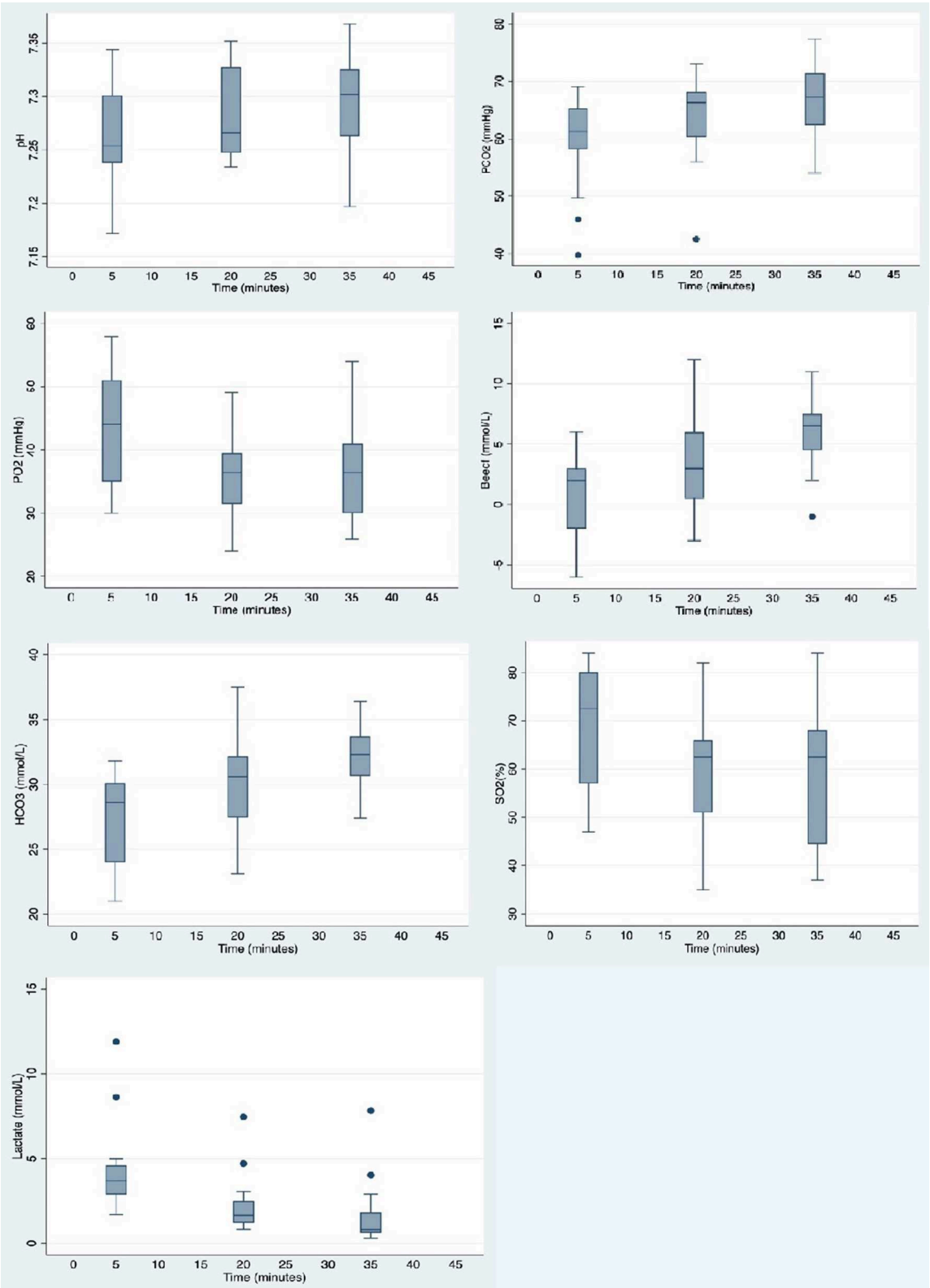

FIGURE 3 | Box plots showing distribution of arterial blood gas values measured at 15 min intervals in warthogs *(Phacochoerus africanus)* immobilized with etorphine, azaperone, and butorphanol. The box represents the interquartile range (25th and 75th percentile) with the horizontal bars inside the box representing median values. The bars represent the lower and upper adjacent values, and outside values are represented by dots.

resulted in immobilization in a similar time frame (∼6 min) (9). These induction times are also similar to those reported using cyclohexylamine and alpha2-agonist immobilization combinations in wild and domestic suids (10–12). Therefore, the use of an opioid immobilization drug combination may not have any advantage over cyclohexylamine-based combinations in terms of faster induction times.

Etorphine can cause significant adverse effects including muscle rigidity, hypertension, and hypoventilation (4, 13). Therefore, etorphine is usually administered in combination with other drugs such as azaperone, alpha2-agonists, butorphanol, or benzodiazepines. In a pilot study, etorphine and azaperone resulted in immobilization in free-ranging warthogs but resulted in severe hypoxia and hypercapnia that required intervention (unpublished data). Since butorphanol administration in etorphine-immobilized white rhinoceros (*Ceratotherium simum*). has been shown to partially reverse these adverse effects, butorphanol was added to the warthog immobilization protocol (4).

Restraint and analgesia are important factors to consider when evaluating immobilization drug combinations. In this study at $t = 20$, 55% of warthogs immobilized with etorphine, azaperone, and butorphanol had reached an immobilization score of 3 (light), with 30% reaching a score of 4 (moderate). Using the same immobilization scoring system to assess responses to stimuli and degree of relaxation, 95% of warthogs immobilized with MBTZK had an immobilization score of 5 (surgical) at $t = 20$ (9). Both drug combinations resulted in a stable immobilization plane for the remaining 20 min of the study. Warthogs administered etorphine, azaperone, and butorphanol never reached a deeper level of immobilization than a score of 4 (moderate–no voluntary movement, reduced palpebral and pedal reflexes, relaxed jaw tone, no reaction to sampling). Most of the observations (54%) were scored at 3, which permitted safe handling, with muscle tone present in jaw and limbs, palpebral and laryngeal reflexes present. In contrast, 79% of total scores for warthogs immobilized with MBTZK were 5, consistent with a surgical plane of anesthesia. These animals had a loss of palpebral and pedal reflexes, absent jaw tone, regular breathing, and no reaction to sampling or ear notching (9). In other studies, warthogs receiving tiletamine-zolazepam and xylazine retained their reflexes (similar to immobilization score 3) (12). However, medetomidine, ketamine, and butorphanol resulted in muscle relaxation, analgesia and loss of reflexes in domestic pigs (similar to immobilization score 4–5) (11). Therefore, the degree of analgesia and restraint required for a procedure will impact the choice of immobilizing drugs.

Tachycardia is commonly observed in animals administered etorphine (13). Although normal values for warthogs are unknown, the mean heart rate values measured in etorphine, azaperone, and butorphanol immobilized animals were considered to be higher than normal with an overall mean of 95 bpm (14). In MBTZK-immobilized warthogs, the overall mean HR was 65 bpm (9). Anesthetized pigs in other studies had reported HR in the range of 70–150 bpm, with bradycardia considered to be <50–70 bpm (14, 15). Butorphanol administration has been shown to significantly reduce overall heart rate in white rhinoceros immobilized with etorphine and azaperone, although still considered tachycardic compared to HR in conscious resting rhinoceros (13). Therefore, although HR appeared elevated in the warthogs, it may be expected that HR would have been higher without the administration of butorphanol.

Respiratory depression is also a common adverse effect of etorphine. In this study, warthogs maintained a stable respiratory rate, with an overall mean value of 15 btpm, during the 40 min monitoring period. In a previous study, MBTZK-immobilized warthogs also had a mean RR of 15 btpm (9). Both of these values were slightly lower than those reported for conscious non-sedated pigs (mean 20, range 16–25 btpm) (14). Higher RR were seen in warthogs anesthetized with a TZ and xylazine combination (range 29 ± 11–32 ± 11 btpm) (12). Although RR appeared to be within acceptable ranges, values for hemoglobin saturation (SpO_2) and arterial blood gases ($PaCO_2$, PaO_2) were consistent with respiratory depression in the immobilized warthogs in this study.

Pulse oximeters are useful tools for monitoring oxygen saturation in immobilized suids; however, skin or mucous membrane pigmentation can lead to inaccuracy (16). Lower SpO_2 values have been reported in conscious domestic pigs (mean 94%, range 92–95%), which may be due to species-specific differences in hemoglobin affinity (14). In a previous study, MBTZK-immobilized warthogs had SpO_2 values between 60 and 100% (9). Similarly, a tiletamine-zolazepam and xylazine combination in warthogs produced SpO_2 varying between 88 ± 5 and 91 ± 4% (12). Therefore, the low values in etorphine-immobilized warthogs in the current study are likely a true reflection of poor oxygenation. However, in order to determine whether these readings were accurate, blood gas analyses were performed to evaluate ventilation.

In our study, median $PaCO_2$ values were elevated at the initial measurement and continued to increase over time ($p = 0.017$). Similarly, low median PaO_2 values worsened over time (44–36.5 mmHg, $p = 0.045$), which was consistent with significant hypoventilation, likely due to the administration of etorphine (13). In contrast, PaO_2 values in MBTZK-immobilized warthogs significantly increased over time (median 50 mmHg at $t = 5$–65 mmHg at $t = 20$) (9). However, values for PaO_2 in conscious domestic pigs ranged from 73 to 92 mmHg, which suggests that the changes may be less severe (14). The low arterial pH in etorphine-immobilized warthogs appeared to be due to respiratory acidosis, consistent with hypoventilation. Values for domestic pigs are reported to be 7.4–7.53 (14). Therefore, significant hypoventilation is a serious adverse effect of the etorphine, azaperone, and butorphanol combination in warthogs, although assisted ventilation could be used to overcome this.

Exertion during induction can exacerbate acidosis and hyperthermia in darted suids. In this study, warthogs had lactate values within normal reported ranges for domestic pigs (0.5–5.5 mmol/L) (17). Body temperatures in this study were also within

normal ranges for domestic pigs and provide additional support that the warthogs did not exert themselves post-darting (18). However, these warthogs were habituated to people which may have influenced their response.

Rough recoveries are also a common cause of trauma and hyperthermia in immobilized suids (3, 8). Use of specific reversals for selected immobilizing drugs have been shown in previous studies to improve recovery in suids (10, 11). Administration of atipamezole and naltrexone in MBTZK-immobilized warthogs resulted in rapid smooth recoveries (mean time to walking 7.3 ± 4.9 min) (9). In the current study, the majority of warthogs had excellent recovery scores, with rapid recoveries (mean time to walking <2 min), since naltrexone was used to antagonize the effects of etorphine. The etorphine, azaperone, butorphanol combination may therefore, be especially useful for short procedures in free-ranging warthogs that need to be fully recovered to avoid predation.

Overall, etorphine, azaperone, and butorphanol administration to free-ranging warthogs was an effective immobilizing drug combination with rapid induction and recoveries. However, the adverse cardiorespiratory changes associated with these drugs may increase the risk of morbidity and mortality in compromised warthogs. Therefore, this combination may be useful in free-ranging healthy warthogs for short duration procedures that require rapid restraint and recovery with minimal analgesia, such as snare removal or sampling. This study also provides other alternatives to cyclohexylamine-based combinations for immobilization of this species in zoos.

DATA AVAILABILITY STATEMENT

The datasets generated for this study are available on request to the corresponding author.

ETHICS STATEMENT

The animal study was reviewed and approved by SAN Parks Animal Use and Care committee.

AUTHOR CONTRIBUTIONS

DN, PB, JH, FO-P, and MM responsible for study design, data collection, analyses, and drafting manuscript. GH, LR, TM, BG, ET, and FO-P participated in data collection and analyses. ET and FO-P were responsible for statistical calculations. All authors assisted with writing and editing the manuscript.

FUNDING

This work was supported by Kruger National Park Veterinary Wildlife Services, South African Medical Research Council, National Research Foundation of South Africa (grant #86949), and Smithsonian Institution National Zoological Park. The content is the sole responsibility of the authors and does not necessarily represent the official views of South African National Parks, South African Medical Research Council, National Research Foundation, or Smithsonian Institution National Zoological Park.

ACKNOWLEDGMENTS

The authors would also like to thank Christine Preto for assistance with field immobilizations.

SUPPLEMENTARY MATERIAL

The Supplementary Material for this article can be found online at: https://www.frontiersin.org/articles/10.3389/fvets.2019.00402/full#supplementary-material

REFERENCES

1. Kock MD, Burroughs R. *Chemical and Physical Restraint of Wild Animals*. 2nd ed. Greyton: International Wildlife Veterinary Services (Africa) (2012). p. 235–6.
2. Kreeger TJ, Arnemo JM. *Handbook of Wildlife Chemical Immobilization*. 4th ed. Private Publication (2012). p. 307–8.
3. Padilla LR, Ko JCH. Non-domestic suids. In: West G, Heard D, Caulkett N, editors. *Zoo and Wildlife Anaesthesia*. Ames, IA: Blackwell Publishing (2007). p. 567–77.
4. Buss P, Miller M, Fuller A, Haw A, Stout E, Olea-Popelka F, et al. Post-induction butorphanol administration alters oxygen consumption to improve blood gases in etorphine-immobilized white rhinoceros. *Vet Anaesth Analg*. (2018) 45:57–67. doi: 10.1016/j.vaa.2017.03.008
5. Burroughs REJ. Chemical capture of the warthog *Phacochoerus aethiopicus*. In: McKenzie AA, editor. *The Capture and Care Manual: Capture, Care, Accommodation and Transportation of Wild African Animals*. Lynnwood: Wildlife Decision Support Services CC (1993). p. 621–3.
6. Jones DM. A rational approach to the use of drugs for sedation and restraint of the larger mammals. *Vet Anaesth Analg*. (1973) 4:33–42. doi: 10.1111/j.1467-2995.1973.tb00220.x
7. Kock MD, Metzler D, Burroughs R. *Chemical and Physical Restraint of Wild Animals*. 1st ed. Greyton: International Wildlife Veterinary Services (Africa) (2006). p. 189–90.
8. Sutherland-Smith M. Suidae and tayassuidae (wild pigs, peccaries). In: Miller RE, Fowler ME, editors. *Fowler's Zoo and Wild Animal Medicine*, Vol. 8. St Louis, MO: Elsevier (2015). p. 568–83.
9. Hewlett, J., Buss, P., Olea-Popelka, F., Koeppel, K., Neiffer, D., Hausler, G., et al. (in press). Evaluation of a partially reversible immobilization protocol using medetomidine, butorphanol, zolazepam-tiletamine, and ketamine in free-ranging warthogs (*Phacochoerus africanus*) in Kruger National Park, South Africa. *J Zoo Wildl Med*. 51.
10. Barasona JA, Lopez-Olvera JP, Vicente J. Trap-effectiveness and response to tiletamine-zolazepam and medetomidine anaesthesia in Eurasian wild boar captured with cage and corral traps. *BMC Vet Res*. (2013) 9:107. doi: 10.1186/1746-6148-9-107
11. Sakaguchi M, Nishimura R, Sasaki N, Ishiguro T, Tamura H, Takeuchi A. Anaesthesia induced in pigs by use of a combination of medetomidine, butorphanol and ketamine and its reversal by administration of atipamezole. *Am J Vet Res*. (1996) 57:529–34.
12. Sonntag S, Hackenbroich C, Boer M. Tiletamine-zolazepam-xylazine immobilisations in warthogs (*Phacochoerus aethiopicus*). *Proc Eur Assoc Zoo Wildl Vet*. (2004) 2004:105–6.

13. Buss P, Miller M, Fuller A, Haw A, Wanty R, Olea-Popelka F, et al. Cardiovascular effects of etorphine, azaperone, and butorphanol combinations in chemically immobilized captive white rhinoceros (*Ceratotherium simum*). *J Zoo Wildl Med*. (2016) 47:834–43. doi: 10.1638/2015-0298.1
14. Hannon JP, Bossone CA, Wade CE. Normal physiological values for conscious pigs used in biomedical research. *Lab Anim Sci*. (1990) 40:293–8.
15. Thurmon JC, Smith GW. Swine anaesthesia. In: Tranquilli WJ, Thurmon JC, Grimm KA, editors. *Lumb and Jones's Veterinary Anesthesia and Analgesia*. Baltimore, MD: Williams and Wilkins (1996). p. 747–63.
16. Moseby C, Gunkel C. Cardiovascular and pulmonary support. In: West G, Heard D, Caulkett N, editors. *Zoo and Wildlife Anaesthesia*. Ames, IA: Blackwell Publishing (2007). p. 93–102.
17. Hofmaier F, Dinger K, Braun R, Sterner-Kock A. Range of blood lactate values in farm pigs prior to experimental surgery. *Lab Anim*. (2013) 47:130–2. doi: 10.1177/0023677213476857
18. Littledike ET, Witzel DA, Riley JL. Body temperatures changes in sows during the periparturient period. *Lab Anim Sci*. (1979) 29:621–4.

Conflict of Interest: The authors declare that the research was conducted in the absence of any commercial or financial relationships that could be construed as a potential conflict of interest.

Copyright © 2019 Neiffer, Buss, Hewlett, Hausler, Rossouw, Manamela, Grenus, Thulson, Olea-Popelka and Miller. This is an open-access article distributed under the terms of the Creative Commons Attribution License (CC BY). The use, distribution or reproduction in other forums is permitted, provided the original author(s) and the copyright owner(s) are credited and that the original publication in this journal is cited, in accordance with accepted academic practice. No use, distribution or reproduction is permitted which does not comply with these terms.

frontiers in Veterinary Science

ORIGINAL RESEARCH
published: 19 November 2019
doi: 10.3389/fvets.2019.00405

Effects of External Oiling and Rehabilitation on Hematological, Biochemical, and Blood Gas Analytes in Ring-Billed Gulls (*Larus delawarensis*)

Nicholas G. Dannemiller[1,2], Katherine E. Horak[1], Jeremy W. Ellis[1], Nicole L. Barrett[1], Lisa L. Wolfe[3] and Susan A. Shriner[1]*

[1] US Department of Agriculture, Animal Plant Health Inspection Service, Wildlife Services, National Wildlife Research Center, Fort Collins, CO, United States, [2] Department of Clinical Sciences, Colorado State University, Fort Collins, CO, United States, [3] Wildlife Health Program, Colorado Parks and Wildlife, Fort Collins, CO, United States

OPEN ACCESS

Edited by:
Nicole Indra Stacy, University of Florida, United States

Reviewed by:
Lorelei Schwacke, National Marine Mammal Foundation, United States
Nuno Santos, University of Porto, Portugal

***Correspondence:**
Nicholas G. Dannemiller
dannemillern@gmail.com

Specialty section:
This article was submitted to Zoological Medicine, a section of the journal Frontiers in Veterinary Science

Received: *12 June 2019*
Accepted: *31 October 2019*
Published: *19 November 2019*

Citation:
Dannemiller NG, Horak KE, Ellis JW, Barrett NL, Wolfe LL and Shriner SA (2019) Effects of External Oiling and Rehabilitation on Hematological, Biochemical, and Blood Gas Analytes in Ring-Billed Gulls (Larus delawarensis). Front. Vet. Sci. 6:405. doi: 10.3389/fvets.2019.00405

Avian species experience extensive morbidity and mortality following large-scale oil spills, often resulting in oiled birds being rescued, and admitted to rehabilitation. Our objective was to experimentally establish time-specific, descriptive blood analyte data following sublethal oil exposure and subsequent rehabilitation. Thirty wild Ring-billed Gulls (*Larus delawarensis*) were randomly allocated to three treatment groups of 10 birds each. One treatment group served as controls and two treatment groups were externally oiled daily for 3 days with weathered MC252 oil collected from the Deepwater Horizon oil spill, mimicking the upper threshold of the US Fish and Wildlife Service's moderate oiling classification. Following external oiling, one oiled treatment group was cleaned via standard rehabilitation practices. Serial venous blood samples were collected for a month to measure packed cell volume, total solids, blood gas and select plasma biochemistry analytes, total white blood cell estimates and differentials, and reticulocyte estimates. We found that both sublethal oil exposure and aspects of captivity were associated with a mild non-regenerative anemia. No other differences in venous blood gas and biochemical analytes as well as white blood cell concentrations were observed among the three groups. These findings suggest that the mild anemia seen in oiled birds undergoing rehabilitation is possibly multifactorial and that moderately oiled gulls have subtle, but potentially not insignificant clinicopathological abnormalities following sublethal oil exposure. Oiled gulls did not develop any clinicopathological derangements post-rehabilitation, suggesting current standard practices for rehabilitation cause minimal morbidity in clinically stable, moderately oiled gulls.

Keywords: oil toxicity, wildlife rehabilitation, hemolytic anemia, immune suppression, blood gas, Ring-billed Gull

INTRODUCTION

The negative impact of oil spills on wildlife, particularly birds, has been widely recognized. Aquatic and semi-aquatic avian populations have experienced extensive morbidity and mortality following many large-scale oil spills, such as the Exxon Valdez (1), Prestige (2), and most recently, Deepwater Horizon (3, 4). However, crude oil's true impact on birds is likely larger than the reported acute mortality estimates (5, 6). Chronic oil exposure has been implicated in avian population declines long after the initial mass mortality following an oil spill, slowing population recovery despite clean up and environmental restoration (7). Thus, a stronger understanding of the effects of sublethal external oil exposure (i.e., external oiling that does not lead to acute death) on individual birds is warranted to better characterize avian oil toxicosis as well as the broader impacts of oil spills.

Sublethal oil exposure on birds causes a wide range of adverse effects including: hemolytic anemia; decreased nutrient absorption; altered physiological stress responses; renal, hematopoietic, and hepatic damage; and immunosuppression (8–12). Of these adverse effects, hemolytic anemia has been most frequently demonstrated in birds exposed to crude oil. Hemolytic anemia secondary to oil exposure is likely caused by oxidative damage mediated by metabolites of polycyclic aromatic hydrocarbons generated from cytochrome P450 enzymes in the livers of oiled birds (13, 14). Oil induced hemolytic anemia is characterized by red blood cell (RBC) regeneration, increased numbers of reticulocytes, and the development of Heinz bodies from oxidative damage to hemoglobin; however, the kinetics of these abnormalities is not well-characterized. Although the adverse effect of oil exposure on RBCs has been well-investigated, there are limited reports on the effect of oil on white blood cells (WBC) (15, 16). Previous studies have shown birds exposed to oil often exhibit reduction in total WBC counts and lymphocytes suggestive of immunosuppression as well as markedly elevated heterophil counts and heterophil/lymphocyte ratios (15, 16). There are currently no reports on the effect of oil exposure on the blood gas and acid-base status of birds.

Due to the development of protocol-driven response and recovery efforts, oiled birds are increasingly rescued and admitted to rehabilitation following oil spills (17). While on-going research continues to target aspects of emergency medicine and critical care for improvement, rehabilitation alone is an inherently stressful sequence of events for oiled birds. To date, no studies have evaluated the effect of current rehabilitation procedures on oiled birds. Knowledge of the clinicopathological abnormalities observed in birds following prolonged sublethal oil exposure, the effect rehabilitation has on these abnormalities, and the overall chronology of these abnormalities would be invaluable to veterinarians treating and managing oiled birds. However, given the temporal and spatial unpredictability of oil spills, this knowledge is difficult to acquire from wild birds *in situ*. While most experimental research on oil exposure has traditionally focused on oral dosing, less work has been conducted on sublethal external oiling. A recent suite of papers assessing avian exposure to Deepwater Horizon crude oil (18) has shown myriad impacts from sublethal external oiling, including flight impairment, reduced weight gain, altered metabolome, oxidative damage, changes in plasma biochemistry, changes in organ weights and histopathology, and cardiac dysfunction (19–24). Consequently, further exploration of the impacts of external oiling is warranted.

The objective of our study was to establish time-specific estimates of hematological, biochemical, and venous blood gas analytes to not only improve the point-of-care assessment of oiled birds, but also help better understand the pathogenesis of oil toxicosis from external oiling. Under experimental conditions and through serial blood sampling, our study characterizes post-exposure and post-rehabilitation changes in select blood analytes for birds externally oiled with weathered crude oil from the Deepwater Horizon oil spill. We also establish reference intervals for wild Ring-billed Gulls (*Larus delawarensis*), a common species found in coastal areas at risk of oil spills. We hypothesized that sublethal oil exposure would cause anemia and immunosuppression in externally oiled birds and that rehabilitated birds would return to pre-exposure values more quickly than post-exposure, non-rehabilitated birds.

METHODS

Gull Capture and Husbandry

All aspects of this study, including bird capture, transport, quarantine, husbandry, oiling, and sampling, were performed according to procedures approved by the Institutional Animal Care and Use Committee of the US Department of Agriculture, Animal and Plant Health Inspection Service, National Wildlife Research Center (NWRC; Approval 2806). Thirty-five Ring-billed Gulls (RBGU) were captured in Larimer County, CO using air cannon nets and net guns and transported to the NWRC, Fort Collins, CO in large ventilated crates. Birds were not captured in extreme weather conditions and transport time was <1 h. Capture was conducted under the authority of US Fish and Wildlife Service (USFWS) Migratory Bird Permit #MB019065 as well as Colorado Parks and Wildlife scientific collection license #18TRb2433.

Upon arrival at the NWRC, captured RBGUs were given a complete and thorough physical exam by the NWRC attending veterinarian, weighed, individually marked with a unique leg band, and a baseline blood sample was collected. Body temperature was also measured using a VetOne digital cloacal thermometer (MWI Animal Health, Aurora, CO). Given RBGUs are not sexually dimorphic, the sex distribution of the captured birds was unknown. Most birds were characterized as breeding adults based on plumage, but a few had markings that were consistent with either non-breeding adult or second winter plumage. Throughout the study, birds were group housed in large, netted outdoor flight pens (18.29 × 37.80 m) that contained artificial pools, heat lamps, as well as platforms and other objects that allowed for natural perching and loafing. During testing, RBGUs were offered a maintenance diet of commercial avian cubes (Mazuri Fish Analog 50/10 Frozen 5T8, St. Louis, MO), raw golden shiner minnows (*Notemigonus crysoleucas*, I.F. Anderson Farms, Inc., Lonoke, AR), and canned mackerel *ad libutum* two times per day. At the conclusion of this study, all surviving birds

were transferred as study animals to other research projects or released near the capture site in Larimer County, CO.

Oil Source

MC252 oil collected during the Deepwater Horizon oil spill and artificially weathered (i.e., weathered in the laboratory prior to receipt for use in studies) was used to moderately externally oil two of the three treatments groups. Oil was artificially weathered by TDI-Brooks International, Inc. and B&B Laboratories (College Station, TX) and shipped to NWRC by Ecochem, Inc. (Tukwila, WA) under chain of custody.

External Oiling and Rehabilitation

After acclimation, 30 RBGUs were randomly allocated to three treatment groups of 10 birds each. *A priori* power analyses determined 10 birds per treatment group would adequately minimize a Type II statistical error (power = 0.996, given effect size = 0.8 and $\alpha = 0.05$). Two treatment groups were externally oiled daily for 3 days with 5–7 mL of oil applied per day with a paintbrush to the breast, wing edges, and tail feathers mimicking the upper threshold of the USFWS moderate oiling classification for birds. This level of oiling is generally described as 14–40% surface area coverage. In general, oil was applied to body areas that would be exposed to an oil sheen for surface feeding birds such as RBGUs. After 3 days, oiled RBGUs received a cumulative total of 15–21 mL of oil. The third treatment group served as controls and were handled in the same manner as the other two groups but were painted with water instead of oil for 3 days. Nine days after initial oiling, one of the oiled treatment groups was cleaned following standard practices for rehabilitating oiled birds over a 48-h period. Briefly, oiled birds were washed in sequential tubs filled with diluted detergent (1-2%) in softened water (2–3 grains of hardness) heated to 106-110°F (41–43°C) until the water remained clear. Birds were then rinsed with softened water at a temperature of 106-112°F and allowed to rest in a clean and well-ventilated brooder box lined with warm towels and equipped with water for drinking while being dried with heat lamps. During the drying process, air temperature was maintained between 90 and 95°F (32-35°C), with the birds being carefully monitored for signs of hypothermia or hyperthermia. The second oiled treatment group remained externally oiled until the conclusion of the study and then was cleaned using the same methods as previously described.

Serial Venous Blood Sampling

In order to characterize changes over time, blood samples (200–300 μL), weights, and temperatures were collected from RBGUs immediately prior to the external oiling and then 7, 15, 22, and 31 days post-oiling (DPO). Venous blood was anaerobically and aseptically collected using a 1.0 inch, 22-gauge needle, and heparinized syringes from either the left or right brachial, distal metatarsal, or external jugular veins. Blood samples were immediately divided into two subsamples. The first subsample was stored in microtainers to later measure packed cell volume (PCV) and total solids using a PCV chart and refractometer as well as visually assess for presence of plasma hemolysis, following high-speed centrifugation of blood-filled microhematocrit tubes. The second subsample was used for instant venous blood gas and select plasma biochemistry analysis, using the Element POC Blood Gas & Electrolyte Analyzer (EPOC; Heska Corporation, Loveland, CO), a handheld veterinary point-of-care analyzer.

Venous blood gas and plasma biochemistry analytes of interest included: hematocrit; plasma concentrations of sodium, potassium, chloride, ionized calcium, lactate, glucose, and bicarbonate; pH; and venous pO_2 and pCO_2. Because the EPOC performed all analyses at 37°C, pH, pCO_2, pO_2, were temperature corrected (TC) to reflect the RBGU's respective body temperatures via the following equations:

$$TC\,pH = pH + (0.0147 * \Delta\,T)$$
$$TC\,pCO_2 = pCO_2 * 10^{(-0.019 * \Delta\,T)}$$
$$TC\,pO_2 = pO_2 * 10^{(-0.0058 * \Delta\,T)}$$

where $\Delta T = 37°C - $body temperature (25). The TC bicarbonate concentration was calculated via the Henderson-Hesselbach equation using TC pH and pCO_2 values as well as the solubility coefficient for CO_2 and pK (logarithmic acid dissociation constant) (25). Due to the effects of pH on ionized calcium, the following correction was applied (26):

$$TC\ Ionized\ Calcium = Ionized\ Calcium * (1 + (0.53\,(pH - TC\,pH)))$$

Anion gap was calculated via the following equation:

$$Anion\ Gap = (Sodium + Potassium) - (Chloride + TC\ Bicarbonate)$$

Two duplicate blood smears were also made each time blood was drawn and subsequently submitted to the Colorado State University Veterinary Diagnostic Lab (Fort Collins, Colorado) for processing. Total WBC estimates were derived using an internal standard operating procedure for avian WBC estimates due to the unavailability of a whole blood sample. Briefly, all WBCs seen in ten 50× oil fields were counted and then divided by 10 to obtain the average WBC count per 50× oil field. This average was then used in the following equation:

$$\text{Total WBC}/\mu\text{l} = 5,000\ \text{WBC} + 3,000\ \text{WBC x (Average WBC}/50 \times\ \text{oil field} - 1)$$

This WBC estimate formula was developed from internal unpublished studies at the Colorado State University Veterinary Diagnostic Laboratory and has not been validated or verified. WBC differential was performed by calculating the percentage of each leukocyte type seen in a sample of 100 leukocytes under 1,000× oil immersion (27). Reticulocyte estimates were generated by enumerating aggregate reticulocytes and ring forms using previously described methods (28).

Statistical Analysis

Physical, hematological, biochemical, and blood gas data collected from all 30 RBGUs immediately prior to the external

oiling were aggregated to generate reference intervals. Given our small sample size and that some analytes had non-parametric distributions, robust estimation of the 90% confidence interval of reference limits was employed as suggested by Friedrichs et al. (29). Robust estimation of the 90% confidence interval was done using a bias corrected bootstrap method based on 10,000 bootstrap replicates. Median, minimum, and maximum values were also calculated and reported to allow informed clinical decision-making (29). For subsequent DPO, mean, median, standard deviation, minimum, and maximum were calculated for each treatment group separately. Data were also analyzed using multiple linear mixed models (LMM) for repeated measures with treatment group, DPO, and the interaction between treatment group and DPO as predictor variables, each of the various clinical analytes as the response variable, and the individual RBGU as a random effect. A separate LMM was run for each clinical analyte with the false discovery rate controlled via the Benjamini–Hochberg procedure (30). Hematocrit as determined by EPOC, hereafter HCT (EPOC), and PCV determined manually, hereafter PCV (spun), were compared using a paired *t*-test, Lin's concordance correlation coefficient (31), and a Bland-Altman plot (32). All statistics were performed in the statistical software program R version 3.5 (33) with the 90% confidence intervals being generated with the "boot" package and LMMs being fitted using the "lme4" package (34).

RESULTS

Physical, hematological, biochemical, and blood gas analyte values from baseline (0 DPO) sampling showed no obvious clinical abnormalities in the RBGUs (**Table 1**). Of the 30 RBGUs included in this study, 28 survived through its conclusion: one rehabilitated-oiled RBGU died between 7 and 15 DPO and one non-rehabilitated-oiled RBGU died between 22 and 31 DPO. Necropsies and histopathology of the deceased birds found the cause of death was not due to sublethal external oil exposure. LMMs were not run for monocytes, eosinophils, and basophils given their mean and median were $0 \times 10^3/\mu L$ on 7, 15, 22, and 31 DPO.

PCV (spun) and HCT (EPOC) of both the rehabilitated and non-rehabilitated-oiled groups were significantly lower when compared to the control group (**Table 2**). On average, non-rehabilitated-oiled RBGUs had 4 ± 0.8% lower PCV (spun) than controls and rehabilitated-oiled RBGUs had 3 ± 0.8% lower PCV (spun) than controls. Similarly, non-rehabilitated-oiled RBGUs had 5 ± 0.8% lower HCT (EPOC) than controls and rehabilitated-oiled RBGUs had 4 ± 0.8% lower HCT (EPOC) than controls on average. PCV (spun) and HCT (EPOC) were also significantly lower over time for all groups (**Table 2**). All treatment groups had lower PCV (spun) and HCT (EPOC) on 7, 15, 22, and 31 DPO compared to 0 DPO (**Table 3**). HCT (EPOC), but not PCV (spun), exhibited a significant interaction between non-rehabilitated-oiled group and time (**Table 2**); when compared to the control group, non-rehabilitated-oiled RBGUs' HCT (EPOC) decreased 0.2% more over time. Obvious plasma hemolysis was not visually observed following high-speed centrifugation of blood-filled microhematocrit tubes for any treatment group.

TABLE 1 | Reference intervals and summary statistics for body temperature and select venous blood analytes of wild Ring-billed Gulls (*Larus delawarensis*).

Analytes	Reference interval	Median	Mean ± SD	(Min, Max)
Body temperature (°C)	42.2–42.5	42.4	42.4 ± 0.5	(41.4, 43.4)
PCV (spun) (%)	51–54	52	53 ± 5	(43, 60)
Hematocrit (EPOC) (%)	42–43	43	43 ± 3	(36, 48)
Total Solids (g/dL)	4.2–4.5	4.1	4.3 ± 0.6	(3.2, 5.8)
Sodium (mmol/L)	156–157	156	156 ± 2	(152, 160)
Potassium (mmol/L)	2.7–2.9	2.8	2.8 ± 0.4	(2.2, 3.7)
Chloride (mmol/L)	120–122	120	121 ± 4	(113, 129)
TC ionized calcium (mmol/L)	1.1–1.2	1.1	1.1 ± 0.1	(0.8, 1.3)
TC anion gap	20–22	22	21 ± 3	(14, 31)
Lactate (mmol/L)	4.4–5.7	4.6	4.9 ± 2.1	(2.4, 12.7)
Glucose (mg/dL)	322–351	334	336 ± 48	(244, 424)
TC pH	7.39–7.43	7.40	7.41 ± 0.06	(7.30, 7.60)
TC pCO_2 (mmHg)	29–32	30	31 ± 5	(21, 40)
TC pO_2 (mmHg)	48–52	49	50 ± 6	(39, 62)
TC bicarbonate (mmol/L)	16–18	16	17 ± 3	(9, 23)
Total WBC ($\times 10^3/\mu L$)	10.0–11.0	11.0	10.6 ± 1.8	(7.0, 13.0)
Heterophils ($\times 10^3/\mu L$)	4.7–5.3	4.9	5.0 ± 1.1	(3.0, 7.7)
Lymphocytes ($\times 10^3/\mu L$)	2.3–2.6	2.6	2.5 ± 0.4	(1.7, 3.3)
Monocytes ($\times 10^3/\mu L$)	0.0–0.1	0.1	0.1 ± 0.1	(0, 0.2)
Eosinophils ($\times 10^3/\mu L$)	0.0–0.0	0.0	0.0 ± 0.0	(0.0, 0.0)
Basophils ($\times 10^3/\mu L$)	0.0–0.0	0.0	0.0 ± 0.0	(0.0, 0.0)
Reticulocytes (%)	0.7–1.0	1.0	1.0 ± 0.4	(0.0, 2.0)

Reference intervals are based on 30 wild caught birds (weight range = 404–550 g, median = 471 g, mean = 466 g) sampled immediately prior to external oiling. Reference intervals are 90% confidence intervals estimated via a bias corrected bootstrap method based on 10,000 bootstrap replicates. TC, temperature corrected; SD, standard deviation.

Estimated reticulocytes significantly differed among treatment groups but did not change over time nor exhibit an interaction between group and time (**Table 2**). Non-rehabilitated-oiled RBGUs had a 1.3 ± 0.1% higher estimated reticulocyte percentage than both rehabilitated-oiled and control RBGUs. Body weight, body temperature, total solids, sodium, potassium, chloride, TC ionized calcium, lactate, glucose, TC anion gap, TC pH, TC pO_2, TC bicarbonate, total WBC, heterophils, and lymphocytes did not differ among treatment groups, change over time, or exhibit an interaction between group and time.

HCT (EPOC) and PCV (spun) were significantly different [$t_{(145)} = 28.78$, $p < 0.001$]—the HCT (EPOC) was on average 8.2% (95% CI: 1.5–14.9%) less than PCV (spun). The concordance correlation coefficient between HCT (EPOC) and PCV (spun) was 0.35 (95% CI: 0.28–0.41) suggesting low concordance in their results. A Bland-Altman plot of the relationship between HCT (EPOC) and PCV (spun) shows considerable variability in the discrepancy between the two methods, but no obvious trend (**Figure 1**).

TABLE 2 | Linear mixed model results for clinical analytes of Ring-billed Gulls (*Larus delawarensis*) in three treatment groups (Control gulls, Oiled/Non-Rehabilitated gulls, and Oiled/Rehabilitated gulls).

	Treatment Non-rehab	SE	DF	*t*	*p*-value	Treatment Rehab	SE	DF	*t*	*p*-value
Weight	−37.1	21.1	30.7	−1.8	0.088	3.2	21.1	30.8	0.2	0.882
Body temperature	0.0	0.2	56.9	−0.1	0.928	−0.1	0.2	57.3	−0.6	0.547
PCV (spun)	−4.2	1.1	142.0	−3.7	<0.001*	−3.5	1.1	142.0	−3.1	0.003*
Hematocrit (EPOC)	−5.1	1.1	24.3	−4.5	<0.001*	−4.1	1.1	24.8	−3.6	0.001*
Total solids	0.0	0.0	0.0	−0.3	0.729	0.0	0.0	0.0	−0.7	0.468
Sodium	0.6	0.8	18.6	0.8	0.439	−0.2	0.8	19.0	−0.2	0.827
Potassium	0.0	0.2	114.9	−0.1	0.900	0.1	0.2	115.4	0.7	0.508
Chloride	0.4	1.2	74.2	0.4	0.711	1.1	1.2	74.8	0.9	0.364
TC ionized calcium	0.0	0.0	98.5	0.9	0.382	0.0	0.0	99.2	−1.2	0.239
TC anion gap	−1.0	1.0	115.9	−1.0	0.339	−1.7	1.0	116.5	−1.6	0.104
Lactate	0.2	0.7	59.8	0.3	0.746	−0.7	0.7	60.2	−0.9	0.347
Glucose	−27.3	18.5	67.8	−1.5	0.146	−40.7	18.6	68.3	−2.2	0.032
TC pH	0.0	0.0	0.0	−0.4	0.699	0.0	0.0	0.0	−0.1	0.928
TC pCO_2	0.6	2.0	69.4	0.3	0.800	−0.8	2.0	69.9	−0.4	0.689
TC pO_2	−0.4	1.7	113.0	−0.2	0.828	1.7	1.7	113.7	1.0	0.310
TC bicarbonate	0.1	0.9	91.1	0.1	0.926	−0.5	0.9	91.7	−0.5	0.600
Total WBC	0.7	0.6	138.0	1.1	0.268	−0.7	0.6	138.0	−1.2	0.252
Heterophils	0.0	0.0	0.0	1.1	0.278	0.0	0.0	0.0	−0.3	0.759
Lymphocytes	0.1	0.2	112.6	0.4	0.691	−0.2	0.2	113.0	−1.5	0.128
Reticulocytes	0.0	0.0	0.0	2.4	0.018*	0.0	0.0	0.0	0.6	0.562

Analytes	DPO	SE	DF	*t*	*p*-value	Non-rehab: DPO	SE	DF	*t*	*p*-value	Rehab: DPO	SE	DF	*t*	*p*-value
Weight	0.0	0.2	113.1	1.8	0.078	0.6	0.4	113.2	1.8	0.078	−0.1	0.4	113.5	−0.3	0.777
Body temperature	0.0	0.0	110.6	−0.4	0.686	0.0	0.0	111.0	1.8	0.069	0.0	0.0	113.0	0.9	0.349
PCV (spun)	−0.1	0.0	142.0	−2.2	0.032*	−0.1	0.1	108.3	−1.1	0.294	0.0	0.1	109.8	−0.2	0.871
Hematocrit (EPOC)	−0.1	0.0	114.5	−3.6	<0.001*	−0.2	0.1	110.5	−2.9	0.005*	0.0	0.1	112.6	−0.3	0.733
Total solids	0.0	0.0	0.0	0.8	0.449	0.0	0.0	0.0	0.2	0.819	0.0	0.0	0.0	−0.1	0.938
Sodium	0.0	0.0	105.8	−1.0	0.315	0.1	0.0	101.8	1.7	0.095	0.1	0.0	104.4	1.8	0.078
Potassium	0.0	0.0	112.1	0.9	0.363	0.0	0.0	113.0	0.4	0.677	0.0	0.0	115.5	0.6	0.551
Chloride	0.0	1.2	74.8	0.9	0.364	0.1	0.1	108.2	1.0	0.306	0.0	0.1	110.9	−0.8	0.399
TC ionized calcium	0.0	0.0	112.5	1.3	0.192	0.0	0.0	113.2	0.4	0.692	0.0	0.0	115.7	1.4	0.158
TC anion gap	0.0	0.0	112.9	−0.6	0.579	0.0	0.1	113.8	0.9	0.377	0.1	0.1	116.2	1.5	0.130
Lactate	0.0	0.0	112.7	0.7	0.483	0.0	0.0	113.1	0.2	0.834	0.0	0.0	115.0	1.2	0.244
Glucose	−0.3	0.6	112.4	−0.6	0.547	0.0	0.8	112.8	0.1	0.955	1.0	0.8	115.0	1.2	0.241
TC pH	0.0	0.0	0.0	−0.6	0.568	0.0	0.0	0.0	−1.8	0.083	0.0	0.0	0.0	−1.6	0.108
TC pCO_2	0.1	0.1	112.0	1.0	0.314	0.1	0.1	112.5	1.2	0.234	0.2	0.1	114.7	2.4	0.016
TC pO_2	0.1	0.1	111.0	1.0	0.315	0.0	0.1	112.0	−0.2	0.830	−0.1	0.1	114.5	−1.2	0.235
TC bicarbonate	0.0	0.0	112.7	0.4	0.667	0.0	0.0	113.4	−0.7	0.497	0.0	0.0	115.8	1.0	0.311
Total WBC	0.0	0.0	138.0	0.1	0.931	0.0	0.0	138.0	−1.0	0.301	0.0	0.0	138.0	0.4	0.687
Heterophils	0.0	0.0	0.0	−0.3	0.792	0.0	0.0	0.0	0.0	0.989	0.0	0.0	0.0	1.4	0.168
Lymphocytes	0.0	0.0	112.6	−0.5	0.649	0.0	0.0	114.4	−0.2	0.844	0.0	0.0	114.6	0.7	0.500
Reticulocytes	0.0	0.0	0.0	1.9	0.066	0.0	0.0	0.0	0.0	0.975	0.0	0.0	0.0	−0.7	0.516

*Repeated measures of each analyte were modeled with Treatment (Control, Non-Rehab, Rehab), days post-oiling (DPO), and the interaction between Treatment and DPO as predictor variables and individual gulls as a random effect. A separate mixed model was run for each analyte with statistical significance determined via the Benjamini–Hochberg. p-values with an * are statistically significant. TC, temperature corrected; SE, standard error; DF, degrees of freedom.*

DISCUSSION

Brought to near extinction due to anthropogenic forces in the late nineteenth century, RBGUs have rebounded and become one of the most common and widespread gull species in North America. We are the first to report blood data reference intervals for wild RBGUs, a potential resource for future comparative studies or clinical work. RBGU PCV (spun) was similar to PCV

TABLE 3 | Post-oiling summary statistics for Ring-billed Gull (*Larus delawarensis*) weight, body temperature, and select venous blood analytes stratified by treatment group (Control gulls, Oiled/Non-Rehabilitated gulls, and Oiled/Rehabilitated gulls) and days post-oiling (DPO).

		7 DPO			15 DPO		
Analytes	**Group**	**Median**	**Mean ± SD**	**(Min, Max)**	**Median**	**Mean ± SD**	**(Min, Max)**
Weight (g)	Control	435	462 ± 59	(402, 552)	449	487 ± 62	(416, 580)
	Oiled	418	424 ± 41	(372, 484)	425	428 ± 43	(380, 496)
	Rehab	449	447 ± 40	(394, 530)	468	465 ± 46	(400, 456)
Body temperature (°C)	Control	42.3	42.5 ± 0.6	(41.8, 43.8)	42.0	42.5 ± 0.4	(42, 43)
	Oiled	42.2	42.2 ± 0.3	(41.8, 42.7)	43.0	43 ± 0.6	(41.6, 43.7)
	Rehab	42.4	42.3 ± 0.6	(41.3, 43.3)	43.0	43 ± 0.5	(42, 43.5)
PCV (spun) (%)	Control	48	47 ± 2	(44, 51)	48	49 ± 3	(43, 56)
	Oiled	43	42 ± 3	(35, 48)	47	46 ± 5	(32, 51)
	Rehab	43	42 ± 3	(35, 47)	41	42 ± 4	(38, 50)
Hematocrit (EPOC) (%)	Control	41	41 ± 2	(39, 43)	42	41 ± 3	(37, 45)
	Oiled	37	36 ± 3	(29, 39)	38	36 ± 5	(23, 41)
	Rehab	38	37 ± 3	(30, 40)	36	36 ± 3	(32, 40)
Total Solids (g/dL)	Control	4.0	3.9 ± 0.5	(3, 4.8)	4.4	4.5 ± 0.8	(3.4, 6.2)
	Oiled	4.0	3.9 ± 0.5	(3.2, 4.6)	5.3	4.9 ± 0.9	(3.4, 5.9)
	Rehab	3.5	3.7 ± 0.6	(3, 4.8)	4.3	4.4 ± 0.8	(3, 5.6)
Sodium (mmol/L)	Control	156	156 ± 1	(155, 158)	156	155 ± 2	(152, 158)
	Oiled	157	156 ± 1	(154, 158)	158	157 ± 2	(155, 159)
	Rehab	157	155 ± 7	(137, 160)	156	156 ± 2	(154, 160)
Potassium (mmol/L)	Control	3.0	3 ± 0.3	(2.5, 3.4)	2.9	3 ± 0.2	(2.7, 3.4)
	Oiled	3.0	3.1 ± 0.3	(2.8, 3.7)	3.1	3 ± 0.3	(2.7, 3.5)
	Rehab	3.2	3.3 ± 0.5	(2.6, 4.4)	3.5	3.9 ± 1.4	(3, 7.4)
Chloride (mmol/L)	Control	119	119 ± 2	(114, 121)	117	117 ± 2	(113, 120)
	Oiled	119	120 ± 1	(117, 121)	121	120 ± 2.3	(117, 124)
	Rehab	121	118 ± 6	(104, 123)	117	118 ± 3.6	(114, 124)
TC ionized calcium (mmol/L)	Control	1.3	1.2 ± 0.1	(1.1, 1.4)	1.3	1.2 ± 0.1	(1, 1.4)
	Oiled	1.2	1.2 ± 0.1	(1.1, 1.4)	1.4	1.4 ± 0.1	(1.2, 1.4)
	Rehab	1.2	1.2 ± 0.1	(1, 1.3)	1.3	1.3 ± 0.1	(1, 1.4)
TC anion gap	Control	24	25 ± 24	(20,36)	24	24 ± 2.6	(19, 28)
	Oiled	24	23 ± 2	(20, 25)	23	23 ± 4	(19, 31)
	Rehab	23	23 ± 3	(15, 27)	24	23 ± 2	(20, 26)
Lactate (mmol/L)	Control	5.8	5.5 ± 1.9	(2.1, 9.3)	5.5	5.9 ± 2.3	(2.4, 9.4)
	Oiled	5.4	5.2 ± 1.9	(2.7, 7.3)	5.9	6.1 ± 1.9	(3.3, 9.9)
	Rehab	5.4	5.1 ± 2	(1.7, 2.5)	5.8	5.7 ± 1.5	(3.1, 7.2)
Glucose (mg/dL)	Control	314	318 ± 59	(230, 409)	334	337 ± 45	(251, 393)
	Oiled	310	312 ± 35	(274, 377)	299	297 ± 30	(240, 334)
	Rehab	276	288 ± 47	(232, 383)	293	302 ± 46	(237, 367)
TC pH	Control	7.40	7.4 ± 0.05	(7.3, 7.5)	7.40	7.38 ± 0.04	(7.3, 7.4)
	Oiled	7.35	7.35 ± 0.05	(7.3, 7.4)	7.35	7.35 ± 0.05	(7.3, 7.4)
	Rehab	7.40	7.36 ± 0.05	(7.3, 7.4)	7.40	7.36 ± 0.05	(7.3, 7.4)
TC pCO_2 (mmHg)	Control	32	30 ± 7	(21, 40)	35	35 ± 3	(32, 41)
	Oiled	35	35 ± 3	(32, 42)	36	36 ± 7	(27, 50)
	Rehab	34	35 ± 6	(46, 19)	37	38 ± 5	(31, 46)
TC pO_2 (mmHg)	Control	52	53 ± 7	(45, 66)	50	49 ± 4	(43, 57)
	Oiled	50	50 ± 2	(47, 53)	51	50 ± 5	(42, 62)
	Rehab	52	51 ± 6	(42, 60)	51	52 ± 3	(48, 57)
TC bicarbonate (mmol/L)	Control	16	16 ± 3	(11, 22)	18	18 ± 2	(14, 20)
	Oiled	17	17 ± 2	(14, 20)	19	17 ± 3	(12, 21)

(Continued)

TABLE 3 | Continued

Analytes	Group	7 DPO			15 DPO		
		Median	Mean ± SD	(Min, Max)	Median	Mean ± SD	(Min, Max)
	Rehab	17	17 ± 3	(11, 23)	19	18 ± 3	(14, 23)
Total WBC ($\times 10^3/\mu L$)	Control	10.0	10.1 ± 1.1	(9, 12)	11.0	10.9 ± 1.7	(8, 13)
	Oiled	11.0	10.9 ± 1.1	(9, 13)	10.0	10.1 ± 2	(7, 13)
	Rehab	10.0	9.8 ± 1.3	(7, 11)	9.0	9.2 ± 1.6	(7, 12)
Heterophils ($\times 10^3/\mu L$)	Control	4.5	4.5 ± 0.6	(3.4, 5.3)	4.9	5.1 ± 1.2	(3.8, 7.2)
	Oiled	5.0	5.1 ± 1	(4, 7)	5.5	5.4 ± 1.9	(2.1, 7.8)
	Rehab	4.5	4.3 ± 1.2	(2.3, 5.5)	4.7	5.1 ± 1.1	(3.6, 7)
Lymphocytes ($\times 10^3/\mu L$)	Control	2.4	2.3 ± 0.1	(2.2, 2.4)	2.7	2.6 ± 0.4	(1.8, 3.1)
	Oiled	2.5	2.5 ± 0.3	(2.2, 3.1)	2.3	2.3 ± 0.6	(1.4, 3.2)
	Rehab	2.3	2.2 ± 0.4	(1.4, 2.7)	1.9	2.1 ± 0.7	(0.8, 3)
Monocytes ($\times 10^3/\mu L$)	Control	0.0	0 ± 0.1	(0, 0.1)	0.0	0 ± 0.1	(0, 0.1)
	Oiled	0.1	0.1 ± 0.1	(0, 0.1)	0.0	0 ± 0	(0, 0)
	Rehab	0.0	0 ± 0.1	(0, 0.1)	0.0	0 ± 0	(0, 0.1)
Eosinophils ($\times 10^3/\mu L$)	Control	0.0	0 ± 0	(0, 0)	0.0	0 ± 0	(0, 0)
	Oiled	0.0	0 ± 0	(0, 0)	0.0	0 ± 0	(0, 0)
	Rehab	0.0	0 ± 0	(0, 0)	0.0	0 ± 0	(0, 0)
Basophils ($\times 10^3/\mu L$)	Control	0.0	0 ± 0	(0, 0)	0.0	0 ± 0	(0, 0)
	Oiled	0.0	0 ± 0	(0, 0)	0.0	0 ± 0	(0, 0)
	Rehab	0.0	0 ± 0	(0, 0)	0.0	0 ± 0	(0, 0)
Reticulocytes (%)	Control	0.7	0.8 ± 0.3	(0.5, 1.6)	0.7	0.6 ± 0.2	(0.3, 0.9)
	Oiled	1.6	1.5 ± 0.5	(0.7, 2.1)	1.1	1.3 ± 0.7	(0.4, 3)
	Rehab	1.0	1 ± 0.4	(0.3, 1.7)	0.6	0.8 ± 0.4	(0.3, 1.4)
		22 DPO			31 DPO		
Analytes	**Group**	**Median**	**Mean ± SD**	**(Min, Max)**	**Median**	**Mean ± SD**	**(Min, Max)**
Weight (g)	Control	440	473 ± 55	(414, 552)	428	458 ± 54	(396, 546)
	Oiled	430	437 ± 41	(396, 500)	444	468 ± 57	(410, 576)
	Rehab	488	477 ± 43	(412, 556)	472	472 ± 45	(408, 544)
Body temperature (°C)	Control	42.8	42.7 ± 0.4	(42.1, 43.2)	42.2	42.1 ± 0.8	(40.5, 43.4)
	Oiled	43.4	43.1 ± 1	(40.3, 43.9)	42.6	42.8 ± 0.4	(42.3, 43.5)
	Rehab	43.0	43 ± 0.3	(43, 44)	42.1	42.1 ± 0.6	(40.7, 42.7)
PCV (spun) (%)	Control	48	48 ± 4	(42, 53)	53	52 ± 3	(46, 55)
	Oiled	47	43 ± 11	(12, 49)	46	46 ± 2	(43, 49)
	Rehab	47	46 ± 3	(40, 49)	50	49 ± 3	(43, 44)
Hematocrit (EPOC) (%)	Control	41	41 ± 2	(36, 43)	43	43 ± 2	(40, 46)
	Oiled	38	35 ± 9	(9, 39)	36	36 ± 2	(34, 38)
	Rehab	38	37 ± 2	(34, 39)	39	39 ± 3	(33, 44)
Total Solids (g/dL)	Control	4.2	4.2 ± 0.8	(3, 5.8)	4.9	4.6 ± 0.5	(3.8, 5.2)
	Oiled	4.4	4.1 ± 1	(1.4, 5)	4.3	4.5 ± 0.4	(4, 5.1)
	Rehab	4.2	4.3 ± 0.8	(3.5, 6)	4.2	4.2 ± 0.3	(3.6, 4.6)
Sodium (mmol/L)	Control	156	156 ± 2	(153, 158)	155	155 ± 1	(153, 157)
	Oiled	157	157 ± 2	(153, 160)	155	156 ± 2	(153, 159)
	Rehab	156	156 ± 2	(153, 159)	158	157 ± 2	(153, 159)
Potassium (mmol/L)	Control	3.2	3.2 ± 0.1	(2.9, 3.3)	3.2	3.1 ± 0.2	(2.8, 3.6)
	Oiled	3.3	3.4 ± 0.4	(2.9, 4.1)	3.0	3 ± 0.4	(2.1, 3.5)
	Rehab	3.4	3.4 ± 0.4	(2.9, 4.1)	3.0	3 ± 0.4	(2.3, 3.4)
Chloride (mmol/L)	Control	118	118 ± 3	(115, 124)	120	119 ± 3	(115, 122)
	Oiled	120	120 ± 2	(118, 123)	120	120 ± 3	(116, 124)

(Continued)

TABLE 3 | Continued

Analytes	Group	22 DPO			31 DPO		
		Median	Mean ± SD	(Min, Max)	Median	Mean ± SD	(Min, Max)
	Rehab	117	118 ± 3	(113, 121)	120	119 ± 3.2	(113, 123)
TC ionized calcium (mmol/L)	Control	1.2	1.2 ± 0.1	(1.1, 1.3)	1.2	1.2 ± 0.1	(1.1, 1.3)
	Oiled	1.3	1.3 ± 0.1	(1.1, 1.4)	1.2	1.2 ± 0.1	(1.1, 1.3)
	Rehab	1.3	1.3 ± 0.1	(1.2, 1.4)	1.2	1.2 ± 0.1	(0.9, 1.3)
TC anion gap	Control	23	23 ± 2.4	(19, 27)	21	22 ± 3	(19, 27)
	Oiled	23	24 ± 2	(22, 27)	22	22 ± 2	(19, 27)
	Rehab	24	24 ± 2	(21, 27)	23	22 ± 3	(17, 25)
Lactate (mmol/L)	Control	4.5	5.1 ± 1.6	(3.3, 8.1)	4.8	5.7 ± 2.2	(3.2, 9.6)
	Oiled	5.3	5.7 ± 2.3	(2.8, 10.7)	5.9	6.1 ± 1.4	(3.7, 8.2)
	Rehab	5.6	5.4 ± 1.9	(1.7, 7.8)	6.2	5.8 ± 1.4	(3.6, 7.6)
Glucose (mg/dL)	Control	326	314 ± 65	(214, 409)	325	346 ± 41	(297, 425)
	Oiled	251	264 ± 33	(221, 321)	337	343 ± 56	(238, 419)
	Rehab	302	293 ± 48	(235, 353)	348	341 ± 30	(296, 371)
TC pH	Control	7.40	7.39 ± 0.03	(7.3, 7.4)	7.40	7.39 ± 0.06	(7.3, 7.5)
	Oiled	7.35	7.36 ± 0.07	(7.3, 7.5)	7.30	7.32 ± 0.04	(7.3, 7.4)
	Rehab	7.30	7.34 ± 0.05	(7.3, 7.4)	7.30	7.35 ± 0.08	(7.3, 7.5)
TC pCO_2 (mmHg)	Control	33	34 ± 3	(30, 38)	34	33 ± 3	(26, 37)
	Oiled	38	36 ± 7	(20, 45)	36	36 ± 3	(33, 40)
	Rehab	35	38 ± 5	(32, 47)	37	38 ± 7	(26, 48)
TC pO_2 (mmHg)	Control	52	51 ± 4	(45, 56)	52	52 ± 3	(47, 58)
	Oiled	51	51 ± 5	(46, 58)	49	50 ± 6	(45, 63)
	Rehab	49	51 ± 4	(48, 60)	49	49 ± 3	(45, 55)
TC bicarbonate (mmol/L)	Control	17	18 ± 2	(15,20)	17	17 ± 1	(15,19)
	Oiled	16	17 ± 3	(12, 22)	15	16 ± 2	(14, 20)
	Rehab	18	17 ± 2	(15, 20)	18	18 ± 2	(16, 20)
Total WBC ($\times 10^3/\mu L$)	Control	11.0	11.2 ± 1.1	(10,13)	10.5	10 ± 2.2	(7, 13)
	Oiled	11.0	10.6 ± 1.7	(8, 13)	11.0	10.4 ± 2.5	(7, 13)
	Rehab	12.0	11.1 ± 2	(7, 13)	10.0	10 ± 2.4	(7, 13)
Heterophils ($\times 10^3/\mu L$)	Control	5.0	5 ± 1.5	(2.8, 7)	3.7	4.3 ± 1.9	(1.9, 7.8)
	Oiled	5.0	5.4 ± 1.8	(2.7, 8)	5.6	5.1 ± 1.3	(2.9, 6.8)
	Rehab	6.6	6.2 ± 2.1	(3.2, 9.1)	5.0	5.2 ± 1.7	(3.2, 9)
Lymphocytes ($\times 10^3/\mu L$)	Control	2.5	2.5 ± 0.4	(2, 3.3)	2.2	2.2 ± 0.5	(1.4, 3.1)
	Oiled	2.4	2.4 ± 0.4	(1.9, 3)	2.7	2.5 ± 0.6	(1.7, 3.3)
	Rehab	2.5	2.4 ± 0.4	(1.7, 2.8)	2.2	2.3 ± 0.5	(1.7, 3.1)
Monocytes ($\times 10^3/\mu L$)	Control	0.0	0 ± 0	(0, 0.1)	0.0	0 ± 0	(0, 0.1)
	Oiled	0.0	0 ± 0	(0, 0.1)	0.0	0 ± 0	(0, 0)
	Rehab	0.0	0 ± 0	(0, 0)	0.0	0 ± 0	(0, 0.1)
Eosinophils ($\times 10^3/\mu L$)	Control	0.0	0 ± 0	(0, 0)	0.0	0 ± 0	(0, 0)
	Oiled	0.0	0 ± 0	(0, 0)	0.0	0 ± 0	(0, 0)
	Rehab	0.0	0 ± 0	(0, 0)	0.0	0 ± 0	(0, 0)
Basophils ($\times 10^3/\mu L$)	Control	0.0	0 ± 0	(0, 0)	0.0	0 ± 0	(0, 0)
	Oiled	0.0	0 ± 0	(0, 0)	0.0	0 ± 0	(0, 0)
	Rehab	0.0	0 ± 0	(0, 0)	0.0	0 ± 0	(0, 0)
Reticulocytes (%)	Control	1.1	1.2 ± 0.4	(0.7, 2)	0.9	1.1 ± 0.8	(0.3, 2.7)
	Oiled	1.6	1.5 ± 0.6	(0.4, 2.3)	1.5	1.5 ± 0.5	(0.7, 2.6)
	Rehab	0.8	1.1 ± 0.6	(0.4, 2)	0.9	1 ± 0.6	(0.4, 2.2)

TC, temperature corrected; SD, standard deviation.

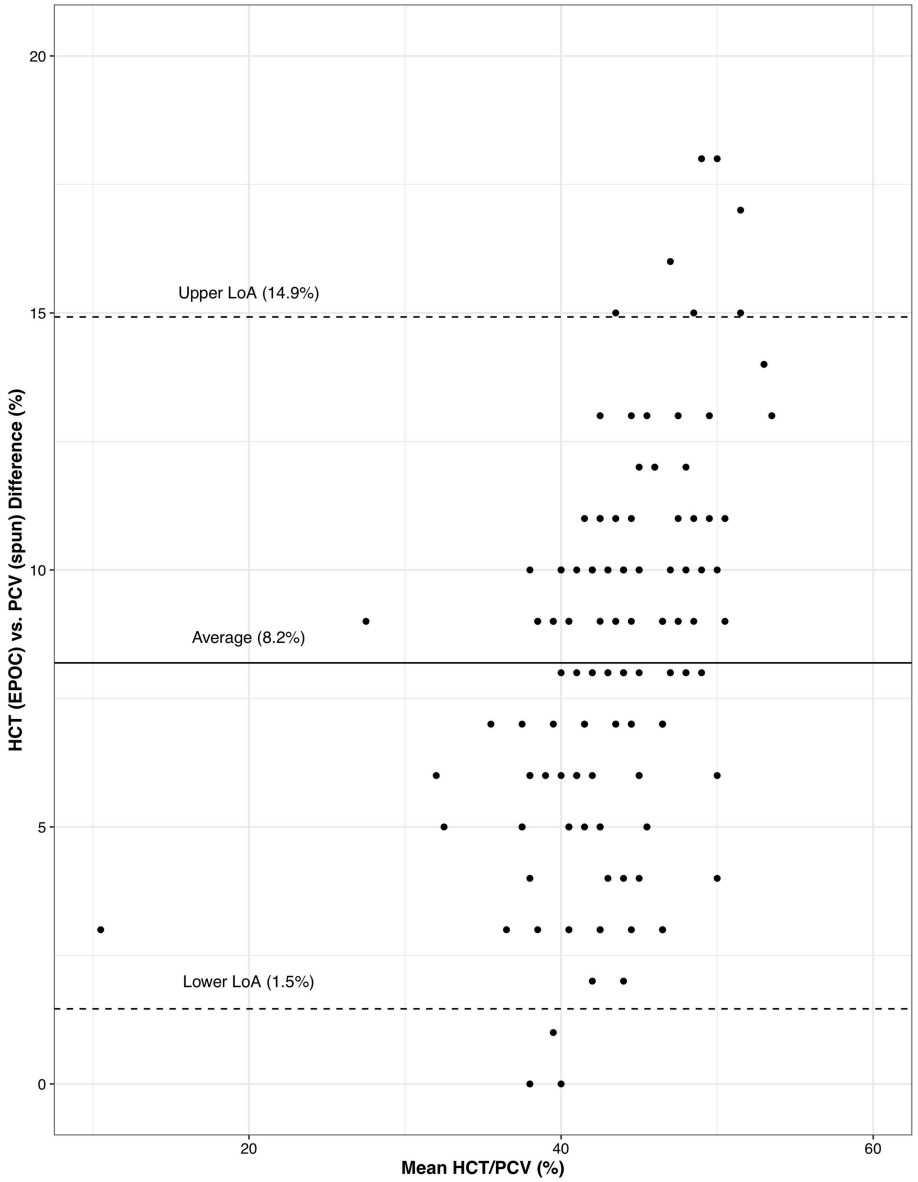

FIGURE 1 | A Bland-Altman plot of the diagnostic difference between hematocrit as measured by the Element POC Blood Gas and Electrolyte Analyzer—HCT (EPOC)—and PCV determined manually following high-speed centrifugation of microhematocrit tubes—PCV (spun). Values on the x-axis represent the mean HCT/PCV between the two methods for a given Ring-billed Gull (*Larus delawarensis*) and values on the y-axis represent the difference between the two methods for the same Ring-billed Gull. Levels of agreement (LoA) represent a 95% confidence interval around the average difference.

data previously reported for other gull species (35–38). Total solids were lower than means reported in Kelp Gulls (*Larus dominicanus*) (37, 38), but birds sampled in both of these studies foraged on high-protein discards from the fishing industry which likely resulted in higher plasma protein concentrations. Glucose concentrations were within the range observed in Kelp Gulls and other seabirds (35, 37, 38). On average, RBGUs had a higher lymphocytes compared to heterophils, a finding seen in Great Black-backed Gulls (*L. marinus*) and Herring Gulls (*L. argentatus*) (39), but opposite of a pattern seen in Kelp Gulls (37).

Our results support our hypothesis that RBGUs develop some degree of anemia secondary to external oil exposure, similar to other avian species. The anemia seen in oiled RBGUs falls within the range of anemia found in externally oiled birds sampled shortly after the Deepwater Horizon oil spill which had on average a 4–19% lower PCV than non-oiled birds (40). Oiled RBGUs may have had a milder anemia compared to some of the birds sampled after Deepwater Horizon due to their easy access to nutritious, oil-free food, and limited need to expend energy foraging. Although control RBGUs had higher HCT (EPOC) than both non-rehabilitated and rehabilitated-oiled RBGUs over the

study period, all RBGUs exhibited anemia after 0 DPO suggesting that both external oiling and aspects of captivity or repeated handling cause persistent mild anemia. The implication that captivity can induce anemia in wild birds over time supports previous experimental work; both orally exposed to oil and non-exposed Rhinoceros Auklets (*Cerorhinca monocerata*) had on average a 10% lower PCV after 3 weeks in captivity (41). Given our RBGUs were group housed in large outdoor flight pens that encouraged natural behaviors, the development of anemia secondary to captivity, regardless of oil exposure, is potentially due to alterations in physiological demands or the stress of repeated handling, rather than the sedentary nature of captivity.

While non-rehabilitated-oiled RBGUs had a higher estimated reticulocyte percentage than both rehabilitated-oiled RBGUs and control RBGUs, all three treatment groups failed to show increased RBC regeneration in the face of a persistent mild anemia, given reticulocyte percentages vary between 1 and 5% in healthy birds (27). This finding contrasts our hypothesis that rehabilitated birds would return to pre-exposure values quicker than non-rehabilitated birds as well as field observations made after the Deepwater Horizon oil spill that found externally oiled birds had on average 27-40% higher reticulocyte percentages (40). However, the absence of a regenerative response is similar to results from previous experimental studies. Rhinoceros Auklets orally exposed to oil as well as Double-crested Cormorants (*Phalacocorax auritis*) orally and externally exposed to oil showed regenerative, but inadequately compensated, responses to anemia with PCV never returning to levels recorded post-capture and pre-oiling (41, 42). The lack of compensatory RBC regeneration despite persistent anemia suggests a lack of production in hematopoietic tissue which may be caused by oil-induced bone marrow suppression or potential changes in physiological demands wild birds experience in captivity resulting in a "resetting" of homeostatic RBC levels.

Although sublethal oil exposure has long been suspected of causing immunosuppression in birds, the effects of oil toxicosis in rehabilitated or experimental birds is confounded with captivity-related stress. RBGUs showed low heterophil to lymphocyte ratios on 0 DPO, suggesting the birds were well-acclimated to captivity prior to external oiling given heterophils increase and lymphocytes decrease in response to stress (43). Following oil exposure, no difference in total WBC, heterophil, lymphocyte, monocyte, eosinophil, and basophil counts were found among treatment groups. This is inconsistent with our hypothesis and implies that moderate external oiling does not alter circulating WBCs. Laughing Gulls (*Leucophaeus atricilla*) offered fish injected with oil also showed no changes in circulating WBCs (44), whereas Common Terns (*Sterna hirundo*), sampled 14–21 days after the Buzzards Bay oil spill, exhibited severely depressed total WBC and lymphocyte counts as well as markedly elevated heterophil counts and heterophil/lymphocyte ratios (15). While further research is warranted, the acute stress of capturing and handling wild birds is potentially a factor in explaining the discrepancy between experimental studies showing no oil-induced immunosuppression and field observations showing some degree of immunosuppression. It is also possible that immunosuppression in experimentally oiled birds is mitigated by the adequate husbandry and nutrition provided during experimental studies. The WBC estimate methodology used herein was developed from unpublished studies and has not been validated or verified by independent review. Therefore, comparisons of our WBC data to other studies needs to be done cautiously.

The significant interaction between non-rehabilitated-oiled RBGUs' HCT (EPOC) suggests that chronic sublethal external oil exposure may result in ongoing anemia. While the control and rehabilitated-oiled RBGUs' HCT (EPOC) gradually increased toward baseline levels between 15 and 31 DPO, the non-rehabilitated-oiled RBGUs' HCT (EPOC) continued to decrease. The diagnostic disagreement between the EPOC and PCV determined manually is not surprising given the difference in methodologies. Veterinary point-of-care analyzers measure hematocrit via whole blood conductometry in which a higher proportion of RBCs decreases electrical conductivity. Consequently, many veterinary point-of-care analyzers likely underestimate avian hematocrit due to the difference in conductivity between avian nucleated RBCs and mammalian non-nucleated RBCs. Measurements of hematocrit performed by the VetScan i-STAT 1 Analyzer (Abaxis Inc., Union City, California) have been previously shown to be on average 15% lower than PCV determined manually in Bar-headed Geese (*Anser indicus*) (45) suggesting that the magnitude of underestimating hematocrit may vary amongst species or veterinary point-of-care analyzers. In addition to our limited sample size, possible limitations of our study include significant differences in weather across the study period, Element POC cartridge temperature, and/or observer effects, given sampling was conducted outside and multiple observers performed WBC differentials. Other limitations of our study include the RBGUs' aforementioned easy access to nutritious, oil-free food and limited need to expend energy foraging as well as the availability of heat lamps minimizing the adverse effects of oil on thermoregulation. Despite accounting for the heterogeneity of individual RBGUs in our LMMs as a random effect, the small sample size per treatment group could explain the significant interaction found with HCT (EPOC) but not PCV (spun) or the lack of differences among treatment groups for some analytes.

CONCLUSIONS

Our study is the first to report hematological, biochemical, and blood gas analytes in birds following sublethal oil exposure and rehabilitation. We found that both sublethal oil exposure and aspects of captivity caused a mild non-regenerative anemia, suggesting the etiology of anemia seen in oiled birds undergoing rehabilitation is possibly multifactorial. Given that moderately oiled gulls in our study had subtle, but potentially not insignificant clinicopathological abnormalities, gulls affected by sublethal external oiling are likely strong candidates for rescue and rehabilitation. Furthermore, oiled gulls did not develop any clinicopathological derangements post-rehabilitation, suggesting current standard practices for rehabilitation cause minimal morbidity in stable, moderately oiled gulls.

DATA AVAILABILITY STATEMENT

The datasets generated for this study are available on request to the corresponding author.

ETHICS STATEMENT

This animal study was reviewed and approved by the USDA/APHIS/WS National Wildlife Research Center Institutional Animal Care and Use Committee.

AUTHOR CONTRIBUTIONS

ND, KH, and SS developed this study's design and oversaw all aspects of the project. JE lead efforts to capture study animals and assisted with their routine husbandry. LW provided the veterinary point of care analyzer used in this study as well as veterinary expertise. ND was responsible for statistical analysis and primarily writing this manuscript. All authors assisted with data collection and played a significant role in editing/reviewing this manuscript.

FUNDING

This research was supported by the intramural research program of the US Department of Agriculture, Animal Plant Health Inspection Service.

ACKNOWLEDGMENTS

The authors would like to thank Kevin Bentler, Katherine Dirsmith, and Mikaela Samsel for their assistance with data collection. The authors would also like to thank the animal care staff of the National Wildlife Research Center for their dedicated animal husbandry as well as the clinical pathology staff of the Colorado State University Veterinary Diagnostic Lab for processing the collected blood smears. Earlier versions of this manuscript were greatly improved through the thoughtful feedback from two reviewers and the editor.

REFERENCES

1. Piatt JF, Lensink CJ, Butler W, Marshal K, Nysewander DR. Immediate impact of the 'Exxon Valdez' oil spill on marine birds. *Auk.* (1990) 107:387–97. doi: 10.2307/4087623
2. Munilla I, Arcos JM, Oro D, Álvarez D, Leyenda PM, Velando A. Mass mortality of seabirds in the aftermath of the Prestige oil spill. *Ecosphere.* (2011) 2:art83. doi: 10.1890/ES11-00020.1
3. Haney JC, Geiger HJ, Short JW. Bird mortality from the Deepwater Horizon oil spill. I. Exposure probability in the offshore Gulf of Mexico. *Mar Ecol-Prog Ser.* (2014) 513:225–37. doi: 10.3354/meps10991
4. Haney JC, Geiger HJ, Short JW. Bird mortality from the Deepwater Horizon oil spill. II. Carcass sampling and exposure probability in the coastal Gulf of Mexico. *Mar Ecol-Prog Ser.* (2014) 513:239–52. doi: 10.3354/meps10839
5. Velando A, Álvarez D, Mouriño J, Arcos F, Barros Á. Population trends and reproductive success of the European shag *Phalacrocorax aristotelis* on the Iberian Peninsula following the Prestige oil spill. *J Ornithol.* (2005) 146:116–20. doi: 10.1007/s10336-004-0068-z
6. Votier SC, Hatchwell BJ, Beckerman A, McCleery RH, Hunter FM, Pellatt J, et al. Oil pollution and climate have wide-scale impacts on seabird demographics. *Ecol Lett.* (2005) 8:1157–64. doi: 10.1111/j.1461-0248.2005.00818.x
7. Peterson CH, Rice SD, Short JW, Esler D, Bodkin JL, Ballachey BE, et al. Long-term ecosystem response to the Exxon Valdez oil spill. *Science.* (2003) 302:2082–6. doi: 10.1126/science.1084282
8. Alonso-Alvarez C, Pérez C, Velando A. Effects of acute exposure to heavy fuel oil from the Prestige spill on a seabird. *Aquat Toxicol.* (2007) 84:103–10. doi: 10.1016/j.aquatox.2007.06.004
9. Leighton FA. Morphological lesions in red blood cells from herring gulls and Atlantic puffins ingesting Prudhoe Bay crude oil. *Vet Pathol.* (1985) 22:393–402. doi: 10.1177/030098588502200415
10. Leighton FA. Clinical, gross, and histological findings in herring gulls and Atlantic puffins that ingested Prudhoe Bay crude oil. *Vet Pathol.* (1986) 23:254–63. doi: 10.1177/030098588602300305
11. Peakall DB, Norstrom RJ, Jeffrey DA, Leighton FA. Induction of hepatic mixed function oxidases in the herring gull (*Larus argentatus*) by Prudhoe Bay crude oil and its fractions. *Comp Biochem Physiol C Toxicol Pharmacol.* (1989) 94:461–3. doi: 10.1016/0742-8413(89)90098-4
12. Peakall DB, Tremblay J, Kinter WB, Miller DS. Endocrine dysfunction in seabirds caused by ingested oil. *Environ Res.* (1981) 24:6–14. doi: 10.1016/0013-9351(81)90126-2
13. Troisi GM, Bexton S, Robinson I. Polyaromatic hydrocarbon and PAH metabolite burdens in oiled common guillemots (*Uria aalge*) stranded on the east coast of England (2001–2002). *Environ Sci Technol.* (2006) 40:7938–43. doi: 10.1021/es0601787
14. Troisi G, Borjesson L, Bexton S, Robinson I. Biomarkers of polycyclic aromatic hydrocarbon (PAH)-associated hemolytic anemia in oiled wildlife. *Environ Res.* (2007) 105:324–9. doi: 10.1016/j.envres.2007.06.007
15. Nisbet ICT, Tseng FS, Fiorello CV, Apanius V. Changes in white blood cell parameters of common terns (*Sterna hirundo*) exposed to low levels of oil. *Waterbirds.* (2015) 38:415–9. doi: 10.1675/063.038.0405
16. Briggs KT, Gershwin ME, Anderson DW. Consequences of petrochemical ingestion and stress on the immune system of seabirds. *ICES J Mar Sci.* (1997) 54:718–25. doi: 10.1006/jmsc.1997.0254
17. Mazet JAK, Newman SH, Gilardi KVK, Tseng FS, Holcomb JB, Jessup DA, et al. Advances in oiled bird emergency medicine and management. *J Avian Med Surg.* (2002) 16:146–9. doi: 10.1647/1082-6742(2002)016[0146:AIOBEM]2.0.CO;2
18. Bursian SJ, Alexander CR, Cacela D, Cunningham FL, Dean KM, Dorr BS, et al. Overview of avian toxicity studies for the deepwater horizon natural resource damage assessment. *Ecotox Environ Safe.* (2017) 146:4–10. doi: 10.1016/j.ecoenv.2017.05.014
19. Dean KM, Cacela D, Carney MW, Cunningham FL, Ellis C, Gerson AR, et al. Testing of an oral dosing technique for double-crested cormorants, *Phalacocorax auritus*, laughing gulls, *Leucophaeus atricilla*, homing pigeons, *Columba livia*, and western sandpipers, *Calidris mauri*, with artificially weather MC252 oil. *Ecotox Environ Safe.* (2017) 146:11–8. doi: 10.1016/j.ecoenv.2017.07.003
20. Perez CR, Moye JK, Cacela D, Dean KM, Pritsos CA. Low level exposure to crude oil impacts avian flight performance: the Deepwater Horizon oil spill effect on migratory birds. *Ecotox Environ Safe.* (2017) 146:98–103. doi: 10.1016/j.ecoenv.2017.05.028
21. Perez CR, Moye JK, Cacela D, Dean KM, Pritsos CA. Homing pigeons externally exposed to Deepwater Horizon crude oil change flight performance and behavior. *Environ Pollut.* (2017) 230:530–9. doi: 10.1016/j.envpol.2017.07.008
22. Harr KE, Reavill DR, Bursian SJ, Cacela D, Cunningham FL, Dean KM, et al. Organ weights and histopathology of double-crested cormorants (*Phalacrocorax auritus*) dosed orally or dermally with artificially weathered Mississippi Canyon 252 crude oil. *Ecotox Environ Safe.* (2017) 146:52–61. doi: 10.1016/j.ecoenv.2017.07.011

23. Harr KE, Rishniw M, Rupp TL, Cacela D, Dean KM, Dorr BS, et al. Dermal exposure to weathered MC252 crude oil results in echocardiographically identifiable systolic myocardial dysfunction in double-crested cormorants (*Phalacrocorax auritus*). *Ecotox Environ Safe.* (2017) 146:76–82. doi: 10.1016/j.ecoenv.2017.04.010
24. Dorr BS, Hanson-Dorr KC, Assadi-Porter FM, Selen ES, Healy KA, Horak KE. Effects of repeated sublethal external exposure to Deepwater Horizon oil on the avian metabolome. *Sci Rep.* (2019) 9:371. doi: 10.1038/s41598-018-36688-3
25. Ashwood ER, Kost G, Kenny M. Temperature correction of blood-gas and pH measurements. *Clin Chem.* (1983) 29:1877–85.
26. Fogh-Andersen N. Ionized calcium analyzer with a built-in pH correction. *Clin Chem.* (1981) 27:1264–7.
27. Campbell TW. *Exotic Animal Hematology and Cytology*. Ames, IA: John Wiley & Sons (2015). doi: 10.1002/9781118993705
28. Johns JL, Shooshtari MP, Christopher MM. Development of a technique for quantification of reticulocytes and assessment of erythrocyte regenerative capacity in birds. *Am J Vet Res.* (2008) 69:1067–72. doi: 10.2460/ajvr.69.8.1067
29. Friedrichs KR, Harr KE, Freeman KP, Szladovits B, Walton RM, Barnhart KF, et al. ASVCP reference interval guidelines: determination of *de novo* reference intervals in veterinary species and other related topics. *Vet Clin Path.* (2012) 41:441–53. doi: 10.1111/vcp.12006
30. Benjamini Y, Hochberg Y. Controlling the false discovery rate: a practical and powerful approach to multiple testing. *J R Stat Soc Series B Stat Methodol.* (1995) 57:289–300. doi: 10.1111/j.2517-6161.1995.tb02031.x
31. Lin LI. A concordance correlation coefficient to evaluate reproducibility. *Biometrics.* (1989) 45:255–68. doi: 10.2307/2532051
32. Bland JM, Altman DG. Statistical methods for assessing agreement between two methods of clinical measurement. *Lancet.* (1986) 1:307–10. doi: 10.1016/S0140-6736(86)90837-8
33. Team RC. *R: A Language and Environment for Statistical Computing*. Vienna: R Foundation for Statistical Computing (2019).
34. Bates D, Mächler M, Bolker B, Walker S. Fitting linear mixed-effects models using lme4. *J Stat Softw.* (2015) 67:1–48. doi: 10.18637/jss.v067.i01
35. Newman SH, Piatt JF, White J. Hematological and plasma biochemical reference ranges of Alaskan seabirds: their ecological significance and clinical importance. *Waterbirds.* (1997) 20:492–504. doi: 10.2307/1521600
36. Garcia MTA, Hermosa Y, Aguirre JI. Does breeding status influence haematology and blood biochemistry of yellow-legged gulls? *Acta Biol Hung.* (2010) 61:391–400. doi: 10.1556/ABiol.61.2010.4.3
37. Doussang D, Merino V, Moreno L, Islas A, Barrientos C, Mathieu C, et al. Hematologic and biochemical parameters of kelp gulls (*Larus dominicanus*) captured in the city of Talcahuano, Chile. *J Zoo Wildl Med.* (2015) 46:447–55. doi: 10.1638/2012-0080.1
38. D'Amico VL, Fazio A, Palacios MG, Carabajal E, Bertellotti M. Evaluation of physiological parameters of kelp gulls (*Larus dominicanus*) feeding on fishery discards in Patagonia, Argentina. *Waterbirds.* (2018) 41:310–5. doi: 10.1675/063.041.0311
39. Averbeck C. Haematology and blood chemistry of healthy and clinically abnormal great black-backed gulls (*Larus Marinus*) and herring gulls (*Larus Argentatus*). *Avian Pathol.* (1992) 21:215–23. doi: 10.1080/03079459208418837
40. Fallon JA, Smith EP, Schoch N, Paruk JD, Adams EA, Evers DC, et al. Hematological indices of injury to lightly oiled birds from the Deepwater Horizon oil spill. *Environ Toxicol Chem.* (2018) 37:451–61. doi: 10.1002/etc.3983
41. Newman SH, Mazet JK, Ziccardi MH, Lieske CL, Fauquier DA, Gardner IA, et al. Haematological changes and anaemia associated with captivity and petroleum exposure in seabirds. *Comp Clin Path.* (1999) 9:60–7. doi: 10.1007/BF02585537
42. Harr KE, Cunningham FL, Pritsos CA, Pritsos KL, Muthumalage T, Dorr BS, et al. Weathered MC252 crude oil-induced anemia and abnormal erythroid morphology in double-crested cormorants (*Phalacrocorax auritus*) with light microscopic and ultrastructural description of Heinz bodies. *Ecotox Environ Safe.* (2017) 146:29–39. doi: 10.1016/j.ecoenv.2017.07.030
43. Davis AK. Effect of handling time and repeated sampling on avian white blood cell counts. *J Field Ornithol.* (2005) 76:334–8. doi: 10.1648/0273-8570-76.4.334
44. Horak KE, Bursian SJ, Ellis CK, Dean KM, Link JE, Hanson-Dorr KC, et al. Toxic effects of orally ingested oil from the Deepwater Horizon spill on laughing gulls. *Ecotox Environ Safe.* (2017) 146:83–90. doi: 10.1016/j.ecoenv.2017.07.018
45. Harter TS, Reichert M, Brauner CJ, Milsom WK. Validation of the i-STAT and Hemocue systems for the analysis of blood parameters in the bar-headed goose, *Anser indicus*. *Conserv Physiol.* (2015) 3:cov021. doi: 10.1093/conphys/cov021

Conflict of Interest: The authors declare that the research was conducted in the absence of any commercial or financial relationships that could be construed as a potential conflict of interest.

Copyright © 2019 Dannemiller, Horak, Ellis, Barrett, Wolfe and Shriner. This is an open-access article distributed under the terms of the Creative Commons Attribution License (CC BY). The use, distribution or reproduction in other forums is permitted, provided the original author(s) and the copyright owner(s) are credited and that the original publication in this journal is cited, in accordance with accepted academic practice. No use, distribution or reproduction is permitted which does not comply with these terms.

frontiers in Veterinary Science

BRIEF RESEARCH REPORT
published: 22 November 2019
doi: 10.3389/fvets.2019.00412

Mortality in Three-Toed Box Turtles (*Terrapene mexicana triunguis*) at Two Sites in Missouri

Jamie L. Palmer[1]*, *Maris Brenn-White*[1], *Stephen Blake*[2] and *Sharon L. Deem*[1]

[1] Institute for Conservation Medicine, Saint Louis Zoo, St. Louis, MO, United States, [2] Department of Biology, Saint Louis University, St. Louis, MO, United States

Once ubiquitous, North American box turtles are experiencing reductions in abundance and range, but the magnitude of these losses is largely unknown. In Missouri, native box turtles (*Terrapene mexicana triunguis* and *Terrapene ornata ornata*) are declining across the state due to anthropogenic disturbances such as urbanization, habitat fragmentation, and vehicle collisions. Through radio-tracking over a period of 7 years, we documented the survival of adult three-toed box turtles at two sites in Missouri: Forest Park (urban park) and Tyson Research Center (TRC) (a protected rural forest). Estimated annual survival of adult turtles in Forest Park was 79% (95% CI: 0.68–0.87) while at TRC annual survival was 93% (95% CI: 0.83–0.97). The odds of annual survival for a turtle at TRC were 3.5 times that of a turtle living in Forest Park. "Winter kill," which refers to box turtles found dead on the surface during brumation or within 2 weeks of emergence, was the most frequently documented category of mortality in Forest Park. At TRC, winter kill was not documented; however, the reasons for most deaths were unknown. These data raise questions about the potential of large urban parks as refuges for box turtles, which we may answer by future studies that compare box turtles living in multiple urban and rural settings. Our preliminary data suggest that even the largest urban parks may not be able to sustain populations of box turtles which has severe implications as urbanization continues to degrade and eliminate box turtle habitat throughout their range.

Keywords: chelonian, urban ecology, winter kill, telemetry, survival estimate, brumation

OPEN ACCESS

Edited by:
Robert James Ossiboff, University of Florida, United States

Reviewed by:
Laura Adamovicz, University of Illinois at Urbana-Champaign, United States
Russell L. Burke, Hofstra University, United States

***Correspondence:**
Jamie L. Palmer
jpalmer@stlzoo.org

Specialty section:
This article was submitted to Veterinary Experimental and Diagnostic Pathology, a section of the journal Frontiers in Veterinary Science

Received: *21 August 2019*
Accepted: *05 November 2019*
Published: *22 November 2019*

Citation:
Palmer JL, Brenn-White M, Blake S and Deem SL (2019) Mortality in Three-Toed Box Turtles (Terrapene mexicana triunguis) at Two Sites in Missouri. Front. Vet. Sci. 6:412. doi: 10.3389/fvets.2019.00412

INTRODUCTION

The Chelonia (turtles and tortoises) is the most imperiled vertebrate order, with more than half (61%) of the 356 known species threatened with extinction (1). Threats to the long-term survival of land turtles, including North American box turtles, come from anthropogenic disturbances that include habitat change (loss, fragmentation, and pollution), infectious and non-infectious disease, vehicle collisions, over-exploitation for the pet trade, and a combination of environmental impacts due to climate change (1–8). Box turtles (*Terrapene* spp.) are widespread throughout much of the United States. Most studies on box turtle ecology and health have focused on *Terrapene carolina carolina* (eastern box turtles); however two taxa that occur west of the Mississippi River,

Terrapene mexicana triunguis [three-toed box turtle, previously *Terrapene carolina triunguis* (9)] and *Terrapene ornata ornata* (ornate box turtle), have received less attention. In Missouri, both taxa occur, and despite the state's relatively low human population density and large tracts of forest and grassland, human impacts are thought to threaten their survival (10–13). The extent of population declines for three-toed and ornate box turtles is largely unknown. Historically, the range of the three-toed box turtle in Missouri extended across the state, with the species preferring forested landscapes. Ornate box turtles favor the more open prairie habitat. Today, Missouri is a mosaic of fragmented forests and small isolated prairies intersected by highways, roads, farmland, and urban and suburban areas. The three-toed box turtle is likely in decline in Missouri due to anthropogenic change. However, it is not currently listed as a state species of conservation concern, most likely due to data deficiency (14).

The life-history strategy of box turtles involves slow maturation and reliance on high juvenile survivorship and low adult mortality to maintain stable populations (15). In long-lived turtles, high adult survival is essential to the conservation of the species (6). Turtles will limit any recovery in a population due to these life history traits. Determining survival estimates and cause of mortality at the population level are important for three-toed box turtle management and conservation given the fragmentation through most of their historic range. The only previously existing survivorship estimate for this species is over 30 years old (12) and is unlikely to reflect the current population dynamics and challenges that three-toed box turtles face today, particularly in an urban environment. Knowledge of the extent to which anthropogenic changes affect box turtle populations would be valuable for understanding the ability of these animals to respond to urbanization.

As part of a larger health and movement ecology study, we estimated annual survival rates and documented causes of mortality of radio-tagged native Missouri box turtles at two sites over a 7-year period.

MATERIALS AND METHODS

Since March 2012, we have monitored the movements and health of two populations of three-toed box turtles: one at an urban site and one at a rural site. Forest Park (FP), the urban site, is a 556 ha park in St. Louis, Missouri consisting of a mosaic of land use including fragmented habitats suitable for box turtles (**Figure 1**). Tyson Research Center (TRC), the rural site, is an 809 ha fenced and protected oak-hickory forest and biological field station (**Figure 1**). Research team members opportunistically located box turtles during weekly searches at both sites.

Once located, we determined sex based on morphology (16), marked each turtle with three "v" shaped notches filed into the marginal scutes (17) and placed very high frequency (VHF) telemetry tags (Holohil Systems, Ltd., Carp, Ontario, Canada) on a subset of turtles at each site (FP $n = 23$, TRC $n = 18$). We placed VHF tags only on adult box turtles considered healthy upon visual examination and weighing more than 400 g to minimize potential negative impacts of tag placement (18). The number of turtles with VHF tags varied due to turtle mortality or tag malfunction. When active, we visited each tagged turtle every 1–4 weeks to perform a visual exam, collect body weight, and record environmental data. We disinfected equipment with 10% bleach and hands with alcohol-based hand sanitizer between each turtle to minimize risk of pathogen transfer.

During brumation, usually occurring in November through March, we visited each hibernaculum every 2–4 weeks to record environmental data, disruptions in brumation, and rare instances of movement of turtles to new hibernacula. When VHF tagged turtles exhibited clinical signs, including nasal and ocular discharge, palpebral edema, lethargy, traumatic injuries, or abnormal brumation, we checked these turtles weekly to ensure retrieval of any carcasses within 1 week of death. We received wildlife collector permits through the Missouri Department of Conservation and approval from the Saint Louis Zoo Institutional Animal Care and Use Committee for this work.

Mortality data were recorded whenever a dead turtle was encountered. Cause of death was determined based on gross

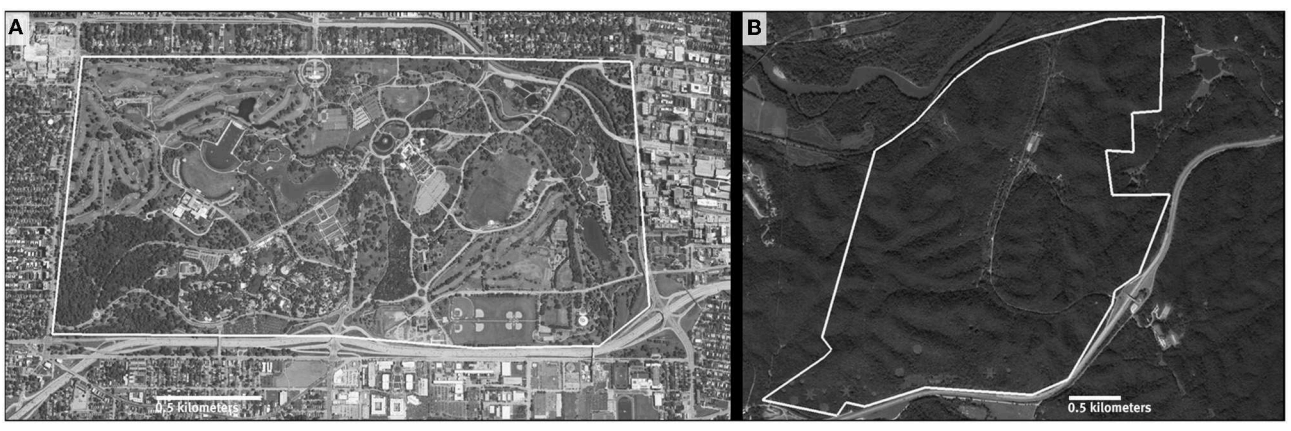

FIGURE 1 | Maps of the field sites, Forest Park **(A)** and Tyson Research Center **(B)** in the mortality study of box turtles in Missouri. White line indicates site perimeter.

necropsy findings and time in relation to brumation. Five categories were used: winter kill, lawnmower, predation, non-specific trauma, or unknown. The term winter kill refers to mortality that occurs during or after brumation (15). For this study, we defined winter kill as death of a turtle found above ground during the over-wintering period or within 2 weeks of emergence from brumation and without obvious signs of trauma. Turtles found in open lawn with adjacent lawnmower tracks and/or severely fractured carapaces were classified as lawnmower mortalities. We defined predation as injury inflicted by another animal as demonstrated by trauma to limbs, head and shell with characteristics of prey interaction. Turtles with evidence of trauma that was not characteristic of either lawnmowers or predation were classified as non-specific trauma. Unknown refers to turtles found dead outside of the winter kill time period with no sign of trauma or other obvious cause of death.

We calculated an observed mortality rate as the number of confirmed deaths out of the number of total box turtles tagged. We tested for differences in observed mortality rates between sites using the Fisher exact method (fisher.exact) in R (19). To account for staggered entry of individual turtles into the study and unknown outcomes for some tagged turtles, we also estimated survival using the known-fate model, a binomial generalized linear model, in the statistical program MARK (20) and the R interface "RMark" (19, 21). As turtles were not directly observed during the months of brumation, we summarized survival data at quarterly intervals for the purposes of this analysis. To evaluate the effects of site and sex on survival in our study population, we proposed a set of four candidate models: (1) survival held constant across sites and sexes, (2) survival allowed to vary by site, (3) survival allowed to vary by sex, and (4) survival allowed to vary by both site and sex. We used Akaike's information criteria adjusted for small sample size (AICc) to compare candidate models and selected the most parsimonious model based on ΔAICc and weight. Using the selected model, we estimated annual survival probabilities and associated 95% confidence intervals. We tested for differences in survival estimates using the program CONTRAST v2.0 (22, 23).

To evaluate the different causes of mortality at each site, we calculated an observed proportionate mortality ratio for the duration of the study as the number of deaths within a specific category out of the number of deaths in all categories, including those where the cause of death was unknown. We tested for differences in proportionate mortality within and between sites using the Fisher exact method as described above.

RESULTS

Between March 2012 and February 2019, we deployed telemetry tags on 41 three-toed box turtles (FP: 11 female and 12 male; TRC: 11 female and seven male). The sex ratio of tagged turtles was comparable at each site (Fisher exact: $p = 0.54$). Over the 7 year period, the observed mortality rate in FP was 60.9% (14 out of 23) (**Figure 2**) consisting of eight males and six females. During this same period, the mortality rate at TRC was 22.2% (4 out of 18) (**Figure 2**) with three females and one male. The observed mortality rate was significantly greater at FP than TRC (Fisher exact: $p = 0.03$).

Similarly, the odds of annual survival for box turtles at TRC (93%, 95% CI: 83–97%) were 3.5 times that of box turtles in FP (79%, 95% CI: 0.68–0.87%). Of the candidate models, the model that allowed survival to vary by site was best supported with the lowest AICc, 62% of the combined model weight, and ΔAICc > 2 between it and the next best supported model (**Table 1**). Confidence limits for sex broadly overlapped zero in the remaining models, suggesting that sex is uninformative as a predictor of survival. We therefore used the model that allowed survival to vary only by site to predict estimated annual survival probabilities (**Table 2**). The model estimated coefficient for site with FP as the baseline was 1.25, which corresponds to an odds ratio of 3.49 (1.08–11.33). The difference in estimated survival probabilities between sites is statistically significant (chi-square = 5.33, $p = 0.02$).

In FP, the leading category of death was winter kill at 43%, whereas at TRC the leading category was "unknown" at 75%

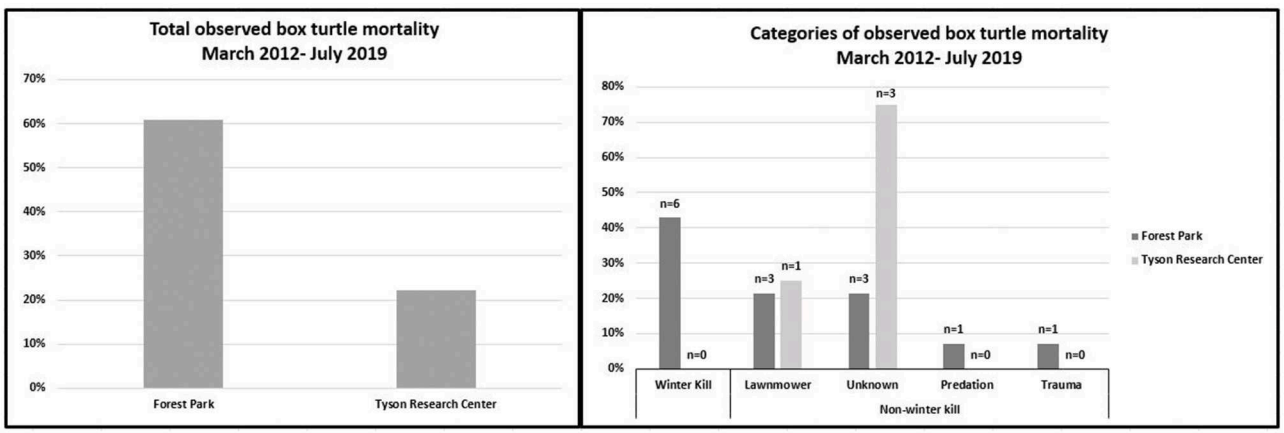

FIGURE 2 | Total observed mortality in box turtles at Tyson Research Center and Forest Park. Categories of observed mortality in the mortality study of box turtles in Missouri.

TABLE 1 | Model selection results of candidate models used to estimate survival from mortality of VHF-tagged three-toed box turtles in Forest Park (urban) and Tyson Research Center (rural) in Missouri, March 2012–February 2019.

Model[a]	K	AICc	ΔAICc	w_i
S (site)	2	101.75	0.00	0.62
S (site + sex)	3	103.79	2.04	0.22
S (.)	1	104.76	3.01	0.13
S (sex)	2	106.74	4.99	0.05

[a]*Models allow survival (S) to remain constant (.) or vary by site and/or sex. We report the number of parameters estimated (K), Akaike's information criterion adjusted for small sample size (AICc), difference in AICc relative to smallest value (ΔAICc) and Akaike weights (w_i).*

TABLE 2 | Best fit model [S (site)] estimated annual survival probabilities of VHF-tagged three-toed box turtles in Forest Park (urban) and Tyson Research Center (rural) in Missouri, March 2012–February 2019.

Site	Annual survival	95% CI
Forest Park	0.79	0.68–0.87
Tyson Research Center	0.93	0.83–0.97

(**Figure 2**). There were no statistically significant differences in proportionate mortality between categories either within or between sites.

DISCUSSION

Survival estimates in our study populations are consistent with those for telemetry followed eastern box turtles (*T. c. carolina*) in Delaware and Indiana (24, 25). Specifically, the annual survival estimate at TRC (93%) is similar to those previously documented in other protected natural settings (95–98%) (24, 25), whereas FP (79%) is similar to a site with relatively high human disturbance (81%) (24).

These differences in mortality may be due to local environmental factors, including anthropogenic impacts, at both sites. TRC is a contiguous, oak-hickory forest managed by Washington University in St. Louis with one paved road and perimeter fencing that does not impede turtle movement, but does control human presence in the site. FP is bordered on one side by a highway and on three sides by city neighborhoods. The park contains a variety of habitats including fragmented forest patches, golf courses, recreational sport fields, and a number of landscaped gardens. Forest fragments are the main habitat utilized by box turtles in FP, and all are bordered by park roads and grass lawns that are regularly mowed.

Research on reptiles living in urban environments suggests that urban box turtles and other urban-dwelling reptiles are more vulnerable to mortality than less urbanized populations (24, 26–29). Threats to box turtles that may be heightened in an urban environment include collection for use in the pet trade and vehicle and lawnmower-related morbidity and mortality (24, 26). Future survival analyses conducted at multiple urban and rural sites while explicitly measuring variation in land use and habitat features would be valuable for understanding the extent to which these anthropogenic changes affect box turtle populations.

Winter kill was the most documented category of mortality in FP but was not observed for any turtles at TRC. Winter kill is thought to be caused by long periods of frigid temperatures without snow or leaf litter of sufficient depth to provide adequate insulation during brumation (15) and is not uncommon in box turtles and other turtle species (15, 30–32). Possible explanations for the observed difference in winter kill between sites include that turtles in FP have poor insulation or ability to burrow deep enough to avoid the harsh winters given the small patch size, human removal of leaf litter, and lack of canopy cover during winter months. Additionally, anthropogenic habitat disruption may adversely affect box turtle brumation. For example, many habitats in FP are managed for restoration of native vegetation and invasive species removal (honeysuckle, *Lonicera* spp. and winter creeper, *Euonymus fortunei*) or modified for human use. These practices may disrupt the microclimates of brumating turtles by removing insulating materials during key winter months. Turtles at TRC usually overwinter in the low portion of ravines under thick leaf litter and therefore may experience different microclimates during the winter than FP turtles. We are currently collecting hibernaculum and surface temperature during brumation for all tagged turtles to determine if differences in insulation efficacy exist between the two sites.

FP is also a site that we believe is popular for pet turtle drop-offs based on observations of non-native eastern box turtles and by personal communication with FP visitors. We also occasionally encounter turtles with shell deformities that are typical of captive kept box turtles (32). These released turtles might be unprepared to brumate depending on their previous husbandry; their potential inability to do so efficiently may be cause for some winter kill cases.

Box turtles are susceptible to vehicle mortality, especially females moving in search of suitable nest sites (26, 33–35). Contrary to expectation, females did not experience greater mortality due to any cause, and no road mortality occurred in tagged turtles at either site, though we did observe road mortality in non-tagged box turtles (TRC $n = 0$, FP $n = 5$). Lawnmower strikes, however, were an important cause of mortality at both sites representing 21% ($n = 3/14$) and 25% ($n = 1/4$) of proportionate mortality at FP and TRC, respectively. This demonstrates that this anthropogenic threat may affect turtles wherever human management of grasslands may occur.

Predation and non-vehicular or lawnmower trauma were only documented in FP and at low proportions at 7% ($n = 1/14$) for each. Cause of death was unknown for the majority of tagged turtles at TRC at 75% ($n = 3/4$) and a significant proportion of tagged turtles in FP with 21% of the mortality. Possible explanations for these cases include death from natural causes or diseases we could not diagnose based on gross necropsy alone depending on carcass condition. We cannot rule out the possibility of infectious disease or exposure to environmental toxins as a contributing factor or cause of death for any

individual, as we did not specifically test for either at the time of death.

Limitations to our study include small sample size and inability to determine cause of death for six out of 18 turtles, thus making it difficult to interpret differences in cause-specific mortality. Testing for pathogens, toxins, and diagnostic procedures that we did not perform may help identify the cause of death in these undetermined cases and provide further data for cause of death in all the turtles. Lack of known history of these animals before tracking and the potential for some to have previously been pets may have affected data in these turtle populations that were presumed to be wild. Also, several tagged individuals at FP ($n = 3$) were lost to follow-up due to either human removal or radio-tag malfunction. Lastly, as there are no replicate urban and rural sites in our study design, associations between mortality rates and site characteristics cannot be explicitly tested and, instead, are best used for hypothesis generation for future research.

Of the identified categories of mortality, winter kill and lawnmower are both important in FP. The leading category was winter kill (43%), suggesting that successful brumation may be difficult for box turtles living in FP, but further data on habitat characteristics and quality are necessary. Because we do not know the history of these individuals, it is possible that some turtles in this study had been pets and were therefore unable to overwinter properly. Human disturbances causing habitat loss and fragmentation, however, are documented causes of population decline in box turtles (12, 24, 27, 36) and may impact the ability of turtles to successfully brumate. Environmental variation due to climate change is predicted to further intensify the rate of box turtle decline, because as ectotherms they and reliant on appropriate temperature throughout the year, including the brumation period (37). As compared to other, more long-term studies on rural Missouri box turtle survival, the higher mortality in FP box turtles may imply that urbanization may increase risk of mortality (12). While high, we do not know the impact of the observed mortality rate on box turtle population stability in FP. We recommend box turtles living in urban parks, such as FP, are monitored for population structure, reproductive success, and survival and that these data are compared to rural populations to determine whether urban parks serve as viable habitat for turtle conservation at a time of increasing urbanization throughout the U.S.

DATA AVAILABILITY STATEMENT

The datasets generated for this study are available on request to the corresponding author.

ETHICS STATEMENT

The animal study was reviewed and approved by Saint Louis Zoo Research Animal Use Committee.

AUTHOR CONTRIBUTIONS

JP substantially contributed to the design of the project, field data collection, and drafting of this manuscript for publication. As the field and lab technician for this research she is involved in every aspect of the box turtle program on a day to day and program level basis. MB-W is a veterinarian for this box turtle research and provided all statistical analysis as well as contribution to the manuscript in content and edits. SB is Co-PI for the box turtle research described here and provided substantial contributions to the research design, implementation, data collection, manuscript editing, and interpretation of the work. SD is the PI for the box turtle research described here, provided substantial contributions to the research design, implementation, data collection, manuscript editing, and interpretation of the work, is the lead veterinarian for the research, and approves all research questions and implementation.

FUNDING

This research was supported by the Saint Louis Zoo Institute for Conservation Medicine and through the National Science Foundation grant DEB1258062. Funding for student field staff was provided by the Tyson Research Center Undergraduate Research Fellow program and the Tyson Environmental Research Fellowship.

ACKNOWLEDGMENTS

We thank Kathleen Apakupakul, Keri Lammering, and all Institute for Conservation Medicine students and volunteers for their help in data collection. Additionally, we thank John Winter and Leah Fine for providing feedback on an early draft of this article. Thank you to project partners Forest Park Forever and Tyson Research Center for all assistance and support for this study.

REFERENCES

1. Turtle Taxonomy Working Group: Rhodin AGJ, Iverson JB, Bour, R. Fritz U, Georges A, Shaffer HB, et al. Turtles of the World: Annotated Checklist and Atlas of Taxonomy, Synonymy, Distribution, and Conservation Status, 8th Ed. In: Rhodin AGJ, Iverson JB, van Dijk PP, Saumure RA, Buhlmann KA, Pritchard PCH, et al. editors. *Conservation Biology of Freshwater Turtles and Tortoises: A Compilation Project of the IUCN/SSC Tortoise and Freshwater Turtle Specialist Group*. Chelonian Research Monographs (2017). p. 1–292.
2. Allender MC, Abd-Eldaim M, Schumacher J, McRuer D, Christian LS, Kennedy M. PCR prevalence of Ranavirus in free-ranging eastern box turtles (*Terrapene carolina carolina*) at rehabilitation centers in three south-eastern US states. *J Wildl Dis*. (2011) 47:759–64. doi: 10.7589/0090-3558-47.3.759
3. Dodd K, Ozgul A, Oli MK. The influence of disturbance events on survival and dispersal rates of Florida box turtles. *Ecol Appl*. (2006) 16:1936–44. doi: 10.1890/1051-0761(2006)016[1936:TIODEO]2.0.CO;2
4. Ernst CH, Lovich JE. *Turtles of the United States and Canada*. 2nd ed. Baltimore: The Johns Hopkins University Press (2009).

5. Gibbons JW, Scott DE, Ryan TJ, Buhlmann KA, Tuberville TD, Metts BS, et al. The global decline of reptiles, déjà vu amphibians. *Bioscience*. (2000) 50:653–66. doi: 10.1641/0006-3568(2000)050[0653:TGDORD]2.0.CO;2
6. Heppell SS. Application of life-history theory and population model analysis to turtle conservation. *Copeia*. (1998) 2:367–75. doi: 10.2307/1447430
7. Rees M, Roe JH, Georges A. Life in the suburbs: behavior and survival of a freshwater turtle in response to drought and urbanization. *Biol Conserv*. (2009) 142:3172–81. doi: 10.1016/j.biocon.2009.08.019
8. van Dijk PP. *Terrapene carolina (Errata Version Published in 2016). The IUCN Red List of Threatened Species 2011:e.T21641A97428179*. (2011). doi: 10.2305/IUCN.UK.2011-1.RLTS.T21641A9303747.en
9. Martin BT, Bernstein NP, Birkhead RD, Koukl JF, Mussmann SM, Placyk JS, Jr. On the reclassification of the terrapene (Testudines: *Emydidae*): a response to Fritz & Havaš. *Zootaxa*. (2014) 3835:292–4. doi: 10.11646/zootaxa.3835.2.9
10. Briggler JT, Johnson TR. *Missouri's Turtles*. Jefferson City, MO: Missouri Department of Conservation. (2006) 12 p.
11. Schwartz ER, Schwartz CW, Kiester AR. The *Three-Toed Box Turtle in Central Missouri, Part II: a Nineteen-Year Study of Homerange, Movements, and Population*. Ibid. Terr Ser. No. 12. Jefferson City, MO: Conservation Commission of the state of Missouri (1984).
12. Schwartz ER, Schwartz CW. A quarter-century study of survivorship in a population of three-toed box turtles in Missouri. *Copeia*. (1991) 1991:1120–3. doi: 10.2307/1446111
13. Carpenter CC. Hibernation, hibernacula and associated behavior of the three-toed box turtle (*Terrapene carolina triunguis*). *Copeia*. (1957) 1957:278–82. doi: 10.2307/1439153
14. Missouri Natural Heritage Program. *Missouri Species and Communities of Conservation Concern Checklist*. Jefferson City, MO: Missouri Department of Conservation (2018) 44 p.
15. Dodd CK. *North American Box Turtles: A Natural History*. Norman: University of Oklahoma Press (2001).
16. Schwartz CW, Schwartz ER. *The Three-Toed Box Turtle in Central Missouri: Its Population, Home Range and Movements*. Terrestrial Series 5. Jefferson City, MO: Missouri Department of Conservation. (1974).
17. Dorcas ME. *Herpetology Laboratory Guidelines and Protocols*. Davidson, NC: Department of Biology; Davidson College (2005).
18. Rittenhouse CD, Millspaugh JJ, Washburn BE, Hubbard MW. Effects of radiotransmitters on fecal glucocorticoid metabolite levels of three-toed box turtles in captivity. *Wildl Soc Bull*. (2005) 33:706–13. doi: 10.2193/0091-7648(2005)33[706:EOROFG]2.0.CO;2
19. R Core Team. *R: A Language and Environment for Statistical Computing*. R Foundation for Statistical Computing, Vienna, Austria. (2018). Available online at: https://www.R-project.org/
20. White GC, Burnham KP. Program MARK: survival estimation from populations of marked animals. *Bird Study*. (1999) 46 (Suppl. 1):S120–39. doi: 10.1080/00063659909477239
21. Laake JL. *RMark: An R Interface for Analysis of Capture-Recapture Data With MARK*. AFSC Processed Report 2013-01, 25 p. Alaska Fish. Sci. Cent., NOAA, Natl. Mar. Fish. Serv. Seattle, WA, United States. (2013).
22. Hines JE, Sauer JR. *Program CONTRAST - A General Program for the Analysis of Several Survival or Recovery Rate Estimates*. US Fish & Wildlife Service, Fish & Wildlife Technical Report 24, Washington, DC, United States (1989).
23. Sauer JR, Williams BK. Generalized procedures for testing hypotheses about survival or recovery rates. *J Wildl Manag*. (1989) 53:137–42. doi: 10.2307/3801320
24. Nazdrowicz NH, Bowman JL, Roth RR. Population ecology of the eastern box turtle in a fragmented landscape. *J Wildl Manag*. (2008) 72:745–53. doi: 10.2193/2005-521
25. Allard HA. The eastern box turtle and its behavior. *J Tenn Acad Sci*. (1948) 23:307–21.
26. Gibbs JP, Shriver WG. Estimating the effects of road mortality on turtle populations. *Conserv Biol*. (2002) 16:1647–52. doi: 10.1046/j.1523-1739.2002.01215.x
27. Bowen KD, Colbert PL, Janzen FJ. Survival and recruitment in a human-impacted population of ornate box turtles, *Terrapene ornata*, with recommendations for conservation and management. *J Herpetol*. (2004) 38:562–8. doi: 10.1670/78-04A
28. Farrell TM, Dodd CK, May PG. Terrapene carolina - Eastern box turtle. In: Meylan PA, editor. *Biology and Conservation of Florida Turtles*. Lunenburg, MA: Chelonian Research Foundation (2006). p. 235–48.
29. Wolf AJ, Hellgren EC, Bogosian V III, Moody RW. Effects of habitat disturbance on Texas horned lizards: an urban case study. *Herpetologica*. (2013) 69:256–81. doi: 10.1655/HERPETOLOGICA-D-12-00062.1
30. Metcalf EL, Metcalf AL. Mortality in hibernating ornate box turtles, *Terrapene ornata*. *Herpetologica*. (1979) 35:93–6. doi: 10.2307/3627283
31. Christiansen JL, Bickham JW. Possible historic effects of pond drying and winterkill on the behavior of *Kinosternon flavescens* and *Chrysemys picta*. *J Herpetol*. (1989) 23:91–4. doi: 10.2307/1564327
32. Meyer J, Selleri P. Dermatology—Shell. In: Saunders WB, editor. *Mader's Reptile and Amphibian Medicine and Surgery*. St. Louis, MO: Elsevier (2019). p. 712–20. doi: 10.1016/B978-0-323-48253-0.00070-2
33. Haxton T. Road mortality of snapping turtles, *Chelydra serpentina*, in central Ontario during their nesting period. *Can Field Nat*. (2000) 114:106–10.
34. Rosen PC, Lowe CH. Highway mortality of snakes in the Sonoran Desert of southern Arizona. *Biol Conserv*. (1994) 68:143–8. doi: 10.1016/0006-3207(94)90345-X
35. Shepard DB, Dreslik MJ, Jellen BC, Phillips CA. Reptile road mortality around an oasis in the Illinois corn desert with emphasis on the endangered eastern massasauga. *Copeia*. (2008) 2008:350–9. doi: 10.1643/CE-06-276
36. Budischak SA, Hester JM, Price SJ, Dorcas ME. Natural history of *Terrapene carolina* (box turtles) in an urbanized landscape. *Southeast Nat*. (2006) 5:191–204. doi: 10.1656/1528-7092(2006)5[191:NHOTCB]2.0.CO;2
37. McCallum ML, McCallum JL, Trauth SE. Predicted climate change may spark box turtle declines. *Amphibia Reptilia*. (2009) 30:259–64. doi: 10.1163/156853809788201072

Conflict of Interest: The authors declare that the research was conducted in the absence of any commercial or financial relationships that could be construed as a potential conflict of interest.

Copyright © 2019 Palmer, Brenn-White, Blake and Deem. This is an open-access article distributed under the terms of the Creative Commons Attribution License (CC BY). The use, distribution or reproduction in other forums is permitted, provided the original author(s) and the copyright owner(s) are credited and that the original publication in this journal is cited, in accordance with accepted academic practice. No use, distribution or reproduction is permitted which does not comply with these terms.

frontiers in Veterinary Science

ORIGINAL RESEARCH
published: 29 November 2019
doi: 10.3389/fvets.2019.00425

Trichomonosis in Greenfinches (*Chloris chloris*) in the Netherlands 2009–2017: A Concealed Threat

Jolianne M. Rijks[1]*, *Andrea A. G. Laumen*[1], *Roy Slaterus*[2], *Julia Stahl*[2], *Andrea Gröne*[1,3] *and Marja L. Kik*[1,3]

[1] Dutch Wildlife Health Centre (DWHC), Department of Pathobiology, Faculty of Veterinary Medicine, Utrecht University, Utrecht, Netherlands, [2] Dutch Centre for Field Ornithology (Sovon), Nijmegen, Netherlands, [3] Pathology Division, Department of Pathobiology, Faculty of Veterinary Medicine, Utrecht University, Utrecht, Netherlands

Finch trichomonosis in Europe is caused by a *Trichomonas gallinae* subtype A1 strain, considered to be clonal because lacking genetic heterogeneity in partial genotyping. The disease recently emerged and has been associated with a 66% reduction of the British breeding greenfinch (*Chloris chloris*) population. In contrast, in the Netherlands, where trichomonosis was detected in 2009, the breeding greenfinch population continued to grow in subsequent years. This study aimed to elucidate whether this discrepancy in population trends is because Trichomonas infection in Dutch greenfinches is associated with less severe disease, i.e., disease being less fatal. Therefore, it characterized and quantified trichomonosis in a convenience sample of greenfinches found dead and examined post-mortem between 2009 and 2017 and compared results to published data from Great Britain. Trichomonads were detected by cytology, histology, or culture in 95/101 greenfinches. The birds with trichomonads all had microscopic lesions in the upper digestive tract consistent with trichomonosis, indicating the trichomonads caused disease. The occurrence of significant lesions due to other causes was low. Some greenfinches with trichomonosis showed no macroscopic lesions. These birds showed significantly less ulceration of the mucosa and less extensive heterophil infiltration, but extent of macrophage infiltration and presence of bacteria was similar to that of birds with macroscopic lesions, and significant lesions due to other causes were equally rare. Therefore, trichomonosis was considered similarly fatal in both groups. The frequency of fatal trichomonosis in the Dutch greenfinches did not differ significantly from that reported from Great Britain. Partial genotyping of the ITS1-5,8S-ITS2 and Fe-hydrogenase regions of *T. gallinae* was performed to detect genetic heterogeneity, that could indicate the presence of other, possibly less virulent, strains. In 60/63 samples there was full alignment of sequences with the clonal strain of *T. gallinae* subtype A1. The remaining three samples had the same single synonymous nucleotide difference in the Fe-hydrogenase region; however, pathology is these three was identical to the others. Collectively, the results provide no clear evidence for less severe disease as explanation for the discrepancy in census data trends. We conclude that trichomonosis is a threat concealed in Dutch breeding greenfinch census data.

Keywords: *Trichomonas gallinae*, trichomonosis, greenfinch (*Chloris chloris*), finch, bird census data, wildlife, the Netherlands

OPEN ACCESS

Edited by:
Francesco Carlo Origgi, University of Bern, Switzerland

Reviewed by:
Ettore Napoli, University of Messina, Italy
Tatjana Sitt, United States Department of Agriculture, United States

***Correspondence:**
Jolianne M. Rijks
j.m.rijks@uu.nl

Specialty section:
This article was submitted to Veterinary Experimental and Diagnostic Pathology, a section of the journal Frontiers in Veterinary Science

Received: *27 August 2019*
Accepted: *11 November 2019*
Published: *29 November 2019*

Citation:
Rijks JM, Laumen AAG, Slaterus R, Stahl J, Gröne A and Kik ML (2019) Trichomonosis in Greenfinches (Chloris chloris) in the Netherlands 2009–2017: A Concealed Threat. Front. Vet. Sci. 6:425. doi: 10.3389/fvets.2019.00425

INTRODUCTION

Trichomonosis is a potentially fatal disease of columbids (*Columbiformes*), raptors (mainly *Falconiformes*), owls (*Strigiformes*) and other selected bird species. It can cause host population declines when emerging in susceptible populations and thus present a serious threat for endangered species (1–3).

The protozoal parasite *Trichomonas gallinae* is the prime etiological agent of trichomonosis, and columbid species are considered primary hosts (4). The transfer of a single trichomonad is enough to cause infection (5). The parasite invades the mucosa of the upper digestive tract, causing damage to the epithelium and then invading mucosa and submucosa (6). There are multiple strains of *T. gallinae,* that can be classified into clades based on partial genome sequences (7). The strains vary in pathogenicity, but there is no molecular assay to distinguish virulent from non-virulent strains (1). The most virulent strains can cause death within 4 days after infection (8). Birds infected early in life by avirulent or moderately virulent strains can develop protective immunity to virulent strains, and may be able to carry virulent strains (1, 4, 8–10). Co-evolution between host and pathogen is probable, given the strong selective pressure (11).

Wild passerine species are not commonly infected by trichomonads (1, 12). However, recently a strain of *T. gallinae* subtype A1 has been infecting finches (*Fringillidae*) in Great Britain (GB) and elsewhere Europe (13–18, 20–23). This strain has unique sequences in partial genotyping (22), suggesting that finch trichomonosis is possibly caused by a single, clonal strain. The emergence of the disease in finches is associated with high mortality and population declines (13–18, 20–23). Trichomonosis accounted for 80–100% of the deaths caused by infectious disease in finches examined post-mortem in GB during 2006–2016 (14, 24). Greenfinches (*Chloris chloris*) have especially been affected (14), and the breeding greenfinch population in GB has declined steadily since the disease was detected from approximately 4.3 million in 2006 to 1.5 million in 2016 (24). This marked decline by 66% has shown no sign of leveling off. As a result of the decline, the breeding greenfinch population in GB was classified as endangered in an assessment based on the International Union for Conservation of Nature (IUCN) guidelines for extinction risk (24, 25). In contrast, in the Netherlands (the NL), where trichomonosis was first detected in greenfinches in 2009[1], the Dutch breeding greenfinch population continues to grow. Only in wintering (including migrating) greenfinches was there a decline in numbers (**Supplemental Material 1**).

The cause for this discrepancy in breeding greenfinch population trends between the NL and GB in the presence of trichomonosis is unclear. Therefore, trichomonas-associated mortality in greenfinches in the NL was compared to trichomonas-associated mortality in greenfinches elsewhere, specifically in GB, to answer the question whether infection in Dutch greenfinches caused less severe disease, i.e., disease being less fatal. The aim of this study was therefore to characterize and quantify trichomonosis in a convenience sample of greenfinches found dead and examined post-mortem between 2009 and 2017 in the NL. These data were then compared to data published on *T. gallinae* subtype A1 finch trichomonosis in greenfinches in GB. The hypotheses were that in the Dutch sample trichomonosis would account significantly less frequently for greenfinch deaths than in greenfinches examined post-mortem in GB, and that the partially typed trichomonas genomes would show genetic heterogeneity.

MATERIALS AND METHODS

Materials

Since 2009, greenfinches found dead have been submitted to the Dutch Wildlife Health Centre (DWHC) for post-mortem examination in the context of wildlife disease scanning (under permit no. FF/75A/2008/075). In 2016, submissions of greenfinches found dead were actively encouraged through media. The greenfinches were examined as soon as possible after the call from the submitter, which usually meant the next day. The birds were kept cool by the submitter and refrigerated at 4°C during transport and overnight. They were never frozen. Post-mortem examination was performed using a standard examination protocol including histology to identify lesions and probable cause of death.

Trichomonad Status

Trichomonads were detected microscopically using one to three of the following methods: cytological examination of smears of macroscopic trichomonas-like lesions; histological examination of predilection tissues (hematoxylin-eosin staining); and trichomonas culture on gape, pharynx, esophagus and/or crop tissues. For the latter, tissues were incubated at 30°C (22) in DMEM (Gibco; Thermofisher, the NL) with 10% fetal bovine serum, supplemented with 1% penicillin/streptomycin (Gibco). The cultures were checked daily for the presence of motile trichomonads using the hanging drop technique. When 10–15 or more trichomonads were observed per image at 100X magnification, the tissue sample was removed, and the remaining cultures were centrifuged (5 min, 3,500 rpm). The supernatants were poured off and the pellets were suspended in approximately 100 μL clinging medium and stored at −80°C.

For analysis, the proportion of greenfinches infected with trichomonads was first assessed. Birds were classified into "trichomonads present," "trichomonads absent," and "inconclusive" specimens. "Trichomonads present" was a greenfinch with trichomonads detected by at least one test. The assumption was made that all trichomonads observed belonged to the genus *Trichomonas*. "Trichomonads absent" was a greenfinch tested by at least two methods to account for the limited negative predictive value of the tests and conclusively negative in all tests performed (12, 18). The specimens for which the trichomonad status could not be concluded according to the above definitions were considered "inconclusive" and excluded from the subsequent investigation steps. Greenfinches that were found on one day at one location were considered to belong to one mortality event.

Presence of trichomonads does not necessarily indicate disease, but it is assumed that the presence of lesions characteristic of trichomonosis and its complications, and the

[1]Dutch Wildlife Health Centre. https://www.dwhc.nl/groenling-het-geel/.

absence of other significant lesions, strongly support fatal trichomonosis. To be able to investigate whether greenfinches without macroscopic lesions were more likely to be cases of mild, subclinical or non-clinical disease, a distinction was made throughout the analysis between specimens with and without macroscopic lesions in the upper digestive tract.

Microscopic Lesions Upper Digestive Tract

To assess presence and severity of microscopic lesions at trichomonad-predilection sites in infected specimens, four characteristic attributes of trichomonad infections were scored in affected tissues (pharynx, esophagus or crop): the depth of the ulceration (0 if no ulceration; 1 if erosion of the epithelium only; 2 if ulceration of epithelium and submucosa only; 3 if transmural ulceration), the extent of macrophage and heterophilic granulocyte infiltration assessed on the basis of five high power fields (0 if no or just one inflammatory cells; 1 if the inflammatory cells comprised <5% of the analyzed tissue; was seen; 1 if the inflammatory cell comprised <5% of the analyzed tissue; 2 if the inflammatory cells comprised 5–50% of the analyzed tissue; 3 if the inflammatory cells comprised >50% of the analyzed tissue), and the presence of bacteria (0 if not present; 1 if present). In addition, the visibility of trichomonads was noted (0 if not visible; 1 if visible). The slides were evaluated by two persons, including one veterinary pathologist. When there were discrepancies, the parties met to reach a consensus. One-sided Fisher exact tests ($p = 0.05$) were performed in R Core Team (19) to investigate if the scored attributes were more severe in specimens with macroscopic lesions than without.

Contribution of Trichomonosis to Mortality

The proportions of trichomonad-infected specimens with and without other significant lesions was then determined to conclude the relative contribution of trichomonosis to greenfinch mortality in the NL. For this analysis, hemorrhagic diathesis in trichomonad-infected specimens with upper digestive tract lesions was considered a complication of trichomonosis and not a distinct lesion. The reason is that lesions in the mucosa of the upper digestive tract can result in reduced food intake and starvation, which results in hemorrhagic diathesis in passerine birds (26). Chi-square tests ($p = 0.05$) were performed in R to compare the contribution of hemorrhagic diatheses to death in trichomonad-infected specimens with and without other significant lesions, and to examine if there was a significant difference in presence of substantial lesions due to other causes between greenfinches with and without macroscopic trichomonosis lesions.

Statistical Comparison With GB Mortality Data

The mortality data from the NL was then compared to a study on greenfinches examined post-mortem in GB from 1 April to 30 September 2006, i.e., the two seasons when most cases occur. Trichomonosis was diagnosed in 70 of 125 specimens based on macroscopic lesions (termed "necrotic ingluvitis" in the study) and *T. gallinae* detection by culture, PCR or both, and trichomonosis was considered probable in 20 of 125 specimens based on macroscopic lesions consistent with trichomonosis with negative *Salmonella* sp. culture (23). This total of 90 of 125 specimens was used for comparison to the proportion of trichomonad-infected greenfinches with macroscopic lesions in the NL.

In addition, the ratio of deaths due to trichomonosis over the total of deaths due to infectious disease was compared between GB (372/426, 2010–2016) (24) and the NL (the NL data, 2009–2017). For consistency with the criteria used in the GB study, the numerator of the NL sample consisted of the trichomonosis birds with no concurrent other infectious disease, and the denominator of all specimens with infectious disease. The Chi-square tests were performed in R.

Trichomonad Partial Genome Sequencing

The genetic heterogeneity of the trichomonads present in the greenfinches was investigated based on the partial sequence identity of the ITS region and the Fe-hydrogenase gene. The ITS1-5,8S-ITS2 locus served to distinguish *T. gallinae* from other trichomonad species (1) and to determine the major clade, A or B (2, 7), the more variable Fe-hydrogenase gene for further differentiation among strains (2). The obtained sequences were compared to those of the epizootic "clonal" strain (22).

In brief, DNA was extracted from frozen and subsequently thawed trichomonad pellets using the QiaAmp DNA Mini Kit (Qiagen, UK) following the manufacturer's instructions. Isolated DNA was stored at 4°C for a short period (a few days) or at −80°C for a longer period (week to months). The concentration and purity of the DNA isolates were checked using the Nanodrop 1000 Spectrophotometer V3.8.1. For amplification of the ITS1-5.8S-ITS2 gene, previously established primers were used: TFR1 primer with minor modifications, as indicated in bold [5′ TGCTTCAGTTCAGCGGGT**TC**TCC 3′] and TFR2 (27). For the amplification of the Fe-dehydrogenase gene the previously established primers TrichhydFOR and TrichhydREV were used (22). PCR amplification was performed with a PCR Master Mix (Phusion). The ITS1/5,8S/ITS2 cycling parameters consisted of an initial denaturation at 98°C for 30 s, followed by 35 cycles at 98°C for 10 s and at 72°C for 30 s, and 72°C for 7 min for the final extension step. The Fe-hydrogenase cycling parameters for Fe-hydrogenase consisted initial denaturation at 98°C for 30 s, followed by 35 cycles at 98°C for 10 s, 65°C for 30 s, 72°C for 60 s, and 72°C for 7 min for the final extension step. Positive and negative controls (distilled water) were included in all PCR runs. The PCR products were purified and were sequenced by Macrogen (the NL). The obtained sequences were aligned with the SeqMan Pro program of Lasergene version 12.0 (DNAStar Inc., Madison Wisconsin) and were analyzed manually. BLAST was used for comparison. Sequences were deposited in GenBank under the following accession numbers: MN385401 (for ITS1/5,8S/ITS2 region of greenfinch no 3), MN385402, MN385403, MN385404 and MN385405 (for Fe-hydrogenase region of greenfinches no 3, 38, 84, and 94, respectively).

Spatial Distribution and Seasonal Occurrence

Results were mapped and plotted per season for overview, against a background of reports of diseased greenfinches made to the

TABLE 1 | Significant lesions and probable cause of death of the 123 greenfinches grouped according to trichomonad presence and macroscopic lesion detection.

Trichomonads	Macroscopic lesions upper digestive tract	Condition	Significant lesions, probable cause of death*
Present (95)	Detected (56)	Cachectic (22), poor (17), moderate (2), good (2)	Trichomonosis (43): trichomonosis only (15), with HD (26); trichomonads only (1), with HD (1)
		Cachectic (4), poor (7), moderate (1)	Trichomonosis and other (13): trichomonosis and trauma (4), and campylobacter enteritis (1), and pneumonia unknown etiology (1), and pneumonia and hepatitis unknown etiology (1), with HD and trauma (3), with HD and coccidiosis (1), with HD and fungal pneumonia (1); trichomonads and salmonellosis (ingluvitis, pneumonia; 1)
	Not detected (37)	Cachectic (16), poor (10), moderate (3)	Trichomonosis (29): trichomonosis only (8), with HD (15); trichomonads only (1), with HD (5)
		Cachectic (4), poor (2), moderate (2)	Trichomonosis and other (8): trichomonosis and trauma (3), and trauma and bacterial pneumonia (1); trichomonads and atoxoplasmosis (1), and trauma (1), with HD and trauma (1), with HD and campylobacter enteritis (1)
	Not determined (2)	Not determined (2)	Not determined (2): too autolytic, but trichomonads cultured (2)
Absent (6)	Detected (1)	Poor (1)	Salmonellosis (sepsis; 1)
	Not detected (5)	Cachectic (1), poor (2), moderate (2), good (1)	Yersiniosis (sepsis; 1), trauma (3), unknown (1)
Inconclusive (22)	Detected (5)	Cachectic (4), poor (1)	Salmonellosis (sepsis; 1), avipox ingluvitis with bacterial sepsis (1), stomatitis unknown etiology (1), avian malaria (1), unknown (1)
	Not detected (14)	Cachectic (6), poor (3), moderate (2), good (2)	Salmonellosis (sepsis; 1), HD (3), pharyngitis or ingluvitis with HD (2), avian malaria with HD (1), trauma (2), cardiopathy (1), unknown (4)
	Not determined (3)	Not determined (3)	Unknown (3)

*HD, Hemorrhagic diathesis G.I. tract. *"Trichomonads" indicates the specimen was infected with trichomonads but trichomonas-associated lesions at predilection sites could not be assessed histologically, generally due to autolysis. These specimens are indicated separately for completeness but viewed as trichomonosis cases in this table since in specimens where histological examination was possible, the microscopic lesions that are indicative of trichomonas-associated disease were always found, even when there were no apparent macroscopic lesions.*

Dutch Center for Field Ornithology (Sovon) during 2009–2017. The spatial distribution was mapped using ArcGIS© software. The seasons were spring (21 March−20 June), summer (21 June−20 September), autumn (21 September−20 December) and winter (21 December−20 March).

RESULTS

Trichomonad Status

In total, 123 greenfinches submitted from 95 mortality events were examined post-mortem between 1 August 2009 and 1 June 2017 (**Supplemental Material 2**). The presence or absence of trichomonads could be determined for 101/123 greenfinches (**Table 1**; **Supplemental Materials 2, 3**). These 101 greenfinches were found during 78 mortality events. In the remaining 22/123 specimens, the trichomonad status was "inconclusive." This was generally due to the autolytic state of the specimen and they were excluded. Excluding the inconclusive results, the concordance between tests was 80% (**Supplemental Material 3**). The hanging drop following culture was more sensitive than histology and cytology (**Supplemental Material 3**).

Trichomonads were absent in 6/101 specimens. These six specimens were found dead in six (6/78) mortality events. Their deaths were associated with bacterial sepsis (2/6), trauma (3/6) or due to an unknown cause (1/6) (**Table 1**). Trichomonads were present in the remaining 95/101 greenfinches (**Table 1**). These 95 specimens were found dead in 72 of the 78 mortality events.

Macroscopic lesions, consisting of caseous yellowish material on the hyperemic mucosa of the gape, pharynx, esophagus or crop or several of these (**Figure 1A**), could be assessed for 93/95 specimens (**Table 1**), and were observed in 56/93 (60%). Seeds adhered firmly to the mucosa in 14/56 of the birds with macroscopic lesions (**Figure 1A**). No macroscopic lesions were present in 37/93 (40%) birds. Seeds adhered firmly to the mucosa in 4/37 specimens without visible lesions. In summary, trichomonads were present in a high proportion of the greenfinches, but these birds did not always have macroscopic lesions indicative of trichomonosis.

Microscopic Lesions Upper Digestive Tract

Trichomonad infection in the examined greenfinches was observed only in the mucosa of the upper digestive tract. No trichomonas-associated lesions were observed elsewhere in the head (sinuses, orbital regions, brain, or neck), lung, or liver.

Characteristically, the affected mucosa was thickened due to epithelial hyperplasia and covered by a mixture consisting of fibrin or serum, cellular debris, erythrocytes and trichomonads, occasionally also with bacteria. The trichomonads were visible in most infected specimens as leaf-shaped to ovoid pale pink organisms among epithelial cells, in the submucosa and muscular layers (**Figure 1B**). Areas of multifocal to widespread

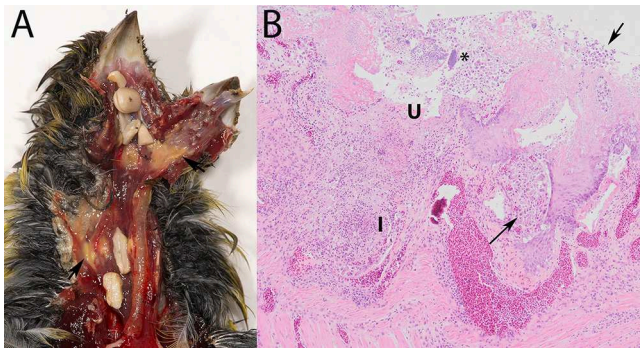

FIGURE 1 | Trichomonosis in a greenfinch (*Chloris chloris*). **(A)** Macroscopic lesions, consisting of caseous yellowish material on the hyperemic mucosa of the upper digestive tract, with seeds stuck. **(B)** Lesions associated with trichomonads (arrows) in the crop, demonstrating the scored microscopic characteristics depth of ulceration (U), extent of macrophage and of heterophilic granulocyte infiltration (I) and presence of bacteria (*) (HE stain, 10x).

necrosis, erosion or ulceration, interrupted the hyperplastic epithelium (**Figure 1B**).

Such microscopic lesions were present in all trichomonad-infected specimens, that were histologically examined (**Table 2**). However, the depth of ulceration was significantly less profound in cases without macroscopic lesions, i.e., those with microscopic lesions only ($p = 0.032$, **Table 2**). Variable degrees of submucosal and occasionally transmural inflammation, composed of heterophilic granulocytes and macrophages, lymphocytes and plasma cells were present (**Figure 1B**). The extent of heterophilic granulocyte infiltration was significantly less in cases without macroscopic lesions ($p = 0.019$; **Table 2**). In contrast, macrophage infiltration was similar between both groups ($p = 0.313$; **Table 2**). Bacterial colonization (**Figure 1B**) was also comparable in in both groups ($p = 0.139$; **Table 2**). In summary, all histologically examined trichomonad-infected greenfinches had microscopic necrotizing lesions in the upper digestive tract. Those without macroscopic lesions had significantly less deep ulcerative lesions and less extensive heterophil infiltration, but extent of macrophage infiltration and presence of bacteria was similar to that of specimens with macroscopic lesions.

Contribution of Trichomonosis to Mortality

Trichomonosis was often severe enough to have caused death, with or without reaching the stage of macroscopically visible lesions. Based on post-mortem examination, 72/93 (77%) trichomonad-infected greenfinches died from trichomonosis alone or from trichomonosis with hemorrhagic diathesis (**Table 1**). Among these, 43/72 had macroscopic lesions in the upper digestive tract, whereas 29/72 had not. The remaining 21/93 (23%) birds had other significant lesions in addition to trichomonosis or trichomonosis with hemorrhagic diathesis. These other significant lesions were associated with bacterial (4/21), protozoal (2/21) or fungal (1/21) infections, pneumonia (2/21) or hepatitis (1/21) of unknown etiology, or trauma (13/21). Of the 21 trichomonad-infected birds that also had other significant lesions, 13/21 had macroscopic lesions in the upper digestive tract and 8/21 had not (**Table 1**). Hemorrhagic diathesis occurred significantly more frequently in the trichomonad-infected birds without lesions due to other causes (47/72; 65%) than in those with (7/21; 33%) ($X^2 = 6.813$; $p = 0.009$), consistent with a contribution of this complication to fatal trichomonosis. The specimens without macroscopic lesions did not have significantly more other lesions (8/37; 21%) than specimens with macroscopic lesions (13/56; 23%) ($X^2 < 0.001$; $p = 1$), suggesting that trichomonosis can be equally fatal in cases with or without macroscopic lesions.

Statistical Comparison With GB Mortality Data

Statistical comparison with published GB mortality data provided no evidence for significant differences in trichomonosis disease in greenfinches between the NL and GB. The proportion of specimens in the Dutch cohort with trichomonads and macroscopic lesions (56/93, 60%) did not differ significantly from the published proportion of greenfinches with macroscopic lesions associated with trichomonosis in GB (90/125, 72%; Chi-square test $X^2 = 2.837$; $p = 0.092$) (23). Also, the ratio of the number of trichomonosis cases with no concurrent other infectious disease ($82 = 93–9$) over the total number of greenfinches with infectious disease ($95 = 93 + 2$; **Table 1**) is 86% (82/95). This ratio does not differ significantly from that of GB (372/426; 87%) ($X^2 = 0.009$; $p = 0.924$) (24).

Trichomonad Partial Genome Sequencing

PCR products were obtained from the trichomonad pellets of 63 greenfinches belonging to 50 mortality events occurring in 2010 (1/63), 2013 (2/63), 2014 (1/63), 2015 (1/63), and 2016 (58/63) (**Supplemental Material 2**). The sample consisted of birds with or without macroscopic lesions of trichomonosis and with or without significant lesions due to other causes (**Table 3**).

All trichomonads were *T. gallinae*. All 63 PCR products (326 bp) obtained for the ITS1-5,8S-ITS2 region showed 100% sequence identity (100% query coverage) with recent GenBank accessions for *T. gallinae* in greenfinches (MK172847) (20). The nucleotide sequences also had 100% sequence identity (66% query coverage) to GenBank accession number GQ150752, the sequence obtained for the ITS1-5,8S-ITS2 region from an infected greenfinch in GB (214 bp) (23).

There was restricted evidence for genetic heterogeneity in the Fe-hydrogenase gene. The sequences of 60/63 PCR products (901 bp) obtained for the Fe-hydrogenase gene fully aligned with the sequence of the of 901 bp of the "clonal" strain (Genbank accession number JF681136). In the other three cases, all from 2016, one nucleotide difference was seen when compared to the same clonal strain (99.89% identity). In all three, there was a synonymous T-to-C substitution at position 135 compared to JF681136. Pathology in these three birds was not distinct from other trichomonas-infected specimens (**Table 3**; **Supplemental Material 2**).

TABLE 2 | Presence and severity of microscopic lesions in the upper digestive tract of 51 greenfinches infected with trichomonads, distinguishing between specimens with and without macroscopic lesions in the upper digestive tract.

Characteristic	Scoring category	Trichomonas infection with visible macroscopic lesions ($n = 39$)	Trichomonas infection without visible macroscopic lesions ($n = 12$)	*P*-value one sided Fisher's exact test
Ulceration	Absent	0	0	0.032
	Epithelium only (erosion)	3	4	
	Epithelium and submucosa	17	6	
	Transmural	19	2	
Macrophages	None or just one	9	1	0.313
	<5% of tissue	14	8	
	5–50% of tissue	7	2	
	>50% of tissue	9	1	
Heterophilic granulocytes	None or just one	4	4	0.019
	<5% of tissue	10	6	
	5–50% of tissue	6	1	
	>50% of tissue	19	1	
Bacteria	Absent	1	2	0.139
	Present	38	10	

TABLE 3 | Overview of the partial genotyping results for *Trichomonas* according to the lesions observed in the 63 tested greenfinches.

Trichomonosis-associated macroscopic lesions	Significant lesions due to other causes	ITS1/5,8/ITS2 gene 100% sequence identity	Fe-hydrogenase gene 100% sequence identity	Fe-hydrogenase gene 99.89% sequence identity (1 synonymous T-to-C substitution at position 135)
Yes	No	31	29	2
Yes	Yes	10	10	
No	No	15	14	1
No	Yes	5	5	
No pathology performed	Not determined	2	2	
Total		63	60	3

The sequences were compared to the "clonal" finch trichomonosis T. gallinae subtype A1 strain present in the GB (GenBank accession numbers GQ150752 for the ITS1/5,8/ITS2 gene and JF681136 for the Fe-hydrogenase gene).

Spatial Distribution and Seasonal Occurrence

The disease occurs widespread and has a seasonal peak. The greenfinches infected with trichomonosis were found widely across the NL (**Figure 2**). Trichomonosis cases were mostly reported during the spring and summer months; however, some cases did occur in autumn and winter (**Supplemental Material 4**).

DISCUSSION

The Dutch greenfinch breeding population continued to grow in the years following the first detection of finch trichomonosis in 2009, unlike the GB population where a decline set in directly when the disease emerged in 2005 and where the disease is perceived as a threat to greenfinches (24, 25). One of the possible explanations for this discrepancy is that the emergence of *Trichomonas* infection in Dutch greenfinches is associated with less severe disease, i.e., disease being less fatal. This possibility was investigated in this study by analyzing the contribution of trichomonosis to greenfinch mortality and the genetic heterogeneity of *Trichomonas* strains. This was done in a convenience sample of greenfinches found dead between 2009 and 2017 in the NL, and through comparison of data to those published from GB. The investigation found no evidence that trichomonosis in the Dutch sample accounted significantly less frequently for greenfinch deaths than in greenfinches examined post-mortem in GB, and only restricted evidence for genetic heterogeneity. Within the limits of partial genetic genotyping, the presence of the same strain that causes finch trichomonosis in GB was confirmed. In addition, a strain with a single synonymous substitution was detected in very few samples. However, the strain with the substitution was also associated with severe disease. Collectively, the results provide no clear evidence for less severe disease as explanation for the discrepancy in census data trends. It is concluded that trichomonosis in NL and GB is similarly fatal for greenfinches. The potential impact on the Dutch greenfinch breeding population may not (yet) be visible in the census data, but the threat is present.

To establish whether trichomonosis in the Dutch sample accounted significantly less frequently for greenfinch deaths than in greenfinches examined post-mortem in GB, it was first necessary to detect the causative agent, then to assess

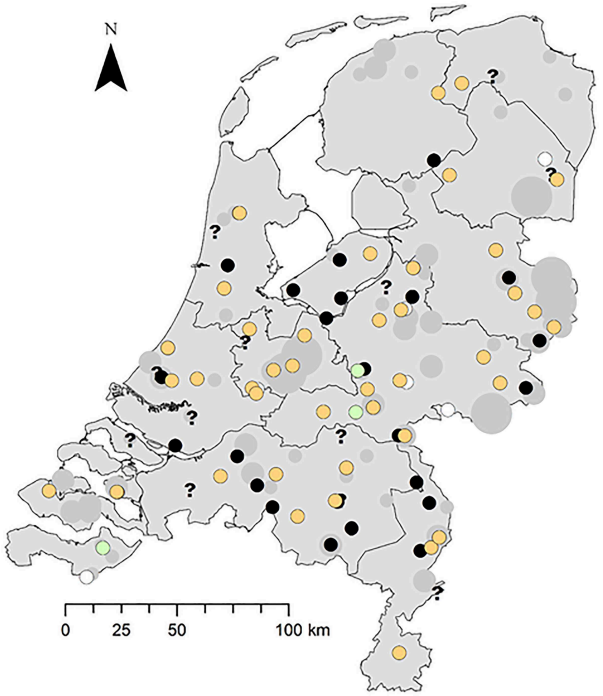

FIGURE 2 | Spatial distribution of trichomonosis cases in the period 2009–2017 against the background of diseased greenfinches reported to Sovon. Trichomonad status: trichomonads subtype A1 present, orange circle; trichomonads subtype A1 with one substitution, green circle; trichomonads present, not genotyped, black circle; trichomonads absent, white circle; inconclusive, question mark. Number of diseased specimens reported to Sovon: 1, small gray dot; 2–10, middle-sized gray dot; >10 large gray dot.

the contribution of the disease to death and compare the data to GB data. This study used three methods that detect trichomonads microscopically: cytological examination, histological examination and culture with hanging-drop examination. Culture with hanging-drop examination has been used as a diagnostic "gold standard" (12), and concordantly had relatively greater sensitivity for detecting trichomonads microscopically than cytology and histology. Trichomonads were present in many of the birds examined. The PCR-tests and sequencing on the cultured products confirmed that these trichomonads were *T. gallinae*, the causal agent of trichomonosis. Only a small number of birds classified as "trichomonads absent" based on "a minimum of two examination methods performed and conclusively negative by all examination methods performed." These are rather demanding criteria for demonstrating absence. They were used because time of death in wildlife is often unknown, and with time after death and autolysis, the probability of false negatives with these detection methods increases (18). However, these criteria may have led to an underestimation of the number of birds without trichomonads, but this would not exceed the number of inconclusive birds in this study and therefore still be a minority. Collectively, even though study design does not allow for inference on prevalence, these data showed that *T. gallinae* is commonly detected in greenfinches found dead in NL since 2009.

To assess the contribution of trichomonosis to the death of the greenfinches, the sample of NL birds was examined macroscopically and microscopically, distinguishing between lesions consistent with trichomonosis and lesions due to other causes. Trichomonads and associated lesions were only seen in the upper digestive tract, confirming the upper digestive tract as predilection site for trichomonosis in greenfinches, as described elsewhere (18). A fair proportion of the specimens with trichomonads in this Dutch convenience sample had no macroscopic lesions in the upper digestive tract, raising the question whether these were specimens with or without disease. Other studies have detected trichomonads by PCR in dead greenfinches in absence of macroscopic lesions, but without performing histology (28). Therefore, they could not distinguish between presence of disease or no disease (28). Here histology showed that the specimens with trichomonads all had microscopic ulcerative necrotic changes in the upper digestive tract, including those without macroscopic lesions. This provides evidence for disease. Further, there is no evidence for presence of the parasite in absence of disease. Therefore, histology is an essential part of the post-mortem examination process: all the greenfinches in the Dutch study in which trichomonads were detected can be considered to have the disease trichomonosis.

The comparison of the scores of the microscopic lesions at trichomonas predilection sites determined that ulceration was less deep and heterophil infiltration less extensive in the trichomonas-infected greenfinches with microscopic lesions only, compared to those with macroscopic lesions. The extent of macrophage infiltration and presence of bacteria was similar. These results collectively suggest a shorter, more acute disease course in the cases without macroscopic lesions, rather than less severe disease. Had there been less severe disease, one could also expect birds without macroscopic lesions to have other significant lesions due to other causes to explain their death. This was not the case. Rather, significant other lesions were equally rare in the trichomonad-infected groups with and without macroscopic lesions in the upper digestive tract. Therefore, there was no evidence that this difference in scores indicated less severe disease in greenfinches without macroscopic lesions. Fatal trichomonosis infections without macroscopic lesions (caseous changes) have been documented in other studies in birds of prey (29, 30).

Only a handful of greenfinches in this study was not infected with *T. gallinae*, and only a quarter of the birds with trichomonosis also had significant lesions due to other causes. The remainder only had trichomonosis, with hemorrhagic diathesis as a complication contributing to the deaths. Taking into consideration that not all studies include histology, trichomonosis was as frequently the cause of death in these Dutch greenfinches as in comparable published GB studies (23, 24). The hypothesis that in the Dutch sample trichomonosis would account significantly less frequently for greenfinch deaths than in greenfinches examined post-mortem in GB was rejected.

The second hypothesis in this study was that the partially typed trichomonas genomes would show genetic heterogeneity.

The *T. gallinae* subtype A1 strain associated with finch trichomonosis in GB has been described as a very pathogenic strain (22). One possibility for less fatal disease in the NL, as in less impact of the disease at population level, is the presence of one or several strains of *T. gallinae* in Dutch greenfinches, that are different from the GB strain. Protective immunity to the virulent strain could possibly be acquired in birds infected early in life by less virulent strains (1, 4, 8–10). Assuming that strain diversity would be detected in greenfinches found dead, the study aimed to detect the presence of such a strain or strains by demonstrating genetic heterogeneity in sequences of the ITS1-5.8S-ITS2 gene region and the Fe-hydrogenase gene. The greenfinches infected with trichomonosis in GB and elsewhere in Europe have shown no genetic heterogeneity in the sequences of these two genes (22). The partial genotyping performed in this study showed the sequences in most of the strains cultured from Dutch greenfinches were identical to those of the GB strain. In three strains however there was a synonymous T-to-C substitution in the Fe-hydrogenase gene at position 135 compared to the "clonal" strain. This substitution is unlikely to be a reading error, as this study has used a high-fidelity DNA polymerase to limit reading errors, and the same substitution was found when the PCR test was repeated in each case.

The importance of this restricted genetic heterogeneity is unclear. A substitution that occurred during the culture process may be a possibility; however, it is not known if mutations occur during the culture process, but strains have been documented to lose their pathogenicity and infectivity while being cultured (1). Other studies have reported one or several single substitutions in the Fe-hydrogenase gene sequence compared to that of the GB finch strain, although not in greenfinches but in other bird species (7, 21, 30). One study hypothesized that this is due to multiple spill-over events among bird species (7). The three greenfinch cases in this study with the synonymous substitution were found in 2016 in different locations (**Figure 2**), and one of them belonged to an incident in which another and one of them belonged to an incident in which another greenfinch was typed as the clonal *T. gallinae* subtype A1 (**Supplemental Material 2**). To further elucidate the importance of this finding, other genes would need to be sequenced, preferably more variable than the SSU rRNA gene and the rpb1 gene, which are very conserved (21) and were therefore not used in this study. Primers have just been published for performing a parallel 19 locus multilocus sequence typing test that showed good discriminatory ability for distinguishing *T. gallinae* strains (31).

Trichomonosis cases were mostly reported during the spring and summer months; however, some cases did occur in autumn and winter. This is consistent with reports on finch trichomonosis in greenfinches in GB (24). Greenfinches infected with trichomonads were found widely across the NL. No inferences could be made on geographical spread over years, and this was never the focus of this study based on convenience sampling. It was not possible to perform robust fine-scale spatial analysis of trends and to identify spatial risk factors. This would require long-term garden bird health monitoring data, which may come within reach in the near future through a generally broad volunteer acceptance of the garden bird monitoring scheme in the NL. In addition, there were only a handful of the submitted dead greenfinches that were not *Trichomonas* cases. This lack of "negatives" also made it impossible to identify risk areas and risk factors.

Despite the numerous sources of bias in this study (convenience sample, depending on public for submission; applied case definitions; use of a culture step before PCR; and limited number of genes sequenced), the results imply that finch trichomonosis could be a threat to Dutch greenfinches that is temporarily masked by other factors in census data. Bird population dynamics are complex, and populations may show lagged responses to disturbance (32). There is still a poor understanding of the demographic, environmental, genetic and behavioral, factors that shape pathogen transmission and bird susceptibility (2). Bird density or garden bird feeding practices in the NL most likely differ from those in GB, affecting the transmission rate (24, 33). Creation of suitable habitat in urban areas could be boosting the Dutch greenfinch population in a positive direction. In addition, Dutch and British greenfinches may differ genetically from each other, affecting their immunity to disease. Alternatively, migrating greenfinches could temporarily be filling up niches emptied by the disease in the Dutch breeding population. For a better understanding of the threat and possible mitigation measures, it is relevant to investigate finch trichomonosis taking a multidisciplinary approach on a European scale.

DATA AVAILABILITY STATEMENT

The dataset generated for this study can be found in Supplemental material 2 and sequences were deposited in GenBank under the following accession numbers: MN385401, MN385402, MN385403, MN385404, and MN385405.

ETHICS STATEMENT

Ethical review and approval was not required for the animal study because the animals were found dead and investigated in the context of a general wildlife disease surveillance programme.

AUTHOR CONTRIBUTIONS

JR, AL, MK, and AG: manuscript writing. JR: conception of study. AL, MK, and AG: pathology. AL: laboratory work. RS and JS: bird census data. JR and AL: data analysis. All authors critically reviewed the manuscript.

FUNDING

The general wildlife disease surveillance programme was funded by the Dutch Ministry of Agriculture, Nature and Food Quality, the Dutch Ministry of Health, Welfare and Sport, and Utrecht University (grants 1400006202/2010, 1400008946/2011, 1300011172/2012, 1300014843/2013, 1300017645/2014, 1300020238/2015, 1300022600/2016, and 1300024982/2017). AL performed her work in the study as a student in the Honors Programme of Utrecht University.

ACKNOWLEDGMENTS

We acknowledge all persons who assisted with the collection of the greenfinches, their post-mortem examination and the laboratory diagnostics.

SUPPLEMENTARY MATERIAL

The Supplementary Material for this article can be found online at: https://www.frontiersin.org/articles/10.3389/fvets.2019.00425/full#supplementary-material

REFERENCES

1. Forrester DJ, Foster GW. Trichomonosis. In: Atkinson CT, Thomas NJ, and Hunter DB, editors. *Parasitic Diseases of Wild Birds*. Ames, IO: Wiley-Blackwell (2008). p. 120–53.
2. Girard YA, Rogers KH, Woods LW, Chouicha N, Miller WA, Johnson CK. Dual-pathogen etiology of avian trichomonosis in a declining band-tailed pigeon population. *Infect Genet Evol.* (2014) 24:146–56. doi: 10.1016/j.meegid.2014.03.002
3. Bunbury N, Jones CG, Greenwood AG, Bell DJ. Epidemiology and conservation implications of *Trichomonas gallinae* infection in the endangered Mauritian pink pigeon. *Biol Conserv.* (2008) 141:153–61. doi: 10.1016/j.biocon.2007.09.008
4. Stabler RM. *Trichomonas gallinae*: a review. *Exp Parasitol.* (1954) 3:368–402. doi: 10.1016/0014-4894(54)90035-1
5. Stabler RM. Kihara JT. Infection and death in the pigeon resulting from the oral implantation of single individuals of *Trichomonas gallinae*. *J Parasitol.* (1954) 40:706. doi: 10.2307/3273726
6. Kietzmann GE. Relationships of *Trichomonas gallinae* to the palatal-esophageal junction of ring doves (*Streptopelia risoria*) as revealed by scanning electron microscopy. *J Parasitol.* (1993) 79:408–15. doi: 10.2307/3283578
7. McBurney S, Kelly-Clark WK, Forzán MJ, Lawson B, Tyler KM, Greenwood SJ. Molecular characterization of *Trichomonas gallinae* isolates recovered from the Canadian Maritime provinces' wild avifauna reveals the presence of the genotype responsible for the European finch trichomonosis epidemic and additional strains. *Parasitology*. (2015). 142:1053–62. doi: 10.1017/S0031182015000281
8. Kocan RM, Herman CM. Trichomoniasis. In: Davis JW, Anderson RC, Karstad L, and Trainer DO, editors. *Infectious and Parasitic Diseases of Wild Birds*. Ames, IO: Iowa State University Press (1971). p. 282–90.
9. Kocan RM, Knisley JO. Challenge infection as a means of determining the rate of disease resistant *Trichomonas gallinae*-free birds in a population *J Wildl Dis*. (1970) 6:13–5. doi: 10.7589/0090-3558-6.1.13
10. BonDurant RH, Honigberg BM. Trichomonads of veterinary importance. In: Kreier JP, editor. *Parasitic Protozoa*. London: Academic Press (1994). p. 113–31.
11. Krone O, Altenkamp R, Kenntner N. Prevalence of *Trichomonas gallinae* in northern goshawks from the Berlin area of northeastern Germany. *J Wildl Dis.* (2005) 41:304–9. doi: 10.7589/0090-3558-41.2.304
12. Anderson NL, Grahn RA, Van Hoosear K, Bondurant RH. Studies of trichomonad protozoa in free ranging songbirds: prevalence of *Trichomonas gallinae* in house finches (*Carpodacus mexicanus*) and corvids and a novel trichomonad in mockingbirds (*Mimus polyglottos*). *Vet Parasitol.* (2009) 161:178–86. doi: 10.1016/j.vetpar.2009.01.023
13. Lawson B, Robinson RA, Neimanis A, Handeland K, Isomursu M, Agren EO, et al. Evidence of spread of the emerging infectious disease, finch trichomonosis, by migrating birds. *EcoHealth*. (2011) 8:143–53. doi: 10.1007/s10393-011-0696-8
14. Lawson B, Robinson RA, Colvile KM, Peck KM, Chantrey J, Pennycott TW, et al. The emergence and spread of finch trichomonosis in the British Isles. *Philos Trans R Soc Lond B Biol Sci.* (2012) 367:2852–63. doi: 10.1098/rstb.2012.0130
15. Lehikoinen A, Lehikoinen E, Valkama J, Väisänen RA, Isomursu M. Impacts of trichomonosis epidemics on Greenfinch *Chloris chloris* and Chaffinch *Fringilla coelebs* populations in Finland. *Ibis.* (2013) 155:357–66. doi: 10.1111/ibi.12028
16. Peters M, Kilwinski J, Reckling D, Henning K. Gehäufte Todesfälle von wild lebenden Grünfinken an Futterstellen infolge *Trichomonas-gallinae*-Infektionen-ein aktuelles Problem in Norddeutschland. *Kleintierpraxis.* (2009) 54:433−38.
17. Zadravec M, Marhold C, Slavec B, Rojs OZ, Răcnik J. Trichomonosis in finches in Slovenia. *Vet Rec.* (2012) 171:253–54. doi: 10.1136/vr.e5973
18. Neimanis AS, Handeland K, Isomursu M, Ågren E, Mattsson R, Hamnes IS, et al. First report of epizootic trichomoniasis in wild finches (family *Fringillidae*) in southern Fennoscandia. *Avian Dis.* (2010) 54:136–41. doi: 10.1637/8952-060509-Case.1
19. R Core Team (2013). R: A language and environment for statistical computing. *R Foundation for Statistical Computing*, Vienna, Austria.
20. Chavatte JM, Giraud P, Esperet D, Place G, Cavalier F, Landau I. An outbreak of trichomonosis in European greenfinches *Chloris chloris* and European goldfinches *Carduelis carduelis* wintering in Northern France. *Parasite.* (2019) 26:21. doi: 10.1051/parasite/2019022
21. Ganas P, Jaskulska B, Lawson B, Zadravec M, Hess M, Bilic I. Multi-locus sequence typing confirms the clonality of *Trichomonas gallinae* isolates circulating in European finches. *Parasitology.* (2014) 141:652–661. doi: 10.1017/S0031182013002023
22. Lawson B, Cunningham AA, Chantrey J, Hughes LA, John SK, Bunbury N, et al. A clonal strain of *Trichomonas gallinae* is the aetiologic agent of an emerging avian epidemic disease. *Infect Genet Evol.* (2011) 11:1638–45. doi: 10.1016/j.meegid.2011.06.007
23. Robinson RA, Lawson B, Toms MP, Peck KM, Kirkwood JK, Chantrey J, et al. Emerging infectious disease leads to rapid population declines of common British birds. *PLoS ONE.* (2010) 5:e12215. doi: 10.1371/journal.pone.0012215
24. Lawson B, Robinson RA, Toms MP, Risely K, MacDonald S, Cunningham AA. Health hazards to wild birds and risk factors associated with anthropogenic food provisioning. *Philos Trans R Soc Lond B Biol Sci.* (2018) 373:20170091. doi: 10.1098/rstb.2017.0091
25. Stanbury A, Brown A, Eaton M, Aebischer N, Gillings S, Hearn R, et al. The risk of extinction for birds in Great Britain. *Br. Birds.* (2017) 110:502–17. Available online at: https://britishbirds.co.uk/article/risk-extinction-birds-great-britain/.
26. Stenkat J, Krautwald-Junghanns ME, Schmidt V. Causes of morbidity and mortality in free-living birds in an urban environment in Germany. *EcoHealth.* (2013) 10:352–65. doi: 10.1007/s10393-013-0868-9
27. Felleisen RSJ. Comparative sequence analysis of 5.8S rRNA genes and internal transcribed spacer (ITS) regions of trichomonadid protozoa. *Parasitology.* (1997) 115 (Pt2):111–9. doi: 10.1017/S0031182097001212
28. Zu Ermgassen EK, Durrant C, John S, Gardiner R, Alrefaei AF, Cunningham AA, et al. Detection of the European epidemic strain of *Trichomonas gallinae* in finches, but not other non-columbiformes, in the absence of macroscopic disease. *Parasitology.* (2016) 143:1294–300. doi: 10.1017/S0031182016000780
29. Stabler RM. *Trichomonas gallinae*, pathogenic trichomonad of birds. *J Parasitol.* (1947) 33:207–13. doi: 10.2307/3273551
30. Chi JF, Lawson B, Durrant C, Beckmann K, John S, Alrefaei AF, et al. The finch epidemic strain of *Trichomonas gallinae* is predominant in British non-passerines. *Parasitology.* (2013) 40:1234–45. doi: 10.1017/S0031182013000930

31. Alrefaei AF, Low R, Hall N, Jardim R, Dávila A, Gerhold R, et al. Multilocus analysis resolves the European Finch epidemic strain of *Trichomonas gallinae* and suggests introgression from divergent trichomonads. *Genome Biol Evol.* (2019) 11:2391–402. doi: 10.1093/gbe/evz164
32. Preston ND, Daszak P, Colwell RR. The human environment interface: applying ecosystem concepts to health. *Curr Top Microbiol Immunol.* (2013) 365:83–100. doi: 10.1007/978-3-662-45792-4_317
33. Hofle U, Gortazar C, Ortiz JA, Knispel B, Kaleta EF. Outbreak of trichomoniasis in a woodpigeon (*Columba palumbus*) wintering roost. *Eur J Wildl Res.* (2004) 50:73–7. doi: 10.1007/s10344-004-0043-2

Conflict of Interest: The authors declare that the research was conducted in the absence of any commercial or financial relationships that could be construed as a potential conflict of interest.

Copyright © 2019 Rijks, Laumen, Slaterus, Stahl, Gröne and Kik. This is an open-access article distributed under the terms of the Creative Commons Attribution License (CC BY). The use, distribution or reproduction in other forums is permitted, provided the original author(s) and the copyright owner(s) are credited and that the original publication in this journal is cited, in accordance with accepted academic practice. No use, distribution or reproduction is permitted which does not comply with these terms.

frontiers in Veterinary Science

REVIEW
published: 13 December 2019
doi: 10.3389/fvets.2019.00444

Health Assessments of Common Bottlenose Dolphins (*Tursiops truncatus*): Past, Present, and Potential Conservation Applications

Ashley Barratclough[1], Randall S. Wells[2], Lori H. Schwacke[1], Teresa K. Rowles[3], Forrest M. Gomez[1], Deborah A. Fauquier[3], Jay C. Sweeney[4], Forrest I. Townsend[5], Larry J. Hansen[1], Eric S. Zolman[1], Brian C. Balmer[1] and Cynthia R. Smith[1]*

[1] National Marine Mammal Foundation, San Diego, CA, United States, [2] Chicago Zoological Society's Sarasota Dolphin Research Program, Mote Marine Laboratory, Sarasota, FL, United States, [3] NOAA, National Marine Fisheries Service, Office of Protected Resources, Silver Spring, MD, United States, [4] Dolphin Quest, San Diego, CA, United States, [5] Bayside Hospital for Animals, Fort Walton Beach, FL, United States

OPEN ACCESS

Edited by:
Robert James Ossiboff, University of Florida, United States

Reviewed by:
Alex M. Costidis, Virginia Aquarium & Marine Science Center, United States
Juan Manuel Campos Krauer, University of Florida, United States

***Correspondence:**
Ashley Barratclough
ashley.barratclough@nmmf.org

Specialty section:
This article was submitted to Zoological Medicine, a section of the journal Frontiers in Veterinary Science

Received: 06 September 2019
Accepted: 26 November 2019
Published: 13 December 2019

Citation:
Barratclough A, Wells RS, Schwacke LH, Rowles TK, Gomez FM, Fauquier DA, Sweeney JC, Townsend FI, Hansen LJ, Zolman ES, Balmer BC and Smith CR (2019) Health Assessments of Common Bottlenose Dolphins (Tursiops truncatus): Past, Present, and Potential Conservation Applications. Front. Vet. Sci. 6:444. doi: 10.3389/fvets.2019.00444

The common bottlenose dolphin (*Tursiops truncatus*) is a global marine mammal species for which some populations, due to their coastal accessibility, have been monitored diligently by scientists for decades. Health assessment examinations have developed a comprehensive knowledge base of dolphin biology, population structure, and environmental or anthropogenic stressors affecting their dynamics. Bottlenose dolphin health assessments initially started as stock assessments prior to acquisition. Over the last four decades, health assessments have evolved into essential conservation management tools of free-ranging dolphin populations. Baseline data enable comparison of stressors between geographic locations and associated changes in individual and population health status. In addition, long-term monitoring provides opportunities for insights into population shifts over time, with retrospective application of novel diagnostic tests on archived samples. Expanding scientific knowledge enables effective long-term conservation management strategies by facilitating informed decision making and improving social understanding of the anthropogenic effects. The ability to use bottlenose dolphins as a model for studying marine mammal health has been pivotal in our understanding of anthropogenic effects on multiple marine mammal species. Future studies aim to build on current knowledge to influence management decisions and species conservation. This paper reviews the historical approaches to dolphin health assessments, present day achievements, and development of future conservation goals.

Keywords: dolphin, *Tursiops truncatus*, conservation, health assessment, veterinary medicine

INTRODUCTION

Assessment of marine mammal health is complex, both from an accessibility standpoint and from the diverse array of factors influencing both individual and population survival. Baseline data are particularly crucial to evaluate whether population, or in some cases species, health is deteriorating by providing points of comparison to assess trends in disease, mortality, and reproductive rates (1). From a veterinary perspective, a hands-on physical exam is the optimal approach to provide critical

information for a comprehensive understanding of both individual and population-level health status. Knowledge gained from physically examining smaller cetaceans can be extrapolated to larger, less-accessible cetaceans to improve understanding of the complexities of adverse health impacts on marine mammal conservation. The common bottlenose dolphin (*Tursiops truncatus*) is an effective model species for understanding both cetacean and marine ecosystem health.

The overarching aim of conservation is to actively preserve habitats and the diversity of species dwelling therein (2). Effective conservation benefits from a foundation of sound scientific understanding of species' biology, population dynamics, and stressors impacting the ecosystem (3). Marine ecosystem health is particularly challenging to assess due to immense biological diversity, as well as the vast scale and connectivity of the ocean environment. Multiple factors threaten marine mammal health (4); therefore, improving knowledge of the interplay of these factors and predicting their long-term effects are essential for successful conservation.

The emerging discipline of conservation physiology is particularly important in the marine environment, as it allows a mechanistic understanding of the drivers of conservation obstacles at an ecosystem level, in addition to species-specific challenges. Understanding how species physiologically respond to environmental alterations is important for successful tailored conservation strategies (5). The rate of expansion of the human population is exacerbating the challenges faced by wildlife with frequently detrimental consequences to their health (6). The unprecedented changes occurring in the environment on a global scale require novel mitigation strategies to ensure effective conservation actions and sustainable wildlife populations (7).

There is limited understanding of the scale of the negative anthropogenic impact on marine mammal biodiversity. Currently 29.2% of marine mammal species are classified as data deficient according to the International Union for the Conservation of Nature (8). As a result, shifts in population viability can be difficult to detect, as the basic natural history of the species has not been documented (9). Intrinsic traits of species can be more important predictors of risk than extrinsic environmental factors, as they provide a measure of the species' inherent susceptibility to human impacts and the ability of species to recover from them (10). The bottlenose dolphin is one of the most closely studied and widely distributed marine mammal species and provides an opportunity to extrapolate knowledge and understanding to other marine mammal species.

HISTORICAL PERSPECTIVE

Initially the first common bottlenose dolphin captures occurred for acquisition for public display, research, or for stock assessment prior to collection. Over time health assessments of inshore dolphins have been utilized to better understand endemic disease, establish baseline physiological measures, and evaluate exposure to, and potential effects of, chemical, biological, and physical stressors. Historically, health assessments developed as additions to existing capture-release efforts for other purposes, such as marking/tagging and population-level studies to understand movement patterns and site fidelity. Starting in 1979, Hubbs/SeaWorld Research Institute began collecting bottlenose dolphin health data in the Indian River Lagoon of east Florida during capture-release operations to assess potential population-level impacts in advance of upcoming zoologic collections (**Figure 1**) (11). Analyses from the samples and data collected included morphometrics, blood biochemistry, hematology and reproductive endocrinology, microbiology, genetics, and life history studies (12). Similar research was initiated by Marine Animal Productions in 1982 in Mississippi Sound, with the inclusion of skin, blubber, and liver tissue sampling in some cases, to establish a health baseline for dolphins inhabiting this area, again prior to collections and for comparison with managed animals (13).

The Sarasota Dolphin Research Program (SDRP) began incorporating additional biological samples and measurements in 1984 to their original capture-release program. This supported tagging and telemetry studies in Sarasota Bay, Florida, which were initiated in 1970. The inclusion of additional biological samples shifted the focus from studies of population range and social patterns to broader scientific investigations of life history, population dynamics, body condition and health, social structure, communication, reproductive success, and effects of human interactions. Samples and measurements included in-depth bloodwork analyses, genetic tests for population structure and paternity, ultrasonic measurement of blubber thickness, weight measurement, age determination (tooth growth layer group counts), further development of tags and tag attachments, and post-release population monitoring (14–19).

In 1992, the Marine Mammal Health and Stranding Response Program was formalized within the National Marine Fisheries Service (NMFS) through an amendment to the Marine Mammal Protection Act (MMPA), establishing the standards for sample collections and promoting collaboration and standardization of bottlenose dolphin health assessments (20). In 1995, NMFS conducted health assessments in response to the 1987–88 mortality event along the east coast of the U.S., in which over 600 bottlenose dolphins stranded as a result of a large-scale morbillivirus epizootic (21–25). Additional studies were also conducted to investigate unusual increases in dolphin strandings near Matagorda Bay, Texas in 1992 (26), and in the Florida Panhandle in 2005–2006 (27) (**Figure 1**) (**Table 1**).

Supplementary capture-release studies were initiated by the National Oceanic and Atmospheric Administration (NOAA) in support of stock assessment on the east coast, which was by that time a requirement for NOAA's NMFS (23, 24). Subsequent capture-release studies used telemetry to understand population structure along the Atlantic coast (39) following increased dolphin mortality (40) which was eventually determined to be associated with morbillivirus (22, 30). The studies found positive morbillivirus titers in some dolphins sampled in estuarine and coastal waters near Beaufort, NC, with no positive titers observed in dolphins sampled in estuaries near Charleston, SC (30). This provided crucial information to understanding dolphin population structure and interaction along the U.S. east coast, with a mosaic of migratory, non-migratory but coastal, and

FIGURE 1 | Bottlenose dolphin capture-release health assessment locations in the U.S.

small estuarine stocks rather than a single large population as initially presumed. In addition utilizing archived Sarasota Bay samples to retrospectively assess morbillivirus titers facilitated further understanding of virus exposure, seroconversion, and population naivety (41). Incorporating health assessments informed scientists that at least some small, estuarine stocks along the Atlantic coast were naïve to morbillivirus and therefore particularly vulnerable (38).

In 2003, the Health and Environmental Risk Assessment (HERA) population monitoring project was initiated for bottlenose dolphins in the Indian River Lagoon, Florida (IRL), and waters surrounding Charleston, South Carolina (CHS) (42). For both the IRL and CHS field sites, health assessments were conducted to establish baseline data and to compare morbidity temporally and across two geographic sites (34, 43). Higher concentrations of persistent organic pollutants (POPs) including legacy [e.g., dichlorodiphenyltrichloroethanes (DDTs), polychlorinated biphenyls (PCBs)] as well as "emerging" contaminants [polybrominated diphenyl ethers (PBDEs) and perfluorooctane sulfonate (PFOS) compounds] were detected in CHS dolphins as compared to IRL dolphins (43, 44). Mercury concentrations in the blood and skin of IRL dolphins were extremely high, approximately five times higher than those in CHS dolphins. Higher exposure to many pathogens (e.g., morbillivirus and lobomycosis) was also observed for the IRL dolphins (34).

The incorporation of health assessments into existing capture-release protocols provided the collection of baseline health data across multiple populations, thus allowing for investigation of geographic variability in health parameters (32, 42). The methodologies established and samples collected during these earlier projects formed the basis for developing a risk assessment framework to quantify the impacts for dolphins affected by anthropogenic threats (e.g., *Deepwater Horizon* oil spill) in geographical areas where baseline data were not available (36).

THREAT IDENTIFICATION AND ASSESSMENT

Dolphin capture-release projects provide a unique perspective to assess individual animal health and extrapolate to overall health of the surrounding population, species, and ecosystem. Over the past 40 years in the U.S., there have been numerous stressors that have impacted bottlenose dolphin populations, for which dolphin capture-release projects have been integral to threat identification and quantification of impacts from a given stressor (e.g., biotoxins, disease, environmental contaminants, oil spills, etc.).

TABLE 1 | Historical list of previous capture locations according to **Figure 1** including number of animals examined or health assessments (HA) performed, purpose of captures, and references.

Date	Location	Number of dolphins	Purpose	References
1979–1981	Indian River Lagoon FL	27 109 total HA	Population assessment	(11)
1982	Mississippi Sound MS	57	Commercial assessment	(13, 28)
1984–2019 (ongoing)	Sarasota FL	289 individuals 811 total HA	Biological sampling, technique development, reference population	(29)
1987	Virginia Beach VA	23	Mass mortality investigation	(21)
1992	Matagorda Bay TX	36	Mortality investigation	(26)
1995	Beaufort NC	31	HA post CeMV outbreak	(24)
1998	Virginia Beach VA	1	Stock assessment	NOAA unpublished data
1999	Charleston SC	14	Stock assessment	(30)
1999* 2000* 2006*	Beaufort NC	6 11 19	Stock assessment	(31) (30) (32)
2002–2003	Brigantine NJ	12	Stock assessment	(30)
2004	Holden Beach NC	10	Persistent organic pollutant assessment	(33)
2003–2018	Charleston SC Indian River Lagoon FL	118 246	Comparative health studies	(34)
2005–2006	St. Joseph Bay FL	30	UME investigation	(27)
2009	Brunswick GA	29	HA legacy environmental contamination	(35)
2011–2018	Barataria Bay LA	202	DWH investigation	(36)
2013	Mississippi Sound MS	20	DWH investigation	(37)
2015	Brunswick GA	19	UME investigation	(38)
2018	Dauphin Island AL	18	DWH investigation	

**The numbers provided are for those where samples were used and published it does not necessarily provide a list of the total numbers of animals handled in this location.*

Unusual Mortality Events

An unusual mortality event (UME) is defined under the U.S. Marine Mammal Protection Act as "a stranding that is unexpected; involves a significant die-off of any marine mammal population; and demands immediate response." The UME program was officially established under Title IV of the MMPA in 1992. Increased recognition of the occurrence of large scale dolphin mortality events in the late 1980s spurred the application of dolphin health assessments beyond population monitoring, to investigating causes and effects of such mortality events (21, 24).

Since 1999, a series of UMEs occurred along the northwestern Florida coastline (Florida Panhandle) including St. Joseph Bay (45). NOAA conducted two dolphin health assessments during 2005 and 2006 in response to these UMEs in which 30 dolphins were sampled and subsequently tagged (27) (**Table 1**). The initial mortalities were tentatively attributed to biotoxins from red tide algae (*Karenia brevis*) (46). Eosinophilia was observed in 23% of sampled dolphins, with associated increased neutrophil phagocytosis and T-lymphocyte proliferation (27). Chronic low-level exposure to another algal toxin, domoic acid, produced by the diatom *Pseudo-nitzschia* spp., previously linked to eosinophilia, was also identified (47). Prior to these UMEs, little was known about dolphin abundance, distribution, and site fidelity in this region, and thus, it was unclear which population(s) of dolphins were impacted (48, 49). Post-health assessment tagging data suggested that the timing and spatial extent of biotoxin events and other potential stressors in the Florida Panhandle may greatly influence the severity of future UMEs (50). Cetacean post-mortem examinations can provide insight into identifying the underlying cause of a UME in addition to baseline data on disease presence and anthropogenic causes of mortality (51–53). Increased integration of live animal assessment with post-mortem findings encourages the transfer of information from the dead to the living, informing scientists of the underlying pathophysiological mechanisms faced within free-ranging populations (54).

Chemical Pollutants

The presence of PCBs and other lipophilic contaminants have been recorded to be accumulating in the tissues of bottlenose dolphins and other odontocetes for decades (31, 55–59). Many marine mammals, particularly piscivorous species, have a high potential to biomagnify pollutants (33), with increased levels resulting from the high trophic position and blubber acting as a reservoir for lipophilic contaminants (60). Both experimental and observational studies support the correlation between

increased PCB levels and endocrine dysfunction, compromised immunity, and/or reproductive failure (61–66). However, the common co-occurrence of similarly acting compounds and uncertainty regarding species-specific dose response functions makes assessment of the effects of these contaminants at a population level challenging (60, 67).

In addition to their applicability to investigating UMEs, dolphin health assessments have also been used to investigate health of populations at risk from environmental contaminants. For example, dolphins along the Georgia coast have been identified with some of the highest concentrations of PCBs in the world, and these levels are site-specific to a Superfund Site in Brunswick, Georgia (60, 68, 69). In 2009, NOAA conducted health assessments on 29 dolphins in the region and identified a high proportion (26%) of sampled individuals suffered from anemia (66). In addition, these dolphins had reduced thyroid hormone levels with total thyroxine, free thyroxine, and triiodothyronine negatively correlated with increased blubber PCB concentrations. T-lymphocyte proliferation and indices of innate immunity decreased with blubber PCB concentration, suggesting an increased susceptibility to infectious disease (66). As with previously described health assessments, telemetry and photo-ID data provided perspective on ranging patterns relative to exposure, subsequent reproductive success, and effects of long-term impacts from cumulative stressors (70). In 2015, another health assessment was conducted in Georgia to look at potential impacts associated with a recent morbillivirus-caused UME and extremely high levels of PCBs that were identified from previous studies. Dolphin morbillivirus titers differed between dolphins sampled in coastal and estuarine waters, and tagging data identified some degree of overlap between these individuals. This study suggested that estuarine dolphins in this region may be highly susceptible to future morbillivirus infections as a result of elevated PCB levels and spatial overlap between coastal and estuarine dolphins that would facilitate disease transmission (50).

Petroleum Toxicity

In 2010, the largest marine oil spill in the history of the U.S., the *Deepwater Horizon* oil spill (DWH), occurred in the northern Gulf of Mexico (GoM). Subsequently a multidisciplinary approach for evaluating the impacts upon cetaceans was undertaken (71, 72). Bottlenose dolphins were the focal cetacean species examined due to the accessibility of dolphins in shallow coastal and estuarine waters, and the heavy oiling in some of those same nearshore areas. Health assessments in heavily oiled areas, particularly Barataria Bay, Louisiana, were initiated as part of NOAA's Natural Resource Damage Assessment (NRDA). Veterinary clinical assessment of dolphins living within the oil spill footprint found significant lung pathology, impaired stress responses, high reproductive failure, and altered functional immunity, as compared to findings from un-oiled reference populations (35, 73–75). After the DWH oil spill, an abnormally high prevalence of lung and adrenal gland pathologies were documented in post-mortem examinations (73, 76). Identifying the baseline incidence of disease in stranded dolphins and diagnosing pathology in live dolphins through the application of enhanced health assessment protocols was required to determine if these findings were correlated with the recent environmental exposure (75, 77, 78).

Determining a causal link for the multiple pathologies observed post DWH oil exposure has been via a diagnosis of exclusion; concluding the toxic effects of the oil spill as the primary differential to both the observed pathologies and the increased dolphin mortality (71, 75). Other differential diagnoses that were the potential causes of previous GoM UMEs were also ruled out including biotoxins (79), POPs (68), and infectious disease (45, 73, 80, 81). Successive health assessments during 2016–2018 have provided additional insight into the chronic health effects. Longitudinal photo-ID surveys allowed estimation of post-spill survival rate (0.80–0.85) and reproductive success (20%), the latter was very low for this population (82, 83). Long-term consequences from oil contamination are difficult to assess but have been suggested in other marine mammals such as the killer whale (*Orcinus orca*) and the sea otter (*Enhydra lutris nereis*) (84–87). Future research efforts will aim to improve understanding of the transgenerational or *in utero* exposure effects in addition to the direct exposure of those animals alive at the time of the oil spill.

Currently there is limited knowledge of the pathophysiology of reproductive failure in bottlenose dolphins. Improved understanding of the normal physiological changes occurring during gestation in successful pregnancies will aim to elucidate possible mechanisms of reproductive failure and identify abnormalities occurring during failed pregnancies. This knowledge will be essential to help understand reproductive challenges, not only for common bottlenose dolphins, but also for the future management of other cetaceans, some critically endangered, to help to understand the reproductive challenges faced in these species and improve future conservation management.

CAPTURE AND HANDLING METHODOLOGY

The standard approach to capture small (1–5) numbers of bottlenose dolphins in shallow waters is by encirclement with a seine net up to 500 m long and 7 m deep (88, 89). Shallow water (<1.5 m), minimal currents, and a solid seafloor are optimum for safe capture and restraint. The seine net is deployed from a specially designed boat at high speed around the target dolphin(s), creating a compass (**Figure 2A**), with well-trained handlers distributed around the circumference to provide aid and restraint when the dolphins contact the net (**Figure 2B**) (29). If capture occurs in deep water (>1.5 m), the net compass can be pulled into nearby shallow water, or the dolphins are handled from the side of response vessels and moved onto specially designed floating mats that are either towed to shallow water or directly onto a processing vessel for sample collection (**Figure 2C**). Capture of individual dolphins in waters exceeding the depth of seine nets has been performed via tail grabs or hoop-nets, which are placed over the head of bow-riding bottlenose dolphins or smaller cetacean species as they surface to

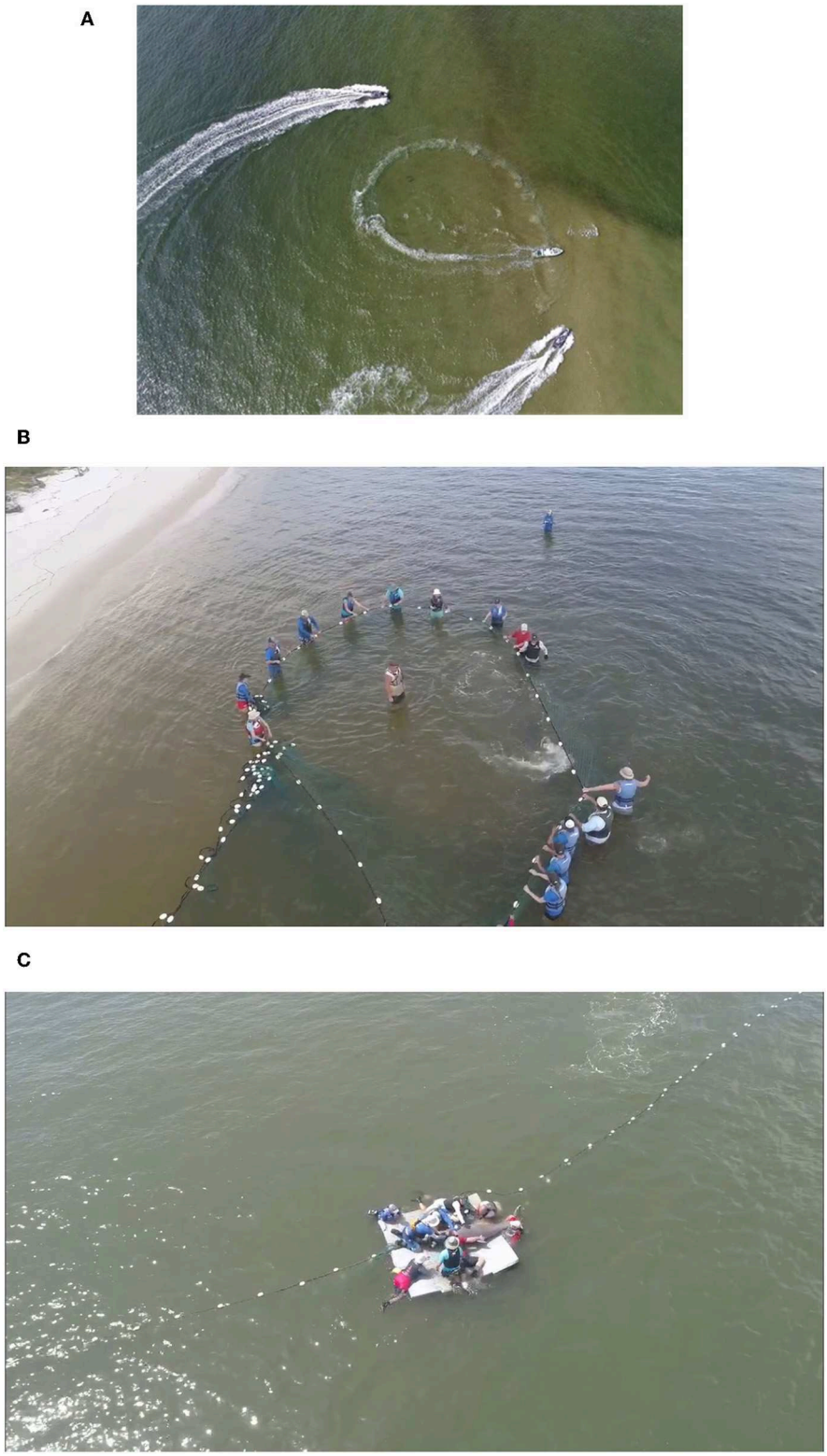

FIGURE 2 | Capture methodology with **(A)** seine net deployed from a specially designed boat creating a compass in the center of the image, with chase boats circling outside to help contain the animals before completion of the compass and to deliver handlers to the net (two dolphins are visible inside the compass on the left side). **(B)** Shallow water set, well-trained handlers distributed around the circumference of the compass to provide aid and restraint when the dolphins contact the net. **(C)** Deep water set, dolphin is placed onto a floating mat and disentangled from the net for transport to the processing vessel. All photos taken under NMFS MMPA/EAS permit No. 18786-03.

breathe (88–90). Once dolphins are safely restrained, veterinary examinations and sampling are performed.

VETERINARY PROCESSING

Current health assessment examinations require collaboration among scientists from multiple disciplines and veterinary specialties to obtain the maximum amount of information from a single snapshot in time while the animal is in-hand. The development of veterinary field techniques was enhanced by the successful management of dolphins in human care. Sampling varies according to research questions, but typically a suite of baseline data are collected to maximize knowledge obtained from a single veterinary exam (**Table 2**) (91). Ensuring a standardized approach to highlight the importance of inter-lab comparability and sharing information between multiple institutions has been paramount in the success of developing field collection methodologies and subsequent sample analysis procedures (32, 113). As described below, additional field procedures have been incorporated over the decades as technology, field techniques, and analytical assays have advanced, and as management needs have evolved.

Determination of reproductive status (e.g., pregnancy, ovarian activity, or testis size as an indicator of sexual maturity) using diagnostic ultrasound was first applied in Sarasota Bay in 1989 (26, 114). Full-body ultrasound has subsequently been proven to be an invaluable, real-time tool during dolphin health assessments, pioneered by the National Marine Mammal Foundation and the U.S. Navy Marine Mammal Program (**Figure 3**) (77, 97, 101–103). In addition, pregnancy may also be diagnosed remotely by using blubber biopsy hormone levels (115, 116). In some cases, post-release visual monitoring and photographic-identification (photo-ID) have allowed researchers to track the outcome of the pregnancy (that was determined by ultrasound or remotely) and determine whether a viable calf was produced (82, 116, 117).

A holistic approach of including dietary assessment into the health exam along with urinalysis, blood (**Figure 4**), and blubber sampling can aim to elucidate underlying causes of health abnormalities. In the field, urinary catheterization has enabled comparison with dolphins in managed care and further developed the understanding of the development of renal pathology in dolphins, especially when differences in diets have been considered (91, 97–99). Important ecological perspectives can be obtained from dietary assessments, along with information regarding prey availability and potential shifts in environmental pressure affecting the ecosystem (118–121). Further research is needed in this area to develop a more standardized nutritional status indicator which can integrate multiple measures. This could be used for example to improve understanding of the effects of prey instability or environmental stressors (122).

Electronic tagging technology to assess individual movement or habitat use has rapidly advanced over the past 40 years so that now small satellite-linked tags can be attached via a single-pin to the dorsal fin and have minimal to no long-term effects on the tagged individual (70, 111). These tags provide fine-scale data on individual animal movements for several months, post-release, and can provide additional insight into the cause of health effects identified during the veterinary examination (37, 38, 117). The movement pattern data from these electronic tags can also be used to conduct follow-up monitoring to assess individual animal health, survival, reproductive success, habitat use, and exposure to threats (82).

MULTIDISCIPLINARY APPROACHES FOR ASSESSING POPULATION HEALTH

Utilizing a multidisciplinary approach to combine clinical veterinary knowledge with epidemiological analyses and population modeling enables long-term forecasting of population trajectories (36). In UMEs, modeling to estimate mortality based on the number of stranded carcasses can provide insight into the immediate losses to the population (71, 123–125). However, integration of available health information and veterinary interpretation of sublethal, chronic conditions, which are likely to influence long-term survival and reproductive potential, can provide a more accurate interpretation of the likely long-term impacts on the population (36). Aside from impacts from acute events such as oil spills, modeling has been used to simulate the likely population-level consequences from sublethal effects of chronic contaminant exposure (60, 67). Estimation of long-term population effects resulting from mortality or morbidity events is critical to inform restoration or recovery plans, and also to appreciate the magnitude of the impact of UMEs on population numbers or of environmental contaminants on the surrounding ecosystem. Advances in modeling application to marine mammal stock assessments will greatly shape the future of marine mammal conservation.

ADVANCES IN TECHNOLOGY AND CONSIDERATIONS FOR ANIMAL WELL-BEING

Dolphin health assessments provide fine-scale information on individual animals that can be extrapolated to evaluate overall population health. While much can be learned from hands-on health assessments, a major driver of current research is to develop techniques to obtain maximum health assessment information from remote sampling and observations. The methodology for safely handling, sampling, and releasing dolphins is continually evolving to minimize the risk to both the dolphins and researchers, as well as maximize the data collected. However, health assessments are still expensive, logistically challenging, have limited target populations, and there is an inherent risk when handling large animals (126, 127). The development of remote sampling technologies is essential to build upon the data collected during hands-on studies and to expand our ability to efficiently and comprehensively assess the health of dolphin populations beyond nearshore waters, as well as the health of larger, less tractable cetacean species.

TABLE 2 | List of veterinary processing sample collection from hands-on physical examinations during common bottlenose dolphin health assessments.

Procedure	Description	Use	References
Blood sample (**Figure 4**)	Obtained from the periarterial rete on the ventral aspect of the tail fluke	Biochemistry Hematology Blood gas analysis Endocrinology Immunology Serology Genetics	(23, 29, 30, 74, 91–93)
Surgical biopsy	Full thickness wedge biopsies of skin and blubber are routinely taken via an inverted "L" block under local anesthesia from the left lateral body wall caudal to the dorsal fin	Genetic population structure (skin) Foraging ecology (skin) Chemical contaminants (blubber) Hormone levels (blubber) Microbiome	(31, 33, 49, 57, 94–96)
Urinalysis	Bladder catheterization	Renal function assessment Dietary analysis	(91, 97–99)
Tooth extraction	Single tooth extracted under local anesthesia	Age determination	(17, 100)
Ultrasonography (**Figure 3**)	Thoracic and abdominal internal assessment	Lung pathology Reproductive Assessment Full abdominal exam including renal assessment Blubber thickness	(77, 97, 101–103)
Electrocardiography (**Figure 6**)	Adapted field use in and out of water	Cardiac assessment	(104)
Morphometrics (**Figure 7**)	Standardized full body measurements: lengths, girths, weight	Assess body condition and growth rates	(105)
Auditory evoked potential	Portable unit adapted for field assessment audiograms	Assess hearing range and sensitivity	(106)
Lesion biopsy	Sample of abnormal skin lesions e.g., pox or freshwater lesions	Histopathology	(57, 93)
Blow analysis (**Figure 5**)	Exhaled breath vapor	Pathogen and hormonal analysis Metabolites Respiratory function testing	(107, 108)
Microbiology	Swabs/culture plates from oral respiratory or genital orifices	Bacteriology Virology	(109)
Freeze brand	Dorsal Fin	Identification	(110)
Feces and urine collection	Swabs or catheter	Biotoxin analysis	(46)
Skin biopsy Electronic and/or roto tagging	Skin sample from biopsy or during dorsal fin tagging	Genetics, sex, stable isotopes identification Ranging patterns reproductive status Survival	(70, 111, 112)

Application of new technologies to improve remote sampling opportunities and maximize information obtained from cetacean health assessments is pushing the boundaries of current marine mammal science. Blow samples previously established when in-hand (**Figure 5**) can now be obtained remotely utilizing UAVs (unmanned aerial vehicles). Drones can be used to obtain aerial images to perform photogrammetry to assess health via body condition in large whales unable to be examined physically (107, 128). Drones can also be used in cetacean disentanglement approaches to provide accurate assessment of exact entanglement points and facilitate more informed decisions on disentanglement methodology. Thermography has been used to assess dolphin dorsal fin temperatures, as a measure of individual health status representing appropriate integumentary thermoregulation (129), and now thermal imaging from drones is being developed to apply to large whale health assessments. Remote temperature assessment will be of increased value in the future when potential climate change impacts could result in cetaceans being exposed to higher or lower environmental temperatures (130–132).

Historically, the standard method of estimating the age in dolphin health assessments is via tooth extraction under local anesthesia and counting the growth layer groups present on longitudinal section (17). Dental radiography has been pioneered in an effort to replace the tooth extraction technique, and validation of the technique is ongoing. Bone density assessment has also been explored as a possible aging method, however correlation with age across the entire lifespan was limited (133). A promising new methodology is the use of pectoral flipper radiography to assess bone maturation (134).

FIGURE 3 | Ultrasound examination of a lymph node on board the veterinary examination and sampling vessel (MMPA ESA Permit No. 18786-03).

FIGURE 4 | Blood sample collection from the peri-arterial rete on the ventral aspect of the tail fluke (MMPA ESA Permit No. 18786-01).

The dolphin pectoral flipper displays both hyperphalangy and paedomorphosis enabling this method to be applied throughout the entire lifespan due to the predictable chronological osteogenic changes occurring to the metacarpal and phalangeal bones. This non-invasive technology could facilitate age estimation for older animals, replacing tooth extraction.

Additional biological information from remote biopsy dart sampling is expanding on the knowledge gained from each individual sample (135). Currently, sex and population structure of the animal can be determined from genetic analyses of skin (112), and contaminant concentrations and stress and reproductive hormone levels can be measured from blubber biopsy (33, 116, 136). Present efforts are working toward using skin to assess the epigenetics of the individual to give an estimation of age (137). The NMMF are expanding on this even further in line with recent human advancements to provide an

FIGURE 5 | Exhaled breath sample collection for cytology (MMPA ESA Permit No. 18786-03).

FIGURE 6 | ECG leads attached during sampling and processing to closely monitor the dolphin's heart rate and assess cardiac function (MMPA ESA Permit No. 18786-03).

FIGURE 7 | Dolphin suspended in a stretcher for weight measurement via load cell on board the veterinary processing vessel. This image was published with permission of MMPA ESA Permit No. 18786-01 for the identifiable individuals in the image.

indication of biological age (138). This emerging technology could provide a means to assess increased environmental pressure or poor health status (139–141).

Remotely deployed suction cup satellite-linked tags can provide short-term (<24 h) data on bioenergetics, respiratory measures and cardiac data (142, 143). An additional remote

tool in development is the use of remotely attached single-pin satellite-linked tags. These techniques will be particularly useful in marine mammals where capture-release is impractical due to size, species intolerance to handling or cost restraints. Future research aims to combine different disciplines to expand scientific knowledge further and inter-species application of new technologies, for example, studying acoustic communication as a proxy to changes in health status (144, 145).

DISCUSSION

Health assessments with an epidemiological focus can aim to understand the pathophysiology of disease and interpret the demographic, anthropogenic, and ecological pressures contributing to individual disease susceptibility (146). Extrapolating from individual health assessments to accurately understand population health status, requires a strategic epidemiological approach (41, 147, 148). Integration of post-mortem examinations within the health assessment framework can provide additional projections from both diagnostic and scientific perspectives aiming to contribute to identifying the underlying cause of mortality and also predicting the future impacts on the population. Performing pro-active marine mammal health assessment examinations allows an opportunity to examine population health under natural environmental conditions, as opposed to during a mass stranding or UMEs. This baseline knowledge of population health status can aid understanding of post-mortem examinations during UMEs and ultimately aim to drive mitigation strategies for successful conservation and species management. Health assessments are facilitating a pro-active approach to marine mammal conservation in addition to a reactive response to UMEs.

The primary role of wildlife veterinarians is shifting from management of high mortality disease epidemics to preventative management and mitigation of anthropogenic causes of mortality (7). Unlike terrestrial species where mass mortalities garner a lot of public attention, marine species can die in large numbers, and the impact can go unnoticed (149). Sharing information regarding health and threats to local populations can facilitate public interest in coastal and estuarine bottlenose dolphin populations. Increased public awareness and reporting of marine mammals in distress can aid understanding of the current global changes and interactions between humans and wildlife, dictating the efforts required to conserve future marine populations globally.

Continuous monitoring of specific populations over time has the benefit of providing both cross-sectional analyses on an annual basis, as well as longitudinal analysis over several decades. Collecting health data consistently across multiple populations facilitates an understanding of geographic variability, can help to establish reference ranges that are generalizable across populations, and can provide a gradient of stressor exposures for cross-sectional or correlational studies. The combined approaches support a robust framework for epidemiological studies to investigate the causal factors for disease. The collection of decades of archival samples from multiple populations facilitates retrospective studies to discern between sublethal pathogen levels, assess temporal and spatial trends, and elucidate the intricacies of disease susceptibility at a population health level. For example, dolphins in Florida are frequently exposed to various levels of *K. brevis* red tides (150, 151). Examining samples from 1994 to 2003 enabled knowledge of baseline levels of brevetoxin in the dolphin population and demonstrated that dolphin carcasses not associated with large scale mass mortality could also contain comparably high levels of brevetoxins (79). This information is invaluable for future research when the duration and intensity of red tides in Florida appears to be increasing (152, 153).

An additional benefit of long-term studies and sample archives generated by health assessments is the ability to apply new technology and diagnostic tests retrospectively enabling advanced monitoring of health changes over time. Identification of emerging infectious causes of mortality such as cetacean morbillivirus requires continued monitoring of levels of herd immunity over long periods of time (81). Sample archives can be used to establish normal levels and improve understanding of emergence, dynamics, and history of pathogens such as morbillivirus or retrospective analysis of brucella (23, 30, 73). Established baseline data can aid interpretation of normal or increased prevalence of positive antibody titers within the population.

Stress of Health Assessments (Alternative Perspective)

Prior to considering health assessments for a project, there should be an in-depth discussion of research priorities and if the short-term capturing of individual dolphins is truly the best tool to address the goals of the study. The value of the data obtained from health assessments of free-ranging dolphins needs to be balanced against the potential stress and risk to the individual from the capture, handling, and sampling process (154–157). The stress of capture often influences baseline data such as blood cortisol and aldosterone levels (158). If baseline hormone values are the focus of a study, remote biopsy sampling of blubber can give an accurate indication of baseline stress hormone levels without the elevation caused by the stress of capture (159). However, the adrenal response to a stimulus such as capture may be of interest (35), and capture-release studies enable the evaluation of an individual's hypothalamic pituitary axis and whether or not the animal is capable of mounting an appropriate stress response (75).

In general, the molecular physiological response to the stress of the veterinary examination is well-documented across species; it is transient and the valuable information obtained from the exam typically offsets any acute stress that may be caused. Based on ongoing population monitoring, long-term health consequences of repeated captures have not been found for individuals examined as many as 15 times or more (160). Ensuring capture and restraint are relatively brief and as calm as possible is important, as it has been shown that short holding times do not induce a significant neuroendocrine stress

response (154). An experienced team and ongoing training opportunities among organizations, in both managed and free-ranging dolphin populations, promote this high standard of assessment.

Globally, free-ranging dolphins are exposed to a wide range of anthropogenic stressors including environmental contaminants, acoustic shipping disturbances, fisheries interactions, habitat degradation or even loss altogether, exposure to biotoxins, climate disruption, and human interactions (161–168). Variability in the level of anthropogenic stress occurs across geographical locations. Health assessments provide a portal into the individual and population health status to facilitate understanding of ecosystem health, and drive conservation and management decisions. The cost of each individual health assessment is offset by the biological information obtained from each examination. Combining these data with additional stranding information, such as post-mortem examinations and field observations, helps to improve understanding and interpretation of biological health assessment data from a conservation perspective.

International Perspective

Biologists and veterinarians from around the world have had the opportunity to partake in dolphin health assessments across U.S. waters with the aim of facilitating capacity building for global cetacean conservation (92). Established dolphin health parameter reference ranges enable comparison between international locations in an effort to tease apart the health effects of different stressors. Throughout the majority of the world, health monitoring of dolphins primarily involves post-mortem exams of stranded cetaceans in Europe, physical exams during translocations such as out-of-habitat animals in Asia and South America such as the recent intervention in Bolivia, or during remote biopsy sampling in photo-identification studies in the Mediterranean (169–173).

Increased international collaboration is essential for mitigating conservation crises and aiming to reduce the number of marine mammals becoming extinct such as the recent loss of the Yangtze River dolphin, the baiji (*Lipotes vexillifer*), or the high-risk Mediterranean monk seal (*Monachus monachus*) and vaquita porpoise (*Phocoena sinus*) (4, 174). Knowledge of capture techniques gained from dolphin health assessments in the U.S. has been applied to alternative species conservation approaches, such as with the vaquita, in an effort to temporarily remove animals from a dangerous habitat and relocate them to a protected environment (175). Marine mammal stranding networks exist world-wide with varying capacity dependent on funding, degree of public interest, number of strandings per year, facilities available, and the extent of inter-agency cooperation (176). Sharing knowledge and organizational structure from locations with financial support can aid capacity building in areas where marine mammal stranding networks are currently limited.

From examining dolphin communication to understanding energetics, lung capacity, respiratory metabolomics, and the mechanisms involved in deep diving physiology, health assessments are contributing to advancing scientific knowledge (108, 177–179). Scientists have improved our understanding of dolphin anatomy and physiology by observing natural behavior during health assessments and monitoring activity and behavior post handling. Collaboration among scientists, veterinarians, and biologists at different health assessments enables a synergistic approach to understanding marine mammal health.

Universally, comprehensive cetacean conservation benefits from an integration of all available cetacean assessment techniques; hands on veterinary health assessments, post-mortem examinations, photo-ID surveys, and field observer data. Ideally a collaborative approach among scientists, biologists, fishers, local community members, and government officials would achieve maximum success from a management perspective. Increased discussion will aim to improve future inter-disciplinary approaches and address anthropogenic impacts on marine mammals.

CONCLUSION

The advancement of common bottlenose dolphin health assessments, transitioning from initial population assessments to endangered species conservation applications has occurred over several decades, expanding knowledge of marine mammal medicine and science. As veterinary standards for dolphins in human care have evolved, so have the standard protocols for handling and monitoring free-ranging dolphins, and diagnostics such as clinicopathology, ultrasonography, radiography, electrocardiography, respirometry, microbiology, and morphometry (29, 32, 43, 77, 104, 108, 180, 181). Dolphin health assessments are a valuable tool to extrapolate from the individual to understanding both population and ecosystem health. Combining scientific investigation with longitudinal population monitoring over multiple dolphin populations provides information to facilitate informed decisions regarding conservation, regulations, and protection of marine mammals.

Social education regarding the presence, longevity, and residence of bottlenose dolphins also allows the public to engage with the species and appreciate their intrinsic value within the ecosystem; dolphins share the same habitat and are impacted by some of the same stressors as local human communities. Citizen science and public interest peaks during UMEs when multiple carcasses are observed on the beaches in a short time frame. This is an opportunity to engage with people to highlight the environmental pressures faced by these apex predators and explain the anthropogenic impacts on these charismatic species.

An interdisciplinary and interagency approach is needed to fully understand the complexities of the challenges faced by marine mammals. Shifts in the tide of social attitudes, interests, regulations, and funding will have consequences to marine mammal populations both free-ranging as well as managed. Understanding the current global challenges and increasing human and wildlife interactions will dictate the mitigation efforts required to conserve future marine populations. Remaining at the cutting edge of science and advancing the field will aim to facilitate conservation of marine mammal populations for future generations.

AUTHOR CONTRIBUTIONS

All authors contributed to the past, present, or future development of dolphin health assessments. AB and RW completed the manuscript writing with significant contributions from LS and CS. All authors provided edits and contributed to the final submitted manuscript.

FUNDING

Waiver received for publication fees to Dr. Randy Wells.

ACKNOWLEDGMENTS

Dolphin health assessments would not have been possible without the vast scientific collaboration from a large global team of scientific colleagues, research assistants, post-docs, graduate students, and volunteers. The authors would like to thank Larry Fulford, who was the dolphin catcher for the majority of health assessments in the southeastern U.S. for 35 years. The authors would also like to thank the significant program support for each health assessment in addition to NOAA's Marine Mammal Health and Stranding Response Program and the Office of Naval Research. In addition, significant program support for health assessments has been received from the Chicago Zoological Society, NOAA's Fisheries Service, National Science Foundation, Environmental Protection Agency, Marine Mammal Commission, Dolphin Quest, Inc., Disney's Animal Programs, Earthwatch, Inc., and the International Whaling Commission. The authors also wish to thank the involvement of the U.S. Navy Marine Mammal Program. This manuscript was made possible in part by a grant from The Gulf of Mexico Research Initiative. The scientific results and conclusions, as well as any views or opinions expressed herein, are those of the authors and do not necessarily reflect the views of NOAA. Dolphin health assessments were conducted under various NMFS research permits for the projects described. This is scientific contribution 246 of the National Marine Mammal Foundation.

REFERENCES

1. Gulland FMD, Hall AJ. Is marine mammal health deteriorating? Trends in the global reporting of marine mammal disease. *EcoHealth.* (2007) 4:135–50. doi: 10.1007/s10393-007-0097-1
2. Myers N, Mittermeier RA, Mittermeier CG, Da Fonseca GA, Kent J. Biodiversity hotspots for conservation priorities. *Nature.* (2000) 403:853. doi: 10.1038/35002501
3. Aguirre AA, Ostfeld RS, Tabor GM, House C, Pearl MC. *Conservation Medicine: Ecological Health in Practice.* New York, NY: Oxford University Press (2002).
4. Reynolds JE, Marsh H, Ragen TJ. Marine mammal conservation. *Endang Species Res.* (2009) 7:23–8. doi: 10.3354/esr00179
5. Wikelski M, Cooke SJ. Conservation physiology. *Trends Ecol Evol.* (2006) 21:38–46. doi: 10.1016/j.tree.2005.10.018
6. Daszak P, Cunningham AA, Hyatt AD. Emerging infectious diseases of wildlife–threats to biodiversity and human health. *Science.* (2000) 287:443–9. doi: 10.1126/science.287.5452.443
7. Deem SL, Karesh WB, Weisman W. Putting theory into practice: wildlife health in conservation. *Conserv Biol.* (2001) 15:1224–33. doi: 10.1046/j.1523-1739.2001.00336.x
8. Iucn. *The IUCN Red List of Threatened Species. Version 2019-2.* (2019). Available online at: http://www.iucnredlist.org
9. Taylor BL, Martinez M, Gerrodette T, Barlow J, Hrovat YN. Lessons from monitoring trends in abundance of marine mammals. *Mar Mamm Sci.* (2007) 23:157–75. doi: 10.1111/j.1748-7692.2006.00092.x
10. Davidson AD, Boyer AG, Kim H, Pompa-Mansilla S, Hamilton MJ, Costa DP, et al. Drivers and hotspots of extinction risk in marine mammals. *Proc Natl Acad Sci USA.* (2012) 109:3395–400. doi: 10.1073/pnas.1121469109
11. Asper ED, Odell DK. *Bottlenose Dolphin Local Herd Monitoring: Captive Marking, Collection of Biological Data, and Follow-Up Observations of Marked Animals.* Final Report to National Marine Fisheries Service, Contract NA79-6A-C-00027. Hubbs/Sea World Research Institute (1980).
12. Odell DK, Asper ED. Distribution and movements of freeze-branded bottlenose dolphins in the Indian and Banana Rivers, Florida. In: Leatherwood S, Reeves R, editors. *The Bottlenose Dolphin.* Elsevier (1990). p. 515–40.
13. Solangi MA, Dukes GE. *Atlantic Bottlenose Dolphin, Tursiops Truncatus Herd Studies in the Mississippi Sound, USA: Capture, Freeze Marking and Biological Sampling.* Biloxi, MS: Marine Animal Productions (1983).
14. Irvine B, Wells RS. Results of attempts to tag atlantic bottlenosed dolphins (*Tursiops truncatus*). *Biol Syst.* (1972) 13:1–5.
15. Irvine AB, Scott M, Wells RS, Kaufman JH. Movements and activities of the Atlantic bottlenose dolphin, *Tursiops truncatus*, near Sarasota, Florida. *Fishery Bull.* (1981) 79:135–43.
16. Wells RS, Scott MD, Irvine AB. The social structure of free-ranging bottlenose dolphins. In: Genoways HH, editor. *Current Mammalogy.* New York, NY: Springer (1987). p. 247–305.
17. Hohn AA, Scott MD, Wells RS, Sweeney JC, Irvine AB. Growth layers in teeth from known-age, free-ranging bottlenose dolphins. *Mar Mamm Sci.* (1989) 5:315–42. doi: 10.1111/j.1748-7692.1989.tb00346.x
18. Wells RS, Scott MD. Estimating bottlenose dolphin population parameters from individual identification and capture-release techniques. *Rep Int Whal Commission.* (1990) 12:407–15.
19. Duffield DA, Wells RS. The combined application of chromosome, protein and molecular data for the investigation of social unit structure and dynamics in Tursiops truncatus. In: Hoelzel AR, editor. *Genetic Ecology of Whales and Dolphins.* Cambridge, UK (1991). p. 155–69.
20. Becker PR, Wilkinson DM, Lillestolen TI. *Marine Mammal Health and Stranding Response Program: Program Development Plan.* NOAA Technical Memorandum NMFS-OPR-94-2, National Oceanic and Atmospheric Administration, Silver Spring, MD (1994).
21. Geraci JR. *Clinical Investigation of the 1987-88 Mass Mortality of Bottlenose Dolphins Along the US Central and South Atlantic Coast.* Final report to National Marine Fisheries Service and US Navy Office of Naval Research and Marine Mammal Commission (1989).
22. Lipscomb TP, Schulman FY, Moffett D, Kennedy S. Morbilliviral disease in Atlantic bottlenose dolphins (*Tursiops truncatus*) from the 1987-1988 epizootic. *J Wildl Dis.* (1994) 30:567–71. doi: 10.7589/0090-3558-30.4.567
23. Duignan PJ, House C, Odell DK, Wells RS, Hansen LJ, Walsh MT, et al. Morbillivirus infection in bottlenose dolphins: evidence for recurrent epizootics in the western Atlantic and Gulf of Mexico. *Mar Mamm Sci.* (1996) 12:499–515. doi: 10.1111/j.1748-7692.1996.tb00063.x
24. Hansen LJ, Wells RS. *Bottlenose Dolphin Health Assessment: Field Report on Sampling Near Beaufort, North Carolina, During July, 1995.* NOAA Technical Memorandum NMFS-SEFSC-382 (1996).
25. Mclellan WA, Friedlaender AS, Mead JG, Potter CW, Pabst DA. Analysing 25 years of bottlenose dolphin (*Tursiops truncatus*) strandings along the Atlantic coast of the USA: do historic records support the coastal migratory stock hypothesis? *J Cetacean Res Manag.* (2002) 4:297–304. Available online at: https://pdfs.semanticscholar.org/1ec1/4350253d6e3276a4d1d0021959b20fc59706.pdf

26. Sweeney JC, Stone LR, Townsend FI, Casper D, Hansen L. *Population Health Assessment on Tursiops truncatus From Matagorda Bay, Texas, Following a Mortality Event, 1992*. NOAA-NMFS, SEFSC Contribution MIA-92/93-41, 10 pp + appendices (1992).
27. Schwacke LH, Twiner MJ, De Guise S, Balmer BC, Wells RS, Townsend FI, et al. Eosinophilia and biotoxin exposure in bottlenose dolphins (*Tursiops truncatus*) from a coastal area impacted by repeated mortality events. *Environ Res.* (2010) 110:548–55. doi: 10.1016/j.envres.2010.05.003
28. Lohoefener R, Hoggard W, Mullin K, Ford R, Benigno J. *Studies of Mississippi Sound Bottlenose Dolphins: Estimates of Bottlenose Dolphin density in Mississippi Sound From Small Boat Surveys*. Pascagoula, MS: National Marine Fisheries Service (1990).
29. Wells RS, Rhinehart HL, Hansen LJ, Sweeney JC, Townsend FI, Stone R, et al. Bottlenose dolphins as marine ecosystem sentinels: developing a health monitoring system. *EcoHealth.* (2004) 1:246–54. doi: 10.1007/s10393-004-0094-6
30. Rowles T, Schwacke L, Wells R, Saliki J, Hansen L, Hohn A, et al. Evidence of susceptibility to morbillivirus infection in cetaceans from the United States. *Mar Mamm Sci.* (2011) 27:1–19. doi: 10.1111/j.1748-7692.2010.00393.x
31. Hansen LJ, Schwacke LH, Mitchum GB, Hohn AA, Wells RS, Zolman ES, et al. Geographic variation in polychorinated biphenyl and organochlorine pesticide concentrations in the blubber of bottlenose dolphins from the US Atlantic coast. *Sci Total Environ.* (2004) 319:147–72. doi: 10.1016/S0048-9697(03)00371-1
32. Schwacke LH, Hall AJ, Townsend FI, Wells RS, Hansen LJ, Hohn AA, et al. Hematologic and serum biochemical reference intervals for free-ranging common bottlenose dolphins (*Tursiops truncatus*) and variation in the distributions of clinicopathologic values related to geographic sampling site. *Am J Vet Res.* (2009) 70:973–85. doi: 10.2460/ajvr.70.8.973
33. Kucklick J, Schwacke L, Wells R, Hohn A, Guichard A, Yordy J, et al. Bottlenose dolphins as indicators of persistent organic pollutants in the western North Atlantic Ocean and northern Gulf of Mexico. *Environ Sci Cons.* (2011) 45:4270–7. doi: 10.1021/es1042244
34. Bossart GD, Fair P, Schaefer AM, Reif JS. Health and Environmental Risk Assessment Project for bottlenose dolphins *Tursiops truncatus* from the southeastern USA. I Infectious diseases. *Dis Aquat Org.* (2017) 125:141–53. doi: 10.3354/dao03142
35. Schwacke LH, Smith CR, Townsend FI, Wells RS, Hart LB, Balmer BC, et al. Health of common bottlenose dolphins (*Tursiops truncatus*) in Barataria Bay, Louisiana, following the deepwater horizon oil spill. *Environ Sci Technol.* (2014) 48:93–103. doi: 10.1021/es403610f
36. Schwacke LH, Thomas L, Wells RS, Mcfee WE, Hohn AA, Mullin KD, et al. Quantifying injury to common bottlenose dolphins from the Deepwater Horizon oil spill using an age-, sex-and class-structured population model. *Endang Species Res.* (2017) 33:265–79. doi: 10.3354/esr00777
37. Mullin KD, Mcdonald T, Wells RS, Balmer BC, Speakman T, Sinclair C, et al. Density, abundance, survival, and ranging patterns of common bottlenose dolphins (*Tursiops truncatus*) in Mississippi Sound following the Deepwater Horizon oil spill. *PLoS ONE.* (2017) 12:e0186265. doi: 10.1371/journal.pone.0186265
38. Balmer B, Zolman E, Rowles T, Smith C, Townsend F, Fauquier D, et al. Ranging patterns, spatial overlap, and association with dolphin morbillivirus exposure in common bottlenose dolphins (*Tursiops truncatus*) along the Georgia, USA coast. *Ecol Evol.* (2018) 8:12890–4. doi: 10.1002/ece3.4727
39. Garrison LP, Hohn AA, Hansen LJ. *Seasonal Movements of Atlantic Common Bottlenose Dolphin Stocks Based on Tag Telemetry Data*. Southeast Fisheries Science Center, Protected Resources and Biodiversity Division (2017). p. 75.
40. Scott GP, Burn DM, Hansen LJ. *The Dolphin Dieoff: Long-Term Effects and Recovery of the Population*. IEEE (1998). p. 819–23.
41. Rowles TK, Schwacke LH, Hall AJ, Barbieri M. Population health assessment study design. In: Gulland FMD, Whitman KL, Dierauf LA, editors. *CRC Handbook of Marine Mammal Medicine*. CRC Press (2018). p. 813–22.
42. Goldstein JD, Reese E, Reif JS, Varela RA, Mcculloch SD, Defran RH, et al. Hematologic, biochemical, and cytologic findings from apparently healthy atlantic bottlenose dolphins (*Tursiops truncatus*) Inhabiting the Indian River Lagoon, Florida, USA. *J Wildl Dis.* (2006) 42:447–54. doi: 10.7589/0090-3558-42.2.447
43. Reif JS, Fair PA, Adams J, Joseph B, Kilpatrick DS, Sanchez R, et al. Evaluation and comparison of the health status of Atlantic bottlenose dolphins from the Indian River Lagoon, Florida, and Charleston, South Carolina. *J Am Vet Med Ass.* (2008) 233:299–307. doi: 10.2460/javma.233.2.299
44. Reif JS, Schaefer AM, Bossart GD, Fair PA. Health and environmental risk assessment project for bottlenose dolphins *Tursiops truncatus* from the southeastern USA. II Environmental aspects. *Dis Aquat Org.* (2017) 125:155–66. doi: 10.3354/dao03143
45. Litz JA, Baran MA, Bowen-Stevens SR, Carmichael RH, Colegrove KM, Garrison LP, et al. Review of historical unusual mortality events (UMEs) in the Gulf of Mexico (1990-2009): providing context for the multi-year northern Gulf of Mexico cetacean UME declared in 2010. *Dis Aquat Org.* (2014) 112:161–75. doi: 10.3354/dao02807
46. Twiner MJ, Flewelling LJ, Fire SE, Bowen-Stevens SR, Gaydos JK, Johnson CK, et al. Comparative analysis of three brevetoxin-associated bottlenose dolphin (*Tursiops truncatus*) mortality events in the Florida panhandle region (USA). *PLoS ONE.* (2012) 7:e42974. doi: 10.1371/journal.pone.0042974
47. Gulland FMD, Haulena M, Fauquier D, Langlois G, Lander ME, Zabka T, et al. Domoic acid toxicity in Californian sea lions (*Zalophus californianus*): clinical signs, treatment and survival. *Vet Rec.* (2002) 150:475–80. doi: 10.1136/vr.150.15.475
48. Balmer BC, Wells RS, Nowacek SM, Nowacek DP, Schwacke LH, Mclellan WA, et al. 157 Seasonal abundance and distribution patterns of common bottlenose dolphins (*Tursiops truncatus*) near St. Joseph Bay, Florida, USA. *J Cetacean Res Manage.* (2008) 10:157–67. Available online at: https://uncw.edu/mmsp/documents/balmer_et_al_2008.pdf
49. Vollmer NL, Rosel PE. A review of common bottlenose dolphins (*Tursiops truncatus truncatus*) in the northern Gulf of Mexico: population biology, potential threats, and management. *Southeastern Natural.* (2013) 12:1–44. doi: 10.1656/058.012.m601
50. Balmer B, Mcdonald T, Hornsby F, Adams J, Allen J, Barleycorn A, et al. Long-term trends in a northern Gulf of Mexico common bottlenose dolphin (*Tursiops truncatus*) population in the wake of the Deepwater Horizon oil spill. *J Cetacean Res Manage.* (2018) 18:1–9. Available online at: https://www.researchgate.net/profile/Brian_Balmer/publication/328076117_Long-term_trends_in_a_northern_Gulf_of_Mexico_common_bottlenose_dolphin_Tursiops_truncatus_population_in_the_wake_of_the_Deepwater_Horizon_oil_spill/links/5bb6324e4585159e8d86662f/Long-term-trends-in-a-northern-Gulf-of-Mexico-common-bottlenose-dolphin-Tursiops-truncatus-population-in-the-wake-of-the-Deepwater-Horizon-oil-spill.pdf
51. Fauquier D, Kinsel M, Dailey M, Sutton G, Stolen M, Wells R, et al. Prevalence and pathology of lungworm infection in bottlenose dolphins *Tursiops truncatus* from southwest Florida. *Dis Aquat Org.* (2009) 88:85–90. doi: 10.3354/dao02095
52. Bogomolni AL, Pugliares KR, Sharp SM, Patchett K, Harry CT, Larocque JM, et al. Mortality trends of stranded marine mammals on Cape Cod and southeastern Massachusetts, USA, 2000 to 2006. *Dis Aquat Org.* (2010) 88:143–55. doi: 10.3354/dao02146
53. Wells RS, Allen JB, Lovewell G, Gorzelany J, Delynn RE, Fauquier DA, et al. Carcass-recovery rates for resident bottlenose dolphins in Sarasota Bay, Florida. *Mar Mamm Sci.* (2015) 31:355–68. doi: 10.1111/mms.12142
54. Moore MJ, Mclellan WA, Daoust PY, Bonde RK, Knowlton AR. Right whale mortality: a message from the dead to the living. In: Kraus SD, Rolland R, editors. *The Urban Whale: North Atlantic Right Whales at the Crossroads*. Cambridge, MA: Harvard University Press (2007).
55. Martineau D, Béland P, Desjardins C, Lagacé A. Levels of organochlorine chemicals in tissues of beluga whales (*Delphinapterus leucas*) from the St. Lawrence Estuary, Quebec, Canada. *Environ Contamin Toxic.* (1987) 16:137–47. doi: 10.1007/BF01055795
56. Kuehl DW, Haebler R. Organochlorine, organobromine, metal, and selenium residues in bottlenose dolphins (*Tursiops truncatus*) collected during an unusual mortality event in the Gulf of Mexico, 1990. *Arch Environ Contam Toxicol.* (1995) 28:494–9. doi: 10.1007/BF00211632
57. Wells RS, Tornero V, Borrell A, Aguilar A, Rowles TK, Rhinehart HL, et al. Integrating life-history and reproductive success data to examine potential relationships with organochlorine compounds for bottlenose

dolphins (*Tursiops truncatus*) in Sarasota Bay, Florida. *Sci Total Environ.* (2005) 349:106–19. doi: 10.1016/j.scitotenv.2005.01.010
58. Yordy JE, Pabst DA, Mclellan WA, Wells RS, Rowles TK, Kucklick JR. Tissue-specific distribution and whole-body burden estimates of persistent organic pollutants in the bottlenose dolphin (*Tursiops truncatus*). *Environ Toxicol Chem.* (2010) 29:1263–73. doi: 10.1002/etc.152
59. Jepson PD, Law RJ. Persistent pollutants, persistent threats. *Science.* (2016) 352:1388–9. doi: 10.1126/science.aaf9075
60. Schwacke LH, Voit EO, Hansen LJ, Wells RS, Mitchum GB, Hohn AA, et al. Probabilistic risk assessment of reproductive effects of polychlorinated biphenyls on bottlenose dolphins (*Tursiops truncatus*) from the southeast United States coast. *Environ Toxicol Chem.* (2002) 21:2752–64. doi: 10.1002/etc.5620211232
61. Reijnders PJ. Reproductive failure in common seals feeding on fish from polluted coastal waters. *Nature.* (1986) 324:456–7. doi: 10.1038/324456a0
62. Ross PS, Ellis G, Ikonomou M, Barrett-Lennard L, Addison R. High PCB concentrations in free-ranging Pacific killer whales, *Orcinus orca*: effects of age, sex and dietary preference. *Mar Poll Bull.* (2000) 40:504–15. doi: 10.1016/S0025-326X(99)00233-7
63. Reddy ML, Reif J, Bachand A, Ridgway S. Opportunities for using Navy marine mammals to explore associations between organochlorine contaminants and unfavorable effects on reproduction. *Sci Tot Environ.* (2001) 274:171–82. doi: 10.1016/S0048-9697(01)00741-0
64. Hall AJ, Hugunin K, Deaville R, Law RJ, Allchin CR, Jepson PD. The risk of infection from polychlorinated biphenyl exposure in the harbor porpoise (*Phocoena phocoena*): a case–control approach. *Environ Health Persp.* (2006) 114:704–11. doi: 10.1289/ehp.8222
65. Mori C, Morsey B, Levin M, Nambiar PR, De Guise S. Immunomodulatory effects of *in vitro* exposure to organochlorines on T-cell proliferation in marine mammals and mice. *J Tox Environ Health A.* (2006) 69:283–302. doi: 10.1080/15287390500227472
66. Schwacke LH, Zolman ES, Balmer BC, De Guise S, George RC, Hoguet J, et al. Anaemia, hypothyroidism and immune suppression associated with polychlorinated biphenyl exposure in bottlenose dolphins (*Tursiops truncatus*). *Proc Biol Sci.* (2012) 279:48–57. doi: 10.1098/rspb.2011.0665
67. Hall AJ, Mcconnell BJ, Rowles TK, Aguilar A, Borrell A, Schwacke L, et al. Individual-based model framework to assess population consequences of polychlorinated biphenyl exposure in bottlenose dolphins. *Environ Health Persp.* (2005) 114:60–4. doi: 10.1289/ehp.8053
68. Balmer BC, Ylitalo GM, Mcgeorge LE, Baugh KA, Boyd D, Mullin KD, et al. Persistent organic pollutants (POPs) in blubber of common bottlenose dolphins (*Tursiops truncatus*) along the northern Gulf of Mexico coast, USA. *Sci Total Environ.* (2015) 527:306–12. doi: 10.1016/j.scitotenv.2015.05.016
69. Balmer JE, Ylitalo GM, Rowles TK, Mullin KD, Wells RS, Townsend FI, et al. Persistent organic pollutants (POPs) in blood and blubber of common bottlenose dolphins (*Tursiops truncatus*) at three northern Gulf of Mexico sites following the Deepwater Horizon oil spill. *Sci Total Environ.* (2018) 621:130–7. doi: 10.1016/j.scitotenv.2017.11.209
70. Balmer BC, Wells RS, Howle LE, Barleycorn AA, Mclellan WA, Ann Pabst D, et al. Advances in cetacean telemetry: a review of single-pin transmitter attachment techniques on small cetaceans and development of a new satellite-linked transmitter design. *Mar Mamm Sci.* (2014) 30:656–73. doi: 10.1111/mms.12072
71. Takeshita R, Sullivan L, Smith C, Collier T, Hall A, Brosnan T, et al. The Deepwater Horizon oil spill marine mammal injury assessment. *Endanger Species Res.* (2017) 33:95–106. doi: 10.3354/esr00808
72. Wallace BP, Brosnan T, Mclamb D, Rowles T, Ruder E, Schroeder B, et al. Effects of the Deepwater Horizon oil spill on protected marine species. *Endang Species Res.* (2017) 33:1–7. doi: 10.3354/esr00789
73. Venn-Watson S, Colegrove KM, Litz J, Kinsel M, Terio K, Saliki J, et al. Adrenal gland and lung lesions in Gulf of Mexico common bottlenose dolphins (*Tursiops truncatus*) found dead following the Deepwater Horizon oil spill. *PLoS ONE.* (2015) 10:e0126538. doi: 10.1371/journal.pone.0126538
74. De Guise S, Levin M, Gebhard E, Jasperse L, Hart LB, Smith CR, et al. Changes in immune functions in bottlenose dolphins in the northern Gulf of Mexico associated with the Deepwater Horizon oil spill. *Endang Species Res.* (2017) 33:291–303. doi: 10.3354/esr00814
75. Smith CR, Rowles TK, Hart LB, Townsend FI, Wells RS, Zolman ES, et al. Slow recovery of Barataria Bay dolphin health following the Deepwater Horizon oil spill (2013-2014), with evidence of persistent lung disease and impaired stress response. *Endang Species Res.* (2017) 33:127–42. doi: 10.3354/esr00778
76. Venn-Watson S, Garrison L, Litz J, Fougeres E, Mase B, Rappucci G, et al. Demographic clusters identified within the northern Gulf of Mexico common bottlenose dolphin (*Tursiops truncates*) unusual mortality event: January 2010-June 2013. *PLoS ONE.* (2015) 10:e0117248. doi: 10.1371/journal.pone.0117248
77. Smith CR, Solano M, Lutmerding BA, Johnson SP, Meegan JM, Le-Bert CR, et al. Pulmonary ultrasound findings in a bottlenose dolphin *Tursiops truncatus* population. *Dis Aquat Organ.* (2012) 101:243–55. doi: 10.3354/dao02537
78. Venn-Watson S, Daniels R, Smith C. Thirty year retrospective evaluation of pneumonia in a bottlenose dolphin *Tursiops truncatus* population. *Dis Aquat Org.* (2012) 99:237–42. doi: 10.3354/dao02471
79. Fire SE, Fauquier D, Flewelling LJ, Henry M, Naar J, Pierce R, et al. Brevetoxin exposure in bottlenose dolphins (*Tursiops truncatus*) associated with *Karenia brevis* blooms in Sarasota Bay, Florida. *Mar Biol.* (2007) 152:827–34. doi: 10.1007/s00227-007-0733-x
80. Colegrove KM, Venn-Watson S, Litz J, Kinsel MJ, Terio KA, Fougeres E, et al. Fetal distress and *in utero* pneumonia in perinatal dolphins during the Northern Gulf of Mexico unusual mortality event. *Dis Aquat Org.* (2016) 119:1–16. doi: 10.3354/dao02969
81. Fauquier DA, Litz J, Sanchez S, Colegrove K, Schwacke LH, Hart L, et al. Evaluation of morbillivirus exposure in cetaceans from the northern Gulf of Mexico 2010-2014. *Endang Species Res.* (2017) 33:211–20. doi: 10.3354/esr00772
82. Lane SM, Smith CR, Mitchell J, Balmer BC, Barry KP, Mcdonald T, et al. Reproductive outcome and survival of common bottlenose dolphins sampled in Barataria Bay, Louisiana, USA, following the Deepwater Horizon oil spill. *Proc Biol Sci.* (2015) 282:20151944. doi: 10.1098/rspb.2015.1944
83. Mcdonald TL, Hornsby FE, Speakman TR, Zolman ES, Mullin KD, Sinclair C, et al. Survival, density, and abundance of common bottlenose dolphins in Barataria Bay (USA) following the Deepwater Horizon oil spill. *Endang Species Res.* (2017) 33:193–209. doi: 10.3354/esr00806
84. Monson DH, Doak DF, Ballachey BE, Johnson A, Bodkin JL. Long-term impacts of the Exxon Valdez oil spill on sea otters, assessed through age-dependent mortality patterns. *Proc Nat Acad Sci USA.* (2000) 97:6562–7. doi: 10.1073/pnas.120163397
85. Bodkin JL, Ballachey BE, Dean T, Fukuyama AK, Jewett S, Mcdonald L, et al. Sea otter population status and the process of recovery from the 1989 'Exxon Valdez'oil spill. *Mar Ecol Prog Ser.* (2002) 241:237–54. doi: 10.3354/meps241237
86. Matkin C, Saulitis E, Ellis G, Olesiuk P, Rice S. Ongoing population-level impacts on killer whales *Orcinus orca* following the'Exxon Valdez'oil spill in Prince William Sound, Alaska. *Mar Ecol Prog Ser.* (2008) 356:269–81. doi: 10.3354/meps07273
87. Helm RC, Costa DP, Debruyn TD, O'shea TJ, Wells RS, Williams TM. Overview of effects of oil spills on marine mammals. In: Fingus MF, editor. *Handbook of Oil Spill Science and Technology*. John Wiley & Sons, Inc. (2015). p. 455–75.
88. Asper ED. Techniques of live capture of smaller Cetacea. *J Fish Res Board Can.* (1975) 32:1191–6. doi: 10.1139/f75-138
89. Loughlin T, Cunningham L, Gales N, Wells RS, Boyd I. Marking and capturing. In: Boyd IL, Don Bowen W, Iverson SJ, editors. *Marine Mammal Ecology and Conservation: A Handbook of Techniques.* Oxford: Oxford University Press (2010). p. 16–41.
90. Klatsky LJ, Wells RS, Sweeney JC. Offshore bottlenose dolphins (*Tursiops truncatus*): movement and dive behavior near the Bermuda Pedestal. *J Mammal.* (2007) 88:59–66. doi: 10.1644/05-MAMM-A-365R1.1
91. Townsend FI, Smith CR, Rowles T. Health assessment of bottlenose dolphins in capture-release studies. In: Gulland FMD, Whitman KL, Dierauf LA, editors. *CRC Handbook of Marine Mammal Medicine.* CRC Press (2018). p. 823–33.

92. Wells RS. Learning from nature: bottlenose dolphin care and husbandry. *Zoo Biol.* (2009) 28:635–51. doi: 10.1002/zoo.20252
93. Ridgway SH. Medical care of marine mammals. *J Am Vet Med Ass.* (1965) 147:1077–85.
94. Kellar NM, Trego ML, Chivers SJ, Archer FI. Pregnancy patterns of pantropical spotted dolphins (*Stenella attenuata*) in the eastern tropical Pacific determined from hormonal analysis of blubber biopsies and correlations with the purse-seine tuna fishery. *Mar Biol.* (2013) 160:3113–24. doi: 10.1007/s00227-013-2299-0
95. Rossman S, Barros NB, Ostrom PH, Stricker CA, Hohn AA, Gandhi H, et al. Retrospective analysis of bottlenose dolphin foraging: a legacy of anthropogenic ecosystem disturbance. *Mar Mamm Sci.* (2013) 29:705–18. doi: 10.1111/j.1748-7692.2012.00618.x
96. Boggs ASP, Schock TB, Schwacke LH, Galligan TM, Morey JS, Mcfee WE, et al. Rapid and reliable steroid hormone profiling in *Tursiops truncatus* blubber using liquid chromatography tandem mass spectrometry (LC-MS/MS). *Analyt Bioanalyt Chem.* (2017) 409:5019–29. doi: 10.1007/s00216-017-0446-z
97. Smith CR, Venn-Watson S, Wells RS, Johnson SP, Maffeo N, Balmer BC, et al. Comparison of nephrolithiasis prevalence in two bottlenose dolphin (*Tursiops truncatus*) populations. *Front Endocrinol.* (2013) 4:145. doi: 10.3389/fendo.2013.00145
98. Smith CR, Poindexter JR, Meegan JM, Bobulescu IA, Jensen ED, Venn-Watson S, et al. Pathophysiological and physicochemical basis of ammonium urate stone formation in dolphins. *J Urol.* (2014) 192:260–6. doi: 10.1016/j.juro.2014.01.008
99. Ardente A, Wells R, Smith C, Walsh M, Jensen E, Schmitt T, et al. Dietary cation–anion difference may explain why ammonium urate nephrolithiasis occurs more frequently in common bottlenose dolphins (*Tursiops truncatus*) under human care than in free-ranging common bottlenose dolphins. *J Anim Sci.* (2017) 95:1396–406. doi: 10.2527/jas.2016.1113
100. Sweeney JC, Ridgway SH. Procedures for the clinical management of small cetaceans. *J Am Vet Med Assoc.* (1975) 167:540–5.
101. Smith CR, Jensen ED, Blankenship BA, Greenberg M, D'agostini DA, Pretorius DH, et al. Fetal omphalocele in a common bottlenose dolphin (*Tursiops truncatus*). *J Zoo Wildlife Med.* (2013) 44:87–92. doi: 10.1638/1042-7260-44.1.87
102. Seitz KE, Smith CR, Marks SL, Venn-Watson SK, Ivancic M. Liver ultrasonography in dolphins: use of ultrasonography to establish a technique for hepatobiliary imaging and to evaluate metabolic disease-associated liver changes in bottlenose dolphins (*Tursiops truncatus*). *J Zoo Wildl Med.* (2016) 47:1034–43. doi: 10.1638/2015-0173.1
103. Martony ME, Ivancic M, Gomez FM, Meegan JM, Nollens HH, Schmitt TL, et al. Establishing marginal lymph node ultrasonographic characteristics in healthy bottlenose dolphins (*Tursiops truncatus*). *J Zoo Wildl Med.* (2017) 48:961–71. doi: 10.1638/2016-0251.1
104. Harms CA, Jensen ED, Townsend FI, Hansen LJ, Schwacke LH, Rowles TK. Electrocardiograms of bottlenose dolphins (*Tursiops truncatus*) out of water: habituated collection versus wild postcapture animals. *J Zoo Wildl Med.* (2013) 44:972–81. doi: 10.1638/2013-0093.1
105. Read A, Wells R, Hohn A, Scott M. Patterns of growth in wild bottlenose dolphins, *Tursiops truncatus*. *J Zool.* (1993) 231:107–23. doi: 10.1111/j.1469-7998.1993.tb05356.x
106. Houser DS, Finneran JJ. Variation in the hearing sensitivity of a dolphin population determined through the use of evoked potential audiometry. *J Acoutic Soc Am.* (2006) 120:4090–9. doi: 10.1121/1.2357993
107. Apprill A, Miller CA, Moore MJ, Durban JW, Fearnbach H, Barrett-Lennard LG. Extensive core microbiome in drone-captured whale blow supports a framework for health monitoring. *mSystems.* (2017) 2:e00119–17. doi: 10.1128/mSystems.00119-17
108. Fahlman A, Brodsky M, Wells R, Mchugh K, Allen J, Barleycorn A, et al. Field energetics and lung function in wild bottlenose dolphins, *Tursiops truncatus*, in Sarasota Bay Florida. *R Soc Open Sci.* (2018) 5:171280. doi: 10.1098/rsos.171280
109. Buck JD, Wells RS, Rhinehart HL, Hansen LJ. Aerobic microorganisms associated with free-ranging bottlenose dolphins in coastal Gulf of Mexico and Atlantic Ocean waters. *J Wildl Dis.* (2006) 42:536–44. doi: 10.7589/0090-3558-42.3.536
110. Wells RS. Identification methods. In: Würsig B, Thewissen JGM, Kovacs K, eitors. *Encyclopedia of Marine Mammals*. 3rd ed. San Diego, CA: Academic Press (2018). p. 503–9.
111. Scott MD, Wells RS, Irvine AB, Mate BR. Tagging and marking studies on small cetaceans. In: Appel MJ, editor. *The Bottlenose Dolphin*. New York, NY: Elsevier (1990). p. 489–514.
112. Rosel PE. PCR-based sex determination in Odontocete cetaceans. *Conserv Genet.* (2003) 4:647–9. doi: 10.1023/A:1025666212967
113. Schwacke L, Hall AJ, Wells RS, Bossart GD, Fair P, Hohn AA, et al. Health and risk assessment for bottlenose dolphin (*Tursiops truncatus*) populations along the southeast United States coast: current status and future plans. *Paper SC/56/E20 Presented to the IWC Scientific Committee.* Sorrento (2004).
114. Wells RS, Smith CR, Sweeney JC, Townsend FI, Fauquier DA, Stone R, et al. Fetal survival of common bottlenose dolphins (*Tursiops truncatus*) in Sarasota Bay, Florida. *Aquat Mamm.* (2014) 40:252. doi: 10.1578/AM.40.3.2014.252
115. Kellar NM, Trego ML, Marks CI, Dizon AE. Determining pregnancy from blubber in three species of delphinids. *Mar Mamm Sci.* (2006) 22:1–16. doi: 10.1111/j.1748-7692.2006.00001.x
116. Kellar NM, Speakman TR, Smith CR, Lane SM, Balmer BC, Trego ML, et al. Low reproductive success rates of common bottlenose dolphins *Tursiops truncatus* in the northern Gulf of Mexico following the Deepwater Horizon disaster (2010-2015). *Endang Species Res.* (2017) 33:143–58. doi: 10.3354/esr00775
117. Wells RS, Schwacke LH, Rowles TK, Balmer BC, Zolman E, Speakman T, et al. Ranging patterns of common bottlenose dolphins *Tursiops truncatus* in Barataria Bay, Louisiana, following the Deepwater Horizon oil spill. *Endang Species Res.* (2017) 33:159–80. doi: 10.3354/esr00732
118. Heithaus MR, Dill LM. Food availability and tiger shark predation risk influence bottlenose dolphin habitat use. *Ecology.* (2002) 83:480–91. doi: 10.1890/0012-9658(2002)083[0480:FAATSP]2.0.CO;2
119. Mccabe EJB, Gannon DP, Barros NB, Wells RS. Prey selection by resident common bottlenose dolphins (*Tursiops truncatus*) in Sarasota Bay, Florida. *Mar Biol.* (2010) 157:931–42. doi: 10.1007/s00227-009-1371-2
120. Santos MB, German I, Correia D, Read FL, Cedeira JM, Caldas M, et al. Long-term variation in common dolphin diet in relation to prey abundance. *Mar Ecol Prog Ser.* (2013) 481:249–68. doi: 10.3354/meps10233
121. Wells R, Mchugh KA, Douglas DC, Shippee S, Berens Mccabe EJ, Barros NB, et al. Evaluation of potential protective factors against metabolic syndrome in bottlenose dolphins: feeding and activity patterns of dolphins in Sarasota Bay, Florida. *Front Endocrinol.* (2013) 4:139. doi: 10.3389/fendo.2013.00139
122. Jodice PGR, Roby DD, Turco KR, Suryan RM, Irons DB, Piatt JF, et al. Assessing the nutritional stress hypothesis: relative influence of diet quantity and quality on seabird productivity. *Mar Ecol Prog Ser.* (2006) 325:267–79. doi: 10.3354/meps325267
123. Hohn AA, Thomas L, Carmichael RH, Litz J, Clemons-Chevis C, Shippee SF, et al. Assigning stranded bottlenose dolphins to source stocks using stable isotope ratios following the Deepwater Horizon oil spill. *Endang Species Res.* (2017) 33:235–52. doi: 10.3354/esr00783
124. Rosel PE, Wilcox LA, Sinclair C, Speakman TR, Tumlin MC, Litz JA, et al. Genetic assignment to stock of stranded common bottlenose dolphins in southeastern Louisiana after the Deepwater Horizon oil spill. *Endang Species Res.* (2017) 33:221–34. doi: 10.3354/esr00780
125. Thomas L, Booth CG, Rosel PE, Hohn A, Litz J, Schwacke LH. Where were they from? Modelling the source stock of dolphins stranded after the Deepwater Horizon oil spill using genetic and stable isotope data. *Endang Species Res.* (2017) 33:253–64. doi: 10.3354/esr00754
126. Wilson RP, Mcmahon CR. Measuring devices on wild animals: what constitutes acceptable practice? *Frontiers Ecol Environ.* (2006) 4:147–54. doi: 10.1890/1540-9295(2006)0040147:MDOWAW2.0.CO;2
127. Balmer BC, Wells RS, Schwacke LH, Schwacke JH, Danielson B, George RC, et al. Integrating multiple techniques to identify stock boundaries of common bottlenose dolphins (*Tursiops truncatus*). *Aquat Conserv Mar Freshw Ecosyst.* (2014) 24:511–21. doi: 10.1002/aqc.2357

128. Pirotta V, Smith A, Ostrowski M, Russell D, Jonsen ID, Grech A, et al. An economical custom-built drone for assessing whale health. *Front Mar Sci.* (2017) 4:425. doi: 10.3389/fmars.2017.00425
129. Barbieri MM, Mclellan WA, Wells RS, Blum JE, Hofmann S, Gannon J, et al. Using infrared thermography to assess seasonal trends in dorsal fin surface temperatures of free-swimming bottlenose dolphins (*Tursiops truncatus*) in Sarasota Bay, Florida. *Mar Mamm Sci.* (2010) 26:53–66. doi: 10.1111/j.1748-7692.2009.00319.x
130. Learmonth JA, Macleod CD, Santos MB, Pierce GJ, Crick H, Robinson R. Potential effects of climate change on marine mammals. *Oceanogr Mar Biol.* (2006) 44:431. doi: 10.1201/9781420006391.ch8
131. Burek KA, Gulland FMD, O'hara TM. Effects of climate change on Arctic marine mammal health. *Ecol Appl.* (2008) 18:126–34. doi: 10.1890/06-0553.1
132. Edwards HH. Potential impacts of climate change on warmwater megafauna: the Florida manatee example (*Trichechus manatus latirostris*). *Clim Change.* (2013) 121:727–38. doi: 10.1007/s10584-013-0921-2
133. Powell JWB, Duffield DA, Kaufman JJ, Mcfee W. Bone density cannot accurately predict age in the common bottlenose dolphin, *Tursiops truncatus*. *Mar Mam Sci.* (2019) 35:1597–602. doi: 10.1111/mms.12591
134. García-Párraga D, Schmitt TL, Jensen E. Use of radiographic parameters for age estimation in bottlenose dolphins (*Tursiops truncatus*). In: *International Association of Aquatic Animal Health Conference Proceedings*. (2011).
135. Weller DW, Cockcroft VG, Würsig B, Lynn SK, Fertl D. Behavioral responses of bottlenose dolphins to remote biopsy sampling and observations of surgical biopsy wound healing. *Aquat Mamm.* (1997) 23:49–58.
136. Boggs ASP, Ragland JM, Zolman ES, Schock TB, Morey JS, Galligan TM, et al. Remote blubber sampling paired with liquid chromatography tandem mass spectrometry for steroidal endocrinology in free-ranging bottlenose dolphins (*Tursiops truncatus*). *Gen Comp Endocrinol.* (2019) 281:164–72. doi: 10.1016/j.ygcen.2019.06.006
137. Beal A, Kiszka JJ, Wells RS, Eirin-Lopez JM. The Bottlenose dolphin Epigenetic Aging Tool (BEAT): a molecular age estimation tool for small cetaceans. *Front Mar Sci*. (2019) 6:561. doi: 10.3389/fmars.2019.00561
138. Horvath S. DNA methylation age of human tissues and cell types. *Genome Biol.* (2013) 14:3156. doi: 10.1186/gb-2013-14-10-r115
139. Levine ME, Hosgood HD, Chen B, Absher D, Assimes T, Horvath S. DNA methylation age of blood predicts future onset of lung cancer in the women's health initiative. *Aging.* (2015) 7:690–700. doi: 10.18632/aging.100809
140. Perna L, Zhang Y, Mons U, Holleczek B, Saum KU, Brenner H. Epigenetic age acceleration predicts cancer, cardiovascular, and all-cause mortality in a German case cohort. *Clin Epigenet.* (2016) 8:64. doi: 10.1186/s13148-016-0228-z
141. Roetker NS, Pankow JS, Bressler J, Morrison AC, Boerwinkle E. Prospective study of epigenetic age acceleration and incidence of cardiovascular disease outcomes in the ARIC study (atherosclerosis risk in communities). *Circ Genom Precis Med.* (2018) 11:e001937. doi: 10.1161/CIRCGEN.117.001937
142. Shorter KA, Shao Y, Ojeda L, Barton K, Rocho-Levine J, Van Der Hoop J, et al. A day in the life of a dolphin: Using bio-logging tags for improved animal health and well-being. *Mar Mamm Sci.* (2017) 33:785–802. doi: 10.1111/mms.12408
143. Mcdonald BI, Johnson M, Madsen PT. Dive heart rate in harbour porpoises is influenced by exercise and expectations. *J Experim Biol.* (2018) 221:jeb168740. doi: 10.1242/jeb.168740
144. Sayigh LS, Tyack PL, Wells RS, Scott MD. Signature whistles of free-ranging bottlenose dolphins *Tursiops truncatus*: stability and mother-offspring comparisons. *Behav Ecol Sociobiol.* (1990) 26:247–60. doi: 10.1007/BF00178318
145. Jones B, Zapetis M, Samuelson MM, Ridgway S. Sounds produced by bottlenose dolphins (*Tursiops*): a review of the defining characteristics and acoustic criteria of the dolphin vocal repertoire. *Bioacoustics.* (2019) 18:1–42. doi: 10.1080/09524622.2019.1613265
146. Bossart G. Marine mammals as sentinel species for oceans and human health. *Vet Path.* (2011) 48:676–90. doi: 10.1177/0300985810388525
147. Hall AJ, Gulland FM, Hammond JA, Schwacke LH, Boyd I, Bowen W, et al. Epidemiology, disease, and health assessment. In: Boyd IL, Don Bowen W, Iverson SJ, editors. *Marine Mammal Ecology and Conservation.* New York, NY: Oxford University Press (2010). p. 144–64.
148. Gulland FM, Dierauf LA, Whitman KL. *CRC Handbook of Marine Mammal Medicine.* 3rd ed. Boca Raton, FL: CRC Press. (2018).
149. Hall MA, Alverson DL, Metuzals KI. By-catch: problems and solutions. *Mar Poll Bull.* (2000) 41:204–19. doi: 10.1016/S0025-326X(00)00111-9
150. Fire SE, Wang Z, Byrd M, Whitehead HR, Paternoster J, Morton SL. Co-occurrence of multiple classes of harmful algal toxins in bottlenose dolphins (*Tursiops truncatus*) stranding during an unusual mortality event in Texas, USA. *Harmful Algae.* (2011) 10:330–6. doi: 10.1016/j.hal.2010.12.001
151. Mchugh KA, Allen JB, Barleycorn AA, Wells RS. Severe *Karenia brevis* red tides influence juvenile bottlenose dolphin (*Tursiops truncatus*) behavior in Sarasota Bay, Florida. *Mar Mamm Sci.* (2011) 27:622–43. doi: 10.1111/j.1748-7692.2010.00428.x
152. Weisberg RH, Liu Y, Lembke C, Hu C, Hubbard K, Garrett M. The coastal ocean circulation influence on the 2018 West Florida Shelf *K. brevis* red tide bloom. *J Geophys Res Oceans.* (2019) 124:2501–12. doi: 10.1029/2018JC014887
153. Zohdi E, Abbaspour M. Harmful algal blooms (red tide): a review of causes, impacts and approaches to monitoring and prediction. *Int J Environ Sci Tech.* (2019) 16:1789–806. doi: 10.1007/s13762-018-2108-x
154. Ortiz RM, Worthy GA. Effects of capture on adrenal steroid and vasopressin concentrations in free-ranging bottlenose dolphins (*Tursiops truncatus*). *Comp Biochem Phys A Phys.* (2000) 125:317–24. doi: 10.1016/S1095-6433(00)00158-6
155. Norman SA, Hobbs RC, Foster J, Schroeder JP, Townsend FI. A review of animal and human health concerns during capture-release, handling and tagging of odontocetes. *J Cetacean Res Manag.* (2004) 6:53–62. Available online at: https://pdfs.semanticscholar.org/e0dc/57f496a9434514ea187083bf672c7d10eeeb.pdf
156. Mancia A, Warr GW, Chapman RW. A transcriptomic analysis of the stress induced by capture–release health assessment studies in wild dolphins (*Tursiops truncatus*). *Mol Ecol.* (2008) 17:2581–9. doi: 10.1111/j.1365-294X.2008.03784.x
157. Fair PA, Schaefer AM, Romano TA, Bossart GD, Lamb SV, Reif JS. Stress response of wild bottlenose dolphins (*Tursiops truncatus*) during capture–release health assessment studies. *Gen Comp Endocrinol.* (2014) 206:203–12. doi: 10.1016/j.ygcen.2014.07.002
158. Hart LB, Wells RS, Kellar N, Balmer BC, Hohn AA, Lamb SV, et al. Adrenal hormones in common bottlenose dolphins (*Tursiops truncatus*): influential factors and reference intervals. *PLoS ONE.* (2015) 10:e0127432. doi: 10.1371/journal.pone.0127432
159. Champagne CD, Kellar NM, Trego ML, Brendan D, Rudy B, Wasser SK, et al. Comprehensive endocrine response to acute stress in the bottlenose dolphin from serum, blubber, and feces. *Gen Comp Endocrin.* (2018) 266:178–93. doi: 10.1016/j.ygcen.2018.05.015
160. Wells RS. Social structure and life history of bottlenose dolphins near Sarasota Bay, Florida: insights from four decades and five generations. In: Yamagiwa J, Karczmarski L, editors. *Primates and Cetaceans*. Tokyo: Springer (2014). p. 149–72.
161. Broadhurst MK. Bottlenose dolphins, *Tursiops truncatus*, removing by-catch from prawn-trawl codends during fishing in New South Wales, Australia. *Mar Fish Rev.* (1998) 60:9–14.
162. Ingram SN, Rogan E. Identifying critical areas and habitat preferences of bottlenose dolphins *Tursiops truncatus*. *Mar Ecol Prog Ser.* (2002) 244:247–55. doi: 10.3354/meps244247
163. Díaz López B. Interactions between Mediterranean bottlenose dolphins (*Tursiops truncatus*) and gillnets off Sardinia, Italy. *J Mar Sci.* (2006) 63:946–51. doi: 10.1016/j.icesjms.2005.06.012
164. Read AJ, Drinker P, Northridge S. Bycatch of marine mammals in US and global fisheries. *Conserv Biol.* (2006) 20:163–9. doi: 10.1111/j.1523-1739.2006.00338.x
165. Brotons JM, Grau AM, Rendell L. Estimating the impact of interactions between bottlenose dolphins and artisanal fisheries around the Balearic Islands. *Mar Mamm Sci.* (2008) 24:112–27. doi: 10.1111/j.1748-7692.2007.00164.x
166. Wells RS, Allen JB, Hofmann S, Bassos-Hull K, Fauquier DA, Barros NB, et al. Consequences of injuries on survival and reproduction of common

bottlenose dolphins (*Tursiops truncatus*) along the west coast of Florida. *Mar Mamm Sci.* (2008) 24:774–94. doi: 10.1111/j.1748-7692.2008.00212.x
167. Pulster EL, Smalling KL, Zolman E, Schwacke L, Maruya KA. Persistent organochlorine pollutants and toxaphene congener profiles in bottlenose dolphins (*Tursiops truncatus*) frequenting the Turtle/Brunswick River Estuary, Georgia, USA. *Environ Contamin Toxic.* (2009) 28:1390–9. doi: 10.1897/08-240.1
168. Wells RS. Feeling the heat: potential climate change impacts on bottlenose dolphins. *Whalewatcher.* (2010) 39:12–7. Available online at: https://iucn-csg.org/wp-content/uploads/2010/03/Whalewatcher-Climate-Change-2010.pdf
169. Bearzi G, Agazzi S, Bonizzoni S, Costa M, Azzellino A. Dolphins in a bottle: abundance, residency patterns and conservation of bottlenose dolphins *Tursiops truncatus* in the semi-closed eutrophic Amvrakikos Gulf, Greece. *Aquat Conserv Mar Freshw Ecosyst.* (2008) 18:130–46. doi: 10.1002/aqc.843
170. Aliaga-Rossel E. Conservation of the river dolphin (*Inia boliviensis*) in Bolivia. In: Garcia M, Shostell J, editors. *Biology, Evolution and Conservation of the River Dolphins in South America and Asia: Unknown Dolphins in Danger.* New York, NY: Nova Science Publishers (2010). p. 55–70.
171. Braulik GT, Noureen U, Arshad M, Reeves RR. Review of status, threats, and conservation management options for the endangered Indus River blind dolphin. *Biol Conserv.* (2015) 192:30–41. doi: 10.1016/j.biocon.2015.09.008
172. Khan MS. Factors affecting the survival of Indus River dolphin and species tolerance towards anthropogenic pressures. *Mar Freshwat Res.* (2017) 68:1245–50. doi: 10.1071/MF16001
173. Centelleghe C, Da Dalt L, Marsili L, Zanetti R, Fernandez A, Arbelo M, et al. Insights into dolphins' immunology: immuno-phenotypic study on Mediterranean and Atlantic stranded cetaceans. *Front Immunol.* (2019) 10:888. doi: 10.3389/fimmu.2019.00888
174. Turvey ST, Pitman RL, Taylor BL, Barlow J, Akamatsu T, Barrett LA, et al. First human-caused extinction of a cetacean species? *Biol Lett.* (2007) 3:537–40. doi: 10.1098/rsbl.2007.0292
175. Rojas-Bracho L, Gulland FMD, Smith CR, Taylor B, Wells RS, Thomas PO, et al. A field effort to capture critically endangered vaquitas *Phocoena sinus* for protection from entanglement in illegal gillnets. *Endang Species Res.* (2019) 38:11–27. doi: 10.3354/esr00931
176. Wilkinson D, Worthy GAJ. Marine mammal stranding networks. *Conserv Manage Mar Mamm.* (1999) 2:396–411.
177. Watwood SL, Tyack PL, Wells RS. Whistle sharing in paired male bottlenose dolphins, *Tursiops truncatus*. *Behav Ecol Sociobiol.* (2004) 55:531–43. doi: 10.1007/s00265-003-0724-y
178. Bejarano AC, Wells RS, Costa DP. Development of a bioenergetic model for estimating energy requirements and prey biomass consumption of the bottlenose dolphin (*Tursiops truncatus*). *Ecol Model.* (2017) 356:162–72. doi: 10.1016/j.ecolmodel.2017.05.001
179. Pasamontes A, Aksenov AA, Schivo M, Rowles T, Smith CR, Schwacke LH, et al. Noninvasive respiratory metabolite analysis associated with clinical disease in cetaceans: a deepwater horizon oil spill study. *Environ Sci Technol.* (2017) 51:5737–46. doi: 10.1021/acs.est.6b06482
180. Hall AJ, Wells RS, Sweeney JC, Townsend FI, Balmer BC, Hohn AA, et al. Annual, seasonal and individual variation in hematology and clinical blood chemistry profiles in bottlenose dolphins (*Tursiops truncatus*) from Sarasota Bay, Florida. *Comp Biochem and Phys Part A Phys.* (2007) 148:266–77. doi: 10.1016/j.cbpa.2007.04.017
181. Houser DS, Finneran JJ, Ridgway SH. Research with navy marine mammals benefits animal care, conservation and biology. *Int J Comp Psych.* (2010) 23:249–68. Available online at: https://escholarship.org/uc/item/3pm7v89g

Conflict of Interest: JS was employed by the company Dolphin Quest.

The remaining authors declare that the research was conducted in the absence of any commercial or financial relationships that could be construed as a potential conflict of interest.

Copyright © 2019 Barratclough, Wells, Schwacke, Rowles, Gomez, Fauquier, Sweeney, Townsend, Hansen, Zolman, Balmer and Smith. This is an open-access article distributed under the terms of the Creative Commons Attribution License (CC BY). The use, distribution or reproduction in other forums is permitted, provided the original author(s) and the copyright owner(s) are credited and that the original publication in this journal is cited, in accordance with accepted academic practice. No use, distribution or reproduction is permitted which does not comply with these terms.

frontiers in Veterinary Science

BRIEF RESEARCH REPORT
published: 17 December 2019
doi: 10.3389/fvets.2019.00466

Saxitoxin Poisoning in Green Turtles (*Chelonia mydas*) Linked to Scavenging on Mass Mortality of Caribbean Sharpnose Puffer Fish (*Canthigaster rostrata*-Tetraodontidae)

*Rocío González Barrientos[1], Gabriela Hernández-Mora[2], Fernando Alegre[3], Theresa Field[4], Leanne Flewelling[5], Sara McGrath[6], Jonathan Deeds[6], Yajaira Salazar Chacón[7], Karla Rojas Arrieta[7], Emilia Calvo Vargas[8], Karen Berrocal Artavia[8] and Brian A. Stacy[9]**

[1] Section of Anatomic Pathology, Department of Biomedical Sciences, College of Veterinary Medicine, Cornell University, Ithaca, NY, United States, [2] Área de Bacteriología, Laboratorio Nacional de Servicios Veterinarios, Servicio Nacional de Salud Animal (SENASA), Ministerio de Agricultura y Ganadería, Heredia, Costa Rica, [3] Jaguar Rescue Center, Playa Chiquita, Limón, Costa Rica, [4] Ceiba Consulting Inc., Tampa, FL, United States, [5] Florida Fish and Wildlife Conservation Commission, Fish and Wildlife Research Institute, St. Petersburg, FL, United States, [6] US Food and Drug Administration, Center for Food Safety and Applied Nutrition, College Park, MD, United States, [7] Unidad de Residuos y Contaminantes en Alimentos de Origen Acuático, Servicio Nacional de Salud Animal (SENASA), Laboratorio Nacional de Servicios Veterinarios, Departamento de Inocuidad de Alimentos, Ministerio de Agricultura y Ganadería, Heredia, Costa Rica, [8] Laboratorio de Fitoplancton Marino, Escuela de Ciencias Biológicas, Estación de Biología Marina Juan Bertoglia Richards, Universidad Nacional, Puntarenas, Costa Rica, [9] National Oceanic and Atmospheric Administration, National Marine Fisheries Service, Office of Protected Resources, University of Florida, Gainesville, FL, United States

OPEN ACCESS

Edited by:
Peter James O'Brien,
University College Dublin, Ireland

Reviewed by:
Kris Helke,
Medical University of South Carolina, United States
Jennifer Landolfi,
University of Illinois at Urbana-Champaign, United States

***Correspondence:**
Brian A. Stacy
brian.stacy@noaa.gov

Specialty section:
This article was submitted to Veterinary Experimental and Diagnostic Pathology, a section of the journal Frontiers in Veterinary Science

Received: 17 October 2019
Accepted: 02 December 2019
Published: 17 December 2019

Citation:
Barrientos RG, Hernández-Mora G, Alegre F, Field T, Flewelling L, McGrath S, Deeds J, Chacón YS, Rojas Arrieta K, Vargas EC, Artavia KB and Stacy BA (2019) Saxitoxin Poisoning in Green Turtles (Chelonia mydas) Linked to Scavenging on Mass Mortality of Caribbean Sharpnose Puffer Fish (Canthigaster rostrata-Tetraodontidae). Front. Vet. Sci. 6:466. doi: 10.3389/fvets.2019.00466

Fish within the family Tetraodontidae are potential sources of both endogenous tetrodotoxins (TTXs) and dietary derived saxitoxins (STXs). Ingestion of fish tissues containing these toxins by other vertebrates can lead to severe illness and death. The Caribbean sharpnose puffer (*Canthigaster rostrata*) is a widespread tetraodontid species within the western Atlantic. Mass settlement of juveniles into foraging habitats have been associated with large-scale puffer fish mortality events. In 2013, 2014, and 2017, puffer mortality events on the southern Caribbean coast of Costa Rica were also associated with strandings of green turtles (*Chelonia mydas*) found to have fed on *C. rostrata*. Stranded sea turtles were found dead without apparent cause or alive with severe neurological signs that resolved during short periods of captivity. Puffer fish and turtle organ samples were analyzed for both TTXs and STXs. Concentrations of TTXs were extremely low in the fish (0.5–0.7 μg/g) and undetectable in turtle stomach contents. However, concentrations of STXs in whole fish (16.6–47.5 μg STX-eq/g) exceeded the 0.8 μg STX-eq/g human seafood safety threshold for STXs by orders of magnitude. Saxitoxins were also detected in samples of stomach contents (ingested fish), brain, lung, kidney, and serum from three affected turtles. Study results indicate that saxitoxicosis resulting from opportunistic foraging on *C. rostrata* during fish mortality events may be a significant factor in episodic stranding of green sea turtles in this region.

Keywords: paralytic shellfish poisoning, sea turtle, biotoxin, fish kill, stranding, neurotoxin

INTRODUCTION

The Caribbean sharpnose puffer (*Canthigaster rostrata*: Tetraodontidae) is a common reef fish found in the western Atlantic. They are omnivorous and feed on a variety of benthic invertebrates (1). Large *C. rostrata* mortality events have been described in Costa Rica and other areas of the Caribbean (2, 3). Similar mass mortality is described in another *Canthigaster* species, Bennett's sharpnose puffer (*C. bennetti*) (4). These events involve juveniles of similar size and are hypothesized to result from stress, resource limitation, diseases, or other environmental factors during mass settlement events (2–4).

The tissues of tetraodontid puffers may contain tetrodotoxins (TTXs) (5) and also the chemically similar saxitoxins (STXs) (6, 7), which may result in morbidity or death if ingested in sufficient quantity. Tetrodotoxins are found naturally in some species of puffers and are hypothesized to be derived by certain marine bacteria, whereas STXs are produced in the marine environment by select dinoflagellates of the genus *Alexandrium* and *Pyrodinium* and bioaccumulate in higher trophic levels through the food chain. The occurrence, concentration, and relative tissue distribution of TTX and STX in puffers can vary greatly by species, even within the same system (8). Both of these toxins are a well-known human seafood safety concern in products intended for human consumption (9). To our knowledge, with the exception of laboratory studies in mammals, toxicosis from ingestion of tetraodontid puffers has only been observed in humans.

During 2013, 2014, and 2017, residents of the Limón Province on the southern Caribbean coast of Costa Rica observed mass mortality of *C. rostrata* coincident with strandings of green turtles (*Chelonia mydas*). Stranded turtles were found dead or alive with abnormal neurological signs. Here we present evidence that the turtles were exposed to and suffered ill effects of STXs, and not TTX, as the result scavenging on *C. rostrata* during fish mortality events.

MATERIALS AND METHODS

Sea Turtle Evaluation and Sampling

Local residents of the Limón Province opportunistically record observations related to sea turtles and other marine life, including sea turtle strandings and other wildlife mortality. During the 2013 event, a recently deceased green sea turtle and fish samples were submitted to National Veterinary Service (SENASA) pathology laboratory for analysis. During the 2014 and 2017 events, live and deceased green turtles found during the events of this report were examined by a veterinarian from the Jaguar Rescue Center. Complete gross necropsies were performed both at SENASA and Jaguar Rescue Center on deceased turtles using standard techniques. Samples of gastric content and organs from dead turtles and puffers found on the beach were collected and frozen at −80°C until analysis.

Biotoxin Analyses

We performed biotoxin analyses at different laboratories during the years of these events based on availability to receive samples and regional capability. A description of all samples, analyses, and laboratories is provided in **Table 1**. Puffers ($n = 3$) and samples collected from affected green turtles ($n = 2$) in 2013 and 2014 were imported into the U.S. (CITES permit nos. 13US724540/9, 2014-CR432/SJ, and 2014-CR433/SJ) for analyses at the Florida Fish and Wildlife Conservation Commission, Florida Fish and Wildlife Fish and Wildlife Research Institute (FWRI) and US Food and Drug Administration, Center for Food Safety and Applied Nutrition (CFSAN). A pooled sample of approximately 10 juvenile puffers and stomach contents (partially digested puffers) from a deceased green turtle collected during a subsequent mortality event in April-May 2017 were analyzed for STXs in Costa Rica by the Unit of Residues and Contaminants in Food of Aquatic Origin of the Department of Food Safety of the National Laboratory of Veterinary Services (LANASEVE), National Service of Animal Health, Ministry of Agriculture and Livestock. In total, samples analyzed for STX included gastric contents (partially digested pufferfish) from single turtles collected during events in 2013, 2014, and 2017, serum and tissues from the turtle necropsied from the 2013 event, and analysis of puffers collected from the environment during the 2013 and 2017 events. Analysis for TTX was only conducted on puffers collected during the 2013 event.

For STX analysis at FWRI, tissues were homogenized, and 5 ml of 0.1 M HCl was added to a 5 g aliquot of each sample. The mixture was adjusted to pH 2.5–4, boiled for 5 min in a water bath, and centrifuged at 3,000 × g for 10 min. The supernatant was retained, and a 0.5 g equivalent was passed through a pre-conditioned SPE C18 cartridge (3 ml, 500 mg). The effluent was collected, the cartridge was rinsed with 2 ml deionized water, and the rinse water was combined with the effluent. Extracts were assayed for STXs using the Abraxis Saxitoxin (PSP) ELISA (enzyme-linked immunosorbent assay). Samples analyzed at LANASEVE were extracted using 0.1 M HCl as described above and were deproteinated using trichloroacetic acid (30% v/v) as described in Rourke et al. (10). At both labs, samples were analyzed using high performance liquid chromatography with fluorescence detection (HPLC-FL) and post-column oxidation (10, 11). Saxitoxin congeners were identified and quantified by comparison to certified reference solutions of saxitoxin (STX), neosaxitoxin (neoSTX), gonyautoxin-1/4 (GTX-1/4), GTX-2/3, 21-N-sulfocarbamoyl saxitoxin (GTX-5/B1), decarbamoyl saxitoxin (dcSTX), dcGTX-2/3, and C1/2 purchased from National Research Council Canada.

Analyses of puffer fish from the 2013 mortality event for both TTX and STX was conducted at CFSAN using high-performance liquid chromatography-tandem mass spectrometry (LC-MS/MS). Three fish ranging in size from 0.8 to 1.5 g were analyzed independently for toxin content by extracting twice with 10 mL each of 1% acetic acid/water through homogenization with a Polytron model PT 10–35 immersion dispenser fitted with a model PTA 20/2W generator (Kinematica, Switzerland). Combined supernatants were brought up to 20 mL with 1% acetic acid/water. Samples were then filtered by syringe fitted with a 0.22 mm filter and diluted 1:10 with 1% acetic acid/water before analyzing by LC-MS/MS. Contents from one turtle stomach collected in 2013 (30 g total) were analyzed for toxin content

TABLE 1 | Inventory of samples analyzed for saxitoxins (STXs) and tetrodotoxin (TTX) by mortality event, laboratory, and method.

Year	No. of turtle strandings	Sampled	Sample type	Laboratory	Method(s)
2013	52	Turtle ($n = 1$)	Stomach content, serum, lung, kidney, brain	FWRI, CFSAN	STX ELISA, STX-HPLC-FL[a], LC-MS/MS (STX and TTX)[a]
		Puffers ($n = 3$)	Whole—individual	FWRI, CFSAN	LC-MS/MS (STX and TTX)
2014	Unknown	Turtle ($n = 1$)	Stomach content	FWRI	STX ELISA, STX-HPLC-FL
2017	37	Turtle ($n = 1$)	Stomach content	LANASEVE	STX-HPLC-FL
		Puffers ($n = 10$)	Whole—pooled	LANASEVE	STX-HPLC-FL

Laboratories included the Florida Fish and Wildlife Conservation Commission, Florida Fish and Wildlife Fish, and Wildlife Research Institute (FWRI), US Food and Drug Administration, Center for Food Safety and Applied Nutrition (CFSAN), and Unit of Residues and Contaminants in Food of Aquatic Origin of the Department of Food Safety of the National Laboratory of Veterinary Services (LANASEVE), National Service of Animal Health, Ministry of Agriculture and Livestock. Methods included enzyme-linked immunosorbent assay (ELISA) and high-performance liquid chromatography with fluorescence detection (HPLC-FL) for detection of STXs and high-performance liquid chromatography-tandem mass spectrometry (LC-MS/MS) for detection of STXs and TTX. Stomach contents consisted of ingested puffers.

[a]*Stomach contents only.*

by homogenizing as described above followed by extraction as described in Deeds et al. (8). Due to the more complex nature of the sample, 2 g of homogenized stomach contents (containing mainly partially digested puffers) were extracted twice with 10 ml each of 1% acetic acid/methanol followed by centrifugation at 3,000 × g. Combined supernatants were taken to dryness under a stream of N_2 and reconstituted in 10 mL of 1% acetic acid/water. Two mL of the final suspension were defatted with 7 ml of chloroform by vortexing followed by centrifugation at 2,500 × g. The aqueous extract was then filtered and diluted 1:10 with 1% acetic acid/water as described above. Extracts were analyzed by LC-MS/MS using a Shimadzu Nexera X2 LC30 UPLC coupled to an 8,050 triple quadrupole mass spectrometer. The UPLC was equipped with a TSK-gel amide 80 column (2.1 × 15 cm) and operated in isocratic mode, with a mobile phase of 65% acetonitrile/35% water/50 mM formic acid/2 mM ammonium formate flowing at 0.4 mL/min. Based on initial HPLC-FL findings, the mass spectrometer was configured to monitor 3 transitions each of toxins TTX, STX, dcSTX, and GTX-5, with a single transition for each used for quantitation (m/z: 320.1 –> 161.95 for TTX, 300.1 –> 282.1 for STX, 257.1 –> 126.1 for dcSTX, 380.1 –> 300.15 for GTX-5).

Phytoplankton Analyses

Water samples were collected from the area of the puffer mortality in October 2013 (09.63847, −82.69389) and analyzed at the Laboratorio de Fitoplancton Marino, Escuela de Ciencias Biológicas, Universidad Nacional. Surface water samples were collected at 1 and 5 m and preserved with Lugol's solution. The quantitative analysis of microalgae was carried out using the Utermöhl method with 10 mL columns and an inverted microscope. The concentration of the microalgae were expressed in number of cells/L. To our knowledge, no water samples were collected during the other events.

RESULTS

Field Observations and Sampling

In September 2013, large-scale mortality involving thousands of *C. rostrata* was reported in Limón Provence, first in Punta Uva and then involving beaches in Cocles and Gandoca. Concurrent with these reports were observations of stranded green turtles and dogs and cats becoming ill after feeding on dead puffers. Based on information obtained from a local Sistema Nacional de Áreas de Conservación (SINAC) official, we estimate that approximately 52 green turtles were found stranded during the period of puffer mortality. Most were found dead and in various states of decomposition. Two live green turtles exhibiting paralysis or extreme paresis were taken into captivity and placed into shallow water to prevent drowning. Both animals recovered within 24–48 h to the degree that they could be released. Additional diagnostic evaluation and treatment was not pursued due to limited resources in the area. One juvenile male green turtle (43 cm from nuchal notch to tip of the suprapygal) in good postmortem was found floating and was collected for necropsy. This animal was in good nutritional condition and had abundant froth throughout the respiratory tract (interpreted as seawater aspiration). Multiple *C. rostrata* were found within the caudal esophagus and partially digested remains of the same species filled the stomach (**Figure 1**). Histopathological findings were regarded as incidental to the cause of death and included moderate numbers of spirorchiid trematode ova embolized within multiple tissues with mild associated histiocytic inflammation, as well as gastric and enteric lymphoplasmacytic inflammation attributable to endoparasitism.

Three additional pufferfish mortality events concurrent with green turtle strandings were reported in the same region in 2014 and 2017. Thirty-seven green sea turtles were found dead during April and May 2017 between Playa Negra de Puerto Viejo to Gandoca. Two of these animals, one very decomposed and one recently deceased, were necropsied (gross examination only) and found to have many partially digested *C. rostrata* within the esophagus and stomach. Samples of partially digested puffers from the non-decomposed turtle and a few *C. rostrata* found in the area were collected for biotoxin analysis. The other two events occurred during May 2014 and November 2017 but reliable data on numbers of turtles affected are not available. A single decomposed green turtle was collected during the 2014 event and upon necropsy *C. rostrata* were found in its stomach and

were sampled for analysis. No turtle carcasses or pufferfish were collected for analysis during the event in November 2017.

Biotoxin Analysis

Results of analyses for STXs and TTX for samples collected during all events are shown in **Tables 2** and **3**. Saxitoxins were detected in all of the turtle organs and stomach contents analyzed by ELISA, and were confirmed in turtle stomach contents and in all puffer fish analyzed using HPLC-FL or LC-MS/MS, depending on the year (**Table 1**). For both HPLC-FL and LC-MS/MS analyses of samples collected in 2013 and 2014, the saxitoxin toxin profile observed was dominated by STX (57–99%), with GTX-5 present in all samples (trace-40%), and low levels in dcSTX (trace-9%) found in all but one sample (**Tables 2**, **3**). Tetrodotoxin concentrations were extremely low in whole puffer fish, and TTX was not detected in the puffers retrieved from the stomach contents of the single green turtle collected in 2013 as determined by LC-MS/MS. In 2017 samples analyzed by LANASEVE, saxitoxin (51–57%), GTX-5 (6–9%), and dcSTX (4–6%) were also observed as well as C1 (21–25%) and C2 (9–12%) (**Table 2**).

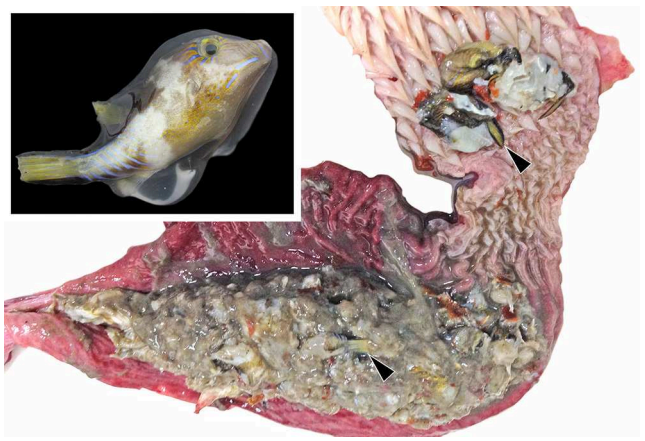

FIGURE 1 | The esophagus and stomach of a green turtle (*Chelonia mydas*) found dead during mass mortality of Atlantic sharpnose puffer fish (*Canthigaster rostrata*, inset) on the Caribbean coast of Costa Rica in November 2013. The lumen is opened showing the remains of multiple puffers, the tails of which are recognizable (arrowheads).

Phytoplankton Analyses

No algal blooms or water discoloration events were reported during the mortality events. Low concentrations (100 cells per L) of two species of dinoflagellate, *Prorocentrum micans* and *Protoperidium divergens*, were present in water samples collected near the end of the 2013 event.

DISCUSSION

Although our sample sizes were very small due to logistical constraints within the study area, we were able to identify a probable cause of the sea turtle strandings and link them with episodic mass mortality of *C. rostrata*. Our evidence includes demonstration of foraging on puffers by green turtles, detection of relatively high concentrations of STXs in the dead puffers, toxin absorption by turtles, documentation of neurological abnormalities in live stranded turtles, and exclusion of other apparent causes of sea turtle stranding based on a limited number of examined animals. Affected turtles ultimately may have died from neurological dysfunction or drowning secondary to toxicosis as evidenced in our necropsy findings. Saxitoxicosis in green turtles during these events appears to have resulted from opportunistic foraging on puffers that died or were moribund. The affected life phase of green turtle is primarily herbivorous; however, they will opportunistically consume easily available sources of fish in some circumstances and readily take fish in captivity (Stacy pers. obs).

The concentration of STXs measured in *C. rostrata* ranged from 16.64 to 47.45 μg STX-eq/g. These concentrations exceed the human seafood safety threshold (0.8 μg/g) by orders of magnitude (9) and are within the range of concentrations

TABLE 2 | Results of high-performance liquid chromatography with fluorescence detection (HPLC-FL) analyses of samples from stranded green sea turtles (*Chelonia mydas*) collected in 2013, 2014, and 2017 and puffer fish (*Canthigaster rostrata*) from 2017.

Specimen	Sample	ELISA STX eq	HPLC-FL total STX eq[a]	Toxin molar %
Turtle (2013)	Stomach content	0.69	0.53	STX 64%; GTX-5 36%; trace dcSTX
	Serum	0.05	–	–
	Lung	0.05	–	–
	Kidney	0.04	–	–
	Brain	0.04	–	–
Turtle (2014)	Stomach content	0.40	0.44	STX >99%; GTX-5 trace; dcSTX 0%
Turtle (2017)	Stomach content	–	1.93	STX 51%; C1 25%; C2 12%; GTX-5 6%; dcSTX 4%
Pooled puffer fish (2017)		–	7.86	STX 57%; C1 21%; C2 9%; GTX-5 7%; dcSTX 6%

Individual organs from turtles were first analyzed for saxitoxins (STXs) by enzyme-linked immunosorbent assay (ELISA) (reported as saxitoxin equivalents, 2013 and 2014 only). Values shown are micrograms of saxitoxins per gram of homogenized sample or per ml of serum. Dashes indicate those samples that were not analyzed using a given method.
[a]Converted using the toxicity equivalency factors of Oshima (12) of STX: 1, dcSTX: 0.51, GTX-5: 0.06, C1: 0.006, C2: 0.096.

TABLE 3 | Results of high-performance liquid chromatography-tandem mass spectrometry (LC-MS/MS) analyses of Caribbean sharpnose puffer fish (*Canthigaster rostrata*) collected during a mortality in 2013 that was concurrent with strandings of green sea turtles (*Chelonia mydas*).

Specimen	LC-MS/MS Total STX eq[a]	Toxin molar %	TTX
Puffer 1 (2013)	16.64	STX 72%; GTX-5 24%; dcSTX 4%	0.07
Puffer 2 (2013)	22.79	STX 67%; GTX-5 30%; dcSTX 3%	0.05
Puffer 3 (2013)	47.45	STX 57%; GTX-5 40%; dcSTX 3%	0.07
Ingested puffers (2013)	0.78	STX 62%; GTX-5 31%; dcSTX 7%	ND

Whole dead fish collected from the beach and ingested fish removed from the stomach of a deceased turtle were analyzed for paralytic shellfish toxins (saxitoxin [STX], decarbamoyl saxitoxin [dcSTX], and GTX-5) and tetrodotoxin (TTX). Values shown are micrograms of toxin per gram of homogenized sample (ND-not detected).

[a]*Converted using the toxicity equivalency factors of Oshima (12) of STX: 1, dcSTX: 0.51, GTX-5: 0.06.*

reported in other saxitoxin contaminated tetraodontid puffers responsible for human poisoning events (6–8). Lethal doses for STXs have not been defined for sea turtles or other reptiles, but comparative data from other taxa provide some context for our observations. Oral LD50 values for STXs in mammals and birds range from 91 to 263 μg/kg (13). Based on the average concentration of STXs detected by LC-MS/MS in homogenized fish tissues [29.0 μg STX-eq/g, calculated using experimentally derived toxicity factors for each congener as reported in (12)] and the average body weight of individual dead fish [0.9 g, (3)], ingestion of 3–9 fish per kg would provide enough toxin to reach the LD50 range determined for other taxa. We estimate that number of fish ingested by turtles easily exceeded this dose as the stomachs of necropsied turtles contained the remains of dozens of *C. rostrata* in addition to an unknown number that likely were digested beyond recognition. Toxin concentrations were lower in gastric contents than whole fish, which could reflect degradation or absorption.

Sea turtle mortality associated with STX-producing dinoflagellate blooms is reported from the Pacific coast of Mexico and Central America, and Papua New Guinea (14–17). These published accounts reported higher STX toxin concentrations in individual turtle tissues (1.16–4.78 μg STX eq/g) than STXs we detected in green turtles feeding on *C. rostrata* (approximately 0.04 μg STXs/g). Mortality due to suspected saxitoxicosis also has been reported in an estuarine turtle, the diamondback terrapin (*Malaclemys terrapin*), with lower concentration of STXs (0.002–0.12 μg STX eq/g) than we detected in green turtle tissue and gastric contents (18). The differences in toxin concentrations among reports could be attributable to methodology, metabolism, as well as dose, timing, and duration of exposure. Data are too limited at this time to inform interpretation of toxin values alone with regard to toxicological effect; rather they serve to demonstrate toxin exposure that should be interpreted in the context of clinical signs, postmortem findings, and environmental data.

Due to their genetic resistance to TTX and STX (19), tetraodontid puffer fish are potential reservoirs of both STXs and TTXs (8). The biological origin of STX in puffer fish has not been defined, but may result from ingestion of toxin-containing prey species or STX-producing dinoflagellates (7). Studies have measured these toxins in puffers caught for research or consumption; there are no reported ill effects on the fish themselves.

To our knowledge, no STX-producing blooms were reported during the period and area of our observations and water samples associated with the 2013 event did not contain STX-producing dinoflagellates; however, sampling was very limited, and we were unable to find any other available data on phytoplankton monitoring for these areas. Documented STX producers in the Caribbean Sea include *Pyrodinium bahamense*, *Gymnodinium catenatum,* and *Alexandrium tamarense* (20, 21). Notably, the limited STX profile observed in 2013 and 2014 samples (STX, dcSTX, and GTX-5) correspond to a similar report of STX accumulation in southern puffers (*Sphoeroides nephalus*) in Florida, USA responsible for human poisonings (7). This report linked STXs in southern puffers to blooms of the dinoflagellate *Pyrodinium bahamense* based on co-occurrence and the similar toxin composition in both algae and puffer tissues. The profiles reported in 2017 samples also included C1 and C2, which may indicate a different PSP species played a role in this event. The Landsberg et al. (7) study showed that STX containing *S. nephalus* retained toxicity in captivity for an extended period, suggesting that the STX observed in *C. rostrata* reported here could have originated from an undetected dinoflagellate bloom that occurred prior to the mortality events.

The cause of episodic or periodic mass mortality of *C. rostrata* has not been specifically defined but may be related to mass recruitment of juveniles into foraging areas, as has been reported in other tetraodontid puffers (3, 4). This mortality may be part of species natural history; however, reports of mortality during mass settlement of various fishes cite other considerations in need of further study, including diseases and environmental factors (3, 22).

Our report describes a unique pathway of saxitoxin exposure, linking mass mortality of a common reef fish and biotoxin reservoir with morbidity and death of scavenging sea turtles. Additionally, saxitoxin poisoning has not been previously documented in sea turtles in the Caribbean. Further studies of the drivers of *C. rostrata* mass mortality and opportunistic scavenging by green turtles, as well as the sources of the STXs themselves, are needed in order to better understand the occurrence of these events.

DATA AVAILABILITY STATEMENT

All datasets generated for this study are included in the article/supplementary material.

ETHICS STATEMENT

The animal study was reviewed and approved by University of Florida Institutional Care and Use Committee.

AUTHOR CONTRIBUTIONS

All authors contributed to data and sample collection and review and preparation of the manuscript. Sample and data analyses were conducted by BS, LF, RB, GH-M, SM, JD, YC, KR, KA, and EV.

ACKNOWLEDGMENTS

We are grateful to the residents of Limón Province for sharing observations and assisting stranded sea turtles. We greatly appreciate the efforts Jaguar Rescue Center, SENASA, and LANASEVE staff for their work with animals, samples, and laboratory analyses. Furthermore, we thank the Archie Carr Center for Sea Turtle Research and Natalia Corrales of Parque Marino del Pacifico for invaluable assistance with CITES permits.

REFERENCES

1. Randall JE. Reef fish, food habits. *Stud Trop Oceanogr.* (1967) 5:655–847.
2. Jordán-Garza AG, Díaz-Almeyda EM, Iglesias-Prieto R. Mass mortality of *Canthigaster rostrata* at the northeast coast of the Yucatan Peninsula. *Coral Reefs.* (2009) 28:661. doi: 10.1007/s00338-009-0492-x
3. Piedra-Castro L, Araya-Vargas A. Mass mortality of *Canthigaster rostrata* (Tetraodontiformes: *Tetraodontidae*) on the southern Costa Rican Caribbean coast. *Rev Mar Cost*. (2018) 10:31–7.doi: 10.15359/revmar.10-1.2
4. Vail AL, Sinclair-Taylor T. Mass schooling and mortality of *Canthigaster bennetti* in Sulawesi. *Coral Reefs.* (2011) 30:251. doi: 10.1007/s00338-010-0706-2
5. Bane V, Lehane M, Dikshit M, O'Riordan A, Furey A. Tetrodotoxin: chemistry, toxicity, source, distribution and detection. *Toxins.* (2014) 6:693–755. doi: 10.3390/toxins6020693
6. Abbott JP, Flewelling LJ, Landsberg JH. Saxitoxin monitoring in three species of Florida puffer fish. *Harmful Algae.* (2009) 8:343–8. doi: 10.1016/j.hal.2008.07.005
7. Landsberg JH, Hall S, Johannessen JN, White KD, Conrad SM, Abbott JP, et al. Saxitoxin Puffer fish poisoning in the United States, with the first report of *Pyrodinium bahamense* as the putative toxin source. *Environ Health Perspect*. (2006) 114:1502–7. doi: 10.1289/ehp.8998
8. Deeds JR, White KD, Etheridge SM, Landsberg JH. Concentrations of saxitoxin and tetrodotoxin in three species of puffers from the Indian River Lagoon, Florida, the location for multiple cases of saxitoxin puffer poisoning from 2002-2004. *Trans Am Fish Soc*. (2008) 137:1317–26. doi: 10.1577/T07-204.1
9. US Department of Health, and Human Services Food and Drug Administration Center for Food Safety and Applied Nutrition (2019). *Fish and Fishery Products Hazards and Controls Guidance.* 4th ed. Available online at: https://www.fda.gov/food/seafood-guidance-documents-regulatory-information/fish-and-fishery-products-hazards-and-controls-guidance (accessed October 14, 2019).
10. Rourke A, Murphy CJ, Pitcher G, van de Riet JM, Burns BG. Rapid postcolumn methodology for determination of paralytic shellfish toxins in shellfish tissue. *J AOAC Int*. (2008) 91:589–97.
11. Van de Riet J M, Gibbs RS, Chou FW, Muggah PM, Rourke WA, Burns G, et al. Liquid chromatographic post-column oxidation method for analysis of paralytic shellfish toxins in mussels, clams, scallops, and oysters: single-laboratory validation. *J AOAC Int*. (2009) 92:1690–704.
12. Oshima Y. Postcolumn derivation liquid chromatographic method for paralytic shellfish toxins. *J AOAC Int*. (1995) 78:528–32.
13. Llewellyn LE. Saxitoxin, a toxic marine natural product that targets a multitude of receptors. *Nat Prod Rep*. (2006) 23:200–22. doi: 10.1039/b501296c
14. Maclean JL. Red tide and paralytic shellfish poisoning in Papua New Guinea. *Papua New Guinea Agricult J*. (1975) 24:131–8.
15. Licea S, Navarrete A, Rodriguez R, Bustillos J, Martínez B. Monitoring a bloom of *Pyrodinium bahamense* var. *compressus* occurring in El Salvador, Guatemala and Mexico (November 2005-March 2006). In: Moestrup Ø, Doucette G, Enevoldsen H, Godhe A, Hallegraeff G, Luckas B, Lundholm N, Lewis J, Rengefors K, Sellner K, Steidinger K, Tester P, Zingone A, editors. *International Society for the Study of Harmful Algae and Intergovernmental Oceanographic Commission of UNESCO, Proceedings of the 12th International Conference on Harmful Algae.* Copenhagen (2008). p. 219–20.
16. Meave del Castillo ME, Rodríguez R, Vargas M. Blooms of *Pyrodinium bahamense* var. *compressum* along the Pacific coast of Central America and southern Mexico. In: Moestrup Ø, Doucette G, Enevoldsen H, Godhe A, Hallegraeff G, Luckas B, Lundholm N, Lewis J, Rengefors K, Sellner K, Steidinger K, Tester P, Zingone A, editors. *Proceedings of the 12th International Conference, Harmful Algae, International Society for the Study of Harmful Algae and Intergovernmental Oceanographic Commission of UNESCO.* Copenhagen (2008). p. 212–5.
17. Amaya O, Quintanilla R, Stacy BA, Dechraoui Bottein MY, Flewelling L, Hardy R, et al. Large-scale sea turtle mortality events in El Salvador attributed to paralytic shellfish toxin-producing algae blooms. *Front Mar Sci*. (2018) 5:411. doi: 10.3389/fmars.2018.00411
18. Hattenrath-Lehmann TK, Ossiboff RJ, Burnell CA, Rauschenberg CD, Hynes K, Burke RL, et al. The role of a PSP-producing Alexandrium bloom in an unprecedented diamondback terrapin (*Malaclemys terrapin*) mortality event in Flanders Bay, New York, USA. *Toxicon.* (2017) 129:36–43. doi: 10.1016/j.toxicon.2017.02.006
19. Jost MC, Hillis DM, Lu Y, Kyle JW, Fozzard HA, Zakon HH. Toxin-resistant sodium channels: parallel adaptive evolution across a complete gene family. *Mol Biol Evol*. (2008) 25:1016–24. doi: 10.1093/molbev/msn025
20. Usup G, Ahmad A, Matsuoka K, Lim PT, Leaw CP. Biology, ecology and bloom dynamics of the toxic marine dinoflagellate *Pyrodinium bahamense*. *Harmful Algae*. (2012) 14:301–12. doi: 10.1016/j.hal.2011.10.026
21. Cuellar-Martinez T, Ruiz-Fernández AC, Alonso-Hernández C, Amaya-Monterrosa O, Quintanilla R, Carrillo-Ovalle HL, et al. Addressing the problem of harmful algal blooms in Latin America and the Caribbean- a regional network for early warning and response. *Front Mar Sci*. (2018) 5:409. doi: 10.3389/fmars.2018.00409
22. Stier AC, Idjadi JA, Geange SW, White JS. High mortality in a surgeonfish following an exceptional settlement event. *Pac Sci*. (2013) 67:533–8. doi: 10.2984/67.4.4

Disclaimer: The statements and findings are those of the authors and do not necessarily reflect the view of NOAA or the US Department of Commerce. Mention of products and trade names does not imply endorsement by the US Government.

Conflict of Interest: TF works for Ceiba Consulting, Inc.

The remaining authors declare that the research was conducted in the absence of any commercial or financial relationships that could be construed as a potential conflict of interest.

Copyright © 2019 Barrientos, Hernández-Mora, Alegre, Field, Flewelling, McGrath, Deeds, Chacón, Rojas Arrieta, Vargas, Artavia and Stacy. This is an open-access article distributed under the terms of the Creative Commons Attribution License (CC BY). The use, distribution or reproduction in other forums is permitted, provided the original author(s) and the copyright owner(s) are credited and that the original publication in this journal is cited, in accordance with accepted academic practice. No use, distribution or reproduction is permitted which does not comply with these terms.

frontiers in Veterinary Science

CASE REPORT
published: 20 December 2019
doi: 10.3389/fvets.2019.00476

Skeletal and Cardiac Rhabdomyolysis in a Live-Stranded Neonatal Bryde's Whale With Fetal Distress

Nakita Câmara, Eva Sierra, Antonio Fernández, Cristian Manuel Suárez-Santana, Raquel Puig-Lozano, Manuel Arbelo and Pedro Herráez*

Department of Veterinary Histology and Pathology, Veterinary School, Institute of Animal Health and Food Safety, University of Las Palmas de Gran Canaria, Las Palmas de Gran Canaria, Spain

The main objective of wildlife forensic investigation is to recognize pathologic changes and cause of death. Even though it may not always be possible to determine the specific illness and/or etiology, the description and subsequent interpretation of the injuries provide an invaluable understanding of pathology in cetacean post-mortem investigations. Although pathological studies have been previously reported in various cetacean species, such descriptions of the infraorder *Mysticeti* remain rare. A live-stranded neonatal Bryde's whale (*Balaenoptera edeni*) which subsequently died soon after the stranding, was assessed by physical exam, blood examination, gross necropsy evaluation, histopathology, and immunohistochemistry. It presented with elevated serum levels of creatine kinase, cardiac troponin I, urea, and creatinine. Microscopically, we observed keratin spicules (squamous epithelial cells) and areas of atelectasis in the lungs. Acute degeneration in the myocytes and cardiomyocytes were comparable to the findings previously described in cases of capture myopathy in live-stranded cetaceans. Immunohistochemistry biomarkers such as myoglobin, fibrinogen, and troponin were analyzed. Skeletal and myocardial damage has been documented in several cetacean species. However, this is the first reported case of skeletal and cardiac rhabdomyolysis associated with live-stranding in a newborn Bryde's whale that suffered from fetal distress.

Keywords: Bryde's whale (*Balaenoptera edeni*), cetaceans, rhabdomyolysis, live-stranding, *Mysticeti*, neonate, stress cardiomyopathy

OPEN ACCESS

Edited by:
Robert James Ossiboff, University of Florida, United States

Reviewed by:
Michael Thomas Walsh, University of Florida, United States
Molly E. Church, University of Pennsylvania, United States

****Correspondence:***
Eva Sierra
eva.sierra@ulpgc.es

Specialty section:
This article was submitted to Veterinary Experimental and Diagnostic Pathology, a section of the journal Frontiers in Veterinary Science

Received: *12 August 2019*
Accepted: *05 December 2019*
Published: *20 December 2019*

Citation:
Câmara N, Sierra E, Fernández A, Suárez-Santana CM, Puig-Lozano R, Arbelo M and Herráez P (2019) Skeletal and Cardiac Rhabdomyolysis in a Live-Stranded Neonatal Bryde's Whale With Fetal Distress. Front. Vet. Sci. 6:476. doi: 10.3389/fvets.2019.00476

BACKGROUND

Pathological study of wildlife fauna has the disadvantage of an unknown clinical history of the animal. The complexity is enhanced in cetaceans because of the difficulty of performing clinical exams and/or other analyses on live animals. The most feasible technique for health assessment in dead cetaceans is by detection of injuries in these animals, through pathological study. The importance of these studies is recognized worldwide to promote conservation of these animals. Unfortunately, the description of pathological entities and/or causes of death in the infraorder *Mysticeti* remains rare (1–8).

Live-stranding is a pathological state with severe acute stress and physical damage central to its etiopathogenesis. It presents clinical and traumatic findings that can cause death of the animal, or can seriously aggravate an existing condition over the period of stranding, capture, handling, restraint, transportation and/or captivity (1, 2, 9–15). The response mechanisms and resultant damage to multiple systems involved in live-stranded cetaceans are comparable to exertional rhabdomyolysis (capture myopathy) in many animals, including birds and terrestrial or marine wild mammals (1, 9–11, 14, 16). Although pathological findings may vary among individuals, biochemical changes and histopathological lesions, consisting of ischemia-reperfusion injuries, are often observed. These changes result in local-to-generalized vasospasms and vasodilation (catecholamine surge, neurogenic shock, and impeded venous flow return by body compression), which is analogous to the stress cardiomyopathy in humans and in direct traumatic injury to muscles, resulting in acute to subacute degeneration (rhabdomyolysis). Acute renal failure associated with myoglobinuric nephrosis secondary to muscle damage and areas of necrosis in viscera are also observed (1, 9, 10, 12, 16–27).

In both wild and captive cetaceans, neonatal mortality is a recognized concern (28–31). The main causes of stranding and/or death in newborns are related with problems in pregnancy (abortion, prematurity), childbirth (fetal distress, dystocia), nursing (missed transfer of passive immunity), behavior (maternal-filial separation/maternal neglect), or intra and interspecific interactions with a fatal outcome. All these above are enclosed in the category of neonatal and/or perinatal pathologies (1, 2). In the case of asphyxia, the fetus responds with redistribution of the blood flow, which limits the deleterious effects of oxygen deprivation in vital organs. This enables the fetus to survive intact unless the asphyxia is profound or prolonged (32).

This report describes the biochemical analysis and gross, histopathological, histochemical, and immunohistochemical features in a live-stranded neonatal Bryde's whale.

CASE PRESENTATION

Stranding Circumstances

A 393-cm-long newborn male Bryde's whale was stranded on the coast of Fuerteventura, Canary Island, Spain, in September 2016. Observations between the high and low tide revealed that the animal appeared to be alive and few meters from the coast. At low tide, the animal was stranded on the beach and died before specialized assistance could be given.

Biochemical Analysis

A sample of whole blood was collected from the tail flukes, immediately post-mortem, for analysis of the serum. Biochemical markers of acute skeletal and heart muscle damage, creatine kinase (CK 460.0 U/L), and cardiac troponin I (0.20 μg/L), were analyzed. Kidney function was also assessed via blood urea nitrogen (BUN 162 mg/dL) and creatinine (2.4 mg/dL).

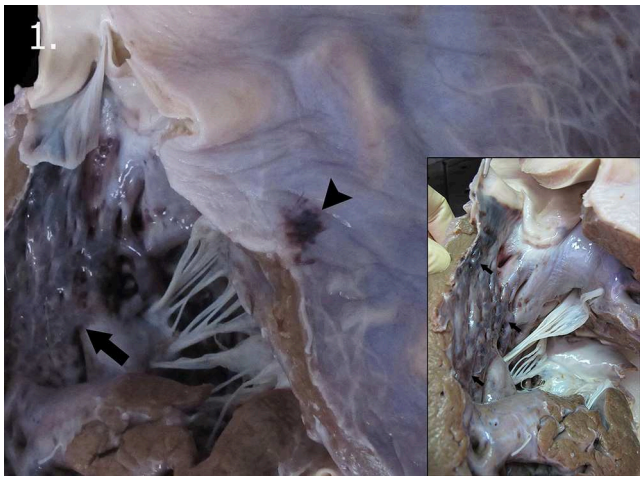

FIGURE 1 | Macroscopic vascular changes observed in the heart. Subepicardial (arrow head) and subendocardial hemorrhage (arrow) in the left ventricle. Detail of the subendocardial hemorrhages present in the left ventricle (arrows).

Gross Anatomic Analysis

A thorough necropsy was performed on the calf, following the standard protocol published by the European Society of Cetaceans and with the addition of some procedures detailed in the *Marine Mammals Ashore* manual, to determine the cause of death (14, 33). The animal was in poor body/nutritional condition with several linear erosions, distributed in a multifocal manner on the ventral abdomen (attributed to direct active stranding damage). While several vestigial hairs were noted in the lateral part of the maxilla, the navel was not healed and contained an internal white exudate. During dissection of the subcutaneous planes, moderate diffuse hemorrhages were observed, especially in the ventral region. The muscles were pale yellow-to-orange. The epiglottis was flaccid at the rostral level, the trachea showed mild-to-moderate foam, and the main and secondary bronchi and bronchioles presented abundant foam, representing pulmonary edema. Both lungs had multifocal and local extensive areas of dark reddish color and were firm (compatible with pulmonary atelectasis). Mild-to-moderate exudation of blood was noted at the incision. Some serous fluid was detected in the pericardial space. On sectioning, both ventricles presented moderate-to-severe subepicardial and subendocardial hemorrhage (**Figure 1**). The ductus arteriosus was also present. Moderate and diffuse mucosal congestion was observed in the stomach, liver, bladder, sclera, and meningeal and subarachnoid vessels. The cerebellum displayed moderate and diffuse congestion, edema, and mild-to-moderate hemorrhage.

Histopathological Analysis

Representative tissue samples were fixed in 10% formalin for ∼48 h and processed using standard protocol. The skeletal (*longissimus dorsi* and *rectus abdominis*) and heart muscles (both atria and ventricles), atrioventricular valves (bicuspid or mitral and tricuspid), semilunar valves (sigmoid, aortic, and

pulmonary with the corresponding arteries), and kidneys were examined for the potential presence of rhabdomyolysis and myoglobinuric nephrosis. Tissue sections (4-μm-thick) were used for hematoxylin and eosin and periodic Acid-Schiff staining, while 5-μm-thick layers were used for phosphotungstic acid, hematoxylin, and Masson's trichrome techniques.

On histopathologic and histochemical examinations, the skeletal and heart muscles presented with injuries consistent with vascular changes (i.e., hemorrhages and interstitial edema) and acute degenerative lesions (i.e., contraction band necrosis, wavy fibers, segmental hypercontraction, hypereosinophilia, cytoplasmic vacuolization, and nuclear pyknosis). Contraction band necrosis was observed in the *longissimus dorsi* and *rectus abdominis* (**Figure 2A**). Long and thin undulated fibers (wavy fibers) were noted (**Figure 2A**). Hypereosinophilia (**Figures 2B,C**) was usually associated with either segmental hypercontraction or segmental necrosis. The above-mentioned changes in the skeletal muscle were moderate and illustrated a multifocal pattern with smaller diameter fibers (presumably type I fibers). Atria and ventricles displayed a multifocal, moderate-to-severe degree of interstitial edema, wavy fibers, hypereosinophilia, and cytoplasmic vacuolization with pyknotic nucleus (**Figure 2D**). Both ventricles demonstrated mild-to-moderate, multifocal, subepicardial, and subendocardial hemorrhage (**Figure 2E**).

Additional histopathological findings include (a) discrete capsular hemorrhage and mild-to-moderate, diffuse congestion in the kidneys with (b) mild, multifocal dilatation of the renal tubules; (c) in the lungs, severe, multifocal presence of keratin spicules (squamous epithelial cells) in alveolar spaces (**Figure 2F**) and (d) severe, multifocal, local extensive areas of atelectasis and moderate, multifocal alveolar hemorrhages; (e) severe, diffuse macro and microvacuolar degeneration (hyaline globules) in the hepatocytes; (f) moderate, focal suppurative omphalitis with the presence of coccoid bacterial colonies in the most superficial areas of the navel, (g) mild congestion and hemorrhage in multiple organs.

Immunohistological Analysis

Tissue sections (3 μm thick) were immunolabeled with anti-myoglobin (skeletal and cardiac muscles, and the kidneys), anti-fibrinogen (skeletal and cardiac muscles), anti-cardiac troponin I (cardiac muscle), and anti-cardiac troponin C (cardiac muscle) primary antibodies. They were visualized using the VECTASTAIN® Elite ABC-Peroxidase Kit (PK-6100) from Vector Laboratories (Peterborough, United Kingdom). The immunohistochemical methodology is summarized in **Supplementary Table 1**. The negative control for the latter consisted of serial sections of the heart without the primary antibody. In contrast, the positive control for myoglobin and fibrinogen were from a cetacean heart sample of a striped dolphin (*Stenella coeruleoalba*). The dolphin had been stranded alive and developed CM owing to capture and human interaction during the rehabilitation process (9, 10). Heart samples from a pig and cetacean, with no apparent acute macroscopic and/or histological lesions, were used as positive controls for cardiac troponin I and cardiac troponin C.

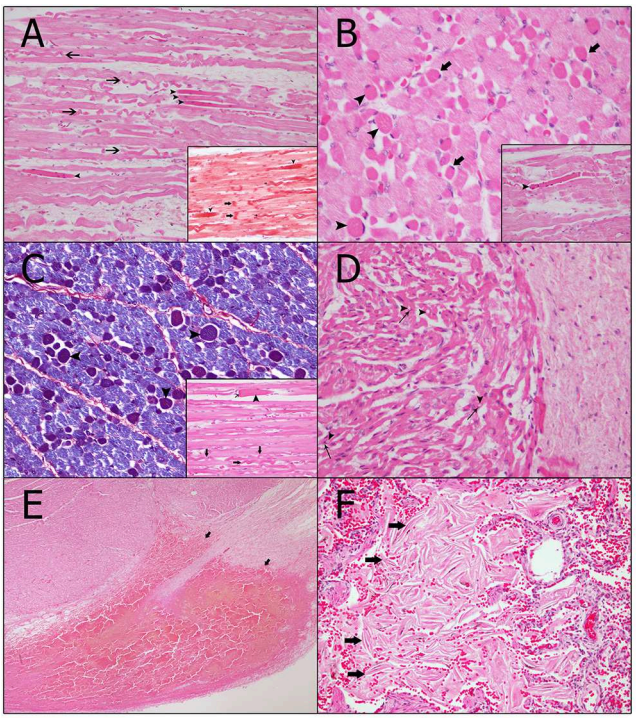

FIGURE 2 | Vascular and acute degenerative changes observed in the skeletal and heart muscles. **(A)** Long and thin undulated fibers, also referred to as wavy fibers (arrows), can be seen in the myocytes. In addition, the myocytes demonstrate hypereosinophilia, i.e., an increase in staining of necrotic muscular cells (arrow heads) with different histochemical techniques, which is usually associated with segmental hypercontraction (arrow heads) (hematoxylin and eosin technique, magnification: 40×). Inset: The contraction band necrosis (arrows) runs transversely throughout the myocytes and is identified via the increasing red color intensity (Masson's trichrome technique). Furthermore, both hypereosinophilia and wavy fibers can be observed (thin arrows) (magnification: 40×). **(B)** In the transversal cut, myocytes of minor caliber (most likely type I fibers) are affected and present hypereosinophilia with segmental hypercontraction (arrow heads). Moreover, endomysia edema (thin arrows) can be seen (hematoxylin and eosin technique, magnification: 60×). Inset: Detail of the segmental hypercontraction of a myocyte (hematoxylin and eosin technique, magnification: 40×). **(C)** More intense blue coloring of the damaged myocytes of minor caliber, which identifies hypereosinophilia and segmental hypercontraction (arrow heads) (phosphotungstic acid hematoxylin technique, magnification: 40×). Inset: Detail of a myocyte with segmental hypercontraction (arrow head) and segmental necrosis of the fiber with the retraction cap (thin arrow). Wavy fibers can also be observed (arrows) (hematoxylin and eosin technique, magnification: 40×). **(D)** Cardiomyocytes show vacuolar degeneration (arrow heads) and pyknotic nucleus (thin arrows) (hematoxylin and eosin technique, magnification: 40×). **(E)** Vascular changes present in the heart consistent with a subepicardial hemorrhage in the left ventricle (arrows) (hematoxylin and eosin technique, magnification: 4×). **(F)** Detail of the intra-alveolar keratin spicules (arrows) (hematoxylin and eosin technique, magnification: 40×).

Immunohistochemically, the degenerated/necrotic muscular and heart cells showed homogenous, intrafibrillar depletion of cardiac troponin I, cardiac troponin C (**Figure 3A**), and myoglobin. Damaged cells from the skeletal and cardiac muscles were found to exhibit several concentrations of immunolabeling for fibrinogen (**Figure 3B**). The kidneys did not exhibit any accumulation of myoglobin.

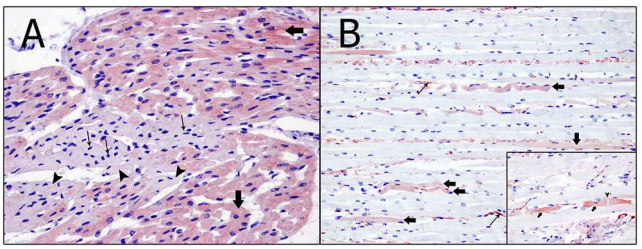

FIGURE 3 | Immunohistochemical techniques in skeletal and heart muscles. **(A)** Degenerated/necrotic cardiomyocytes (arrow heads), with pyknotic nucleus (thin arrows), show intrafibrillar depletion of cardiac troponin C. In contrast, normal cardiomyocytes (arrows) present an intense immunolabeling (immunohistochemical technique: anti-troponin C, magnification: 60×). **(B)** Expression of fibrinogen (arrows) in the myocytes presenting changes, including wavy fibers, hypereosinophilia and segmental hypercontraction. Immunolabeling of fibrinogen in the interior of the blood vessels can also be seen (thin arrows) (immunohistochemical technique: anti-fibrinogen, magnification: 40×). Inset: Necrotic myocytes (arrows) strongly expressed alongside the contraction band necrosis (arrow head) and inside the blood vessels (thin arrows) (immunohistochemical technique: anti-fibrinogen, magnification: 40×).

DISCUSSION

Discussion of the Animal Characteristics

Cetacean newborns/neonates are defined as having a compatible total length, displaying "fetal folds" over the body, soft and folded dorsal fin and tail flukes, vibrissal hairs or vibrissal crypts, and a healing (or closing) navel (34). Our animal was 393 cm long, slightly under the normal range (395–430 cm) (35). The animal did not present any "fetal folds" but we identified some vibrissal hairs; the navel was not healed and contained inflammatory exudate. This suggested an infection after birth; therefore, the animal would most likely be a few days old (34).

Discussion of the Biochemical Results

Clinico-pathological evaluation was challenging in this case as biochemical values, such as that for cardiac troponin I, are rarely reported. They may not exist in the scientific database for various species of cetaceans, particularly the infraorder *Mysticeti*. Our biochemical data was compared with published papers assessing different mammals, including humans, dogs, and other species of cetaceans [e.g., bottlenose dolphins (*Tursiops truncatus*) belonging to the infraorder *Odontoceti* and a stranded baby gray whale (*Eschrichtius robustus*) of the infraorder *Mysticeti*]; this is summarized in **Table 1** (13, 36–39).

In concordance with the results obtained from other species (i.e., 107–255 U/L in a neonatal gray whale), injury to the skeletal muscle was supported by an increase in CK (460 U/L), which is one of the useful indicators of both skeletal and cardiac muscle damage (12, 13, 16, 39–41). After myocardial injury, CK begins to rise in 4 to 9 h, peaks at 24 h, and returns to baseline 48 to 72 h after the stress event (42). This increase in CK was correlated with histological and immunohistochemical changes, thus supporting the presence of muscle damage.

Cardiac troponin I, measured by conventional assays, is elevated in >90% of patients with stress cardiomyopathy (43).

TABLE 1 | Comparison between the biochemical results of the studied animal and normal laboratory values of other mammals.

	Class *Mammalia*							
	Order *Primates*	**Order *Carnivora***		**Order *Cetartiodactyla***				
	Suborder *Haplorhini*			**Suborder *Cetacea***				
	Infraorder *Simiformes*			**Infraorder *Odontoceti***		**Infraorder *Mysticeti***		
	Family *Hominidae*	**Family *Canidae***		**Family *Delphinidae***		**Family *Eschrichtiidae***	**Family *Balaenopteridae***	
	HUMANS (*Homo sapiens*) (17)	**DOG (*Canis lupus familiaris*) (19, 20)**		**BOTTLENOSE DOLPHIN (*Tursiops truncatus*) (9)**		**NEONATAL GRAY WHALE (*Eschrichtius robustus*) (9)**	**NEONATAL BRYDE'S WHALE (*Balaenoptera edeni*)**	
				Captive (*n* = 38)	**Wild Atlantic Juvenile (*n* = 96)**	**Stranded (*n* = 1)**	Stranded (n = 1)	
Creatine Kinase (U/L)	30–170	0–190		100–250	47–455	107–255		**460**
Troponin I (μg/L)	≤0.1	≤0.03–0.07		ND	ND	ND		**0.20**
Blood Urea Nitrogen (mg/dL)	8–20	7–20.72		42–58	42–77	21–75		**162**
Creatinine (mg/dL)	0.7–1.3	0.44–1.595		1.0–2.0	0.68–1.49	1.0–2.0		**2.4**

Our animal presented with 0.20 μg/L cardiac troponin I in the serum; this is higher than the reference values in both humans (≤0.1 μg/L) and dogs (≤0.03–0.07 μg/L) (36–38). The release of troponin from injured cardiomyocytes usually occurs 3 to 9 h after ischemic damage, peaks in 12 to 48 h, and remains elevated for 4 to 7 days (42, 44, 45). Hence, the above laboratory values cannot aid in early detection of myocardial necrosis (1–3 h). These markers do not assist in accurate diagnosis until 6 or more hours after the onset of the event. In order to obtain a satisfactory clinical picture in humans, blood should be drawn 6–9 h after the onset of the stress event and/or symptom onset (44). The increase in cardiac troponin I serum levels and the decrease in myocyte troponin immunoreaction is caused by the early release of cardiac troponin I and troponin C by damaged cardiomyocytes. This was verified by immunohistochemistry (22, 46).

In this case, pre-renal azotemia is likely related to hypovolemic shock, and was reasonably supported by higher BUN values (162 mg/dL) than the reference values from the other species (i.e., 21 to 75 mg/dL in the stranded gray whale). Hypovolemic shock can be originated by a relative decrease in the effective circulating volume without a loss of total body fluid (i.e., decreased in venous return) and/or a direct intravascular fluid loss (i.e., dehydration or hemorrhage) (12, 40). In our case, we can associate this clinical finding with various causes, such as compartment syndrome, heart failure, and dehydration. Moreover, creatinine was slightly above (2.4 mg/dL) the normal values seen in other species (i.e., 1.0 to 2.0 mg/dL in a stranded neonatal gray whale). In order to confirm the hypothesis that the increase in creatinine we observed could be within the normal ranges for the Bryde's whale species, more accurate age and species-specific normal values would be needed. Small elevation of creatinine and high levels of urea can be associated with pre-renal azotemia caused by dehydration. This is a possible interpretation for our case. Since dehydration is associated with prolonged fasting, it is important to consider this aspect in stranded animals, especially young ones (47).

Discussion of the Histopathological Results

With the anatomopathological findings, the morphological diagnoses include (1) severe multifocal fetal atelectasis with presence of severe multifocal keratin spicules and a moderate alveolar hemorrhage; (2) multifocal moderate-to-severe acute degeneration of cardiomyocytes; (3) moderate multifocal acute skeletal muscle degeneration; and (4) mild congestion and hemorrhage in various organs.

Atelectasis is a relatively frequent finding in fetal and neonatal (*atelectasis neonatorum*) deaths (perhaps associated with aspiration of amniotic fluid or meconium), it is found incidentally or in non-specific forms in young or adult individuals (1, 48–50). In contrast, pulmonary edema with intra-alveolar keratin spicules (*pulmonary vernix caseosa*), either isolated or in aggregates of stratified epithelium, keratinized and with nuclear retention, can be observed in fetal distress. Considering non-specific findings, without knowledge of the primary cause, and after discarding lesions compatible with other etiological diagnoses, we considered the macro and microscopic findings as a whole to be typical of fetal distress (1).

Acute degenerative changes, such as contraction band necrosis, were observed in both the *longissimus dorsi* and the *rectus abdominis*. This represents a skeletal and myocardial lesion characteristic of transient ischemia and reperfusion, which is associated with high concentrations of endogenous catecholamines (23, 51, 52). This condition has been reported in humans after stressful events, as well as in other animals after acute death, including seals and cetaceans (1, 9–12, 16–23, 53–56). Wavy fibers were also detected in the skeletal and heart muscles. Considering that they are the first histologic abnormality associated with ischemia, this condition may be used as a morphological indicator of early myocardial injury (9–11, 22, 23, 53, 57). In addition, hypereosinophilia was observed in the skeletal and cardiac muscles, respectively. Animals that die following a stressful situation present with this cytoplasmic alteration (9–11, 22, 53, 57, 58). The animal also presented with vacuolization in the cardiomyocytes. Previous studies commonly associate this with areas that experience severe, chronic, and fatal ischemia as a result of acute death due to stressful situations (11, 22, 53, 59).

Vascular changes, including congestion, interstitial edema, and hemorrhage, are generally detected through histological approaches and form part of the stress cardiomyopathy pathology (17). In the current case, all the heart sections showed separated fibers, with interstitial edema. Following the introduction of catecholamines, interstitial edema is usually associated with subendocardial and subepicardial hemorrhage, found in both ventricles of this neonate (57). These lesions are occasionally detected in humans with stress cardiomyopathy and have been previously demonstrated in animals that died after live-stranding and handling (1, 9, 10, 17, 20).

The sequence of changes in an acute ischemic injury begins within 5 min. The myocardium reveals long, thinned, wavy fibers separated by spaces, characterizing edema and microvascular congestion at the borders of the ischemic myocardium. In 2 to 3 h, early changes of cardiomyocyte coagulation necrosis with nuclear pyknosis, color change, more specifically "brick red change" or cytoplasm hypereosinophilia, focal contraction bands, and subtle interstitial edema are evident. Hypereosinophilia and edema become more pronounced and more easily recognizable 3 to 6 h after the event. Six to 12 h later changes accelerate and more extensive contraction band necrosis with reperfusion is noted (25). Based on the acute degenerative findings in both skeletal and cardiac muscle of our case, we propose that the ischemic injury, which caused these lesions, occurred between 6 and 12 h prior to death, coinciding with the live-stranding.

Discussion of the Immunohistochemical Results

Previous studies demonstrated the necessity of corroborating histopathological findings with specific markers to better determine the amount of damage present in cells. The immunohistochemical confirmation ante-mortem showed depletion of myoglobin, cardiac troponin I, and cardiac troponin C as well as intrafibrillar fibrinogen deposition (9, 10, 12, 22, 45, 58, 60–63). Depletion of myoglobin (a

marker used for skeletal and cardiac damage), troponin I and C (specific markers to detect injury to the heart), as well as accumulation of fibrinogen (used to identify skeletal and cardiac damage) in injured cells was confirmed in the present study.

Although this animal presented with clinical and pathological findings resembling rhabdomyolysis, which can lead to a secondary myoglobinuric nephrosis, lesions associated with acute kidney injury (i.e., intrinsic kidney disease/ damage or acute tubular necrosis) were not detected through the histopathological and immunohistochemical studies (1, 9, 10, 12, 16–27, 64).

Discussion of the Cause of Death

Considering the biochemical results and the macro and microscopic findings which concur with the etiological diagnoses of fetal distress and skeletal and cardiac rhabdomyolysis, we propose that the most probable cause of death in this animal is active stranding pathology which aggravated a previous neonatal/perinatal pathology.

The active stranding pathology is defined by a set of lesions and biochemical findings in animals that were stranded alive and leads to both a catecholaminergic crisis (stress cardiomyopathy) and multi-organ ischemic-reperfusion damage with rhabdomyolysis with myoglobinuric nephrosis secondary to muscle damage. The severity of this syndrome usually causes the death of the animal, occasionally as a result of the intensification of preexisting pathologies (1, 9, 10, 22).

Neonatal/perinatal pathology in cetaceans comprises a wide constellation of etiologic factors, including fetal distress (1, 2). A severe disturbance in the oxygen supply to the fetus can have effects on the newborn's cardiac function. Elevated levels of cardiac troponin I, cardiac troponin T, CK and its fraction MB can be observed in full-term infants after intrauterine hypoxia and respiratory distress (65). Limited studies have shown premature infants and various breeds of stillborn cow calves to present with acute degenerative changes, such as myocardial necrosis, which may result from antepartum or intrapartum asphyxia (hypoxia) (65–67).

CONCLUSIONS

Although we cannot confirm that the elevated serum values (CK, cTnI, BUN, and creatinine) were due to post stranding or fetal distress, but based on the histological findings, we can conclude that these lesions are due to live stranding. Therefore, we suggest that the animal assessed here probably died because of an exacerbation of preceding injuries (fetal distress) and the final complications of stranding. Since description of pathological entities and/or causes of death in the *Mysticeti* infraorder is still scarce, we consider this article to be an important contribution to improve conservation efforts by reducing the mortality of these animals.

DATA AVAILABILITY STATEMENT

All data reported in this work is classified and stored in the tissue bank of the Institute of Animal Health and Food Safety (IUSA), Veterinary School, University of Las Palmas de Gran Canaria (ULPGC).

ETHICS STATEMENT

Ethical review and approval was not required for the animal study because no experiments were performed on live animals. Required permission for the management of stranded cetaceans was issued by the environmental department of the Canary Islands' Government and the Spanish Ministry of Environment. No experiments were performed on live animals.

AUTHOR CONTRIBUTIONS

NC wrote the article, collected the blood sample, performed the necropsy of the animal, and contributed toward the biochemical analysis, gross, histological, histochemical, and immunohistological description and diagnosis of the case. ES and PH contributed toward the biochemical analysis, gross, histological, histochemical, and immunohistological description and diagnosis of the case, and guided NC during the drafting and publication processes. AF, CS-S, RP-L, and MA performed the necropsy of the animal and contributed toward the gross and histological description and diagnosis of the case. All authors read and approved the final manuscript.

FUNDING

This study was part of a Ph.D. thesis of the Universidad de Las Palmas de Gran Canaria (ULPGC) supported by the Ministry of Economy and Competitiveness (MINECO) through a predoctoral grant for training of research personnel (BES-2016-076907). Furthermore, this research work was part of the National Project titled Embolic Pathology (gas/fat) in cetaceans supported by the Ministry of Economy and Competitiveness (MINECO) (CGL2015-71498-P) as well as part of the Project titled Stress Cardiomyopathies in Cetaceans supported by the Ministry of Science, Innovation and Universities, and subsided by the Government of Gran Canaria (CABILDO2018: CABILDO2018-04). Finally, the Canary Islands Government funded and provided support to the stranding research network.

ACKNOWLEDGMENTS

We would like to thank all the people who indirectly participated in the production of this work, including the staff of the Animal Lab, our laboratory technician, all the members and volunteers of the Cetacean Stranding Network, as well as Marisa Tejedor and the associated non-governmental organization (SECAC) who collaborated in the necropsy.

SUPPLEMENTARY MATERIAL

The Supplementary Material for this article can be found online at: https://www.frontiersin.org/articles/10.3389/fvets.2019.00476/full#supplementary-material

REFERENCES

1. Díaz-Delgado J, Fernández A, Sierra E, Sacchini S, Andrada M, Vela AI, et al. Pathologic findings and causes of death of stranded cetaceans in the Canary Islands (2006-2012). *PLoS ONE.* (2018) 13:e0204444. doi: 10.1371/journal.pone.0204444
2. Arbelo M, Los Monteros AE, Herráez P, Andrada M, Sierra E, Rodríguez F, et al. Pathology and causes of death of stranded cetaceans in the Canary Islands (1999-2005). *Dis Aquat Organ.* (2013) 103:87–99. doi: 10.3354/dao02558
3. Cornaglia E, Rebora L, Gili C, Di Guardo G. Histopathological and immunohistochemical studies on cetaceans found stranded on the Coast of Italy between 1990 and 1997. *J Vet Med Ser A.* (2000) 47:129–42. doi: 10.1046/j.1439-0442.2000.00268.x
4. Kemper C, Flaherty A, Gibbs S, Hill M, Long M, Byard RW. Cetacean captures, strandings and mortalities in South Australia 1881-2000, with special reference to human interactions. *Aust Mammal.* (2005) 27:37–47. doi: 10.1071/AM05037
5. Martineau D, Lagacé A, Béland P, Higgins R, Armstrong D, Shugart LR. Pathology of stranded beluga whales (*Delphinapterus leucas*) from the St. Lawrence Estuary, Québec, Canada. *J Comp Pathol.* (1988) 98:287–310. doi: 10.1016/0021-9975(88)90038-2
6. Dhermain F, Soulier L, Bompar J-M. Natural mortality factors affecting cetaceans in the Mediterranean Sea. *Cetaceans Mediterr Black Seas State Knowl Conserv Strateg A Rep to ACCOBAMS Secr Monaco* (2002).
7. McAloose D, Rago MV, Di Martino M, Chirife A, Olson SH, Beltramino L, et al. Post-mortem findings in southern right whales Eubalaena Australis at Península Valdés, Argentina, 2003-2012. *Dis Aquat Organ.* (2016) 119:17–36. doi: 10.3354/dao02986
8. Groch KR, Díaz-Delgado J, Marcondes MCC, Colosio AC, Santos-Neto EB, Carvalho VL, et al. Pathology and causes of death in stranded humpback whales (*Megaptera novaeangliae*) from Brazil. *PLoS ONE.* (2018) 13:e0194872. doi: 10.1371/journal.pone.0194872
9. Herráez P, Espinosa de los Monteros A, Fernández A, Edwards JF, Sacchini S, Sierra E. Capture myopathy in live-stranded cetaceans. *Vet J.* (2013) 196:181–8. doi: 10.1016/j.tvjl.2012.09.021
10. Herráez P, Sierra E, Arbelo M, Jaber JR, Espinosa De Los Monteros A, et al. Rhabdomyolysis and myoglobinuric nephrosis (Capture Myopathy) in a striped dolphin. *J Wildl Dis Wildl Dis Assoc.* (2007) 43:770–4. doi: 10.7589/0090-3558-43.4.770
11. Cowan DF, Curry BE. Histopathology of the alarm reaction in small odontocetes. *J Comp Pathol.* (2008) 139:24–33. doi: 10.1016/j.jcpa.2007.11.009
12. Bonsembiante F, Centelleghe C, Rossi G, Giglio S, Madeo E, Gelain ME, et al. Clinico-pathological findings in a striped dolphin (*Stenella coeruleoalba*) affected by rhabdomyolysis and myoglobinuric nephrosis (capture myopathy). *J Vet Med Sci.* (2017) 79:1013–18. doi: 10.1292/jvms.17-0023
13. Gulland FMD, Dierauf LA, Whitman KL. *CRC Handbook of Marine Mammal Medicine*. Florida, FL: CRC Press (2018).
14. Geraci JR, Lounsbury VJ. *Marine Mammals Ashore: A Field Guide for Strandings*. Baltimore, MD: National Aquarium (2005).
15. Wilkinson DM. *Report to Assistant Administrator for Fisheries: Program Review of the Marine Mammal Stranding Networks* (1991).
16. Seguel M, Paredes E, Pavés H, Gottdenker NL. Capture-induced stress cardiomyopathy in South American fur seal pups (*Arctophoca australis gracilis*). *Mar Mammal Sci.* (2014) 30:1149–57. doi: 10.1111/mms.12079
17. Jiang JP, Downing SE. Catecholamine cardiomyopathy: review and analysis of pathogenetic mechanisms. *Yale J Biol Med.* (1990) 63:581–91.
18. Kawai S. Pathology of takotsubo (ampulla) cardiomyopathy. In: Veselka J, editor. *Cardiomyopathies - From Basic Research to Clinical Management*. London: IntechOpen (2012). p. 709–26. doi: 10.5772/29050
19. Maréchaux S, Fornes P, Petit S, Poisson C, Thevenin D, Le Tourneau T, et al. Pathology of inverted takotsubo cardiomyopathy. *Cardiovasc Pathol.* (2008) 17:241–3. doi: 10.1016/j.carpath.2007.08.002
20. Mitchell A, Marquis F. Can takotsubo cardiomyopathy be diagnosed by autopsy? Report of a presumed case presenting as cardiac rupture. *BMC Clin Pathol.* (2017) 17:4. doi: 10.1186/s12907-017-0045-0
21. Miura M, Kawano H, Yoshida T, Yamagata Y, Nakata T, Koga S, et al. The histological features of a myocardial biopsy specimen in a patient in the acute phase of reversible catecholamine-induced cardiomyopathy due to pheochromocytoma. *Intern Med.* (2017) 56:665–71. doi: 10.2169/internalmedicine.56.7454
22. Câmara N, Sierra E, Fernández-Maldonado C, Espinosa de los Monteros A, Arbelo M, Fernández A, et al. Stress cardiomyopathy in stranded cetaceans: a histological, histochemical and immunohistochemical study. *Vet Rec.* (2019) 185:694. doi: 10.1136/vr.105562
23. Fineschi V, Michalodimitrakis M, D'Errico S, Neri M, Pomara C, Riezzo I, et al. Insight into stress-induced cardiomyopathy and sudden cardiac death due to stress. a forensic cardio-pathologist point of view. *Forensic Sci Int.* (2010) 194:1–8. doi: 10.1016/j.forsciint.2009.10.025
24. Spraker T. Stress and capture myopathy in artiodactylids. *Zoo Wild Anim Med Curr Ther.* (1993).
25. Buja LM, Butany J. *Cardiovascular Pathology*. Elsevier Science (2015). Available at: https://books.google.es/books?id=rdqcBAAAQBAJ
26. Buja LM. Myocardial ischemia and reperfusion injury. *Cardiovasc Pathol.* (2005) 14:170–5. doi: 10.1016/j.carpath.2005.03.006
27. Sachdeva J, Dai W, Kloner RA. Functional and histological assessment of an experimental model of takotsubo's cardiomyopathy. *J Am Heart Assoc.* (2019) 3:e000921. doi: 10.1161/JAHA.114.000921
28. Mann J, Connor RC, Barre LM, Heithaus MR. Female reproductive success in bottlenose dolphins (Tursiops sp.): life history, habitat, provisioning, and group-size effects. *Behav Ecol.* (2000) 11:210–9. doi: 10.1093/beheco/11.2.210
29. Wells R, Scott M, Irvine AB. The social structure of free-ranging bottlenose dolphins. In: Genoways HH, editor. *Current Mammalogy*. New York, NY: Springer Science; Business Media, LLC (1987). p. 247–305. doi: 10.1007/978-1-4757-9909-5_7
30. Sweeney J, Stone R, Campbell M, McBain J, Leger J, Xitco M, et al. Comparative survivability of tursiops neonates from three U.S. institutions for the decades 1990-1999 and 2000-2009. *Aquat Mamm.* (2010) 36:248–61. doi: 10.1578/AM.36.3.2010.248
31. Flower J, Langan J, Nevitt B, Chinnadurai S, Stacey R, Ivančić M, et al. Neonatal critical care and hand-rearing of a bottlenose dolphin (*Tursiops truncatus*) calf. *Aquat Mamm.* (2018) 43:482–90. doi: 10.1578/AM.44.5.2018.482
32. Parer JT, Livingston EG. What is fetal distress? *Am J Obstet Gynecol.* (1990) 162:1421–7. doi: 10.1016/0002-9378(90)90901-I
33. Kuiken T, Hartmann MG. *Proceedings of the First ECS Workshop on Cetacean Pathology: Dissection Techniques and Tissue Sampling: Leiden, the Netherlands, 13-14 September 1991*. European Cetacean Society (1991).
34. Puig-Lozano R, Bernaldo de Quirós Y, Díaz-Delgado J, García-Álvarez N, Sierra E, De la Fuente J, et al. Retrospective study of foreign body-associated pathology in stranded cetaceans, Canary Islands (2000–2015). *Environ Pollut.* (2018) 243:519–27. doi: 10.1016/j.envpol.2018.09.012
35. Perrin WF, Würsig BG, Thewissen JGM. *Encyclopedia of Marine Mammals*. Amsterdam; Boston, MA: Elsevier/Academic Press (2009).
36. Padilla O *Texas THSC. Normal Laboratory Values: Blood, Plasma, and Serum*. Available online at: https://www.msdmanuals.com/professional/resources/normal-laboratory-values/blood-tests-normal-values#v8508814
37. Sleeper MM, Clifford CA, Laster LL. Cardiac troponin I in the normal dog and cat. *J Vet Intern Med.* (2001) 15:501–3. doi: 10.1111/j.1939-1676.2001.tb01582.x
38. Wray J. *Canine Internal Medicine: What's Your Diagnosis?*. Oxford: John Wiley & Sons (2017).
39. Reidarson T, Mcbain J, Yochem P. Medical and nutritional aspects of a rehabilitating California gray whale calf. *Aquat Mamm.* (2001) 27:215–21.
40. Stockham SL, Scott MA. *Fundamentals of Veterinary Clinical Pathology*. Iowa: John Wiley & Sons (2013).
41. St Aubin DJ, Austin TP, Geraci JR. Effects of handling stress on plasma enzymes in harp seals, *Phoca groenlandica*. *J Wildl Dis.* (1979) 15:569–72. doi: 10.7589/0090-3558-15.4.569
42. Lewandrowski K, Chen A, Januzzi J. Cardiac markers for myocardial infarction: a brief review. *Am J Clin Pathol Pathol Patterns Rev.* (2002) 118:93–9. doi: 10.1309/3EK7-YVV9-228C-E1XT
43. Lyon AR, Bossone E, Schneider B, Sechtem U, Citro R, Underwood SR, et al. Current state of knowledge on takotsubo syndrome: a position statement

from the taskforce on takotsubo syndrome of the heart failure association of the European society of cardiology. *Eur J Heart Fail.* (2016) 18:8–27. doi: 10.1002/ejhf.424
44. Khan MS. Diagnostic efficacy of cardiac troponin in post-mortem examination of acute myocardial infarction. *Int J Eth Trauma Vict.* (2015) 1:2. doi: 10.18099/ijetv.v1i1.27
45. Hansen SH, Rossen K. Evaluation of cardiac troponin I immunoreaction in autopsy hearts: a possible marker of early myocardial infarction. *Forensic Sci Int.* (1999) 99:189–96. doi: 10.1016/S0379-0738(98)00193-5
46. Mikaelian I, Coluccio D, Morgan KT, Johnson T, Ryan AL, Rasmussen E, et al. Temporal Gene expression profiling indicates early up-regulation of interleukin-6 in isoproterenol-induced myocardial necrosis in rat. *Toxicol Pathol.* (2008) 36:256–64. doi: 10.1177/0192623307312696
47. Cubas ZS, Silva JCR, Catão-Dias JL. *Tratado de Animais Selvagens: Medicina Veterinária*. São Paulo: Roca (2014).
48. Moore MJ, Knowlton A, Kraus S, Mclellan WA, Bonde R. Morphometry, gross morphology and available histopathology in North Atlantic right whale (eubalaena glacialis) mortalities. J Cetac Res Manage. (2004) 6:199–214.
49. Fernández A, Edwards JF, Rodríguez F, de los Monteros AE, Herráez P, Castro P, et al. "Gas and fat embolic syndrome" involving a mass stranding of beaked whales (Family Ziphiidae) exposed to anthropogenic sonar signals. *Vet Pathol.* (2005) 42:446–57. doi: 10.1354/vp.42-4-446
50. Alstrup AKO, Hedayat A, Jensen TH, Hammer AS, Munk OL, Jensen HE. Necropsy report of a fin whale (*Balaenoptera physalus*) stranded in Denmark in 2010. *Aquat Mamm.* (2013) 39:385. doi: 10.1578/AM.39.4.2013.385
51. Reichenbach DD, Benditt EP. Catecholamines and cardiomyopathy: the pathogenesis and potential importance of myofibrillar degeneration. *Hum Pathol.* (1970) 1:125–50. doi: 10.1016/S0046-8177(70)80007-7
52. Turnbull BS, Cowan DF. Myocardial contraction band necrosis in stranded cetaceans. *J Comp Pathol.* (1998) 118:317–27. doi: 10.1016/S0021-9975(07)80007-7
53. Cowan DF, Curry BE. *Histopathological Assessment of Dolphins Necropsies Onboard Vesssels in the Eastern Tropical Pacific Tuna Fishery*. La Jolla, CA: Southwest Fisheries Science Center, National Marine Fisheries Service, NOAA (2002). p. 31.
54. Akashi YJ, Nef HM, Möllmann H, Ueyama T. Stress cardiomyopathy. *Annu Rev Med.* (2010) 61:271–86. doi: 10.1146/annurev.med.041908.191750
55. Pascual I, Abó AI, Piqué M. Hallazgos histológicos en el síndrome de takotsubo. *Rev Española Cardiol.* (2015) 68:625. doi: 10.1016/j.recesp.2014.08.013
56. Lyon AR, Rees PS, Prasad S, Poole-Wilson PA, Harding SE. Stress (Takotsubo) cardiomyopathy—A novel pathophysiological hypothesis to explain catecholamine-induced acute myocardial stunning. *Nat Clin Pract Cardiovasc Med.* (2008) 5:22–9. doi: 10.1038/ncpcardio1066
57. Fishbein MC. Early evolution from ischemia to myocardial necrosis. *Cardiovasc Toxicol.* (2001) 1:83–6. doi: 10.1385/CT:1:2:083
58. Sierra E, Fernández A, de los Monteros A, Arbelo M, Díaz J, Andrada Borzollino M, et al. Histopathological muscle findings may be essential for a definitive diagnosis of suspected sharp trauma associated with ship strikes in stranded cetaceans. *PLoS ONE.* (2014) 9:e88780. doi: 10.1371/journal.pone.0088780
59. Adegboyega PA, Haque AK, Boor PJ. Extensive myocytolysis as a marker of sudden cardiac death. *Cardiovasc Pathol.* (1996) 5:315–21. doi: 10.1016/S1054-8807(96)00041-5
60. Ortmann C, Pfeiffer H, Brinkmann B. A comparative study on the immunohistochemical detection of early myocardial damage. *Int J Legal Med.* (2000) 113:215–20. doi: 10.1007/s004149900094
61. Xiaohong Z, Xiaorui C, Jun H, Qisheng Q. The contrast of immunohistochemical studies of myocardial fibrinogen and myoglobin in early myocardial ischemia in rats. *Leg Med.* (2002) 4:47–51. doi: 10.1016/S1344-6223(01)00054-2
62. Martínez-Díaz F, Rodríguez-Morlensín M, Pérez-Cárceles MD, Noguera J, Luna A, Osuna E. Biochemical analysis and immunohistochemical determination of cardiac troponin for the postmortem diagnosis of myocardial damage. *Histol Histopathol.* (2005) 20:475–81. doi: 10.14670/HH-20.475.
63. Fishbein MC, Wang T, Matijasevic M, Hong L, Apple FS. Myocardial tissue troponins T and I: an immunohistochemical study in experimental models of myocardial ischemia. *Cardiovasc Pathol.* (2003) 12:65–71. doi: 10.1016/S1054-8807(02)00188-6
64. Malkina A. *Acute Kidney Injury (AKI).* San Francisco, CA: University of California. Available online at: ttps://www.msdmanuals.com/professional/genitourinary-disorders/acute-kidney-injury/acute-kidney-injury-aki?query=acute kidney injury
65. Correale M, Nunno L, Ieva R, Rinaldi M, Maffei G, Biase RM, et al. Troponin in newborns and pediatric patients. *Cardiovasc Hematol Agents Med Chem.* (2009) 7:270–8. doi: 10.2174/187152509789541927
66. Murray RD, Williams AJ, Sheldon IM. Field investigation of perinatal mortality in friesian cattle associated with myocardial degeneration and necrosis. *Reprod Domest Anim.* (2008) 43:339–45. doi: 10.1111/j.1439-0531.2007.00911.x
67. Waldner CL, Kennedy RI, Rosengren LB, Pollock CM, Clark ETG. Gross postmortem and histologic examination findings from abortion losses and calf mortalities in western Canadian beef herds. *Can Vet J La Rev Vet Can.* (2010) 51:1227–38.

Conflict of Interest: The authors declare that the research was conducted in the absence of any commercial or financial relationships that could be construed as a potential conflict of interest.

Copyright © 2019 Câmara, Sierra, Fernández, Suárez-Santana, Puig-Lozano, Arbelo and Herráez. This is an open-access article distributed under the terms of the Creative Commons Attribution License (CC BY). The use, distribution or reproduction in other forums is permitted, provided the original author(s) and the copyright owner(s) are credited and that the original publication in this journal is cited, in accordance with accepted academic practice. No use, distribution or reproduction is permitted which does not comply with these terms.

frontiers in Veterinary Science

ORIGINAL RESEARCH
published: 31 January 2020
doi: 10.3389/fvets.2020.00033

Cutaneous Lesions in Freshwater Turtles (*Emydura macquarii krefftii* and *Myuchelys latisternum*) in a Rainforest Creek in North Queensland, Australia

Wytamma Wirth[1], *Elizabeth Elliott*[2†], *Donna Rudd*[1], *Linda Hayes*[1], *Alicia Maclaine*[1], *Narges Mashkour*[1], *Shamim Ahasan*[1,3], *Jakob Gorm Dahl*[1], *Kezia Drane*[1] *and Ellen Ariel*[1*]

[1] College of Public Health, Medical and Veterinary Sciences, James Cook University, Douglas, QLD, Australia, [2] AusPhage, Rasmussen, QLD, Australia, [3] Faculty of Veterinary and Animal Sciences, Hajee Mohammad Danesh Science and Technology University, Rangpur, Bangladesh

OPEN ACCESS

Edited by:
Robert James Ossiboff,
University of Florida, United States

Reviewed by:
Hannah Bender,
Taronga Conservation Society Australia, Australia
Mark S. Flint,
The Ohio State University, United States

***Correspondence:**
Ellen Ariel
ellen.ariel@jcu.edu.au

†Present address:
Elizabeth Elliott,
Australian Crayfish Hatchery, Mount St John, QLD, Australia

Specialty section:
This article was submitted to Veterinary Experimental and Diagnostic Pathology, a section of the journal Frontiers in Veterinary Science

Received: 26 September 2019
Accepted: 14 January 2020
Published: 31 January 2020

Citation:
Wirth W, Elliott E, Rudd D, Hayes L, Maclaine A, Mashkour N, Ahasan S, Gorm Dahl J, Drane K and Ariel E (2020) Cutaneous Lesions in Freshwater Turtles (Emydura macquarii krefftii and Myuchelys latisternum) in a Rainforest Creek in North Queensland, Australia. Front. Vet. Sci. 7:33. doi: 10.3389/fvets.2020.00033

Freshwater turtles inhabit most rivers and creeks on the east coast of Australia, but some species are only found in specific catchments, which makes them vulnerable to extinction. During annual fieldtrips to Alligator Creek, North Queensland, the resident population of *Myuchelys latisternum* and *Emydura macquarii krefftii* in a natural pond, just outside Bowling Green National Park, have been surveyed for a number of years and demographic data recorded against tagged turtles. Rounded, cutaneous lesions on individual animals were first noted in August 2016, three years after the first survey of the population. Turtles living in the upstream sections of the creek were not affected. An initial investigation into the cause of the lesions ruled out pollutants and although the bacterial communities appeared to be different on turtles with lesions, a causative agent was not identified. Attempts to isolate virus in culture was not successful and specific PCRs for ranavirus, papillomavirus, adenovirus and herpesvirus did not identify their presence. Blood biochemical parameters, body condition and activity levels were not significantly different between affected turtles and those without lesions. The turtles in this pond were monitored regularly over the following three years with 249 *M. latisternum* and 192 *E. m. krefftii* captured, tagged and released. The prevalence of the lesions fluctuated with season from 0 to 77 and 68% respectively, but did not vary significantly between species or sex in adults. There was a tendency for larger animals to be more likely to have lesions. The position of the lesions on the turtles was mostly on dorsal surfaces, distally on the legs and proximal on the tales of males, indicating that the initial lesion may have been associated with a behaviourally induced trauma. Recaptured animals ($n = 43$) during this period, provided records of lesion progression over time and while some healed up between capture events, others persisted for up to 24 months. Some turtles were repeatedly captured without lesions. Intra-species aggression associated with seasonal behaviours could potentially be the primary cause of skin trauma, followed by a secondary invasion of an unusual pathogen present in the environment.

Keywords: freshwater turtles, cutaneous lesions, disease, wildlife, outbreak

INTRODUCTION

Freshwater turtles are vulnerable to many human and natural factors and a systematic analysis of tortoise and freshwater turtle global distribution identified coastal Australia as one of three areas of priority for freshwater turtle conservation (1). In Australia, there are 25 species of freshwater turtles, 11 of which have a conservation status of vulnerable or worse (2). Most of the Australian freshwater turtles belong to the family Chelidae that retract their neck and head under the shell by folding it to one side and are therefore referred to as side-necks (3). They are a totem animal in some Indigenous Australian cultures and although they are collected and consumed, such traditional harvest is not of conservation concern (4). The major risks to Australia turtles include: invasive species, drought, habitat modification, and disease (2).

Due to their longevity and close association with the aquatic environment, freshwater turtles can be considered indicators of aquatic environmental health. In addition to being sentinel species for long term pollution exposure, they are also at risk of habitat loss or degradation, invasive species and diseases among other threats (5–8). The limited range of many Australian freshwater turtle species and the risk of extirpation from any of the abovementioned threats, means that conservation is a very real and urgent issue. Recently, the vulnerability of the range restricted Bellinger River Snapping Turtle (*Myuchelys georgesi*), became apparent when a novel disease affecting the turtles drove the population close to extinction in <1 month (9, 10) and highlights the need for a focus on factors affecting the health of Australian freshwater turtles.

In August 2016, cutaneous lesions were noted on a proportion of freshwater turtles captured as part of regular monitoring of wild living turtles in Alligator Creek, North Queensland. Here we report on the characteristics of the lesions, the spatial and temporal extent of the epidemic and the impact on the population through a longitudinal study.

MATERIALS AND METHODS

All handling of turtles were carried out under permits from James Cook University (JCU) Animal Ethics Committee (A2309) and Department of Environment and Science (WISP13270413 and WA0012830).

Study Site

For the past six years in July/August the JCU Turtle Health Research Team has monitored a pond on Alligator Creek just outside the Bowling Green Bay National Park for freshwater turtle presence, demographics and general health. Alligator Creek originates in the Mt Elliott complex, inside the national park, where there is no industry, agriculture or human dwellings. The pond of interest, the Craill pond, is a hollow in the bedrock, ∼30 m at the widest part, 90 m at its longest and 5 m at its deepest. Alligator Creek runs into and out of this pond. The Craill pond is inhabited by two species of turtles, *Emydura macquarii krefftii* and *Myuchelys latisternum* and a number of freshwater fish species as well as freshwater crustaceans and crocodiles (*Crocodylus johnstoni*). No unusual natural or anthropogenic event preceded the first observations of lesions in this population of turtles.

Turtles

Approximately 50 turtles are captured annually by a combination of baited cathedral traps (passive sampling) and hand-capture (active sampling) to minimize any bias that might arise due to using only one method. *Emydura macquarii krefftii* tend to frequent the downstream reaches of large river systems or creeks, where they forage in the water and are considered omnivorous (11). *Myuchelys latisternum* are chiefly carnivorous and inhabit mainly the headwaters of rivers and tributaries, but can also be found in lagoons and billabongs (11). Both species can grow to 30 cm curved carapace length (CCL) and have a life-span of 20–30 years (12). In early August 2016, during the annual fieldtrip, cutaneous lesions on the soft tissue were recorded in the neck and tail region and on legs and feet of turtles ($n = 15/50$).

Fieldtrips

Field monitoring of the Craill pond (Site 5) was continued at intervals during the next 2 years. Any turtle above 15 cm CCL was tagged with a small titanium tag (National Wing Tags, Jiffy 893) in the webbing of one of the hind-feet and re-captures could therefore be identified and disease progression recorded if relevant. Morphometrics of captured turtles and records of cutaneous lesions were collected from the turtles captured. The size at which male tails start to elongate varies between species and individuals (12). Turtles less than the median CCL of the 10 smallest identifiable males of each species were classed as juveniles, unless their tail was obviously differentiated (13). Physical examinations were performed on all captured turtles, this process included: freshwater leech counts, eye/oral/nasal examination, soft-tissue exam for swelling or bruising, activity level (high, medium, low), damage to shell or missing claws, and adult female turtles were palpated for eggs to assess breeding status. Disease investigation as well as water quality monitoring were also performed to develop an understanding of the etiology of the lesions.

Spatial Pattern

In order to determine the spatial extent of this disease, turtle populations in four ponds upstream from Site 5 were also investigated during September/October 2016, starting with the pond at the highest elevation above mean sea level that the terrain allowed access to (Site 1). The five sites were at least 1 km apart and between 10 and 25 m difference in elevation (https://www.freemaptools.com/elevation-finder.htm), with Site 1 being at the highest elevation and the downstream sites gradually lower. See **Table 1** for GPS location and elevation of study sites. To avoid spreading an un-identified agent upstream, we disinfected all equipment with 5% bleach after each site and moved in a downstream direction between sites on any given day. Turtle populations downstream from Site 5 were not investigated as it is assumed that they will be exposed via the flow to a given pathogen in the water (14). Additionally, the creek below this

TABLE 1 | GPS locations and elevation in meters (m) above mean sea level for the five sites investigated for lesions on turtles following the outbreak at Site 5 in July 2016.

Site	Latitude	Longitude	Elevation	Description
1	−19.4456	146.9746	95	Pond
2	−19.4417	146.9623	82	Pond
3	−19.4408	146.9541	69	Stream
4	−19.4367	146.9477	44	Pond
5	−19.429	146.9437	34	Pond

pond is frequented by saltwater crocodiles, which makes trapping and underwater hand capture too risky.

Environmental Measurements

Conductivity, pH, and macro invertebrate counts and identity were recorded in the Craill pond when the lesions were first noticed (Site 5), as well as upstream from the outbreak. Air temperature historical data for the nearest weather station at Cape Ferguson was obtained from the Australian Bureau of Meterology (www.bom.gov.au) and mapped against proportion of turtles with lesions on the various fieldtrips.

Data Analysis

All analysis was performed using the Statsmodels module (version 0.10.0) and Pandas library (0.24.2) in Python 3.6 (15, 16). Chi Square tests were used to compare the proportion on turtles (post-outbreak) with lesions in each species, sex and age class. The association of CCL with probability of having lesions (odds-ratio) was calculated by logistic regression. Pearson correlation was used to determine the relationship between mean maximum air temperature and the portion of animals with lesions grouped by month of capture.

Laboratory Analysis

Pathology

With permission from relevant authorities, one male *E. m. krefftii* (14.0 cm CCL; 235 g), one male *M. latisternum* (14.8 cm CCL; 280 g) and one juvenile *M. latisternum* (12.0 cm CCL; 145 g) with lesions, were euthanized with MS222 according to Conroy et al. (17). A full necropsy and pathology investigation was performed, with emphasis on the lesions, but samples from all internal organs were collected from all three turtles. Samples were preserved in 10% neutral buffered formalin, embedded in paraffin, sectioned at 5 μm and stained with Haematoxylin and Eosin as well as Gomori's Methenamine-Silver (GMS), Ziehl-Neilsen (ZN), and Periodic Acid-Schiff (PAS) stains for examination (18).

Bacterial Culture and Initial Identification

Swab samples were collected in the field from 20 lesions of affected turtles and chins of 20 turtles without lesions. These areas were rinsed well with sterile saline before being sampled using dry swabs. Swab samples were also taken directly from liver, spleen, heart and heart blood during necropsy. All samples were immediately cultured on a range of media including Sheep Blood Agar (non-selective, aerobic and anaerobic) and MacConkey (selective for Gram negative bacteria) using standard culture methods. Bacterial identifications were determined using Biolog system and API20NE according to the manufacturer's instructions. All incubations were performed at 28 and 37°C for 48 h.

Bacterial Identification by Sequencing

Bacterial isolates that could not be identified using traditional methods were extracted to isolate genomic DNA using High Pure PCR Template Preparation Kit Version 20 (Cat. 11796828001 Roche, NSW) and Lysozyme (Cat. 10837059001 Roche, NSW) as per manufacturer's instructions. The concentrations of the resulting purified DNA samples were quantified using a Qubit 2.0 fluorimeter (Invitrogen) prior to storage in a −20°C freezer. The bacterial 16S rRNA gene was amplified with a set of universal primers, 27F and 1391R (5′-AGAGTTTGATCMTGGCTCAG-3′ and 5′-GACGGGCGGTGTGTRCA-3′; 1350bp) under standard PCR conditions consisting of an initial denaturation of 1 min at 95°C; followed by 30 cycles of denaturation at 95°C for 30 s; annealing at 55°C for 15 s; extension at 72°C for 15 s; and final elongation step at 72°C for 5 min. The PCR products were run on a 1.5% agarose gel to confirm amplification. Following confirmation, the PCR products were sent to Macrogen Inc., Seoul, South Korea for Sanger sequencing. Later, the nucleotide sequences were processed and aligned in Geneious (Biomatters Ltd.) followed by identification using NCBI nucleotide BLAST (https://blast.ncbi.nlm.nih.gov/Blast.cgi).

Blood Biochemical Parameters

Blood was collected in the field (1 ml) from the femoral vein of 20 turtles with and 20 without lesions using a 1 ml syringe and 27 gauge needle into a lithium heparin paediatric tube. The samples were transported back to the JCU Pathology Laboratory on ice. The samples were separated as soon as possible and the plasma samples stored frozen (−20°C) until analysed within 24 h on an automated Clinical Biochemistry analyser (Beckman Coulter AU480). The blood biochemical parameters were assessed and analysed using a student *T*-Test to determine significant difference in biochemical parameters associated with presence and absence of skin lesions and severity of infection.

Viral Culture

Samples from select organs (lung, spleen, liver, kidney and heart) from the turtles that underwent necropsy were stored at −80°C for viral isolation. Samples were homogenised with 1 ml Dulbecco's modified Eagle's medium (DMEM) supplemented with 100X Antibiotic-Antimycotic and subjected to three freeze/thaw cycles at −20°C before clarification by centrifugation at 12,000 rpm for 5 min. The swabs from lesions were soaked in the same culture medium and treated similar to the necropsy samples. A total of 500 μl supernatant from each sample was added to 80% confluent monolayers of FHM (fathead minnow) cells in a 24-well tissue culture plate (SARSTEDT®). The plates were incubated at 25°C and checked daily for cytopathic effects. Two blind passages were performed for each sample at weekly

intervals, by transferring 100 µl of cell culture supernatant from inoculated wells to corresponding wells with new, non-infected FHM cell monolayers on a separate plate.

Viral Molecular Investigation

DNA extraction was carried out on swabs from lesions by NucleoMag® VET DNA isolation Kit (Macherey-Nagel) according to manufacturer's protocol. PCR was performed on lesion swabs using primers for various viral infections. The swabs were screened for herpesvirus, adenovirus, papillomavirus and ranavirus genome by PCR following the respective methods described by Vandevanter et al. (19), Wellehan et al. (20), Manire et al. (21), and Ariel et al. (22). Any samples that reacted in the assays were sequenced using BigDye v.3.1 Sanger sequencing (Macrogen, Korea) following gel extraction. Non-specific reactors (determined by sequence) were disregarded.

RESULTS

Spatial Extent of Outbreak

During September / October 2016, 23 *M. latisternum* and four *E. m. krefftii* were captured at the four upstream sites investigated for spatial extent of the outbreak (**Table 2**). None of the 27 turtles caught upstream from the Craill pond had cutaneous lesions. *M. latisternum* was the only species found at the three sites at highest altitude. At the site closest to the Craill pond, both species were present. A gravid female was identified at sites 1, 3, and 4, indicating that the turtles were actively involved in reproduction and nesting during this time.

TABLE 2 | Number, sex and age-class of *M. latisternum* and *E. m. krefftii* captured at upstream sites (1-4), during September/October 2016 fieldtrips to Alligator Creek.

	E.latisternum			*E. m. krefftii*	
Site	**Male**	**Female**	**Juvenile**	**Male**	**Female**
1	3	4*	1		
2	4	6	1		
3		2*	1		
4			1	1	3*

*Indicates that one of the females captured were gravid with hard-shelled eggs.

Water Quality

The pH levels were close to neutral for all sites (mean pH: 6.96, 7.22, 7.46, and 7.1 for sites 1-2, 3, 4, and 5 respectively). The water conductivity values at all sites were low (mean µS/cm: 64, 43, 74, and 63 for sites 1-2, 3, 4, and 5 respectively). The macro invertebrate populations were different at Site 5 (the Craill pond). Site 1, 2, 3, and 4 all had highly sensitive macro invertebrates which indicates undisturbed water conditions, while Site 5 only had medium or lower sensitive invertebrates typically associated with creeks found near urban settings.

Season and Proportion of Turtles With Lesions

The proportion of turtles captured with lesions varied over time in a regular manner that appeared to be seasonal (**Figure 1**). Air temperature was overlaid on the graph showing proportion of turtles with lesions over time. The proportion of turtles with lesions is negatively correlated with the mean maximum air temperature during the sampling month ($P < 0.05$, $r = -0.7$).

Gross Pathology

Lesions are characterized by focal areas of white-tan discoloration varying in size from 1 to 3 cm diameter, with irregular to rounded margins, which are occasionally firm, white and contracted, reflecting fibrosis (**Figures 2A,B**). The discolouration of the skin caused the lesions to look white against the darker skin and these white rounded patches were also noticeable when watching a turtle surface in the water. Position of 58 lesions on the skin of turtles were categorized using available photos from 22 females, 24 males, and 3 juveniles. Ninety three % of these type of lesions were on the dorsal surface of tails, legs and necks, the rest

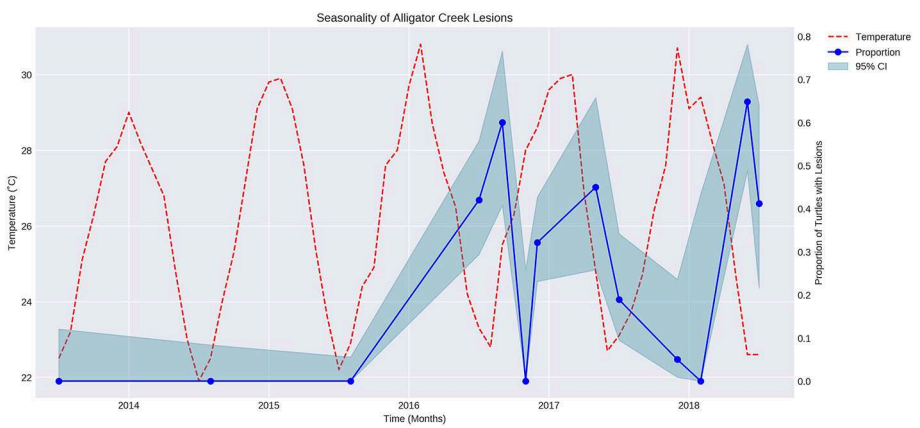

FIGURE 1 | Fluctuation of mean maximum air temperature (red broken line) and proportion of turtles with cutaneous lesions at Alligator Creek (blue dots) at 95% CI (blue shading) over time from 2013 to 2018.

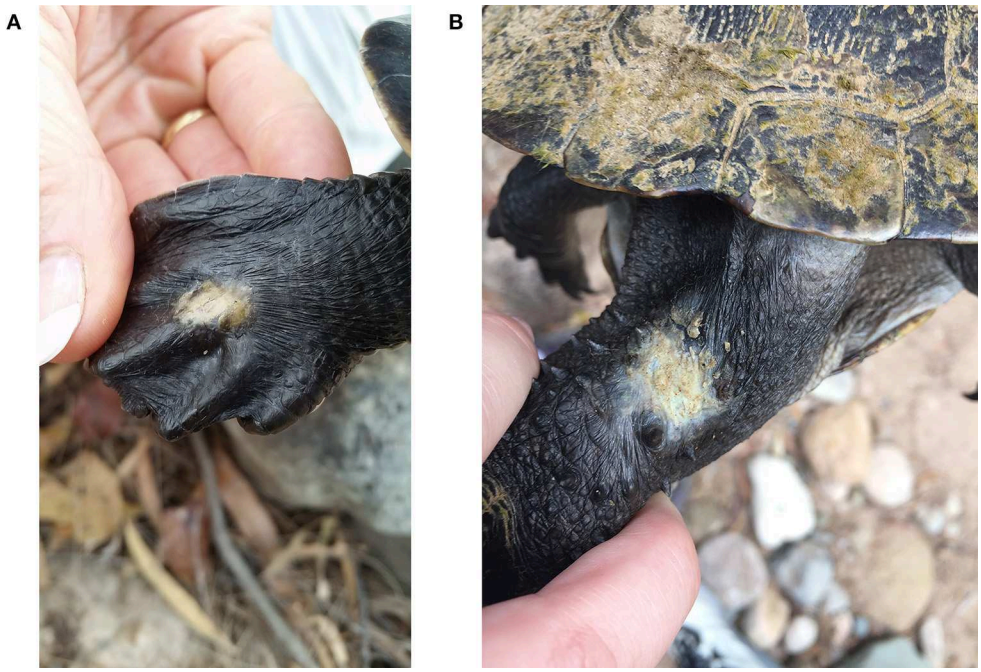

FIGURE 2 | Typical appearance and location of skin lesions on turtles captured at Alligator Creek. **(A)** Skin lesions on top of foot of *E. m. krefftii*. **(B)** Skin lesion on neck of *M. latisternum*.

were lateral, except for lesions near the cloaca on two adult females. The lesions on the tails were mostly proximal (92%), predominantly distal on the legs (93%) and either proximal (43%) or middle of the neck (43%). Lesions were fairly evenly distributed between adult males and females for neck and leg lesions, but the tail lesions were recorded predominantly on males (92%). Turtles with lesions did not otherwise appear affected in terms of body condition and activity levels. The three turtles euthanized for necropsy were in good health with full gastro-intestinal tracts, plenty of body fat and no lesions other than the cutaneous lesions.

Histopathology

Skin samples from all three turtles were similar, with each demonstrating a severe, subacute to chronic, multifocal, necrotizing, suppurative epidermitis and dermatitis. The epidermis was multifocally eroded to ulcerated and overlain by a dense serocellular crust embedded with colonies of coccobacilli and rods (predominantly Gram negative) (**Figure 3**) and filamentous organisms (Gomori's methenamine silver stain (GMS) positive) (**Figure 4**). No organisms were observed with Ziehl-Neelsen stain. In some areas there was also a layering effect of keratin and exudate. At the dermo-epidermal junction, there was a band of inflammation and often, granulation tissue; the former consisted largely of granulocytes and macrophages. In the dermis, there was patchy infiltration of granulocytes and small blood vessels were congested and frequently cuffed by moderate numbers of lymphocytes and plasma cells. Vascular fibrinoid degeneration was occasionally observed, but rare. In the adjacent intact epidermis, there was frequently spongiosis of the basal cell layer. No significant abnormalities were noted in other organs.

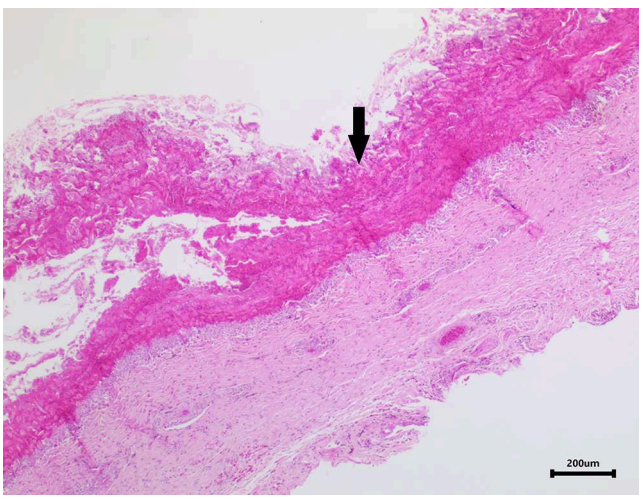

FIGURE 3 | Image of turtle skin showing a dense serocellular crust (arrow) overlying the severely ulcerated epidermis.

Bacteriology

Bacterial culture of swabs from internal organs during necropsy were negative, while a number of bacterial strains were cultured and identified from swaps of normal skin in turtles with and without lesions as well as directly from lesions (**Table 3**).

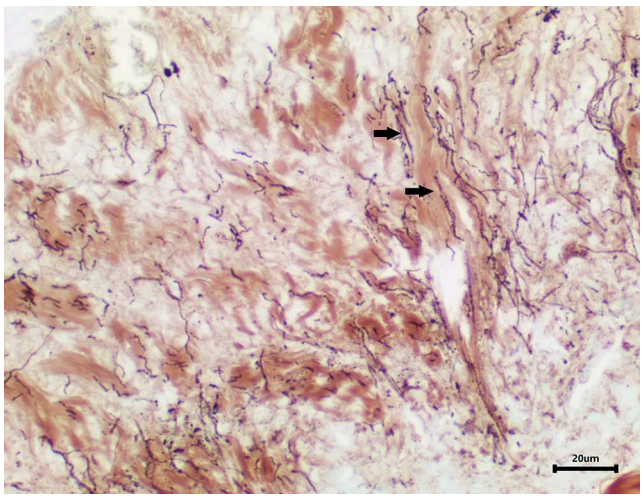

FIGURE 4 | Area of epidermal necrosis and ulceration embedded with filamentous organisms (GMS stain).

TABLE 3 | Number of bacterial strains isolated for 14 species of bacteria from 20 turtles without lesions and normal skin and lesions in 20 diseases freshwater turtles.

	Turtle without lesion	Turtle with lesion	
	Normal skin	Normal skin	Lesion
Serratia marcescens	2	3	9
Staphylococcus capitis	1	2	4
Fictibacillus and *Bacillus*	1	1	4
Aeromonas sobria		2	3
Aeromonas hydrophila		4	1
Chryseobacterium			1
Acinetobacter		3	
Aquitalea		1	
Diaphorobacter and *Acidovorax*		1	
Microbacterium sp.		1	
Pseudomonas fluorescens		1	
Bacillus	1		
Citrobacter youngae	1		
Pseudomonas aeruginosa	1		

Blood Biochemical Parameters

No statistically significant differences were observed in the blood parameters of turtles from different species, age groups, sex, sites, and presence or absence of lesions.

Virology

There was no development of CPE in cell cultures after three blind passages and the PCRs to detect ranavirus, herpesvirus, adenovirus, and papillomavirus genome were also negative for the samples collected.

TABLE 4 | The total number of *M. latisternum* and *E. m. krefftii* captured as well as those presenting with lesions in the Craill pond, during fieldtrips to Alligator Creek at various dates from 2013 to 2018.

Date	*M. latisternum*		*E. m. krefftii*	
	Total	Lesions	Total	Lesions
21/07/2013	15	0	13	0
10/08/2014	25	0	17	0
2/08/2015	44	0	21	0
31/07/2016	26	12	24	9
10/09/2016	13	10	12	5
6/11/2016	10	0	1	0
10/12/2016	45	17	39	10
5/05/2017	13	5	7	4
30/07/2017	21	4	16	3
10/12/2017	9	1	11	0
10/02/2018	1	0	4	0
28/06/2018	18	11	19	13
29/07/2018	9	2	8	5
	249	62	192	49

Turtles Captured

In the period from July 2013 to July 2018, 249 *M. latisternum* and 192 *E. m. krefftii* were captured in Alligator Creek at Site 5 (**Table 4**). All size groups of turtles were continuously captured over the period for both species (**Figure 5**).

The Curved Carapace Length (CCL) of turtles captured ranged in size from 7.8 to 30.0 cm for *M. latisternum* and 8.4 to 28.5 cm for *E. m. krefftii*. For both species, juveniles comprised approximately 1/3 of the captured turtles, while females dominated the *M. latisternum* captures (ratio male: female = 54 : 119) and males the *E. m. krefftii* turtles (male: female = 99 : 39) (**Table 5**).

Presence of Lesions Over Time

Cutaneous lesions were not recorded in this sub-population of freshwater turtles before July 2016, nor in any other freshwater turtles studied in the region, before or since. The number of turtles caught on each fieldtrip varied, as did the proportion of animals with lesions (**Figures 6A,B**). Presence of cutaneous lesions on turtles captured on fieldtrips since July 2016 varied from 0 to 77% for *M. latisternum* and 0 to 68% for *E. m. krefftii*.

Considering data from the first records of the outbreak in July 2016 and onwards from Site 5 only, there was no significant difference in proportion of turtles with cutaneous lesions between the two species (X^2 (1, N = 306) 0.262296; $p > 0.05$), nor was there any significant difference between sex in adult *M. latisternum* (X^2 (1, N = 108) 0.908654; $p > 0.05$), nor for *E. m. krefftii* (X^2 (1, N = 102) 0.728571; $p > 0.05$).

There was however, a significant difference in proportion of turtles with lesions between adults and juveniles (X^2 (1, N =306) 16.67154; $p < 0.001$), with juveniles being less likely to have lesions than adults for the two species combined. For a 1 cm

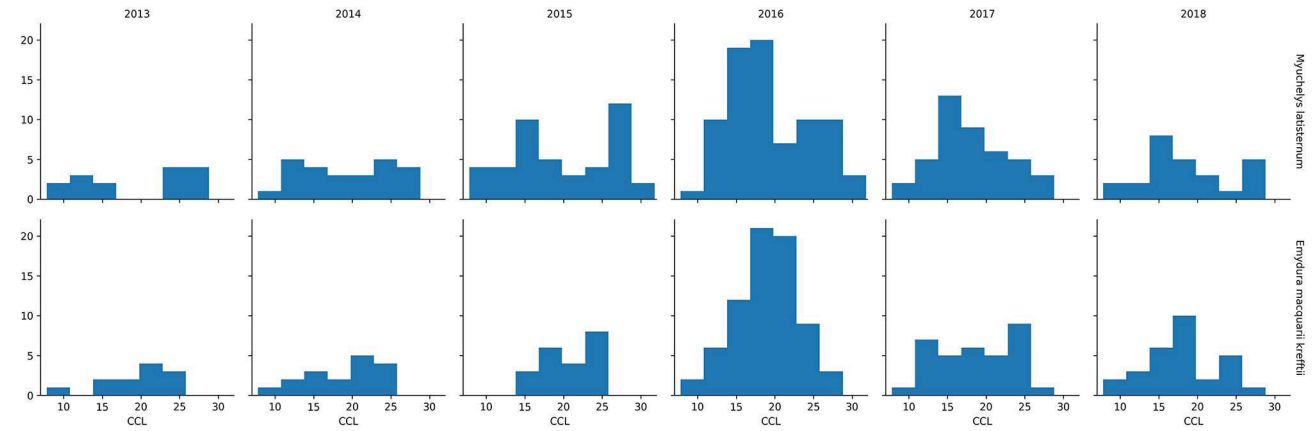

FIGURE 5 | Number of *M. latisternum* and *E. m. krefftii* recorded in each size class of curved carapace length (CCL) from 2013 to 2018.

TABLE 5 | Male, female and juvenile *M. latisternum* and *E. m. krefftii* captured at Alligator creek from 2013 to 2018.

	M. latisternum	*E. m. krefftii*
Males	54	99
Females	119	39
Juveniles	76	54

increase in CCL there is a 15.2% ($p < 0.001$, 95% CI 8.9–21.9) increase in odds of having a lesion.

Lesion Progression Over Time

In order to assess the progression of the disease over time, a subset of the data from 2013 to 2018 was investigated using turtles ($n = 43$) that had been recaptured since the initial recorded outbreak in July 2016. Spanning 11 fieldtrips over 2.5 years, 15 turtles remained without lesions on subsequent fieldtrips spaced from 2 to 30 months apart. Two of these turtles were previously recorded with lesions, but had recovered. Fourteen turtles that were registered with lesions, still had lesions 2–24 months later. One of these turtles (number 52854, **Figure 7**) was initially registered with lesions, which appeared to heal over a 3-month period, but it was recaptured with lesions 22 and 24 months later. Eight of the recaptured turtles were initially registered without lesions, but were recapture with them between 3 and 24 months later. On the other hand, five turtles with lesions were found to have healed on subsequent fieldtrips 2 to 5 months later (see **Figure 7**).

DISCUSSION

Several threats to freshwater turtles have been identified as contributors to their decline, including urban development (23–26) and introduced predators (4, 27), however, the study on the impact of disease on wild animals including populations of freshwater turtles is hampered by their cryptic and often remote habitats (22). Occasionally, spectacular outbreaks in public areas draw the attention of the general public and scientists alike and spur in-depth investigations with a multi-disciplinary approach (9, 10). The appearance of cutaneous lesions on a proportion of freshwater turtles captured as part of regular monitoring of wild living turtles in Alligator Creek, North Queensland was likewise an opportunity to study the course of disease development in a wild population over time.

Spatial and Temporal Extent of the Epidemic

The epidemic was confined to a natural pond on Alligator Creek, the Craill pond (Site 5), and although turtles were found upstream from the pond, these did not have lesions during the initial stages of the outbreak in 2016. Downstream populations were not investigated due to presence of saltwater crocodiles and associated risk, but were considered infected according to general principles guiding zoning for diseases in streams (14). Prior to July 2016, there were no records of such lesions in this area or other streams or rivers in the region despite regular annual sampling, but turtles were continuously caught with lesions in this pond for the 3-year monitoring that followed.

Water quality parameters tested did not indicate an acute contamination event although the Craill pond was considered more disturbed than the upstream sites, based on the macro invertebrates found there. However, it was not possible to completely rule out a pollution, contamination, or other toxic event as water was only sampled at one timepoint (during the initial outbreak).

An inverse relationship between temperature and the proportion of turtles captured with lesions throughout the year was identified. The relationship may not be a direct one, but temperature fluctuate with season and other seasonal factors such as migration and aggression in response to reproduction, basking sites or food availability (28) may also have increased the risk in this pond at certain times of the year.

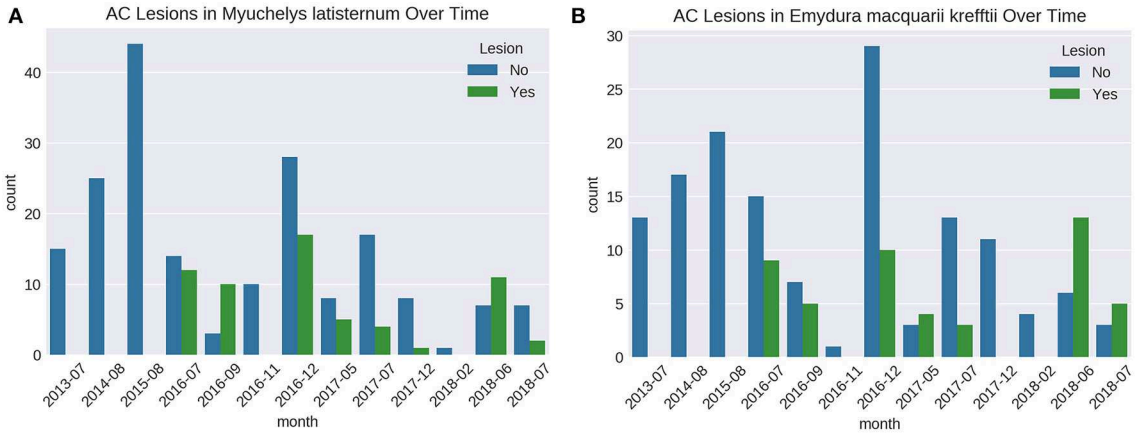

FIGURE 6 | Number of captured *M. latisternum* **(A)** and *E. m. krefftii* **(B)** turtles without cutaneous lesions (blue) and with lesions (green) on fieldtrips to Alligator Creek from 2013 to 2018.

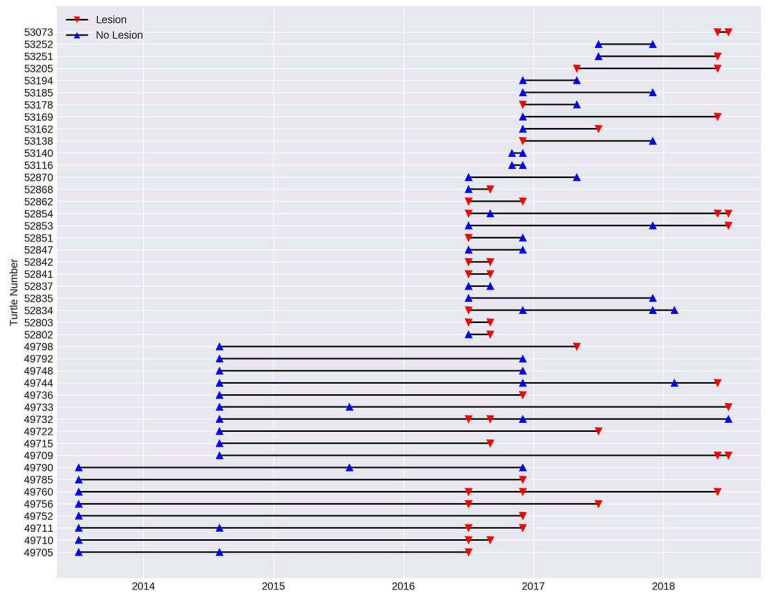

FIGURE 7 | Presence of lesions (red triangle) and no lesions (blue triangle) in the 43 turtles recaptured at Site 5, Alligator Creek between 2013 and 2018. Individual turtles are identified with tag number.

Characteristics of the Lesions

Histological examination revealed that the condition was largely confined to the epidermis, while all other organs in the animals investigated appeared normal. Skin lesions associated with ranaviral infection have been reported in lizards and turtles, but in most cases internal organs were also infected (29–32). While there was no detectable bias toward sex or species of turtles, the odds ratio indicates that the larger the turtle, the higher the risk of a lesion, and juveniles were rarely affected. The position of the lesions on the turtles indicated a non-random distribution on the skin and it is therefore likely that the initial skin lesion may have been caused by trauma and associated with a behavior where certain parts of the body would be at higher risk. The lesions were predominantly dorsal indicating that the trauma may have originated from above the turtle rather than below. The lesions on legs were mostly distal, while neck lesions were both proximal and middle of the neck. Tail lesions were essentially all proximal and on males apart from lesions near the cloaca on two females.

Given that peak lesion prevalence (May-September) precedes the nesting season of in this region, which is October to January for *E. m. krefftii* and September to March for *M. latisternum* according to Cann (12) and as evidenced by hard-shelled eggs detected via palpation on fieldtrips, it is possible that courtship behavior would put adult turtles in a higher risk group, either through intra-species aggression during courtship and mating (28) or because this behavior favors another risk factor such as a

predator. Biting during courtship and mating could also explain the lesions on the male tails as they may be targeted by competing males as seen in other freshwater turtles and sea turtles (28, 33). Alternatively, the males have larger tails than the females and would therefore be an easier target, but lesions on legs were mostly distal and on the feet, while the tail lesions were primarily proximal, which indicates that male tails are somehow a different target from legs. The lesions on the cloaca of two females could be associated with skin trauma during mating.

Courtship and mating is a natural occurrence and by itself would not cause such lesions. The investigation therefore focused on identifying a unique infectious agent, which could have gained entry following skin trauma.

Agent Causing the Lesions

Occasionally there are reports of wild populations of turtles succumbing to unknown pressures: several hundred *E. macquarii*, for instance, were unaccountably found dead at Lake Boga, South Australia, during the first half of 1976, while many others were clearly emaciated (12). Such mass mortalities are possibly caused by intoxication or infectious diseases. Most publications concerning the influence of disease on freshwater turtle populations in Australia are based on mass mortality events or general health problems in a population (7, 34). It is therefore challenging to interpret the presence of microorganisms in sick turtles as pathogenic or commensal due to lack of baseline data.

A number of bacterial strains were cultured and identified from swaps of normal skin in turtles with and without lesions as well as directly from lesions. The only bacteria isolated only from a lesion and not normal skin on any of the turtles was *Chryseobacterium*. This was only isolated in one instance, and is therefore not considered a causative agent. Some of the other bacteria are normal skin flora (*Aeromonas sobria, Aeromonas hydrophila, Serratia marcescens, Staphylococcus capitis, Fictibacillus,* and *Bacillus*), but they can on occasion turn pathogenic (22). In this study they were isolated at a higher rate from lesions and could therefore be secondary pathogens. There seemed to be a different composition of bacteria on skin of some turtles with and without lesions, but again, they do not appear to have any causation effect.

The blood biochemical parameters in turtles with lesions did not differ from turtles without lesions and none of the swab samples reacted in the virological assays for ranavirus, herpesvirus, adenovirus, or papillomavirus, which have been reported in reptiles on previous occasions (35). Ranaviral infections in turtles have been associated with intra-cytoplasmic inclusion bodies (36, 37), but these were not detected. A toxic etiology would also seem unlikely in this case, based on the distribution of the lesions, as it would be expected that the lesions would be random and affect all areas of the animal, rather than just the dorsum.

The Impact on the Population Through a Longitudinal Study

The lesions in the turtles at Alligator Creek, did not appear to have a dramatic impact on their overall health over the 3-year monitoring period following the first appearance of the lesions. There was no obvious decline or change in the demographics of the turtle populations and some turtles recorded with lesions were recaptured the following years, indicating that the affliction was not definitively lethal, but slow progressing. In addition, the post mortem examination following euthanasia of three adult males in clinically good health, but with skin lesions, revealed a good amount of body fat and a gastro intestinal tract full of ingesta, indicating that the animals were thriving, despite the winter temperatures and presumed mating season.

Field monitoring was intensified in the months after the initial reports of lesions so there are more data from late 2016 than other years, and fieldtrips in 2016–2018 were also spaced over more months and seasons. Following the initial outbreak in 2016, we continued to capture turtles of all sizes and both species of turtles, including recapture of 43 tagged turtles. This sub-sample of recaptured turtles was very useful in defining disease progression in the population. It revealed that some turtles stayed free of lesions over several years even if they co-existed with animals with lesions. Some turtles were repeatedly registered with lesions over several fieldtrips, while others had healed between captures. Other turtles were initially registered without lesions, but developed them between subsequent fieldtrips. Future monitoring will be required to determine if the population will fully heal over time.

This pattern of disease progression suggests that the agent is not a lethal one and that healing may occur naturally. It also suggests that exposure to the agent in the environment is not sufficient to cause disease, but there must be a contributing risk factor involved to create a portal of entry in a non-random fashion. These findings fits into the theory of an initial skin trauma associated with certain seasons, followed by entry and establishment of a pathogen present in the local environment. The seasonal aggression associated with courtship and mating could potentially be the cause of the skin trauma, but the identity and drivers for the appearance of a unique pathogen in this population is still under investigation.

DATA AVAILABILITY STATEMENT

The datasets generated for this study are available on request to the corresponding author.

ETHICS STATEMENT

The animal study was reviewed and approved by James Cook University Animal Ethics Committee.

AUTHOR CONTRIBUTIONS

EA and WW contributed conception and design of the study. All authors contributed to the acquisition, analysis and interpretation of data for the work. WW and KD organized the database and photos. WW performed the statistical analysis. EA wrote the first draft of the manuscript. All authors wrote individual sections of the manuscript and revising it

critically for important intellectual content and approved the submitted version.

FUNDING

This investigation was partly funded by the National Significant Disease Investigation Program (NSDI), Wildlife Health Australia (WHA), Worldwide Fund for Nature (WWF), and JCU.

ACKNOWLEDGMENTS

For directly facilitating and commenting on the investigation Dr. Mark Read, Dr. Col Limpus, and Dr. Alastair Freeman deserves special thanks. The Gudjuda rangers, Townsville Skin Divers, Leigh Benson (NPSR) and numerous volunteers were invaluable in their assistance in the field.

REFERENCES

1. Buhlmann KA, Akre TSB, Iverson JB, Karapatakis D, Mittermeir RA, George A, et al. A global analysis of tortoise and freshwater turtle distributions with identification of priority conservation areas. *J Informat.* (2009) 8:116–49. doi: 10.2744/CCB-0774.1
2. Van Dyke JU, de Ferronato BO, Spencer RJ. Current conservation status of Australian freshwater turtles. *Aust J Zool.* (2018) 66:1. doi: 10.1071/ZOv66n1_IN
3. Wilson S, Swan G. *A Complete Guide to Reptiles of Australia*. Sydney, NSW: Reed New Holland (2003).
4. Fordham DA, Georges A, Brook BW. Indigenous harvest, exotic pig predation and local persistence of a long-lived vertebrate: managing a tropical freshwater turtle for sustainability and conservation. *J Appl Ecol.* (2008) 45:52–62. doi: 10.1111/j.1365-2664.2007.01414.x
5. Rowe CL. "The calamity of so long life": life histories, contaminants, and potential emerging threats to long-lived vertebrates. *Bioscience.* (2008) 58:623–31. doi: 10.1641/B580709
6. Doupé RG, Knott MJ, Schaffer J, Burrows DW. Investigational piscivory of some juvenile Australian freshwater fishes by the introduced *Mozambique tilapia Oreochromis mossambicus. J Fish Biol.* (2009) 74:2386–400. doi: 10.1111/j.1095-8649.2009.02254.x
7. Flint M, Limpus DJ, Limpus CJ, Patterson-Kane JC, Eales JA, Mills PC. Biochemical and hematological reference intervals for Krefft's turtles *Emydura macquarii krefftii* from the Burnett River Catchment, Australia. *Dis Aquatic Organ.* (2011) 95:43. doi: 10.3354/dao02352
8. Lovich JE, Ennen JR, Agha M, Gibbons JW. Where have all the turtles gone, and why does it matter? *BioScience.* (2018) 68:771–81. doi: 10.1093/biosci/biy095
9. Spencer RJ, Van Dyke J, Petrov K, Ferronato B, McDougall F, Austin M, et al. Profiling a possible rapid extinction event in a long-lived species. *Biol Conserv.* (2018) 221:190–7. doi: 10.1016/j.biocon.2018.03.009
10. Zhang J, Finlaison DS, Frost MJ, Gestier S, Gu X, Hall J, et al. Identification of a novel nidovirus as a potential cause of large scale mortalities in the endangered Bellinger River snapping turtle (*Myuchelys georgesi*). *PLoS ONE.* (2018) 13:e0205209. doi: 10.1371/journal.pone.0205209
11. Tucker AD, Guarino F, Priest TE. Where lakes were once rivers: contrasts of freshwater turtle diets in dams and rivers of Southeastern Queensland. *Chelonian Conserv Biol.* (2012) 11:12–23. doi: 10.2744/CCB-0906.1
12. Cann J. *Australian Freshwater Turtles*. Beaumont Pub (1998).
13. Spencer R. *The Murray River Turtle, Emydura macquarii: Population Dynamics, Nesting Ecology and Impact of the Red Fox, Vulpes Vulpes*. University of Sydney (2001).
14. Anonymous. *Aquatic Animal Health Code*. (2019). Available online at: https://www.oie.int/international-standard-setting/aquatic-code/ (accessed August 1, 2019).
15. Seabold S, Perktold J. Statsmodels: econometric and statistical modeling with python. In: *Proceedings of the 9th Python in Science Conference,* Vol. 57 (2010).
16. McKinney W. Data structures for statistical computing in python. In: *Proceedings of the 9th Python in Science Conference,* Vol. 57 (2010).
17. Conroy CJ, Papenfuss T, Parker J, Hahn NE. Use of tricaine methanesulfonate (MS222) for euthanasia of reptiles. *J Am Assoc Lab Anim Sci.* (2009) 48:28–32.
18. Bancroft JD, Gamble M. *Theory and Practice of Histological Techniques*. Elsevier Health Sciences (2008).
19. Vandevanter DR, Warrener P, Bennett L, Schultz ER, Coulter S, Garber RL, et al. Detection and analysis of diverse herpesviral species by consensus primer PCR. *J Clin Microbiol.* (1996) 34:1666–71. doi: 10.1128/JCM.34.7.1666-1671.1996
20. Wellehan JFX, Johnson AJ, Harrach B, Benko M, Pessier AP, Johnson CM, et al. Detection and analysis of six lizard adenoviruses by consensus primer PCR provides further evidence of a reptilian origin for the atadenoviruses. *J Virol.* (2004) 78:13366–9. doi: 10.1128/JVI.78.23.13366-13369.2004
21. Manire CA, Stacy BA, Kinsel MJ, Daniel HT, Anderson ET, Wellehan JFX. Proliferative dermatitis in a loggerhead turtle, Caretta caretta, and a green turtle, *Chelonia mydas*, associated with novel papillomaviruses. *Vet Microbiol.* (2008) 130:227–37. doi: 10.1016/j.vetmic.2008.01.013
22. Ariel E, Freeman AB, Elliott E, Wirth W, Mashkour N, Scott J. An unusual mortality event in Johnstone River snapping turtles *Elseya irwini* (Johnstone) in Far North Queensland, Australia. *Aust Vet J.* (2017) 95:355–61. doi: 10.1111/avj.12627
23. Spinks PQ, Pauly GB, Crayon JJ, Shaffer HB. Survival of the western pond turtle (*Emys marmorata*) in an urban California environment. *Biol Conserv.* (2003) 113:257–67. doi: 10.1016/S0006-3207(02)00392-0
24. Aresco MJ. The effect of sex-specific terrestrial movements and roads on the sex ratio of freshwater turtles. *Biol Conserv.* (2005) 123:37–44. doi: 10.1016/j.biocon.2004.10.006
25. Beaudry F, deMaynadier PG, Hunter ML. Identifying road mortality threat at multiple spatial scales for semi-aquatic turtles. *Biol Conserv.* (2008) 141:2550–63. doi: 10.1016/j.biocon.2008.07.016
26. Crawford BA, Maerz JC, Nibbelink NP, Buhlmann KA, Norton TM. Estimating the consequences of multiple threats and management strategies for semi-aquatic turtles. *J Appl Ecol.* (2014) 51:359–66. doi: 10.1111/1365-2664.12194
27. Spencer R-J, Thompson MB. Experimental analysis of the impact of foxes on freshwater turtle populations. *Conserv Biol.* (2005) 19:845–54. doi: 10.1111/j.1523-1739.2005.00487.x
28. Rovero F, Lebboroni M, Chelazzi G. Aggressive Interactions and Mating in Wild Populations of the European Pond Turtle *Emys orbicularis*. *J Herpetol.* (1999) 33:258. doi: 10.2307/1565723
29. Stohr AC, Blahak S, Heckers KO, et al. Ranavirus infections associated with skin lesions in lizards. *Vet Res.* (2013) 44:84. doi: 10.1186/1297-9716-44-84
30. Maclaine A, Mashkour N, Scott J, Ariel E. Susceptibility of eastern water dragons *Intellagama lesueurii lesueurii* to Bohle iridovirus. *Dis Aquatic Organ.* (2018) 127:97–105. doi: 10.3354/dao03193
31. Maclaine A, Forzán MJ, Mashkour N, Scott J, Ariel E. Pathogenesis of Bohle iridovirus (Genus Ranavirus) in experimentally infected juvenile eastern water dragons (*Intellagama lesueurii lesueurii*). *Vet Pathol.* (2019) 56:465–75. doi: 10.1177/0300985818823666
32. Wirth W, Schwarzkopf L, Skerratt LF, Tzamouzaki A, Ariel E. Dose-dependent morbidity of freshwater turtle hatchlings, *Emydura macquarii krefftii*, inoculated with Ranavirus isolate (*Bohle iridovirus*, Iridoviridae). *J Gen Virol.* (2019) 100:jgv001324. doi: 10.1099/jgv.0.001324
33. Jessop TS, FitzSimmons NN, Limpus CJ, Whittier JM. Interactions between behavior and plasma steroids within the scramble mating system of the promiscuous green turtle, *Chelonia mydas*. *Hormones Behav.* (1999) 36:86–97. doi: 10.1006/hbeh.1999.1527

34. Tucker AD, Kelly WR, Limpus CJ, Priest TE, Guarino F. Prevalence of ulcerative disease in free-ranging Krefft's turtle. *Memoirs Queensland Museum*. (2002) 48:233–7.
35. Marschang RE. Viruses infecting reptiles. *Viruses*. (2011) 3:2087–126. doi: 10.3390/v3112087
36. Marschang RE, Becher P, Posthaus H, et al. Isolation and characterization of an iridovirus from Hermann's tortoises (*Testudo hermanni*). *Arch Virol*. (1999) 144:1909–22. doi: 10.1007/s007050050714
37. Allender MC, Fry MM, Irizarry AR, Craig L, Johnson AJ, Jones M, et al. Intracytoplasmic inclusions in circulating leukocytes from an eastern box turtle (*Terrapene carolina carolina*) with iridoviral infection. *J Wildl Dis*. (2006) 42:677–84. doi: 10.7589/0090-3558-42.3.677

Conflict of Interest: EE was employed by the company Ausphage.

The remaining authors declare that the research was conducted in the absence of any commercial or financial relationships that could be construed as a potential conflict of interest.

Copyright © 2020 Wirth, Elliott, Rudd, Hayes, Maclaine, Mashkour, Ahasan, Gorm Dahl, Drane and Ariel. This is an open-access article distributed under the terms of the Creative Commons Attribution License (CC BY). The use, distribution or reproduction in other forums is permitted, provided the original author(s) and the copyright owner(s) are credited and that the original publication in this journal is cited, in accordance with accepted academic practice. No use, distribution or reproduction is permitted which does not comply with these terms.

frontiers in Veterinary Science

CASE REPORT
published: 31 January 2020
doi: 10.3389/fvets.2020.00025

A Novel *Exophiala* Species Associated With Disseminated Granulomatous Inflammation in a Captive Eastern Hellbender (*Cryptobranchus alleganiensis alleganiensis*)

Cynthia Hopf[1], Erin A. Graham[2], Connie F. C. Gibas[3], Carmita Sanders[3], James Mele[3], Hongxin Fan[2], Michael M. Garner[4], Nathan P. Wiederhold[3], Robert Ossiboff[2,5] and Noha Abou-Madi[1]*

[1] Department of Clinical Sciences, Cornell University College of Veterinary Medicine, Ithaca, NY, United States, [2] Department of Comparative Diagnostic and Population Medicine, University of Florida College of Veterinary Medicine, Gainesville, FL, United States, [3] Fungus Testing Laboratory & Molecular Diagnostics Laboratory, Department of Pathology and Laboratory Medicine, University of Texas Health Science Center at San Antonio, San Antonio, TX, United States, [4] Northwest ZooPath, Monroe, WA, United States, [5] Department of Population Medicine and Diagnostic Sciences, Cornell University College of Veterinary Medicine, Ithaca, NY, United States

OPEN ACCESS

Edited by:
Chris Walzer,
University of Veterinary Medicine
Vienna, Austria

Reviewed by:
Randy Junge,
Columbus Zoo and Aquarium,
United States
Kathryn Christine Gamble,
Lincoln Park Zoo, United States

***Correspondence:**
Cynthia Hopf
crh245@cornell.edu

Specialty section:
This article was submitted to Zoological Medicine, a section of the journal Frontiers in Veterinary Science

Received: 31 May 2019
Accepted: 13 January 2020
Published: 31 January 2020

Citation:
Hopf C, Graham EA, Gibas CFC, Sanders C, Mele J, Fan H, Garner MM, Wiederhold NP, Ossiboff R and Abou-Madi N (2020) A Novel Exophiala Species Associated With Disseminated Granulomatous Inflammation in a Captive Eastern Hellbender (Cryptobranchus alleganiensis alleganiensis). Front. Vet. Sci. 7:25. doi: 10.3389/fvets.2020.00025

The genus *Exophiala* is composed of ubiquitous, pigmented, saprotrophic fungi and includes both terrestrial and waterborne species. Though *Exophiala* species are generally considered opportunistic pathogens, exophialosis can be an important cause of morbidity and mortality in aquatic and semi-aquatic species. Over a 6-year period, a captive 32-year-old male eastern hellbender (*Cryptobranchus alleganiensis alleganiensis*), was treated for recurring, slow growing, ventral midline cutaneous masses. Excisional biopsies were characterized histologically by granulomatous dermatitis with low numbers of intralesional, pigmented fungal conidia and hyphae. Bacterial and fungal cultures of the masses and skin were negative on two separate submissions. Polymerase chain reaction amplification of a short fragment of the fungal 28S large subunit (LSU) ribosomal RNA was positive with 100% nucleotide sequence identity to several species of *Exophiala*. Following recurrence after successive rounds of antifungal therapy, euthanasia was elected. At necropsy, similar dermal granulomatous inflammation and intralesional pigmented fungal elements as observed in excisional biopsies formed a thick band in the dermis and extended through the coelomic body wall. Visceral dissemination was noted in the lung and kidney. Postmortem DNA sequence analysis of a large portion of the fungal LSU as well as the internal transcribed spacer (ITS) from a portion of frozen affected dermis identified the fungus as a novel species, *Exophiala* sp. 1 (UTHSCSA R-5437).

Keywords: amphibian, chromoblastomycosis, chromomycosis, cryptobranchid, exophialosis, fungus, phaeohyphomycosis, salamander

INTRODUCTION

Native to the United States, hellbenders (*Cryptobranchus alleganiensis*) are large aquatic salamanders represented by two subspecies: the eastern hellbender (*C. a. alleganiensis*) and the Ozark hellbender (*C. a. bishopi*). *Cryptobranchus a. alleganiensis* ranges from New York to Georgia, through Tennessee and the Ohio River Valley to the Ozarks and inhabit clear, swift-flowing streams with rocky bottoms (1). Wild populations have been declining due to historical overharvesting for the pet trade, and are now threatened by habitat deterioration and infectious disease outbreaks (*Batrachochytrium dendrobatidis* [*Bd*]) (1–4). The eastern hellbender was designated as a species of special concern in New York State in 1983 and is listed as near-threatened by the IUCN Red List. Conservation efforts have focused on head-start and reintroduction programs, habitat restoration, and disease surveillance (1, 5). Some reported health problems in the eastern hellbender include traumatic injuries, neoplasia (epidermal papilloma, squamous cell carcinoma, Sertoli cell tumor, and poorly differentiated sarcoma), and infections with *Saprolegnia* or *Bd* (1).

Phaeohyphomycosis is a disease caused by a heterogenous group of septate dark-walled phaeoid fungi that can cause both subcutaneous and systemic infections. Over 100 species of melanized fungi are in this category, including *Exophiala* and *Cladophialophora*, that both belong to the order *Chaetothyriales* (6). *Exophiala* species can be opportunists or pathogens of immunocompetent humans and have also caused disease in fish, amphibians, and invertebrates (7). Study of the taxonomy and clinical disease characteristics of *Exophiala* species is ongoing with updates in their classification. This report characterizes a unique morphologic presentation of fatal phaeohyphomycosis in an eastern hellbender associated with an undescribed species of *Exophiala*.

CASE PRESENTATION

A 32-year-old male eastern hellbender (*C. a. alleganiensis*), wild caught as a juvenile, was examined following the discovery of a chain of small, nodular masses noted along the ventral midline. The masses were slow-growing and initially involved only the skin. Two excisional surgeries were performed 31 months apart due to the recurrence of the condition.

For surgical procedures the hellbender was anesthetized in a bath solution of 0.1% MS222 (Ethyl 3-aminobenzoate methanesulfonate, Millipore Sigma, Darmstadt, Germany) buffered with sodium bicarbonate. Induction was achieved after 15 min and anesthesia was maintained by covering the body of the hellbender with gauzes soaked with a buffered 0.05% solution of MS222. Heart rate was monitored using a Doppler ultrasonic flow detector and depth of anesthesia was gauged by the lack of righting reflex and response to surgical stimulation. No increase in the concentration of MS222 was required throughout the procedure. For both anesthetic procedures, the hellbender recovered completely after 2 fresh water bath changes and 20 min after the anesthesia was discontinued.

During the first surgery, the ventral midline masses involved only the skin. The larger masses were excised for diagnostic purposes. Post-operative treatment included enrofloxacin (Baytril 22.7 mg/ml, Bayer, Shawnee Mission, Kansas 66201 USA) 5 mg/kg given intra-coelomically. Butorphanol (0.5 mg/L) bath solution (Dolorex 10 mg/ml, Merck, Madison, New Jersey, 07940 USA) was used for analgesia for the first 24 h. Eleven days post-operatively, the skin wound dehisced over 2–3 mm but the coelomic wall closure remained intact and the skin healed by second intention without further complication. Microscopically the lesions consisted of dermal granulomatous inflammation. A Fite's acid fast stain revealed no acid fast positive bacteria within the lesions. A Gomori methenamine silver (GMS) stain identified scattered and infrequent spherical yeast-like structures that were difficult to find in foci of inflammation. Culture and PCR were not attempted at this time and treatment was declined as euthanasia was considered. The hellbender healed and no recrudescence of the masses was noted for several years.

Three and a half years after the initial surgery, new masses were discovered, and a second surgery was performed. The masses had invaded into the coelomic wall. They were excised using radiosurgery and blunt dissection in the anesthetized animal. The chain of masses removed measured 9 × 4.5 × 2 cm. Sections of the mass were submitted for aerobic bacterial culture, fungal culture, and histologic analysis.

Cultures for bacteria and fungi were negative. Histologic findings were similar to the previous biopsy and were characterized by granulomatous dermatitis with epidermal ulceration, edema, and hyperplasia (**Figures 1A,B**). Low numbers of pigmented, round to oval-shaped conidia (6.5 to 8.5 μm diameter) were present in small clusters within granulomatous foci (**Figure 1B**). Rare non-branching hyphae with thin, non-parallel, pigmented walls ranging from 5 to 10 μm in diameter and sporadic septation were also noted. A GMS stain revealed that the conidia and hyphae were intensely argyrophilic (**Figure 1C**) and demonstrated positive cytochemical reactivity with a Fontana-Masson stain for melanin, consistent with a pigmented fungus (phaeohyphomycosis) (**Figure 1D**). No acid-fast bacteria were highlighted with Ziehl-Neelsen or Fite-Faraco staining.

Nucleic acids were extracted from scrolls of paraffin-embedded skin using a commercially available kit (DNeasy Blood and Tissue Kit, QIAGEN, Germantown, Maryland, USA), and fungal DNA was amplified by polymerase chain reaction (PCR) using universal primers that target a variable region within the large 28S subunit (8). An amplicon of approximately 260 bp was sequenced bidirectionally (Genomics Facility, Biotechnology Resource Center, Cornell University), assembled and edited of primer sequence (Geneious R10; Auckland, New Zealand) for a final product size of 224 bp, and compared for homology with sequences in GenBank (https://www.ncbi.nlm.nih.gov/genbank/). The resultant product exhibited 100% nucleotide identity to a number of *Exophiala* species, including *Exophiala opportunistica* (KP347962.1), *E. bonariae* (KR781083.1), and *E. cancerae* (KF928502.1).

Post-operative treatment consisted of 5 mg/kg of enrofloxacin injected subcutaneously (SC) in a pocket of electrolyte solution

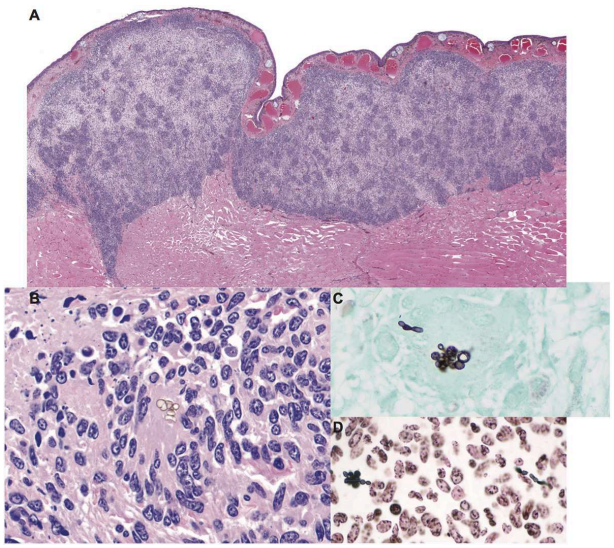

FIGURE 1 | Granulomatous mycotic dermatitis in an eastern hellbender (*Cryptobranchus alleganiensis alleganiensis*). **(A)** The dermis is expanded by a band of nodular to diffuse granulomatous inflammation with focal epidermal attenuation and extension through underlying striated muscle fibers. Hematoxylin and eosin (HE). **(B)** Small, sporadic, clusters of extracellular pigmented conidia are surrounded by numerous epithelioid macrophages and multinucleated giant cells amid scattered pyknotic and karyorrhectic cellular debris (HE). **(C)** Fungal elements are argyrophilic; conidia are accompanied by rare hyphae with thin, non-parallel walls and sporadic septation. Gomori methenamine silver (GMS). **(D)** Conidia and hyphae exhibit positive cytochemical reactivity within the fungal wall, consistent with a pigmented (melanin) fungus. Fontana-Masson.

FIGURE 2 | Multicentric granulomatous mycotic inflammation in an eastern hellbender (*Cryptobranchus alleganiensis alleganiensis*). **(A)** The ventral dermis is expanded by multinodular coalescing granulomas with ulceration of the overlying epidermis. **(B)** Similar nodular granulomas are present within the lungs.

(Normosol-R, Hospira Inc, Lake Forest, IL 60045 USA), and meloxicam (Metacam 5 mg/ml, Boehringer Ingelheim, St. Joseph, MO 64506 USA) 0.2 mg/kg also given SC every other day for 8 and 6 days respectively. In light of the histology and PCR results, itraconazole (Sporanox, 10 mg/ml, Janssen Pharmaceutica N.V. Beerse, Belgium) was added at a dose of 5 mg/kg once daily hidden in the prey food item. A total of only 18 treatments of itraconazole over the course of 30 days were successfully administered due to hypophagia and poor compliance. Itraconazole was discontinued after the 18th successful administration. The surgical wound healed without complication. The hellbender's appetite improved. Two years after the second surgery, the masses recurred at the same location with ulceration of the skin. Due to the recurrence of the lesions and the extent of the masses, euthanasia was elected.

POST-MORTEM DIAGNOSTICS

Gross necropsy revealed a chain of multinodular, coalescing, and ulcerated dermal masses of the ventral coelomic body wall (**Figure 2A**). The masses had a gross appearance similar to those of previous surgical excisions, and were concentrated in the region of the two previous surgical incisions. The masses extended through the body wall and were multifocally visible through the coelomic mesothelium. Multiple, white-tan nodular masses were also present in the lungs (**Figure 2B**) and the kidneys. No gross abnormalities were noted in other visceral organs. Several tissues were sampled and fixed in 10% neutral buffered formalin for microscopic examination and frozen for further testing, including the body wall sections of granulomatous lesion, sections of skin and mass, left distal thoracic limb, eye, brain, heart, urinary bladder, lungs, liver, spleen, kidneys, pancreas, intestines, segments of small and large intestine, and testicular tissue.

Histologic examination confirmed the presence of generalized granulomatous dermatitis associated with pigmented fungal elements as noted in historical excisional biopsies (**Figures 1A–D**). Granulomatous inflammation extended into the muscle of the coelomic body wall, but did not penetrate into the coelomic cavity. Evidence of visceral mycotic dissemination was noted in the lung and kidney and was characterized by moderate to severe granulomatous pneumonia and nephritis with low numbers of intralesional pigmented fungi as described in the skin lesions.

A 1 cm^3 sample of frozen, affected dermis collected at the time of necropsy was lysed in a Precellys® Evolution tissue homogenizer (Bertin Technologies, Montigny-le-Bretonneux FRANCE) and genomic DNA was extracted using EZ1 DNA

tissue kit with a BioRobot EZ1 instrument (QIAGEN) following manufacturer's instructions. PCR amplification of the internal spacer region (ITS) and partial large subunit gene of the nuclear rDNA (LSU) were done using primers specifically designed for *Exophiala*: EXO1 and EXO2 (9), and U1 and U2 (8), respectively. Sequencing was done with the same primers using BigDye Terminator v. 3.1 Cycle Sequencing Kit (Applied Biosystems, Foster City, CA, USA). The sequences generated were deposited in GenBank, https://www.ncbi.nlm.nih.gov/ with the accession nos. MK253014 (ITS) and MK253015 (LSU).

Using the obtained ITS sequence, identification was done by an in-house BLASTn search within a sequence dataset compiled in Bioedit v7.0.5 program comprising short barcode identifiers located in the ITS2 region of reference and authentic strains of *Exophiala* and related species (10, 11). A 100% match was not found with any of the strains in the dataset. Subsequently, BLASTn searches in GenBank were performed using partial ITS and partial LSU sequences. The top ITS results showed that the isolate (UTHSCSA R-5437) matched 100% with an unidentified *Exophiala* sp. S4.3 (KY322615), 96% with *E. cancerae* CBS 120420^T (NR_1377664), 95.69% with *E. opportunistica* CBS 109811^T (KF928435) and 95.32% with *E. bonariae* CBS 139957^T (NR_144964). In the partial LSU BLASTn search, a 100% match was observed with *E. cancerae* (KF928502), and type strains of *E. opportunistica* (KF928501) and *E. bonariae* (KR781083), 98-99% matches with *E. psychrophila* CBS 191.87^T (MH873750), *E. salmonis* CBS 157.67^T (MH870616), *E. radicis* P2854^T (KT723448) and *E. pisciphila* CBS 537.73^T (MH870790). Phylogenetic analysis was then conducted using only the ITS sequence because the LSU sequence obtained was short and was unreliable, and repeat sequencing of LSU failed to obtain a longer sequence for use.

The ITS sequences of representative *Exophiala* species and relatives were obtained from GenBank based on BLASTn searches and on the datasets of Yong et al. (12) and Borman et al. (13). The sequences were assembled and aligned using MUSCLE (14) as implemented in Sequencher version 5.4.6-Build 46289 (Gene Codes Corp., MI USA) and refined visually using SE-AL (15). The best fit evolutionary model for this dataset was determined using the Find Best DNA Models for maximum likelihood (ML) as implemented in MEGA version 7 (16). General Time Reversible model with Gamma distributed rate variation and an estimated proportion of invariable sites (GTR+G+I) (17) was found to be the best fit evolutionary model for this dataset having the lowest Bayesian Information Criterion score (BIC) (18). Maximum likelihood analysis was conducted with GTR+G+I substitution model and 1000 bootstrap (19) iterations. Bayesian inference was done using MrBayes v3.2.5 (20) applying the same substitution model. The Markov Chain Monte Carlo (21) started from a random tree topology and lasted 6 million generations, where every 100th tree was retained and the first 25% of the trees were discarded as burn in. A 50% majority rule consensus tree and posterior probabilities were calculated. Bayesian posterior probabilities (BPP) $>$ 0.90 and bootstrap (BT) values $>$ 70% were considered significant.

The phylogenetic tree inferred from maximum likelihood (**Figure 3**) showed our isolate within a monophyletic clade (BPP 0.99/ BT 93%) comprising mostly of waterborne species, i.e., *E. opportunistica*, *E. lacus*, *E. cancerae*, *E. psychrophila*, *E. salmonis*, *E. aquamarina*, *E. pisciphila* (7) and other species originally isolated from non-aquatic sources, i.e., *E. bonariae* (22) and *E. equina* (7). Within the clade, it is closest to *E. cancerae* with high support (BPP 1.00 / BT 86%). ITS pairwise comparison of UTHSCSA R-5437 with *E. cancerae* CBS 120420^T (NR_1377664) however, showed 15 nucleotide base pair differences.

DISCUSSION

Phaeohyphomycosis is caused by pigmented filamentous fungi including *Exophiala* species (23). Waterborne *Exophiala* species are important pathogens in fish including *E. salmonis* in cut-throat trout (*Salmo clarkii*) and the Atlantic salmon (*Salmo salar*). *Exophiala pisciphila* caused an epizootic in the channel catfish (*Ictalurus punctatus*), and brain and skin lesions in smooth dogfish (*Mustelus canis*) (7). In amphibians, infection with *Exophiala* are reported in marine toads (*Bufo marinus*) and European blind cave salamanders (*Proteus anguinus*) (24). Case reports of dermal or disseminated disease in reptiles are described in a Galapagos tortoise (*Geochelone nigra*) (25), Eastern box turtle (*Terrapene carolina carolina*) (26), and Aldabra tortoise (*Geochelone gigantean*) (27). *Exophiala dermatitidis* and *E. oligosperma* have both been reported to cause infections in humans (7).

Melanized fungi including *Exophiala* spp. can cause disease more frequently in aquatic animals than in terrestrial animals. Further, dry, thicker skin, the presence of fur or feathers, and the absence of sweat glands are thought to provide a degree of protection against infection in reptiles, birds, and mammals (7). Infections may occur secondary to traumatic percutaneous inoculation (23, 27, 28). Immunosuppression may be a factor in producing infection, but phaeohyphomycosis has been reported in immunocompetent animals (7, 27–29).

Pathogenicity associated with *Exophiala* is not described in *C. a. alleganiesis*. The source of infection in this case is unknown but may be percutaneous invasion of the fungus associated with ventral abrasions. Concurrent diseases that may have contributed were not identified in this animal. It is considered possible that the fungus of this report was a primary pathogen.

The initially observed nodular dermatitis spread to deeper structures of the body wall and eventually spread systemically. Over time lesions were identified in the dermis, skeletal muscle of the body wall, lungs, and kidneys. The lesions in the viscera suggested hematogenous spread from the skin. The lesions in this animal were first noted 6 years prior to the first surgery and had not appeared to change, until a progressive growth was noted. No observed changes in the hellbender's environment or health justified the change in the masses. Detailed reports of lesions from *Exophiala* infections are rare and include systemic mycosis with *E. angulospora* in an Atlantic halibut (*Hippoglossus hippoglossus*), and disseminated mycosis in a colony of Ornate-horned frogs (*Ceratophrys ornata*) with cutaneous and visceral lesions

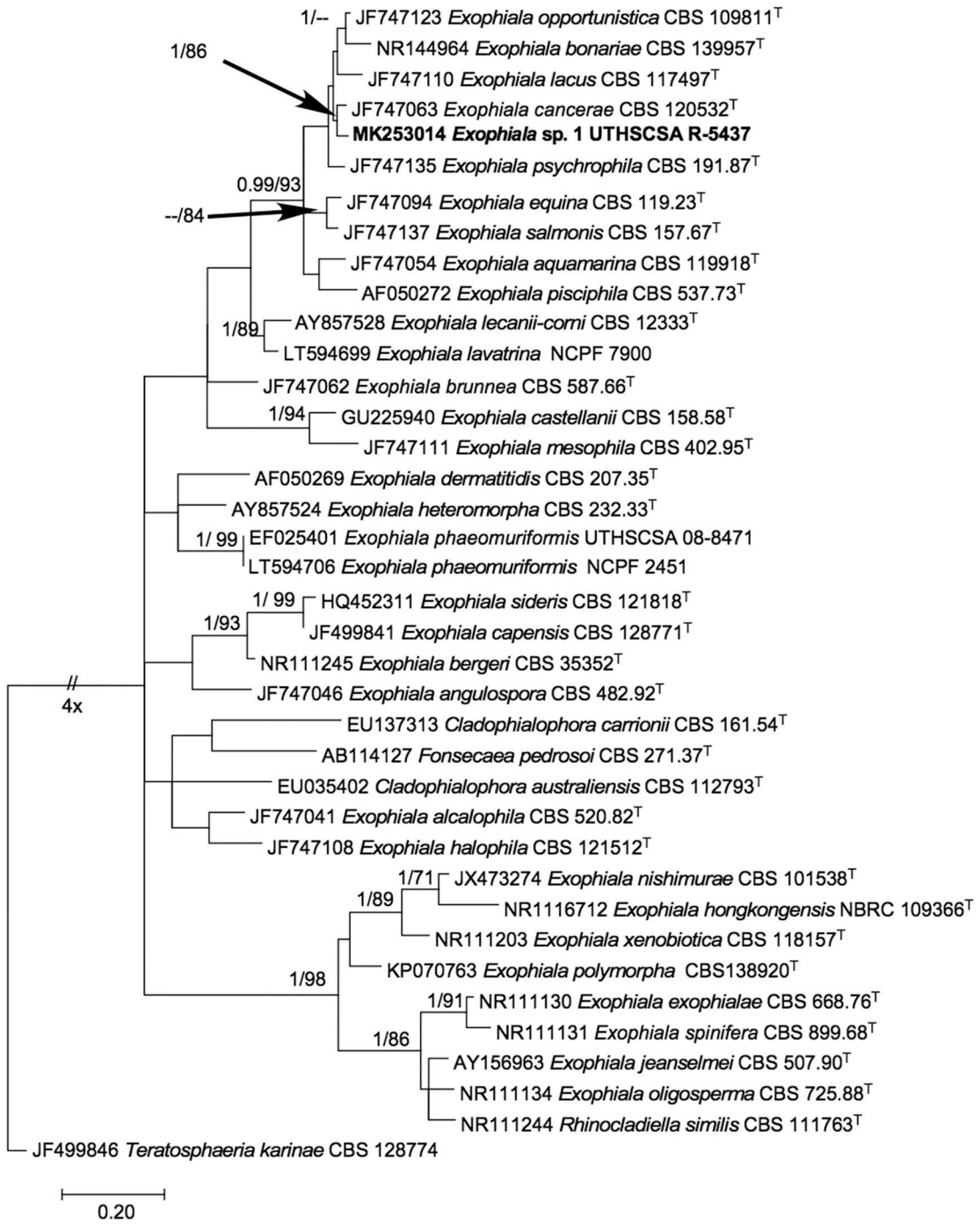

FIGURE 3 | Phylogenetic tree inferred from ITS sequences showing the relationship of *Exophiala* sp. UTHSCSA R-5437 to known *Exophiala* species. Branch lengths are proportional to phylogenetic distance. ML bootstrap support values (1000 resampling, Right) >70% and posterior probability values from Bayesian inference (Left) > 0.90 are shown above the branches. *Teratosphaeria karinae* CBS 128774^T was designated as outgroup. ^{T}, type strain; CBS, CBS-KNAW Fungal Biodiversity Center culture collection, The Netherlands; NBRC, National Biological Resource Center, Japan; NCPF, UK National Collection of Pathogenic Fungi, PHE UK National Mycology Reference Laboratory and School of Biological Sciences, University of Bristol, Bristol, United Kingdom; UTHSCSA, Fungus Testing Lab, University of Texas Health Science Center at San Antonio, Texas USA. Sequence accession numbers are indicated in front of species names.

(28, 29); however, *Exophiala* species infections are commonly encountered in fish and amphibians during routine diagnostic investigations of captive collections (personal observations, MG).

Diagnostic techniques used in cases of phaeohyphomycoses include impression smear cytologic exam, histologic exam, culture, molecular identification, and phylogenetic analysis

(23, 28, 29). In the present case, the fungus was identified histologically followed by molecular screening. Initial antemortem PCR results on a short segment of the 28S ribosomal large subunit identified the species as an *Exophiala*. Differentiation from other closely related species was not possible based on the short size and conserved nature of the targeted region. Attempts to culture the organism were unsuccessful. Different *Exophiala* species have similar morphologic and physiologic characteristics and can be difficult to differentiate based on clinical signs, gross necropsy, and histologic examination. The organism of this report had unique features in histologic section that differed considerably from the more commonly observed infections. In hematoxylin and eosin stained sections of infected tissue, *Exophiala* typically forms long, streaming, yellow, slender hyphae and occasional branching elements with parallel cell walls. In this salamander, the lesions were chronic, with minimal necrosis, and the fungal agent was present in low numbers primarily as small yeast-like or septate conidial forms, with only rare hyphae observed. In this regard, infection with this organism in hellbenders or other species could possibly misconstrued as a different fungus, or be overlooked due to the low density of organism in tissue sections.

Identification of *Exophiala* species is challenging because they are highly pleomorphic and produce synanamorphs in their life cycles (10, 30, 31). Although these species are generally recognizable as *Exophiala*, identification is difficult using morphological and other phenotypic criteria because almost identical structures are observed even with phylogenetically distantly related species (10). DNA sequencing and the increasing availability of sequences in public databases (e.g., GenBank) improved fungal identification and led to the discovery of novel species as well as reclassification of species in their natural groupings. ITS sequences in *Exophiala* and related species have been found to have variabilities caused by stutter formation in PCR products making this target unreliable for identification (10). However, short fragments in the ITS2 region have differences in nucleotide composition that are stable allowing them to be used as barcodes by clinical diagnostic laboratories for the identification of medically important black yeasts and relatives (10). In this case, the barcode did not give a species identity because the *Exophiala* strain in this study did not match with any of the species in the database and could represent a new species. ITS phylogenetic analysis showed that this sequence is closely related with *E. cancerae* (BPP1.00/ BT 86%); however pairwise ITS sequence comparison with that of *E. cancerae* showed 15 base pair differences. Based on the in-house Bioedit barcode identifier sequence BLASTn result, BLASTn results in GenBank and phylogenetic analysis, this organism is as a putatively novel *Exophiala* species closely related to *E. cancerae*. Confirmation and description of this organism as a new species is not possible at this time because of the lack of viable culture of the organism and failure to sequence other gene loci for a multi-gene phylogenetic analysis.

Treatment options for *Exophiala* species are limited. In humans, this includes radiation therapy, amputation, resection followed by skin grafts, and systemic administration of amphotericin B and 5-fluorocytosine (32). Ketoconazole and acridine dyes combined with excisional surgery were unsuccessful in a marine toad (*Bufo marinus*) (33). Treatment was successful in an Aldabra tortoise (*Geochelone gigantean)* infected with *Exophiala oligosperma* (27). In the present case, two surgeries with aggressive debridement of the masses, followed by oral itraconazole failed to resolve the infection. Without a culture, the appropriateness of itraconazole therapy could not be confirmed. Poor compliance may have been caused by post-operative stress, the increased feeding frequency to match the treatment schedule, or a side effect of the drug. Decreased frequency of the treatment was attempted, but the hellbender remained hypophagic and the treatment was ultimately discontinued. Treatment in bath water might have been successful and was considered but declined due to husbandry considerations.

DATA AVAILABILITY STATEMENT

The datasets generated for this study can be found in the GenBank, https://www.ncbi.nlm.nih.gov/.

ETHICS STATEMENT

The care and treatment of this animal, as well as the testing performed post-mortem were approved by the Rosamond Gifford Zoo (Syracuse, NY, USA) Animal Care Committee and the Rosamond Gifford Zoo (Syracuse, NY, USA) IACUC committee.

AUTHOR CONTRIBUTIONS

CH, and NA-M performed the medical and surgical management of this case, the submission of the samples to necropsy, writing of the manuscript. CG, CS, JM, HF, and NW performed the molecular and genetic analysis on the samples provided. MG, RO, and EG processed the tissues for histopathologic examination, and performed the analysis of the results. All authors discussed the results and commented on the manuscript.

REFERENCES

1. Junge RE. Hellbender medicine. In: Miller RE, Fowler M, editor. *Fowler's Zoo and Wild Animal Medicine Current Therapy*. (2012). p. 260–4.
2. Souza MJ, Gray MJ, Colclough P, Miller DL.Prevalence of infection by *Batrachochytrium dendrobatidis* and ranavirus in Eastern hellbenders (*Cryptobranchus alleganiensis alleganiensis*) in eastern Tennessee. *J Wildl Dis*. (2012) 48:560–6. doi: 10.7589/0090-3558-48.3.560
3. Bales EK, Hyman OJ, Loudon AH, Harris RN, Lipps G, Chapman E, et al. Pathogenic chytrid fungus *Batrachochytrium dendrobatidis*, but not, *B. salamandrivorans,* detected on Eastern Hellbendersz. *PLoS ONE.* (2015) 10:e0116405. doi: 10.1371/journal.pone.0116405

4. Wheeler BA, Prosen E, Mathis A, Wilkinson RF. Population declines of a long-lived salamander: a 20+-year study of hellbenders, *Cryptobranchus alleganiensis*. *Biol Conserv*. (2003) 109:151–6. doi: 10.1016/S0006-3207(02)00136-2
5. New York State Department of Conservation. *Eastern Hellbender Fact Sheet*. Available online at: https://www.dec.ny.gov/animals/7160.html (accessed January 29, 2019).
6. Nyaoke A, Weber ES, Innis C, Stremme D, Dowd C, Hinckley L. Disseminated phaeohyphomycosis in weedy, *Phyllopteryx taeniolatus*, and leafy, *Phycodurus eques*, seadragons caused by species of Exophiala, including a novel species. *J Vet Diagnos Investig.* (2009) 21:69–79. doi: 10.1177/104063870902100111
7. de Hoog GS, Vicente VA, Najafzadeh MJ, Harrak MJ, Badali H, Seyedmousavi S. Waterborne Exophiala species causing disease in cold-blooded animals. *Persoonia*. (2011) 27:46–72. doi: 10.3767/003158511X614258
8. Sandhu GS, Kline BC, Stockman L, Roberts GD. Molecular probes for diagnosis of fungal infections. *J Clin Microbiol*. (1995) 33:2913–9. doi: 10.1128/JCM.33.11.2913-2919.1995
9. Porteous NB, Grooters AM, Redding SW, Thompson EH, Rinaldi MG, De Hoog GS, et al. Identification of *Exophiala mesophila* isolated from treated dental unit waterlines. *J Clin Microbiol.* (2003) 41:3885–89. doi: 10.1128/JCM.41.8.3885-3889.2003
10. Heinrichs G, de Hoog GS, Haase G. Barcode identifiers as a practical tool for reliable species assignment of medically important black yeast species. *J Clin Microbiol*. (2012) 50:3023–30. doi: 10.1128/JCM.00574-12
11. Hall TA. BioEdit: a user-friendly biological sequence alignment editor and analysis program for windows 95/98/NT. *Nucleic Acids Symp Series.* (1999) 41:95–8.
12. Yong LK, Wiederhold NP, Sutton DA, Sandoval-Denis M, Lindner JR, Fan H, et al. Morphological and molecular characterization of *Exophiala polymorpha* sp. nov. isolated from *Sporotrichoid lymphocutaneous* lesions in a patient with *Myasthenia gravis*. *J Clin Microbiol.* (2015) 53:2816–22. doi: 10.1128/JCM.00622-15
13. Borman AM, Fraser M, Szekely A, Larcombe DE, Johnson EM. Rapid identification of clinically relevant members of the genus exophiala by matrix-assisted laser desorption ionization–time of flight mass spectrometry and description of two novel species, *Exophiala campbellii* and *Exophiala lavatrina*. *J Clin Microbiol.* (2017) 55:1162–76. doi: 10.1128/JCM.02459-16
14. Edgar RC. Muscle: a multiple sequence alignment method with reduced time and space complexity. *BMC Bioinformatics*. (2004) 5:113. doi: 10.1186/1471-2105-5-113
15. Rambaut A. *Se-Al: Sequence Alignment Editor, version 2.0 alpha 11 Carbon [Computer program]*. Oxford Univercitry (2002). Available online at: http://tree.bio.ed.ac.uk/software/seal/ (accessed May 21, 2019).
16. Kumar S, Stecher G, Tamura K. MEGA7: molecular evolutionary genetics analysis version 7.0 for bigger datasets. *Mol Biol Evol*. (2016) 33:1870–74. doi: 10.1093/molbev/msw054
17. Nei M, Kumar S. *Molecular Evolution and Phylogenetics*. New York, NY: Oxford University Press (2000).
18. Posada D, Crandall KA. Selecting the best-fit model of nucleotide substitution. *Syst Biol.* (2001) 50:580–601. doi: 10.1080/10635150118469
19. Felsenstein J. Confidence limits on phylogenies: an approach using the bootstrap. *Evolution.* (1985) 39:783–91. doi: 10.1111/j.1558-5646.1985.tb00420.x
20. Ronquist F, Huelsenbeck JP. MRBAYES 3: Bayesian phylogenetic inference under mixed models. *Bioinformatics.* (2003) 19:1572–4. doi: 10.1093/bioinformatics/btg180
21. Metropolis NA, Rosenbluth W, Rosenbluth MN, Teller AH, Teller E. Equations of state calculations by fast computing machines. *J Chem Phys*. (1953) 21:1087–91. doi: 10.1063/1.1699114
22. Crous PW, Schumacher RK, Akulov A, Thangavel R, Hernández-Restrepo M, Carnegie AJ. New and interesting fungi. 2. *Fungal Syst Evol*. (2019) 3:57–34. doi: 10.3114/fuse.2019.03.06
23. Pare JA. Fungal diseases of amphibians: an overview. *Vet Clin Exot Anim.* (2003) 6:315–26. doi: 10.1016/S1094-9194(03)00006-9
24. Bizjak-Mali L, Zalar P, Turk M, Babič MN, Kostanjšek R, Gunde-Cimerman N. Opportunistic fungal pathogens isolated from a captive individual of the European blind cave salamander *Proteus anguinus*. *Dis Aquat Organ.* (2018) 129:15–30. doi: 10.3354/dao03229
25. Manharth A, Lemberger K, Mylniczenko N, Pinkerton M, Pessier AP, Kammeyer P, et al. Disseminated phaeohyphomycosis due to Exophiala species in a *Galapagos tortoise*, *Geochelone nigra*. *J Herp Med Surg.* (2005) 15:20–6. doi: 10.5818/1529-9651.15.2.20
26. Joyner PH, Shreve AA, Spahr J, Fountain AL, Sleeman JM. Phaeohyphomycosis in a free-living eastern box turtle (Terrapene Carolina Carolina). *J Wildl Dis*. (2006) 42:883–8. doi: 10.7589/0090-3558-42.4.883
27. Stringer EM, Garner MM, Proudfoot JS, Ramer JC, Bowman MR, Heng HG, et al. Phaeohyphomycosis of the Carapace in an Aldabra Tortoise (*Geochelone gigantean*). *J Zoo Wildl Med*. (2009) 40:160–7. doi: 10.1638/2008-0035.1
28. Miller EA, Montali RJ, Ramsay EC, Rideout RA. Disseminated chromoblastomycosis in a colony of ornate-horned frogs (*Ceratophrys ornata*). *J Zoo Wildl Med*. (1992) 23:433–8.
29. Overy DP, Groman D, Giles J, Duffy S, Rommens M, Johnson G. *Exophiala angulospora* causes systemic mycosis in atlantic halibut: a case report. *J Aquat Anim Health*. (2015) 27:12–9. doi: 10.1080/08997659.2014.953266
30. Cañete-Gibas CF, Wiederhold NP. The black yeasts: an update on species identification and diagnosis. *Curr Fungal Infect Rep*. (2018) 12:59–65. doi: 10.1007/s12281-018-0314-0.
31. de Hoog GS, Takeo K, Yoshida S, Gottlich E, Nishimura K, Miyaji M. Pleoanamorphic life cycle of Exophiala (Wangiella) dermatitidis. *Antonie Van Leeuwenhoek*. (1994) 65:143–53. doi: 10.1007/BF00871755
32. Sudduth EJ, Crumbley AJ. Phaeohyphomycosis due to exophiala species: clinical spectrum of disease in humans. *Clin Infect Dis*. (1992) 15:639–44. doi: 10.1093/clind/15.4.639
33. Bube A, Burkhardt E, Weiss R. Spontaneous chromomycosis in the marine toad (*Bufo marinus*). *J Comp Pathol*. (1992) 106:73–7. doi: 10.1016/0021-9975(92)90069-7

Conflict of Interest: The authors declare that the research was conducted in the absence of any commercial or financial relationships that could be construed as a potential conflict of interest.

The handling Editor declared a past co-authorship with one of the authors RO.

Copyright © 2020 Hopf, Graham, Gibas, Sanders, Mele, Fan, Garner, Wiederhold, Ossiboff and Abou-Madi. This is an open-access article distributed under the terms of the Creative Commons Attribution License (CC BY). The use, distribution or reproduction in other forums is permitted, provided the original author(s) and the copyright owner(s) are credited and that the original publication in this journal is cited, in accordance with accepted academic practice. No use, distribution or reproduction is permitted which does not comply with these terms.

frontiers in Veterinary Science

ORIGINAL RESEARCH
published: 04 February 2020
doi: 10.3389/fvets.2020.00034

Evaluation of Severity and Factors Contributing to Foot Lesions in Endangered Ozark Hellbenders, *Cryptobranchus alleganiensis bishopi*

Rebecca H. Hardman[1], Kelly J. Irwin[2], William B. Sutton[3] and Debra L. Miller[1]*

[1] Center for Wildlife Health, University of Tennessee, Knoxville, Knoxville, TN, United States, [2] Arkansas Game and Fish Commission, Benton, AR, United States, [3] Wildlife Ecology Laboratory, Department of Agricultural and Environmental Sciences, Tennessee State University, Nashville, TN, United States

OPEN ACCESS

Edited by:
Nicole Indra Stacy, University of Florida, United States

Reviewed by:
Kris Helke, Medical University of South Carolina, United States
Elena Elena Gorman, Oregon State University, United States

***Correspondence:**
Rebecca H. Hardman
rhardman@tennessee.edu

Specialty section:
This article was submitted to Veterinary Experimental and Diagnostic Pathology, a section of the journal Frontiers in Veterinary Science

Received: *10 September 2019*
Accepted: *14 January 2020*
Published: *04 February 2020*

Citation:
Hardman RH, Irwin KJ, Sutton WB and Miller DL (2020) Evaluation of Severity and Factors Contributing to Foot Lesions in Endangered Ozark Hellbenders, Cryptobranchus alleganiensis bishopi. Front. Vet. Sci. 7:34. doi: 10.3389/fvets.2020.00034

Arkansas populations of Ozark Hellbenders, *Cryptobranchus alleganiensis bishopi* have declined precipitously over the past few decades and are now limited to a single river. Biologists have also observed an increase of distal limb lesions with unidentified etiology and unknown role in morbidity and mortality of the species in this location. We documented lesions and collected associated individual size class data and pathogen samples in Ozark Hellbenders of Arkansas ($n = 73$) from 2011 to 2014 with the following two objectives: (1) document spatiotemporal patterns and severity of lesions present in this last remaining Arkansas Ozark Hellbender population, and (2) determine if host factors and infection status are associated with lesion severity. A scoring system was created from 0 to 7 based on lesion observations. Linear mixed model regressions followed by AICc model evaluation were used to determine associations among infection status for amphibian pathogens *Batrachochytrium dendrobatidis* (*Bd*) and Ranavirus as well as individual biometrics on lesion score. We discovered 93.2% of Hellbenders had lesions characterized by digit swelling that often progressed toward toe-tip ulceration. In severe cases we observed digital necrosis progressing to digit loss. Any recaptured individuals had the same or worse lesion score from previous captures. The top predictive model for lesion severity included individual mass and *Bd* infection status with a significant, positive association of *Bd* with increased lesion severity ($\beta = 0.87 \pm 0.39$ S.E., C.I.: 0.11, 1.63). Our findings highlight a widespread and progressive disease that is an important factor to consider for the future of Ozark Hellbenders. This syndrome is presumptively multifactorial, and future studies will benefit from investigating several factors of host, infectious agents, and environment and their roles in disease manifestation for the purpose of developing effective, multi-faceted conservation strategies. A summary of potential etiologies and mechanisms is provided that may explain observed lesion distribution and that will be applicable to future disease and epidemiological investigations.

Keywords: Hellbender, salamander, chytrid, *Bd*, amphibian disease

INTRODUCTION

Human alteration of habitat has been linked to increased disease prevalence in many wildlife systems [see (1)]. Stream dwelling amphibians have been commonly used as biological indicators of environmental degradation due to their susceptibility to a variety of anthropogenic disturbances (2, 3). Specific consequences of degraded watersheds such as chemical runoff and increased sedimentation are known to negatively impact amphibian health [see (4, 5)].

Hellbenders (*Cryptobranchus alleganiensis*) are large, fully aquatic salamanders that inhabit cool, rocky, well-oxygenated rivers and streams in the eastern United States (6). The eastern subspecies (*C. a. alleganiensis*) inhabits a majority of the range with Ohio, Tennessee, and Mississippi River drainages extending from northeastern Mississippi to southern New York, and between southeastern Indiana and central West Virginia, with a disjunct population in central Missouri, while the Ozark Hellbender (*Cryptobranchus a. bishopi*) is a disjunct subspecies restricted to Ozark highland rivers of southern Missouri and northern Arkansas (7). Hellbenders may be particularly susceptible to increased sedimentation and other changes in water quality because they are fully aquatic and respire cutaneously (8). They require large cover rocks or crevices for breeding sites (6) and sediment-free interstitial spaces in gravel for larval and juvenile growth (9, 10).

Over the past few decades, population numbers have decreased appreciably in both subspecies. Many historical Hellbender populations are now extirpated or are functionally extinct (only large, senescent individuals remain) (11, 12). These drastic declines have resulted in federal listing of *C. a. bishopi* as an endangered subspecies (13) and inclusion of both *C. a. alleganiensis* and *C. a. bishopi* in appendix III of the Convention on International Trade in Endangered Species (CITES) of Wild Fauna (14). Ozark Hellbenders in Arkansas are believed to be extirpated from all but one river located in the northern portion of the state. Habitat degradation is hypothesized as the primary driver behind the declines of this subspecies. In one study in Missouri, decreased population densities of both subspecies were linked to decreased watershed buffers and associated change in stream parameters of temperature, conductivity, pH, and percent pebble (% of substrate in transect to be rocks of 4–64 mm diameter) (15). Moreover, Ozark Hellbenders in Arkansas (and populations in Missouri) have also been documented with distal limb lesions (16). These include feet with swollen, fused, or missing digits, and occasionally, exposed phalanges. A few cases are documented with partial to near complete foot loss. Similar but much less severe lesions have been observed in Eastern Hellbenders in Tennessee, but at lower frequency (17, 18).

Primary pathogens may also be negatively impacting *C. a. bishopi* populations and may contribute fully or in part to abnormalities, even if they are only part of a multifactorial process. Chytrid fungus (*Batrachochytrium dendrobatidis* or *Bd*) is present in *C. a. bishopi* (19, 20), and *C. a. alleganiensis* (21–23), but *Bd* prevalence is similar among both healthy and declining populations. However, in captive settings, *Bd* infection has resulted in mortality (24, 25), revealing its potential to cause disease in Hellbenders, especially in altered environments. The role of *Bd* in the morbidity and mortality of toe lesions remains unknown.

An emerging chytrid fungus, *Batrachochytrium salamandrivorans* (*Bsal*), has also been implicated in cases of skin lesions and mortalities in Europe. In addition, this pathogen appears to be more pathogenic to salamanders as opposed to frogs (26). Although *Bsal* has not been found in North America to date (21, 27), it is imperative to test salamanders with skin lesions to rule out a novel introduction.

Ranavirus is another emerging amphibian pathogen that is responsible for dramatic mortality events in captive colonies of the related Chinese Giant Salamander *Andrias davidianus* (28). Lesions from Ranavirus outbreaks in *A. davidianus* are identified by distal limb swelling, necrosis, and ulceration (29), which are similar to lesions observed in *C. a. bishopi*. Ranavirus has been found to infect wild Hellbenders, but without any obvious clinical signs at the time of sampling (18). However, Ranavirus infection in wild adult Hellbenders is negatively associated with calculated body condition score (BCS) (Hardman, unpublished data), highlighting the possibility that this virus may have unknown sublethal effects in Hellbenders.

Bacterial pathogens should also be considered, particularly opportunistic species associated with aquatic environments known to cause disease in immunosuppressed hosts. Two such species, *Citrobacter freundii* and *Aeromonas hydrophila* have been cultured from some, but not all lesions sampled in *C. a. bishopi* in Missouri (30). *C. freundii* is an opportunistic pathogen associated with aquatic ectotherms and is documented to produce a variety of sequelae including septicemic cutaneous ulcerative disease (SCUD) in turtles and necrotizing fasciitis in humans (31). *A. hydrophila* represents another opportunistic bacterium associated with mixed-pathogen infections that involves skin ulcerations and septicemia in both fish (32) and amphibians (33). However, when another study (34) applied culture-independent methods (16S amplicon sequencing) to identify bacteria from these lesions, they did not determine any consistent association between lesions and a particular bacterial species, further supporting this syndrome is likely of complex etiology.

Consequently, it remains unclear how host, pathogen, and environment may interact to produce a high prevalence of distal limb lesions. Further, no study has yet quantified lesion severity and applied an epidemiological evaluation of lesion presence. We documented lesions and collected associated individual size class data and pathogen samples in Ozark Hellbenders of Arkansas from 2011 to 2014 with the following two objectives: (1) document spatiotemporal patterns and severity of lesions present in this last remaining Arkansas Ozark Hellbender population, and (2) determine if host factors and infection status are associated with lesion severity.

MATERIALS AND METHODS

Collection

Within Arkansas, Hellbenders are currently restricted to only one river, which we have chosen to not identify to prevent potential poaching. We performed 1 week intensive surveys

each summer from 2011 to 2014. Surveys fell within a 3 week sampling window from late July to early August except for 2013 when high water levels prevented sampling, and sampling was delayed until September. These surveys were done before the onset of full breeding season which begins in early September. Disease sampling protocols were added to ongoing surveys for population monitoring. All sampling occurred under USFWS permit TE66039A-0 issued to KJI and Arkansas Game and Fish Commission. We sampled shallow and deep-water habitats (up to 4 m) using a hookah dive system (i.e., gasoline powered air compressor with tethered air supply lines to dive regulators). We also performed standard snorkeling to locate individuals in shallower water only. We also sampled Hellbenders via previously placed artificial nest boxes (35). Any animals encountered under cover objects or nest boxes were captured and placed in a clean soft cotton or mesh bag. Bags remained submerged in the river before and after animals were processed (University of Tennessee IACUC protocol # 2481-0916). We changed dive gloves between animal captures to reduce pathogen transfer and contamination of pathogen samples.

Standard measurements were recorded for total length (TL; cm), snout-vent length (SVL; cm), and mass (g). Captured animals were scanned for presence of a passive integrated transponder (PIT) tag, and number was recorded if present. New captures were marked subcutaneously with a PIT tag at the base of the tail as described in Hecht-Kardasz et al. (36), except without the use of post-injection adhesive. After processing, which took between 10 and 20 min per animal, all individuals were released at their point of capture. New containers, bags, and gloves were used between individuals. All equipment (including diving gloves) was cleaned with soap and soaked in 5% solution of either bleach or chlorhexidine for at least 10 min and rinsed thoroughly before use at another site. This protocol provides more than sufficient disinfection to prevent the spread of both Ranavirus (37) and *Bd* (38).

Pathogen Sampling

Swabs for *Bd* quantitative PCR (qPCR) and tail tissue for Ranavirus qPCR were collected for another study evaluating disease prevalence (Hardman et al., unpublished data) and those results were incorporated into our lesion severity analysis. The methods for this were as follows:

To sample for chytrids (*Bd* and *Bsal*), we ran a sterile cotton swab (Fisherbrand product# 23400111) five times over each body region in the following order: dorsum, ventrum, inguinal areas, and all portions of the feet including toe-tips as described by Brem et al. (39). Although standard *Bd* swabbing protocol in frogs generally does not include the dorsum [see (39)], we included it because of unpublished reports of suspicious dorsal skin lesions associated with *Bd* infection in Hellbenders. We collected tissue samples for Ranavirus via a sterile punch biopsy (6×3 mm) or forceps and blade to remove a small tissue section of the dorsal tailfin near the tail-tip. We immediately placed swabs and tissue in sterile 1.5 mL microcentrifuge tubes with 70% ethanol for field storage and transport.

In 2012 we collected additional swabs exclusively from foot lesions in a subset of animals and sent these samples to Zoologix Inc. (Chatsworth CA) for additional targeted qPCR for *Citrobacter freundii* and *Aeromonas hydrophila*.

Quantitative PCR (qPCR) of *Bd, Bsal*, and Ranavirus

Ethanol was removed via centrifugation under a fume hood to dry samples prior to extraction. We extracted DNA from swabs and tail tissue using a DNeasy Blood and Tissue Kit (Qiagen Inc., Valencia, CA, USA) and stored at −80°C. Separate qPCR singleplex assays were performed for each target pathogen (Ranavirus, *Bd*, *Bsal*) with the following 15 μL protocol: 7.5 μL 2X TaqMan™ Universal PCR Master Mix (Applied Biosystems™), 1 μL Forward Primer at 10 μM, 1 μL Reverse Primer at 10 μM, 0.5 μL Probe at 10 μM, 1 μL molecular grade water, and 4 μL sample DNA. Reaction temperatures were as follows for Ranavirus and *Bd*: 50°C for 2 min, 95°C for 10 min, and 45 cycles of the following: 95°C for 15 s and 60°C for 60 s. *Bsal* reaction temperatures were identical except with increased annealing temperatures of 62°C. We used primer and probe combinations published from Picco et al. (40) for Ranavirus qPCR reactions and Blooi et al. (41) for *Bd* and *Bsal* reactions. Each 15 μL reaction was performed in a 96-well plate via the QuantStudio™ 6 Flex Real-Time PCR System (Applied Biosystems) with a positive control from DNA extracted from pure culture for each pathogen and a water negative control. We performed separate singleplex assays for *Bd* and *Bsal* as opposed to the published duplex (41) assay to avoid potential inter-assay competition and subsequent false negatives (42). Each sample was run in duplicate and rerun when duplicates did not match within two cycle threshold (Ct) values. If a rerun continued to have a discrepancy, we removed the sample from our analysis. We determined animals to be positive for a pathogen with an average Ct value < 45.

Lesion Scores

Based on previous surveys we knew that lesions reported to be increasing in prevalence were generally restricted to distal limbs, and this is where we focused lesion quantification. Lesion scores were based on observations of chronic, non-healing, ulcerative areas of the feet and toes. We and others had noted several Ozark Hellbenders with various abnormal toes that were swollen, sometimes ulcerated, and in other cases semi-necrosed or missing. Some individuals had severe digit loss, while others had mild swelling. We wanted to quantify this difference as opposed to use a presence/absence approach to lesion prevalence. A lesion scoring system was further necessary because traumatic wounds to the feet and rest of body can occur from conspecific interactions during the breeding season. We wanted to prevent these healed scars and wounds from potentially confounding lesion assessment in Ozark Hellbenders by adhering to lesion score criteria that only evaluated non-healed lesions in the distal limbs (**Table 1**). Using a preprinted baseline drawing, individuals were recorded for lesion sub-type and anatomic location. Digits were noted as either "Healthy" (**Figure 1A**), "Bulbous" or "Swollen" (**Figure 1B**), "Shortened" (**Figure 1C**), or "Missing" (**Figure 1C**), with accompanying ulcerations on foot pads (**Figure 1D**), ulcerations on toe tips (**Figures 1B,D**),

TABLE 1 | Lesion scoring system used to quantify distal limb lesions in Ozark Hellbenders, *Cryptobranchus alleganiensis bishopi*.

SCORE	No. foot pads ulcerated	No. toes missing	No. toes shortened	No. toes swollen	Description
0	0	0	0	0	No observable distal limb lesions. Healed scars may be present. No active ulcerations or swelling.
1	0	0	0	1–5	1–5 swollen toes in one or two feet. No ulcerations on feet or toes. No shortened, fused, or missing toes
2	0	0	0	6–10	6–10 swollen toes affecting two feet. Toe tip ulcerations may be present. No shortened, fused, or missing toes
3	0–1	0	0	11–18	11–18 swollen toes affecting three or four feet. Toe tip ulcerations may be present. No shortened, fused, or missing toes. May have one footpad ulceration
4	0–1	0–1	1–5	1–17	1–5 shortened toes with 0–1 missing toes. Remaining toes swollen. May have one footpad ulceration
5	0–2	0–4	1–16	1–15	1–5 shortened toes with 2–4 missing toes OR 6+ shortened toes with zero missing toes. Remaining toes swollen. May have up to two footpad ulcerations.
6	0–2	5–18	1–13	1–13	5+ missing toes with up to two foot pad ulcerations
7	3–4	5–18	1–13	1–13	5+ missing toes with 3+ foot pad ulcerations.

Scores are from 0–7. A score of 0 (blue) represents no distal limb lesions observed. Mild scores in green (1–2) have some swollen toes only, moderate scores in yellow (3–4) have most toes swollen and some shortened. Severe scores in red (5–7) denote several toes shortened or missing.

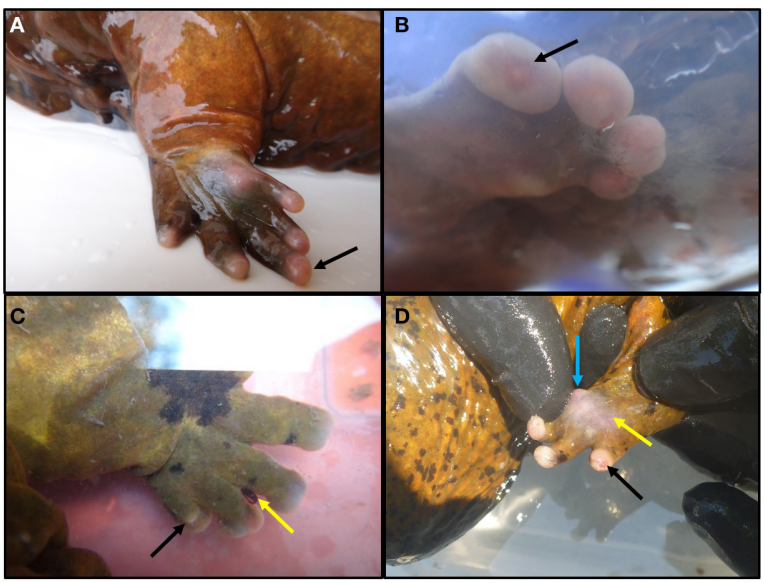

FIGURE 1 | Examples of various degrees of lesions observed in Ozark Hellbenders *Cryptobranchus alleganiensis bishopi* in Arkansas. **(A)** Foot with all toes intact and slight erythema with digit III slightly swollen (black arrow). This clinical presentation equals a score of one if all four feet were in this condition. **(B)** Front foot with all swollen digits with a toe tip ulceration on digit IV (black arrow). This clinical presentation equals a score of three if all four feet were in this condition. **(C)** Toes have become flattened and are beginning to shorten. Digit IV is almost completely missing, and bone is beginning to protrude through the dorsal skin (black arrow). Note an attached leech in the interdigital space between digits II and III (yellow arrow). This clinical presentation equals a score of five if all four feet were in this condition. If any more toes were completely missing along with two or more foot pad ulcerations, a score of 6–7 would be given. **(D)** Digit IV is swollen and slightly erythematous with toe tip ulceration (black arrow). Skin on foot pad is thin, turned white gray, slightly transparent, and is close to ulcerating (yellow arrow). Underlying tissue is swollen and erythematous with an apparent nodule forming at the medial aspect (blue arrow). This clinical presentation equals a score of three if all four feet were in this condition.

or completely missing limbs (picture not available). All drawings were created by the same field observer.

A lesion scoring system with eight levels ranging from scores of 0–7 (**Table 1**) was created and scores were based on the number of toes affected, type of sub-lesion on each toe, and presence or absence of foot-pad ulcerations. A score of 0 denoted an individual with no digital lesions, whereas a score of 7 denoted an individual with very severe lesions in all four feet. These eight levels were determined based on natural breaks in lesion severity by number of toes swollen, progressing to number of toes shortened, and number missing. This allowed levels to account for differential amounts of toes affected by these three

TABLE 2 | List of Linear Mixed Models (LMM) included in AICc analysis in order of smallest to largest ΔAICc.

Model name	Fixed effects	Random effects	K	LL	AICc	ΔAICc	AICcWt
Chytrid + Size	***Bd* (0/1) + Mass**	**Indv ID, Site, Year**	**7**	**−137.25**	**290.22**	**0.00**	**0.26**
Chytrid + Condition	***Bd* (0/1) + BCS**	**Indv ID, Site, Year**	**7**	**−137.58**	**290.88**	**0.66**	**0.18**
Chytrid only	***Bd* (0/1)**	**Indv ID, Site, Year**	**6**	**−138.82**	**290.92**	**0.70**	**0.18**
Global	***Bd* (0/1) + BCS + Mass**	**Indv ID, Site, Year**	**8**	**−136.66**	**291.57**	**1.34**	**0.13**
Size only	Mass	Indv ID, Site, Year	6	−139.60	292.47	2.25	0.08
Condition only	BCS	Indv ID, Site, Year	6	−139.83	292.93	2.70	0.07
Size + Condition	Mass + BCS	Indv ID, Site, Year	7	−138.79	293.30	3.08	0.05
Random	—	Indv ID, Site, Year	5	−141.35	293.60	3.38	0.05

Models evaluated individual and site factors on lesion severity (scored 0–7) of Ozark Hellbenders, Cryptobranchus alleganiensis bishopi in Arkansas. Fixed effects included presence/absence of chytrid fungus Batrachochytrium dendrobatids, Bd (0/1), mass (g), and body condition score (BCS). Random effects included Individual ID (Indv ID), site, and year. Top models of ΔAICc < 2.0 are noted in bold and were used for subsequent variable model averaging. Presence of Bd determined via qPCR from skin swab.

lesion subtypes without excessive levels to allow for quantitative analysis. Individuals receiving lesion scores of 1–2 primarily had toe swelling only. Scores 3–4 had most toes shortened and some missing. Scores 5–7 had several toes or even entire feet missing with remaining toes swollen or shortened. Score level cutoff and score designations to each animal were based on the standardized field drawings and were done blind to any other information of that animal.

Lesion Severity Models

A linear mixed model was used to evaluate effects of infection status and individual factors on lesion severity. We originally chose the following fixed effect parameters: mass, TL, and presence or absence of *Bd* and Ranavirus. We created a third individual parameter of body condition score (BCS) by calculating residuals for each individual from residuals of the fitted polynomial plot of TL and mass. Total length was subsequently removed from our analysis because of its correlation with mass. Because of few detections of Ranavirus, it was excluded from our models. All models included a combination of our individual fixed effects listed and the following three random effects of: Individual ID, Year, and Site ID. Our model list is described in **Table 2** which includes the following seven predictive models: Chytrid + Size, Chytrid + Condition, Chytrid only, Global, Size only, Condition only, Size + Condition, Random. All mixed models were created from the lme4 package (43) in RStudio (44). We evaluated relative model fit from AICc for all possible combinations of fixed effects to determine the top performing model via the AICcmodavg package (45) and considered models competitive when ΔAICc was < 2.0. Variables that appeared in more than one of the top models were model-averaged as recommended in Burnham and Anderson (46) to determine relative variable contribution in those models.

RESULTS

Pathogen Prevalence

Of the 73 individuals evaluated in this analysis, 23 (31.5%) were positive for *Bd, four* (5.5%) positive for Ranavirus, and 0% positive for *Bsal*. Two Ranavirus positive individuals were also infected with *Bd* (50.0%). For the subset of eight lesion-only swabs tested for opportunistic bacteria, 0% were positive for C. *freundii* and 0% positive for *A. hydrophila*.

Lesion Severity Distribution

A total of 73 animals were assessed during this study with an average lesion score of 4.27 and a median score of five. Only five animals were considered lesion free (Lesion Score = 0; 6.8%), and all these five were negative for *Bd*. Lesion-free animals were generally smaller, falling within the ten smallest individuals captured (15th percentile in mass), weighing <300 g. Of the 12 recaptured individuals nine had progressively greater lesion scores from the previous recapture, whereas three maintained the same score (**Table 3**). We recaptured one individual twice, with an initial score of four in 2011, followed by a lesion score of six in both 2012 and 2014 (**Table 3**).

Linear Mixed Models and AICc

Of the model sets evaluated, the Chytrid + Size, Chytrid + Condition, Chytrid only, and Global model sets were competitive based on AICc evaluation (**Table 2**). Of the model averaged coefficients from these model sets, *Bd* infection status was the only variable to have a significant effect on lesion severity ($\beta = 0.87 \pm 0.39$ S.E., C.I.: 0.11, 1.63; **Table 4**). Lesions in *Bd*-positive animals had an average score of 4.78 in contrast to 4.06 in *Bd*-negative animals (**Figure 2**). Random effects also did not explain variation well with the following variances in the top model for Individual ID (0.6524 ± 0.8077 S.D.), Site (0.8336 ± 0.9130 S.D.), and Year (0.0 ± 0.0 S.D.). However, because site explained the most variation among random effects, we created a table showing average lesion score and pathogen prevalence by site location in order from most upstream to downstream (**Table 5**). This reveals no clear pattern with lesion score but does highlight two sites for further investigation which had the lowest average lesion scores of 2.3 and 1.5 for sites 8 and 13, respectively.

DISCUSSION

This work presents novel data on the complexity and epidemiology of foot lesions in the remaining Arkansas Ozark Hellbender population. These lesions have only been mentioned

TABLE 3 | Twelve recaptured individuals and subsequent change in lesion score between final and initial captures.

Data ID	Recap no.	Final capture year	Final lesion score	Years between recap	Total score Δ	Score Δ per year
151	1	2014	5	3	+0	+0.0
153	1	2015	7	4	+2	+0.5
158	1	2014	6	1	+2	+2.0
158	2	2014	6	3	+2	+0.7
161	1	2014	5	3	+0	+0.0
166	1	2012	4	3	+3	+1.0
168	1	2012	5	1	+0	+0.0
169	1	2014	7	1	+1	+1.0
177	1	2014	5	2	+4	+2.0
180	1	2015	4	1	+4	+4.0
190	1	2015	4	1	+0	+0.0
191	1	2015	7	1	+1	+1.0
Average			5.4	2	+1.6	+1.0

Averages for scores listed at bottom. Note all lesion score changes are positive.

TABLE 4 | Fixed effect variables in top models (ΔAICc < 2) listed with model-averaged results.

Variable	*β* coeff	S.E.	95% C.I.
***Bd* (0/1)**	**0.87**	**0.39**	**0.11, 1.63**
Mass	0.35	0.21	−0.05, 0.76
BCS	0.27	0.19	−0.11, 0.65

Significant effects (based on 95% C.I.) noted in bold.

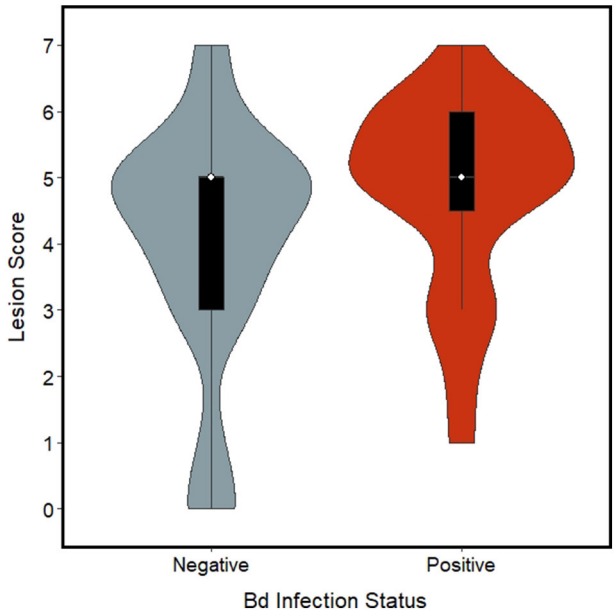

FIGURE 2 | Violin plot with box plots embedded for lesion scores (ranging 0–7) from foot lesions of Ozark Hellbenders, grouped by *Batrachochytrium dendrobatidis* (*Bd*) infection status. *Bd* negative Hellbenders (blue-gray) had an average score of 4.06 whereas *Bd* positive Hellbenders (red) had an average score of 4.78.

to occur but have never been evaluated or fully described in published literature to date. Our results demonstrate these distal limb lesions are prevalent (93.2%) in *C. a. bishopi* in Arkansas. This is a larger percentage of affected animals than previously reported in Ozark Hellbenders in Missouri (49% in 2004 and 67–90% in 2006) (13). Lesions appear inflammatory in nature, although we do not have histological data to confirm presence of inflammation. They are non-healing and progressive, and we hypothesize that lesions start within soft tissues of the digits and then progress to the skin surface as grossly visible ulcerative lesions, followed by loss of tissue integrity, and necrosis. In recaptured individuals, we found that lesions are maintained or worsen in severity over several years and were always restricted to distal limbs.

Only five individuals from a total of 73 (6.8%) sampled were lesion free. These apparently healthy individuals were represented by some of the smallest individuals. Interestingly, our top predictive model included mass. Although this was not a significant effect in our model averaging analysis, mass was positively correlated with lesion severity. If this represents a true trend, it may reveal that older, larger individuals are more likely to have severe lesions. One interpretation of this phenomenon would be that lesions result from long term sequelae from a single historical event such as a chemical runoff or single pathogen outbreak, and younger individuals were simply not alive during the exposure period. A second interpretation is the etiological agent(s) that is/are responsible for these lesions require(s) long-term exposure to produce disease and younger Hellbenders are not old enough to have reached a certain critical exposure time for lesion development. Both hypotheses imply a chronic and progressive disease process which is supported by our recapture data showing individuals had either the same or worse lesion scores upon successive captures.

Our most important finding was that *Bd* infection status was in all top predictive models and represents the only statistically significant predictor to explain lesion severity. We confirmed a significant positive correlation of *Bd* infection with lesion severity. However, the causation behind this relationship remains unclear. Previous surveys of *Bd* in wild Hellbenders have been of little apparent value in population assessments, as *Bd* is present in this and several other Hellbender populations with no clear disease association (18, 21–23, 47). Still, *Bd* is an introduced pathogen to the United States, only to appear in Hellbenders after 1969 (20), and may be causing more damage to Hellbender health than understood. In captive Hellbenders, chytridiomycosis is considered a serious health threat, and both adults and juveniles have experienced mortality due to *Bd* (24, 25). Furthermore, mortality events appeared to follow times of stress such as with juvenile captive to wild translocations (25) where *Bd* may have been able to take advantage of weakened skin immunity. Although current literature does not support

TABLE 5 | List of capture sites (exact location not disclosed) sampled for Ozark Hellbenders (*Cryptobranchus alleganiensis bishopi*) in Arkansas.

Site order	Total captures	Ranavirus pos.	*Bd* pos.	*Bd* % pos.	Avg lesion score
1	6	0	1	16.7	3.2
2	4	0	0	0.0	5.8
3	4	0	3	75.0	4.5
4	13	0	6	46.2	4.8
5	5	0	0	0.0	4.6
6	2	0	1	50.0	5.0
7	2	0	1	50.0	5.5
8	3	0	1	33.3	2.3
9	3	0	2	66.7	3.0
10	12	0	0	0.0	4.1
11	3	1	2	66.7	5.7
12	1	0	0	0.0	3.0
13	4	1	2	50.0	1.5
14	7	2	2	28.6	4.7
15	4	0	2	50.0	5.3
Total	**73**	**4**	**23**	**31.5**	**4.3**

Site number represents relative location along stream from most upstream (Site 1) moving in order to most downstream (Site 15). Listed for each site are total captures, total positive samples for Ranavirus or Bd, and average lesion score. Total counts or averages across all sites shown in bottom row.

immunosuppression via chronic stress as a driver of classic *Bd* mortality events in amphibians (48), stress may play a role in *Bd* susceptibility of more tolerant species (49). Laboratory trials have shown that *Bd* infection intensity and incidence of chytridiomycosis can increase after alterations in host immunity via glucocorticoid administration in plethodontid salamanders (50) and Northern Leopard Frogs (51). Therefore, if wild *C. a. bishopi* are experiencing immunosuppression associated with lesion severity, *Bd* may have a greater chance of maintaining infection, and should still be considered a health threat in the wild.

Our data may underestimate the impact *Bd* has on *C. a. bishopi* because of our sampling time. In Crawfish Frogs, *Lithobates areolatus*, *Bd* infection prevalence and intensity has seasonal patterns where individuals often clear infection by late summer only to become reinfected in winter and spring (52). If *Bd* follows the same infection pattern in *C. a. bishopi,* it could be an important factor preventing wound healing and promoting progressive disease in cooler months when prevalence is much greater than when we sample in late summer. Still, we do not propose *Bd* as a primary or necessary etiologic agent for manifestation of these lesions, but stress that *Bd* may be important in progression of lesion severity through disruption of skin function and healing, especially in more severe cases.

We hypothesize that lesion formation occurs through a multifactorial process. Synergistic effects of introduced agents and altered or degraded habitat have been shown to produce disease in an otherwise resistant population. For instance, red tide blooms can affect sea turtle immune function and potentially drive increased prevalence of fibropapillomatosis (53). In amphibians, increased use of the herbicide atrazine can negatively affect health directly (54), but also indirectly though potentiating trematode infestations (55). Ozark Hellbenders in Arkansas are experiencing heavy sediment loads from agricultural land uses and subsequent decreased watershed buffers, which could result in concomitant increases of agricultural runoff (e.g., pesticides, herbicides, contaminants of poultry litter). All sites sampled for this study fall along one river with little forested buffer remaining and constantly eroding stream banks. We cannot ignore the fact that habitat degradation is likely contributing to the lesions in Ozark Hellbenders in Arkansas and may be causing chronic stress with long term consequences of immunosuppression. Further, in laboratory experiments of another salamander species, *Desmognathus ochrophaeus*, increased plasma corticosterone was associated with increased wound healing time (56), which supports a potential mechanism between chronic stress and lesions.

Ozark Hellbenders are likely immunocompromised from decreased genetic diversity. Low immunogenetic diversity is linked to increased disease incidence in other wildlife species e.g., malaria in great reed warblers (57), and facial tumors in Tasmanian Devils (58). *C a. bishopi* have lower MHC IIb diversity than their Eastern counter parts in Missouri (59) and combined with other factors, may have reached a threshold to become less resistant to one or more pathogens. Further, genetic bottlenecking could also increase frequency of rare alleles and chances for genetically driven disease. Rare alleles are hypothesized to play an important role in complex diseases in humans such as with autism (60) and warrants further investigation for Ozark Hellbenders.

Opportunistic bacteria are hypothesized to contribute to these digit and foot lesions once host immune systems are weakened, however, no specific opportunistic pathogen has yet been identified (30, 34). Our subset of lesion swabs was negative for both *C. freundii* and *A. hydrophila*, which lowers support for their role in lesion development. Several other pathogens including viruses and parasites still need to be considered. For instance, a case of progressive ulcerative dermatitis was reported in a captive treefrog, *Phyllomedusa bicolor*, associated with both viral and microsporidial systemic infection, showing potential for either to contribute to skin ulcerations (61).

Ranavirus should still be considered as a potential pathogen in producing these lesions despite having a low prevalence in our samples (5.5%). Lesions of ranavirosis in juveniles of related Chinese Giant Salamanders (*Andrias davidianus*) include inflammation, ulceration, and necrosis of the distal limbs (28, 29) that appear to be very similar to those observed in *C. a. bishopi.* Ranavirus infection in *C. a. bishopi* adults may result in sublethal disease with long term sequelae as opposed to dramatic mortality events observed in juvenile *A. davidianus*. If only a single Ranavirus infection event is needed to cause damage to begin lesion formation, and a typical Hellbender has a life expectancy of 20–30 years in the wild, probability of exposure and subsequent long-term sequelae may be fairly high. This concept could hold true for many other pathogens that cause damage

to skin and vasculature, making the causative agent difficult to detect without long term monitoring.

It will be critical to understand the pathophysiology of this disease to determine the most effective course of action. Examples from domestic animals show us that complex diseases can be treated successfully if critical factors in disease manifestation are identified. For parvoviral disease in domestic dogs, the main etiologic agent is a virus (Parvoviridae), which cannot be targeted directly using antiviral drugs. Although disease can be prevented via vaccination, in unvaccinated dogs, mortality rates can be significantly reduced with antimicrobial treatment to prevent effects of secondary bacterial translocation of the gastrointestinal tract (62). Feline lower urinary tract disease (FLUTD) is a multifactorial process in domestic cats that can result in chronic urinary tract disease. Currently, the most effective treatment is not treating the animals, but rather treating the environment by removing sources of stress at home (63). Hellbender conservation managers should, therefore, focus attention not on a single factor but on an ecosystem. We may not be able to remove pathogens from these river systems, but we may be able to help reduce transmission between animals and reduce environmental stress. First, we can reduce artificially increased transmission and subsequent pathogen burden by adhering to aseptic sampling protocols in the field and in repatriation efforts. Second, we can focus efforts on habitat restoration. If bank restoration efforts decrease erosion and runoff, this may not only improve living and breeding space but simultaneously decrease disease incidence by reducing negative effects of environmental factors on host health.

This study documents a progressive disease affecting almost all sampled individuals in the remaining Ozark Hellbender population in Arkansas. The presentation of progressive lesions with a long differential list suggests that this disease is complex, and we highlight areas that need further research to fully understand factors in Ozark Hellbender health. Many questions still exist on the exact etiology of these lesions, and why they progress, but we do know that increased lesion severity is associated with *Bd* infection. We acknowledge that lack of histopathological data limits our inference into completely describing these lesions and recommend future studies to include histopathology to complement gross findings. Still, our lesion scoring system can be used to monitor changes in overall population health including response to restoration efforts. It can also be used to evaluate similar distal extremity lesions observed in other Ozark and Eastern Hellbender populations. Finally, Hellbenders are large, long-lived animals and may serve as sentinels for long term exposure to sublethal agents. The high prevalence of these lesions should not only motivate continued research in Hellbender health but should also raise concerns for potential health risks to other wildlife and human populations sharing these watersheds.

DATA AVAILABILITY STATEMENT

The datasets generated for this study are available on request to the corresponding author.

ETHICS STATEMENT

The animal study was reviewed and approved by University of Tennessee IACUC.

AUTHOR CONTRIBUTIONS

RH, KI, and DM contributed to conception and design of the study. RH, KI, and WS completed filed sampling. RH and WS performed the statistical analysis. RH organized the database. RH wrote the first draft of the manuscript. All authors contributed to manuscript revision, read, and approved the submitted version.

FUNDING

This work was supported by the Arkansas Game and Fish Commission.

ACKNOWLEDGMENTS

The authors would like to thank T. Inebit, USFWS, and all AGFC staff that assisted in monitoring over the years. Partial funding for open access to this research was provided by University of Tennessee's Open Publishing Support Fund.

REFERENCES

1. Hing S, Narayan EJ, Thompson RCA, Godfrey SS. The relationship between physiological stress and wildlife disease: consequences for health and conservation. *Wildlife Res.* (2016) 43:51–60. doi: 10.1071/WR15183
2. Southerl MT, Jung RE, Baxter DP, Chellman IC, Mercurio G, Vølstad JH. Stream salamanders as indicators of stream quality in Maryland, USA. *Appl Herpetol.* (2004) 2:23–46. doi: 10.1163/1570754041231596
3. Welsh HH Jr, Ollivier LM. Stream amphibians as indicators of ecosystem stress: a case study from California's redwoods. *Ecol Appl.* (1998) 8:1118–32. doi: 10.1890/1051-0761(1998)008[1118:SAAIOE]2.0.CO;2
4. Egea-Serrano A, Relyea RA, Tejedo M, Torralva M. Understanding of the impact of chemicals on amphibians: a meta-analytical review. *Ecol Evol.* (2012) 2:1382–97. doi: 10.1002/ece3.249
5. Brannon MP, Purvis BA. Effects of sedimentation on the diversity of salamanders in a southern Appalachian headwater stream. *J N C Acad Sci.* (2008) 124:118–22. Available online at: https://dc.lib.unc.edu/cdm/singleitem/collection/jncas/id/3892/rec/4
6. Nickerson MA, Mays CE. The hellbenders: North American giant salamanders. *Biol Geol.* (1973) 1:1–106.
7. Powell R, Conant R, Collins JT. *Peterson Field Guide to Reptiles and Amphibians of Eastern and Central North America*. 4th ed. New York, NY: Houghton Mifflin Co. (2016). 494 p.
8. Guimond RW, Hutchison VH. Aquatic respiration: An unusual strategy in the hellbender *Cryptobranchus alleganiensis alleganiensis* (Daudin). *Science.* (1973) 182:1263–5. doi: 10.1126/science.182.4118.1263
9. Da Silva Neto JG, Sutton WB, Freake M. Life-stage differences in microhabitat use by hellbenders (*Cryptobranchus alleganiensis*). *Herpetologica.* (2019) 75:21–9. doi: 10.1655/0018-0831-75.1.21
10. Keitzer SC. *Habitat preferences of the eastern hellbender in West Virginia* (Master's Thesis). Marshall University, Huntington, WV, United States (2007).
11. Wheeler BA, Prosen E, Mathis A, Wilkinson RF. Population declines of a long- lived salamander: a 20+ year study of hellbenders, *Cryptobranchus alleganiensis. Biol Conserv.* (2003) 109:151–6. doi: 10.1016/S0006-3207(02)00136-2

12. Graham SP, Soehren EC, Cline GR, Schmidt CM, Sutton WB, Rayburn JR, et al. Conservation status of hellbenders (*Cryptobranchus alleganiensis*) in Alabama, USA. *Herpetol Conserv Biol.* (2011) 6:242–9.
13. USFWS. Endangered and threatened wildlife and plants; endangered status for the Ozark Hellbender Salamander. 50 CFR part 23. *Fed. Regist.* (2011) 76:61956−78.
14. USFWS. Inclusion of the hellbender, including the eastern hellbender and the Ozark Hellbender, in appendix III of the convention on international trade in endangered species of wild fauna and flora (CITES). 50 CFR Part 23. *Fed. Regist.* (2011) 76:61978–85.
15. Bodinof-Jachowski CM, Hopkins WA. Loss of catchment-wide riparian forest cover is associated with reduced recruitment in a long-lived amphibian. *Biol Conserv.* (2018) 202:215–27. doi: 10.1016/j.biocon.2018.02.012
16. Hiler WR, Wheeler BA, Trauth SE. Abnormalities in the Ozark Hellbender, (*Cryptobranchus alleganiensis bishopi*) in Arkansas: a comparison between two rivers with a historical perspective. *J Ark Acad Sci.* (2005) 59:88–94.
17. Miller BT, Miller JL. Prevalence of physical abnormalities in Eastern Hellbender (*Cryptobranchus alleganiensis alleganiensis*) populations of middle Tennessee. *Southeastern Naturalist.* (2005) 4:513–20. doi: 10.1656/1528-7092(2005)004[0513:POPAIE]2.0.CO;2
18. Souza MJ, Gray MJ, Colclough P, Miller DL. Prevalence of *Batrachochytrium dendrobatidis* and ranavirus in eastern hellbenders (*Cryptobranchus alleganiensis alleganiensis*) in eastern Tennessee. *J Wildl Dis.* (2012) 48:560–6. doi: 10.7589/0090-3558-48.3.560
19. Briggler JT, Larson KA, Irwin KJ. Presence of the amphibian chytrid fungus (*Batrachochytrium dendrobatidis*) on hellbenders (*Cryptobranchus alleganiensis*) in the Ozark highlands. *Herpetol Rev.* (2008) 39:443–4.
20. Bodinof CM, Briggler JT, Duncan MC, Beringer J, Millspaugh JJ. Historic occurrence of the amphibian chytrid fungus *Batrachochytrium dendrobatidis* in hellbender *Cryptobranchus alleganiensis* populations from Missouri. *Dis Aquat Org.* (2011) 96:1–7. doi: 10.3354/dao02380
21. Bales EK, Hyman OJ, Loudon AH, Harris RN, Lipps G, Chapman E, et al. Pathogenic chytrid fungus *Batrachochytrium dendrobatidis*, but not *B. salamandrivorans*, detected on Eastern Hellbenders. *PLoS ONE.* 10:e0116405. doi: 10.1371/journal.pone.0116405
22. Williams LA, Groves JD. Prevalence of the amphibian pathogen *Batrachochytrium dendrobatidis* in Eastern Hellbenders (*Cryptobranchus alleganiensis*) in western North Carolina, USA. *Herpetol Conserv Biol.* (2014) 9:454−67.
23. Goyner JL, Yabsley MJ, Jensen JB. A preliminary survey of *Batrachochytrium dendrobatidis* exposure in hellbenders from a stream in Georgia, USA. *Herpetol Rev.* (2011) 42:58–9.
24. Dean N, Ossiboff R, Bunting E, Schuler K, Rothrock A, Roblee K. The Eastern Hellbender and *Batrachochytrium dendrobatidis* (*Bd*) in western New York. *Presented at the 65th Annual International Conference of the Wildlife Disease Association.* Cortland, NY (2016).
25. Dusick A, Flatland B, Craig L, Ferguson S. What is your diagnosis? Skin scraping from a hellbender. *Vet Clin Pathol.* (2016) 46:183–4. doi: 10.1111/vcp.12428
26. Martel A, Blooi M, Adriaensen C, Van Rooij P, Beukema W, Fisher MC, et al. Recent introduction of a chytrid fungus endangers western palearctic salamanders. *Science.* (2014) 346:630–1. doi: 10.1126/science.1258268
27. Klocke B, Becker M, Lewis J, Fleisher RC, Muletx-Wolz CR, Rockwood L, et al. *Batrachochytrium salamandrivorans* not detected in U.S. survey of pet salamanders. *Sci Rep.* (2017) 7:13132. doi: 10.1038/s41598-017-13500-2
28. Geng Y, Wang KY, Zhou ZY, Li CW, Wang J, He M, et al. First report of a ranavirus associated with morbidity and mortality in farmed Chinese giant salamanders (*Andrias davidianus*). *J Comp Pathol.* (2011) 145:95–102. doi: 10.1016/j.jcpa.2010.11.012
29. Zhou ZY, Geng Y, Liu XX, Ren SY, Zhou Y, Wang KY, et al. Characterization of a ranavirus isolated from the Chinese giant salamander (*Andrias davidianus*, Blanchard, 1871) in China. *Aquaculture.* (2014) 384–7:66–73. doi: 10.1016/j.aquaculture.2012.12.018
30. Nickerson CA, Ott CM, Castro SL, Garcia VM, Molina TC, Briggler JT, et al. Evaluation of microorganisms cultured from injured and repressed tissue regeneration sites in endangered giant aquatic Ozark Hellbender Salamanders. *PLoS ONE.* (2011) 6:e28906. doi: 10.1371/journal.pone.0028906
31. Chuang YM, Tseng SP, Teng LJ, Ho YC, Hsueh PR. Emergence of cefotaxime resistance in *Citrobacter freundii* causing necrotizing fasciitis and osteomyelitis. *J Infect.* (2006) 53:e161–3. doi: 10.1016/j.jinf.2005.11.002
32. Gudmundsdottir BK, Bjornsdottir B. *Aeromonas salmonicida* and *A. hydrophila*. In: Woo PTK, Cipriano RC, editors. *Fish Viruses and Bacteria: Pathobiology and Protection.* Boston, MA: CABI (2017). p. 173–89. doi: 10.1079/9781780647784.0173
33. Miller DL, Rajeev S, Brookins M, Cook J, Whittington L, Baldwin CA. Concurrent infection with Ranavirus, *Batrachochytrium dendrobatidis*, and *Aeromonas* in a captive anuran colony. *J Zoo Wildlife Med.* (2008) 39:445–9. doi: 10.1638/2008-0012.1
34. Hernández-Gómez O, Kimble, SJA, Briggler JT, Williams RN. Characterization of the cutaneous bacterial communities of two giant salamander subspecies. *Microb Ecol.* (2017) 73:445–54. doi: 10.1007/s00248-016-0859-9
35. Briggler JT, Ackerson JR. Construction and use of artificial shelters to supplement habitat for hellbenders (*Cryptobranchus alleganiensis*). *Herpetol. Rev.* (2012) 43:412–6.
36. Hecht-Kardasz KA, Nickerson MA, Freake M, Colclough P. Ecology and population structure of Hellbenders in the Great Smoky Mountains. *Bull Fla Mus Nat Hist.* (2012) 51:227–41.
37. Bryan L, Baldwin CA, Gray MJ, Miller DL. Efficacy of select disinfectants at inactivating Ranavirus. *Dis Aquat Org.* (2009) 84:89–94. doi: 10.3354/dao02036
38. Johnson ML, Berger L, Philips L, Speare R. Fungicidal effects of chemical disinfectants, UV light, desiccation and heat on the amphibian chytrid *Batrachochytrium dendrobatidis*. *Dis Aquat Org.* (2003) 57:255–60. doi: 10.3354/dao057255
39. Brem F, Mendelson JR III, Lips KR. *Field-Sampling Protocol for Batrachochytrium dendrobatidis From Living Amphibians, Using Alcohol Preserved Swabs. Version 1.0*. Arlington, TX: Conservation International. (2007). Available online at: http://www.amphibians.org (accessed July 18, 2007).
40. Picco AM, Brunner JL, Collins JP. Susceptibility of the endangered California tiger salamander, *Ambystoma californiense*, to ranavirus infection. *J Wildl Dis.* (2007) 43:286–90. doi: 10.7589/0090-3558-43.2.286
41. Blooi M, Pasmans F, Longcore JE, Spitzen-van der Sluijs A, Vercammen F, Martel A. Duplex real-time pcr for rapid simultaneous detection of *Batrachochytrium dendrobatidis* and *Batrachochytrium salamandrivorans* in amphibian samples. *J Clin Microbiol.* (2013) 51:4173–7. doi: 10.1128/JCM.02313-13
42. Thomas V, Blooi M, Van Rooij P, Van Praet S, Verbrugghe E, Grasselli E, et al. Recommendations on diagnostic tools for *Batrachochytrium salamandrivorans*. *Transbound Emerg Dis.* (2018) 65:478–88. doi: 10.1111/tbed.12787
43. Bates D, Maechler M, Bolker B, Walker S. Fitting linear mixed-effects models using lme4. *J Stat Softw.* (2015) 67:1–48. doi: 10.18637/jss.v067.i01
44. R Core Team. *R: A Language and Environment for Statistical Computing*. Vienna: R Foundation for Statistical Computing (2013). Available online at: http://www.R-project.org/ (accessed March 10, 2019).
45. Mazerolle MJ. *AICcmodavg: Model Selection and Multimodel Inference Based on (Q)AIC(c).* R Package Version 2.2-1. (2019). Available online at: https://cran.r-project.org/package=AICcmodavg (accessed July 01, 2019).
46. Burnham KP, Anderson DR. *Model Selection and Inference: A Practical Information-Theoretic Approach*. 2nd ed. New York, NY: Springer-Verlag (2002).
47. Seeley KE, D'Angelo M, Gowins C, Greathouse J. Prevalence of *Batrachochytrium dendrobatidis* in Eastern Hellbender (*Cryptobranchus alleganiensis*) populations in West Virginia, USA. *J Wildl Dis.* (2016) 52:391–4. doi: 10.7589/2015-02-052
48. Grogan LF, Robert J, Berger L, Skerratt LF, Scheele BC, Castley JG, et al. Review of the Amphibian immune response to Chytridiomycosis, and future directions. *Front Immunol.* (2018) 9:2536. doi: 10.3389/fimmu.2018.02536
49. Rollins-Smith LA. Amphibian immunity-stress, disease, and climate change. *Dev Comp Immunol.* (2017) 66:111–9. doi: 10.1016/j.dci.2016.07.002
50. Fonner CW, Patel SA, Boord SM, Venesky MD, Woodley SK. Effects of corticosterone on infection and disease in salamanders exposed to the

amphibian fungal pathogen *Batrachochytrium dendrobatidis*. *Dis Aquat Org.* (2017) 123:159–71. doi: 10.3354/dao03089
51. Tatiersky L, Rollins-Smith LA, Lu R, Jardine C, Barker IK, Clark ME, et al. Effect of glucocorticoids on expression of cutaneous antimicrobial peptides in northern leopard frogs (*Lithobates pipiens*). *BMC Vet Res.* (2015) 11:191. doi: 10.1186/s12917-015-0506-6
52. Kinney VC, Heemeyer JL, Pessier AP, Lannoo MJ. Seasonal patterns of *Batrachochytrium dendrobatidis* infection and mortality in *Lithobates areolatus*: affirmation of Vrendenberg's "10,000 zoospore rule". *PLoS ONE.* (2011) 6:e16708. doi: 10.1371/journal.pone.0016708
53. Perrault JR, Stacy NI, Lehner AF, Mott CR, Hirsch S, Gorham JC, et al. Potential effects of brevetoxins and toxic elements on various health variables in Kemp's ridley (*Lepidochelys kempii*) and green (*Chelonia mydas*) sea turtles after a red tide bloom event. *Sci Total Environ.* (2017) 605–6:967–79. doi: 10.1016/j.scitotenv.2017.06.149
54. Hayes TB, Anderson LL, Beasley VR, de Solla SR, Iguchi T, Ingraham H, et al. Demasculinization and feminization of male gonads by atrazine: consistent effects across vertebrate classes. *J Steroid Biochem Mol Biol.* (2011) 127:64–73. doi: 10.1016/j.jsbmb.2011.03.015
55. Rohr JR, Schotthoefer AM, Raffel TR, Carrick HJ, Halstead N, Hoverman JT, et al. Agrochemicals increase trematode infections in a declining amphibian species. *Nature.* (2008) 455:1235–9. doi: 10.1038/nature07281
56. Thomas JR, Woodley SK. Treatment with corticosterone delays cutaneous wound healing in male and female salamanders. *Gen Comp Endocrinol.* (2015) 216:33–8. doi: 10.1016/j.ygcen.2015.04.013
57. Westerdahl H, Waldenström J, Hansson B, Hasselquist D, von Schantz T, Bensch S. Associations between malaria and MHC genes in a migratory songbird. *Proc R Soc B.* (2005) 272:1511–8. doi: 10.1098/rspb.2005.3113
58. Morris KM, Wright B, Grueber CE, Hogg C, Belov K. Lack of genetic diversity across diverse immune genes in an endangered mammal, the Tasmanian devil (*Sarcophilus harrisii*). *Mol Ecol.* (2015) 24:3860–72. doi: 10.1111/mec.13291
59. Hernández-Gómez O, Briggler JT, Williams RN. Influence of immunogenetics, sex and body condition on the cutaneous microbial communities of two giant salamanders. *Mol Ecol.* (2018) 27:1915–29. doi: 10.1111/mec.14500
60. Griswold AJ, Dueker ND, Van Booven D, Rantus JA, Jaworski JM, Slifer SH, et al. Targeted massively parallel sequencing of autism spectrum disorder-associated genes in a case control cohort reveals rare loss-of-function risk variants. *Mol Autism.* (2015) 6:43. doi: 10.1186/s13229-015-0034-z
61. Graczyk TK, Cranfield MR, Bicknese EJ, Wisnieski AP. Progressive ulcerative dermatitis in a captive, wild-caught South American giant tree fog (*Phyllomedusa bicolor*) with microsporidial septicemia. *J Zoo Wildlife Med.* (1996) 27:522–7.
62. Goddard A, Leisewitz AL. *Canine parvovirus*. *Vet Clin N Am.* (2010) 40:1041–53. doi: 10.1016/j.cvsm.2010.07.007
63. Westropp JL, Delgado M, Buffington CAT. Chronic lower urinary Tract signs in cats: current understanding of pathophysiology and management. *Vet Clin N Am.* (2019) 49:187–209. doi: 10.1016/j.cvsm.2018.11.001

Conflict of Interest: The authors declare that the research was conducted in the absence of any commercial or financial relationships that could be construed as a potential conflict of interest.

Copyright © 2020 Hardman, Irwin, Sutton and Miller. This is an open-access article distributed under the terms of the Creative Commons Attribution License (CC BY). The use, distribution or reproduction in other forums is permitted, provided the original author(s) and the copyright owner(s) are credited and that the original publication in this journal is cited, in accordance with accepted academic practice. No use, distribution or reproduction is permitted which does not comply with these terms.

frontiers in Veterinary Science

CASE REPORT
published: 07 February 2020
doi: 10.3389/fvets.2020.00024

Clinical Manifestation and Molecular Characterization of a Novel Member of the *Nannizziopsiaceae* in a Pulmonary Granuloma From a Galapagos Tortoise (*Chelonoidis nigra*)

Jane E. Christman[1], *Amy B. Alexander*[1], *Kyle A. Donnelly*[1], *Robert J. Ossiboff*[1], *Nicole I. Stacy*[1], *Rebecca L. Richardson*[1], *J. Brad Case*[2], *April L. Childress*[1] *and James F. X. Wellehan*[1]*

[1] *Department of Comparative, Diagnostic and Population Medicine, College of Veterinary Medicine, University of Florida, Gainesville, FL, United States,* [2] *Department of Small Animal Clinical Sciences, College of Veterinary Medicine, University of Florida, Gainesville, FL, United States*

OPEN ACCESS

Edited by:
David K. Meyerholz, University of Iowa, United States

Reviewed by:
Amanda Jezek Martinot, Beth Israel Deaconess Medical Center, Harvard Medical School, United States
Matt Allender, University of Illinois at Urbana-Champaign, United States

***Correspondence:**
James F. X. Wellehan
wellehanj@ufl.edu

Specialty section:
This article was submitted to Veterinary Experimental and Diagnostic Pathology, a section of the journal Frontiers in Veterinary Science

Received: *07 September 2019*
Accepted: *13 January 2020*
Published: *07 February 2020*

Citation:
Christman JE, Alexander AB, Donnelly KA, Ossiboff RJ, Stacy NI, Richardson RL, Case JB, Childress AL and Wellehan JFX (2020) Clinical Manifestation and Molecular Characterization of a Novel Member of the Nannizziopsiaceae in a Pulmonary Granuloma From a Galapagos Tortoise (Chelonoidis nigra). Front. Vet. Sci. 7:24. doi: 10.3389/fvets.2020.00024

Nannizziopsiaceae is a family of fungal organisms within the order Onygenales containing two genera of important reptile pathogens, *Nannizziopsis* and *Paranannizziopsis*. A captive Galapagos tortoise (*Chelonoidis nigra*) from Boca Raton, Florida, United States, was presented for a clinical history of chronic progressive lethargy and inappetence. At initial presentation, the tortoise had a moderate non-regenerative anemia, leukocytosis, whip-like heterophil projections, erythrocyte fragmentation, and fibrin strands, with the latter two raising concern for disseminated intravascular coagulation. A single large encapsulated pulmonary granuloma was identified through imaging, including plain film radiography and bronchoscopy. Direct intralesional samples were obtained from transcarapacial celioscopy for fungal culture, cytology, histopathology, and polymerase chain reaction. Amplification and sequencing of the ITS2 region of the rRNA genes with Bayesian and maximum likelihood analyses placed the fungus in the family Nannizziopsiaceae within the order Onygenales, representing a novel fungal species.

Keywords: onygenales, *Nannizziopsiaceae*, fungal pneumonia, *Chelonoidis nigra*, Galapagos tortoise

INTRODUCTION

Galapagos tortoises (*Cheloinidis nigra*) are the largest tortoise species and are listed in CITES Appendix I. They appear prone to fungal infections in captivity, with reported organisms including *Beauveria bassiana* (1), *Exophiala equina* (2), and *Aphanoascella galapagosensi* (3).

The fungal order Onygenales in the class Eurotiomycetes contains the majority of the most significant fungal pathogens of vertebrates, including *Ajellomyces* (*Blastomyces* and *Histoplasma*), *Coccidioides*, *Paracoccidioides, Microsporum, Trichophyton, Ophidiomyces,* and *Lacazia*. Within the order Onygenales, members of the family Nannizziopsiaceae contain the genera *Nannizziopsis* and *Paranannizziopsis*, which cause significant morbidity and mortality in reptiles (4). While many cases were initially misidentified as *N. vriesii* based on morphology, and the initial isolation of

Nannizziopsis (*Rollandina*) *vriesii* was from an *Amieva* sp., the authors are not aware of any reptile isolates other than the one in 1970, and it does not appear to be a common reptile pathogen. *N. guarroi* is the most widespread in captive reptiles, and most significantly impacts squamates in Iguania (Agamidae, Chamaeleonidae, Iguanidae, and relatives), where it is commonly known as "yellow fungus disease" (5). *N. arthrosporioides, N. barbata, N. chlamydospora*, and *N. draconii* reportedly cause cutaneous infections in agamids, albeit less commonly, while *N. dermatitidis* displays a similar clinical presentation in chameleons and leopard geckos. *N. crocodili* has been associated with disease in crocodiles and is the only member of the genus primarily known to cause infections in non-squamate reptiles (6). *N. obscura* has been linked to osteomyelitis in humans (7) and a *N. obscura*-like fungus has been found to cause fungal disease in a Bryde's whale (*Balaenoptera edeni*) (8). The genus *Paranannizziopsis* causes disease primarily in aquatic snakes, although disease has also been seen in tuatara and a coastal bearded dragon (9). To date, disease due to Nannizziopsiaceae has not been described in the Testudines.

CASE PRESENTATION

A captive, ∼80-year-old male Galapagos tortoise (*Chelonoidis nigra*) from Boca Raton, Florida, USA, presented for 8 months of progressive lethargy and a 2-week duration of inappetence. The tortoise was originally wild caught from the Galapagos Islands in the 1940s and had been maintained in the current collection for over 30 years while housed in close proximity to several other chelonian species in intermixed groups. Prior to presentation, the animal was treated with three courses of unknown doses of fenbendazole separated 3 months apart.

On presentation, the tortoise was severely lethargic and unable to lift his head. He was subjectively considered in adequate body condition based on musculature. A moderate amount of opaque tan mucoid discharge was noted on the nasal planum and oral cavity. A corneal opacity was also present in the left eye, and ophthalmic examination noted intracorneal hemorrhage and corneal edema. A complete blood count at initial presentation revealed a mild to moderate leukocytosis (18.2K cells/μl; expected reference 0.5–15.9 × 10^3 cells/μl (10) with a mild heterophil left shift (0.9 × 10^3 cells/μl) as well as severe, non-regenerative anemia [PCV 14%; expected reference 8-29.8%; (10)] with occasional erythrocyte fragments. Initial blood film review resulted in identification of variably sized aggregates of fine linear strands suggestive of fibrin with entrapped thrombocytes (**Figure 1A**); these linear strands were confirmed as fibrin based on Fraser Lendrum stain (**Figure 1B**). The initial and subsequent blood films showed variable numbers of whip-like heterophil projections suggestive of inflammation (11). Together, the presence of fibrin strands and evidence of erythrocyte fragmentation raised concern for developing disseminated intravascular coagulation. Plasma chemistry results did not show any abnormal findings.

Transcarapacial radiographs pursued 48 h after admission showed an expansile soft tissue opacity in the right dorsal lung with a mild to moderate faveolar to interstitial pattern in the left lung. Blood culture performed at the time of ultrasound grew aerobic, fastidious, Gram-positive bacilli that could not be identified biochemically. Sensitivity could not be performed due to fastidious growth. On bronchoscopy, just past the branch to the right bronchi, a large, tan mass was identified. Superficial biopsy samples were submitted for cytology, histopathology, fungal culture, and fungal polymerase chain reaction (PCR). Fungal culture was negative. Cytology showed abundant mucus with mixed heterophilic and histiocytic inflammation with focal aggregates of coccobacilli, and a single fragment of fungal hypha stained argyrophilic with Gomori methenamine stain. Histologically the biopsy consisted of a ciliated respiratory epithelium overlying a submucosa mildly expanded with fibrillar to homogenous eosinophilic material and multifocal aggregates of lymphocytes, plasma cells, macrophages, and heterophils; no fungal elements were identified, and no microbes were identified on Gram, Gomori methenamine-silver (GMS), periodic acid-Schiff, or Fite's acid fast stained slides.

Five days after initial presentation, transcarapacial surgical pulmonoscopy was performed. Two adjacent 5 mm pilot holes were created in the right cranial carapace at the second pleural scute. A large (∼10 cm in diameter) round tan granuloma was observed along the dorsal pulmonary parenchyma within the right lung (**Figure 1C**). The capsule was debrided and deep tissue biopsies were collected. Voriconazole (0.2 mg/kg, VFend, Pfizer, New York, NY) and amphotericin B (0.1 mg/kg, X-Gen Pharmaceuticals Inc., Horseheads, NY) were injected directly into the center of the granuloma. A 12-french, 11 cm polypropylene intralesional port (Boston Scientific, Marlborough, MA) was placed directly within the granuloma. Histology showed granulomatous and heterophilic inflammation with mixed proteinaceous cellular debris, reactive faveolar pneumocytes, and low numbers of fungal hyphae (**Figure 1D**). GMS staining highlighted fungal hyphae with septate parallel walls 4-6 μm in diameter and infrequent dichotomous acute angle branching (**Figure 1E**). No acid fast organisms were seen on Fite's acid fast staining.

The lung granuloma sample was plated onto Chocolate agar, Columbia Blood agar (BAP), MacConkey agar (MAC), Colistin with Nalidixic acid (CNA), Potato Flake agar (PFA), and Inhibitory Mold agar (IMA). The Chocolate, BAP, MAC, and CNA plates were incubated at 25 ± 2°C for 5 days. Plates were reviewed every 18-24 h for bacterial growth. On day 5, a very scant amount of filamentous growth appeared around the tissue that was embedded into the Chocolate, BAP and CNA agar plates. No bacterial colonies appeared after 5 days. The fungal colony was isolated to a PFA and incubated at 25 ± 2°C, along with the original PFA plates that were set-up for the fungal culture, to ensure growth from the aerobic culture matched what was growing on the fungal culture.

The PFA and IMA plates were incubated at 25 ± 2° and reviewed at day 7. Very scant growth of a white, dense fungus appeared on each plate. Microscopic morphology was reviewed using the cellophane tape mount method. Hyphae were septate and produced arthroconidia-like structures. Conidia were tear-drop shaped with blunt or straight bases. Some were shaped like

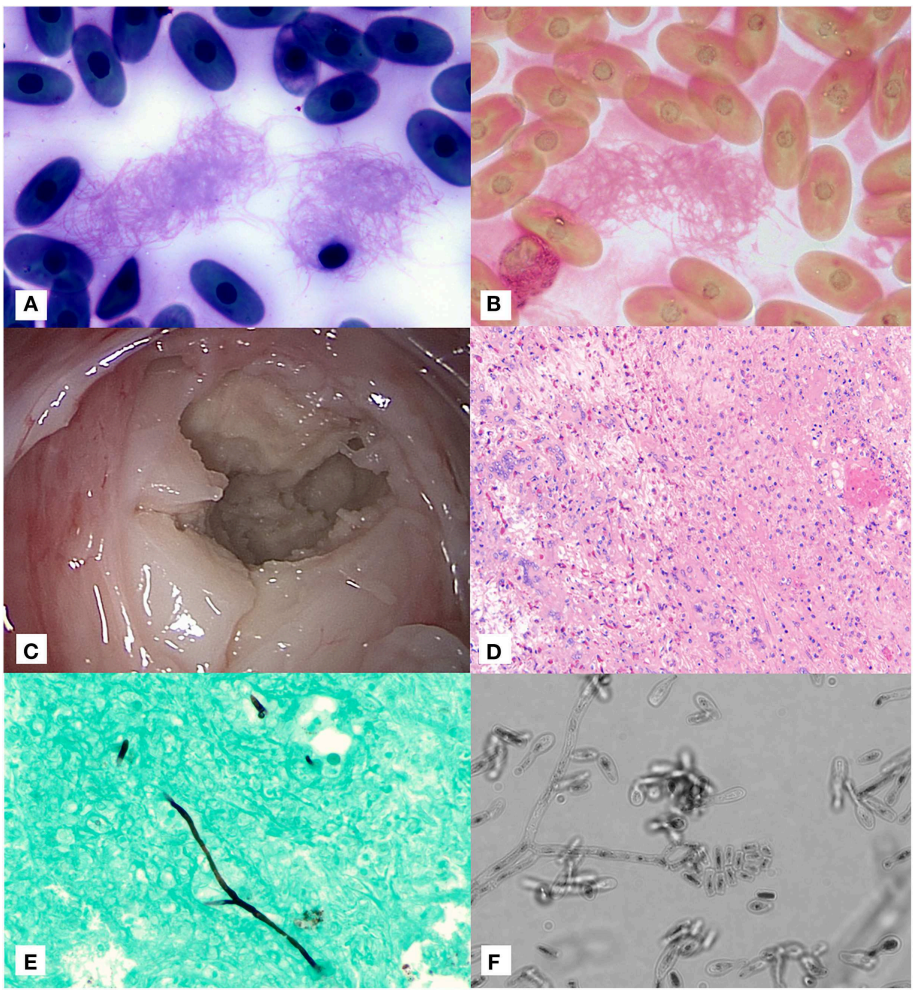

FIGURE 1 | Image composite of diagnostic findings in a Galapagos tortoise (*Chelonoidis nigra*) with a pulmonary fungal granuloma caused by a novel Nannizziopsiaceae. **(A)** Aggregates of fine linear fibrin strands in a blood film at time of initial presentation stained with Wright-Giemsa (×100 objective). **(B)** Fraser-Lendrum stain of fibrin strands (×100 objective). **(C)** Gross image of encapsulated pulmonary mass through transcarapacial pulmonoscopy. **(D)** Hematoxyin/Eosin staining of pulmonary granuloma. **(E)** Gomori methenamine silver staining of rare branching, parallel walled fungal hyphae within the pulmonary granuloma as sampled by direct intralesional sampling (×20 objective). **(F)** Direct light microscopy of fungal microconidia and hyphae as grown in culture (×60 objective).

glass bottles, with a spherical base and long, straight neck. Most conidia were single celled, and some had 2 cells (**Figure 1F**).

DNA was extracted from a biopsy of the pulmonary granuloma and from a fungal culture with a commercial extraction kit (DNeasy® Blood and Tissue Kit, Qiagen, Valencia, CA) following manufacturer's instructions. Polymerase chain reaction amplification of the internal transcribed spacer 2 (ITS2) domain of the rRNA gene was undertaken using previously described methods with primers ITS4 and ITS86 (12) on both the direct sample taken directly from the celioscopy as well as from fungal colonies taken from the fungal culture. To obtain additional sequence, polymerase chain reaction amplification of the actin gene using primers Act-l b and Act-4r was done on the samples (13). Products were electrophoresed on a 1% agarose gel and PCR products were purified using a commercial extraction kit (QIAquick gel extraction kit, Qiagen Inc., Valencia, CA) followed by direct sequencing using a commercial kit (Big-Dye terminator kit, Applied Biosystems, Foster City, CA) on an automated DNA sequencer (ABI 3130, Applied Biosystems, Foster City, CA). Primer sequences were trimmed off prior to further analysis, and the ITS2 sequence was 248 nucleotides and the actin sequence was 852 nucleotides. Sequences were submitted to GenBank under accession numbers MN403040 and (submitted, to be added prior to publication).

Homologous nucleotide sequences for fungal ITS2 and actin were retrieved from GenBank and aligned using the program Multiple Alignment using Fast Fourier Transform (MAFFT) (14). All *Paranannizziopsis* and several *Nannizziopsis* species had no available actin sequences. *Penicillium_digitatum* (GenBank accession numbers NW_014574615 and NW_014574576), a

fungus in the order Eurotiales in the class Eurotiomycetes, was designated as the outgroup. Bayesian phylogenetic analyses of nucleotide alignments were performed using MrBayes 3.1.2 on the CIPRES server, with a general time reversible model, gamma distributed rate variation, and a proportion of invariant sites (15, 16). The first 25% of 2,000,000 iterations were discarded as burn in. There were no significant topological differences when each gene was run individually, so the genes were concatenated, with ambiguities used for actin in the 2 *Paranannizziopsis* and 4 *Nannizziopsis* that had no available sequence. The Bayesian phylogenetic tree is shown (**Figure 2**).

Maximum likelihood analysis was performed using RAxML on the CIPRES server, using a gamma distributed rate variation, a proportion of invariant sites, and a general time reversible model (17). Again, *Penicillium digitatum* (GenBank accession numbers NW_014574615 and NW_014574576) was used as an outgroup. To test the strength of the tree topology, bootstrap analysis was used (1000 re-samplings) (18). ML bootstrap values are shown on the Bayesian tree (**Figure 2**).

Samples were submitted to the University of Texas San Antonio for fungal susceptibility, which showed the organism was inhibited by itraconazole at 0.06 μg/ml, posaconazole at ≤0.03 μg/ml, and terbinafine at ≤0.004 μg/ml. While there are no CLSI standards, these values were interpreted by the authors as likely to be clinically efficacious. Inhibition by amphotericin B occurred at 0.25 μg/ml, by fluconazole at 32 μg/ml, and by voriconazole at 0.125 μg/ml. The patient was discharged on itraconazole (6.5 mg/kg q24h, Par Pharmacueticals, Chestnut Ridge, NY) and terbinafine (3.8 mg/kg q24h, Harris Pharmaceutical Inc., Fort Myers, FL). While follow-up imaging was declined, the moribund state of the state of the tortoise resolved and spontaneous hemorrhage was no longer seen. The patient is known to be doing well 2 years after discharge.

DISCUSSION

Fungi in the order Onygenales (class Eurotiomycetes) show significant genomic adaptation to utilizing animal hosts, with

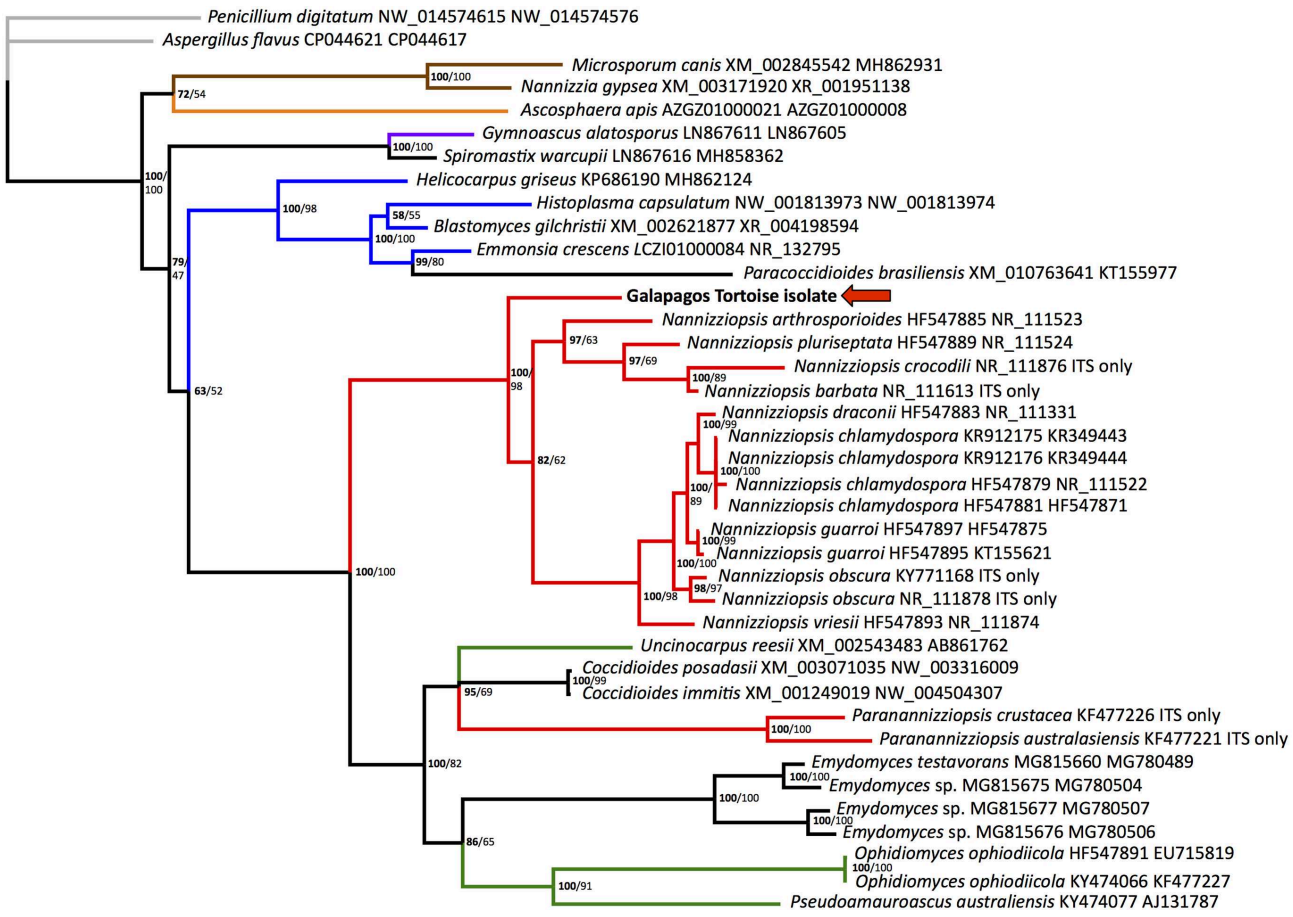

FIGURE 2 | Bayesian tree depicting the relationship of the Galapagos tortoise fungus to other members of the order Onygenales, based on the ITS2 region. Numbers at each node represent the posterior probability in bold, and ML bootstrap values are given unbolded to the right. *Penicillium digitatum* is used as an outgroup, and the order Eurotiales is in gray. The family Arthrodermataceae is in brown, Ascosphaeraceae is in orange, Gymnoascaceae is in purple, Ajellomycetaceae is in blue, Nannizziopsiaceae are in red, Onygenaceae are in green, and taxa not currently assigned to a family are in black. The Galapagos tortoise fungus is marked with an arrow.

reduction in cellulose binding genes for digesting plants and an increase in keratinase genes for digesting animals (19, 20). Despite the clinical significance of the Onygenales in diverse vertebrate hosts, there is little data on disease due to the Onygenales in Testudines to date. *Aphanoascella galapagoensis*, a member of the Onygenales in the family Onygenaceae, was isolated from a Galapagos tortoise with carapacial keratitis (3). Recently, *Emydomyces testavorans*, a member of the Onygenales that does not cluster with the Nannizziopsiaceae, was reported in shell lesions from diverse aquatic turtles (21).

The ITS2 region is transcribed with the highly conserved rRNA genes but does not have an apparent function and is therefore not highly conserved. This results in utility for distinguishing closely related organisms but presents challenges with longer-range phylogenetic analyses. Actin is an important structural gene and is more conserved. Support for some family-level relationships was fairly strong, with Arthrodermataceae and Ajellomycetaceae (shown in **Figure 2** in brown and blue, respectively) showing 100% posterior probability and 98-100% ML bootstrap values. However, the monophyly of *Nannizziopsis* and *Paranannizziopsis* was not identified using this region. Our analysis found moderate support for *Paranannizziopsis* clustering within Onygenaceae, with 100% posterior probability and 82% ML bootstrap support. It should be noted that we did not have actin sequence for *Paranannizziopsis*, so this placement is based solely on ITS2 data. Even with additional gene sequences, strong support for this was not found in some other analyses (21). Use of additional genes would resolve placement of *Paranannizziopsis*. However, the support for clustering of the Galapagos tortoise isolate with *Nannizziopsis* is strong; the Bayesian posterior probability is 100% and the ML bootstrap value is 98%. This organism should be classified either in *Nannizziopsis* or as a novel sister genus. The genetic distances seen within the genus in our analysis are greater than distances between some other genera, suggesting a novel sister genus may be more appropriate.

While reported *Nannizziopsis* cases in squamates and crocodilians presented initially as cutaneous lesions, pulmonary disease has been reported in an *Amieva* sp. (22) and a carpet chameleon (*Furcifer* [*Chamaeleo*] *lateralis*) (23). *Nannizziopsis hominis* has been isolated from fungal lesions in the lungs of humans (4). The findings in this tortoise were most consistent with a primary pulmonary infection, as no cutaneous lesions were identified.

Giant tortoises represent a diagnostic challenge. The shell of tortoises is a significant impediment to interpretation of traditional radiographic imaging, and advanced imaging such as computed tomography (CT) or magnetic resonance imaging (MRI) is often needed to image soft tissue structures (24, 25). As are many giant tortoises, this patient was too large to fit in available CT or MRI equipment. Endoscopy represents an alternative methodology for visualization of lesions in tortoises (26). Pulmonary fungal disease is not uncommon in Galapagos tortoises (1, 27). Transcarapacial pulmonoscopy has been used for fungal pneumonia in a smaller tortoise species (28); without its use in this case, a definitive diagnosis could not have been made and direct treatment of the lesion would not have been possible.

Other factors may have contributed to the development of clinical disease in this patient. Benzimidazole toxicosis affects rapidly dividing cells, especially those of hematopoietic tissue; Hermann's tortoises (*Testudo hermanni*) given two 5-day courses of 50 mg/kg of fenbendazole 2 weeks apart showed significant heteropenia for 70 days (29). The fenbendazole treatment prior to admission may have predisposed this tortoise to immunosuppression and fungal infection. The climate in Boca Raton, FL, may also have played an immunosuppressive role. Puerto Ayora, in the Galapagos Islands, has average temperatures of 26.4°C during the hottest month of the year, and 21.4°C during the coolest month of the year (https://en.climate-data.org). Palm Beach, 45 km north of Boca Raton, has average temperatures of 28°C during the hottest month of the year, and 18.6°C during the coolest month of the year (https://en.climate-data.org). Temperatures outside the range for which ectotherms are adapted to can be expected to result in suboptimal immune function (30, 31).

The non-regenerative anemia on initial bloodwork reflects the patient's debilitated status and suggested bone marrow suppression secondary to chronic inflammation and/or from presumptive drug toxicity. The observation of fibrin strands on blood films at initial presentation was an unusual finding and raised concern for developing intravascular coagulation, although thrombocytes were considered adequate and observed in variably sized clumps, some of which were entrapped in fibrin aggregates. This may also explain the presence of the intracorneal hemorrhage and subjectively prolonged bleeding at the site of collection during venipuncture at admission. Disseminated intravascular coagulation has been previously reported in other chelonians, including a softshell turtle and sea turtles in response to mycobacteriosis (32) and cold stunning (33), respectively. Significant improvement was noted during the 4 weeks of hospitalization at the clinic. The patient was discharged and has been clinically stable at time of writing of this manuscript (18 months after admission).

The relatively low concentration at which itraconazole inhibited this fungus *in vitro* may have been important for the response to therapy. This does not appear to be the case for all members of the *Nannizziopsiaceae*. In one report, two of three bearded dragons treated for *N. guarroi* with itraconazole died (34). In another report, six of seven bearded dragons treated for *N. guarroi* with itraconazole and clotrimazole died (35) Only one of two chameleons treated for *N. dermatitidis* with itraconazole survived (23). Phenotypic differences between species in the *Nannizziopsiaceae* may be clinically significant, emphasizing the importance of accurate and precise fungal identification for patient care. This case report describes the clinical manifestation and medical management of Nanniziomycotic infection in a tortoise and documents the identification and molecular characterization of a novel fungal pathogen in a clinically significant clade.

DATA AVAILABILITY STATEMENT

The sequence data from this study can be found in GenBank under accession number MN403040.

AUTHOR CONTRIBUTIONS

Clinical management of the case by JEC, AA, KD, JW. Transcarapacial pulmonoscopy, sample collection, and port placement by JBC, KD. Fungal culture and morphologic characterization by RR. Histologic interpretation performed by RO. Cytologic interpretation performed by NS. PCR and sequencing performed by AC. Sequence interpretation and phylogenetic analysis by JW. Initial draft written by JEC. All authors contributed to the writing and editing of this manuscript.

ACKNOWLEDGMENTS

The authors would like to thank the veterinary technicians and the diagnostic laboratory staff of the University of Florida Veterinary Teaching Hospital for their dedicated work with this patient.

REFERENCES

1. Georg LK, Williamson WM, Tilden EB, Getty RE. Mycotic pulmonary disease of captive giant tortoises due to *Beauvaria bassiana* and *Paecilomyces fumosoroseus*. *Sabouraudia*. (1963) 2:80–6. doi: 10.1080/00362176385190161
2. Manharth A, Lemberger K, Mylniczenko N, Pinkerton M, Pessier AP, Kammeyer P, et al. Disseminated phaeohyphomycosis due to an *Exophiala* species in a Galapagos tortoise, *Geochelone nigra*. *J Herpetol Med Surg*. (2005) 15:20–6. doi: 10.5818/1529-9651.15.2.20
3. Sutton DA, Marin Y, Thompson EH, Wickes BL, Fu J, Garcia D, et al. Isolation and characterization of a new fungal genus and species, *Aphanoascella galapagosensis*, from carapace keratitis of a Galapagos tortoise (*Chelonoidis nigra* microphyes). *Med Mycol*. (2013) 51:113–20. doi: 10.3109/13693786.2012.701767
4. Sigler L, Hambleton S, Paré JA. Molecular characterization of reptile pathogens currently known as members of the *Chrysosporium* anamorph of *Nannizziopsis vriesii* complex and relationship with some human-associated isolates. *J Clin Microbiol*. (2013) 51:3338–57. doi: 10.1128/JCM.01465-13
5. Le Donne V, Crossland N, Brandao J, Sokolova Y, Fowlkes N, Nevarez JG, et al. *Nannizziopsis guarroi* infection in 2 Inland Bearded Dragons (*Pogona vitticeps*): clinical, cytologic, histologic, and ultrastructural aspects. *Vet Clin Pathol*. (2016) 45:368–75. doi: 10.1111/vcp.12345
6. Hill AG, Sandy JR, Begg A. Mycotic dermatitis in juvenile freshwater crocodiles (*Crocodylus johnstoni*) caused by *Nannizziopsis crocodili*. *J Zoo Wildl Med*. (2019) 50:225–30. doi: 10.1638/2018-0133
7. Stillwell WT, Rubin BD, Axelrod JL. Chrysosporium, a new causative agent in osteomyelitis. A case report. *Clin Orthop Relat Res*. (1984) 190–2. doi: 10.1097/00003086-198404000-00032
8. Groch KR, Diaz-Delgado J, Sacristan C, Oliveira DE, Souza G, Sanchez-Sarmiento AM, et al. Pulmonary and systemic fungal infections in an Atlantic spotted dolphin and a Bryde's whale, Brazil. *Dis Aquat Organ*. (2018) 128:73–9. doi: 10.3354/dao03207
9. Masters NJ, Alexander S, Jackson B, Sigler L, Chatterton J, Harvey C, et al. Dermatomycosis caused by *Paranannizziopsis australasiensis* in five tuatara (*Sphenodon punctatus*) and a coastal bearded dragon (*Pogona barbata*) in a zoological collection in New Zealand. *N Z Vet J*. (2016) 64:301–7. doi: 10.1080/00480169.2016.1177473
10. Teare A. *ZIMS Expected Test Results for Chelonoidis nigra*. (2019). Species360 Zoological Information Management System. Retrieved from: http://zims.Species360.org [filters: All_ages_combined_All_sexes_Standard_International_Units]
11. Stacy NI, Fredholm DV, Rodriguez C, Castro L, Harvey JW. Whip-like heterophil projections in consecutive blood films from an injured gopher tortoise (*Gopherus polyphemus*) with systemic inflammation. *Vet Quart*. (2017) 37:162–5. doi: 10.1080/01652176.2017.1325538
12. Turenne CY, Sanche SE, Hoban DJ, Karlowsky JA, Kabani AM. Rapid identification of fungi by using the ITS2 genetic region and an automated fluorescent capillary electrophoresis system. *J Clin Microbiol*. (1999) 37:1846–51. doi: 10.1128/JCM.37.6.1846-1851.1999
13. Voigt K, Wöstemeyer J. Reliable amplification of actin genes facilitates deep-level phylogeny. *Microbiol Res*. (2000) 155:179–95. doi: 10.1016/S0944-5013(00)80031-2
14. Katoh K, Toh H. Improved accuracy of multiple ncRNA alignment by incorporating structural information into a MAFFT-based framework. *BMC Bioinform*. (2008) 9:212. doi: 10.1186/1471-2105-9-212
15. Miller MA, Schwartz T, Pickett BE, He S, Klem EB, Scheuermann RH, et al. A RESTful API for access to phylogenetic tools via the CIPRES science gateway. *Evol Bioinform*. (2015) 11:43–8. doi: 10.4137/EBO.S21501
16. Ronquist F, Teslenko M, Van Der Mark P, Ayres DL, Darling A, Höhna S, et al. MrBayes 3.2: efficient Bayesian phylogenetic inference and model choice across a large model space. *Syst Biol*. (2012) 61:539–42. doi: 10.1093/sysbio/sys029
17. Stamatakis A, Hoover P, Rougemont J. A rapid bootstrap algorithm for the RAxML web servers. *Syst Biol*. (2008) 57:758–71. doi: 10.1080/10635150802429642
18. Felsenstein J. Confidence limits on phylogenies: an approach using the bootstrap. *Evolution*. (1985) 39:783–91. doi: 10.1111/j.1558-5646.1985.tb00420.x
19. Sharpton TJ, Stajich JE, Rounsley SD, Gardner MJ, Wortman JR, Jordar VS, et al. Comparative genomic analyses of the human fungal pathogens Coccidioides and their relatives. *Genome Res*. (2009) 19:1722–31. doi: 10.1101/gr.087551.108
20. Burmester A, Shelest E, Glöckner G, Heddergott C, Schindler S, Staib P, et al. Comparative and functional genomics provide insights into the pathogenicity of dermatophytic fungi. *Genome Biol*. (2011) 12:R7. doi: 10.1186/gb-2011-12-1-r7
21. Woodburn DB, Miller AN, Allender MC, Maddox CW, Terio KA. *Emydomyces testavorans*, a new genus and species of onygenalean fungus isolated from shell lesions of freshwater aquatic turtles. *J Clin Microbiol*. (2019) 57:e00628-18. doi: 10.1128/JCM.00628-18
22. Stchigel AM, Sutton DA, Cano-Lira JF, Cabañes FJ, Abarca L, Tintelnot K, et al. Phylogeny of chrysosporia infecting reptiles: proposal of the new family Nannizziopsiaceae and five new species. *Persoonia*. (2013) 31:86–100. doi: 10.3767/003158513X669698
23. Paré JA, Sigler L, Hunter DB, Summerbell RC, Smith DA, Machin KL. Cutaneous mycoses in chameleons caused by the *Chrysosporium* anamorph of *Nannizziopsis vriesii* (Apinis) Currah. *J Zoo Wildl Med*. (1997) 28:443–53.
24. Croft LA, Graham JP, Schaf SA, Jacobson ER. Evaluation of magnetic resonance imaging for detection of internal tumors in green turtles with cutaneous fibropapillomatosis. *J Am Vet Med Assoc*. (2004) 225:1428–35. doi: 10.2460/javma.2004.225.1428
25. Ricciardi M, Franchini D, Valastro C, Ciccarelli S, Caprio F, Eyad Assad A, et al. Multidetector computed tomographic anatomy of the lungs in the loggerhead sea turtle (*Caretta caretta*). *Anat Rec*. (2018) 302:1658–65. doi: 10.1002/ar.24030
26. Divers SJ, Stahl SJ, Camus A. Evaluation of diagnostic coelioscopy including liver and kidney biopsy in freshwater turtles (*Trachemys scripta*). *J Zoo Wildl Med*. (2010) 41:677–87. doi: 10.1638/2010-0080.1
27. Heard D, Cantor G, Jacobson E, Purich B, Ajello L, Padhye, A. Hyalohyphomycosis caused by *Paecilomyces lilacinus* in an Aldabra tortoise. *J Am Vet Med Assoc*. (1986) 189:1143.
28. Hernandez-Divers SJ. Pulmonary candidiasis caused by *Candida albicans* in a Greek tortoise (*Testudo graeca*) and treatment with

intrapulmonary amphotericin B. *J Zoo Wildl Med*. (2001) 32:352–9. doi: 10.1638/1042-7260(2001)032<0352:PCCBCA>2.0.CO;2
29. Neiffer DL, Lydick D, Burks K, Doherty D. Hematologic and plasma biochemical changes associated with fenbendazole administration in Hermann's tortoises (*Testudo hermanni*). *J Zoo Wildl Med*. (2005) 36:661–73. doi: 10.1638/04003.1
30. Ferguson LV, Kortet R, Sinclair BJ. Eco-immunology in the cold: the role of immunity in shaping the overwintering survival of ectotherms. *J Exp Biol*. (2018) 221(Pt 13):jeb163873. doi: 10.1242/jeb.163873
31. Zimmerman LM, Wilson Carter A, Bowden RM, Vogel LA. Immunocompetence in a long-lived ectothermic vertebrate is temperature dependent but shows no decline in older adults. *Funct Ecol*. (2017) 31:1383–9. doi: 10.1111/1365-2435.12867
32. Murray M, Waliszewski NT, Garner MM, Tseng FS. Sepsis and disseminated intravascular coagulation in an eastern spiny softshell turtle (*Apalone spinifera spinifera*) with acute mycobacteriosis. *J Zoo Wildl Med*. (2009) 40:572–5. doi: 10.1638/2008-0125.1
33. Innis CJ, Staggs LA. Cold-stunning. In: Manire CA, Norton TM, Stacy BA, Innis CJ, Harms CA, editors. *Sea Turtle Health and Rehabilitation*. Plantation, FL: J. Ross Publishing, Inc. (2017). p. 675–87.
34. Bowman MR, Paré JA, Sigler L, Naeser JP, Sladky KK, Hanley CS, et al. Deep fungal dermatitis in three inland bearded dragons (*Pogona vitticeps*) caused by the *Chrysosporium* anamorph of *Nannizziopsis vriesii*. *Med Mycol*. (2007) 45:371–6. doi: 10.1080/13693780601188610
35. Hedley J, Eatwell K, Hume L. Necrotising fungal dermatitis in a group of bearded dragons (*Pogona vitticeps*). *Vet Rec*. (2010) 166:464–5. doi: 10.1136/vr.b4816

Conflict of Interest: The authors declare that the research was conducted in the absence of any commercial or financial relationships that could be construed as a potential conflict of interest.

Copyright © 2020 Christman, Alexander, Donnelly, Ossiboff, Stacy, Richardson, Case, Childress and Wellehan. This is an open-access article distributed under the terms of the Creative Commons Attribution License (CC BY). The use, distribution or reproduction in other forums is permitted, provided the original author(s) and the copyright owner(s) are credited and that the original publication in this journal is cited, in accordance with accepted academic practice. No use, distribution or reproduction is permitted which does not comply with these terms.

frontiers in Veterinary Science

REVIEW
published: 21 February 2020
doi: 10.3389/fvets.2020.00003

Infectious Wildlife Diseases in Austria—A Literature Review From 1980 Until 2017

Nina Eva Trimmel[1]* *and Chris Walzer*[1,2]

[1] Department of Integrative Biology and Evolution, Research Institute of Wildlife Ecology, University of Veterinary Medicine Vienna, Vienna, Austria, [2] Wildlife Conservation Society, Bronx, NY, United States

This literature review examines infectious wildlife disease research in Austria. We analyzed 226 research papers, published between 1980 and 2017. We determined that wildlife disease papers increased significantly from 0.8 ± 0.8 publications per year in the first decade (1980–1989) when compared to 2008–2017 with an average of 12.9 ± 4.1 publications per year. We illustrate information about the most investigated diseases and highlight the lack of research into certain wildlife pathogens. A special emphasis was given to diseases with zoonotic potential. The review showed that research focused on a few select species like the red fox (*Vulpes vulpes*), red deer (*Cervus elaphus*), and wild boar (*Sus scrofa*), all game species. Moreover, diseases affecting livestock and human health were seen more often. The review also found that only a low number of publications actually stated disease prevalence and confidence interval data. The reported diseases identified were classified according to their notifiable status and the distribution at the wildlife–human and wildlife–livestock interface. Furthermore, we try to argue why research into some diseases is prioritized, and why other diseases are underrepresented in current Austrian research. While spatiotemporal indicators could not be assessed due to the variability in methodologies and objectives of various studies, the information provided by this review offers the first comprehensive evaluation of the status of infectious wildlife disease research in Austria. Therefore, this study could assist investigators to identify further areas of priorities for research and conservation efforts and for wildlife management professionals to inform policy and funding strategies. With this review, we want to encourage research in the field of wildlife diseases in Austria to enhance current knowledge in the prevention of further loss in biodiversity and to find new measures to promote "One Health" on a global scale.

Keywords: wildlife, infectious, diseases, zoonosis, Austria, game, one health, EID

OPEN ACCESS

Edited by:
Nicole Indra Stacy,
University of Florida, United States

Reviewed by:
Martha Weber,
Riverbanks Zoo and Garden, United States
Karoly Erdelyi,
National Food Chain Safety Office, Hungary

***Correspondence:**
Nina Eva Trimmel
nina.trimmel@gmail.com

Specialty section:
This article was submitted to Zoological Medicine, a section of the journal Frontiers in Veterinary Science

Received: *26 August 2019*
Accepted: *02 January 2020*
Published: *21 February 2020*

Citation:
Trimmel NE and Walzer C (2020) Infectious Wildlife Diseases in Austria—A Literature Review From 1980 Until 2017. Front. Vet. Sci. 7:3. doi: 10.3389/fvets.2020.00003

INTRODUCTION

We determined the status of infectious wildlife disease research in Austria based on a 37-year literature review between 1980 and 2017. The literature review was modeled on a similar study from the Republic of Korea in 2017 (1). One reason for conducting this review was to determine if an increase in so-called emerging infectious diseases (EIDs) had been noted in Austrian wildlife. It has previously been determined that that ∼70% of EIDs have their origin in wildlife, and an estimated 60–80% of all EIDs also have zoonotic potential (2, 3). Increases in EIDs are related to the human

impacts on landscapes (3, 4). In our constantly changing world, ecosystems continuously transform and offer pathogens novel opportunities to evolve, resulting in a greater diversity of adaptable and rapidly spreading infectious agents (5). Pathogens that can infect several species of hosts, so-called multihost pathogens, can also represent cause for concern with regard to wildlife conservation (6). Wildlife potentially contributes to the spread and maintenance of infectious diseases, and knowing the status supports addressing and mitigating impacts.

Austria has a population of ∼8.8 million people (2017) with an average population density of 105 people/km^2. The gross domestic product per capita is 37,100 euros (2016), which makes Austria one of the wealthiest countries in the European union (EU). A member of the European Union (EU) since 1995, the federal state of Austria is located in Central Europe and divided into nine provinces. Austria is a landlocked country with a land area of 83,879 km^2 and a diversity of landscapes. About two-thirds of the land mass are mountainous, encompassing the Alps, the Carpathians, as well as the gneiss and granite highlands of the Bohemian Massif. The remaining third consists of the Vienna Basin and the Pannonian border regions of the Hungarian lowlands (7–9). The Austrian Fauna consists of roughly 45,870 different species, of which 626 are vertebrates. One hundred and ten vertebrates belong to the mammalian class, 418 to the avian class, 16 to the class of reptiles, 21 are amphibian species, and 60 species are fish (10).

Both active and passive surveillance programs for wildlife diseases exist in Austria (11, 12). Control programs were successful in eradicating rabies using widespread oral immunization of red fox (*Vulpes vulpes*). The last known rabies case occurred in 2003, and in 2008, Austria was declared rabies free. As of 2013, indicator animals (e.g., fox, badger, racoon dog, and raccoon) opportunistically were found dead, and all animals suspected of being rabid are examined at the National Reference Laboratory. Additional epizootic monitoring programs for Aujesky disease, bovine spongiform encephalopathy (BSE), scrapie, bluetongue virus, *Brucella melitensis*, bovine brucellosis, enzootic bovine leucosis, infectious bovine rhinotracheitis and infectious pustular vulvovaginitis, classical swine fever, and avian influenza are implemented. Only one zoonotic disease in wildlife is routinely monitored, namely, trichinosis in wild boars (*Sus scrofa*). In addition, in livestock animals, campylobacteriosis, echinococcosis, salmonellosis, trichinosis, and verotoxin-producing *Escherichia coli* are routinely monitored (13).

Abbreviations: ADNS, Animal Disease Notification System; AGES, Austrian Agency for Health and Food Safety; ASF, African swine fever; AT, Austria; AVR, Annual Veterinary Report; BSE, Bovine spongiform encephalopathy; BVD, Bovine viral diarrhea; CI, Confidence interval; CWD, Chronic wasting disease; EFSA, European Food Safety Authority; EID, Emerging infectious disease; EU, European Union; KVG, Kommunikationsplattform VerbraucherInnengesundheit; MRSA, *Methicillin-resistant Staphylococcus aureus;* NA, Not applicable; NCBI, National Center for Biotechnology Information; NRL, National Reference Laboratory of the AGES; OIE, World Organization for Animal Health; RZZA, Report of Zoonoses and Zoonotic Agents; TSE, Transmissible spongiform encephalopathy; TSG, Tierseuchengesetz, Federal law on epizootics; WNV, West Nile Virus.

The wildlife-human interface in Austria consists of a number of critical points, such as game meat consumption, the hunting industry (e.g., direct contact between hunters, hunting dogs, and game animals) and tourism (e.g., hikers and recreational athletes). Occupations that involve a constant exposure to animals are related to a higher risk of infection, and this risk may be intensified through contact with livestock sharing pastures with wildlife. Risk groups include farmers, veterinarians, hunters, forestry workers, veterinary technicians, animal keepers, taxidermists, zookeepers, and people who prepare or consume game meat (14–18).

Wildlife diseases are often not included in epidemiological reflections, as the main focus remains on diseases in livestock and transmission to humans. It is important to note that the wildlife-livestock interface is bidirectional and dynamic with frequent pathogen exchange through shared resources, such as habitats, water, and feed (19, 20). These factors increase the risk of transmitting infectious diseases from wildlife to domestic animals and subsequently to humans (19). Our review serves not only as an overview but also as a reminder that research on wildlife diseases is important and must be encouraged. This review is the first and only comprehensive review of infectious wildlife diseases in Austria.

MATERIALS AND METHODS

A detailed literature search was conducted between October 2018 and December 2018 using the following literature data bases: "vetmedseeker" (vetmedseeker, University of Veterinary Medicine Vienna, Austria), "Scopus" (Scopus, Elsevier, Netherlands), "Ovid" ("Ovid Technologies," Wolters Kluwer, Netherlands), "Web of Science" (Web of Science Core Collection, Clarivate Analytics, United States), and "PubMed" (NCBI Pubmed, National Center for Biotechnology Information, United States). Search terms used included "wildlife," "diseases," "infectious," and "zoonosis" adjusted by setting the time frame to 1980–2017 and the affiliation to Austria. This resulted in 2,696 hits on "Scopus," 1,284 hits on the "vetmedseeker," 755 on "Ovid," 473 on "PubMed," and 180 on "Web of Science." Only articles published in peer-reviewed journals were retained. Papers that addressed wildlife-human or wildlife-domestic disease transmission were also included. Additional articles found manually from the respective citations were included as well. A schematic step-by-step of the literature search can be found in **Figure 1**.

Following abstract review, 518 publications from "Scopus" appeared relevant. Papers were then compiled using a reference managing software (End Note Version X7.8, Thomson Reuters, United States). Duplicates, non-peer reviewed articles, book chapters, and conference proceedings were excluded in a first round. In a second round, we focused on infectious pathogens and diseases occurring in wild species. We excluded papers describing non-infectious, autoimmune, or idiopathic diseases. In addition, we restricted the search to vertebrates. Multicountry studies were only included in our review if "Austria" was mentioned in the materials and methods. In a third

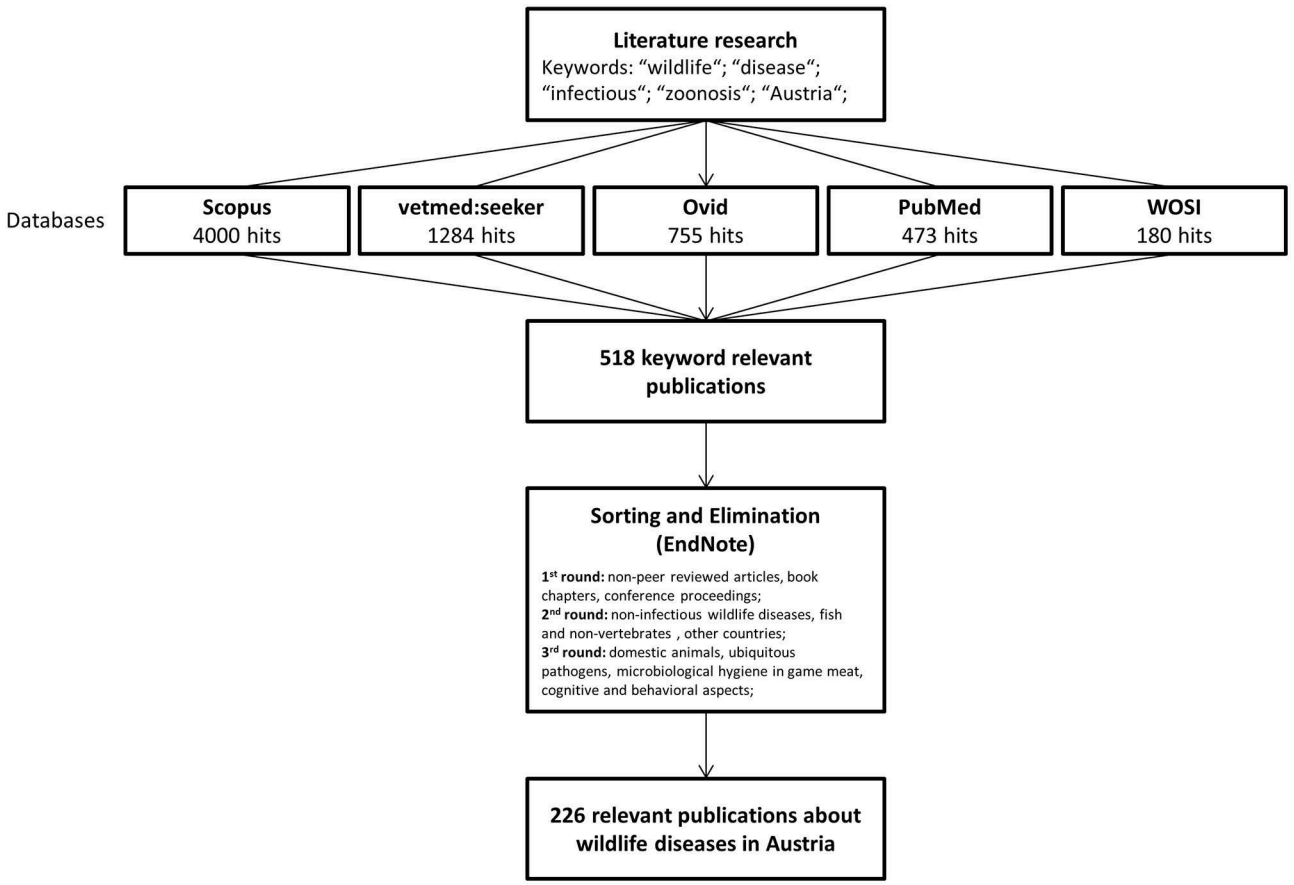

FIGURE 1 | Overview of the work steps for drafting this review.

round, we excluded publications that addressed microbiological hygiene aspects in game meat. Subsequent to this process, it was clear that "Scopus" was the most efficient database for wildlife diseases, revealing 219 out of a total of 226 relevant publications. "PubMed," in contrast, only showed 76 relevant articles. Finally, from all databases surveyed, 226 papers were retained and entered into a Microsoft Excel file for descriptive statistical analysis.

Publications were classified according to definitions by "Springer Nature" concerning article type (21) into original research articles, reviews, case reports, and short reports or letters. Original research articles were further subdivided into controlled studies and retrospective studies. Subsequently papers were categorized according to year of publication, type of pathogen, affected animal species, and group interface. The classification of group interfaces describes the primary group of interest (e.g., wildlife, humans, or livestock animals). Furthermore, we recorded whether the disease was notifiable according to the OIE List of notifiable diseases or the current Austrian legislation. If the paper covered various infectious agents, it was assigned to the categories "Notifiable in Austria" or "OIE-listed disease," if at least one notifiable disease was included. In addition, it was noted if the prevalence and confidence intervals of the pathogen(s) were stated in the article.

Infectious agents were divided into parasitic, viral, bacterial, and fungal pathogens, and articles covering more than one pathogen or addressing more than one species were classified as "multiple infectious agents" or "multiple species affected." Furthermore, agents were classified as zoonotic or having zoonotic potential. To determine the zoonotic potential of the diseases, the OIE list for infectious diseases, the "Merck Veterinary Manual" (22), as well as various textbooks (23–26) were consulted. Diseases that are not yet known to have zoonotic potential or are currently being researched have been labeled as "unknown."

RESULTS

Publication Frequency

After review, we retained 226 publications, published between 1980 and 2017 (**Figure 2**). With the exception of the years 1981–1982, 1986, 1988, 1991, and 1993–1994, numerous wildlife disease papers were published. From 1995 onwards, there was a continuous increase in wildlife disease publications, with the most articles ($n = 19$) published in 2014. In 2007 and 2015, a drop in publications was noted, followed by an increase in the subsequent year. During the 37 years reviewed, 2000–2017 was most productive period with 89.4% of the retained articles

published during this time period. Comparing the average yearly number of publications in the first decade (1980–1989 = 0.8 ± 0.8) to the last decade (2008–2017 = 12.9 ± 4.1) clearly shows a significant increase in interest in wildlife diseases (normality of data was tested by Shapiro-Wilk; two-tailed *t*-test: $p = 0.01$, *t*-statistics = −9.1178). Of the 226 papers, 146 publications were empirical studies, more specifically, 109 controlled studies, and 37 retrospective analyses. The rest was composed of 30 review articles, 34 case reports, and 16 letters or short reports (**Figure 3**).

Infectious Agents

The largest proportion of publications, namely 84 (37%), addressed infectious diseases caused by parasites (endoparasites: protozoa and helminths, or ectoparasites: arachnids and insects). A total of 67 (30%) of publications discussed viral diseases and 53 (23%) bacterial diseases, 9 (4%) dealt with diseases of fungal origin, and 13 (6%) papers mentioned multiple infectious agents (27–41). We found no studies concerning diseases caused by prions (see **Figure 4**). In summary, we found 136 pathogens discussed in the 226 publications. For the complete list of all diseases and pathogens found in this study, see **Table 1**. Of these 136 infectious agents, 84 (62%) were only featured once, 23 (17%) were mentioned twice, and 12 (9%) were discussed three times. The remaining pathogens, namely 17 (12%), were featured more than three times. No clear trend was determined as to changes in which pathogenic agents were reported over the years (see **Figure 5**). Beyond the publications that discussed multiple pathogens ($N > 10$), Usutu virus was the most studied

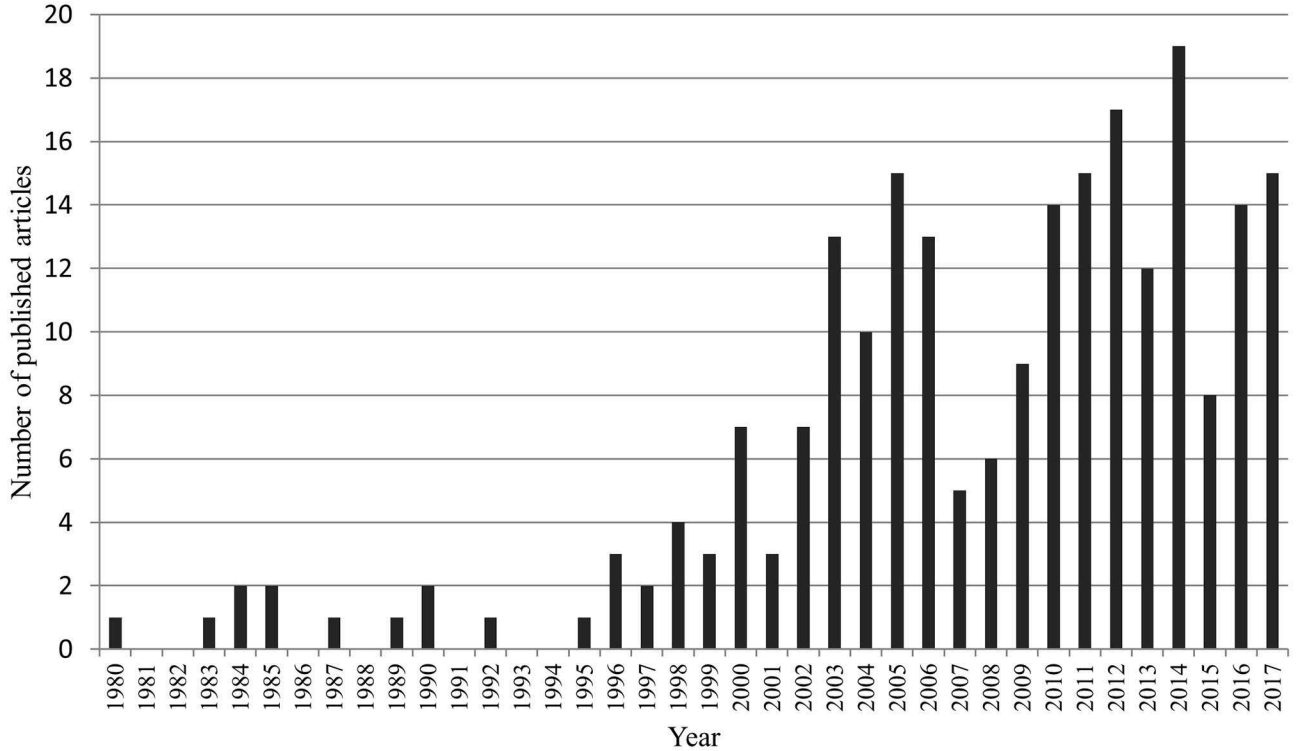

FIGURE 2 | Frequency of publications addressing wildlife diseases in Austria between 1980 and 2017.

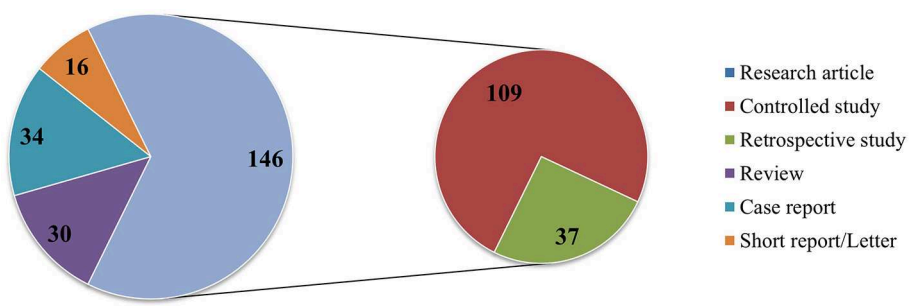

FIGURE 3 | Numerical amount of the different types of scientific publications according to the Springer classification.

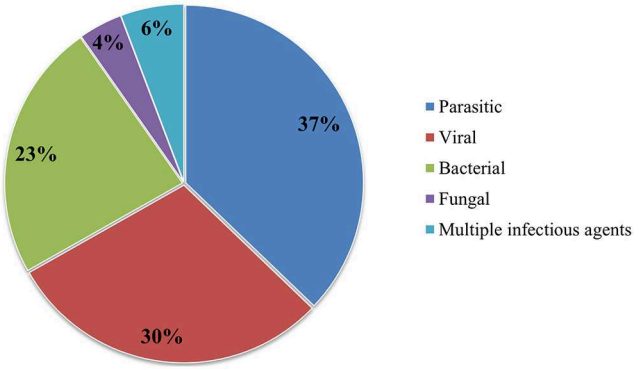

FIGURE 4 | Percentage of the infectious agents mentioned in all publications.

agent in Austria, with 14 published papers. It was followed by *Echinococcus multilocularis* (n = 11), West Nile Virus (n = 9), *Trichinella* sp. (n = 8), *Toxoplasma gondii*, *Salmonella* sp., *Mycobacterium caprae*, and *Mycobacterium avium* subsp. *paratuberculosis* with seven publications each. Also noteworthy are *Fascioloides magna* and *Anaplasma phagocytophilum* with six publications each, as well as *Francisella tularensis*, which was mentioned in five papers (see **Figure 6**).

Zoonotic Potential

The review shows that 61% of papers discussed pathogens that have zoonotic potential, 21% of papers discussed diseases without zoonotic potential, and 5% discussed diseases with unclear zoonotic potential that would need further research (see **Figures 7, 8**).

Notifiable Status

A total of 77 publications addressed diseases notifiable in Austria according to Austrian legislation including the § 16. Federal law on epizootics, the Tuberculosis Act (1968), the Epidemic Act (1950), the Sexually Transmitted Diseases Act (1945), the BVD Regulation (2007), and the Paratuberculosis Ordinance (2006), while 67 publications mentioned OIE notifiable diseases (See **Supplementary Tables 1, 2**). Of the 77 publications addressing notifiable diseases in Austria, 48 also addressed notifiable diseases according to the OIE list. For 19 publications, our criteria were not applicable, as they did not mention an exact pathogen but multiple pathogens ($N > 10$) (see **Figure 9**). Of the 136 diseases detected, 24 diseases are notifiable according to current Austrian law. Six of these 24 diseases are notifiable as per the Austrian § 16. Federal law on epizootics, the remaining diseases are notifiable according to the above-mentioned laws (See **Supplementary Tables 1, 2**). Moreover, 20 diseases were found to be OIE-listed diseases (see **Figure 10**). Lastly, of the 24 diseases notifiable in Austria, 11 are also notifiable according to the OIE list.

Prevalence and Confidence Interval

Prevalence was indicated in a total of 99 (44%) publications. The confidence intervals, on the other hand, were only mentioned in 20 (9%) publications (see **Figure 11**).

Animal Species

Both red deer (*Cervus elaphus*) and red foxes (*V. vulpes*) were each mentioned in 32 papers. These numbers were followed by wild boar (*S. scrofa*) (n = 25), chamois (*Rupicapra rupicapra*) (n = 21), roe deer (*Capreolus capreolus*) (n = 20), European brown hare (*Lepus europeus*) (n = 16), blackbird (*Turdus merula*) (n = 12), and fallow deer (*Dama dama*) (n = 10). Among the 10 most frequently described animal species, the domestic dog (*Canis lupus familiaris*) was the only domestic animal species. It occurred in a total of 12 papers. Furthermore, in 14 papers, multiple bird species were listed (see **Figure 12**).

In summary, we found 131 animal species or groups (e.g., genera, families, and orders) in the 226 publications. Of these, 58 were birds, followed by 55 mammal species, and 2 marsupial species. Reptiles and amphibians appear underrepresented by nine species or groups and seven species, respectively. Thirteen more categories were formed to describe those papers addressing more than 10 species or not stating an exact species. These included multiple bird, rodent, reptile psittacine bird, snake, amphibian and mammalian species, and domestic ruminants, wild ruminants, wild carnivores, wild ungulates, and game animals. Ninety six species or categories were mentioned once, whereas 12 were mentioned twice.

Risk Group Interfaces

A total of 163 publications addressed diseases that occurred exclusively in wild animals, conducted research solely with wild animals or took samples only from wildlife. In contrast, 12 papers dealt with diseases at the wildlife-human interface, and all of these diseases were zoonotic. In these 12 studies, humans and animals were sampled or results reported in humans and animals were discussed. Moreover, 25 publications addressed transmission and prevalence of diseases at the wildlife-livestock interface. Last but not least, 26 publications pertained to all interfaces, i.e., between wild animals, domesticated animals, and humans (see **Figure 13**).

Distinct Study Features

A total of 74 papers did not exhibit a specific trait according to our classification and were categorized under "No distinct feature." In 53 publications, more than one specific pathogenic agent was mentioned. Furthermore, 46 papers referenced countries other than Austria. Diseases that emerged in captive wildlife were discussed in 44 publications. Thirteen studies addressed diseases emerging in wildlife but centered on human medicine (**Figure 14**). These included sampling of specific at-risk groups (e.g., hunters, veterinarians, animal keepers). Moreover, six papers dealt with game meat hygiene, and lastly, three publications were about environmental sampling for ubiquitous pathogens (e.g., *Clostridium botulinum*, avian botulism).

DISCUSSION

According to the WHO, 75% of new EIDs or emerging diseases originate from animal reservoirs and thus have zoonotic potential. In the last 30 years, these EIDs have appeared as a consequence of the intensifying codependence in multiuse

TABLE 1 | Infectious pathogens in alphabetical order, listing their zoonotic potential, notifiable status, animals affected, and authors, as found through our study.

Disease or pathogen	Disease agent	Notifiable in Austria	OIE notifiable disease	Zoonotic potential	Affected species	References
Agamid adenovirus 1	Viral	No	No	No	Bearded dragon *(Pogona vitticeps)*	(42)
Alaria alata	Parasitic	No	No	Yes	Red fox *(Vulpes vulpes),* Wild boar *(Sus scrofa)*	(43–45)
Anaplasma phagocytophilum	Parasitic	No	No	Yes	Chamois *(Rupicapra rupicapra),* Ibex *(Capra ibex*), Mouflon *(Ovis gmelini musimon*), Red deer *(Cervus elaphus*), Roe deer *(Capreolus capreolus),* Timber wolf *(Canis Lupus Occidentalis)*	(46–51)
Ankylostoma spp.	Parasitic	No	No	Yes	Cheetah *(Acinonyx jubatus)*	(52)
Arboviruses	Viral	No	No	Yes	Multiple species*	(53)
Ascaris suum	Parasitic	No	No	Yes	Racoon *(Procyon lotor),* Red fox *(Vulpes vulpes*), Wild boar *(Sus scrofa)*	(54)
Ascaridia spp.	Parasitic	No	No	NA	Northern bald ibis *(Geronticus eremita)*	(55)
Aspergillus fumigates	Fungal	No	No	Yes	Falcon *(Falco)*	(56)
Aspergillus spp.	Fungal	No	No	Yes	Cheetah *(Acinonyx jubatus)*	(52)
Aujeszky's disease[a]	Viral	Yes	Yes	No	Dog *(Canis lupus familiaris),* Wild boar *(Sus scrofa)*	(57–59)
Avian Borna disease virus	Viral	No	No	No	Canary bird *(Serinus canaria*) and multiple psittacine species*	(60–63)
Avian hepatitis E virus	Viral	No	No	Yes	Common buzzard *(Buteo buteo),* Feral pigeon *(Columba livia domestica),* Little owl *(Athene noctua),* Song thrush *(Turdus philomelos)*	(64)
Avian influenza virus[a,b]	Viral	Yes	Yes	Yes	Coot *(Fulica atra),* Duck *(Anatidae),* Egret *(Ardeidae),* Goose *(Anatidae),* Grebe *(Podicipedidae*), Swan *(Cygnus),* and other wild bird species	(65, 66)
Avian pox virus	Viral	No	No	No	Bald eagle *(Haliaeetus leucocephalus),* Great Bustard *(Otis tarda),* Great tit *(Parus major),* and multiple bird species*	(67–70)
Babesia canis	Parasitic	No	No	No	Eurasian golden jackal *(Canis aureus)*	(71)
Babesia capreoli	Parasitic	No	No	Unknown	Chamois *(Rupicapra rupicapra),* Ibex *(Capra ibex*), Mouflon *(Ovis gmelini musimon*), Red deer *(Cervus elaphus),* Roe deer *(Capreolus capreolus)*	(48)
Babesia divergens	Parasitic	No	Yes	Yes	Chamois *(Rupicapra rupicapra),* Ibex *(Capra ibex),* Mouflon *(Ovis gmelini musimon),* Red deer *(Cervus elaphus),* Roe deer *(Capreolus capreolus)*	(48, 51)
Babesia microti	Parasitic	No	No	Yes	Red fox *(Vulpes vulpes*) and other wild carnivores	(72, 73)
Babesia vesperuginis	Parasitic	No	No	Unknown	Bat *(Chiroptera)*	(74)
Babesia spp.	Parasitic	No	No	NA	Chamois *(Rupicapra rupicapra),* Fallow deer *(Dama dama),* Mouflon *(Ovis gmelini musimon);* Père David's deer *(Elaphurus davidianus),* Red deer *(Cervus elaphus),* Roe deer *(Capreolus capreolus),* Sika deer *(Cervus nippon)*	(75)
Bartonella spp.	Bacterial	No	No	Yes	Bank vole *(Clethrionomys glareolus),* Common vole *(Microtus arvalis),* Wood mouse *(Apodemus sylvaticus),* Yellow-necked field mouse *(Apodemus flavicollis)*	(76)
Batrachochytrium dendrobatidis	Fungal	No	Yes	Unknown	Alpine newt *(Ichthyosaura alpestris),* Alpine salamander *(Salamandra atra),* Crested newt *(Triturus cristatus, T. carnifex, T. dobrogicus),* Fire and yellow bellied toad *(Bombina bombina, B. variegata),* Poison dart frogs *(Dendrobatidae),* Smooth newt *(Lissotriton vulgaris),* Water frogs *(Pelophylax)*	(77–79)
Baylisascaris procyonis	Parasitic	No	No	Yes	Racoon *(Procyon lotor),* Red fox *(Vulpes vulpes),* Wild boar *(Sus scrofa)*	(54)
Baylisascaris spp.	Parasitic	No	No	Yes	Skunk *(Mephitis mephitis)*	(80)
Borna Disease Virus[c]	Viral	Yes	No	Yes	Bicolored shrew *(Crocidura leucodon*), Cheetah *(Acinonyx jubatus),* Domestic horse *(Equus ferus caballus),* and multiple other species*	(81–83)
Borrelia spp.	Bacterial	No	No	Yes	Bank vole *(Clethrionomys glareolus),* Common vole *(Microtus arvalis*), Wood mouse *(Apodemus sylvaticus),* Yellow-necked field mouse *(Apodemus flavicollis)*	(76)
Bot fly larvae "*Cephenemyia auribarbis"*	Parasitic	No	No	Unknown	Red deer *(Cervus elaphus)*	(84)

(Continued)

TABLE 1 | Continued

Disease or pathogen	Disease agent	Notifiable in Austria	OIE notifiable disease	Zoonotic potential	Affected species	References
Bovine viral diarrhea virus[d]	Viral	Yes	Yes	No	Chamois *(Rupicapra rupicapra),* Fallow deer *(Dama dama),* Red deer *(Cervus elaphus),* Roe deer *(Capreolus capreolus)*	(85, 86)
Brucella microti	Bacterial	No	No	Unknown	Red fox *(Vulpes vulpes)*	(87, 88)
Brucella suis[a]	Bacterial	Yes	Yes	Yes	Red fox *(Vulpes vulpes)*	(89)
Brucella vulpis	Bacterial	No	No	Unknown	Red fox *(Vulpes vulpes)*	(90)
Brucella spp.[b]	Bacterial	Yes	No	NA	European brown hare *(Lepus europaeus),* Red fox *(Vulpes vulpes)*	(91, 92)
Campylobacter spp.[b]	Bacterial	Yes	No	Yes	Multiple wild bird species*	(93, 94)
Candidatus neoehrlichia spp.	Bacterial	No	No	Yes	Red fox *(Vulpes vulpes)*	(95)
Capillaria spp.	Parasitic	No	No	NA	Northern bald ibis *(Geronticus eremita)*	(55)
Capillaria boehmi	Parasitic	No	No	Unknown	Red fox *(Vulpes vulpes)*	(96)
Capillaria hepatica/Calodium hepaticum	Parasitic	No	No	Yes	Multiple species*	(97–99)
Chelonid Herpesvirus (ChHV)	Viral	No	No	No	Leopard tortoise *(Stigmochelys pardalis)*	(100)
Chlamydiaceae spp.	Bacterial	No	No	NA	Multiple wild rodent species*	(101)
Chrysosporium guarroi	Fungal	No	No	Unknown	Bearded dragon *(Pogona vitticeps)*	(102)
Clostridium botulinum[b], *Avian botulism*	Bacterial	Yes	No	No	Garganey *(Anas querquedula),* Mallard *(Anas platyrhynchos),* Northern lapwing *(Vanellus vanellus)* and multiple other wild bird species*	(103, 104)
Clostridium perfringens	Bacterial	No	No	Yes	Blackbuck *(Antilope cervicapra),* Collared peccary *(Pecari tajacu),* Domestic goat *(Capra aegagrus hircus),* Domestic sheep *(Ovis aries),* Domestic swine *(Sus scrofa domesticus),* European reindeer *(Rangifer tarandus),* Japanese serow *(Capricornis crispus),* Lechwe *(Kobus leche),* Waterbuck *(Kobus ellipsiprymnus)*	(105)
Clostridium septicum	Bacterial	No	No	Yes	Chamois *(Rupicapra rupicapra)*	(106)
Coccidia	Parasitic	No	No	NA	Common hill myna *(Gracula religiosa)*	(107)
Collyriclum faba	Parasitic	No	No	Unknown	Starling *(Sturnus vulgaris)*	(108)
Coxiella burnetii	Bacterial	No	No	Yes	Bank vole *(Clethrionomys glareolus),* Common vole *(Microtus arvalis),* Wood mouse *(Apodemus sylvaticus),* Yellow-necked field mouse *(Apodemus flavicollis)*	(76)
Crane hepatitis herpesviruses	Viral	No	No	Unknown	Gray crowned crane *(Balearica regulorum)*	(109)
Cryptococcus spp.	Fungal	No	No	Yes	Feral pigeon *(Columba livia domestica)*	(110)
Cryptosporidium spp.	Parasitic	No	No	Yes	Corn snake *(Pantherophis guttatus),* Leopard gecko *(Eublepharis macularius),* and multiple reptile and snake species*	(111, 112)
Cryptosporidium suis	Parasitic	No	No	Yes	Wild boar *(Sus scrofa)*	(113)
Cryptosporidium scrofarum	Parasitic	No	No	Yes	Wild boar *(Sus scrofa)*	(113)
Demodex spp.	Parasitic	No	No	No	Cheetah *(Acinonyx jubatus)*	(52)
Dermatophilus congolensis	Bacterial	No	No	Yes	Orangutan *(Pongo pygmaeus pygmaeus)*	(114)
Dermatophytosis (Trichopphyton, Microsporum)	Fungal	No	No	Yes	Small mammals	(115)
Devriesea agamarum	Bacterial	No	No	Unknown	Bearded dragon *(Pogona vitticeps)*	(102)
Dirofilaria repens	Parasitic	No	No	Yes	Dog *(Canis lupus familiaris),* Red fox *(Vulpes vulpes)*	(116)
Dirofilaria immitis	Parasitic	No	No	Yes	Dog *(Canis lupus familiaris),* Red fox *(Vulpes vulpes)*	(116)

(Continued)

TABLE 1 | Continued

Disease or pathogen	Disease agent	Notifiable in Austria	OIE notifiable disease	Zoonotic potential	Affected species	References
Distemper virus	Viral	No	No	No	Badger *(Meles meles),* Beech marten *(Martes foina),* Cheetah *(Acinonyx jubatus),* Dog *(Canis lupus familiaris)*	(82, 117–119)
Echinococcus multilocularis[b]	Parasitic	Yes	Yes	Yes	Beaver *(Castor fiber),* Dog *(Canis lupus familiaris),* Domestic cat *(Felis silvestris catus),* Red fox *(Vulpes vulpes),* and multiple mammalian or rodent species*	(54, 99, 120–128)
Eimeria leporis	Parasitic	No	No	No	European brown hare *(Lepus europaeus)*	(123)
Encephalitozoon cuniculi	Parasitic	No	No	Yes	Bearded dragon *(Pogona vitticeps),* Common vole *(Microtus arvalis),* European brown hare *(Lepus europaeus),* European water vole *(Arvicola terrestris)*	(129–131)
Encephalitozoon spp.	Parasitic	No	No	Yes	Multiple species*	(132)
Encephalomyocarditis virus	Viral	No	No	Yes	Domestic cat *(Felis silvestris catus)* and wild rodents	(133)
Entamoeba invadens	Parasitic	No	No	No	Boa constrictor *(Boa constrictor)*	(134)
Entamoeba spp.	Parasitic	No	No	NA	Multiple snake species*	(112)
ESBL/AmpC producing Enterobacteriaceae	Bacterial	No	No	Yes	Rook *(Corvus frugilegus)*	(135)
Escherichia coli	Bacterial	No	No	Yes	Mouflon *(Ovis gmelini musimon)* and multiple wild bird species*	(93, 94, 136)
European brown hare *(Lepus europaeus)* syndrome	Viral	No	No	No	European brown hare *(Lepus europaeus),* Rabbit *(Oryctolagus cuniculus)*	(137, 138)
Fascioloides magna	Parasitic	No	No	No	Fallow deer *(Dama dama),* Red deer *(Cervus elaphus),* Roe deer *(Capreolus capreolus),* and otherwild ungulates and ruminants	(139–144)
Feline Herpes Virus 1	Viral	No	No	No	Cheetah *(Acinonyx jubatus)*	(82, 145)
Flavivirus, mosquito-borne	Viral	No	No	Yes	Multiple species*	(146)
Francisella tularensis[b]	Bacterial	Yes	Yes	Yes	Dog *(Canis lupus familiaris),* European brown hare *(Lepus europaeus),* Red fox *(Vulpes vulpes)*	(18, 89, 91, 147, 148)
Fur mites (Lynxacarus mustelae)	Parasitic	No	No	Unknown	Beech marten *(Martes foina)*	(149)
Geopetitia aspiculata	Parasitic	No	No	Unknown	Bearded barbet *(Lybius dubius),* Black-faced dacnis *(Dacnis lineata),* Brown-breasted barbet *(Lybius melanopterus),* Sociable weaver *(Philetairus socius),* Steere's liocichla *(Liocichla steerii)*	(150)
Hantavirus/Puumala Virus[b]	Viral	Yes	No	Yes	Bank vole *(Clethrionomys glareolus),* Common vole *(Microtus arvalis),* Domestic cat *(Felis silvestris catus*), House mouse *(Mus musculus),* Wood mouse *(Apodemus sylvaticus),* Yellow-necked field mouse *(Apodemus flavicollis),* and other wild rodents	(76, 133, 151, 152)
Hepatozoon canis	Parasitic	No	No	No	Eurasian golden jackal *(Canis aureus),* Red fox *(Vulpes vulpes)*	(71, 72, 153)
Herpesvirus	Viral	No	No	NA	Tortoises *(Testudinidae)*	(154)
Histoplasma capsulatum var. *Capsulatum*	Fungal	No	No	Yes	Badger *(Meles meles)*	(155)
*Iridovirus (*Genus *Ranavirus)*	Viral	No	No	Unknown	Leopard tortoise *(Stigmochelys pardalis)*	(100)
Klebsiella pneumoniae	Bacterial	No	No	Yes	Mouflon *(Ovis gmelini musimon)*	(136)
Koala retrovirus (KoRV)	Viral	No	No	Unknown	Koala *(Phascolarctos cinereus)*	(156)
Leishmania infantum	Parasitic	No	Yes	Yes	Eurasian golden jackal *(Canis aureus)*	(71)
Leptospira interrogans[b]	Bacterial	Yes	No	Yes	European brown hare *(Lepus europaeus),* Wild boar *(Sus scrofa)*	(91, 157)
Leptospira spp.	Bacterial	No	No	Yes	Bank vole *(Clethrionomys glareolus*), Common vole *(Microtus arvalis),* Wood mouse *(Apodemus sylvaticus),* Yellow-necked field mouse *(Apodemus flavicollis)*	(76)

(Continued)

TABLE 1 | Continued

Disease or pathogen	Disease agent	Notifiable in Austria	OIE notifiable disease	Zoonotic potential	Affected species	References
Listeria monocytogenes[b]	Bacterial	Yes	No	Yes	Water fowl *(Anatidae),* Red deer *(Cervus elaphus),* Roe deer *(Capreolus capreolus*), Chamois *(Rupicapra rupicapra),* Wild boar *(Sus scrofa),* Mouflon *(Ovis gmelini musimon),* and other wild and domestic ruminants	(158, 159)
Listeria spp.	Bacterial	No	No	NA	Water fowl *(Anatidae*) and wild and domestic ruminants	(159)
Lymphocytic choriomeningitis virus	Viral	No	No	Yes	Bank vole *(Clethrionomys glareolus),* Common vole *(Microtus arvalis),* Wood mouse *(Apodemus sylvaticus),* Yellow-necked field mouse *(Apodemus flavicollis)*	(76)
Malignant catarrhal fever virus	Viral	No	No	No	Chamois *(Rupicapra rupicapra),* Fallow deer *(Dama dama),* Red deer *(Cervus elaphus*), Roe deer *(Capreolus capreolus)*	(160)
Methicillin-resistant *Staphylococcus aureus* (MRSA)	Bacterial	No	No	Yes	Eurasian Lynx *(Lynx lynx*), European brown hare *(Lepus europaeus),* Hedgehog *(Erinaceus europaeus),* Otter *(Lutra lutra),* Rook *(Corvus frugilegus)*	(93, 135, 161, 162)
Monocercomonas spp.	Parasitic	No	No	Unknown	Multiple snake species*	(112)
Mycobacterium avium ssp. *Paratuberculosis*[e]	Bacterial	Yes	Yes	Yes	Capercaillie *(Tetrao urogallus),* Cattle *(Bos taurus),* Chamois *(Rupicapra rupicapra*), European brown hare *(Lepus europaeus),* Fallow deer *(Dama dama),* Ibex *(Capra ibex),* Mouflon *(Ovis gmelini musimon),* Mountain hare *(Lepus timidus),* Red deer *(Cervus elaphus),* Roe deer *(Capreolus capreolus),* Red fox *(Vulpes vulpes),* Yellow-necked field mouse *(Apodemus flavicollis)*	(163–169)
Mycobacterium avium subsp. *silvaticum*	Bacterial	No	Yes	Yes	Ural owl *(Strix uralensis)*	(170)
Mycobacterium bovis[a,b]	Bacterial	Yes	Yes	Yes	Badger *(Meles meles),* Red deer *(Cervus elaphus),* Wild boar *(Sus scrofa)*	(171)
Mycobacterium caprae[b]	Bacterial	Yes	Yes	Yes	Camel *(Camelus),* Cattle *(Bos taurus),* Domestic goat *(Capra aegagrus hircus),* Red deer *(Cervus elaphus),* Wild boar *(Sus scrofa)*	(16, 172–177)
Mycoplasma conjunctivae	Bacterial	No	No	Yes	Chamois *(Rupicapra rupicapra),* Domestic goat *(Capra aegagrus hircus),* Domestic sheep *(Ovis aries),* Domestic swine *(Sus scrofa domesticus),* Ibex *(Capra ibex)*	(178, 179)
Myxozoa	Parasitic	No	No	NA	Mole *(Talpa europaea)*	(180)
Neospora caninum	Parasitic	No	No	No	Common vole *(Microtus arvalis),* Dog *(Canis lupus familiaris),* European brown hare *(Lepus europaeus),* European water vole *(Arvicola terrestris),* Red fox *(Vulpes vulpes),* Parma wallaby *(Macropus parma)*	(129, 181–183)
Orthopoxvirus	Viral	No	No	Yes	Domestic cat *(Felis silvestris catus)* and wild rodents	(133)
Parapoxvirus	Viral	No	No	Yes	Domestic cat *(Felis silvestris catus*) and wild rodents	(133)
Parvovirus	Viral	No	No	No	Badger *(Meles meles),* Cheetah *(Acinonyx jubatus)*	(52, 82, 118)
Pasteurella spp.	Bacterial	No	No	NA	Chamois *(Rupicapra rupicapra)*	(184)
Pharyngomyia picta	Parasitic	No	No	Unknown	Red deer *(Cervus elaphus)*	(84)
Plasmodium spp.[b]	Parasitic	Yes	No	No	Humboldt penguins *(Spheniscus humboldti),* King penguins *(Aptenodytes patagonicus),* Puffins *(Fratercula arctica),* Rockhopper penguins *(Eudyptes chrysocome),* and multiple wild bird species*	(185–187)
Psittacine beak and feather disease virus	Viral	No	No	Unknown	Budgerigar *(Melopsittacus undulatus)*	(188)
Rabies[a,b]	Viral	Yes	Yes	Yes	Red fox *(Vulpes vulpes)*	(189–191)
Rabbit hemorrhagic disease	Viral	No	Yes	No	European brown hare *(Lepus europaeus),* Rabbit *(Oryctolagus cuniculus)*	(137, 138, 192)
Rat hepatitis E virus	Viral	No	No	Yes	Black rat *(Rattus rattus),* Norway rat *(Rattus norvegicus)*	(193)
Rickettsia spp.	Bacterial	No	No	Yes	Bank vole *(Clethrionomys glareolus),* Common vole *(Microtus arvalis),* Wood mouse *(Apodemus sylvaticus),* Yellow-necked field mouse *(Apodemus flavicollis)*	(76)

(Continued)

TABLE 1 | Continued

Disease or pathogen	Disease agent	Notifiable in Austria	OIE notifiable disease	Zoonotic potential	Affected species	References
Roe deer *(Capreolus capreolus)* papillomavirus	Viral	No	No	No	Red deer *(Cervus elaphus)*	(194)
Salmonella enterica[b]	Bacterial	Yes	No	Yes	Red fox *(Vulpes vulpes)* and multiple reptile species*	(195, 196)
Salmonella spp.[b]	Bacterial	Yes	No	NA	Chamois *(Rupicapra rupicapra),* Lizards *(Squamata),* Mouflon *(Ovis gmelini musimon),* Red deer *(Cervus elaphus),* Roe deer *(Capreolus capreolus),* Snakes *(Serpentes),* Tortoises *(Testudinidae),* Turtles *(Chelonii),* Wild boar *(Sus scrofa),* and multiple wild bird, amphibian, reptile and other species*	(93, 94, 158, 197–200)
Scabies/Sarcoptic mange[a]	Parasitic	Yes	No	Yes	Chamois *(Rupicapra rupicapra),* Ibex *(Capra ibex)*	(201, 202)
Staphylococcus aureus	Bacterial	No	No	Yes	Multiple species*	(203)
Syngamus trachea	Parasitic	No	No	Yes	Northern bald ibis *(Geronticus eremita)*	(55)
Taenia crassiceps	Parasitic	No	No	Yes	Common vole *(Microtus arvalis),* European water vole *(Arvicola terrestris)*	(99, 204)
Taenia taeniaeformis	Parasitic	No	No	Yes	Common vole *(Microtus arvalis),* European water vole *(Arvicola terrestris)*	(99, 204)
Taenia spp.	Parasitic	No	No	Yes	Cheetah *(Acinonyx jubatus)*	(52)
Theileria spp.	Parasitic	No	Yes	No	Chamois *(Rupicapra rupicapra),* Fallow deer *(Dama dama),* Mouflon *(Ovis gmelini musimon),* Père David's deer *(Elaphurus davidianus),* Red deer *(Cervus elaphus),* Roe deer *(Capreolus capreolus),* Sika deer *(Cervus nippon)*	(75, 205)
Tickborne encephalitis virus[b] (TBEV)	Viral	Yes	No	Yes	Mouflon *(Ovis gmelini musimon),* Roe deer *(Capreolus capreolus)*	(206, 207)
Toxascaris leonina	Parasitic	No	No	No	Cheetah *(Acinonyx jubatus)*	(52)
Toxocara canis		No	No	Yes	Dog *(Canis lupus familiaris),* Domestic cat *(Felis silvestris catus),* Racoon *(Procyon lotor),* Red fox *(Vulpes vulpes),* Wild boar *(Sus scrofa)*	(54, 208, 209)
Toxocara cati	Parasitic	No	No	Yes	Dog *(Canis lupus familiaris),* Domestic cat *(Felis silvestris catus),* Red fox *(Vulpes vulpes)*	(208, 209)
Toxocara mystax	Parasitic	No	No	Yes	Cheetah *(Acinonyx jubatus)*	(52)
Toxoplasma gondii	Parasitic	No	No	Yes	Bank vole *(Clethrionomys glareolus),* Common vole *(Microtus arvalis),* European water vole *(Arvicola terrestris),* Pallas cat *(Otocolobus manul),* Racoon *(Procyon lotor),* Red fox *(Vulpes vulpes),* Wild boar *(Sus scrofa),* Wood mouse *(Apodemus sylvaticus),* Yellow-necked field mouse *(Apodemus flavicollis)* and multiple other species*	(54, 76, 99, 181, 182, 210, 211)
Treponema spp.	Bacterial	No	No	Unknown	European brown hare *(Lepus europaeus)*	(212)
Trichinella britovi	Parasitic	No	Yes	Yes	Red fox *(Vulpes vulpes)*	(213)
Trichinella pseudospiralis	Parasitic	No	Yes	Yes	Wild boar *(Sus scrofa)*	(214)
Trichinella spp.	Parasitic	No	Yes	Yes	Domestic swine *(Sus scrofa domesticus),* Racoon *(Procyon lotor),* Red fox *(Vulpes vulpes),* Wild boar *(Sus scrofa)*	(54, 215–221)
Trichomonas gallinae	Parasitic	No	No	No	Bearded vulture *(Gypaetus barbatus),* Budgerigar *(Melopsittacus undulatus),* Canary bird *(Serinus canaria),* Eurasian collared dove *(Streptopelia decaocto),* European greenfinch *(Chloris chloris),* Feral pigeon *(Columba livia domestica),* Hawfinch *(Coccothraustes coccothraustes),* Racing pigeons *(Columba livia domestica),* Yellowhammer *(Emberiza citrinella)*	(222, 223)
Trichophyton terrestre	Fungal	No	No	Unknown	Madagascar day gecko *(Phelsuma m. madagascariensis)*	(224)
Trichostrongylus tenius	Parasitic	No	No	Yes	Northern bald ibis *(Geronticus eremita)*	(55)
Tritrichomonas fetus	Parasitic	No	No	No	Quail *(Coturnix coturnix)*	(225)

(Continued)

TABLE 1 | Continued

Disease or pathogen	Disease agent	Notifiable in Austria	OIE notifiable disease	Zoonotic potential	Affected species	References
Usutu Virus	Viral	No	No	Yes	Black bird *(Turdus merula)*, Blue tit *(Cyanistes caeruleus)*, Egyptian vulture *(Neophron percnopterus)*, Eurasian eagle owl *(Bubo bubo)*, Great gray owl *(Strix nebulosa)*, House sparrow *(Passer domesticus)*, Owls *(Strigiformes)*, Snowy owl *(Bubo scandiacus)*, Swallow *(Hirundinidae)*, White stork *(Ciconia ciconia)*, Ural owl *(Strix uralensis)*, and multiple wild bird and other species*	(226–239)
Verocytotoxin-producing *Escherichia coli*[b]	Bacterial	Yes	No	Yes	Chamois *(Rupicapra rupicapra)*, Cattle *(Bos taurus)*	(240)
West Nile Virus[b,c]	Viral	Yes	Yes	Yes	Bearded vulture *(Gypaetus barbatus)*, Domestic horse *(Equus ferus caballus)*, Goshawk *(Accipiter gentilis)*, Gyrfalcon *(Falco rusticolus)*, Kea *(Nestor notabilis)*, Snowy owl *(Bubo scandiacus)*, and multiple other bird species*	(237, 241–248)
Yersinia pseudotuberculosis	Bacterial	No	No	Yes	Cheetah *(Acinonyx jubatus)*	(52)

[a]*Notifiable diseases according to the § 16. Federal law on epizootics in Austria.*
[b]*Notifiable diseases according to the Tuberculosis Act, Epidemic Act 1950, and Sexually Transmitted Diseases Act in Austria.*
[c]*Notifiable disease in Austria, as part of the Equine encephalitis disease complex.*
[d]*Notifiable according to the BVD Regulation 2007, BGBl. II No. 178/2007.*
[e]*Notifiable according to the Paratuberculosis Ordinance, BGBl. II No. 48/2006*.*
**Multiple species/other species, indicates more than 10 (N > 10) mentioned animal species.*

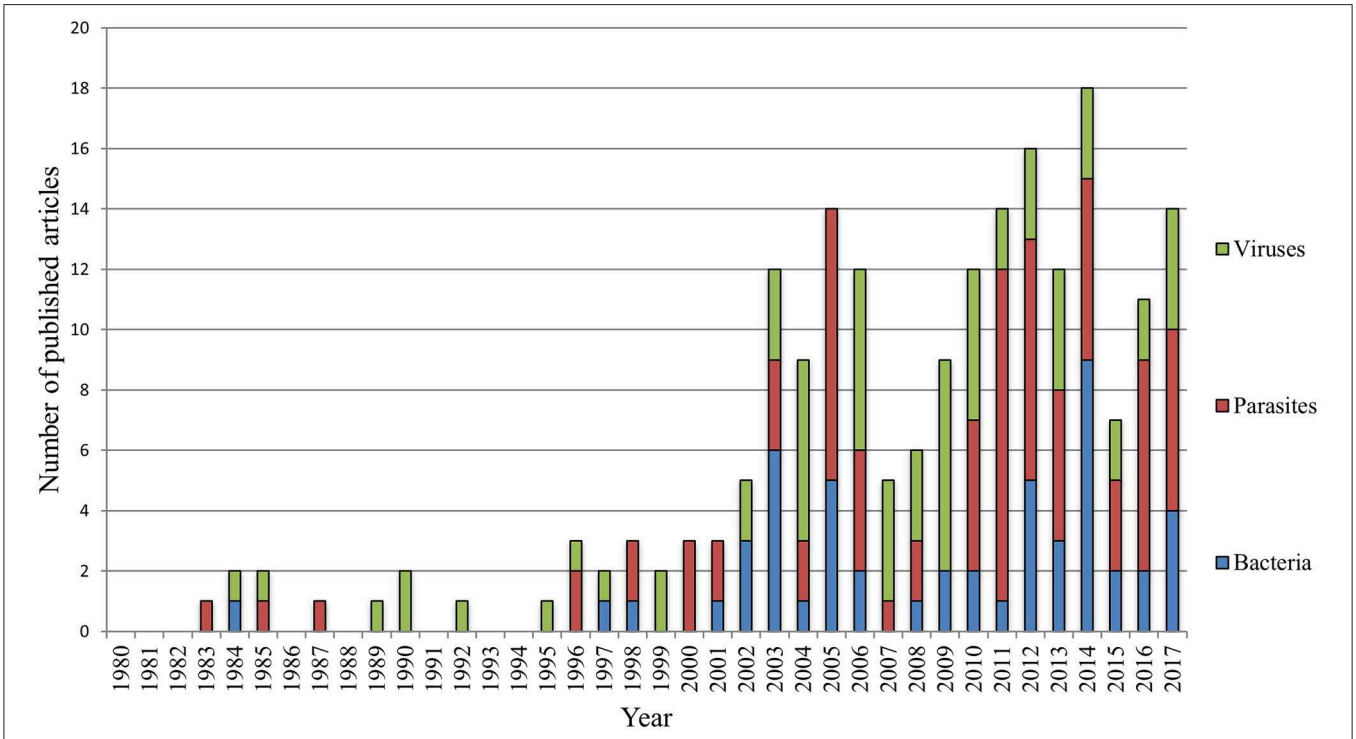

FIGURE 5 | Distribution of publications addressing either bacterial, viral, or parasitic diseases between 1980 and 2017.

landscapes at the interface between animals and humans (249). This review provides a first insight into the state of knowledge on wildlife diseases in Austria between 1980 and 2017.

This literature review identified 226 publications between 1980 and 2017. More than half of the publications (65%) involved actively conducted research. The review also revealed that 15% of all papers were case reports. A majority of these case reports were based on pathology reports from the NRL of the AGES, the Institute of Pathology and the Research Institute of Wildlife Ecology at the University of Veterinary Medicine in Vienna. The

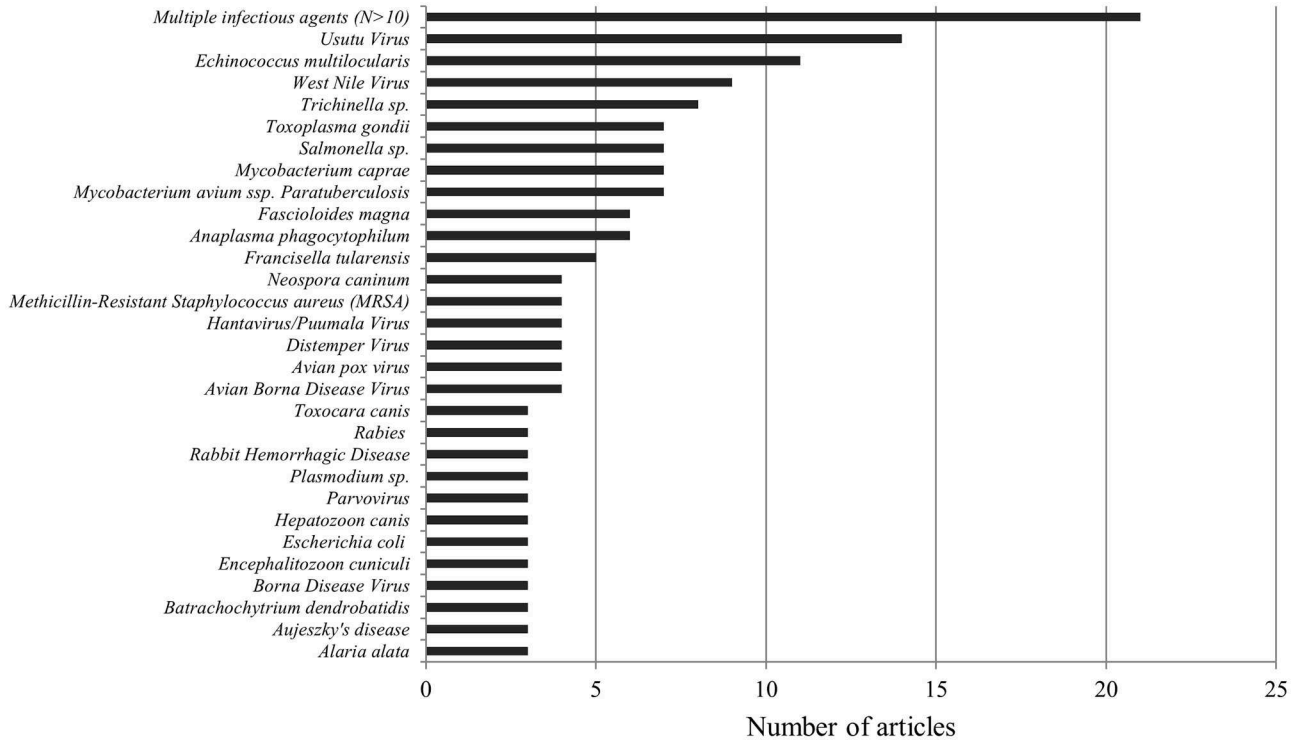

FIGURE 6 | Numerical depiction of diseases mentioned in all publications three times or more.

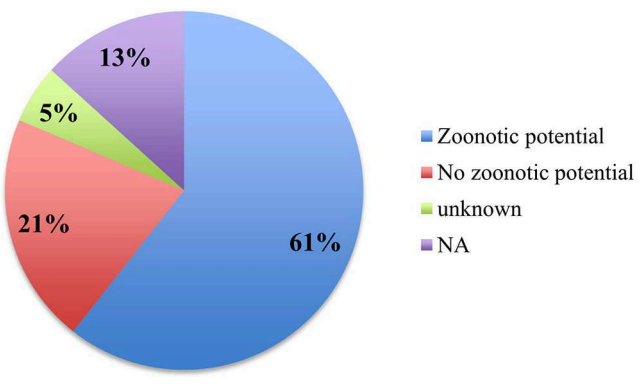

FIGURE 7 | Percentage of publications discussing the zoonotic potential of diseases.

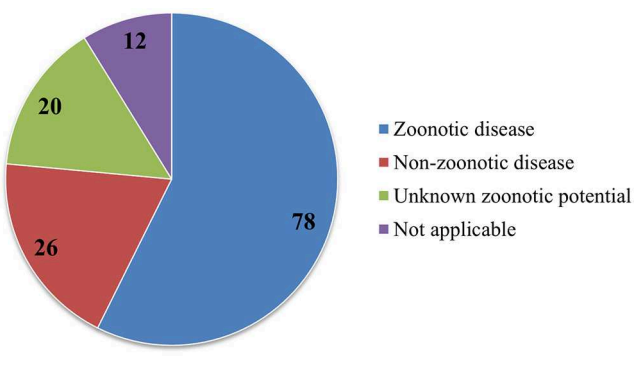

FIGURE 8 | Numbers of diseases with or without zoonotic potential, as well as diseases with currently unknown zoonotic potential.

existence of several facilities addressing wildlife pathogens and disease appears to have had a positive impact on the generation of knowledge in this field.

In comparison to a similar study from the Republic of Korea, which focused on the time span between 1982 and 2014 and found an average rate of 6.1 publications per year, our review yielded a higher total number of publications as well as a higher average amount of publications per year. (1). However, it has to be mentioned that our study covered a longer period of time. In the Korean review, viral diseases were reported on more often than in Austria. The most frequently researched diseases in Korea were avian influenza virus and rabies. In Austria, Usutu virus and *E. multilocularis* clearly dominated. As far as interfaces are concerned, research in Korea focused primarily on human and livestock diseases, whereas in Austria the main focus was on diseases in wildlife. In Korea, 24 zoonotic diseases were reported, whereas in Austria 78 have been investigated since 1980. Fifteen diseases that are notifiable according to the OIE list were mentioned in the Korean review; in contrast, 20 were reported in Austria. Birds dominated in the Korean review, while mammals, namely the red fox (*V. vulpes*) and the red deer (*C. elaphus*), were most reported on in Austria (1).

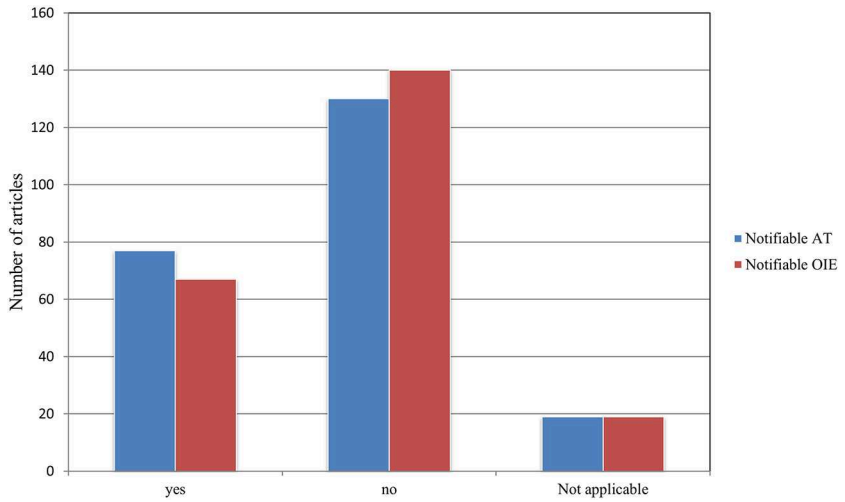

FIGURE 9 | Number of publications addressing diseases which are notifiable according to Austrian legislation and/or the OIE–World Organization for Animal Health compared to those addressing non-notifiable diseases.

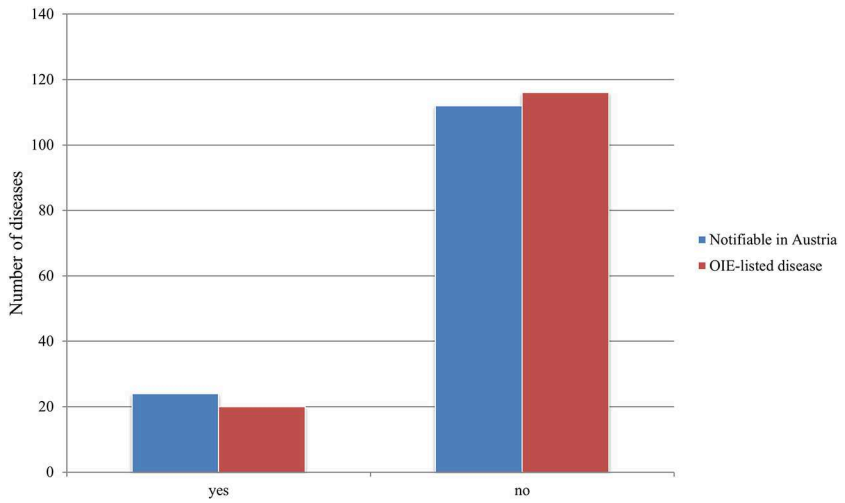

FIGURE 10 | Number of notifiable diseases described in retained papers according to Austrian legislation and the OIE compared to non-notifiable diseases.

Infectious Agents

Parasitic diseases accounted for 37% of the papers, 30% were viral, and 23% were bacterial. Fungal diseases were only mentioned in 4% of all studies. Furthermore, we did not find a single study on transmissible spongiform encephalopathies or other diseases caused by prions. This may be due to the fact that only eight cases of BSE were detected in Austria between 2001 and 2010 (250). Austria was also declared as a country with negligible BSE risk by the OIE in 2012. However, it is prudent not to ignore TSEs in wildlife in view of the sudden emergence of chronic wasting disease in reindeer (*Rangifer tarandus*) and moose (*Alces alces*) in Finland and Norway in April 2016 (251).

Viral diseases were addressed in 30% of publications. The most studied viral pathogens were Usutu Virus and West Nile Virus. Since its first detection in 2001, Usutu Virus has been responsible for massive die-off of blackbirds (*T. merula*) in Europe. The first two human cases of Usutu Virus were detected in 2003 in Austria, generating a greater interest in this vector-borne disease (252). To a much lesser extent, avian Borna disease virus, avian pox virus, distemper virus, and Hantavirus/Puumala virus were also investigated.

Parasitic diseases accounted for 37% of papers. *E. multilocularis*, *Trichinella* sp., *T. gondii*, *F. magna*, *A. phagocytophilum*, and *Neospora caninum* were most often reported on. With the exception of *F. magna* and *N. caninum,* all of these are zoonotic.

When it comes to the bacterial pathogens, the most reported bacteria were *Salmonella* sp., *M. caprae* and *M. avium*

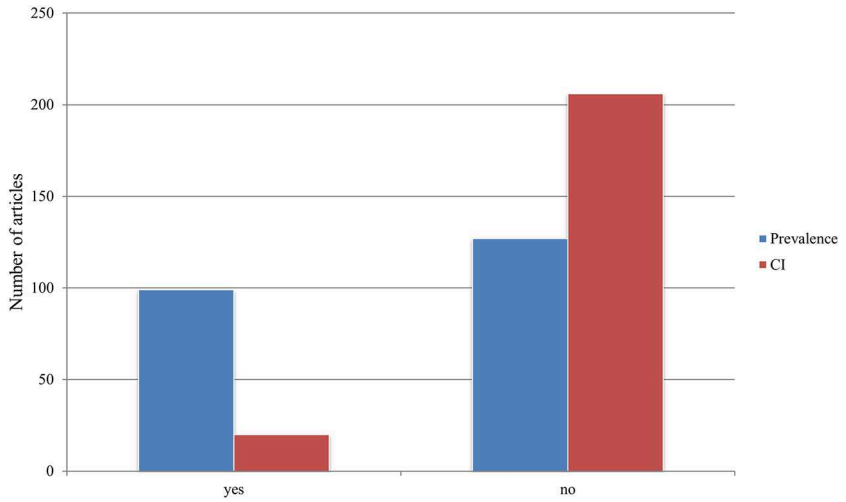

FIGURE 11 | Representation of the specification of prevalence and confidence interval (CI) in all the publications.

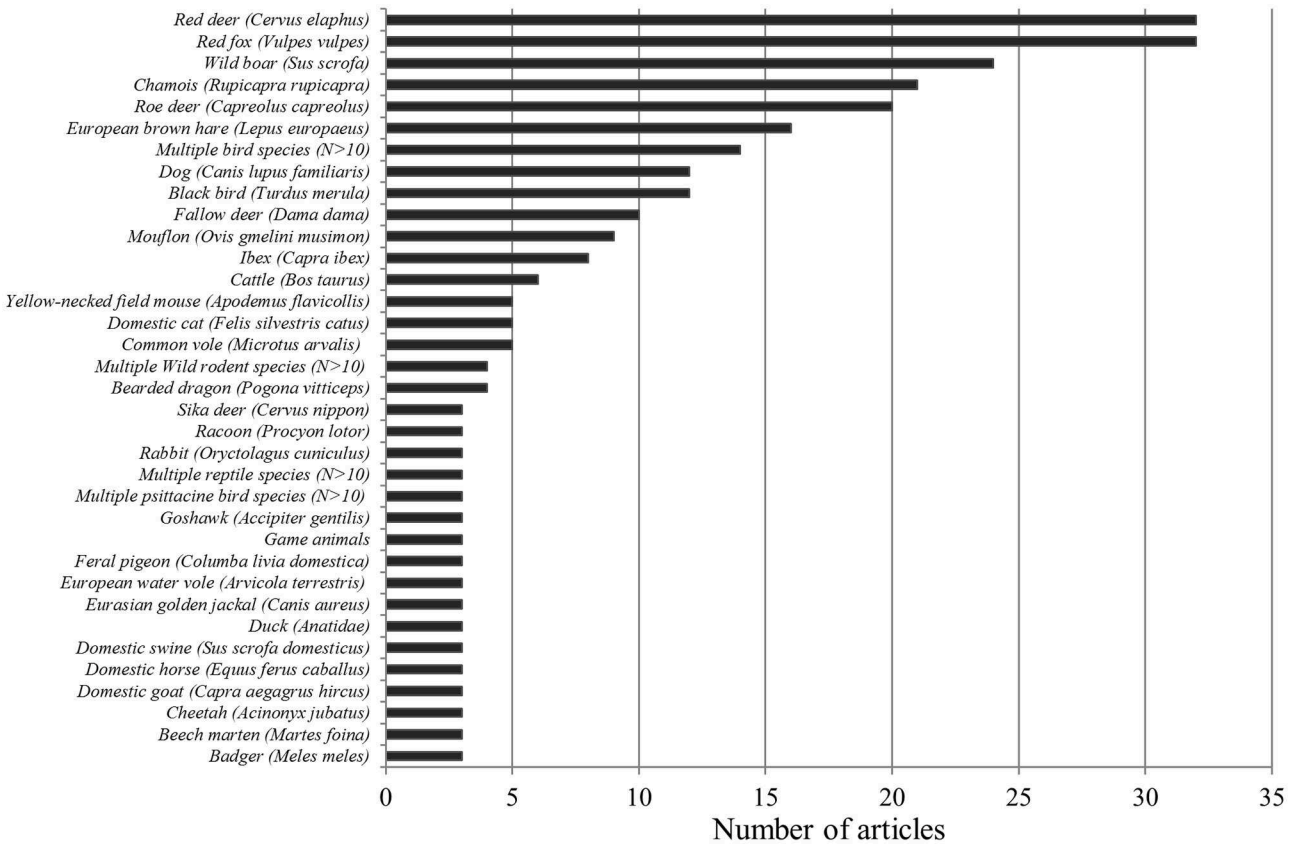

FIGURE 12 | Numerical occurrence of the individual wild animal species or group in the investigated literature.

subsp. *paratuberculosis*, *F. tularensis*, and methicillin-resistant *Staphylococcus aureus*. These are all zoonotic, potentially food borne and thus of high relevance to human health. The risk of a spillover or spillback of these bacterial diseases from wildlife to livestock is potentially quite high, as livestock and wildlife share mountain pastures in Austria.

Batrachochytrium dendrobatidis, a fungus that infects amphibians and is responsible for the global decline and even

extinction of amphibians, was the most reported fungi and a classic EIDs (253).

Zoonotic Potential

The recovered papers are biased toward zoonotic diseases (61% $n = 78$). This is most likely due to funding being more readily available for diseases representing a human health risk. However, wildlife diseases without zoonotic potential should not be ignored, as they can also pose a risk to society, for example by causing major direct economic losses (e.g., ASF) and the loss of ecosystem services through species loss.

Notifiable Status

Of the 35 notifiable animal diseases in the Austrian federal law on epizootics, 7 were reported in the examined literature. In addition, the BVD Regulation 2007, BGBl. II No. 178/2007, and the Paratuberculosis Ordinance, BGBl. II No. 48/2006*, were of relevance, as both BVD and paratuberculosis were reported in wildlife (See **Supplementary Tables 1, 2**). The OIE list includes 117 diseases that can possibly infect or infest animals (254). In this review, we noted 20 diseases that are notifiable according to the OIE. Of the 29 diseases discussed more than two times, seven are notifiable according to the OIE list and the Austrian legislation, four are only notifiable in Austria, and three are only notifiable according to the OIE list.

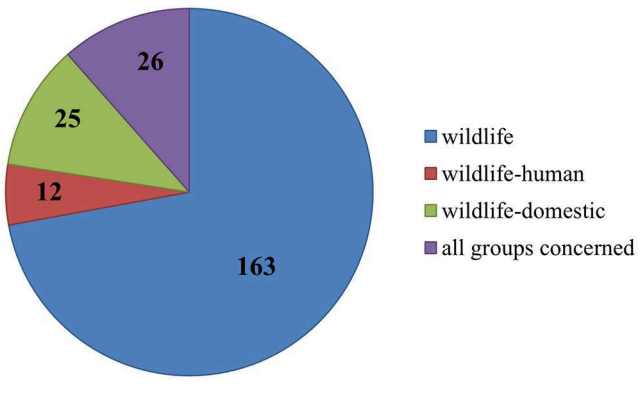

FIGURE 13 | Numerical allocation of the observed interfaces addressed in all publications.

Prevalence and Confidence Interval

Reporting prevalence is essential and provides insight into the epidemiological situation of a pathogen or disease entity in the sampled region. The disease prevalence was stated in 44% of publications. Of concern is that CI were only mentioned in 9% of the papers, thereby seriously limiting the significance of most studies and respective results. We found that 17 publications that provided a confidence interval for their results were research articles (e.g., controlled studies or retrospective studies). Providing confidence intervals did not increase over the 37 years reviewed. The authors of this study are of the opinion that appropriate descriptive statistics are not sufficiently employed in Austrian wildlife disease research at the present time.

Animal Species

Of roughly 626 different vertebrate species (including fish) native to Austria, only 21% have been addressed in this review. This demonstrates a huge untapped research potential in wildlife health research.

Mammals

The most studied mammalian species were the red fox (*V. vulpes*), the red deer (*C. elaphus*), the wild boar (*S. scrofa*), the chamois (*R. rupicapra*), the roe deer (*C. capreolus*), and

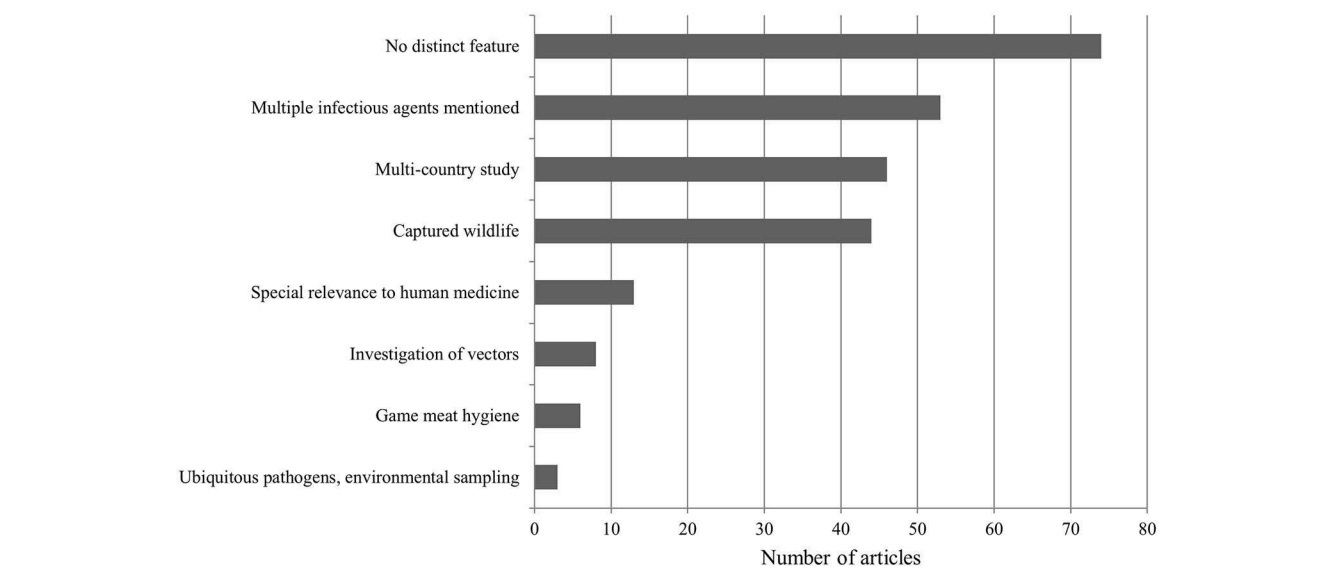

FIGURE 14 | Distribution of different distinct features exhibited by all publications.

the European brown hare (*L. europeus*). It is worth mentioning that these species represent the main game species in Austria. Again, it becomes clear that the primary focus of research has lain on species that serve as food source and offer recreational opportunities for humans. These animals pose a higher risk of transmitting zoonoses, generate funding, and therefore are more interesting to research. The wild boar is a species that has been of great interest to research, as populations are rapidly expanding both in absolute numbers and spatial distribution. Similar to many European countries, wild boar population management is increasingly difficult in Austria. One reason for the rapid reproduction of wild boar is climate change, resulting in increased food availability from beech nuts and acorns coupled with an increased number of litters and offspring survival. Since infection pressure potentially increases with population density, the wild boar population poses an important potential risk for domesticated pigs and humans from ASF or *Trichinella* spp. (214, 255).

Birds

The most studied bird species in Austria was the blackbird (*T. merula*) with references in 12 publications. Interestingly, all studies about blackbirds focused on Usutu virus related to the outbreak in Europe in 2000–2001. The mosquito-borne zoonotic Usutu virus has caused widespread deaths in blackbirds. Before the emergence of the disease in Austria, no previous research on this virus existed. Besides blackbirds, goshawks (*Accipiter gentilis*), feral pigeons (*Columba livia domestica*), and ducks were also of special interest to research. The Usutu virus highlights the fact that a large proportion of research related to wildlife diseases is opportunistic and initially reactive.

Reptiles and Amphibians

The captive bearded dragon (*Pogona vitticeps*) was the most studied reptile in Austria between 1980 and 2017 and appeared in four studies. However, no disease was mentioned more than once. Moreover, we were not able to identify any individual amphibian species that appeared more than once in the investigated publications. The reason for this low number of studies could be the scarcity of amphibian and reptile species in Austria. There are only 21 known native amphibian species and 16 reptile species in Austria (10).

Risk Group Interfaces

The majority (72%) of publications either prospectively sampled wild animal species or evaluated research results in retrospective studies. Numerous publications address the possibility of transmission of pathogens between the different interfaces (e.g., wildlife-livestock, wildlife-human). The remaining studies (28%) dealt with diseases affecting the interfaces between wildlife, livestock, and humans. These papers actively collected samples or performed retrospective studies on existing data across different interfaces. Our study shows that most of the publications addressed the fact that wildlife diseases can emerge in and cross various interfaces.

Distinct Study Features

We were able to identify seven categories within which we could further classify a subset of the papers. Publications could also exhibit more than one distinct feature. Fifty-three publications addressed more than one pathogen of which 42 were research papers. Six publications represented reviews. Furthermore, in 46 studies, countries other than Austria were mentioned. Only 44 studies dealt with captive wildlife or exotic pets. Research at the wildlife-human interface was documented in 13 studies, and these sampled both animals and humans. As the interface between wildlife and humans expands across Austria, it appears prudent to increase research and facilitate human and veterinary medical collaborations. Disease research on trichinosis, tularemia, tuberculosis, and echinococcosis would especially benefit from such collaborative one-health approaches.

CONCLUSION

Wildlife diseases will challenge research and medicine alike for years to come, as major changes due to the growing human population and environmental impacts increase. These impacts contribute to increased occurrence of diseases originating in wild animal species spilling over to humans. This review shows that increasing numbers of studies are being conducted in Austria. However, there is still room for further research. With the exception of prions, all infectious agents (viruses, bacteria, parasites, and fungi) have been investigated. Although there have been numerous studies on zoonoses, we have to stress the importance for future research to focus more strongly on disease dynamics and transmission at the wildlife-human interface. We acknowledge that wildlife disease studies frequently lack prevalence data, or data are of poor quality, to perform robust prevalence calculations. However, it appears that data essential to prevalence statement are not always available, especially in single case reports or due to the bias produced by passive surveillance sampling. Therefore, researchers may often decide not to include prevalence data, since it could be misinterpreted or even speculative. We would suggest that future wildlife disease-related studies should include prevalence data if possible, or state other appropriate measures and methods for statistical and epidemiological characterization of a disease event. Similarly, it appears important to expand the scope of the species investigated in the future. Funding is most often only available during impactful events, such as outbreaks, but is notably lacking for baseline research on wildlife, ecosystems, and diseases. Our assumption that there would be an increase in the number of publications on wildlife diseases in Austria over the period examined was confirmed. Considering our hypothesis, spatiotemporal indicators would have been beneficial to our review. However, due to the quality of the available data, its variability in consistency regarding study design, objectives, and methodologies of the investigated studies (e.g., multiple sampling sites, sampling across longer periods of time, multiple diseases in the same study), stating spatiotemporal indicators would have exceeded the clearly defined scope of this initial study. We believe this question would be best addressed in a separate and future analysis. We hope that this review provides information about the current research status for wildlife ecologists, veterinarians, and officials alike and incentivizes further research that employs "One Health" approaches.

AUTHOR CONTRIBUTIONS

NT did the literature research and wrote the manuscript. CW planned the review concept and working steps, and edited the manuscript.

FUNDING

Funding was provided internally by the University of Veterinary Medicine of Vienna.

ACKNOWLEDGMENTS

We would like to thank Dr. P. K. Walzer for improving and revising our manuscript in terms of grammar and style.

SUPPLEMENTARY MATERIAL

The Supplementary Material for this article can be found online at: https://www.frontiersin.org/articles/10.3389/fvets.2020.00003/full#supplementary-material

REFERENCES

1. Hwang J, Lee K, Kim YJ, Sleeman JM, Lee H. Retrospective analysis of the epidemiologic literature, 1990–2015, on wildlife-associated diseases from the republic of Korea. *J Wildlife Dis.* (2017) 53:5–18. doi: 10.7589/2015-12-348
2. Hassell JM, Begon M, Ward MJ, Fèvre EM. Urbanization and disease emergence: dynamics at the wildlife–livestock–human interface. *Trends Ecol Evol.* (2017) 32:55–67. doi: 10.1016/j.tree.2016.09.012
3. Jones KE, Patel NG, Levy MA, Storeygard A, Balk D, Gittleman JL, et al. Global trends in emerging infectious diseases. *Nature.* (2008) 451:990–3. doi: 10.1038/nature06536
4. McFarlane R, Sleigh A, McMichael T. Synanthropy of wild mammals as a determinant of emerging infectious diseases in the Asian-Australasian region. *EcoHealth.* (2012) 9:24–35. doi: 10.1007/s10393-012-0763-9
5. Coker R, Rushton J, Mounier-Jack S, Karimuribo E, Lutumba P, Kambarage D, et al. Towards a conceptual framework to support one-health research for policy on emerging zoonoses. *Lancet Infect Dis.* (2011) 11:326–31. doi: 10.1016/S1473-3099(10)70312-1
6. Gortázar C, Ferroglio E, Höfle U, Frölich K, Vicente J. Diseases shared between wildlife and livestock: a European perspective. *Eur J Wildlife Res.* (2007) 53:241–56. doi: 10.1007/s10344-007-0098-y
7. StatistikAustria. *Bevölkerung.* (2019). Available online at: https://www.statistik.at/web_de/statistiken/menschen_und_gesellschaft/bevoelkerung/index.html (accessed February 8, 2019).
8. Statisitk Austria. *Austria. Data Figures Facts.* (2018). Available online at: https://eu2018.statistik.at/fileadmin/euratspraesidentschaft/downloads/austria._data._figures._facts.pdf (accessed February 8, 2019).
9. Wikipedia. *Austria.* (2019). Available online at: https://en.wikipedia.org/wiki/Austria#Geography (accessed February 08, 2019).
10. Geiser E. Wie viele tierarten leben in österreich? Erfassung, Hochrechnung und Abschätzung. *Vcrii Zool Bot Ges Österreich.* (1998) 135:81–93.
11. Herzog U, Damoser J, Höflechner-Pöltl A. *Annual Veterinary Report 2017.* Federal Ministry of Labour, Social Affairs, Health and Consumer Protection and Austrian and Agency for Health and Food Safety (AGES), Vienna (2017). p. 1–84.
12. Federal Ministry of Labour, Social Affairs, Health and Consumer Protection and Austrian Agency for Health and Food Safety. *Zoonoses and Zoonotic agents in Austria. Report 2017.* Vienna (2018). p. 1–84.
13. Kommunikationsplattform VerbraucherInnengesundheit (KVG). *Überwachung.* (2019). Available online at: https://www.verbrauchergesundheit.gv.at/tiere/krankheiten/ueberwachung/ueberwachung.html (accessed May 8, 2019).
14. Deutz A, Fuchs K, Auer H, Schuller W, Nowotny N, Kerbl U, et al. Zoonoses, seroepidemiological examination of different persons for selected contact zoonoses: seroprevalences, risk factors and preventive measures. *Fleischwirtschaft.* (2002) 82:101–4.
15. Deutz A, Köfer J. Small game (fox, brown hare, pheasant and duck) as carriers of zoonoses. *Berl Mun Tierarztl Wochenschr.* (2000) 113:401–6. doi: 10.7748/paed.12.3.11.s15
16. Fink M, Schleicher C, Gonano M, Prodinger WM, Pacciarini M, Glawischnig W, et al. Red deer as maintenance host for bovine tuberculosis, alpine region. *Emerg Infect Dis.* (2015) 21:464–7. doi: 10.3201/eid2103.141119
17. Kainz R, Paulsen P. Changes in EU hygiene legislation for meat from hunted game. *Wien Tierarztl Monatsschr.* (2005) 92:150–6.
18. Posautz A, Gyuranecz M, Denes B, Knauer F, Dier H, Walzer C. Seroprevalence of *Francisella tularensis* in Austrian hunting dogs. *Vector Borne Zoon Dis.* (2017) 18:117–9. doi: 10.1089/vbz.2017.2193
19. Wiethoelter AK, Beltrán-Alcrudo D, Kock R, Mor SM. Global trends in infectious diseases at the wildlife-livestock interface. *Proc Natl Acad Sci USA.* (2015) 112:9662–7. doi: 10.1073/pnas.1422741112
20. Daszak P, Cunningham AA, Hyatt AD. Anthropogenic environmental change and the emergence of infectious diseases in wildlife. *Acta Trop.* (2001) 78:103–16. doi: 10.1016/S0001-706X(00)00179-0
21. Springer. *Types of Journal Articles.* (2019). Avaialble online at: https://www.springer.com/gp/authors-editors/authorandreviewertutorials/writing-a-journal-manuscript/types-of-journal-articles/10285504 (accessed February 8, 2019).
22. Aiello SE, Moses MA. *The Merck Veterinary Manual.* 11th ed. Kenilworth, NJ: Merck & Co., Inc. (2016).
23. Boch J, Supperer R. *Veterinärmedizinische Parasitologie.* 3rd ed. Berlin: Parey (2006).
24. Deplazes P, Eckert J, Samson-Himmelstjerna GV, Zahner H. *Lehrbuch der Parasitologie für die Tiermedizin.* 3rd ed. Stuttgart: Enke (2013).
25. Rolle M, Mayr A, Büttner M. *Medizinische Mikrobiologie, Infektions- und Seuchenlehre.* 8th ed. Stuttgart: Enke (2007).
26. Selbit, H-J, Truyen U, Valentin-Weigand P, Alber G. *Tiermedizinische Mikrobiologie, Infektions- und Seuchenlehre.* 9th ed. Stuttgart: Enke (2011).
27. Rehbein S, Visser M. Die Endoparasiten des Sikawildes (*Cervus nippon*) in Österreich. *Wien Klin Wochenschr.* (2007) 119:96–101. doi: 10.1007/s00508-007-0865-5
28. Winkelmayer R, Paulsen P. Parasites in free-living wild game: relevance for meat hygiene and possibilities of detection. *Wien Tierarztl Monatsschr.* (2011) 98:239–44.
29. Schwarz L, Frena M, Skalicky M, Prosl H. Endoparasite infestation of roe deer from a hunting ground in Lower Austria. *Wien Tierarztl Monatsschr.* (2011) 98:285–91.
30. Hoby S, Walzer C, Slotta-Bachmayr L, Segner H, Robert N. Pathological investigations in free-ranging ungulates in the National Park Hohe Tauern, Austria. *Wien Tierarztl Monatsschr.* (2006) 93:104–12.
31. Juncker-Voss M, Prosl H, Lussy H, Enzenberg U, Auer H, Lassnig H, et al. Screening for antibodies against zoonoses among employees of the Zoological Garden of Vienna, Schönbrunn, Austria. *Berl Munch Tierarztl Wochenschr.* (2004) 117:404–9.
32. Duscher G, Leschnik M, Führer HP, Joachim A. Wildlife reservoirs for vector-borne canine, feline and zoonotic infections in Austria. *Int J Parasitol.* (2015) 4:88–96. doi: 10.1016/j.ijppaw.2014.12.001
33. Deutz A, Fuchs K, Schuller W, Nowotny N, Auer H, Aspock H, et al. Seroepidemiological studies of zoonotic infections in hunters in southeastern Austria - prevalences, risk factors, and preventive methods. *Berl Munch Tierarztl Wochenschr.* (2003) 116:306–11.
34. Duscher T, HodŽić A, Glawischnig W, Duscher G. The raccoon dog (*Nyctereutes procyonoides*) and the raccoon (*Procyon lotor*) - their role and impact of maintaining and transmitting zoonotic diseases in Austria, Central Europe. *Parasitol Res.* (2017) 116:1411–6. doi: 10.1007/s00436-017-5405-2

35. Deutz A, Hinterdorfer F. Diseases in brown hare: Post-mortem findings, range of pathogens and zoonotic aspects. *Tierarztl Umschau.* (2000) 55:628–35.
36. Khayal B, Hess M, Bagó Z. Pathomorphological investigations on wild birds during the winter season 2005/2006. *Wien Tierarztl Monatsschr.* (2010) 97:125–34.
37. Wascher CAF, Bauer AC, Holtmann AR, Kotrschal K. Environmental and social factors affecting the excretion of intestinal parasite eggs in graylag geese. *Behav Ecol.* (2012) 23:1276–83. doi: 10.1093/beheco/ars113
38. Rehbein S, Visser M, Jekel I, Silaghi C. Endoparasites of the fallow deer (*Dama dama*) of the Antheringer Au in Salzburg, Austria. *Wien Klin Wochenschr.* (2014) 126 (Suppl.1):37–41. doi: 10.1007/s00508-014-0506-8
39. Schmidt-Ukaj S, Hochleithner M, Richter B, Hochleithner C, Brandstetter D, Knotek Z. A survey of diseases in captive bearded dragons: a retrospective study of 529 patients. *Vet Med.* (2017) 62:508–15. doi: 10.17221/162/2016-VETMED
40. Hoby S, Schwarzenberger F, Doherr MG, Robert N, Walzer C. Steroid hormone related male biased parasitism in chamois, *Rupicapra rupicapra*. *Vet Parasitol.* (2006) 138:337–48. doi: 10.1016/j.vetpar.2006.01.028
41. Deutz A, Köfer J. Pig and wild boar as carriers of zoonoses. *Berl Munch Tierarztl Wochenschr.* (1999) 112:305–10.
42. Kübber-Heiss A, Benetka V, Filip T, Benyr G, Schilcher F, Pallan C, et al. First detection of an adenovirus infection in a bearded dragon (*Pogona vitticeps*) in Austria. *Wien Tierarztl Monatsschr.* (2006) 93:68–72.
43. Duscher G. Duncker's muscle fluke—*Alaria alata* in red foxes from Austria in relation to the occurrence of wild boars. *Wien Tierarztl Monatsschr.* (2011) 98:251–4.
44. Paulsen P, Ehebruster J, Irschik I, Lücker E, Riehn K, Winkelmayer R, et al. Findings of *Alaria alata mesocercariae* in wild boars (*Sus scrofa*) in eastern Austria. *Eur J Wildlife Res.* (2012) 58:991–5. doi: 10.1007/s10344-012-0642-2
45. Sailer A, Glawischnig W, Irschik I, Lücker E, Riehn K, Paulsen P. Findings of *Alaria alata mesocercariae* in wild boar in Austria: current knowledge, identification of risk factors and discussion of risk management options. *Wien Tierarztl Monatsschr.* (2012) 99:346–52.
46. Petrovec M, Sixl W, Schweiger R, Mikulašek S, Elke L, Wüst G, et al. Infections of wild animals with *Anaplasma phagocytophila* in Austria and the Czech republic. *Ann NY Acad Sci.* (2003) 990:103–6. doi: 10.1111/j.1749-6632.2003.tb07345.x
47. Polin H, Hufnagl P, Haunschmid R, Gruber F, Ladurner G. Molecular evidence of *Anaplasma phagocytophilum* in *Ixodes ricinus* ticks and wild animals in Austria. *J Clin Microbiol.* (2004) 42:2285–6. doi: 10.1128/JCM.42.5.2285-2286.2004
48. Silaghi C, Hamel D, Pfister K, Rehbein S. *Babesia* species and co-infection with *Anaplasma phagocytophilum* in free-ranging ungulates from tyrol (Austria). *Wien Tierarztl Monatsschr.* (2011) 98:268–74.
49. Silaghi C, Hamel D, Thiel C, Pfister K, Friche Passos LM, Rehbein S. Genetic variants of *Anaplasma phagocytophilum* in wild caprine and cervid ungulates from the alps in tyrol, Austria. *Vector-Borne Zoonotic Dis.* (2011) 11:355–62. doi: 10.1089/vbz.2010.0051
50. Leschnik M, Kirtz G, Virányi Z, Wille-Piazzai W, Duscher G. Acute granulocytic anaplasmosis in a captive timber wolf (*Canis lupus occidentalis*). *J Zoo Wildlife Med.* (2012) 43:645–8. doi: 10.1638/2011-0224R.1
51. Cezanne R, Mrowietz N, Eigner B, Duscher G, Glawischnig W, Führer HP. Molecular analysis of *Anaplasma phagocytophilum* and *Babesia divergens* in red deer (*Cervus elaphus*) in Western Austria. *Mol Cell Probes.* (2016) 31:55–8. doi: 10.1016/j.mcp.2016.07.003
52. Kotsch V, Kübber-Heiss A, Url A, Walzer C, Schmidt P. Diseases of captive cheetahs (*Acinonyx jubatus*) within the European endangered species program (EEP)—A 22-year retrospective histopathological study. *Wien Tierarztl Monatsschr.* (2002) 89:341–50.
53. Pfeffer M, Dobler G. Emergence of zoonotic arboviruses by animal trade and migration. *Parasit Vect.* (2010) 3:35. doi: 10.1186/1756-3305-3-35
54. Auer H. Parasites of huntable game dangerous for people in Austria. *Wien Tierarztl Monatsschr.* (2011) 98:245–50.
55. Frigerio D, Cibulski L, Ludwig SC, Campderrich I, Kotrschal K, Wascher CAF. Excretion patterns of coccidian oocysts and nematode eggs during the reproductive season in Northern Bald Ibis (*Geronticus eremita*). *J Ornithol.* (2016) 157:839–51. doi: 10.1007/s10336-015-1317-z
56. Pardeike J, Weber S, Zarfl HP, Pagitz M, Zimmer A. Itraconazole-loaded nanostructured lipid carriers (NLC) for pulmonary treatment of aspergillosis in falcons. *Eur J Pharm Biopharm.* (2016) 108:269–76. doi: 10.1016/j.ejpb.2016.07.018
57. Thaller D, Bilek A, Revilla-Fernández S, Bagó Z, Schildorfer H, Url A, et al. Diagnosis of aujeszky's disease in a dog in Austria. *Wien Tierarztl Monatsschr.* (2006) 93:62–7.
58. Leschnik M, Gruber A, Kübber-Heiss A, Bagó Z, Revilla-Fernández S, Wodak E, et al. Epidemiological aspects of aujeszky's disease in Austria by the means of six cases in dogs. *Wien Tierarztl Monatsschr.* (2012) 99:82–90.
59. Steinrigl A, Revilla-Fernández S, Kolodziejek J, Wodak E, Bagó Z, Nowotny N, et al. Detection and molecular characterization of *Suid herpesvirus* type 1 in Austrian wild boar and hunting dogs. *Vet Microbiol.* (2012) 157:276–84. doi: 10.1016/j.vetmic.2011.12.033
60. Weissenböck H, Bakonyi T, Sekulin K, Ehrensperger F, Doneley RJT, Dürrwald R, et al. *Avian bornaviruses* in psittacine birds from Europe and Australia with proventricular dilatation disease. *Emerg Infect Dis.* (2009) 15:1453–9. doi: 10.3201/eid1509.090353
61. Weissenböck H, Sekulin K, Bakonyi T, Högler S, Nowotny N. Novel *Avian bornavirus* in a nonpsittacine species (canary; *Serinus canaria*) with enteric ganglioneuritis and encephalitis. *J Virol.* (2009) 83:11367–71. doi: 10.1128/JVI.01343-09
62. Weissenböck H, Fragner K, Nedorost N, Mostegl MM, Sekulin K, Maderner A, et al. Localization of avian bornavirus RNA by *in situ* hybridization in tissues of psittacine birds with proventricular dilatation disease. *Vet Microbiol.* (2010) 145:9–16. doi: 10.1016/j.vetmic.2010.02.030
63. Nedorost N, Maderner A, Kolodziejek J, Lussy H, Nowotny N, Weissenböck H. Identification of mixed infections with different genotypes of avian bornaviruses in psittacine birds with proventricular dilatation disease. *Avian Dis.* (2012) 56:414–7. doi: 10.1637/10026-112911-ResNote.1
64. Zhang X, Bilic I, Troxler S, Hess M. Evidence of genotypes 1 and 3 of *Avian hepatitis E virus* in wild birds. *Virus Res.* (2017) 228:75–8. doi: 10.1016/j.virusres.2016.11.028
65. Globig A, Baumer A, Revilla-Fernández S, Beer M, Wodak E, Fink M, et al. Ducks as sentinels for avian influenza in wild birds. *Emerg Infect Dis.* (2009) 15:1633–6. doi: 10.3201/eid1510.090439
66. Fink M, Fernández SR, Schobesberger H, Koefer J. Geographical spread of highly pathogenic *avian influenza virus* H5N1 during the 2006 outbreak in Austria. *J Virol.* (2010) 84:5815–23. doi: 10.1128/JVI.01642-09
67. Loupal G, Schönbauer M, Jahn J. Pocken bei Zoo - und wildvögeln: licht - und elektronenmikroskopische untersuchungen. *Z Vet Reihe B.* (1985) 32:326–36. doi: 10.1111/j.1439-0450.1985.tb01969.x
68. Reiter AS, Loupal G. A case of pox in the great bustard (*Otis tarda*) of the hanság population in Austria. *J Ornithol.* (1995) 136:221–3. doi: 10.1007/BF01651245
69. Gruber A, Grabensteiner E, Kolodziejek J, Nowotny N, Loupal G. *Poxvirus* infection in a great tit (*Parus major*). *Avian Dis.* (2007) 51:623–5. doi: 10.1637/0005-2086(2007)51[623:PIIAGT]2.0.CO;2
70. Pichler R, Posautz A, Beer T. *Avian pox virus* in a female bald eagle (*Haliaeetus leucocephalus*) - a case report. *Wien Tierarztl Monatsschr.* (2016) 103:321–5.
71. Mitková B, Hrazdilová K, D'Amico G, Duscher G, Suchentrunk F, Forejtek P, et al. Eurasian golden jackal as host of canine vector-borne protists. *Parasit Vect.* (2017) 10:183. doi: 10.1186/s13071-017-2110-z
72. Duscher G, Führer HP, Kubber-Heiss A. Fox on the run - molecular surveillance of fox blood and tissue for the occurrence of tick-borne pathogens in Austria. *Parasit Vect.* (2014) 7:521. doi: 10.1186/PREACCEPT-1542240345144663
73. HodŽić A, Zörer J, Duscher G. *Dermacentor reticulatus*, a putative vector of *Babesia cf.* microti (syn. theileria annae) piroplasm. *Parasitol Res.* (2017) 116:1075–7. doi: 10.1007/s00436-017-5379-0
74. Corduneanu A, Hrazdilová K, Sándor AD, Matei IA, Ionică AM, Barti L, et al. *Babesia vesperuginis*, a neglected piroplasmid: new host and geographical records, and phylogenetic relations. *Parasit Vect.* (2017) 10:598. doi: 10.1186/s13071-017-2536-3
75. Hinaidy HK. Blutparasiten der wildlebenden wiederkäuer österreichs. *J Veterin Med Ser B.* (1987) 34:81–97. doi: 10.1111/j.1439-0450.1987.tb00374.x

76. Schmidt S, Essbauer SS, Mayer-Scholl A, Poppert S, Schmidt-Chanasit J, Klempa B, et al. Multiple infections of rodents with zoonotic pathogens in Austria. *Vector Borne Zoo Dis.* (2014) 14:467–75. doi: 10.1089/vbz.2013.1504
77. Richter B, Kübber-Heiss A. First detection of chytridiomycosis associated with fatalities in poison dart frogs (*Dendrobates tinctorlus*) in Austria. *Wien Tierarztl Monatsschr.* (2010) 97:157–60.
78. Sztatecsny M, Glaser F. From the eastern lowlands to the western mountains: first records of the chytrid fungus *Batrachochytrium dendrobatidis* in wild amphibian populations from Austria. *Herpetol J.* (2011) 21:87–90.
79. Lötters S, Kielgast J, Sztatecsny M, Wagner N, Schulte U, Werner P, et al. Absence of infection with the amphibian chytrid fungus in the terrestrial alpine salamander (*Salamandra atra*). *Salamandra.* (2012) 48:58–62. doi: 10.5167/uzh-62111
80. d'Ovidio D, Pantchev N, Noviello E, Del Prete L, Maurelli MP, Cringoli G, et al. Survey of *Baylisascaris spp.* in captive striped skunks (mephitis mephitis) in some European areas. *Parasitol Res.* (2017) 116:483–6. doi: 10.1007/s00436-016-5307-8
81. Dürrwald R, Kolodziejek J, Muluneh A, Herzog S, Nowotny N. Epidemiological pattern of classical Borna disease and regional genetic clustering of *Borna disease viruses* point towards the existence of to-date unknown endemic reservoir host populations. *Microb Infect.* (2006) 8:917–29. doi: 10.1016/j.micinf.2005.08.013
82. Shibly S, Schmidt P, Robert N, Walzer C, Url A. Immunohistochemical screening for viral agents in cheetahs (*Acinonyx jubatus*) with myelopathy. *Veterin Rec.* (2006) 159:557–61. doi: 10.1136/vr.159.17.557
83. Weissenböck H, Bagó Z, Kolodziejek J, Hager B, Palmetzhofer G, Dürrwald R, et al. Infections of horses and shrews with *Bornaviruses* in upper Austria: a novel endemic area of borna disease. *Emerg Microb Infect.* (2017) 6:e52. doi: 10.1038/emi.2017.36
84. Leitner N, Schwarzmann L, Zittra C, Palmieri N, Eigner B, Otranto D, et al. Morphological and molecular identification of nasopharyngeal bot fly larvae infesting red deer (*Cervus elaphus*) in Austria. *Parasitol Res.* (2016) 115:4417–22. doi: 10.1007/s00436-016-5206-z
85. Krametter R, Nielsen SS, Loitsch A, Froetscher W, Benetka V, Moestl K, et al. *Pestivirus* exposure in free-living and captive deer in Austria. *J Wildlife Dis.* (2004) 40:791–5. doi: 10.7589/0090-3558-40.4.791
86. Glawischnig W, Schoepf K, Matt M. Monitoring for *Bovine viral diarrhea virus* in Austrian red deer (*Cervus elaphus elaphus*) by using ear-notch samples. *J Wildlife Dis.* (2010) 46:1269–73. doi: 10.7589/0090-3558-46.4.1269
87. Scholz HC, Hofer E, Vergnaud G, Fleche PL, Whatmore AM, Dahouk SA, et al. Isolation of *Brucella microti* from mandibular lymph nodes of red foxes, (*Vulpes vulpes*), in lower Austria. *Vector Borne Zoo Dis.* (2009) 9:153–5. doi: 10.1089/vbz.2008.0036
88. Al Dahouk S, Hofer E, Tomaso H, Vergnaud G, Le Flèche P, Cloeckaert A, et al. Intraspecies diodiversity of the genetically homologous species *Brucella microti*. *Appl Environ Microbiol.* (2012) 78:1534–43. doi: 10.1128/AEM.06351-11
89. Hofer E, Reisp K, Revilla-Fernández S, Plicka H, Romanek G, Bagó Z, et al. Isolation of *Francisella tularensis* and *Brucella suis* from red foxes (*Vulpes vulpes*). *Tierarztli Umschau.* (2010) 65:229–32.
90. Scholz HC, Revilla-Fernández S, Dahouk SA, Hammerl JA, Zygmunt MS, Cloeckaert A, et al. *Brucella vulpis* sp. nov, isolated from mandibular lymph nodes of red foxes (*Vulpes vulpes*). *Intl J Syst Evol Microbiol.* (2016) 66:2090–8. doi: 10.1099/ijsem.0.000998
91. Winkelmayer R, Vodnansky M, Paulsen P, Gansterer A, Treml F. Explorative study on the seroprevalence of *Brucella-, Francisella- and Leptospira* antibodies in the European hare (*Lepus europaeus*) of the Austrian—Czech border region. *Wien Tierarztl Monatsschr*. (2005) 92:131–5.
92. Hofer E, Revilla-Fernández S, Al Dahouk S, Riehm JM, Nöckler K, Zygmunt MS, et al. A potential novel *Brucella* species isolated from mandibular lymph nodes of red foxes in Austria. *Vet Microbiol.* (2012) 155:93–9. doi: 10.1016/j.vetmic.2011.08.009
93. Konicek C, VodráŽka P, Barták P, Knotek Z, Hess C, Račka K, et al. Detection of zoonotic pathogens in wild birds in the cross-border region Austria—Czech republic. *J Wildlife Dis.* (2016) 52:850–61. doi: 10.7589/2016-02-038
94. Troxler S, Hess C, Konicek C, Knotek Z, Barták P, Hess M. Microdilution testing reveals considerable and diverse antimicrobial resistance of *Escherichia coli,* thermophilic *Campylobacter spp*. and *Salmonella spp*. isolated from wild birds present in urban areas. *Eur J Wildlife Res.* (2017) 63:68. doi: 10.1007/s10344-017-1125-2
95. HodŽić A, Cezanne R, Duscher G, Harl J, Glawischnig W, Führer HP. Candidatus Neoehrlichia sp. in an Austrian fox is distinct from candidatus neoehrlichia mikurensis, but closer related to candidatus neoehrlichia lotoris. *Parasit Vectors.* (2015) 8:1163. doi: 10.1186/s13071-015-1163-0
96. HodŽić A, Bruckschwaiger P, Duscher G, Glawischnig W, Führer HP. High prevalence of *Eucoleus boehmi* (syn. Capillaria boehmi) in foxes from western Austria. *Parasitol Res.* (2016) 115:3275–8. doi: 10.1007/s00436-016-5145-8
97. Führer HP. An overview of the host spectrum and distribution of *Calodium hepaticum* (syn. *Capillaria hepatica*): part 1 - *Muroidea*. *Parasitol Res.* (2014) 113:619–40. doi: 10.1007/s00436-013-3691-x
98. Führer HP. An overview of the host spectrum and distribution of *Calodium hepaticum* (syn. *Capillaria hepatica*): part 2 - *Mammalia* (excluding *Muroidea*). *Parasitol Res.* (2014) 113:641–51. doi: 10.1007/s00436-013-3692-9
99. Führer HP, Schneider R, Walochnik J, Auer H. Extraintestinal helminths of the common vole (*Microtus arvalis*) and the water vole (*Arvicola terrestris*) in Western Austria (Vorarlberg). *Parasitol Res.* (2010) 106:1001–4. doi: 10.1007/s00436-010-1753-x
100. Benetka V, Grabensteiner E, Gumpenberger M, Neubauer C, Hirschmüller B, Möstl K. First report of an *iridovirus* (*Genus Ranavirus*) infection in a leopard tortoise (*Geochelone pardalis pardalis*). *Wien Tierarztl Monatsschr.* (2007) 94:243–8.
101. Stephan S, Guerra D, Pospischil A, Hilbe M, Weissenböck H, Novotný L, et al. *Chlamydiaceae* and chlamydia-like organisms in free-living small mammals in Europe and Afghanistan. *J Wildlife Dis.* (2014) 50:195–204. doi: 10.7589/2013-08-194
102. Schmidt-Ukaj S, Loncaric I, Klang A, Spergser J, Häbich AC, Knotek Z. Infection with *Devriesea agamarum* and *Chrysosporium guarroi* in an inland bearded dragon (*Pogona vitticeps*). *Vet Dermatol.* (2014) 25:555–97. doi: 10.1111/vde.12146
103. Kissling R, Krocza W. On the diagnosis of duck-sickness in an area near illmitz, Austria. *Wien Tierarztl Monatsschr.* (1984) 71:327–9.
104. Zechmeister TC, Kirschner AKT, Fuchsberger M, Gruber SG, Süß B, Rosengarten R, et al. Prevalence of botulinum neurotoxin C1 and its corresponding gene in environmental samples from low and high risk avian botulism areas. *Altex.* (2005) 22:185–95.
105. Sipos W, Fischer L, Schindler M, Schmoll F. Genotyping of *Clostridium perfringens* isolated from domestic and exotic ruminants and swine. *J Veterin Med Ser B Infect Dis Veterin Pub Health.* (2003) 50:360–2. doi: 10.1046/j.1439-0450.2003.00690.x
106. Burgstaller J, Burgstaller A, Mansfeld MD. Infection with *Clostridium septicum* in a chamois (*Rupicapra rupicapra*). *Wien Tierarztl Monatsschr.* (2014) 101:98–102.
107. Burtscher H. Große coccidien-gewebszysten im gehirn von *Gracula religiosa* (*Aves*: *Sturnidae*). *Zentralblatt Veterinärmedizin Reihe B.* (1983) 30:590–9. doi: 10.1111/j.1439-0450.1983.tb01885.x
108. Prosl H, Loupal G. Diagnosis of an infestation with *Collyriclum faba* (Bremser, 1831) in a starling (*Sturnus vulgaris L.*) in Vienna. *Tierarztli Praxis.* (1985) 13:177–179.
109. Foerster S, Chastel C, Kaleta EF. Crane hepatitis herpesviruses. *J Veterin Med Ser B.* (1989) 36:433–41. doi: 10.1111/j.1439-0450.1989.tb00625.x
110. Kielstein P, Hotzel H, Schmalreck A, Khaschabi D, Glawischnig W. Occurrence of *Cryptococcus spp.* in excreta of pigeons and pet birds. *Mycoses.* (2000) 43:7–15. doi: 10.1046/j.1439-0507.2000.00534.x
111. Richter B, Nedorost N, Maderner A, Weissenböck H. Detection of *Cryptosporidium* species in feces or gastric contents from snakes and lizards as determined by polymerase chain reaction analysis and partial sequencing of the 18S ribosomal RNA gene. *J Vet Diagn Invest.* (2011) 23:430–5. doi: 10.1177/1040638711403415
112. Richter B, Kübber-Heiss A, Weissenböck H, Schmidt P. Detection of *Cryptosporidium* spp., *Entamoeba* spp. and *Monocercomonas* spp. in the gastrointestinal tract of snakes by *in-situ* hybridization. *J Compar Pathol.* (2008) 138:63–71. doi: 10.1016/j.jcpa.2007.11.001
113. Nemejc K, Sak B, Kvetonova D, Hanzal V, Janiszewski P, Forejtek P, et al. *Cryptosporidium suis* and *Cryptosporidium scrofarum* in Eurasian wild boars (*Sus scrofa*) in central Europe. *Vet Parasitol.* (2013) 197:504–8. doi: 10.1016/j.vetpar.2013.07.003
114. Brack M, Hochleithner C, Hochleithner M, Zenker W. Suspected dermatophilosis in an adult orangutan (*Pongo pygmaeus pygmaeus*). *J Zoo Wildlife Med.* (1997) 28:336–41.

115. Otcenásek M, Hubálek Z, Sixl W. Survey of dermatophytes in the hair of small mammals from Austria. *Folia Parasitol.* (1980) 27:83–7.
116. Führer HP, Auer H, Leschnik M, Silbermayr K, Duscher G, Joachim A. Dirofilaria in humans, dogs, and vectors in Austria (1978-2014)—from imported pathogens to the endemicity of *Dirofilaria repens*. *PLoS Negl Trop Dis.* (2016) 10:e0004547. doi: 10.1371/journal.pntd.0004547
117. Kölbl S, Schnabel H, Mikula M. Distemper as the cause of death in badgers in Austria. *Tierarztliche Praxis.* (1990) 18:81–4.
118. Burtscher H, Url A. Evidence of canine distemper and suggestion of preceding parvovirus-myocarditis in a eurasian badger (*Meles meles*). *J Zoo Wildlife Med.* (2007) 38:139–42. doi: 10.1638/05-016.1
119. Benetka V, Leschnik M, Affenzeller N, Mösti K. Phylogenetic analysis of Austrian *canine distemper virus* strains from clinical samples from dogs and wild carnivores. *Vet Rec.* (2011) 168:377. doi: 10.1136/vr.c6404
120. Kreidl P, Allerberger F, Judmaier G, Auer H, Aspock H, Hall AJ. Domestic pets as risk factors for alveolar hydatid disease in Austria. *Am J Epidemiol.* (1998) 147:978–81. doi: 10.1093/oxfordjournals.aje.a009388
121. Eckert J, Conraths FJ, Tackmann K. Echinococcosis: an emerging or re-emerging zoonosis? *Int J Parasitol.* (2000) 30:1283–94. doi: 10.1016/S0020-7519(00)00130-2
122. Vuitton DA, Zhou H, Bresson-Hadni S, Wang Q, Piarroux M, Raoul F, et al. Epidemiology of alveolar echinococcosis with particular reference to China and Europe. *Parasitology.* (2003) 127(Suppl.):87–107. doi: 10.1017/S0031182003004153
123. McCulloch CR, Prosl H, Schmidt P. A spontaneous and fatal jejunal intussusception in a European brown hare associated with *Eimeria leporis*. *J Vet Med B Infect Dis Vet Public Health.* (2004) 51:470–2. doi: 10.1111/j.1439-0450.2004.00806.x
124. Duscher G, Steineck T, Günter P, Prosl H, Joachim A. *Echinococcus multilocularis* in foxes in Vienna and surrounding territories. *Wien Tierarztl Monatsschr.* (2005) 92:16–20.
125. Duscher G, Pleydell D, Prosl H, Joachim A. *Echinococcus multilocularis* in Austrian foxes from 1991 until 2004. *J Vet Med Series B.* (2006) 53:138–44. doi: 10.1111/j.1439-0450.2006.00930.x
126. Schneider R, Aspöck H, Auer H. Unexpected increase of alveolar echincoccosis, Austria, 2011. *Emerg Infect Dis.* (2013) 19:475–7. doi: 10.3201/eid1903.120595
127. Gottstein B, Frey CF, Campbell-Palmer R, Pizzi R, Barlow A, Hentrich B, et al. Immunoblotting for the serodiagnosis of alveolar echinococcosis in alive and dead Eurasian beavers (*Castor fiber*). *Vet Parasitol.* (2014) 205:113–8. doi: 10.1016/j.vetpar.2014.06.017
128. Posautz A, Parz-Gollner R, Hölzler G, Gottstein B, Schwaiger L, Beiglböck C, et al. First record of *Echinococcus multilocularis* in Austrian beavers (*Castor fiber*). *Wien Tierarztl Monatsschr.* (2015) 102:74–9.
129. Führer HP, Blöschl I, Siehs C, Hassl A. Detection of *Toxoplasma gondii, Neospora caninum*, and *Encephalitozoon cuniculi* in the brains of common voles (*Microtus arvalis*) and water voles (*Arvicola terrestris*) by gene amplification techniques in western Austria (Vorarlberg). *Parasitol Res.* (2010) 107:469–73. doi: 10.1007/s00436-010-1905-z
130. Richter B, Csokai J, Graner I, Eisenberg T, Pantchev N, Eskens HU, et al. Encephalitozoonosis in two inland bearded dragons (*Pogona vitticeps*). *J Comp Pathol.* (2013) 148:278–82. doi: 10.1016/j.jcpa.2012.05.009
131. Bartova E, Markova J, Sedlak K. Prevalence of antibodies to *Encephalitozoon cuniculi* in European hares (*Lepus europaeus*). *Ann Agric Environ Med.* (2015) 22:674–6. doi: 10.5604/12321966.1185773
132. Hinney B, Sak B, Joachim A, Kváč M. More than a rabbit's tale – *Encephalitozoon* spp. in wild mammals and birds. *Int J Parasitol.* (2016) 5:76–87. doi: 10.1016/j.ijppaw.2016.01.001
133. Nowotny N. Serological examinations in domestic cats for virus infections of wild rodents with potential human pathogenicity. *Zentralbl Hyg Umweltmed.* (1996) 198:452–61.
134. Richter B, Kübber-Heiss A, Weissenböck H. Diphtheroid colitis in a *Boa constrictor* infected with amphibian *Entamoeba* sp. *Vet Parasitol.* (2008) 153:164–7. doi: 10.1016/j.vetpar.2008.01.013
135. Loncaric I, Stalder GL, Mehinagic K, Rosengarten R, Hoelzl F, Knauer F, et al. Comparison of ESBL - and AmpC producing *enterobacteriaceae* and Methicillin-Resistant *Staphylococcus aureus* (MRSA) isolated from migratory and resident population of rooks (*Corvus frugilegus*) in Austria. *PLoS ONE.* (2013) 8:e84048. doi: 10.1371/journal.pone.0084048
136. Loncaric I, Beiglböck C, Feßler AT, Posautz A, Rosengarten R, Walzer C, et al. Characterization of ESBL- and AmpC-producing and fluoroquinolone-resistant *Enterobacteriaceae* isolated from mouflons (*Ovis orientalis musimon*) in Austria and Germany. *PLoS ONE.* (2016) 11:e0155786. doi: 10.1371/journal.pone.0155786
137. Fuchs A, Weissenböck H. Comparative histopathological study of Rabbit haemorrhagic disease (RHD) and European brown hare syndrome (EBHS). *J Comp Pathol.* (1992) 107:103–13. doi: 10.1016/0021-9975(92)90100-9
138. Nowotny N, Ros Bascuñana C, Ballagi-Pordány A, Gavier-Widén D, Uhlén M, Belák S. Phylogenetic analysis of rabbit haemorrhagic disease and European brown hare syndrome viruses by comparison of sequences from the capsid protein gene. *Arch Virol.* (1997) 142:657–73. doi: 10.1007/s007050050109
139. Ursprung J, Joachim A, Prosl H. Epidemiology and control of the giant liver fluke, *Fascioloides magna*, in a population of wild ungulates in the Danubian wetlands east of Vienna. *Berl Munch Tierarztl Wochenschr.* (2006) 119:316–23.
140. Haider M, Hörweg C, Liesinger K, Sattmann H, Walochnik J. Recovery of *Fascioloides magna* (*Digenea*) population in spite of treatment programme? Screening of Galba truncatula (Gastropoda, Lymnaeidae) from Lower Austria. *Vet Parasitol.* (2012) 187:445–51. doi: 10.1016/j.vetpar.2012.01.032
141. Hörweg C, Prosl H, Wille-Piazzai W, Joachim A, Sattmann H. Prevalence of *Fascioloides magna* in *Galba truncatula* in the Danube backwater area east of Vienna, Austria. *Wien Tierarztl Monatsschr.* (2011) 98:261–7.
142. Ursprung J, Prosl H. The American Giant Liver Fluke (*Fascioloides magna*) in the Danube floodplain forests east of Vienna, Austria. Occurrence and control 2000 - 2010. *Wien Tierarztl Monatsschr.* (2011) 98:275–84.
143. Sattmann H, Hörweg C, Gaub L, Feix AS, Haider M, Walochnik J, et al. Wherefrom and whereabouts of an alien: the American liver fluke *Fascioloides magna* in Austria: an overview. *Wiener klinische Wochenschrift.* (2014) 126 (Suppl.1):23–31. doi: 10.1007/s00508-014-0499-3
144. Husch C, Sattmann H, Hoerweg C, Ursprung J, Walochnik J. Genetic homogeneity of *Fascioloides magna* in Austria. *Vet Parasitol.* (2017) 243:75–8. doi: 10.1016/j.vetpar.2017.06.007
145. Walzer C, Url A, Robert N, Kübber-Heiss A, Nowotny N, Schmidt P. Idiopathic acute onset myelopathy in cheetah (*Acinonyx jubatus*) cubs. *J Zoo Wildlife Med.* (2003) 34:36–46. doi: 10.1638/1042-7260(2003)34[0036:IAOMIC]2.0.CO;2
146. Weissenböck H, Hubálek Z, Bakonyi T, Nowotny N. Zoonotic mosquito-borne flaviviruses: Worldwide presence of agents with proven pathogenicity and potential candidates of future emerging diseases. *Vet Microbiol.* (2010) 140:271–80. doi: 10.1016/j.vetmic.2009.08.025
147. Hubálek Z, Sixl W, Halouzka J. *Francisella tularensis* in *Dermacentor reticulatus* ticks from the Czech Republic and Austria. *Wiener klinische Wochenschrift.* (1998) 110:909–10.
148. Deutz A, Guggenberger T, Gasteiner J, Steineck T, Bagó Z, Hofer E, et al. Investigation of the prevalence of tularaemia under the aspect of climate change. *Wien Tierarztl Monatsschr.* (2009) 96:107–13.
149. Visser M, Messner C, Rehbein S. Massive infestation with fur mites (*Lynxacarus mustelae*) of a stone marten (*Martes foina*) from Tyrol. *Wiener klinische Wochenschrift.* (2011) 123 (Suppl. 1):36–42. doi: 10.1007/s00508-011-0005-0
150. Juncker-Voss M, Kübber-Heiss A, Kutzer E, Kanzler P, Schratter D, Prosl H. *Geopetitia aspiculata*: Endemic in zoobirds in Austria. *Wien Tierarztl Monatsschr.* (2001) 88:106–13.
151. Aberle SW, Lehner P, Ecker M, Aberle JH, Arneitz K, Khanakah G, et al. *Nephropathia epidemica* and *Puumala virus* in Austria. *Eur J Clin Microbiol Infect Dis.* (1999) 18:467–72. doi: 10.1007/s100960050325
152. Plyusnina A, Aberle S, Aberle J, Plyusnin A. Genetic analysis of *Puumala hantavirus* strains from Austria. *Scand J Infect Dis.* (2006) 38:512–9. doi: 10.1080/00365540600585040
153. Duscher G, Kubber-Heiss A, Richter B, Suchentrunk F. A golden jackal (*Canis aureus*) from Austria bearing *Hepatozoon canis* - import due to immigration into a non-endemic area? *Ticks Tick Borne Dis.* (2013) 4:133–7. doi: 10.1016/j.ttbdis.2012.10.040
154. Kübber-Heiss A, Schilcher F, Möstl K. *Herpesvirus*-infections in tortoises in Austria. *Wien Tierarztl Monatsschr.* (1999) 86:78–82.
155. Bauder B, Kübber-Heiss A, Steineck T, Kuttin ES, Kaufman L. Granulomatous skin lesions due to histoplasmosis in a badger

(*Meles meles*) in Austria. *Medical Mycology.* (2000) 38:249–53. doi: 10.1080/mmy.38.3.249.253
156. Tsangaras K, Siracusa MC, Nikolaidis N, Ishida Y, Cui P, Vielgrader H, et al. Hybridization capture reveals evolution and conservation across the entire *koala retrovirus* genome. *PLoS ONE.* (2014) 9:e95633. doi: 10.1371/journal.pone.0095633
157. Deutz A, Fuchs K, Schuller W, Müller M, Kerbl U, Klement C. Studies on the seroprevalence of antibodies against *Leptospira interrogans* in hunters and wild boar from south-eastern Austria. *Eur J Wildlife Res.* (2002) 48:60–5. doi: 10.1007/BF02285358
158. Paulsen P, Winkelmayer R. Seasonal variation in the microbial contamination of game carcasses in an Austrian hunting area. *Eur J Wildlife Res.* (2004) 50:157–9. doi: 10.1007/s10344-004-0054-z
159. Linke K, Rückerl I, Brugger K, Karpiskova R, Walland J, Muri-Klinger S, et al. Reservoirs of *Listeria* species in three environmental ecosystems. *Appl Environ Microbiol.* (2014) 80:5583–92. doi: 10.1128/AEM.01018-14
160. Benetka V, Krametter-Froetscher R, Baumgartner W, Moestl K. Investigation of the role of Austrian ruminant wildlife in the epidemiology of malignant catarrhal fever viruses. *J Wildl Dis.* (2009) 45:508–11. doi: 10.7589/0090-3558-45.2.508
161. Loncaric I, Kübber-Heiss A, Posautz A, Stalder GL, Hoffmann D, Rosengarten R, et al. Characterization of methicillin-resistant *Staphylococcus* spp. *carrying the mecC gene, isolated from wildlife. J Antimicrob Chemother.* (2013) 68:2222–5. doi: 10.1093/jac/dkt186
162. Loncaric I, Kübber-Heiss A, Posautz A, Stalder GL, Hoffmann D, Rosengarten R, et al. mecC- and mecA-positive meticillin-resistant *Staphylococcus aureus* (MRSA) isolated from livestock sharing habitat with wildlife previously tested positive for mecC-positive MRSA. *Vet Dermatol.* (2014) 25:147–8. doi: 10.1111/vde.12116
163. Deutz A, Spergser J, Rosengarten R, Köfer J. First detection of intrauterine transmission of paratuberculosis in red deer and chamois. *Z Jagdwiss.* (2003) 49:314–9. doi: 10.1007/BF02189639
164. Deutz A, Spergser J, Wagner P, Steineck T, Köfer J, Rosengarten R. Paratuberculosis in wild animals - An observed increase in the clinical incidence. *Tierarztl Umsch.* (2003) 58:482–9.
165. Deutz A, Spergser J, Wagner P, Rosengarten R, Köfer J. *Mycobacterium avium* subsp. paratuberculosis in wild animal species and cattle in Styria/Austria. *Berl Munch Tierarztl Wochenschr.* (2005) 118:314–20.
166. Glawischnig W, Steineck T, Spergser J. Infections caused by *Mycobacterium avium* subspecies *avium, hominissuis,* and *paratuberculosis* in free-ranging red deer (*Cervus elaphus hippelaphus*) in Austria, 2001-2004. *J Wildlife Dis.* (2006) 42:724–31. doi: 10.7589/0090-3558-42.4.724
167. Spergser J, Fuchs K, Deutz A. Molecular characterisation of *M. avium* subsp paratuberculosis isolated from cattle and wild animal species from Styria. *Wien Tierarztl Monatsschr.* (2006) 93:47–52.
168. Gerritsmann H, Stalder GL, Spergser J, Hoelzl F, Deutz A, Kuebber-Heiss A, et al. Multiple strain infections and high genotypic diversity among *Mycobacterium avium* subsp. paratuberculosis field isolates from diseased wild and domestic ruminant species in the eastern Alpine region of Austria. *Infect Genet Evol.* (2014) 21:244–51. doi: 10.1016/j.meegid.2013.11.009
169. Glawischnig W, Khaschabi D. Paratuberculosis in a free living red deer (*Cervus elaphus hippelaphus*) from Vorarlberg. *Wien Tierarztl Monatsschr.* (2001) 88:66–9.
170. Scope A, Spergser J, Vobornik A, Gumpenberger M, Hooijberg EH, Reifinger M. Atypical mycobacteriosis in a ural owl (*Strix uralensis*, PALLAS 1771) from the Austrian reintroduction project. *Wien Tierarztl Monatsschr.* (2013) 100:85–92.
171. Rivière J, Carabin K, Le Strat Y, Hendrikx P, Dufour B. Bovine tuberculosis surveillance in cattle and free-ranging wildlife in EU Member States in 2013: A survey-based review. *Vet Microbiol.* (2014) 173:323–31. doi: 10.1016/j.vetmic.2014.08.013
172. Prodinger WM, Eigentler A, Allerberger F, Schönbauer M, Glawischnig W. Infection of red deer, cattle, and humans with *Mycobacterium bovis* subsp. *caprae in western Austria. J Clin Microbiol.* (2002) 40:2270–2. doi: 10.1128/JCM.40.6.2270-2272.2002
173. Glawischnig W, Allerberger F, Messner C, Schönbauer M, Prodinger WM. Tuberculosis in free-living red deer (*Cervus elaphus hippelaphus*) in the northern Alps. *Wien Tierarztl Monatsschr.* (2003) 90:38–44.
174. Prodinger WM, Brandstatter A, Naumann L, Pacciarini M, Kubica T, Boschiroli ML, et al. Characterization of *Mycobacterium caprae* isolates from Europe by mycobacterial interspersed repetitive unit genotyping. *J Clin Microbiol.* (2005) 43:4984–92. doi: 10.1128/JCM.43.10.4984-4992.2005
175. Weikel J, Glawischnig W, Hofer E, Schoepf K. Tuberculosis in a deer (*Capreolus capreolus*) detected in Tyrol (Austria). *Wien Tierarztl Monatsschr.* (2010) 97:287–9.
176. Schoepf K, Prodinger WM, Glawischnig W, Hofer E, Revilla-Fernandez S, Hofrichter J, et al. A two-years' survey on the prevalence of tuberculosis caused by *Mycobacterium caprae* in red deer (*Cervus elaphus*) in the Tyrol, Austria. *Vet Sci.* (2012) 2012:245138. doi: 10.5402/2012/245138
177. Rettinger A, Broeckl S, Fink M, Prodinger WM, Blum H, Krebs S, et al. The region of difference four is a robust genetic marker for subtyping *mycobacterium caprae* isolates and is linked to spatial distribution of three subtypes. *Transbound Emerg Dis.* (2017) 64:782–92. doi: 10.1111/tbed.12438
178. Belloy L, Janovsky M, Vilei EM, Pilo P, Giacometti M, Frey J. Molecular epidemiology of *Mycoplasma conjunctivae* in *Caprinae*: Transmission across species in natural outbreaks. *Appl Environ Microbiol.* (2003) 69:1913–9. doi: 10.1128/AEM.69.4.1913-1919.2003
179. Zimmermann L, Jambresic S, Giacometti M, Frey J. Specificity of *Mycoplasma conjunctivae* strains for alpine chamois *Rupicapra r.* rupicapra. *Wildlife Biol.* (2008) 14:118–24. doi: 10.2981/0909-6396(2008)14[118:SOMCSF]2.0.CO;2
180. Friedrich C, Ingolic E, Freitag B, Kastberger G, Hohmann V, Skofitsch G, et al. A myxozoan-like parasite causing xenomas in the brain of the mole, *Talpa europaea L.*, 1758 (*Vertebrata, Mammalia*). *Parasitology.* (2000) 121:483–92. doi: 10.1017/S0031182099006769
181. Wanha K, Edelhofer R, Gabler-Eduardo C, Prosl H. Prevalence of antibodies against *Neospora caninum* and *Toxoplasma gondii* in dogs and foxes in Austria. *Vet Parasitol.* (2005) 128:189–93. doi: 10.1016/j.vetpar.2004.11.027
182. Bartova E, Sedlak K, Treml F, Holko I, Literak I. *Neospora caninum* and *Toxoplasma gondii* antibodies in European brown hares in the Czech Republic, Slovakia and Austria. *Vet Parasitol.* (2010) 171:155–8. doi: 10.1016/j.vetpar.2010.03.002
183. Cronstedt-Fell A, Richter B, Voracek T, Kübber-Heiss A. Neosporosis in a Captive Parma Wallaby (*Macropus parma*). *J Comp Pathol.* (2012) 146:274–7. doi: 10.1016/j.jcpa.2011.05.002
184. Posautz A, Loncaric I, Kübber-Heiss A, Knoll A, Walzer C. Acute die-off of chamois (*Rupicapra rupicapra*) in the eastern Austrian alps due to bacterial bronchopneumonia with *Pasteurellaceae. J Wildlife Dis.* (2014) 50:616–20. doi: 10.7589/2013-04-090
185. Loupal G, Kutzer E. Infections with *Plasmodium spec*, in puffins (*Fractercula arctica*). *Kleintierpraxis.* (1996) 41:901–6.
186. Dinhopl N, Mostegl MM, Richter B, Nedorost N, Maderner A, Fragner K, et al. Application of *in-situ* hybridization for the detection and identification of avian malaria parasites in paraffin wax-embedded tissues from captive penguins. *Avian Pathol.* (2011) 40:315–20. doi: 10.1080/03079457.2011.569533
187. Dinhopl N, Nedorost N, Mostegl MM, Weissenbacher-Lang C, Weissenbock H. *In situ* hybridization and sequence analysis reveal an association of *Plasmodium* spp. with mortalities in wild passerine birds in Austria. *Parasitol Res.* (2015) 114:1455–62. doi: 10.1007/s00436-015-4328-z
188. Hess M, Scope A, Heincz U. Comparitive sensitivity of polymerase chain reaction diagnosis of psittacine beak and feather disease on feather samples, cloacal swabs and blood from budgerigars (*Melopsittacus undulates*, Shaw 18005). *Avian Pathol.* (2004) 33:477–81. doi: 10.1080/03079450400003619
189. Jahn J, Timischl W. Mathematical-analysis of the spread of wildlife rabies in Austria. Empirical and theoretical background. *Wien Tierarztl Monatsschr.* (1984) 71:149–55.
190. Kollaritsch H, Maurer W. Tollwut: Epidemiologie, prä- und postexpositionelle Immunisierung. *Wien Klinis Wochenschr.* (2006) 118:312–20. doi: 10.1007/s00508-006-0606-1
191. Müller T, Bätza HJ, Beckert A, Bunzenthal C, Cox JH, Freuling CM, et al. Analysis of vaccine-virus-associated rabies cases in red foxes (*Vulpes vulpes*) after oral rabies vaccination campaigns in Germany and Austria. *Arch Virol.* (2009) 154:1081–91. doi: 10.1007/s00705-009-0408-7

192. Kölbl S, Settele J, Schönbauer M. The first appearance of infectious hemorrhagic disease of rabbits in Austria. *Berl Munch Tierarztl Wochenschr.* (1990) 103:261–6.
193. Ryll R, Bernstein S, Heuser E, Schlegel M, Dremsek P, Zumpe M, et al. Detection of *Rat hepatitis E virus* in wild Norway rats (*Rattus norvegicus*) and Black rats (*Rattus rattus*) from 11 European countries. *Vet Microbiol.* (2017) 208:58–68. doi: 10.1016/j.vetmic.2017.07.001
194. Erdélyi K, Gál J, Sugár L, Ursu K, Forgách P, Szeredi L, et al. *Papillomavirus*-associated fibropapillomas of red deer (*Cervus elaphus*). *Acta Vet Hungar.* (2009) 57:337–44. doi: 10.1556/AVet.57.2009.2.14
195. Geue L, Löschner U. *Salmonella enterica* in reptiles of German and Austrian origin. *Vet Microbiol.* (2002) 84:79–91. doi: 10.1016/S0378-1135(01)00437-0
196. Glawischnig W, Lazar J, Wallner A, Kornschober C. Cattle-derived *Salmonella enterica* serovar dublin infections in red foxes (*Vulpes vulpes*) in Tyrol, Austria. *J Wildlife Dis.* (2017) 53:361–3. doi: 10.7589/2016-04-087
197. Pfleger S, Benyr G, Sommer R, Hassl A. Pattern of *Salmonella* excretion in amphibians and reptiles in a vivarium. *Int J Hyg Environ Health.* (2003) 206:53–9. doi: 10.1078/1438-4639-00184
198. Awad-Masalmeh M, Romanik G, Herkal C. The occurrence of *Salmonellae* in reptiles kept privateley or in zoos in Austria. *Tierarztliche Umschau.* (2005) 60:70–4.
199. Paulsen P, Smulders FJM, Hilbert F. *Salmonella* in meat from hunted game: a Central European perspective. *Food Res Int.* (2012) 45:609–16. doi: 10.1016/j.foodres.2011.06.055
200. Hilbert F, Smulders FJM, Chopra-Dewasthaly R, Paulsen P. *Salmonella* in the wildlife-human interface. *Food Res Int.* (2012) 45:603–8. doi: 10.1016/j.foodres.2011.08.015
201. Fuchs K, Deutz A, Gressmann G. Detection of space-time clusters and epidemiological examinations of scabies in chamois. *Vet Parasitol.* (2000) 92:63–73. doi: 10.1016/S0304-4017(00)00269-7
202. Gressmann G, Deutz A. Considerations on reducing the risk of scabies infestation in chamois by targeted hunting of individual age classes. *Z Jagdwiss.* (2001) 47:34–42. doi: 10.1007/BF02242412
203. Monecke S, Gavier-Widén D, Hotzel H, Peters M, Guenther S, Lazaris A, et al. Diversity of *Staphylococcus aureus* isolates in european wildlife. *PLoS ONE.* (2016) 11:e0168433. doi: 10.1371/journal.pone.0168433
204. Führer HP, Siehs C, Schneider R, Auer H. Morphometrical analysis of *Taenia taeniaeformis* and *Taenia crassiceps* in the common vole (*Microtus arvalis*) and the water vole (*Arvicola terrestris*) in Vorarlberg, Austria. *Helminthologia.* (2012) 49:169–73. doi: 10.2478/s11687-012-0034-x
205. Führer HP, Biro N, Harl J, Worliczek HL, Beiglbock C, Farkas R, et al. Molecular detection of *Theileria sp.* ZS TO4 in red deer (*Cervus elaphus*) and questing *Haemaphysalis concinna* ticks in Eastern Austria. *Vet Parasitol.* (2013) 197:653–7. doi: 10.1016/j.vetpar.2013.07.005
206. Bag,ó Z, Bauder B, Kolodziejek J, Nowotny N, Weissenböck H. Tickborne encephalitis in a mouflon (*Ovis ammon musimon*). *Vet Rec.* (2002) 150:218–20. doi: 10.1136/vr.150.7.218
207. Duscher G, Wetscher M, Baumgartner R, Walder G. Roe deer sera used for TBE surveillance in Austria. *Ticks Tick Borne Dis.* (2015) 6:489–93. doi: 10.1016/j.ttbdis.2015.03.018
208. Deutz A, Fuchs K, Auer H, Kerbl U, Aspöck H, Köfer J. *Toxocara*-infestations in Austria: a study on the risk of infection of farmers, slaughterhouse staff, hunters and veterinarians. *Parasitol Res.* (2005) 97:390–4. doi: 10.1007/s00436-005-1469-5
209. Auer H, Aspöck H. The diagnosis of *Toxocara* infestations and of human toxocarosis. *Lab Med.* (2006) 30:1–12. doi: 10.1515/JLM.2006.001
210. Basso W, Edelhofer R, Zenker W, Möstl K, Kübber-Heiss A, Prosl H. Toxoplasmosis in Pallas' cats (*Otocolobus manul*) raised in captivity. *Parasitology.* (2005) 130:293–9. doi: 10.1017/S0031182004006584
211. Edelhofer R, Prossinger H. Infection with *Toxoplasma gondii* during pregnancy: seroepidemiological studies in Austria. *Zoonoses Public Health.* (2010) 57:18–26. doi: 10.1111/j.1863-2378.2009.01279.x
212. Posautz A, Leidinger E, Knauer F, Hoffmann D, Suchentrunk F, Walzer C, et al. Seroprevalence of *Treponema* sp. in European brown hares *(Lepus europaeus)* in Austria and Germany. *Wien Tierarztl Monatsschr.* (2014) 101:281–5.
213. Krois E, Nöckler K, Duscher G, Joachim A, Kapel CMO, Prosl H. *Trichinella britovi* in Austrian red foxes (*Vulpes vulpes*). *Wien Tierarztl Monatsschr.* (2005) 92:308–14.
214. Glawischnig W, Wunsch A, Fötschl H, Bagó Z, Vanek E. First report of *Trichinella pseudospiralis* in wild boar in Austria. *Wien Tierarztl Monatsschr.* (2016) 103:183–187.
215. Edelhofer R, Prosl H, Kutzer E. Trichinellosis and toxoplasmosis in wild pigs of Eastern Austria. *Wien Tierarztl Monatsschr.* (1996) 83:225–9.
216. Pozio E. Trichinellosis in the European union: epidemiology, ecology and economic impact. *Parasitol Today.* (1998) 14:35–8. doi: 10.1016/S0169-4758(97)01165-4
217. Paulsen P, Winkelmayer R, Gneist M, Riedl C., Gansterer A, Gabler C, et al. Establishing a *Trichinella* proficiency testing scheme in Austria. First communication: a preliminary study on Trichinella inspection of wild boar meat in Lower Austria by authorized trained hunters employing the compression method. *Wien Tierarztl Monatsschr.* (2003) 90:91–7.
218. Auer H. Human trichinellosis in Austria. *Wien Tierarztl Monatsschr.* (2005) 92:288–94.
219. Sattmann H, Prosl H. History of early research on *trichinellae* and trichinelloses. *Wien Tierarztl Monatsschr.* (2005) 92:283–7.
220. Winkelmayer R, Paulsen P. *Trichinella* examination of free range wild boar in Lower Austria. *Wien Tierarztl Monatsschr.* (2005) 92:322–4.
221. Duscher G, Winkelmayer R, Prosl H. Wild boar distribution in Austrian areas with *Trichinella* spp. findings in red foxes. *Wien Tierarztl Monatsschr.* (2005) 92:315–21.
222. Grabensteiner E, Bilic I, Kolbe T, Hess M. Molecular analysis of clonal trichomonad isolates indicate the existence of heterogenic species present in different birds and within the same host. *Vet Parasitol.* (2010) 172:53–64. doi: 10.1016/j.vetpar.2010.04.015
223. Ganas P, Jaskulska B, Lawson B, Zadravec M, Hess M, Bilic I. Multi-locus sequence typing confirms the clonality of *Trichomonas gallinae* isolates circulating in European finches. *Parasitology.* (2014) 141:652–61. doi: 10.1017/S0031182013002023
224. Schilcher F, Kübber-Heiss A, Breuer-Strosberg R, Barth S. Dermatomycosis due to *Trichphyton terrestre* in Madagascar Day Geckos (*Phelsuma m. madagascariensis*). *Wien Tierarztl Monatsschr.* (1998) 85:131–5.
225. Mostegl MM, Richter B, Nedorost N, Maderner A, Dinhopl N, Kübber-Heiss A, et al. Identification of a putatively novel trichomonad species in the intestine of a common quail (*Coturnix coturnix*). *Vet Parasitol.* (2012) 183:369–72. doi: 10.1016/j.vetpar.2011.07.036
226. Weissenböck H, Kolodziejek J, Url A, Lussy H, Rebel-Bauder B, Nowotny N. Emergence of *Usutu virus*, an African mosquito-borne Flavivirus of the Japanese encephalitis virus group, central Europe. *Emerg Infect Dis.* (2002) 8:652–6. doi: 10.3201/eid0807.020094
227. Weissenböck H, Kolodziejek J, Fragner K, Kuhn R, Pfeffer M, Nowotny N. *Usutu virus* activity in Austria, 2001-2002. *Microb Infect.* (2003) 5:1132–6. doi: 10.1016/S1286-4579(03)00204-1
228. Chvala S, Kolodziejek J, Nowotny N, Weissenböck H. Pathology and viral distribution in fatal *Usutu virus* infections of birds from the 2001 and 2002 outbreaks in Austria. *J Comp Pathol.* (2004) 131:176–85. doi: 10.1016/j.jcpa.2004.03.004
229. Bakonyi T, Gould EA, Kolodziejek J, Weissenböck H, Nowotny N. Complete genome analysis and molecular characterization of *Usutu virus* that emerged in Austria in 2001: comparison with the South African Strain SAAR-1776 and other flaviviruses. *Virology.* (2004) 328:301–10. doi: 10.1016/S0042-6822(04)00525-2
230. Hassler D, Pfeffer M, Weissenbock H, Nowotny N. *Usutu virus* in Austria reminds one of the *West Nile virus* in the USA. *Dtsch Med Wochenschr.* (2004) 129:2339–40.
231. Weissenböck H, Bakonyi T, Chvala S, Nowotny N. Experimental *Usutu virus* infection of suckling mice causes neuronal and glial cell apoptosis and demyelination. *Acta Neuropathol.* (2004) 108:453–60. doi: 10.1007/s00401-004-0916-1
232. Chvala S, Bakonyi T, Bukovsky C, Meister T, Brugger K, Rubel F, et al. Monitoring of *Usutu virus* activity and spread by using dead bird surveillance in Austria, 2003-2005. *Vet Microbiol.* (2007) 122:237–45. doi: 10.1016/j.vetmic.2007.01.029

233. Meister T, Lussy H, Bakonyi T, Sikutova S, Rudolf I, Vogl W, et al. Serological evidence of continuing high *Usutu virus* (*Flaviviridae*) activity and establishment of herd immunity in wild birds in Austria. *Vet Microbiol.* (2008) 127:237–48. doi: 10.1016/j.vetmic.2007.08.023
234. Rubel F, Brugger K, Hantel M, Chvala-Mannsberger S, Bakonyi T, Weissenböck H, et al. Explaining *Usutu virus* dynamics in Austria: Model development and calibration. *Prev Vet Med.* (2008) 85:166–86. doi: 10.1016/j.prevetmed.2008.01.006
235. Brugger K, Rubel F. Simulation of climate-change scenarios to explain *Usutu-virus* dynamics in Austria. *Prev Vet Med.* (2009) 88:24–31. doi: 10.1016/j.prevetmed.2008.06.023
236. Buchebner N, Zenker W, Wenker C, Steinmetz HW, Sós E, Lussy H, et al. Low *Usutu virus* seroprevalence in four zoological gardens in central Europe. *BMC Vet Res.* (2013) 9:153. doi: 10.1186/1746-6148-9-153
237. Stiasny K, Aberle SW, Heinzl FX. Retrospective identification of human cases of *West nile virus* infection in Austria (2009 to 2010) by serological differentiation from *Usutu* and other *flavivirus* infections. *Eurosurveillance.* (2013) 18:20614. doi: 10.2807/1560-7917.ES2013.18.43.20614
238. Bakonyi T, Busquets N, Nowotny N. Comparison of complete genome sequences of *Usutu virus* strains detected in Spain, Central Europe, and Africa. *Vector Borne Zoon Dis.* (2014) 14:324–9. doi: 10.1089/vbz.2013.1510
239. Bakonyi T, Erdélyi K, Brunthaler R, Dán Á, Weissenböck H, Nowotny N. *Usutu virus*, Austria and Hungary, 2010-2016. *Emerg Microb Infect.* (2017) 6:85. doi: 10.1038/emi.2017.72
240. Freidl G, Stalder G, Kostić T, Sessitsch A, Beiglböck C, Walzer C. Verocytotoxin-producing *Escherichia coli* in chamois (*Rupicapra rupicapra*) and cattle in Austria. *J Wildlife Dis.* (2011) 47:704–8. doi: 10.7589/0090-3558-47.3.704
241. Weissenböck H, Hubálek Z, Halouzka J, Pichlmair A, Maderner A, Fragner K, et al. Screening for *West Nile virus* infections of susceptible animal species in Austria. *Epidemiol Infect.* (2003) 131:1023–7. doi: 10.1017/S0950268803001031
242. Linke S, Muehlen M, Niedrig M, Ellerbrok H, Kaiser A, Fiedler W, et al. Assessing the exposure of German and Austrian bird ringers to *West Nile virus* (Flavivirus) and evaluating their potential risk of infection. *J Ornithol.* (2008) 149:271–5. doi: 10.1007/s10336-007-0270-x
243. Wodak E, Richter S, Bagó Z, Revilla-Fernández S, Weissenböck H, Nowotny N, et al. Detection and molecular analysis of *West Nile virus* infections in birds of prey in the eastern part of Austria in 2008 and 2009. *Vet Microbiol.* (2011) 149:358–66. doi: 10.1016/j.vetmic.2010.12.012
244. Bakonyi T, Ferenczi E, Erdelyi K, Kutasi O, Csorgo T, Seidel B, et al. Explosive spread of a neuroinvasive lineage 2 *West Nile virus* in Central Europe, 2008/2009. *Vet Microbiol.* (2013) 165:61–70. doi: 10.1016/j.vetmic.2013.03.005
245. Beck C, Jimenez-Clavero MA, Leblond A, Durand B, Nowotny N, Leparc-Goffart I, et al. Flaviviruses in europe: complex circulation patterns and their consequences for the diagnosis and control of west nile disease. *Int J Environ Res Public Health.* (2013) 10:6049–83. doi: 10.3390/ijerph10116049
246. Hernández-Triana LM, Jeffries CL, Mansfield KL, Carnell G, Fooks AR, Johnson N. Emergence of *West Nile virus* lineage 2 in Europe: a review on the introduction and spread of a mosquito-borne disease. *Front Public Health.* (2014) 2:271. doi: 10.3389/fpubh.2014.00271
247. Rizzoli A, Jiménez-Clavero MA, Barzon L, Cordioli P, Figuerola J, Koraka P, et al. The challenge of West nile virus in Europe: knowledge gaps and research priorities. *Eurosurveillance.* (2015) 20:21135. doi: 10.2807/1560-7917.ES2015.20.20.21135
248. Bakonyi T, Gajdon GK, Schwing R, Vogl W, Häbich AC, Thaller D, et al. Chronic *West Nile virus* infection in kea (*Nestor notabilis*). *Vet Microbiol.* (2016) 183:135–9. doi: 10.1016/j.vetmic.2015.12.012
249. Bidaisee S, Macpherson CNL. Zoonoses and one health: a review of the literature. *J Parasitol Res.* (2014) 2014:874345. doi: 10.1155/2014/874345
250. Austrian Agency for Health and Food Safety (AGES). *Transmissible Spongiforme Enzephalopathie (TSE)*. (2019). Available online at: https://www.ages.at/themen/krankheitserreger/tse-bsescrapiecwd/tab/3/ (accessed May 10, 2019).
251. European Food Safety Authority (EFSA). *Chronic Wasting Disease: Addressing Risks for the EU (CWD)*. (2017). Available online at: https://www.efsa.europa.eu/en/press/news/170118 (accessed May 6, 2019).
252. Austrian Agency for Health and Food Safety (AGES). *Usutu Virus*. (2019). Available online at: https://www.ages.at/themen/krankheitserreger/usutu-virus/tab/1/ (accessed May 9, 2019).
253. Dobson A, Foufopoulos J. Emerging infectious pathogens of wildlife. *Philo Trans R Soc B Biol Sci.* (2001) 356:1001–12. doi: 10.1098/rstb.2001.0900
254. World Organisation for Animal Health (OIE). *OIE Listed Diseases*. (2019). Available online at: http://www.oie.int/en/animal-health-in-the-world/oie-listed-diseases-2019/ (accessed May 7, 2019).
255. Vetter SG, Ruf T, Bieber C, Arnold W. What is a mild winter? Regional differences in within-species responses to climate change. *PLoS ONE.* (2015) 10:e0132178. doi: 10.1371/journal.pone.0132178

Conflict of Interest: The authors declare that the research was conducted in the absence of any commercial or financial relationships that could be construed as a potential conflict of interest.

Copyright © 2020 Trimmel and Walzer. This is an open-access article distributed under the terms of the Creative Commons Attribution License (CC BY). The use, distribution or reproduction in other forums is permitted, provided the original author(s) and the copyright owner(s) are credited and that the original publication in this journal is cited, in accordance with accepted academic practice. No use, distribution or reproduction is permitted which does not comply with these terms.

frontiers in Veterinary Science

CASE REPORT
published: 27 February 2020
doi: 10.3389/fvets.2020.00069

Diagnosis and Surgical Management of a Paratesticular Cyst in a Rehabilitating Juvenile Male Green Turtle (*Chelonia mydas*)

Tatiana C. Weisbrod[1]*, *Nicole I. Stacy*[1], *Nancy L. Stedman*[2] and *Terry M. Norton*[3]

[1] Department of Comparative, Diagnostic, and Population Medicine, College of Veterinary Medicine, University of Florida, Gainesville, FL, United States, [2] Busch Gardens Tampa, Tampa, FL, United States, [3] Georgia Sea Turtle Center/Jekyll Island Authority, Jekyll Island, GA, United States

A juvenile green turtle (*Chelonia mydas*) undergoing rehabilitation for cold stunning exhibited an asymmetric bulging of the left caudal plastron and was diagnosed with a large intra-coelomic mass based on radiographical findings. Ultrasonography further identified a fluid-filled structure within the caudal coelom. Cytological evaluation of fluid obtained from the structure was consistent with a transudate, and thus, a cyst of unknown origin was suspected. Computed tomography imaging was pursued to further characterize the extent and location of the mass, which occupied ∼50% of the total coelomic cavity volume. Conservative management with monitoring and occasional drainage of the mass did not result in improvements; thus, an exploratory laparoscopy for further investigation and surgical planning was elected. Intra-coelomic surgery was performed to remove a thick-walled cystic mass associated with the left gonad. Histopathology confirmed a paratesticular cyst continuous with, and possibly originating from, the epididymis. Post-surgical recurrence of the cyst was not appreciated, and the animal was successfully released 1 year after admission. Unrelated to the cyst, the turtle developed acute severe anemia on two occasions throughout rehabilitation that responded to modification of antimicrobial treatment and subsequent steroid administration. To the authors' knowledge, this is the first report of a paratesticular cyst in a reptile.

Keywords: anemia, developmental abnormality, epididymal cyst, Mullerian duct, surgery

OPEN ACCESS

Edited by:
Tracy Stokol,
Cornell University, United States

Reviewed by:
James Steeil,
Smithsonian Institution, United States
Maria De Jesus Forzan,
Long Island University, United States

***Correspondence:**
Tatiana C. Weisbrod
tweisbrod@ufl.edu

Specialty section:
This article was submitted to Veterinary Experimental and Diagnostic Pathology, a section of the journal Frontiers in Veterinary Science

Received: *09 December 2019*
Accepted: *28 January 2020*
Published: *27 February 2020*

Citation:
Weisbrod TC, Stacy NI, Stedman NL and Norton TM (2020) Diagnosis and Surgical Management of a Paratesticular Cyst in a Rehabilitating Juvenile Male Green Turtle (Chelonia mydas). Front. Vet. Sci. 7:69. doi: 10.3389/fvets.2020.00069

INTRODUCTION

A free-ranging juvenile green turtle (*Chelonia mydas*) of unknown sex, weighing 2.4 kg was admitted to the Georgia Sea Turtle Center on Jekyll Island, Georgia, for rehabilitation after cold stunning at Fernandina Beach, Florida, in February 2016. The turtle was found to be thin (body condition score 2/5) with mild algae and epibiota coverage on the carapace. Hematological and plasma biochemical analyses were consistent with typical findings in cold-stunned green turtles (1), including heterophilia consistent with systemic inflammation; hypoglycemia, hypoproteinemia, hypoalbuminemia, and hypocalcemia likely secondary to emaciation and anorexia; elevated uric acid presumably from dehydration or possibly renal disease; and elevated creatine kinase from muscle injury or exertion (**Table 1**). Packed cell volume (PCV) was normal at this time. Initial whole-body radiographs were unremarkable. Medical treatment was initiated with ceftazidime

TABLE 1 | Select hemogram and plasma biochemical findings over time in a cold-stunned green turtle (*Chelonia mydas*).

Days from admission	0	56	81	98	270	297	345	Reported data
Clinical time point	**Admit**	**First anemic event**	**Diagnosis of mass**	**Second anemic event**	**Pre-operative**	**2 weeks post-operative**	**Pre-release**	
Creatine kinase, μmol/L	80.9	18.5	6.1	10	7.7	54.9	20.4	NR
Albumin, g/L	5	12	16	14	12	8	8	6–21
Total protein, g/L	17	33	50	41	31	23	25	26–69
Globulin, g/L	12	21	34	27	19	15	17	19–52
Uric acid, μmol/L	273.6	47.6	83.3	77.3	47.6	53.5	41.6	29.7–208.2
Glucose, mmol/L	1.4	6.1	12.4	6.9	5.4	5.4	5.8	4.8–9.3
Calcium, mmol/L	1	1.3	1.7	1.5	1.2	1.2	1.1	0.4–3
Phosphorus, mmol/L	2.4	3.2	2.8	3.1	3.3	3.2	2.3	1.2–3.5
Potassium, mmol/L	4.6	4.1	3.7	4.8	4.6	3.6	4.7	4.1–6.9
Chloride, mmol/L	121	124	106	130	115	124	116	100–130
Sodium, mmol/L	155	158	158	157	155	156	156	157–183
PCV L/L	0.28	0.10/0.11	0.18	0.13	0.31	0.12	0.32	0.17–0.38
TS g/L	16	36	51	44	34	20	26	NR
Immature RBC/100 (PCV < 25)	NR	32	84	76	NR	22	NR	NR
WBC estimate $\times 10^9$/L	24.50	9.30	34.50	33.00	14.10	89.00	10.20	1.76–22.40
Absolute heterophils $\times 10^9$/L	18.00	3.50	19.00	20.00	7.50	71.00	6.20	0.23–2.59
Absolute immature heterophils $\times 10^9$/L	0.00	0.00	0.69	2.00	0.00	0.89	0.00	NR
Absolute lymphocytes $\times 10^9$/L	4.90	3.90	10.00	7.30	4.50	12.00	2.10	3.42*
Absolute monocytes $\times 10^9$/L	1.70	1.70	4.80	3.30	1.40	2.70	0.51	0.18–2.92
Absolute eosinophils $\times 10^9$/L	0.25	0.09	0.00	0.66	0.42	1.80	0.92	0.37–5.16
Absolute basophils $\times 10^9$/L	0.00	0.19	0.00	0.00	0.28	0.00	0.51	0–0.13
Thrombocytes	Adequate	Adequate	Adequate	Adequate	Adequate	Adequate	Adequate	NA
Erythrocyte morphology	Occ. fragments	Moderate anisocytosis and polychromasia	Moderate anisocytosis and polychromasia	Moderate anisocytosis and polychromasia	NSCF	Moderate anisocytosis and polychromasia	NSCF	NA
WBC morphology	NSCF	NSCF	Mild left-shift, 1+ toxicity	Moderate left-shift, 1+ toxicity	NSCF	Mild left shift	NSCF	NA

*Plasma biochemical reference ranges are minimum and maximum values from 100 free-ranging juvenile green turtles (2). Hemogram reference ranges are minimum and maximum values (unless otherwise noted) from 23 juvenile and 5 mature free-ranging green turtles (3); NR, not reported; NA, not available; NSCF, no significant cytological findings; *number represents the mean.*

(20 mg/kg BW, every 3 days for 39 days, subcutaneously), lactated Ringer's solution (LRS) with 5% dextrose (5 ml/kg BW, as indicated by daily bloodwork monitoring, intravenously), and 23% calcium gluconate (0.2 ml/kg BW, once daily until normalized, subcutaneously).

Bloodwork, appetite, and weight steadily improved over the first 4 weeks after admission; however, 8 weeks from initial presentation, the turtle developed an acute, regenerative, non-hemolytic anemia (**Table 1**). A blood culture was negative, ceftazidime administration was discontinued, and broad-spectrum antimicrobial therapy was instituted with amikacin (5 mg/kg BW first dose followed by 3 mg/kg BW, every 3 days for 46 days, subcutaneously) and ampicillin (30 mg/kg BW, once daily for 17 days, subcutaneously) followed by amoxicillin/clavulanic acid (30 mg/kg BW, once daily for 29 days, orally), and dexamethasone sodium phosphate at an immunosuppressive dose (0.5 mg/kg BW, once daily for 10 days, then every other day for 6 days). The turtle developed hyperglycemia with concurrent steroid administration, which normalized upon its discontinuation, and PCV improved over 3 weeks.

During routine physical examinations, about 1 month following the development of the acute anemia, the left side of the plastron was noted to bulge asymmetrically compared to the right side. Whole-body radiographs identified a large round soft tissue mass within the caudal left coelom that was not appreciated on prior images (**Figure 1A**). Follow-up CT imaging confirmed the presence of a large mass comprising ∼50% of the total coelomic volume within the left caudal coelom (**Figure 1B**). Differentials included cyst, abscess, hematoma, neoplasia (e.g., fibropapillomatosis), or much less likely an anatomical abnormality. Ultrasound of the region from the left pre-femoral window showed multiple anechoic structures with cystic appearance. An ultrasound-guided fine-needle aspirate of the fluid-filled structure yielded a clear pale-yellow, low protein (total solids 4 g/dl), acellular (white blood cell estimate 0/μl) fluid

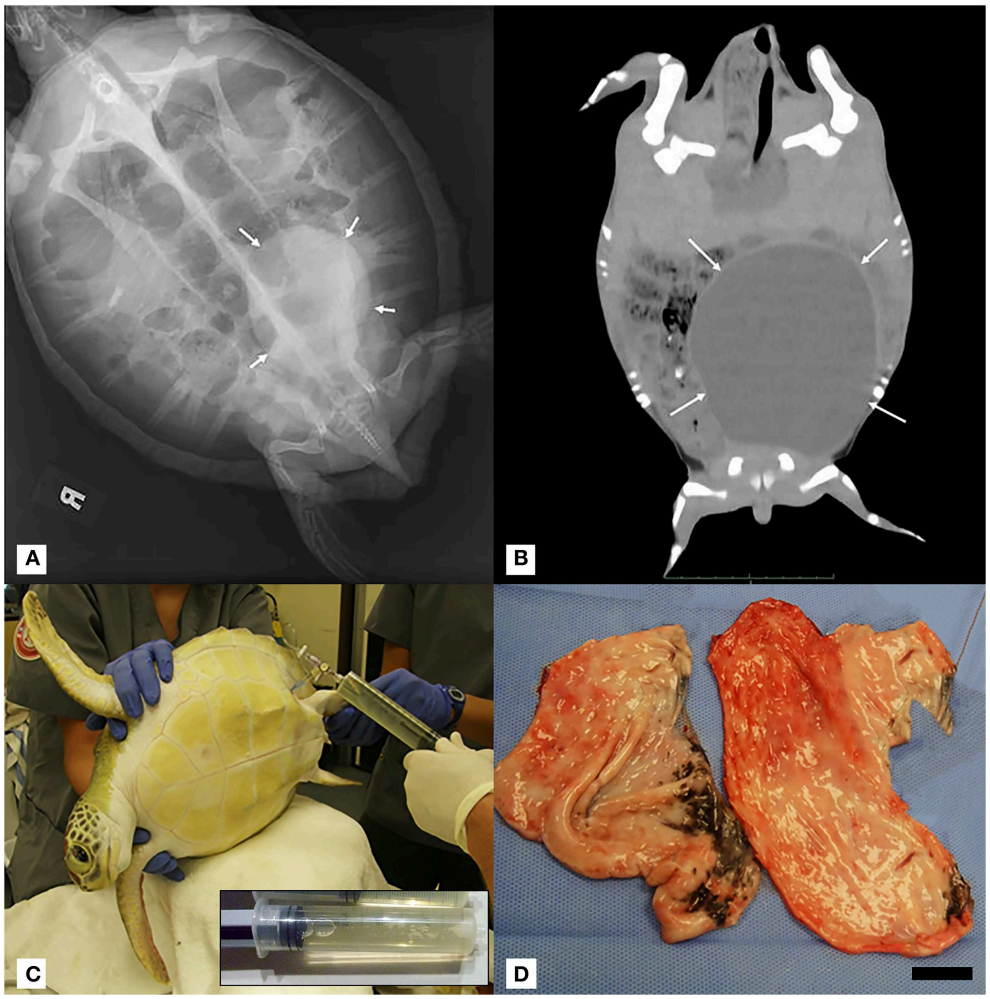

FIGURE 1 | (A) Dorsoventral projection full-body radiograph of a juvenile green turtle (*Chelonia mydas*) showing a large rounded well-demarcated mass with soft tissue opacity within the left caudal coelom (white arrows). **(B)** Coronal mid-coelomic CT section of a green turtle (*Chelonia mydas*) showing a large rounded soft tissue/fluid opacity mass (white arrows) within the left caudal coelom displacing gastrointestinal contents dorsally and to the right. CT was performed 2 weeks after initial radiographic diagnosis of mass, and no fluid was aspirated during this interval. Progression of gross left-sided plastron distention was noted. **(C)** Positioning of turtle in right lateral recumbency for left pre-femoral fine-needle fluid aspiration of intra-coelomic cyst. Inset: Representative 60-ml syringe filled with transudate fluid from cyst aspiration. **(D)** Gross image of cyst in two sections post-surgical removal. Scale bar = 2.5 cm.

most consistent with a transudate (**Figure 1C**). Coinciding with the administration of steroids and the diagnosis of the mass were marked heterophilia, lymphocytosis, and monocytosis with left shift and mild toxic change (**Table 1**), consistent with chronic-active inflammation, which improved slowly over 4 weeks. The turtle developed anemia a second time about 6 weeks after the first (**Table 1**), and a second blood culture was obtained and was negative. This event resolved without medical intervention over 3 weeks.

Repeat fluid aspirations from the mass were performed on a near-weekly interval for both therapeutic and diagnostic monitoring purposes. The fluid was similar in consistency and color to the initially diagnosed transudate, and when successful, an average of 100 ml was removed during each aspiration attempt. One of the samples appeared cloudy and cytologically disclosed marked histiocytic and heterophilic inflammation with the presence of extracellular and phagocytized bacteria. It is unclear whether this sample represented fluid from the coelomic mass or coelomic effusion. Accidental intestinal aspiration was not considered a possibility given the location of fluid aspiration. Based on these findings, antimicrobial administration with metronidazole (20 mg/kg BW, once daily for 40 days, orally) and enrofloxacin (5 mg/kg BW, once daily for 40 days, orally) was initiated for coverage against enteric pathogens. Next, further diagnostics to delineate the origin of the mass were pursued.

The turtle was anesthetized for exploratory laparoscopy with dexmedetomidine (74 μg/kg BW, intravenously), butorphanol (0.45 mg/kg BW, intravenously), and alfaxalone (0.5 mg/kg BW, intravenously). The patient was intubated (4 mm uncuffed endotracheal tube) and maintained with sevoflurane (variable from 0.5 to 3%). A 2-cm, left pre-femoral skin incision was made, and an examination trocar/cannula was inserted followed by a

2.7-mm 30° video laparoscope. A single large mass was visualized within the caudal coelom as well as three to four cystic structures in the region of the left gonad. These were initially interpreted as ovarian tissue; however, it was later determined histologically that the turtle was male. It was impossible to determine the origin of the mass by laparoscopy, and no free coelomic fluid was appreciated. The surgical site was closed with 4-0 polydioxanone (PDSII, Ethicon, Sommerville, NJ, USA) using a horizontal mattress suture pattern. The dexmedetomidine was reversed with atipamezole (0.74 mg/kg BW, intravenously; then 0.22 mg/kg BW, intravenously 2 h later due to slow recovery), and the turtle recovered uneventfully. Two weeks later, the turtle was briefly sedated with dexmedetomidine (50 μg/kg BW, intravenously) for cloacoscopy and contrast cystogram. Iodinated contrast media (20 ml, Iohexol) was instilled into the cloaca through the rigid endoscope. Results of this examination showed normal cloacal, ureteral, and urinary bladder anatomy without evidence of an associated mass.

Given the persistence of the mass and the need for repeated fluid aspirations, surgical removal was performed ∼6 months after the initial discovery. Pre-operative bloodwork revealed a mildly low calcium (1.2 mmol/L) (**Table 1**) so a single dose of calcium gluconate (calcium gluconate 23%, 0.2 ml/kg BW, subcutaneously) was administered. The turtle was anesthetized with dexmedetomidine (75 μg/kg BW, intravenously), ketamine (1 mg/kg BW, intravenously), and butorphanol (0.4 mg/kg BW, intravenously), received 30 ml LRS IV at the time of induction, and a local anesthetic block was performed on the left pre-femoral surgical site (0.5 ml lidocaine, 2% solution, in 0.5 ml sodium bicarbonate). The turtle was intubated with a 5-mm uncuffed endotracheal tube, maintained on inhalant sevoflurane (0.5–1%), and manually ventilated at a rate of two breaths per minute. A surgical approach was made to the left pre-femoral region with the turtle in right lateral recumbency. A combination of laparoscopic and standard surgical instrumentation was used to visualize and completely excise the mass. The structure appeared to be in close association with the left kidney and gonad, but a definitive origin could not be determined. Heavy bleeding occurred during the procedure, and hemostasis was achieved via direct ligation of blood vessels. Sectioning of the mass into two portions facilitated its removal, and the coelomic cavity was thoroughly flushed with normal saline and suctioned prior to closure (**Figure 1D**). The incision was closed in two layers with 4-0 PDS in a simple interrupted pattern. Dexmedetomidine was reversed with atipamezole (75 mg/kg BW, intravenously), and the turtle recovered slowly, but smoothly. The turtle received tramadol (5 mg/kg BW, every other day for two doses, subcutaneously) and meloxicam (0.5 mg/kg BW, once daily for 5 days, subcutaneously) post-operatively. Bloodwork performed post-operatively showed an increase in creatine kinase activity, anemia, hypoproteinemia, and an extreme leukocytosis characterized by heterophilia, lymphocytosis, monocytosis, and eosinophilia (**Table 1**), consistent with post-surgical chronic-active inflammation, blood loss, and muscle injury. The severe anemia with concurrent hypoproteinemia was likely secondary to blood loss and/or systemic inflammation post-surgery. Histopathological evaluation of the cystic mass confirmed a 3- to 4-mm-thick wall of vascular dense collagenous connective tissue rarely covered by necrotic and sloughing cuboidal to columnar epithelium arranged in a single layer. The connective tissue was continuous with the stroma of the immature epididymis but did not involve the testis. Rarely, the connective tissue entrapped small ducts lined by a single layer of cuboidal epithelial cells with occasional hyperplasia (**Figure 2**). Connective tissue was arranged concentrically around some entrapped ducts. Ducts were morphologically similar to those of the immature epididymis. Cilia were not identified on any epithelial cells of the cystic mass. The cyst wall and adjacent testicular and epididymal tissue were stained immunohistochemically for smooth muscle actin using a commercially available mouse monoclonal antibody and an automated staining platform following the manufacturer's recommendations (clone 1A4; Roche Diagnostics, Indianapolis, IN, USA). Vascular smooth muscle in these tissues exhibited strong cytoplasmic immunoreactivity, but positive reactivity was not detected elsewhere in the tissues. A granuloma surrounding remnants of a degenerate metazoan parasite was also present within the connective tissue.

Following surgery, the turtle received supportive care including iron dextran supplementation (5 mg/kg BW,

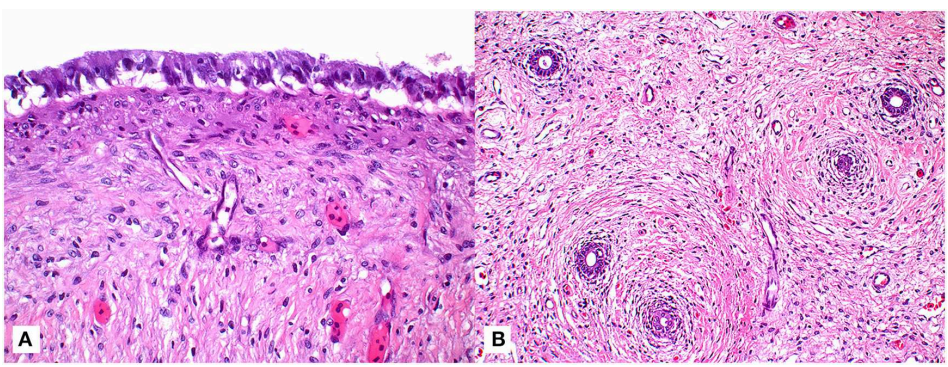

FIGURE 2 | Tissue sections of a paratesticular cyst surgically removed from a male green turtle (*Chelonia mydas*). **(A)** Photomicrograph of tissue section demonstrating columnar epithelial cells overlying maturing fibroplasia of cyst wall (63x; hematoxylin and eosin stain). **(B)** Lower magnification photomicrograph highlighting the presence of ducts (arrows) entrapped within the connective tissue of cyst wall (20x; hematoxylin and eosin stain).

subcutaneously), and antimicrobial administration with amoxicillin/clavulanic acid (30 mg/kg BW, once daily for 30 days, orally) and amikacin (3 mg/kg BW, every 3 days for 36 days, subcutaneously) was continued. Over 2 months, the patient improved steadily, and the anemia fully resolved. Physical examination and recheck radiographs revealed that the cyst had not regrown 2 months following the surgery. Pre-release bloodwork was normal, and the turtle was released near his original stranding location off the coast of Anastasia State Park, St. Augustine, Florida, about 1 year (i.e., 348 days) after admission.

DISCUSSION

This is the first report of a cyst of reproductive origin in a reptile species, specifically a marine turtle, which represented an unusual clinical challenge given the unprecedented finding and the extent of the intra-coelomic extension of the mass. Furthermore, we describe the medical management of acute anemia in this green turtle patient.

Reproductive cysts are infrequently reported in the veterinary literature, and information is limited to case reports in mammalian species. Reports of intra-coelomic cysts in reptiles are rare and limited to non-reproductive renal cysts. In mammalian species, epididymal cysts and testicular cysts have been reported most frequently and were largely incidental findings as they are rarely associated with reproductive disorders (4–9). Gartner duct (Wolffian duct) cysts have been reported in female dogs and have been associated with urinary dysfunction and/or additional congenital anomalies (10, 11). This latter condition occurs due to failure of Wolffian duct regression in females, and an analogous condition can occur in males. Mullerian duct cysts can result from failure of this embryological structure to fully regress in males. In humans, Mullerian duct cysts are relatively rare occurring in only 1–5% of the young, adult male population and are not typically associated with additional urogenital abnormalities (12). Cysts are typically benign and compared to other described cyst types, which arise from adjacent reproductive structures, can be relatively large, fluid-filled, and non-communicating with other organs (13, 14). Mullerian duct formation and regression in reptiles, including chelonians, seem to occur in a fashion analogous to mammals with full regression seen by hatching in red-eared sliders (*Trachemys scripta elegans*) (15, 16). In marine turtles, however, Mullerian ducts are recognized to occasionally persist as non-functioning tubular structures adjacent to the testes or kidneys (17). The anatomical location of the cyst in this case could be consistent with either an epididymal cyst or a Mullerian duct cyst, although the latter may be less likely based upon the absence of smooth muscle and presence of epididymal-like ducts in the cyst wall. A congenital, rather than acquired, cyst is considered to be most likely based on the age of the animal, histological appearance, and lack of evidence for prior trauma. Cyst detection due to enlargement was coincident with convalescence, and it is presumed that correction of initial dehydration and poor nutritional plane, in addition to return to normal behaviors, resulted in continuous fluid accumulation within the cyst. Although such cysts are considered incidental findings in many species, the size, extent, and continued enlargement of the cyst in this case was concerning for potential complications. In humans, urinary retention, recurrent infections, urogenital inflammation, and reduced fertility have been associated with various cyst types (14). Surgical removal of the entire cyst is typically curative as was considered to be in this case (18). In marine turtles, the testes are attached to the kidneys via the mesorchium and lie in close proximity to renal arteries and veins (17). This anatomical relationship makes urogenital surgical intervention challenging as there is a high risk of marked blood loss. Blood loss was significant during surgery in this case; however, meticulous dissection and prompt hemostasis helped reduce the risk of potentially fatal hemorrhage. Owing to close association with the cyst, a small section of immature epididymis was removed. The potential impact of partial, unilateral epididymectomy on reproductive capacity in reptiles is unknown, and changes in testicular architecture, spermatogenesis, or ejaculate sperm concentration are possible (19). Normal functioning and fertility may be maintained provided that the contralateral reproductive tract remains unaffected (20). Long-term follow-up was not possible as this turtle was released, but cyst recurrence was absent several months prior to release, and the PCV had normalized (**Table 1**).

Unrelated to the diagnosis and management of the cyst were the two episodes of anemia in this animal. Anemia of varying severity can be observed in cold-stunned marine turtles of any species admitted to rehabilitation and typically becomes more apparent upon rehydration (1). The acute severe regenerative anemia that occurred 2 months into rehabilitation in this patient, however, was not a typical finding for cold-stunned marine turtles. Several authors have identified cases of acute hemolytic anemia at facilities with convalescing marine turtles, although no clear cause has been identified to date (TN, NS). Light gray/greenish plasma indicative of biliverdinemia was reported for blood samples collected during anemic events of the current patient, presumptively suggesting extravascular hemolysis resulting in the release of biliverdin from heme degradation (21). Possible causes for acute hemolytic anemia seen in cold-stunned marine turtles include underlying septicemia, adverse drug reaction, and/or an association with cold stunning (e.g., increased osmotic fragility or other unknown causes). Two blood cultures obtained during anemic events in this case were negative; however, given antimicrobial administration concurrent with sampling as well as the likely differing susceptibility of certain bacterial species at varying incubation temperatures, this does not exclude septicemia as a possible underlying cause (22). Leukogram findings also supported systemic inflammation for which considerations include non-infectious and infectious causes. Cephalosporins, including ceftazidime, have been associated with both immune-mediated hemolytic anemias as well as changes to bone marrow microenvironments both *in vitro* and *in vivo* in mammals (23–25). The turtle in this case received ceftazidime for ∼6 weeks prior to the onset of the first anemic event. In order to address the potential for both adverse drug reactions as well as

septicemia, ceftazidime was discontinued, a blood culture was obtained, broad-spectrum antimicrobial coverage was initiated with amikacin and ampicillin, and a course of steroids was trialed. The authors have found that some acute anemias in green turtles, as in this case, have been steroid responsive; however, in addition to the immunomodulatory effects of steroids, a possible resolving infection and the cessation of the cephalosporin may have also contributed to improvement. Given that penicillins have also been associated with hemolytic anemia in mammals, it is unlikely, but possible, that this contributed to the second anemic event in this patient (26). There was no clinical evidence of hemorrhage or coagulopathy in either instance. Further investigation into the underlying causes for acute anemias in rehabilitating green turtles is needed in order to aid therapeutic decision making.

DATA AVAILABILITY STATEMENT

The raw data supporting the conclusions of this article will be made available by the authors, without undue reservation, to any qualified researcher.

ETHICS STATEMENT

Sea turtle rehabilitation was conducted in accordance with Georgia Department of Natural Resources Wildlife Rehabilitation Permit # OS4 CN 1000450736 and Florida Fish and Wildlife Commission's Marine Turtle Permit # MTP-17-135 following general principles of veterinary medicine and animal care.

AUTHOR CONTRIBUTIONS

TW contributed to the early clinical case management and completed the first manuscript draft. NIS provided the processing and interpretation for all clinical pathology samples. NLS provided the processing and interpretation for all histological samples. TN managed and oversaw all clinical and surgical aspects of this case. All authors assisted in writing and editing of the manuscript.

FUNDING

All expenses related to the diagnosis, treatment, and care of this turtle were funded by the Georgia Sea Turtle Center.

ACKNOWLEDGMENTS

The authors would like to acknowledge the rehabilitation staff at the Georgia Sea Turtle Center, Dr. Douglas Mader for his case management input, and Dr. Vincent K. Arlauskas for his assistance with the surgical procedure in this case.

REFERENCES

1. Anderson ET, Harms CA, Stringer EACZMM, Cluse WM. Evaluation of hematology and serum biochemistry of cold-stunned green sea turtles (*Chelonia mydas*) in North Carolina, USA. *J Zoo Wildlife Med*. (2011) 42:247–55 doi: 10.1638/2010-0217.1
2. Bolten AB, Bjorndal KA. Blood profiles for a wild population of green turtles (*Chelonia mydas*) in the southern Bahamas: size-specific and sex-specific relationships. *J Wildl Dis*. (1992) 28:407–13. doi: 10.7589/0090-3558-28.3.407
3. Lewbart GA, Hirschfeld M, Denkinger J, Vasco K, Guevara N, García J, et al. Blood gases, biochemistry, and hematology of galapagos green turtles (*Chelonia mydas*). *PLoS ONE*. (2014) 9:1–8. doi: 10.1371/journal.pone.0096487
4. Gelberg HB, McEntee K. Cystic rete testis in a cat and fox. *Vet Pathol*. (1983) 20:634–6. doi: 10.1177/030098588302000516
5. Kafi M, Oryan A, Morgan-Azghadi N. Pathology of testis and epididymis in native goats in southern Iran. *Comp Clin Path*. (2007) 16:201–5. doi: 10.1007/s00580-006-0662-y
6. Schumacher J, Lenz SD, Walker W. Cystic rete testis associated with cryptorchidism in a horse. *Vet Pathol*. (1994) 31:115–7. doi: 10.1177/030098589403100117
7. Matuszewska M, Sysa PS. Epididymal cysts in European bison. *J Wildl Dis*. (2013) 38:637–40. doi: 10.7589/0090-3558-38.3.637
8. Kutzler MA, Shoemaker M, Valentine BA, Bildfell RJ, Tornquist SJ. Bilateral cystic rete testis in an alpaca (*Lama pacos*). *J Vet Diagnostic Investig*. (2006) 18:303–6. doi: 10.1177/104063870601800315
9. Hesser AC, Davidson AP. Spermatocele in a South African boerboel dog. *Top Companion Anim Med*. (2015) 30:28–30. doi: 10.1053/j.tcam.2015.03.001
10. Kim HJ, Kim JK, Choi JH, Jang JY, Ban HJ, Seo JM, et al. A Gartner duct cyst of the vagina causing dysuria and dyschezia in a Yorkshire Terrier. *J Vet Sci*. (2007) 8:427–9. doi: 10.4142/jvs.2007.8.4.427
11. Fujita A, Tsuboi M, Uchida K, Nishimura R. Complex malformations of the urogenital tract in a female dog: gartner duct cyst, ipsilateral renal agenesis, and ipsilateral hydrometra. *Jpn J Vet Res*. (2016) 64:147–52. doi: 10.14943/jjvr.64.2.147
12. Yogeswaran C, Srinivasan V, Ekwueme KC. Mullerian duct cyst treated with template-guided transperineal aspiration: a case report and review of the literature. *JRSM Open*. (2018) 9:1–4. doi: 10.1177/20542704177 25497
13. Kachewar SG, Sankaye SB. Mullerian duct cyst. *J Mahatma Gandhi Inst Med Sci*. (2013) 18:64–6.
14. Shebel HM, Farg HM, Kolokythas O, El-Diasty T. Cysts of the lower male genitourinary tract: embryologic and anatomic considerations and differential diagnosis. *Radiographics*. (2013) 33:1125–43. Available online at from: www.rsna.org/rsnarights. doi: 10.1148/rg.334125129
15. Austin HB. Mullerian-duct regression in the American alligator (*Alligator mississippiensis*): its morphology and testicular induction. *J Exp Zool*. (1989) 251:329–38. doi: 10.1002/jez.1402510309
16. Wibbels T, Wilson C, Crews D. Mullerian Duct development and regression in a turtle with temperature-dependent sex determination. *J Herpetol*. (1999) 33:149. doi: 10.2307/1565558
17. Wyneken, J. *The Anatomy of Sea Turtles*. U.S. Department of Commerce NOAA Technical Memorandum NMFS-SEFSC-470. Miami, FL (2001). p. 1–172.
18. Desautel MG, Stock J, Hanna MK. Müllerian duct remnants: surgical management and fertility issues. *J Urol*. (1999) 162(3 Pt 2):1008–13; discussion: 1014. doi: 10.1016/S0022-5347(01)68050-9
19. Osman AM, Monzaly MEM. Effect of unilateral vasectomy, epididymectomy and epididymal ligation on the reproductive capacity of growing rams. *Zentralbl Veterinarmed A*. (1976) 23:373–83. doi: 10.1111/j.1439-0442.1976.tb01716.x
20. Gygax AP, Donawick WJ, Gledhill BL. Haematocoele in a stallion and recovery of fertility following unilateral castration. *Equine Vet J*. (1973) 5:128–30. doi: 10.1111/j.2042-3306.1973.tb03210.x
21. Anderson ET, Valente ALS, Stacy BA, Wyneken J. Hepatobiliary system. In: Manire CA, Norton TM, Stacy BA, Innis CJ, Harms CA, editors. *Sea Turtle*

Health and Rehabilitation. 1st ed. Plantation, FL: J. Ross Publishing (2017). p. 367–79.
22. Mader DR, Conzelman GM, Baggot JD. Effects of ambient temperature on the half-life and dosage regimen of amikacin in the gopher snake. *J Am Vet Med Assoc.* (1985) 187:1134–6.
23. Chen F, Zhan Z. Severe drug-induced immune haemolytic anemia due to ceftazidime. *Blood Transfus*. (2014) 12:435–7. doi: 10.2450/2014.0237-13
24. Charak BS, Louie R, Malloy B, Twomey P, Mazumder A. The effect of amphotericin b, aztreonam, imipenem and cephalosporins on the bone marrow progenitor cell activity. *J Antimicrob Chemother*. (1991) 27:95–104. doi: 10.1093/jac/27.1.95
25. Gore C, David TJ. Drug-induced fever and bone marrow suppression in a 12-year-old girl with cystic fibrosis. *J R Soc Med*. (2001) 94(Suppl. 40):35–7. doi: 10.1177/014107680109440s09
26. Garratty G. Immune hemolytic anemia associated with drug therapy. *Blood Rev*. (2010) 24:143–50. doi: 10.1016/j.blre.2010.06.004

Conflict of Interest: The authors declare that the research was conducted in the absence of any commercial or financial relationships that could be construed as a potential conflict of interest.

Copyright © 2020 Weisbrod, Stacy, Stedman and Norton. This is an open-access article distributed under the terms of the Creative Commons Attribution License (CC BY). The use, distribution or reproduction in other forums is permitted, provided the original author(s) and the copyright owner(s) are credited and that the original publication in this journal is cited, in accordance with accepted academic practice. No use, distribution or reproduction is permitted which does not comply with these terms.

frontiers in Veterinary Science

ORIGINAL RESEARCH
published: 05 March 2020
doi: 10.3389/fvets.2020.00120

Epidemiological Investigation of a Mortality Event in a Translocated Gopher Tortoise (*Gopherus polyphemus*) Population in Northwest Florida

Rebecca A. Cozad[1,2]*, *Sonia M. Hernandez*[1,3], *Terry M. Norton*[4,5], *Tracey D. Tuberville*[6], *Nicole I. Stacy*[7], *Nancy L. Stedman*[8] *and Matthew J. Aresco*[2]

[1] Warnell School of Forestry and Natural Resources, University of Georgia, Athens, GA, United States, [2] Nokuse Plantation, Bruce, FL, United States, [3] Southeastern Cooperative Wildlife Disease Study, College of Veterinary Medicine, University of Georgia, Athens, GA, United States, [4] St. Catherines Island Foundation, Midway, GA, United States, [5] Georgia Sea Turtle Center, Jekyll Island Authority, Jekyll Island, GA, United States, [6] University of Georgia's Savannah River Ecology Laboratory, Aiken, SC, United States, [7] Department of Comparative, Diagnostic, and Population Medicine, College of Veterinary Medicine, University of Florida, Gainesville, FL, United States, [8] Busch Gardens, Tampa, FL, United States

OPEN ACCESS

Edited by:
Arvo Viltrop, Estonian University of Life Sciences, Estonia

Reviewed by:
Kristin H. Berry, United States Geological Survey, United States
Lora L. Smith, University of Georgia, United States

***Correspondence:**
Rebecca A. Cozad
racozad@gmail.com

Specialty section:
This article was submitted to Zoological Medicine, a section of the journal Frontiers in Veterinary Science

Received: *15 September 2019*
Accepted: *18 February 2020*
Published: *05 March 2020*

Citation:
Cozad RA, Hernandez SM, Norton TM, Tuberville TD, Stacy NI, Stedman NL and Aresco MJ (2020) Epidemiological Investigation of a Mortality Event in a Translocated Gopher Tortoise (Gopherus polyphemus) Population in Northwest Florida. Front. Vet. Sci. 7:120. doi: 10.3389/fvets.2020.00120

Nokuse Plantation, a 22,055 ha private conservation preserve in northwest Florida, is a recipient site for gopher tortoises translocated from development sites in Florida. Since 2006, Nokuse has received over 5,000 tortoises from multiple development sites. During 2013–2015, 52 tortoises were found sick ($n = 14$) or dead ($n = 38$) in multiple soft-release enclosures in which tortoises consistently exhibited clinical signs, with additional sick ($n = 5$) and dead ($n = 5$) tortoises presenting similarly during 2016–2017. When found alive, tortoises behaved abnormally (e.g., frequently out of burrows during cold weather, pacing along enclosure fencing), appeared emaciated, were lethargic, and had developed redness under plastron scutes. Similar numbers of male ($n = 28$) and female ($n = 32$) tortoises were recovered along with two of unidentified sex, including mainly adults ($n = 59$) and three subadults. Physical examination, blood analysis, and other diagnostics were indicative of starvation and dehydration. Most sick tortoises provided with supportive care recovered. Necropsy findings generally confirmed starvation, with no evidence of infectious pathogens or contaminants. There were no apparent differences in quality of habitat, plant community, or soil or water among affected and unaffected enclosures. Botanical surveys indicated adequate forage quality and quantity, with no poisonous exotic or native plants detected. No land management practices changed prior to this event. Analysis of epidemiological data and demographic factors from before and during this mortality event identified initial density of tortoises in the enclosures as exerting the strongest influence on detection of tortoise morbidity and mortality. We believe that the stress associated with mixing tortoises from different populations and at higher densities during translocation impacted an individual tortoise's ability to obtain or absorb adequate nutrients from foraging, ultimately leading to a wasting condition

consistent with starvation. Based on our findings, we recommend a maximum of 3 gopher tortoises per ha in soft-release enclosures for translocation, but further research is warranted to investigate the complexity of stress and social pressures associated with translocation.

Keywords: density, *Gopherus polyphemus*, habitat loss, reptile, starvation, stress, translocation

INTRODUCTION

The gopher tortoise (*Gopherus polyphemus*) once occurred throughout most of the southeastern United States, particularly in areas where longleaf pine savannas were historically present (1). Direct habitat loss, habitat degradation, and historical harvesting of tortoises for their meat have caused a serious range-wide population decline, leading to federal protection of the species in the western portion of its range, and status as a candidate for federal listing in the eastern portion of the range (2–5). Over the last two decades, translocation of gopher tortoises has been increasingly used as a mitigation strategy when land development is planned, making the gopher tortoise the most widely translocated animal in the southeastern United States (6–8). Translocation, or the intentional moving of individuals from one location to another, is used in the conservation efforts for many species, although reviews of translocation programs in general have reported various levels of failure or success (6, 9–12). There have been extensive debates regarding ethical issues associated with translocation, especially for mitigation-driven translocations (13, 14).

The greatest number of gopher tortoise translocations throughout their range occur in Florida due to large-scale development of gopher tortoise habitat (15). From 1991 to 2007, Florida's mitigation policy, known as Incidental Take Permits, allowed developers to pay a mitigation fee to develop gopher tortoise habitat. This practice caused the legal entombment or killing of gopher tortoises on development sites, with estimates for number of tortoises "taken" ranging from ∼84,000 to over 100,000 individuals (16–18). Although Florida Fish and Wildlife Conservation Commission (FFWCC) stopped issuing Incidental Take Permits in 2007 due to public pressure, existing permits were grandfathered at sites already slated for future development. Some gopher tortoises impacted by Incidental Take Permits are being voluntarily relocated to conservation lands and new policies since 2007 require that all gopher tortoises are translocated away from development sites. An estimated 180,000 tortoises will be translocated from new development sites in Florida by 2022 (3, 8). These mitigation-driven translocations prevent mortality of individual tortoises on the development sites by moving them to protected and managed sites with either depleted or extirpated tortoise populations (4).

Post-translocation monitoring is important for determining whether properly planned and executed translocations can successfully augment or reestablish populations of gopher tortoises. A critical component for evaluating success of translocations is the inclusion of health assessments and surveillance for pathogens (19–21). In early 2013, biologists conducting routine monitoring at one of the largest translocation sites in Florida began finding sick and dead tortoises within several soft-release enclosures. When found alive, tortoises appeared emaciated and lethargic, behaved abnormally (frequently found outside of burrows in cold weather), and had developed redness under their scutes on the plastron. Intact tortoise carcasses found fresh with no signs of predation damage also displayed the aforementioned clinical signs, suggesting that they died of disease. Other dead tortoises were also found with an intact shell, suggesting that predation was not involved. However, these carcasses were found too late to investigate the cause of death because there was little to no soft tissue remaining.

To aid future translocation and management practices at this designated recipient site, we investigated the epidemiology and potential cause(s) of the mortality event that occurred in this population of translocated gopher tortoises in northwest Florida. We analyzed gross necropsy and histopathology results from dead tortoises, diagnostic assays and the response to treatment of live tortoises, and testing for infectious pathogens. Additionally, we explored differences in soil and plant nutritional composition between two sites with different mortality rates. Finally, we used a modeling approach to determine the factors useful in predicting which individual tortoises will develop clinical signs of disease.

METHODS

Study Site

Nokuse Plantation, a 22,055 ha private nature preserve in the Florida panhandle, is one of the largest recipient sites for translocated gopher tortoises in the state of Florida. Initial density of resident tortoises was 0.004 individuals per ha due to past habitat conversion and a long history of collection by humans for their meat before current legal protections were in place. All release sites are in sandhill communities with deep, well-drained sands [e.g., Lakeland soil; (22)] and open canopy of longleaf pine (*Pinus palustris*) and scattered turkey oak (*Quercus laevis*) with very little woody midstory. The herbaceous understory is primarily native grasses and forbs dominated by bluestem grasses (*Andropogon* spp.) and Bahia grasses (*Paspalum* spp.). Much of the sandhill was converted to farmland with varied management practices (e.g., use of center pivot irrigation and length of time that phosphate fertilizer was applied) in the late 1960s−1980s but has undergone significant restoration in the last 18 years. The abundance of herbaceous groundcover plants provide ample forage for gopher tortoises. Nokuse typically maintains a burn rotation of 3–5 years to reduce presence of a hardwood midstory, prevent succession into a mixed hardwood forest, and stimulate growth of native grasses and herbs (the main food source for tortoises). One of the sites (SR1) had not been burned for ∼10

years prior to the initiation of this study, although there was not significant hardwood encroachment.

From 2006 to 2019, 5,097 gopher tortoises were translocated from development sites across Florida and released into 23 large (4–136 ha) soft-release enclosures, which has previously been shown to encourage site fidelity (23). These enclosures were constructed using a 1 m tall silt fence (temporary barrier constructed of porous fabric, typically used for sediment control) buried ∼0.3 m into the ground to prevent immediate tortoise dispersion, with the silt fence removed 1–2 years after the last individual was released into the enclosure. Prior to translocation, resident tortoise density in areas where the enclosures were constructed was estimated to be 0–0.1 individuals per ha. Tortoise density inside release enclosures ranged between 0.56 and 16.36 adults per ha (**Table 1**). There was a roughly 1:1 ratio for adult males and females overall. Each tortoise was permanently marked with a unique notch ID [modified from Cagle (24)], and sex, donor site, and standard morphometric measurements including body weight to nearest 0.001 kg and straight carapace length (SCL) to nearest 1 mm (25) were recorded before release. Body condition indices (BCI) were calculated using the formula BCI = mass (in kg)/SCL (in mm) ^3 [modified from Nagy et al. (26)]. Due to predation-related mortalities attributed to coyotes (*Canis latrans),* 1.5 m high electric fences were installed around the perimeters of five release enclosures starting in early 2014. After the electric fences were installed, predation by coyotes was virtually eliminated without negative effects or mortality for tortoises.

Mortality Surveillance and Investigation

During 2011–2017, surveys for tortoise mortality were conducted during routine monitoring of the five enclosures with electric fences (**Figure 1**). Monitoring included walking the interior side of the silt fence enclosures (daily for newly constructed enclosures and weekly for others), periodic transects through interior portions of the pens (monthly), and walking the exterior of the enclosure for electric fence maintenance (weekly). Additional monitoring with high search effort in two of these enclosures (DB1 and SR1) occurred during 2016–2017, as part of a project involving trapping and radiotelemetry. When a dead tortoise was found, GPS coordinates were recorded, and the carcass or shell was recovered and brought

TABLE 1 | Release densities within soft-release enclosures and penning durations of translocated gopher tortoises at Nokuse Plantation.

Release enclosure	Size (ha)	First tortoise released	Last tortoise released	Max penning duration (months)	Adults released	Density (adults/ha)	Diseased tortoises
SN	10	5/2006	11/2006	22	29	2.87	
SS	10	5/2006	8/2006	22	36	3.56	
C1	25	10/2006	12/2007	21	57	2.27	
CB1	8	11/2006	7/2007	38	34	4.20	
CB4	134	5/2007	4/2008	34	507	3.77	
CB2	24	6/2007	10/2007	31	15	0.62	
CB5	31	6/2007	7/2007	33	183	5.87	
CB7	19	9/2007	6/2008	28	79	4.15	
C2	13	10/2007	9/2008	13	50	3.86	
CB6	89	11/2007	7/2009	29	313	3.52	
D1	7	11/2007	3/2012	13	43	6.25	
D2	4	10/2008	11/2008	7	15	3.71	
BC1	13	12/2008	9/2009	22	7	0.56	
CB9	23	10/2009	11/2011	33	251	10.88	
SR1*	**13**	**6/2011**	**11/2015**	**94**	**105**	**8.37**	**5**
DB1*	**17**	**3/2012**	**7/2013**	**40**	**278**	**16.36**	**36**
M1	**10**	**3/2013**	**10/2014**	**27**	**82**	**8.10**	**3**
DB2	**24**	**5/2013**	**6/2014**	**30**	**209**	**8.61**	**4**
DB3	**28**	**5/2014**	**4/2015**	**18**	**254**	**8.97**	**2**
M2	13	10/2014	7/2018	53	132	10.52	
SR2	**24**	**5/2015**	**3/2016**	**37**	**223**	**9.18**	**1**
WC1**	20	3/2016	9/2017	n/a	143	7.07	
WC2**	7	6/2017	5/2019	n/a	59	8.10	
M3**	4	10/2019	11/2019	n/a	6	1.50	
M4**	8	11/2019	n/a	n/a	4	0.5	

Maximum penning duration was defined as time between when the first tortoise was released into the enclosure and when the silt fence was removed. Mortality surveillance occurred in enclosures denoted in bold.

** Denotes release sites with increased monitoring efforts during 2016–2017.*

*** Denotes sites with intact silt fences and/or ongoing releases at time of publication.*

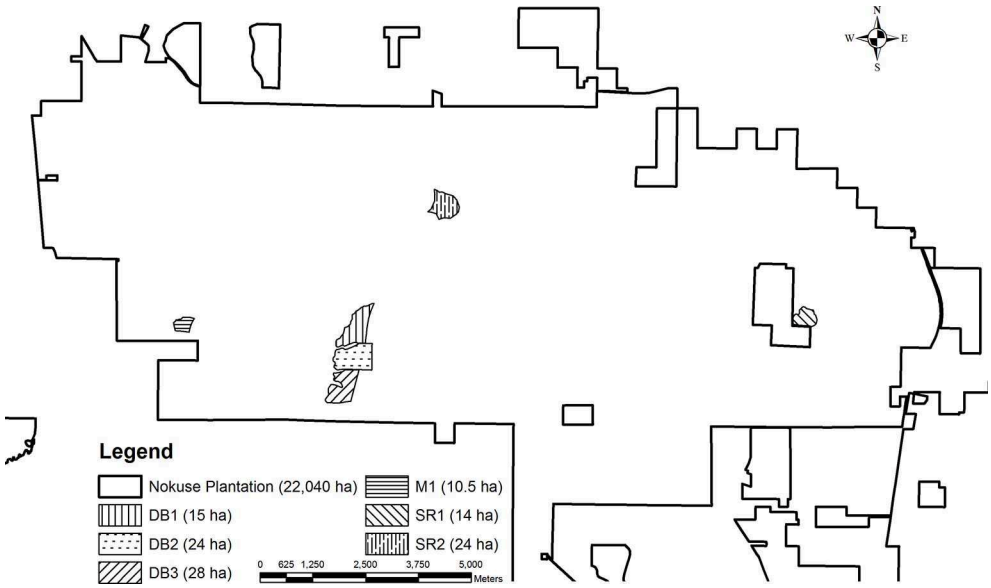

FIGURE 1 | Gopher tortoise translocation release enclosures and mortality surveillance sites at Nokuse Plantation, a private conservation preserve in northwest Florida.

to the field lab for individual identification (based on shell notches and morphometric measurements) and processing. Tortoises found within ∼24–48 h of death based on the visual degree of decomposition were sent to a wildlife veterinarian who conducted a necropsy (TMN). If possible, live tortoises found during monitoring were captured and given a physical examination, including examination for external injuries and clinical signs of disease. If abnormalities were found, the tortoise was brought to the field office for monitoring or transported to a rehabilitation center (Georgia Sea Turtle Center [GSTC], Jekyll Island, GA) for diagnostics and treatment. Mortality and health monitoring occurred throughout the year. Analyses were performed on subsets of the total number of sick or dead tortoises encountered with clinical signs.

Necropsy and Histopathology

A gross necropsy was completed on 21 recently dead tortoises found during mortality surveys and tortoises that died or were euthanized during rehabilitation (see section 2.6). Histopathology was only conducted on tortoises that were not autolyzed. Samples from all major tissues (skeletal muscle, heart, lung, brain, liver, kidney, spleen, gastrointestinal tract, bladder, tongue, skin, bone, and keratin) were collected for histopathological analysis. All tissues were examined microscopically by a board-certified veterinary anatomic pathologist with expertise in chelonians (NLS). Additional representative tissue samples were also collected and frozen for further testing, such as for toxicology and testing for infectious pathogens.

Testing for Infectious Pathogens

Select tissues (liver, kidney, spleen, gastrointestinal tract, and tongue) from six dead tortoises were submitted to the University of Florida ZooMed Diagnostic Laboratory (Gainesville, FL) for screening of infectious agents common in chelonians (adenovirus, herpesvirus, and *Mycoplasma* spp.) using PCR. DNA was extracted using a DNeasy blood and tissue kit (QIAGEN Inc., Redwood City, CA) following the manufacturer's instructions and run for the agents listed above. The PCR products (DNA fragments), including a negative and previously identified positive control, were run on a 1.5% agarose gel with ethidium bromide and were visualized under ultraviolet light. Successfully amplified products were excised and purified using the QIAquick® Gel Extraction kit (QIAGEN Inc., Redwood City, CA) following the manufacturer's instructions. The purified gel pieces, including the primer, were submitted to the University of Florida Interdisciplinary Center for Biotechnology Research for Sanger sequencing. The final product was edited and compared with sequences previously entered in GenBank.

Tissues (pooled gastrointestinal tract, kidney, liver, spleen and tongue for each individual) from four tortoises were submitted to the University of Florida Wildlife and Aquatic Veterinary Disease Laboratory for ranavirus screening using quantitative PCR (qPCR).

Tissues from another 13 of the 21 necropsied tortoises were submitted to the University of Illinois Wildlife Epidemiology Laboratory (Urbana, IL), including gastrointestinal tract ($n = 12$), kidney ($n = 11$), liver ($n = 11$), spleen ($n = 5$), and tongue ($n = 5$). Tissues were screened for nine pathogens (*Anaplasma phagocytophilum*, *Borrelia burgdorferi*, *Ambystoma tigrinum* virus, Bohle iridovirus, epizootic hematopoietic necrosis virus, *Frog virus 3* [FV3-like ranavirus; FV3], *M. agassizii*, *M. testudineum*, *Salmonella enteritidis*, *S. typhimurium*, Testudinid herpesvirus 2, intranuclear coccidiosis) using Fluidigm qPCR (27).

Ticks were collected from tortoises during rehabilitation ($n = 3$) and during necropsy ($n = 2$). Tick samples were submitted to the University of Florida Department of

Wildlife Ecology and Conservation. Conventional PCR and gel electrophoresis followed by Sanger sequencing on positive samples were used to determine the presence and identity of *Anaplasma* and *Ehrlichia* using previously published primers (28). Similarly, conventional PCR and sequencing were used to determine the presence and identity of *Rickettsia* spp. present in the tick specimens (29).

Toxicants in Liver Tissues

Liver samples from six dead tortoises were also submitted to the Veterinary Diagnostic Laboratory (Michigan State University, East Lansing, MI) to test for presence of toxicants that were: (1) considered likely to cause the clinical signs and lesions noted; and/or (2) were potentially applied to the soils on Nokuse lands during past agricultural and silvicultural activities under previous ownership. This panel was run using inductively coupled plasma mass spectrometry and included arsenic (As), cadmium (Cd), cobalt (Co), copper (Cu), iron (Fe), lead (Pb), manganese (Mn), mercury (Hg), molybdenum (Mo), selenium (Se), thallium (Tl), and zinc (Zn). Concentrations based on wet weight are reported in parts per million (ppm). These samples were additionally evaluated by gas chromatography mass spectrometry and screened against the Wiley 9 Mass Spectrometry library, which includes >500,000 common agricultural pesticides and herbicides, as well as persistent organic pollutants.

Diagnostics and Rehabilitation of Live Tortoises

Nineteen tortoises found alive but sick (displaying clinical signs such as emaciation, lethargy, abnormal behavior, and/or redness under the plastron scutes) were transported to the GSTC for diagnostics and treatment. Standard morphometrics were recorded at admission. Each tortoise received a complete health assessment by a zoological medicine board-certified specialist (TMN). Body condition indices were calculated for comparison with data from initial release. Ectoparasites were documented and, if present, collected, and stored in alcohol.

Using a sodium heparinized syringe, blood was collected from either the jugular or brachial vein for a suite of blood analyses to assess overall health of the individual tortoise. The volume of blood collected did not exceed 0.5% of the tortoise's body weight. Whole blood was transferred to a microhematocrit tube and centrifuged (Hemata-Stat II, Separation Technology Inc., EKF Diagnostics) to measure packed cell volume (PCV) and plasma color, and a refractometer was used to measure plasma total solids (TS). Within 30 min of collection, a small amount of heparinized whole blood was used to make blood films for review, including white blood cell (WBC) estimate and differential, and morphological evaluation, performed by a board-certified veterinary clinical pathologist (NIS). Remaining blood was centrifuged (Triac centrifuge, Primary Care Diagnostics, Becton Dickinson Company) to harvest plasma. A biochemical panel was performed on all plasma samples with an AU480 chemical analyzer (Beckman Coulter Inc., Brea, CA) by IDEXX Laboratories (Westbrook, ME): aspartate aminotransferase (AST), creatine kinase (CK), albumin, total protein, globulin, blood urea nitrogen (BUN), cholesterol, glucose, calcium, phosphorus, chloride, potassium, sodium, uric acid, and triglycerides.

During rehabilitation, tortoises were kept in housing maintained between 23 and 32°C (30). All tortoises received antimicrobials [enrofloxacin (Baytril, Bayer HealthCare LLC., Shawnee Mission, KS)] and fluid therapy [Lactated Ringer's Solution (Abbott Laboratories Inc., Chicago, IL)]. Dependent on initial diagnostics, tortoises also received supplementation with B vitamins and/or iron. Tortoises suspected to have gastric ulcers were treated with sucralfate (TEVA Pharmaceuticals USA Inc., North Water, PA), and tortoises with ocular discharge or palpebral edema were treated with tetracycline ophthalmic ointment (Terramycin, Zoetis Inc., Kalamazoo, MI). All tortoises were closely monitored for eating and defecation and were frequently soaked in shallow water to promote hydration. Tortoises that did not eat on their own were provided nutritional support through a red rubber feeding tube with a reptile herbivore complete diet (Emeraid IC Herbivore, Emeraid LLC., Cornell, IL).

Forage and soil sampling and testing

Forage and soil samples were collected at approximately 30 active gopher tortoise burrows in each of two enclosures, DB1 and SR1 (see **Figure 1**), during July and August 2017. DB1 was a site of high disease-related mortality, while SR1 had no documented disease-related mortality and was chosen as a site for comparison. At each selected burrow, a 1-m^2 quadrat was placed ∼5 m away at a randomly selected angle (0–180°) from the mouth of the burrow. If the randomized angle resulted in placement around the base of a tree or shrub, the next angle was chosen.

All above-ground herbaceous vegetation within the quadrat was cut at the soil line, collected, and transported to the lab for processing. Vegetation samples from each enclosure were separated into two types: (1) grasses and grass-like plants and (2) non-grass mixed forbs and legumes. For each enclosure, samples of each vegetation type collected from individual burrows were thoroughly mixed by group to create a composite mixture (e.g., DB1 mixed grasses, DB1 mixed forbs and legumes, etc.). Two composite samples from each forage group from each site were submitted for analysis through wet chemistry procedures (Dairy One Forage Laboratory, Ithaca, NY, see **Appendix A** in **Supplementary Material** for specific procedure details).

Soil cores of 30 cm were collected from the center of each quadrat using a soil auger. Each soil core sample was then separated into a top (depth = 0–15 cm) and bottom (depth = 16–30 cm) layer. Samples were then pooled by enclosure and depth layer and thoroughly mixed to create a composite sample ($n = 4$). Total elemental analysis of soils was performed for each composite sample by the University of Georgia Soils Lab (Athens, GA), where levels of the following elements were measured through acid digestion: phosphorus (P), potassium (K), calcium (Ca), Fe, magnesium (Mg), Mn, Mo, boron (B), Cu, nickel (Ni), sodium (Na), sulfur (S), Zn, aluminum (Al), As, Cd, chromium (Cr), and Pb. Element concentrations based on dry weight are reported in ppm.

Statistics and Modeling for Predictor Variables for Disease

Sex of diseased tortoises was compared using a Welch two sample *t*-test in statistical program R [version 3.4.2; (31)]. All blood data for rehabilitated tortoises were compared with data from free-ranging (translocated) healthy gopher tortoises from Nokuse Plantation using a Welch two sample *t*-test in R. Forage data were compared using Analysis of Variance (ANOVA) in *R* to test for effects of site, forage type, and a site*type interaction. Soil data were compared between sites (DB1, SR1) using a Welch two sample *t*-test in *R*.

To identify potential variables useful for predicting morbidity and mortality, all data collected for tortoises translocated to five of the release enclosures (including enclosures with known disease-related mortalities) was compiled. Individual tortoises encountered either dead or alive during mortality surveillance were designated as either "diseased" or "healthy." Diseased animals were those tortoises that experienced disease-related mortality or underwent rehabilitation. Individuals detected after January 2016 were excluded from this modeling analysis, as they were encountered during non-routine monitoring with high search effort (e.g., trapping and radiotracking). Data for the models included donor site location and characteristics, recipient site (release enclosure) characteristics, and individual tortoise data. Donor site variables (when available) included donor site, donor county, number of tortoises in cohort (in this study defined as tortoises collected from the same donor site and moved at the same time), donor site latitude, change in latitude from donor site to recipient site, presence of a "sick" cohort member (binary response), and number of sick tortoises in the cohort. Recipient site variables included initial stocking density (tortoises/ha), number of distinct donor populations in enclosure, and days since last burn. Individual tortoise variables included sex, SCL, initial BCI at time of release (calculated using SCL and mass), days since release (into soft-release enclosure; includes time after silt fence was removed), month encountered, and season encountered (assigned using month encountered; spring = March, April, May; summer = June, July, August; fall = September, October, November; winter = December, January, February).

Biologically relevant combinations of variables within each candidate set of models were estimated with logistic regression, and model fit was assessed using Akaike Information Criterion [AIC; (32)] as a ranking variable in R. These were run in a fixed-effects model with a binomial distribution to determine relationship between the variables and the binomial response outcome of detection (1) or absence (0) of disease.

Three separate sets of candidate models were evaluated initially to determine whether any of these sets of characteristics were important for predicting the detection of disease (**Supplementary Table**). Each set of candidate models was focused on a set of characteristics—e.g., donor site, recipient site, or host (tortoise). Highly correlated variables (such as static categorical variables pertaining to site) were excluded from use in the same model. Results from these models were also compared with a null model (intercept only). A global model was not included, as there were correlated variables that could not be run in the same model.

Variables included in the top model(s) for each candidate set were then compiled to create a final set of combination models. Models that were tested in this final set included only variables that made biological sense when combined. Model results were evaluated using AIC for top model selection.

RESULTS

Between April 2013 and April 2017, 62 tortoises were found sick or dead with the cause attributed to disease. We defined the morbidity and mortality event as the period between April 2013 and November 2015, during which most diseased tortoises (n = 52; 84%) were encountered, although there were additional diseased tortoises (n = 10; 16%) found between January 2016 and April 2017 that are also included in some analyses. Tortoises were found sick or dead in all months except February, and almost all (59/62) were adults. There was no difference (p = 0.2) in number of males (n = 28) and females (n = 32) found sick or dead, and mean SCL was 271 ± 35 mm SD. The timing between a tortoise's release and when it was found sick or dead varied between 0 and 5 years. Two tortoises were assessed and determined to be sick upon arrival and was transported for rehabilitation instead of being released; all others were found sick or dead years after their initial release. Mortalities were initially confined to one site (DB1; 15 ha; April to December 2013) but several tortoises were later found sick or dead in an adjacent site, DB2 (24 ha; December 2013). Sporadic mortalities also occurred in other release sites, sometimes several miles away from DB1 and DB2. Most tortoises during the event were found in DB1 (36/52; 69%), with the others found in DB2 (n = 4), DB3 (n = 2), and M1 (n = 3). Other tortoises were from unidentified enclosures (n = 3), other sites on Nokuse (n = 2), or were never released (n = 2).

Gross Necropsies and Histopathology

Of the 21 animals that were submitted for necropsy, histopathology, and ancillary testing, we observed signs consistent with inanition or malnutrition [e.g., poor body condition (n = 17), hepatic (n = 4) and/or skeletal muscle (n = 14) atrophy, atrophy of adipose tissue within the bone marrow (n = 1)], mild to severe osteopenia of the plastron (n = 2), hemosiderosis (accumulation of iron) in the liver (n = 13), or no gross or microscopic evidence of infectious disease (n = 21). Emaciation, muscle atrophy, empty (or nearly empty) gastrointestinal tract, and liver hemosiderosis were the most common findings for dead tortoises.

The esophagus, stomach and small intestine of many tortoises that died were devoid of forage contents: seven had completely empty stomachs, five had distended stomachs filled with gas or clear fluid, and an additional two had abnormal material and mucous present in the stomach. Two tortoises had only tube-feeding formula in the intestinal tract (from supportive care), and only one necropsied tortoise had grass present in the stomach. One tortoise also had necrotic mucosa and another had necrotic-like material present in the gastrointestinal tract. Some of the tortoises had fecal material in the colon and gas in

the gastrointestinal tract which was attributed to gastrointestinal stasis or ileus, a common finding in sick chelonians. None of the gastrointestinal tracts contained unusual plants or foreign objects. An enlarged or distended urinary bladder with amber colored urine and gray urates was also documented in 10 (48%) of the necropsied tortoises, which is consistent with dehydration and/or starvation in tortoises (33).

Testing for Infectious Pathogens

The only pathogen detected in samples submitted to the University of Florida was *Mycoplasma* spp., where DNA was detected in three of six tortoises. Histopathology of the upper respiratory tract of two tortoises was consistent with mild to severe upper respiratory tract disease (URTD).

Low levels of FV3 DNA (mean = 0.1433 copies/ng DNA, SD ± 0.085) were detected in the gastrointestinal tract of three tortoises, while other samples submitted to the University of Illinois were negative for all other pathogens tested (34). No other pathogens were detected in tissue samples.

Ticks were identified as gopher tortoise ticks (*Amblyomma tuberculatum*). No tortoise pathogens were detected in any of the submitted tick samples.

Liver Toxicants

Liver concentrations for As, Cd, Co, Cu, Fe, Pb, Mn, Hg, Mo, Se, and Tl were within the expected range based on the limited reference ranges for liver mineral values in tortoises for the Michigan State University Veterinary Diagnostic Laboratory (**Table 2**; Buchweitz, pers. comm.). No toxic organic compounds screened for in the Wiley 9 MS library were detected in any of the liver samples.

Tortoises in Rehabilitation

Nineteen tortoises were found sick but still alive between August 2014 and April 2017 and admitted to the GSTC for medical care. Physical examinations of all tortoises indicated poor body condition, lethargy, and severe weakness. Some also had obstructed nares, nasal discharge, pale mucous membranes, and varying degrees of red discoloration under the scutes of the plastron suggestive of hemorrhage (**Figure 2**); no other consistent clinical abnormalities were found. The neurological function of tortoises was assessed frequently and considered normal. Body condition indices and CBCs were obtained on 11/19 tortoises and plasma biochemistry testing was performed on 11/19 tortoises within 14 days of arrival at the GSTC and compared with previously published blood analyte data from other studies (**Table 3**). One tortoise had blood drawn on two sample dates (day 0 and day 14). Blood sampling was delayed to avoid further stressing of severely compromised tortoises. Compared to clinically normal free-ranging tortoises from Nokuse Plantation, tortoises admitted for rehabilitation had, on average, significantly lower body weight ($p < 0.01$), BCI ($p < 0.01$), PCV ($p = 0.02$), immature heterophils ($p < 0.01$), lymphocytes ($p < 0.01$), total solids ($p < 0.01$), total protein ($p < 0.001$), albumin ($p < 0.01$), globulin ($p < 0.01$), cholesterol ($p = 0.03$), glucose ($p < 0.01$), calcium ($p = 0.02$), and potassium ($p = 0.02$), and significantly higher AST ($p = 0.04$) and BUN ($p < 0.01$) (**Table 4**). The anemia in these tortoises was moderate to severe and non-regenerative. No hemoparasites or other infectious agents were identified in any of the blood films and plasma color, when noted, was clear. Seven of 12 tortoises had mild to moderate heterophil left-shifting.

When tortoises were treated with supportive care (fluid therapy, warmth, vitamins, and other supplements), nutritional support, and antibiotics, some improved and showed increasing appetite and normal food consumption. Seven animals (37%) died or were ultimately euthanized because of their deteriorating condition, while the other 12 (63%) recovered at the GSTC. Once recovered, tortoises were returned to Nokuse Plantation, where they were released into a separate, smaller enclosure and provided with supplemental food. After 11–15 months, seven of the 12 recovered tortoises (58%) were successfully recaptured, reassessed, and released in a new larger enclosure. Two of the tortoises that were rehabilitated and released were later found dead in or near their burrows, but the cause of their death remains undetermined.

Nutrients in Forage Plants and Minerals in Soils

Only significant differences in the plant nutritional composition between the two study sites (DB1, SR1) are reported here.

TABLE 2 | Liver toxicant concentrations in parts per million (ppm) for selected elements (arsenic [As], cadmium [Cd], cobalt [Co], copper [Cu], iron [Fe], lead [Pb], manganese [Mn], mercury [Hg], molybdenum [Mo], selenium [Se], thallium [Tl], and zinc [Zn]) in liver tissue of six translocated gopher tortoises (*Gopherus polyphemus*) that died during a mortality event from 2013 to 2015 at Nokuse Plantation, a private preserve in northwest Florida.

		Selected elements (ppm)											
ID	SEX	As	Cd	Co	Cu	Fe	Pb	Mn	Hg	Mo	Se	Tl	Zn
2021	F	<0.03	0.12	<0.03	2	1,397	0.03	2.64	<0.13	0.8	0.09	<0.03	39
2172	M	<0.03	0.19	<0.03	4.4	1,577	<0.03	2.11	<0.13	1.12	0.72	<0.03	93
2197	F	0.05	0.22	<0.03	2.1	2,772	0.09	3.7	0.06	1.03	0.18	<0.03	42
2274	F	<0.03	0.93	<0.03	3	1,271	<0.03	7.64	<0.13	0.62	0.19	<0.03	88
2552	M	<0.03	0.37	<0.03	4.4	1,133	<0.03	1.34	<0.13	0.7	0.18	<0.03	20
307	F	<0.03	0.93	<0.03	3	1,271	<0.03	7.64	<0.13	0.62	0.19	<0.03	88

Concentrations based on wet weight values.

FIGURE 2 | Clinical presentation documented in gopher tortoises during rehabilitation at the Georgia Sea Turtle Center included emaciation (**Left**) and hemorrhaging under the scutes on the plastron (**Right**). Photos provided by T. Norton.

Starch ($p < 0.03$), Ethanol Soluble Carbohydrates (ESC, simple sugars; $p = 0.007$), crude fat ($p < 0.03$), potassium ($p < 0.001$), manganese ($p = 0.03$), and Dietary Cation-Anion Difference (DCAD; $p = 0.001$) were all higher in the DB1 site. Phosphorus ($p < 0.02$), magnesium ($p < 0.02$), sulfur ($p = 0.007$), and chloride ion ($p < 0.001$) values were higher in the SR1 site. There were no significant differences between sites for any of the soil minerals analyzed.

Models Exploring Predictors of Disease

The top model for the recipient site candidate set included initial density and days since burn as variables, with a model weight of 0.972. Within the candidate set for donor site, two models captured most of the weight, with the number of diseased tortoises in cohort included as a variable in both models. That variable alone accounted for the majority of the weight (0.726), followed by the secondary model which also included donor region (model weight = 0.257). The top model in the host candidate set included initial BCI, season encountered, and days since release (model weight = 0.459) followed by just season encountered as a variable (model weight = 0.278).

Three models with the combined variable types captured almost all of the weight of the models, with the two variables of initial density and season encountered included in all three (**Table 5**). The variables of initial BCI, days since release, and days since burn were also included in one or more of the models that captured most of the weight. Sick tortoises were detected more frequently in enclosures with higher initial densities (8.1–16.36 adults/ha) than those with lower initial densities (0.56–8.1 adults/ha). Disease was detected most frequently in the fall and winter, indicating that there is likely a seasonal component in presence of disease or its detection. There was a bimodal effect from days since last burn, where tortoises were also more likely to be detected either 1–3 years before a prescribed burn, or within the first 2 years following a burn. Tortoises were more likely to be detected with disease within the first 3 years after release. Tortoises detected with disease had an initial BCI of 0.15–0.20, which was in the intermediate range of individuals represented in the data.

DISCUSSION

This study documents the investigation of a mortality event of gopher tortoises exhibiting evidence of starvation and dehydration presumptively resulting from higher tortoise density and associated chronic stress after translocation. Previous studies have demonstrated that translocated gopher tortoise populations with appropriate management can have very high rates of retention and nearly 98% annual apparent survival more than 10 years post-release (7, 37). Current approaches for gopher tortoise translocation rely on previous studies to improve short-term translocation success, such as soft-release enclosures to increase site fidelity (23, 38). While the mortality event was pronounced enough to warrant an investigation, the apparent annual survival of adults for the affected enclosures (and Nokuse as a whole) is 0.89–0.98 (Aresco, unpubl. data), which is on par with or greater than apparent annual survival rates of 0.87–0.99 reported for adult wild (39–41) and translocated (7, 37, 42) gopher tortoise populations. The time from introducing a tortoise to Nokuse Plantation to the tortoise becoming ill or being found dead did not seem to affect likelihood of mortality during this event, as tortoises both recently introduced and those that had been there for years died. There was also no significant difference between number of diseased males and females, suggesting that detection of disease was not biased by sex. The majority of tortoises were also found during the cooler months, when they would be expected to be less active. However, aberrant thermoregulatory behavior may have been easier to detect during cooler months, as tortoises with poor health may spend significantly more time basking or being out of their burrows at inappropriate temperatures (43–45) rather than undergoing winter dormancy (46). This behavior of emergence or basking in cooler weather may suggest that the tortoises found in the fall and winter were potentially attempting to behaviorally induce a fever, which gopher tortoises have been shown to do when their immune system is challenged (47).

There were several commonalities among tortoise necropsy results. Tortoises were emaciated, had moderate to severe muscle atrophy, a mostly empty gastrointestinal tract, and hemosiderin

TABLE 3 | Comparative hematology and blood chemistry data from gopher tortoises (*Gopherus polyphemus*) translocated to Nokuse Plantation sampled during rehabilitation within 14 days after admission in comparison to a free-ranging population translocated from Georgia to South Carolina (35) and a free-ranging population in Georgia (36).

Hematology	**Rehab (<14 days) (*n* = 12)**			**Hernandez et al. (35) (*n* = 10)**			**Taylor and Jacobson (36) (*n* = 13)**		
	Mean	**Min**	**Max**	**Mean**	**Min**	**Max**	**Mean**	**Min**	**Max**
Packed Cell Volume	15	8	25	25	14	29	23	15	30
White blood cell concentration ($\times 10^3$/ul)	12.79	3.80	32.00	10.28	4.20	17.6	15.70	10.00	22.00
Heterophils ($\times 10^3$/ul)	6.75	1.50	21.00	4.81	1.60	10.9	**4.76	1.57	8.95
Immature Heterophils ($\times 10^3$/ul)	0.31	0	1.70						
Lymphocytes ($\times 10^3$/ul)	2.71	0.34	4.60	1.43	0.29	5.46	8.89	5.02	12.4
Monocytes ($\times 10^3$/ul)	1.60	0.13	3.70	0.19	0	0.72	1.16	0.47	20.88
Eosinophils ($\times 10^3$/ul)	0.81	0	2.60	0.56	0	1.51	** (see heterophils)		
Basophils ($\times 10^3$/ul)	0.77	0	1.90	3.37	1.25	7.92	0.90	0.31	1.73
Heterophil:Lymphocyte Ratio	2.70	0.71	8.08	5.23	1.61	10.69			

Blood chemistry	**Rehab (<14 days) (*n* = 11)**			**Hernandez et al. (35) (*n* = 14)**				**Taylor and Jacobson (36) (*n* = variable)**		
	Mean	**min**	**max**	**Mean**	**min**	**max**	**n**	**Mean**	**min**	**max**
Total Protein (g/dL)	2.6	1.5	3.9	4.5	3.5	5.8	17	3.1	1.3	4.6
Albumin (g/dL)	0.4	0.1	0.9	1.2	1.0	1.5	17	1.5	0.5	2.6
Globulins (g/dL)	2.2	0.9	3.3							
AST (U/L)	240	53	650	163	87	252	17	136	57	392
Creatine Kinase (U/L)	3,117	31	27,231	1,408	55	5,705	13	160	32	628
Blood Urea Nitrogen (mg/dL)	89	15	229					30	1	130
Cholesterol (mg/dL)	36	9	70	121	10	282	13	76	19	150
Glucose (mg/dL)	72	8	134	131	81	197	16	75	55	128
Calcium [Ca] (mg/dL)	9.4	8.2	11.7	15.7	11.4	23.2	10	12	10	14
Phosphorus [P] (mg/dL)	2.0	1.0	4.1	2.8	1.7	6.1	17	2.1	1.0	3.1
Ca/P ratio	5.4	2.2	8.4							
Chloride (mEq/L)	93	24	121	92	88	98	17	102	35	128
Potassium (mEq/L)	4.0	0.9	6.8	4.0	3.3	5.3	17	5.0	2.9	7.0
Sodium (mEq/L)	119	30	151	126	121	130	17	138	127	148
Uric Acid (mg/dL)	7.2	2.0	26.7	2.6	1.4	4.8	17	3.5	0.9	8.5
Triglycerides (mg/dL)	14	2	33	177	29	523	12	32	0	178

*** Heterophils and eosinophils combined as reported in reference.*

accumulation in the liver. The combination of these factors suggests that these animals had not been eating for an extended time prior to death, although the cause remains unknown. When found alive, individuals exhibited muscle atrophy, had poor body condition, sub-keratin hemorrhage of the plastron, and bloodwork findings consistent with a catabolic state and consequent starvation. Although starvation due to lack of adequate forage within the release sites seems unlikely given the abundance and diversity of suitable forage plants present in all of the known affected sites and the fact that many other tortoises were unaffected, underlying disease and/or chronic stress could lead to decreased foraging and consequent malnutrition (48, 49).

There are no other published studies that include data for minerals in livers for gopher tortoises; thus, comparisons were drawn from the closely related desert tortoise (*Gopherus agassizii*), which occurs in southwestern US deserts. Hepatic iron concentrations from necropsied gopher tortoises were similar to those in desert tortoises with clinical signs of URTD (p=0.99) but significantly higher than a control group of healthy desert tortoises ($p = 0.01$) (50). Increased hepatic iron concentrations may be attributed to iron accumulation from red blood cell breakdown and inability to reabsorb the iron from hemoglobin (50). This is consistent with our necropsy findings of hepatic hemosiderosis and could result from cachexia, or weakness and muscle wasting due to severe chronic illness (51). A mortality investigation for desert tortoises in the Mojave Desert following periods of drought found similar necropsy and histopathology results, including hepatic hemosiderosis (52). Based on the toxicological assays of liver tissues, ingestion of toxicants due to past agricultural and silviculture practices seems unlikely as the cause of disease and mortality in these tortoises.

TABLE 4 | Differences in body condition, plasma biochemistry, and hematology data between clinically abnormal translocated gopher tortoises (*Gopherus polyphemus*) in rehabilitation and clinically normal free-ranging tortoises at Nokuse Plantation.

	Rehab (n = 12)			Free-Ranging (n = 83)			
Parameter	**Mean**	**Min**	**Max**	**Mean**	**Min**	**Max**	***p***
Weight (kg)	2.77	1.90	4.00	3.76	1.56	5.73	*<0.01*
Carapace length (cm)	25.97	23.10	30.80	27.70	21.00	31.70	*0.04*
Body condition index	0.16	0.14	0.19	0.18	0.14	0.22	*<0.01*
Packed cell volume (%)	15	8	25	26	12	43	*0.02*
White blood cell concentration ($\times 10^3$/ul)	12.79	3.80	32.00	16.25	7.20	35.60	*0.2*
Heterophils ($\times 10^3$/ul)	6.75	1.50	21.00	7.80	1.70	21.00	0.56
Immature heterophils ($\times 10^3$/ul)	0.31	0	1.70	0.65	0	3.50	*<0.01*
Lymphocytes ($\times 10^3$/ul)	2.71	0.34	4.60	4.27	1.60	9.40	*<0.01*
Monocytes ($\times 10^3$/ul)	1.60	0.13	3.70	1.40	0	4.30	*0.64*
Eosinophils ($\times 10^3$/ul)	0.81	0	2.60	1.48	0	23.00	*0.11*
Basophils ($\times 10^3$/ul)	0.77	0	1.90	0.96	0	3.50	*0.41*
Heterophil:Lymphocyte ratio	2.70	0.71	8.08	1.98	0.38	5.24	*0.30*
	Rehab (n=11)			**Free-Ranging (n=88)**			
Total Solids (g/dL)	2.6	1.0	4.0	3.6	2.1	5.6	*<0.01*
Total Protein (g/dL)	2.6	1.5	3.9	3.7	1.3	6.4	*<0.01*
Albumin (g/dL)	0.4	0.1	0.9	0.8	0.1	1.9	*<0.01*
Globulin (g/dL)	2.2	0.9	3.3	3.0	1.2	5	*<0.01*
AST (U/L)	240	53	650	96	11	241	*0.04*
CK (U/L)	3,117	31	27,231	1,357	33	8,341	*0.49*
BUN (mg/dL)	89	15	229	4	0	70	*<0.01*
Cholesterol (mg/dL)	36	9	70	54	6	139	*0.03*
Glucose (mg/dL)	72	8	134	117	22	264	*< 0.01*
Calcium [Ca] (mg/dL)	9.4	8.2	11.7	10.6	0	18.1	*0.02*
Phosphorus [P] (mg/dL)	2.0	1.0	4.1	2.6	0.7	9.1	*0.06*
Ca/P ratio	5.4	2.2	8.4	4.5	0	10.9	*0.22*
Chloride (mEq/L)	93	24	121	103	35	270	*0.26*
Potassium (mEq/L)	4.0	0.9	6.8	5.0	2.0	9.9	*0.02*
Sodium (mEq/L)	119	30	151	135	49	276	*0.15*
Uric Acid (mg/dL)	7.2	2.0	26.7	3.4	0.6	9.9	*0.12*
Triglycerides (mg/dL)	14	2	33	21	2	252	*0.19*

AST, aspartate aminotransferase; CK, creatine kinase; BUN, blood urea nitrogen.

Other than *Mycoplasma* spp., the causative agent linked to URTD, there is scant information on the diseases and pathogens of wild gopher tortoises. However, none of the histopathological findings or infectious pathogen assays provide evidence to suspect an infectious pathogen as the cause of these mortalities. We did detect *Mycoplasma* spp. DNA in tissue from three tortoises and FV3 DNA at low levels in the gastrointestinal tracts of three tortoises. However, the severity and the inconsistent frequency of lesions noted in necropsied tortoises do not indicate that mortalities were caused by URTD or by *Mycoplasma* spp. infection. Additionally, as ranavirus was not detected in other organs, the low number of copies present in the three positive samples, and most importantly, the lack of a demonstrable host response, it is also unlikely that ranavirus was the cause of mortality. The three tortoises instead may have been asymptomatic carriers of ranavirus, or the virus was simply passing through the gastrointestinal tract (34). Novel pathogens remain a possibility and continued testing to eliminate infectious agents as the cause of future mortalities is recommended.

The data on body condition, physical examination, plasma biochemistry, and hematology of gopher tortoises evaluated during rehabilitation are consistent with chronic malnutrition. Blood chemistry data revealed that total protein, total solids, albumin, globulins, cholesterol, glucose, calcium, and potassium were significantly lower when compared with free-ranging clinically normal tortoises of the same study population, and AST and BUN were higher. Similar trends were observed for these analytes when comparing diseased tortoises from this study with previously reported blood analytes data for free-ranging tortoises elsewhere, with the additional observation of comparatively higher CK and uric acid in our study tortoises (35, 36). The following interpretations are based on general principles of blood data interpretation in reptiles (53). Anemia in reptiles can be the sequela of various underlying causes, such as chronic disease

TABLE 5 | Akaike Information Criterion (AIC) table for top logistic regression models demonstrating variables for predicting detection of disease in translocated gopher tortoises (*Gopherus polyphemus*) at Nokuse Plantation, a private conservation preserve in northwest Florida.

Model	K	AIC	ΔAIC	Model Wt
initial_bci+days_since_release+initial_density+season	8	153.5	0	0.405
days_since_release+initial_density+season+days_since_burn	8	153.8	0.2	0.36
initial_bci+days_since_release+initial_density+season+days_since_burn	9	155.1	1.6	0.184
null model (intercept only)	1	368.8	215.3	0

BCI, body condition index.

and/or inflammatory disease (e.g., from infectious or non-infectious causes), but also has been associated with starvation and dehydration in desert tortoises (52). Considerations for generalized low plasma proteins (i.e., panhypoproteinemia which is defined as low concentrations of total protein, albumin, and globulins) in context of other abnormalities in blood variables include chronic malnutrition resulting from decreased protein synthesis and/or increased catabolism, in addition to malabsorption and/or maldigestion, and less likely hepatic insufficiency or protein loss from renal disease. Hypocalcemia and hypokalemia are often also associated with anorexia or malnutrition in reptiles. Cholesterol was lower in sick tortoises admitted for treatment when compared to free-ranging tortoises, presumptively due to anorexia, malnutrition and/or malabsorption. Increased BUN may be the result of increased protein catabolism or intestinal hemorrhage. Although both AST and CK were mildly elevated in tortoises during rehabilitation, only AST was significantly higher, possibly due to the longer half-life of AST, suggesting muscle wasting. Hyperuricemia (>3 mg/dL uric acid) was observed in 10 of 12 tortoises, indicating dehydration. Given the evidence of dehydration, the observed panhypoproteinemia was likely more severe than actually reflected in plasma protein concentrations. Hematological data of rehabilitating tortoises was consistent with anemia of chronic and/or inflammatory disease. Clinically normal free-ranging Nokuse tortoises had higher immature heterophils and lymphocytes than rehabilitating tortoises, suggesting active immune stimulation. The presence of comparatively higher immature heterophils, monocytes, and eosinophils and wide range of leukocytes indicating leukopenia or leukocytosis in rehabilitating tortoises compared to free-ranging tortoises from other studies suggest possible immunosuppression from bone marrow depression to active systemic inflammation, respectively, presumptively reflecting various stages of being affected by stress, non-specific inflammation, and/or immunosuppression. Given the context of necropsy and histopathological findings of tortoises that died in which there was no evidence of infectious disease, the clinicopathological abnormalities and clinical findings in rehabilitating tortoises are consistent with chronic malnutrition, starvation, and dehydration. Together these results support that these tortoises were not eating sufficient amounts, were eating nutritionally deficient forage, or were unable to properly absorb nutrients from the forage.

There are no apparent differences in the quality of habitat, gopher tortoise forage, or soil type and composition among release sites (Aresco, pers. comm.). Examination of the affected enclosures (i.e., those experiencing mortalities) by a botanist did not detect any poisonous exotic or native plants (A. Schotz, AL Natural Heritage Program, unpubl. report) and there is an ongoing investigation on the plant community composition. Forage nutritional assays showed that the forage tested from DB1 (the site with the highest mortality) had higher amounts of non-fibrous carbohydrates such as starches and sugars, which suggests more readily available energy was present in plants from that site when compared to those from the site where no mortalities occurred (SR1). No land management practices had recently changed prior to this mortality event. Although the specific historical farm practices differed among sites, no discernible correlation between farming practice and tortoise mortality has yet to emerge (Aresco, pers. comm.), and soil and liver samples tested did not contain elevated levels of agriculture-related toxicants. The only habitat management related factor that emerged as important for detection of disease was the time since last prescribed burn. This variable had a bimodal effect on probability of detection of disease. Tortoises were likely to be detected with disease within the year following a prescribed burn, although this is likely due to their increased visibility following the removal of the understory vegetation, similar to the increased detection of tortoise burrows post-burn (54). Additionally, diseased tortoises were also more likely to be detected within 1 year prior to the last prescribed burn, which is functionally 3–5 years after a burn based on the current burn rotation. This suggests that burn frequency should at the very least be maintained at 3–5 years, although it may be beneficial to burn more frequently. Fire or other frequent disturbance is required within this ecosystem to maintain the open canopy and sparse midstory that gopher tortoises prefer, and lack of frequent fire on the landscape can lead to suboptimal habitat and foraging conditions (41, 55).

Our highest ranked models suggest that certain recipient site, donor site and individual tortoise characteristics were important in detecting diseased tortoises. Season was an important component of several of the top models, with diseased tortoises more likely to be detected in fall and winter than in other seasons. As previously discussed, diseased tortoises may have been more detectable when abnormal thermal behavior is more apparent. Although no biological cause for a seasonal pattern in actual disease status could be determined, seasonal differences in immunity have been reported in ectotherms, which may be particularly susceptible during times of thermal instability such as onset of dormancy (56, 57). In gopher tortoises, the number of circulating lymphocytes and bactericidal ability are significantly reduced in fall and winter compared to other seasons (58).

Initial tortoise density in release pens was the most important variable for detecting disease. The models indicated that diseased tortoises were found most frequently in enclosures with higher densities. Although we did not detect a pathogen responsible for the mortalities, holding animals at higher densities increases the probability of pathogen transmission and disease, which can be exacerbated in highly social species with complex social structures, such as the gopher tortoise (59, 60). Gopher tortoise

movement and behavior patterns are affected by density, and translocated individuals also tend to have increased movements and home ranges (23, 61, 62). The increased movement exhibited by translocated tortoises also leads to increased contact opportunities for transmission of potential pathogens (21). Given the complex social structure of gopher tortoise populations, it is logical that density may influence the stress (and health) exhibited by individuals after translocation (21). Overcrowding was also believed to be a contributing factor in mortalities of desert tortoises exhibiting similar clinical signs as in this study (52).

Other variables included in the top models included days since release and initial BCI. Tortoises were more likely to be detected with disease within the first 3–4 years after release, with the probability of detection of disease decreasing after that time point. The initial time post-translocation while a tortoise is acclimating to a novel environment ("establishment phase") is also a time of high stress, and therefore higher health risk (49, 63). Our models suggest that once a tortoise survives more than 3–4 years post-translocation, the likelihood that they will be found diseased is much lower.

Condition indices have been used to quantify health and estimate energy reserves in various taxa, but may not be the most reliable assessment of body condition, especially in chelonians (64, 65). The method used to calculate BCI in this study (using only SCL and mass) does not accurately represent the approximate volume of the tortoise. Additionally, BCIs can be affected by several factors, including hydration and reproductive status (26, 64). The variable size and shape of individual tortoises also suggests that weight alone is not a good indicator of health and condition, such that a method that evaluates muscle mass and fat deposits may be a better option (66). Regardless, individuals with a low initial body condition (and therefore energy reserves) may be more likely to remain at a lower body condition, especially under stressful conditions. Tortoises with lower energy reserves may also be at a higher risk for deteriorating health, particularly when evaluated in conjunction with the other highlighted variables.

Our results may serve as a cautionary tale for future translocation efforts, as new pathogens and diseases continue to be discovered. A specific etiology was not found to be the cause of the mortalities. However, higher density in the translocation enclosures, which may induce social disruption and stress, appears to be strongly associated with the detection of clinical signs and deaths of tortoises. Other factors, such as initial body condition, may also have contributed. This retrospective study has revealed important factors that appear correlated with probability of disease, and therefore provide guidance regarding both important data to collect as part of translocation and factors to consider when planning releases. For example, more information regarding donor site, such as habitat or vegetation type and quality, were not available for most donor sites but may be important determinants of tortoise health at release, as well as for evaluating and understanding translocation success.

In Florida, the primary objective for gopher tortoise translocation is usually to avoid direct and immediate mortality due to development, with the secondary objective of reintroducing tortoises to an area where they were previously extirpated or to augment existing populations (15). While both objectives are met with translocation to Nokuse Plantation, this study has underscored the importance of both long-term monitoring health and disease following translocation and incorporating an adaptive management approach. Disease screening (or at least collection of samples for later pathogen testing if an issue subsequently arises) is an important consideration when combining tortoises from multiple source populations. In some cases, health problems that may arise after a translocation event are not a result of the translocated animals introducing diseases or pathogens, but rather that these naïve animals are exposed to local pathogens or contaminants (20, 67). Stress, such as that associated with the translocation process, is an additional factor that may lead to increased susceptibility to disease and infection in tortoise species (21, 44, 45, 49, 68). Should monitoring reveal elevated disease prevalence or mortality in a translocated or augmented population, translocation practices merit review and modification before implementation elsewhere.

Although gopher tortoises possess many characteristics that make them a difficult species for which to measure long-term post-translocation success (e.g., long-lived with long generation times) (69), continued surveillance and improvements in future translocation and release protocols can increase the likelihood of maintaining a stable population. One of the most important tasks is to ensure that the recipient site continues to be managed to maintain optimal habitat for gopher tortoises, such as through the frequent application of prescribed fire. Additionally, increased monitoring during the inactive season, particularly following prescribed burning, may also lead to early detection of tortoises in poor health, which could then receive early treatment. Managers should also ensure that density of gopher tortoises within release enclosures is maintained below a set maximum density to reduce the potential for additional chronic stress associated with social disruption, especially when combining tortoises from multiple sources or for confining to pens for multiple years. Based on 14 years of experience with large-scale gopher tortoise translocations and the findings of this mortality event, we recommend a site density of no more than 3 adult tortoises per ha, even in areas with high forage quality. This recommended maximum density is lower than another translocated population, in which 13 adults and subadults from the same source population were penned in a 1-ha enclosure for 6–9 mo. (23). However, our recommended density is higher than documented in many wild populations (0.02–3.08 tortoises/ha; all size classes) of gopher tortoises (61, 62, 70–72). The penning density we recommend may need to be reduced further pending additional research into the effects of translocation on social networks and effects of density on the health and behavior of translocated gopher tortoises.

DATA AVAILABILITY STATEMENT

The datasets generated for this study are available on request to the corresponding author.

ETHICS STATEMENT

The animal study was reviewed and approved by University of Georgia IACUC.

AUTHOR CONTRIBUTIONS

SH, TN, and MA contributed to project design. RC, TN, NLS, and MA contributed to data collection. RC, SH, and NIS contributed to data analysis. RC wrote the manuscript. SH, TN, TT, NIS, NLS, and MA edited and reviewed the manuscript.

FUNDING

Funding was provided by the Nokuse Plantation and the Georgia Sea Turtle Center.

ACKNOWLEDGMENTS

This work was done under FFWCC scientific collection permit LSSC-15-00118 and the University of Georgia's Institutional Animal Care and Use Committee animal use protocol A2015 09-008-R1. Thank you to the staff and AmeriCorps volunteers at the GSTC for their assistance with rehabilitated tortoises and sample collection, Shawn McMahon for assistance with data compilation, and Dr. Matt Allender for performing pathogen assays. Support for TDT was provided by Department of Energy through award number DE-EM0004391 to the University of Georgia Research Foundation.

SUPPLEMENTARY MATERIAL

The Supplementary Material for this article can be found online at: https://www.frontiersin.org/articles/10.3389/fvets.2020.00120/full#supplementary-material

REFERENCES

1. Auffenberg W, Franz R. The status and distribution of the gopher tortoise *Gopherus polyphemus*. In: Bury RB, editor. *North American tortoises: Conservation and Ecology*. Research Report No. 12. Washington, DC: U.S. Department of the Interior, Fish and Wildlife Service (1982). p. 95–126.
2. US Fish and Wildlife Service (USFWS). Determination of threatened status for the gopher tortoise (*Gopherus polyphemus*). *Fed Reg.* (1987) 52:25376–80.
3. Florida Fish and Wildlife Conservation Commission (FFWCC). *Gopher Tortoise Management Plan, Gopherus polyphemus*. Tallahassee, FL: Florida Fish and Wildlife Conservation Commission (2007).
4. US Fish and Wildlife Service (USFWS). Endangered and Threatened wildlife and plants: 90-day finding on a petition to list the eastern population of gopher tortoise (*Gopherus polyphemus*) as Threatened. *Fed Reg.* (2009) 74:46401–6.
5. US Fish and Wildlife Service (USFWS). Endangered and Threatened wildlife and plants; 12-month finding on a petition to list the gopher tortoise as Threatened in the eastern portion of its range. *Fed Reg.* (2011) 76:45130–62.
6. Seigel RA, Dodd CK. Manipulation of turtle populations for conservation: halfway technologies or viable options? In: Klemens MW, editor. *Turtle Conservation*. Washington, DC: Smithsonian Institution Press (2000). p. 218–38.
7. Tuberville TD, Norton TM, Todd BD, Spratt JS. Long-term apparent survival of translocated gopher tortoises: a comparison of newly released and previously established animals. *Biol Conserv*. (2008) 141:2690–7. doi: 10.1016/j.biocon.2008.08.004
8. Berry KH, Aresco MJ. Threats and conservation needs for North American tortoises. In: Rostal DC, McCoy ED, Mushinsky HR, editors. *Biology and Conservation of North American Tortoises*. Baltimore, MD: Johns Hopkins University Press (2014). p. 143–58.
9. IUCN. *The IUCN Position Statement on Translocation of Living Organisms: Introductions, Re-Introductions and Restocking*. Gland: IUCN (1987). Available online at: http://www.iucn.org/dbtw-wpd/edocs/PP-002.pdf. (accessed May 2016).
10. Wolf CM, Griffith B, Reed C, Temple SA. Avian and mammalian translocations: update and reanalysis of 1987 survey data. *Conserv Biol.* (1996) 10:1142–54. doi: 10.1046/j.1523-1739.1996.10041142.x
11. Germano JM, Bishop PJ. Suitability of amphibians and reptiles for translocation. *Conserv Biol.* (2009) 23:7–15. doi: 10.1111/j.1523-1739.2008.01123.x
12. Sullivan BK, Nowak EM, Kwiatkowski MA. Problems with mitigation translocation of herpetofauna. *Conserv Biol.* (2015) 29:12–8. doi: 10.1111/cobi.12336
13. McCoy ED, Berry KH. Using an ecological ethics framework to make decisions about the relocation of wildlife. *Sci Eng Ethics.* (2008) 14:505–21. doi: 10.1007/s11948-008-9091-4
14. Germano JM, Field KJ, Griffiths RA, Clulow S, Foster J, Harding G, et al. Mitigation-driven translocations: are we moving wildlife in the right direction? *Front Ecol Environ*. (2015) 13:100–5. doi: 10.1890/140137
15. Florida Fish and Wildlife Conservation Commission (FFWCC). *Gopher Tortoise Management Plan, Gopherus polyphemus*. Tallahassee, FL: Florida Fish and Wildlife Conservation Commission (2012).
16. Flescher D. *Facing a Slow Death: Florida Allows Developers to Bury Alive or Kill Gopher Tortoises in Return for Protection of Habitat Elsewhere in the State, but Officials Warn That the Species Now Faces a "Very High Risk Of Extinction."* Fort Lauderdale, FL: Sun-Sentinel (2005).
17. Mushinsky HR, McCoy ED, Berish JS, Ashton R, Wilson DS. Biology and conservation of Florida turtles: *Gopherus polyphemus* — the gopher tortoise. *Chelonian Res Monogr*. (2006) 3:350–75.
18. Myrkalo RJ, Caruso KA, Hughes EA. State listed species permits. *Fla Sci*. (2010) 73:196–202.
19. Corn JL, Nettles VF. Health protocol for translocation of free-ranging elk. *J Wildl Dis*. (2001) 37:413–26. doi: 10.7589/0090-3558-37.3.413
20. Kock RA, Woodford WH, Rossiter PB. Disease risks associated with the translocation of wildlife. *Rev Sci Tech.* (2010) 29:329–50. doi: 10.20506/rst.29.2.1980
21. Aiello CM, Nussear KE, Walde AD, Esque TC, Emblidge PG, Sah P, et al. Disease dynamics during wildlife translocations: disruptions to the host population and potential consequences for transmission in desert tortoise social networks. *Anim Conserv*. (2014) 17:27–39. doi: 10.1111/acv.12147
22. Overing JD, Watts FC. *Soil Survey of Walton County, Florida*. Gainesville, FL: United States Department of Agriculture, Soil Conservation Service (1989).
23. Tuberville TD, Clark EE, Buhlmann KA, Gibbons JW. Translocation as a conservation tool: site fidelity and movement of repatriated gopher tortoises (*Gopherus polyphemus*). *Anim Conserv*. (2005) 8:349–58. doi: 10.1017/S1367943005002398
24. Cagle FR. A system of marking turtles for future identification. *Copeia*. (1939) 3:170–3. doi: 10.2307/1436818
25. McRae WA, Landers JL, Cleveland GD. Sexual dimorphism in the gopher tortoise (*Gopherus polyphemus*). *Herpetologica.* (1981) 37:46–52.
26. Nagy KA, Henen BT, Vyas DB, Wallis IR. A condition index for the Desert Tortoise (*Gopherus agassizii*). *Chelonian Conserv Biol.* (2002) 4:425–9.
27. Archer GA, Phillips CA, Adamovicz L, Band M, Byrd J, Allender MC. Detection of copathogens in free-ranging eastern box turtles (*Terrepene carolina carolina*) in Illinois and Tennessee. *J Zoo Wildl Med*. (2017) 48:1127–34. doi: 10.1638/2017-0148R.1

28. Loftis AD, Reeves WK, Szumlas DE, Abbassy MM, Helmy IM, Moriarity JR, et al. Surveillance of Egyptian fleas for agents of public health significance: *Anaplasma*, *Bartonella*, *Coxiella*, *Ehrlichia*, *Rickettsia*, and *Yersinia pestis*. *Am J Trop Med Hyg*. (2006) 75:41–8. doi: 10.4269/ajtmh.2006.75.41
29. Kidd L, Maggi R, Diniz PP, Hegarty B, Tucker M, Breitschwerdt E. Evaluation of conventional and real-time PCR assays for detection and differentiation of spotted fever group Rickettsia in dog blood. *Vet Microbiol*. (2008) 129:294–303. doi: 10.1016/j.vetmic.2007.11.035
30. Norton TM, Allender MC. Natural history and medical management of terrestrial and aquatic chelonians. In: Hernandez SM, Barron HW, Miller EA, Aguilar RF, and Yabsley MJ, editors. *Medical Management of Wildlife Species: A Guide for Practitioners*. 1st ed. (Hoboken, NJ: Wiley-Blackwell) (2019). p. 363–82.
31. R Core Team. *R: A Language and Environment for Statistical Computing*. Vienna, Austria: R Foundation for Statistical Computing (2013). Available online at: http://www.R-project.org/. (accessed October 2017).
32. Akaike H. A new look at the statistical identification model. *IEEE Trans Automat Contr*. (1974) 19:716–23. doi: 10.1109/TAC.1974.1100705
33. Boyer TH, Innis CJ. Chelonian taxonomy, anatomy, and physiology. In: Divers SJ, Stahl SJ, editors. *Mader's Reptile and Amphibian Medicine and Surgery*. 3rd ed. Philidelphia, PA: Saunders (2019). p. 31–49.
34. Cozad RA, Norton TM, Aresco MJ, Allender MC, Hernandez SH. Detection of ranavirus (*Frog virus 3*) in translocated gopher tortoises (*Gopherus polyphemus*). *J Wildl Dis*. (2020). doi: 10.7589/2019-02-053
35. Hernandez SM, Tuberville TD, Frank P, Stahl SJ, McBride MM, Buhlmann KA, et al. Health and reproductive assessment of a free-ranging gopher tortoise (*Gopherus polyphemus*) population following translocation. *J Herpetol Med Surg*. (2010) 20:84–93. doi: 10.5818/1529-9651-20.2.84
36. Taylor RW Jr, Jacobson ER. Hematology and serum chemistry of the gopher tortoise (*Gopherus polyphemus*). *Comp. Biochem. Physiol. A*. (1982) 72:425–8. doi: 10.1016/0300-9629(82)90241-9
37. Ashton KG, Burke RL. Long-Term retention of a relocated population of gopher tortoises. *J Wildl Manag*. (2007) 71:783–7. doi: 10.2193/2005-583
38. Aresco MJ, Walker RN, Greene M. *Site Fidelity, Movements, Survival, and Minimum Area Required of Gopher Tortoises (Gopherus polyphemus) Translocated From Development Sites to Managed Conservation Lands*. Tallahassee, FL: Status Report to the Florida Fish and Wildlife Conservation Commission, Permit WX06116b (2010).
39. Ozgul A, Oli MK, Bolker BM, Perez-Heydrich C. Upper Resiratory Tract Disease, force of infection, and effects on survival of gopher tortoises. *Ecol Appl*. (2009) 19:786–98. doi: 10.1890/08-0219.1
40. Tuberville TD, Todd BD, Hermann SM, Michener MK, Guyer C. Survival, demography, and growth of gopher tortoises (*Gopherus polyphemus*) from three different study sites with different management histories. *J Wildl Manag*. (2014) 78:1151–60. doi: 10.1002/jwmg.773
41. Howell HJ, Rothermel BB, White KN, Searcy CA. Gopher tortoise demographic responses to a novel disturbance regime. *J Wildl Manag*. (2020) 84:56–65. doi: 10.1002/jwmg.21774
42. McKee RK. *An Island of Misfit Tortoises: Evaluating the Use of Waif Animals to Recover Populations on the Brink*. [master's thesis], Athens GA: University of Georgia (2019).
43. Berry KH, Christopher MM. Guidelines for the field evaluation of desert tortoise health and disease. *J Wildl Dis*. (2001) 37:427–50. doi: 10.7589/0090-3558-37.3.427
44. Jacobson ER. Health issues of North American tortoises. In: Rostal DC, McCoy ED, Mushinsky HR, editors. *Biology and Conservation of North American Tortoises*. Baltimore, MD: Johns Hopkins University Press (2014). p. 60–76.
45. McGuire JL, Smith LL, Guyer C, Yabsley MJ. Effects of mycoplasmal upper-respiratory-tract disease on movement and thermoregulatory behavior of gopher tortoises (*Gopherus polyphemus*) in Georgia, USA. *J Wildl Dis*. (2014) 50:745–56. doi: 10.7589/2013-11-306
46. DeGregorio BA, Buhlmann KA, Tuberville TD. Overwintering of gopher tortoises (*Gopherus polyphemus*) translocated to the northern limit of their geographic range: temperatures, timing, and survival. *Chelonian Cons Biol*. (2012) 11:84–90. doi: 10.2744/CCB-0921.1
47. Goessling JM, Guyer C, Mendonca MT. More than fever: thermoregulatory responses to immunological stimulation and consequences of thermoregulatory strategy on innate immunity in gopher tortoises (*Gopherus polyphemus*). *Physiol Biochem Zool*. (2017) 90:484–93. doi: 10.1086/692116
48. Herzog CJ, Czéh B, Corbach S, Wuttke W, Schulte-Herbrüggen O, Hellweg R, et al. Chronic social instability stress in female rats: a potential animal model for female depression. *Neuroscience*. (2009) 159:982–92. doi: 10.1016/j.neuroscience.2009.01.059
49. Dickens MJ, Delehanty DJ, Romero LM. Stress: An inevitable component of animal translocation. *Biol Conserv*. (2010) 143:1329–41. doi: 10.1016/j.biocon.2010.02.032
50. Jacobson ER, Gaskin JM, Brown MB, Harris RK, Gardiner CH, LaPointe JL, et al. Chronic Upper Respiratory Tract Disease of free-ranging desert tortoises (*Xerobates Agassizii*). *J Wildl Dis*. (1991) 27:296–316. doi: 10.7589/0090-3558-27.2.296
51. Donoghue S. Nutrition. In: Mader DR, editor. *Reptile Medicine and Surgery*. 2nd ed. Philadelphia, PA: Saunders Elsevier Inc. (2006). p. 251–98.
52. Berry KH, Spangenberg EK, Homer BL, Jacobson ER. Deaths of desert tortoises following periods of drought and research manipulation. *Chelonian Conserv Biol*. (2002) 4:436–48.
53. Campbell TW. Clinical chemistry of reptiles. In: Thrall MA, Weiser G, Allison RW, Campbell TW, editors. *Veterinary Hematology and Clinical Chemistry*. 2nd edn. Ames, IA: John Wiley & Sons, Inc (2012). p. 599–606.
54. Howze JM, Smith LL. Detection of gopher tortoise burrows before and after a prescribed fire: implications for surveys. *J. Fish Wildl. Manag*. (2019) 10:62–8. doi: 10.3996/052018-JFWM-045
55. Aresco MJ, Guyer C. Burrow abandonment by gopher tortoises in slash pine plantations of the Conecuh National Forest. *J Wildl Manag*. (1999) 63:26–35. doi: 10.2307/3802484
56. Raffel TR, Rohr JR, Kieseck JM, Hudson PJ. Negative effects of changing temperature on amphibian immunity under field conditions. *Funct Ecol*. (2006) 20:819–28. doi: 10.1111/j.1365-2435.2006.01159.x
57. Schwanz L, Warner DA, McGaugh S, Di Terlizzi R, Bronikowski A. State-dependent physiological maintenance in a long-lived ectotherm, the painted turtle (*Chrysemys picta*). *J Exp Biol*. (2011) 214:88–97. doi: 10.1242/jeb.046813
58. Goessling JM, Guyer C, Mendonca MT. Seasonal acclimation of constitutive immunity in gopher tortoises *Gopherus polyphemus*. *Physiol Biochem Zool*. (2016) 89:487–97. doi: 10.1086/688694
59. Wendland LD, Wooding J, White CL, Demcovitz D, Littell R, Berish JED, et al. Social behavior drives the dynamics of respiratory disease in threatened tortoises. *Ecology*. (2010) 91:1257–62. doi: 10.1890/09-1414.1
60. Guyer C, Hermann SM, Johnson VM. Social behaviors of North American tortoises. In: Rostal DC, McCoy ED, Mushinsky HR, editors. *Biology and Conservation of North American Tortoises*. Baltimore, MD: Johns Hopkins University Press (2014). p. 102–9.
61. Guyer C, Johnson VM, Hermann SM. Effects of population density on patterns of movement and behavior of gopher tortoises (*Gopherus polyphemus*). *Herpetol Monogr*. (2012) 26:122–34. doi: 10.1655/HERPMONOGRAPHS-D-10-00004.1
62. Bauder JM, Castellano C, Jensen JB, Stevenson DJ, Jenkins CL. Comparison of movements, body weight, and habitat selection between translocated and resident gopher tortoises. *J Wildl Manag*. (2014) 78:1444–55. doi: 10.1002/jwmg.790
63. Armstrong DP, Seddon PJ. Directions in reintroduction biology. *Trends Ecol. Evol*. (2008) 23:20–5. doi: 10.1016/j.tree.2007.10.003
64. Jacobson ER, Weinstein M, Berry K, Hardenbrook B, Tomlinson C, Freitas D. Problems with using weight versus carapace length relationships to assess tortoise health. *Vet Rec*. (1993) 132:222–3. doi: 10.1136/vr.132.9.222
65. Stevenson RD, Woods WA Jr. Condition indices for conservation: new uses for evolving tools. *Integr. Comp. Biol*. (2006) 46:1169–90. doi: 10.1093/icb/icl052
66. Lamberski N. *Body condition scores of desert tortoises*. U.S. Fish and Wildlife Service report (2013). Available online at: https://www.fws.gov/nevada/desert_tortoise/documents/reports/2013/assess/DesertTortoise-BCS-2013-lamberski-po.pdf (accessed April 2016).
67. Wolff PL, Seal US. Implications of infectious disease for captive propagation and reintroduction of threatened species. *J Zoo Wildl Med*. (1993) 24:229–30.
68. Drake KK, Nussear KE, Esque TC, Barber AM, Vittum KM, Medica PA, et al. Does translocation influence physiological stress in the desert tortoise. *Anim Conserv*. (2012) 15:560–70. doi: 10.1111/j.1469-1795.2012.00549.x

69. Riedl SC, Mushinsky HR, McCoy ED. Translocation of the gopher tortoise: difficulties associated with assessing success. *Appl Herpetol*. (2008) 5:145–60. doi: 10.1163/157075408784648844
70. Eubanks JO, Michener WK, Guyer C. Patterns of movement and burrow use in a population of gopher tortoises (*Gopherus polyphemus*). *Herpetologica*. (2003) 59:311–21. doi: 10.1655/01-105.1
71. Berish JED, Kiltie RA, Thomas TM. Long-term population dynamics of gopher tortoises (*Gopherus polyphemus*) in a pine plantation in northern Florida. *Chelonian Cons Biol*. (2012) 11:50–8. doi: 10.2744/CCB-0904.1
72. McGuire JL, Smith LL, Guyer C, Lockhart JM, Lee GW, Yabsley MJ. Surveillance for upper respiratory tract disease and *Mycoplasma* in free-ranging gopher tortoises (*Gopherus polyphemus*) in Georgia, USA. *J Wildl Dis*. (2014) 50:733–44. doi: 10.7589/2013-11-300

Conflict of Interest: NS was employed by Busch Gardens.

The remaining authors declare that the research was conducted in the absence of any commercial or financial relationships that could be construed as a potential conflict of interest.

Copyright © 2020 Cozad, Hernandez, Norton, Tuberville, Stacy, Stedman and Aresco. This is an open-access article distributed under the terms of the Creative Commons Attribution License (CC BY). The use, distribution or reproduction in other forums is permitted, provided the original author(s) and the copyright owner(s) are credited and that the original publication in this journal is cited, in accordance with accepted academic practice. No use, distribution or reproduction is permitted which does not comply with these terms.

frontiers in Veterinary Science

ORIGINAL RESEARCH
published: 06 March 2020
doi: 10.3389/fvets.2020.00131

Coelomic Fluid Evaluation in *Pisaster ochraceus* Affected by Sea Star Wasting Syndrome: Evidence of Osmodysregulation, Calcium Homeostasis Derangement, and Coelomocyte Responses

Sarah J. Wahltinez[1], Alisa L. Newton[2], Craig A. Harms[3], Lesanna L. Lahner[4] and Nicole I. Stacy[1]**

[1] Department of Comparative, Diagnostic, and Population Medicine, College of Veterinary Medicine, University of Florida, Gainesville, FL, United States, [2] Wildlife Conservation Society, Bronx, NY, United States, [3] Department of Clinical Sciences and Center for Marine Sciences and Technology, College of Veterinary Medicine, North Carolina State University, Morehead, NC, United States, [4] Seattle Aquarium, Seattle, WA, United States

OPEN ACCESS

Edited by:
Justin J. Greenlee, National Animal Disease Center (USDA ARS), United States

Reviewed by:
José Silva, Universidade de São Paulo São Carlos, Brazil
Katherine Buckley, Auburn University, United States
Weiwei Zhang, Ningbo University, China

***Correspondence:**
Sarah J. Wahltinez
swahltinez@ufl.edu
Nicole I. Stacy
stacyn@ufl.edu

Specialty section:
This article was submitted to Veterinary Experimental and Diagnostic Pathology, a section of the journal Frontiers in Veterinary Science

Received: 28 October 2019
Accepted: 20 February 2020
Published: 06 March 2020

Citation:
Wahltinez SJ, Newton AL, Harms CA, Lahner LL and Stacy NI (2020) Coelomic Fluid Evaluation in Pisaster ochraceus Affected by Sea Star Wasting Syndrome: Evidence of Osmodysregulation, Calcium Homeostasis Derangement, and Coelomocyte Responses. Front. Vet. Sci. 7:131. doi: 10.3389/fvets.2020.00131

Sea Star Wasting Syndrome (SSWS) is one of the largest marine wildlife die-offs ever recorded, killing millions of sea stars from more than 20 Asteroid species from Alaska to Mexico from 2013 to 2015 from yet undetermined cause(s). Coelomic fluid surrounds the sea star's organs, playing critical roles in numerous systemic processes, including nutrient transportation and immune functions. Coelomocytes, which are cellular components of coelomic fluid and considered functionally equivalent to vertebrate leukocytes, are responsible for innate cell-mediated immunity. The objectives of this study were to (1) evaluate changes in coelomic fluid chemistry, coelomocyte counts, and cytology from ochre sea stars (*Pisaster ochraceus*) ($n = 55$) with clinical signs consistent with SSWS at varying intensity (SSWS score 1: $n = 4$, score 2: $n = 2$, score 3: $n = 3$, score 4: $n = 18$, score 5: $n = 26$) in comparison to coelomic fluid from clinically normal sea stars ($n = 26$) and to (2) correlate SSWS score with cellular and biochemical analytes. SSWS-affected sea stars had wider ranges of all electrolytes, except calcium; statistically significantly higher chloride, osmolality, and total protein; lower calcium; and higher coelomocyte counts when compared to clinically normal sea stars maintained under identical environmental conditions. Free and/or phagocytized bacteria were noted in 29% (16 of 55) coelomic fluid samples from SSWS-affected sea stars but were absent in clinically normal sea stars. SSWS score correlated significantly with increasing chloride concentration, osmolality, and coelomocyte counts. These chemistry and cytological findings in coelomic fluid of SSWS-affected sea stars provide insight into the pathophysiology of SSWS as these results suggest osmo- and calcium dysregulation, coelomocyte responses, and presumptive opportunistic bacterial

infection in SSWS-affected sea stars. This information provides potential future research applications for the development of treatment strategies for sea stars in managed care and for understanding the complexity of various biochemical and cellular pathophysiological mechanisms involved in sea star wasting.

Keywords: chemistry, cytology, echinoderm disease, invertebrate, ochre sea star, osmolality

INTRODUCTION

Sea star wasting or mass stranding events have been reported since the 1960s along the North American Pacific (1, 2) and Atlantic Coasts (3–6) as well as the Mediterranean Sea (7), Atlantic coast of Europe (8), and East China Sea (9). These historical wasting events were limited in geographic scope and impacted only a few species. Sea Star Wasting Syndrome (SSWS) is one of the largest recorded marine wildlife die-offs, resulting in death of millions of sea stars from more than 20 species from 2013 until 2015 (10). Sea Star Wasting Syndrome was first noted off the coast of the Pacific Northwest in mid-2013 and later impacted sea stars from Southern Alaska to Baja California, Mexico (11, 12). The ochre sea star (*Pisaster ochraceus*), the keystone species of the rocky intertidal zone (13), was among the most heavily affected species. The resulting collapse of sea star populations caused a trophic cascade with large scale, complex effects on marine invertebrate population dynamics along the Pacific Coast (14).

Sea Star Wasting Syndrome impacted sea stars begin to show behavioral changes of abnormally curled rays and inability to grasp substrate, progressing to exhibit white epidermal lesions, ray autotomy, loss of turgor (deflation), and loss of structural integrity leading to disintegration and eventual death (11, 12). The progression of clinical observations can be rapid, typically leading to death within days (15). Histologically, wasting sea stars consistently exhibit epidermal degeneration, necrosis, and ulceration with dermal separation, necrosis, and inflammation (16). The etiology for these histological changes has not been determined to date.

There is evidence that marine echinoderm mass mortality events may be associated with pathogens and/or environmental stressors and it is presumed that various underlying etiologies or inciting causes may result in similar clinical signs characteristic for SSWS (10). For this reason, we have chosen to use the terminology Sea Star Wasting Syndrome rather than Sea Star Wasting Disease as it was initially referred to in previous publications by various authors (11, 12). Due to limited types of tissue reactions to pathogens and other stressors in echinoderms, various disease processes reportedly result in similar clinical and histopathological manifestations (16). The ultimate cause(s) of the 2013–2015 SSWS event as well as most historical and more recent observations of sea star wasting in various geographical areas are still unknown. No infectious causes were definitively linked to SSWS, although a densovirus and a novel circular DNA virus were isolated from *Pycnopodia helianthoides* (11) and *Asterias forbesi* (17), respectively. Associations between increased ocean temperature and clinical signs of wasting have been identified for *P. helianthoides* (18), *P. ochraceus* (19, 20), and *Astropecten johnstoni* (7). In contrast to those reports, wasting of *P. ochraceus* along the Oregon coast was linked to decreased temperature (12), but no clear association between temperature and SSWS was found based on an analysis of 20 years of data from 88 geographical sites (15).

Coelomic fluid fills the coelomic cavity and surrounds the internal organs of asteroid sea stars, so it can provide information on systemic biochemical and cellular processes and potential response mechanisms to disease. Coelomocytes, the invertebrate counterpart to vertebrate leukocytes, are an integral part of the sea star immune system and circulate in coelomic fluid. They are responsible for cellular innate immune defense through interactions with the complement system, cytokines, lectins, antimicrobial peptides, proteins, clotting factors, and protein mediators that facilitate cellular adhesion (21–23). Sea stars are osmoconformers when placed in hypertonic and hypotonic sea water, equilibrating inorganic ions within 24 h (24). Sea stars are isoionic with seawater and appear capable of minimally maintaining ionic homeostasis for potassium and calcium (25–27). They are able to regulate their coelomic fluid volume through unknown mechanisms (28, 29).

While coelomocyte concentrations (30–32) and chemistry data (24, 32) have been published for clinically normal sea stars, no comparisons between SSWS affected and clinically normal sea stars have been published to date. The objectives of this study were to (1) evaluate changes in coelomic fluid chemistry, coelomocyte counts, and cytology from ochre sea stars ($n = 55$) with clinical signs consistent with SSWS at varying intensity score on a grading scale of 1–5 in comparison to coelomic fluid from clinically normal sea stars ($n = 26$) and to (2) correlate SSWS score with cellular and biochemical analytes.

MATERIALS AND METHODS

Coast-inhabiting ochre sea stars were collected from Puget Sound ranging from several days to several weeks prior to this study during spring 2015. Sea stars were categorized as early-adult if their arm radius was 8–10 cm and late-adult if their arm radius was >10 cm. The sea stars were clinically normal at time of collection and the entire cohort of these collected sea stars began to show signs consistent with SSWS once under managed care. This was expected and considered a progression of disease in these animals collected from areas knowingly affected by this syndrome. The occurrence and progression of clinical signs observed for these sea stars was consistent with those concurrently reported for free-ranging sea stars (20). The sea

stars were adults of unknown age at time of coelomic fluid sampling when showing clinical evidence of SSWS in June and July 2015. The sea stars were maintained in several well-established, natural sea water flow-through quarantine tanks with an average temperature 10°C (50°F) and average pH 7.8 and species-appropriate husbandry (33) at the Seattle Aquarium, an Association of Zoo and Aquariums-accredited facility. Water quality parameters, including salinity, were measured at least every 7 days. Clinically normal sea stars ($n = 26$) that were collected several years before SSWS in the area and well-established at the aquarium were maintained in a similar manner but in display tanks separate from the sea stars with clinical evidence of wasting (32).

Sea stars were scored at the time of coelomic fluid sampling on a SSWS grading scale of 1–5 adapted from a scoring system proposed by Bates et al. (19) as briefly outlined in the following and **Table 1**. Grade 0 sea stars were clinically normal on visual and physical examination and displayed appropriate activity and feeding behaviors. Grade 1 sea stars had mild disease without white lesions. These sea stars often displayed central disc flattening, lack of adherence to substrate, mild swelling of arms, and abnormal wrapping of arms at rest. Grade 2 sea stars had mild disease with small white lesions. These lesions were restricted to one arm or only the central disc. Grade 3 sea stars had moderate disease with white lesions found on one arm plus the central disc or two arms or an arm/disc interface. Grade 4 sea stars had severe disease. These sea stars had lesions found on three or more arms or two arms plus central disc or arm/disc interface plus arm or central disc or more than one arm/disc interface lesion. Grade 5 sea stars had severe disease with one or more arms detached from the central disc or the sea star was found unresponsive, unattached to the substrate and with no tube foot movement.

Native coelomic fluid was collected from the perivisceral coelomic cavity using a 23-ga. 2.5 cm needle and syringe ∼1 cm from the distal tip of a ray on the aboral surface of the sea star. A total volume of at least 1.0 ml was collected per individual. Prior to performing necropsies of deceased sea stars (SSWS score 5), all collectable coelomic fluid was aspirated. Coelomic fluid was transferred into aliquots with and without additives as outlined in the following.

TABLE 1 | Clinical observations based on a 1–5 grading scale in sea stars affected by Sea Star Wasting Syndrome, adapted from Bates et al. (19).

Score	Description
0	Clinically normal
1	Mild disease, no white lesions; often central disc flattening, lack of adherence to substrate, mild swelling of arms, and abnormal wrapping of arms at rest
2	Mild disease with small white lesions restricted to one arm or only the central disc
3	Moderate disease with white lesions on one arm plus the central disc OR two arms OR an arm/disc interface
4	Severe disease; white lesions on three or more arms OR two arms plus central disc OR arm/disc interface plus arm or central disc OR more than one arm/disc interface lesion
5	Severe disease; one or more arms detached from the central disc OR non-responsive, detached from substrate and lacking tube foot movement

Samples of 200 µl native, undiluted coelomic fluid were transferred into lithium heparin microtubes and analyzed for magnesium, sodium, potassium, chloride, calcium, and total protein (Ortho Vitros 250 analyzer, Ortho Clinical Diagnostics, Rochester, New York 14626 USA). Osmolality was measured in coelomic fluid aliquots without any additives or anticoagulants using a freezing point depression osmometer (Advanced Instruments Osmometer, model 3320, Norwood, MA) at Cornell University's Animal Health Diagnostic Center.

After coelomic fluid collection, direct smears were immediately prepared for dry mount cytology using native coelomic fluid. Coelomic fluid was placed in both lithium heparin and ethylenediaminetetraacetic acid (EDTA) micro tubes (Sarstedt Inc., Princeton, NJ). Formalin preparations of 50 µl coelomic fluid in 200 µl 10% neutral buffered formalin and 50 µl EDTA coelomic fluid in 200 µl 10% neutral buffered formalin were prepared for coelomocyte counts for comparison (34). Sediment smears were prepared after centrifugation of 200 µl of coelomic fluid at 605 relative centrifugal force (RCF) for 10 min, drawing off the supernatant, re-suspending the pellet in 50 µl supernatant, and preparation of smears from this concentrated cellular material for dry mount cytology. Direct and sediment dry mount smears were air-dried and stained with Wright-Giemsa (Harleco®, EMD Millipore, Billerica, Massachusetts, USA) for cytological evaluation by one investigator who was blinded to animal ID and SSWS score. Manual coelomocyte counts were performed on native (non-EDTA preserved) and EDTA-anticoagulated formalin fixed preparations as described for lobster hemolymph and fish blood in due consideration of the dilution factor resulting from formalin dilution (34).

Statistical analyses were performed in the programming language Python (Version 3.7.3) using the numerical library SciPy (Version 1.3.0). The full source code is freely available for review at https://bit.ly/2OmrMt1. To determine if there was a statistically significant difference in salinity between different systems and sampling dates, a Kruskal Wallis H-test (one-way ANOVA on ranks) was performed as this data did not meet the assumption of normality. The assumption of normality was only met in clinically normal sea stars for magnesium, sodium, potassium, chloride, and calcium (32) and for sodium, chloride and calcium in SSWS-affected sea stars per D'Agostino and Pearson's test. To determine if there was a statistically significant difference ($P \leq 0.05$) between the distributions of tested analytes, osmolality, and coelomocyte counts from SSWS-affected sea stars and those from clinically normal sea stars, a Welch's t-test was selected for analytes that met the assumption of normality and a non-parametric Kruskal-Wallis H-test for those that did not. A paired t-test was used to evaluate if there was a difference in cell counts between formalin preparations with EDTA and those with native coelomic fluid. To evaluate the correlation between SSWS-score and analytes, a Spearman's rank-order correlation coefficient was computed and its statistical significance was determined using the t-distribution.

RESULTS

Coelomic fluid was collected from 55 SSWS-affected early-adult ($n = 22$) and late-adult ($n = 33$) sea stars. The following SSWS scores were identified: score 1: $n = 4$, score 2: $n = 2$, score 3: $n = 3$, score 4: $n = 18$, score 5: $n = 26$. The distribution of sea stars among SSWS scores represented the rapid disease progression (typically within several days) and severity observed in the collection.

Coelomic Fluid Chemistry

Biochemical analysis was performed of coelomic fluid from 41 and of osmolality from 8 SSWS-affected sea stars (**Figure 1**). Diseased sea stars demonstrated wider ranges of all chemistry data than clinically normal sea stars, except for calcium. SSWS-affected sea stars had wider ranges of electrolytes, with statistically significantly higher chloride ($P = 1.3 \times 10^{-7}$). Total protein ($P = 0.03$) was significantly higher and calcium ($P = 0.048$) significantly lower when compared to clinically normal sea stars. SSWS-affected sea stars ($n = 8$) had higher osmolality ($P = 3.4 \times 10^{-3}$) than clinically normal sea stars ($n = 6$). SSWS-affected sea star coelomic fluid chemistry and coelomocyte count data are presented in **Table 2**.

Coelomocyte Counts

Coelomocyte counts of SSWS-affected sea stars were highly variable, ranged from 0 to 60,750/μl (median: 900; mean: 6,126), and had significantly higher coelomocyte counts ($P = 1.5 \times 10^{-7}$) compared to clinically normal sea stars (median: 0; mean: 13; **Table 2**). Both formalin preparations (with and without EDTA) were consistent with each other across all samples for cell counts ($P = 0.36$). Several ($n = 15$, 27%) SSWS-affected sea stars had 0/μl coelomocyte counts; their SSWS scores were score 1: $n = 3$; score 2: $n = 1$; score 3: $n = 2$; score 4: $n = 7$; score 5: $n = 2$.

Cytological Evaluation

Cytological evaluation was performed on all 55 SSWS-affected sea stars. There was consistently one coelomocyte type present with morphology of the mononuclear phagocyte morphotype based on previous descriptions of coelomocyte morphology (23, 31). The coelomocytes were vacuolated in 10 samples (18%) and/or had phagocytized pink or basophilic material of undetermined origin in 32 samples (58%). Free ($n = 3$), phagocytized ($n = 5$), or both free and phagocytized ($n = 8$) bacteria were present in 16 samples (29%). The bacteria were predominantly plump or bipolar bacilli ($n = 14$), coccobacilli with concurrent bacilli ($n = 1$), or coccobacilli with concurrent bacilli and diplococci ($n = 1$). Unknown extracellular basophilic material was noted in 20 samples (36%) and material suggestive of proteinaceous origin or nucleoproteinaceous necrotic debris in 36 samples (65%). There were frequently lysed and disintegrated cells in 35 samples (64%). Crystals suggestive of cholesterol crystals were seen in 9 samples (16%), crystals suggestive of salt origin in 17 samples (31%), and mineral material in 7 samples (13%). Representative images of cytological findings are included in **Figure 2**.

Clinically normal sea stars reportedly have the same predominant coelomocyte morphotype suggestive of the mononuclear phagocyte morphotype, extracellular crystals suggestive of salt origin, and no bacteria or other microorganisms (32).

Sea Star Wasting Syndrome Score

SSWS score was significantly correlated with higher chloride concentration (rho = 0.63, $P = 2.44 \times 10^{-8}$), coelomocytes (rho = 0.67, $P = 1.54 \times 10^{-11}$), and osmolality (rho = 0.85, $P = 2.54 \times 10^{-4}$). The association between SSWS score and analytes is included in **Figure 3**.

Tank Water Salinity

Salinity was maintained between 29 and 32 ppt during the sampling period. There was no significant difference in salinity between different systems and sampling dates ($P = 0.12$), including comparisons of tank systems of SSWS-affected seas stars and those holding clinically normal sea stars.

DISCUSSION

This is the first report of comprehensive coelomic fluid analysis in SSWS-affected sea stars showing evidence of biochemical and cellular alterations pointing toward potential underlying pathophysiological processes associated with the syndrome.

Dysregulation of Critical Biochemical Regulatory Processes Are Presumptively Involved in Sea Star Wasting Syndrome Pathophysiology

The significant increases in chloride, total protein, and osmolality suggest osmodysregulation. The increase in coelomic fluid osmolality may indicate that SSWS-affected sea stars are actively concentrating one or more active osmolytes; additional considerations include that energy-dependent cross-membranal transport mechanisms and/or pumps may be affected by wasting, or that protein may leak into the coelom due to cellular apoptosis and/or necrosis. If sea stars are truly becoming hyperosmotic to seawater by a yet unknown mechanism or cumulative mechanisms, this could explain why relatively hypoosmotic seawater could penetrate tissues and cause biochemical homoeostatic imbalances as seen in SSWS. Histopathology of sea stars with clinical signs consistent with SSWS showed extensive necrosis, epidermal ulceration, and dermal separation (16). In a study with ochre sea stars exposed to changes in salinity, coelomic fluid chloride concentrations approximated those of seawater, thus suggesting sea stars may not actively regulate chloride homeostasis (27). Although the sample size tested for osmolality was limited, our results provide evidence for osmodysregulation in sea stars affected by SSWS and an incentive for further study of osmoregulatory pathways.

Season and reproductive cycle stage have been associated with effects on the ionic regulation in *Asterias* (25, 35, 36).

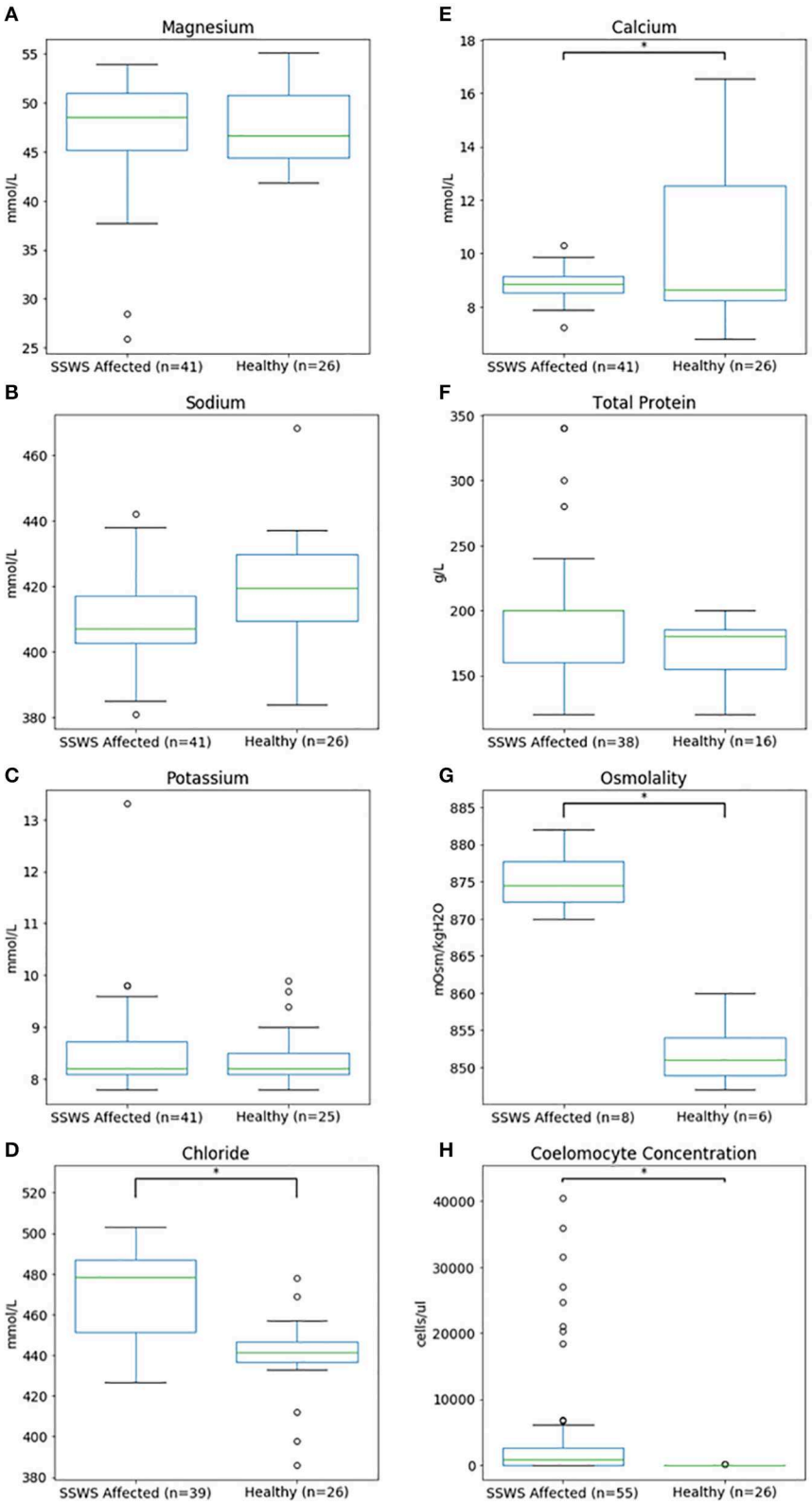

FIGURE 1 | Box plots comparing coelomic fluid chemistry data **(A–F)**, osmolality **(G)**, and coelomocyte counts **(H)** of *Pisaster ochraceus* showing clinical signs consistent with Sea Star Wasting Syndrome compared to clinically normal *P. ochraceus*. *Denotes statistical significance ($P < 0.05$).

TABLE 2 | Coelomic fluid chemistry data and coelomocyte counts of *Pisaster ochraceus* showing clinical signs consistent with Sea Star Wasting Syndrome.

Analyte	Units	*n*	Mean	SD	Median	Range	90% CI*
Magnesium	mmol/L	41	46	7.5	48	16–54	43–53
Sodium	mmol/L	41	412	15.8	407	381–463	396–442
Potassium	mmol/L	41	8.8	1.9	8.2	7.8–19.1	8.0–9.0
Chloride	mmol/L	39	473	25.7	479	427–553	416–461
Calcium	mmol/L	41	8.7	1.0	8.9	4.2–10.3	7.4–13.7
Total Protein	g/L	38	21	69.6	20	<10–50	Range: <10–20
Coelomocytes	#/μl	55	6126	12393.1	900	0–60,750	Range: 0–180
Osmolality	mOsm/kgH_2O	8	875	4.3	875	870–882	NA

CI, Confidence Interval for clinically normal sea stars; NA, not available.*
**Wahltinez et al. (32). #Number of cells.*

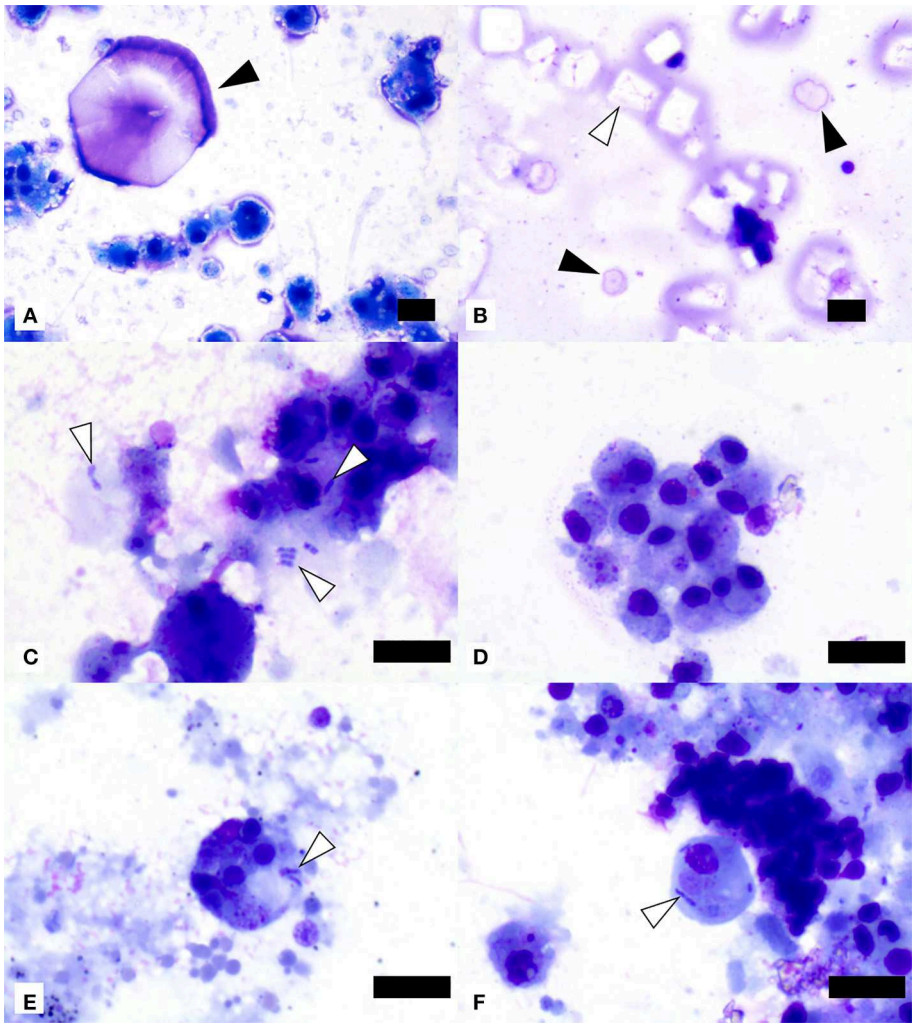

FIGURE 2 | Image composite of coelomic fluid sediment smear preparations from ochre sea stars (*Pisaster ochraceus*) affected by Sea Star Wasting Syndrome. **(A)** Presumptive salt crystal (black arrowhead) and mononuclear phagocyte morphotype cells showing variable vacuolation. **(B)** Presumptive cholesterol crystals (one example shown by white arrowhead) and two presumptive salt crystals (black arrowheads). **(C)** Extracellular and phagocytized bacilli (white arrowheads) in close association with mononuclear phagocyte morphotype cells. **(D)** Mononuclear phagocyte morphotype cells with variable amounts of phagocytized material of undetermined origin. **(E,F)** Two mononuclear phagocyte morphotype cells with phagocytized small bacilli (white arrowheads). Scale bars = 10 μm.

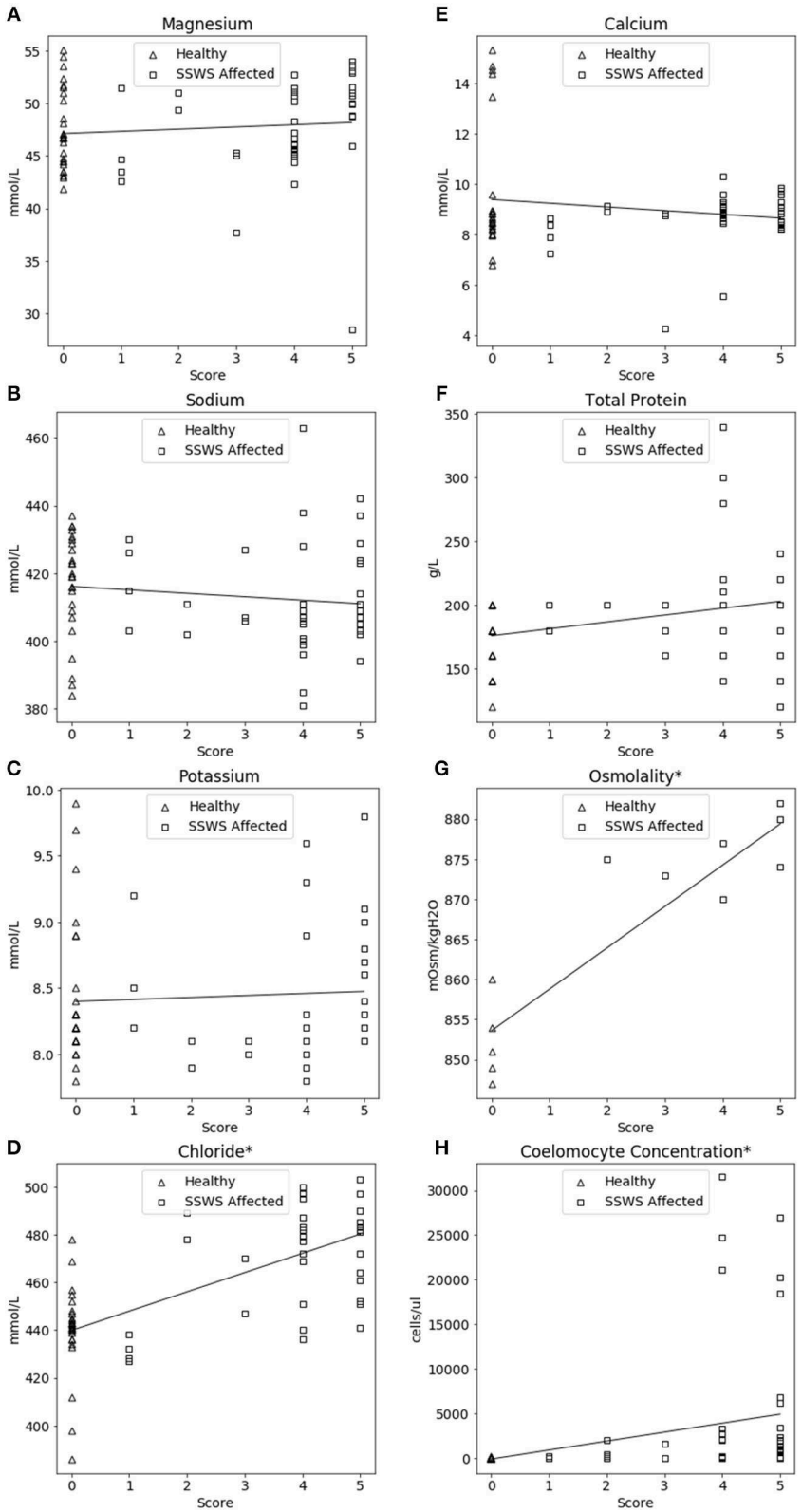

FIGURE 3 | Correlation plots comparing coelomic fluid chemistry data **(A–F)**, osmolality **(G)**, and coelomocyte counts **(H)** of *Pisaster ochraceus* showing clinical signs consistent with Sea Star Wasting Syndrome (SSWS) compared with clinically normal *P. ochraceus* grouped by SSWS Score (0–5). *Denotes statistical significance ($P < 0.05$).

Season is unlikely to have contributed to the differences described in this study as coelomic fluid from SSWS and clinically normal sea stars was sampled in the boreal summer. Sea stars with clinical signs consistent with SSWS were often noted to spawn in later stages of wasting. Spawning may occur as a terminal behavior in response to electrolyte changes or other stressors.

Mutable collagenous tissue (MCT) is unique to echinoderms and capable of rapid, neuronal-mediated changes in tensile strength that are not due to muscle fibers (37–39). In sea stars, MCT has been found in the body wall (40, 41), in ligaments at spine joints, and in the stem of tube feet (42). The effect of ion concentrations on MCT variable tensility has been studied extensively on *in-vitro* preparations, primarily of holothurian dermis. Samples of MCT placed in solutions with higher calcium concentrations display stiffening, while MCT samples placed in solutions with decreased calcium concentrations result in softening (43–48). The SSWS-affected sea stars with significantly lower coelomic fluid calcium concentrations all displayed softening of the body wall and lesions of the integument, suggesting MCT involvement in SSWS progression. However, clinically normal sea stars had wider ranges of coelomic fluid calcium concentrations, including some calcium values lower than the SSWS-affected sea stars, and all clinically normal sea stars displayed normal MCT stiffness. Given the altered calcium regulation in SSWS-affected sea stars in this study, further studies could investigate the effect of ion concentrations on MCT *in-vivo*, how ion channels impact MCT mutability and integrity, and mechanisms for changes to ion concentrations in coelomic fluid.

Sea Star Wasting Syndrome-Affected Sea Stars Show Active Cellular Immune Responses

The observed higher coelomocyte counts in SSWS sea stars suggest active cellular immune responses similar to studies that have demonstrated that environmental stressors and disease can result in increased circulating coelomocytes in echinoderms (30, 49, 50). The lack of differences in coelomocyte counts in EDTA- and heparin-preserved samples indicate that either anticoagulant can be used. At this time, it is unknown whether the use of anticoagulants is necessary for coelomic fluid analysis and if native coelomic fluid can be used for coelomocyte counts. Further study is warranted.

Several (n = 15, 27%) SSWS-affected sea stars had coelomocyte counts of 0/μl which was inconsistent with increased coelomocyte numbers observed in the majority of SSWS-affected sea stars. This may represent an artificial decrease due to cellular clumping or aggregation (51); however, cell clumping was only noted in 12 samples with counts above 810/μl, none of which had a zero coelomocyte count. In addition, the observed low coelomocyte counts in SSWS-affected sea stars may have resulted from individual variation in disease progression or an individual's inability to mount an effective immune response due to external factors resulting in immunocompromise. Previous studies have shown that temperature, salinity, and/or parasitism impact coelomocyte response and sea star immunity, although none of these factors were noted in the sea stars in the current study (30).

The free and phagocytized bacteria presumptively represent secondary infection due to disturbance(s) in body wall integrity as they were not identified in the majority of SSWS coelomic fluid samples, but in none from unaffected sea stars. Culture of coelomic fluid was beyond the scope of this study and not attempted. The basophilic and proteinaceous material as well as the presumptive cholesterol crystals noted on cytology are probably due to apoptosis or necrosis as described by meta-transcriptomic analysis (52) and histopathology (16) in SSWS-affected sea stars.

Sea Star Wasting Syndrome Severity Correlates With Biochemical and Cellular Changes

The significant correlations between SSWS score with chloride, osmolality, and coelomocyte counts are consistent with the direct comparison of SSWS-affected and clinically normal sea stars. However, due to the low sample size for osmolality those results should be interpreted cautiously. The SSWS score appears to have a predictive ability with chloride, osmolality, and coelomocyte counts and reflect severity of clinical disease.

CONCLUSIONS

The results of this study provide guidance for future studies of sea star osmo- and calcium regulatory pathways and cellular immune functions. This study provides information on chemical and basic cellular components in coelomic fluid of SSWS- affected sea stars, furthering our understanding of the pathophysiology of this devastating syndrome. Evaluation of calcium, chloride, total protein, osmolality, and coelomocyte counts in individuals or a cohort of sea stars, in comparison with the biochemical composition of their surrounding water, may provide an earlier diagnosis of onset of disease and advanced disease states. By understanding that osmoregulation is impacted by SSWS, therapeutic targets and interventions may be created to stop or reverse disease progression in individuals under managed care. The evidence of an opportunistic bacterial infection suggests why there are anecdotal reports of SSWS-affected sea stars responding to antimicrobial therapy but failing to respond in other cases. Treating these secondary infections may allow individual sea stars to more effectively compensate for the primary problem. Enrofloxacin has been shown to reach therapeutic levels via intracoelomic injection (53) and may be useful depending on antimicrobial sensitivity testing. Furthermore, the application of the information provided herein provide insight into potential complex pathophysiological mechanisms of SSWS and lays the groundwork for future research strategies

relevant to the conservation of sea stars as keystone species in marine ecosystems.

DATA AVAILABILITY STATEMENT

The datasets generated for this study are available on request to the corresponding author.

ETHICS STATEMENT

Although Institutional Animal Care and Use Committee review is not required for non-cephalopod invertebrates, this study was conducted in adherence to general ethical principles.

AUTHOR CONTRIBUTIONS

LL and AN were responsible for study design. SW collected coelomic fluid samples with the oversight of LL. SW and NS drafted the manuscript. All authors assisted in writing and editing of the manuscript and performed data analysis and interpretation.

FUNDING

This work was supported by the Boeing Company through a private grant for Sea Star Wasting Syndrome-related research through the Seattle Aquarium. Routine biochemistry analyses were funded by the University of Miami Avian and Wildlife Laboratory.

ACKNOWLEDGMENTS

The authors thank Dr. Carolyn Cray and the University of Miami Avian and Wildlife Laboratory for performing electrolyte analyses, Oscar Wahltinez for computational/statistical analysis support, and Amy Olsen and Angela Smith of Seattle Aquarium for their help with water quality data.

REFERENCES

1. Dungan ML, Miller TE, Thomson DA. Catastrophic decline of a top carnivore in the Gulf of California rocky intertidal zone. *Science.* (1982) 216:989–91. doi: 10.1126/science.216.4549.989
2. Eckert GL, Engle JM, Kushner DJ. Sea star disease and population declines at the channel Islands. In: *Proceedings of the Fifth California Islands Symposium.* (Santa Barbara, CA) (2000). p. 390–3.
3. Sieling FW. Mass mortality of the starfish, Asterias forbesi, on the Atlantic coast of Maryland. *Chesap Sci.* (1960) 1:73–4. doi: 10.1007/BF02688260
4. Tiffany WJ. Mass mortality of Luidia senegalensis (Lamarck, 1816) on Captiva Island, Florida, with a note on its occurrence in Florida Gulf coastal waters. *Florida Sci.* (1978) 41:63–4.
5. Menge B. Coexistence between the seastars *Asterias vulgaris* and *A. forbesi* in a heterogenous environment: a non-equilibrium explanation. *Oecologia.* (1979) 272:245–72. doi: 10.1007/BF00377430
6. Bucci C, Francoeur M, McGreal J, Smolowitz R, Zazueta-Novoa V, Wessel GM, et al. Sea star wasting disease in *Asterias forbesi* along the Atlantic coast of North America. *PLoS ONE.* (2017) 12:1–20. doi: 10.1371/journal.pone.0188523
7. Staehli A, Schaerer R, Hoelzle K, Ribi G. Temperature induced disease in the starfish Astropecten jonstoni. *Mar Biodivers Rec.* (2009) 2:1–6. doi: 10.1017/S1755267209000633
8. Thorpe JP, Spencer EL. A mass stranding of the asteriod *Asterias rubens* on the Isle of man. *J Mar Biol Assoc UK.* (2000) 80:749–50. doi: 10.1017/S0025315499002659
9. Suzuki G, Kai S, Yamashita H. Mass stranding of crown-of-thorns starfish. *Coral Reefs.* (2012) 31:821. doi: 10.1007/s00338-012-0906-z
10. Hewson I, Sullivan B, Jackson EW, Xu Q, Long H, Lin C, et al. Perspective: something old, something new? review of wasting and other mortality in asteroidea (echinodermata). *Front Mar Sci.* (2019) 6:1–8. doi: 10.3389/fmars.2019.00406
11. Hewson I, Button JB, Gudenkauf BM, Miner B, Newton AL, Gaydos JK, et al. Densovirus associated with sea-star wasting disease and mass mortality. *Proc Natl Acad Sci USA.* (2014) 111:17278–83. doi: 10.1073/pnas.1416625111
12. Menge B, Cerny-Chipman E, Johnson A, Sullivan J, Gravem S, Chan F. Sea star wasting disease in the keystone predator Pisaster ochraceus in Oregon: insights into differential population impacts, recovery, predation rate, and temperature effects from long-term research. *PLoS ONE.* (2016) 11:e0153994. doi: 10.1371/journal.pone.0153994
13. Paine RT. Food web complexity and species diversity. *Am Nat.* (1966) 100:65–75. doi: 10.1086/282400
14. Schultz JA, Cloutier RN, Côté IM. Evidence for a trophic cascade on rocky reefs following sea star mass mortality in British Columbia. *PeerJ.* (2016) 4:e1980. doi: 10.7717/peerj.1980
15. Miner CM, Antrim L, Fradkin SC, Miner BG, Murray SN, Smith JR, et al. Large-scale impacts of sea star wasting disease (SSWD) on intertidal sea stars and implications for recovery. *PLoS ONE.* (2018) 13:e0192870. doi: 10.1371/journal.pone.0192870
16. Newton AL, Smolowitz R. Invertebrates. In: Terio KA, McAloose D, St. Leger J, editors. *Pathology of Wildlife and Zoo Animals.* (Cambridge, MA: Elsevier Inc.) (2018). p. 1019–52. doi: 10.1016/B978-0-12-805306-5.00041-9
17. Fahsbender E, Hewson I, Rosario K, Tuttle AD, Varsani A, Breitbart M. Discovery of a novel circular DNA virus in the Forbes sea star, Asterias forbesi. *Arch Virol.* (2015) 160:2349–51. doi: 10.1007/s00705-015-2503-2
18. Harvell CD, Montecino-Latorre D, Caldwell JM, Burt JM, Bosley K, Keller A, et al. Disease epidemic and a marine heat wave are associated with the continental-scale collapse of a pivotal predator (*Pycnopodia helianthoides*). *Sci Adv.* (2019) 5:eaau7042. doi: 10.1126/sciadv.aau7042
19. Bates AE, Hilton BJ, Harley CDG. Effects of temperature, season and locality on wasting disease in the keystone predatory sea star Pisaster ochraceus. *Dis Aquat Organ.* (2009) 86:245–51. doi: 10.3354/dao02125
20. Eisenlord ME, Groner ML, Yoshioka RM, Elliott J, Maynard J, Fradkin S, et al. Ochre star mortality during the 2014 wasting disease epizootic: role of population size structure and temperature. *Philos Trans R Soc Lond B Biol Sci.* (2016) 371:20150212. doi: 10.1098/rstb.2015.0212
21. Beck G, Habicht GS. Isolation and characterization of a primitive interleukin-1-like protein from an invertebrate, Asterias forbesi. *Proc Natl Acad Sci USA.* (2006) 83:7429–33. doi: 10.1073/pnas.83.19.7429
22. Leonard LA, Strandberg JD, Winkelstein JA. Complement-like activity in the sea star, Asterias forbesi. *Dev Comp Immunol.* (1990) 14:19–30. doi: 10.1016/0145-305X(90)90004-X
23. Smith LC, Ghosh J, Buckley KM, Clow LA, Dheilly NM, Haug T, et al. Echinoderm immunity. In: Soderhall K, editor. *Invertebrate Immunity*. Boston: Springer Publishing (2010). p. 260–301. doi: 10.1007/978-1-4419-8059-5_14
24. Diehl WJ, Lawrence JM. The effect of salinity on coelomic fluid osmolyte concentration and intracellular water content in Luidia clathrata (Say) (Echinodermata: Asteroidea). *Comp Biochem Physiol Part A Physiol.* (1984) 79:119–26. doi: 10.1016/0300-9629(84)90718-7
25. Binyon J. Ionic regulation and mode of adjustment to reduced salinity of the starfish Asterias rubens L. *J Mar Biol Assoc UK.* (1962) 42:49–64. doi: 10.1017/S0025315400004458

26. Stickle WB, Denoux GJ. Effects of *in situ* tidal salinity fluctuations on osmotic and ionic composition of body fluid in Southeastern Alaska rocky intertidal fauna. *Mar Biol.* (1976) 37:125–35. doi: 10.1007/BF00389123
27. Held MBE, Harley CDG. Responses to low salinity by the sea star Pisaster ochraceus from high- and low-salinity populations. *Invertebr Biol.* (2009) 128:381–90. doi: 10.1111/j.1744-7410.2009.00175.x
28. Pearse JS. Coelomic water volume control in the antarctic sea-star Odontaster validus. *Nature.* (1967) 216:1118–9. doi: 10.1038/2161118a0
29. Ellington WR, Lawrence JM. Coelomic fluid volume regulation and isosmotic intracellular regulation by Luidia clathrata (Echinodermata: Asteroidea) in response to hyposmotic stress. *Biol Bull.* (1974) 146:20–31. doi: 10.2307/1540394
30. Coteur G, Corriere N, Dubois P. Environmental factors influencing the immune responses of the common European starfish (*Asterias rubens*). *Fish Shellfish Immunol.* (2004) 16:51–63. doi: 10.1016/S1050-4648(03)00030-5
31. Pinsino A, Thorndyke MC, Matranga V. Coelomocytes and post-traumatic response in the common sea star Asterias rubens. *Cell Stress Chaperones.* (2007) 12:331–41. doi: 10.1379/CSC-288.1
32. Wahltinez SJ, Stacy NI, Lahner LL, Newton AL. Coelomic fluid evaluation in clinically normal Ochre sea stars Pisaster ochraceus: cell counts, cytology, and biochemistry reference intervals. *J Aquat Anim Health.* (2019) 31:239–43. doi: 10.1002/aah.10072
33. Böttger SA, Walker CW, Unuma T. Care and maintenance of adult echinoderms. In: Ettnsohn CA, Wray GA, Wessel GM, editors. *Methods in Cell Biology*, 74th edn. Cambridge: Academic Press (2006). p. 17–38. doi: 10.1016/S0091-679X(04)74002-9
34. Arnold JE, Matsche MA, Rosemary K. Preserving whole blood in formalin extends the specimen stability period for manual cell counts for fish. *Vet Clin Pathol.* (2014) 43:613–20. doi: 10.1111/vcp.12214
35. Robertson JD. The inorganic composition of the body fluids of three marine invertebrates. *J Exp Biol.* (1939) 16:387–97.
36. Robertson JD. Ionic regulation in some marine invertebrates. *J Exp Biol.* (1949) 26:182–200.
37. Motokawa T. Connective tissue catch in echinoderms. *Biol Rev.* (1984) 59:255–70. doi: 10.1111/j.1469-185X.1984.tb00409.x
38. Wilkie IC. Is muscle involved in the mechanical adaptability of echinoderm mutable collagenous tissue? *J Exp Biol.* (2002) 205:159–65.
39. Wilkie IC. Mutable collagenous tissue: overview and biotechnological perspective. *Prog Mol Subcell Biol.* (2005) 39:221–50. doi: 10.1007/3-540-27683-1_10
40. Wilkie I, Griffiths G, Glennie S. Morphological physiological aspects of the autotomy plane in the aboral integument of *Asterias rubens* L. (Echinodermata). In: Jangoux M, editor. *Echinoderm Research.* Rotterdam: Balkema AA (1990). p. 301–13.
41. Motokawa T. Mechanical mutability in connective tissue of starfish body wall. *Biol Bull.* (2011) 221:280–9. doi: 10.1086/BBLv221n3p280
42. Motokawa T. Morphology of the spines and spine joint in the crown-of-thorns starfish *Acantaster planci* (Echinodermata, Asteroida). *Zoomorphology.* (1986) 106:247–53. doi: 10.1007/BF00312046
43. Wilkie IC. Nervously mediated change in the mechanical properties of a brittlestar ligament. *Mar Behav Physiol.* (1978) 5:289–306. doi: 10.1080/10236247809378544
44. Smith DS, Wainwright SA, Baker J, Cayer ML. Structural features associated with movement and "catch" of sea-urchin spines. *Tissue Cell.* (1981) 13:299–320. doi: 10.1016/0040-8166(81)90007-0
45. Hidaka M. Effects of certain physico-chemical agents on the mechanical properties of the catch apparatus of the sea-urchin spine. *J Exp Biol.* (1983) 103:15–29.
46. Diab M, Gilly WF. Mechanical properties and control of nonmuscular catch in spine ligaments of the sea urchin, *Strongylocentrotus franciscanus. J Exp Biol.* (1984) 111:155–70.
47. Byrne M. The mechanical properties of the autotomy tissues of the holothurian Eupentacta quinquesemita and the effects of certain physico-chemical agents. *J Exp Biol.* (1985) 117:69–86.
48. Hayashi Y, Motokawa T. Effects of ionic environment on viscosity of catch connective tissue in holothurian body wall. *J Exp Biol.* (1986) 125:71–84.
49. Grand A, Pratchett M, Rivera-Posada J. The immune response of *Acanthaster planci* to oxbile injections and antibiotic treatment . *J Mar Biol.* (2014) 2014:1–1. doi: 10.1155/2014/769356
50. Matranga V, Pinsino A, Celi M, Natoli A, Bonaventura R, Schröder HC, et al. Monitoring chemical and physical stress using sea urchin immune cells. *Prog Mol Subcell Biol.* (2005) 39:85–110. doi: 10.1007/3-540-27683-1_5
51. Kanungo K. The coelomocytes of asteroid echinoderms. In: Cheng TC, editor. *Invertebrate Blood.* Berlin: Springer (1984). p. 7–39. doi: 10.1007/978-1-4684-4766-8_2
52. Gudenkauf BM, Hewson I. Metatranscriptomic analysis of *Pycnopodia helianthoides* (Asteroidea) affected by sea star wasting disease. *PLoS ONE.* (2015) 10:1–11. doi: 10.1371/journal.pone.0128150
53. Rosenberg JF, Haulena M, Phillips BE, Harms CA, Lewbart GA, Lahner LL, et al. Population pharmacokinetics of enrofloxacin in purple sea stars (*Pisaster ochraceus*) following an intracoelomic injection or extended immersion. *Am J Vet Res.* (2016) 77:1266–75. doi: 10.2460/ajvr.77.11.1266

Conflict of Interest: The authors declare that this study received funding from Boeing Company. The funder was not involved in the study design, collection, analysis, interpretation of data, the writing of this article or the decision to submit it for publication.

Copyright © 2020 Wahltinez, Newton, Harms, Lahner and Stacy. This is an open-access article distributed under the terms of the Creative Commons Attribution License (CC BY). The use, distribution or reproduction in other forums is permitted, provided the original author(s) and the copyright owner(s) are credited and that the original publication in this journal is cited, in accordance with accepted academic practice. No use, distribution or reproduction is permitted which does not comply with these terms.

frontiers in Veterinary Science

ORIGINAL RESEARCH
published: 24 March 2020
doi: 10.3389/fvets.2020.00156

Leukocyte and Platelet Characteristics of the Giant Panda (*Ailuropoda melanoleuca*): Morphological, Cytochemical, and Ultrastructural Features

Spencer P. Kehoe[1]*, *Nicole I. Stacy*[2], *Salvatore Frasca Jr.*[2], *Tracy Stokol*[3], *Chengdong Wang*[4], *Kathryn Strayer Leach*[1], *Li Luo*[4] and *Sam Rivera*[1]

[1] Department of Veterinary Services, Zoo Atlanta, Atlanta, GA, United States, [2] Department of Comparative, Diagnostic, and Population Medicine, College of Veterinary Medicine, University of Florida, Gainesville, FL, United States, [3] Department of Population Medicine and Diagnostic Sciences, College of Veterinary Medicine, Cornell University, Ithaca, NY, United States, [4] Chengdu Research Base of Giant Panda Breeding, Northern Suburb Chengdu, Sichuan, China

OPEN ACCESS

Edited by:
Jennifer Johns,
Oregon State University, United States

Reviewed by:
Diana Schwartz,
Kansas State University, United States
Tatjana Sitt,
United States Department of Agriculture, United States

***Correspondence:**
Spencer P. Kehoe
spencerpkehoe@gmail.com

Specialty section:
This article was submitted to Veterinary Experimental and Diagnostic Pathology, a section of the journal Frontiers in Veterinary Science

Received: 17 January 2020
Accepted: 04 March 2020
Published: 24 March 2020

Citation:
Kehoe SP, Stacy NI, Frasca S Jr, Stokol T, Wang C, Leach KS, Luo L and Rivera S (2020) Leukocyte and Platelet Characteristics of the Giant Panda (Ailuropoda melanoleuca): Morphological, Cytochemical, and Ultrastructural Features. Front. Vet. Sci. 7:156. doi: 10.3389/fvets.2020.00156

The giant panda (*Ailuropoda melanoleuca*) is a vulnerable species and a charismatic member of zoological collections worldwide. Despite its importance as a representative species for global wildlife conservation efforts, no studies to date have described normal cell morphology or cytoplasmic constituents by traditional techniques such as cytochemical staining and evaluation of ultrastructural features. The objective of this study was to accurately identify and characterize the leukocytes and platelets of clinically healthy giant pandas using routine Wright-Giemsa stain, eight cytochemical stains, immunocytochemistry (CD3), and transmission electron microscopy (TEM) to further the collective understanding of normal cellular morphological features, cytochemical reactivity, and cytoplasmic contents found in health. Voluntary venipuncture was performed on four healthy individual animals (two adults and two juveniles), as part of routine preventive health evaluation. Blood was collected for routine and cytochemical stains, and into 2.5% glutaraldehyde for TEM. On Wright-Giemsa-stained blood films, leukocytes were differentiated into granulocytes (neutrophils, eosinophils, basophils) and mononuclear cells (lymphocytes, monocytes). Cytochemical staining revealed similar leukocyte and platelet staining patterns to those reported in other mammals, with some notable differences. By TEM, leukocytes with nuclear and cytoplasmic features of mononuclear cells were readily differentiated from granulocytes, and platelets had similar ultrastructural features to those reported in other mammals. Neutrophils were the predominant cell type followed by lymphocytes, while basophils were rare. Rare large or reactive lymphocytes, rare reactive monocytes, and rare large platelets were noted in apparently healthy giant pandas of this study. A unique mononuclear cell, with a moderately indented nucleus and shared cytochemical and ultrastructural characteristics of lymphocytes and monocytes, was discovered in this species. The combined cytochemical, immunocytochemical (CD3), and ultrastructural features of these unique cells more closely resemble those of monocytes, but the definitive cell

lineage remains unknown at this time. This study provides novel information on giant panda leukocyte morphology and cellular constituents in health, shows the importance of manual blood film review, has important implications for hemogram interpretation in future clinical cases and research, and provides a baseline for future characterization and understanding of hemogram changes in response to disease.

Keywords: *Ailuropoda melanoleuca*, cytochemistry, giant panda, hematology, immunocytochemistry, leukocyte morphology, transmission electron microscopy, *Ursidae*

INTRODUCTION

The giant panda (*Ailuropoda melanoleuca*) is an endemic species to China, living in small populations isolated by fragmented landscapes and mountain ranges (1). Despite being an iconic animal and flagship species for global conservation efforts, the International Union for the Conservation of Nature's (IUCN) Red List recently downgraded the giant panda's status from endangered to vulnerable in 2016. Previously, the most prominent threat to the population was deforestation and consequent habitat loss. However, China's efforts to protect and restore the native forests where these animals live have been a major driving factor for the increasing population trend of giant pandas in the wild from ∼1,596 in 2003 to 1,864 in 2016, and the subsequent reduction in their status (2–5). Despite no longer being classified as endangered, concern remains regarding their status as habitat fragmentation, population isolation, increasing livestock encroachment, infrastructure development, and tourism have emerged as new threats to the survival of the species (1, 2, 5–11). Of particular concern is the rapid rate of climate change and associated habitat changes, which may lead to additional loss of habitat by more than 50% according to some models (6, 8–10).

Given the continued concern for the conservation status of the giant panda, it is imperative to monitor these animals for infectious diseases of concern to the species and relevant environmental and anthropogenic risks. An essential requirement of any monitoring or disease identification program is knowledge of basic health parameters, such as behavior, morphometrics, physical findings, and results of clinical pathological and infectious disease testing. These parameters allow for the comprehensive evaluation of individuals or groups of animals under managed care or in the wild (12). One useful and readily available tool utilized for this purpose is hematological evaluation, as changes in hematological analytes can support the diagnosis of stress or various infectious or inflammatory conditions that might affect these animals.

Despite the importance of the giant panda, only two studies to date have provided limited descriptions of hematological findings and reference ranges (13, 14) in a low number of apparently healthy giant pandas ($n = 17$ and $n = 7$, respectively). However, neither of these studies provided a detailed description of normal white blood cell (WBC) morphological features or cytoplasmic constituents, as determined by cytochemical staining and electron microscopy. These techniques have been utilized successfully in various other non-domestic mammalian and non-mammalian species (15–17) to assist with accurate identification of cell lineages and detailed morphological characterization of blood cells, and to facilitate understanding of their functions. Correct leukocyte identification in turn allows for more accurate hemogram interpretation, which has clinical implications for the management and care of these animals. It is important to have baseline information on the morphological features, cytochemical staining characteristics, and cellular constituents of leukocytes in healthy pandas, so that deviations from the norm may be readily recognized. This will allow clinicians to better understand how the giant panda responds at the cellular level to disease, stress, and physiological conditions, such as growth, ageing, reproduction, and changes in habitat/diet in wild animals or husbandry in captive animals.

The purpose of this study was to describe and characterize leukocytes and platelets in the blood of clinically healthy captive giant pandas using Wright-Giemsa (a routine Romanowsky hematological stain), eight cytochemical stains, and transmission electron microscopy (TEM). With this data, we sought to establish baseline data for the typical morphological features and cytoplasmic constituents of leukocytes and platelets in the blood of healthy giant pandas. The information gained from this work will impact hemogram interpretation in future clinical cases and research, allow for more accurate hematological reference interval determination following the guidelines set forth by the American Society of Veterinary Clinical Pathology (18), and improve our understanding of leukocyte changes in response to disease, stress, and physiological changes in free-ranging and captive giant pandas.

MATERIALS AND METHODS

Ethics Statement: This study was carried out in accordance with all state, federal, international, and institutional guidelines, with an approved institutional animal care and use committee protocol (UF IACUC# 201706823).

Four clinically healthy giant pandas, consisting of one adult male and female and two juvenile females, were utilized for this study. All animals were housed at Zoo Atlanta, an Association of Zoos and Aquariums-accredited institution, which is one of only three institutions currently housing the eight giant pandas in the United States. Blood collection was performed

Abbreviations: TEM, transmission electron microscopy; EDTA, ethylenediaminetetraacetic acid; PVC, polyvinyl chloride; ALP, alkaline phosphatase; ANBE, α-naphthyl butyrate esterase; MPx, myeloperoxidase; SBB, sudan black; CAE, chloroacetate esterase; PAS, Periodic-Acid-Schiff; TB, Toluidine blue.

as part of their annual preventive medical assessment, with all animals having been trained for phlebotomy while awake. Collection was accomplished via behavioral restraint, with each animal voluntarily placing their antebrachium into a modified phlebotomy sleeve made from polyvinyl chloride (PVC) tubing and grasping a horizontal bar (**Figure 1**). With the aid of positive reinforcement, they remained in position until shaving, alcohol preparation, and phlebotomy was complete. Blood was collected from the median antebrachial vein using a 22-gauge butterfly needle, and placed into a blood tube containing ethylenediamine tetraacetic acid (EDTA) for anticoagulation. All four animals were assessed as healthy based on a lack of reported or observed clinical abnormalities, and results of routine hematological and serum biochemical testing performed as part of their annual preventative health assessment, which were within previously published intervals for the species (13, 14).

Numerical results for hematological tests were obtained from the EDTA-anticoagulated blood with an automated Sysmex XN-10 series hematology analyzer (Sysmex America, Inc., Lincolnshire, IL). Ten standard wedge-type direct blood films were prepared from the blood and air-dried, and were used to assess leukocyte morphological characteristics via light microscopy using a Wright-Giemsa stain (Harleco®, EMD Millipore, Billerica, Massachusetts, USA) and cytochemical staining characteristics using eight stains. A board-certified clinical pathologist (NIS) performed the leukocyte differential by counting 200 WBC on two Wright-Giemsa stained blood films per animal (100 WBC per smear) and conversion to absolute numbers, as per standard laboratory practice (**Table 1**). Cytochemical staining for alkaline phosphatase (ALP), α-naphthyl butyrate esterase (ANBE), myeloperoxidase (MPx), chloroacetate esterase (CAE), and Sudan black (SBB) were performed using commercial kits (ALP, Procedure No. 85; ANBE, Procedure No. 181; MPx, Procedure No. 390; CAE, Procedure No. 91; SBB, Procedure No. 380; Sigma-Aldrich, St. Louis, MO, USA) as previously described (19), with blood from a horse (ALP and ANBE) and dog (MPx, CAE, and SBB) as positive controls. Periodic-Acid-Schiff (PAS), Toluidine blue (TB, pH 2.5–3.0), and Luna stains were performed using established protocols (20, 21), with histological sections of eosinophilic infiltrates, gastrointestinal tract, and a mast cell tumor used as positive controls. All cytochemical stains were performed at the Clinical Pathologic Laboratory in the Animal Health Diagnostic Center (AHDC) at Cornell University, and examined independently by two authors (TS and NS). The strength of the staining reaction (negative, equivocal, 1+ to 3+) and pattern of staining (diffuse in cytoplasm, granular, etc.) were subjectively graded. Only positive cytochemical reactions are provided in the text for ease of reading.

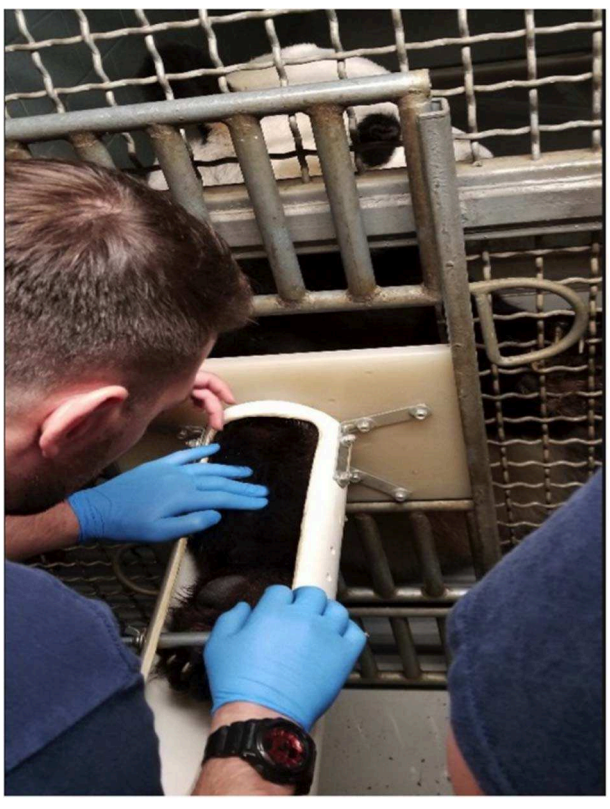

FIGURE 1 | Modified phlebotomy sleeve made from polyvinyl chloride tubing and plastic housing, locked into the metal mesh of the enclosure, with the giant panda (*Ailuropoda melanoleuca*) reaching into the sleeve and grasping a horizontal metal bar. The patient remained in this position voluntarily, utilizing behavioral restraint and positive reinforcement while the antebrachium was clipped, alcohol was applied, and phlebotomy was performed.

Immunocytochemical staining for CD3 was conducted at the Histology Laboratory of the University of Florida College of Veterinary Medicine to aid in the differentiation of the unique mononuclear cells as monocytes or lymphocytes. A rabbit polyclonal anti-human CD3 antibody (CD3Σ chain; RB-9039-P0, LabVision, Fremont, CA) with cross-reactivity across mammalian and non-mammalian species was applied to wedge-type direct blood films from all four study animals as previously described (22, 23). The slides were counterstained with Harris Hematoxylin (Fisher Scientific, Pittsburgh, PA, USA) and cover slipped. The above procedure was followed to obtain negative controls, except that primary antibody was not applied to the blood films. For positive controls, domestic dog blood films were used. Positive and negative controls were run concurrently with each set of processed slides.

For TEM, a tube of EDTA-anticoagulated blood was centrifuged at 2,500 rpm for 20 min, the plasma was removed, and the remaining buffy coat was preserved by replacing the plasma volume with 2.5% glutaraldehyde in 0.1M phosphate buffer (Electron Microscopy Services, Hatfield, PA 19440). The samples were placed vertically in a refrigerator (4°C) for 24 h, undisturbed. They were then post-fixed in 1% osmium tetroxide, dehydrated through a graded ethanol series (16) and propylene oxide, followed by embedding (EMBED 812, Epon 812 substitute, Electron Microscopy Sciences, Hatfield, PA). Ultrathin sections were prepared with an ultramicrotome (EM UC6, Leica Microsystems, Inc., Buffalo Grove, IL), counterstained with uranyl acetate and lead citrate, and imaged on a transmission electron microscope (Hitachi 7600, Hitachi High Technologies America, Inc., Clarksburg,

TABLE 1 | Comparative hematology data from four healthy captive giant pandas (*Ailuropoda melanoleuca*), one adult male and female and two juvenile females, used in this study and housed at the same AZA-accredited institution.

Hematology	Adult male	Adult female	Juvenile female #1	Juvenile female #2
Hematocrit (%)	40	45	45	35
Hemoglobin (g/dL)	14.0	15.1	14.3	12.1
RBC ($x10^{12}$/L)	6.52	7.24	7.28	5.93
MCV (fL)	61	62	62	59
MCH (pg)	21.5	20.9	19.6	20.4
MCHC (g/dL)	35.0	33.6	31.8	34.6
WBC $x10^3$/uL	6.70	6.80	7.40	11.90
Band Neutrophils ($x10^3$/uL)	0	0	0	0
Segmented Neutrophils ($x10^3$/uL)	4.30	5.20	4.80	7.60
Lymphocytes ($x10^3$/uL)	1.80	1.20	2.20	3.10
Monocytes ($x10^3$/uL)	0.13	0.14	0.22	0.36
Unique mononuclear cells ($x10^3$/uL)	0.20	0.07	0.15	0.48
Eosinophils ($x10^3$/uL)	0.27	0.20	0.07	0.36
Basophils ($x10^3$/uL)	0	0	0	0
Band Neutrophils (%)	0	0	0	0
Segmented Neutrophils (%)	64	76	65	64
Lymphocytes (%)	27	18	29	26
Monocytes (%)	2	2	3	3
Unique mononuclear cells (%)	3	1	2	4
Eosinophils (%)	4	3	1	3
Basophils (%)	0	0	0	0
Platelets ($x10^3$/uL)	428	406	542	566

Numerical results for standard hematological tests were obtained from the EDTA-anticoagulated blood with an automated Sysmex XN-10 series hematology analyzer (Sysmex America, Inc., Lincolnshire, IL). A 200 leukocyte differential count was obtained by manual blood film review and conversion to absolute numbers. RBC, red blood cell count; MCV, mean cell volume; MCH, mean cell hemoglobin; MCHC, mean cell hemoglobin concentration; WBC, white blood cell count.

MD) at the Electron Microscopy Core Facility, University of Florida College of Medicine. Identification of blood cells by TEM was based on nuclear morphology, e.g., non-lobulated or lobulated, and cytoplasmic features, e.g., the relative number, size, shape, and distribution of granules and organelles.

RESULTS

The blood cells lacked overt morphological abnormalities and hemoparasites were not identified in blood films from all 4 bears. Typical granulocytes (i.e., neutrophils, eosinophils, basophils), mononuclear cells (i.e., lymphocytes, monocytes), and platelets were identified in blood films stained with Wright-Giemsa (**Figure 2**). In addition, a mononuclear cell with overlapping features of lymphocytes and monocytes, having a moderately indented to occasionally bilobed nucleus was identified in low numbers in the blood film from each bear (termed "unique" mononuclear cell; see below for more detail). Cytochemical staining revealed consistent patterns in leukocytes and platelets, which are described in detail below and summarized (**Table 2**). Neutrophils, lymphocytes, monocytes, and platelets were identified on TEM; eosinophils and basophils were not identified on TEM, given their low concentrations in the blood of clinically normal giant pandas of this study.

Neutrophils

Neutrophils were the predominant leukocyte in study animals (**Table 1**). On Wright-Giemsa-stained blood films, they were ∼12–15 μm in diameter with colorless cytoplasm. The nuclei were segmented with clumped chromatin, similar to those in other mammalian species. They showed diffuse cytoplasmic reactivity, ranging from weak to strongly positive for ANBE. They showed strong cytoplasmic staining in a granular pattern for MPx, SBB, and PAS, and moderate to strong, diffuse to chunky multifocal cytoplasmic reactivity for CAE (**Figure 2**, **Table 2**). Ultrastructurally, neutrophils were identified by their nuclear lobulation with wide accumulations of heterochromatin along the inner leaflets of the nuclear membrane and relatively less centrally located euchromatin, and their cytoplasm contained primary and secondary granules, as seen in other species (**Figure 3A**).

Eosinophils

Eosinophils were slightly larger than neutrophils at ∼12–18 μm in diameter and had a segmented nucleus with variable numbers of orange to pink, small round cytoplasmic granules on blood films stained with Wright-Giemsa. They had moderate to strong cytoplasmic positivity for ANBE, which outlined the granules and had stronger staining than monocytes, including chunky deposits. Eosinophil granules were strongly positive for MPx, and moderately positive for SBB (albeit weaker than neutrophils).

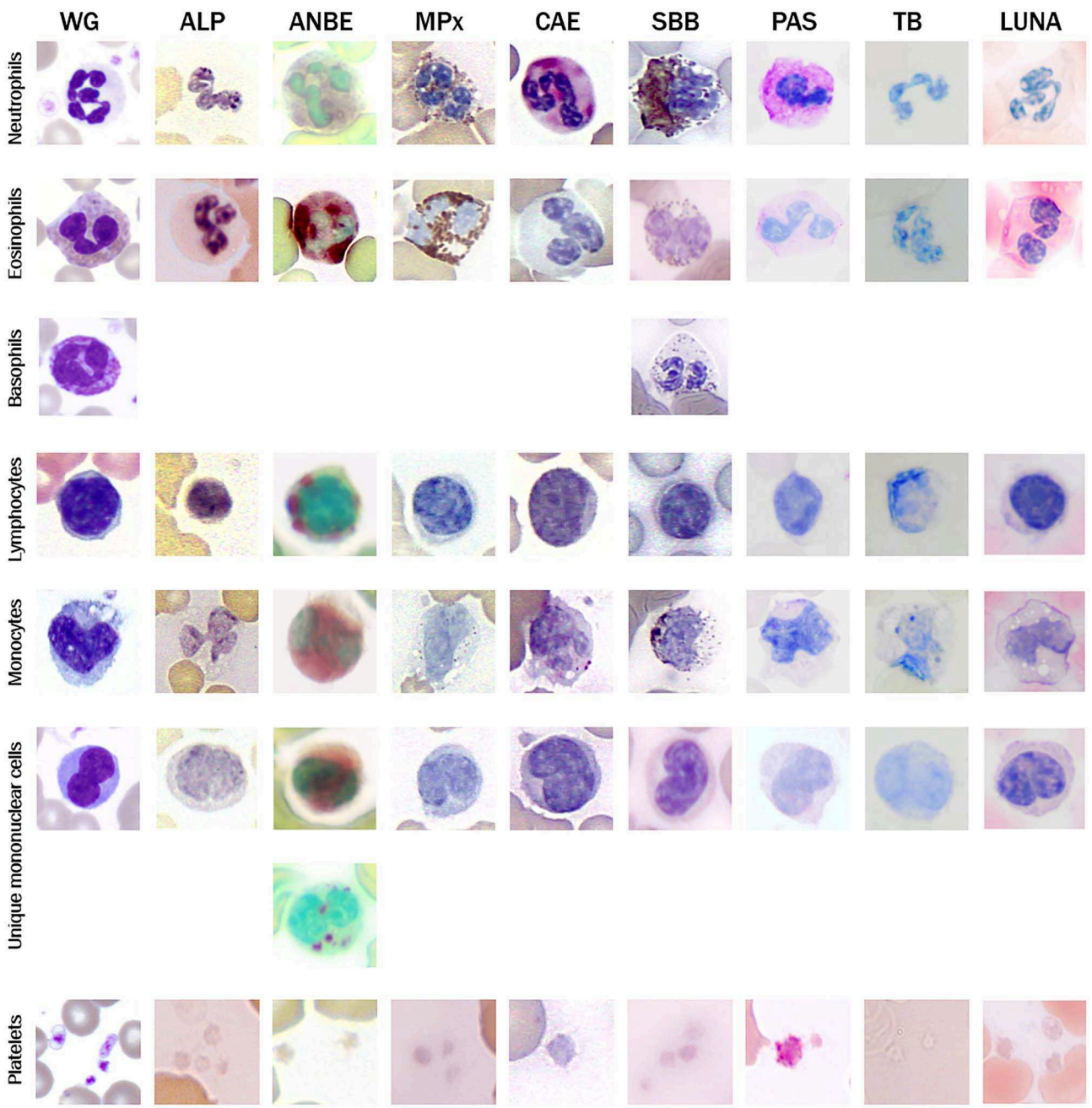

FIGURE 2 | Image composite of representative morphological features of giant panda (*Ailuropoda melanoleuca*) leukocytes in Wright-Giemsa (WG)-stained blood films and blood films stained with eight cytochemical stains (ALP, alkaline phosphatase; ANBE, α-naphthyl butyrate esterase; MPx, myeloperoxidase; CAE, chloroacetate esterase; SBB, Sudan black B; PAS, Periodic-Acid-Schiff; TB, Toluidine blue (pH 2.5-3.0). Basophils were not identified with most of the cytochemical stains.

Eosinophils had weaker granular cytoplasmic positivity for PAS than neutrophils and light patchy grainy cytoplasmic staining for Luna (**Figure 2**, **Table 2**). Eosinophils were not definitively identified on TEM.

Basophils

Rare basophils were identified in Wright-Giemsa-stained blood films (**Figure 2**). Their morphological features were similar to that observed in other mammalian species with a diameter of 14–16 μm, a segmented nucleus and colorless cytoplasm filled with numerous small round purple granules. No basophils were positively identified using most of the cytochemical stains, making it difficult to determine their cytochemical staining pattern. Two presumptive basophils were positive for SBB (**Figure 2**) and PAS (not shown), respectively (**Table 2**). Similarly, basophils were not definitively identified in the examined TEM ultrathin buffy coat sections.

TABLE 2 | Cytochemical staining patterns of giant panda (*Ailuropoda melanoleuca*) leukocytes and platelets.

n = 4	ALP	ANBE	MPx	CAE	SBB	PAS	TB	Luna
Neutrophils	-	C: +/– to + + +; some –	C (granular): + + +	C (diffuse to chunky multifocal): ++ to + + +, rare + focal	C (granular): + + +	C (granular): + + +	–	–
Eosinophils	-	C: + to + + + (outlining granules)	C (granules): + + +	–	C (granular): ++	C: + (cytoplasmic to granular: granules negative)	–	C (grainy, diffuse, outlining granules): +
Basophils	N/A	N/A	N/A	N/A	N/A	N/A	N/A	N/A
Lymphocytes	-	C (multifocal to focal granular): + + +; some small and rare large lymphocytes: –	–	–	–	–	–	–
Monocytes	-	C (diffuse): + to ++	C (few granules): +/–	Mostly negative, a few cells in some pandas (1+ granular)	C (few granules): +/–	C (granules): +/–	–	–
Unique mononuclear cells	-	Variable: C either diffuse + to ++ or multifocal to focal granular + + +	–	Mostly negative, rare cells in some pandas (1+ granular)	–	–	–	–
Platelets	-	–	–	–	–	C (diffuse to granular): + to ++	–	–

Staining was subjectively scored by two authors (NS, TS) as negative (–), equivocal (negative or weakly positive, +/–), and weakly (1+), moderately (2+), or strongly (3+) positive with results consolidated between the authors. C, Cytoplasm; ALP, Alkaline phosphatase; ANBE, Alpha-naphthyl butyrate esterase; MPx, Myeloperoxidase; CAE, Chloroacetate esterase; SBB, Sudan black B; PAS, Periodic Acid Schiff; TB, Toluidine blue.

Lymphocytes

Lymphocytes were the second most abundant WBC type in the study animals (**Table 1**). They were small to large, ranging from ∼7–16 μm in diameter, with small well-differentiated lymphocytes being predominant. Lymphocytes were round to oval, typically with a round or minimally clefted nucleus with smooth to clumped chromatin, a high nuclear to cytoplasmic ratio, and a scant to small amount of colorless or light blue cytoplasm. There were rare to low numbers of large and/or reactive lymphocytes with bluer cytoplasm. Rare lymphocytes appeared to have more deeply clefted to lobulated nuclei. On cytochemical staining, small lymphocytes generally showed strong multifocal to focal granular reactivity for ANBE (**Figure 2**, **Table 2**). Some small lymphocytes (up to 26%) in 3 animals, and rare large lymphocytes in 1 animal, stained negative for ANBE. Immunocytochemical staining with CD3 showed that most of the giant panda lymphocytes, including rare clefted small lymphocytes, stained positively for CD3 (70–90% of lymphocytes), consistent with T lymphocytes (**Figure 4**), with low numbers (<15%) being negative for this stain. With TEM, lymphocytes had a round nucleus with a smoothly curved nuclear membrane and a rim of heterochromatin along its inner leaflet, surrounding more centrally located euchromatin. These cells had a high nuclear-to-cytoplasmic ratio and a few cytoplasmic organelles, such as mitochondria (**Figure 3B**).

Monocytes

Monocytes ranged from 12 to 18 μm in diameter, had pale blue-grey cytoplasm with a ground glass texture, and a reniform to oval nucleus with lighter less clumped chromatin than lymphocytes on blood films stained with Wright-Giemsa. Some monocytes appeared to have indented to bilobed nuclei. A few monocytes contained low numbers of small clear cytoplasmic vacuoles consistent with reactive monocytes and/or dust-like red-to-pink cytoplasmic granules. On cytochemical staining, monocytes showed diffuse light to moderate cytoplasmic positivity for ANBE. They had variable staining for MPx and SBB, with around 10–20% showing multifocal granular positivity for CAE or PAS (**Figure 2**, **Table 2**). Ultrastructurally, monocytes had lower nuclear-to-cytoplasmic ratios compared to lymphocytes, as well as deeply indented nuclear profiles with more cytoplasmic organelles, such as mitochondria, than that seen in lymphocytes. Additionally, there were low numbers of small-diameter membrane-bound vacuoles within the cytoplasm (**Figure 3C**).

"Unique" Mononuclear Cells

Low numbers of cells had morphological features that overlapped between lymphocytes and monocytes in Wright-Giemsa-stained blood films. These cells comprised 1–4% of all leukocytes (**Table 1**). These cells had a nucleus with moderate indentation and variable chromatin features, including smooth or finely stippled chromatin. Several cells had a distinct bilobed nucleus. They ranged in size from 12 to 18 μm in diameter and had a variable amount of pale blue to blue-gray cytoplasm, with a variable nuclear to cytoplasmic ratio. On cytochemical staining, rare cells showed multifocal granular positivity for CAE (**Figure 2**, **Table 2**). Although the vast majority (99%) of unique mononuclear cells had lighter diffuse cytoplasmic positivity for ANBE, more consistent with staining characteristics of monocytes, rare (1%) smaller bilobed cells with intense multifocal cytoplasmic staining for ANBE also existed, resembling the staining pattern of lymphocytes (**Figure 2**).

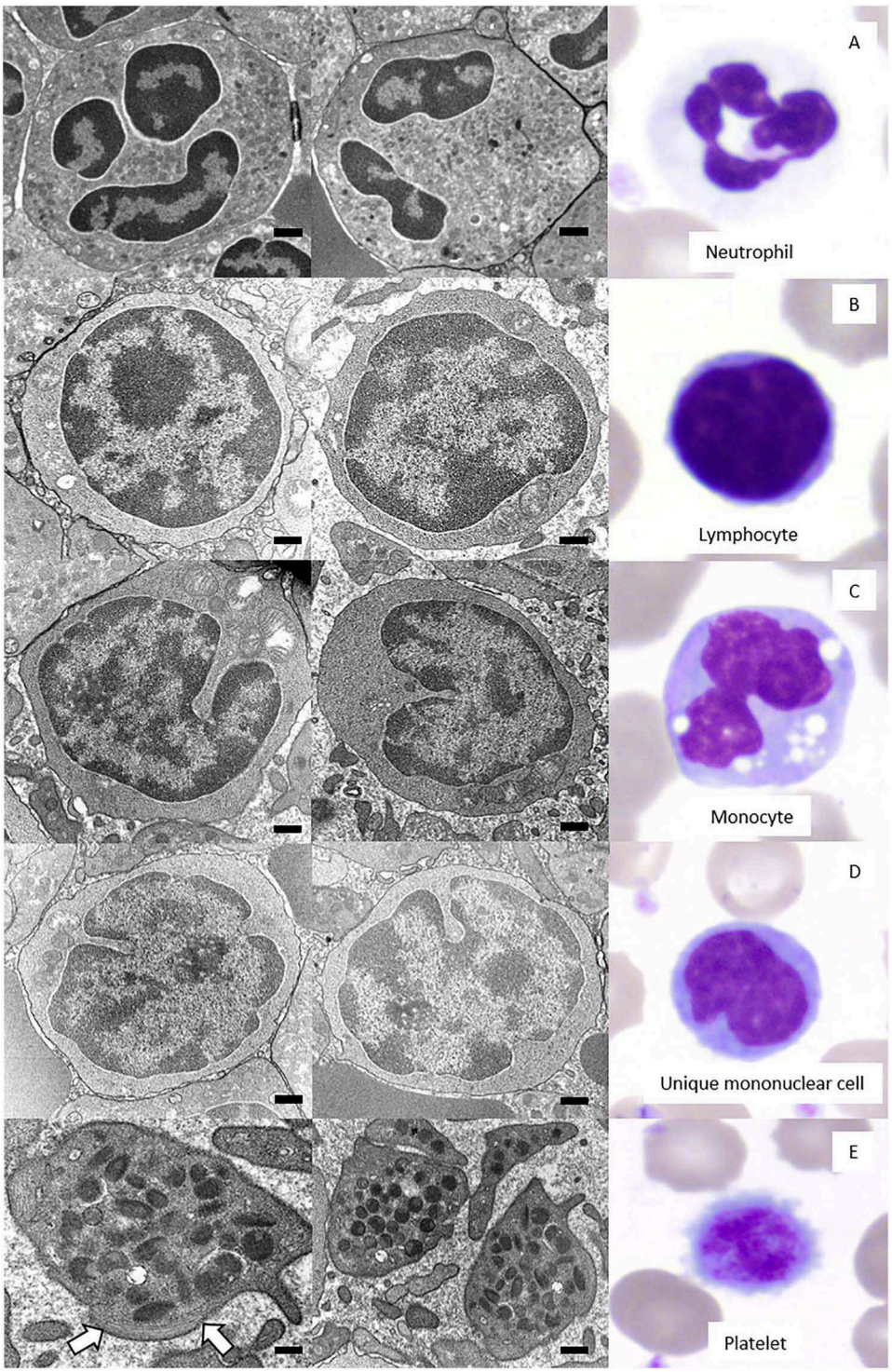

FIGURE 3 | Two-image composite (left and middle panel) of the ultrastructural features of giant panda (*Ailuropoda melanoleuca*) leukocytes and platelets as observed by transmission electron microscopy (TEM) with corresponding Wright-Giemsa-stained images of the relevant cell (right panel). Black size bars = 500 nm for TEM images. **(A)** Neutrophils had a lobulated nucleus predominantly composed of heterochromatin and abundant cytoplasm with numerous granules. **(B)** Lymphocytes had a high nuclear-to-cytoplasmic ratio, a round nucleus with a smoothly curved nuclear membrane, and a thin rim of cytoplasm with a scarcity of organelles, including mitochondria. **(C)** Monocytes had a lower nuclear-to-cytoplasmic ratio compared to lymphocytes, a deeply indented nucleus, and a cytoplasm containing organelles, such as mitochondria. **(D)** Unique mononuclear cells had a nuclear-to-cytoplasmic ratio subjectively between that of lymphocytes and monocytes, with an undulating nuclear membrane that was moderately indented and a cytoplasm containing low numbers of organelles, such as mitochondria. **(E)** Platelets were without a nucleus and had numerous electron-dense cytoplasmic granules and a band of microtubules (arrows) in the peripheral cytoplasm.

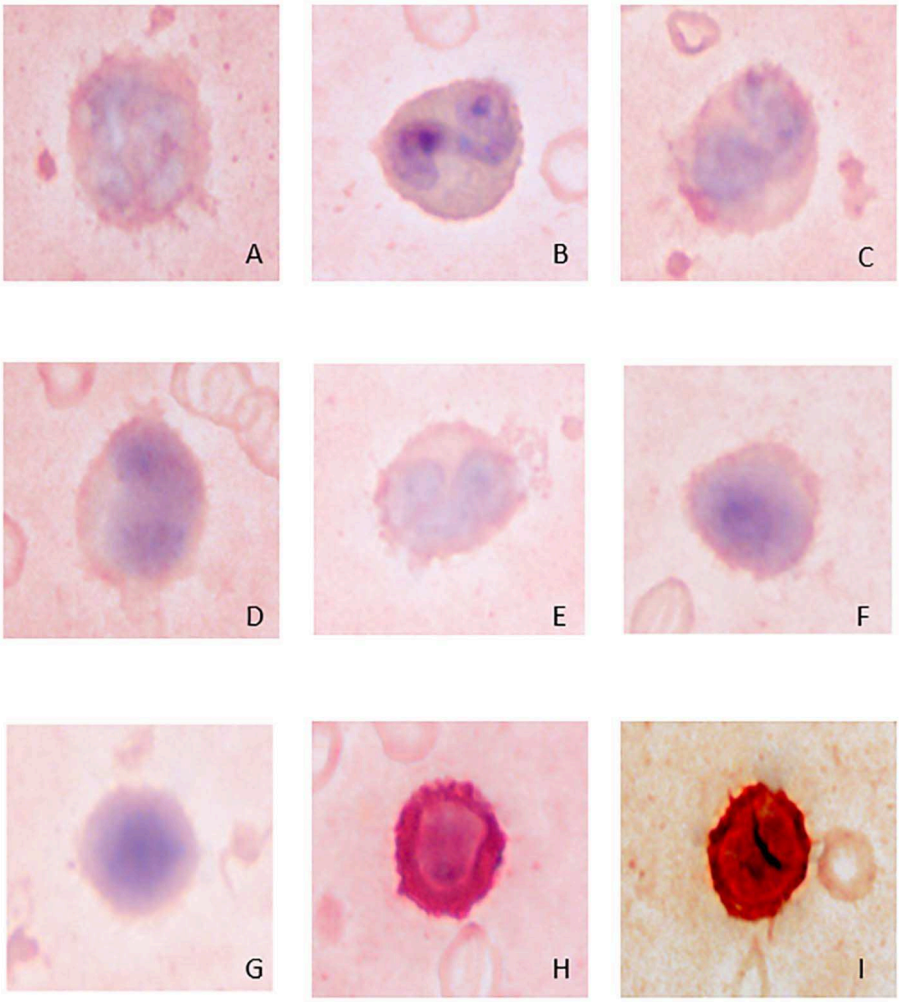

FIGURE 4 | Image composite of immunocytochemical staining reactions for CD3 in giant panda (*Ailuropoda melanoleuca*) leukocytes. **(A)** neutrophil (negative); **(B)** eosinophil (negative); **(C)** monocyte (negative); **(D,E)** unique mononuclear cell (negative); **(F,G)** lymphocytes (negative); **(H)** positive-staining T-lymphocyte; **(I)** canine control showing a positive-staining T-lymphocyte.

In an attempt to clarify lineage, CD3 immunocytochemical staining was performed since antibodies directed against the zeta chain react across taxa (22–24). We did not perform immunostaining for B cell markers (e.g., CD79a, Pax-5), because available reagents display less species cross-reactivity and require validation prior to use, which was beyond the scope of this study. While rare CD3-positive lymphocytes did have clefted nuclei, most of the cells with moderately indented or bilobed nuclei were negative for CD3, suggesting they were either of monocytic or B cell lineage. The few unique mononuclear cells identified on TEM tended to have a moderately indented nucleus, with a nuclear to cytoplasmic ratio and number of cytoplasmic organelles intermediate between the identified lymphocytes and monocytes of this species. The contour of the nuclear membrane of these cells was undulating, rather than smooth like that of lymphocytes, and less deeply indented than that of monocytes. There were occasional examples of unique mononuclear cells with cytoplasmic organelles aggregated in the area of nuclear indentation, similar to that of the monocytes (**Figure 3D**). While TEM provided for ultrastructural descriptions of these cells and supported that they were mononuclear cells, the characteristics ascribed to them were based on a small population of cells and did not further differentiate the type of mononuclear cell (i.e., monocytic vs. lymphocytic).

Platelets

Platelets were negative for ALP, ANBE, CAE, Luna, MPx, SBB, and TB stains. They showed weak to moderate, diffuse to granular cytoplasmic reactivity for PAS (**Figure 2**), which is typical for platelets across the animal kingdom in mammalian and non-mammalian taxa (15). Rare large platelets were also noted. On TEM, platelets were ovoid to elongated and non-nucleated. Their cytoplasm contained numerous electron-dense, membrane-bound structures consistent with dense secretory granules, i.e. dense bodies, which were largely located in a wide central zone of the cytoplasm, while segments of a circumferential

bundle of microtubules were located in the periphery of the cytoplasm (**Figure 3**), as expected in this cell type (25–27).

DISCUSSION

This report is the first to characterize normal leukocyte and platelet morphology using routine light microscopy, cytochemistry, immunocytochemistry, and electron microscopy in healthy giant pandas, establishing a baseline for these cell types in this species. With cytochemical staining, reaction patterns seen in other species cannot be directly extrapolated to giant pandas, due to inherent species differences. For example, eosinophils in domestic cats do not normally stain positive with MPx or SBB, while those of other mammals will stain positive for both of these stains (15). In contrast, ultrastructural features of cells are generally conserved across species. By using this combination of routine and specialized modalities, we were able to better characterize the leukocyte lineages of the giant panda. Some leukocytes, such as the unique mononuclear cells noted herein, were potentially misidentified in previous studies that sought to establish hematological ranges for this species. One of these studies utilized the rapid stain, Diff-Quik® (Baxter Healthcare Corp., Dade Division, Miami, Florida 33152, USA), which is inferior to Wright-Giemsa in staining quality with the potential for missing subtle cellular features and staining characteristics (13). The other study derived reference ranges for the different leukocytes using an automated analyzer only, without manual blood film review for morphological assessment and verification of results (14). Additionally, compared to light microscopic blood film review, an automated analyzer likely cannot reliably differentiate unique or different cells found in a given species, such as the unique mononuclear cells identified in the giant pandas of this study.

Leukocyte morphological features were similar for all four healthy giant pandas, both juveniles and adults, in the Wright-Giemsa-stained blood films. Neutrophils were the predominant leukocyte type and basophils were rare, consistent with humans and other members of the order Carnivora (28, 29). Since all giant pandas remained calm and unreactive during voluntary and conditioned phlebotomy, the predominance of neutrophils is unlikely to be related to a stress response. The low number of circulating basophils in the giant pandas of our study is consistent with previous studies in the giant panda and Asiatic black bear (13, 14, 17). Wright-Giemsa also revealed rare large or reactive lymphocytes, rare reactive monocytes, and rare large platelets in both juvenile and adult giant pandas, indicating that rare numbers of antigenically stimulated mononuclear cells can be expected in healthy pandas (25).

Neutrophils had the typical cytochemical reactions seen in most animals, with positive reactions for SBB, CAE, MPx and PAS (15). The results for PAS and SBB are similar to that reported for the Asiatic black bear (17). MPx is the standard stain used to identify neutrophils, while SBB stains lipids in neutrophils. The CAE stain is more specific but less sensitive than MPx or SBB in neutrophils of other mammalian species (15, 30) and was strongly positive in the giant panda neutrophils. Giant panda neutrophils did have a notable difference in cytochemical staining compared to most other mammals, however. They had positive diffuse cytoplasmic reactivity when stained with a substrate for ANBE (a commonly used non-specific esterase). The few other taxa with non-specific esterase positive neutrophils include equine and caprine species which reportedly showed variable positivity, and Asiatic black bears which had moderate to strong positive staining reactions for alpha-naphthyl acetate esterase (ANAE, another non-specific esterase) (15, 17, 29–31). Unlike neutrophils of humans, primates, rabbits, rats, guinea pigs, horses, and ruminants, mature neutrophils from the giant panda were negative for ALP, similar to those of the dog and cat (15, 32). Ultrastructurally, neutrophils had a granular cytoplasm similar to that expected in other mammalian species.

Eosinophils were readily identified on Wright-Giemsa-stained blood films, but were not always easy to differentiate from neutrophils or monocytes in the cytochemical stains that lacked staining in the granules. As expected, they were the only leukocyte to stain positively with the Luna stain, an eosinophil-specific stain (15). Overall, giant panda eosinophils had similar cytochemical staining reactions to other mammals with positive reactions for SBB and MPx, and negative reactions for CAE (15). They shared some cytochemical similarities with the Asiatic black bear (positive for SBB and non-specific esterase) and elephant (positive for MPx and ANBE, negative for ALP and CAE negative), but unlike the Asiatic black bear, eosinophils of the giant panda were PAS positive (17, 33). The ultrastructural features of eosinophils are expected to be similar to that of other species (34), but since none were observed by TEM due to their low number in this study, this assumption cannot be verified.

Lymphocytes and monocytes of giant pandas were morphologically and cytochemically similar to those of other animals. Most of the small lymphocytes of the giant panda showed focal to multifocal strong granular reactivity for non-specific esterase (ANBE used in this study) and lacked reactivity to the other cytochemical stains, similar to that in other species, including the Asiatic black bear (15, 17). This pattern of ANBE positivity has been associated with lymphocytes of T cell origin in other studies (35–38). Interestingly, up to 26% of the small lymphocytes and rare large lymphocytes were ANBE negative. This could be due to weak staining, the presence of only a few small granules, which could be readily missed on cursory review, or non-T cell lineage cells. In contrast, monocytes had diffuse light to moderate cytoplasmic positivity for ANBE, suggesting that ANBE may help differentiate these two mononuclear cells in the giant panda, as in other species. However, it is acknowledged that the staining patterns are quite subjective and staining intensity will also be influenced by pH and other methodological factors, such as reaction times (15). The reactions noted with the rest of the cytochemical stains in the giant panda monocytes were consistent with monocytes of other species, such as the Asiatic black bear (15, 17). The immunocytochemical staining showed that the antibody against CD3 identified T cells in the study animals, with expected negative reactions in the other cell lineages, including monocytes. Ultrastructurally, monocytes had lower nuclear-to-cytoplasmic ratios, more deeply indented nuclear profiles, and were often noted to have slightly more cytoplasmic organelles than lymphocytes.

The different staining patterns in lymphocytes and monocytes with respect to the ANBE stain were helpful when trying

to determine the lineage of the "unique" mononuclear cells discovered in the giant panda. Individual cells had light microscopical and ultrastructural features that were seen in lymphocytes and monocytes, making them difficult to categorize with confidence. Most of these cells had moderately indented nuclei, while a few had a more distinctly bilobed nucleus, the latter of which is a feature also seen in monocytic leukocytes of elephants, hyraxes and manatees (members of *Afrotheria*) (33, 39, 40). Although rare cells had ANBE staining characteristics consistent with T lymphocytes (i.e., multifocal cytoplasmic staining), most of the cells in question displayed ANBE staining characteristics consistent with giant panda monocytes, in addition to rare cells showing multifocal granular CAE positivity (15). Additionally, the results of CD3 immunostaining revealed the vast majority of these cells were negative for this T cell marker, supporting the possibility that these cells may in fact be of monocytic lineage. Although B cell origin is also a consideration and can only be excluded by negative staining with validated antibodies (which was beyond the scope of this study), the ANBE staining characteristics make this cell type less likely to be of B cell origin. Due to their low number in blood, it was difficult to conclusively identify defining ultrastructural features of these cells using TEM. While we suspect the unique cell in question should be classified as a monocyte, we acknowledge the limitations of the tools utilized in this study, and recommend that further testing (e.g., double immunostaining using flow cytometry with molecular lymphocyte and monocyte markers) will be required to definitively prove that these cells are not lymphocytes, e.g., B lymphocytes or non-B non-T lymphocytes; however, reagents for such further testing have not yet been identified or validated for this species. In addition to this limitation, we acknowledge that the number of animals included in this study consists of only 4 individuals, due to limited access to individuals of this high-profile species. However, our number of study animals is comparable to other studies on cytochemical staining and morphological leukocyte characterization of various nondomestic species (17, 41–43).

Platelets of the giant panda had classic morphological features and only showed positive cytochemical staining for PAS. The latter is a consistently positive stain in these cells of most species, including avian and reptilian thrombocytes, the mammalian platelet equivalent (15, 44, 45). The negative reactions for the other cytochemical stains mirror that seen in most other species, with some exceptions (e.g., canine platelets are usually positive for non-specific esterases, including ANBE) (15, 17, 35, 46, 47). Ultrastructurally, giant panda platelets had cytoplasmic electron dense granules similar to those seen in other mammals, including the Asiatic black bear (17), as well as a marginal band of microtubules, like that described in humans and other non-human primates (26).

CONCLUSIONS

The results herein will be a useful resource for the expected normal morphological, cytochemical, and ultrastructural findings of leukocytes in this vulnerable and high profile species, and will provide a basis for more accurate hematological interpretation. This information can be used to help clinicians detect deviations from the norm earlier in the course of disease or in response to environmental or physiological changes, as well as with monitoring trends in captive and wild populations over time. We showed that a polyclonal antibody against the epsilon chain of CD3 yielded the expected positive and negative staining reactions in giant panda leukocytes and would be a useful stain for identifying T lymphocytes in cytological or histological samples from this species. Furthermore, the combined use of Wright-Giemsa, cytochemistry, immunocytochemistry, and (to a lesser degree) TEM allowed for the identification of a unique indented to bilobed mononuclear cell found in low numbers in the giant panda, suspected to be of monocyte cell lineage. While cytochemical staining was helpful in determining the cell lineage of unique mononuclear cells, routine Wright-Giemsa evaluation was generally adequate for differential counting of leukocytes. This study also highlights the importance and clinical value of manual blood film review, as it is superior to automated leukocyte differentials in species with unique leukocyte types. Without the detailed leukocyte characterization presented herein, these cells may have otherwise remained unnoticed or been misidentified in clinical cases and future studies, as was the case for the bilobed monocytes of elephants, prior to their accurate identification. Future studies are needed to further characterize and identify this cell type, given the limitations of the tools utilized in this study, as well as identify the hematological changes that occur in giant panda leukocytes in response to specific diseases of concern or to physiological or environmental changes. Additionally, studies focused on validating additional molecular markers for leukocyte phenotyping are warranted.

DATA AVAILABILITY STATEMENT

All datasets generated for this study are included in the article/supplementary material.

ETHICS STATEMENT

The animal study was reviewed and approved by UF IACUC# 201706823. Written informed consent was obtained from the individual(s) for the publication of any potentially identifiable images or data included in this article.

AUTHOR CONTRIBUTIONS

SK, primary and corresponding author and primary scientific investigator, performed phlebotomy on giant pandas, prepared samples, and compiled tables for manuscript. Wrote and edited manuscript. NS performed Wright-Giemsa and immunocytochemical (CD3) staining of giant panda leukocytes and platelets, performed detailed light microscopical assessment of Wright-Giemsa-stained blood films and is one of the two authors who evaluated the cytochemical staining reactions, took photomicrographs, compiled image composites and tables for the manuscript, and reviewed and edited manuscript. SF performed

and compiled transmission electron microscopy images of giant panda leukocytes and platelets, and reviewed and edited the manuscript. TS oversaw cytochemical staining of blood films and is one of the two authors who evaluated the cytochemical staining reactions in all the pandas, and reviewed and edited the manuscript. All co-authors contributed to manuscript revision, and read and approved the submitted version.

FUNDING

Funding for this project was provided by internal funds from Zoo Atlanta.

ACKNOWLEDGMENTS

The authors would like to thank the animal care staff working with the giant pandas at Zoo Atlanta, and Sharon Debose, RVT, for technical assistance. We would like to thank the staff of the University of Florida, College of Medicine, Electron Microscopy Core Facility, particularly Dr. Jill W. Verlander, Dr. Sharon W. Matthews, and Chao Chen, for advice and technical assistance, Martha Shuman with the Animal Health Diagnostic Center at the University of Cornell who performed the cytochemical staining, and the University of Florida Histology Laboratory staff for their technical assistance.

REFERENCES

1. Zhang B, Li M, Zhang Z, Goossens B, Zhu L, Zhang S, et al. Genetic viability and population history of the giant panda, putting an end to the "evolutionary dead end"? *Mol Biol Evol.* (2007) 24:1801–10. doi: 10.1093/molbev/msm099
2. Swaisgood R, Wang D, Wei F. *Ailuropoda melanoleuca. The IUCN Red List of Threatened Species.* (2016) 2016:e-T712A102080907. doi: 10.2305/IUCN.UK.2016-2.RLTS.T712A45033386.en
3. Swaisgood RR, Wang D, Wei F. Panda downlisted but not out of the woods. *Conserv Lett.* (2018) 11:e12355. doi: 10.1111/conl.12355
4. Loucks CJ, Lü Z, Dinerstein E, Wang H, Olson DM, Zhu C, et al. Giant pandas in a changing landscape. *Science.* (2001) 294:1465. doi: 10.1126/science.1064710
5. Liu J, Hull V, Yang W, Viña A, Chen X, Ouyang Z, et al. *Pandas and People: Coupling Human and Natural Systems For Sustainability*. New York, NY: Oxford University Press. (2016) doi: 10.1093/acprof:oso/9780198703549.001.0001
6. Tuanmu MN, Viña A, Winkler JA, Li Y, Xu W, Ouyang Z, et al. Climate-change impacts on understory bamboo species and giant pandas in China's Qinling Mountains. *Nat Clim Chang.* (2013) 3:249. doi: 10.1038/nclimate1727
7. Wang F, McShea WJ, Wang D, Li S. Shared resources between giant panda and sympatric wild and domestic mammals. *Biol Conserv.* (2015) 186:319–25. doi: 10.1016/j.biocon.2015.03.032
8. Songer M, Delion M, Biggs A, Huang Q. Modeling impacts of climate change on giant panda habitat. *Int J Ecol.* (2012) 2012:1–12. doi: 10.1155/2012/108752
9. Fan J, Li J, Xia R, Hu L, Wu X, Li G. Assessing the impact of climate change on the habitat distribution of the giant panda in the Qinling Mountains of China. *Ecol Modell.* (2014) 274:12–20. doi: 10.1016/j.ecolmodel.2013.11.023
10. Li R, Xu M, Wong MH, Qiu S, Sheng Q, Li X, et al. Climate change-induced decline in bamboo habitats and species diversity: Implications for giant panda conservation. *Divers Distrib.* (2015) 21:379–91. doi: 10.1111/ddi.12284
11. Xu W, Viña A, Kong L, Pimm SL, Zhang J, Yang W, et al. Reassessing the conservation status of the giant panda using remote sensing. *Nat Ecol Evol.* (2017) 1:1635. doi: 10.1038/s41559-017-0317-1
12. Deem L, Karesh B, Weisman W. Putting theory into practice: Wildlife health in conservation. *Conserv Biol.* (2001) 15:1224–33. doi: 10.1111/j.1523-1739.2001.00336.x
13. Mainka SA, He T, Chen M, Dierenfeld ES. Hematologic and serum biochemical values for healthy captive giant pandas (*Ailuropoda melanoleuca*) at the Wolong Reserve, Sichuan, China. *J Zoo Wildl Med.* (1995) 26:377–81.
14. Burrell C, Zhang H, Li D, Wang C, Li C, Aitken-Palmer C. Hematology, serum biochemistry, and urinalysis values in the adult giant panda (*Ailuropoda melanoleuca*). *J Zoo Wildl Med.* (2017) 48:1072–6. doi: 10.1638/2016-0215.1
15. Raskin RR. Cytochemical staining. In: Weiss DJ, Wardrop KJ, editors. *Schalm's Veterinary Hematology, sixth edition*. Ames, IA: Blackwell Publishing Ltd (2010). p. 1141–54.
16. Salakij C, Salakij J, Apibal S, Narkkong NA, Chanhome L, Rochanapat N. Hematology, morphology, cytochemical staining, and ultrastructural characteristics of blood cells in king cobras (*Ophiophagus hannah*). *Vet Clin Pathol.* (2002) 31:116–26. doi: 10.1111/j.1939-165X.2002.tb00290.x
17. Salakij C, Salakij J, Narkkong NA, Trongwonsa L, Pattanarangsan R. Hematology, cytochemistry and ultrastructure of blood cells from Asiatic black bear (*Ursus thibetanus*). *Kasetsart J (Nat Sci).* (2005) 39:247–61.
18. Friedrichs KR, Harr KE, Freeman KP, Szladovits B, Walton RM, Barnhart KF, et al. ASVCP reference interval guidelines: Determination of de novo reference intervals in veterinary species and other related topics. *Vet Clin Path.* (2012) 41:441–53. doi: 10.1111/vcp.12006
19. Stokol T, Schaefer M, Shuman M, Belcher N, Dong L. Alkaline phosphatase is a useful cytochemical marker for the diagnosis of acute myelomonocytic and monocytic leukemia in the dog. *Vet Clin Path.* (2015) 44:79–93. doi: 10.1111/vcp.12227
20. Luna LG. *Manual of Histologic Staining Methods of the Armed Forces Institute of Pathology, third edition*. New York, NY: McGraw-Hill. (1968). p. 111–2.
21. MacManus JF, Mowry RW. *Staining Methods: Histologic and Histochemical.* New York, NY: Hoeber Med Div Harper & Row. (1960). p. 132–261.
22. Bricker NK, Raskin RE, Densmore CL. Cytochemical and immunocytochemical characterization of blood cells and immunohistochemical analysis of spleen cells from 2 species of frog, Rana (*Aquarana*) catesbeiana and Xenopus laevis. *Vet Clin Path.* (2012) 41:353–61. doi: 10.1111/j.1939-165X.2012.00452.x
23. Muñoz FA, Estrada-Parra S, Romero-Rojas A, Work TM, Gonzalez-Ballesteros E, Estrada-Garcia I. Identification of CD3+ T lymphocytes in the green turtle Chelonia mydas. *Vet Immunol Immunop.* (2009) 131:211–7. doi: 10.1016/j.vetimm.2009.04.015
24. Park CI, Hirono I, Aoki T. Molecular characterization of the Japanese flounder, *Paralichthys olivaceus*, CD3ε and evolution of the CD3 cluster. *Dev Comp Immunol.* (2005) 29:123–33. doi: 10.1016/j.dci.2004.06.004
25. Harvey JW. *Veterinary Hematology-E-Book: A Diagnostic Guide and Color Atlas*. Missouri: Elsevier Health Sciences. (2012) p. 157–58 & 192–208.
26. Young B, O'Dowd G, Woodford P (editors). Blood, haematopoiesis and bone marrow. In: *Wheater's Functional Histology: A Text and Colour Atlas, sixth edition*. Philadelphia, PA: Churchill Livingstone, Elsevier Ltd (2014). p. 46–64.
27. Fawcett DW, Raviola E (editors). Blood. In: *Bloom and Fawcett, A Textbook of Histology, twelfth edition*. New York, NY: Chapman & Hall (1994). p. 108–32.
28. Hawkey CM. *Comparative Mammalian Haematology: Cellular Components and Blood Coagulation of Captive Wild Animals*. London: Butterworth-Heinemann. (2017). p. 87–8.
29. Nunn CL, Gittleman JL, Antonovics J. A comparative study of white blood cell counts and disease risk in carnivores. *Proc R Soc Lond Ser Biol Sci.* (2003) 270:347–56. doi: 10.1098/rspb.2002.2249
30. Sheehan HL, Storey GW. An improved method of staining leukocyte granules with Sudan black B. *J Pathol Bacteriol.* (1947) 59:336–7. doi: 10.1002/path.1700590142
31. Tschudi P, Archer RK, Gerber H. Cytochemical staining of equine blood and bone marrow cells. *Equine Vet J.* (1977) 9:205–7. doi: 10.1111/j.2042-3306.1977.tb04032.x
32. Jain NC (editor). Cytochemistry of normal and leukemic leukocytes. In: *Schalm's Veterinary Hematology, 4 Edn*. Philadelphia, PA: Lea & Febiger (1986). p. 909–39.

33. Harr KE, Isaza R, Blue JT. Hematology of Elephants. In: Weiss DJ, Wardrop KJ, editors. *Schalm's Veterinary Hematology, sixth edition*. Ames, IA: Blackwell Publishing Ltd (2010). p. 942–9.
34. Young KM, Meadows RL. Eosinophils and Their Disorders. In: Weiss DJ, Wardrop KJ, editors. *Schalm's Veterinary Hematology, sixth edition*. Ames, IA: Blackwell Publishing Ltd (2010). p. 281–9.
35. Facklam NR, Kociba GJ. Cytochemical characterization of leukemic cells from 20 dogs. *Vet Pathol.* (1985) 22:363–69. doi: 10.1177/030098588502200411
36. Dulac RW, Yang TJ. Differential sodium fluoride sensitivity of alpha-naphthyl acetate esterase in human, bovine, canine, and murine monocytes and lymphocytes. *Exp Hematol.* (1991) 19:59–62.
37. Wulff JC, Sale GE, Deeg HJ, Storb R. Nonspecific acid esterase activity as a marker for canine T lymphocytes. *Exp Hematol.* (1981) 9:865–70.
38. Yang K, Bearman RM, Pangalis GA, Zelman RJ, Rappaport H. Acid phosphatase and alpha-naphthyl acetate esterase in neoplastic and non-neoplastic lymphocytes: A statistical analysis. *Am J Clin Pathol.* (1982) 78:141–9. doi: 10.1093/ajcp/78.2.141
39. Stacy NI, Isaza R, Wiedner E. First report of changes in leukocyte morphology in response to inflammatory conditions in Asian and African elephants (*Elephas maximus* and *Loxodonta africana*). *PLoS ONE.* (2017) 12:e0185277. doi: 10.1371/journal.pone.0185277
40. Stacy NI, Hollinger C. Introduction to comparative clinical pathology. In: Terio KA, McAloose D, St. Leger J, editors. *Pathology of Wildlife and Zoo Animals*. San Diego, CA: Elsevier Inc (2018). p. 55–115.
41. Salakij C, Salakij J, Rattanakunuprakarn J, Tengchaisri N, Tunwattana W, Apibal S. Morphology and cytochemistry of blood cells from Asian wild dog (*Cuon alpinus*). *Kasetsart J Soc Sci.* (2000) 34:518–25.
42. Cannon MS. The morphology and cytochemistry of the blood leukocytes of Kemp's ridley sea turtle (*Lepidochelys kempi*). *Can J Zool.* (1992) 70:1336–40. doi: 10.1139/z92-188
43. Henkel KA, Swenson CL, Richardson B, Common R. Morphology, cytochemical staining and ultrastructural characteristics of reindeer (*Rangifer tarandus*) leukocytes. *Vet clin path.* (1999) 28:8–15. doi: 10.1111/j.1939-165X.1999.tb01035.x
44. Mateo MR, Roberts ED, Enright FM. Morphologic, cytochemical, and functional studies of peripheral blood cells of young healthy American alligators (*Alligator mississippiensis*). *Am J Vet Res.* (1984) 45:1046–53.
45. Swayne DE, Stockham SL, Johnson GS. Cytochemical properties of chicken blood cells resembling both thrombocytes and lymphocytes. *Vet Clin Path.* (1986) 15:17–24. doi: 10.1111/j.1939-165X.1986.tb00639.x
46. Facklam NR, Kociba GJ. Cytochemical characterization of feline leukemic cells. *Vet Pathol.* (1986) 23:155–61. doi: 10.1177/030098588602300208
47. Raskin RE, Valenciano A. Cytochemistry of normal leukocytes. In: Feldman BF, Zinkl JG, Jain NC, editors. *Schalm's Veterinary Hematology, fifth edition*. Philadelphia, PA: Lippincott Williams & Wilkins (2000). p. 337–46.

Conflict of Interest: The authors declare that the research was conducted in the absence of any commercial or financial relationships that could be construed as a potential conflict of interest.

Copyright © 2020 Kehoe, Stacy, Frasca, Stokol, Wang, Leach, Luo and Rivera. This is an open-access article distributed under the terms of the Creative Commons Attribution License (CC BY). The use, distribution or reproduction in other forums is permitted, provided the original author(s) and the copyright owner(s) are credited and that the original publication in this journal is cited, in accordance with accepted academic practice. No use, distribution or reproduction is permitted which does not comply with these terms.

frontiers in Veterinary Science

CASE REPORT
published: 02 April 2020
doi: 10.3389/fvets.2020.00166

Mandibular Ossifying Fibroma and Multiple Oral Papillomas in a Roe Deer (*Capreolus capreolus*)

Samoa Zürcher-Giovannini[1], *Thomas-Daniel Ruder*[2,3†], *Roy Pool*[4], *Karoly Erdelyi*[5] *and Francesco C. Origgi*[1*]

[1] Centre for Fish and Wildlife Health, Vetsuisse Faculty, University of Bern, Bern, Switzerland, [2] Centre of Forensic Imaging and Virtopsy, Institute of Forensic Medicine, University of Bern, Bern, Switzerland, [3] Department of Forensic Medicine and Imaging, Institute of Forensic Medicine, University of Zurich, Zurich, Switzerland, [4] Department of Pathobiology, College of Veterinary Medicine & Biomedical Sciences, Texas A&M University, College Station, TX, United States, [5] Veterinary Diagnostic Directorate, National Food Chain Safety Office, Budapest, Hungary

OPEN ACCESS

Edited by:
Michele Ann Miller,
Stellenbosch University, South Africa

Reviewed by:
Nikolaus Huber,
University of Veterinary Medicine, Austria
Jana Kvicerova,
University of South Bohemia, Czechia

***Correspondence:**
Francesco C. Origgi
francesco.origgi@vetsuisse.unibe.ch

†Present address:
Thomas-Daniel Ruder,
Department of Diagnostic, Interventional and Pediatric Radiology Inselspital, University of Bern, Bern, Switzerland

Specialty section:
This article was submitted to Zoological Medicine, a section of the journal Frontiers in Veterinary Science

Received: 17 December 2019
Accepted: 10 March 2020
Published: 02 April 2020

Citation:
Zürcher-Giovannini S, Ruder T-D, Pool R, Erdelyi K and Origgi FC (2020) Mandibular Ossifying Fibroma and Multiple Oral Papillomas in a Roe Deer (Capreolus capreolus). Front. Vet. Sci. 7:166. doi: 10.3389/fvets.2020.00166

An emaciated, adult, free-ranging roe deer (*Capreolus capreolus*) presenting a large mandibular mass, was shot by a game warden in Sissach, Switzerland. The head of the roe deer was submitted to the Center for Fish and Wildlife Health for examination. Grossly, the mass consisted of a 6 × 7 × 4 cm mandibular exophytic growth, associated with loss of incisors teeth. On cut section, a hard, light-tan core was rimmed by a thick layer of soft tissue. Computed tomography examination confirmed the mandibular origin of the mass. Histologically, the mass consisted of an unencapsulated fibro-osseous neoplasm. The bony portion was composed of multiple haphazardly arranged spicules rimmed by osteoblasts with no associated periosteal layer. Embedding the bony spicules were short anastomosing and branching streams and bundles of spindled cells. The overlaying partially ulcerated mucosa, showed prominent rete ridges deepening into the submucosa. In addition to the mandibular mass, multiple soft cauliflower-like proliferations were expanding from the gingival surface. Histologically, these masses were arranged in papillary elements composed of pluristratified squamous epithelium with long rete ridges extending into a rich underlying fibrovascular supportive stroma. Neither papillomaviral DNA nor antigen could be identified in association with the oral masses. The gross, histological and radiological features of the mandibular mass are consistent with an ossifying fibroma, while the cauliflower oral masses were diagnosed as papillomas.

Keywords: roe deer, ossifying fibroma, computed tomography, papilloma, wildlife

BACKGROUND

Ossifying fibroma is a benign fibro-osseous neoplasm, which most frequently develops within the mandible. This tumor is considered a rare occurrence in veterinary medicine and it has been reported mainly in young horses (1). Other species including cats (2), Anglo-Nubian goats (3), greater kudu (4), sheep (5), miniature Rex rabbits (6) and dogs (7) may also, but more rarely, develop the tumor.

Papillomas and fibropapillomas have been reported in a wide range of domestic and wild animals including several cervid species, such as white-tailed (*Odocoileus virginianus*) and mule

deer (*Odocoileus hemionus*) in North America (8), European elk (*Alces alces*) (9) and reindeer (*Rangifer tarandus*) in Sweden (10), red deer (*Cervus elaphus*) in Scotland (11), as well as red deer and roe deer (*Capreolus capreolus*) in Hungary (12, 13). Species-specific papillomaviruses (PV), whose origin has been recently traced to the European continent (14), were frequently detected in association with these tumors. Fibropapillomas in roe deer most commonly develop on the skin of the head, neck, abdomen and limbs of the affected animal (15).

In this short communication, we describe the simultaneous occurrence of a mandibular ossifying fibroma and multiple oral papillomas in a wild ruminant. To the best of our knowledge, this is the first documented description of an ossifying fibroma in a roe deer (*Capreolus capreolus*). Additionally, the papillomas described in this study, developed within the oral cavity differently from the more common cutaneous papilloma and fibropapillomas reported in deer up to date.

CASE HISTORY

A weak and emaciated free-ranging adult (estimated age 4, 5 years old, according to the feature of the dentition), female roe deer (*Capreolus capreolus*) presenting a large mass expanding from the cranial aspect of the mandible, was culled by a game-warden in Sissach, Switzerland. A field necropsy was performed by the game warden who did not observe any additional gross abnormalities. The head of the roe deer was submitted to the Center for Fish and Wildlife Health (FIWI) at the University of Bern, Switzerland, for a full pathology investigation. During the examination of the submitted head, additionally to the mandibular mass, multiple proliferative growths were observed expanding from the upper and lower gingiva.

Samples of the masses were fixed in 10% buffered formalin, decalcified for about 1 h and then processed routinely for histological examination. Paraffin sections (5 µm thick) were stained with hematoxylin and eosin (H&E).

A computed tomography (CT) scan of the whole head was performed at the Institute of Forensic Medicine in Bern, Switzerland.

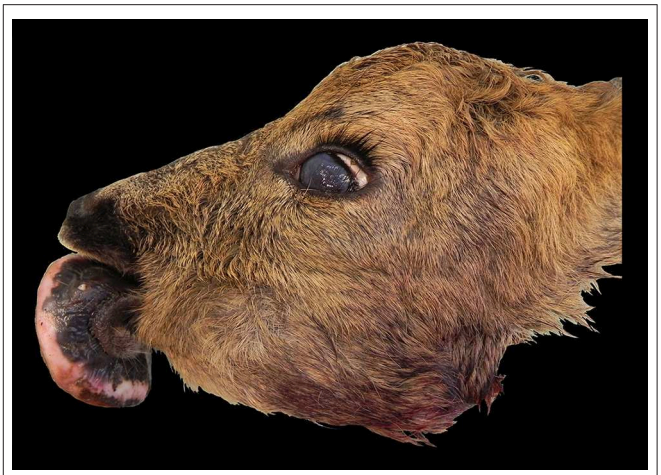

FIGURE 1 | Head, roe deer (*Capreolus capreolus*); a mass is expanding from the rostral aspect of the mandible.

FIGURE 2 | Skull, roe deer; the mass is composed of a bony center.

DESCRIPTION OF LABORATORY INVESTIGATIONS AND DIAGNOSTIC TESTS

Pathology and Imaging

Macroscopically, the mandibular mass consisted of a 6 × 7 × 4 cm exophytic growth, expanding from the rostral aspect of the mandible and associated with loss of incisors teeth (**Figures 1**, **2**). The mass was covered laterally and dorso-caudally by intact mucosa contiguous to that of the oral cavity, while a local-extensive mucosal ulceration was present on its rostral aspect. On cut section, the mass was composed of a hard, light-tan core rimmed by a thick layer of soft tissue. CT examination revealed the presence of both osseous and soft tissue components, and confirmed that the neoplasm was originating from the mandible (**Figures 3**, **4**). The portion of the mandible contiguous to the mass showed local bone destruction. Both bodies of the mandible were unaffected.

Histologically, the mass consisted of an unencapsulated fibro-osseous neoplasm, expanding the oral submucosa and elevating the partially ulcerated mucosa (**Figure 5**). The bony portion was composed of multiple haphazardly arranged spicules of woven bone rimmed by polygonal cells (osteoblasts). This cancellous bone mass was not surrounded by a layer of periosteum, consistent with the edge of an expanding fibrous stromal tumor mass (**Figure 6**). Embedding the bony spicules were short anastomosing and branching streams and bundles of spindled cells supported by an abundant eosinophilic matrix (**Figures 7**, **8**). The spindled cells had indistinct margins, and contained a scant amount of eosinophilic cytoplasm. Nuclei were elongated to ovoid and frequently hyperchromatic. Anisokaryosis and anisocytosis were moderate. Mitoses were less than one per ten high power fields. Multiple foci of mild lymphocytic to plasmacytic infiltration were also present. The mucosa overlaying

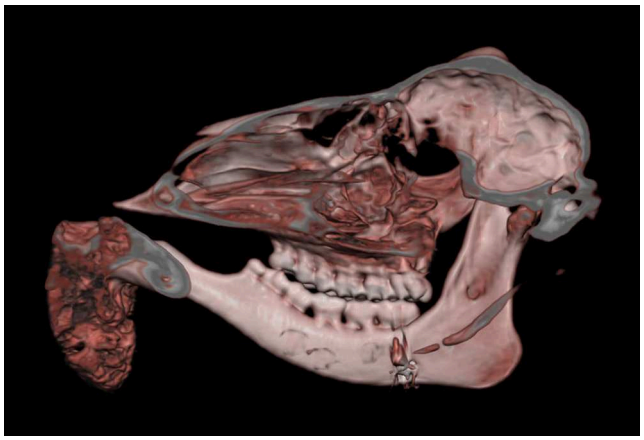

FIGURE 3 | Head, roe deer; computed tomography scan showing the contiguity of the bony mass with the mandible and the effacement of the latter by the tumor. This figure uses *volume-rendering* technique to provide a three-dimensional image of the skull.

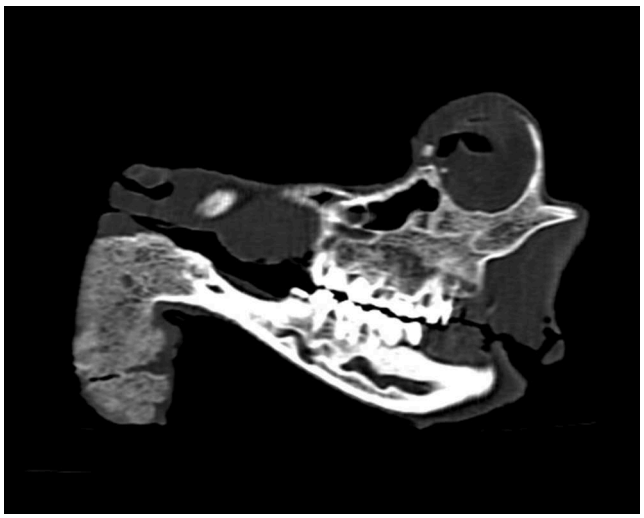

FIGURE 4 | Head, roe deer; computed tomography scan showing the contiguity of the bony mass with the mandible and the effacement of the latter by the tumor. This figure features a single sagittal MPR (multi-planar reconstruction) image through the skull at the level of the tumor.

FIGURE 5 | Mandibular mass, roe deer (*Capreolus capreolus*); a proliferative fibrous-osseous mass comprising cancellous bone in the absence of a periosteal layer is elevating the ulcerated labial mucosa; H&E stain.

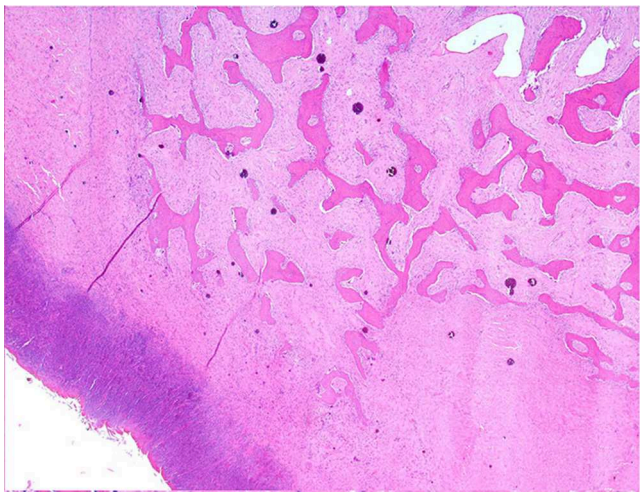

FIGURE 6 | Mandibular mass, roe deer; the bony spicules increase in size from the periphery to the center of the mass; H&E stain.

the mass was partially ulcerated. The surrounding viable mucosa was composed of a hyperplastic hyperkeratotic pluristratified squamous epithelium with prominent rete ridges deepening into the submucosa, while the ulcerated portion presented a thick band of degenerating neutrophils admixed with lymphocytes and cellular debris.

Additionally to the mandibular mass, multiple soft cauliflower-like proliferations (from ca. 3.5 × 2 × 1 cm to 7.5 × 4 × 2 cm) were present over the gingival surface, rimming the lateral and lingual aspects of the upper and lower premolars and molars and extending caudally up to the proximal tract of the pharynx (**Figure 9**). The tumor masses were shiny and light tan on cut surface.

Histologically, the soft oral masses were arranged in papillary elements composed of keratinized pluristratified squamous epithelium with long rete ridges extending into a rich underlying fibrovascular supportive stroma (**Figure 10**). The epithelial neoplastic cells were polygonal to cuboidal, had distinct cell borders and moderate to large amount of eosinophilic cytoplasm. The nuclei were round to oval with stippled chromatin and contained one variably distinct nucleolus. Anisokaryosis and anisocytosis were moderate. Mitoses were less than one per ten high power fields. In between the neoplastic cells, the intercellular bridges, separated by clear

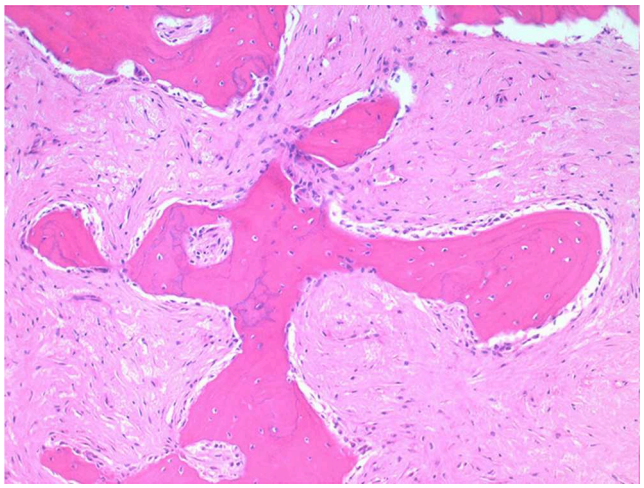

FIGURE 7 | Mandibular mass, roe deer; embedding the bony spicules were streams and bundles of spindled cells supported by an abundant eosinophilic matrix; H&E stain.

FIGURE 9 | Mandible, roe deer (*Capreolus capreolus*); cauliflower-like proliferations expanding from the gingival surface and rimming the lower premolars and molars.

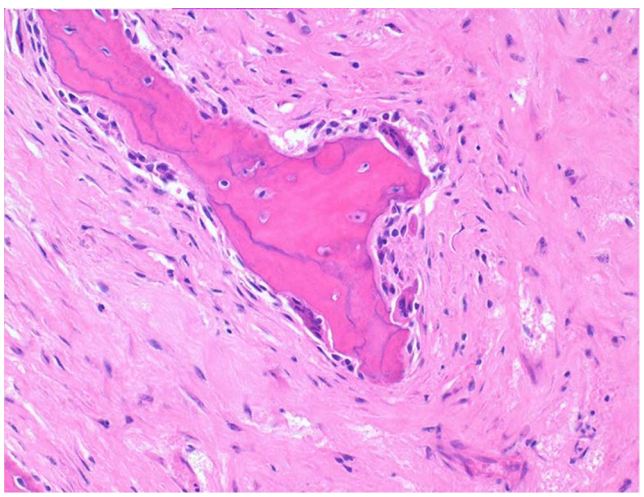

FIGURE 8 | Mandibular mass, roe deer; spicules are lined by osteoblasts and those larger and deeper seated in the mass undergo bone remodeling at their surfaces; H&E stain.

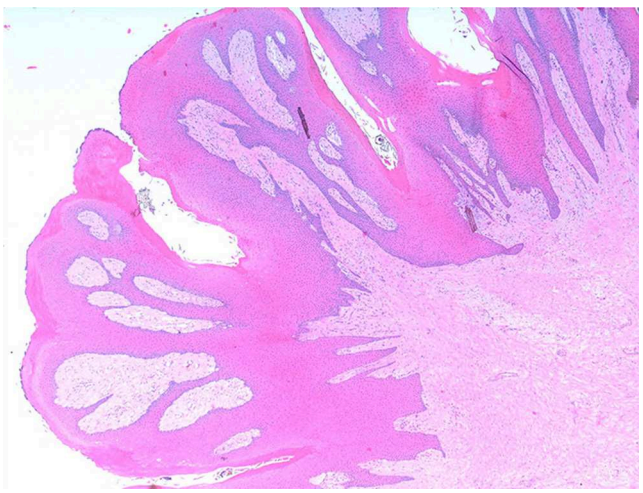

FIGURE 10 | Gingival mass, roe deer; cross section of the papillary projection; H&E stain.

spaces, were relatively prominent (spongiosis). Multiple clear intracytoplasmic vacuoles, occasionally filled with amphophilic material and pushing the nuclei peripherally, were seen within the *stratum basale* and *stratum spinosum*, while larger vacuoles, containing eosinophilic material, were seen in the *stratum spinosum* only. The upper portion of the underlying submucosal layer was poorly cellular and was composed of loose collagen fibers separated by variably extensive clear spaces, while in the deeper portion thicker fibrous bundles, more densely arranged, were seen. Multifocally, mononuclear inflammatory infiltrates composed mainly by lymphocytes and plasma cells were also observed.

Molecular and Immunohistochemical Investigation

Given that papillomas in wild ruminants have been frequently associated with papillomaviruses (PV), the cauliflower oral masses observed in the submitted roe deer were tested for the presence of Roe deer PV DNA and antigen through PCR and immunohistochemistry, respectively. Briefly, total DNA was extracted from a section of fresh tissue excised from the oral masses using the DNeasy extraction kit (Quiagen, Hombrechtikon, CH) according to the instructions of the manufacturer. A PCR reaction was performed with a pair of PCR primers (Pap1f and Pap1r) designed for the detection of cervid PV DNA and a second PCR

with broader detection spectrum capable of detecting all Delta PVs was carried out using the primers UPV1 and UPV2 (12, 15). In addition, sections of paraffin-embedded tissue of the oral masses were mounted on Xylene treated slides and processed by immunohistochemistry for the detection of PV antigen as described earlier (15). Briefly, the immunohistochemical reaction was performed using rabbit antibodies B0580 (DAKO, Glostrup, Denmark) raised against BPV1 L1 capsid protein and the reaction was visualized with a horseradish peroxidase-labeled polymer system (EnVisionTM+ Kit; Dako, Glostrup, Denmark). Cutaneous papillomas were used as control. Both PCR and immunohistochemistry yielded negative results, suggesting the absence of both Delta papillomavirus DNA and antigen in the examined lesion.

DISCUSSION

The gross, histological and radiological features of the mandibular mass along with its anatomic localization are consistent with an ossifying fibroma. The cauliflower oral masses were diagnosed as papillomas.

Ossifying fibroma is a slow-growing, benign, expansile fibro-osseous tumor that most commonly develops within the rostral mandible of animals (16). Its histological features are intermediate between those typical of an osteoma and of fibrous dysplasia, respectively. Morphologically it resembles a fibroma where bone forms by osseous metaplasia. The proliferative element consists of spindle cells undergoing transformation to osteoblasts producing spicules of developing bone (17). The cancellous bone is not associated with periosteum and there is a sudden transition between the fibroblastic stroma and the bony trabeculae. The latter are better developed than the bone and osteoid produced in osteosarcomas and are bordered by a layer of osteoblasts lacking the classic perpendicular arrangement to the surface of the spicules seen in osteomas. Ossifying fibromas lack cartilage formation and do not metastasize. Other characteristics include low cellularity, low pleomorphism and low mitotic index. Ossifying fibromas most frequently affect the mandible of young horses (1) but they have also been described in the lower and upper jaw of other species (2–7, 18, 19). Relatively unusual locations including the tibia (20, 21) and os penis (22) have also been reported. Other infrequent locations include that of a white-tailed deer (*Odecoileus virginianus*) affected by a debilitating ossifying fibroma of the ear (23). The ear lesion was suggested to be associated with ear tagging and with a possible virus transmission occurring during the procedure. Diagnosis of ossifying fibromas can be challenging especially when the examined lesions share significant morphological features with similar but distinct fibrous-osseous neoformations. In the case presented here, the location associated with the local invasiveness assessed through the CT scan, the absence of periosteum, the morphology and arrangements of the osteoblasts and the sharp demarcation between the fibrous and osseous components are strongly suggestive of an ossifying fibroma.

Papillomas are benign tumors usually occurring within the skin of many domestic animals but have also been described within the oral cavity, especially in dogs (24), and within the esophagus and forestomachs of cattle (25). The distinction between papilloma and fibropapilloma can be difficult especially when the papilloma is in a regressing phase. While papillomas consist of hyperkeratotic epidermal or mucosal exuberant exophytic masses supported by a fine fibrovascular stroma, fibropapillomas consist predominantly in fibroblastic neoproliferations overlaid by a hyperplastic, hyperkeratotic epidermis/mucosa (16). In this case report, although the fibrous stroma of some of the masses was relatively prominent, there were no clear groups of proliferating fibroblasts, consistent with papillomas. Cutaneous papillomas and fibropapillomas have been reported in several cervids species. These skin tumors have been repeatedly associated with species-specific PV, although this association might be more complex than previously considered (14). Genomes of deer- (White-tailed deer, *Odocoileus virginianus*) (26), Reindeer- (*Rangifer tarandus*) (10), European Elk- (*Alces alces*) (27), Roe deer- (*Capreolus capreolus*) (15), and Red deer- (*Cervus elaphus*) *papillomavirus* (12) have been sequenced and they have all been demonstrated to be member of the *Delta-papillomavirus* genus. Differently, *Bovine papillomavirus type* 4 of cattle (usually causing lesion within the esophagus and forestomach) has been determined to be a *Xipapillomavirus* (25). The PCR amplification of Delta PV DNA from a tissue sample of the oral papillomas and the immunohistochemistry directed to the detection of PV antigen were negative. Additionally, the cytopathic changes known to occur secondary to the presence of the virus, such as nuclear size reduction, perinuclear clearing (koilocytosis) and increased amounts of amphophilic foamy cytoplasm, were not obviously observed within the mucosa of this roe deer. These results suggest the absence of papillomavirus association in the observed oral masses. Alternatively, the putative presence of a PV might not have been detected because of a significant divergence with that of the best characterized PVs of wild ruminants or for the presence of an amount of viral genomic DNA under the limit of detection of the adopted protocol.

DATA AVAILABILITY STATEMENT

All the data collected during this investigation are reported in the present article.

AUTHOR CONTRIBUTIONS

SZ-G and FO performed the study and wrote the manuscript. T-DR performed the computed tomography examination, carried out the image analysis and interpretation and contributed to the manuscript. RP contributed to the interpretation of the bone lesions, to the diagnosis and to the manuscript. KE performed the molecular and the immunohistochemical analyses, their interpretation and contributed to the manuscript.

ACKNOWLEDGMENTS

The investigation described in this manuscript was partially summarized in an abstract entitled: Ossifying fibroma in a roe deer (*Capreolus capreolus*), which was submitted to the 2011 Annual Conference of the European College of Veterinary Pathologists. The authors would like to thank all the personnel of the Center for Fish and Wildlife Health (FIWI) at the Vetsuisse Faculty, University of Bern and in particular Marie-Pierre Ryser-Degiorgis and Helmut Segner for their constant support.

REFERENCES

1. Morse CC, Saik JE, Richardson DW, Fetter AW. Equine juvenile mandibular ossifying fibroma. *Vet Pathol*. (1988) 25:415–21. doi: 10.1177/030098588802500603
2. Turrel JM, Pool R. Primary bone tumors in the cat: a retrospective study of 15 cats and a literature review. *Vet Radiol*. (1982) 23:152–66. doi: 10.1111/j.1740-8261.1982.tb01099.x
3. Pritchard GC. Ossifying fibroma in an Anglo-Nubian goat. *Goat Vet Soc J*. (1984) 5:31.
4. Boever WJ, Kennedy S, Kane KK. Ossifying fibroma in a greater kudu. *Vet Med Small Anim Clin*. (1977) 72:1483–6.
5. Rogers AB, Gould DH. Ossifying fibroma in a sheep. *Small Rum Res*. (1998) 28:193–7. doi: 10.1016/S0921-4488(97)00082-5
6. Whitten KA, Popielarczyk MM, Belote DA, McLeod GC, Mense MG. Ossifying fibroma in a miniature rex rabbit (*Oryctolagus cuniculus*). *Vet Pathol*. (2006) 43:62–4. doi: 10.1354/vp.43-1-62
7. Miller MA, Towle HA, Heng HG, Greenberg CB, Pool RR. Mandibular ossifying fibroma in a dog. *Vet Pathol*. (2008) 45:203–6. doi: 10.1354/vp.45-2-203
8. Lancaster WD, Sundberg JP. Characterization of papillomaviruses isolated from cutaneous fibromas of white-tailed deer and mule deer. *Virology*. (1982) 123:212–6. doi: 10.1016/0042-6822(82)90307-5
9. Moreno-Lopez J, Pettersson U, Dinter Z, Philipson L. Characterization of a papilloma virus from the European elk (EEPV). *Virology*. (1981) 112:589–95. doi: 10.1016/0042-6822(81)90304-4
10. Moreno-Lopez J, Ahola H, Eriksson A, Bergman P, Pettersson U. Reindeer papillomavirus transforming properties correlate with a highly conserved E5 region. *J Virol*. (1987) 61:3394–400. doi: 10.1128/JVI.61.11.3394-3400.1987
11. Moar MH, Jarrett WF. A cutaneous fibropapilloma from a red deer (*Cervus elaphus*) associated with a papillomavirus. *Intervirology*. (1985) 24:108–18. doi: 10.1159/000149626
12. Erdelyi K, Gal J, Sugar L, Ursu K, Forgach P, Szeredi L, et al. Papillomavirus-associated fibropapillomas of red deer (*Cervus elaphus*). *Acta Vet Hung*. (2009) 57:337–44. doi: 10.1556/AVet.57.2009.2.14
13. Takács A, Nagy-Bozsoki J. Occurence of cutaneous fibromatosis in roe deer (*Capreolus capreolus*) populations on the great plain of Ungary. *Magy Allatorv Lapja*. (1988) 120:431–433.
14. Frias-De-Diego A, Jara M, Escobar LE. Papillomavirus in wildlife. *Front Ecol Evol*. (2019) 7:406. doi: 10.3389/fevo.2019.00406
15. Erdelyi K, Balint A, Dencso L, Dan A, Ursu K. Characterisation of the first complete genome sequence of the roe deer (*Capreolus capreolus*) papillomavirus. *Virus Res*. (2008) 135:307–11. doi: 10.1016/j.virusres.2008.03.002
16. Thompson KG, Dittmer KE. Tumors of bone. In: Meuten DJ, editor. *Tumors in Domestic Animals*. Fifth ed. Ames, IA: Wiley Blackwell (2017). p. 356–424. doi: 10.1002/9781119181200.ch10
17. Slayter MW, Boosinger TR, Pool RR, Dämmrich K, Misdrop W, Larsen S. *Histological Classification of Bone and Joint Tumors of Domestic Animals*, Vol. 1, Washington, DC: Armed Forces Institute of Pathology (1994). p. 1–50.
18. McCauley CT, Campbell GA, Cummings CA, Drost WT. Ossifying fibroma in a llama. *J Vet Diagn Invest*. (2000) 12:473–6. doi: 10.1177/104063870001200517
19. Schmelting B, Zoller M, Kaspareit J. Peripheral ossifying fibroma and juxtacortical chondrosarcoma in cynomolgus monkeys (*Macaca fascicularis*). *J Am Assoc Lab Anim Sci*. (2011) 50:98–104.
20. Collins JA. Ossifying fibroma/osteoma in the proximal tibia of a mature gelding. *Vet Rec*. (1998) 143:367–8. doi: 10.1136/vr.143.13.367
21. Razmyar J, Dezfoulian O, Peighambari SM. Ossifying fibroma in a canary (*Serinus canaria*). *J Avian Med Surg*. (2008) 22:320–2. doi: 10.1647/2007-027.1
22. Mirkovic TK, Shmon CL, Allen AL. Urinary obstruction secondary to an ossifying fibroma of the os penis in a dog. *J Am Anim Hosp Assoc*. (2004) 40:152–6. doi: 10.5326/0400152
23. Roscoe DE, Veikley LR, Mills M Jr, Hinds L, 3rd. Debilitating ossifying fibromas of a white-tailed deer associated with ear tagging. *J Wildl Dis*. (1975) 11:62–5. doi: 10.7589/0090-3558-11.1.62
24. Bregman CL, Hirth RS, Sundberg JP, Christensen EF. Cutaneous neoplasms in dogs associated with canine oral papillomavirus vaccine. *Vet Pathol*. (1987) 24:477–87. doi: 10.1177/030098588702400602
25. Mauldin EA, Peters-Kennedy J. Integumentary system. In: Jubb KVF, Kennedy PC, Palmer N, editors. *Pathology of Domestic Animals*. Sixth ed. St. Louis, MO: Elsevier. (2016). p 509–736. doi: 10.1016/B978-0-7020-5317-7.00006-0
26. Groff DE, Lancaster WD. Molecular cloning and nucleotide sequence of deer papillomavirus. *J Virol*. (1985) 56:85–91. doi: 10.1128/JVI.56.1.85-91.1985
27. Ahola H, Bergman P, Strom AC, Moreno-Lopez J, Pettersson U. Organization and expression of the transforming region from the European elk papillomavirus (EEPV). *Gene*. (1986) 50:195–205. doi: 10.1016/0378-1119(86)90324-0

Conflict of Interest: The authors declare that the research was conducted in the absence of any commercial or financial relationships that could be construed as a potential conflict of interest.

Copyright © 2020 Zürcher-Giovannini, Ruder, Pool, Erdelyi and Origgi. This is an open-access article distributed under the terms of the Creative Commons Attribution License (CC BY). The use, distribution or reproduction in other forums is permitted, provided the original author(s) and the copyright owner(s) are credited and that the original publication in this journal is cited, in accordance with accepted academic practice. No use, distribution or reproduction is permitted which does not comply with these terms.

frontiers in Veterinary Science

ORIGINAL RESEARCH
published: 30 April 2020
doi: 10.3389/fvets.2020.00229

Epitheliotropic Infections in Wildlife Ruminants From the Central Alps and Stelvio National Park

Laura Gallina[1], Federica Savini[1], Giovanni Casà[1], Irene Bertoletti[2], Alessandro Bianchi[2], Lucia Rita Gibelli[2], Davide Lelli[2], Antonio Lavazza[2] and Alessandra Scagliarini[3]*

[1] *Dipartimento di Scienze Mediche Veterinarie, Alma Mater Studiorum, Università di Bologna, Bologna, Italy,* [2] *Istituto Zooprofilattico Sperimentale della Lombardia e dell'Emilia-Romagna, Brescia, Italy,* [3] *Dipartimento di Medicina Specialistica Diagnostica e Sperimentale, Alma Mater Studiorum, Università di Bologna, Bologna, Italy*

The mountain chain of the Alps, represents the habitat of alpine fauna where the red deer (*Cervus elaphus*) population is the outmost numerous, followed by the chamois (*Rupicapra rupicapra*) and the alpine ibex (*Capra ibex*) at higher altitudes. Previous reports showed the circulation of epitheliotropic viruses, belonging to the families *Papillomaviridae* and *Poxviridae,* causing skin and mucosal lesions in wild ruminants of the Stelvio National Park, situated in the area. To deepen our knowledge on the natural dynamics of the infections, a passive surveillance on all the cases of proliferative skin and mucosal lesions in wild ruminants was performed. Twenty-seven samples (11 chamois, 10 red deer and 6 ibex) collected from 2008 to 2018 were analyzed by negative staining electron microscopy, histology, and PCR followed by genome sequencing and phylogenetic analyses. Results confirmed the spread of Parapoxvirus of Red Deer in New Zealand (PVNZ) in Italy, and its ability to cause severe lesions i.e., erosions and ulcers in the mouth. We showed for the first time a PVNZ/CePV1v (C. *elaphus* papillomavirus 1 variant) co-infection identified in one red deer. This result supports previous evidence on the ability of papillomavirus and parapoxvirus to mutually infect the same host tissue. Interestingly two ibex and one chamois showing orf virus (OV) skin lesions were shown to be co-infected with bovine papillomavirus type 1 and 2. The presence of bovine papillomavirus, in orf virus induced lesions of chamois and ibex raises the question of its pathogenetic role in these animal species. For the first time, OV/CePV1v co-infection was demonstrated in another chamois. CePV1v is sporadically reported in red deer throughout Europe and is considered species specific, its identification in a chamois suggests its ability of cross-infecting different animal species. Poxviruses and papillomavirus have been simultaneously detected also in the skin lesions of cattle, bird and human suggesting a possible advantageous interaction between these viruses. Taken together, our findings add further information on the epidemiology and pathogenetic role of epitheliotropic viruses in wild ruminants living in the central Alps and in Stelvio National Park.

Keywords: coinfection, papillomavirus, poxvirus, ruminants, wildlife, epitheliotropic, phylogenesis

OPEN ACCESS

Edited by:
Francesco Carlo Origgi, University of Bern, Switzerland

Reviewed by:
Carlo Vittorio Citterio, Istituto Zooprofilattico Sperimentale delle Venezie, Italy
Karoly Erdelyi, National Food Chain Safety Office, Hungary

****Correspondence:***
Laura Gallina
laura.gallina@unibo.it

Specialty section:
This article was submitted to Veterinary Experimental and Diagnostic Pathology, a section of the journal Frontiers in Veterinary Science

Received: *17 January 2020*
Accepted: *03 April 2020*
Published: *30 April 2020*

Citation:
Gallina L, Savini F, Casà G, Bertoletti I, Bianchi A, Gibelli LR, Lelli D, Lavazza A and Scagliarini A (2020) Epitheliotropic Infections in Wildlife Ruminants From the Central Alps and Stelvio National Park. Front. Vet. Sci. 7:229. doi: 10.3389/fvets.2020.00229

INTRODUCTION

Epitheliotropic viruses belonging to the *Poxviridae* and *Papillomaviridae* families include a number of viral species which are known to infect wild ruminants in many parts of the world. According to ICTV in the *Poxviridae* family, *Chordopoxvirinae* subfamily, the genera Deerpoxvirus and Parapoxvirus include several species able to cause diseases in wild ruminants (1). The viruses belonging to the genus Deerpoxvirus (DPV) are responsible for non-parapoxvirus-like infections in the members of two subfamilies of cervids, American deer (*Odocoileinae*) and reindeer (*Rangiferinae*). These viruses, resembling orthopoxviruses in shape, have been reported in North America in wild mule deer (*Odocoileus hemionus*) in Wyoming (2), black-tailed deer (*O. h. columbianus*) (3) and pudu (*Pudu puda*) (4) in California, in wild cervid species in the Northwest Pacific (5), in farmed white-tailed deer in Mississipi (6) and in a goitered gazelle (*Gazella subgutturosa*) (7). The first genome sequence of Mule Deerpoxvirus (MDPV), from a farmed white-tailed deer fawn in Florida, has been recently published by Sayler et al. (8). A sero-survey, performed in Oregon, indicated that the exposure to DPV is common in Odocoileus populations leading to speculate that the high antibody prevalence and the low rate of observed DPV-related disease may suggest a low virulence of these pathogens (9).

To date, in the genus Parapoxvirus (PPV) there are four confirmed PPV species recognized by the ICTV: the prototype member orf virus (ORFV) endemic in most sheep- and goat-raising countries, the bovine popular stomatitis virus (BPSV) and pseudocowpox virus (PCPV) mainly infecting cattle. The Parapoxvirus of Red Deer in New Zealand (PVNZ), described by Robinson and Mercer (10) has now become the fourth PPV species (11). OV, PCPV, and PVNZ have been detected in several deer species including: white-tailed deer from the United States (12, 13), red deer (*Cervus elaphus*) in New Zealand, Italy and Germany (10, 11, 14, 15), chamois (*Rupicapra rupicapra*) in Italy and Austria (16, 53) and ibex (*Capra ibex*) in Italy (14) and reindeer (*Rangifer tarandus*) in Scandinavia (17, 18). In 2018, Tryland and collaborators reported parapoxvirus infections in caribou and Sitka black-tailed deer confirming that most of the wild ruminant species in Alaska can be affected by OV. Human infection from cervid-borne parapoxviruses (OV and PCPV) has been reported in America and in Europe (12, 16, 19, 20). These findings showed that hunters, wildlife inspectors, subsistence harvesters, and biologists are the professional categories most exposed to PPV infections from wild animals.

The family *Papillomaviridae* comprises 330 PV types currently listed as Reference Genomes for animals in the Papillomavirus Episteme (http://pave.niaid.nih.gov). Only 39 ruminant PV types are recognized up to now [Papillomavirus Episteme, (21)]. Within the large group of ungulates (diverse group of mammals that includes odd-toed and even-toed ungulates), bovine papillomavirus (BPV) plays a major role in a variety of diseases in domestic and wild ruminants (22). PV DNAs have been detected in Europe and North America in papilloma lesions of several wild deer species (23–31). The majority of papillomaviruses detected in wild deer belong to the Delta genus and cause fibropapillomatosis. This disease has been reported in roe deer (*Capreolus capreolus*) in Hungary and the Czech Republic (28, 29) and in red deer in Italy and Portugal (32, 33). The causative agents CcaPV1 and CePV1v are closely related PV variants of the Delta papillomavirus genus. At present, in all the European countries where red deer fibropapillomas have been reported, there was no evidence of a similar infection in roe deer. To date, Hungary is the only European country in which there is a coexistence of CePV1v and CcaPV1 infection in local deer population (32). A new papillomavirus, RtPV2, genus Xi, was identified in the eye swab samples of semi-domesticated reindeer (*R. tarandus tarandus)* in Norway (34). More recently, multiple persistent pigmented squamous papillomas (warts) on the chins in European red (*C. elaphus elaphus*) X wapiti (*C. e. canadensis*) deer stags were shown to be caused by CePV1 belonging to the Epsilon genus (35).

Wildlife disease surveillance is a complementary component of human and animal disease surveillance, monitoring, prevention and control programs, as well as conservation efforts (36). Smits et al. (34) underlined the importance of studying the virus diversity in wildlife to provide important epidemiological baseline information about pathogens and their evolutionary patterns in different host species. A collaboration network of hunters, wildlife rangers, Istituto Zooprofilattico Sperimentale della Lombardia e dell'Emilia Romagna (IZSLER) and University of Bologna was established to better understand the natural dynamics and possibility for interspecies transmission of the infections and clinical diseases caused by the epitheliotropic viruses circulating in wildlife population of the central Alps and Stelvio Park. With this purposes, a range of testing were employed for confirmatory diagnosis and the main findings on viral genomic characterization are presented.

MATERIALS AND METHODS

Sampling

The study was performed in northern Italy, Lombardia region in the Valtellina valley (province of Sondrio), Brembana and Seriana valley (province of Bergamo) and in Camonica valley (province of Brescia) where wild ruminants such as chamois (*R. rupicapra*), red deer (*C. elaphus*) and ibex (*C. ibex*) are present. samples were taken from carcasses of necropsied animals, during the diagnostic activities of the IZSLER. In fact, chamois and ibex found dead are commonly submitted to IZSLER and examined in the framework of the regional health monitoring and control plan for wildlife (DDG, 5 December 2012, no. 11358).

A certain number of red deer were randomly culled during a program aimed at controlling its population density in the Stelvio National Park (Lombardia Region).

Moreover, selective hunting of wild ungulates is legal during the September-December period. In accordance with Italian Law (N. 157 of 11/02/1992), hunters must carry culled wild ruminants to the control centers where age, sex and morpho-biometric measurements are registered and gross lesions inspection of carcass and organs are also performed.

For this study, cutaneous pathological samples with proliferative lesions such as epithelial or fibroepithelial

neoplasms were collected from animals of every age group and adult animals during post-mortem inspection and stored at −20°C for 1–2 weeks in the control center facility and subsequently transferred at −80°C to the laboratory until further processing. Cutaneous samples ($n = 27$) were collected during seven (2008, 2010–2013, 2016, 2018) hunting seasons (**Table 1**). In particular, during the same period a total of 1,572 carcasses were examined 1,119 of which were red deer, 400 were chamois and 53 were ibex. The number of cases presenting skin and mucosal lesions were 19 for red deer, 20 for chamois and 9 for ibex. Samples were obtained only from legally hunted animals or animals found dead. No animal was deliberately culled for this study.

Histopathology

Tissue samples were fixed by immersion in 10% neutral buffered formalin and embedded in paraffin wax. Sections were cut at 4 μm, stained with hematoxylin and eosin (HE) and examined by light microscopy.

Negative Staining Electron Microscopy

Tissue samples were subjected to negative staining electron microscopy using the Airfuge method (37). Samples were ultracentrifuged (Airfuge, Beckman Coulter Inc. Life Sciences, Indianapolis, Indiana, USA) for 15 min at 82,000 × g using a rotor holding six 175-μl test tubes in which specific adapters for 3 mm carbon-coated Formvar copper grids were placed. The grids were then stained using 2% sodium phosphotungstate (pH 6.8) for 1.5 min and observed under a Tecnai G2 Spirit Biotwin transmission electron microscope (FEI, Hillsboro, Oregon, USA) at 20,500–43,000× for at least 15 min before being considered negative. Attempts to identify the observed viral particles were based on their morphological characteristics.

PCR and Sequencing

DNA from 25 mg of each fresh sample was extracted using NucleoSpin Tissue kit (Macherey-Nagel GmbH, Duren, Germany). The PCR reactions were performed with a Taq PCR Master Mix Kit (Qiagen, Hilden, Germany) on a final volume of 25 ul containing 1x PCR buffer, 5 μL of Q-solution, 0.8 uM deoxynucleotide mix (Thermo Scientific, Waltham, Massachusetts, USA), 0.4 uM of sense and antisense primer, 2.5 μL of DNA template, and 0.65 units of Taq DNA polymerase. Each reaction included a no-template control and an appropriate positive control (a previously sequenced sample). The presence of BPV1 and BPV2 was tested by amplification of the L1 ORF encoding the L1 major capsid protein. The entire genome of CePV1v was obtained from two red deer samples (376 and 377) as already described (32) while for the samples 1,601, 1,635, and 1,636 only the L1 and partial L2 samples were amplified and sequenced. Detection of parapoxvirus was performed amplifying the B2L gene encoding the homolog of the vaccinia virus major envelope antigen p37K. Further genomic characterization of the Parapoxvirus positive samples was accomplished through amplification of three virulence genes GIF, vIL-10, vVEGF. Primers used and target genes amplified are listed in **Table 2**. Sanger sequencing was performed on both strands of the amplified DNA (ABI Prism 3100 Genetic Analyzer, Perkin-Elmer Applied Biosystems, Foster City, California, USA) and chromatograms were assembled using 4Peaks 1.7.1 (Nucleobytes 2015). Sequences were deposited in GenBank using the National Center for Biotechnology Information (NCBI) BankIt v3.0 submission tool (NCBI 2015) under accessions (see **Table 1**).

Phylogenetic Analysis

Phylogenetic analyses were performed by MEGA 7. The evolutionary history for the B2L and vVEGF genes and concatenated B2L, GIF, vIL-10, and vVEGF genes were inferred by using the maximum Likelihood method based on Tamura 3-parameter model and gamma-distribution. Statistical support for branches of the trees was evaluated by bootstrapping with 1,000 replications. The concatenated phylogenetic tree has been performed based on the alignment of 19 amino acid sequences, there were a total of 569 positions in the final dataset. The analysis of the B2L gene involved 62 nucleotide sequences and there were a total of 489 positions in the dataset. The vVEGF phylogenetic tree has been performed based on 53 deduced amino acid sequences. There were a total of 111 positions in the final dataset.

RESULTS

Gross Pathology and Histopathology

Overall, a 3% prevalence of skin and mucosal lesions attributable to PPV or PV was calculated in the years considered. The prevalence for each animal species is different, ibexes showed the highest prevalence (17%) followed by chamois (5%) and deer (1.7%). The lesions are distributed differently depending on the age groups, in particular animals of the year ($N = 8$, 36%) and up to 2 years of age ($N = 11$, 50%) account for 86% of positive cases, while in adults PPV and PV lesions are less frequent ($N = 3$, 14%).

Post-mortem inspection showed different size firm cutaneous tumors with rough hairless pigmented surface, resembling papillomas (**Figures 1A,B**), on the hind legs of 5 hunted red deer (376, 377, 1,601, 1,635, 1,636). On histological examination, exophytic proliferation with hyperparakeratosis and pseudo-epitheliomatous hyperplasia was observed. The stratum granulosum was prominent with presence of large, rounded and irregular keratohyalin granules in the epidermis and the dermis showed a proliferation of fibroblasts and connective tissue with multifocal mononuclear inflammatory infiltrate in all the papilloma-like lesions of Red deer. The histopathological findings were consistent with red deer fibropapillomatosis.

Proliferative lesions, erosions, and ulcers, resembling parapoxvirus infections, on the lips and on the hard palate (**Figures 1C,D**) were reported in 5 Red Deer found dead (1126B, 1126C, 1126D, 1126E, 523), in seven Chamois (45, 265, 520, 521, 1,637, 257/09, 485/09) and three ibexes (47, 7/11, 373/08) (found dead). Ulcerative and crusting lesions on the coronary band as well as the mucocutaneous tissues of the head (**Figures 1E,F**)

TABLE 1 | List of examined cases.

Animal ID	Animal species	EM	PPV (GenBank accession n.)	PV (GenBank accession n.)	Site of collection	Date of collection
1126B	Red deer (F, 6 m)	PPV	MN977289 MN977284	–	Bormio (So)	08/11/2010 dead
1126C	Red deer (M, 6 m)	–	MN977290 MN977285	MN977312 MN977315	Bormio (So)	08/11/2010 dead
1126D	Red deer (F, 10 Y)	PPV	MN977293	–	Bormio (So)	08/11/2010 dead
1126E	Red deer (M, 10 m)	–	MN977291	–	Bormio (So)	08/11/2010 dead
523	Red deer (M, U)	PPV	MN977292 MN977286	–	Ponte di Legno (Bs)	23/04/2013 U
376	Red deer (M, 2 Y)	PV	–	MN985322	Vione (Bs)	03/11/2012 dead
377	Red deer (U, U)	PV	–	MN985323	Lenno (Co)	29/10/2012 hunted
1601	Red deer (U, U)	PV	–	MN977311 MN977318	Monno (Bs)	23/09/2018 hunted
1635	Red deer (M, 1 Y)	PV	–	MN977310 MN977317	Gravedona (Co)	02/09/2016 hunted
1636	Red deer (M, 1 Y)	PV	–	MN977316 MN977309	Valdidentro (So)	03/09/2016 hunted
45	Chamois (M, 2 Y)	PPV	MN977219 MN977305 MN977270 MN977209	MN977319	Sondalo (So)	03/03/2018 dead
115	Chamois (F, 1 Y)	PPV	MN977216 MN977299 MN977279 MN977210	–	Carona (Bg)	19/10/2011 hunted
265	Chamois (U, 6 m)	PPV	MN977217 MN977278 MN977200	–	Lenna (Bg)	29/11/2011 U
375	Chamois (M, 1,5 Y)	PPV	MN977221 MN977302 MN977272 MN977201	MN977313 MN977314	Val Masino (So)	08/10/2012 dead
519	Chamois (F, 6 m)	PPV	MN977222 MN977295 MN977273 MN977202	–	Ponte in Valtellina (So)	09/01/2013 dead
520	Chamois (F, 1 Y)	PPV	MN977223 MN977303 MN977274 MN977203	–	Ponte di Legno (Bs)	22/01/2013 dead
521	Chamois (F, 1 Y)	PPV	MN977224 MN977307 MN977275 MN977204	–	Ponte di Legno (Bs)	23/02/2013 dead
522	Chamois (M, 6 m)	PPV	MN977225 MN977297 MN977276 MN977205	MN977322	Val Masino (So)	27/02/2013 dead
1637	Chamois (M, 2 Y)	PPV	MN977226 MN977308 MN977287 MN977208	–	Valdidentro (So)	22/10/2018 hunted
257/09	Chamois (M, 1 Y)	PPV	HQ239071* MN977294 MN977283 MN977196	–	Valdidentro (So)	19/02/2008 hunted

(Continued)

TABLE 1 | Continued

Animal ID	Animal species	EM	PPV (GenBank accession n.)	PV (GenBank accession n.)	Site of collection	Date of collection
485/09	Chamois (F, 6 m)	PPV	HQ239073* MN977298 MN977280 MN977197	–	Fusine (So)	06/03/2008 dead
07/11	Ibex (M, 8 m)	PPV	MN977213 MN977277 MN977198	–	Valbondione (Bg)	19/01/2011 dead
116	Ibex (M, 3 m)	PPV	MN977214 MN977300 MN977288 MN977211	–	Gerola Alta (So)	21/08/2011 dead
264	Ibex (U, U)	PPV	MN977215 MN977301 MN977282 MN977199	–	Valbondione (Bg)	24/10/2011 dead
44	Ibex (M, 13 Y)	PPV	MN977218 MN977304 MN977269 MN977206	MN977321	Livigno (So)	03/03/2018 dead
373/08	Ibex (M, 6 m)	PPV	HQ239072* MN977296 MN977281 MN977212	–	Ponte di Lgno (Bs)	19/02/2008 dead
47	Ibex (F, 3 Y)	–	MN977220 MN977306 MN977271 MN977207	MN977320	Valfurva (So)	05/06/2018 dead

Electron microscopy (EM) results, GenBank accession numbers of the sequenced samples, site of collection and date and cause (hunted or found dead) of death of the animals. (–): negative result. (*): sequence already published in Scagliarini et al. (14). F, Female; M, Male; m, months; Y, years old; U, unknown.

TABLE 2 | Primers targeting different gene regions were used to detect the papillomavirus CePV1v, BPV1, BPV2, and the parapoxvirus OV and PVNZ from 27 skin lesions' samples.

Gene	Acronym	Primers	Product (bp)	References
Putative viral envelope antigen (OV)	B2L	PPP-1 5′-GTCGTCCACGAGCAGCT-3′ PPP-4 5′-TACGTGGGAAGCGCCTCGCT-3′	595	(38)
Granulocyte–macrophage-colony-stimulating factor/ interleukin-2 inhibition factor (OV)	GIF	GIF 5 5′-GCTCTAGGAAAGATGGCGTG-3′ GIF 6 5′-GTACTCCTGGCTGAAGAG CG-3′	408	(39)
Viral interleukin 10 ortholog (OV)	vIL-10	vIL-10-3 5′-ATGCTACTCACACAGTCGCTCC-3′ vIL-10-4 5′-TATGTCGAACTCGCTCATGGCC-3′	300	(39)
Vascular endothelial growth factor gene of OV NZ-2 like (OV)	VEGF-E	VEGF_forNZ2 5′ATGARGTTGCTCGTCKGCATAC-3′ VEGF_rev1NZ2 5′-CGTCTTCTGGGCGGCCTTGT-3′ VEGF_rev2NZ2 5′-CTTCGGCGCCGTCTAGGC-3′	399	This study
Vascular endothelial growth factor gene of (OV)	VEGF-E	GF1 5′-GCGGGATCCGCCATGAAGTTGCTCGT-3′ GF2 5′-GCGGAATTCCTAGCGGCGTCTTCTGG-3′	399	(40)
Vascular endothelial growth factor gene of (PVNZ)	VEGF-E	5′-TTTGGCGCGCCAGAGACTTCTAATACAGTGTAGCG-3′ 5′-TCACCCGAACGCGTACGTCTTGGAGGCATAG-3′	447	(41)
Vascular endothelial growth factor NZ7 like gene (OV)	VEGF-E	GF3 5′-GCGGGATCCACGATGAAGTTAACAGC-3′ GF4 5′-GCGGAATTCTTATCGTCTAGGTTCCCTA-3′	450	(40)
minor capsid protein (CePV1v)	L2	CePVL2F 5′-TAGACTACTACTACCTGTGACACAC-3′ CePVL2R 5′-TGGTCACAGGTGTAGGTGGCA-3′	250	(33)
major capsid protein (CePV1v)	L1	CePVL1F5731 5′-TATTTGCCACCTACACCTGTGAC-3′ CePVR7253 5′-CAGCTGGACAGCTCATTAG-3′	1522	(33)
E5 oncoprotein (BPV1 and BPV2)	E5	5′B1/2-E5: 5′-CACTACCTCCTGGAATGAACATTTCC-3′ 3′B1/2-E5: 5′-CTACCTTWGGTATCACATCTGGTGG-3′	499	(42)
major capsid protein (BPV1)	L1	BPV1estL1f 5′-TGATGGGCACACAGTTGATTTGTAC-3′ BPV1estL1r 5′-GGTGCAGTTGACTTACCTTCTGT-3′	1621	This study

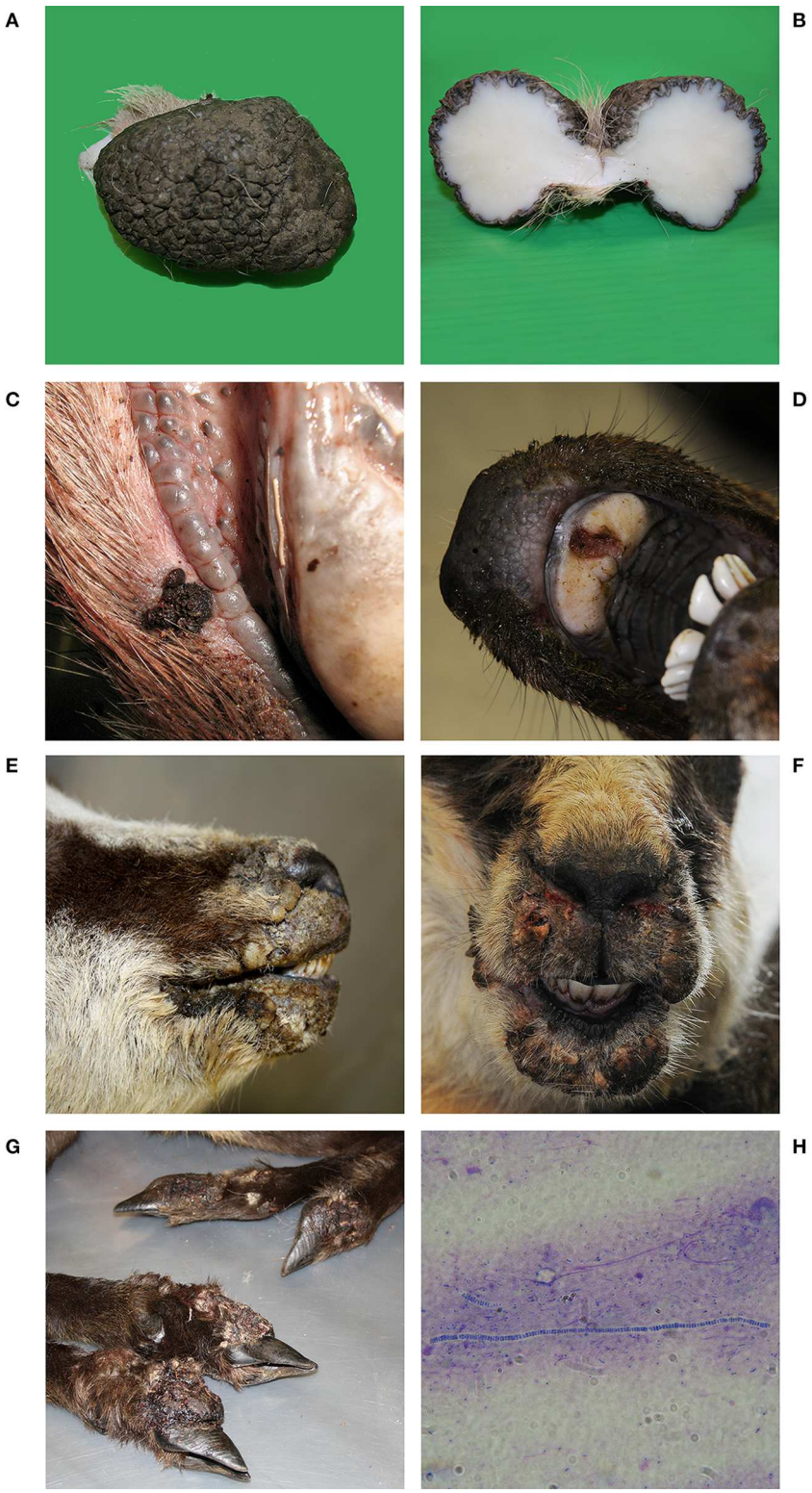

FIGURE 1 | Red deer N° 1635. **(A)** Pedunculated, oval cutaneous neoformation of dimensions 7 × 5 × 5 cm. Hyperkeratotic, glabrous, black, irregular, and fissured surface. **(B)** When cut, lardaceous consistency, white color and uniform, regular appearance. **(C)** Red deer N°1126D and **(D)** Red deer N° 523. Proliferative lesions, erosions, and ulcers on the lips and on the hard palate. **(E)** Chamois N° 522 and **(F)** Chamois N° 520. Ulcerative and crusting lesions on the mucocutaneous tissues of the head: Chamois N° 375. **(G)** Severe proliferative pododermatitis of all four limbs with coronary hyperplasia. **(H)** Microscopic detection of *Dermatophilus congolensis*. Gram staining, 1000x.

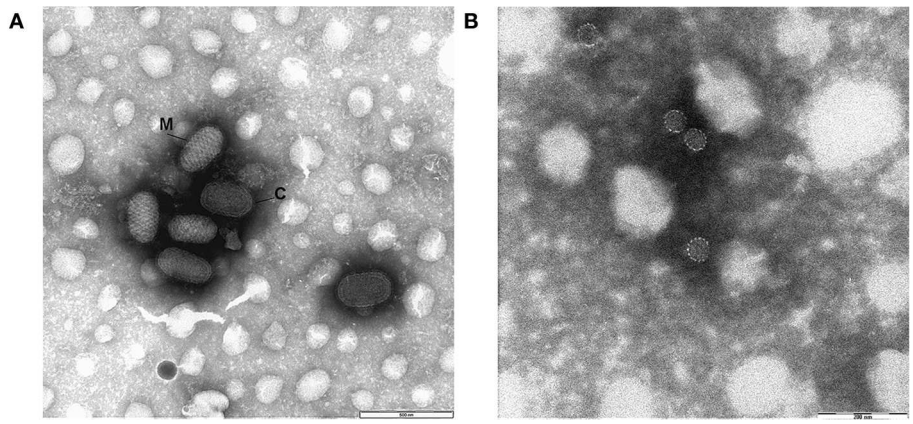

FIGURE 2 | Negative-staining EM micrographs of **(A)** Parapoxvirus showing the typical morphology: oblong, rounded, or ovoid large particles of around 140–170 nm wide and 220–300 nm long. M (mulberry) form, C (capsule) form. Bar = 500 nm. **(B)** Papillomavirus: non-enveloped icosahedral particles of around 50–55 nm in diameter. Bar = 200 nm.

have been shown in four chamois (115, 375, 519, 522) and two ibexes (116, 264). PPVs' typical hyperplastic and proliferative epidermal lesions with vacuolation and swelling of keratinocytes in the stratum spinosum and intracytoplasmic eosinophilic inclusion bodies were observed in all the affected animals. In chamois 375 proliferative dermatitis generally referred to as strawberry footrot (43) was observed in the four lower legs (**Figure 1G**). The bacteriological examination confirmed the isolation of *Dermatophilus congolensis* (**Figure 1H**).

Negative Staining Electron Microscopy

Negative-staining EM showed the presence of parapoxvirus in 19 samples (3 red deer, 11 chamois, 5 ibex) out of 27 cases examined (**Table 1**). PPV identification was based on the typical morphology: oblong, rounded, or ovoid large particles (140–170 nm wide and 220–300 nm long). Either the characteristic M (mulberry) form, showing regular surface structure where tubules with a diameter of 10–20 nm form a criss-cross pattern, and less frequently the C (capsule) form showing a smooth uniform surface and a thick membrane were observed (**Figure 2A**).

Indeed, with the same technique non-enveloped icosahedral particles of around 50–55 nm in diameter, morphologically referable to PVs (**Figure 2B**) were found in 5 red deer samples. Only in three samples, 2 red deer and 1 ibex, we did not observe any viral particles by NSEM.

PCR and Sequencing

PCR amplification and subsequent sequencing of red deer samples revealed PVNZ and CePV1v infections in 5 and 6 samples respectively. Sequencing of a 550 bp of the B2L gene showed 100% nucleotide identity not only among the four PVNZ isolates but also with the cases previously reported in the same geographical area (14). The analysis of the PVNZ VEGF gene revealed 100% amino acidic identity between the samples1126B and 1126C and 95.9% with the sample 523. It was not possible to amplify PVNZ VEGF from the samples 1126E and 1126D. CePV-1v was detected in the form of a single infection in five skin samples (376, 377, 1,601, 1,635, 1,636) and as coinfecting agent together with PVNZ in the sample 1126C. The entirely sequenced 376 and 377 samples showed 100% nucleotide identity with the IT-1127 CePV1v (GenBank n. JQ744282.1). Sequencing of the entire L1 gene (1,524 bp) of the samples 1601, 1635, 1636, 1126C, showed nucleotide identity ranging from 99.9 to 100% among all the analyzed sequences. The amplification and sequencing of 274 bp of the CePV1v L2 gene revealed a nine-nucleotide deletion, causing the lack of three amino acids of the encoded capsid protein. All samples obtained from chamois and ibex tested positive for parapoxvirus infection. Sequencing of the 550 bp of the B2L gene identified OV as the causative agent of the lesions with nucleotide and amino acid identity ranging from 96.3 to 100% in the chamois strains and 97.2 to 100% for the ibex strains. Sequencing of the vIL-10 gene from chamoix and ibex samples allowed to obtain 410 bp sequences displaying 89.1 to 100% and 80.1 to 100% nucleotide and amino acid identity, respectively. The GIF gene was sequenced from all the ibex and chamois samples producing 350 nucleotide sequences showing 83.5 to 100% identity among all isolates. Amplification and sequencing of the entire vVEGF gene identified NZ-2-like VEGF variants in all samples but one (257) that showed high similarity to NZ7-like VEGF (GenBank n. S67522). Ibex and chamois vVEGF gene showed high rate sequence variation in particular, samples 116, 264, 265, 7/11 revealed a 21 nucleotides insertion in the N-terminal region while a 12 nucleotides insertion was evidenced in the C-terminal region of the 115, 116, 44, 1,637 samples. In two chamois (45, 522) and two ibexes (44, 45) it was possible to detect BPV1 co-infecting an OV lesion by sequencing the L1 gene. Finally, in chamois 375 showing echtyma lesion on the nasolabial rim, it was possible to identify and sequence the entire L1 sequence of CePV1v.

Phylogenetic Analysis

The phylogenetic analysis of the partial B2L gene of the 22 parapoxvirus samples compared to the sequences of the four

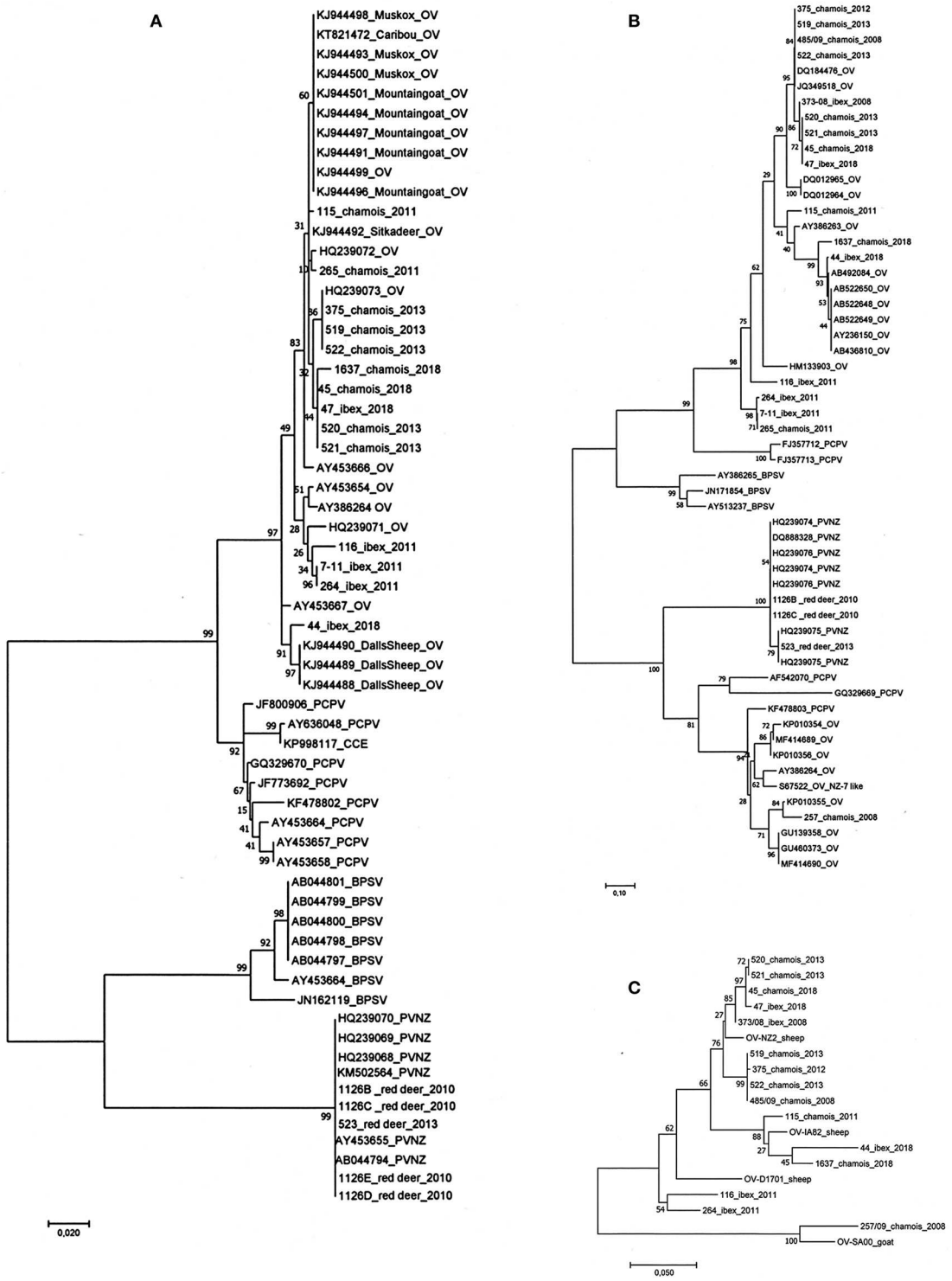

FIGURE 3 | Phylogenetic analysis performed on the parapoxvirus genes sequenced. **(A)** The phylogenetic tree of the partial B2L gene of the 22 parapoxvirus samples showing clusters corresponding to the four species of the parapoxvirus genus, all the OV sequences from ibex and chamois cluster with other strains isolated from sheep and goats. Five PVNZ isolates grouped into a separate cluster with other PVNZ. **(B)** The phylogenetic analysis of the vVEGF showed an expected high variability of the vVEGF variant of isolates from chamois and ibex. The chamois sample 257 grouped with the OV NZ7 like vVEGF variants. **(C)** Phylogenetic tree based on the concatenated B2L, GIF, vVEGF, and vIL10 amino acid sequences. No host-dependent clustering was identified instead two main clusters of NZ2 and NZ7 OV variants. (OV-NZ-2: GenBank n. DQ184476 OV-IA82 GenBank n. AY386263 D1701 GenBank n. HM133903 OV-SA00 GenBank n. AY386264).

species of the parapoxvirus genus, grouped them in two viral species' clusters (**Figure 3A**). Comparison of the 17 sequences from ibex and chamois showed that they were OV and that they cluster with other OV strains isolated from sheep and goats regardless of the infected animal species as already reported for other wildlife species such as Mountain goat (*Oreamnos americanus*), Dall's sheep (*Ovis dalli dalli*), muskoxen (*Ovibos moschatus*), caribou (*R. tarandus*). As expected the five PVNZ cases grouped into a separate cluster with three other PVNZ isolated from red deer in the Stelvio National park (14). The phylogenetic analysis of the deduced amino acid sequences obtained from the vVEGF gene showed the high variability of viral isolates from chamois and ibex confirming clustering with OVs (data are showed in **Figure 3B**). In particular, the sample from chamois 257 grouped with the OV NZ7 like VEGF variants (**Figure 3B**). In accordance with previous data, vVEGF from PVNZ demonstrated a lower degree of sequence variability compared to the other parapoxvirus species grouping in a separate cluster (**Figure 3B**). Despite the variability identified in the B2L, GIF, vVEGF, and vIL10 genes from OV infecting ibex and chamois, the phylogenetic analysis performed on the deduced amino acid sequences of the four OV concatenated genes did not show host-dependent clusterization and revealed two main clusters with the chamois 257 grouping with the NZ7 like strain SA00 isolated from a goat (**Figure 3C**).

DISCUSSION

Wildlife infectious diseases play a major role in regulating natural populations and may seriously threaten the health and welfare of wildlife, livestock and humans. We and others previously reported the circulation of epitheliotropic viruses in wild ruminant populations in different European countries. Several cases of proliferative skin and mucosal diseases associated to CePV1v (32, 33), PVNZ and OV (14) have been reported in wild ruminants of the Stelvio Park which is located in the central Alps. These diseases have been sporadically detected in hunted animals and carcasses of animals found dead during passive surveillance showing that there is a need for broadening the investigations. This study has been carried out to further investigate the etiological aspects of these diseases and collect more data on the natural disease dynamics and the inter-species disease transmission that still remain unclear. Twenty-seven samples have been collected from a larger territory, including the Stelvio National Park but also the mountain valleys of the neighboring provinces of Brescia, Bergamo, and Sondrio (Central Alps) during the period 2008–2018. The limited morbidity rate registered, are probably due to the origin of the cases collected during passive surveillance. A higher prevalence of PPV and PV infected animals can be supported by serological data that showed high antibody prevalence toward another epitheliotropic virus (DPV), indicating that the exposure to theses pathogens is common but the virulence is low with a consequent low rate of disease in Odocoileus populations (9).

Our analyses showed typical parapoxvirus-like particles observed by EM in three red deers found dead showing proliferative lesions covered by crusts, ulcers and erosions on the muco-cutaneous junction of nose and lips. The histologic features were consistent with a parapoxvirus infection in all the cases. Molecular analyses confirmed that the identified virus was the parapoxvirus PVNZ based on the B2L gene and the vVEGF sequences and subsequent phylogenetic analyses. The high level of identity with the same genomic regions of all the available sequences from Italy, Germany and New Zealand further confirms that these parapoxvirus strains are all members of the same species. In contrast the vVEGF gene sequences of all the OV strains responsible of the proliferative lesions of the 11 diseased chamois and five ibexes showed the expected level of genomic variability confirming to be highly hyper-variable as previously reported in OV (46, 47). The low genomic variability of PVNZ might suggest a low selection pressure due to a limited number of susceptible host species, it is in fact known that genomic variants can be a response to increase the fitness of a virus to adapt to immune and antiviral response elicited from different host species (48). The larger host range of OV infecting different domestic and wild animal species and humans may have induced adaptive mutations to allow successful colonization of new animal species (49) contributing to its genomic diversity.

After the first demonstration of PVNZ as the causative agent of the disease in cases of pustular stomatitis in red deer (14), Friederichs et al. (11) isolated PVNZ from tonsils of asymptomatic deer showing that the virus may persist in a small number of healthy looking animals within the population. This data lead us to speculate that, despite the low rate of morbidity, PVNZ may be circulating in persistently infected red deer populations as it was reported in calves (50). Thus, only in a small number of cases, likely in association with other stress factors and/or infectious synergic agents, the PVNZ infections of the mucosal epithelium cause a serious debilitation to the affected animals with reduced ability to feed and death as might have happened to the red deer found dead in our study Persistent infections could allow periodical shedding and clinical manifestations that facilitate the virus survival and spread under favorable conditions (11). Poxvirus-borne life-threatening illnesses, involving the upper alimentary tract occurring in a proportion of affected young and adult deer had been attributed to an immunocompromised state (4). In one of the PVNZ pathological samples (1126C) it was possible to demonstrate also the genome of a papillomavirus and the genetic characterization showed a CePV1v co-infection. CePV1 is the causative agent of red deer fibropapillomatosis and it has not been previously reported as coinfectant agent in a PVNZ induced lesion. The presence of CePV1v is compatible with the ability of PVs to cause latent infection (44). Although the mechanism has not yet been elucidated, following infection they can maintain their genome as episome in the basal layer cells. The lack of detection of mature particles by EM in this sample could support such hypothesis. Our results further confirm the simultaneous presence of different epitheliotropic viruses as already reported in animal and human skin lesions (51–53).

CePV1v was associated with single or multiple fibropapilloma collected from the inner limb of five hunted red deer in agreement with previous reports (14, 33). While there is evidence that Bovine papillomaviruses are not restricted to any anatomical site in cattle (45), fibropapillomas of Red deer associated to CePV1 were always localized in the inner hind leg. This constant localization could be the result of a transmission through arthropod vectors that might play a significant role in the ecology of the virus (28). Indeed, a demonstration of roe deer papillomavirus (CcaPV) DNA in deer keds (*Lipoptena cervi*) and ticks (*Ixodes ricinus*) was reported (29).

The CePV1v confirms to be associated to all the red deer fibropapillomas as previously pointed out and our data further confirm that the pathogen is circulating in Central Alps and in the Stelvio Park being only sporadically reported. The detection of the nucleotide deletion in the L2 gene in all samples is confirmed to be a genomic distinctive characteristic of the CePV1v supporting its classification as a variant of the CcaPV1 that infects roe deer.

More evidence of PPV/PV co-infections is given by the detection of BPV1 and BPV2 in contagious ecthyma samples of two chamois and two ibexes confirming what was previously found in the healthy skin of chamois and ibexes in the Italian Alps (54). The presence of BPV in PPV induced lesions of chamois and ibex poses the question on its pathogenetic role. Poxvirus and Papillomavirus have been simultaneously detected also in skin lesions of cattle (55, 56), birds (57), and humans (51), suggesting that both viruses can complete a replication cycle in the same lesion, providing important data on the host-range of these infectious agents. The skin is the primary barrier to the external environment where groups of viruses sharing cell tropism may be present and not necessarily indicative of a pathology, instead co-infections may represent a degree of commensal interactions (58). Previous report (54) identified bovine papillomavirus DNA in the healthy skin of wild ruminants, documenting coinfection of BPV-1 and CePV1v in healthy red deer in Italy.

Another PPV and PV coinfection was identified in a chamois ecthyma lesion where CePV1v was detected only by molecular biology. This data confirms the ability of this further viral species of the Delta PV genus to infect different animal species beside its natural host. The mechanism of inter species transmission of CePV1v should be studied further in the light of the fact that other Delta papillomaviruses have already shown to be transmissible even to phylogenetically distant animal species thus host tropism of papillomaviruses is not as species-specific as previously thought (22). The genetic characterization of the PPV infecting chamois and ibex suggested that OV has an ecological niche in chamois and ibex as reported for other wildlife species worldwide (39). Nevertheless, phylogenetic analysis of the conserved B2L gene showed that all strains of chamois and ibex grouped with other isolates from sheep and goats instead of clustering by animal species confirming the high genomic variability of the OV species and the susceptibility of wildlife species. In the study area, domestic livestock share pastures with wildlife and it's not uncommon to observe goats among ibexes during the summer season, suggesting the possibility for viral spread among domestic and wild animals.

The same results were obtained by phylogenetic analysis performed on the variable virulence genes vIL10 and GIF that suggested a diverse OV population spreading among chamois and ibex of the Stelvio Park and Central Alps. It was also possible to identify a NZ7 like VEGF variant gene in the isolate from chamois 257, this variant is less widespread and more conserved and often associated with proliferative forms of contagious ecthyma of sheep and goats (40, 59).

Dermatophilus congolensis was isolated from one chamois presenting a clinical condition generally referred to as strawberry footrot (43). This animal was in poor general condition presenting massive proliferative OV lesions over the muzzle which might have predisposed the subject to infection and eventually led to the development of severe disease form. Dermatophilosis and contagious ecthyma in wildlife share clinical signs and predisposing factors like traumatic abrasions so they can co-infect host's skin. Due to their zoonotic potential it is important to identify and report these skin diseases (14, 60–63). The persistence of PPV and other zoonotic pathogens in Alpine wild ruminants indicates a source for virus transmission to susceptible livestock and hunters (12, 19, 20, 64). Farmers and veterinarians represent high-risk groups, as their repeated contact with livestock and wild animals expose them to a possible infection. Our findings provide a further example of wildlife animals playing a role as reservoir of zoonotic diseases. Taken all together our results add further information on the microbial populations inhabiting the skin of wild ruminants. Recent studies have demonstrated that interactions between the skin microbiome and the immune system can maintain a healthy skin vs. the establishment of a disease status (65). Metagenomic analyses would be required to further characterize the skin microbiome of these animal species to better understand their cutaneous ecosystem.

CONCLUSION

This study reports skin epithelitropic lesions of wild ruminants describing pathologiacal finding and the viral associated agents like CePV1v and PVNZ in red deer and OV in chamois and ibex. Sequences obtained from PPV affected red deer revealed a high degree of identity between individuals examined suggesting that PVNZ is strictly species specific. On the other hand, CePV1v was detected as infectant agent in fibropapilloma of red deer but also as coinfectant of a PPV lesion in a chamois. This evidence leads us to speculate that, like other delta papillomavirus, also CePV1v could gain new hosts and change the epidemiology of an infection that it is only sporadically reported. The high genomic variability of OV affecting chamois and ibex suggests the possibility of transmission of OV from wildlife to livestock. Wild ruminants might be a further source of viruses during the summer season for domestic ruminants and humans. These findings show that active surveillance plan are indeed crucial to collect data on the real spread of epitheliotropic infections in wildlife species and domestic target hosts.

DATA AVAILABILITY STATEMENT

The original contributions presented in the study are included in the article/supplementary files, further inquiries can be directed to the corresponding author/s.

ETHICS STATEMENT

Ethical review and approval was not required for the animal study because samples were taken from carcasses of necropsied animals, during the diagnostic activities of the IZSLER. In fact, chamois and ibex found dead are commonly submitted to IZSLER and examined in the framework of the regional health monitoring and control plan for wildlife (DDG, 5 December 2012, no. 11358). A certain number of red deer were randomly culled during a program aimed at controlling its population density in the Stelvio National Park (Lombardia Region). Moreover, wild ungulates are legally selective-hunted during the period September-December. In accordance with Italian Law (N. 157 of 11/02/1992), hunters must carry culled wild ruminants to the control centers where age, sex and morpho-biometric measurements are registered and gross lesions inspection of carcass and organs are also performed.

AUTHOR CONTRIBUTIONS

LG and FS performed genetic characterization and molecular analyses and wrote the manuscript. GC performed genetic characterization and molecular analyses. AB and IB performed necropsy, coordinated field sampling, and contributed to the preparation of the manuscript. LRG performed histopathological investigation. AL and DL performed electron microscopy and contributed to the preparation of the manuscript. AS assisted in project conception, wrote and edited various parts of the manuscript.

ACKNOWLEDGMENTS

Giovanni Bozzoni for technical assistance and Giusppe Bertocchi for artwork (figures) preparation.

REFERENCES

1. ICTV. Available online at: https://talk.ictvonline.org/
2. Williams ES, Becerra VM, Graham TJ, Owens MJ, Nunamaker CE. Spontaneous poxviral dermatitis and keratoconjunctivitis in free-ranging mule deer (*Odocoileus hemionus*) in Wyoming. *J Wildl Dis*. (1985) 21:430–3. doi: 10.7589/0090-3558-21.4.430
3. Patton JF, Nordhausen RW, Woods LW, MacLachlan NJ. Isolation of a poxvirus from a black-tailed deer (Odocoileus hemionus columbianus). *J Wildl Dis*. (1996) 32:531–3. doi: 10.7589/0090-3558-32.3.531
4. Junge RE, Duncan MC, Miller E, Gregg D, Kombert M. Clinical presentation and antiviral therapy for poxvirus infection in pudu (*Pudu puda*). *J Zoo Wildl Med*. (2003) 31:412–8. doi: 10.1638/1042-7260(2000)031[0412:CPAATF]2.0.CO;2
5. Moerdyk-Schauwecker M, Eide K, Bildfell R, Baker RJ, Black W, Graham et al. Characterization of cervidpoxvirus isolates from Oregon, California and eastern Canada. *J Vet Diagn Investig*. (2009) 21:487–92. doi: 10.1177/104063870902100409
6. Baughman B, Zhang S, Jin L, Pace LW, Cooley J, Yan L, et al. Diagnosis of deerpox virus infection in a white tailed deer (Odocoileus virginianus) fawn. *J Vet Diagn Investig*. (2011) 23:965–70. doi: 10.1177/1040638711416621
7. Bracht AJ, Armién AG, Carrillo C, O'Hearn ES, Fabian AW, Moran KE, et al. Isolation and characterization of a Cervidpoxvirus from a goitered gazelle (*Gazella subgutturosa*) from a zoologic park in Minnesota. *J Zoo Wildl Med*. (2013) 44:589–95. doi: 10.1638/2012-0090R2.1
8. Sayler KA, Subramaniam K, Jacob JM, Loeb JC, Craft WF, Farina LL, et al. Characterization of mule deerpox virus in Florida white-tailed deer fawns expands the known host and geographic range of this emerging pathogen. *Arch Virol*. (2019) 164:51–61. doi: 10.1007/s00705-018-3991-7
9. Jin L, McKay A, Green R, Xu L, Bildfell R. Serosurvey for antibody to Deerpox virus in five Cervid species in Oregon, USA. *J Wildl Dis*. (2013) 49:186–9. doi: 10.7589/2011-12-353
10. Robinson AJ, Mercer AA. Parapoxvirus of red deer: evidence for its inclusion as a new member in the genus parapoxvirus. *Virology*. (1995) 208:812–5. doi: 10.1006/viro.1995.1217
11. Friederichs S, Krebs S, Blum H, Lang H, Buttner M. Parapoxvirus (PPV) of red deer reveals subclinical infection and confirms a unique species. *J Gen Virol*. (2015) 96:1446–62. doi: 10.1099/vir.0.000080
12. Roess AA, Galan A, Kitces E, Li Y, Zhao H, Paddock CD, et al. Novel deer-associated parapoxvirus infection in deer hunters. *N Engl J Med*. (2010) 363:2621–7. doi: 10.1056/NEJMoa1007407
13. Roess AA, McCollum AM, Gruszynski K, Zhao H, Davidson W, Lafon N, et al. Surveillance of parapoxvirus among ruminants in Virginia and Connecticut. *Zoonoses Public Health*. (2013) 60:543–8. doi: 10.1111/zph.12036
14. Scagliarini A, Vaccari F, Turrini F, Bianchi A, Cordioli P, Lavazza A. Parapoxvirus infections of red deer. *Italy Emerg Infect Dis*. (2011) 17:684–7. doi: 10.3201/eid1704.101454
15. Horner GW, Robinson AJ, Hunter R, Cox BT, Smith R. Parapoxvirus infections in New Zealand farmed red deer. *N Z Vet J*. (1987) 35:41–5. doi: 10.1080/00480169.1987.35376
16. Kitchen M, Müller H, Zobl A, Windisch A, Romani N, Huemer H. ORF virus infection in a hunter in Western Austria, presumably transmitted by game. *Acta Derm Venereol*. (2014) 94:212–4. doi: 10.2340/00015555-1643
17. Tikkanen MK, McInnes CJ, Mercer AA, Büttner M, Tuimala J, Hirvelä-Koski V, et al. Recent isolates of parapoxvirus of Finnish reindeer (*Rangifer tarandus* tarandus) are closely related to bovine pseudocowpox virus. *J Gen Virol*. (2004) 85:1413–8. doi: 10.1099/vir.0.79781-0
18. Klein J, Tryland M. Characterisation of parapoxviruses isolated from Norwegian semi-domesticated reindeer (*Rangifer tarandus* tarandus). *Virol J*. (2005) 79:422–32. doi: 10.1186/1743-422X-2-79
19. Smith KJ, Skelton HG, James WD, Lupton GP. Parapoxvirus infections acquired after exposure to wildlife. *Arch Dermatol*. (1991) 127:79–82. doi: 10.1001/archderm.1991.01680010089014
20. Kuhl JT, Huerter CJ, Hashish H. A case of human orf contracted from a deer. *Cutis*. (2003) 71:288–90.
21. National Institute of Allergy and Infectious Diseases. *Papilloma Episteme. The Papillomavirus Knowledge Source*. (2019). Available online at: http://pave.niaid.nih.gov (accessed January 17, 2020).
22. Daudt C, Da Silva FRC, Lunardi M, Alves CBDT, Weber MN, Cibulski SP, et al. Papillomaviruses in ruminants: an update. *Transbound Emerg Dis*. (2018) 65:1381–95. doi: 10.1111/tbed.12868
23. Shope RE, Mangold R, Macnamara LG, Dumbell KR. An infectious cutaneous fibroma of the Virginia whitetailed deer (*Odocoileus virginianus*). *J Exp Med*. (1958) 108:797–802. doi: 10.1084/jem.108.6.797
24. Lancaster WD, Sundberg JP. Characterization of papillomaviruses isolated from cutaneous fibromas of white-tailed deer and mule deer. *Virology*. (1982) 123:212–6. doi: 10.1016/0042-6822(82)90307-5
25. Moreno-Lopez J, Pettersson U, Dinter Z, Philipson L. Characterization of a papilloma virus from the European elk (EEPV). *Virology*. (1981) 112:589–95. doi: 10.1016/0042-6822(81)90304-4
26. Moar MH, Jarrett WF. A cutaneous fibropapilloma from a red deer (*Cervus elaphus*) associated with a papillomavirus. *Intervirology*. (1985) 24:108–18. doi: 10.1159/000149626
27. Erdélyi K, Bálint A, Dencso L, Dán A, Ursu K. Characterisation of the first complete genome sequence of the roe deer (*Capreolus capreolus*) papillomavirus. *Virus Res*. (2008) 135:307–11. doi: 10.1016/j.virusres.2008.03.002

28. Erdélyi K, Gál J, Sugár L, Ursu K, Forgách P, Szeredi L, et al. Papillomavirus-associated fibropapillomas of red deer (*Cervus elaphus*). *Acta Vet Hung*. (2009) 57:337–44. doi: 10.1556/AVet.57.2009.2.14
29. Král J, Bandouchová H, Brichta J, Kováčová V, Ondráček K, Osičková J, et al. Papillomavirus infection of roe deer in the Czech Republic and fibropapilloma-associated levels of metallothionein, zinc, and oxidative stress. *Acta Vet Brno*. (2015) 84:105–11. doi: 10.2754/avb201584020105
30. Mengual-Chuliá B, Wibbelt G, Gottschling M, Bravo I. Distantly related papillomaviruses isolated from healthy skin of the timor deer (Rusa timorensis). *Genome Announc*. (2018) 14:24. doi: 10.1128/genomeA.00505-18
31. Mengual-Chuliá B, Wittstatt U, Olias P, Bravo I. Genome sequences of two novel papillomaviruses isolated from healthy skin of *Pudu puda* and *Cervus elaphus* deer. *Genomic Announc*. (2018) 3:18. doi: 10.1128/genomeA.00298-18
32. Scagliarini A, Gallina L, Battilani M, Turrini F, Savini F, Lavazza A, et al. *Cervus elaphus* papillomavirus (CePV1): new insights on viral evolution in deer. *Vet Microbiol*. (2013) 165:252–9. doi: 10.1016/j.vetmic.2013.03.012
33. Garcês A, Pires I, Savini F, Scagliarini A, Gallina L. Cutaneous fibropapilloma in a red deer associated with *Cervus elaphus* papillomavirus: the first Portuguese case. *J Wild Dis*. (2020) doi: 10.7589/2019-03-070. [Epub ahead of print].
34. Smits SL, Schapendonk CME, van Leeuwen M, Kuiken T, Bodewes R, et al. Identification and Characterization of Two Novel Viruses in Ocular Infections in Reindeer. *PLoS ONE*. (2013) 8:e69711. doi: 10.1371/journal.pone.0069711
35. Munday J, Vaatstra B, Dunowska M, Laurie R, Hills S. Genomic characterization of a novel Epsilonpapillomavirus associated with pigmented papillomas in a red deer (*Cervus elaphus*). *Virus Genes*. (2016) 52:633–9. doi: 10.1007/s11262-016-1340-z
36. OIE. *Guidelines for Wildlife Disease Surveillance: An Overview*. (2015).
37. Lavazza A, Pascucci S, Gelmetti D. Rod-shaped virus-like particles in intestinal contents of three avian species. *Vet Rec*. (1990) 126:581.
38. Inoshima Y, Morooka A, Sentsui H. Detection and diagnosis of parapoxvirus by the polymerase chain reaction. *J Virol Methods*. (2000) 84:201–8. doi: 10.1016/S0166-0934(99)00144-5
39. Tryland M, Beckmen KB, Burek-Huntington KA, Breines EM, Klein J. Orf virus infection in Alaskan mountain goats, Dall's sheep, muskoxen, caribou and Sitka black-tailed deer. *Acta Vet Scand*. (2018) 60:12. doi: 10.1186/s13028-018-0366-8
40. Lyttle DJ, Fraser KM, Fleming SB, Mercer AA, Robinson AJ. Homologs of vascular endothelial growth factor are encoded by the poxvirus orf virus. *J Virol*. (1994) 68:84–92. doi: 10.1128/JVI.68.1.84-92.1994
41. Ueda N, Inder MK, Wise LM, Fleming SB, Mercer AA. Parapoxvirus of red deer in New Zealand encodes a variant of viral vascular endothelial growth factor. *Virus Res*. (2007) 124:50–8. doi: 10.1016/j.virusres.2006.09.012
42. Brandt S, Haralambus R, Shafti-Keramat S, Steinborn R, Stanek C, Kirnbauer R. A subset of equine sarcoids harbours BPV-1 DNA in a complex with L1 major capsid protein. *Virology*. (2008) 375:433–41. doi: 10.1016/j.virol.2008.02.014
43. Stewart GH. Dermatophilosis: a skin disease of animals and man Part II. *Vet Rec*. (1972) 91:537–44. doi: 10.1136/vr.91.22.537
44. Maglennon GA, Doorbar J. The biology of papillomavirus latency. *Open Virol J*. (2012) 6:190–7. doi: 10.2174/1874357901206010190
45. Batista MV, Silva MA, Pontes NE, Reis MC, Corteggio A, Castro RS, et al. Molecular epidemiology of bovine papillomatosis and the identification of a putative new virus type in Brazilian cattle. *Vet J*. (2013) 197:368–73. doi: 10.1016/j.tvjl.2013.01.019
46. Mercer AA, Wise LM, Scagliarini A, McInnes CJ, Büttner M, Rziha HJ, et al. Vascular endothelial growth factors encoded by Orf virus show surprising sequence variation but have a conserved, functionally relevant structure. *J Gen Virol*. (2002) 83(Pt. 11):2845–55. doi: 10.1099/0022-1317-83-11-2845
47. Delhon G, Tulman ER, Afonso CL, Lu Z, de la Concha-Bermejillo A, Lehmkuhl et al. Genomes of the parapoxviruses ORF virus and bovine papular stomatitis virus. *J Virol*. (2004) 78:168–77. doi: 10.1128/JVI.78.1.168-177.2004
48. Spielman SJ, Weaver S, Shank SD, Rife Magalis B, Li M, Kosakovsky Pond S. Evolution of viral genomes: interplay between selection, recombination, and other forces. In: Anisimova M, editors. *Evolutionary Genomics: Statistical and Computational Methods, Methods in Molecular Biology*. New York, NY: Springer. (2019). p. 427–68.
49. Hatcher EL, Hendrickson RC, Lefkowitz EJ. Identification of Nucleotide-Level Changes Impacting Gene Content and Genome Evolution in Orthopoxviruses. *J Virol*. (2014) 88:13651–13668. doi: 10.1128/JVI.02015-14
50. Dal Pozzo F, Martinelle L, Gallina L, Mast J, Sarradin P, Thiry E, et al. Original findings associated with two cases of bovine papular stomatitis. *J Clin Microbiol*. (2011) 49:4397–400. doi: 10.1128/JCM.05281-11
51. Payne D, Yen A, Tyring S. Coinfection of molluscum contagiosum with human papillomavirus. *J Am Acad Dermatol*. (1997) 36:641–4. doi: 10.1016/S0190-9622(97)70261-5
52. Chaudhari S, Guo Y, Chaudhari P. Simultaneous infection of human papillomavirus and poxvirus. *J Cutan Pathol*. (2015) 42:916–8. doi: 10.1111/cup.12554
53. Scagliarini A, Casà G, Trentin B, Gallina L, Savini F,MorentM, et al. Evidence of zoonotic Poxviridae coinfection clinically diagnosed papillomas using a newly developed mini-array test. *J Vet Diagn Invest*. (2016) 28:59–64. doi: 10.1177/1040638715614604
54. Savini F, Dal Molin E, Gallina L, Casà G, Scagliarini A. Papillomavirus in healthy skin and mucosa of wild ruminants in the Italian Alps. *J Wildl Dis*. (2016) 52:82–7. doi: 10.7589/2015-03-065
55. Zhu W, Haga T, Yuan D, Watanabe KI, Chambers JK, Gao N, et al. Coinfection of a lingual lesion with bovine papular stomatitis virus and bovine papillomavirus. *Arch Virol*. (2019) 164:1441–4. doi: 10.1007/s00705-019-04199-9
56. Gallina L, Savini F, Lavazza A, Di Marco P, Puleio R, Roccaro M, et al. Bovine papillomatosis in Sicily: virus identification, diagnosis and co-infections. *Large Anim Rev*. (2017) 23:171–4.
57. Pérez-Tris J, Williams RA, Abel-Fernández E, Barreiro J, Conesa JJ, Figuerola J, et al. A multiplex PCR for detection of poxvirus and papillomavirus in cutaneous warts from live birds and museum skins. *Avian Dis*. (2011) 55:545–53. doi: 10.1637/9685-021411-Reg.1
58. Virgin HW. The virome in mammalian physiology and disease. *Cell*. (2014) 157, 142–50. doi: 10.1016/j.cell.2014.02.032
59. Scagliarini A, Dal Pozzo F, Gallina L, Guercio A, Vaccari F, Battilani M, et al. *In vitro* activity of VEGF-E produced by orf virus strains isolated from classical and severe persistent contagious ecthyma. *Vet Microbiol*. (2006) 114:142–7. doi: 10.1016/j.vetmic.2005.11.052
60. Alejo-Cancho I, Bosch J, Vergara A, Mascaro JM, Marco F, Vila J. Dermatitis by Dermatophilus congolensis. *Clin Microbiol Infect*. (2015) 21:e73–74. doi: 10.1016/j.cmi.2015.06.013
61. Bianchi L, Tramontana M, Biondi F, Hansel K, Gallina L, Scagliarini A, et al. Image gallery: recurrent bovine papular stomatitis virus infection diagnosed by nested polymerase chain reaction. *Br J Dermatol*. (2019) 180:e67. doi: 10.1111/bjd.17399
62. De Meneghi D, Ferroglio E, Bollo E, Vizcaino LL, Moresco A, Rossi L, et al. Dermatophilosis of Alpine Chamois (*Rupicapra rupicapra*) in Italy. *Schweiz Arch Tierheilkd*. (2002) 144:131–6. doi: 10.1024/0036-7281.144.3.131
63. Gallina L, Veronese F, Farinelli P, Boldorini R, Delrosso G, Colombo E, et al. Erythema multiforme after orf virus infection. *Epidemiol Infect*. (2016) 144:88–9. doi: 10.1017/S0950268815001077
64. Caravaglio JV, Khachemoune A. Orf virus infection in humans: a review with a focus on advances in diagnosis and treatment. *J Drugs Dermatol*. (2017) 16:684–9.
65. Hoffman RA. The cutaneous ecosystem: the roles of the skin microbiome in health and its association with inflammatory skin conditions in humans and animals. *Vet Dermatol*. (2017) 28:60–e15. doi: 10.1002/9781119278368.ch4.1

Conflict of Interest: The authors declare that the research was conducted in the absence of any commercial or financial relationships that could be construed as a potential conflict of interest.

The reviewer KE declared a past co-authorship with one of the authors AL, to the handling editor.

Copyright © 2020 Gallina, Savini, Casà, Bertoletti, Bianchi, Gibelli, Lelli, Lavazza and Scagliarini. This is an open-access article distributed under the terms of the Creative Commons Attribution License (CC BY). The use, distribution or reproduction in other forums is permitted, provided the original author(s) and the copyright owner(s) are credited and that the original publication in this journal is cited, in accordance with accepted academic practice. No use, distribution or reproduction is permitted which does not comply with these terms.

frontiers in Veterinary Science

REVIEW
published: 05 May 2020
doi: 10.3389/fvets.2020.00193

Sarcoptic Mange in Wild Caprinae of the Alps: Could Pathology Help in Filling the Gaps in Knowledge?

*Sara Turchetto[1], Federica Obber[2], Luca Rossi[3], Stefano D'Amelio[4], Serena Cavallero[4], Alessandro Poli[5], Francesca Parisi[5], Paolo Lanfranchi[6], Nicola Ferrari[6], Debora Dellamaria[7] and Carlo V. Citterio[2]**

[1] Freelance Veterinary Pathologist, Belluno, Italy, [2] Istituto Zooprofilattico Sperimentale delle Venezie—SCT2 Belluno—U.O. Ecopatologia, Belluno, Italy, [3] Dipartimento di Scienze Veterinarie, Università degli Studi di Torino, Grugliasco, Italy, [4] Dipartimento di Sanità Pubblica e Malattie Infettive, Università di Roma "La Sapienza", Rome, Italy, [5] Dipartimento di Scienze Veterinarie, Università di Pisa, Pisa, Italy, [6] Dipartimento di Medicina Veterinaria, Università degli Studi di Milano, Lodi, Italy, [7] Istituto Zooprofilattico Sperimentale delle Venezie—SCT5 Trento, Trento, Italy

Sarcoptic mange represents the most severe disease for wild Caprinae individuals and populations in Europe, raising concerns for both conservation and management of these ungulates. To date, this disease has been investigated in different wild caprine species and under many different perspectives including diagnostics, epidemiology, impact on the host populations, and genetics of both hosts and parasite, with the aim to disentangle the host–*Sarcoptes scabiei* relationship. Notwithstanding, uncertainty remains and basic questions still need an answer. Among these are the effect of immune responses on mange severity at an individual level, the main drivers in host–parasite interactions for different clinical outcomes, and the role of the immune response in determining the shift from epidemic to endemic cycle. A deeper approach to the pathology of this disease seems therefore advisable, all the more reason considering that immune response to *S. scabiei* in wild Caprinae, generally classified as a hypersensitivity, remains poorly understood. In this paper, we reviewed the pathological features associated to sarcoptic mange in wildlife, exploring different kinds of hypersensitivity and outcomes, with the objective of highlighting the major drivers in the different responses to this disease at an individual level and proposing some key topics for future research, with a particular attention to Alps-dwelling wild caprines.

Keywords: ***Sarcoptes scabiei*, caprinae, pathology, sarcoptic mange, immune response, hypersensitivity**

OPEN ACCESS

Edited by:
Robert James Ossiboff, University of Florida, United States

Reviewed by:
Scott Carver, University of Tasmania, Australia
Danielle Darracq Nelson, Washington State University, United States

****Correspondence:***
Carlo V. Citterio
ccitterio@izsvenezie.it

Specialty section:
This article was submitted to Veterinary Experimental and Diagnostic Pathology, a section of the journal Frontiers in Veterinary Science

Received: *17 December 2019*
Accepted: *24 March 2020*
Published: *05 May 2020*

Citation:
Turchetto S, Obber F, Rossi L, D'Amelio S, Cavallero S, Poli A, Parisi F, Lanfranchi P, Ferrari N, Dellamaria D and Citterio CV (2020) Sarcoptic Mange in Wild Caprinae of the Alps: Could Pathology Help in Filling the Gaps in Knowledge? Front. Vet. Sci. 7:193. doi: 10.3389/fvets.2020.00193

INTRODUCTION

Sarcoptic mange (or scabies) due to the burrowing mite *Sarcoptes scabiei* is reported worldwide in domestic and wild mammals, in the latter often representing a threat to conservation due to evident effects on population dynamics. Some varieties of this mite have been described as being able to infect a specific range of zoologically related hosts. Mites infecting the Northern chamois (*Rupicapra r. rupicapra*), a scabies sensitive caprine (Fam. Caprinae) on which this paper is mainly focused, are referred to as *S. scabiei* var. *rupicaprae* (**Figure 1**). Besides chamois, they are experimentally and/or naturally cross-transmissible to the Alpine ibex (*Capra ibex*) and the

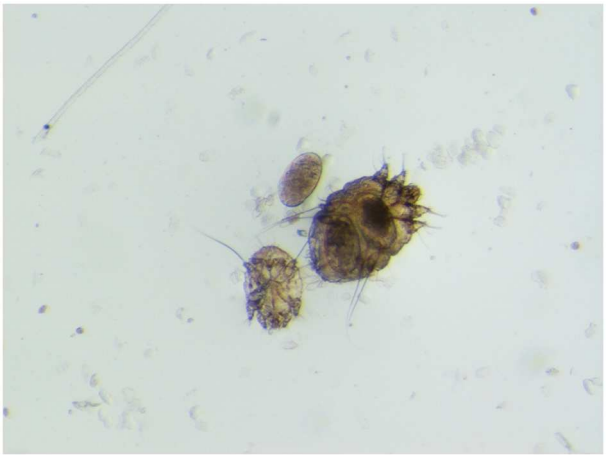

FIGURE 1 | *Sarcoptes scabiei* var. *rupicaprae* (stereomicroscope 60×) from a mangy northern chamois (*Rupicapra r. rupicapra*) in northeast Italy.

BOX 1 | Gaps in knowledge to fill concerning sarcoptic mange in wildlife in Europe (26).

Which dynamics are actually involved in the shift from epidemic to endemic cycle of sarcoptic mange in wildlife populations?
How do factors such as coinfections, health condition, and genetic background influence mange infestation in wildlife?
How can mortality due to mange be properly assessed and differentiated from other causes of death?
Is sarcoptic mange a threat for biodiversity conservation? Which species or populations should be considered for intervention?

domestic goat, while sporadically to domestic sheep, mouflon (*Ovis aries musimon*), roe deer (*Capreolus capreolus*), and red deer (*Cervus elaphus*) (1, 2).

Sarcoptic mange is probably the most severe disease affecting wild Caprinae in Europe (3), as evidenced by the epizootics affecting the Spanish ibex (*Capra pyrenaica*) in the southeast of Spain (4, 5), and the northern chamois and Alpine ibex in the Eastern Alps in Italy, Austria, Germany, and Slovenia (6–8). Moreover, sarcoptic mange has been severely affecting two other wild Caprinae hosts in Southern Europe, namely the western subspecies of the southern chamois [*Rupicapra pyrenaica parva;* (9)] and the exotic Barbary sheep [*Ammotragus lervia*; (10)].

Besides serious consequences for endangered taxa, where losing even a few individuals can be critical for conservation (11), this disease may also raise concern over the wildlife-based economy, due to the setbacks of population downturns. This is well-represented in the Eastern Alps, where recent mange outbreaks have caused doubt over 30 years of commendable conservation efforts of the locally fragile Alpine ibex (an easy to spot symbol for mountain hikers), and a sympatric game, the alpine subspecies of the northern chamois, currently ranked "Least concern" by IUCN due to its wide and abundant distribution, has also experienced significant population crashes, which have led to a sharp reduction and even the banning of any harvest in affected game management units (3, 7).

Due to its impact on wild caprine populations and the related conservation issues, sarcoptic mange has been investigated from a range of perspectives. In Europe, research has been performed on epidemiology [e.g., (1, 3–7, 9, 10)], including spatial epidemiology (12), immunodiagnosis (13, 14), experimental infection (15–18), mite genetics (19, 20), and host genetics. Concerning this latter topic, special emphasis has been given to the major histocompatibility complex (MHC), deemed crucial to cope with infectious agents including *S. scabiei* and other pathogens (21–23). Studies on host genetics are believed to be of particular interest also due to the typical pattern of sarcoptic mange in these species, where the first epidemic peak in naïve populations may exert a significant demographic impact (up to more than 80% reduction of the population size), followed by less severe outbreaks ("waves") at 10- to 15-years intervals with a low mortality rate rarely exceeding 25% (3). Such a cyclic pattern could be suggestive of dynamics based on the presence of an advantageous genetic background in those animals surviving the exposition, determining a selection of individuals with higher genetic resistance (24), which, combined with the lowered population density, could explain the minor waves after the introduction of the pathogen. In addition, balancing selection may favor, at the same time, heterozygosity and the retaining of rare alleles. To investigate this hypothesis, adaptive processes need to be explored, and for this purpose, MHC genes are excellent candidates (21), representing a promising research field to explore the Caprinae-*S. scabiei* relationship. In fact, intracellular and extracellular pathogens trigger a strong immune response in such species, and the study of the genetic background of the MHC molecules may assist the identification of resistance-associated or rare alleles, which may be involved in the survival of individuals with peculiar polymorphisms in these genetic regions. Under this hypothesis, however, it would be expected that different genetic backgrounds are reflected in different kinds and/or degrees of immune response and consequent pathological pictures. Indeed, pathology should precede and inform studies on the host–parasite relationship and coevolution, including genetics, but in the case of sarcoptic mange, the investigation path is not so linear. In our opinion, however, pathology can give a remarkable contribution to the study of mange ecology and epidemiology in wildlife, and in particular in Caprinae, thus helping to fill the longtime gap in knowledge in Europe (25) resumed by the research questions in **Box 1** (26).

In recent years, studies on the pathology of sarcoptic mange in European wild ruminants have been focused on the impact of this disease on individuals and populations (18, 27) or on early diagnostics (28), while less attention has been paid to characterizing mange lesions and ranking them according to severity and chronology of the pathological process (29, 30). Assuming that traits of genetic resistance may underlie diverse immune response type and intensity among different individuals (31), a fine-tuned pathological description could help answer some of the questions in **Box 1**, e.g., by correlating

selected macroscopic and histopathological frames to specific epidemiological phases (epidemic vs. endemic), coinfections, and genetic backgrounds. Hence, in this paper, we have explored the pathology of sarcoptic mange in wildlife, with the objective of highlighting the major drivers in the range of host responses to the disease and proposing some key issues for future research at both an individual and a population level, with a particular attention to Alps-dwelling wild Caprinae.

HYPERSENSITIVITY AS THE BASIS OF TISSUE DAMAGE IN SARCOPTIC MANGE

Ectoparasites are known to cause a range of unfavorable effects, as damage to skin and predisposition to secondary infection. Moreover, they can serve as vectors of infectious agents such as viruses, bacteria, spirochetae, rickettsiae, and protozoans. The cutaneous reaction to parasites, often mediated by immune mechanisms, varies with parasite abundance, location, feeding habits, and host immune recognition (32).

Diseases associated with excessive or aberrant immune responses are classified as either hypersensitive (allergy) or autoimmune. Microscopically, evidence in all studied host species indicates that sarcoptic mange is a complex hypersensitivity reaction to various mite antigens, as proteins in the cuticle and feces, producing most of the clinical features (33–37). Actually, the mechanisms of tissue injury in hypersensitivity reactions are the same as the effector mechanisms of defense against infectious pathogens, but in hypersensitivity reactions, they are poorly controlled, excessive, or misdirected (31). Hypersensitivity can be classified into four basic immune reaction types (I, II, III, and IV), which mediate the tissue damage in response to normally harmless foreign compounds (e.g., antiserum, pollen, insect venoms). In the skin, hypersensitivity in most cases is the result of either type I or type IV reactions, or comes from a combination of two or more of the four reaction types (32).

Type I hypersensitivity is mediated by the reaction between a foreign antigen and a specific antibody (usually IgE), enabling the release of pharmacologically active substances as histamine, chemotactic factors for eosinophils and neutrophils, and cytokines by mast cells and basophils. It can be either systemic (anaphylaxis), or localized to the skin, or both and include, as an example, atopic dermatitis, urticaria, angioedema, or hypersensitivity to bites of insects and mites as *Sarcoptes* sp. This reaction is characterized by mast cell degranulation, capillary dilation, edema, and infiltrates of eosinophils (32).

On the other hand, type IV reactions are mediated by antigen-specific effector T lymphocytes, which include sensitized T-helper lymphocytes (Th1 or Th2). Th1-mediated reactions develop after contact with a specific persistent antigen and cause the recruitment of other lymphocytes and macrophages to eliminate the targeted antigen. In Th2-mediated reactions, contact with soluble antigen bound to MHC class II (MHC II) causes inflammatory responses dominated by eosinophils (32).

SARCOPTIC MANGE FROM MACROSCOPIC LESIONS TO MICROSCOPIC FEATURES

Itching is a frequent symptom in cutaneous hypersensitivity reactions and represents the first clinical feature also for sarcoptic mange. An erythematous maculopapular eruption with alopecia, hyperkeratosis, and the formation of crusts is accompanied by self-traumatic excoriations, leading to secondary pyoderma. In general, lesions first affect the margins of the pinnae, followed by ventral truncal abdomen, chest, lateral elbows, and face involvement (38). However, localization of the early lesions also depends on the skin area first exposed to the infection. Extensive alopecia, lichenification, and hyperpigmentation may be seen in chronic cases (29) (**Figure 2**).

Studies have shown that the response to mange is different among host species. For instance, dogs, humans, and rabbits acquire full immunity, while in the red fox, immune response appears to be less effective at restricting infection due to lack of memory T-cells after initial phases. Additionally, the immune response can be uneven within the same species according to the sex of the individual or its previous exposure status (26). Field evidence suggests, however, that such an unevenness could also depend on other still unknown factors: namely, in both northern chamois and Alpine ibex, it is renowned that the impact of mange has been higher in some populations than in others. For example, the impact of *S. scabiei* on the demography of the Alpine ibex colonies in northeastern Italian Alps has ranged from extinction and dramatic crashes to relatively low population reduction, so that ibex individuals from the latter are used *ex juvantibus* for the restocking of the former (39).

In the northern chamois, histological skin lesions due to sarcoptic mange have been recently classified in three grades (40) according to crust thickness, alopecia, mite counts, infiltration of eosinophils, lymphocytes, and mast cells. Grades 1 and 2 are characterized by slight to moderate crust formation and a

FIGURE 2 | Severe sarcoptic mange in a northern chamois *Rupicapra r. rupicapra* (NE Italy). Particularly of the chest. Macroscopically, lesions are characterized by severe diffuse chronic hyperplastic and hyperkeratotic dermatitis with alopecia and crusting.

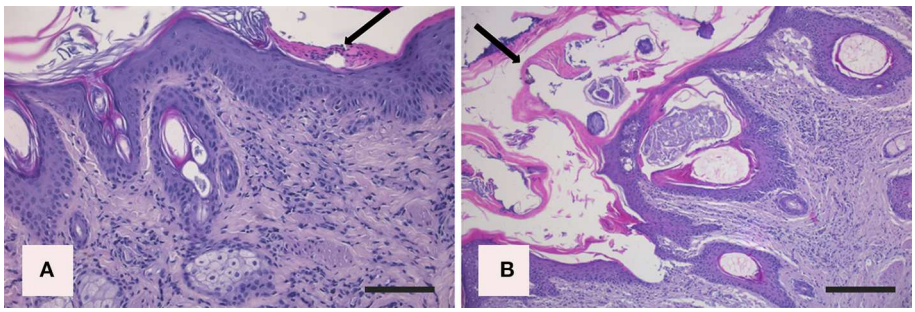

FIGURE 3 | Histopathologic lesions in northern chamois (*Rupicapra r. rupicapra*) affected by sarcoptic mange. The following pictures are further evidenced by black arrows: **(A)** Moderate, diffuse, irregular epidermal hyperplasia with neutrophilic serocellular crust in grade 2 sarcoptic mange (hematoxylin and eosin, bar = 300 μm). **(B)** Severe, diffuse, orthokeratotic to compact hyperkeratosis with thick neutrophilic serocellular crusts in a grade 3 sarcoptic mange, which correlate with the increased number of mites (hematoxylin and eosin, bar = 300 μm). Further details available in Salvadori et al. (40).

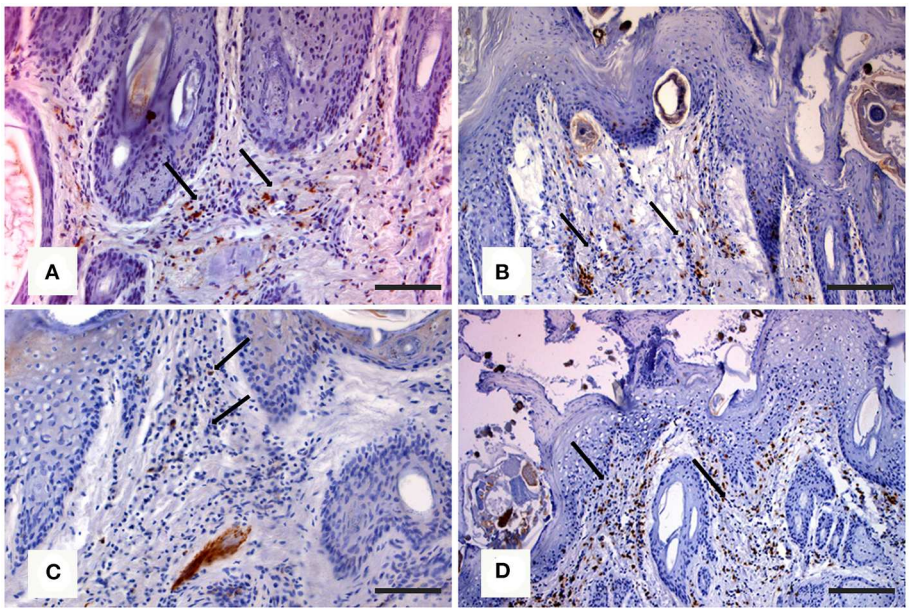

FIGURE 4 | Immunohistochemical staining of skin in northern chamois (*Rupicapra r. rupicapra)* affected by sarcoptic mange. The following pictures are further evidenced by black arrows: **(A)** Diffuse macrophages infiltration in the superficial dermis in grade 2 sarcoptic mange (IHC, anti CD68 antibody, DAB chromogen, and hematoxylin counterstain, bar = 300 μm). **(B)** Numerous T lymphocytes in the superficial dermis of a chamois with grade 2 sarcoptic mange (IHC, anti CD3 antibody, DAB chromogen, and hematoxylin counterstain, bar = 300 μm). **(C)** Increased B lymphocytes infiltration in the superficial dermis in a grade 3 sarcoptic mange (IHC, anti CD79a antibody, DAB chromogen, and hematoxylin counterstain, bar = 300 μm). **(D)** Scattered T lymphocytes among B cells in a grade 3 lesion (IHC, anti CD3 antibody, DAB chromogen, and hematoxylin counterstain, bar = 300 μm). Further details available in Salvadori et al. (40).

low number of mites, while grade 3 represents the most severe stage with crust thickness of more than 3.5 mm (**Figures 3A,B**), which correlates with a very high number of mites and severe parakeratosis with diffuse bacterial aggregates. The presence of numerous and thick serocellular crusts is apparently a mechanism destroying mites or inhibiting their burrowing into the skin, as these crusts contain specific antibodies and other toxic components leading to mite intoxication (18). In all stages, an increased number of eosinophils, mast cells, T and B lymphocytes, and macrophages are associated with diffuse severe epidermal hyperplasia, suggesting both type I and type IV hypersensitivity. Analogously to human scabies, grades 1 and 2 could be suggestive of skin immune response to *S. scabiei* with adequate presence of macrophages (**Figure 4A**), T lymphocytes (**Figure 4B**), and eosinophils that allow parasite control through a reduction in mite numbers and limitation of lesions. Moreover, numbers of eosinophils in the dermis are correlated with the density of mites, suggesting that recruitment of eosinophils is influenced by the parasites or their products (41). In contrast, grade 3 lesions seem to be characterized by a significant increase of B lymphocytes (**Figure 4C**) and a decrease in eosinophils without a significant increase in

macrophages and T lymphocytes (**Figure 4D**) (40). Infiltration of Langerhans cells is also observed in the epidermis of mangy chamois, and it is assumed that epidermal dendritic cells with captured sarcoptic antigen migrate through lymphatic vessels into the draining regional lymph nodes. Here, they present it to naïve T cells and induce their differentiation into Th1 and Th2. Th1-type reactions tend to produce proinflammatory and microbicidal responses, counteracted with Th2-type reactions including molecules promoting IgE production (IL-4, IL-5, IL-10, and IL-13) and eosinophilic responses in allergies, and also an anti-inflammatory response (42). Antigen presentation is likely to be increased in the dermis of chamois with sarcoptic mange, as suggested by the increased number of T and B lymphocytes, macrophages, and eosinophils in grade 3 lesions compared to grade 1: in particular, the increased B lymphocyte and eosinophil numbers in grade 3 compared to grade 1 appears the most significant (40). Grades 1 and 2 lesions with slight to moderate crust formation and a lower abundance of mites could therefore be thought of as the initial stages, while grade 3 could be interpreted as the following, generalized, severe stage. As in human scabies, grades 1 and 2 could be suggestive of adequate skin immune response to *S. scabiei*, allowing parasite control and limitation of lesions. In contrast, grade 3 lesions, characterized by significant B lymphocyte and eosinophils increase, could suggest a Th2 weighted imbalance, involving an IgE-driven nonprotective Th2 response, that could affect the control and reduction of the mite burden particularly in sequential infestations (40). The role of Langerhans cells in the pathogenesis of chamois mange, however, remains obscure, and research is needed on the distributional changes of these cells in response to infection (29).

For *Alpine ibex*, although gross lesions in mangy animals are often dramatic (**Figure 5**), no detailed histological data are available at the moment. The histological picture has been instead described in the *Spanish ibex* (18), where the skin lesions observed closely match the classical picture of wild and domestic animals affected by sarcoptic mange. The cellular response is largely dominated by mononuclear cells and marginally by eosinophils and mast cells, which may explain the presence of less obvious marked hyperkeratosis. Similarly to chamois, ibex skin lesions are compatible with a combined type I and type IV hypersensitivity reaction. Type I hypersensitivity is characterized by cytotoxicity signs (e.g., spongiosis), positively correlated with the number of inflammatory cells. Subsequently, these signs decrease along with the cellular infiltrate, which suggests type IV hypersensitivity. As in all other species, the number of plasma cells in mangy ibex is low, which may be linked to a reduced role of the humoral response. Moreover, also in ibex, the overexpression of eosinophils, mast cells, and neutrophils is associated with a detrimental and non-protective response, unable to control the infection.

For comparison among different taxa, it is worthwhile reporting the skin features of European mangy *carnivores*. In *red foxes* (*Vulpes vulpes*) infected with *S. scabiei* var. *vulpes*, skin lesions associated with necropsy findings have also been classified in three types (43). In this host after an early stage A, characterized by focal-extensive skin lesions, thin crusts, mild to moderate alopecia, few mites, and numerous eosinophils, the subject either enters stage B (hyperkeratotic, "fatal" form) with generalized skin lesions, thick crusts, and increased mite number, lymphocytes, and mast cells, leading in most cases to death; or stage C (alopecic, "healing" form), characterized by focal severe alopecia, hyperpigmentation and lichenification, absence of mites, and mixed cell infiltration, leading to possible survival. As both mast cell and mite counts increase in foxes showing type B lesions compared to type A, unknown extrinsic or intrinsic factors, such as a dysregulation of the immune system, may result in impairment of the eosinophilic function, affecting the host's ability to control mite infestation and thus playing an important role in determining the disease course. The scarce number of mites detected in the skin of red foxes with the alopecic form contrasts with the numerous mites observed in individuals showing the hyperkeratotic form, and it is interesting to point out that the latter generally represents the typical picture in mountain caprines. A further interesting comparison can be made with another carnivore, the *wolf* (*Canis lupus*) where, in contrast to the chamois, the abundance of mites decreases in the lesions as the hypersensitivity reaction progresses (44). In animals showing the alopecic form, neutrophils establish the inflammatory infiltrate: although neutrophils can be related to secondary infections or skin damage, the oxidation burst of these cells may be important in eliminating mites (34). Both macroscopical and microscopical skin lesions by sarcoptic mange in wolves suggest a prevalence of the alopecic form (**Figures 6A,B**) rather than the hyperkeratotic one; the coincidence in wolves of this presentation with the apparent higher ability of this species to control the parasite (45) could suggest that the immune response in the alopecic form represents a more effective defense mechanism against *S. scabiei* (44). A higher efficiency of the wolf immune system in controlling the mite proliferation could also allow this host to reduce the number of mite generations on itself. Actually, the detection in a wolf of both "ungulate-like" and "red fox-like" mites suggests that repeated infestations are possible with mites from any of

FIGURE 5 | Severe sarcoptic mange in an Alpine ibex (*Capra ibex*) from NE Italy. Macroscopically, lesions are characterized by severe, multifocal to coalescing, chronic hyperplastic dermatitis with alopecia and lichenification. Courtesy of Mr. Vittorio Fusinato.

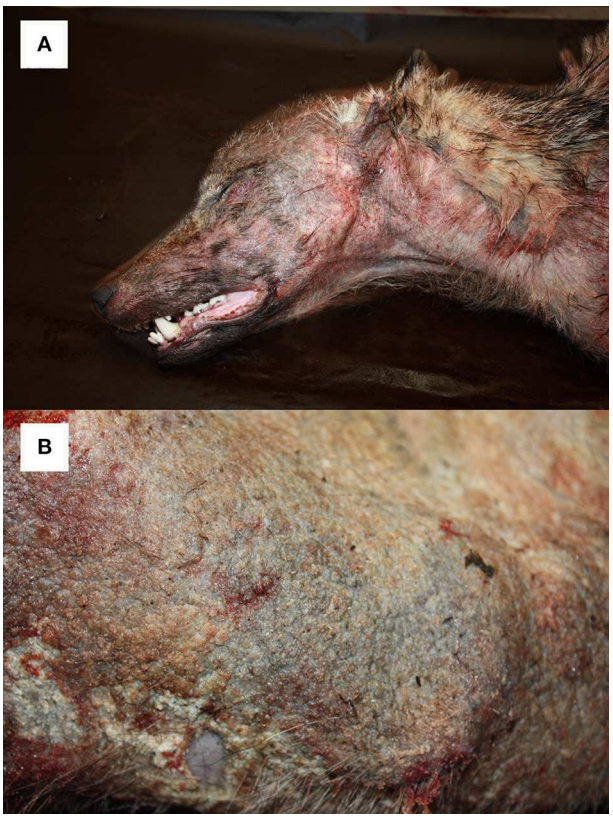

FIGURE 6 | Alopecic form of sarcoptic mange affecting a young (1–2 years) female wolf (*Canis lupus*) from NE Italy. Particularly of the head **(A)** and the trunk **(B)**.

FIGURE 7 | A follow-up in the field led to the hypothesis that the northern chamois in this picture (NE Italy) was healing from sarcoptic mange. This adult female is characterized by moderate, focally extensive, chronic hyperplastic dermatitis with alopecia and lichenification. Monitoring healing processes in wild animals are challenging due to difficulties in regularly observing specific individuals. At the same time, capturing or culling of such individuals should be absolutely avoided, since under the hypothesis of a genetic resistance to *S. scabiei*, they could represent an essential resource for the population. Healing of Alpine ibex individuals have also been reported anecdotally. Courtesy of Mr. Vittorio Fusinato.

BOX 2 | Research questions about immune response to *S. scabiei* in wildlife (26).

How can the effect of immunological responses on mange severity be studied in wildlife?
Which factors are the primary drivers in host–parasite interactions for both positive and negative clinical outcomes of mange in wildlife?

the sympatric species this canid may get in contact with. These features may inhibit host adaptation, thus facilitating gene flow among mite populations and preventing genetic selection, finally determining the high variability reported in *C. lupus*–derived mites. In the case of the wolf, its wide spatial range and the large number of species this canid can potentially contact (both as a predator and as a scavenger) are additional subjects favoring repeated infestations by genetically different mites from different host species (20).

An important remark is finally related to lethality, since for Spanish ibex (46) and red fox (43), there is evidence that some free-ranging individuals are able to heal from sarcoptic mange, whereas for northern chamois and Alpine ibex, evidence of recovery remains anecdotal (**Figure 7**).

PERSPECTIVES IN THE PATHOLOGY OF SARCOPTIC MANGE IN ALPINE WILD CAPRINAE

Although uncertainty remains for mange pathology in wild Caprinae, steps to understand immune responses to *S. scabiei* [(26), **Box 2**] are being made, and therefore prospects for a deeper understanding are positive. Key areas that we consider research priorities include the following:

Role of the Oxidative Burst

As seen in previous studies, numerous mononuclear cells, mast cells, and plasma cells may play a key role in protective immunity. Observation about preferential infiltration of neutrophils, due not only to the presence of mites but also to potential secondary bacterial infections or excoriations, and evaluation of the progression or regression of the disease may inform on the oxidative burst role in effective protection.

Role of Different Types and Degrees of Hypersensitivity

Under field conditions, evaluating skin lesions in chamois/ibex from different epidemiological scenarios (e.g., individuals from scabies naïve vs. endemically infected populations) could help to elucidate inflammatory responses to the first and subsequent infestations. Experimentally, identifying the subpopulations of mononuclear cells in scabietic lesions during the sensitization

and challenge infection phases, and characterizing the timing and intensity of the immunological response during the challenge phase, could help to elucidate their role and the mechanism for the immune response in these hosts (34).

Role of the Intensity of the Immunologic Reaction

Skin biopsy details of inflammatory response to scabies mite antigens may inform about variability in severity of clinical signs, development of asymptomatic carriers, and decrease in mite numbers as the disease progresses. Individuals with compromised immune system (due to coexistent immunosuppressive disease and/or poor condition) may harbor much larger populations of mites. Similarly, high mite counts associated to severe clinical presentation, including the notorious crusted (or Norwegian) scabies (https://www.cdc.gov/parasites/scabies/disease.html), are seen most commonly in human patients who are immunocompromised due to many causes, among which the acquired immunodeficiency syndrome (AIDS) (47). It should be noted, however, that although variability of spongiosis and inflammation in the immediate vicinity of individual mites is postulated to be indicative of the stage of the inflammatory reaction to these parasites, histological features may vary depending upon the fortuitous presence of mites in the histological sections, as observed in dogs (48). Therefore, comparison between histological pictures among individuals and/or species should include a representative number of sections both including and not including mites.

Role of Langerhans Cells

Distributional studies in humans have shown a preference of mites for sparsely haired skin, resulting in a predominantly ventral truncal distribution of lesions and relatively spare on the dorsum of the trunk, that could be explained by the rarity of epidermal Langerhans cells in certain regions, e.g., neck and shoulder (49). Moreover, experimental manipulation with UV radiation clearly showed abrogation of epidermal Langerhans cells in mice (50), which could explain the beginning of sensitization in certain parts of human and animal skin depending on the frequency and morphological identity of Langerhans cells, unevenly distributed (51, 52). The implementation of an immunohistochemical study on skin biopsies from healthy and mangy chamois could help to evaluate the distributional changes of these cells in the body regions and the reflections of these variations on the disease.

Role of the MHC of the Host

It is accepted that the evaluation of genetic polymorphisms in chamois, in particular of the MHC II molecules specifically involved in reactions against extracellular pathogens, may greatly contribute to estimating the adaptive potential of populations, as well as to identifying alleles potentially related to susceptibility and resistance. Studies that combine pathology and genetics could therefore be useful to investigate genetic diversity in infected individuals, and Northern alpine chamois represents a suitable model for such studies. However, observations and data collection should be undertaken over time by the comparison between MHC class II sampled under different conditions (e.g., healthy chamois before the first epidemic wave; mangy and healthy chamois during the first outbreak; survived and younger chamois after the first and during the second epidemic wave). In fact, only a consistent and longitudinal sample could be representative to clarify whether some animals are genetically prone to allergic reactions against the mite, as well as if others are actually protected from the disease. A comparable study design investigated the chamois population dynamics in relation to different exposure levels to several pathogens, including pneumonia, Pestivirus, and sarcoptic mange (22, 53, 54). The study of MHC class II polymorphisms revealed genetic drift and balancing selection in response to the diseases: high polymorphisms and numbers of alleles were observed in individuals who survived pneumonia outbreaks, even with a high mortality rate. Similarly, genetic polymorphisms of DRB1 genes of chamois populations with different epidemiological pictures of sarcoptic mange were monitored for seven years, revealing (i) the presence of few alleles at a very high frequency in all populations, most likely selected as favorable; (ii) the presence of a higher than expected level of polymorphisms; and (iii) several alleles at low frequency observed only in populations with peculiar epidemiological scenarios (endemic, epidemics, healthy populations).

In conclusion, pathology could represent a significant clue in understanding the relationships between host and *S. scabiei*, particularly as part of the "Sarcoptes-World Molecular Network" (55, 56), aimed at harmonizing *Sarcoptes* epidemiology, diagnosis, treatment, and molecular studies from all over the world. Undoubtedly, the establishment of a similar framework focused on pathology and immune response to this parasite, besides improving the knowledge on this disease, could inform wildlife management and, in a perspective of comparative pathology, contribute to mitigation of sarcoptic mange in domestic animals and humans.

AUTHOR CONTRIBUTIONS

ST and CC conceived the paper. ST, LR, SC, SD'A, AP, FP, FO, DD, NF, PL, and CC wrote the manuscript. All authors contributed to manuscript revision, read, and approved the submitted version.

FUNDING

This paper has been partly supported by the results of these research projects:

PRIN 2010P7LFW4_004—Genomics and host–pathogen interactions: a model study in the One-Health perspective.

Ricerca corrente IZSVE 14/07—Sorveglianza su patologie prioritarie ed emergenti nella fauna selvatica dell'Arco Alpino centro-orientale.

ACKNOWLEDGMENTS

We acknowledge all institutions and persons that across the years contributed to the study of sarcoptic mange by collecting samples and sharing information. An honorable mention goes to the Belluno Province Police, whose territory surveillance action allowed us to get samples and images in this paper. We are also grateful to Marta Vascellari and Claudia Zanardello (SCS3-IZSVe) for support in histological sampling, to Mirko Ruzza (SCS7-IZSVe) for support in editing the images, to Isabella and Philip McGuinness for English supervision, and to Olivia Francione for her inspirational support.

REFERENCES

1. Alasaad S, Oleaga A, Casais R, Rossi L, Molinar Min A, Soriguer RC, et al. Temporal stability in the genetic structure of Sarcoptes scabiei under the host-taxon law: empirical evidences from wildlife-derived Sarcoptes mite in Asturias, Spain. *Parasit. Vect*. (2011) 4:151–7. doi: 10.1186/1756-3305-4-151
2. Kutzer E. Zur epidemiologie de Sarcoptes-raeude. *Angew Parasitol*. (1996) 7:241–8.
3. Rossi L, Tizzani P, Rambozzi L, Moroni B, Meneguz PG. Sanitary emergencies at the wild/domestic caprines interface in Europe. *Animals*. (2019) 9:922. doi: 10.3390/ani9110922
4. Pérez JM, Ruiz-Martínez I, Granados JE, Soriguer RC, Fandos P. The dynamics of sarcoptic mange in the ibex population of Sierra Nevada in Spain – influence of climatic factors. *J Wildlife Res*. (1997) 2:86–9.
5. León-Vizcaíno L, Ruíz de Ybáñez MR, Cubero MJ, Ortíz MJ, Espinosa J, Pérez L, et al. Sarcoptic mange in spanish ibex from Spain. *J Wildl Dis*. (1999) 35:647–59. doi: 10.7589/0090-3558-35.4.647
6. Rossi L, Meneguz P, De Martin P, Rodolfi M. The epizootiology of sarcoptic mange in chamois Rupicapra rupicapra from the Italian Eastern Alps. *Parassitologia*. (1995) 37:233–40.
7. Rossi L, Fraquelli C, Vesco U, Permunian R, Sommavilla GM, Carmignola G, et al. Descriptive epidemiology of a scabies epidemic in chamois in the Dolomite alps, Italy. *Eur J Wildl Res*. (2007) 53:131–41. doi: 10.1007/s10344-006-0067-x
8. Schaschl H. *Gamsräude*. Wien: österreichischer Jagd- und Fischerei-verlag. Vienna (2003). p. 160.
9. Fernández-Morán J, Gómez S, Ballesteros F, Quirós P, Benito JL, Feliu C, et al. Epizootiology sarcoptic mange in a population of cantabrian chamois Rupicapra pyrenaica parva in northwestern Spain. *Vet Parasitol*. (1997) 115:163–71. doi: 10.1016/S0304-4017(97)00061-7
10. Gonzalez-Candela M, Leon Vizcaìno L, Cubero-Pablo MJ. Population effects of sarcoptic mange in Barbary sheep (*Ammotragus lervia*) from Sierra Espuna Regional Park, Spain. *J Wildl Dis*. (2004) 40:456–65. doi: 10.7589/0090-3558-40.3.456
11. Pence DB, Ueckermann E. Sarcoptic mange in wildlife. *Revue Scient Techn*. (2002) 21:385–98. doi: 10.20506/rst.21.2.1335
12. Turchetto S, Obber F, Permunian R, Lorenzetto M, Ferr,è N, Stancampiono L, et al. Spatial and temporal explorative analysis of sarcoptic mange in Alpine chamois (Rupicapra r. rupicapra). *Hystrix Ital J Mammal*. (2014) 25, 25–30. doi: 10.4404/hystrix-25.1-9460
13. Rambozzi L, Menzano A, Lavin S, Rossi L. Biotin-avidin amplified ELISA for detection of antibodies to Sarcoptes scabiei in chamois (Rupicapra spp.). *Vet Res*. (2004) 35:701–8. doi: 10.1051/vetres:2004039
14. Raez-Bravo A, Granados JE, Serrano E, Dellamaria D, Casais R, Rossi L, et al. Evaluation of three enzyme-linked immunosorbent assays for sarcoptic mange diagnosis and assessment in the Iberian ibex, Capra pyrenaica. *Parasit Vect*. (2016) 9:558. doi: 10.1186/s13071-016-1843-4
15. Lavin S, Ruiz-Bascaran M, Marco I, Fondevila MD, Ramis AJ. Experimental infection of chamois (*Rupicapra pyrenaica parva*) with Sarcoptes scabiei derived from naturally infected goats. *J. Vet. Med. B*. (2000) 47:693–9. doi: 10.1046/j.1439-0450.2000.00406.x
16. Menzano A, Rambozzi L, Molinar Min A, Rossi L. Experimental infection of chamois with Sarcoptes scabiei. *In: Mange and myiasis of livestock. Proceedings of Workshop EU-COST Action 833*. Toulouse (2002). p. 60–4. Available online at: http://op.europa.eu/en/publication-detail/-/publication/f6b03401-1939-4aed-a24a-5a5062e9d3e7/language-en/format-PDF/source-124957428
17. Sarasa M, Rambozzi L, Rossi L, Meneguz PG, Serrano E, Granados JE, et al. Sarcoptes scabiei: specific immune response to sarcoptic mange in the Iberian ibex Capra pyrenaica depends on previous exposure and sex. *Exp Parasitol*. (2010) 124:265–71. doi: 10.1016/j.exppara.2009.10.008
18. Espinosa J, Ráez-Bravo A, López-Olvera JR, Pérez JM, Lavín S, Tvarijonaviciute A, et al. Histopathology, microbiology and the inflammatory process associated with Sarcoptes scabiei infection in the Iberian ibex, Capra pyrenaica. *Paras Vec*. (2017) 10:596–606. doi: 10.1186/s13071-017-2542-5
19. Rasero R, Rossi L, Soglia D, Maione S, Sacchi P, Rambozzi L, et al. Host taxon-derived Sarcoptes mite in European wild animals revealed by microsatellite markers. *Biol Conserv*. (2010) 143:1269–77. doi: 10.1016/j.biocon.2010.03.001
20. Oleaga A, Alasaad S, Rossi L, Casais R, Vicente J, Maionee S, et al. Genetic epidemiology of Sarcoptes scabiei in the Iberian wolf in Asturias, Spain. *Vet Parasitol*. (2013) 196:453–9. doi: 10.1016/j.vetpar.2013.04.016
21. Mona S, Crestanello B, Bankhead-Dronnet S, Pecchioli E, Ingrosso S, D'Amelio S, et al. Disentangling the effects of recombination, selection, and demographyon the genetic variation at a major histocompatibility complex class II gene in the alpine chamois. *Mol Ecol*. (2008) 17:4053–67. doi: 10.1111/j.1365-294X.2008.03892.x
22. Cavallero S, Marco I, Lavín S, D'Amelio S, López-Olvera JR. Polymorphisms at MHC class II DRB1 exon 2 locus in Pyrenean chamois (Rupicapra pyrenaica pyrenaica). *Infect Genet Evol*. (2012) 12:1020–6. doi: 10.1016/j.meegid.2012.02.017
23. Schaschl H, Suchentrunk F, L., Morris D, Slimen HB, Smith S, et al. (2012). Sex-specific selection for MHC variability in Alpine chamois. *BMC Evol Biol* 12:20. doi: 10.1186/1471-2148-12-20
24. Guberti V, Zamboni L. Can the host resistance hypothesis explain the cyclic patterns observed in *Sarcoptes scabiei in chamois (Rupicapra rupicapra)? Parassitologia*. (2000) 42(Suppl. 1):72.
25. Guberti V, Rossi L. The wild mammals/parasite relationship: a review of the Italian literature 1970-1994. *Suppl Ricerche Biol Selvagg*. (1996) 17–26.
26. Astorga F, Carver S, Almberg ES, Sousa GR, Wingfield K, Niedringhaus KD, et al. International meeting on sarcoptic mange in wildlife, June 2018, Blacksburg, Virginia, USA. *Paras Vect*. (2018) 11:449. doi: 10.1186/s13071-018-3015-1
27. Espinosa J, Granados JE, Cano-Manuel FJ, López-Olvera JR, Ráez-Bravo A, Romero D, et al. Sarcoptes scabiei alters follicular dynamics in female Iberian ibex through a reduction in body weight. *Vet Parasitol*. (2017) 243:151–6. doi: 10.1016/j.vetpar.2017.06.022
28. Rahman MM, Lecchi C, Fraquelli C, Sartorelli P, Ceciliani F. Acute phase protein response in Alpine ibex with sarcoptic mange. *Vet Parasitol*. (2010) 168:293–8. doi: 10.1016/j.vetpar.2009.12.001
29. Rode B, Bavdek SV, Lackovic G, Fazarinc G, Bidovec A. Immunohistochemical study of normal and mange (S. scabiei var rupicaprae) infested chamois (Rupicapra rupicapra L) skin. *Anat Histol Embryol*. (1998) 27:187–92. doi: 10.1111/j.1439-0264.1998.tb00178.x
30. Salvadori C, Finlayson J, Trogu T, Formenti N, Lanfranchi P, Citterio C, et al. Characterization of immune system cell subsets in fixed tissues from alpine chamois (*Rupicapra rupicapra*). *J Compar Pathol*. (2016) 155:207–12. doi: 10.1016/j.jcpa.2016.06.012
31. Kumar V, Abbas AK, Aster JC. (editors). Diseases of the immune system. In: *Robbins and Cotran Pathologic Basis of Disease*. 9th edn. Philadelphia, PA: Elsevier (2015). p. 200–11.
32. Hargis AM, Myers S. The integument. In: Zacary JF, editor. *Pathologic Basis of Veterinary Disease*. St. Louis: Elsevier. (2017). p.1040–2.
33. Bornstein S, Zakrisson G. Humoral antibody response to experimental Sarcoptes scabiei var. vulpes infection in the dog. *Vet Dermatol*. (1993) 4:107–10. doi: 10.1111/j.1365-3164.1993.tb00202.x

34. Arlian LG, Morgan MS, Rapp CM, Vyszenski-Moher DL. The development of protective immunity in canine scabies. *Vet Parasitol*. (1996) 62:133–42. doi: 10.1016/0304-4017(95)00854-3
35. Lower KS, Medleau LM, Hnilica K, et al. Evaluation of an enzyme-linked immunosorbent assay (ELISA) for the serological diagnosis of sarcoptic mange in dogs. *Vet Dermatol*. (2001) 12:315–20. doi: 10.1046/j.0959-4493.2001.00265.x
36. Scott DW, Miller WH, Griffin CE. *Muller & Kirk's Small Animal Dermatology, 6th ed.*. Philadelphia, PA: W.B. Saunders (2001). p. 476–83.
37. Walton SF. The immunology of susceptibility and resistance to scabies. *Parasite Immunol*. (2010) 32:532–40. doi: 10.1111/j.1365-3024.2010.01218.x
38. Gross TL, Ihrke PJ, Walder EJ, Affolter VK. (editors). Perivascular diseases of the dermis. In: *Skin Diseases of the Dog and Cat: Clinical and Histopathologic Diagnosis*. 2nd edn. Oxford: Blackwell Publishing (2005). p. 217.
39. Partel P, Citterio CV, Cavallero S. *Alpine ibex* (Capra ibex) versus *Sarcoptes scabiei*: field evidence of possible resistance as a driver for management and research. *Hystrix*. (2016) 27(ATIt Congress Supplement):21. doi: 10.4404/hystrix-27.0-11877
40. Salvadori C, Rocchigiani G, Lazzarotti C, Formenti N, Trogu T, Lanfranchi P, et al. *Histological Lesions and Cellular Response in the Skin of Alpine Chamois (Rupicapra r. rupicapra) Spontaneously Affected by Sarcoptic Mange*. London: Hindawi Publishing Corporation, BioMed Research International (2016). p. 1–8. doi: 10.1155/2016/3575468
41. Skerratt LF. Cellular response in the dermis of common wombats (Vombatus ursinus) infected with Sarcoptes scabiei var. wombat. *J Wildl Dis*. (2003) 39:193–202. doi: 10.7589/0090-3558-39.1.193
42. Berger A. Th1 and Th2 responses: what are they? *BMJ*. (2000) 321:424. doi: 10.1136/bmj.321.7258.424
43. Nimmervoll H, Hoby S, Robert N, Lommano E, Welle M, Ryser-Degiorgis MP. Pathology of sarcoptic mange in red foxes (vulpes vulpes): macroscopic and histologic characterization of three disease stages. *J Wildl Dis*. (2013) 49:91–102. doi: 10.7589/2010-11-316
44. Oleaga A, Casais R, Prieto JM, Gortázar C, Balseiro A. Comparative pathological and immunohistochemical features of sarcoptic mange in five sympatric wildlife species in Northern Spain. *Eur J Wildl Res*. (2012) 58:997–1000. doi: 10.1007/s10344-012-0662-y
45. Oleaga A, Casais R, Balseiro A, Esp,í A, Llaneza L, Hartasánchez A, et al. (2011). New techniques for an old disease: sarcoptic mange in the Iberian wolf. *Vet. Parasitol.* 181, 255–266. doi: 10.1016/j.vetpar.2011.04.036
46. Alasaad S, Granados JE, Fandos P, Cano-Manuel FJ, Soriguer RC, Pérez JM. The use of radio-collars for monitoring wildlife diseases: a case study from Iberian ibex affected by Sarcoptes scabiei in Sierra Nevada, Spain. *Paras Vect*. (2013) 6:242. doi: 10.1186/1756-3305-6-242
47. Stone SP. Scabies and pediculosis. In: Freedberg IM, et al., editors. *Fitzpatrick's Dermatology in General Medicine*, *6th edn.* New York, McGraw-Hill (2003). p. 2283–9.
48. Morris DO, Dunstan RW. A histomorphological study of sarcoptic acariasis in the dog: 19 cases. *J Am Anim Hosp Assoc*. (1996) 32:119–24. doi: 10.5326/15473317-32-2-119
49. Mikuloaska A, Falck B. Distributional changes of Langerhans cells in human skin during irritant contact dermatitis. *Arch Dermatol Res*. (1994) 286:429–33. doi: 10.1007/BF00371567
50. Gurish MF, Lynch DH, Yowell R, Daynes RA. Abrogation of epidermal antigen-presenting cell function by ultraviolet radiation administered in vivo. *Transplantation*. (1983) 36:304–9. doi: 10.1097/00007890-198309000-00015
51. Rico MJ, Streilen JW. Comparison of alloimmunogenicity of Langerhans cells and keratinocytes from mouse epidermis. *J Invest Dermatol*. (1987) 89:607–10. doi: 10.1111/1523-1747.ep12461373
52. Schweizer J. Langerhans cell-free regions in orthokeratinizing sole-of-foot epidermis of adult mouse. *Arch Dermatol Res*. (1980) 268:157–60. doi: 10.1007/BF00403800
53. Cavallero S, Citterio C, Lanfranchi P, Rossi L, Obber F, D'Amelio S. Host-pathogen interaction in modulating variability at MHC DRB1 locus in alpine chamois. In: *Proceeding of the II Rupicapra Symposium. Biology, Health, Monitoring and Management*. Catalonia: Bellver de Cerdanya (2013). p. 24–25.
54. Luzzago C, Ebranati E, Cabezón O, Fernández-Sirera L, Lavín S, Rosell R, et al. Spatial and temporal phylogeny of border disease virus in pyrenean chamois (*Rupicapra p. pyrenaica). PLoS ONE*. (2016) 11:e0168232. doi: 10.1371/journal.pone.0168232
55. Alasaad S, Rossi L, Heukelbach J, Pérez JM, Hamarsheh O, Otiende M, et al. The neglected navigating web of the incomprehensibly emerging and re-emerging Sarcoptes mite. *Infect Genet Evol*. (2013) 17:253–9. doi: 10.1016/j.meegid.2013.04.018
56. Alasaad S, Walton S, Rossi L, Bornstein S, Abu-Madi M, Soriguer R, et al. Sarcoptes-world molecular network (Sarcoptes-WMN): integrating research on scabies. *Int J Infect Dis*. (2011) 15:e294–7. doi: 10.1016/j.ijid.2011.01.012

Conflict of Interest: The authors declare that the research was conducted in the absence of any commercial or financial relationships that could be construed as a potential conflict of interest.

Copyright © 2020 Turchetto, Obber, Rossi, D'Amelio, Cavallero, Poli, Parisi, Lanfranchi, Ferrari, Dellamaria and Citterio. This is an open-access article distributed under the terms of the Creative Commons Attribution License (CC BY). The use, distribution or reproduction in other forums is permitted, provided the original author(s) and the copyright owner(s) are credited and that the original publication in this journal is cited, in accordance with accepted academic practice. No use, distribution or reproduction is permitted which does not comply with these terms.

frontiers in Veterinary Science

CASE REPORT
published: 07 May 2020
doi: 10.3389/fvets.2020.00235

Health Impacts and Recovery From Prolonged Freshwater Exposure in a Common Bottlenose Dolphin (*Tursiops truncatus*)

Alissa C. Deming[1], Noel L. Wingers[1], Debra P. Moore[2], David Rotstein[3], Randall S. Wells[4], Ruth Ewing[5], Matthew R. Hodanbosi[1,6] and Ruth H. Carmichael[1,6]*

[1] Marine Mammal Research Center, Dauphin Island Sea Lab, Alabama Marine Mammal Stranding Network, Dauphin Island, AL, United States, [2] College of Veterinary Medicine, Mississippi State University, Mississippi State, MS, United States, [3] Marine Mammal Pathology Services, Olney, MD, United States, [4] Chicago Zoological Society's Sarasota Dolphin Research Program, Sarasota, FL, United States, [5] Southeast Fisheries Science Center, National Marine Fisheries Service, U.S. Department of Commerce, Miami, FL, United States, [6] Department of Marine Sciences, University of South Alabama, Mobile, AL, United States

OPEN ACCESS

Edited by:
Francesco Carlo Origgi, University of Bern, Switzerland

Reviewed by:
Tatjana Sitt, United States Department of Agriculture, United States
Francisco Ruben Carvallo Chaigneau, Virginia Tech, United States

***Correspondence:**
Alissa C. Deming
alissademing@gmail.com

Specialty section:
This article was submitted to Veterinary Experimental and Diagnostic Pathology, a section of the journal Frontiers in Veterinary Science

Received: 31 December 2019
Accepted: 06 April 2020
Published: 07 May 2020

Citation:
Deming AC, Wingers NL, Moore DP, Rotstein D, Wells RS, Ewing R, Hodanbosi MR and Carmichael RH (2020) Health Impacts and Recovery From Prolonged Freshwater Exposure in a Common Bottlenose Dolphin (Tursiops truncatus). Front. Vet. Sci. 7:235. doi: 10.3389/fvets.2020.00235

Common bottlenose dolphins (*Tursiops truncatus)* exposed to freshwater or low salinity (<10 practical salinity units; PSU) for prolonged periods of time have been documented to develop skin lesions, corneal edema and electrolyte abnormalities, and in some instances they have died. Here we review a case of an out-of-habitat subadult, female common bottlenose dolphin that remained in a freshwater lake in Seminole, Alabama for at least 32 days. Due to concerns for the dolphin's health a rescue was initiated. At the time of rescue bloodwork results indicated minor electrolyte abnormalities (hyponatremia, hypochloremia, hypoosmolality). Renal function was not affected (normal creatinine and urea nitrogen) and all other bloodwork parameters (hemogram; serum biochemistry analytes) were within normal limits. The dolphin was deemed healthy enough for immediate relocation and release. A satellite-linked tag was attached to the dorsal fin to track the dolphin following its relocation to a nearby brackish water bay (Perdido Bay, AL), a known habitat for bottlenose dolphins. Twelve weeks following release, the dolphin was found dead as a result of a fisheries interaction (peracute underwater entrapment). A full necropsy was conducted and there was complete resolution of the skin pallor and skin lesions and no evidence of chronic renal or central nervous system lesions. Post-mortem analysis of vitreous humor (used as a proxy for serum analytes and to determine post-mortem interval) was challenging to interpret and has not been validated in dolphins. This supports the need for future research in cetaceans to establish a species-specific approach. Elevated barium (Ba) concentrations in tooth dentin corresponded to increased seasonal freshwater discharge patterns, confirming repeated annual exposure to low salinity conditions prior to death and indicating freshwater exposure may pose an ongoing threat to dolphins in the region. This case provides a unique opportunity to follow the progression of prolonged freshwater exposure and recovery in a bottlenose dolphin and highlights that dolphins in nearshore habitats face a combination of persistent natural and human associated threats.

Keywords: Gulf of Mexico, freshwater skin lesions, corneal edema, out-of-habitat, human interaction

INTRODUCTION

Prolonged exposure to freshwater or low salinity water (<10 practical salinity units; PSU) in common bottlenose dolphins (*Tursiops truncatus*; hereafter referred to as dolphins) has been recognized to cause negative health impacts, and in some cases, death (1–4). Dolphins have evolved to live in a marine environment where salinities maintain above 30 PSU. Cetaceans have developed the ability to excrete strongly hypertonic urine to conserve water and aid in fluid homeostasis in a marine environment (5–7). Some populations of dolphins that reside in bays, sounds and estuaries are known to be exposed to lower salinity water (15–25 PSU) and, on occasion, experience short periods of lower salinity (<15 PSU) as a result of freshwater runoff from watersheds, rivers and large storm events [e.g., floods and hurricanes; (3, 8, 9)]. Recent studies in Barataria Bay, Louisiana found that dolphins exhibited a preferred salinity threshold of >8 PSU and avoided waters of <5 PSU (10). Little is known about the effects of prolonged freshwater exposure in dolphins, including the length of exposure time necessary to cause negative health impacts and the ability of a dolphin to recover following prolonged low salinity exposure.

Exposure to excessive freshwater causes a range of pathologies in mammals. In terrestrial mammals, freshwater intoxicosis can occur if large quantities of freshwater are consumed in a short period of time as seen in psychogenic polydipsia (described in canines, hoofstock, and humans), self-imposed overhydration in Army recruits following heat-related injuries, iatrogenic causes (as seen in fluid overloading with intravenous fluids in hospitalized animal and human patients) and child abuse (11–16). In humans, the early stages of water intoxication include confusion, disorientation and vomiting, with progressive exposure resulting in hyponatremia, seizures, coma, and death (15). In wild dolphins, prolonged exposure to freshwater causes generalized skin pallor, various degrees of proliferative, erosive and ulcerative skin lesions with possible secondary bacterial, fungal and protozoal infections, corneal edema, and electrolyte imbalances (including hyponatremia, hypochloremia, and low calculated osmolality) (1, 3, 4). In cases of freshwater exposure and dolphins, however, there is little documentation of the clinical signs antemortem or the pathophysiology post-mortem, primarily due to the lack of *a priori* knowledge of freshwater exposure of stranded dolphins and the availability of fresh post-mortem specimens to examine histologically.

Several approaches to determine whether a dolphin had been exposed to prolonged freshwater prior to death have been proposed or are currently being investigated. These approaches include the use of vitreous humor post-mortem as a proxy for serum electrolytes and trace elements analyses of teeth, which can have distinct freshwater and marine patterns (4, 6, 17–19). Currently the most common means to assess freshwater exposure in stranded dolphin carcasses is evaluation of the skin for lesions consistent with prolonged freshwater exposure and known exposure to low salinity water (1, 3).

To date, the vast majority of prolonged freshwater exposure reports in dolphins have been associated with out-of-habitat dolphins that traveled to and remained in freshwater systems for prolonged periods of time or were displaced as a result of natural disasters such as flooding or hurricanes (1, 3, 9). In the Southeast United States from 1992 to 2005, there were 12 documented cases of bottlenose dolphins that were classified as out-of-habitat because they were free-swimming in low salinity or freshwater systems for prolonged periods of time (1). Six of the 12 cases resulted in death attributed to prolonged freshwater exposure and the remaining cases required lifesaving intervention (rescue, relocation, or rehabilitation). Due to a limited understanding of how long dolphins can tolerate exposure to low salinity water, it can be challenging for authorities to determine at what point life-saving intervention is necessary for out-of-habitat dolphins. Stranding responders and authorities often encourage dolphins to leave an area through various herding techniques and monitor for signs of decreased foraging, skin pallor, or skin lesions. Once a dolphin is deemed to be in distress, rescue, and relocation or rehabilitation is pursued. Most of the knowledge of the physiological impacts of prolonged freshwater exposure has been gained during these efforts (1, 4). Following rescue and relocation, stranding responders attempt to track the dolphin to determine success of the rescue, but there is limited information in the literature about the ability of a dolphin to recover from prolonged low salinity exposure. Here we review a case of a common bottlenose dolphin that recovered following rescue from prolonged freshwater exposure but ultimately died from human interaction. This case gives a unique opportunity to assess the progression and resolution of freshwater skin lesions following relocation to more appropriate habitat conditions.

CASE DESCRIPTION AND ANALYTICAL METHODS

On 23 February 2016, a member of the public reported to the Alabama Marine Mammal Stranding Network (ALMMSN) that two dolphins (suspected mother with older calf) were swimming in a small freshwater lake in Seminole, Alabama (30.502990°N, −87.442926°W) (**Figure 1A**-map; **Figure 2**-timeline of case). The complainant provided photos of the dolphins and reported they were traveling together in the lake, observed foraging and appeared healthy. The lake is connected to the Perdido Bay estuary system approximately 25-km south, via a small, shallow canal (**Figure 1A**). Perdido Bay (salinity average 15–25 PSU) is a region considered by the National Oceanographic and Atmospheric Association, National Marine Fisheries Service (NOAA/NMFS) to be suitable habitat for bottlenose dolphins, and NOAA/NMFS is responsible for their management (20). Under the direction of NOAA/NMFS, the dolphins were monitored with anticipation that they would leave the area on their own volition.

Thirteen days later (07 March 2016), the dolphins were still in the lake and were no longer observed feeding. On 08 March 2016, ALMMSN staff assessed the dolphins onsite and both had mild erosive skin lesions and slight generalized skin pallor. Otherwise they appeared to be in good body condition and behaving normally. During monitoring, the larger dolphin exited the lake through a 2-meter wide canal that connected

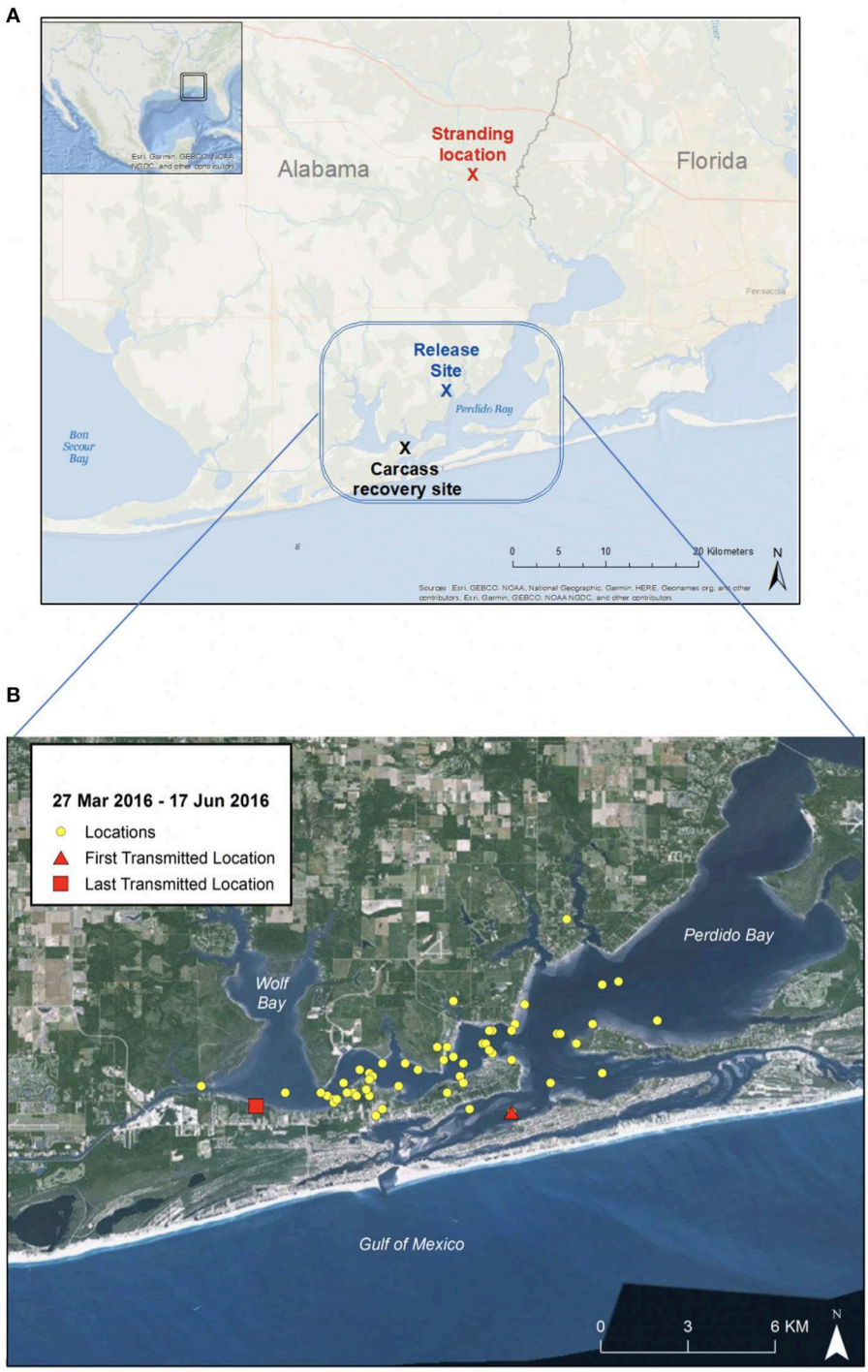

FIGURE 1 | Maps of Perdido Bay, Alabama. **(A)** Rescue location (red), release site (blue), and site of carcass recovery (black) with blue rectangle region indicating area dolphin spent time during 12-week recovery period. **(B)** Close-up map of Perdido Bay showing satellite tracking signal locations (27 March 2016 to 17 June 2016). The dolphin remained within Perdido Bay, a known estuarine habitat for bottlenose dolphins, and did not appear to travel south into the Gulf of Mexico during the post-release period.

to Perdido River and southward to Perdido Bay. The larger dolphin was not observed in the lake again and the fate of this dolphin is unknown. The smaller dolphin remained in the lake. On 13 March 2016 ALMMSN, Emerald Coast Wildlife Refuge (ECWR), and NOAA/NMFS responders attempted to herd the remaining dolphin from the lake using bubblenet,

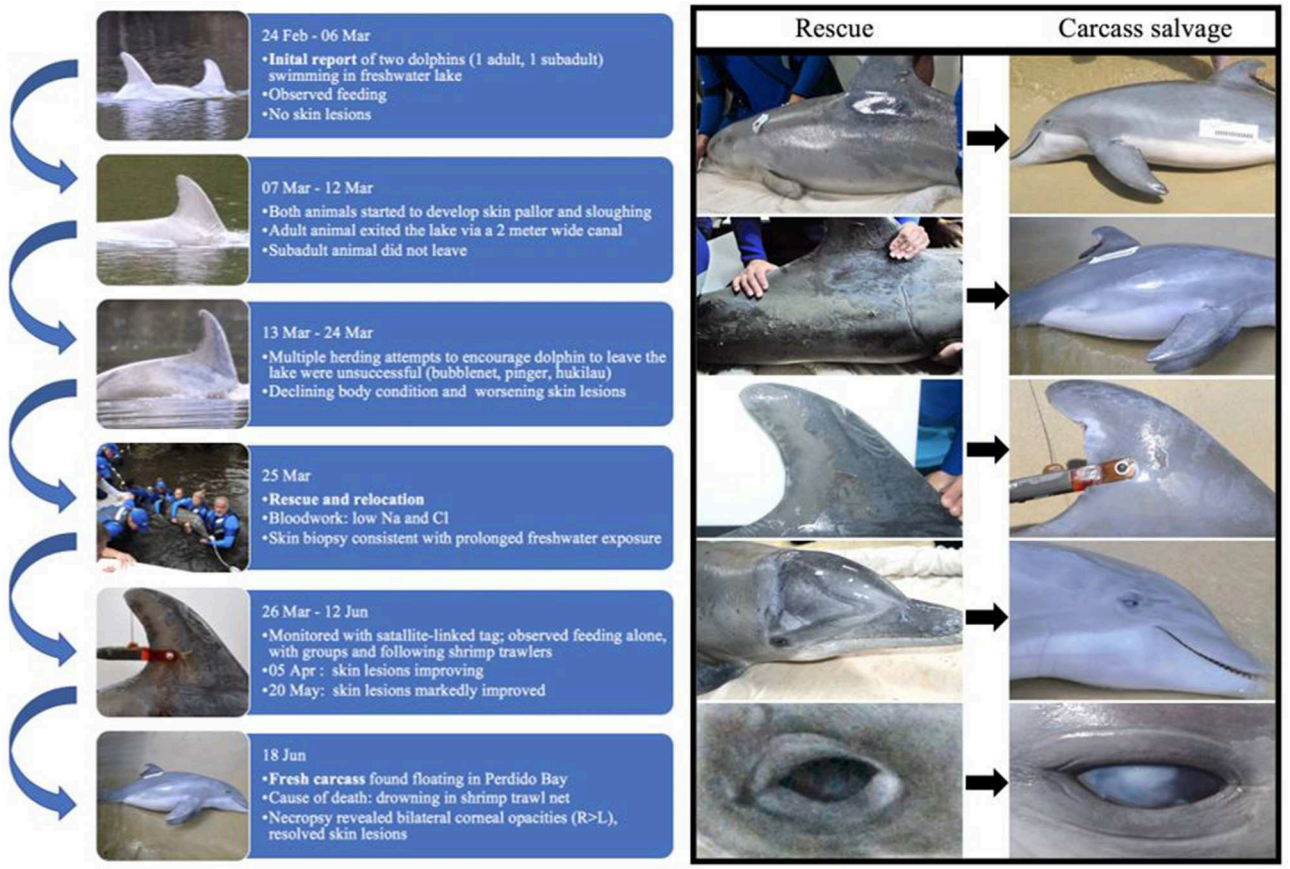

FIGURE 2 | Timeline of case from initial report (24 February 2016) to time of death (18 June 2016) and photographs of skin lesions taken at time of rescue (25 March 2016; left column **A–E**) and time of carcass recovery (18 June 2016; right column **F–J**). During the 12-week period following rescue from a freshwater lake and release into a brackish water estuary, skin lesions markedly improved, with almost complete resolution. Corneal opacities were worse at time of death than at time of rescue. Left lateral body **(A,F)**; right flank **(B,G)**; right dorsal fin **(C,H)**; right lateral head **(D,I)**; and right eye **(E,J)**.

pingers, and a hukilau, but efforts were unsuccessful. Due to the decrease in observed foraging, deteriorating body condition and worsening skin lesions, officials deemed the dolphin was in need of rescue and either relocation or rehabilitation if indicated at time of rescue.

On 25 March 2016, ALMMSN, regional collaborators, and NOAA/NMFS initiated a rescue (**Figure 2**). The dolphin was captured using a boat-based, net capture technique (21–23). Once secured, the dolphin was brought to land and veterinarians performed a thorough physical examination, collected blood samples (heparinized whole blood and serum) from the ventral fluke vessel, skin culture (fungal only), and skin biopsies for histologic evaluation and molecular analysis. Fungal skin culture swabs were collected from an area with moderate skin sloughing (left and right dorsolateral thorax). Local anesthesia (lidocaine with epinephrine; L-block) was administered and two skin/blubber biopsies extending the full thickness of the blubber were collected with an 8-mm biopsy punch, near the location of culture swab collection. The skin/blubber biopsies were cut in half longitudinally and one section of each was fixed in 10% neutral buffered formalin for histologic evaluation and the remaining sample was frozen for fungal culture and/or molecular analysis as needed (−20°C). Following skin biopsy fixation, the tissues were embedded in paraffin, sectioned at 5-μm thickness, stained histochemically with hematoxylin and eosin (H&E), gram, giemsa, acid fast bacteria (AFB) stain, Grocott's methenamine silver (GMS) stains, and evaluated by a veterinary pathologist.

Point of care electrolyte analysis (iStat CG8+) was performed on heparinized whole blood (**Table 1**), which showed a mild hyponatremia (146 mEq/L; reference range: 149–157 mEq/L) and hypochloremia (98 mEq/L; reference range: 110–119 mEq/L) with normal creatinine (0.9 mg/dL; reference range: 0.68–1.49 mg/dL) and low urea nitrogen (34 mg/dL; reference range: 42–77 mg/dL) (24). Hemogram and serum biochemistry profiles were also performed, and with the exception of the above-mentioned electrolyte abnormalities, all other parameters were within normal limits for a wild subadult bottlenose dolphin (24). It was determined that the dolphin was in suitable condition for immediate relocation and release. The dolphin was transported by vehicle to the mouth of Palmetto Creek (30.34691°N, −87.51409°W) in Perdido Bay, AL (**Figure 1A**).

TABLE 1 | Biochemical analytes of serum (red) from apparently healthy wild Atlantic juvenile bottlenose dolphins (24); and biochemical analytes from this case at time of rescue (serum) and post-mortem (vitreous).

Biochemical analyte	Healthy (24)	Rescue (this case)	Post-mortem (this case)
Sodium (mEq/L)	149–157	147	145 (149.4)*
Chloride (mEq/L)	110–119	96	123 (127.4)*
Potassium (mEq/L)	3.2–4.4	4.2	41.5
Creatinine (mg/dL)	0.68–1.49	0.9	1.7
Urea Nitrogen (mg/dL)	42–77	34	104

Value was corrected using potassium to determine a post-mortem interval of 48 h (25) and applying the post-mortem sodium and chloride correction factors established by Zilg et al. (19).

Salinity at the release location was 6.2 PSU. A satellite-linked SPOT-299B Single-point Finmount, 2-Lay tag (Wildlife Computers, Redmond, WA, USA) was applied to the trailing edge of the dorsal fin and the dolphin was released (23, 26). The tag was programmed to transmit 250 times each day, during five periods of suitable satellite overflight. Post-release, the dolphin's movements were monitored via satellite-linked tag transmissions, boat observations and communication with local dolphin watching tour operators. Throughout the 85-day tracking period the dolphin remained in Perdido Bay (**Figure 1B**). During this time, salinity levels measured at the closest environmental monitoring buoy in Bon Secour Bay (Alabama Real-time Coastal Observing System; https://arcos.disl.org/stations/disl_stations?stationnew=106) were relatively low, particularly at the time of relocation (3.7 PSU on 25 March 2016), and steadily increased throughout the post-release period (18.5 PSU on 18 June 2016; **Figure 4**).

On 18 June 2016, ALMMSN received a call from Orange Beach Coastal Resources regarding a fresh-dead dolphin with a satellite-linked tag on the dorsal fin, floating in the surf (Orange Beach, AL; 30.301585°N, −87.559443°W; **Figure 1A**). ALMMSN responded, took photographs (**Figure 2**), and transported the carcass to Dauphin Island Sea Lab. The carcass was placed in a refrigerated cold room (4°C) overnight, and on 19 June 2016 a necropsy was performed. The carcass was fresh dead (Code 2) at time of salvage and in early decomposition (Code 3, early) at the time of necropsy. A full suite of tissues was collected and fixed in 10% neutral buffered formalin. Following fixation, the tissues were embedded in paraffin, sectioned at 5-μm thickness, stained with H&E, and evaluated by a pathologist. Additionally, a small piece of green net material caught in the right attachment screw of the satellite-linked tag and a small hook found free-floating in the forestomach were submitted to the NOAA/NMFS Gear Research Team for analysis.

At necropsy, 24-h following the carcass report, vitreous humor was collected to serve as a proxy for serum (19, 27, 28). The vitreous was red-tinged, indicating possible blood contamination, most likely related to retinal or fundic hemorrhage associated with drowning/asphyxiation (29). Vitreous was centrifuged for 10 min at 1,800 g and the liquid supernatant collected, frozen (−20°C) and shipped overnight on dry ice to Cornell University's Animal Health Diagnostic Center for electrolyte analysis. Results were compared to published references for serum chemistry analytes in wild juvenile bottlenose dolphins (24). There was no urine in the bladder for urinalysis.

Because this dolphin experienced a known period of prolonged freshwater exposure, trace element analysis and age estimation were performed on a tooth to determine if a freshwater elemental signature could be identified in the most recent growth layer group (GLG) (17, 18, 30–32). For trace element analysis, a 2-mm mid-sagittal tooth section was cut using a Buehler IsoMet 1000 Precision saw with a diamond blade. Trace element data were collected along the cut surface through laser ablation inductively coupled plasma mass spectrometry (LA-ICPMS) using a NWR213 Nd:YAG laser coupled with an Agilent 7700x quadrupole ICPMS. Trace element values for ^{43}Ca, ^{137}Ba, ^{208}Pb were collected. Laser scan parameters were set as 30 μm s^{-1} scan speed, 10 μm spot size at 20 Hz, with ablation fluence of 45% (15–17 J cm^{-2}). SRM612 glass (National Institute of Standards and Technology) and MAPS-4 phosphate pellet (United States Geological Survey) were used as tuning and reference standards, respectively. The concentrations of all elements were normalized to ^{43}Ca, and data were analyzed using 2-point reference calibration in Microsoft Excel. To relate trace element ratios to the time of elemental incorporation, we estimated the dolphin's age using established sclerochronological age determination methods (31, 32). Briefly, the 2-mm tooth section was decalcified with RDO decalcifying solution, then further sectioned into 25-μm slices. These slices were stained with a hematoxylin solution and placed onto microscope slides. Age was estimated by counting the number of GLG in the post-natal dentin of the tooth (31, 32).

DIAGNOSTIC ASSESSMENT

At the time of rescue, following 32 days of freshwater exposure, the dolphin was slightly thin. The skin was diffusely pale grey and sloughing (>70%) with superficial erosive lesions on the flukes, head, mid-epaxial region, and dorsal fin (**Figure 2**). Skin biopsies collected at time of rescue were examined histologically and there was epithelial erosion, edema, hydropic degeneration of superficial epithelial cells, and separation of superficial epithelial layers with serum accumulation (**Figure 3A**). Special stains (H&E, gram, giemsa, AFB, GMS) for fungi, bacteria and protozoa were negative, and no fungal hyphae were identified. Fungal culture grew *Curvularia* sp. (Fungus Testing Laboratory, UT, USA), a pigmented environmental hyphomycete found in the soil and plant debris, but fungal PCR from frozen skin biopsy was negative. The organism was likely a superficial saprophyte and was not present within the epidermal layers.

When the carcass was recovered, 85 days after being relocated to brackish water (range = 3.7–20.7 PSU; mean = 13.4; *SD* = 4.4 PSU), the freshwater skin lesions were markedly improved to completely resolved (**Figure 2**) and the epidermis was normal on histologic evaluation. The most significant finding on necropsy

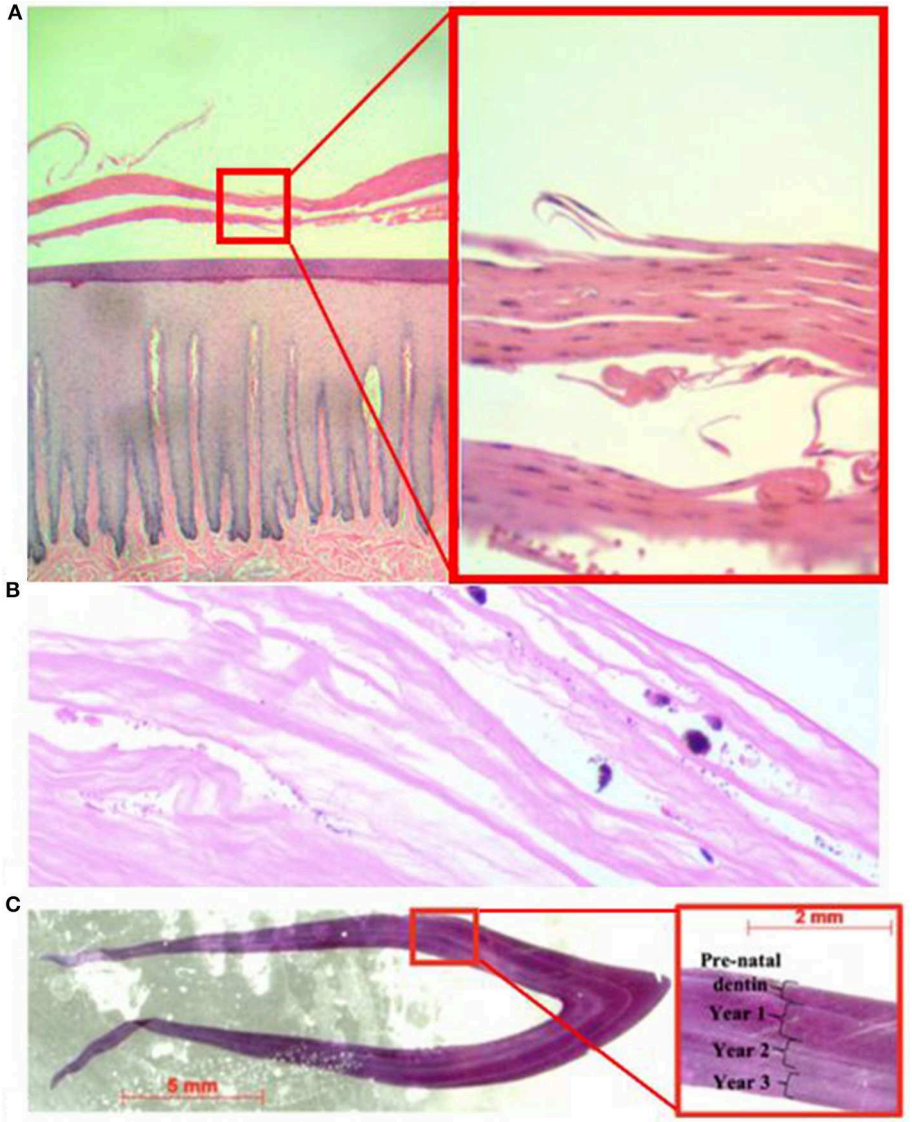

FIGURE 3 | Photomicrograph of hematoxylin and eosin stained tissue slides including **(A)** skin biopsy at time of rescue (left = 4X; right = 20X). The stratum externum is separated by eosinophilic fluid and epithelium is separated and curled; **(B)** corneal edema of the right eye at time of necropsy (20X); and **(C)** cross-section of tooth used for trace element analysis and close-up (red box) showing annual growth layer groups used to estimate the dolphin's age.

included a small piece of net remnant on the satellite-linked tag, several minimally digested fish and invertebrates in the forestomach, and superficial criss-cross linear impressions on the skin of the rostrum, melon and leading edges of the pectoral fins and flukes. Additional gross findings included a moderate amount of red-tinged froth in the bronchi and bronchioles, occasional petechiae, and ecchymosis on the intestinal mucosa, a free-floating bait hook in the forestomach and a mild to moderate trematode (*Braunina cordiformis*) burden in the main (glandular) stomach. Both eyes had mild (left) to marked (right) corneal opacities (**Figure 2**), that were worse at time of carcass recovery compared to time of rescue and had moderate corneal edema on histologic evaluation (**Figure 3B**).

The majority of histologic findings were considered incidental and included few protozoal cysts (*Sarcocystis* sp.) in the skeletal muscle without an inflammatory response, mild lymphoplasmacytic pneumonia and pulmonary fibrosis and gastric *B. cordiformis*. There were no histopathologic lesions in the kidneys, integument, adrenal glands or central nervous system that would indicate prolonged or chronic effects associated with the freshwater exposure. The net material evaluated by NMFS Gear Research Team was identified to be trawl net #7 or #9 (twisted nylon twine) that had been dipped and is used in inshore recreational and commercial shrimp trawls. The small hook recovered from the forestomach was a 3/0 offset live bait hook, sometimes called a "Mosquito Hook." Cause of

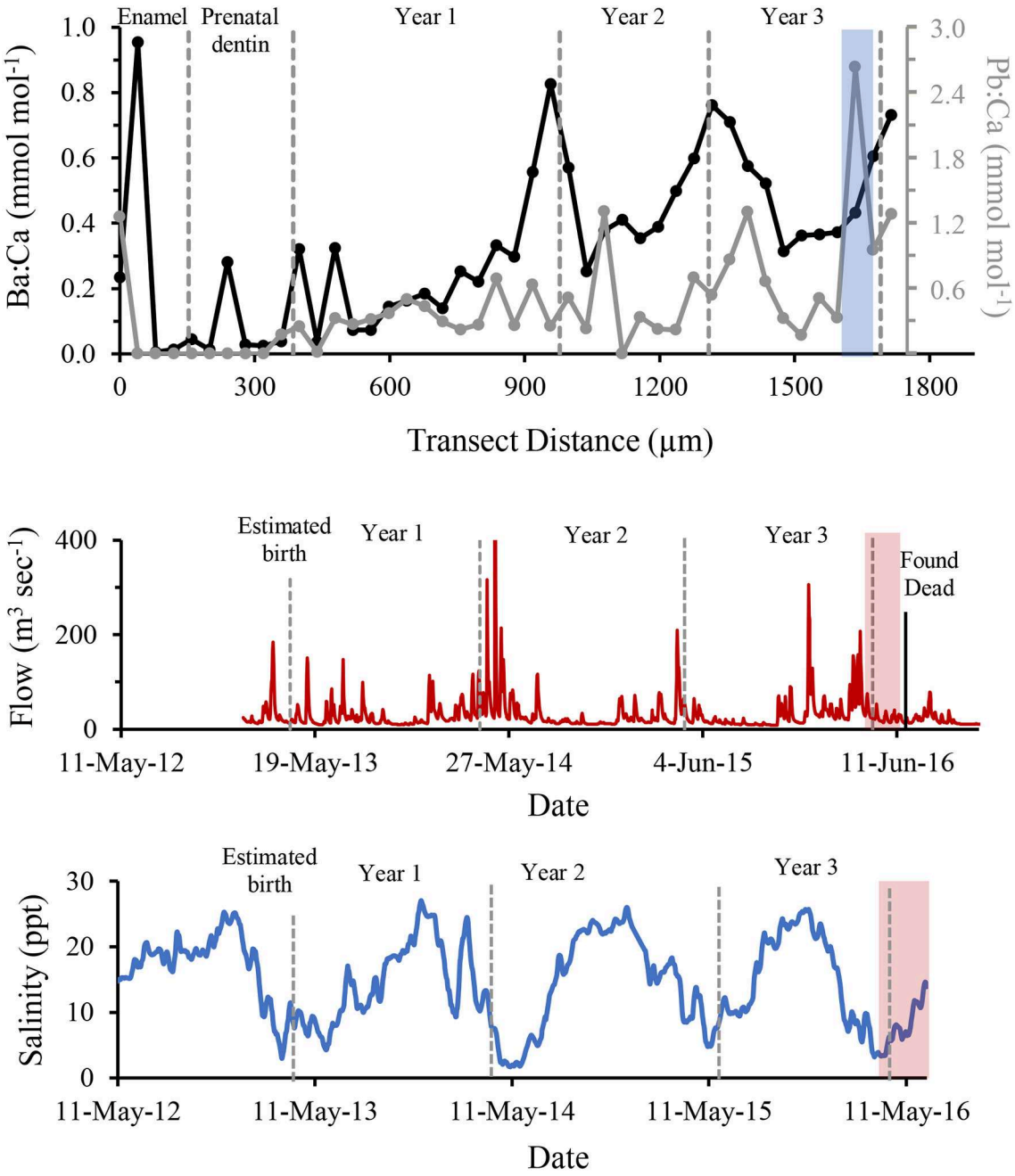

FIGURE 4 | Ba (black) and Pb (grey) concentrations normalized to Ca and compared to years of life of a known freshwater-exposed dolphin, determined by LA-ICPMS across growth layer groups in a tooth **(Top)**. Freshwater discharge to the area from the Perdido and Styx Rivers is shown for the same time period **(Middle)**. Historical salinity levels measured at closest environmental monitoring buoy (Bon Secour) to relocation site **(Bottom)**. Dashed grey bars indicate boundaries of annual growth layer groups (shown in this figure), the period of known stranding within a freshwater canal is indicated by light blue shaded regions, and red shaded region marks period from relocation to time if death. Discharge data were obtained from publicly available United States Geological Survey data at monitoring sites USGS02377750 (Styx River, Seminole, AL) and USGS02376500 (Perdido River, Barrineau Park, FL). Salinity data were obtained from Alabama Real-time Coastal Observing System, Bon Secour monitoring station (https://arcos.disl.org/stations/disl_stations?stationnew=106).

death was peracute underwater entrapment in a shrimp trawl net supported by the presence of net material and criss-cross net impression on the body along with tracheobronchial froth and enteric petechiae (33).

The post-mortem electrolyte analysis of the vitreous had a severely elevated potassium (41.5 mEq/L), mildly low sodium (145 mEq/L), mildly low chloride (123 mEq/L), mildly elevated creatinine (1.7 mg/dL), and mildly elevated urea nitrogen (104

mg/dL). Based on equations developed in human forensics using vitreous potassium levels (34), the post-mortem interval (PMI) was estimated to range from 42 h [(PMI = $1.076(K^+)-2.815$ with K = 41.5 mEq/L; (25)] to >120 h [(PMI = $6.15(K^+)-38.1$ with K = 41.5 mEq/L; (35)] at time of vitreous collection. Post-mortem changes in sodium and chloride of 2.2 mEq/L every 24 h following death have been documented in humans (19) and represent the best available data for making similar estimates in marine mammals. To apply Zilg et al. (36) sodium and chloride correction factor, we used the conservative PMI estimate of 42 h and rounded up to 48 h to enable application of the sodium and chloride correction factor, which is calculated for 24-h intervals. This estimates the vitreous sodium at time of death to be 149.4 mEq/L and chloride equivalent to 127.4 mEq/L. No similar approaches have been developed to apply to PMI increases in creatinine or urea nitrogen.

Based on the number of GLGs present in the post-natal dentin, we estimate the dolphin was slightly over 3 years old at death (**Figure 3C**). Ontogenetic shifts occurred in Ba:Ca and Pb:Ca indicated by differences in elemental composition between enamel, pre-natal dentin and post-natal dentin (**Figure 4**, top). Post-natal peaks in Ba:Ca correlated with seasonal freshwater inputs to the system and salinity (**Figure 4**, middle and bottom, respectively). Peaks in Pb:Ca followed Ba:Ca, particularly in years 2–3, with a spike in Pb:Ca during the period of known freshwater exposure prior to death.

DISCUSSION

This report describes a case of prolonged freshwater exposure in a common bottlenose dolphin that remained in a freshwater lake for at least 32 days, prior to successful rescue and recovery. The prolonged freshwater exposure resulted in diffuse skin lesions, mild electrolyte abnormalities, corneal edema, and decreased body condition. Following 85 days in a brackish water bay with somewhat more appropriate salinity (range = 3.7–20.8 PSU; mean = 13.7; *SD* = 4.4), the dolphin was found dead as a result of a fisheries interaction (peracute underwater entrapment). At the time of death, freshwater-related skin lesions were resolved and there were no chronic renal or central nervous system lesions on histologic examination, but corneal edema worsened, likely affecting vision in at least one eye. It is difficult to determine if the corneal edema was sequelae of the freshwater exposure, the result of trauma to the cornea either during the rescue capture, transport or during the 12-weeks following relocation, or some combination of these.

A typical treatment for corneal edema in dolphins managed under human care is topical application of hypertonic saline drops (5% NaCl). Therefore, moving a dolphin from freshwater to higher salinity brackish water should improve conditions relative to the corneal edema. However, it may be that the brackish water in Perdido Bay was still too hypotonic to allow the already compromised corneal epithelium to heal, and the corneal edema continued to worsen. This observation warrants close monitoring of dolphin eyes following transition between low and higher salinity water and stresses the importance of protecting the eyes during capture and transport. If a dolphin with prolonged freshwater exposure is brought into rehabilitation, application of hypertonic saline eye drops may be indicated to decrease corneal edema and likelihood of corneal fibrosis that could impact long-term vision. This case provides valuable insight into the health effects of a dolphin during a known period of freshwater exposure and supports that relocation to higher salinity habitat may enable successful recovery from some symptoms (skin lesions) but not others (corneal edema).

The analysis of tooth GLGs indicated this dolphin was 3–4 years old, which corresponds to the age class associated with its straight length [190 cm; (37)]. The observed seasonal increases in Ba:Ca in the tooth coincided with seasonal pulses of low-salinity water and is consistent with expected elevated Ba content in freshwater. A negative correlation between Ba:Ca in water and salinity has been shown for the northern Gulf of Mexico (38), and thus, Ba:Ca ratio is often used as an indicator of freshwater residency for a variety of finfish (39–41). Our data demonstrate that this application may be effective in dolphins to trace regular seasonal exposure to freshwater. The elevated Pb:Ca values at the time of acute freshwater exposure in the enclosed lake indicate the dolphin was exposed to higher concentrations of Pb, either conveyed in freshwater discharge or through consumption of contaminated fish (42). This finding suggests freshwater has potential to affect dolphin health through increased exposure to local anthropogenic contaminants, as seen elsewhere in the southeastern U.S. (43), and merits further study. Importantly, these data suggest resident dolphins along the northern Gulf of Mexico coast repeatedly endure at least seasonal low-salinity conditions and exposure to elements conveyed via freshwater discharge throughout their lifetime.

The electrolyte analysis on the post-mortem vitreous humor is challenging to interpret. There is a lack of validation using this technique in cetaceans, and there can be significant variability associated with ante- and post-mortem factors (including autolysis, ambient temperature, drowning in low salinity water, blood contamination, and/or corneal disease potentially impacting the permeability of the cornea- all potential confounding variables in this case). Vitreous analytes in humans and some animals (cows, dogs, and cats) have been used to determine the PMI, specifically using potassium. Vitreous humor acts as a proxy for antemortem serum chemistry analyte analysis including sodium, chloride and nitrogenous compounds (creatinine and urea nitrogen) (19, 27, 44, 45). It is generally accepted that potassium, urea nitrogen, and creatinine increase with increasing PMI (27, 34, 44, 45), and sodium and chloride decrease with increasing PMI (19). Using the calculated PMI, the vitreous sodium was corrected using the method described by Zilg et al. (19), which gave a sodium value of 149.4 mEq/L (within normal limits). However, chloride appeared elevated both before and after applying the correction factor. The slight elevation in vitreous creatinine and urea nitrogen may reflect a post-mortem increase as seen in other species, or could be the result of antemortem abnormalities, possibly associated with chronic renal disease and/or rhabdomyolysis associated with struggle prior to death. Due to the various confounding variables with this case

and lack of established methodology in cetacean species, the error associated with these values cannot be quantified at this time. Future work on post-mortem vitreous analytes in cetacean species is needed and has the potential to serve as a useful tool in confirming prolonged freshwater exposure once established.

Post-mortem evaluation determined the cause of death to be drowning in a shrimp trawl net. Although the freshwater effects on the skin improved through time, visual impairment secondary to prolonged freshwater exposure may have resulted from progressive corneal edema, perhaps connected to interactions with fisheries for easier prey procurement, resulting in death. The combination of natural and anthropogenic influences on the life of this animal alludes to a larger story. Combined threats from anthropogenically-exacerbated influences, such as climate-related changes to rainfall or pulse storm events, and increased fishery pressures or freshwater diversion, have the potential to synergistically impact vulnerable bay, sound, and estuary bottlenose dolphin populations. These factors may further cause animals to stray out-of-habitat or endure changes to habitat that make it less suitable. This study highlights the likelihood of these multiple or cumulative stressors to negatively affect nearshore dolphins.

DATA AVAILABILITY STATEMENT

The datasets generated for this study are available on request to the corresponding author.

ETHICS STATEMENT

This animal study was reviewed and approved by National Oceanographic and Atmospheric Association, National Marine Fisheries Service under a Stranding Agreement issued to the Dauphin Island Sea Lab.

AUTHOR CONTRIBUTIONS

All contributing authors have approved this work for publication. Individual contributions were distributed as follows: AD, NW, DM, DR, RE, RW, MH, and RC: study concept and design, sample and data acquisition, and data interpretation. AD, DR, RW, RE, and RC: manuscript preparation. NW, DM, and MH: manuscript review.

FUNDING

This work was funded in part by the National Fish & Wildlife Foundation (#45720), the Alabama Department of Conservation and Natural Resources, and the University of South Alabama graduate student fellowship program (to MH). The satellite-linked tag and tracking were supported by NOAA's John H. Prescott Program Grant No. NA14NMF4390187.

ACKNOWLEDGMENTS

ALMMSN conducts marine mammal rescue, monitoring, and stranding response, as authorized by NOAA/NMFS, by way of a Letter of Authorization. Additional animal response assistance were provided by Emerald Coast Wildlife Refuge, Institute for Marine Mammal Studies, NOAA/NMFS, Dr. Scott Gearhart, J. P. Peterson, and the SeaWorld Orlando Rescue Team, University of Central Florida and University of South Alabama. Satellite-linked tracking, sighting reports, monitoring, and assistance were provided by the Chicago Zoological Society's Sarasota Dolphin Research Program, Alabama Department of Conservation and Natural Resources, Wade Stevens and the City of Orange Beach, and Orange Beach area dolphin tour boat operators. Thanks to NOAA NMFS Gear Research Team Southeast Fisheries Science Center, Pascagoula Lab, D. Foster, K. Falana, W. Hoggard, M. Hendon, for analysis of the net and hook collected from the carcass. We thank Elizabeth Hieb, Kayla DaCosta, and Katie Witlicki for their hard work associated with this case.

REFERENCES

1. Mase-Guthrie B, Townsend F, Mcfee W, Manire C, Ewing RY. *Cases of Prolonged Freshwater Exposure in Dolphins Along the Southeast United States. Poster Presentation at Society of Marine Mammalogy* (San Diego, CA), (2005).
2. Carmichael RH, Graham WM, Aven A, Worthy G, Howden, S. Were multiple stressors a 'perfect storm' for northern Gulf of Mexico bottlenose dolphins (*Tursiops truncatus*) in 2011? *PLoS ONE.* (2012) 7:e41155. doi: 10.1371/journal.pone.0041155
3. Mullin KD, Barry K, Sinclair C, Litz J, Maze-Foley K, Fougeres E, et al. *Common Bottlenose Dolphins (Tursiops truncatus) in Lake Pontchartrain, Louisiana: 2007 to Mid-2014.* NOAA Technical Memorandum NMFS-SEFSC-673. (2015) p. 43.
4. Ewing RY, Mase-Guthrie B, Mcfee W, Townsend F, Manire CA, Walsh M, et al. Evaluation of serum for pathophysiological effects of prolonged low salinity water exposure in displaced bottlenose dolphins. *Front Vet Sci.* (2017) 4:80. doi: 10.3389/fvets.2017.00080
5. Kjeld M. Concentrations of electrolytes, hormones, and other constituents in fresh postmortem blood and urine of fin whales (*Balaenoptera physalus*). *Can J Zool.* (2001) 79:438–46. doi: 10.1139/z00-222
6. Birukawa N, Ando H, Goto M, Kanda N, Pastene LA, Nakatsuji H, et al. Plasma and urine levels of electrolytes, urea and steroid hormones involved in osmoregulation of cetaceans. *Zoolog Sci.* (2005) 22:1245–57. doi: 10.2108/zsj.22.1245
7. Ridgway S, Venn-Watson, S. Effects of fresh and seawater ingestion on osmoregulation in Atlantic bottlenose dolphins (*Tursiops truncatus*). *J Comp Physiol B.* (2010) 180:563–76. doi: 10.1007/s00360-009-0439-0
8. Colbert A, Scot G, Fulton M, Wirth E, Daugomah J, Key P, et al. *Investigation of Unusual Mortalities of Bottlenose Dolphins along the Mid-Texa Coastal Bay Ecosystem During 1992.* Charleston, SC: NOAA Technical Memorandum NMFS 147 (1999). p. 23.
9. Rosel P, Watts H. Hurricane impacts on bottlenose dolphins in the Northern Gulf of Mexico. *Gulf Mexico Sci.* (2008) 1:88–94. doi: 10.18785/goms.2501.07
10. Hornsby F, Mcdonald T, Balmer B, Speakman T, Mullin K, Rosel P, et al. Using salinity to identify common bottlenose dolphin habitat in Barataria Bay, Louisiana, USA. *Endangered Spec Res.* (2017) 33:181–92. doi: 10.3354/esr00807
11. Gilchrist, F. Water intoxication in weaned beef calves. *Can Vet J.* (1996) 37:490–1.
12. Njoroge EM, Maribei JM, Mbugua PN, Njiru SM. Water intoxication in cattle. *J S Afr Vet Assoc.* (1999) 70:177–9. doi: 10.4102/jsava.v70i4.792

13. Umansky L, Sella A. Psychogenic polydipsia leading to water intoxication. *Harefuah.* (2000) 138:9–12, 87.
14. O'Brien KK, Montain SJ, Corr WP, Sawka MN, Knapik JJ, Craig, S. C. Hyponatremia associated with overhydration in U.S. Army trainees. *Mil Med.* (2001) 166:405–10. doi: 10.1093/milmed/166.5.405
15. Farrell DJ, Bower, L. Fatal water intoxication. *J Clin Pathol.* (2003) 56:803–4. doi: 10.1136/jcp.56.10.803-a
16. Kawahara N, Ofuji S, Abe S, Tanaka A, Uematsu M, Ogata, Y. Water intoxication in adult cattle. *Jpn J Vet Res.* (2016) 64:159–64.
17. Botta S, Albuquerque C, Hohn A, Da Silva V, Santos MCO, Meirelles C, et al. Ba/Ca ratios in teeth reveal habitat use patterns of dolphins. *Mar Ecol Prog Ser.* (2015) 521:249–63. doi: 10.3354/meps11158
18. Buddhachat K, Klinhom S, Siengdee P, Brown JL, Nomsiri R, Kaewmong P, et al. Elemental analysis of bone, teeth, horn and antler in different animal species using non-invasive handheld X-ray fluorescence. *PLoS ONE.* (2016) 11:e0155458. doi: 10.1371/journal.pone.0155458
19. Zilg B, Alkass K, Berg S, Druid, H. Interpretation of postmortem vitreous concentrations of sodium and chloride. *Forensic Sci Int.* (2016) 263:107–13. doi: 10.1016/j.forsciint.2016.04.006
20. Rosel P, Mullin K, Garrison L, Schwacke L, Adams J, Balmer B, et al. *Photo-Identification Capture-Mark-Recapture Techniques for Estimating Abundance of Bay, Sound Estuary Populations of Bottlenose Dolphins along the U.S. East Coast and Gulf of Mexico: A Workshop Report.* NOAA Technical Memorandum NMFS-SEFSC-621 (2011).
21. Asper, E. Techniques of live capture of smaller Cetacea. *J Fish Res Board Can.* (1975) 32:1191–6. doi: 10.1139/f75-138
22. Wells RS, Rhinehart HL, Hansen LJ, Sweeney JC, Townsend FI, Stone R, et al. Bottlenose dolphins as marine ecosystem sentinels: developing a health monitoring system. *EcoHealth.* (2004) 1:246–54. doi: 10.1007/s10393-004-0094-6
23. Loughlin T, Cunningham L, Gales N, Wells R, Boyd I. Marking capturing. In: Boyd I, Don Bowen W, Iverson S, editors. *Marine Mammal Ecology Conservation: A Handbook of Techniques.* Oxford: Oxford University Press (2010). p. 16–40.
24. Hall AJ, Wells RS, Sweeney JC, Townsend FI, Balmer BC, Hohn AA, et al. Annual, seasonal and individual variation in hematology and clinical blood chemistry profiles in bottlenose dolphins (*Tursiops truncatus*) from Sarasota Bay, Florida. *Comp Biochem Physiol A Mol Integr Physiol.* (2007) 148:266–77. doi: 10.1016/j.cbpa.2007.04.017
25. Jashnani KD, Kale SA, Rupani AB. Vitreous humor: biochemical constituents in estimation of postmortem interval. *J Forensic Sci.* (2010) 55:1523–7. doi: 10.1111/j.1556-4029.2010.01501.x
26. Wells RS, Schwacke LH, Rowles TK, Balmer BC, Zolman E, Speakman T, et al. Ranging patterns of common bottlenose dolphins (*Tursiops truncatus*) in Barataria Bay, Louisiana, following the deepwater horizon oil spill. *Endangered Spec Res.* (2017) 33:159–80. doi: 10.3354/esr00732
27. Swift PG, Worthy E, Emery, J. L. Biochemical state of the vitreous humour of infants at necropsy. *Arch Dis Child.* (1974) 49:680–5. doi: 10.1136/adc.49.9.680
28. Vanhaebost J, Palmiere C, Scarpelli MP, Abdallah FB, Capron A, Schmit, G. Postmortem diagnosis of hyponatremia: case report and literature review. *Int J Legal Med.* (2018) 132:173–9. doi: 10.1007/s00414-017-1601-y
29. Tsujinaka M, Bunai, Y. Postmortem ophthalmologic examination by endoscopy. *Am J For Med Pathol.* (2006) 27:287–91. doi: 10.1097/01.paf.0000233531.91189.4b
30. Hui C. *Reliability of Using Dentin Layers for Age Determination in "Tursiops truncatus".* Marine Mammal Commissioners Report (No. MMC-77/09). San Diego, CA (1978). p. 25.
31. Hohn AA. Age determination and age related factors in the teeth of Western North Atlantic bottlenose dolphins. *Sci Rep Whales Res Inst.* (1980) 32:39–66.
32. Hohn AA, Scott MD, Wells RS, Sweeney JC, Irvine AB. Growth layers in teeth from known-age, free-ranging bottlenose dolphins. *Mar Mammal Sci.* (1989) 5:315–42. doi: 10.1111/j.1748-7692.1989.tb00346.x
33. Moore M, Van Der Hoop J, Barco S, Costidis A, Gulland F, Jepson P, et al. Criteria and case definitions for serious injury and death of pinnipeds and cetaceans caused by anthropogenic trauma. *Diseases of Aquat Org.* (2013) 103:229–64. doi: 10.3354/dao02566
34. Li W, Chang Y, Cheng Z, Ling J, Han L, Li X, et al. Vitreous humor: a review of biochemical constituents in postmortem interval estimation. *J For Sci Med.* (2018) 4:85–90. doi: 10.4103/jfsm.jfsm_13_18
35. Coe J. Vitreous potassium as a measure of the postmortem interval: an historical review and critical evaluation. *Forensic Sci Int.* (1989) 42:201–13. doi: 10.1016/0379-0738(89)90087-X
36. Zilg B, Bernard S, Alkass K, Berg S, Druid H. A new model for the estimation of time of death from vitreous potassium levels corrected for age and temperature. *Forensic Sci. Int.* (2018). doi: 10.1016/j.forsciint.2015.07.020
37. Wells RS, Scott MD. Bottlenose dolphin Tursiops truncate (Montagu, 1821). In: Ridgeway SH, Harrison R, editors. *Handbook of Marine Mammals. The Second Book of Dolphins and Porpoises,* Vol. 6. San Diego, CA: Academic Press (1999). p. 137–82.
38. He S, Xu, Y. Spatiotemporal distributions of Sr and Ba along an estuarine river with a large salinity gradient to the Gulf of Mexico. *Water.* (2016) 8:323. doi: 10.3390/w8080323
39. Elsdon T, Gillanders B. Alternative life-history patterns of estuarine fish: barium in otoliths elucidates freshwater residency. *Can J Fish Aquat Sci.* (2005) 65:1143–52. doi: 10.1139/f05-029
40. Patterson III W, Cowan Jr J, Wilson C, Chen, Z. Temporal and spatial variability in juvenile red snapper otolith elemental signatures in the northern Gulf of Mexico. *Trans Am Fish Soc.* (2008) 137:521–32. doi: 10.1577/T06-264.1
41. Lewis J, Patterson W, Carlson J, Mclachlin K. Do vertebral chemical signatures distinguish juvenile blacktip shark (*Carcharhinus limbatus*) nursery regions in the northern Gulf of Mexico? *Mar Freshw Res.* (2016) 67:1014–22. doi: 10.1071/MF15088
42. Cheung KC, Leung HM, Wong, M. H. Metal concentrations of common freshwater and marine fish from the Pearl River Delta, south China. *Arch Environ Contam Toxicol.* (2008) 54:705–15. doi: 10.1007/s00244-007-9064-7
43. Balmer B, Zolman E, Bolton J, Fauquier D, Fougeres E, George R, et al. Ranging Patterns and Exposure to Cumulative Stressors of a *Tursiops truncatus* (Common Bottlenose Dolphin) in Georgia. *South Natur.* (2019) 18:N1–9. doi: 10.1656/058.018.0112
44. Hanna PE, Bellamy JE, Donald, A. Postmortem eyefluid analysis in dogs, cats and cattle as an estimate of antemortem serum chemistry profiles. *Can J Vet Res.* (1990) 54:487–94.
45. Lange N, Swearer S, Sturner WQ. Human postmortem interval estimation from vitreous potassium - an analysis of original data from 6 different studies. *Forensic Sci Int.* (1994) 66:159–74. doi: 10.1016/0379-0738(94)90341-7

Disclaimer: The statements, findings, conclusions, and opinions are those of the authors and nothing contained herein constitutes an endorsement in any respect by NFWF.

The scientific results and conclusions, as well as any views or opinions expressed herein, are those of the author(s) and do not necessarily reflect those of NOAA or the Department of Commerce.

Conflict of Interest: The authors declare that the research was conducted in the absence of any commercial or financial relationships that could be construed as a potential conflict of interest.

Copyright © 2020 Deming, Wingers, Moore, Rotstein, Wells, Ewing, Hodanbosi and Carmichael. This is an open-access article distributed under the terms of the Creative Commons Attribution License (CC BY). The use, distribution or reproduction in other forums is permitted, provided the original author(s) and the copyright owner(s) are credited and that the original publication in this journal is cited, in accordance with accepted academic practice. No use, distribution or reproduction is permitted which does not comply with these terms.

frontiers in Veterinary Science

CASE REPORT
published: 04 August 2020
doi: 10.3389/fvets.2020.00467

Case Report: Invasive Pentastomes, *Raillietiella orientalis* (Sambon, 1922), in a Free-Ranging Banded Water Snake (*Nerodia fasciata*) in North Central Florida, USA

Heather D. S. Walden, Marley E. Iredale, April Childress, James F. X. Wellehan Jr. and Robert J. Ossiboff*

Department of Comparative, Diagnostic and Population Medicine, University of Florida College of Veterinary Medicine, Gainesville, FL, United States

OPEN ACCESS

Edited by:
Maria De Jesus Forzan, Long Island University, United States

Reviewed by:
Steven Victor Kubiski, University of California, Davis, United States
Gabriella Gaglio, University of Messina, Italy
Jeff Lorch, National Wildlife Health Center, United States Geological Survey, United States

***Correspondence:**
Heather D. S. Walden
hdstockdale@ufl.edu

Specialty section:
This article was submitted to Veterinary Experimental and Diagnostic Pathology, a section of the journal Frontiers in Veterinary Science

Received: *13 May 2020*
Accepted: *24 June 2020*
Published: *04 August 2020*

Citation:
Walden HDS, Iredale ME, Childress A, Wellehan JFX Jr and Ossiboff RJ (2020) Case Report: Invasive Pentastomes, Raillietiella orientalis (Sambon, 1922), in a Free-Ranging Banded Water Snake (Nerodia fasciata) in North Central Florida, USA. Front. Vet. Sci. 7:467. doi: 10.3389/fvets.2020.00467

Raillietiella orientalis is an obligate, crustacean parasite that resides in the respiratory tract of definitive snake hosts. Common throughout southeastern Asia and Australia, *R. orientalis* is believed to have been introduced into southern Florida, United States along with Burmese pythons (*Python bivittatus*) in the 1990s. While the invasive range of Burmese pythons is restricted to southern Florida, *R. orientalis* has advanced north in the state in native snake species. *R. orientalis* were recovered from the lungs, trachea, oral cavity, and esophagus of an emaciated adult female free-ranging banded water snake (*Nerodia fasciata*) in north central (Alachua County), Florida, USA. Concurrent findings included the recovery of *Ochetosoma* sp. trematodes from the oral cavity, and multifocal dermal lesions consistent with snake fungal disease (*Ophidiomyces ophiodiicola*). This is the first report of *R. orientalis* in north central Florida, well outside the invasive range of the Burmese python, documenting the substantial northward expansion of the known geographical range of this invasive pentastome in Florida.

Keywords: Burmese python, colubrid, parasite, Pentastomida, pentastomiasis, *Raillietiella orientalis*, water snake

INTRODUCTION

Pentastomes are obligate, internal parasites found mainly in the respiratory tracts of their definitive hosts, which include mammals, reptiles, amphibians and birds. Pentastomes have indirect life cycles, and use mammals, reptiles, amphibians, fish, or coprophagous insects as intermediate hosts (1). Large eggs are found in the feces of the definitive host; when ova are mature, they contain a larva which will develop in the tissues of the intermediate host. Nymphal stages are ingested by the definitive host, where they develop to an adult. The anterior ends consist of four chitinized hooks and a buccal cadre that allow the parasite to attach to the host and feed on blood (1). Pentastome species inhabit the lungs of reptiles more than any other host clade, and the openness of the reptile lung may make it an easy niche to populate (2). These parasites can become very large (up to 10 cm long) in the host lung. Morbidity and mortality due to pentastome infections in reptiles are usually associated with pneumonia. Migration of larval and nymphal stages can cause disease in definitive, intermediate, and aberrant hosts (1).

An adult, female, free-ranging banded water snake (*Nerodia fasciata*) was found emaciated, extremely weak, and with no righting reflex after being eaten and regurgitated by another snake [a black racer (*Coluber constrictor*)] in Alachua, County, Florida in May of 2019. The snake was treated with fluids, antibiotics, and supportive care. During hospitalization, fecal flotation revealed pentastome ova; the snake was found dead on day 4 before the planned endoscopic exam and removal of adult pentastomes could be performed. A complete postmortem examination was performed. On gross necropsy, numerous adult metazoan parasites were recovered from the oral cavity, esophagus, and respiratory tract (**Figure 1**). In the oral cavity and choana, there were six adult pentastomes and approximately seven dark black-red trematodes (renifers). In the esophagus there were three adult pentastomes and approximately seven trematodes (**Figure 1**). In the trachea there were three adult pentastomes (**Figure 1**, inset), and in the lungs there were approximately five adult pentastomes. There were also five adult pentastomes in the connective tissue ventral to the spine and dorsal to the liver. There were multifocal dark brown ovoid discolorations of the ventral scales, measuring 0.3–0.5 cm in diameter, that were associated with roughening of the scale margins distributed along the length of the ventrum.

Histologically, within the lumen of the glottis/trachea there were multiple longitudinal and transverse sections of pentastome parasites (**Figure 2A**). Male pentastomes measured up to 1,500 microns in diameter, and were characterized by the presence of a buccal cadre and hooks (**Figure 2B**), acidophilic glands (**Figure 2B**), a digestive tract lined by ciliated uninucleate enterocytes and containing brown-orange pigment (digested blood; **Figure 2B**), and an eosinophilic cuticle with refractile, round spiracles. Female pentastomes measured up to 2,250 microns in diameter, and sections were dominated by a reproductive tract filled with dozens of 50–100 micron diameter ovoid ova with a translucent, slightly refractile shell (**Figure 2C**). The trachea itself had mild, multifocal tracheal epithelial attenuation and heterophilic to mucoid tracheitis with intraluminal pentastome ova. Few granulomas with central cores of eosinophilic debris and slightly refractile, translucent, yellow material were also present adjacent to the trachea and deep to the oral mucosa. Other concurrent systemic findings included bacterial bronchopneumonia, chronic necrotizing and granulomatous hepatitis, and generalized cutaneous and facial dermatitis with intralesional fungal hyphae and arthroconidia. PCR of formalin-fixed paraffin embedded ribbons of affected skin were confirmed to contain *Ophidiomyces ophiodiicola* by quantitative PCR by the Zoological Medicine Diagnostic Laboratory, College of Veterinary Medicine, University of Florida, confirming a diagnosis of ophidiomycosis (snake fungal disease).

Adult male and female pentastomes (five female, one male) were preserved in 70% ethanol and examined morphologically

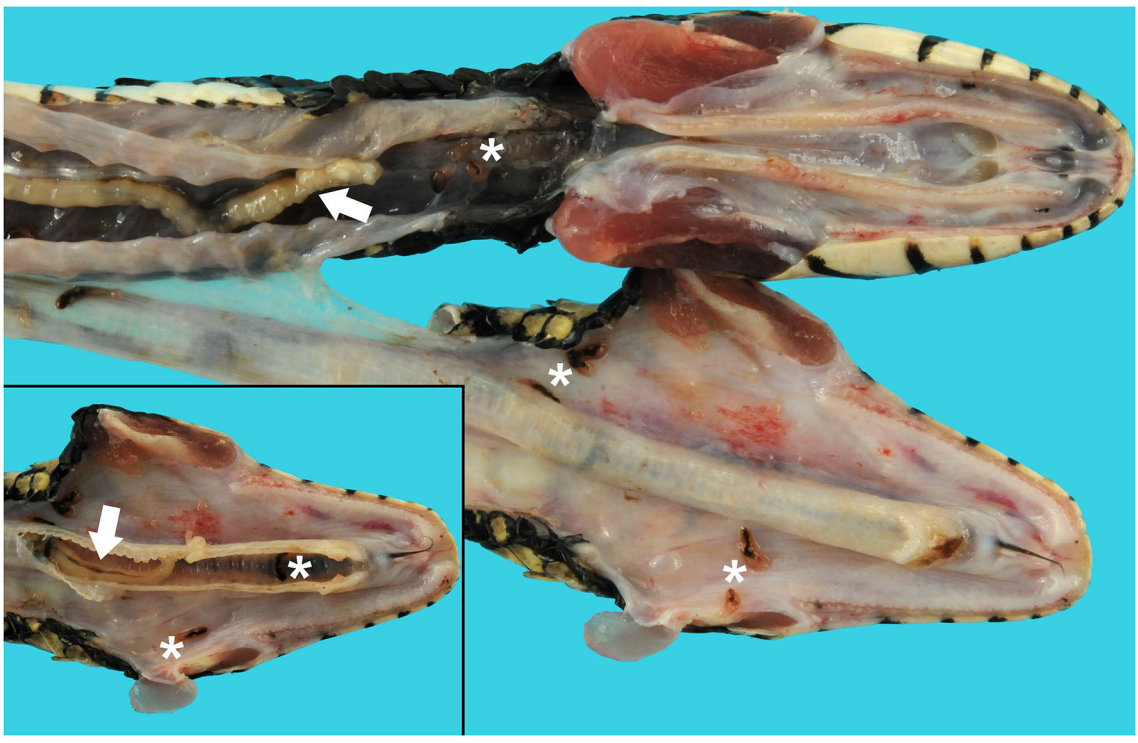

FIGURE 1 | Tracheal and esophageal pentastomes and trematodes in a banded water snake (*Nerodia fasciata*). The jaw is unilaterally disarticulated and positioned laterally to expose the oral cavity, glottis, and esophagus. *Raillietiella orientalis* pentastomes (white arrows) and *Ochetosoma* sp. trematodes (white asterisks) are present in the oral cavity, esophagus, and lumen of the trachea (inset).

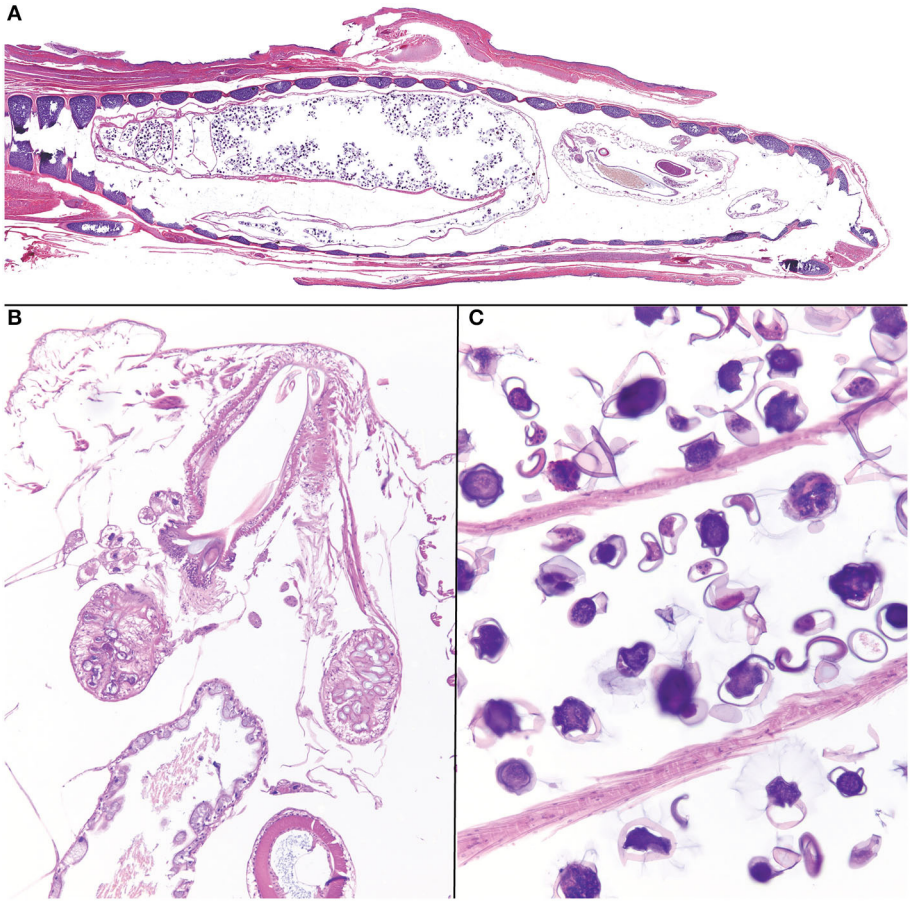

FIGURE 2 | Photomicrographs of *Raillietiella orientalis* pentastomes within the trachea of a banded water snake (*Nerodia fasciata*). **(A)** On subgross examination, cross and longitudinal male and female parasites fill the lumen of the trachea. **(B)** The buccal cadre of a male parasite with hooks and acidophilic glands. **(C)** Ova within the lumen of a female *Raillietiella orientalis*.

(**Figure 3A**). Pentastomes were cleared using lactophenol, and species were identified based on total body length as well as measurements and characteristics of the buccal cadre and hook (**Figure 3B**), cephalothorax, and male spicules (3). Female pentastomes ranged from 29 to 51 mm in length, the male was 10 mm long. Posterior AB hook measurement for the largest female was 308 microns, and posterior BC hook measurement was 487 microns. Male spicules consisted of a flared base, with a deeply grooved reticulated pattern (**Figure 3C**). Females were gravid, and eggs recovered from the uterus were ∼96 × 100 µm (**Figure 3D**). Morphologic characteristics were consistent with *Raillietiella orientalis*. Oral trematodes (renifers) were also preserved in 70% ethanol and examined morphologically. Morphologic characteristics were consistent with an *Ochetosoma* species (data not shown).

To confirm the morphologic identification of the parasite, nucleic acids were extracted from an ethanol fixed female pentastome using a DNEasy kit (Qiagen, Valencia, CA), and an approximately 425 bp portion of the small subunit ribosomal RNA gene (18S SSU) was amplified as previously described (4). The PCR product was resolved in a 1.5% agarose gel. Bands were excised and purified using a QIAquick gel extraction kit (Qiagen). The product was sequenced directly in both directions by a commercial sequencing facility (Genewiz, South Plainfield, New Jersey, USA). Primer sequences were trimmed and compared to known sequences using the NCBI Basic Local Alignment Search Tool (5). The amplified 18S sequence was 100% identical to numerous *R. orientalis* isolates, including those previously identified in Florida and reported by Miller et al. (6) and Farrell et al. (7).

DISCUSSION

This is the first report of *R. orientalis* in north central Florida. *Raillietiella orientalis* has been reported in several snake species in Asia and Australia, including those from the families Colubridae, Elaphidae, Viperidae, and Boidae (3, 8, 9). *Raillietiella orientalis* was first identified in the United States in 2017 in free-ranging, invasive Burmese pythons in the Florida Everglades as well as nine native

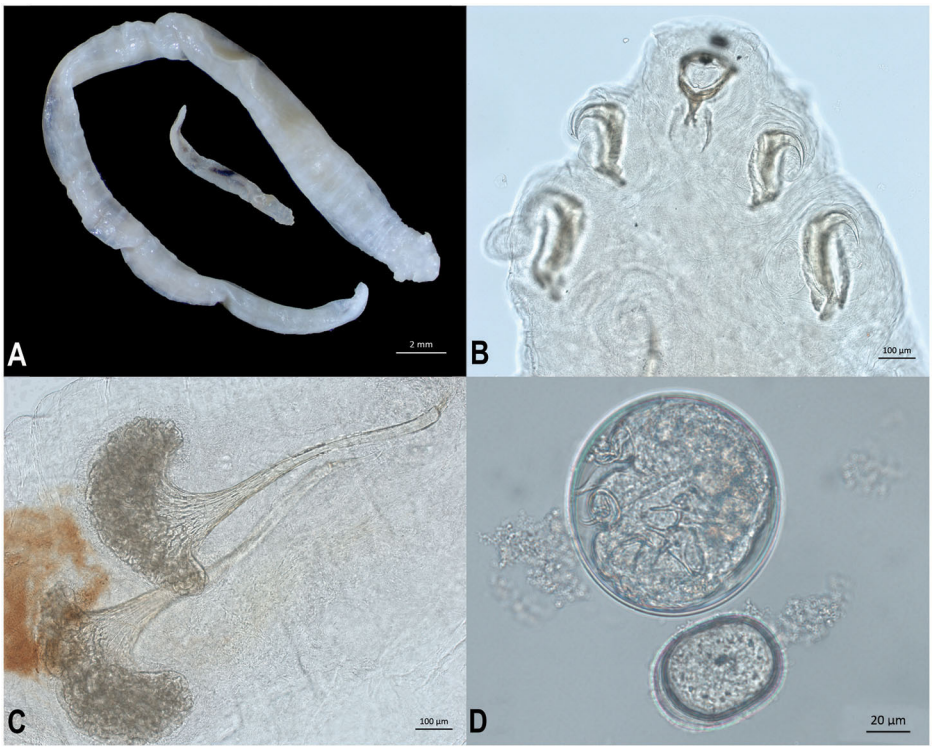

FIGURE 3 | Life stages and morphological characteristics of *Raillietiella orientalis* pentastomes recovered from the lungs of a banded water snake (*Nerodia fasciata*). **(A)** Ethanol-fixed male (smaller) and female (larger) *R. orientalis* adults. **(B)** Male *R. orientalis* anterior hooks and buccal cadre. **(C)** Spicules from male *R. orientalis*. **(D)** Egg recovered from uterus of gravid female *R. orientalis*.

snake species in six southern Florida counties (6) (**Figure 4**, purple counties). In that study, no parasites were identified during surveillance in northern Florida (including Alachua County) and southern Georgia. In 2018, *R. orientalis* were documented in three pygmy rattlesnakes (*Sistrurus miliarus*) more than 160 km north of the known range of Burmese pythons, in central Florida (7) (**Figure 4**, blue county). The spring 2019 identification of *R. orientalis* in a water snake in Alachua County demonstrates an additional range extension of nearly 150 km northward, and a total range extension of nearly 340 km beyond the northernmost range of the Burmese python.

This dramatic extension north suggests the potential of native or invasive species other than pythons serving as both successful intermediate and definitive hosts for the parasite. While the exact intermediate hosts of *R. orientalis* in Florida are unknown, most pentastome species use amphibians or reptiles as intermediate hosts, and definitive hosts for the many *Raillietiella* species include snakes and lizards (1, 8). The natural range of *Nerodia fasciata* is extensive, inhabiting coastal plains from southwest Alabama to North Carolina, along the Gulf States into Texas, and up the Mississippi River to Indiana (10). Along with sympatric species identified by Miller et al. (6) to be susceptible to infection, such as cottonmouths (*Agkistrodon piscivorus*), salt marsh snakes (*Nerodia clarkii*), garter snakes (*Thamnophis sirtalis*), and corn snakes (*Pantherophis guttatus*), there is a substantial risk that *Raillitiella orientalis* may spread throughout the southeastern United States, and potentially further.

The only named *Raillietiella* species for which sequence is available in public databases are *R. orientalis* and *R. indica*. Especially in light of the size variation seen in *R. orientalis*, the lack of reference sequence data for *Raillietiella* is concerning. Moreover, morphological features used for pentastomid identification may be altered by development in a different host (11). In the gecko species *Hemidactylus frenatus*, the species *Raillietiella indica* (syn *R. frenatus*, *R. hebitihamata*) develops hooks that are significantly different from those that *R. indica* develops in the marine toad (*Rhinella marina*), to the extent that they would morphologically identified as different species (11). Similarly, *R. indica* hook measurements vary significantly depending on whether the host is a Mediterranean gecko or a green anole (*Anolis carolinensis*) (12). Feral populations of another member of the gecko genus *Hemidactylus*, *H. turcicus* (Mediterranean gecko) populations are well established in Alachua County (13). *Raillietiella teagueselfi* has been reported from feral Mediterranean geckos in Texas, though this *Raillietiella* species lacks both reference sequence and molecular confirmation of a morphological diagnosis (14). Given the observed morphological plasticity of *Raillietiella* in different hosts, both morphological and genetic identification of

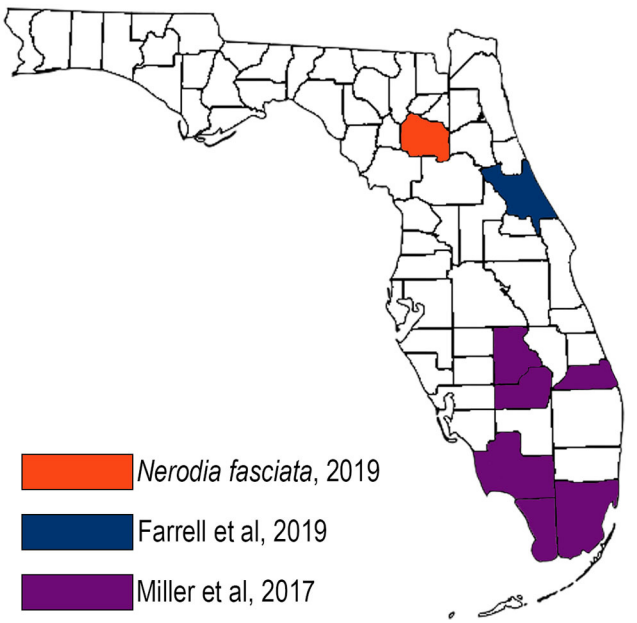

FIGURE 4 | Map of *Raillietiella orientalis* documentations in Florida, United States showing the northward extension of the parasite over time.

Raillietiella species in different host species are warranted for accurate identification.

The spread of this parasite into definitive hosts in northern Florida suggests infection in competent squamate hosts in bordering southeastern states may be imminent. *Raillietiella orientalis* is not the only invasive *Raillietiella* species spreading through the continental US from invasive to native reptile species. *Raillietiella indica* was reported in the Mediterranean gecko, *Hemidactylus turcicus* in Texas in the early 1980s (15). Sakla et al. (12) later reported *R. indica* was not only infecting *H. turcicus*, but that it had also made its way into the native *Anolis carolinensis* in Louisiana, and noted an unpublished report of *R. indica* in *H. frenatus* in New Orleans, Louisiana as early as 2008. The authors speculated the introduction of *R. indica* into Louisiana could be from the Mediterranean gecko, known to New Orleans since 1949, or introduced from the Cuban brown anole, *Anolis sagrei*, another known host of *R. indica* (12). The exact origin of free-ranging Florida Burmese pythons, the natural host(s) for *R. orientalis,* in southern Florida is unknown; however, a prevailing theory is due to the release of animals destined for the pet trade in the 1990s. Although Burmese python sightings date back to approximately 1980, there has been a marked growth in python populations in the Everglades in the past 20 years. This population growth has been accompanied by severe declines in native mammals (16). The introduction of *R. orientalis* into Florida and ultimately, native Florida snakes, most likely occurred with the release of the Burmese pythons in southern Florida. No other reported *Raillietiella* hosts are native to North America or have been previously been reported in Florida (8). This case report highlights that parasites accompanying invasive species can also have a negative impact on native wildlife that can extend far beyond the range of the invasive host.

While *R. orientalis* is of limited clinical significance to the Burmese python, these invasive pentastomes are likely contributing to morbidity and mortality in native snake species (6, 7). Morbidity and mortality associated with these parasitic infections may be due to additional co-infections. Conversely, as North American snakes species have not coevolved with *R. orientalis*, the pathogenic effects may be more severe in a naïve host (17). Interestingly, this water snake had concurrent ophidiomycosis (snake fungal disease). Co-morbidities of ophidiomycosis and raillietielliasis are a significant cause of morbidity and mortality in pygmy rattlesnakes in central Florida (7). The role these two agents play in more widespread wild snake health in general warrants investigation. Moreover, as little is known about the life cycle of R. orientalis, including both the number of and species of viable intermediate hosts as well as the prepatent period, additional studies on the life cycle of *R. orientalis* are also needed.

DATA AVAILABILITY STATEMENT

All datasets generated for this study are included in the article/supplementary material.

ETHICS STATEMENT

Ethical review and approval was not required for the animal study because care, until natural death, of the snake was provided in accordance to current standards of care. The snake was not a research snake and was found in the wild and cared for by UFCVM veterinarians.

AUTHOR CONTRIBUTIONS

HW contributed to gross morphological parasite identification and photographs. RO and MI contributed to postmortem examination and interpretation and photographs. AC, JW, and RO contributed to molecular parasite characterization. All authors contributed to the article and approved the submitted version.

FUNDING

All expenses related to the parasite diagnosis of this snake were funded by HW, JW, and RO laboratories.

ACKNOWLEDGMENTS

The authors thank Nina Thompson, Deborah Usina, and the staff of the Histology Laboratory at University of Florida's College of Veterinary Medicine.

REFERENCES

1. Paré JA. An overview of pentastomiasis in reptiles and other vertebrates. *J Exot Pet Med*. (2008) 17:285–94. doi: 10.1053/j.jepm.2008.07.005
2. Riley J, Henderson RJ. Pentastomids and the tetrapod lung. *Parasitol*. (1999) 119:S89–105. doi: 10.1017/S0031182000084651
3. Ali JH, Riley J, Self JT. A review of the taxonomy and systematics of the pentastomid genus *Raillietiella* Sambon, 1910 with a description of a new species. *Syst Parasitol*. (1985) 7:111–23. doi: 10.1007/BF00009814
4. Brookins MD, Wellehan JFX, Roberts JF, Allison K, Curran SS, Childress AL, et al. Massive visceral pentastomiasis caused by *Porocephalus crotali* in a dog. *Vet. Pathol.* (2009) 46:460–3. doi: 10.1354/vp.07-VP-0246-R-BC
5. Johnson M, Zaretskaya I, Raytselis Y, Merezhuk Y, McGinnis S, Madden TL. NCBIBLAST: a better web interface. *Nucleic Acids Res*. (2008) 36:W5–9. doi: 10.1093/nar/gkn201
6. Miller MA, Kinsella JM, Snow RW, Hayes MM, Falk BG, Reed RN, et al. Parasite spillover: indirect effects of invasive Burmese pythons. *Ecol Evol*. (2018) 8:830–40. doi: 10.1002/ece3.3557
7. Farrell TM, Agugliaro J, Walden HDS, Wellehan JFX, Childress AL, Lind CM. Spillover of pentastome parasites from invasive Burmese pythons (*Python bivittatus*) extends beyond the geographic range of pythons in Florida. *Herp Rev*. (2019) 50:73–6.
8. Christoffersen ML, De Assis JE. A systematic monograph of the recent Pentastomida, with a compilation of their hosts. *Zool Med Leiden*. (2013) 87:1−206.
9. Kelehear C, Spratt DM, O'Meally D, Shine R. Pentastomids of wild snakes in the Australian tropics. *Int J Parasitol Parasites Wildl*. (2014) 3:20–31. doi: 10.1016/j.ijppaw.2013.12.003
10. Gibbons JW, Dorcas ME. *North American Watersnakes: A Natural History*. Norman: University of Oklahoma Press (2004).
11. Kelehear C, Spratt DM, Dubey S, Brown GP, Shine R. Using combined morphological, allometric and molecular approaches to identify species of the genus *Raillietiella* (Pentastomida). *PLoS ONE*. (2011) 6:e24936. doi: 10.1371/journal.pone.0024936
12. Sakla AJ, Detwiler JT, Caballero IC, Kelehear C, Criscione CD. Recognizing the causes of parasite morphological variation to resolve the status of a cryptogenic pentastome. *J Parasitol*. (2019) 105:432–41. doi: 10.1645/18-205
13. Krysko KL, Daniels KJ. A key to the Geckos (Sauria: Gekkonidae) of Florida. *Caribb J Sci*. (2005) 41:28–36.
14. Riley J, McAllister C, Freed P. *Raillietiella teagueselfi* n. sp (Pentastomida: Cephalobaenida) from the Mediterranean Gecko, *Hemidactylus turcicus* (Sauria: Gekkonidae). *Texas J Parasitol*. (1988) 74:481–6. doi: 10.2307/3282059
15. Pence DB, Selcer KW. Effects of pentastome infection on reproduction in a southern Texas population of the Mediterranean Gecko, *Hemidactylus turcicus*. *Copeia*. (1988) 3:565–72. doi: 10.2307/1445374
16. Dorcas ME, Willson JD, Reed RN, Snow RW, Rochford MR, Miller MA, et al. Severe mammal declines coincide with proliferation of invasive Burmese pythons in Everglades National Park. *Proc Natl Acad Sci USA*. (2012) 109:2418–22. doi: 10.1073/pnas.1115226109
17. Lymbery AJ, Morine M, Kanani HG, Beatty SJ, Morgan DL. Co-invaders: the effects of alien parasites on native hosts. *Int J Parasitol Parasites Wildl*. (2014) 3:171–7. doi: 10.1016/j.ijppaw.2014.04.002

Conflict of Interest: The authors declare that the research was conducted in the absence of any commercial or financial relationships that could be construed as a potential conflict of interest.

Copyright © 2020 Walden, Iredale, Childress, Wellehan and Ossiboff. This is an open-access article distributed under the terms of the Creative Commons Attribution License (CC BY). The use, distribution or reproduction in other forums is permitted, provided the original author(s) and the copyright owner(s) are credited and that the original publication in this journal is cited, in accordance with accepted academic practice. No use, distribution or reproduction is permitted which does not comply with these terms.

frontiers in Veterinary Science

ORIGINAL RESEARCH
published: 25 September 2020
doi: 10.3389/fvets.2020.00635

The Iconic Atlantic Goliath Grouper (*Epinephelus itajara*): A Comprehensive Assessment of Health Indices in the Southeastern United States Population

Christopher R. Malinowski[1,2,3]*, *Justin R. Perrault*[4,5], *Felicia C. Coleman*[1], *Christopher C. Koenig*[1], *Justin M. Stilwell*[6], *Carolyn Cray*[7] and *Nicole I. Stacy*[7,8]

[1] Florida State University Coastal and Marine Laboratory, St. Teresa, FL, United States, [2] Department of Biological Science, Florida State University, Tallahassee, FL, United States, [3] Department of Forestry and Natural Resources, Purdue University, West Lafayette, IN, United States, [4] Mote Marine Laboratory, Sarasota, FL, United States, [5] Loggerhead Marinelife Center, Juno Beach, FL, United States, [6] Department of Pathology, College of Veterinary Medicine, University of Georgia, Athens, GA, United States, [7] Division of Comparative Pathology, Department of Pathology & Laboratory Medicine, University of Miami Miller School of Medicine, Miami, FL, United States, [8] Department of Comparative, Diagnostic, and Population Medicine, College of Veterinary Medicine, University of Florida, Gainesville, FL, United States

OPEN ACCESS

Edited by:
Jennifer Johns,
Oregon State University, United States

Reviewed by:
Sean Thomas Spagnoli,
Oregon State University, United States
Rubina Sirri,
University of Bologna, Italy

***Correspondence:**
Christopher R. Malinowski
crmalino@purdue.edu

Specialty section:
This article was submitted to Veterinary Experimental and Diagnostic Pathology, a section of the journal Frontiers in Veterinary Science

Received: *23 June 2020*
Accepted: *04 August 2020*
Published: *25 September 2020*

Citation:
Malinowski CR, Perrault JR, Coleman FC, Koenig CC, Stilwell JM, Cray C and Stacy NI (2020) The Iconic Atlantic Goliath Grouper (Epinephelus itajara): A Comprehensive Assessment of Health Indices in the Southeastern United States Population. Front. Vet. Sci. 7:635. doi: 10.3389/fvets.2020.00635

The Atlantic Goliath Grouper (*Epinephelus itajara*) population has rebounded from near extinction to an international status as vulnerable due in part to regional species recovery efforts. The southeastern US population has been recovering with the main spawning locations off the coasts of Florida. Despite their economic importance to the catch-and-release fishery and the dive industry, and their ecological importance as ecosystem engineers resulting in positive impacts on reefs and species richness, baseline health assessment information is very limited in this species to date. The objectives of this study were to: (1) establish reference intervals for hematological and plasma biochemical analytes, and report immune function, oxidative stress, and vitellogenin in mature males and females; (2) evaluate total length, age, and sex in relation to blood analytes in juvenile and mature fish; (3) assess analytes across sampled months in mature male and female fish; and (4) describe the typical light microscopy findings in liver and gill biopsies, including quantitative assessment of pigmented macrophage aggregates. Health indices are reported as reference intervals when applicable, or otherwise descriptively. Blood analyte correlations with length and age, sex differences, and comparisons across months provided relevant physiological considerations, including differences in protein/energy metabolism, tissue growth, sexual maturation, active reproduction, and antigenic stimulation. Liver histology identified changes associated with life stage, active reproduction, or of subclinically to clinically insignificant infectious and/or inflammatory processes. Hepatocellular vacuolation and pigmented macrophage aggregates were prominent. Pigmented macrophage aggregates correlated with total length, presumably from continuous antigenic stimulation and/or metabolic changes as

fish grow. Gill histological findings were subtle. The data presented herein provide an essential baseline assessment of a suite of health variables in an iconic marine teleost species, serves as a springboard for future studies relevant to conservation physiology, and allows for population-level applications for conservation management and policy.

Keywords: hematology, histology, marine teleost, native immune functions, oxidative stress, plasma biochemistry, conservation ecology

INTRODUCTION

Conservation physiology is a newly emerging discipline that examines the health status and physiological responses of wildlife to environmental disturbances in an effort to better understand factors contributing to population declines (1, 2). These assessments are crucial for conservation efforts, as wildlife are increasingly faced with such anthropogenic threats as climate change, habitat loss, pathogen introduction, contaminant exposure, and overexploitation (3–5). Many of these perturbations are occurring at unprecedented rates and have already resulted in recognizable declines in individual and population health, making conservation and recovery efforts challenging (4, 5). Population-level health assessments involve a combination of physical and physiological examinations in an effort to establish "baselines" for hematological and biochemical analytes (2–4). It is when shifts in these biomarkers occur that physiologically relevant alterations in population health in response to various stressors can be recognized (6, 7). Population health and viability are inseparable, and therefore monitoring the health of organisms and their populations can be used to inform management and to improve upon our understanding of complex conservation issues (2, 3).

Comprehensive health assessments of threatened and endangered wildlife species are much rarer in comparison to domestic and aquaculture species (8–10). Hematological and biochemical analyses can be useful in identifying stress, inflammation, diseases, and nutritional deficiencies, among many other underlying conditions or responses to physiological changes. However, these diagnostic procedures are less frequently utilized in fishes compared to other vertebrate species, whether mammalian or not (9, 10). Baseline health studies in fishes have primarily focused on aquaculture species, including salmon [*Salmo salar*, (11)], tilapia [*Oreochromis* sp., (12)], sturgeon [*Acipenser* spp., (13, 14)], and seabass [*Dicentrarchus labrax*, (9)]. Reports of hematological and biochemical blood analytes are much less common for wild teleosts and elasmobranchs (15–19). Because of the paucity of information on baseline blood analytes in wild fishes, it is crucial to establish reference intervals in marine fish populations to better understand overall health and disease prevalence. These reference intervals can then be used as a basis for investigating spatial and temporal trends and for assessing population dynamics after potential environmental changes, stressors, or specific threats that might occur over time (5).

One internationally vulnerable marine fish species is the Atlantic Goliath Grouper (*Epinephelus itajara*; hereafter, called Goliath Grouper) (20). This species is the largest grouper in the Atlantic (reaching adult sizes of >2 m total length and 360–450 kg), long-lived (at least 37 years), charismatic, and it resides in waters of the western Atlantic Ocean, Gulf of Mexico, and Caribbean south to Brazil (21–24). Goliath Grouper are characterized as slow-maturing, protogynous hermaphrodites (21, 25) with known spawning locations in coastal waters of Florida in the southeastern United States (26, 27) and off the southern coast of Brazil (28). Largely due to overfishing, these animals faced near extinction in the early 1990s. They now show signs of population recovery off the coasts of Florida due to the closing of commercial and recreational fisheries from extractive exploitation but remain in low numbers elsewhere throughout their range. Several factors continue to cast doubt on whether full recovery has occurred and will be possible in Florida, including loss of mangrove habitat, destructive episodic events such as red tide and sudden cold exposure in winter months, and health and reproductive effects of high mercury concentrations in tissues and gonads (29–32). Due to conservation efforts in the United States, Florida now serves as the center of recovery for the remaining Goliath Grouper population (32, 33).

Baseline blood analyses can be used to assess sublethal impacts of environmental contaminants, but it is necessary to first establish reference intervals to gauge what is "physiologically normal" in these animals (34). Such assessments can, and should, be conducted using non-lethal methods whenever possible. Therefore, the objectives of this study were to use non-lethal sampling methods (1) to establish reference intervals for hematological and plasma biochemical analytes, and report immune function, oxidative stress, and vitellogenin in mature males and females; (2) to evaluate total length, age, and sex in relation to blood analytes in juvenile and mature fish; (3) to assess analytes across sampled months in mature male and female fish; and (4) describe the typical light microscopy findings in liver and gill biopsies, including quantitative assessment of pigmented macrophage aggregates.

MATERIALS AND METHODS

Capture, Tissue Sampling and Preparation

This research was performed in accordance with institutional and national guidelines concerning the use of animals in research, and was approved by the Florida State University Institutional Animal Care and Use Committee (IACUC) (protocol #s: 1106, 1411, and 1718); Florida Fish and Wildlife Conservation

Commission permits SAL-15-1244A-SRP, SAL-16-1244A-SRP, SAL-17-1244-SRP; and the National Oceanic and Atmospheric Administration permit F/SER24:PH.

This work was conducted throughout the coastal waters of Florida [for capture and sampling region details see (31)] at depths between 10 and 35 m for adults and <0.1–2 m for juveniles. Juveniles were distinguished from mature adults based on sampling location, size, and age. Juveniles primarily occur in mangrove habitat, while adults occur on offshore reefs. Males mature at 1,100–1,150 mm total length and 4–6 yrs of age, while females mature at 1,200–1,350 mm total length and 6–7 yrs of age (21, 35).

Several of us (26, 31, 35) developed non-lethal capture and sampling efforts that addressed federal and state laws requiring the release of this protected species alive and in good condition. On the deck of the boat, fish were immediately vented with a trocar and cannula to release gas from the swim bladder and to reduce pressure on internal organs, a wet towel placed over their eyes to protect from direct sunlight, a hose with flowing seawater placed over the gills for irrigation, and opercular respiratory rate constantly monitored during the sampling procedure. We did not see overt clinical reactions or evidence of pain caused by incisions or biopsies. While one fish died prior to release, all others were released immediately after sampling and appeared to swim without evidence of abnormal behavior.

From 2014 to 2017, adult Goliath Grouper were caught off the coasts of Florida, in the Gulf of Mexico and Atlantic Ocean. Fish were sampled during the spawning season from mid-July through September ($n = 79$), which are peak spawning months, but also during the pre-spawning month of May ($n = 44$), where they are preparing to spawn, and in October ($n = 16$) where they are still in spawning condition, but past peak spawning. In four cases, the same fish was caught twice over the 4 years of this study, from independent sampling trips. We treated recaptures of fish as independent samples because it was feasible that sufficient time had passed between captures to allow changes in their physiology.

Tissue and blood samples were collected immediately after fish were transferred to the deck of the boat, including (1) samples of dorsal fin rays (rays 6 and 7 excised at their base) for age determination [methods in (36)]; (2) liver tissue and gill filaments for histopathological analysis; (3) gonad tissue for sex determination [methods in (36)]; and (4) blood for analysis of various health variables.

Dorsal fin rays were immediately placed on ice in the field and stored frozen at −20 °C until they were sent to D. Murie (University of Florida) for age determination <12 months after collection.

Liver tissue (<2 g) was obtained using a sterile stainless-steel biopsy tool inserted through a small incision at the base of the pectoral fin, which was then closed using sterile sutures. For cases where the liver was not easily accessible through the incision, a biopsy was not obtained. A small gill filament biopsy was taken near the edge using sterile surgical scissors. Following collection, tissues were immediately fixed in 10% neutrally-buffered formalin, and, following 24 h of fixation, the samples were rinsed and stored in 70% ethanol and shipped to Crowder Histology (Baton Rouge, Louisiana USA) for processing. Tissues were processed according to standard histological methods using a tissue processor. Processed tissues were embedded in paraffin, sectioned to 3–5 μm thickness, and stained with hematoxylin and eosin (H&E) for viewing by light microscopy. Additional sections were stained with periodic acid Schiff (PAS) with and without diastase.

Gonad biopsies were obtained by inserting a polyethylene catheter into the gonoduct as per previously described techniques (27). Gonads were preserved in formalin and then shipped to D. Murie (University of Florida, Florida USA) for sex determination. Because this is a protogynous hermaphrodite, sexes included males, females, transitionals, or unknown (where insufficient gonad tissue was collected).

At the site of blood collection, scales were removed using a blade and the entire area was repeatedly swabbed with sterile 70% isopropyl alcohol pads. Blood was collected via caudal venipuncture using either a 16- or 18-gauge heparin-coated needle and syringe (**Supplemental Figure 1**). To heparinize, a liquid solution of heparin sodium was prepared, drawn into each syringe through the needle, and then thoroughly expelled several times prior to blood collection to avoid dilution of blood by heparin. Collected blood was placed into 10 mL lithium-heparin coated BD Vacutainers® (Becton-Dickinson and Co., Franklin Lakes, New Jersey USA) and was carefully inverted to ensure adequate mixture with anticoagulant and subsequently placed over an ice bath in the field for up to 10 h until processing. Hemolysis was minimized by preventing direct contact between blood tubes and the ice. Upon processing blood samples, a portion of whole blood was centrifuged (Fisher Scientific Model 228, Thermo Fisher Scientific, Waltham, Massachusetts USA) at 300 rpm for 10 min to harvest plasma. Plasma aliquots and remaining whole blood were stored frozen at −80°C, with plasma for no more than 12 months, until further analyses were conducted.

Analysis of Blood Analytes

On the same day as sampling, heparinized whole blood was subsampled in microcapillary tube duplicates and sealed with Critoseal® (Sherwood Medical Co., Deland, Florida USA). Each tube was placed in a microhematocrit centrifuge (Zipocrit® centrifuge, LW Scientific, Lawrenceville, GA, USA) and spun at 11,000 rpm for 5 min. After spinning, packed cell volume (PCV) was assessed as a percentage using a hematocrit microcapillary tube reader. The average of the duplicate samples was reported.

For blood film review, duplicate blood films were prepared for each sample, air-dried, and stained with Wright-Giemsa (Harleco®, EMD Millipore, Billerica, Massachusetts, USA). Blood film evaluation included a white blood cell (WBC) estimate, a 200-WBC differential, and blood cell morphological evaluation.

Frozen plasma samples were sent to the University of Miami Avian and Wildlife Laboratory (UMAW) for protein electrophoresis and quantification of vitellogenin (VTG). Two representative plasma protein electrophoretograms of a female and male Goliath Grouper indicating the 6 fractions of interest are presented in **Supplemental Figure 2**.

We quantified total protein in two ways: (1) using the Biuret method, indicated as "Total protein (B) in **Tables 1–3**"; and using a refractometric method (ReichertR VET360, Reichert R Technologies, Buffalo, New York USA) indicated as "Total protein (R) in **Tables 1–3**. Electrophoresis was carried out using split beta gels and the SPIFE 3,000 system (Helena Laboratories, Beaumont, Texas USA) to measure the concentrations of 6 fractions.

Vitellogenin was quantified using a grouper-specific VTG ELISA kit, which employs the competitive enzyme immunoassay technique in the detection range of 60–1,200 ng/mL (MyBioSource, San Diego, California USA). Vitellogenin was measured by adding standards or samples to appropriate wells containing horseradish peroxidase (HRP) conjugated-rabbit antibody.

Plasma biochemical analytes were measured using the dry chemistry analyzer Vitros 250XR (Ortho, Rochester, New York USA) at UMAW and included alkaline phosphatase (ALP) aspartate aminotransferase (AST), blood urea nitrogen (BUN), calcium, cholesterol, creatine phosphokinase (CK), creatinine, glucose, iron, lactate dehydrogenase (LDH), lipase, magnesium, phosphorus, potassium, sodium, total bilirubin, triglycerides, and uric acid. The calcium:phosphorus ratio was calculated. For glucose, the minimum detection limit was 10 mg/dL. For the two samples that fell below this limit, the low value of "10" was used for statistical purposes.

Immune function, antioxidant capacity, and indicators of oxidative stress were quantified using plasma to measure activities of lysozyme, glutathione peroxidase (GPx), superoxide dismutase (SOD), and concentrations of reactive oxygen and nitrogen species (ROS/RNS). Lysozyme activity was analyzed using standard turbidity assays performed by Walsh et al. (37). At UMAW, GPx was measured using a commercially available glutathione peroxidase assay kit (Cayman Chemical Co., Michigan USA). A spectrophotometer was used to measure GPx activity following the oxidation of NADPH at 340 nm in this reaction. SOD was quantified using a SOD assay kit (Cayman Chemical Co., Ann Arbor, Michigan USA), which detects superoxide radicals generated by xanthine oxidase and hypoxanthine through the use of a tetrazolium salt. SOD was measured as the proportional amount of enzyme needed to exhibit 50% dismutation of the superoxide radical at an absorbance of 450 nm. Concentrations of ROS/RNS were evaluated using an OxiSelectTM *In Vitro* ROS/RNS Assay Kit (Green Fluorescence, Cell Biolabs, Inc., San Diego, California USA), following the manufacturer's instructions (38, 39). This assay universally measured ROS and RON species, which can include, among others, hydrogen peroxide, nitric oxide, peroxynitrite, and peroxyl radicals.

Histopathological Analysis

Prepared liver and gill tissue slides were evaluated using a Leica DM1000LED microscope (Leica Microsystems Inc, Buffalo Grove, Illinois USA) at UGACVM Histology Laboratory.

Additional analyses on liver tissue slides were conducted at Florida State University (Tallahassee, Florida, USA) to evaluate pigmented macrophage aggregates (PMAs), sometimes referred to as melano-macrophage centers, which are aggregates of highly pigmented phagocytes (40, 41). These were a prominent feature of liver tissue identified from preliminary histological analyses in this study. To quantify area and count of PMAs, images were taken from a subset of the fish with liver biopsies collected ($n = 55$) using a Canon EOS equipped with a DSLR adapter for compound microscopes and Digital Photo Professional 4 software. For each prepared microscope slide, five images were taken of random and non-overlapping representative areas at each 100× and 400× total magnification. Counts of PMAs were quantified manually from 100× images, and area of PMA per total image area in pixels and percent area occupied by PMAs were calculated (42) from 400× images using ImageJ software (43). The five counts and area estimates were then averaged per slide and reported as PMA % area and count (44).

Data Analysis

Reference Intervals

Reference intervals for hematology, plasma biochemistry, and protein electrophoresis data were calculated using MedCalc (MedCalc Software v.18.5, Ostend, Belgium) following the American Society of Veterinary Clinical Pathology reference interval guidelines using a combination of non-parametric and parametric methods, depending on sample size and distribution of the data (45). Reference intervals in conventional units were established for all mature male and female fish combined (**Table 1**), and also females (**Table 2**) and males (**Table 3**) individually. These same reference intervals were also converted to Standard International units (**Supplemental Tables 1–3**). Normality was assessed using the D'Agostino-Pearson test, while outliers were detected using the Reed test. Logarithmic or Box-Cox transformation was employed when necessary. Biochemistry and protein electrophoresis samples with visual hemolysis scores of $\geq 1+$ were removed from the dataset prior to calculation of reference intervals given the potential interference of hemolysis on various blood analyte measurements (46).

Statistical Analysis

All analyses were conducted using R (R Development Core Team). To reduce dataset complexity for hematology, plasma biochemistry, and plasma proteins, similar variables were grouped into these respective categories. We used canonical correlation analysis (CCA) as an exploratory analytical method to investigate the relationships between multivariate datasets of size (i.e., total length), age, and sex with health variables in all fish, including juvenile and mature fish and all sexes, to investigate potential morphometrical effects on blood analyte data. Multivariate CCA was carried out separately on analytes of hematology, plasma proteins, and plasma biochemistry to limit the inflation of Type I error rates and to reduce the number of pairwise analyses. Individual parameters of PCV and VTG, along with immune system and oxidative stress, were not tested using CCA due to few parameters relative to the three previously mentioned categories, and lower sample sizes. Tests of dimensionality, to determine which canonical dimensions were statistically significant at the 0.05 level, were conducted using likelihood ratio tests with Wilks' lambda distribution. Zscores

TABLE 1 | Measures of central tendency, range, and reference intervals (with 90% confidence intervals for upper and lower limits) for hematological, plasma biochemical, and plasma protein electrophoretic data for all adult Atlantic Goliath Grouper (*Epinephelus itajara*) in conventional units.

	N	Mean ± SD	SE	Median	Range	95% RI (90% CI)		Data distribution/RI method/Transformation
						Lower limit	Upper limit	
Hematology								
Packed cell volume (%)	32	36 ± 7	1	36	24–52	23 (19–26)	50 (46–53)	G/P/N
White blood cells ($\times10^3/\mu L$)	140	6.21 ± 1.83	0.15	6.05	2.80–9.50	3.01 (2.80–3.60)	9.30 (9.10–9.50)	NA/NP/N
Neutrophils ($\times10^3/\mu L$)	140	1.19 ± 0.53	0.04	1.10	0.29–2.50	0.36 (0.29–0.49)	2.30 (2.10–2.50)	NA/NP/N
Immature neutrophils ($\times10^3/\mu L$)	140	0.080.34	0.03	0	0–3.90	0 (0)	0.26 (0.18–3.90)	NA/NP/N
Lymphocytes ($\times10^3/\mu L$)	140	3.87 ± 1.14	0.10	3.75	1.60 −6.30	2.05 (1.60–2.20)	5.95 (5.70–6.30)	NA/NP/N
Monocytes ($\times10^3/\mu L$)	140	1.08 ± 0.38	0.03	1.00	0.38–2.20	0.47 (0.38–0.53)	1.95 (1.70–2.20)	NA/NP/N
Eosinophils ($\times10^3/\mu L$)	140	0.05 ± 0.05	0	0.05	0–0.23	0 (0)	0.18 (0.16–0.23)	NA/NP/N
Basophils ($\times10^3/\mu L$)	140	0 ± 0.01	0	0	0–0.08	0 (0)	0 (0–0.08)	NA/NP/N
Plasma biochemistry								
Alkaline phosphatase (U/L)	58	68 ± 20	3	65	21–112	28 (21–36)	108 (100–116)	G/P/N
Aspartate aminotransferase (U/L)	58	100 ± 87	11	83	19–652	29 (24–35)	273 (213–353)	G/P/B
Blood urea nitrogen (mg/dL)	58	NA	NA	5	<2–14	<2 (<2)	12 (11–13)	G/P/N
Calcium (mg/dL)	58	15.2 ± 2.9	0.4	14.7	8.3–25.7	8.6 (7.2–10.1)	20.5 (18.9–22.1)	NG/R/N
Calcium: phosphorus ratio	58	1.41 ± 0.34	0.05	1.47	0.77–2.61	0.82 (0.73–0.92)	2.15 (1.99–2.32)	G/P/B
Cholesterol (mg/dL)	58	174 ± 64	8	158	65–432	90 (81–100)	326 (282–378)	G/P/B
Creatine phosphokinase (U/L)	58	NA	NA	148	<20–1,019	<20 (<20–24)	842 (616–1,138)	G/P/B
Creatinine (mg/dL)	58	0.95 ± 0.69	0.09	0.75	0.20–4.10	0.31 (0.27–0.36)	2.62 (2.00–3.50)	G/P/B
Glucose (mg/dL)	58	NA	NA	34	<10–317	NA	NA	NA
Iron ($\mu g/dL$)	58	162 ± 50	7	154	56–270	65 (46–83)	259 (241–278)	G/P/N
Lactate dehydrogenase (U/L)	58	2,963 ± 3,619	475	2048	171–25,067	248 (169–365)	13139 (9,008–19,151)	G/P/B
Lipase (U/L)	58	243 ± 141	18	234	11–546	12 (0–40)	561 (490–634)	G/P/B
Magnesium (mg/dL)	58	4.6 ± 2.2	0.3	4.2	2.5–15.6	2.9 (2.8–3.1)	8.8 (7.1–12.3)	G/P/B
Phosphorus (mg/dL)	58	11.3 ± 3.0	0.4	10.9	4.8–18.2	5.5 (4.3–6.6)	17.1 (16.0–18.2)	G/P/N
Potassium (mEq/L)	58	4.8 ± 1.1	0.1	4.8	2.0–7.3	2.6 (2.2–3.0)	7.0 (6.6–7.4)	G/P/N
Sodium (mEq/L)	58	210 ± 43	6	200	131–433	113 (78–160)	290 (243–326)	NG/R/N
Total bilirubin (mg/dL)	58	NA	NA	<0.1	<0.1–0.5	<0.1 (<0.1)	<0.1 (<0.1)	NG/R/N
Triglycerides (mg/dL)	58	96 ± 57	8	85	15–235	18 (12–26)	242 (202–286)	G/P/B
Uric acid (mg/dL)	58	NA	NA	0.5	<0.2–1.8	<0.2 (<0.2)	1.7 (1.4–2.1)	G/P/B
Plasma proteins								
Total protein (B) (g/dL)	58	6.0 ± 1.0	0.1	6.0	2.7–8.5	3.9 (3.5–4.3)	8.0 (7.6–8.4)	G/P/N
Total protein (R) (g/dL)	23	5.9 ± 1.0	0.2	5.9	3.7–7.4	4.0 (3.5–4.6)	7.8 (7.2–8.4)	G/P/N
Fraction 1 (g/dL)	58	1.08 ± 0.31	0.04	1.11	0.32–1.98	0.46 (0.34–0.58)	1.69 (1.57–1.81)	G/P/N
Fraction 2 (g/dL)	58	1.22 ± 0.32	0.04	1.17	0.54–1.98	0.58 (0.46–0.71)	1.86 (1.73–1.98)	G/P/N
Fraction 3 (g/dL)	58	0.50 ± 0.16	0.02	0.48	0.21–1.02	0.26 (0.23–0.29)	0.87 (0.77–0.97)	G/P/B
Fraction 4 (g/dL)	58	0.68 ± 0.19	0.03	0.66	0.27–1.34	0.36 (0.31–0.41)	1.11 (1.01–1.21)	G/P/B
Fraction 5 (g/dL)	58	1.91 ± 0.44	0.06	1.88	1.01–3.10	1.04 (0.88–1.21)	2.79 (2.62–2.95)	G/P/N
Fraction 6 (g/dL)	58	0.59 ± 0.23	0.03	0.55	0.16–1.24	0.24 (0.20–0.28)	1.15 (1.01–1.30)	G/P/B

Mean ± SD was not calculated for analytes where some values fell below the limits of detection; for calculation of reference intervals, values below the limits of detection were assigned to half of the detection limit. Plasma samples with evidence of hemolysis or lipemia were removed from the dataset for calculation of reference intervals. Total protein (R), total protein using refractometer; Total protein (B), total protein by Biuret; G, Gaussian; P, Parametric; NP, Non-parametric; NG, Non-Gaussian; B, Box-Cox; R, Robust; N, None.

were computed to standardize data prior to CCA analyses. Canonical loading values of ∼0.3 or greater were used to select the variables determined by this approach to have the most meaningful relationship with the canonical variate (47–49). In R, analyses were carried out using packages CanCorr (http://www.statpower.net/R312/CanCorr.r), CCA, and VEGAN.

To test for the relationships between blood analytes, total length and age, and histological parameters, our analyses were generally restricted to the important variables derived from CCA where CCA was performed. Linear regression analyses were carried out on each clinical and histological variable, including those where CCA was not performed, separately. The only

TABLE 2 | Measures of central tendency, range, and reference intervals (with 90% confidence intervals for upper and lower limits) for hematological, plasma biochemical, and plasma protein electrophoretic data for mature female Atlantic Goliath Grouper (*Epinephelus itajara*) in conventional units.

	N	Mean ± SD	SE	Median	Range	95% RI (90% CI)		Data distribution/RI method/Transformation
						Lower limit	Upper limit	
Hematology								
Packed cell volume (%)	12	38 ± 7	2	39	24–47	NA	NA	Cannot calculate RIs for sample sizes <20
White blood cells ($\times 10^3/\mu L$)	65	6.07 ± 1.79	0.22	5.90	2.90–9.30	2.39 (1.56–2.89)	9.64 (8.99–10.24)	NG/R/N
Neutrophils ($\times 10^3/\mu L$)	65	1.16 ± 0.51	0.06	1.10	0.34–2.30	0.39 (0.31–0.48)	2.40 (2.10–2.72)	G/P/B
Immature neutrophils ($\times 10^3/\mu L$)	65	0.05 ± 0.09		0	0–0.65	NA	NA	Cannot calculate RIs
Lymphocytes ($\times 10^3/\mu L$)	65	3.79 ± 1.09	0.13	3.60	2.10–6.00	1.53 (1.23–1.85)	5.98 (5.55–6.33)	NG/R/N
Monocytes ($\times 10^3/\mu L$)	65	1.07 ± 0.39	0.05	1.00	0.38–2.20	0.31 (0.17–0.45)	1.83 (1.69–1.97)	G/P/N
Eosinophils ($\times 10^3/\mu L$)	65	0.04 ± 0.05	0.01	0.04	0–0.21	0 (0)	0.13 (0–0.16)	NG/R/N
Basophils ($\times 10^3/\mu L$)	65	0 ± 0	0	0	0	0 (0)	0 (0)	G/P/N
Plasma biochemistry								
Alkaline phosphatase (U/L)	25	63 ± 17	3	58	42–103	29 (19–39)	97 (87–107)	G/P/N
Aspartate aminotransferase (U/L)	25	77 ± 47	9	73	19–262	21 (14–30)	192 (143–255)	G/P/B
Blood urea nitrogen (mg/dL)	25	NA	NA	5	<1–14	<1 (<1–1.7)	12.7 (10.0–15.7)	G/P/B
Calcium (mg/dL)	25	16.6 ± 3.4	0.7	15.7	12.4–25.7	12.3 (11.6–13.1)	26.7 (21.6–38.2)	G/P/B
Calcium:phosphorus ratio	25	1.55 ± 0.36	0.07	1.52	0.77–2.61	0.86 (0.65–1.06)	2.25 (2.04–2.45)	G/P
Cholesterol (mg/dL)	25	192 ± 84	17	167	110–432	99 (88–112)	479 (313–973)	G/P/B
Creatine phosphokinase (U/L)	25	251 ± 257	51	169	22–1019	21 (12–37)	1208 (653–2251)	G/P/B
Creatinine (mg/dL)	25	0.94 ± 0.84	0.17	0.70	0.20–4.10	0.25 (0.19–0.33)	3.07 (1.87–5.43)	G/P/B
Glucose (mg/dL)	25	NA	NA	39	<10–317	NA	NA	NA
Iron ($\mu g/dL$)	25	169 ± 54	11	171	87–270	64 (33–95)	275 (244–306)	G/P/N
Lactate dehydrogenase (U/L)	25	3,652 ± 4,964	993	1912	427–25067	293 (182–486)	22096 (9,854–54,385)	G/P/B
Lipase (U/L)	25	169 ± 115	23	185	11–446	3 (0–26)	462 (354–583)	G/P/B
Magnesium (mg/dL)	25	5.3 ± 3.1	0.6	4.0	2.9–15.6	1.6 (1.2–2.5)	10.5 (6.8–13.9)	NG/R/Logarithmic
Phosphorus (mg/dL)	25	11.2 ± 2.9	0.6	10.9	5.6–17.0	5.6 (3.9–7.2)	16.8 (15.1–18.4)	G/P/N
Potassium (mEq/L)	25	5.0 ± 1.0	0.2	5.1	2.7–7.3	3.1 (2.6–3.7)	6.9 (6.3–7.5)	G/P/N
Sodium (mEq/L)	25	224 ± 58	12	209	181–433	82 (25–166)	329 (243–388)	NG/R/N
Total bilirubin (mg/dL)	25	NA	NA	<0.1	<0.1–0.5[a]	<0.1 (<0.1)	<0.1 (<0.1)	NG/R/N
Triglycerides (mg/dL)	25	119 ± 70	14	113	15–235	12 (1.7–31)	290 (228–359)	G/P/B
Uric acid (mg/dL)	25	NA	NA	0.4	<0.2–1.8	<0.2 (<0.2)	1.5 (1.1–2.1)	G/P/B
Plasma proteins								
Total protein (B) (g/dL)	25	6.1 ± 1.0	0.2	5.9	4.5–8.5	4.1 (3.5–4.7)	8.0 (7.4–8.6)	G/P/N
Total protein (R) (g/dL)	11	6.0 ± 0.7	0.2	5.9	4.9–7.2	NA	NA	Cannot calculate RIs for sample sizes <20
Fraction 1 (g/dL)	25	1.15 ± 0.33	0.07	1.16	0.32–1.98	0.50 (0.31–0.69)	1.80 (1.61–1.99)	G/P/N
Fraction 2 (g/dL)	25	1.10 ± 0.25	0.05	1.09	0.73–1.59	0.62 (0.47–0.76)	1.59 (1.45–1.74)	G/P/N
Fraction 3 (g/dL)	25	0.56 ± 0.16	0.03	0.54	0.36–1.02[b]	0.28 (0.20–0.36)	0.80 (0.72–0.88)	G/P/N
Fraction 4 (g/dL)	25	0.68 ± 0.21	0.04	0.65	0.41–1.34	0.41 (0.37–0.46)	1.23 (0.97–1.65)	G/P/B
Fraction 5 (g/dL)	25	1.94 ± 0.47	0.09	1.92	1.15–3.10	1.01 (0.74–1.28)	2.86 (2.89–3.14)	G/P/N
Fraction 6 (g/dL)	25	0.64 ± 0.27	0.05	0.60	0.16–1.24	0.10 (0–0.26)	1.18 (1.02–1.34)	G/P/N

[a] *0.5 mg/dL is an outlier. Reference intervals calculated with this value removed. The next highest value was 0.2 mg/dL.*

[b] *1.02 g/dL is an outlier. Reference intervals calculated with this value removed. The next highest value was 0.77 g/dL.*

Mean ± SD was not calculated for analytes where some values fell below the limits of detection; for calculation of reference intervals, values below the limits of detection were assigned to half of the detection limit. Plasma samples with evidence of hemolysis or lipemia were removed from the dataset for calculation of reference intervals. Total protein (R), total protein using refractometer; Total protein (B), total protein by Biuret; G, Gaussian; P, Parametric; NP, Non-parametric; NG, Non-Gaussian; B, Box-Cox; R, Robust; N, None.

TABLE 3 | Measures of central tendency, range, and reference intervals (with 90% confidence intervals for upper and lower limits) for hematological, plasma biochemical, and plasma protein electrophoretic data for mature male Atlantic Goliath Grouper (*Epinephelus itajara*) in conventional units.

	N	Mean ± SD	SE	Median	Range	95% RI (90% CI)		Data distribution/RI method/Transformation
						Lower Limit	Upper Limit	
Hematology								
Packed cell volume (%)	20	35 ± 7	2	34	27–52	22 (18–27)	49 (43–54)	G/P/N
White blood cells ($\times 10^3/\mu L$)	75	6.34 ± 1.86	0.21	6.20	2.80–9.50	3.24 (2.92–3.60)	11.27 (10.15–12.52)	G/P/Logarithmic
Neutrophils ($\times 10^3/\mu L$)	75	1.22 ± 0.55	0.06	1.10	0.29–2.50	0.39 (0.32–0.48)	2.55 (2.26–2.88)	G/P/B
Immature neutrophils ($\times 10^3/\mu L$)	75	0.11 ± 0.45	0.05	0	0–3.90	NA	NA	Cannot calculate RIs
Lymphocytes ($\times 10^3/\mu L$)	75	3.94 ± 1.18	0.14	4.00	1.60–6.30	1.98 (1.78–2.20)	7.11 (6.39–7.92)	G/P/Logarithmic
Monocytes ($\times 10^3/\mu L$)	75	1.09 ± 0.38	0.04	1.10	0.47–2.00	0.34 (0.22–0.47)	1.83 (1.71–1.96)	G/P/N
Eosinophils ($\times 10^3/\mu L$)	75	0.06 ± 0.05	0.01	0.06	0–0.23	0 (0)	0.15 (0.13–0.17)	NG/R/N
Basophils ($\times 10^3/\mu L$)	75	0 ± 0.01	0	0	0–0.08	0 (0)	0 (0)	NG/R/N
Plasma biochemistry								
Alkaline phosphatase (U/L)	33	72 ± 22	4	71	21–112	30 (19–40)	115 (104–125)	G/P/N
Aspartate aminotransferase (U/L)	33	117 ± 105	18	90	34–652	42 (36–50)	331 (219–559)	G/P/B
Blood urea nitrogen (mg/dL)	33	7 ± 3	1	6	3–14	3 (2–4)	14 (11–17)	G/P/Logarithmic
Calcium (mg/dL)	33	14.1 ± 1.9	0.3	14.1	8.3–18.6	10.3 (9.3–11.2)	17.9 (16.9–18.9)	G/P/N
Calcium: phosphorus ratio	33	1.31 ± 0.29	0.05	1.39	0.84–2.01	0.74 (0.59–0.88)	1.88 (1.74–2.03)	G/P/N
Cholesterol (mg/dL)	33	161 ± 40	7	153	65–253	83 (64–103)	239 (219–259)	G/P/N
Creatine phosphokinase (U/L)	33	NA	NA	147	<20–728	<20 (<20–25)	643 (454–886)	G/P/B
Creatinine (mg/dL)	33	0.95 ± 0.56	0.10	0.80	0.40–3.30	0.40 (0.35–0.47)	2.26 (1.74–4.21)	G/P/B
Glucose (mg/dL)	33	NA	NA	33	<10–110	NA	NA	NA
Iron (μg/dL)	33	157 ± 46	8	151	56–259	66 (43–89)	248 (224–271)	G/P/N
Lactate dehydrogenase (U/L)	33	2,440 ± 2,049	357	2,081	171–8,577	199 (94–384)	8,607 (6,021–12,032)	G/P/N
Lipase (U/L)	33	299 ± 133	23	304	56–546	38 (0–105)	560 (493–627)	G/P/N
Magnesium (mg/dL)	33	4.2 ± 0.8	0.1	4.2	2.5–6.8	2.8 (2.5–3.1)	5.9 (5.4–6.5)	G/P/B
Phosphorus (mg/dL)	33	11.3 ± 3.1	0.5	10.9	4.8–18.2	5.3 (3.7–6.8)	17.4 (15.9–19.0)	G/P/N
Potassium (mEq/L)	33	4.6 ± 1.2	0.2	4.7	2.0–6.8	2.2 (1.6–2.9)	7.0 (6.4–7.6)	G/P/N
Sodium (mEq/L)	33	200 ± 23	4	198	131–258	156 (144–167)	244 (233–255)	G/P/N
Total bilirubin (mg/dL)	33	NA	NA	<0.1	<0.1–0.3	<0.1 (<0.1)	<0.1 (<0.1–0.2)	NG/R/N
Triglycerides (mg/dL)	33	78 ± 36	6	76	19–153	7 (0–25)	149 (131–167)	G/P/N
Uric acid (mg/dL)	33	NA	NA	0.5	<0.2–1.6	<0.2 (<0.2)	1.5 (1.3–1.7)	G/P/N
Plasma proteins								
Total protein (B) (g/dL)	33	5.9 ± 1.1	0.2	6.0	2.7–8.0	3.8 (3.2–4.3)	8.0 (7.5–8.6)	G/P/N
Total protein (R) (g/dL)	12	5.8 ± 1.1	0.3	5.7	3.7–7.4	NA	NA	Cannot calculate RIs for sample sizes <20
Fraction 1 (g/dL)	33	1.02 ± 0.29	0.05	1.08	0.37–1.56	0.45 (0.30–0.59)	1.60 (1.45–1.74)	G/P/N
Fraction 2 (g/dL)	33	1.31 ± 0.35	0.06	1.26	0.54–1.98	0.62 (0.45–0.80)	1.99 (1.82–2.17)	G/P/N
Fraction 3 (g/dL)	33	0.45 ± 0.14	0.02	0.44	0.21–0.87	0.24 (0.20–0.28)	0.77 (0.67–0.89)	G/P/B
Fraction 4 (g/dL)	33	0.69 ± 0.18	0.03	0.67	0.27–1.01	0.33 (0.24–0.42)	1.05 (0.95–1.14)	G/P/N
Fraction 5 (g/dL)	33	1.90 ± 0.43	0.07	1.88	1.01–3.06	1.06 (0.84–1.27)	2.74 (2.52–2.95)	G/P/N
Fraction 6 (g/dL)	33	0.55 ± 0.20	0.03	0.54	0.27–1.08	0.28 (0.24–0.33)	1.05 (0.87–1.29)	G/P/B

Mean ± SD was not calculated for analytes where some values fell below the limits of detection; for calculation of reference intervals, values below the limits of detection were assigned to half of the detection limit. Plasma samples with evidence of hemolysis or lipemia were removed from the dataset for calculation of reference intervals. Total protein (R), total protein using refractometer; Total protein (B), total protein by Biuret; G, Gaussian; P, Parametric; NP, Non-parametric; NG, NG; B, Box-Cox; R, Robust, N, None.

exception to this was for PMA count data with age and size, for which a GLM with family Poisson was conducted. Data were transformed (natural-log, square-root, log-10, cube-root) to meet parametric assumptions where appropriate. Where assumptions were not met for linear regression analysis, packages COIN and lmPerm were used for permutation-based statistical tests with

Monte-Carlo simulation as an alternative to classical procedures. The categorical factor "sex" (male, female, transitional) was compared with separate clinical parameters using GLM with family Gaussian. The only exception to this was for PMA count data, for which GLM with family Poisson was conducted. For these GLMs, multiple comparisons were conducted using the glht function with packages emmeans and multcomp to produce Tukey contrasts with adjusted p-values. For linear regressions, the Holm-Bonferroni method was used to correct for multiple comparisons (50).

To test the relationship between VTG and each of the six protein fractions determined by protein electrophoretograms, we used linear regression analysis. Data were transformed (natural-log, square-root) to meet parametric assumptions where appropriate.

The relationship between total length (TL, cm) and age (yrs) for Goliath Grouper was previously shown by Malinowski (31) to be strongly positively correlated ($r^2 = 0.51$, $p < 2 \times 10^{-16}$), but here we also compared size and age between males, females, and transitionals using analysis of variance and Tukey contrasts with adjusted p-values. Because length and age are known to be important factors in determining fish health (51, 52), both were included as factors in this study.

To evaluate trends in blood analytes across months of sample collection for mature males and females, we used analysis of variance and Tukey contrasts with adjusted p-values after transforming (natural-log, square-root) any data that did need meet parametric assumptions. For data that did not meet assumptions after transformation, we used GLMs with the glht function for multiple comparisons. Because some months for mature males or females had little data, not all months of sample collection (May, July, August, September, October) were represented for both sexes. For males, there were only two samples from mid-July so we combined those into the month of Aug. This was justifiable because July and August are the two primary spawning months. For females, there was only one sample in October, and we decided to remove from this analysis because it could not be justifiably combined into the previous month.

RESULTS

Study Animals and Sampling

A total of 510 Goliath Grouper were caught, from which 195 blood samples were collected for hematological analysis. Of those 195 blood samples, 139 were used for blood plasma analyses of various health variables. Of the 139 samples used for blood plasma analyses, the major portion of this study, they were collected from different sexes and age groups ($n_{female} = 58$, $n_{male} = 62$, $n_{transitional} = 6$, $n_{unknown} = 8$, $n_{juvenile} = 5$), with ages (yrs) ranging from 4 to 19 (median = 11, mean = 10.8, SD = 3.1) and total lengths (cm) from 57 to 219 (mean = 163.4, median = 165, SD = 27.5) (**Supplemental Figure 3**). From the 510 fish caught, we also opportunistically collected liver samples ($n = 183$) and gill samples ($n = 44$) for histopathological review, many of which had corresponding blood samples collected, but not all. The number of blood and liver samples collected varied due to logistics of sample collection and handling. A comparison of age and size between sexes for adults showed no difference in age, but a marginally significant difference in total length between males (mean = 163.8, median = 164, SD = 19.2) and females (mean = 173.0, median = 171, SD = 21.2) was observed, with females being larger ($p = 0.03$).

Reference Intervals

Conventional unit measures of central tendency, range, and reference intervals for all fishes, females only, and males only are reported in **Tables 1–3**, respectively. Standard International are reported in **Tables S1–S3**. For plasma biochemical, immune system and oxidative stress analytes with too low of a sample size for reference intervals, descriptive statistics are reported in **Table 4**.

PCV, Hematology, Plasma Proteins, and VTG

There were no significant correlations between hematology data, including PCV and leukogram, and age or total length ($p > 0.05$). Thrombocyte numbers were determined to be adequate in all blood films evaluated, often with variably sized clumps that prevented a more detailed quantitative assessment. Samples from the majority of fish did not show any evidence of red blood cell (RBC) immaturity (i.e., lack of anisocytosis, polychromasia, immature erythroid stages), with only $n = 3$ displaying mild anisocytosis and polychromasia averaging 14 immature RBC/100 mature RBC (range 9–21 immature RBC/100 mature RBC). There were also no significant differences in leukogram data among females, males, and transitionals ($p > 0.05$). Lymphocytes were the predominant WBC type. As described in Materials and Methods, CCA was not performed on PCV or VTG due to few parameters and low sample size.

For plasma proteins, the first CCA (CCA1) was statistically significant ($F = 2.257$, $p = 0.002$) and strongly correlated with a canonical correlation coefficient (CCC) of 0.63 between plasma protein analytes and sex, age, and total length variables (**Supplemental Table 5**). The total variance explained by the CCA1 was 71.8%. In order of CCA loading value, for plasma protein analytes, the first canonical dimension was most strongly influenced by fraction 2 (loading strength = 0.51), fraction 1 (loading strength = −0.49), and fraction 4 (loading strength = −0.27). For sex, age, and length variables, the first dimension was comprised of total length (loading strength = −0.88) and age (loading strength = −0.46).

Linear regression analysis revealed a number of significant results with protein fractions, which are detailed in **Table 5**. Fraction 2 was significantly negatively correlated with total length ($r^2 = 0.18$) and age ($r^2 = 0.06$), while fraction 4 was negatively correlated with age ($r^2 = 0.05$). Although sex had a fairly low canonical loading (loading strength = 0.11), we did find that males had significantly higher fraction 2 concentrations than females and that the concentration of this fraction for females was significantly negatively correlated with total length, with this female-only negative correlation ($r^2 = 0.25$) being stronger than with all sexes combined. The other sex-related result for proteins

TABLE 4 | Descriptive statistics of immune and oxidative stress indicators, and vitellogenin, for adult (male, female, transitional) Atlantic Goliath Grouper (*Epinephelus itajara*) that were not included as reference intervals.

Health index	Mean	SD	SE	Median	Min	Max	N
ALL ADULT							
Immune/oxidative stress							
GPx (nmol/min/ml)	383.25	193.23	28.49	374.39	40.75	784.45	46
Lysozyme (μg/ml)	3.86	1.64	0.19	3.17	1.37	7.74	76
ROS/RNS (nM)	6432.65	1561.47	218.65	6177.36	3431.45	9087.93	51
Superoxide dismutase (U/ml)	15.47	20.16	1.98	7.55	0.82	120.01	104
Protein precursor							
Vitellogenin (ng/ml)	433.89	212.33	32.76	382.76	79.32	1017.28	42
FEMALE							
Immune/oxidative stress							
GPx (nmol/min/ml)	351.98	190.99	42.71	336.19	40.75	652.01	20
Lysozyme (μg/ml)	3.94	1.74	0.30	3.42	1.37	7.11	33
ROS/RNS (nM)	5962.35	1295.73	254.11	5703.19	3431.45	8402.36	26
Superoxide dismutase (U/ml)	15.37	24.06	3.51	5.70	1.33	120.01	47
Protein precursor							
Vitellogenin (ng/ml)	506.44	260.21	59.70	469.80	79.32	1017.28	19
MALE							
Immune/oxidative stress							
GPx (nmol/min/ml)	388.15	207.44	46.38	427.88	40.75	784.45	20
Lysozyme (μg/ml)	3.84	1.60	0.25	3.14	1.78	7.74	41
ROS/RNS (nM)	7010.24	1661.69	339.19	7474.49	3569.95	9087.93	24
Superoxide dismutase (U/ml)	16.95	16.88	2.36	10.32	0.82	79.21	51
Protein precursor							
Vitellogenin (ng/ml)	376.82	136.97	33.22	374.35	201.89	784.88	17

Plasma samples with evidence of hemolysis or lipemia were removed from the dataset for calculation of descriptive statistics. SD, standard deviation; SE, standard error; GPx, glutathione peroxidase; ROS, reactive oxygen species; RNS, reactive nitrogen species.

TABLE 5 | Statistically significant plasma protein electrophoresis fractions and vitellogenin of Atlantic Goliath Grouper (*Epinephelus itajara*) categorized by sex (T, transitional; F, female; M, male) and by continuous variables of total length and age.

Analyte	Sex (T*F)	(Sex M*F)	Sex (M*T)	Total length (cm)	Age (yr)
Plasma protein electrophoresis					
Fraction 2[a]		*p = 0.005* *$n_{M/F}$ = 37/39* *Z = 3.07*		**p < 0.001** **n = 88, r^2 = 0.18** **F = 19.42, df = 86**	**p = 0.009** **n = 86, r^2 = 0.06** **F = 6.78, df = 84**
Female				**p < 0.001** **n = 39, r^2 = 0.25** **F = 13.31, df = 37**	
Fraction 5	**p = 0.049** **$n_{T/F}$ = 4/39** **Z = −2.31**		*p = 0.045* *$n_{M/T}$ = 37/4* *Z = 2.35*		
Fraction 4					**p = 0.025** **n = 86, r^2 = 0.05** **F = 5.30, df = 84**
Protein precursor: Vitellogenin					
Male				**p = 0.030** **n = 18, r^2 = 0.23** **F = 6.04, df = 16**	
Female				*p = 0.021* *n = 19, r^2 = 0.26* *F = 7.43, df = 17*	

[a] *Data were natural-log transformed.*

Where male and female categorical variables were significantly different, respective significant post-hoc linear regression results are shown. The p-value is given with adjusted r^2 value in parentheses. Blank cells indicate no significant difference or correlation. For sex, bolded values indicate the first sex in the pairwise comparison is lower and italicized values indicate the first sex is greater. For total length and age, negative relationships are bolded and positive relationships are italicized.

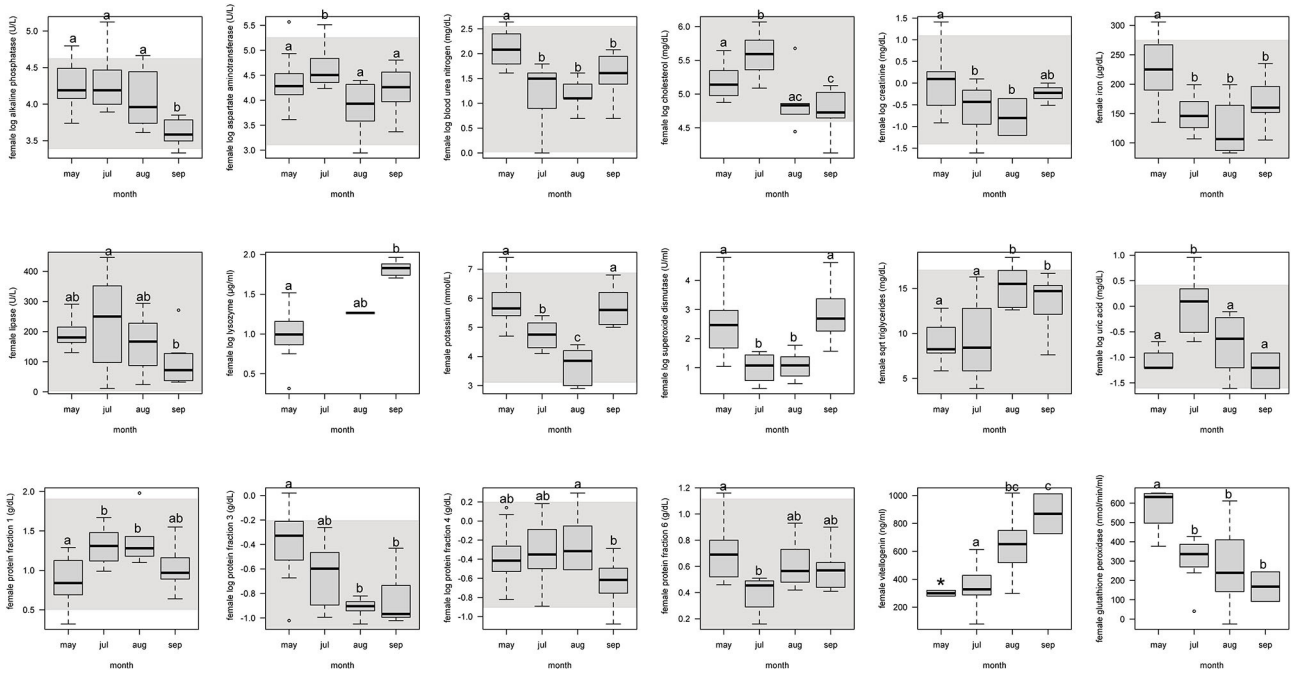

FIGURE 1 | Boxplots showing significant ($p < 0.05$) biochemistry analytes, plasma protein electrophoresis fractions, vitellogenin, and immune system and oxidative stress analytes for female Atlantic Goliath Grouper (*Epinephelus itajara*) across sample collection months (May, July, August, September). There was only one sample in October, and we decided to remove from this analysis because it could not be justifiably combined into the previous month. Shading represents reference intervals. Different letters indicate significant difference. Range = vertical dashed lines, median = bold horizontal lines in box, first quartile = area below the line in the box, third quartile = area above the line in the box. The upper and lower ends of the nominal data range is defined as the respective interquartile distance (IQD) ± 1.5 IQD. Open circles = points that fall outside of this range.

was that fraction five concentrations were significantly lower in transitionals than both males and females. Concentrations of VTG were similar for males, females, and transitionals ($p > 0.05$), but concentrations significantly increased ($p < 0.05$) with total length ($r^2 = 0.26$) for females and total length ($r^2 = 0.23$) for males. PCV did not correlate significantly with total length or age and was not different between sexes ($p > 0.05$).

There were no significant correlations ($p > 0.05$) between VTG and each of the protein fractions.

For females, protein fraction 1 significantly ($p < 0.05$) increased from May to July and August, and then decreased in September (**Figure 1**, **Supplemental Table 4**). Fractions 3 and 6 significantly decreased from May through the following months. Fraction 4 decreased only from September to August. Vitellogenin increased from May through September, but with May not significant because of too few samples ($n = 2$).

For males, protein fraction 3 was significantly ($p < 0.05$) lower from May and September, but August and October were not different (**Figure 2**, **Supplemental Table 4**).

Plasma Biochemistry

The CCA for plasma biochemistry included all biochemical analytes. For those, the first canonical correlation was statistically significant ($F_1 = 1.72$, $p = 0.007$) and strongly correlated with a CCC of 0.76 between blood biochemical analytes and sex, age, and total length variables (**Supplemental Table 5**). The total variance explained by CCA1 was 56.9%. In order of CCA loading value, for plasma biochemical analytes, the first canonical dimension was most strongly influenced by BUN (loading strength = −0.70), creatinine (loading strength = −0.64), glucose (loading strength = −0.48), uric acid (loading strength = −0.47), lipase (loading strength = −0.45), phosphorus (loading strength = −0.42), LDH (loading strength = −0.36), iron (loading strength = −0.34), CPK (loading strength = −0.30), and potassium (loading strength = −0.26). For sex, age, and total length variables, the first dimension was comprised of total length (loading strength = 0.80), age (loading strength = 0.61), and sex (loading strength = 0.70). Significant results for plasma biochemistry pairwise tests and linear regressions are detailed in **Table 6**.

BUN was significantly ($p < 0.05$) higher in males than females and transitionals. There was a significant ($p < 0.05$) negative relationship between BUN and age for males, but not females, with a stronger correlation for males ($r^2 = 0.30$) than for all sexes combined ($r^2 = 0.22$). There was also a significant ($p < 0.05$) negative relationship between BUN and total length for females ($r^2 = 0.08$) and males ($r^2 = 0.34$), with males showing the strongest correlation—similar to that of all sexes combined ($r^2 = 0.37$). Creatinine was significantly ($p < 0.05$) higher in males than females and transitionals, and showed a negative relationship with total length and age. There was a significant ($p < 0.05$) negative relationship between creatinine and age for males, but

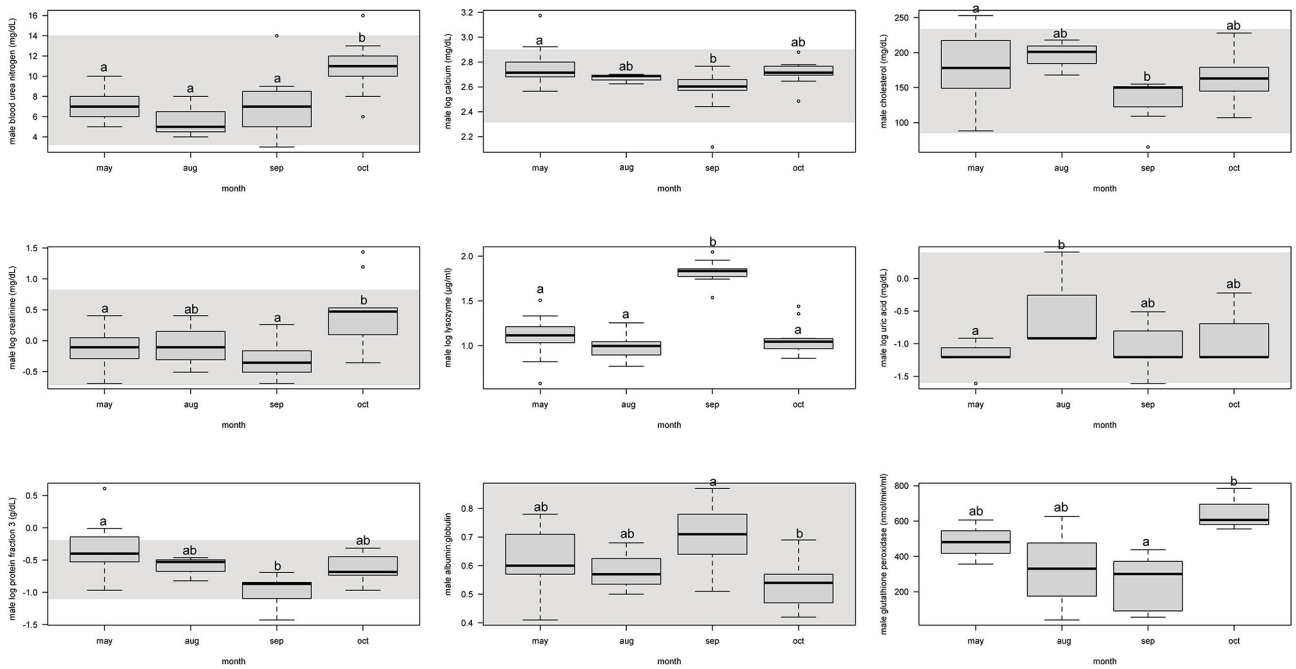

FIGURE 2 | Boxplots showing significant ($p < 0.05$) biochemistry analytes, plasma protein electrophoresis fractions, and immune system and oxidative stress analytes for male Atlantic Goliath Grouper (*Epinephelus itajara*) across sample collection months (May, August, September, October). There were only two samples from mid-July so we combined those into the month of August. Shading represents reference intervals. Different letters indicate significant difference. Range = vertical dashed lines, median = bold horizontal lines in box, first quartile = area below the line in the box, third quartile = area above the line in the box. The upper and lower ends of the nominal data range is defined as the respective interquartile distance (IQD) ± 1.5 IQD. Open circles = points that fall outside of this range.

not females, with a stronger correlation for males ($r^2 = 0.11$) than for all sexes combined ($r^2 = 0.08$). There was also a significant ($p < 0.05$) negative relationship between creatinine and total length for males ($r^2 = 0.18$), with this correlation lower in comparison to all sexes combined ($r^2 = 0.32$).

Glucose ($r^2 = 0.08$) and iron ($r^2 = 0.0.08$) were significantly ($p < 0.05$) negatively correlated with total length, albeit these correlations were weak. Lactate dehydrogenase, potassium, and uric acid all showed significant ($p < 0.05$) differences between sexes. Lactate dehydrogenase activity was significantly lower in transitionals than females, uric acid lower in males than transitionals, and potassium higher in males and females than transitionals ($p < 0.05$ in all cases). Significant ($p < 0.05$) negative relationships occurred for lipase and phosphorus with total length ($r^2_{(lipase)} = 0.17$, $r^2_{(phosphorus)} = 0.06$) and age ($r^2_{(lipase)} = 0.10$, $r^2_{(phosphorus)} = 0.06$).

While glucose is an important metabolite that should be considered, we chose to exclude glucose data from reference interval development because samples were negatively affected by sample processing delay, which could not be avoided in this study. The raw data were included so that future investigations could consider confounding effects of sample handling on glucose concentrations by optimizing handling techniques and analytical methodologies.

Calcium (loading strength = −0.15) and triglycerides (loading strength = 0.07) had low CCA loadings (<0.3), but significant ($p < 0.05$) differences between sexes did occur. Calcium was significantly ($p < 0.05$) lower in males than transitionals, while triglycerides were higher in females than males. No other differences or relationships were observed for plasma biochemistry analytes, including ALP, AST, cholesterol, CK, magnesium, sodium, and total bilirubin.

For females, alkaline phosphatase, BUN, creatinine, iron, and lipase significantly ($p < 0.05$) decreased from May through September (**Figure 1**, **Supplemental Table 4**). Aspartate aminotransferase, cholesterol, and uric acid significantly increased from the pre-spawning month of May to July, one of the peak spawning months, and then significantly decreased in the following months. Potassium significantly decreased from May through August, but then increased in September. Triglycerides significantly increased from May and July to August and September.

For males, BUN and creatinine significantly ($p < 0.05$) increased from September to October, but were similar to each other in previous months (**Figure 2**, **Supplemental Table 4**). Calcium and cholesterol significantly decreased between May and September, but was not different between other months. Uric acid significantly increased from May to August, but the other months were not different.

Immune System and Oxidative Stress

As described in Materials and Methods, CCA was not performed on factors related to immune system and oxidative stress; however, pairwise tests and linear regressions were conducted

TABLE 6 | Statistically significant plasma biochemistry analytes of Atlantic Goliath Grouper (*Epinephelus itajara*) categorized by sex (T, transitional; M, male; F, female) and by continuous variables of total length and age.

Plasma biochemical analyte	Sex (T*F)	(Sex M*F)	Sex (M*T)	Total length (cm)	Age (yr)
Blood urea nitrogen		*p = 0.034* *$n_{M/F}$ = 35/38* *Z = 2.46*	*p = 0.002* *$n_{M/T}$ = 35/4* *Z = 3.32*	**p < 0.001** **n = 85, r^2 = 0.37** **F = 50.33, df = 83**	**p < 0.001** **n = 83, r^2 = 0.22** **F = 23.54, df = 81**
Male				**p < 0.001** **n = 35, r^2 = 0.34** **F = 18.56, df = 33**	**p < 0.001** **n = 35, r^2 = 0.30** **F = 15.52, df = 33**
Female				**p = 0.04** **n = 38, r^2 = 0.08** **F = 4.34, df = 40**	
Calcium	**p = 0.042** **$n_{T/F}$ = 4/38** **Z = −2.38**				
Creatinine[a]		*p = 0.033* *$n_{M/F}$ = 35/38* *Z = 2.46*	*p = 0.002* *$n_{M/T}$ = 35/4* *Z = 3.32*	**p < 0.001** **n = 85, r^2 = 0.32** **F = 39.69, df = 83**	**p = 0.004** **n = 83, r^2 = 0.08** **F = 8.05, df = 81**
Male				**p = 0.008** **n = 35, r^2 = 0.18** **F = 8.05, df = 32**	**p = 0.031** **n = 35, r^2 = 0.11** **F = 5.06, df = 32**
Glucose[a]				**p = 0.004** **n = 85, r^2 = 0.08** **F = 7.87, df = 83**	
Iron				**p = 0.013** **n = 84, r^2 = 0.08** **F = 8.06, df = 82**	
Lactate dehydrogenase[a]	**p = 0.027** **$n_{T/F}$ = 4/38** **Z = −2.26**				
Lipase[b]				**p < 0.001** **n = 85, r^2 = 0.17** **F = 17.79, df = 83**	**p < 0.001** **n = 83, r^2 = 0.10** **F = 10.10, df = 81**
Phosphorus				**p = 0.002** **n = 84, r^2 = 0.06** **F = 6.57, df = 82**	**p = 0.004** **n = 83, r^2 = 0.06** **F = 6.50, df = 81**
Potassium	**p = 0.003** **$n_{T/F}$ = 4/38** **Z = −3.28**		*p < 0.001* *$n_{M/T}$ = 35/4* *Z = 3.82*		
Triglycerides[a]		**p = 0.012** **$n_{M/F}$ = 35/38** **Z = −2.80**			
Uric acid			**p = 0.032** **$n_{M/T}$ = 35/4** **Z = −2.48**		

[a]*Data were natural-log transformed.*

[b]*Data were square-root transformed.*

Where male and female categorical variables were significantly different, respective significant post-hoc linear regression results are shown. The p-value is given with adjusted r^2 value in parentheses. Blank cells indicate no significant difference or correlation. For sex, bolded values indicate the first sex in the pairwise comparison is lower and italicized values indicate the first sex is greater. For total length and age, negative relationships are bolded and positive relationships are italicized.

and significant results are detailed in **Table 7**. Reactive oxygen and nitrogen species were significantly ($p < 0.05$) higher in males than females, and SOD was higher in males than transitionals. Significant ($p < 0.05$) positive linear regressions, albeit fairly weak, occurred for lysozyme with total length ($r^2 = 0.13$) and age ($r^2 = 0.07$).

For females, SOD significantly ($p < 0.05$) decreased from May through July and August, and then increased in September (**Figure 1**, **Supplemental Table 4**). Glutathione peroxidase significantly decreased from May through September. Lysozyme significantly increased from May through September.

TABLE 7 | Statistically significant immune system and oxidative stress analytes of Atlantic Goliath Grouper (*Epinephelus itajara*) categorized by sex (T, transitional; M, male; F, female) and by continuous variables of total length and age.

Immune/oxidative stress analyte	Sex (T*F)	(Sex M*F)	Sex (M*T)	Total length (cm)	Age (yr)
Lysozyme[a]				$p < 0.001$ $n = 82, r^2 = 0.13$ $F = 13.41, df = 80$	$p = 0.010$ $n = 82, r^2 = 0.07$ $F = 6.93, df = 80$
Superoxide dismutase[a]			$p = 0.049$ $n_{M/T} = 51/5$ $Z = 2.30$		
Reactive oxygen/nitrogen species		$p = 0.039$ $n_{M/F} = 24/26$ $Z = 2.38$			

[a] *Data were natural-log transformed.*

Where male and female categorical variables were significantly different, respective significant post-hoc linear regression results are shown. The p-value is given with adjusted r^2 value in parentheses. Blank cells indicate no significant difference or correlation. For sex, bolded values indicate the first sex in the pairwise comparison is lower and italicized values indicate the first sex is greater. For total length and age, negative relationships are bolded and positive relationships are italicized.

For males, lysozyme significantly increased from August to September, but all other months did not differ from each other (**Figure 2**, **Supplemental Table 4**). Glutathione peroxidase significantly increased between September and October, but neither differed from May and August.

Pigmented Macrophage Aggregates

Pigmented macrophages formed dense, round to ovoid aggregates with variable yellow, golden brown, and dark brown pigmentation (**Figure 3**). Total length (range = 57–214 cm) was significantly positively correlated with PMA % area ($r^2 = 0.15$, $df = 51$, $p = 0.004$) and count ($z = 2.278$, $df = 51$, $p = 0.02$). Age (range = 4–18 yrs) and sex were not significant factors in pigmented macrophage aggregate abundance.

Other Histological Changes

The most consistent microscopical change observed was mild to severe, diffuse, indistinct, cytoplasmic vacuolation of hepatocytes, which were PAS positive and diastase sensitive, confirming glycogen content ($n = 164/183$, **Figures 3A–F**). Rare to infrequent changes (**Figures 4A–E**) included minimal to mild lymphocytic hepatitis ($n = 19/183$), periductal fibrosis ($n = 9/183$), lipid vacuolation of hepatocytes ($n = 7/183$), mild, mixed periductal and perivascular inflammation ($n = 4/183$), sinusoidal distension by round, clear, well-delineated spaces suggestive of gas bubbles that displace adjacent hepatocytes ($n = 4/183$, **Figures 4A,B**), and hepatocellular atrophy ($n = 3/183$). In many cases, liver sections contained rare to low numbers of mineralized granulomas ($n = 72/183$). Trematode eggs consisting of a tan, refractile capsule and internal miracidium were rarely to infrequently found within PMAs ($n = 30/183$, **Figure 3D**). Rare cross sections of encysted nematodes ∼120–150 μm in diameter and featuring a ridged, refractile cuticle, coelomyarian musculature, pseudocoelom, lateral cords, intestine, and developing gonads were present within the hepatic parenchyma ($n = 3/183$, **Figure 4C**). Within the gills, the most frequent changes were rare to low numbers of small, mineralized granulomas ($n = 11/45$), few monogeneans in interlamellar troughs ($n = 5/45$, **Figure 4D**), and rare, possible epitheliocystis inclusions ($n = 2/45$, **Figure 4E**).

DISCUSSION

This study reports novel data on a suite of health variables for Goliath Grouper in Florida waters that provide an essential baseline "snapshot" and an important adjunct tool for assessing population recovery. It also advances our knowledge about Goliath Grouper physiology and lays the groundwork for future research on the effects of various natural and human-induced stressors impinging on this species throughout its range where currently no such baseline health data exists. Given the abundance and novelty of data generated by this work, the focus of this current study lays on the animals and their intrinsic factors as no baseline health data of this kind exist to date on this or other Goliath Grouper populations throughout their range. Future investigations into temporal, spatial, and various other aspects of this population will benefit from the baseline data presented herein.

The influence of intrinsic (e.g., size, age, sex) and extrinsic (e.g., water temperature, habitat, diet, capture techniques) factors on various health variables is well-documented for many species [e.g., (53, 54)]. Intrinsic factors are of particular importance regarding their effects on blood data of fishes (55, 56). Identifying and understanding the influence of these factors, which are more variable and less controllable in wild than managed individuals of the same species, are essential for accurate data interpretation. This is often the biggest challenge in wildlife health assessment studies, given the many logistical challenges in sample acquisition (e.g., stress from capture, effects from anesthesia if applicable) and potential confounding factors related to animal handling and sample collection.

In our study, animal capture and handling techniques, as well as analytical methodologies, were consistent for all analyses, thus minimizing possible variability from extrinsic factors. Therefore, we were able to focus interpretation of health assessment data of Goliath Grouper on morphometrics and time period of sampling,

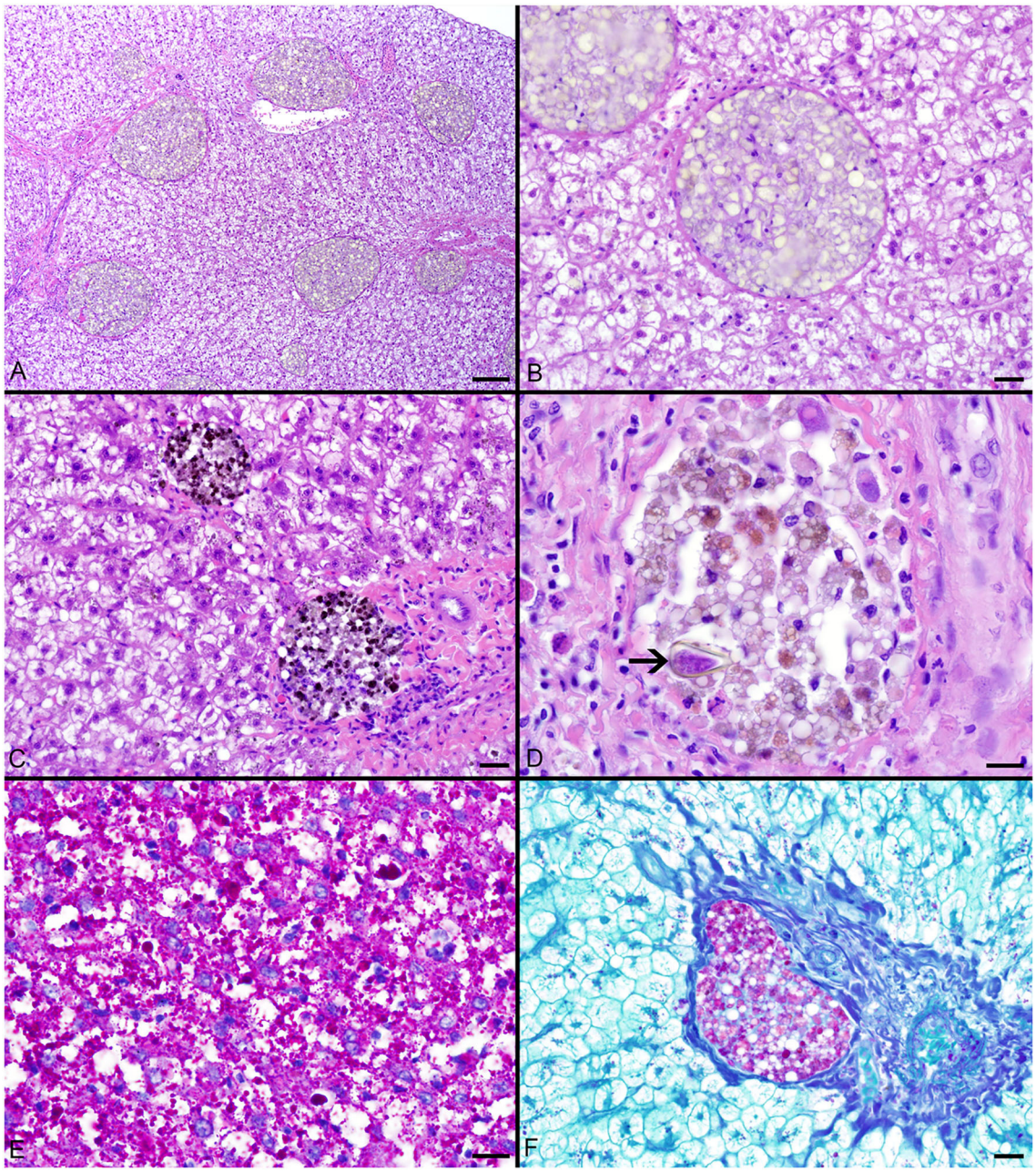

FIGURE 3 | (A–C) Hepatocellular vacuolation and variable pigmented macrophage appearance in livers of Atlantic Goliath Grouper (*Epinephelus itajara*). **(D)** High magnification of a pigmented macrophage aggregate shows the presence of a trematode egg (arrow). **(E)** Variably sized globules of intracytoplasmic glycogen within hepatocytes stain deep magenta with PAS. **(F)** Staining of the hepatocellular cytoplasm with PAS is lost after exposure to diastase, consistent with the presence of glycogen, while pigmented macrophage aggregates retain PAS staining, indicating the presence of glycoproteins, particularly lipofuscin. Scale Bars: A = 100 μm, B-C = 20 μm, D-E = 10 μm, F = 20 μm.

which are among the most important intrinsic and extrinsic factors, respectively. Wildlife health assessments typically include the establishment of reference intervals for blood analytes, and often require partitioning of data into effects from factors such as habitat, season, spawning condition, length, age, and sex when sufficient numbers of samples are available (45, 55, 57). The observed significant difference between males and females in terms of total length, but not age, (**Supplemental Figure 3**) in this study population needs to be taken into account when considering the discussion of sex differences of various analytes.

While there are a number of blood analyte studies of marine elasmobranchs and cultured marine teleosts [e.g., (10, 15–17,

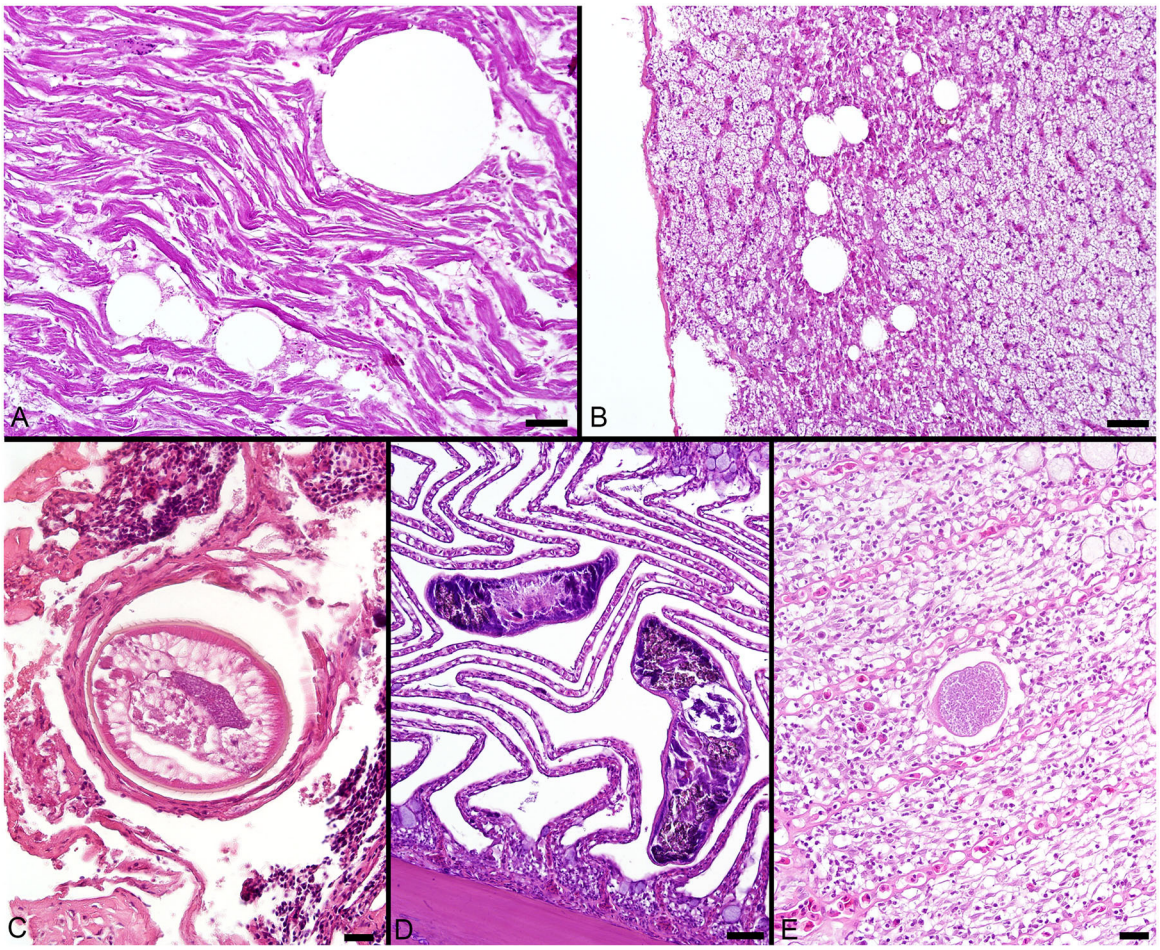

FIGURE 4 | (A) Large, round, clear spaces consistent with air bubbles multifocally displace myofibers in the heart of a fish that died during sampling. **(B)** Similar air bubbles obstruct hepatic sinusoids, resulting in congestion of sinusoids and disruption of the adjacent liver parenchyma. **(C)** Cross section through an encysted nematode adjacent to the liver capsule. **(D)** Monogenean parasites found within interlamellar spaces in the gill. **(E)** A single presumptive epitheliocystis inclusion within the gill lamella. Scale Bars: A-B = 50 μm, C = 20 μm, D = 50 μm, E = 20 μm.

58)], there are few available for wild populations of marine teleosts (59–61), with the data presented herein being the first for Goliath Grouper off Florida. Hence, it is both challenging and inappropriate to make comparisons among studies that use very different analytical methodologies for species that are vastly different physiologically.

Hematology data for Goliath Grouper showed more consistencies than differences across such intrinsic factors as length, age, and sex. PCV was comparable to other teleost species and fell mostly within reported ranges (62); however, the higher range in Goliath Grouper in this study exceeded the common upper limit of 45% PCV in teleosts, especially in males. This suggests either a subtle sex difference and/or effects from stress during capture and handling (e.g., release of catecholamines resulting in hemoconcentration and swelling of RBCs) (55). Only three fish showed evidence of mild erythroid regeneration, two of which with available PCV data were at the lower end of the reference interval (23 and 24%, respectively). This observation may reflect a recent response to either anemia or transiently lower PCV. Regarding leukogram findings in Goliath Grouper, lymphocytes were the predominant WBC type, which is similar to numerous fish species reported in the literature (55, 62). In addition, very low numbers of immature neutrophils were identified and hence are considered a normal finding in this species.

In contrast to the consistencies with hematology data, plasma biochemical analytes showed several correlations in juvenile and mature fish and monthly trends in mature males and females allowing for considerations regarding some physiological aspects of this species. However, since all correlations of blood analytes with morphometrics were overall weak in this study, these considerations are acceptable if interpreted with caution. Most correlations were observed with length and age concurrently, while few were associated with length alone (e.g., vitellogenin, glucose, iron) and only one with age alone (i.e., protein fraction 4). This shows that this population with an average age of 10.8

yrs (range = 4–19 yrs) and an average total length of 163 cm (range = 57–219 cm) likely represents individuals in phases of somatic growth. Albeit study animals were considered sexually mature, they presumably represent a younger population in the recovery stage, since the oldest Goliath Grouper reported to date was 37 yrs old, and, although the life span of Goliath Grouper remains unknown, this species is thought to live to much older ages (21, 32, 33). Goliath Grouper can also reach sizes of at least 250 cm total length (63), so a majority of individuals in this study population have not yet reached their full growth potential. While this study provides a baseline for morphometrical data in this recovering population of Goliath Grouper, to see if these patterns and relationships hold in older and larger Goliath Grouper that reach their full growth and age potential, continued state and federal protection from lethal extraction of this species is necessary. In addition, analyte differences (e.g., fraction 2 "presumptive albumin," BUN) in males and females may be associated with effects of sexual maturation or other associated dietary or physiological changes (e.g., tissue growth). Males mature at slightly smaller sizes and younger ages than females (21, 35), and the spawning season, when many samples were collected, is the only time of year where females would transition to males. Moreover, most individuals from this population transition within the mean age range of individuals in this study (25). The many variations of blood analytes in mature males and females across sampled months suggest sex-specific metabolic and physiological differences in pre-spawning and spawning months in this species.

Several identified differences in plasma biochemical analytes with length, age and/or sex indicate potential significance regarding tissue growth and metabolic and/or nutritional changes in a growing, reproductively active population. These analytes include BUN and phosphorus, which were negatively correlated with length and age, possibly indicating a difference in feeding intensity or protein metabolism. However, a recent meal before capture should also be considered. Higher BUN and creatinine in males compared to females and transitionals, but lower uric acid in males compared to transitionals suggest sex differences in muscle mass and/or protein/energy metabolism. This is further supported by variations in BUN, creatinine, and uric acid between adult males and females across sampled months. Although fish primarily excrete nitrogenous waste as ammonia across their gills, urea is still present in all fish, if only comprising a low percentage of nitrogenous waste, and is often of research interest, along with creatinine, in diagnosing gill or liver disease (64, 65). Future Goliath Grouper research should consider these patterns along with environmental toxicants in diagnosing disease or other negative health effects. The negative correlation of creatinine in males with length and age may suggest that smaller males possibly have higher muscle mass or reflect tissue growth. Creatinine, although similar to BUN in that it occurs in relatively small amounts in teleosts, can also be a good indicator of health and potential renal damage (64). The excretion and metabolism of nitrogenous wastes in fishes is still poorly understood and the clinical and physiological significance of these analytes still remains unknown (55). Observed correlations, sex differences, and monthly trends of other analytes including calcium, cholesterol, iron, enzymes, and potassium may suggest subtle differences or variations in feeding frequency/fasting, diet, metabolic rates, reproductive physiology, or nutritional state of individuals prior to sample collection. In this same Goliath Grouper study population, a concurrent study found that males and females consumed the same prey but at different frequencies, and there was a lot of variation in stomach fullness, with many individuals having empty stomachs at time of capture (66). Future research should directly consider diet and blood plasma analytes to better understand the relationship between these two factors.

The protein electrophoretogram of the Goliath Grouper consistently provided 6 fractions across the analyses of all study samples. The fraction migration was very similar to that seen in mammals with a dominant fraction 2 (presumptive albumin) and prominent fraction 5 (presumptive beta globulin migrating fraction). Previously, 6 and 5 fractions have been described in Rainbow Trout *Oncorhynchus mykiss* (67) and Koi *Cyprinus carpio* (68), respectively. Whereas, Koi electrophoretogram also had dominant fraction 2 and 5, Rainbow Trout samples exhibited a dominant fraction 3. Assigning specific protein fraction labels to fraction 1 to 6 is difficult as very few studies have been conducted on teleosts using modern protein electrophoresis methods. Changes in acute phase proteins in fish with natural or experimental infection and with inflammatory processes have been documented (69) so it is likely that many of these fractions represent proteins, metabolites, and hormones that function similarly to their mammalian counterparts. This conclusion is further supported by the observed variations in protein fractions across months in mature males and females. The negative correlation of fraction 2 with length and age is likely due to the observed significantly lower concentrations in females and the negative correlation for females by length. This sex difference corresponds with trends in other analytes, such as higher BUN and creatinine in males, suggesting differences in protein metabolism by sex. Fraction 4 is the one analyte showing a negative correlation only with age. This is an interesting contrast to the positive correlation of lysozyme with length and age, indicating a tendency to increase in growing Goliath Grouper, potentially suggestive of a greater capacity of the innate immune system and/or greater cumulative exposure to antigens as these fish age. Sex differences were observed through differences of higher SOD in males compared to transitionals, higher ROS/RNS species in males compared to females, and monthly trends of lysozyme, SOD, and GPx in mature males and females, possibly suggesting variations in energy balance, diet, or an association with circulating reproductive proteins.

Vitellogenin was positively correlated with length in females and negatively in males, with a substantial increase in mature females from pre-spawning through spawning months, showing an overt sex difference in a maturing population with growth and sexual development. For a protogynous hermaphrodite (i.e., change sex from female to male), like Goliath Grouper, it would also make sense that any males that transitioned from females would initially have high VTG that would then be reduced as the now-male continues to grow, since VTG is an egg yolk precursor protein normally found only in females (70, 71).

Individuals for this health assessment study are well within the range of sizes and ages of transitional females observed for this population, which were shown in a previous study to range from 108 to 191 cm TL and 4 to 12 yrs of age (25). However, circulating VTG can change rapidly, as has been shown in other grouper species (72), and so changes in plasma VTG during and after sex change in protogynous species should be a focus of future studies. Similar to the pattern in VTG, triglycerides were higher in females compared to males, suggesting a difference in circulating lipids and lipoproteins needed for vitellogenesis (73, 74). Although there was overlap in plasma VTG concentrations in males and females, these findings suggest possible utility of VTG as a non-invasive biomarker for sex determination in consideration of size of fish and month of sampling given that analytical techniques are available via ELISA and proteomics (72, 75). Since VTG did not correlate with any of the plasma protein fractions, traditional protein electrophoresis is presumably insensitive for the identification of VTG variations in this species. The baseline data presented herein may be useful for future studies of the effects of environmental estrogens and reproductive success (76, 77).

Hepatocyte morphology and appearance in fish liver tissue may vary considerably based on species, age, sex, season, nutritional status, and exposure to environmental pollutants (78). The histological changes described in this study reflect either typical, species-related observations, findings associated with life stage or active reproduction, or subclinical to clinically insignificant infectious and/or inflammatory processes. The observed positive correlation of PMA % area and count with total length shows an increase as these fish grow and mature, presumptively from continuous active inflammation (e.g., antigen exposure) and/or metabolic changes over time. The main finding of prominent vacuolation of hepatocytes was consistent with abundant, intracytoplasmic glycogen storage, which was confirmed by diastase sensitive PAS staining. Excess energy intake beyond basal metabolism and other demands is often stored in fish hepatocytes as glycogen and/or lipid and utilized in fasting situations (79–81). Fish species physiology and diet components may predispose the accumulation of glycogen vs. lipid (79–81). Glycogen accumulation is frequently seen in the hepatocytes of captive and occasionally wild fish, particularly trout and seabass, which may reflect carbohydrate rich diets, minimal energy expenditure for foraging, and/or poor utilization of dietary carbohydrates (78–81). Few fish had vacuolation consistent with lipid type which may suggest either mobilization of lipid from adipose stores (e.g., associated with reproduction), excess dietary lipid, or, much less likely, hepatocellular injury and dysfunction. Given the uniformity and diffuse nature of vacuolation and lack of associated tissue or cellular alterations, the vacuolation likely represents typical, physiological glycogen and/or lipid storage for this species (79, 80). Infectious agents, when present, were in very low numbers and likely had little to no impact on the fish. There was no indication of neoplastic or other proliferative processes in the samples.

Microscopical gas bubbles within hepatic sinusoids were suggestive of peracute gas supersaturation similar to decompression sickness rather than traditional gas bubble disease typically seen in fish exposed to excess dissolved gases in water (82). These changes were considered iatrogenic, and potentially due to capture methods bringing the fish up from depth, removal of surrounding pressure, and release of dissolved gases in the blood and highly vascularized tissues (82). This last result is highly important for consideration of the health of Goliath Grouper in the current catch-and-release fishery that has grown into a major non-consumptive enterprise in Florida (32), in addition to optimizing fish capture techniques for health assessment studies. Although a catch-and-release fishery is a far better alternative to that of an extractive fishery, stress and other patho-/physiological effects need to be further considered as this enterprise continues to expand, particularly related to barotrauma and how their dissolved blood gases shift out of solution, resulting in decompression-like embolisms as the fish is pulled rapidly to the surface. For research purposes, and to better understand these effects while minimizing the stress on the animal, improvement to sampling techniques, as we have done in the past, would involve venting swim bladders mid-water prior to surfacing to minimize barotrauma, and/or using descending devices to safely return fish back to depth where expanded gases can contract [e.g., (83)].

This study is the first to report a suite of various health indices of the Atlantic Goliath Grouper off the coasts of Florida, several of which indicate physiologically-relevant differences in length, age, and sex. It adds to the otherwise sparse literature of hematological, biochemical, immune function, and oxidative stress data in free-ranging populations of marine teleost fishes. It also demonstrates that non-invasive blood sampling provides an opportunity to obtain critical endpoint data and a vast amount of health information in a species in need of population and physiological monitoring. Future studies might include additional diagnostic methodologies (e.g., for parasitology, microbiology) that were beyond the scope of this study. Additionally, our study adds to existing data on high muscle and liver tissue concentrations of mercury in this species that are among the highest of any teleost in the Atlantic or Gulf of Mexico (31). The current study provides the necessary health baselines for which to compare health effects related to tissue contaminant concentrations. The health indices reported herein will be critical for monitoring dynamics and demographics of the Florida population and for understanding physiological responses to various stressors and to a changing global oceanic environment specifically relevant to this population and associated organisms within their ecosystem (1). Further, it will facilitate the identification of conservation problems and challenges pertaining to this species and its habitat and provide the opportunity for targeted conservation efforts by state and federal agencies.

DATA AVAILABILITY STATEMENT

The raw data supporting the conclusions of this article will be made available by the authors, without undue reservation.

ETHICS STATEMENT

The animal study was reviewed and approved by Florida State University Institutional Animal Care and Use Committee (IACUC) (protocol #s: 1106, 1411, and 1718).

AUTHOR CONTRIBUTIONS

CM: study design, setup and organization of sampling protocols, field collections and sample processing, preservation and transport, data analyses, histological and blood plasma sample analyses, manuscript writing and editing, and manuscript submission. JP: setup and organization of sampling protocols, blood plasma sample analyses, manuscript writing and editing, and reference intervals. NS: manuscript writing and editing, data interpretation, and blood film review. JS: histopathological analysis, and manuscript writing and editing. CC: blood plasma sample analyses, and manuscript writing and editing. FC and CK: manuscript writing and editing, sample collection protocol, and general project oversight. All authors contributed to the article and approved the submitted version.

FUNDING

Funding for this study was provided by U.S. National Oceanic and Atmospheric Administration grant NA11NMF4330123 awarded to CK and FC, Mote Marine Laboratory's Postdoctoral Research Fellowship to JP, Jack Winn Gramling Research Award in Marine Biology awarded to CM, and Florida State University Coastal and Marine Laboratory scholarships awarded to CM.

ACKNOWLEDGMENTS

We thank D. Murie for aging and histologically confirming sex for all individual fish. We thank W. Hawkins and R. Overstreet for their initial help with histopathological review. Countless volunteers assisted in sample collection, for which this study would not have been possible. Although not an exhaustive volunteer list, we thank S. Adams, S. Briegel, L. Bueno, C. Coppenrath, J. Cusick, R. Ellis, M. Faletti, C. Gabel, T. Grogan, A. Heil, M. Hruby, R. Johnson, B. Keller, J. Locascio, C. Matechik, R. McKenzie, D. McNutt, C. Mott, A. Nardelli, M. Newman, K. Newton, N. Ragbeer, T. Snow, C. Stallings, B. Talwar, B. Tezak, O. Tzadik, M. Violich, K. Wall, and N. Zenzola. We thank C. Dugan for her work in microscopic analysis and quantification of PMAs. We thank Rookery Bay National Estuarine Research Reserve for use of their facilities, which enabled sample collection in the Ten Thousand Islands.

SUPPLEMENTARY MATERIAL

The Supplementary Material for this article can be found online at: https://www.frontiersin.org/articles/10.3389/fvets.2020.00635/full#supplementary-material

REFERENCES

1. Wikelski M, Cooke SJ. Conservation physiology. *Trends Ecol Evol.* (2006) 21:38–46. doi: 10.1016/j.tree.2005.10.018
2. Cooke SJ, O'Connor CM. Making conservation physiology relevant to policy makers and conservation practitioners. *Conserv Lett.* (2010) 3:159–66. doi: 10.1111/j.1755-263X.2010.00109.x
3. Karesh WB, Cook RA. Applications of veterinary medicine to *in situ* conservation efforts. *Oryx.* (1995) 29:244–52. doi: 10.1017/S0030605300021232
4. Deem SL, Karesh WB, Weisman W. Putting theory into practice: wildlife health in conservation. *Conserv Biol.* (2001) 15:1224–33. doi: 10.1046/j.1523-1739.2001.00336.x
5. Deem S, Harris H. Health assessments. In: Manire CA, Norton TM, Stacy BA, Harms CA, Innis CJ, editors. *Sea Turtle Health and Rehabilitation*. Plantation, FL: J. Ross Publishing. (2017). p. 945–957.
6. Pauly D. Anecdotes and the shifting baseline syndrome of fisheries. *Trends Ecol Evol.* (1995) 10:430. doi: 10.1016/S0169-5347(00)89171-5
7. Knowlton N, Jackson JB. Shifting baselines, local impacts, and global change on coral reefs. *PLoS Biol.* (2008) 6:e54. doi: 10.1371/journal.pbio.0060054
8. Wedemeyer GA, Yasutake WT. *Clinical Methods for Assessment of the Effect of Enviromental Stress on Fish Health*. (1977) New York, NY: Technical papers of the U.S Fish and Wildlife Service.
9. Peres H, Santos S, Oliva-Teles A. Selected plasma biochemistry parameters in gilthead seabream (*Sparus aurata*) juveniles. *J Appl Ichthyol.* (2013) 29:630–6. doi: 10.1111/j.1439-0426.2012.02049.x
10. Peres H, Santos S, Oliva-Teles A. Blood chemistry profile as indicator of nutritional status in European seabass (*Dicentrarchus labrax*). *Fish Physiol Biochem.* (2014) 40:1339–47. doi: 10.1007/s10695-014-9928-5
11. Sandnes K, Lie Ø, Waagbø R. Normal ranges of some blood chemistry parameters in adult farmed Atlantic salmon, *Salmo salar*. *J Fish Biol.* (1988) 32:129–36. doi: 10.1111/j.1095-8649.1988.tb05341.x
12. Hrubec TC, Cardinale JL, Smith SA. Hematology and plasma chemistry reference intervals for cultured tilapia (Oreochromis hybrid). *Vet Clin Pathol.* (2000) 29:7–12. doi: 10.1111/j.1939-165X.2000.tb00389.x
13. Knowles S, Hrubec TC, Smith SA, Bakal R. Hematology and plasma chemistry reference intervals for cultured shortnose sturgeon (*Acipenser brevirostrum*). *Vet Clin Pathol.* (2006) 35:434–40. doi: 10.1111/j.1939-165X.2006.tb00160.x
14. Matsche MA, Arnold J, Jenkins E, Townsend H, Rosemary K. Determination of hematology and plasma chemistry reference intervals for 3 populations of captive Atlantic sturgeon (*Acipenser oxyrinchus oxyrinchus*). *Vet Clin Pathol.* (2014) 43:387–96. doi: 10.1111/vcp.12174
15. Harms C, Ross T, Segars A. Plasma biochemistry reference values of wild bonnethead sharks, *Sphyrna tiburo*. *Vet Clin Pathol.* (2002) 31:111–5. doi: 10.1111/j.1939-165X.2002.tb00289.x
16. Cain DK, Harms CA, Segars A. Plasma biochemistry reference values of wild-caught southern stingrays (Dasyatis americana). *J Zoo Wildlife Med.* (2004) 35:471–6. doi: 10.1638/03-107
17. Haman KH, Norton TM, Thomas AC, Dove A. Baseline health parameters and species comparisons among free-ranging Atlantic sharpnose (*Rhizoprionodon terraenovae*), bonnethead (*Sphyrna tiburo*), and spiny dogfish (*Squalus acanthias*) sharks in Georgia, Florida, and Washington, USA. *J Wildlife Dis.* (2012) 48:295–306. doi: 10.7589/0090-3558-48.2.295
18. Satheeshkumar P, Ananthan G, Senthilkumar D, Khan AB, Jeevanantham K. Comparative investigation on haematological and biochemical studies on wild marine teleost fishes from Vellar estuary, southeast coast of India. *Comparative Clin Pathol.* (2012) 21:275–81. doi: 10.1007/s00580-010-1091-5
19. Fazio F, Marafioti S, Arfuso F, Piccione G, Faggio C. Comparative study of the biochemical and haematological parameters of four wild Tyrrhenian fish species. *Vet Med.* (2013) 58:576–81. doi: 10.17221/7139-VETMED
20. Bertoncini AA, Aguilar-Perera A, Barreiros J, Craig MT, Ferreira B, Koenig C. *Epinephelus Itajara* (errata version published in 2019). *The IUCN Red List of Threatened Species 2018:T195409A145206345* (2018). Available

online at: https://www.iucnredlist.org/species/195409/145206345 (accessed May 08, 2020).
21. Bullock LH, Murphy MD, Godcharles MF, Mitchell M. Age, growth, and reproduction of jewfish Epinephelus itajara in the eastern Gulf of Mexico. *Fishery Bull.* (1992) 90:243–9.
22. Sadovy Y, Eklund A-M. Synopsis of biological data on the Nassau grouper, *Epinephelus striatus* (Bloch,1792) and the Jewfish E. Itajara (Lichtenstein, 1822). US Department Commer. NOAA Technical Report NMFS146, and FAO Fisheries Synopsis 157, Seattle, Washington (1999), p. 65.
23. Francesconi J, Schwartz F. Jewfish, *Epinephelus itajara*, from North Carolina, with range correction and body comparisons. *J Elisha Mitchell Sci Soc*. (2000) 116:167–70. Available online at: https://www.jstor.org/stable/24335506?seq=1#metadata_info_tab_contents
24. Ferreira BP, Hostim-Silva M, Bertoncini AA, Coleman FC. Atlantic goliath grouper - *Epinephelus itajara.* In Sadovy de Mitcheson Y, Colin PL, editors. *Reef Fish Spawning Aggregations: Biology, Research and Management*. Dordrecht: Springer (2012). p. 417–422.
25. Koenig C, Coleman F, Malinowski C, Ellis R, Murie D, Parkyn D, et al. *Regional Age Structure, Reproductive Biology and Trophic Patterns of Adult Goliath Grouper in Florida*. St. Petersburg, FL: MARFIN Project (NA11NMF4330123 NOAA/NMFS Final Report (2016).
26. Koenig C, Bueno L, Coleman F, Cusick J, Ellis R, Kingon K, et al. Diel, lunar, and seasonal spawning patterns of the Atlantic goliath grouper, *Epinephelus itajara*, off Florida, United States. *Bull Marine Sci.* (2016) 93:391–406. doi: 10.5343/bms.2016.1013
27. Malinowski C, Coleman F, Koenig C, Locascio J, Murie D. Are Atlantic goliath grouper, *Epinephelus itajara*, establishing more northerly spawning sites? Evidence from the northeast Gulf of Mexico. *Bull Marine Sci.* (2019) 95:371–91. doi: 10.5343/bms.2018.0062
28. Bueno LS, Bertoncini AA, Koenig CC, Coleman FC, Freitas MO, Leite JR, et al. Evidence for spawning aggregations of the endangered Atlantic goliath grouper *Epinephelus itajara* in southern Brazil. *J Fish Biol*. (2016) 89:876–89. doi: 10.1111/jfb.13028
29. SEDAR (SouthEast Data, Assessment, and Review cooperative). *SEDAR 23 Stock Assessment Report. Southeastern U. S. Goliath Grouper*. (2011). Available online at: http://sedarweb.org/sedar-23-final-goliath-grouper-stock-assessment-report.
30. SEDAR (SouthEast Data, Assessment, and Review cooperative). *SEDAR 47 Stock Assessment Report. Southeastern U. S. Goliath Grouper*. (2016). Available online at: http://sedarweb.org/sedar-47-final-stock-assessment-report-southeastern-us-goliath-grouper.
31. Malinowski C. High mercury concentrations in Atlantic Goliath Grouper: spatial analysis of a vulnerable species. *Mar Pollut Bull*. (2019) 143:81–91. doi: 10.1016/j.marpolbul.2019.04.006
32. Koenig CC, Coleman FC, Malinowski CR. Atlantic Goliath Grouper of Florida: to fish or not to fish fisheries. *Fisheries*. (2020) 45:20–32. doi: 10.1002/fsh.10349
33. Koenig CC, Coleman FC, Kingon K. Pattern of recovery of the goliath grouper Epinephelus itajara population in the southeastern US. *Bull Mar Sci.* (2011) 87:891–911. doi: 10.5343/bms.2010.1056
34. Blaxhall PC. The haematological assessment of the health of freshwater fish: a review of selected literature. *J Fish Biol.* (1972) 4:593–604. doi: 10.1111/j.1095-8649.1972.tb05704.x
35. Koenig CC, Coleman FC, Eklund AM, Schull J, Ueland J. Mangroves as essential nursery habitat for goliath grouper (*Epinephelus itajara*). *Bull Mar Sci.* (2007) 80:567–85. Available online at: https://www.ingentaconnect.com/content/umrsmas/bullmar/2007/00000080/00000003/art0000010
36. Murie DJ, Parkyn DC, Koenig CC, Coleman FC, Schull J, Frias-Torres S Evaluation of finrays as a non-lethal ageing method for protected goliath grouper *Epinephelus itajara*. *Endanger Species Res.* (2009) 7:213–20. doi: 10.3354/esr00146
37. Walsh CJ, Leggett SR, Carter BJ, Colle C. Effects of brevetoxin exposure on the immune system of loggerhead sea turtles. *Aquat Toxicol.* (2010) 97:293–303. doi: 10.1016/j.aquatox.2009.12.014
38. Klaren W, Gadupudi G, Wels B, Simmons D, Olivier A, Robertson L. Progression of micronutrient alteration and hepatotoxicity following acute PCB126 exposure. *Toxicology.* (2015) 338:1–7. doi: 10.1016/j.tox.2015.09.004
39. Pawlak M, Baugé E, Lalloyer F, Lefebvre P, Staels B. Ketone body therapy protects from lipotoxicity and acute liver failure upon Ppar α deficiency. *Mol Endocrinol*. (2015) 29:1134–43. doi: 10.1210/me.2014-1383
40. Steinel NC, Bolnick DI. Melanomacrophage centers as a histological indicator of immune function in fish and other poikilotherms. *Front Immunol*. (2017) 8:827. doi: 10.3389/fimmu.2017.00827
41. Manera M, Sayyaf Dezfuli B, DePasquale JA, Giari L. Pigmented macrophages and related aggregates in the spleen of european sea bass dosed with heavy metals: ultrastructure and explorative morphometric analysis. *Microsc Res Tech*. (2018) 81:351–64. doi: 10.1002/jemt.22986
42. Borucinska J, Kotran K, Shackett M, Barker T. Melanomacrophages in three species of free-ranging sharks from the northwestern Atlantic, the blue shark *Prionacae glauca* (L.), the shortfin mako, Isurus oxyrhinchus Rafinesque, and the thresher, *Alopias vulpinus* (Bonnaterre). *J Fish Dis*. (2009) 32:883–91. doi: 10.1111/j.1365-2761.2009.01067.x
43. Rasband W. *ImageJ: Image Processing and Analysis in Java*. Astrophysics Source Code Library (2012).
44. Schwindt AR, Truelove N, Schreck CB, Fournie JW. Quantitative evaluation of macrophage aggregates in brook trout Salvelinus fontinalis and rainbow trout Oncorhynchus mykiss. *Dis Aquatic Organisms*. (2006) 68:101–13. doi: 10.3354/dao068101
45. Friedrichs KR, Harr KE, Freeman KP, Szladovits B, Walton RM, Barnhart KF, et al. ASVCP reference interval guidelines: determination of *de novo* reference intervals in veterinary species and other related topics. *Vet Clin Pathol.* (2012) 41:441–53. doi: 10.1111/vcp.12006
46. Mirghaed AT, Ghelichpour M, Hoseini SM, Amini K. Hemolysis interference in measuring fish plasma biochemical indicators. *Fish Physiol Biochem.* (2017) 43:1143–51. doi: 10.1007/s10695-017-0359-y
47. Lambert ZV, Durand RM. Some precautions in using canonical analysis. *J Mark Res*. (1975) 12:468–75. doi: 10.1177/002224377501200411
48. Thompson B. *Canonical Correlation Analysis: Uses and Interpretation*. Beverly Hills, CA: Sage (1984).
49. Liu J, Drane W, Liu X, Wu T. Examination of the relationships between environmental exposures to volatile organic compounds and biochemical liver tests: application of canonical correlation analysis. *Environ Res*. (2009) 109:193–99. doi: 10.1016/j.envres.2008.11.002
50. Holm S. A simple sequentially rejective multiple test procedure. *Scand J Stat*. (1979) 65–70. doi: 10.2307/4615733
51. Evans DW, Dodoo DK, Hanson PJ. Trace element concentrations in fish livers: implications of variations with fish size in pollution monitoring. *Mar Pollut Bull.* (1993) 26:329–34. doi: 10.1016/0025-326X(93)90576-6
52. Hrubec TC, Smith SA, Robertson JL. Age-related changes in hematology and plasma chemistry values of hybrid striped bass (Morone chrysops× Morone saxatilis). *Vet Clin Pathol.* (2001) 30:8–15. doi: 10.1111/j.1939-165X.2001.tb00249.x
53. Quaglietta L, Mira A, Boitani L. Extrinsic and intrinsic factors affecting the daily rhythms of a semiaquatic carnivore in a Mediterranean environment. *Hystrix Italian J Mammal.* (2018) 29:128–36. doi: 10.4404/hystrix-00022-2017
54. Sequeira AM, Rodríguez J, Eguíluz VM, Harcourt R, Hindell M. Convergence of marine megafauna movement patterns in coastal and open oceans. *Proc Natl Acad Sci USA*. (2018) 115:3072–7. doi: 10.20350/digitalCSIC/8525
55. Campbell T. Hematology of Fish. In: Thrall MA, Weiser G, Allison R, Campbell T, editors. *Veterinary Hematology and Clinical Chemistry*, 2nd ed. Ames, IA: John Wiley & Sons Inc., (2012). p. 298–312.
56. Satheeshkumar P, Ananthan G, Kumar DS, Jagadeesan L. Haematology and biochemical parameters of different feeding behaviour of teleost fishes from Vellar estuary, India. *Comparative Clin Pathol*. (2012) 21:1187–91. doi: 10.1007/s00580-011-1259-7
57. Haws TG, Goodnight CJ. Some aspects of the hematology of two species of catfish in relation to their habitats. *Physiol Zool.* (1962) 35:8–17. doi: 10.1086/physzool.35.1.30152708
58. Fazio F. Fish hematology analysis as an important tool of aquaculture: a review. *Aquaculture*. (2019) 500:237–42. doi: 10.1016/j.aquaculture.2018.10.030
59. Tavares-Dias M, Moraes F. Haematological and biochemical reference intervals for farmed channel catfish. *J Fish Biol*. (2007) 71:383–8. doi: 10.1111/j.1095-8649.2007.01494.x

60. Mozanzadeh MT, Yaghoubi M, Yavari V, Agh N, Marammazi JG. Reference intervals for haematological and plasma biochemical parameters in sobaity sea bream juveniles (*Sparidentex hasta*, Valenciennes 1830). *Comparative Clin Pathol*. (2015) 24:1501–7. doi: 10.1007/s00580-015-2107-y
61. Collins S, Dornburg A, Flores JM, Dombrowski DS, Lewbart G. A comparison of blood gases, biochemistry, and hematology to ecomorphology in a health assessment of pinfish (*Lagodon rhomboides*). *PeerJ*. (2016) 4:e2262. doi: 10.7717/peerj.2262
62. Hrubec T, Smith S. Hematology of Fish. In: Feldman B, Zinkl J, Jain N, editors. *Schalm's Veterinary Hematology* 5th ed. Philadelphia: Lippincott Williams & Wilkins. (2000). p. 1120–5.
63. Heemstra, P. C., Randall, J., E. (1993). Groupers of the world. *FAO Fisheries synopsis* 16:I.
64. Nelson K, Jones J, Jacobson S, Reimschuessel R. Elevated blood urea nitrogen (BUN) levels in goldfish as an indicator of gill dysfunction. *J Aquatic Animal Health*. (1999) 11:52–60. doi: 10.1577/1548-8667(1999)011<0052:EBUNBL>2.0.CO;2
65. Mensinger AF, Walsh PJ, Hanlon RT. Blood biochemistry of the oyster toadfish. *J Aquatic Animal Health*. (2005) 17:170–6. doi: 10.1577/H04-021.1
66. Malinowski C. *Spawning Patterns, Trophic Ecology, and Toxicology: Conservation Related Research of an Iconic Reef Fish, the Atlantic Goliath Grouper*. Dissertation, Florida State University (2019).
67. Manera M, Britti D. Assessment of serum protein fractions in rainbow trout using automated electrophoresis and densitometry. *Vet Clin Pathol*. (2008) 37:452–6. doi: 10.1111/j.1939-165X.2008.00070.x
68. Christiansen EF, Cray C, Lewbart GA, Harms CA. Plasma protein electrophoresis and acute phase proteins in koi carp (*Cyprinus carpio*) following exploratory coeliotomy. *J Exotic Pet Med*. (2015) 24:76–83. doi: 10.1053/j.jepm.2014.11.008
69. Bayne CJ, Gerwick L. The acute phase response and innate immunity of fish. *Dev Comparative Immunol*. (2001) 25:725–43. doi: 10.1016/S0145-305X(01)00033-7
70. Arukwe A, Goksøyr A. Eggshell and egg yolk proteins in fish: hepatic proteins for the next generation: oogenetic, population, and evolutionary implications of endocrine disruption. *Comparative Hepatol*. (2003) 2:4. doi: 10.1186/1476-5926-2-4
71. Crump KL, Trudeau VL. Mercury-induced reproductive impairment in fish. *Environ Toxicol Chem*. (2009) 28:895–907. doi: 10.1897/08-151.1
72. Heppell S, Sullivan C. Gag (*Mycteroperca microlepis*) vitellogenin: purification, characterization and use for enzyme-linked immunosorbent assay (ELISA) of female maturity in three species of grouper. *Fish Physiol Biochem*. (1999) 20:361–74. doi: 10.1023/A:1007730816797
73. Fremont L, Riazi A. Biochemical analysis of vitellogenin from rainbow trout (*Salmo gairdneri*): fatty acid composition of phospholipids. *Reprod Nutr Dév*. (1988) 28:939–52. doi: 10.1051/rnd:19880607
74. Garcia-Garrido L, Muñoz-Chapuli R, De Andres, A. Serum cholesterol and triglyceride levels in *Scyliorhinus canicula* (L.) during sexual maturation. *J Fish Biol*. (1990) 36:499–509. doi: 10.1111/j.1095-8649.1990.tb03552.x
75. Om AD, Jasmani S, Ismail N, Yeong S, Abol-Munafi A. Application MALDI TOF on protein identification of vitellogenin in giant grouper (*Epinephelus lanceolatus*). *Fish Physiol Biochem*. (2013) 39:1277–86. doi: 10.1007/s10695-013-9782-x
76. Sumpter JP. Feminized responses in fish to environmental estrogens. *Toxicol Lett*. (1995) 82:737–42. doi: 10.1016/0378-4274(95)03517-6
77. Mills LJ, Gutjahr-Gobell RE, Horowitz DB, Denslow N, Chow MC, Gerald EZ. Relationship between reproductive success and male plasma vitellogenin concentrations in cunner, *Tautogolabrus adspersus*. *Environ Health Perspectives*. (2003) 111:93–100. doi: 10.1289/ehp.5531
78. Evensen Ø. Liver. In: Ferguson HW, editor. *Systemic Pathology of Fish, 2nd ed*, London: Scotian Press. (2006). p.201–17.
79. Wolf JC, Wolfe MJ. A brief overview of nonneoplastic hepatic toxicity in fish. *Toxicol Pathol*. (2005) 33:75–85. doi: 10.1080/01926230590890187
80. Enes P, Panserat S, Kaushik S, Oliva-Teles A. Nutritional regulation of hepatic glucose metabolism in fish. *Fish Physiol Biochem*. (2009) 35:519–39. doi: 10.1007/s10695-008-9259-5
81. Wolf JC, Baumgartner WA, Blazer VS, Camus A. Nonlesions, misdiagnoses, missed diagnoses, and other interpretive challenges in fish histopathology studies: a guide for investigators, authors, reviewers, and readers. *Toxicol Pathol*. (2015) 43:297–325. doi: 10.1177/0192623314540229
82. Speare D. Disorders associated with exposure to excess dissolved gasses. In: Leatherland JF, Woo PTK (eds) *Fish Deseases and Disorders Vol. 2: Noninfectious Disorders*, 2nd ed. Wallingford: CABI Publishing. (2010). p. 342–56. doi: 10.1079/9781845935535.0342
83. Runde BJ, Buckel JA. Descender devices are promising tools for increasing survival in deepwater groupers. *Mar Coast Fish*. (2018) 10:100–17. doi: 10.1002/mcf2.10010

Conflict of Interest: The authors declare that the research was conducted in the absence of any commercial or financial relationships that could be construed as a potential conflict of interest.

Copyright © 2020 Malinowski, Perrault, Coleman, Koenig, Stilwell, Cray and Stacy. This is an open-access article distributed under the terms of the Creative Commons Attribution License (CC BY). The use, distribution or reproduction in other forums is permitted, provided the original author(s) and the copyright owner(s) are credited and that the original publication in this journal is cited, in accordance with accepted academic practice. No use, distribution or reproduction is permitted which does not comply with these terms.

frontiers in Veterinary Science

ORIGINAL RESEARCH
published: 29 September 2020
doi: 10.3389/fvets.2020.00637

Concentrations of Retinol and α-Tocopherol in Tissue Samples From Anna's Hummingbirds (*Calypte anna*)

Stephanie M. Diao[1], Robert H. Poppenga[2], Gwendolyne Gonzales Alarcio[2], Janet E. Foley[1], Ruta R. Bandivadekar[1], Linda S. Aston[2] and Lisa A. Tell[1]**

[1] Department of Medicine and Epidemiology, School of Veterinary Medicine, University of California, Davis, Davis, CA, United States, [2] California Animal Health and Food Safety Laboratory System, University of California, Davis, Davis, CA, United States

OPEN ACCESS

Edited by:
Robert James Ossiboff, College of Veterinary Medicine, University of Florida, United States

Reviewed by:
Karyn Bischoff, Cornell University, United States
Lisa A. Murphy, University of Pennsylvania, United States

***Correspondence:**
Robert H. Poppenga
rhpoppenga@ucdavis.edu
Lisa A. Tell
latell@ucdavis.edu

Specialty section:
This article was submitted to Zoological Medicine, a section of the journal Frontiers in Veterinary Science

Received: *01 July 2020*
Accepted: *04 August 2020*
Published: *29 September 2020*

Citation:
Diao SM, Poppenga RH, Gonzales Alarcio G, Foley JE, Bandivadekar RR, Aston LS and Tell LA (2020) Concentrations of Retinol and α-Tocopherol in Tissue Samples From Anna's Hummingbirds (Calypte anna). Front. Vet. Sci. 7:637. doi: 10.3389/fvets.2020.00637

Retinol (vitamin A) and α-tocopherol (vitamin E) concentrations were measured in tissue samples (liver, heart, pectoral muscle, and brain) from Anna's Hummingbirds (*Calypte anna*). Hummingbirds were after-hatch year birds that were sourced from various rehabilitation centers throughout California. Tissues samples were analyzed using high-performance liquid chromatography (HPLC). Minimum, maximum, mean, standard deviation (SD), and median ppm concentrations were calculated for each vitamin and tissue sample type. A novel analytical method was developed to analyze small mass tissue samples, with the smallest sample mass being 0.05 g for which analysis can be performed. Mean ± standard deviation (SD) concentrations of retinol in hummingbird livers, hearts, and pectoral muscle samples were 269.0 ± 216.9 ppm, 1.8 ± 2.2 ppm, and 0.3 ± 0.1 ppm, respectively. Mean ± SD α-tocopherol concentrations were 6.9 ± 4.6 ppm, 5.5 ± 4.0 ppm, 3.7 ± 2.2 ppm, and 9.1 ± 3.2 ppm for liver, heart, pectoral muscle, and brain samples, respectively. Vitamin concentrations from varying tissue types were compared to determine which were best associated with liver concentrations, the most commonly analyzed tissue for these vitamins. For both retinol and α-tocopherol, heart samples were most strongly associated with the liver samples. The results of this study provide baseline retinol and α-tocopherol concentrations in different tissue types from Anna's hummingbirds. These baseline values may be utilized in conservation efforts to avoid hypervitaminosis and hypovitaminosis of rehabilitated and/or captive hummingbirds by providing guidelines for nutritional targets which could be assessed on post-mortem examinations. Post-mortem examination of birds and measurement of vitamin concentrations in tissues may allow for dietary changes that aid captive hummingbirds.

Keywords: retinol, α-tocopherol, hummingbird, analytical method, vitamin concentrations, tissue samples

INTRODUCTION

As avian pollinators, hummingbirds play an important role in maintaining the health of a diverse ecosystem (1). Unfortunately, at least 26 hummingbird species are threatened (2). With a decrease in pollinators, there is an increased risk of crop failure and loss of biodiversity (2). Thus, successful rehabilitation of injured or sick hummingbirds and maintenance of healthy captive populations have the potential to be important from a holistic perspective.

Nutritional disorders are the most common non-infectious type of disease described in captive hummingbirds (3). Since hummingbirds have a unique diet of insects and nectar, replicating a hummingbird's diet can be quite difficult. This becomes an issue when hummingbirds enter rehabilitation centers and are fed a prepared commercial diet for other avian species. Many prepared diets are formulated based on the nutritional requirements of poultry (4) which can lead to hypervitaminosis or hypovitaminosis when used for other avian species. Establishing baseline vitamin concentrations in hummingbird tissues may help with formulating more appropriate diets or assess the adequacy of a given diet. However, little research has been conducted on hummingbirds' nutrient requirements (5).

Retinol (vitamin A) and α-tocopherol (vitamin E) in particular may be essential for hummingbird health during the rehabilitation process. Retinol is needed for normal metabolism, cell differentiation, and growth; α-tocopherol is an antioxidant that helps remove free radicals produced from lipid oxidation, metabolism, and tissues under stressful conditions (6, 7).

Analytical methods for measuring tissue vitamin concentrations exist for a variety of species, although most current methods require at least 0.25 g of tissue for α-tocopherol analysis (8) and 0.5 g of liver for retinol analysis[1]. Given that the average Anna's Hummingbird (*Calypte anna*) total body mass is only 4–4.5 g[2], obtaining an adequate amount of tissue for vitamin analysis would be challenging, especially for liver and heart samples which weigh on average 0.07 and 0.09 g, respectively (**Supplemental Table 1**).

The objective of this study was to establish baseline retinol and α-tocopherol tissue concentrations in the Anna's Hummingbird, *C. anna*, and compare vitamin concentrations in different tissues with liver sample concentrations. To achieve this goal, a high-performance liquid chromatography (HPLC) analytical method able to quantify retinol and α-tocopherol in small mass tissue samples (as little as 0.05 g) was developed and validated. This new analytical method was used to quantify retinol and α-tocopherol concentrations in liver, heart, pectoral muscle, and brain samples from deceased hummingbirds.

[1]CAHFS internal procedure, effective date 12/02/2018.

[2]Cornell Lab of Ornithology Birds of the World. Anna's Hummingbird (2020).

MATERIALS AND METHODS

Tissue Samples

Carcasses of 40 Anna's Hummingbirds were obtained from the following wildlife rehabilitation centers: Lindsay Wildlife Center, California Wildlife Center, Santa Barbara Wildlife Care Network, and Wetlands and Wildlife Care Center of Orange County. Only after-hatch year (AHY) birds were utilized in this study. Sex, species, and age were determined as described by The North American Banders' Manual for Hummingbirds (9). Whole brain, liver, heart, and pectoral muscle samples were collected from the carcasses using Iris scissors. Tissues were immediately placed in individual 1.5 mL cryogenic tubes (Thermo Fisher Scientific, Waltham, WA) and stored at −20°C. Tissue (liver, heart, pectoral muscle) samples from 20 hummingbirds (10 females and 10 males) were used for the retinol analysis and tissue (liver, heart, pectoral muscle, and brain) samples from 20 other hummingbirds (10 females and 10 males) were used for α-tocopherol analysis at the California Animal Health and Food Systems Laboratory (CAHFS) in Davis, California. Care was taken to ensure that samples were exposed to the least amount of light possible. Permission for obtaining the hummingbird carcasses for scientific study was approved by the United States Fish and Wildlife Service (Permit: MB55944B-2) and the California Department of Fish and Wildlife (Permit: SC-013066).

Chemicals and Reagents

Retinol (all-trans-retinol, >97% purity) and α-tocopherol (DL-alpha-tocopherol, >97% purity), butylated hydroxytoluene (BHT), and ascorbic acid were purchased from Sigma-Aldrich (St. Louis, MO). BHT and ascorbic acid were used as antioxidants for vitamins A and E, respectively. Ascorbic acid (1%) in ethanol was prepared by dissolving 1.0 g of ascorbic acid in 100 mL of ethanol. BHT (1%) in alcohol was prepared by dissolving 1.0 g of BHT in 100 mL of methanol (used for long term storage of retinol stock standard solutions) or ethanol (used during the α-tocopherol extraction process). HPLC grade methanol, pesticide grade petroleum ether, and potassium hydroxide (KOH) pellets were purchased from Thermo Fisher Scientific (Waltham, WA). Saturated KOH was prepared by adding KOH pellets to a volume of water until precipitation persists. Optima grade, Koptec Pure Ethanol-200-proof was purchased from Decon Laboratories, Inc. (King of Prussia, PA). 18 MΩ water (Aqua Solutions Water Purification System (Jasper, GA) was used throughout the study.

Standard Preparations

The retinol stock standard solution of 1,000 μg/mL was prepared by weighing 25 mg into a 25 mL amber volumetric flask and bringing up to volume with 1% BHT in methanol. All intermediate standards of retinol were made by serial dilutions in 1% BHT in methanol. The α-tocopherol stock standard 1,000 μg/mL was made by weighing 50 mg neat material into a 50 mL volumetric flask and bringing up to volume with methanol. All intermediate standards were made by serial dilutions in methanol. Stock standard solutions and intermediate solutions for both vitamins were stored at −20°C in amber vials to protect from light-induced oxidation. Calibration

curves were prepared fresh daily, in methanol, from the intermediate standards.

Chromatographic Conditions

An Agilent 1200 high-performance liquid chromatography (HPLC) system equipped with 1260 Infinity FLD fluorescence detector (Agilent, Santa Clara, CA) and ChemStation software to control the system were used for the quantitative analysis of both vitamins. For retinol analysis, a Spherisorb ODS2 4.6 × 250 mm, 5 μm particle size (Waters Corporation, Milford, MA) reverse phase column was used. Separation was achieved with isocratic elution using mobile phases consisting of water (solvent A) and methanol (solvent B) at 4:96 ratio. The flow rate was 1 ml/min and total run time was 10 min. Detection was performed using a fluorescence detector with excitation and emission wavelengths at 300 and 470 nm, respectively.

For α-tocopherol analysis, a Spherisorb ODS2 4.6 × 150 mm, 5 μm particle size (Waters Corporation, Milford, MA) reverse phase column was used. A single mobile phase consisting of 100% methanol was used (isocratic) at a flow rate of 1 mL/min. The total run time was 9 min. The fluorescence detector was set to excitation and emission wavelengths of 295 and 340 nm, respectively. The column temperature for both analyses was ambient.

Sample Preparation for Retinol Analysis

Vitamin A was analyzed as total retinol. For liver and heart tissue, sample preparation began by weighing each tissue (wet mass, **Supplemental Table 1**) into individual 50 mL disposable, plastic test tubes. For pectoral muscle tissue, 0.1 g (wet mass) was weighed out into individual 50 mL disposable, plastic test tubes. Ascorbic acid (1%) in ethanol was added to each tube until the total mass was 2.5 g. The sample was vortexed briefly and then homogenized using a GenoGrinder (SPEX Sample Prep, Metuchen, NJ) set to 750 rpm for 5 min with 2 steel grinding balls. A 1.25 g aliquot of the homogenate was weighed into a glass, disposable, screw cap test tube. One milliliter of water, 0.75 mL of 1% ascorbic acid in ethanol, and 150 μL of saturated KOH were added, and the samples were saponified in a 70°C water bath for 20 min. After the samples were cooled to room temperature, 10 mL of petroleum ether was added to each tube. The samples were then vortexed for 1 min followed by centrifugation at 1,300 × g for 3 min. A 5 mL aliquot of each supernatant was transferred to a clean test tube and evaporated to dryness by a gentle flow of nitrogen at 35–45°C. The residue was reconstituted in 0.2 mL of methanol. The extract was sonicated, vortexed, filtered through a 0.45 μm Millipore syringe filter into an autosampler vial, and submitted for HPLC analysis.

Sample Preparation for α-Tocopherol Analysis

Vitamin E was analyzed as α-tocopherol. For liver and heart tissues, sample preparation began by weighing each tissue (wet mass) into individual 50 mL disposable, plastic test tubes (**Supplemental Table 8**). 0.5 mL of 1% BHT in ethanol was added to the sample and vortexed. After the addition of 5 mL of petroleum ether, each sample was homogenized using a GenoGrinder and 2 steel grinding balls at 750 rpm for 5 min. The samples were then centrifuged at 1,300 × g for 3 min and the supernatant collected and filtered through Whatman 1PS filter paper. A 2.5 mL aliquot was transferred into a clean test tube and evaporated to dryness under a gentle flow of nitrogen at 35–45°C. The extract was then reconstituted in 0.2 mL of methanol, which was then sonicated, vortexed, filtered through a 0.45 μm Millipore syringe filter into an autosampler vial, and submitted for HPLC analysis.

The same procedure was followed for brain and pectoral muscle with the following modifications: 0.2 ml of 1% BHT in ethanol was added to a whole brain tissue. One milliliter of 1% BHT in ethanol was added to 0.1 g (wet mass) of pectoral muscle and extracted with 10 mL of petroleum ether. A 5 mL aliquot was taken, and the evaporated sample was reconstituted in 1 mL of methanol. Once placed into autosampler vials, extracts of each of the four tissue types were treated in an identical manner.

Quality Control Sample Preparation and Method Validation

Method validation was performed using chicken tissue homogenates. Quality control sample collection and preparation began by removing tissue (liver, heart, pectoral muscle, and brain) samples from 3 chickens (*Gallus gallus domesticus*) procured from the Hopkins Avian Facility at University of California, Davis. Each tissue type was composited and homogenized using a blender. Two gram aliquots of tissue homogenate were stored in foiled packets at −20°C until analysis.

Multiple sub-aliquots of 0.1 and 0.05 g (wet mass) of liver, heart, and pectoral muscle homogenates were analyzed for both vitamins. 0.05 g aliquots of brain homogenates were analyzed for α-tocopherol only, using the same procedures described above. Established ranges of both vitamins in each of the tissues collected were determined from results of the method validation. Established ranges, defined as the mean concentration ± 2 standard deviations, were used for quality control (QC) purposes.

The established ranges measured for retinol were 482.2 ± 115.3 ppm for liver (n = 11), 0.2 ± 0.1 ppm for heart (n = 15), and 0.3 ± 0.06 ppm for pectoral muscle (n = 14) (**Supplemental Table 2**). For α-tocopherol, the established ranges were 9.3 ± 1.3 ppm for liver (n = 11), 8.3 ± 2.7 ppm for heart (n = 11), 1.2 ± 0.1 ppm for pectoral muscle (n = 11), and 6.2 ± 0.9 ppm for brain (n = 9) (**Supplemental Table 2**). Intra-assay and inter-assay variability (% CV) are reported in **Supplemental Tables 3**, **4** for retinol and α-tocopherol, respectively.

Analyte recoveries were determined by spiking chicken tissue homogenates with a known amount of each vitamin and processing the samples as outlined above. Aliquots of homogenates (n = 8 of each vitamin for each tissue, n = 6 of α-tocopherol for brain) were fortified at 500 ppm retinol and 10 ppm α-tocopherol for liver, 1 ppm retinol and 10 ppm α-tocopherol for heart, 1 ppm retinol and 10 ppm α-tocopherol for pectoral muscle, and 10 ppm α-tocopherol for brain. After analysis, the peak area for each vitamin in the unspiked sample was subtracted from the peak area of the spiked sample. Recovery

was calculated as the percentage of the corrected concentrations of the spiked amount. The spike recoveries, as well as the mean, standard deviation, % CV are listed in **Supplemental Tables 5**, **6**.

To measure absolute recovery of each vitamin, solvent spikes were made by weighing 0.1 g of the 1 and 500 μg/ml retinol standards and 0.1 g of the 1 μg/ml α-tocopherol standard into separate empty tubes and processed using the same procedures described above. The mean recoveries, standard deviations, and ranges for the solvent spikes (n = 5) for each matrix are reported in **Supplemental Table 2**. The established concentration range for the retinol 1 ppm and 500 ppm solvent spikes were 1.1 ± 0.2 ppm and 513.3 ± 106.7 ppm, respectively. The established range for α-tocopherol at 1 ppm was 1.0 ± 0.2 ppm. Intra-assay and inter-assay variability for both retinol and α-tocopherol solvent spikes are reported in **Supplemental Tables 3**, **4**.

Each analytical batch of hummingbird samples was extracted and analyzed with QC samples consisting of duplicate chicken tissue homogenates and a solvent spike at 1 and/or 500 ppm. Based on the results from the analyses of chicken tissue homogenates, the concentration of α-tocopherol, in all of the hummingbird tissue samples, and retinol, in hummingbird pectoral muscle samples, were expected to be low (<10 ppm) that only a 1 ppm solvent spike was used. For retinol analyses of heart and liver hummingbird samples, both 1 and 500 ppm solvent spikes were used as QC.

Standard quality assurance requirements for any batch involved an R^2 of the standard curve equal to or >0.980 and an analyte recovery of the solvent spikes and chicken tissue homogenates to be within the previously established ranges for both vitamins.

Data Analysis

Vitamin quantitation was accomplished by using a 10- to 16-point curve at concentrations of 0.25, 0.5, 1.0, 10, 20, 30, 40, and 50 ng of vitamin standard that were run daily. Some concentrations were run in duplicate. Vitamin concentrations were then interpolated from the regression equation of the trend line of the corresponding standard curve. The theoretical method limits of detection for each vitamin, in each matrix, were calculated as the lowest calibrator injected into the HPLC, in ng, divided by the amount of sample injected, in mg (**Supplemental Table 7**).

How well-values in different tissue types compared to the liver standard was evaluated using linear regression and by examining the R^2 and their p-value. Results with a p-value of 0.05 or less were considered statistically significant.

RESULTS

Vitamin Concentrations in Liver, Heart, and Pectoral Muscle Samples

Minimum, maximum, mean, standard deviation, and median for retinol concentrations for hummingbird liver, heart, and pectoral muscle samples are reported in **Table 1.** Mean ± standard deviation (SD) concentration of retinol in liver samples (n = 20) was 269.0 ± 216.9 ppm. For the heart and pectoral muscle samples (n = 20), the mean ± SD concentrations were 1.8 ± 2.2 ppm and 0.3 ± 0.1 ppm, respectively.

TABLE 1 | Summary statistics for retinol wet mass concentrations in liver, heart, and pectoral muscle samples from after-hatch year Anna's Hummingbird carcasses (n = 20).

Tissue type	Minimum (ppm)	Maximum (ppm)	Mean (ppm)	Standard deviation (ppm)	Median (ppm)
Male liver (n = 10)	69.8	794.4	303.3	208.7	308.5
Female liver (n = 10)	44.2	811.5	234.7	230.5	156.4
Total liver (n = 20)	44.2	811.5	269.0	216.9	202.6
Male heart (n = 10)	0.6	4.7	1.4	1.2	1.1
Female heart (n = 10)	0.2	9.6	2.1	2.9	1.2
Total heart (n = 20)	0.2	9.6	1.8	2.2	1.2
Male pectoral muscle (n = 10)	0.1	0.4	0.3	0.1	0.3
Female pectoral muscles (n = 10)	0.09	0.4	0.3	0.1	0.3
Total pectoral muscle (n = 20)	0.09	0.4	0.3	0.1	0.3

For each tissue type, the minimum (ppm), maximum (ppm), mean (ppm), standard deviation (ppm), and median (ppm) were calculated for samples from male, female, and total hummingbirds (males and females).

Mean ± SD α-tocopherol concentrations in hummingbird samples (n = 20) were 6.9 ± 4.6 ppm, 5.5 ± 4.0 ppm, and 3.7 ± 2.2 ppm for liver, heart, and pectoral muscles, respectively. Minimum, maximum, mean, standard deviation, and median for α-tocopherol concentrations for liver, heart, and pectoral muscle samples are reported in **Table 2**. Only 19 birds were analyzed for α-tocopherol concentrations in the brain because one sample (Bird# 24) was lost during analysis. Mean ± SD α-tocopherol concentration in hummingbird brain samples (n = 19) was 9.1 ± 3.2 ppm.

Vitamin Concentration Relationships Among Liver, Heart, Pectoral Muscle, and Brain Samples

Retinol and α-tocopherol concentrations of heart, pectoral muscle, and brain samples were regressed against the traditional tissue of choice, liver (**Figures 1**, **2**). For retinol concentrations, the regression of values from heart samples on liver values had a statistically significant value R^2 = 0.64 (p = 1.374e-05); the regression of pectoral muscle samples on liver was also significant (p = 0.048), but with a low R^2 = 0.16. For α-tocopherol concentrations, the heart and liver regression also had a significant R^2 = 0.64 (p = 1.278e-05) as did pectoral muscle (R^2

TABLE 2 | Summary statistics for α-tocopherol wet mass concentrations in liver, heart, pectoral muscle, and brain samples from after-hatch year Anna's Hummingbird carcasses ($n = 20$).

Tissue type	Minimum (ppm)	Maximum (ppm)	Mean (ppm)	Standard deviation (ppm)	Median (ppm)
Male liver ($n = 10$)	0.5	17.9	8.8	5.4	8.5
Female liver ($n = 10$)	0.4	9.7	5.0	2.9	5.1
Total liver ($n = 20$)	0.4	17.9	6.9	4.6	5.8
Male heart ($n = 10$)	0.4	14.2	7.4	4.4	7.3
Female heart ($n = 10$)	0.08	7.1	3.6	2.5	3.8
Total heart ($n = 20$)	0.08	14.2	5.5	4.0	4.8
Male pectoral muscle ($n = 10$)	2.3	9.6	4.9	2.1	4.4
Female pectoral muscle ($n = 10$)	0.1	4.8	2.5	1.6	2.3
Total pectoral muscle ($n = 20$)	0.1	9.6	3.7	2.2	3.7
Male brain ($n = 9$)	3.4	13.0	8.7	2.9	8.9
Female brain ($n = 10$)	4.8	15.9	9.5	3.6	8.5
Total brain ($n = 19$)	3.4	15.9	9.1	3.2	8.9

One brain sample was not available for analysis, therefore n = 19 for brain samples. For each tissue type, the minimum (ppm), maximum (ppm), mean (ppm), standard deviation (ppm), and median (ppm) were calculated for samples from male, female, and total hummingbirds (males and females).

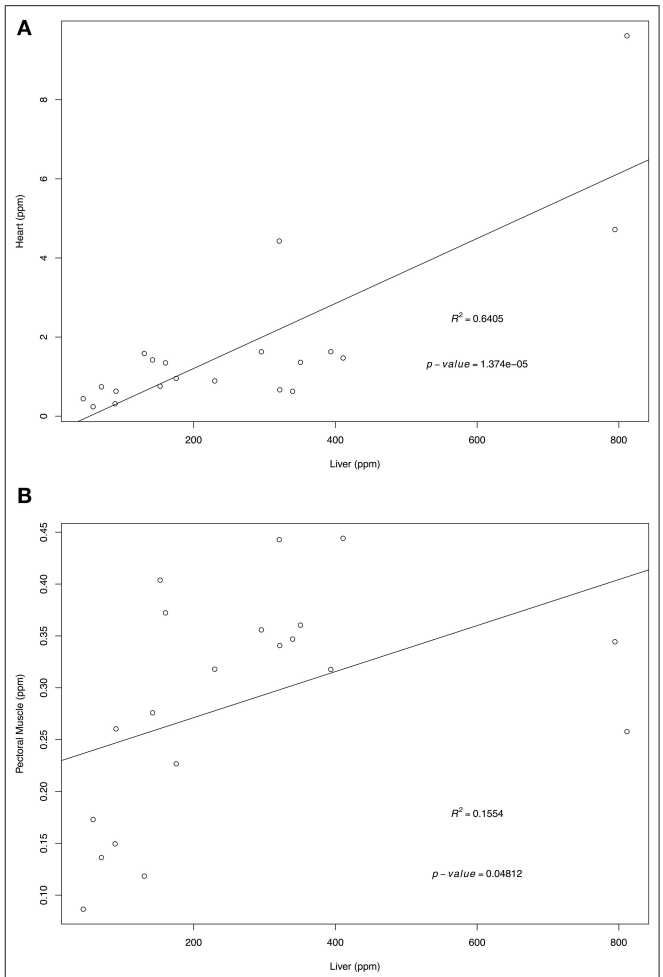

FIGURE 1 | Regression of liver retinol wet mass concentrations (ppm) on heart **(A)** and pectoral muscle **(B)**. Tissues samples were obtained from after-hatch year Anna's Hummingbird carcasses ($n = 20$). Samples were analyzed by high performance liquid chromatography.

$= 0.63$, $p = 1.801e-05$) whereas the regression of brain and liver samples was not significant ($R^2 = 0.02$, $p = 0.263$).

Validating HPLC at a Smaller Tissue Quantity

Means, standard deviations, and CVs were calculated for each chicken control batch and for the total overall batches (**Supplemental Tables 3**, **4**). For all control samples (liver, heart, pectoral muscles, brain, solvent spike 1 ppm, and solvent spike 500 ppm), the CVs were 20% and under for both intra-assay and inter-assay evaluations.

The spiked quality control chicken tissue homogenates all had CVs of 20% or under. Results of the retinol and α-tocopherol concentrations recovered are listed in **Supplemental Tables 5**, **6**.

DISCUSSION

This study developed an accurate analytical assay for quantifying retinol and α-tocopherol concentrations in small mass tissue samples, reported vitamin concentration ranges for hummingbird tissues with the intent that this information could help future rehabilitation efforts, and determined whether brain, heart, and pectoral muscle could accurately inform overall concentrations relative to the standard tissue liver. The brain was only considered for α-tocopherol analysis because hummingbirds commonly experience head trauma. Therefore, the authors were curious as to how α-tocopherol concentrations might be of benefit in the event of an injury. Retinol was not considered due to lack of resources and time.

The first phase of the study was to develop and validate an analytical method for measuring retinol and α-tocopherol in small mass tissue samples because most methods require large sample masses (8). Similar to another study that developed a method for quantifying trace elements in small mass tissue samples (10) the assay method for retinol and α-tocopherol has consistent performance. In addition, regardless of the variability in chicken brain tissue quality control sample masses (lowest

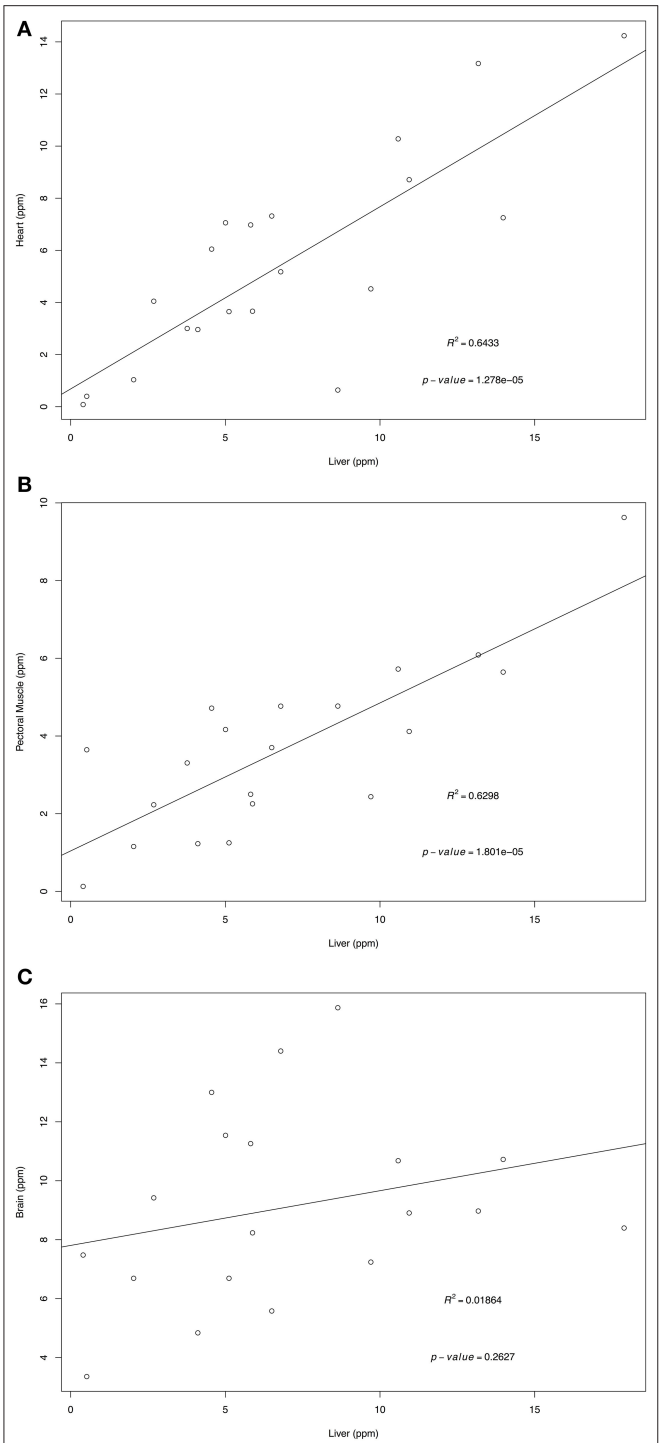

FIGURE 2 | Regression of liver α-tocopherol wet mass concentrations (ppm) on heart **(A)**, pectoral muscle **(B)**, and brain **(C)**. Tissues samples were obtained from after-hatch year Anna's Hummingbird carcasses ($n = 20$). Samples were analyzed by high performance liquid chromatography.

mass of 0.05 g), α-tocopherol concentrations were very close to expected concentrations (CV = 6.7%), thus supporting the precision of the analytical method.

As expected, hummingbird liver samples contained the highest mean concentration of retinol. This finding was expected because retinol is a fat-soluble vitamin, which accumulates mostly in organ tissues (11). Heart and pectoral muscle samples followed in respect to their retinol concentrations. For α-tocopherol, brain samples had the highest mean α-tocopherol concentration. Hummingbirds have a remarkable metabolic rate, one of the highest mass-specific metabolic rates among homoeothermic vertebrates (12). As a result, they also have an increased generation of reactive oxidation species (ROS). Defense against lipid peroxidation and ROS involves many antioxidant components, but mainly α-tocopherol (13). The brain is a highly sensitive organ, and high concentrations of α-tocopherol help combat peroxidation. The original hypothesis was that pectoral muscles would generate more ROS than the brain and liver due to the energy demands needed to sustain a hovering flight pattern, and thus would have higher α-tocopherol concentrations. However, this was not the case as liver, heart, and pectoral muscle samples had the second, third, and fourth highest mean concentrations of α-tocopherol, suggesting the potential degree of lipid peroxidation and ROS generated by those tissues. The authors suspect that the liver is an organ with high metabolic demands, which may explain why the liver had higher α-tocopherol concentrations compared to other tissues. In addition, it was interesting that α-tocopherol concentrations were relatively high in brain tissue samples. The brain is also a metabolically active organ, but the higher α-tocopherol concentrations may have an additional benefit to hummingbirds that experience head trauma. Another theory is that the pectoral muscles have evolved for efficiency, therefore they do not generate as much ROS compared to other organs. Unfortunately, to the authors' knowledge, there are no published studies that have evaluated vitamin concentrations in brain, liver, and pectoral muscle samples from birds for which to compare. However, in sheep, liver was shown to have higher concentration of vitamin E, followed by heart and then skeletal muscle (14). Liver concentration was also increased in comparison to skeletal muscle in pigs (15).

For retinol, when comparing liver concentrations with other tissues, the significant regressions of heart and pectoral muscle samples on liver indicate that both tissues could be potential samples for determining retinol concentrations. Heart and pectoral muscles have the advantage of being more easily salvaged in a small carcass than the liver, and are less prone to tissue autolysis. Based on the R^2-values, heart samples were better substitutes for liver samples compared to pectoral muscle samples.

For α-tocopherol, heart and pectoral muscle samples were also significant predictors of liver values, suggesting that either tissue can be utilized for assessing α-tocopherol status. However, the higher R^2-value for heart samples suggest that they would be a better reflection of the liver concentrations than pectoral muscle samples. The high p-value and low R^2-value for the brain samples indicate that the brain samples are not suitable for estimating liver α-tocopherol concentrations.

To evaluate species difference, the authors compared hummingbird retinol and α-tocopherol concentrations (mean

± SD) with chicken quality control sample concentrations (**Supplemental Table 2**) as quantified by the same analytical method. For retinol, the quality control chicken liver sample mean (482.2 ± 57.7 ppm) was higher than that for hummingbird samples (269.0 ± 216.9 ppm). However, the hummingbird pectoral muscle samples (0.3 ± 0.1 ppm) had the same mean concentration as the chicken quality control samples (0.3 ± 0.03 ppm). Surprisingly, hummingbird heart samples had a higher mean retinol concentration (1.8 ± 2.2 ppm) than the chicken quality control samples (0.2 ± 0.05 ppm), suggesting species differences in retinol storage.

For α-tocopherol, hummingbird pectoral muscle (3.7 ± 2.2 ppm) and brain (9.1 ± 3.2 ppm) samples had higher mean concentrations than chicken quality control samples (pectoral muscle: 1.2 ± 0.05 ppm, brain: 6.2 ± 0.4 ppm). This may be a reflection of a hummingbird's greater need for anti-oxidants compared to chickens (16) Chickens have a lower metabolic rate in comparison (12), so theoretically they would not need as robust of an anti-oxidant system to counteract generation of free-radicals. A surprising finding was that the mean α-tocopherol concentration for hummingbird heart samples (5.5 ± 4.0 ppm) was lower than the chicken samples mean (8.3 ± 1.4 ppm). A hummingbird's heart is a highly efficient and specialized organ, ensuring that oxygenated blood reaches the pectoral muscles to sustain a hovering flight pattern (17). It would be reasonable to expect that a higher anti-oxidant concentration (α-tocopherol) would be necessary to counteract the amount of ROS generated by the heart and the hummingbird's circulatory system, but this is not the case as seen in the data.

Establishing a retinol concentration range for quality control chicken liver samples was necessary as part of the assay validation, but also provided an opportunity to compare retinol chicken liver sample concentration from our study with published data. For our study, the mean retinol chicken liver concentration was 482.2 ± 57.7 ppm. This mean concentration is very different from previously reported values, which may be attributed to our small sample size. Across the literature, there is a large discrepancy in retinol concentrations. One manuscript reported the mean to be 370 ppm (converted from 370 RE mg/kg) (18) while another study found the mean to be 56.0 ± 38.9 ppm (converted from 5.60 ± 3.89 mg RE/100 g) (19). Published concentrations represent total retinol concentrations, including not only trans-retinol, but also retinyl palmitate, oleate, stearate, and linoleate as well. Our study employed a procedure that measured trans-retinol. However, a hydrolysis method was performed so that, in theory if all of the retinyl esters were hydrolyzed in the samples to retinol, the concentrations from our study would be equivalent to the RE seen in reported literature. In addition, the variation may be due to differences in study location, chicken age, amount of dietary retinol, breed of chicken, etc. For example, mean values for chicken livers of Britain was 97 ppm (9.7 mg RE/100 g), of the Slovak Republic was 170-200 ppm (17–20 mg RE/100 g), and of Germany was 335 ppm (33.5 mg RE/100 g) (19).

These same principles could be the source of variability in the hummingbird retinol concentrations as seen by the high standard deviation and the range of values (**Table 1**, **Supplemental Table 8**). Being a migratory species, the hummingbird carcasses probably represented different geographic regions, which would impact their diet. In addition, hummingbirds have age and sex differences in their diets which affect the ratio of nectar to insects consumed. Although the hummingbirds were all determined to be aged "AHY" (adult), we were unable to determine where in the reproductive cycle each bird was in, which can vastly impact the vitamin concentrations.

Vitamin E concentrations were measured as α-tocopherol in this study. Reported chicken liver mean α-tocopherol concentration values are scarce. One report found the mean concentration was 2.1 ppm (0.21 mg/100 g) (20). Again, the value is different from the mean α-tocopherol concentration obtained in this study, which was 9.3 ppm. The difference may be due to variation in diet and how much retinol was supplemented in the chickens' diets. Supplementing with retinol, which is commonly done in commercial feeds, has shown to have a linear depressive effect on α-tocopherol concentrations in the plasma and liver samples from both chicks and adult chickens (21, 22).

A limitation of this study was using free-ranging hummingbirds as animal subjects. This could cause a variation in the diet that the birds consumed and the environment that they inhabited. Dietary consumption can impact vitamin concentrations, especially vitamin E in the form of α-tocopherol. Geographic location and time of year can influence dietary consumption (23) and, since hummingbirds are migratory species, this presents even more of a challenge.

Prior to being presented to wildlife rehabilitation centers, all hummingbirds used in this study were free-ranging. These birds were opportunistically collected, which means they had an unknown health status at time of death. However, the data from this study at least serve as an initial reference point from which to build upon. The birds ($n = 18$) that were dead on presentation or were euthanized within 24 h would most likely better represent the nutrient status of free ranging birds. However, for 22 hummingbirds, the length in captivity could not be determined due to lack of management information. Therefore, these birds could have been fed a commercial diet while in captivity. Liver is a tissue matrix that has been documented to be especially sensitive to changes in dietary vitamin consumption (22). Sheep livers were seen to have a decrease in α-tocopherol liver within a week of being fed an α-tocopherol depleted diet (22). The same is seen for vitamin A when vitamin A was depleted for 3 weeks in turkeys (23). Ten hummingbirds used for retinol analysis and 12 hummingbirds used for α-tocopherol analysis were not documented as dead on arrival or euthanized within 24 h. It is possible that these birds, while in captivity, could have been fed a supplemental diet for an extended period of time, which would impact the results. In a study in which growing pigs experienced vitamin E supplementation and depletion, muscle was less likely to change with changes in vitamin dietary consumption, reflecting long-term nutritional history (24). Therefore, for the 22 cases with unknown histories, it may be more appropriate to use pectoral muscle to accurately reflect the vitamin concentration of free-ranging hummingbirds.

Future studies might benefit from evaluating tissues on a dry mass basis since hummingbird tissues desiccate rapidly following

dissection. In addition, this method could possibly be used with plasma for quantifying vitamin concentrations antemortem, thus enabling determination of real time vitamin concentrations in live hummingbirds.

CONCLUSION

A HPLC analytical method for measuring retinol and α-tocopherol concentrations in small mass tissue samples was established and validated. Baseline wet weight concentrations of retinol and α-tocopherol in hummingbird liver, heart, pectoral muscle, and brain samples were determined. Tissue analysis for any analyte is a challenge in hummingbirds given their small body size and the tendency for their tissues to rapidly autolyze post-mortem. Comparison among various tissue types was performed to determine which tissue best reflected liver sample concentrations so that other tissues could be considered in the case of liver autolysis. Heart samples best reflected liver concentrations for retinol, and both heart and pectoral muscle samples reflected liver concentrations for α-tocopherol. Having methods for quantifying retinol and α-tocopherol concentrations in hummingbird samples might help with conservation efforts and avoid hypervitaminosis and hypovitaminosis in the case of rehabilitated birds or hummingbirds being raised in captivity

DATA AVAILABILITY STATEMENT

All datasets presented in this study are included in the article/**Supplementary Material**.

ETHICS STATEMENT

Ethical review and approval was not required for the animal study because permission for obtaining the hummingbird carcasses for scientific study was approved by the United States Fish and Wildlife Service (Permit: MB55944B-2) and the California Department of Fish and Wildlife (Permit: SC-013066).

AUTHOR CONTRIBUTIONS

LT, RP, LA, and GG contributed to conception and design of the study. SD and GG processed tissue samples and collected data. SD and LT wrote the original manuscript. JF wrote the R codes and guided data analysis. SD performed the statistical analysis. RB aided in specimen selection and collection. All authors contributed to manuscript revision and approved the submitted version.

ACKNOWLEDGMENTS

This project was supported in part by generous donations made by Dr. Grant Patrick, Dr. Terry, and Mrs. Erica Roelofs. The authors would like to thank the staff at the Lindsay Wildlife Experience, California Wildlife Center, Santa Barbara Wildlife Care Network, and Wetlands and Wildlife Care Center of Orange County for their help with acquiring hummingbird carcasses and Michelle Mah for her help with sample dissection. Additionally, the authors would like to thank the California Animal Health and Food Safety Laboratory System (CAHFS) for providing resources and guidance.

SUPPLEMENTARY MATERIAL

The Supplementary Material for this article can be found online at: https://www.frontiersin.org/articles/10.3389/fvets.2020.00637/full#supplementary-material

REFERENCES

1. Stiles FG. Taste preferences, color preferences, and flower choice in hummingbirds. *The Condor.* (1976) 78:10–26.
2. Allen-Wardell G, Bernhardt P, Bitner R, Burquez A, Buchmann S, Cane J, et al. The potential consequences of pollinator declines on the conservation of biodiversity and stability of food crop yields. *Conservat Biol.* (1998) 12:8–17.
3. Godoy LA, Tell LA, Ernest HB. Hummingbird health: pathogens and disease conditions in the family Trochilidae. *J Ornithol.* (2014) 155:1–12. doi: 10.1007/s10336-013-0990-z
4. Peaker M. Nutritional requirements and diets for hummingbirds and sunbirds. *International Zoo Yearbook.* (1990) 29:109–18. doi: 10.1111/j.1748-1090.1990.tb03339.x
5. Brice AT, Grau CR. Hummingbird nutrition: development of a purified diet for long-term maintenance. *Zoo Biol.* (1989) 8:233–7. doi: 10.1002/zoo.1430080304
6. Dierenfeld ES. Vitamin E deficiency in zoo reptiles, birds, and ungulates. *J Zoo Wildlife Med.* (1989) 20:3–11.
7. Cohen A, Klasing K, Ricklefs R. Measuring circulating antioxidants in wild birds. *Comp Biochem Physiol B Biochem Mol Biol.* (2007) 147:110–21. doi: 10.1016/j.cbpb.2006.12.015
8. Desai ID. [16] Vitamin E analysis methods for animal tissues. *Methods Enzymology*. (1984) 105:138–47.
9. Russel SM, Russel RO. *The North American Banders' Manual for Hummingbird.* (2019). Available online at: http://www.nabanding.net/wp-content/uploads/2019/11/Hummingbird-Manual-31_Oct_2019.pdf (accessed June 23, 2020).
10. Mikoni NA, Poppenga R, Ackerman JT, Foley J, Hazlehurst J, Purdin G, et al. Trace element contamination in feather and tissue samples from Anna's hummingbirds. *Ecol Indicat.* (2017) 80:96–105. doi: 10.1016/j.ecolind.2017.04.053
11. Clifford J, Kozil A. *Fat-Soluble Vitamins: A, D, E, and K.* (2017). Available online at: https://extension.colostate.edu/docs/pubs/foodnut/09315.pdf (accessed June 23, 2020).
12. Suarez RK. Hummingbird flight: sustaining the highest mass-specific metabolic rates among vertebrates. *Experientia.* (1992) 48:565–70. doi: 10.1007/BF01920240
13. Surai PF, Noble RC, Speake BK. Relationship between vitamin E content and susceptibility to lipid peroxidation in tissues of the newly hatched chick. *Br Poultry Sci.* (1999) 40:406–10. doi: 10.1080/00071669987520
14. Fry JM, Smith GM, McGrath MC, Speijers EJ, Allen JG. Plasma and tissue concentrations of α-tocopherol during vitamin E depletion in sheep. *Br J Nutr.* (2007) 69:225–32. doi: 10.1079/BJN19930024

15. Jensen M, Lindholm A, Hakkarainen J. The vitamin E distribution in serum, liver, adipose and muscle tissues in the pig during depletion and repletion. *Acta Vet Scand.* (1990) 31:129–36.
16. Dolan E, Saunders B, Dantas WS, Murai IH, Roschel H, Artioli GG, et al. A comparative study of hummingbirds and chickens provides mechanistic insight on the histidine containing dipeptide role in skeletal muscle metabolism. *Sci Rep.* (2018) 8:14788. doi: 10.1038/s41598-018-32636-3
17. Nespolo RF, González-Lagos C, Solano-Iguaran JJ, Elfwing M, Garitano-Zavala A, Mañosa S, et al. Aerobic power and flight capacity in birds: a phylogenetic test of the heart-size hypothesis. *J Exp Biol.* (2018) 221:jeb162693. doi: 10.1242/jeb.162693
18. Howells LC, Livesey CT. A survey of vitamin A concentrations in the liver of food-producing animals. *Food Addit Contam.* (1998) 15:10–8. doi: 10.1080/02652039809374595
19. Majchrzak D, Fabian E, Elmadfa I. Vitamin A content (retinol and retinyl esters) in livers of different animals. *Food Chem.* (2006) 98:704–10. doi: 10.1016/j.foodchem.2005.06.035
20. Lange W. Cholesterol, phytosterol, and tocopherol content of food products and animal tissues. *J Am Oil Chem Soc.* (1950) 27:414–22.
21. Sklan D, Donoghue S. Vitamin E response to high dietary vitamin A in the chick. *J Nutr.* (1982) 112:759–65. doi: 10.1093/jn/112.4.759
22. Yuan J, Roshdy AR, Guo Y, Wang Y, Guo S. Effect of dietary vitamin A on reproductive performance and immune response of broiler breeders. *PLoS ONE.* (2014) 9:e105677. doi: 10.1371/journal.pone.0105677
23. Torregrossa A-M, Puschner B, Tell L, Olsen J, Dierenfeld ES. Circulating concentrations of vitamins A and E in captive psittacine birds. *J Avian Med Surg.* (2005) 19:225–9. doi: 10.1647/2004-004.1
24. Aye PP, Morishita TY, Saif YM, Latshaw JD, Harr BS, Cihla FB. Induction of vitamin A deficiency in turkeys. *Avian Dis.* (2000) 44:809–17. doi: 10.2307/1593053

Conflict of Interest: The authors declare that the research was conducted in the absence of any commercial or financial relationships that could be construed as a potential conflict of interest.

Copyright © 2020 Diao, Poppenga, Gonzales Alarcio, Foley, Bandivadekar, Aston and Tell. This is an open-access article distributed under the terms of the Creative Commons Attribution License (CC BY). The use, distribution or reproduction in other forums is permitted, provided the original author(s) and the copyright owner(s) are credited and that the original publication in this journal is cited, in accordance with accepted academic practice. No use, distribution or reproduction is permitted which does not comply with these terms.

frontiers in Veterinary Science

ORIGINAL RESEARCH
published: 21 October 2020
doi: 10.3389/fvets.2020.567258

Retrospective Study of Fishery Interactions in Stranded Cetaceans, Canary Islands

Raquel Puig-Lozano[1], Antonio Fernández[1], Eva Sierra[1], Pedro Saavedra[2], Cristian M. Suárez-Santana[1], Jesús De la Fuente[1], Josué Díaz-Delgado[3], Ana Godinho[4,5], Natalia García-Álvarez[1], Daniele Zucca[1], Aina Xuriach[1], Marina Arregui[1], Idaira Felipe-Jiménez[1], Francesco Consoli[1], Pablo J. Díaz-Santana[1], Simone Segura-Göthlin[1], Nakita Câmara[1], Miguel A. Rivero[1], Simona Sacchini[1], Yara Bernaldo de Quirós[1] and Manuel Arbelo[1]*

[1] Veterinary Histology and Pathology, Atlantic Center for Cetacean Research, University Institute of Animal Health and Food Safety (IUSA), Veterinary School, University of Las Palmas de Gran Canaria, Las Palmas of Gran Canaria, Spain, [2] Department of Mathematics, University of Las Palmas de Gran Canaria, Las Palmas of Gran Canaria, Spain, [3] TVMDL Texas A&M, Veterinary Medical Diagnostic Laboratory, College Station, TX, United States, [4] Life and Health Sciences Research Institute (ICVS), School of Medicine, University of Minho, Braga, Portugal, [5] ICVS/3B's - PT Government Associate Laboratory, Braga/Guimarães, Portugal

OPEN ACCESS

Edited by:
Robert James Ossiboff, University of Florida, United States

Reviewed by:
Graham Pierce, Higher Council for Scientific Research (CSIC), Spain
Valentín Pérez, Universidad de León, Spain

***Correspondence:**
Yara Bernaldo de Quirós
yara.bernaldo@ulpgc.es

Specialty section:
This article was submitted to Veterinary Experimental and Diagnostic Pathology, a section of the journal Frontiers in Veterinary Science

Received: 29 May 2020
Accepted: 01 September 2020
Published: 21 October 2020

Citation:
Puig-Lozano R, Fernández A, Sierra E, Saavedra P, Suárez-Santana CM, De la Fuente J, Díaz-Delgado J, Godinho A, García-Álvarez N, Zucca D, Xuriach A, Arregui M, Felipe-Jiménez I, Consoli F, Díaz-Santana PJ, Segura-Göthlin S, Câmara N, Rivero MA, Sacchini S, Bernaldo de Quirós Y and Arbelo M (2020) Retrospective Study of Fishery Interactions in Stranded Cetaceans, Canary Islands. Front. Vet. Sci. 7:567258. doi: 10.3389/fvets.2020.567258

Estimating cetacean interactions with fishery activities is challenging. Bycatch and chronic entanglements are responsible for thousands of cetacean deaths per year globally. This study represents the first systematic approach to the postmortem investigation of fishery interactions in stranded cetaceans in the Canary Islands. We retrospectively studied 586 cases necropsied between January 2000 and December 2018. Of the cases with a known cause of death, 7.4% (32/453) were due to fishery interactions, and the Atlantic spotted dolphin (*Stenella frontalis*) was the most affected species [46.9% (15/32)]. Three types of fishery interactions were recognized by gross findings: bycatch [65.6% (21/32)], chronic entanglements [18.8% (6/32)], and fishermen aggression [15.6% (5/32)]. Among the bycaught cases, we differentiated the dolphins that died because of ingestion of longline hooks [23.8% (5/21)] from those that died because of fishing net entrapments [76.2% (16/21)], including dolphins that presumably died at depth due to peracute underwater entrapment (PUE) [37.5% (6/16)], dolphins that were hauled out alive and suffered additional trauma during handling [43.8% (7/16)], and those that were released alive but became stranded and died because of fishery interactions [18.7% (3/16)]. Gross and histologic findings of animals in each group were presented and compared. The histological approach confirmed gross lesions and excluded other possible causes of death. Cetaceans in good-fair body condition and shallow diving species were significantly more affected by fishery interactions, in agreement with the literature. Low rates of fishery interactions have been described, compared with other regions. However, within the last few years, sightings of entangled live whales, especially the minke whale (*Balaenoptera acutorostrata*) and Bryde's whale (*B. edeni*), have increased. This study contributes to further improvement of the evaluation of different types of fishery interactions and may facilitate the enforcement of future conservation policies to preserve cetacean populations in the Canary Islands.

Keywords: fisherman aggressions, peracute underwater entrapment, entanglement, bycatch, Bryde's whale, Atlantic spotted dolphin, longline hooks, minke whale

INTRODUCTION

Fishery activities are a major threat to cetacean populations globally (1). Bycatch is a major cause of mortality and poses the highest widespread risk (2, 3). Detection of bycatch among cetaceans is challenging, as there are typically no pathognomonic lesions (4, 5).

Bycaught dolphins in gillnets or trawls are often reportedly healthy individuals in good body condition, with pathological findings that are usually consistent with peracute underwater entrapment (PUE) (5). The most common findings in this type of bycatch are net cuts and impressions on the skin (mainly over the head, but also affecting the flippers and body), changes in the lung (edema, multifocal emphysema, and atelectasis), recently ingested food, reddish or bulging eyes, congestion, and disseminated gas bubbles (6). Other bycatch findings include those produced by fishermen, such as gunshots, stabs over the body, or amputations to disentangle the animal from fishing nets, and abdominal cuts to sink the carcasses (5, 7). To identify bycatch as a cause of death, it is essential to rule out other possible causes of death.

Another type of fishery interaction is chronic entanglement with an active net, or with abandoned, lost or otherwise discarded fishing gear, which form part of the marine debris, and cause ongoing "ghost-fishing" for years (8, 9). At least 14 cetacean species have been reportedly entangled, and 97% of the cases were attached to fishing gear (10). Entanglements are considered a global threat, which international entanglement response and monitoring programs urge (11).

The Canary Islands are located in the region of Macaronesia, close to the north-western coast of Africa. With up to 30 cetacean species (Biocan—Banco del Inventario Natural de Canarias[1], seven mysticetes and 23 odontocetes, the Canary Islands hold the greatest cetacean biodiversity among European territories, and its fisheries are mainly artisanal. The Atlantic Center for Cetacean Research has been monitoring the health of free-ranging cetaceans stranded in the Canary Islands over the last 20 years. The three most stranded species are the Atlantic spotted dolphin (*Stenella frontalis*), the short-beaked common dolphin (*Delphinus delphis*), and the striped dolphin (*Stenella coeruleoalba*) (12, 13).

The aim of this study was to retrospectively investigate the prevalence and most common pathological findings of each type of fishery interaction, among stranded cetaceans in the Canary Islands. Our results will likely aid the promotion of adequate conservation policies in the archipelago and improve detection of this anthropic threat.

MATERIALS AND METHODS

Postmortem examinations of 586 cetaceans stranded along the coasts of the Canary Islands were performed from January 2000 to December 2018, following standardized protocols (14). No experiments were performed on live animals. Permission for the handling of stranded cetaceans was granted by the Spanish Ministry of Environment.

For each necropsied cetacean, the epidemiology of the stranding (i.e., location and date); life history data (i.e., species, growth development, sex, and gonad maturation); body condition; and decomposition code, were systematically recorded. Growth development categories (neonate, calf, juvenile, subadult, and adult) were extrapolated from the osteological characteristics of stranded cetaceans in the Canary Islands (15). Gonad maturation was determined, based on histological gonadal examination (16). Body condition (very poor, poor, fair, or good) was estimated, based on anatomical landmarks (17). The decomposition code (1-very fresh, 2-fresh, 3-moderate autolysis, 4-advanced autolysis, and 5-very advanced autolysis) was determined following the classification of IJsseldijk et al. (18). During the necropsy, lesions were described and photographed. In one animal (case 26), the gas score was determined and gas analysis was performed following standardized protocols (19, 20). Representative tissue samples were fixed in 10% neutral buffered formalin, routinely processed, embedded in paraffin, sectioned at thickness of 5 μm, and stained with hematoxylin and eosin for histopathologic analysis.

A conservative approach was adopted to determine fishery interactions, based on previous studies (5–7, 12, 13, 21–24). All stranding cases were reviewed retrospectively, as we looked for individuals with findings that were consistent with fishery interactions, and excluded cases in which other possible traumatic etiologies, such as ship collision, intra-interspecific interactions, or live stranding, could not have been ruled out (25–32). Different types of fishery interactions were determined based on gross findings. Within these various types, histological findings in the skeletal and cardiac muscle, lungs, liver, kidneys, brain, and adrenal glands of the cases with decomposition codes 1–3, were detailed and compared, based on the availability of the samples.

In order to identify factors related to fishery interactions, categorical variables (species, sex, growth development, gonad maturation, body condition, diving behavior, island, and date of stranding) were expressed as frequencies and percentages, and were compared, as appropriate, using the chi-squared (χ^2) test or the Fisher's exact test. Fishing deaths were due to all of the different types of fishery interactions identified: chronic entanglements, fishermen aggressions from the boat, and bycatch (including fishing net entrapments and ingestion of longline hooks). For statistical analyses, some categorical variables were further regrouped as follows: growth development category (neonate/calf, juvenile/subadult, and adult); body condition (very poor/poor and fair/good); and stranding island based on geographical proximities and the presence of high-site fidelity populations [Western Islands (El Hierro and La Palma), La Gomera together with Tenerife, Gran Canaria, and Eastern Islands (Fuerteventura-Lanzarote-La Graciosa)]. All statistical analyses were performed only on those animals with an identifiable cause of death (453/586). Statistical significance was set at $p < 0.05$. Data were analyzed using the R package, version 3.6.1 (33).

[1]https://www.biodiversidadcanarias.es/

TABLE 1 | Gross findings in stranded cetaceans, which died because of fishery interactions (chronic entanglement, aggression, or bycatch) ($n = 32$).

						Bycatch (n = 21)									
		Entanglement (n = 6)		Aggression (n = 5)		Hook ingestion (n = 5)		PUE (n = 6)		Aggression during handling (n = 7)		Returned (n = 3)		Total (n = 21)	
Stranding event	Stranding alive	1	17%	0	0%	0	0%	0	0%	0	0%	3	100%	3	14%
	Stranding death	5	83%	5	100%	5	100%	6	100%	7	100%	0	0%	18	86%
	Fishing gears attached	4	67%	0	0%	5	100%	0	0%	0	0%	2	67%	7	33%
Body condition	Poor-very poor	2	33%	0	0%	0	0%	2	33%	0	0%	0	0%	2	10%
	Good-fair	3	50%	5	100%	5	100%	4	67%	6	86%	3	100%	18	86%
	NE	1	17%	0	0%	0	0%	0	0%	1	14%	0	0%	1	5%
Skin	Net impressions over the body	6	100%	0	0%	2	40%	4	67%	3	43%	1	33%	10	48%
	Net cuts in pectoral flippers	0	0%	0	0%	2	40%	4	67%	2	29%	1	33%	9	43%
	Net cuts in head	1	17%	0	0%	3	60%	5	83%	7	100%	2	67%	17	81%
	Net cuts over the body	1	17%	0	0%	3	60%	3	50%	5	71%	3	100%	14	67%
Subcutaneous	Hematoma	2	33%	5	100%	3	60%	0	0%	6	86%	0	0%	9	43%
Skeletal muscle	Hemorrhages	2	33%	5	100%	2	40%	1	17%	6	86%	0	0%	9	43%
Bones	Mandibles fracture	0	0%	0	0%	2	40%	2	33%	2	29%	2	67%	8	38%
	Maxilla fracture	0	0%	0	0%	1	20%	2	33%	1	14%	2	67%	6	29%
	Neurocranium fracture	0	0%	0	0%	0	0%	0	0%	2	29%	0	0%	2	10%
	Tympanic fracture	0	0%	0	0%	0	0%	0	0%	0	0%	1	33%	1	5%
	Vertebrae fracture	0	0%	2	40%	0	0%	0	0%	1	14%	0	0%	1	5%
	Rib fracture	0	0%	0	0%	0	0%	0	0%	0	0%	1	33%	1	5%
	Teeth lost/fractured	0	0%	2	40%	1	20%	3	50%	3	43%	2	67%	9	43%
Digestive tract	Esophagus Fresh/undigested prey	1	17%	3	60%	0	0%	3	50%	2	29%	0	0%	5	24%
	Stomach Fresh/undigested prey	1	17%	3	60%	2	40%	3	50%	5	71%	0	0%	10	48%
	Digested content	0	0%	0	0%	1	20%	1	17%	0	0%	3	100%	5	24%
	Empty/ND	4	67%	1	20%	2	40%	2	33%	1	14%	0	0%	5	24%
Bubbles	Lymphatic vessels	0	0%	1	20%	0	0%	1	17%	2	29%	0	0%	3	14%
	Blood vessels	1	17%	0	0%	1	20%	5	83%	4	57%	1	33%	11	52%
Blood in cavities	Hemothorax	1	17%	3	60%	2	40%	0	0%	1	14%	0	0%	3	14%
	Hemoabdomen	0	0%	0	0%	3	60%	1	17%	1	14%	0	0%	5	24%
	Hemopericardium	0	0%	0	0%	0	0%	0	0%	1	14%	0	0%	1	5%
Lungs	Hyperinflated	1	17%	0	0%	2	40%	2	33%	5	71%	3	100%	12	57%
	Hemorrhagic parenchyma	0	0%	3	60%	0	0%	1	17%	2	29%	1	33%	4	19%
	Subpleural hemorrhage	0	0%	4	80%	0	0%	3	50%	0	0%	0	0%	3	14%
	Tracheal or bronchial edema	2	33%	0	0%	0	0%	0	0%	2	29%	0	0%	2	10%
	Rib impressions	0	0%	0	0%	0	0%	0	0%	0	0%	2	67%	2	10%
	Rupture of the parenchyma	0	0%	3	60%	0	0%	0	0%	1	14%	0	0%	1	5%

(Continued)

TABLE 1 | Continued

						Bycatch (n = 21)									
		Entanglement (n = 6)		Aggression (n = 5)		Hook ingestion (n = 5)		PUE (n = 6)		Aggression during handling (n = 7)		Returned (n = 3)		Total (n = 21)	
Heart	Hemopericardium	0	0%	0	0%	1	20%	0	0%	0	0%	0	0%	1	5%
	Hemorrhages	0	0%	0	0%	0	0%	0	0%	1	14%	0	0%	1	5%
	Vascular changes in valves	2	33%	0	0%	0	0%	0	0%	0	0%	0	0%	0	0%
Large vessels	Aorta vascular changes	1	17%	0	0%	1	20%	1	17%	4	57%	0	0%	6	29%
	Rete mirabile vascular changes	0	0%	0	0%	0	0%	0	0%	2	29%	0	0%	2	10%
Kidney	Hemorrhages	0	0%	0	0%	0	0%	0	0%	1	14%	0	0%	1	5%
	Retroperitoneal emphysema	1	17%	0	0%	1	20%	2	33%	2	29%	0	0%	5	24%
Lymphatic	Lymph in vessels	0	0%	2	40%	0	0%	3	50%	4	57%	0	0%	7	33%
Brain	Meningeal hemorrhages	0	0%	1	20%	0	0%	0	0%	3	43%	0	0%	3	14%
	Parenchymal hemorrhages	0	0%	0	0%	0	0%	0	0%	1	14%	0	0%	1	5%

Decomposition codes (1–5). For each category, the number and percentage of affected individuals are shown.
The color values correspond to the percentage of a finding or a pathologic feature within each group of studied animals (bycatch, fisherman aggression and chronic entanglement).

RESULTS

A total of 860 cetaceans were stranded along the coasts of the Canary Islands between January 2000 and December 2018. Among them, 586 cetaceans were necropsied. The full anatomopathological study of each case allowed us to identify the most probable cause of death in 453 cases. Of those cases, 32 (7.4%) cetaceans of seven species died because of the pathological consequences of fishery interactions.

Types of Fishery Interactions

Cases of fishery interactions ($n = 32$) were divided into three categories: bycatch (i.e., longline hook ingestion or fishing net entrapment) ($n = 21$); chronic entanglements ($n = 6$); and fisherman aggressions ($n = 5$) (**Supplementary Table 1**).

Bycatch

The bycatch group included cetaceans that were presumably entrapped in active fishing gear. In this group ($n = 21$), four species were affected: the Atlantic spotted dolphin ($n = 12$); striped dolphin ($n = 6$); common dolphin ($n = 2$); and Atlantic bottlenose dolphin (*Tursiops truncatus*) ($n = 1$). All growth development categories were affected by bycatch. The adults were the most affected (11/21), followed by the juveniles (6/21), subadults (3/21), and calves (2/21).

This group was further divided into the following subgroups: dolphins that ingested longline hooks (5/21); dolphins with lesions compatible with forced submersion, which presumably died at depth due to PUE (6/21); dolphins that were stranded alive and later died, exhibiting lesions that were consistent with PUE (3/21); and polytraumatized dolphins that were hauled out alive but suffered additional trauma during handling, including mainly cranioencephalic trauma, and/or perforations produced by fishing equipment (7/21).

Different degrees of chronicity of the lesions were observed; from acute lesions in PUE cases to subacute-chronic lesions in cases of longline hook ingestion. However, some gross findings were common among most cases (**Table 1**). Almost every bycaught case showed fair to good body condition. In addition, many animals exhibited superficial cutaneous lesions caused by contact with fishing nets, mainly on the rostrum, but also on the flippers, and along the sides of the body, as well as net impressions (**Figures 1A,B**). Other common findings included diffuse bilateral hyperinflated lungs (**Figure 1C**, inset upper image), disseminated intravascular gas bubbles in the veins and lymphatic vessels (**Figures 1D,E**). In fewer cases, undigested food was found in the forestomach (**Figure 1C** inset lower image), occasionally in the esophagus, and/or associated with the presence of abundant lymph in the lymphatic mesenteric vessels and chyle in the thoracic duct. Lost teeth (**Figure 1F**), a fractured rostrum and/or maxilla, and retroperitoneal emphysema were also described. Gross findings of each bycatch case are presented in **Supplementary Table 2**.

Histologically, almost all cases showed clear intravascular spaces compatible with gas and/or fat embolism. Common findings included: mild to moderate multifocal acute degenerative changes in skeletal muscle (i.e., segmental degeneration of the muscular fibers); mild multifocal acute degenerative changes in cardiac muscle (i.e., increased acidophilic cytoplasm of the myocardiocytes, contraction

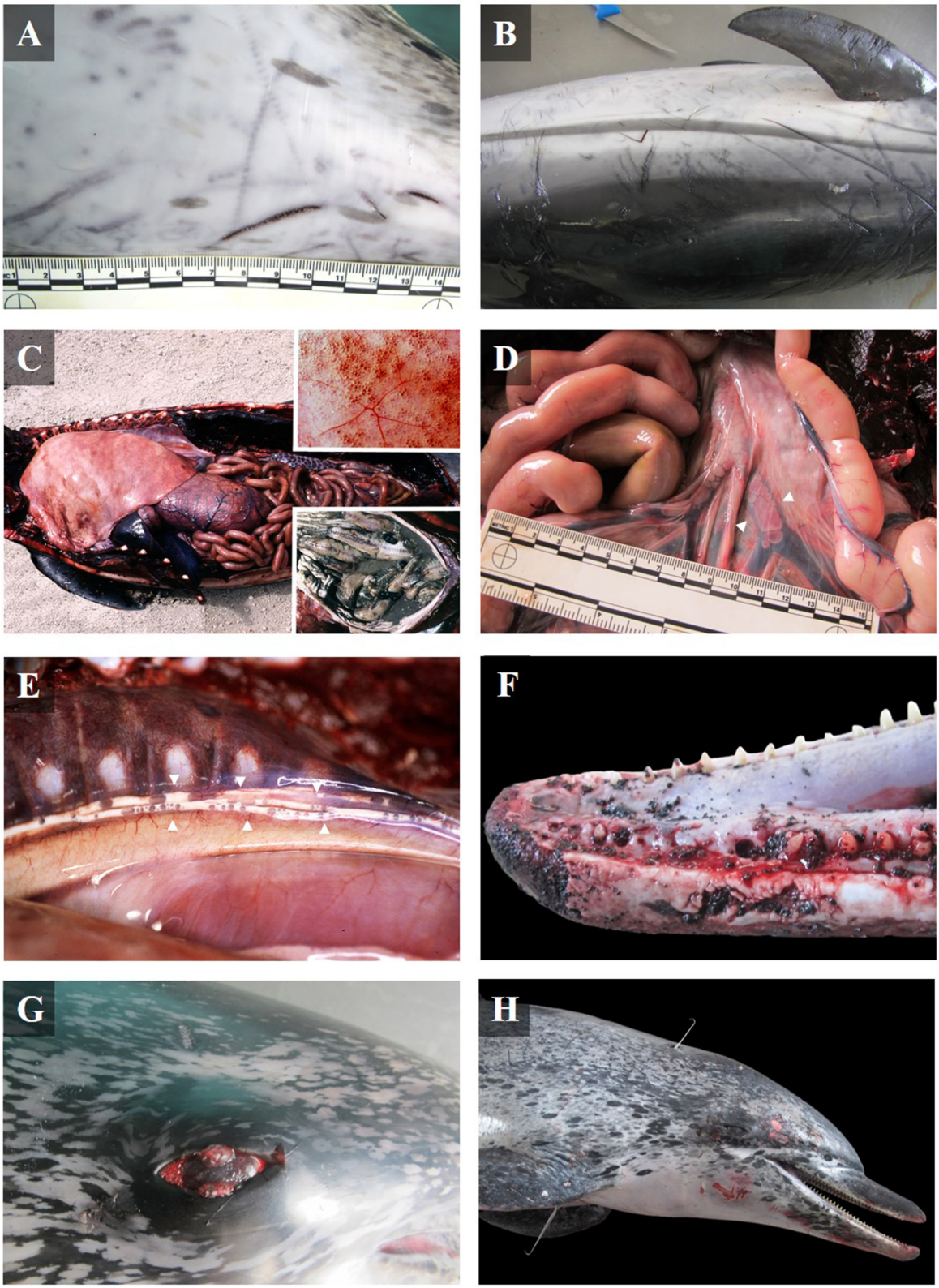

FIGURE 1 | Gross lesions in bycaught dolphins stranded along the Canary Islands. **(A)** Cutaneous impressions presumably produced by a twisted wire net, and **(B)** linear and typical triangular monofilament cuts on an adult Atlantic spotted dolphin (case 29). **(C)** Left lateral view of the thoracic and abdominal cavities of a juvenile

(Continued)

FIGURE 1 | Atlantic bottlenose dolphin (case 7). Severe hyperinflated lungs with emphysema (inset upper image), and full stomach with undigested food, fresh fish (inset lower image). **(D)** Mesenteric veins with severe multifocal intravascular gas bubbles in an adult common dolphin (case 32). **(E)** Thoracic duct (between arrow points) full of lymph and gas bubbles in an Atlantic spotted dolphin calf (case 1). **(F)** Left lateral view of the rostrum with multifocal fracture and lost teeth in the rostral part of the mandible (case 21). **(G)** Reddish eyes with conjunctival emphysema of an adult Atlantic spotted dolphin, found with an ingested longline hook (case 29). **(H)** Right lateral view of an adult Atlantic spotted dolphin with two perforating thoracic wounds. The tracks of the wounds, marked by two steel skewers, probably produced during aggressive handling (case 21).

band necrosis, and juxtanuclear vacuolization of cardiac cells); multifocal lung changes such as alveolar emphysema, hemorrhages, and alveolar edema; systemic leukocytosis; and multifocal intracytoplasmic hepatocellular hyaline globules. In fewer cases, bronchiolar sphincter contraction, multifocal hyaline casts in distal renal tubules and corticomedullary adrenal hemorrhages, intramuscular hemorrhages, and multifocal pigmentary tubulonephrosis were observed. Regarding the central nervous system (CNS), mild changes manifested as multifocal hemorrhages, perivascular edema, and perivascular cuffs mostly associated with glial nodules were observed in a few cases. A severe non-suppurative meningoencephalitis was present in one case (**Table 2**). Histological findings of each bycatch case are presented in **Supplementary Table 3**.

All animals affected by the ingestion of longline hooks ($n = 5$) were adult Atlantic spotted dolphins in fair-good body condition. Ingested hooks had perforated the esophagus (cases 2 and 29), produced fibrinosuppurative pleuritis and pericardial hemorrhages (case 29; **Figure 2D**), pierced the mandibular fossa (cases 18 and 31), and affected the sublingual soft tissue to produce focal, extensive necrosis and hemorrhage (case 20). Hemothorax, hemoabdomen, and hemopericardium were also observed (**Table 1**). In one case, reddened eyes were observed (**Figure 1G**).

Of the six cases showing findings consistent with PUE, four were striped dolphins [one pregnant adult (case 17), two subadults (cases 28 and 30), and one juvenile (case 25)]; one was a Atlantic spotted dolphin calf (case 1); and another, a juvenile Atlantic bottlenose dolphin (case 7). All animals in this category were found dead, and the majority were in good-fair body condition. All had cutaneous lesions associated with contact with fishing nets, as well as disseminated intravascular gas bubbles, cutaneous impressions, lost/fractured teeth, undigested food, hyperinflated lungs with subpleural hemorrhages and hemorrhagic parenchyma, and retroperitoneal emphysema (**Table 1**).

Three other animals showed lesions compatible with PUE. They were likely caught in nets and released alive back into the ocean. They included a striped dolphin calf (case 6), a juvenile striped dolphin entangled in gear with a fishing ball (case 12), and an adult Atlantic spotted dolphin that appeared to have been entangled in a fishing net (case 23). Supposedly, shortly after release, these animals were stranded alive and subsequently died. Two had fractured bones [mandible and maxilla with lost or fractured teeth, tympanic fracture, and rib fracture], which may have been caused by active stranding (**Table 1**). Disseminated intravascular gas bubbles were present in case 23 alone. The same animal had bubbles within the posterior chamber of the eye.

Bycaught cases included seven animals that were probably hauled out and raised to the deck alive but suffered different forms of physical trauma during handling. The affected cases included Atlantic spotted dolphins ($n = 5$) [three adults (cases 11, 21, and 22); one subadult (case 27); and one juvenile (case 9)], and common dolphins ($n = 2$) [one adult (case 32) and one juvenile (case 26)]. All were stranded dead, and most were in fair body condition. These animals were polytraumatized and exhibited skin-muscle perforations (**Figure 1H**) with associated hemorrhages, which affected internal organs in some cases [perforations of the aorta (case 9), trachea and esophagus (case 22)]; neurocranium fractures (2/7) [in the squamous part of the occipital bone (case 27), and in the right occipital condyle (case 32)] with associated hematoma and congestion in the underlying leptomeninges and brain; and fractures of the maxilla and mandible (cases 26 and 32). Case 26 also showed signs of severe trauma to the right caudolateral side of the head with leptomeningeal congestion, severe scoliosis of the peduncle, and an open fracture that affected the caudal vertebrae. Other traumatic findings included hemorrhages on the adventitia of the aorta (cases 9, 11, 22, and 26) and in the rete mirabile (cases 22 and 26); hemothorax (cases 11 and 22); hemoabdomen (case 22); hemopericardium (case 22); and lung perforation (case 11) (**Table 1**).

Disseminated intravascular gas bubbles were present in four out of seven bycaught animals. One was a juvenile female common dolphin (case 26) that was found stranded dead, refrigerated (4°C) for 24 h, and necropsied while still fresh (decomposition code 2). The gas score and gas analyses were evaluated on this animal. The gas score revealed the presence of occasional small bubbles following careful screening of the subcutaneous veins (gas score 1); abundant presence of gas bubbles in the coronary veins and lumbocaudal venous plexus (gas score 5); and gas bubbles occupying complete sections of the mesenteric veins (gas score 6). Emphysema was present exclusively in the perirenal subcapsular region.

Gas analyses were performed in mesenteric veins, the right ventricle, aorta, pulmonary artery, and intestinal lumen (**Figure 3**). Except for samples of the intestine and mesenteric veins, N_2 was the main component of the sampled bubbles [61.0 $\pm$ 9.2 μmol %], followed by CO_2 [30.0 $\pm$ 16.2 μmol %], and O_2 [8.9 $\pm$ 7.1 μmol %]. Both CH_4 and H_2 were absent from these samples. In contrast, gas bubbles from the mesenteric veins contained H_2 [31.2 $\pm$ 10.2 μmol %], in addition to N_2 [54.8 $\pm$ 3.7 μmol %], O_2 [11.6 $\pm$ 3.2 μmol %], and CO_2 [2.4 $\pm$ 3.3 μmol %]. In the intestinal lumen, CO_2 was the main constituent [78.4 $\pm$ 2 μmol %], followed by H_2 [16.4 $\pm$ 1.3 μmol %], N_2 [4.2 $\pm$ 2.6 μmol %], and O_2 [1 $\pm$ 0.5 μmol %].

TABLE 2 | Histological findings in stranded cetaceans, which died because of fishery interactions.

							Bycatch									
			Entanglement		Aggression		Hook ingestion		PUE		Aggression during handling		Returned		Total	
Skeletal muscle	Acute degenerative changes	No	1/5	20%	1/4	25%	1/3	33%	0/5	0%	0/6	0%	0/3	0%	1/17	6%
		Mild	3/5	60%	1/4	25%	1/3	33%	3/5	60%	2/6	33%	3/3	100%	9/17	53%
		Moderate	1/5	20%	2/4	50%	1/3	33%	1/5	20%	3/6	50%	0/3	0%	5/17	29%
		Severe	0/5	0%	0/4	0%	0/3	0%	1/5	20%	1/6	17%	0/3	0%	2/17	12%
	Atrophy		3/5	60%	1/4	25%	0/3	0%	1/5	20%	2/6	33%	0/3	0%	3/17	18%
	Hemorrhages		0/5	0%	1/4	25%	1/3	33%	0/5	0%	4/6	67%	0/3	0%	5/17	29%
Lungs	Alveolar edema		2/5	40%	4/5	80%	3/3	100%	4/6	67%	4/6	67%	0/2	0%	11/17	65%
	Emphysema		3/5	60%	3/5	60%	2/3	67%	5/6	83%	4/6	67%	2/2	100%	13/17	76%
	Muscular bronchiolar sphincter contraction		0/5	0%	4/5	80%	2/3	67%	2/6	33%	2/6	33%	0/2	0%	6/17	35%
	Hemorrhages		1/5	20%	4/5	80%	2/3	67%	4/6	67%	4/6	675	2/2	100%	12/17	71%
Heart	Acute degenerative changes	No	0/5	0%	0/4	0%	0/3	0%	1/5	20%	4/6	67%	1/1	100%	6/15	40%
		Mild	5/5	100%	1/4	25%	1/3	33%	4/5	80%	1/6	17%	0/1	0%	6/15	40%
		Moderate	0/5	0%	0/4	0%	2/3	67%	0/5	0%	1/6	17%	0/1	0%	3/15	20%
		Severe	0/5	0%	0/4	0%	0/3	0%	0/5	0%	0/6	0%	0/1	0%	0/15	0%
	Hemorrhages		2/5	40%	0/4	0%	0/3	0%	0/5	0%	3/6	50%	0/1	0%	3/15	20%
Liver	Intracytoplasmic hyaline globules		4/5	80%	2/3	67%	2/3	67%	4/4	100%	4/5	80%	1/3	33%	11/15	73%
Adrenal glands	Hemorrhages		4/5	80%	2/4	50%	1/3	33%	2/4	50%	1/6	17%	1/3	33%	5/16	31%
Blood vessels	Leukocytosis		4/5	80%	3/5	60%	3/3	100%	5/6	83%	5/6	83%	2/3	67%	15/18	83%
	Intravascular coagulation		2/5	40%	0/5	0%	1/3	33%	1/6	17%	5/6	83%	0/3	0%	7/18	39%
	Intravascular clear spaces		5/5	100%	5/5	100%	3/3	100%	6/6	100%	5/6	83%	3/3	100%	17/18	94%
Reproductive system	Gonadal maturity	Mature	2/5	40%	3/5	60%	3/3	100%	2/6	33%	5/6	83%	1/3	33%	11/18	61%
		Immature	3/5	60%	2/5	40%	0/3	0%	4/6	67%	1/6	17%	2/3	67%	7/18	39%
Kidney	Membranous glomerulonephritis		0/5	0%	2/5	40%	1/3	33%	1/6	17%	1/6	17%	0/3	0%	3/18	17%
	Hyaline cast		1/5	20%	0/5	0%	2/3	67%	1/6	17%	2/6	33%	0/3	0%	5/18	28%
	Pigmentary tubulonephrosis		0/5	0%	1/5	20%	0/3	0%	2/6	33%	1/6	17%	1/3	33%	4/18	22%
	Hemorrhages		2/5	40%	0/5	0%	0/3	0%	0/6	0%	1/6	17%	0/3	0%	1/18	6%
Brain	Perivascular edema		1/4	20%	3/4	75%	1/3	33%	1/6	17%	2/6	33%	1/3	33%	5/18	28%
	Hemorrhages		2/4	50%	1/4	25%	2/3	67%	2/6	33%	3/6	50%	1/3	33%	8/18	44%
	Meningitis/encephalitis		1/4	25%	1/4	25%	0/3	0%	0/6	0%	0/6	0%	1/3	33%	1/18	6%
	Perivascular cuffs		0/4	0%	2/4	50%	0/3	0%	1/6	17%	3/6	50%	0/3	0%	4/18	22%
	Glial nodules		3/4	75%	0/4	0%	1/3	33%	1/6	17%	2/6	33%	0/3	0%	4/18	22%

For cases with decomposition codes 1–3 (n = 28), histological findings in the skeletal and cardiac muscle, lungs, liver, kidneys, adrenal glands, blood vessels, and brain, were detailed and compared, as well as findings of gonad maturation (M, mature; I, immature) upon the availability of samples.
The color values correspond to the percentage of a finding or a pathologic feature within each group of studied animals (bycatch, fisherman aggression and chronic entanglement).

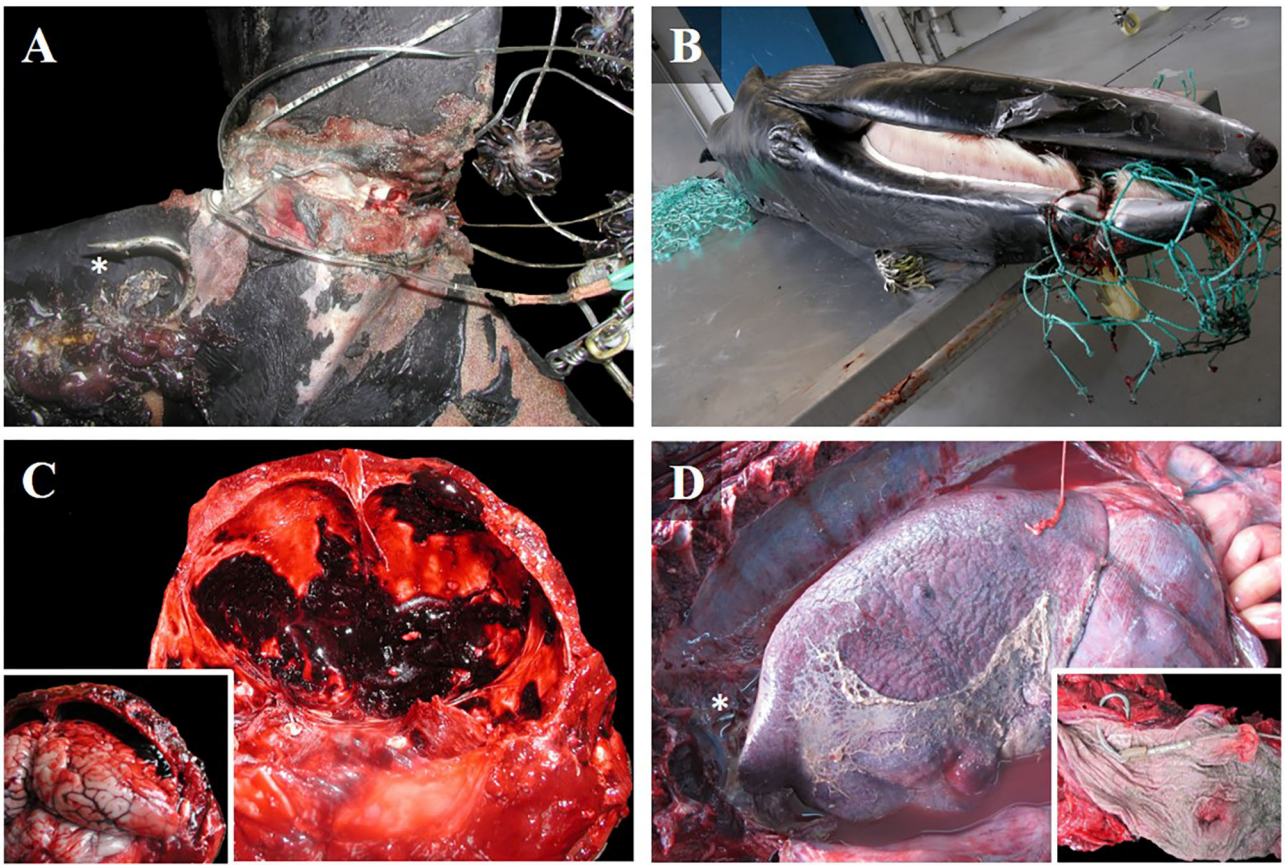

FIGURE 2 | Gross findings in cetacean deaths caused by different types of fishing interactions. **(A)** Dorsal view of the caudal peduncle of a Gervais' beaked whale calf (case 10), entangled in a longline. Cirripeds and a hook (asterisk) were attached to the nylon wire. Severe chronic skin ulcerations were observed, with a loss of soft tissue, and granulation tissue on the borders of the wound. Note that the fluke was almost amputated. **(B)** Lateral view of entangled minke whale calf (case 16) with chronic ulcerative stomatitis affecting the maxilla, and tissue strangulation. **(C)** Caudal view of the cranium of an adult Atlantic spotted dolphin (case 13) with a fatal subdural hematoma, and associated brain compression (inset). **(D)** Left lateral view of the thoracic cavity of an adult Atlantic spotted dolphin (case 29). Fibrinosuppurative pleuritis and pyothorax caused by ingestion of a longline hook (asterisk) that perforated the thoracic portion of the esophagus (inset).

Chronic Entanglement

In this category, we observed six cases with skin wounds that were consistent with chronic entanglement. They included two minke whale calves (*Balaenoptera acutorostrata*) (cases 16 and 19); two short-finned pilot whale calves (*Globicephala macrorhynchus*) (cases 14 and 24); one Gervais' beaked whale calf (*Mesoplodon europaeus*) (case 10); and one subadult Atlantic bottlenose dolphin (case 8). Regarding body condition, three out of six cases showed fair to good body condition (cases 8, 14, and 19), while two were in poor-very poor condition (cases 10 and 16). In case 24, the advanced decomposition (code 5) did not allow us to determine the body condition, nor perform histological evaluation.

All cases exhibited fishing gear impressions, erosions, and/or ulcerative lesions with granulation tissue and fibrosis over the rostrum, flippers, and/or tail. In case 14, the animal was stranded alive with nylon wire attached to a plastic floating bottle. The other five were found dead. Case 8 exhibited rope impressions between the pectoral fins and near the left eye. In case 10, nylon wire with cirripeds and longline hooks were attached to the caudal peduncle (**Figure 2A**). Case 16 had green monofilament nylon fishing gear attached to the maxilla (**Figure 2B**). Case 19 exhibited symmetrical bilateral ulcers and granulation tissue in the mandibular symphysis, consistent with fishing gear impressions. Case 24 had a thick rope (4 cm in diameter) surrounding the thoracic region. Other pathological findings included tracheal edema, hyperinflated lungs with rib impressions, serous atrophy of pericardial fat, hemorrhage in the adventitia of the thoracic aorta, and retroperitoneal emphysema. Only two cases had undigested food in the stomach (**Table 1**). Gross findings of each case are presented in **Supplementary Table 2**.

Histologically, clear intravascular spaces, compatible with intravascular gas and/or fat, mild to moderate multifocal acute muscular degenerative changes in skeletal muscle, and mild degenerative changes in the cardiac muscle, multifocal myofiber atrophy of the skeletal muscle, multifocal corticomedullary adrenal hemorrhages, intracytoplasmic hepatocellular hyaline

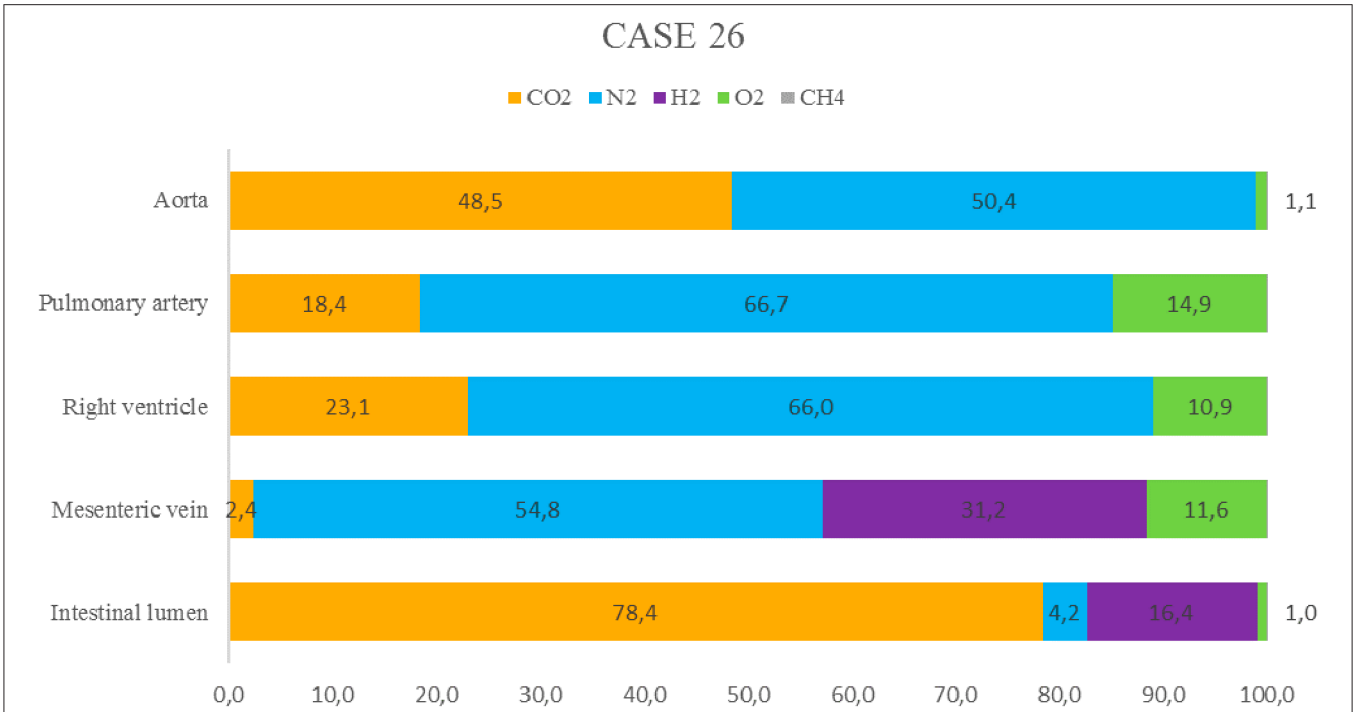

FIGURE 3 | Relative gas composition (% μmol) of samples from the intestine, mesenteric veins, right ventricle, aorta, and pulmonary artery of a juvenile female common dolphin (case 26).

globules, systemic leukocytosis, hemorrhages in multiple organs, intravascular coagulation, multifocal alveolar emphysema, alveolar edema, diffuse hemorrhagic lung parenchyma, multifocal hemorrhages in the cortex of the kidney, and hyaline casts were observed. Regarding the CNS, case 8 showed mild focal non-suppurative meningoencephalitis. Mild multifocal glial nodules and moderate multifocal hemorrhages were occasionally observed (**Table 2**). Histological findings are presented in **Supplementary Table 3**.

Fisherman Aggression

In this category ($n = 5$), we observed three Atlantic spotted dolphins [two adults (cases 3 and 13) and one juvenile (case 15)], and two common dolphins [one adult and one calf, possibly relatives as they were stranded on the same date and location (cases 4 and 5)]. All cetaceans in this group showed fair-good body condition, and a full stomach with undigested prey, as well as signs of anthropogenic trauma, such as unique or multifocal stabs inflicted by sharp instruments, mainly in the laterodorsal area affecting the thoracic region (cases 3, 4, 5, and 15) and dorsal side of the head (cases 3 and 13). Net cuts and impressions were not observed on the skin (**Table 1**). These animals exhibited several lesions associated with incisive trauma, such as vascular changes (i.e., edema, hemorrhage, hematoma) in the skin and muscular tissue, bone fractures [sixth left rib (case 4) and the ninth thoracic vertebrae (case 5)], lung perforations with related focal, extensive hemorrhage, and hemothorax (cases 4, 5, and 15), and hemorrhage in the leptomeninges (case 13; **Figure 2C**) were observed (**Table 1**). Gross findings of each case are presented in **Supplementary Table 2**.

Histologically, mild to moderate multifocal acute segmental myofiber degeneration of skeletal muscle, diffuse hemorrhages within the affected skin and muscles, mild multifocal acute degenerative changes in cardiac muscle, multifocal alveolar edema, hemorrhages in the lung parenchyma, muscular sphincter contraction of the bronchioles, multifocal emphysema, systemic leukocytosis, intracytoplasmic hepatocellular hyaline globules, multifocal corticomedullary adrenal gland hemorrhages, multifocal membranous glomerulonephritis, and multifocal pigmentary tubulonephrosis were observed. Regarding the CNS, multifocal perivascular edema, perivascular cuffs, and hemorrhages in the brain parenchyma were occasionally observed. Mild multifocal granulomatous encephalitis was present in case 3. Clear intravascular spaces were present in all cases (**Table 2**). Histological findings are presented in **Supplementary Table 3**.

Statistical Analysis

Although almost half of the affected animals were Atlantic spotted dolphins [46.9% (15/32)], no statistically significant differences were found in the prevalence of fishery interactions among animals of different species ($p = 0.125$), nor among growth development categories ($p = 0.871$), sex ($p = 0.813$), gonad maturation ($p = 0.704$), or the island of stranding ($p = 0.684$) (**Table 3**).

TABLE 3 | Statistical analysis of the epidemiological data of studied cetaceans during the period 2000–2018 (n = 586).

	Overall N = 586	**Other cause of death N = 421**	**Fishing interactions *N* = 32**	**P-value**
Species				0.125
Balaenoptera acutorostrata	6 (1.3)	4 (1.0)	2 (6.2)	
Balaenoptera borealis	2 (0.4)	2 (0.5)	0 (0.0)	
Balaenoptera edeni	2 (0.4)	2 (0.5)	0 (0.0)	
Balaenoptera physalus	4 (0.9)	4 (1.0)	0 (0.0)	
Delphinus delphis	51 (11.3)	47 (11.2)	4 (12.5)	
Globicephala macrorhynchus	36 (7.9)	34 (8.1)	2 (6.2)	
Grampus griseus	11 (2.4)	11 (2.6)	0 (0.0)	
Kogia breviceps	23 (5.1)	23 (5.5)	0 (0.0)	
Kogia sima	6 (1.3)	6 (1.4)	0 (0.0)	
Lagenodelphis hosei	3 (0.7)	3 (0.7)	0 (0.0)	
Megaptera novaeangliae	2 (0.4)	2 (0.5)	0 (0.0)	
Mesoplodon bidens	1 (0.2)	1 (0.2)	0 (0.0)	
Mesoplodon densirostris	7 (1.5)	7 (1.7)	0 (0.0)	
Mesoplodon europaeus	6 (1.3)	5 (1.2)	1 (3.1)	
Orcinus orca	1 (0.2)	1 (0.2)	0 (0.0)	
Phocoena phocoena	1 (0.2)	1 (0.2)	0 (0.0)	
Physeter macrocephalus	22 (4.9)	22 (5.2)	0 (0.0)	
Pseudorca crassidens	2 (0.4)	2 (0.5)	0 (0.0)	
Stenella coeruleoalba	92 (20.3)	86 (20.4)	6 (18.8)	
Stenella frontalis	89 (19.6)	74 (17.6)	15 (46.9)	
Stenella longirostris	3 (0.7)	3 (0.7)	0 (0.0)	
Steno bredanensis	23 (5.1)	23 (5.5)	0 (0.0)	
Tursiops truncatus	36 (7.9)	34 (8.1)	2 (6.2)	
Ziphius cavirostris	24 (5.3)	24 (5.7)	0 (0.0)	
Sex				0.813
Female	205 (45.8)	191 (45.9)	14 (43.8)	
Male	243 (54.2)	225 (54.1)	18 (56.2)	
Growth development categories				0.871
Neonate/calf	131 (28.9)	123 (29.2)	8 (25.0)	
Juvenile/subadult	130 (28.7)	120 (28.5)	10 (31.2)	
Adult	192 (42.4)	178 (42.3)	14 (43.8)	
Coast				0.684
El Hierro y La Palma	8 (1.8)	7 (1.7)	1 (3.1)	
La Gomera y Tenerife	154 (34.0)	141 (33.5)	13 (40.6)	
Gran Canaria	125 (27.6)	116 (27.6)	9 (28.1)	
Fuerteventura y Lanzarote	166 (36.6)	157 (37.3)	9 (28.1)	
Mature categories				0.704
Immature	225 (50.1)	210 (50.4)	15 (46.9)	
Mature	224 (49.9)	207 (49.6)	17 (53.1)	
Body condition				0.004
Poor/very poor	162 (37.8)	158 (39.6)	4 (13.3)	
Good/fair	267 (62.2)	241 (60.4)	26 (86.7)	
Diving behavior				0.008
Shallow diver	317 (70.0)	288 (68.4)	29 (90.6)	
Deep diver	136 (30.0)	133 (31.6)	3 (9.4)	

The pathological cause of death in 453 cases was determined, among which, 32 cases were due to fishery interactions.

Body Condition

Body condition could have been determined in 94.7% of the individuals, with a known cause of death (429/453). Most of the animals [62.2% (267/429)] showed good/fair body condition, while 37.8% (162/429) were in poor/very poor body condition. The body condition of two dolphins, which died as a result of fishery interactions, could not have been determined owing to artifactual loss of tissue (case 9) and the very advanced state of decomposition of the carcass (code 5) (case 24) (**Supplementary Table 1**). Nonetheless, most dolphins showing signs of fishery interactions were in good/fair body condition 86.7% (26/30), compared with dolphins in poor/very poor condition. This difference was statistically significant ($p = 0.004$) (**Table 3**).

Diving Behavior

Shallow-water species were stranded in greater numbers, representing 70% of the animals with a known cause of death (317/453), while deep divers represented 30% of the cases (136/453). Although we observed more shallow than deep divers stranded during the study period, this difference was even larger when the prevalence of shallow [90.6% (29/32)] vs. deep divers [9.4% (3/32)] was compared with the findings of fishery interactions. This difference was statistically significant ($p = 0.008$) (**Table 3**).

Temporality of Stranding Events

The yearly average number of stranding caused by fishery interactions was 1.7 animals (32 cases over 19 years), indicating a low rate of fishery interactions within the geographical area. In 2001 and 2017, a slight increase in the number of cases ($n = 5$ each year) was noted. No fishery interactions were recorded during the years 2003, 2006, 2010, or 2011.

DISCUSSION

The rates of fishery interactions among cetaceans are underreported worldwide (2, 3). In the case of stranded cetaceans, an advanced decomposition code may hinder the determination of the cause of death. In addition, most fishery interaction findings (except gear cuts and impressions) are not pathognomonic (4, 5). Nonetheless, fisheries are considered a major global threat to cetaceans (34). Bycatch especially affects the harbor porpoise (*Phocoena phocoena*), bottlenose dolphin, common dolphin, and striped dolphin [e.g., (1, 35, 36)]. Furthermore, cases of chronic entanglements appear to be on the rise globally (8, 10), and their effects in certain baleen populations such as the minke whale is concerning (34).

In the Canary Islands, fishing is mainly artisanal and multi-specific, and is characterized by the use of small vessels ($\leq$15 m in total length) and various types of fishing gear. Larger vessels are also used for tuna, but to a lesser extent[2]. Gillnets are allowed during certain periods in some designated areas, whereas trawling is absolutely forbidden in the archipelago. In addition, longlines and traps are forbidden in El Hierro and Fuerteventura, as well as in all marine reserves of the archipelago [Annex 1. Decreto 182/2004 de 21 de diciembre, Reglamento de la Ley de Pesca de Canarias]. These conservative policies may explain the low annual rates of fishing-related deaths in cetaceans stranded along the Canary coasts.

Of the seven cetacean species identified, the Atlantic spotted dolphin was the most affected. This species, together with the Atlantic bottlenose dolphin, Gervais' beaked whale, short-finned pilot whale, and striped dolphin are regularly present year-round. Moreover, common dolphins and minke whales are seasonally present (37, 38).

Bycatch

Fishery interactions were likely recent and occurred close to the Canary coast in animals that were stranded alive or found dead in a fresh or very fresh state. Although local artisanal fisheries might have been responsible for these deaths, other fishing activities in international waters and illegal fishing cannot be ruled out. Until now, no pathognomonic clinical findings have been identified for bycaught animals (4). However, the greater the number of compatible lesions identified in a case, the more consistent the identification of bycatch (5, 39).

In this study, the ingestion of longline hooks affected Atlantic spotted dolphins alone ($n = 5$). Although this interaction with longline fisheries is well-known worldwide (40, 41), its related pathologies have been poorly reported. In this study, we identified two cases of Atlantic spotted dolphins with hooks that pierced the mandibles. To the best of our knowledge, this is also the first report of esophageal perforation with fibrinosuppurative pleuritis caused by hook ingestion in a dolphin species (**Figure 2D**). Although the literature reflects more information about larynx strangulation with longline fishing gear (42, 43), this type of lesions was not observed in the present study.

Different necropsy findings might be observed in cases of fishing net entrapment, depending on the fishery and the affected cetacean species (5, 21, 22, 44). Our results are consistent with those of Bernaldo de Quirós et al. (6), who reported external net marks, evidence of recent feeding (fresh undigested gastric contents), and disseminated intravascular gas bubbles.

In contrast with the findings of Bernaldo de Quirós et al. (6), only one case had reddish eyes (case 29), and another case had bubbles within the posterior chamber of the eye (case 23). In the present study, hyperinflated and hemorrhagic lungs were also identified, with occasional froth and rib impressions, corresponding histologically with areas of marked emphysema and alveolar edema. These findings agreed with those of Moore et al. (5). However, Bernaldo de Quirós et al. (6) found that froth in the airways and other lung changes (i.e., wet, heavy edema, congestion, and hemorrhage) were statistically poor indicators of bycatch.

In the present study, case 26 was one example of a bycaught dolphin with gas embolism. This animal exhibited a large number of gas bubbles (gas score of 18), consistent with the findings of Bernaldo de Quirós et al. (24). In addition, the composition of the gas bubbles was consistent with gases produced by compression and decompression, in which nitrogen is the main component,

[2]https://www.gobiernodecanarias.org/pesca/

and CO_2 can sometimes be present at high concentrations (20). Hydrogen, a marker of putrefaction, was found in the mesenteric veins alone, which is consistent with the findings of Bernaldo de Quirós et al. (24).

Pathological findings in cases of fishing net entrapment often suggest some degree of physical struggle associated with varying degrees of muscular exertion (5). In bycaught dolphins, the adrenocortical response and hyperthermia (45) induce injury to the skeletal muscle, similar to that described in live stranded cetaceans (26, 27, 31). Acute degenerative changes have also been observed in severely polytraumatized free-ranging stranded cetaceans, such as in cases of ship strikes (23, 28) and fatal social traumatic intra-interspecific interactions (23, 32). Previous studies have reported cardiac changes (29, 46, 47), as well as intracytoplasmic hepatocellular hyaline globules (13, 27, 48) in agonal situations. Intravascular coagulation, mostly present in bycaught dolphins that endured aggression during handling, has been described in domestic animals with extensive tissue destruction (49). We also observed a few cases with mild inflammation of the CNS. These findings are consistent with the presence of concomitant infections.

Chronic Entanglement

It is difficult to know the actual number of entangled cetaceans even if the number of entangled individuals within a specific population is known, as the same animal can become entangled multiple times (50), and entangled carcasses tend to sink (8). Even with the limitations of the available data, the number of reported entanglements during the last decade is three times higher than that reported during the 1990s, and 97% of those cases were entangled in fishing gear (10).

In the Atlantic Ocean, at least half of the mysticetes' deaths are caused by fishing gear (51). Minke whales particularly, appear to be less likely to survive entanglements than larger whales (52). The first description of an entangled minke whale in the Canary Islands was reported in 1993 in Morro Jable-Fuerteventura. This stranded animal was found dead, with a fishing net in the rostrum (53). In recent years (2012–2020), entanglements have included seven minke whales, six Bryde's whales (*B. edeni*), one humpback whale (*Megaptera novaeangliae*)[3], two rough-toothed dolphins (*Steno bredanensis*), and one member of the Delphinidae family, sighted close to the Canary coasts (personal communication with the Canary Islands stranding network). Among these, three minke whales and two Bryde's whales were disentangled[4]. Whether those whales survived remains unknown, as no follow-up investigations were conducted after the disentanglement. Consistent with the findings of the present study, we consider chronic entanglements a potential threat to cetacean' populations in the Canary Islands, especially minke and Bryde's whales.

Entangled mysticetes are commonly found with ropes and nets within the oral cavity, or surrounding the flippers, or tail, and entangled odontocetes are usually found with recreational fishing gear, longlines, and fishing lures (5). Even if the gear becomes detached, the scars of healed wounds may remain (54). In chronic entanglements, open and unhealed wounds could lead to septicemia and even death (5). Although no microbiological studies have been conducted on entangled cases in the present study, histological evaluation of the cases revealed intravascular coagulation, leukocytosis (mostly neutrophilic), and multiorgan hemorrhages in most of the affected animals.

In addition, those cases in poor body condition showed atrophy of the skeletal muscle. Case 19 also exhibited severe serous atrophy of pericardial fat, which indicates a catabolic condition. In the present study, only one animal was stranded alive and most cases showed mild degenerative changes in myocardiocytes. The occurrence of cardiac failure in cases of chronic entanglement should be further investigated. Similarly, the presence of hepatocellular hyaline globules in almost all cases was remarkable, previously described in agonal situations of stranded cetaceans (27, 48).

Fisherman Aggression

The predominance of artisanal fisheries in the Canary Islands suggests daily direct contact between cetaceans and fishermen, who are usually in small vessels a few meters above. Our results showed lethal trauma on the dorsal side of the dolphins, which is consistent with the fishermen's position just above, on the water's surface. Stabs and contusions affected mainly the thoracic cavity (with associated hemothorax, bone fractures, lung perforations), and/or the cephalic region (head contusions with associated brain hemorrhages). No other common findings were observed between these cases and the bycatch cases (e.g., net cuts/impressions on the skin, hyperinflated lungs, intravascular disseminated gas bubbles), nor evidence of being brought to deck. Although this category has been previously described, few cases have been reported (7, 55), because the most frequent aggressions inflicted by fishermen (amputations, stabs, and perforations) occur onboard, when animals are trapped in gillnets or trawlnets (5). Another form of human aggression is gunshot wounds (56), which were not observed in the present study. Histological findings, such as severe focal, extensive hemorrhages in the skin and muscles, and hemorrhagic lungs, agreed with the gross findings, which indicated that the various cases of trauma were inflicted while the animals were still alive. Histological findings were associated with agonal perimortem changes in dolphins, as well as systemic leukocytosis, due to open wounds.

Statistical Analysis

Body Condition

The body condition index is a good indirect indicator of the nutritional status of cetaceans (17). Previous studies have described bycaught dolphins in good body condition (4), but this is common in cetacean deaths due to the fatal trauma of ship strikes (5, 7, 12, 13), and social traumatic intra-interspecific interactions (32).

Our results indicate that individuals with good nutritional status may be more susceptible to adverse fishery interactions (especially bycatch), compared with animals exhibiting catabolic metabolism due to energy demanding pathologies (i.e., severe

[3]https://twitter.com/GranCanariaCab/status/1209437122345734145

[4]https://www.eldiario.es/canariasahora/sociedad/Liberada-canarias-ballena-atrapada-marana_0_76292969.html

infections, parasitism, or neoplasia). In contrast, chronic entangled cetaceans typically appear in poor body condition (5, 7). Our results showed only a few necropsied cases of entanglement, only half of which showed poor-very poor body condition. However, observational records along the Canary coasts have confirmed the presence of entangled whales in poor body condition (personal communication with the Canary Islands stranding network).

Diving Behavior

In the present study, shallow diving species were affected by fishery interactions to a significantly greater extent than deep diving species. These findings are consistent with those of previous studies, in which the majority of the affected cetaceans were shallow-water species (5, 10, 40). In the Canary Islands, artisanal fishing activities are mainly pelagic and superficial (0–150 m depth)[5], which is consistent with the swimming patterns of shallow species.

Nonetheless, it is important to highlight the fact that deep divers, especially sperm whales (*Physeter macrocephalus*), have been reported worldwide with considerable amounts of ingested marine debris, including fishing gear (10, 57, 58). The Canary waters contain a great variety of deep divers, which are known to be affected by marine debris (59). We highly recommend more detailed descriptions of ingested foreign bodies, to better understand whether they originate from fishery activities.

Temporality of Stranding Events

Fortunately, our geographical area showed relatively low numbers of deaths due to fishing activities. This might be related to the sustainable artisanal fisheries and restrictive laws in the Canary waters. Similarly, in the Azores of Portugal, bycatch rates are low, with no evidence of any increase over the last 15 years (60). Artisanal fisheries cause a considerable number of deaths worldwide, even though these numbers are typically lower than those caused by industrial fisheries (1, 61).

In recent years, although sightings of live chronic entangled cetaceans have increased along the archipelago, necropsied cases remain scarce. The widespread use of social media to report the consequences of pollution in marine ecosystems has helped us to learn more about these interactions.

CONCLUSIONS

This is the first retrospective study of fishery interactions in stranded cetaceans along the Canary Islands. The determination of different types of fishery interactions as the cause of death was based on a 20-year investigation of stranded cetaceans. We described the most relevant gross and histologic findings in each type of interaction. Three types of fishery interactions were observed according to gross findings, including chronic entanglement, fisherman aggression, and bycatch (longline hook ingestion and fishing net entrapment).

We found that the Atlantic spotted dolphin, regularly seen in our geographical area, was the most affected species. We also found that cetaceans in good-fair body condition and shallow-water species were significantly more affected. The low prevalence of fishery interactions in this region could be attributed to the broad protective legislation applicable to the Canary waters and the most prevalent type of fisheries, artisanal fisheries. However, there is increasing concern about chronic entanglements, especially in minke and Bryde's whales. We encourage continuous pathological studies on stranded cetaceans, to monitor fishing-related deaths and their consequences in cetacean populations. The findings of this study might contribute to the implementation of appropriate conservation policies in the Canary Islands.

[5]http://www.grancanariapescaenred.com/sobre-nosotros/como-pescamos/

DATA AVAILABILITY STATEMENT

All datasets generated for this study are included in the article/**Supplementary Material**.

AUTHOR CONTRIBUTIONS

RP-L, YB, MArb, AF, and ES: conceptualization. RP-L, AF, ES, JD, JD-D, SS, A, NG-Á, DZ, AX, MR, IF-J, FC, PD-S, SS-G, NC, CS-S, MArr, YB, and MArb: sampling and diagnosis of the cause of death of each animal. PS, RP-L, and YB: data analyses. RP-L and MR: image editing. RP-L: writing. YB, MArb, MR, AF, and ES: supervision. All authors: review and editing.

FUNDING

We thank the Canary Islands Government for funding the stranding network. Partial funding came from the national project (ref. CGL2015-71498-P, PGC2018-101226-B-I00, MAC/1.1b/149). The necropsies and sampling were done under permission from the Ministry of Agriculture, Fisheries, Food, and Environment of Spain. This study involved a Ph.D. (RP-L) and one postdoc (YB) fellowship supported by the University of Las Palmas de Gran Canaria.

ACKNOWLEDGMENTS

The authors would like to thank our laboratory technicians, all the members of the Cetacean Stranding Network of the Canary Islands, especially to Marisa Tejedor, Vidal Martín (Society for the Study of Cetaceans in the Canarian Archipelago) and Manuel Carrillo (Canary Islands Conservation).

SUPPLEMENTARY MATERIAL

The Supplementary Material for this article can be found online at: https://www.frontiersin.org/articles/10.3389/fvets.2020.567258/full#supplementary-material

REFERENCES

1. Reeves RR, McClellan K, Werner TB. Marine mammal bycatch in gillnet and other entangling net fisheries, 1990 to 2011. *Endanger Species Res.* (2013) 20:71–97. doi: 10.3354/esr00481
2. Young NM, Iudicello S. *Worldwide Bycatch of Cetaceans. U.S. Dep. Commerce,* National Oceanic Atmospheric Administration Technical Memorandum, National Marine Fisheries Service NMFS-OPR-36 (2007). p. 276.
3. Dolman SJ, Moore MJ. Welfare implications of cetacean bycatch and entanglements. In: *Marine Mammal Welfare.* Cham: Springer (2017). p. 41–65.
4. Kuiken T. Review of the criteria for the diagnosis of bycatch in cetaceans. In: *Proceedings of the 2nd ECS Workshop on Cetacean Pathology*. Saskatoon, SK: European Cetacean Society Newsletter 26 (Spec Issue) (1996). p. 38–43.
5. Moore MJ, Hoop J, Van Der Barco SG, Costidis AM, Gulland FM, Jepson PD, et al. Criteria and case definitions for serious injury and death of pinnipeds and cetaceans caused by anthropogenic trauma. *Dis Aquat Organ.* (2013) 103:229–64. doi: 10.3354/dao02566
6. Bernaldo de Quirós Y, Hartwick M, Rotstein DS, Garner MM, Bogomolni A, Greer W, et al. Discrimination between bycatch and other causes of cetacean and pinniped stranding. *Dis Aquat Organ.* (2018) 127:83–95. doi: 10.3354/dao03189
7. Read AJ, Murray KT. *Gross Evidence of Human-Induced Mortality in Small Cetaceans*. NOAA Technical Memorandum NMFS (2000). p. 21.
8. Laist DW. Impacts of marine debris: entanglement of marine life in marine debris, including a comprehensive list of species with entanglement. In: Coe JM, Rogers DB, editors. *Marine Debris: Sources, Impacts, and Solutions*. New York, NY: Springer-Verlag (1997). p. 99–139.
9. Macfadyen G. Huntington T, Cappell R. *Abandoned, Lost or Otherwise Discarded Fishing Gear*. Rome: Food and Agriculture Organization of the United Nations (2009).
10. Baulch S, Perry C. Evaluating the impacts of marine debris on cetaceans. *Mar Pollut Bull.* (2014) 80:210–21. doi: 10.1016/j.marpolbul.2013.12.050
11. IWC. *Report of the Fourth Workshop on Large Whale Entanglement Issues*. Provincetown: Center for Coastal Studies (2018). Available online at: https://iwc.int/entanglement-response-experts-meet-in-provincetown
12. Arbelo M, Espinosa De Los Monteros A, Herráez P, Andrada M, Sierra E, Rodríguez F, et al. Pathology and causes of death of stranded cetaceans in the canary Islands (1999-2005). *Dis Aquat Organ.* (2013) 103:87–99. doi: 10.3354/dao02558
13. Díaz-Delgado J, Fernández A, Sierra E, Sacchini S, Andrada M, Vela A, et al. Pathologic findings and causes of death of stranded cetaceans in the Canary Islands. *PLoS ONE.* (2018) 13:e0204444. doi: 10.1371/journal.pone.0204444
14. Kuiken T, García-Hartmann M. Proceedings of dissection techniques and tissue sampling. In: *Proceedings of the First ECS Workshop on Cetacean Pathology*. Leiden (1991). p. 13–4.
15. Tejedor M. *Aportaciones a la Osteología y sus Anomalías Asociadas en los Cetáceos Menores Del Archipiélago Canario*. Las Palmas de Gran Canaria: University of Las Palmas de Gran Canaria (2016).
16. Geraci JR, Lounsbury VJ. *Marine Mammals Ashore: A Field Guide for Strandings (N Aquarium, Ed.), 2 nd Edn*. Baltimore, MD (2005).
17. Joblon MJ, Pokras MA, Morse B, Harry CT, Rose KS, Sharp SM, et al. Body condition scoring system for delphinids based on short-beaked common dolphins (*Delphinus delphis*). *J Mar Anim Their Ecol.* (2014) 7:5–13. Available online at: http://www.oers.ca/journal/volume7/issue2/scientific1.pdf
18. IJsseldijk LL, Brownlow AC, Mazzariol S. *European Best Practice on Cetacean Post-Mortem Investigation and Tissue Sampling*. Istanbul: Joint Accobams and Ascobans Document (2019).
19. Bernaldo de Quirós Y. *Methodology and Analysis of Gas Embolism: Experimental Models and Stranded Cetaceans*. Las Palmas de Gran Canaria: University of Las Palmas de Gran Canaria. (2011).
20. Bernaldo de Quirós Y, González-Díaz O, Møllerløkken A, Brubakk AO, Hjelde A, Saavedra P, et al. Differentiation at autopsy between *in vivo* gas embolism and putrefaction using gas composition analysis. *Int J Legal Med.* (2013) 127:437–45. doi: 10.1007/s00414-012-0783-6
21. Kuiken T, Simpson VR, Allchin CR, Bennett PM, Codd GA, Harris EA, et al. Mass mortality of common dolphins (*Delphinus delphis*) in south west England due to incidental capture in fishing gear. *Vet Rec.* (1994) 134:81–9. doi: 10.1136/vr.134.4.81
22. Jepson PD, Deaville R, Acevedo-Whitehouse K, Barnett J, Brownlow A, Brownell RL, et al. What caused the UK's largest common dolphin (*Delphinus delphis*) mass stranding event? *PLoS ONE.* (2013) 8:e60953. doi: 10.1371/journal.pone.0060953
23. Sierra E, Espinosa de los Monteros A, Fernández A, Díaz-Delgado J, Suárez-Santana C, Arbelo M, et al. Muscle pathology in free-ranging stranded cetaceans. *Vet Pathol.* (2017) 54:298–311. doi: 10.1177/0300985816660747
24. Bernaldo de Quiros Y, Seewald JS, Sylva SP, Greer B, Niemeyer M, Bogomolni AL, et al. Compositional discrimination of decompression and decomposition gas bubbles in bycaught seals and dolphins. *PLoS ONE.* (2013) 8:e83994. doi: 10.1371/journal.pone.0083994
25. Campbell-Malone R, Barco SG, Daoust P-Y, Knowlton AR, McLellan WA, Rotstein DS, et al. Gross and histologic evidence of sharp and blunt trauma in north atlantic right whales (*Eubalaena glacialis*) killed by vessels. *J Zoo Wildl Med.* (2008) 39:37–55. doi: 10.1638/2006-0057.1
26. Herráez P, Sierra E, Arbelo M, Jaber JR, de los Monteros AE, Fernández A. Rhabdomyolysis and myoglobinuric nephrosis (capture myopathy) in a striped dolphin. *J Wildl Dis.* (2007) 43:770–4. doi: 10.7589/0090-3558-43.4.770
27. Herráez P, Espinosa de los Monteros A, Fernández A, Edwards JF, Sacchini S, Sierra E. Capture myopathy in live-stranded cetaceans. *Vet J.* (2013) 196:181–8. doi: 10.1016/j.tvjl.2012.09.021
28. Sierra E, Fernández A, Espinosa De Los Monteros A, Arbelo M, Díaz-Delgado J, Andrada M, et al. Histopathological muscle findings may be essential for a definitive diagnosis of suspected sharp trauma associated with ship strikes in stranded cetaceans. *PLoS ONE.* (2014) 9:e88780. doi: 10.1371/journal.pone.0088780
29. Câmara N, Sierra E, Fernandez-Maldonado C, Espinosa de Los Monteros A, Arbelo M, Fernandez A, et al. Stress cardiomyopathy in stranded cetaceans: a histological, histochemical and immunohistochemical study. *Vet Rec.* (2019) 185:694. doi: 10.1136/vr.105562
30. Câmara N, Sierra E, Fernández A, Suárez-santana CM, Puig-lozano R, Arbelo M, et al. Skeletal and cardiac rhabdomyolysis in a live-stranded neonatal Bryde's Whale with fetal distress. *Front Vet Sci.* (2019) 6:476. doi: 10.3389/fvets.2019.00476
31. Câmara N, Sierra E, Fernández A, Arbelo M, Bernaldo de Quirós Y, Arregui M, et al. Capture myopathy and stress cardiomyopathy in a live-stranded Risso's Dolphin (*Grampus griseus*) in rehabilitation. *Anim Open Access J MDPI.* (2020) 10:220. doi: 10.3390/ani10020220
32. Puig-Lozano R, Fernández A, Saavedra P, Tejedor M, Sierra E, De la Fuente J, et al. Retrospective study of traumatic intra-interspecific interactions in stranded cetaceans, Canary Islands. *Front Vet Sci.* (2020) 7:107. doi: 10.3389/fvets.2020.00107
33. R Core Team. *R: A Language and Environment for Statistical Computing.* Vienna: R Foundation for Statistical Computing (2019). Available online at: https://www.R-project.org/
34. Dolman SJ, Brakes P. Sustainable fisheries management and the welfare of bycaught and entangled cetaceans. *Front Vet Sci.* (2018) 5:287. doi: 10.3389/fvets.2018.00287
35. Bjørge A, Skern-Mauritzen M, Rossman MC. Estimated bycatch of harbour porpoise (*Phocoena phocoena*) in two coastal gillnet fisheries in Norway, 2006–2008. Mitigation and implications for conservation. *Biol Conserv.* (2013) 161:164–73. doi: 10.1016/j.biocon.2013.03.009
36. Peltier H, Authier M, Deaville R, Dabin W, Jepson PD, van Canneyt O, et al. Small cetacean bycatch as estimated from stranding schemes: the common dolphin case in the northeast Atlantic. *Environ Sci Policy.* (2016) 63:7–18. doi: 10.1016/j.envsci.2016.05.004
37. Martín V, Servidio A, Tejedor M, Arbelo M, Brederlau B, Neves S, et al. Cetaceans and conservation in the canary islands. In: *18th Biennial Conference on the Biology of Marine Mammals*. Quebec City (2009).
38. Smit V, Ritter F, Ernert A, Strueh N. *Habitat Partitioning by Cetaceans in a Multi-Species Ecosystem Around the Oceanic Island of La Gomera (Canary Islands)*. Stralsund: Poster communication presented at the Annual Conference of the ECS (2010). p. 12161.

39. García Hartmann M, Couperus AS, Addink MJ. The diagnosis of bycatch: preliminary results of research in the Netherlands. *Eur Cetacean Soc Newslett.* (1994) 26:16–26.
40. NOAA. *List-Fisheries-Summary-Tables.* (2020). Available online atAvailable online at @ www.fisheries.noaa.gov
41. Werner TB, Northridge S, Press KM, Young N. Mitigating bycatch and depredation of marine mammals in longline fisheries. *ICES J Mar Sci.* (2015) 72:1576–86. doi: 10.1093/icesjms/fsv092
42. Gomerčić MD, Galov A, Gomerčić T, Škrtić D, Curković S, Lucić H, et al. Bottlenose dolphin (*Tursiops truncatus*) depredation resulting in larynx strangulation with gillnet parts. *Mar Mammal Sci.* (2009) 25:392–401. doi: 10.1111/j.1748-7692.2008.00259.x
43. Levy AM, Brenner O, Scheinln A, Morlck D, Ratner E, Goffman O, et al. Laryngeal snaring by ingested fishing net in a common Bottlenose Dolphin (*Tursiops truncatus*) off the israeli shoreline. *J Wildl Dis.* (2009) 45:834–8. doi: 10.7589/0090-3558-45.3.834
44. Deaville R, Jepson PD., (eds). *CSIP Final Report for the period 1st January 2005–31st December 2010*. London: Institute of Zoology (2011).
45. Curry BE. *Stress in Mammals: The Potential Influence of Fishery-Induced Stress on Dolphins in the Eastern Tropical Pacific Ocean.* La Jolla, CA: NOAA Technical Memorandum. NOAA-TM-NMFS-SWFSC-260 (1999).
46. Cowan DF, Curry BE. *Histopathological Assessment of Dolphins Necropsies Onboard Vessels in the Eastern Tropical Pacific Tuna Fishery.* Santa Cruz, CA: Southwest Fisheries Science Center, National Marine Fisheries Service, National Oceanographic and Atmospheric Administration (NOAA) Administrative Report No. LJ-02-24C (2002). p. 31.
47. Cowan DF, Curry BE. Histopathology of the alarm reaction in small odontocetes. *J Comp Pathol.* (2008) 139:24–33. doi: 10.1016/j.jcpa.2007.11.009
48. Jaber JR, Pérez J, Arbelo M, Andrada M, Hidalgo M, Gómez-Villamandos JC, et al. Hepatic lesions in cetaceans stranded in the Canary Islands. *Vet Pathol.* (2004) 41:147–53. doi: 10.1354/vp.41-2-147
49. Zachary JF. Bone marrow and blood cells. In: Zachary JF, editor. *Pathologic Basis of Veterinary Disease*. 6th ed. St. Louis, MI: Elsevier (2017). p. 724–61.
50. Knowlton AR, Hamilton PK, Marx MK, Pettis HM, Kraus SD. Monitoring North Atlantic right whale Eubalaena glacialis entanglement rates: a 30 yr retrospective. *Mar Ecol Prog Ser.* (2012) 466:293–302. doi: 10.3354/meps09923
51. Northridge S, Cargill A, Smru AC, Mandleberg L, Hwdt SC, Sac BR. Entanglement of minke whales in Scottish waters; an investigation into occurrence, causes and mitigation. Contract Report. Final Report to Scottish Government CR/2007/49 (2010).
52. Lien J. Entrapments of large cetaceans in passive inshore fishing gear in Newfoundland and Labrador (1979-1990). *Rep Int Whal Comm.* (1994) 149—57.
53. van Waerebeek K, André M, Sequeira M, Vidal M, Daniel R, Anne C. Spatial and temporal distribution of the minke whale, Balaenoptera acutorostrata (Lacépède, 1804), in the southern. *J Cetacean Res Manag.* (1999) 1:223–37.
54. Heyning JE, Lewis TD. Entanglements of baleen whales in fishing gear off southern California. *Rep Int Whal Comm.* (1990) 40:427–31.
55. Byard RW, Kemper C, Bossley M, Kelly D, Hill M. Veterinary forensic pathology: the assessment of injuries to dolphins at postmortem. *Forensic Pathol Rev.* (2006) 4:415–33. doi: 10.1007/978-1-59259-921-9_14
56. Goldstein T, Johnson S, Phillips A, Hanni K, Fauquier D. Human-related injuries observed in live stranded pinnipeds along the. *Aquat Mamm.* (1999) 25:43–51.
57. Jacobsen JK, Massey L, Gulland F. Fatal ingestion of floating net debris by two sperm whales (*Physeter macrocephalus*). *Mar Pollut Bull.* (2010) 60:765–7. doi: 10.1016/j.marpolbul.2010.03.008
58. Unger B, Rebolledo ELB, Deaville R, Gröne A, IJsseldijk LL, Leopold MF, et al. Large amounts of marine debris found in sperm whales stranded along the North Sea coast in early 2016. *Mar Pollut Bull.* (2016) 112:134–41. doi: 10.1016/j.marpolbul.2016.08.027
59. Puig-Lozano R, Bernaldo de Quirós Y, Díaz-Delgado J, García-Álvarez N, Sierra E, De la Fuente J, et al. Retrospective study of foreign body-associated pathology in stranded cetaceans, Canary Islands (2000–2015). *Environ Pollut.* (2018) 243:519–27. doi: 10.1016/j.envpol.2018.09.012
60. Cruz MJJ, Machete M, Menezes G, Rogan E, Silva MAMA. Estimating common dolphin bycatch in the pole-and-line tuna fishery in the Azores. *PeerJ.* (2018) 2018:1–18. doi: 10.7717/peerj.4285
61. Mangel JC, Alfaro-Shigueto J, Waerebeek K, Van Cáceres C, Bearhop S, Witt MJ, et al. Small cetacean captures in Peruvian artisanal fisheries: high despite protective legislation. *Biol Conserv.* (2010) 143:136–43. doi: 10.1016/j.biocon.2009.09.017

Conflict of Interest: The authors declare that the research was conducted in the absence of any commercial or financial relationships that could be construed as a potential conflict of interest.

Copyright © 2020 Puig-Lozano, Fernández, Sierra, Saavedra, Suárez-Santana, De la Fuente, Díaz-Delgado, Godinho, García-Álvarez, Zucca, Xuriach, Arregui, Felipe-Jiménez, Consoli, Díaz-Santana, Segura-Göthlin, Câmara, Rivero, Sacchini, Bernaldo de Quirós and Arbelo. This is an open-access article distributed under the terms of the Creative Commons Attribution License (CC BY). The use, distribution or reproduction in other forums is permitted, provided the original author(s) and the copyright owner(s) are credited and that the original publication in this journal is cited, in accordance with accepted academic practice. No use, distribution or reproduction is permitted which does not comply with these terms.

frontiers in Veterinary Science

ORIGINAL RESEARCH
published: 28 October 2020
doi: 10.3389/fvets.2020.570055

Standardization of Dolphin Cardiac Auscultation and Characterization of Heart Murmurs in Managed and Free-Ranging Bottlenose Dolphins (*Tursiops truncatus*)

Barbara K. Linnehan[1], Adonia Hsu[2], Forrest M. Gomez[1], Sharon M. Huston[2], Ryan Takeshita[1], Kathleen M. Colegrove[3], Teri K. Rowles[4], Ashley Barratclough[1], Whitney B. Musser[1], Craig A. Harms[5], Veronica Cendejas[1], Eric S. Zolman[1], Brian C. Balmer[1], Forrest I. Townsend[6], Randall S. Wells[7], Eric D. Jensen[8], Lori H. Schwacke[1] and Cynthia R. Smith[1]*

[1] National Marine Mammal Foundation, San Diego, CA, United States, [2] San Diego Veterinary Cardiology, San Diego, CA, United States, [3] Zoological Pathology Program, University of Illinois at Urbana-Champaign, Brookfield, IL, United States, [4] Office of Protected Resources, National Oceanic and Atmospheric Administration, Silver Spring, MD, United States, [5] Center for Marine Sciences and Technology, North Carolina State University, Morehead City, NC, United States, [6] Bayside Hospital for Animals, Fort Walton Beach, FL, United States, [7] Chicago Zoological Society's Sarasota Dolphin Research Program, c/o Mote Marine Laboratory, Sarasota, FL, United States, [8] U.S. Navy Marine Mammal Program, Naval Information Warfare Center Pacific, San Diego, CA, United States

OPEN ACCESS

Edited by:
Nicole Indra Stacy,
University of Florida, United States

Reviewed by:
Todd Schmitt,
SeaWorld Entertainment, United States
Trevor J. Gerlach,
Veterinary Specialty Center, United States
William George Van Bonn,
Shedd Aquarium, United States

***Correspondence:**
Barbara K. Linnehan
Barb.Linnehan@nmmf.org

Specialty section:
This article was submitted to Zoological Medicine, a section of the journal Frontiers in Veterinary Science

Received: 05 June 2020
Accepted: 24 September 2020
Published: 28 October 2020

Citation:
Linnehan BK, Hsu A, Gomez FM, Huston SM, Takeshita R, Colegrove KM, Rowles TK, Barratclough A, Musser WB, Harms CA, Cendejas V, Zolman ES, Balmer BC, Townsend FI, Wells RS, Jensen ED, Schwacke LH and Smith CR (2020) Standardization of Dolphin Cardiac Auscultation and Characterization of Heart Murmurs in Managed and Free-Ranging Bottlenose Dolphins (Tursiops truncatus). Front. Vet. Sci. 7:570055. doi: 10.3389/fvets.2020.570055

Cardiac auscultation is an important, albeit underutilized tool in aquatic animal medicine due to the many challenges associated with in-water examinations. The aims of this prospective study were to (1) establish an efficient and repeatable in-water cardiac auscultation technique in bottlenose dolphins (*Tursiops truncatus*), (2) describe the presence and characterization of heart murmurs detected in free-ranging and managed dolphins, and (3) characterize heart murmur etiology through echocardiography in free-ranging dolphins. For technique development, 65 dolphins cared for by the Navy Marine Mammal Program (Navy) were auscultated. The techniques were then applied to two free-ranging dolphin populations during capture-release health assessments: Sarasota Bay, Florida (SB), a reference population, and Barataria Bay, LA (BB), a well-studied population of dolphins impacted by the *Deepwater Horizon* oil spill. Systolic heart murmurs were detected at a frequent and similar prevalence in all dolphin populations examined (Navy 92%, SB 89%, and BB 88%), and characterized as fixed or dynamic. In all three populations, sternal cranial and left cranial were the most common locations for murmur point of maximal intensity (PMI). An in-water transthoracic echocardiogram technique was refined on a subset of Navy dolphins, and full echocardiographic exams were performed on 17 SB dolphins and 29 BB dolphins, of which, 40 had murmurs. Spectral Doppler was used to measure flow velocities across the outflow tracts, and almost all dolphins with audible murmurs had peak outflow velocities $\geq$1.6 m/s (95%, 38/40); three dolphins also had medium mitral regurgitation which could be the source of their murmurs. The presence of audible murmurs in most of the free-ranging dolphins (88%) was attributed to high velocity blood flow as seen on echocardiography, similar

to a phenomenon described in other athletic species. These innocent murmurs were generally characterized as Grade I-III systolic murmurs with PMI in the left or sternal cranial region. This study is the first to describe an efficient technique for in-water dolphin cardiac auscultation, and to present evidence that heart murmurs are common in bottlenose dolphins.

Keywords: heart murmur, auscultation, dolphin, *Tursiops truncatus*, cetacean, cardiology, echocardiography

INTRODUCTION

Following the *Deepwater Horizon* (DWH) oil spill in 2010, cardiotoxic effects were documented in a variety of species, including fish (1–5), birds (6), and rodents (7). Cardiac disease has also been identified in oil spill cleanup workers and people living in close proximity to the oil spill (8–11). In bottlenose dolphins (*Tursiops truncatus*) residing in Barataria Bay, LA (BB), numerous studies have described detrimental health impacts linked to DWH oil exposure, including pulmonary, reproductive, and endocrine disease (12–17); however, the cardiac effects associated with oil exposure in dolphins have not previously been examined. Preliminary data collected during capture-release health assessments conducted in 2016 identified a high prevalence of heart murmurs on auscultation. Given the DWH oil exposure of BB dolphins and evidence linking oil to heart disease in other species, there was a clear need to study the cardiac health of this population. In-depth cardiac assessment protocols had not been established or implemented for free-ranging dolphins previously. There is currently a paucity of data regarding normal baselines of clinical cardiac assessment in dolphins, both those managed under human care and free-ranging. Therefore, establishing protocols and normal parameters for cardiac assessment is vitally important to improve the overall medical care and assessment of dolphin health in both settings.

While cardiac disease has not historically been the top cause of mortality in dolphins, it remains a clinically relevant cause of morbidity and mortality (18). There are many anecdotal reports and several published reports of cardiac disease in live dolphins, both in managed care (19–21) and free ranging (22–25). Over the years, the U.S. Navy Marine Mammal Program has diagnosed several dolphins with cardiac disease (unpublished data), both alive and at necropsy, particularly in geriatric animals. Necropsies of stranded free-ranging dolphins have demonstrated a variety of cardiac abnormalities, including valvular disease, myocarditis, aneurysms (26), cardiomyopathy (25), endocarditis (27), congenital malformations (28), and capture cardiomyopathy (22–25, 29). With advances in medicine and husbandry resulting in increased lifespans in managed care dolphins, geriatric diseases such as cardiac disease are likely to become more prevalent. Fine tuning cardiac diagnostic techniques, and understanding normal vs. abnormal, are crucial in order to identify and monitor cardiac disease cases, support healthy aging, and move dolphin cardiac medicine forward.

Given the logistical challenges of auscultation, electrocardiography (ECG), and echocardiography in living cetaceans, much of the knowledge regarding cetacean cardiology has been based on stranding, necropsy, and histologic findings (26–32), as well as circulatory and dive physiology research (33–37). The anatomy of the dolphin heart has been well-described (38, 39). In recent years, initial steps have been taken to develop antemortem diagnostic cardiac tools in an effort to better understand dolphin cardiology. ECG techniques were first described in dolphins in 1970 (40), and comprehensive findings in putatively healthy dolphins were described by Harms et al. (41), with additional reports in managed and free-ranging dolphins and other cetaceans in the last two decades (42–46). Continued research and investigation have laid the foundation for echocardiographic assessment in managed dolphin populations. Sklansky et al. (47) compared transthoracic and transesophageal echocardiography in five managed dolphins and found that transthoracic echocardiograms were difficult due to anatomic and behavioral challenges. However, with a trained breath-hold, it was determined that transesophageal echocardiograms could be reliably performed and valuable for evaluating cardiac health. Miedler et al. (48) described a transthoracic echocardiographic technique and presented measured indices in managed dolphins. Chetboul et al. (49) provided quantitative data on left ventricular morphology and function using anatomic M-mode in four managed dolphins. Miedler et al. (50) used echocardiography to estimate systolic left ventricular function during rest and following exercise in 13 trained dolphins, and provided baseline data for normal stroke volume and cardiac output in awake, managed dolphins.

There have been no peer-reviewed studies to date detailing cardiac auscultation and prevalence of heart murmurs in free-ranging or managed cetacean populations, nor studies describing the use of echocardiography in free-ranging dolphins. As such, the aims of the current study were to (1) establish an efficient and reproducible in-water cardiac auscultation technique in dolphins, (2) describe the presence and characterization of heart murmurs in both free-ranging and managed dolphins, and (3) better characterize heart murmur etiology through echocardiography in free-ranging dolphins.

MATERIALS AND METHODS

Animals

For technique development, 65 dolphins cared for by the U.S. Navy Marine Mammal Program in San Diego, CA participated in voluntary cardiac auscultation exams from March 2018 through August 2019, including 35 males and 30 females, ranging in

age from 2 to 54 years, and 169 to 290 cm in total length, examined to be healthy during the period of the study. A subset of these dolphins ($n = 15$) also received echocardiography exams for technique refinement. Dolphins voluntarily participated in these procedures through positive operant conditioning. Navy dolphin participation was approved by the Navy Marine Mammal Program's Institutional Animal Care and Use Committee (NIWC Pacific IACUC # 128-2018) and from the U.S. Navy Bureau of Medicine and Surgery (NRD-1157). The Navy Marine Mammal Program is accredited by AAALAC International and adheres to the national standards of the U.S. Public Health Service Policy on the Humane Care and Use of Laboratory Animals and the Animal Welfare Act. One geriatric dolphin in this population has known cardiac disease (second degree atrioventricular block and mild aortic insufficiency).

Free-ranging bottlenose dolphins were examined during capture-release health assessments in Sarasota Bay, FL (SB) in June 2018, a non-oiled reference location, conducted under NMFS Scientific Research Permit No. 20455. All dolphins in this study were given complete veterinary examinations as previously described, and were assigned prognostic scores indicative of their overall health status (15, 51). Nineteen dolphins were auscultated in SB, 10 males and 9 females (1 confirmed pregnant on ultrasound), ranging in age from 2 to 47 years, and 168 to 281 cm in total length. Of the 19 SB dolphins auscultated, 17 also received echocardiograms. The SB population is a particularly valuable reference group due to the long-term research on health, ecology, behavior, life history, and human interactions (52).

Capture-released health assessments were performed in BB in July 2018, conducted under NMFS Scientific Research Permit No. 18786. Thirty-four dolphins were auscultated in BB, including 21 males and 13 females (6 confirmed pregnant on ultrasound), ranging from 195 to 267 cm in total length. Of the 34 BB dolphins auscultated, 29 also received echocardiograms. The methods of temporary capture and on-site release in both locations followed those previously described (15, 53).

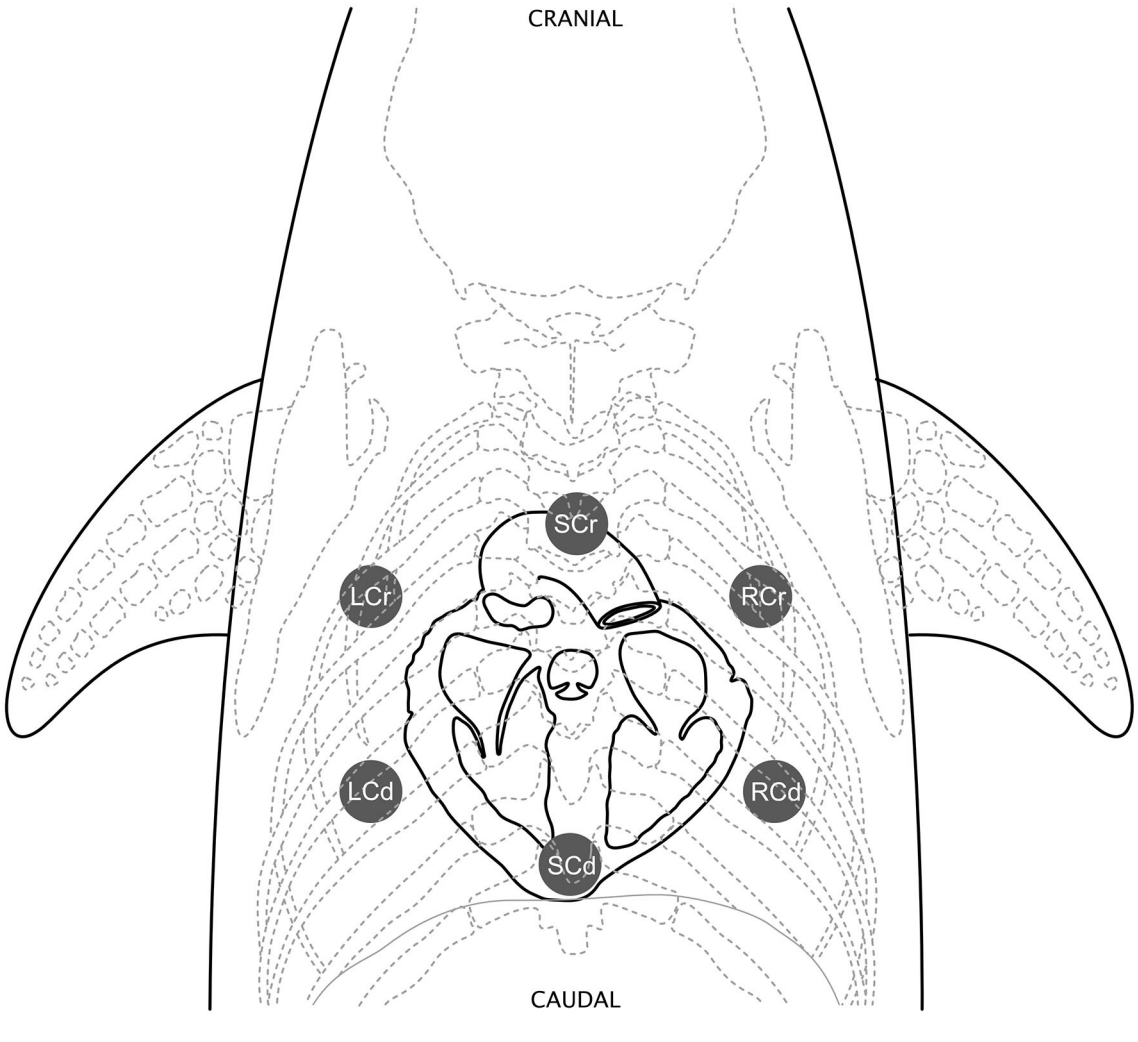

FIGURE 1 | Standardized cardiac auscultation points. Six points of auscultation were standardized: sternal caudal (SCd) over the heart apex, left caudal (LCd), left cranial (LCr), sternal cranial (SCr) over the heart base, right cranial (RCr), and right caudal (RCd). Figure illustrated by Veronica Cendejas.

Cardiac Auscultation

All auscultations were performed in seawater with the 3M™ Littman® Veterinary Master Classic II 32″ (3M™ Littman®, St. Paul, MN, USA). The head of the stethoscope was covered in Parafilm® M laboratory film (Bemis Company, Inc., Oshkosh, WI, USA) and secured with electrical tape along the tubing for waterproofing. The duration of this waterproof seal was variable, and once a leak was identified, the stethoscope was traded out for another waterproofed stethoscope without a leak. The application of Parafilm® to the head did not affect the sound of the stethoscope.

In all dolphins, cardiac auscultation began by manually palpating in between the pectoral flippers for the strongest heartbeat and placing the stethoscope on the body at that location. From there, six points of auscultation were standardized: sternal caudal, left caudal, left cranial, sternal cranial, right cranial, and right caudal (**Figure 1**), listening for several breath cycles. When a cardiac murmur was detected, it was graded by intensity using the conventional Grade I–VI scale (Grade I: low intensity murmur, heard only in a quiet environment after careful auscultation over a localized area; Grade II: low intensity murmur, heard immediately when auscultating over the point of maximal intensity; Grade III: moderate intensity murmur; Grade IV: high intensity murmur, heard over several areas but without a palpable precordial thrill; Grade V: high intensity murmur with a palpable precordial thrill; Grade VI: high intensity murmur with a palpable precordial thrill, heard even when the stethoscope is lifted slightly off the thoracic wall) (54–57). The point of maximal intensity (PMI), or the position on the chest where the murmur could be heard most strongly, was also recorded for each dolphin with a murmur. Based on the ausculting clinician's observation, one of the six standardized areas of auscultation was selected to best describe the murmur PMI.

The timing of the murmur in relation to the heart sounds (systolic or diastolic) and in relation to the cardiac cycle (fixed or dynamic) was also determined. Dolphins normally have a pronounced respiratory sinus arrhythmia, with a "split" between the low and high heart rate phases. The lower heart rate phase occurs before the breath (bradycardic phase), and the heart rate increases transiently after the breath (tachycardic phase). The estimated low and high heart rates heard during auscultation were recorded for each animal. A fixed murmur was defined as one that did not change grade and was heard at the same level during the entire auscultation. A dynamic murmur was defined as one that changed grade within an auscultation period. Since dynamic murmurs fluctuated with the changing heart rates, they were given a grade in the bradycardic phase and in the tachycardic phase to reflect the changing intensity with heart rate.

Navy Dolphins

All Navy dolphins ($n = 65$) were auscultated by authors BKL (marine mammal clinician) and AH (Diplomate, American College of Veterinary Internal Medicine, Cardiology). Trainers held the dolphins in a voluntary right lateral presentation (left lateral recumbency) in the water at the side of the dolphin's sea-pen enclosure. Veterinarians on the side of the enclosure then held the right pectoral flipper with one hand and auscultated the entire cardiac window with the other hand, allowing dolphins to comfortably roll to take breaths as needed (**Figure 2A**).

Free-Ranging Dolphins

Nineteen dolphins were auscultated in SB and 34 in BB. Dolphins were gently restrained in the water by experienced handlers while auscultation was performed by either cardiologist AH or SH (Diplomates, American College of Veterinary Internal Medicine Cardiology) in addition to other authors (BKL, FMG, CRS; marine mammal clinicians). Veterinarians standing in the water beside the dolphin could reach under the water and gain access to the entire cardiac window with the dolphin upright (**Figure 2B**). Auscultations were performed for several minutes and occurred shortly after initial capture (within 1–20 min).

Phonocardiography

A 3M™ Littman® Electronic Stethoscope, Model 3200, was used to record heart sounds of Navy dolphins. Phonocardiograms were downloaded onto StethAssist™ Software (Zargis Medical, Princeton, NJ, USA) for analysis and identification of murmurs. **Figure 3** illustrates phonocardiograms of two dolphins with systolic, soft dynamic murmurs.

Transthoracic Echocardiography

Navy Dolphins

Echocardiograms were performed on a subset of Navy dolphins to aid in technique refinement for free-ranging dolphin applications. Twenty-three in-water transthoracic echocardiograms were performed with 15 Navy dolphins. Dolphins were trained to assume dorsal, lateral, and 45-degree lateral recumbency with a trainer standing on a submerged platform. The examining cardiologist (AH or SH) stood on the platform beside the trainer and was able to scan the cardiac window in one or all of these three positions. Given that the aim of ultrasounding Navy dolphins was technique establishment for applications in the field, many of these exams were partial echocardiograms (i.e., not all of the standard views were obtained).

Free-Ranging Dolphins

In SB, 17 dolphins received in-water transthoracic echocardiograms (of 19 dolphins auscultated). In BB, 29 dolphins received in-water transthoracic echocardiograms (of 34 auscultated). Dolphins were gently restrained by experienced handlers in the water, keeping the dolphin mostly submerged with the blowhole clear of water. Echocardiograms were performed by cardiologists while standing beside the dolphin and reaching under to obtain access to the cardiac window. This was typically performed next to a boat, so that electronic equipment could stay dry and shaded on the boat. Dolphins were examined in dorsal presentation or in a 45-degree tilt to the right or left to allow for better visualization of the cardiac window. Most exams were completed in 5–7 min, and were performed opportunistically in the health assessment process, generally about 30 min from initial capture (range 6–138 min, median 36 min after initial capture).

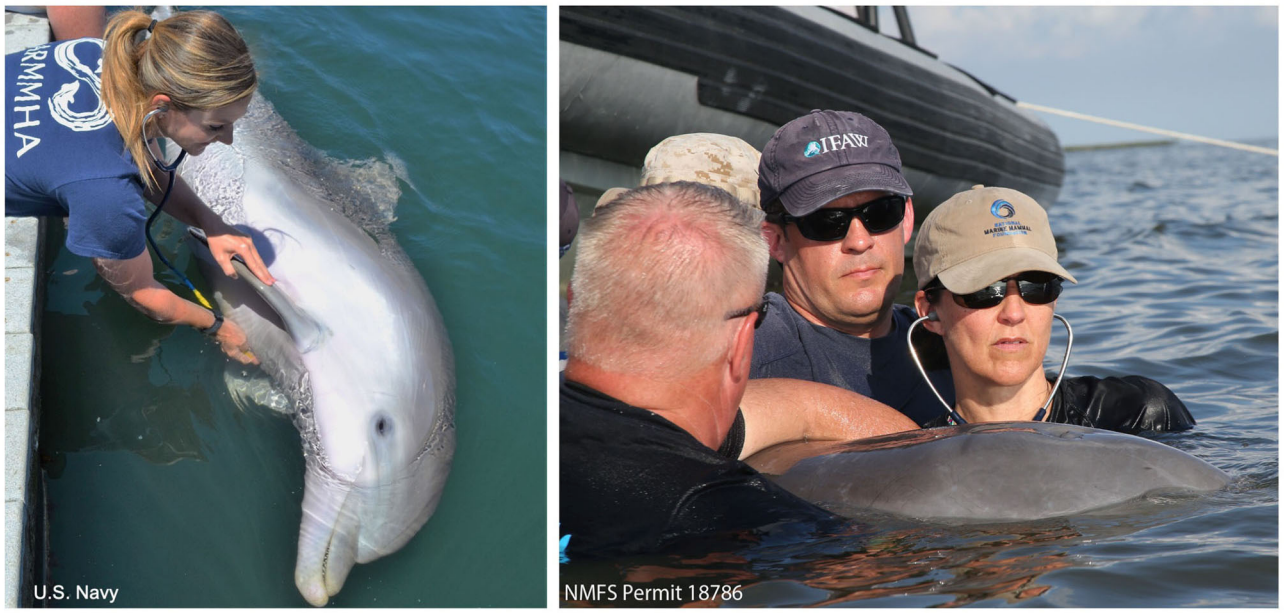

FIGURE 2 | Dolphin cardiac auscultation positioning. **(A)** A trained Navy dolphin assumes a voluntary right lateral present in the water and veterinarians auscultate the cardiac window while holding the pectoral flipper. **(B)** A free-ranging BB dolphin is auscultated while experienced handlers gently restrain the animal in water with the blowhole clear. Veterinarians listen by reaching under, between the pectoral flippers, to access the cardiac window.

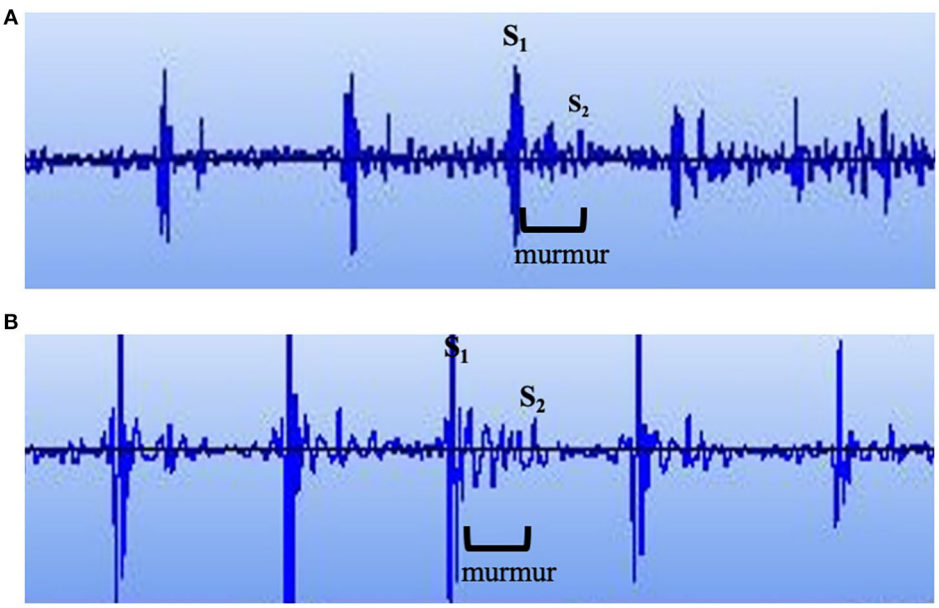

FIGURE 3 | Phonocardiogram. Phonocardiograms of **(A)** a young male Navy dolphin and **(B)** an adult female Navy dolphin with systolic, soft dynamic heart murmurs.

All transthoracic echocardiograms were performed using the GE Vivid-iq ultrasound and GE 3S phased-array transducer cardiac probe (1.5–3.6 MHz) (General Electric Healthcare, Chicago, IL, USA). The following standard echocardiogram images were examined: right parasternal long-axis, right parasternal short-axis, left parasternal apical, left parasternal cranial long-axis, left parasternal short-axis.

Regurgitant jets were classified subjectively as none (absent), trace, small, medium, or large. Trace regurgitation had a barely detectable jet noted on color Doppler (a few color pixels). A small jet was one that was relatively narrow, that did not distend very

TABLE 1 | Prevalence and characteristics of heart murmurs in SB, BB, and Navy dolphins.

	Counts				Prevalence		
			Murmur present			Within murmur cases	
	n	None	Fixed	Dynamic	Any murmur	Fixed	Dynamic
SB	19	2	7	10	0.89	0.41	0.59
BB	34	4	19	11	0.88	0.63	0.37
					$P = 1$		$P = 0.22$
Free-ranging	53	6	26	21	0.89	0.55	0.45
Navy	65	5	9	51	0.92	0.15	0.85
					$P = 0.54$		$P < 0.001$

Murmur prevalence was compared between the three populations (Fisher's Exact Test). The sum of SB and BB is provided (free-ranging) for comparison of free-ranging and managed dolphins.

far from the valve being interrogated, did not persist throughout the entirety of systole and/or appeared only mildly turbulent based on the mosaic color flow pattern. A medium jet was defined as one that appeared turbulent within at least ¼ of the associated chamber. A large jet was defined as one that appeared turbulent within more than ½ of the associated chamber. Classification criteria were defined by the investigators (SH and AH) based on standard evaluation of color flow jet origin, direction and size (58).

To evaluate whether high outflow tract velocity causes murmurs in dolphins, the maximum blood flow velocity was determined across the left and right outflow tracts (the left ventricular outflow tract [LVOT] and aortic valve [AV], the right ventricular outflow tract [RVOT], and pulmonic valve [PV]) and compared to 1.6 m/s, the speed above which high velocity flow typically causes an audible murmur in small animals due to enhanced blood turbulence at high velocity (59–61).

DATA AND STATISTICAL ANALYSIS

Echocardiograms were analyzed using GE Vivid-iq ultrasound software, EchoPAC version 201. Two cardiologists (AH and SH) reviewed each study and made all qualitative and quantitative measurements. When measurements differed between cardiologists, they were discussed to reach a consensus.

Murmur prevalence and type (fixed or dynamic) were compared between dolphin groups using two-sided Fisher's Exact Tests (R version 3.5.0, The R Foundation for Statistical Computing, Vienna, Austria). In the cases where the prevalence of a finding in SB and BB was similar (i.e., no statistical difference between the groups), the data were pooled into one "free-ranging" group for comparison with the Navy managed group. Other parameters were analyzed including murmur intensity grade, murmur PMI, maximum outflow tract velocity, and valvular regurgitation.

RESULTS

Murmur Prevalence and Heart Rate

In Navy dolphins, 60 of 65 (92%) had heart murmurs. In SB, 17 of 19 dolphins (89%) had heart murmurs. In BB, 30 of the 34 dolphins (88%) had heart murmurs. All murmurs were systolic. There was no difference in murmur prevalence between SB and BB ($p = 1$, Fisher's Exact Test), nor between the managed and free-ranging groups ($p = 0.54$) (**Table 1**). In both groups, murmurs were detected in males and females of all age classes.

In Navy dolphins, the mean low heart rate during auscultation (i.e., heart rate during the bradycardic phase of the respiratory sinus arrhythmia) was 49 beats/min (SD ± 12) and the mean high heart rate (i.e., heart rate during the tachycardic phase of the respiratory sinus arrhythmia) was 78 beats/min (±12). In SB dolphins, the mean low heart rate was 73 beats/min (±11) and the mean high heart rate was 97 beats/min (±12). In BB dolphins, the mean low heart rate was 79 beats/min (±16) and the mean high heart rate was 103 beats/min (±15). Pairwise comparisons of the mean heart rates (both high and low) were performed across the three cohorts using *T*-tests and adjusted *p*-values via the Benjamini and Hochberg method (62). While there are no detectable differences between the mean heart rates for SB and BB, the Navy heart rates were significantly lower ($p < 0.001$).

Fixed vs. Dynamic Murmurs

Across the groups studied, murmurs were either fixed or dynamic (**Table 1**). Of the Navy dolphins with murmurs, 9 of 60 (15%) had fixed murmurs and 51/60 (85%) had dynamic murmurs. Of the SB dolphins with murmurs, 7 of 17 (41%) had fixed murmurs and 10 of 17 (59%) had dynamic murmurs. Of the BB dolphins with murmurs, 19 of 30 (63%) had fixed murmurs and 11 of 30 (37%) had dynamic murmurs (**Table 1**). In all dynamic murmur cases, the murmur became louder in the tachycardic phase, and was quieter or absent in the bradycardic phase. The prevalence of fixed vs. dynamic murmurs between the SB and BB was similar ($p = 0.22$, Fisher's Exact Test). However, managed Navy dolphins had a higher prevalence of dynamic murmurs (85% dynamic and 15% fixed) when compared to free-ranging dolphins (45% dynamic and 55% fixed; $p < 0.001$) (**Table 1**).

Murmur Grade

Fixed murmurs ranged from Grade I to IV. Dynamic murmur grades ranged from absent (i.e., unable to be heard) to Grade II in the bradycardic phase and Grade I to III in the tachycardic phase. With increasing heart rates, dynamic murmurs became

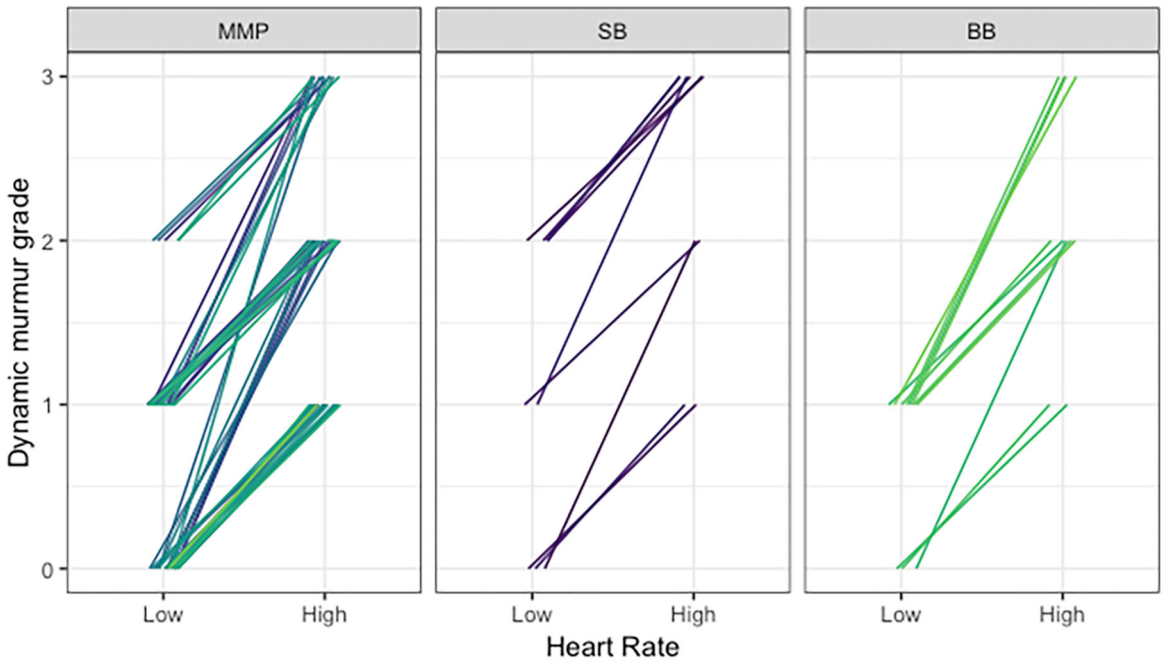

FIGURE 4 | Comparison of dynamic murmur grade and heart rate across Navy and free-ranging populations. Dynamic murmurs were given a grade in the bradycardic phase and the tachycardic phase of the respiratory sinus arrhythmia to reflect the changing intensity with heart rate, using the conventional Grade I–VI scale. With increasing heart rates, dynamic murmurs became louder and grades increased.

louder and grades increased in all cases (**Figure 4**). There were no differences in murmur grade between groups.

Point of Maximal Intensity (PMI)

In both SB and BB, sternal cranial was the most common PMI (SB $n = 7$, BB $n = 7$), followed by left cranial (SB $n = 4$, BB $n = 5$), right cranial (SB $n = 3$, BB $n = 5$), and left caudal (SB $n = 1$, BB $n = 2$). In Navy dolphins, left cranial was the most common PMI ($n = 26$), followed closely by sternal cranial ($n = 21$), then right cranial ($n = 5$), left caudal ($n = 4$), sternal caudal ($n = 3$), and right caudal ($n = 1$). The sternal cranial and left cranial regions correspond to the basilar region of the heart, which was also noted to be the area of the strongest palpable heartbeat in most dolphins, and is in proximity to the aortic and pulmonic valves.

Animal Positioning

The right lateral presentation (left lateral recumbency) was found to be the single best position for efficient auscultation in managed dolphins. With the dolphin upright in the water in a dorsal presentation, veterinarians were unable to reach to the sternum on larger dolphins from the site of the netted enclosure, and clinicians are typically not able to stand beside the dolphin in the water due to the depth of the enclosure. Therefore, a dorsal presentation in this setting was less efficient, as the dolphin and trainer had to reposition to listen to right and left sides of the sternum from the side of the enclosure in order to reach all of the auscultation points. In the right lateral presentation, all auscultation points could easily be reached and auscultated for several breath cycles. Auscultation findings in the right lateral position did not differ from those heard in left lateral positioning or dorsal presentation in the vast majority of dolphins. In two dolphins, right-sided auscultation was difficult in the right lateral present, so the heart was auscultated in both right and left lateral positions to hear both sides as closely as possible. In such instances, the outcome of auscultation (i.e., murmur characterization) was the same regardless of position. Dorsal presentation was found to be the single best position for efficient auscultation in free-ranging dolphins, since veterinarians were standing in the water besides the animal and could easily reach the entire sternum without having to place the dolphins in lateral recumbency. Additionally, the free-ranging animals were not held in lateral recumbency as they are not trained for this behavior.

Echocardiograms

Many of the dolphins exhibited high outflow tract velocities with no apparent stenosis. The maximum velocity ranges for the left and right outflow tracts were 0.98–2.7 m/s and 0.94–2.39 m/s, respectively. No evidence of stenosis (aortic or pulmonic) was seen in any of the dolphins. Of the free-ranging dolphins who had complete echocardiograms 46, 40 had heart murmurs. All but two dolphins with murmurs had outflow velocities $\geq$1.6 m/s (38/40, 95%). **Figure 5** illustrates an example of spectral Doppler measurement of outflow velocity.

In three free-ranging dolphins, there was sufficient valvular regurgitation seen with color flow Doppler to be the potential source of the audible murmur. One dolphin in SB and two dolphins in BB were described as having medium mitral

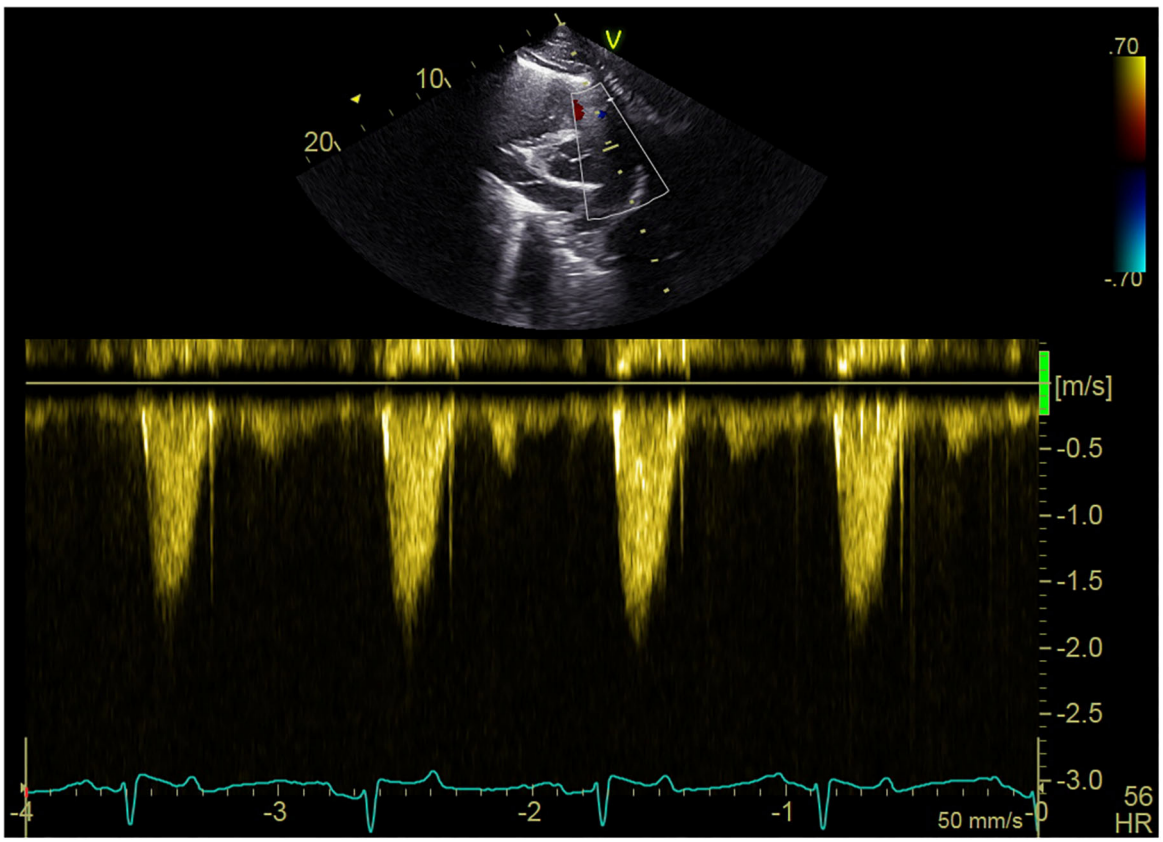

FIGURE 5 | Echocardiogram spectral Doppler. Example of blood flow velocity measurement with spectral Doppler during the echocardiogram of a free-ranging dolphin in BB.

regurgitation based on color flow Doppler signal appearance. The murmurs in these three dolphins had differing classifications: the SB dolphin had a dynamic murmur, Grade II-III systolic, right cranial PMI, one BB dolphin had a fixed murmur, Grade III systolic, sternal cranial PMI, and the other BB dolphin had a fixed murmur, Grade III systolic, left caudal PMI. All three of these dolphins also had maximum outflow velocities ≥1.6 m/s. The vast majority of dolphins, however, had little to no structural or valvular changes on echocardiogram to account for the audible murmurs. Many dolphins were described as having trace or small regurgitant jets across all valves with no obvious evidence of hemodynamic remodeling to suggest significant cardiac disease. Five dolphins had no regurgitation or insufficiency and 39 had trace to small regurgitation or insufficiency at one or more valves.

Therefore, 35/40 (88%) of the murmurs auscultated in free-ranging dolphins were likely due to high velocity blood flow across the outflow tracts. In three dolphins, the etiology of murmurs was potentially mitral regurgitation, though all three of these dolphins also had maximum outflow velocities ≥1.6 m/s.

DISCUSSION

Cardiac auscultation is an important, albeit underutilized, diagnostic tool in aquatic animal medicine. It is an essential part of a complete veterinary physical exam in dolphins and a fundamental part of the cardiac exam. Early descriptions of dolphin cardiac auscultation described the dolphin heart as practically inaudible (63). Dolphin cardiology has long been a gap in our knowledge of dolphin medicine, and there is recent momentum for improved investigations and understanding of dolphin cardiac health. Basic steps such as standardizing in-water cardiac auscultation are crucial for better assessing cardiac health across managed dolphin facilities and free-ranging dolphin assessments. This research describes an efficient technique for in-water dolphin cardiac auscultation, and presents the first evidence that heart murmurs are common in bottlenose dolphins, the majority of which are innocent flow murmurs due to high outflow velocity.

A heart murmur is the audible turbulence caused by disruption of laminar blood flow within or in close proximity to the heart. Echocardiography is the gold standard for investigating the source of a murmur. Causes of heart murmurs can include pathological etiologies, such as primary valvular abnormalities (regurgitation due to degeneration, calcification, or infection of the valves), secondary valve dysfunction (cardiomyopathy, pulmonary hypertension), or congenital defects (valvular dysplasia, stenosis, septal defects, patent ductus arteriosus (55, 56, 64). Murmurs can also be

classified as physiologic, commonly referred to as benign, innocent, or functional murmurs. In domestic animals and humans, these innocent murmurs can be caused by fever, excitement or stress, pregnancy, or anemia (55, 56, 65). Benign systolic ejection murmurs in children are common and usually disappear by adulthood (65, 66). Flow murmurs have also been described commonly in elite athletes due to cardiac adaptations to endurance exercise (67, 68). Whether a murmur is innocent or pathologic, the principle of turbulent blood flow is responsible for causing the audible sound (69).

Studies in dogs, horses, and elite human athletes have demonstrated the presence of innocent flow murmurs in these athletic individuals. In retired racing greyhounds, a soft, Grade I-II systolic murmur is common and of no apparent pathologic consequence, with aortic velocities that are significantly higher than in dogs without murmurs (70). In addition, 40% of heavily trained sled dogs in one study had Grade I to II early to mid-systolic heart murmurs (71), similar to the prevalence of 30–50% reported for human endurance athletes (67). The systolic murmur was most likely a result of increased blood velocity across the aortic valve, and the study observed that heavily trained sled dogs with murmurs tended to be better performers than those without murmurs (71). Similarly, physiologic flow murmurs are common in horses, generated by the fast flow of blood through their large diameter great vessels in systole, and are of no clinical significance (72, 73).

Human cardiology studies show that elite athletes often have innocent murmurs due to functional and morphological adaptations in response to exercise (68). Soft (Grades I-II), mid-systolic, ejection murmurs are heard in 30–50% of endurance athletes at the base of the heart (67) due to high velocity blood flow. It is also well-established that children frequently have innocent murmurs, which often resolve before adulthood and are of no clinical consequence (65, 69). The typical features of innocent murmurs in children and physiologically adapted human athletes have been described as short, early to mid-systolic, and faint (Grades I-III) (74). These characteristics fit the profile for the majority of murmurs auscultated in the dolphins in this study.

In order for normal blood flow across normal valves to cause audible murmurs, there must be turbulent blood flow. The principle of peak outflow velocity causing an audible murmur relies on the Reynolds number. The Reynolds number is a dimensionless value for a given fluid that describes the factors that determine whether flow is laminar or turbulent as it flows through a tube, or in this case, blood through a major blood vessel (65, 75). The equation for the Reynolds number (Re) is: Re = rhoVD/mu, where rho is the blood density, V is the velocity, D is the diameter of the vessel, and mu is the blood viscosity (75). Turbulence only occurs after the Reynolds number increases to a critical value, which can be achieved when any of the equation components vary (75). The higher the Reynolds number, the more likely turbulence will occur. Given the equation, the Reynolds number will increase as velocity increases. It will also increase if the viscosity of the blood decreases, such as with anemia, for example (76). Therefore, if an animal has high velocity and/or low blood viscosity, there is more likely to be turbulent flow, and thus, an audible murmur.

Applying this principle to the dolphins in the current study with dynamic murmurs, the results demonstrated that the velocity of blood flow increases as the heart rate speeds up with the respiratory sinus arrhythmia (**Figure 4**), thus making the high velocity the most likely cause of the turbulence and resulting audible dynamic murmur. Similar murmurs heard in all three sites, regardless of health status, were confirmed as physiologic given the high velocity blood flow and absence of pathological changes present on echocardiography. Dolphins spend a great deal of time free-swimming and diving in the open ocean; therefore, it is possible that these highly athletic dolphins have adapted to exercise to varying degrees, in a similar manner to racing greyhounds, horses, sled dogs, and elite human athletes. In addition, the dolphin flow murmurs observed in this study could be a result of adaptations to the aquatic environment, with variations in buoyancy contributing to unique morphologic and functional changes not observed in terrestrial counterparts.

In small animal medicine, 1.6 m/s is generally the accepted cutoff over which peak velocities cause turbulent blood flow resulting in audible murmurs (59–61). It appears from the data in the current study, that the threshold is similar for audibly high velocity in dolphins, as almost all murmurs auscultated had peak outflow velocities over 1.6 m/s and almost all dolphins without murmurs had peak velocities below 1.6 m/s in BB and SB (**Figure 6**). Two dolphins did not have audible murmurs though their peak velocities were $\geq$1.6 m/s (one in SB and one in BB). There was no observed evidence of stenosis associated with either the aortic or pulmonic valves, however, mild stenosis that may not reveal obvious two-dimensional structural abnormalities (77) cannot be ruled out.

The prevalence and characteristics of murmurs in both free-ranging populations were similar to each other and differed only slightly from the Navy population. Navy dolphins had significantly more dynamic murmurs and free-ranging dolphins more fixed murmurs. One possible explanation for the higher prevalence of fixed murmurs in the free-ranging population is higher sympathetic tone. Dolphins during post-capture restraint exams exhibit a typical mammalian acute stress response (78), which transiently causes increased heart rate and blood pressure. Due to this stress response, heart rates were often higher upon initial auscultation in the free-ranging dolphins, and the heart louder to hear. In contrast, Navy dolphins are trained to calmly participate in husbandry procedures voluntarily, and therefore, did not exhibit a stress response during auscultation. Navy dolphin studies involving pre-stress-test blood draws provided with voluntary participation have demonstrated that these dolphins are not stressed during such behaviors (79, 80). It is suspected that the higher parasympathetic tone in the Navy dolphins, therefore, generally resulted in lower heart rates with pronounced respiratory sinus arrhythmia ("split"), and fainter auscultation in many of the dolphins. Dynamic murmurs were detected when the heart rate transiently sped up after breaths, then became quieter or absent as the heart rate slowed down. In the free-ranging population, dolphins exhibited a stress response

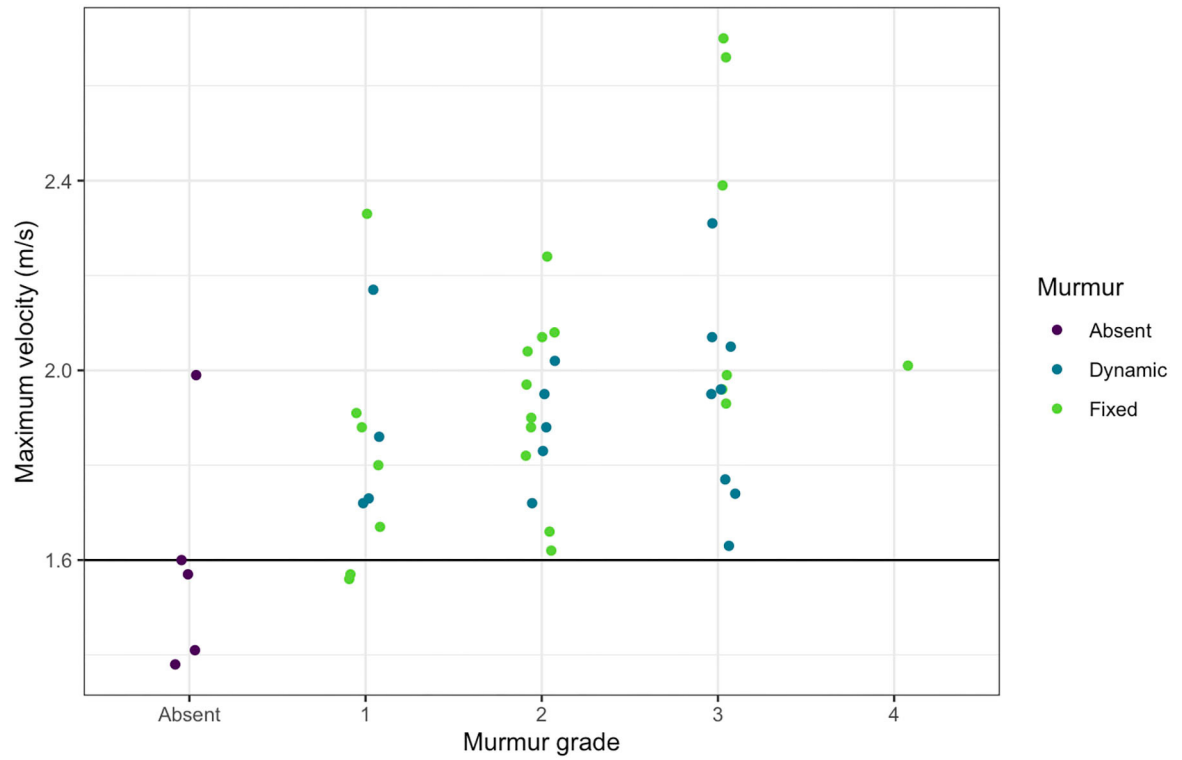

FIGURE 6 | Maximum outflow tract velocities and murmur grades. The maximum outflow velocity for each free-ranging dolphin with a murmur is plotted against the murmur grade, demonstrating that nearly all dolphins with audible murmurs had maximum velocities over 1.6 m/s.

and it is suspected that their murmurs sounded fixed rather than dynamic in many due to increased heart rate and less pronounced split. Although the prevalence of murmurs in the two populations was similar, stress of capture and restraint cannot be completely ruled out as a contributing factor to murmur etiology in the free-ranging population, as studies in dogs have shown that stress of handling can exacerbate murmurs (81, 82).

Animal positioning for auscultation also differed slightly between the free-ranging and Navy dolphins. For Navy dolphins, a voluntary right lateral presentation was found to be the single best position for efficient auscultation when examining from the side of the enclosure. When the dolphins were upright, veterinarians were unable to reach the sternum from the side of the enclosure, and the sea pens are too deep for clinicians to stand in. Therefore, a right lateral presentation was the most efficient and reproducible for clinical applications in this setting. Auscultation findings in the right lateral presentation did not differ from those heard in left lateral presentation or dorsal presentation in the vast majority of dolphins. In instances where right-sided auscultation was difficult with the right side up, the heart was auscultated in both right and left lateral presentations, and the outcome of auscultation was not impacted by the positioning. In contrast, veterinarians standing in the water beside the free-ranging dolphins during health assessments were able to easily reach under the dolphins and gain access to the sternum with the dolphins upright. Therefore, it was not necessary to roll these dolphins into right or left lateral presentation to facilitate auscultation. While it would have been ideal to auscultate Navy dolphins in the same manner for this study, logistically this was not feasible nor efficient for clinical use with the managed population. Despite the differences in positioning for logistical reasons, this did not appear to confound the results, as the murmur PMI locations were similar in both populations.

Comparison of murmur characteristics and echocardiographic findings in the free-ranging dolphins did not yield a clear distinction between physiologic murmurs and pathologic murmurs that could be determined via auscultation alone. Generally, however, most of the innocent flow murmurs were systolic, Grade I-III, dynamic, and PMI was left cranial or sternal cranial (basilar). Many dolphins had trace or small valvular regurgitation; based on the prevalence of high outflow tract velocity and the consistently located PMIs, it is likely these trivial to mild regurgitations did not contribute to the audible murmurs. Trivial or mild regurgitation is often considered a variation of normal in human and veterinary echocardiography, and is also referred to as physiologic regurgitation (58, 61). In the three dolphins with medium mitral regurgitation, the characteristics of their murmurs varied and some characteristics overlapped with the flow murmurs. It is also possible for an animal to have sufficient regurgitation or insufficiency to cause a murmur in addition to having high aortic flow velocity. These

three animals also had comorbidities, including moderate to severe lung disease, and were all classified as guarded to poor prognoses based on overall health assessment data. Therefore, while auscultation is an important tool and the majority of dolphins had innocent murmurs, only echocardiography can definitively distinguish between an innocent, physiologic murmur and a pathologic one.

Given that the aim with Navy dolphins was technique development, many of these dolphins' echocardiograms were partial studies, and therefore the echocardiographic findings were not compared between free-ranging and Navy dolphins in the current study. Continued work to perform echocardiograms on additional Navy dolphins and further corroborate auscultation findings is ongoing. Thus far, the same appears to be true for Navy dolphins: most dolphins have low grade, dynamic, systolic murmurs with PMI left or sternal cranial and echocardiograms performed thus far have established that flow murmurs are also common in this population. In addition, it will be of interest in future work to compare Navy dolphins of varying activity levels, i.e., those who frequently deep dive in the open ocean, vs. those who occasionally swim in the open ocean, vs. those who do not. A flow murmur in these dolphins could be a sign of fitness, like in the highly trained sled dogs. Comparing murmurs between other populations of dolphins, beyond the three studied here and with varying activity levels, would also be of interest for future work.

Using the standardized approach described herein, this study characterized murmurs previously not described in dolphins. It is unlikely that most of the murmurs are new and more plausible that these soft, dynamic murmurs were being missed previously due to brevity of auscultation, environmental factors, and/or lack of standardized technique. Underwater noise, patient movement, echolocating patients, water movement, and saltwater damage to stethoscopes all add difficulty to underwater auscultation. Many of the murmurs described were very subtle (Grades I and II) and could easily be missed due to loud ambient noise or an uncooperative patient. Listening to many dolphins repeatedly aided greatly in training the ears to diagnose these soft murmurs. It is also important to listen in the various locations for multiple breath cycles, as the murmur presence or intensity can change with the changing heart rate in a given location. Full cardiac auscultation as suggested may take several minutes per dolphin due to breath holding. Given these findings, this study highlights that performing auscultation for a longer duration and ideally with minimal ambient noise are the keys to proper cardiac auscultation assessment. Utilizing this technique for routine clinical assessment of Navy dolphins has yielded repeatable results in terms of murmur identification and characterization. While the majority of heart murmurs identified in dolphins in this study were determined to be innocent murmurs, it is important for clinicians in managed care settings to utilize repeated auscultation and monitor for changes over time. Murmurs with differing characteristics or murmurs changing over time may warrant further cardiac assessment, including echocardiography, and should be interpreted in light of other clinical findings.

CONCLUSION

In summary, this report describes an efficient technique for in-water dolphin cardiac auscultation and presents the first evidence that heart murmurs are common in bottlenose dolphins. Heart murmurs were detected in most of the dolphins in this study, both managed and free-ranging, regardless of oil exposure. In the majority of dolphins with murmurs, structural abnormalities, such as valvular lesions or congenital defects were not identified, and the audible murmurs were attributed to high velocity blood flow seen on echocardiography, similar to the phenomenon described in other athletic species. These innocent murmurs generally were characterized as systolic, low grade (I-III), dynamic murmurs with PMI in the left or sternal cranial region; however, echocardiography remains the gold standard to definitively diagnose the etiology of a murmur.

DATA AVAILABILITY STATEMENT

The datasets presented in this study can be found in online repositories. Data are publicly available through the Gulf of Mexico Research Initiative Information & Data Cooperative (GRIIDC) at https://data.gulfresearchinitiative.org/data/R6.x809.000:0001.

ETHICS STATEMENT

The animal study was reviewed and approved by Naval Information Warfare Center Pacific's Institutional Animal Care and Use Committee, U.S. Navy Bureau of Medicine and Surgery, NOAA Animal Care and Use Committee, and Mote Marine Laboratory's Institutional Animal Care and Use Committee. Written informed consent was obtained from the individual(s) for the publication of any potentially identifiable images or data included in this article.

AUTHOR CONTRIBUTIONS

BL, AH, FG, SH, LS, and CS contributed to the design and implementation of the research. BL, AH, FG, SH, RT, KC, VC, TR, AB, WM, CH, EZ, BB, FT, RW, LS, and CS implemented the free-ranging dolphin health assessments and data collection. BL, AH, SH, and VC implemented Navy dolphin exams in collaboration with EJ. RT, BL, AH, FG, SH, AB, WM, and KC performed data analysis. BL wrote the manuscript in consultation with AH, RT, FG, SH, and CS. All authors edited the manuscript.

FUNDING

This research was made possible by a grant from The Gulf of Mexico Research Initiative (Award # SA 18-12). This was scientific contribution number 273 for the National Marine

Mammal Foundation. Barataria Bay health assessments were conducted under NMFS Scientific Research Permit No. 18786, issued to NOAA Fisheries Marine Mammal Health and Stranding Response Program, and approved by the NOAA Animal Care and Use Committee. Sarasota Bay health assessments were performed under NMFS Scientific Research Permit No. 20455 and approved by Mote Marine Laboratory's Institutional Animal Care and Use Committee.

ACKNOWLEDGMENTS

The authors thanked veterinary technicians Jammy Eichman, Anthony Perron, Erin Brodie, and Henry Cao for their assistance, and the animal trainers for their training support. We also thanked Celeste Parry and Sacha Stevenson for assistance with data collection, and the fieldwork teams, especially Larry Fulford, for their help with free-ranging dolphin health assessments.

REFERENCES

1. Brette F, Machado B, Cros C, Incardona JP, Scholz NL, Block BA. Crude oil impairs cardiac excitation-contraction coupling in fish. *Science.* (2014) 343:772–6. doi: 10.1126/science.1242747
2. Incardona JP, Gardner LD, Linbo TL, Brown TL, Esbaugh AJ, Mager EM, et al. Deepwater horizon crude oil impacts the developing hearts of large predatory pelagic fish. *PNAS*. (2014) 111:1510–8. doi: 10.1073/pnas.1320950111
3. Nelson D, Heuer RM, Cox GK, Stieglitz JD, Hoenig R, Mager EM, et al. Effects of crude oil on *in situ* cardiac function in young adult mahi-mahi (*Coryphaena hippurus*). *Aquat Toxicol.* (2016) 180:274–81. doi: 10.1016/j.aquatox.2016.10.012
4. Brette F, Shiels HA, Galli GLJ, Cros C, Incardona JP, Scholz NL, et al. A novel cardiotoxic mechanism for a pervasive global pollutant. *Sci Rep*. (2017) 7:41476. doi: 10.1038/srep41476
5. Heuer RM, Galli GLJ, Shiels HA, Fieber LA, Cox GK, Mager EM, et al. Impacts of deepwater horizon crude oil on mahi-mahi (*Coryphaena hippurus*) heart cell function. *Environ Sci Technol*. (2019) 53:9895–904. doi: 10.1021/acs.est.9b03798
6. Harr KE, Rishniw M, Rupp TL, Cacela D, Dean KM, Dorr BS, et al. Dermal exposure to weathered MC252 crude oil results in echocardiographically identifiable systolic myocardial dysfunction in double-crested cormorants (P*halacrocorax auritus*). *Ecotoxicol Environ Saf*. (2017) 146:76–82. doi: 10.1016/j.ecoenv.2017.04.010
7. Zheng W, McKinney W, Kashon M, Jackson M, Law B, Kan H, Fedan J. The effects of crude oil vapor exposure on the cardiovascular system of rats. In: *Toxicologist, Supplement to Toxicological Sciences. Society of Toxicology 56th Annual Meeting and ToxExpo; 2017 March 12–16*. Baltimore, MD: Oxford University Press (2017). p. 479.
8. Strelitz J, Engel L, Kwok R, Miller A, Blair A, Sandler D. O29–3 Oil spill cleanup work and incident coronary heart disease in the gulf study. *Occup Environ Med*. (2016) 73:A54. doi: 10.1136/oemed-2016-103951.146
9. D'Andrea MA, Reddy GK. The development of long-term adverse health effects in oil spill cleanup workers of the Deepwater Horizon offshore drilling rig disaster. *Front Public Health*. (2018) 6:117. doi: 10.3389/fpubh.2018.00117
10. Strelitz J, Engel LS, Kwok RK, Miller AK, Blair A, Sandler DP. Deepwater Horizon oil spill exposures and nonfatal myocardial infarction in the GuLF STUDY. *Environ Health*. (2018) 17:69. doi: 10.1186/s12940-018-0408-8
11. Strelitz J, Keil AP, Richardson DB, Heiss G, Gammon MD, Kwok RK, et al. Self-reported myocardial infarction and fatal coronary heart disease among oil spill workers and community members 5 years after Deepwater Horizon. *Environ Res*. (2019) 168:70–9. doi: 10.1016/j.envres.2018.09.026
12. Venn-Watson S, Colegrove KM, Litz J, Kinsel M, Terio K, Saliki J, et al. Adrenal gland and lung lesions in Gulf of Mexico common bottlenose dolphins (*Tursiops truncatus*) found dead following the Deepwater Horizon oil spill. *PLoS ONE*. (2015) 10:e0126538. doi: 10.1371/journal.pone.0126538
13. Smith CR, Rowles TK, Hart LB, Townsend FI, Wells RS, Zolman ES, et al. Slow recovery of Barataria Bay dolphin health following the Deepwater Horizon oil spill (2013–2014), with evidence of persistent lung disease and impaired stress response. *Endanger Species Res*. (2017) 33:127–42. doi: 10.3354/esr00778
14. Lane SM, Smith CR, Mitchell J, Balmer BC, Barry KP, McDonald T, et al. Reproductive outcome and survival of common bottlenose dolphins sampled in Barataria Bay, Louisiana, USA, following the Deepwater Horizon oil spill. *P Roy Soc B Biol Sci*. (2015) 282:20151944. doi: 10.1098/rspb.2015.1944
15. Schwacke LH, Smith CR, Townsend FI, Wells RS, Hart LB, Balmer BC, et al. Health of common bottlenose dolphins (*Tursiops truncatus*) in Barataria Bay, Louisiana, Following the Deepwater Horizon oil spill. *Environ Sci Technol*. (2014) 48:93–103. doi: 10.1021/es500134b
16. Dias LA, Litz J, Garrison L, Martinez A, Barry K, Speakman T. Exposure of cetaceans to petroleum products following the Deepwater Horizon oil spill in the Gulf of Mexico. *Endanger Species Res*. (2017) 33:119–25. doi: 10.3354/esr00770
17. Takeshita R, Sullivan L, Smith C, Collier T, Hall A, Brosnan T, et al. The Deepwater Horizon oil spill marine mammal injury assessment. *Endanger Species Res.* (2017) 33:95–106. doi: 10.3354/esr00808
18. St. Leger J, Raverty S, Mena A. Cetacea. In: Terio K, McAloose D, St. Leger J, editors. *Pathology of Wildlife and Zoo Animals*. Cambridge, MA: Academic Press (2018). p. 533–68. doi: 10.1016/B978-0-12-805306-5.00022-5
19. Sweeney JC, SH Ridgway. Common diseases of small cetaceans. *JAVMA*. (1975) 167:533–40.
20. Lutmerding BA, Huston S, Frank K, Smith CR, Jensen ED. Case report: evidence of dilated cardiomyopathy and congestive heart failure in a geriatric bottlenose dolphin (*Tursiops truncatus*). In: *Proceedings of the 46th Annual International Association for Aquatic Animal Medicine Conference; 2015 Apr 6–10*. Chicago, IL: VIN.com (2015). Available online at: https://www.vin.com/apputil/content/defaultadv1.aspx?pId=12676. (accessed September 3, 2020).
21. Miedler S, Schmitt T, Reidarson T, McBain J. Transthoracic cardiac ultrasound examination in bottlenose dolphins (*Tursiops truncatus*). In: *Proceedings of the 38th Annual International Association for Aquatic Animal Medicine Conference; 2007 May 5–9*. Orlando, FL: VIN.com (2007). Available online at: https://www.vin.com/apputil/content/defaultadv1.aspx?pId=11257&catId=32376&id=3865385. (accessed September 3, 2020).
22. Herráez P, Sierra E, Arbelo M, Jaber JR, De Los Monteros AE, Fernández A. Rhabdomyolysis and myoglobinuric nephrosis (capture myopathy) in a striped dolphin. *J Wildl Dis*. (2007) 43:770–4. doi: 10.7589/0090-3558-43.4.770
23. Cowan DF, Curry BE. *Histopathological Assessment of Dolphins Necropsied Onboard Vessels in the Eastern Tropical Pacific Tuna Fishery*. National Marine Fisheries Service, Southwest Fisheries Science Center, NMFS SWFSC Administrative Report LJ-02–24C (2002).
24. Câmara N, Sierra E, Fernández A, Arbelo M, Bernaldo de Quirós Y, Arregui M, et al. Capture myopathy and stress cardiomyopathy in a live-stranded Risso's dolphin (*Grampus griseus*) in rehabilitation. *Animals*. (2020) 10:220. doi: 10.3390/ani10020220
25. Durden WN, Leger JS, Stolen M, Mazza T, Londono C. Lacaziosis in bottlenose dolphins (*Tursiops truncatus*) in the Indian River Lagoon, Florida, USA. *J Wildl Dis.* (2009) 45:849–56. doi: 10.7589/0090-3558-45.3.849
26. Scaglione F, Bollo E, Pregel P, Chiappino L, Sereno A, Mignone W, et al. Heart pathologies in dolphins stranded along the northwestern Italian coast. *Dis Aquat Org*. (2013) 107:31–6. doi: 10.3354/dao02672
27. Diaz-Delgado J, Eva S, Isabel VA, Lucas D, Marisa A, Manuel A, et al. Endocarditis associated with *Wohlfahrtiimonas chitiniclastica* in a short-beaked common dolphin (*Delphinus delphis*). *J Wildl Dis*. (2015) 51:283–6. doi: 10.7589/2014-03-072
28. Powell JWB, Archibald RT, Cross CA, Rotstein DS, Soop VM, McFee WE. Multiple congenital cardiac abnormalities in an Atlantic bottlenose dolphin (*Tursiops truncatus*). *J Wildl Dis.* (2009) 45:839–42. doi: 10.7589/0090-3558-45.3.839
29. Bossart GD, Hensley GT, Goldstein JD, Kroell K, Manire CA, Defran RH, et al. Cardiomyopathy and myocardial degeneration in stranded pygmy

(*Kogia breviceps*) and dwarf (*Kogia sima*) sperm whales. *Aquat Mamm*. (2007) 33:214–22. doi: 10.1578/AM.33.2.2007.214
30. Slijper EJ. Foramen ovale and ductus arteriosus botalli in aquatic mammals. *Mammalia*. (1961) 25:528–70. doi: 10.1515/mamm.1961.25.4.528
31. Ochrymowych C, Lambertsen RH. Anatomy and vasculature of a minke whale heart. *Am J Anat*. (1984) 169:165–75. doi: 10.1002/aja.1001690205
32. Szatmári V, Bunskoek P, Kuiken T, van den Berg A, van Elk C. Echocardiographic diagnosis and necropsy findings of a congenital ventricular septal defect in a stranded harbor porpoise. *Dis Aquat Org*. (2016) 118:177–83. doi: 10.3354/dao02973
33. Elsner R, Kenney DW, Burgess K. Diving bradycardia in the trained dolphin. *Nature*. (1966) 212:407–8. doi: 10.1038/212407a0
34. Kooyman GL. *Diverse Divers: Physiology and Behaviour*. Berlin Heidelberg: Springer-Verlag (1989). doi: 10.1007/978-3-642-83602-2
35. Williams TM, Friedl WA, Haun JE. The physiology of bottlenose dolphins (*Tursiops truncatus*): heart rate, metabolic rate and plasma lactate concentration during exercise. *J Exp Biol*. (1993) 179:31–46.
36. Ponganis PJ, Kooyman GL, Ridgway SH. Comparative diving physiology. In: Brubakk A, Neuman TS, editors. *Bennet and Elliott's Physiology and Medicine of Diving*. 5th ed. Edinburgh: Saunders, Elsevier Science Ltd (2003). p. 211–6.
37. Sommer L. Hemodynamic and coronary angiographic studies in the bottlenose dolphin (*Tursiops truncatus*). *Am J Physiology*. (1968) 215:1498–505. doi: 10.1152/ajplegacy.1968.215.6.1498
38. Macdonald AA, Carr PA, Currie RJ. Comparative anatomy of the foramen ovale in the hearts of cetaceans. *J Anat*. (2007) 211:64–77. doi: 10.1111/j.1469-7580.2007.00743.x
39. Cozzi B, Huggenberger S, Oelschlager HA. Chapter 4, Diving: breathing, respiration, and the circulatory system. In: Cozzi B, Huggenberger S, Oelschläger H, editors. *Anatomy of Dolphins: Insights into Body Structure and Function*. Cambridge, MA: Elsevier Academic Press (2017). p. 106–20. doi: 10.1016/B978-0-12-407229-9.00004-X
40. Hamlin R, Jackson R, Himes J, Pipers F, Townsend A. Electrocardiogram of bottle-nosed dolphin (*Tursiops truncatus*). *Am J Vet Res*. (1970) 31:501.
41. Harms CA, Jensen ED, Townsend FI, Hansen LJ, Schwacke LH, Rowles TK. Electrocardiograms of bottlenose dolphins (*Tursiops truncatus*) out of water: habituated collection versus wild postcapture animals. *J Zoo Wildl Med*. (2013) 44:972–81. doi: 10.1638/2013-0093.1
42. Yaw TJ, Kraus MS, Ginsburg A, Clayton LA, Hadfield CA, Gelzer AR. Comparison of a smartphone-based electrocardiogram device with a standard six-lead electrocardiogram in the Atlantic bottlenose dolphin (*Tursiops truncatus*). *J Zoo Wildl Med*. (2018) 49:689–95. doi: 10.1638/2017-0140.1
43. Williams TM, Fuiman LA, Kendall T, Berry P, Richter B, Noren SR, et al. Exercise at depth alters bradycardia and incidence of cardiac anomalies in deep-diving marine mammals. *Nat Commun*. (2015) 6:6055. doi: 10.1038/ncomms7055
44. Bickett N, Tift M, St. Leger J, Ponganis P. Heart rate regulation in the killer whale. *FASEB J*. (2016) 30:1230.9–1230.9. doi: 10.1096/fasebj.30.1_supplement.1230.9
45. Elmegaard SL, Johnson M, Madsen PT, McDonald BI. Cognitive control of heart rate in diving harbor porpoises. *Curr Biol*. (2016) 26:1175–6. doi: 10.1016/j.cub.2016.10.020
46. Goldbogen JA, Cade DE, Calambokidis J, Czapanskiy MF, Fahlbusch J, Friedlaender AS, et al. Extreme bradycardia and tachycardia in the world's largest animal. *PNAS*. (2019) 116:25329–25332. doi: 10.1073/pnas.1914273116
47. Sklansky M, Levine G, Havlis D, West N, Renner M, Rimmerman C, et al. Echocardiographic evaluation of the bottlenose dolphin (*Tursiops truncatus*). *J Zoo Wildl Med*. (2006) 37:454–63. doi: 10.1638/05-116.1
48. Miedler S, McBain J, Reidarson T, Schmitt T. *Handbook of Transthoracic Cardiac Ultrasound Examination in Bottlenose Dolphins*. Vienna (2008).
49. Chetboul V, Lichtenberger J, Mellin M, Mercera B, Hoffmann A-C, Chaix G, et al. Within-day and between-day variability of transthoracic anatomic M-mode echocardiography in the awake bottlenose dolphin (*Tursiops truncatus*). *J Vet Cardiol*. (2012) 14:511–8. doi: 10.1016/j.jvc.2012.07.002
50. Miedler S, Fahlman A, Valls Torres M, Álvaro Álvarez T, Garcia-Parraga D. Evaluating cardiac physiology through echocardiography in bottlenose dolphins: using stroke volume and cardiac output to estimate systolic left ventricular function during rest and following exercise. *J Exp Biol*. (2015) 218:3604–10. doi: 10.1242/jeb.131532
51. Barratclough A, Wells RS, Schwacke LH, Rowles TK, Gomez FM, Fauquier DA, et al. Health assessments of common bottlenose dolphins (*Tursiops truncatus*): past, present, and potential conservation applications. *Front Vet Sci*. (2019) 6:444. doi: 10.3389/fvets.2019.00444
52. Wells RS. Social structure and life history of bottlenose dolphins near Sarasota Bay, Florida: insights from four decades and five generations. In: Yamagiwa J, Karczmarski L, editors. *Primates and Cetaceans. Primatology Monographs*. Tokyo: Springer (2014). p. 149–72. doi: 10.1007/978-4-431-54523-1_8
53. Wells RS, Rhinehart HL, Hansen LJ, Sweeney JC, Townsend FI, Stone R, et al. Bottlenose dolphins as marine ecosystem sentinels: developing a health monitoring system. *EcoHealth*. (2004) 1:246–54. doi: 10.1007/s10393-004-0094-6
54. Levine SA. The systolic murmur: its clinical significance. *JAMA*. (1933) 101:436–8. doi: 10.1001/jama.1933.02740310020005
55. Zipes DP, Libby P, Bonow RO, Mann DL, Tomaselli GF. *Braunwald's Heart Disease E-Book: A Textbook of Cardiovascular Medicine*. Philadelpha, PA: Elsevier Health Sciences (2018).
56. Tilley LP, Smith FWK, Oyama MA, Sleeper MM. *Manual of Canine and Feline Cardiology*, 4th Edition. St. Louis, MO: Elsevier Health Sciences (2008).
57. Kvart C, Haggstrom J. *Cardiac Auscultation and Phonocardiography in Dogs, Horses and Cats*. Uppsala: Privately printed (2002).
58. Otto CM. *Textbook of Clinical Echocardiography E-Book*. Philadelphia, PA: Elsevier Health Sciences (2013).
59. Bonagura JD. Effective cardiac auscultation. In: *Proceedings of the Latin American Veterinary Conference; 2017 Apr 20–22*. Lima: International Veterinary Information Service (2017).
60. Bonagura JD. Cardiac auscultation. In: Bonagura JD, Fuentes VL, Muers KM, editors. *Proceedings of the the 26th Annual Waltham/OSU Symposium, Small Animal Cardiology*, 2002 Oct 19–20. Lima: VIN.com (2015). Available online at: https://www.vin.com/doc/?id=6693280. (accessed August 20, 2019).
61. Mattoon JS, Nyland TG. *Small Animal Diagnostic Ultrasound - E-Book*. St. Louis, MO: Elsevier Health Sciences (2014).
62. Benjamini Y, Hochberg Y. Controlling the false discovery rate: a practical and powerful approach to multiple testing. *J R Stat Soc B Methodol*. (1995) 57:289–300. doi: 10.1111/j.2517-6161.1995.tb02031.x
63. Lettvin JY, Gruberg ER, Rose RM, Plotkin G. Dolphins and the bends. *Science*. (1982) 216:650–1. doi: 10.1126/science.216.4546.650-a
64. Côté E, Edwards NJ, Ettinger SJ, Luis Fuentes V, MacDonald KA, Scansen BA, Sisson DD, Abbott JA. Management of incidentally detected heart murmurs in dogs and cats. *J Vet Cardiol*. (2015) 17:245–61. doi: 10.1016/j.jvc.2015.05.001
65. Doshi AR. Innocent heart murmur. *Cureus*. (2018) 10:12. doi: 10.7759/cureus.3689
66. Frank JE, Jacobe KM. Evaluation and management of heart murmurs in children. *AFP*. (2011) 84:793–800.
67. Huston TP, Puffer JC, Rodney WM. The athletic heart syndrome. *New Engl J Med*. (1985) 313:24–32. doi: 10.1056/NEJM198507043130106
68. George KP, Wolfe LA, Burggraf GW. The "athletic heart syndrome". A critical review. *Sports Med*. (1991) 11:300–30. doi: 10.2165/00007256-199111050-00003
69. Mejia E, Dhuper S. *Innocent Murmur*. Treasure Island, FL: StatPearls Publishing (2020). http://www.ncbi.nlm.nih.gov/books/NBK507849/. (accessed August 8, 2019).
70. Fabrizio F, Baumwart R, Iazbik MC, Meurs KM, Couto CG. Left basilar systolic murmur in retired racing greyhounds. *J Vet Intern Med*. (2006) 20:78–82. doi: 10.1111/j.1939-1676.2006.tb02826.x
71. Constable PD, Hinchcliff KW, Olson J, Hamlin RL. Athletic heart syndrome in dogs competing in a long-distance sled race. *J Appl Phys*. (1994) 76:433–8. doi: 10.1152/jappl.1994.76.1.433
72. Reef VB. Review article: heart murmurs in horses: determining their significance with echocardiography. *Equine Vet J*. (1995) 27:71–80. doi: 10.1111/j.2042-3306.1995.tb04992.x
73. Bonagura JD. Equine heart disease: an overview. *Vet Clin N Am-Equine*. (1985) 1:267–88. doi: 10.1016/S0749-0739(17)30755-1
74. Rich BSE, Havens SA. The athletic heart syndrome. *Curr Sports Med Rep*. (2004) 3:84–8. doi: 10.1249/00149619-200404000-00006
75. Murgo JP. Systolic ejection murmurs in the era of modern cardiology: what do we really know? *J Am Coll Cardiol*. (1998) 32:1596–602. doi: 10.1016/S0735-1097(98)00425-2

76. Pollock JD, Makaryus AN. *Physiology, Cardiovascular Hemodynamics*. Treasure Island, FL: StatPearls Publishing (2020). http://www.ncbi.nlm.nih.gov/books/NBK470310/. (accessed August 8, 2019).
77. Pyle RL, Patterson DF, Chacko S. The genetics and pathology of discrete subaortic stenosis in the Newfoundland dog. *Am Heart J*. (1976) 92:324–34. doi: 10.1016/S0002-8703(76)80113-5
78. Fair P, Schaefer A, Romano T, Bossart G, Lamb S, Reif J. Stress response of wild bottlenose dolphins (*Tursiops truncatus*) during capture-release health assessment studies. *Gen Comp Endocrinol*. (2014) 206:203–12. doi: 10.1016/j.ygcen.2014.07.002
79. Houser DS, Martin S, Crocker DE, Finneran JJ. Endocrine response to simulated U.S. Navy mid-frequency sonar exposures in the bottlenose dolphin (*Tursiops truncatus*). *J Acoust Soc Am*. (2020) 147:1681–7. doi: 10.1121/10.0000924
80. Champagne CD, Kellar NM, Trego ML, Delehanty B, Boonstra R, Wasser SK, et al. Comprehensive endocrine response to acute stress in the bottlenose dolphin from serum, blubber, and feces. *Gen Comp Endocrinol*. (2018) 266:178–93. doi: 10.1016/j.ygcen.2018.05.015
81. Pradelli D, Quintavalla C, Crosta MC, Mazzoni L, Oliveira P, Scotti L, et al. The influence of emotional stress on Doppler-derived aortic peak velocity in boxer dogs. *J Vet Int Med*. (2014) 28:1724–30. doi: 10.1111/jvim.12434
82. Pedersen HD, Häggström J, Falk T, Mow T, Olsen LH, Iversen L, et al. Auscultation in mild mitral regurgitation in dogs: observer variation, effects of physical maneuvers, and agreement with color Doppler echocardiography and phonocardiography. *J Vet Int Med*. (1999) 13:56–64. doi: 10.1111/j.1939-1676.1999.tb02166.x

Conflict of Interest: The authors declare that the research was conducted in the absence of any commercial or financial relationships that could be construed as a potential conflict of interest.

The handling editor declared a past co-authorship with AB and CH.

The reviewer WV declared past-publications with KC to the handling editor.

Copyright © 2020 Linnehan, Hsu, Gomez, Huston, Takeshita, Colegrove, Rowles, Barratclough, Musser, Harms, Cendejas, Zolman, Balmer, Townsend, Wells, Jensen, Schwacke and Smith. This is an open-access article distributed under the terms of the Creative Commons Attribution License (CC BY). The use, distribution or reproduction in other forums is permitted, provided the original author(s) and the copyright owner(s) are credited and that the original publication in this journal is cited, in accordance with accepted academic practice. No use, distribution or reproduction is permitted which does not comply with these terms.

frontiers in Veterinary Science

CASE REPORT
published: 24 November 2020
doi: 10.3389/fvets.2020.569185

Case Report: Suppression of Harem Stallion Behavior and Fertility Following Anti-Gonadotropin-Releasing Hormone Vaccination of a Captive Wild Przewalski's Horse (*Equus ferus przewalskii*)

Jérôme Ponthier[1*†], *Goulven Rigaux*[2†], *Sonia Parrilla-Hernandez*[3], *Sophie Egyptien*[1], *Carine Gatez*[3], *Carla Carrasco Leroy*[2] *and Stéfan Deleuze*[1,3]

[1] Equine and Companion Animal Reproduction Pathologies Clinic, Veterinary Medicine Faculty, University of Liège, Liège, Belgium, [2] Domaine des Grottes de Han, Han sur Lesse, Rochefort, Belgium, [3] Animal Physiology, Veterinary Medicine Faculty, University of Liège, Liège, Belgium

This report describes an option to modulate the testicular function of wild horses and field methods to assess it. Non-surgical castration of a captive wild Przewalski's stallion with anti-gonadotropin-releasing hormone (GnRH) immunization was performed by sub-cutaneous injection of two doses of 450 μg (3 ml) of GnRH conjugated to diphtheria toxin, further repeated every 6 months. Semen quality was assessed after collection by electro-ejaculation under general anesthesia. Endocrine and behavioral consequences were studied during a 2-year follow-up period. The procedure of electro-ejaculation was safe and effective to collect spermatozoa. Motility was low but was improved by a significant dilution of sample (1*v*/4*v*−1*v*/5*v*) after collection. Immuno-neutering resulted in a decrease of the total spermatozoa number and motility 1 month after primary vaccination. However, infertility could not yet be guaranteed. Six months post-vaccination, serum testosterone concentrations had decreased and the treated stallion had lost his harem stallion role. Moreover, at the same time, the total spermatozoa number was near zero with no motile spermatozoa, and offspring was no longer observed. As a conclusion, electro-ejaculation under general anesthesia is suitable on wild horses to obtain spermatozoa that should be washed or largely diluted before use for artificial insemination (AI) programs. Anti-GnRH immuno-neutering protocol led to a dramatic decrease of spermatozoa number, motility, and testosterone production. This also induced deep changes in the social structure of the band. Such technique could be considered as an alternative to surgical castration in wild horses.

Keywords: wildlife preservation, Przewalski horse (*Equus ferus przewalskii*), anti-GnRH immunization, neutering, castration, electro-ejaculation

OPEN ACCESS

Edited by:
Francesco Carlo Origgi, University of Bern, Switzerland

Reviewed by:
Nikolaus Huber, University of Veterinary Medicine, Austria
Malgorzata Pozor, University of Florida College of Veterinary Medicine, United States

***Correspondence:**
Jérôme Ponthier
Jerome.Ponthier@uliege.be

†These authors have contributed equally to this work

Specialty section:
This article was submitted to Zoological Medicine, a section of the journal Frontiers in Veterinary Science

Received: *03 June 2020*
Accepted: *08 October 2020*
Published: *24 November 2020*

Citation:
Ponthier J, Rigaux G, Parrilla-Hernandez S, Egyptien S, Gatez C, Carrasco Leroy C and Deleuze S (2020) Case Report: Suppression of Harem Stallion Behavior and Fertility Following Anti-Gonadotropin-Releasing Hormone Vaccination of a Captive Wild Przewalski's Horse (Equus ferus przewalskii). Front. Vet. Sci. 7:569185. doi: 10.3389/fvets.2020.569185

INTRODUCTION

In zoos and safari parks, modulation of reproduction is required to limit the offspring of some over-represented species or inbreeding within herds. However, neutering of captive wild animals is challenging: any intervention is time consuming and life threatening when a general anesthesia is required. Moreover, any surgery is including risks of wound infection that would be difficult to treat.

Modulation of the equine hypothalamic–pituitary axis can be an alternative to surgical neutering (1). Vaccination against gonadotropin-releasing hormone (GnRH) induces a decrease of testosterone and spermatozoa production in domestic stallions, and commercial contraception protocols are available (2). The main adverse effects are a local inflammation after injection and a persistent infertility in males or anestrus in mares, sometimes lasting long after the last vaccination (2, 3). Inhibition of testosterone secretion interferes with the social behavior in gregarious species (4–8). In wild horses, the harem stallion may be challenged by other males, and rapid changes in hierarchy may cause severe injuries after fights (9, 10).

This report aims to describe the effects of an anti-GnRH vaccination in a captive wild Przewalski's horse (*Equus ferus przewalskii*) on semen quality, testosterone concentrations, and social interactions over a long period.

CASE DESCRIPTION

"Le Domaine des Grottes de Han" (Han sur Lesse, Belgium) is a safari park housing Przewalski's horses roaming freely. Depending on the season, hay supplementation is distributed once or twice a day in the only feeder available in the park. Castration of the 18-year-old harem role stallion was considered to limit the band's inbreeding, as he was keeping two bachelors away from the three or four mares, their foals (one or two, depending on the year), and the food. The immuno-neutering with an anti-GnRH vaccine was preferred over surgical procedures. The vaccine consisted in a 3-ml dose of Improvac® (vaccine initially developed for porcine by Zoetis, Louvain-la-Neuve, Belgium) containing a minimum of 450 μg of GnRH agonist conjugated to diphtheria toxin, as specified by the manufacturer leaflet. On day 0 (May 26th 2016), day 32, and day 177, the vaccine was subcutaneously administrated in the chest, during the procedures performed under general anesthesia to assess the effects of immuno-neutering on semen quality and testicular endocrine activity with semen and blood samples (**Figure 1**). Then, for a 2-year period, 3-ml boosters were darted every 6 months. Social behavior with younger stallions and reproductive interactions with mares of the treated stallion were observed twice daily. The treated stallion's paternity was genetically excluded in foals born during these 2 years (**Figure 1**).

Anesthesia

The stallion's bodyweight was estimated at 300 kg. The protocol consisted of a tele-anesthesia with a pressurized

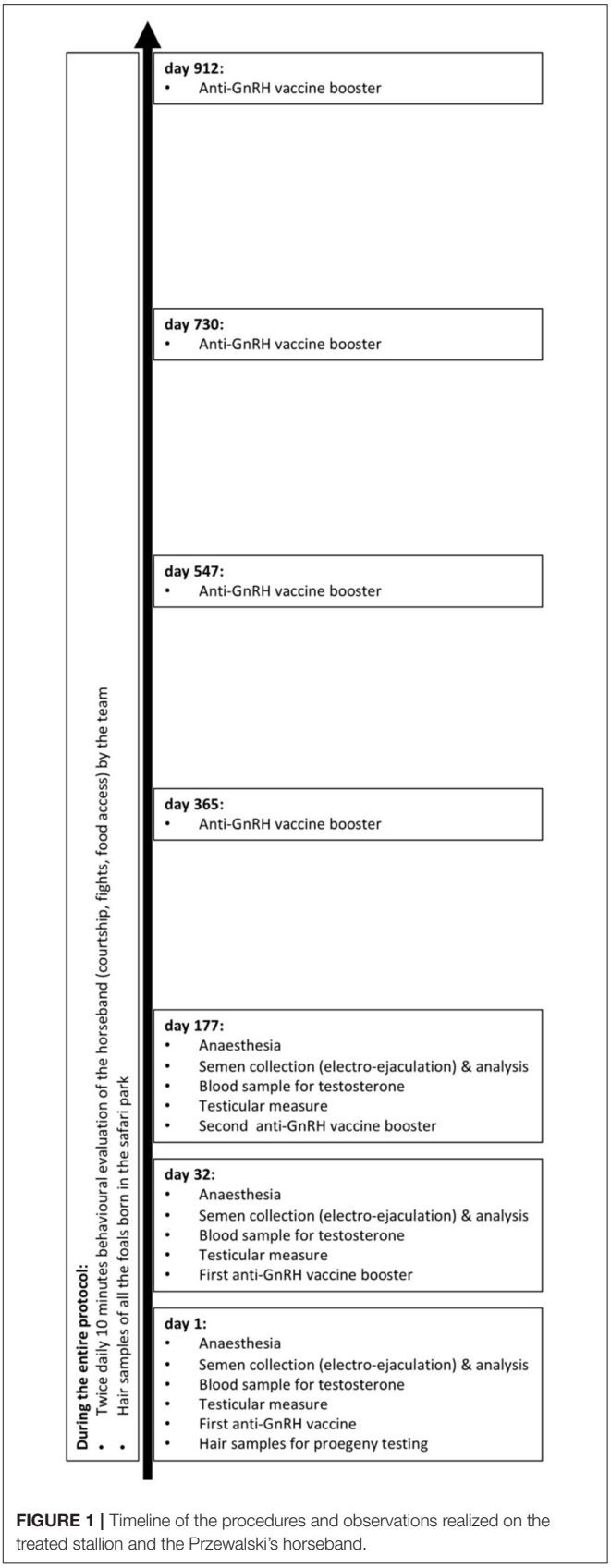

FIGURE 1 | Timeline of the procedures and observations realized on the treated stallion and the Przewalski's horseband.

air dart containing detomidine (10 mg), butorphanol (12 mg), and etorphine (5.6 mg). Once in a recumbent position, the premedication dart was removed, a catheter (14G) was placed in the jugular vein, and intravenous balanced anesthesia (glycerol guaiacolate 500 ml, ketamine 1 g, and xylazine 250 mg) was given on demand until the end of procedures. Oxygen was given via an endotracheal tube. When the procedures were completed, naltrexone (125 mg) and atipamezole (between 25 and 50 mg) were injected intra-muscularly to accelerate recovery.

Breeding Soundness Examination, Semen Collection, and Analysis

At days 0, 32, and 177, the testicular transverse circumference was measured perpendicularly to the testis long axis with a tape: with three measures of each testis, the mean value was calculated. To decrease the urinary contamination of semen, the bladder was emptied by catheterization before electro-ejaculation. The prostate was manually stimulated during 2 min by rectal palpation.

Ejaculation was induced with an electro-ejaculator using a lubricated bovine rectal probe (Minitübe, Tiefenbach, Germany, 40-cm long, 7-cm diameter, three longitudinal electrodes). Four cycles of stimulations separated by 3 min of rest were performed, with these sequences:

- Cycle 1: 10 stimulations 0.5 V−10 stimulations 1.5 V−15 stimulations 2.5 V;
- Cycle 2: 10 stimulations 0.5 V−10 stimulations 1.5 V−10 stimulations 2.5 V−15 stimulations 3.5 V;
- Cycle 3: 10 stimulations 1.5 V−10 stimulations 2.5 V−10 stimulations 3.5 V−15 stimulations 4.5 V;
- Cycle 4: 10 stimulations 0.5 V−10 stimulations 2.5 V−10 stimulations 3.5 V−15 stimulations 4.5 V.

Semen samples were collected after each cycle. After the last cycle, the bladder was catheterized and the urine was centrifuged to determine the spermatozoa concentration in the pellet.

The following analysis were performed on each semen sample. In the field, immediately after collection, subjective evaluation of spermatozoa motility was performed under light microscopy (×400), with 10 μl of semen on a warmed slide (37°C). To determine the concentration of spermatozoa, 10 μl of semen were diluted in 390 μl of 40% formaldehyde in the field. This sample was then shipped to the laboratory where concentration was determined under microscopy, using a Thoma cell (IMV, Laigle, France). Fractions of the ejaculate were then largely (1*v*/4*v*−1*v*/5*v*) extended with INRA 96® (IMV, Laigle, France) to dilute possible urine contamination of the semen. It was shipped within 4 h to the laboratory, where total and progressive motilities were determined (11) with a Makler® cell in a semen analyzer (IVOS with 2006 software, Hamilton Thorn®, Beverly, USA) using semen re-diluted to 20 × 10^6 spz/ml with INRA 96® (IMV, Laigle, France). Percent of morphologically abnormal spermatozoa was determined by counting 200 spermatozoa after Diff-Quick® staining (RAL, Martillac, France).

Endocrinology

Blood samples were collected on days 0, 32, and 177 and assayed for testosterone with an automated spectrography by a commercial laboratory (LabForVet, Les Isnes, Belgium).

Behavioral Evaluation

Since the beginning of the protocol (day 0), and for 2.5 years, the animal nursing team managers of the safari park recorded interactions between the old treated Przewalski's stallion and the rest of the horse band during the twice-daily 10-min surveillance duty (early morning and afternoon): fights, fights for access to hay in feeders, and aggressions when the treated male was approaching the rest of the group. Courtship behaviors expressed by the males of the band were also reported twice daily in a standardized form.

Progeny Testing

An equine commercial progeny test was used to determine if the foals born in the park between 2017 and 2019 were the offspring of the treated stallion. These assays used 13 DNA markers, and filiation was excluded when more than five markers differed (Progenus, Gembloux, Belgium).

RESULTS

Semen Quality

Table 1 summarizes the volume and semen parameters of four fractions collected by electro-ejaculation on day 0. Repetition of cycles was associated with decreased concentrations and motility in the samples. Few spermatozoa were observed in urine. The total semen volume was 133 ml and the total spermatozoa number was 4,110 × 10^6 spz. The morphology analysis showed 82.6% of normal spermatozoa and 11.4% of broken mid-pieces. Left and right testis circumferences were 13.5 and 12.5 cm, respectively.

At day 32, only three cycles of electro-ejaculation were performed, due to anesthesia instability. Data about collected fractions are summarized in **Table 1**. The total collected volume was 44 ml, with a total spermatozoa number of 1,517 × 10^6 spz. Day 32 motility parameters were reduced and morphological analysis only showed 58.7% of normal spermatozoa, with high proportions of abnormal mid-pieces (32.5%). No spermatozoa were observed in the urine. The mean testicular circumference was 11 cm for both testes.

At day 177, the total collected volume of semen was 37 ml, with no spermatozoa under light microscopy. Fractions were centrifuged (1,000 × *g*, 20 min), to obtain 1-ml pellets for analysis: 10 μl of these undiluted samples were injected in the Thoma cell, using a correction factor to calculate the concentration. The first and third fractions contained no spermatozoa and the second fraction (15 ml) contained very few (**Table 1**). A dramatic decrease in the total number of collected spermatozoa was observed, with only 49,500 spz, and no observed spermatozoa was motile (**Figures 2**, **3**). Normal spermatozoa were absent (main abnormalities were mid-piece defects and separated heads). The left testis circumference was

TABLE 1 | Evolution of semen parameters.

	Volume (ml)	Spermatozoa concentration ($\times 10^6$ spz/ml)	Total spermatozoa number ($\times 10^6$ spz)	CASA total motility after dilution in INRA 96® (%)	CASA progressive motility after dilution in INRA 96® (%)
DAY 0 SEMEN ANALYSIS					
Cycle 1	30	65	1,950	89	70
Cycle 2	52	28	1,456	70	48
Cycle 3	22	18	396	76	62
Cycle 4	28	11	308	59	45
Total	**132**		**4,110**		
Bladder	*181*	*1*	*181*		
DAY 32 SEMEN ANALYSIS					
Cycle 1	12	31	372	47	29
Cycle 2	15	48	720	61	37
Cycle 3	17	25	425	41	25
Total	**44**		**1,517**		
DAY 177 SEMEN ANALYSIS					
Cycle 1	12			No cellular liquid	
Cycle 2	15	<0.0033		No motile cells	
Cycle 3	10			No cellular liquid	
Total	**37**		**49,500**		

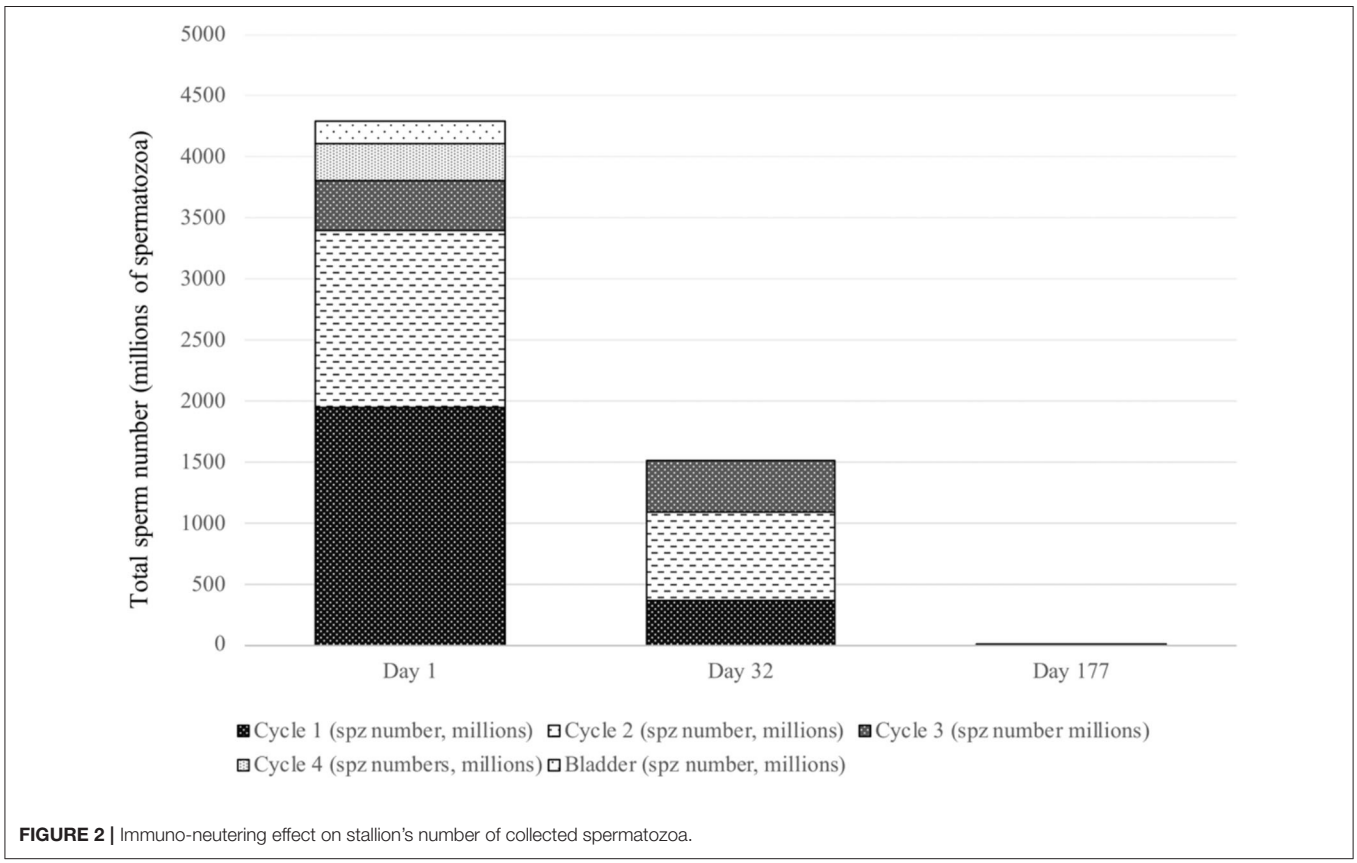

FIGURE 2 | Immuno-neutering effect on stallion's number of collected spermatozoa.

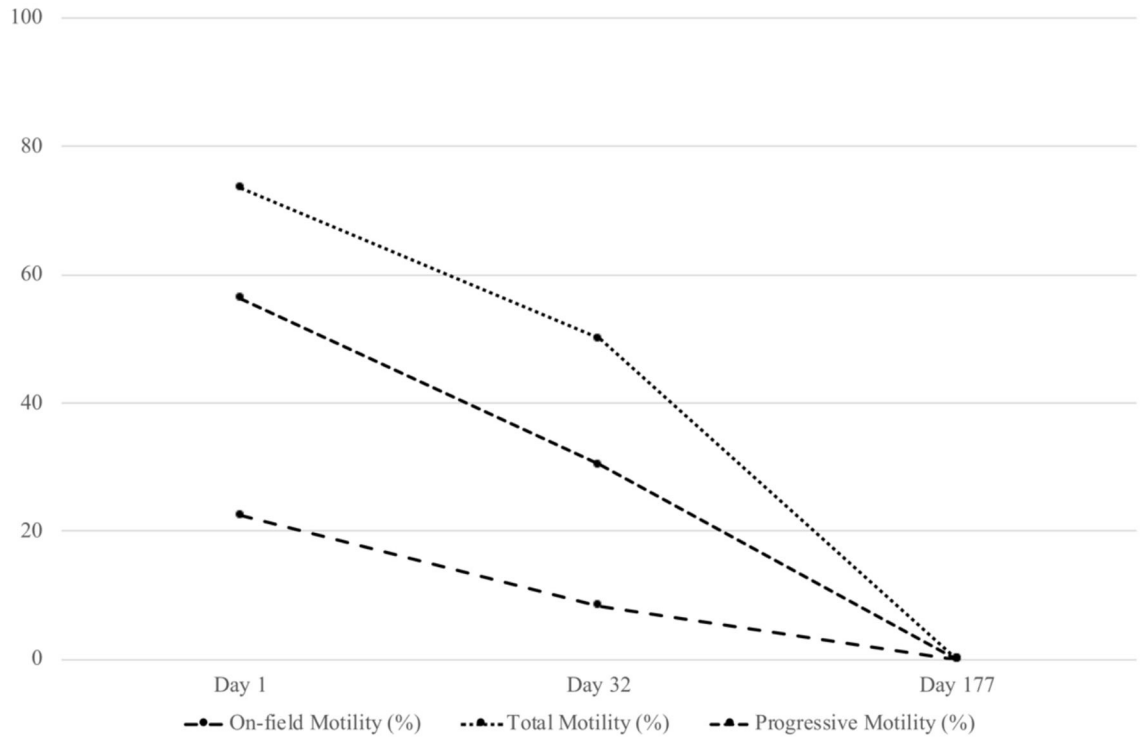

FIGURE 3 | Immuno-neutering effect on stallion's on-field observed motility, total (CASA), and progressive motility (CASA).

10 cm. The right testis seemed smaller, but could not be measured because it was high-up in the inguinal region.

Between 2017 and 2019, no offspring of the treated stallion was genetically identified in the park.

Endocrine and Behavioral Evolution

On days 0 and 32, basal blood testosterone concentrations were 105 and 133 ng/dl, respectively. On day 177, it dropped to 29 ng/dl.

Between days 0 and day 32, no behavioral changes were observed: the treated stallion remained the harem stallion, and its body condition was good. The younger stallions were not allowed to eat at the same time or to mate. Between the first and the second booster injections (days 32 and 177), clear changes in the males' hierarchy appeared. Within 2–4 weeks, the treated stallion no longer fought for the leadership and no longer covered the mares. The younger stallions kept him away from the females and the entire band during feeding. His body condition decreased (ribs easy to see, reduced back muscles thickness), reducing his chances to keep the leadership.

After day 177, the anti-GnRH vaccine (3 ml) was darted every 6 months without necessitating a general anesthesia. During these 2 years, the old stallion did not fight to keep his harem stallion role and remained isolated from the band, especially during feeding times. However, 1–2 weeks before the planned time for the booster, the treated stallion showed feces marking and made attempts to fight the leaders, but the vaccine rapidly (2–3 days) suppressed these behaviors.

DISCUSSION

Our electro-ejaculation protocol under general anesthesia is suitable for semen evaluation and artificial insemination (AI) programs of captive wild Przewalski's horses and, potentially, of other wild equids. As an example, electro-ejaculations were concomitantly performed to include other Przewalski's stallions in an exchange program: motile spermatozoa were also collected (12). Analysis performed before our immuno-neutering protocol showed a low raw semen quality, but the large dilution ($1v/4v-1v/5v$) with a commercial extender improved motility. This reversible effect was also observed by our team (12) and in another report of wild Przewalski's horses electro-ejaculations (13). This could be explained by the dilution of urine contamination: further studies should assay urea and creatinine in raw semen and correlate it with the semen quality. However, the motility improvement observed after dilution suggested that electro-ejaculated spermatozoa of wild equids are suitable for AI after washing with two or three centrifugations in an extender, as described for toxic plasma (14).

The first three doses of anti-GnRH vaccines were given during anesthesia, which was needed to monitor the evolution of semen quality of this wild stallion. Tele-injection was then easily performed every 6 months on this stallion because the vaccine volume was low (3 ml). In agreement with the previous reports on equine domestic breeds, total azoospermia and a nearly complete aspermia were observed after 6 months (1–3, 15–17), when this can require up to 1 year in elephants (7, 8).

Basal blood testosterone concentrations showed a dramatic decrease between days 32 and 177. No dynamic exploration of testosterone production after an hCG stimulation was performed due to short-time general anesthesia performed in the field. Thus, the low testosterone concentration observed on day 177 could only be a temporary decrease between the 4 to 6 peaks daily observed in stallions (18–21). However, the dramatic decrease in testicular size, spermatozoa number and quality, and the absence of offspring during the follow-up all confirm the reduced testicular functions after an anti-GnRH immuno-neutering.

The treated stallion's behavior also highly suggested a decreased testosterone production. Changes in hierarchy were observed after the first booster injection (day 32), leading to the loss of harem stallion role by the immuno-neutered animal. This effect was already documented in wolves, which are also living in complex social structures (4, 5). In wild equids bands, immuno-neutering affects not only the treated stallion's interactions with other horses but also his feeding behavior and body condition. This could be related to the new harem stallions' roles forbidding the old one to access to the feeders or to the observed testosterone decrease. Resumption of fights between the new harem stallions' roles and the old one before the booster injection supports a rapid reversibility of the vaccination effect.

Surgical castration or immuno-neutering have behavioral effects that should be compared to the risk and benefits of a surgical vasectomy. In the present case, avoiding inbreeding was getting urgent and this old stallion could not be included in an exchange program. As euthanasia was not an option for the park team, they were informed about each option's risks. Castration or vasectomy post-operative cares seemed impossible to perform for the team on a free roaming wild horse, and immuno-neutering was chosen as the best solution. The staff still manages the consequences for the treated stallion by feeding him separately.

The effects of immuno-neutering are well-described in stallions (1–3). This non-surgical option is an effective, easy, safe, cheap, and possibly reversible means to control wild horse populations and only requires darting every 6 months. It could improve animal welfare by avoiding euthanasia when control of the equid's population is becoming imperative: not only in parks but also where free groups of wild horses, wild ass, donkeys, or zebra cause troubles to their environment. However, reproduction data in the larger bands of immuno-neutered stallions and mares could help to understand the long-term effects of this technique.

To conclude, the electro-ejaculation protocol performed under general anesthesia was effective to collect spermatozoa for semen quality assessment of a captive wild Przewalski's horse. Dilution and/or washing of the raw semen could increase its quality for fresh semen AI procedures. Vaccination against GnRH resulted in an efficient fertility suppression in this Przewalski's stallion and induced anatomical, endocrine, and behavioral changes, contributing to the loss of his harem stallion role. Such technique should always be considered before performing any kind of castration in groups of wild animals.

DATA AVAILABILITY STATEMENT

The raw data supporting the conclusions of this article will be made available by the authors, without undue reservation.

ETHICS STATEMENT

Ethical review and approval was not required for the animal study because the procedures were performed on an animal on the demand of the owner (a safari park). The study was realized on the basis of this clinical situation, required by the owner of the animal. Written informed consent was obtained from the owners for the participation of their animals in this study.

AUTHOR CONTRIBUTIONS

All authors performed all the on-field procedures, including anesthesia, and electro-ejaculation. JP, SP-H, SE, and SD performed the semen analysis. GR and CCL collected the comportemental information during all the follow-up period. They also darted the stallion for booster vaccines after day 177. JP wrote the manuscript. All authors reviewed and corrected the manuscript. All authors contributed to the article and approved the submitted version.

FUNDING

This study was funded by the Equine & Companion Animal Reproduction Pathologies Clinic, Veterinary Medicine Faculty, University of Liège, Liège, Belgium for the assays; le Domaine des Grottes de Han for the procedures, the medications, and the nursing team assistance.

ACKNOWLEDGMENTS

The authors thank the animal nursing team of Le Domaine des Grottes de Han, especially Mr. Etienne Brunelle and Mr. Anthony Kohler, their managers.

REFERENCES

1. Stout TA. Modulating reproductive activity in stallions: a review. *Anim Reprod Sci.* (2005) 89:93–103. doi: 10.1016/j.anireprosci.2005.06.015
2. Bailly-Chouriberry L, Loup B, Popot MA, Dreau ML, Garcia P, Bruyas JF, et al. Two complementary methods to control gonadotropin-releasing hormone vaccination (Improvac(R)) misuse in horseracing: enzyme-linked immunosorbent assay test in plasma and steroidomics in urine. *Drug Test Anal.* (2017) 9:1432–40. doi: 10.1002/dta.2187
3. Janett F, Stump R, Burger D, Thun R. Suppression of testicular function and sexual behavior by vaccination against GnRH (Equity) in the adult stallion. *Anim Reprod Sci.* (2009) 115:88–102. doi: 10.1016/j.anireprosci.2008.11.011
4. Kirkpatrick JF, Lyda RO, Frank KM. Contraceptive vaccine in wildlife: a review. *Am J Reprod Immunol.* (2011) 66:40–50. doi: 10.1111/j.1600-0897.2011.01003.x

5. Rabb GB, Woolpy JH, Ginsburg BE. Social relationship in a group of captive wolves. *Am Zool.* (2015) 7:305–11. doi: 10.1093/icb/7.2.305
6. Asa CS, Mech LD, Seal US, Plotka ED. The influence of social and endocrine factors on urine-marking by captive wolves (*Canis lupus*). *Horm Behav.* (1990) 24:497–509. doi: 10.1016/0018-506X(90)90038-Y
7. Lueders I, Hildebrandt TB, Gray C, Botha S, Rich P, Niemuller C. Supression of testicular function in a male Asian elephant (*Elephas maximus*) treated with gonadotropin-releasing hormone vaccines. *J Zoo Wildl Med.* (2014) 45:611–9. doi: 10.1638/2013-0233R.1
8. Lueders I, Young D, Maree L, van der Horst G, Luther I, Botha S, et al. Effects of GnRH vaccination in wild and captive African elephant bulls (*Loxodonta africana*) on reproductive organs and semen quality. *PLoS ONE.* (2017) 12:e0178270. doi: 10.1371/journal.pone.0178270
9. Burger D, Dolivo G, Wedekind C. Ejaculate characteristics depend on social environment in the Horse (*Equus caballus*). *PLoS ONE.* (2015) 10:e0143185. doi: 10.1371/journal.pone.0143185
10. McDonnell SM, Murray SC. Bachelor and harem stallion behavior end endocrinology. *Biol Reprod Mono.* (1995) 1:577–90. doi: 10.1093/biolreprod/52.monograph_series1.577
11. Ponthier J, Franck T, Detilleux J, Mottart E, Serteyn D, Deleuze S. Association between myeloperoxidase concentration in equine frozen semen and post-thawing parameters. *Reprod Domest Anim.* (2010) 45:811–6. doi: 10.1111/j.1439-0531.2009.01357.x
12. Rigaux G, Parrilla-Hernandez S, Egyptien S, Gatez C, Carrasco Leroy C, Deleuze S, et al. On-field electro-ejaculation of wild prezwalski horses: results and perspectives. *J Equ Vet Sci.* (2018) 66:83. doi: 10.1016/j.jevs.2018.05.050
13. Pukazhenthi BS, Johnson A, Guthrie HD, Songsasen N, Padilla LR, Wolfe BA, et al. Improved sperm cryosurvival in diluents containing amides versus glycerol in the Przewalski's horse (*Equus ferus przewalskii*). *Cryobiology.* (2014) 68:205–14. doi: 10.1016/j.cryobiol.2014.01.013
14. Loomis PR. Advanced methods for handling and preparation of stallion semen. *Vet Clin Equine.* (2006) 22:663–76. doi: 10.1016/j.cveq.2006.07.002
15. Janett F, Gerig T, Tschuor AC, Amatayakul-Chantler S, Walker J, Howard R, et al. Effect of vaccination against gonadotropin-releasing factor (GnRF) with Bopriva(R) in the prepubertal bull calf. *Anim Reprod Sci.* (2012) 131:72–80. doi: 10.1016/j.anireprosci.2012.02.012
16. Janett F, Gerig T, Tschuor AC, Amatayakul-Chantler S, Walker J, Howard R, et al. Vaccination against gonadotropin-releasing factor (GnRF) with Bopriva significantly decreases testicular development, serum testosterone levels and physical activity in pubertal bulls. *Theriogenology.* (2012) 78:182–8. doi: 10.1016/j.theriogenology.2012.01.035
17. Schulman ML, Botha AE, Muenscher SB, Annandale CH, Guthrie AJ, Bertschinger HJ. Reversibility of the effects of GnRH-vaccination used to suppress reproductive function in mares. *Equine Vet J.* (2013) 45:111–3. doi: 10.1111/j.2042-3306.2012.00577.x
18. Cox JE. The castration of horses: or castration of half a horse? *Vet Rec.* (1973) 93:425–6. doi: 10.1136/vr.93.15.425-a
19. Cox JE, Redhead PH, Dawson FE. Comparison of the measurement of plasma testosterone and plasma oestrogens for the diagnosis of cryptorchidism in the horse. *Equine Vet J.* (1986) 18:179–82. doi: 10.1111/j.2042-3306.1986.tb03589.x
20. Illera JC, Silvan G, Munro CJ, Lorenzo PL, Illera MJ, Liu IK, et al. Amplified androstenedione enzymeimmunoassay for the diagnosis of cryptorchidism in the male horse: comparison with testosterone and estrone sulphate methods. *J Steroid Biochem Mol Biol.* (2003) 84:377–82. doi: 10.1016/S0960-0760(03)00057-8
21. Senger PL. *Pathways to Pregnancy and Parturition*. 3rd ed. Pullman, WA (2015).

Conflict of Interest: The authors declare that the research was conducted in the absence of any commercial or financial relationships that could be construed as a potential conflict of interest.

Copyright © 2020 Ponthier, Rigaux, Parrilla-Hernandez, Egyptien, Gatez, Carrasco Leroy and Deleuze. This is an open-access article distributed under the terms of the Creative Commons Attribution License (CC BY). The use, distribution or reproduction in other forums is permitted, provided the original author(s) and the copyright owner(s) are credited and that the original publication in this journal is cited, in accordance with accepted academic practice. No use, distribution or reproduction is permitted which does not comply with these terms.

Advantages of publishing in Frontiers

OPEN ACCESS
Articles are free to read for greatest visibility and readership

FAST PUBLICATION
Around 90 days from submission to decision

HIGH QUALITY PEER-REVIEW
Rigorous, collaborative, and constructive peer-review

TRANSPARENT PEER-REVIEW
Editors and reviewers acknowledged by name on published articles

Frontiers
Avenue du Tribunal-Fédéral 34
1005 Lausanne | Switzerland

Visit us: www.frontiersin.org
Contact us: frontiersin.org/about/contact

REPRODUCIBILITY OF RESEARCH
Support open data and methods to enhance research reproducibility

DIGITAL PUBLISHING
Articles designed for optimal readership across devices

FOLLOW US
@frontiersin

IMPACT METRICS
Advanced article metrics track visibility across digital media

EXTENSIVE PROMOTION
Marketing and promotion of impactful research

LOOP RESEARCH NETWORK
Our network increases your article's readership